



FRIEDA RIVER

Frieda River Limited

Sepik Development Project

Environmental Impact Statement

Appendix 2a – Frieda River Hydroelectric Project
Selection Phase Study

FRP-2-D-00-01-D-084-002



Frieda River Hydroelectric Project Selection Phase Study

Main Report

Report Prepared for

Frieda River Limited



Report Prepared by



SRK Consulting (Australasia) Pty Ltd

PNA009

November 2018

Frieda River Hydroelectric Project

Selection Phase Study

Main Report

Frieda River Limited

PO Box 2297, Fortitude Valley Business Centre
Brisbane QLD 4006

SRK Consulting (Australasia) Pty Ltd

Level 1, 10 Richardson Street
West Perth WA 6005

e-mail: perth@srk.com.au
website: asia-pacific.srk.com

Tel: +61 08 9288 2000
Fax: +61 08 9288 2001

PNA009

November 2018

Compiled by

Claude Prinsloo
Senior Consultant

Email: jmoreno@srk.com.au

Peer Reviewed by

Pepe Moreno
Principal Consultant

Authors:

Claude Prinsloo; Peter Robinson; John Chapman; Ian de Bruyn, Greg Brown, Alejo Sfriso, Heather Thompson, Dave Luppnow, Andrew Lim, Ognjen Kotur, Daryl Hockley and Rebecca Getty.

Executive Summary

Introduction and project design/overview

Frieda River Limited (FRL), a wholly owned subsidiary of PanAust Limited, commissioned SRK Consulting (Australasia) Pty Ltd (SRK) to undertake a Selection Phase Study (SPS) for the Frieda River Hydroelectric Project (FRHEP), will be developed with the Frieda River Copper-Gold Project (FRCGP).

The FRCGP, as currently envisaged, will mine a large copper porphyry deposit that lies in rugged jungle-covered upland terrain of the West Sepik Province in Papua New Guinea (PNG). The project is remote and has no road access or power supply. The site experiences high rainfall and seismic activity.

The functions of the proposed hydroelectric power facility are to supply power for planned mining activities and potential third-party customers and to store the 33-year Life of Mine tailings and waste rock produced. The combined total volume of tailings and waste generated (2.13 Bm³) will be deposited subaqueously in the FRHEP reservoir. Over the LOM, it is expected that a further 44 Mt of fugitive sediment will inundate the FHREP reservoir.

The total power demand for the mine, once fully operational, ranges between 165 MW and 277 MW, and it is planned that excess power generation will be distributed to the export grid for sale to other customers.

SRK collaborated with Robinson Energy Limited (REL) and Stantec New Zealand Ltd (Stantec) to design a 190.5 m high asphalt core rockfill dam (ACRD) embankment capable of supplying the required flow to 10 turbines housed directly downstream of the embankment.

Independent external review was provided by the Tailings Independent Review Panel (TIRP), which is appointed by FRL. The TIRP undertook three reviews of the design.

SRK prepared a forward works plan, with a specific focus on the Definition Phase Study (DPS), as well as an overview of requirements for project implementation.

Design Objectives, Standards and Criteria

The design of the FRHEP is dual-purpose: the facility will produce economic and renewable power, as well as provide permanent, safe and stable storage of tailings and waste rock from the FRCGP.

The facility is required to store a total of 2.17 Bm³ (1.5 Bt tailings, 1.6 Bt waste rock and 44 Mt fugitive sediment) over a 33-year LOM. This will require a single raise embankment with a crest level of RL 238.5 m (190.5 m high).

The SPS objectives were to consider alternative options and identify the optimum design solution for the FRHEP.

To produce power, the reservoir must provide a supply of water to the hydroelectric facility. To protect the integrity of the embankment, inflow flood volumes must either be stored or safely diverted. To prevent acid generation, the tailings and waste rock must be kept in a fully saturated state under a cover of water.

The embankment is classified as Extreme Consequence under guidelines provided by the Australian National Committee on Large Dams (ANCOLD), and design standards and criteria have been selected to align with these guidelines.

Given the scale of the FRHEP, the inter-related operating requirements of the FRHEP, and the hazard rating, SRK recommends an FRHEP stewardship program be developed along with the engineering design.

Design inputs

Geology

The FRCGP is located on the northern flank of the Central Highlands. The embankment site is on Exploration Licence (EL)1212, in an area dominated by three major WNW–ESE to NW–SE, northward dipping thrust faults. These faults are splays of the Leonard Schulze Fault, which lies about 100 km to the east. From south to north, the major thrust splays are the Fiak, Frieda and Saniap faults. The Saniap Fault forms the boundary between rocks of the Wogamush Formation to the north and Ok Binai Phyllite to the south. The Saniap Fault lies approximately 2 km north of the embankment site and the Frieda Fault lies some 7 km to the south of the embankment site.

The oldest rocks in the area are the Jurassic- to Middle Eocene-aged Ok Binai Phyllite, which grades into the equivalent of the Wabia beds and Wahagi Group slate. The sequences comprise phyllitic mudstone, sandstone and volcanolithic rocks. The overlying Wogamush Formation consists of volcanogenic sequences and forms part of the Late Oligocene- to Miocene-aged Maramuni Igneous Complex. The sequences consist of andesite to basaltic volcanics, volcanolithic sandstone, mudstone and limestone. In some places, the sequences have been intruded by numerous plutons.

Major slices of April Ophiolites have been thrust over the sequences of Ok Binai Phyllite and Wogamush Formation. The April Ophiolite is of Paleogene age and consists of undifferentiated ultrabasic igneous rocks of basalt, gabbro and peridotite. These rocks represent the erosional remnants of a thrust sheet of oceanic crust that was once more extensive. The rocks are variably serpentinised and comprise layered to massive cumulate dunite – the bedrock at the FRHEP site – harzburgite and wehrlite. The embankment is situated in a klippe of April Ophiolite, separated from the underlying Ok Binai Phyllite to the south and the underlying sedimentary Wogamush Formation to the north by a low angle thrust fault.

Probabilistic and deterministic seismic hazard assessments (PSHAs and DSHAs) were developed for the nearby Nena integrated storage facility (ISF) site in an earlier design. The results from these assessments were used to estimate design ground motions, including peak ground acceleration (PGA) of 1.09g for the maximum credible earthquake (MCE) at the FRHEP.

Climate and Hydrology

The climate of the FRHEP site is classified as a tropical wet climate. The average annual rainfall is in the order of 8,000 mm. The climate is dominated by local weather effects rather than by synoptic-scale monsoonal effects or the movement of the inter-tropical convergence zone. The terrain controls patterns of air circulation, with the result that the rainfall pattern exhibits very weak seasonality.

The FRHEP catchment area is approximately 1,033 km². The 72-hour, 1:100 average recurrence interval (ARI) rainfall and probable maximum precipitation (PMP) are 367 mm and 1,350 mm, and results in peak flows of 7,640 m³/s and 30,000 m³/s, respectively.

Geochemistry and Water Quality

As part of the FRCGP, several geochemical testing programs have been completed on ore, tailings and waste rock samples. The results indicated that all lithological units are potentially acid-forming (PAF), with the acid potential (AP) values exceeding the generally low acid neutralisation capacity (ANC) values; therefore, the waste rock would quickly become acidic if left exposed to air. In addition, the results indicated short lag times to net acid generation and high rates of oxidation. The leachate

chemistries further indicated that elevated concentrations of metals (particularly copper, iron and aluminium) would be expected under oxidising conditions.

The implication is that oxidation should be minimised by depositing the waste rock subaqueously as soon after it is mined as practicable.

Testing of representative tailings samples indicated that the tailings are also likely to be PAF; although lag times to acidification may be slightly longer. If the tailings oxidise, copper, cobalt, manganese and nickel would leach at significant concentrations. Subaqueous deposition will prevent acid generation and minimise solute release from the tailings.

FRHEP scheme configuration and performance

With the dam crest elevation at RL 238.5 m, a key objective of the SPS was to optimise the FRHEP's power generation potential while ensuring first power was available for the FRCGP commissioning (initially) and for full production thereafter.

The following major factors have been taken into account:

- The FRCGP and export grid reliability targets are achieved, taking the generating plant reliability and water supply reliability into account
- The maximum operating level permitted is met, while ensuring the freeboard requirements for water level rises in the event of a probable maximum flood (PMF) and a 1:1000 annual exceedance probability (AEP) are met and accounting for the possible slumping of the dam crest following a large seismic event.
- The optimum live storage range for maximising energy production.

The resulting powerstation installed capacity details are set out in Table ES-1. Details of the combined maximum load required by the FRCGP and remote export grid are provided in Table ES-2 for Year 17 which is the year of peak electricity demand at the FRCGP.

Table ES-1: Key turbine generator and auxiliary plant design details

Turbine	Units	Large unit	Small unit
Number of units		8	2
Rated power output at generator terminals	MW	69.2	19.3
Rated generator output at generator terminals	MVA	81.4	22.7
Synchronous speed	rpm	300	500
Generator flywheel effect GD ²	T-m ²	1,750 (minimum); in excess of 2,250 preferred	130 (minimum); in excess of 160 preferred
Generator efficiency at peak output and unit power factor		>98.5%	>98.5%
Generator efficiency at peak output and 0,85 power factor		>97.0%	>97.0%
Transformer efficiency at rated output		>99.3%	>99.3%
Auxiliary power losses		<0.5% of station output	<0.5% of station output
Unit rated power output at HV transformer Terminals	MW	68.3	19.1
Rated generator output at HV transformer terminals	MVA	80.0	22.3
Station installed capacity at HV transformer terminals	MW	584.8	

Table ES-2: Optimised power generation for dam crest height of RL 238.5 m (Year 17)

Parameter	Units	Values
FRCGP peak demand	MW	277.2
FRCGP energy demand	GWh/a	2,159
Indicative supply losses	%	0.2%
Net FRCGP energy supply	GWh/a	2,155
Export grid peak demand	MW	100.0
Export grid energy demand	GWh/a	630
Supply losses	%	1.5%
Net export grid energy supply	GWh/a	621
FRHEP peak demand	MW	377.2
FRHEP energy demand	GWh/a	2,789
Supply losses	%	0.5%
Net FRHEP energy supply	GWh/a	2,775

The bulk of the FRHEP design was completed and a draft report submitted in early June 2018 prior to the second TIRP review (12–15 June 2018). The draft report submitted did not consider the revised FRCGP electrical demand which was received in late May.

SRK/Stantec addressed the most critical areas identified by the TIRP only; the remaining issues raised during the TIRP review will be addressed as part of forward works.

FRHEP design components

The main FRHEP design components are the embankment and hydroelectric power facility. Subcomponents of the hydroelectric power facility are the intakes, conveyance tunnels, powerhouse and associated equipment.

Embankment

The embankment is designed as a zoned rockfill dam with an impermeable asphalt core in the centre of the embankment. The embankment includes the following main features:

- Foundation – unsuitable material must be removed
- Filter/ transition zones – upstream and downstream of the asphalt core and horizontal filter and transition zones on the downstream segment
- Embankment seepage cut-off – impermeable asphalt core in the centre of the embankment
- Foundation seepage cut-off – plastic concrete cut-off wall and grout curtain (includes pressure grouting to seal fault structures)
- Downstream toe drain
- Concrete plinths – in the valley section and on the left and right abutments
- Rockfill shell.

Residual flow intake

The residual flow intake is located at a low level to allow river flow once the embankment diversion tunnels are closed and plugged. As soon as the water level reaches RL 171.20 m, allowing the main conveyance system to be used, the residual flow system will be shut down. Once the reservoir level rises above RL 200 m and the bypass valves are operating correctly, the residual flow intake will be

plugged. It may be decided that the plugging of the residual flow valve tunnel can be delayed until the spillway is commissioned.

The residual flow system has the following components/ features:

- An intake structure
- Tunnel
- Valve shaft and flow control valves
- Stilling chamber and connection to one of the diversion tunnels.

Lower intake

The design includes a lower intake to enable early operation of the hydroelectric power generation facility once filling of the reservoir commences. This lower intake arrangement also provides initial access to the main conveyance tunnels, allowing construction to be undertaken from both ends. Once the upper intake is operating correctly, the lower intake will be decommissioned and plugged. The lower intake will be in use for a short period – nominally two years.

The lower intake has the following components/ features:

- A simple bell-mouthed concrete intake structure
- A screen
- 62 m gate access shaft with a platform at RL 205 m
- A single set of hydraulically controlled wheeled gates and stoplogs.

Upper intake

The upper intake structure will feed two parallel conveyance tunnels, and includes:

- 50 m high concrete intake structure
- Two sets of hydraulically controlled wheeled gates and stoplogs
- A screen
- An automated screen cleaner
- An access bridge at RL 235 m.

Conveyance tunnels

The two parallel conveyance tunnels have the following features:

- Each tunnel is 7.1 m in diameter, including power shafts and surge chambers.
- Each tunnel will be fully concrete lined.
- Each tunnel will be steel-lined at the outlet end and connected to the main penstocks.

Penstocks and manifold

Two 7.1 m diameter epoxy lined penstocks will connect the powerhouse to the conveyance tunnels. Each penstock is then split via a manifold to provide water to each turbine and the bypass valves.

Powerhouse

The powerhouse contains the generating and switching equipment, and has the following features:

- The powerhouse building is 196 m long by 35 m wide and located on the original river bank of the Frieda River, just downstream of the embankment toe.
- The powerhouse has multiple levels to access the equipment, and a loading/ erection bay to allow installation (and future maintenance) of the equipment.

- On the river side of the powerhouse, a submerged tailrace allows water from the turbines to be discharged to the river.
- The tailrace contains a series of closure stoplogs for flood protection.

Bypass valves

Two other major structures, the bypass valves and flow chambers are located adjacent to the powerhouse. They have the following features:

- The bypass structures are connected to each penstock and consist of four large (2.3 m) cone valves, housed in an energy dissipation/ anchor chamber.
- The bypass valves will bypass flood flows around the powerhouse during early filling and before completion of the right abutment spillway.
- The bypass valves allow flows to enter the Frieda River immediately below the embankment to maintain a navigable river during construction, which is required prior to completion of the main access road.

Generation equipment

The powerhouse contains a series of 10 turbine generator units – eight turbines rated at 69.2 MW and two smaller units at 19.3 MW. Each penstock/ conveyance tunnel is connected to four large units plus one small unit which is available, if required, to ensure load requirements are met.

The operation of the four large units on each penstock will generally be operated as follows:

- 2 or 3 units will be available for generation
- 1 unit will be available as a spinning reserve on one of the penstocks
- 1 unit can be out of service for maintenance.

The key performance rules for the turbine generator and auxiliary plant are set out in Table ES-1.

Load banks

The function of the load banks, located adjacent to the powerhouse, is to commission the turbine generators and conveyance system when there is insufficient or no electrical demand from the FRCGP.

Cofferdams

An initial diversion dam will be required upstream of the main cofferdam to allow construction of the upstream cofferdam in the river course to be completed. The upstream cofferdam will provide flood protection to the downstream embankment works – a geomembrane cut-off on the upstream face of the cofferdam embankment is included. The upstream cofferdam will be integrated with the main embankment.

The downstream cofferdam will provide flood protection to the upstream works by preventing backwater once the diversion tunnels have been commissioned.

Surface water management structures

The Frieda River is a river of significant size and the FRHEP will require extensive water management works. Management of large runoff volumes requires a robust system to assure stability of the embankment while limiting environmental impacts and allowing facility closure. In addition, within design storm parameters, safety and access must be assured to protect personnel undertaking construction of the embankment cut-off system, foundation stripping and plinth development.

Surface water management structures have been integrated in the FRHEP design. The function of the water management structures is to manage the upstream catchment runoff, precipitation falling on the facility, plus any tailings supernatant water, throughout progressive periods of the FRHEP life, as follows:

- Construction: A diversion dam, main cofferdam, downstream cofferdam, two diversion tunnels, a residual flow tunnel and associated power shaft
- Operation: Two conveyance tunnels with integrated lower and upper intakes and surge chambers, and a right abutment spillway
- Closure: Right abutment spillway.

To maintain a minimum residual flow of 50 m³/s downstream of the embankment, a residual flow tunnel will be installed and integrated with the western diversion tunnel. This tunnel will be permanently closed once it has served its purpose.

To expedite commissioning of the FRHEP, the design incorporates a supplementary lower intake that links to the final conveyance tunnel system. This initiative is referred to as 'early filling'.

Quarry

A quarry has been designed to supply 30.5 million LCM of clean rock for construction of the FRHEP and appurtenant structures. Quarry operations have been designed in four phases to incorporate civil infrastructure scheduling and access requirements and to accommodate water level rise. The quarry has been extended to provide the bulk of excavations needed for construction of the intake structures.

The geotechnical investigation identified rock of suitable quality for FRHEP construction on the east bank of the Frieda River and directly south of the embankment location. To meet construction volume demand, rock from the spillway excavation works, which is of similar quality to the rock from the quarry will also be used. The spillway excavation has therefore been designed as an extension of the quarry.

The proposed quarry and spillway excavations will be operated as a single source of supply that can supply the required volumes of rock for the FRHEP. The quarry design includes an allowance of unsuitable material that would be spoiled or used for temporary construction infrastructure, 16% from the quarry and 18% from the spillway. It is understood that this spoil material is mainly NAF.

SRK recommends CAT 785 haul trucks be used for haulage of rock materials.

Sediment management

Sediment management plans were developed to prevent sediment contamination of the embankment filter and transition layers and to limit sediment transported away from the site. The site experiences high rainfall that causes erosion and movement of sediments, and on-site management is required. The basic sediment management philosophy involves limiting the extent of disturbed areas as far as is practical, diverting runoff from the excavation and spoil piles, and constructing sedimentation ponds to capture sediment downstream of key construction activity areas.

The construction plan includes two temporary spoil storage areas south of the embankment: on the east and west banks of the Frieda River respectively. The spoil storage areas will be flooded once the reservoir has been filled.

Paired sedimentation ponds have been designed at each key sediment generation site allowing maintenance to be carried out on one pond while the other is in operation. One pair of sedimentation ponds is required downstream of the embankment site and one at each of the two spoil storage areas.

Construction, operation and closure

Opportunities and risks associated with the project have been analysed to support the SPS design and are addressed in a supporting report.

Construction methodology

The FRHEP is a large, complex project that requires the expertise of Tier 1 dam building contractor. Some construction risks have been ranked as High to Extremely High and careful planning and control will be required to ensure compliance with the FRHEP objectives.

FRL requires the FRHEP to be completed safely and effectively, within a predetermined construction timeframe. Personnel safety and meeting safety performance targets are key project objectives. All construction activities must be executed in accordance with PNG regulatory requirements. The construction works will result in significant disturbance of the natural environment. All environmental impacts, including impacts on downstream water sources and users, must be managed in line with an approved Environmental Management Plan (EMP).

Among many other challenges, the contractor will face wet conditions, steep terrain, shallow rock, and accessibility and spatial constraints. Due to the site's remote location, it is assumed that no bulk infrastructure, such as access roads, will exist for the first 18 months of construction. Materials will need to be brought to site by barges using the Sepik and Frieda rivers.

The embankment construction will require placement of rockfill, filter and transition zones, and an asphalt core. The placement of these materials will occur at different times and rates, requiring the use of different equipment and facing different challenges.

Due to the considerable load exerted by the contents of the reservoir on the embankment, each material must meet specific standards with regard to density, strength, permeability, compressibility and resistance to deformation. Tailings, sediment and fine waste is likely to mobilise and settle against the embankment, contributing additional load. The compaction specifications for the rockfill, filter and transition materials and asphalt core will be determined based on field tests carried out prior to construction and on experience from similar projects. The construction materials will also have to meet the technical specifications.

Stewardship

Given the scale and hazard rating of the FRHEP, and its dual function of generating power and serving as storage for waste rock and tailings, SRK recommends that stewardship program be developed in conjunction with the engineering design. Key stewardship components include a dam safety program, associated corporate systems, role descriptions and commercial structuring.

Deposition strategy

The waste rock and tailings generated over the 33-year LOM will be disposed of and stored subaqueously to prevent acid generation. Tailings will be deposited subaqueously via a floating pipeline system in dedicated storage compartments within the Ok Binai and Frieda River compartments, and single-stage crushed waste rock will be dumped via barges in the Nena, Ok Binai and Frieda River compartments.

An emergency compartment for deposition of any material during emergency or maintenance conditions has been sited near the plant.

Water quality and suspended sediment estimates indicate that deposition of the tailings and waste rock must be restricted to a maximum level below the surface of the reservoir. This will prevent exposure of fines to the epilimnion layer where streamflow and currents cause water movement and

may result in re-suspension and/ or transportation of particles past the embankment. The waste rock may not be dumped within 1 km of the embankment.

The waste rock generated during early filling of the reservoir will be dumped at the headwaters of the reservoir in the Nena compartment closest to the plant.

The mechanical design of the pipelines, pumps and barges is part of the FRCGP and does not form part of the scope of this study

Embankment and Reservoir Operating Rules

The reservoir and embankment crest rules shown in Table ES-3 were determined following completion of the Water Balance and Energy Model and the Energy Production analysis.

Table ES-3: Water Management operating rules

Item	Values	Comment
Embankment crest level	RL 238.5 m	Final embankment crest elevation
Embankment spillway crest level	RL 212.44 m	Crest level for spillway four gates 7.5 m (W) × 16.2 m (H) to achieve spillway discharge required in a PMF event
Maximum PMF water level with four spillway gates operating	RL 231.8 m	Maximum level during the PMF with all four spillway gates operating correctly
Maximum PMF water level with three spillway gates operating	RL 232.40 m	Maximum level during the PMF with three of the four gates operating correctly; the fourth spillway gate remains fully closed
Normal reservoir maximum operating level	RL 226.14 m	Maximum operating level with spillway gates closed (no spill)
Minimum reservoir operating level for full power to FRCGP alone	RL 199.39 m	Reservoir level below which power supply to the FRCGP shuts down
Lower intake invert	RL 143.30 m	In support of early power
Upper intake invert	RL 185.60 m	Permanent intake
Maximum tailings and waste rock level	RL 159.40 m	Based on 33-year LOM at the FRCGP

Closure

Conceptual FRHEP closure plans were developed for:

- i) the temporary suspension of mining
- ii) early permanent closure
- iii) permanent closure
- iv) closure during construction.

Critical closure requirements include:

- minimisation of the risk of failure for the embankment and spillway
- prevention of uncontrolled release of the tailings and waste rock
- prevention of oxidation and contaminant release from the stored tailings and waste rock.

Unlike conventional hydroelectric power dams, the requirement to maintain a permanent water cover over the reactive tailings and waste rock precludes the reservoir being drained. The embankment is expected to exist in perpetuity and will require monitoring and maintenance over the long term.

The conditions applicable to temporary suspension are less onerous than for long-term closure, which would include removal of radial gates, closure of tunnels and removal of the powerhouse.

Water quality predictions

Once fully submerged, the waste rock will not undergo any further oxidation. However, as the waste rock falls through the water, solutes generated from the time the waste rock is first exposed and the time it is deposited could be released. Depending on the mining schedule and methods, the period of exposure prior to deposition may vary – solute release from the waste rock was estimated conservatively based on an average exposure time of 12 weeks, using the oxidation and metal release rates determined from kinetic testing. During operations, exposure times before inundation will be kept as short as practicable. Secondary mitigation strategies to limit solute release may include blending the waste rock with limestone or lime to neutralise acidity and precipitate metals.

Subaqueous deposition will also prevent oxidation of the tailings. Solutes from the process water will be released into the reservoir when the tailings are deposited. Solute release was estimated from results of locked cycle metallurgical testing.

A limnological assessment by HydroNumerics Pty Limited (HydroNumerics) assessed the layer stability within the reservoir and the transport of sediments from natural sources as a result of barge dumping of waste rock and pipeline deposition of tailings. Results indicated that development of the reservoir will attenuate flows downstream of the FRHEP in the Frieda River (but will have no impact on flows in the Sepik River) during operations and after closure, and will effectively regulate transport of suspended solids.

Other results of the limnological assessment were integrated with the water balance and source terms developed for the open pit, waste rock and tailings to develop a combined water and load balance model. The results indicated that contact water in the open pits is likely to become acidic during early operations and would remain acidic after flooding of the open pits at closure. Metal concentrations, copper and iron in particular, are expected to be elevated relative to background levels, and direct release without treatment would result in unacceptable concentrations downstream of the FRHEP. Treatment of open-pit water runoff will therefore commence from Year 1 of operations, using an engineered water treatment plant, to mitigate poor water quality downstream. Treated open-pit water will be discharged to Ubai Creek, where it will flow into the ISF. Discharge treatment residues will be comingled with the tailings and deposited to the bottom of the ISF. Treatment will continue during operations and for approximately 50 years after closure, or until closure criteria are met.

The control measures for waste rock and tailings in the reservoir, in conjunction with the pit water treatment system, are predicted to maintain compliance with the *PNG Environment (Water Quality) Regulations (2002)* and the PNG drinking water guidelines downstream of a proposed mixing zone in the Frieda River. The FRHEP reservoir outflows are predicted to result in increases in constituent concentrations in the Frieda River, and may lead to exceedance of corresponding Australian guidelines¹ receiving water quality trigger values. The predicted increases will vary depending on the flow conditions, stage of operations and water treatment strategy. Copper concentrations in the Sepik River are predicted to remain comparable to background levels. Naturally occurring dissolved organic carbon is expected to complex with copper and other metals to various degrees, which would reduce the concentrations of labile metals and reduce toxicity. Copper speciation calculations indicate that, on average, between 68% and 87% of the dissolved copper may be complexed by organic species.

Waste rock deposition within the FRHEP reservoir is expected to generate locally elevated concentrations of total suspended solids (TSS). Modelling results indicate that the TSS can be regulated by controlling the rate and location of deposition. TSS concentrations downstream of the embankment are expected to range to a maximum of 445 mg/L, with a mean of ~158 mg/L for the

¹ ANZECC & ARMCANZ 2000, Australian and New Zealand Guidelines for Fresh and Marine Water Quality

operational period (compared to the baseline mean TSS concentrations of 208 mg/L). Additional mitigation may be required for meeting the International Finance Corporation (IFC) discharge point criterion of 50 mg/L. Potential measures may include rescheduling of waste rock deposition and the use of silt curtains at the deposition sites or at the intakes to the hydroelectric power plant.

Water Balance

During operations, flows downstream of the reservoir embankment show less variability between minimum and maximum values, and between 10th and 90th percentile values, due to the regulation of flows from the FRHEP reservoir. The altered flow regime extends along the entire Frieda River to its confluence with the Sepik River. However, there are unlikely to be significant changes to the Sepik River flow regime.

The modelling results further suggest that water levels in the FRHEP reservoir may not be sufficient to support the planned hydroelectric power production during extended dry periods, with interruptions to operations possible during extended low rainfall realisations (typically below the 10th percentile), particularly during periods of high water demand for hydroelectric power generation.

Limnology

Modelling results suggest that the FRHEP reservoir is likely to be persistently stratified with no regular periods of complete mixing, and that the addition of waste rock and tailings to the reservoir beneath the epilimnion is unlikely to alter the top-down stratification structure. Modelled inflows from the major rivers form intrusions through the reservoir at a depth of neutral buoyancy following an initial plunge near their headwaters. In addition to the inflows, the hydroelectric power intake rate and depth play an important role in shaping the stratification and promoting short-circuiting of inflow waters through the reservoir.

Supporting reports

The SPS design is supported by extensive investigations and analyses undertaken during the SPS, including:

- Embankment optimisation
- Hydroelectric power scheme design
- Limnology study
- Dam break assessment
- Wave size assessment
- Site wide water and load balance
- Multiple accounts analysis (MAA)
- Implementation
- Risk analysis
- Basis of Estimate
- Forward works plan.

Additional investigation is required to support further design of the FRHEP, which may lead to changes in designs and costs.

The FRHEP key parameters are listed in Table ES-4. Full details of are presented in the accompanying technical reports, which should be consulted prior to undertaking any analysis or review of the proposed design.

Table ES-4: Key parameters

Element	Key parameter	New Values
Hydrology	24 hr PMP rainfall depth	790 mm
	Mean annual rainfall	8,000 mm
	PMF peak flow (72 hr)	30,000 m ³ /s
	1:100 AEP flood peak flow (24 hr)	7,640 m ³ /s
	Mean annual discharge	220 m ³ /s
	Catchment area	1,033 km ²
Seismicity	MCE	1.09g
Reservoir	Footprint at maximum operating level	123 km ²
	Storage capacity at maximum operating level	9.6 Bm ³
Diversion dam	Flood protection	<1:2 AEP (design)
	Crest elevation	RL 74.5 m
	Crest width	10 m
	Crest length	160 m
	Fill volumes	113,000 m ³
	Construction materials	Large rocks and selected fine-grained fill
	Maximum height	27 m
	Average upstream slope	1:3 (V:H)
	Downstream slope	1:2.5 (V:H)
Upstream cofferdam	Flood protection	AEP 1:100
	Crest elevation	RL 83 m
	Crest width	15 m
	Crest length	300 m
	Fill volumes	380,000 m ³
	Construction materials	Rockfill and selected fine-grained fill
	Maximum height	35.5 m
	Average upstream slope	1:2.5 (V:H)
	Downstream slope	1:2.5 (V:H)
Downstream cofferdam	Flood protection	AEP 1:100
	Crest elevation	RL 55.5 m
	Crest width	3 m (each)
	Crest length	62 m
	Fill volumes	21,000 m ³
	Construction materials	Rockfill and selected fine-grained fill
	Maximum height	8 m
	Upstream slope	1:3 (V:H)
	Downstream slope	1:3 (V:H)
	Number	2
Diversion tunnels	Length	1,375 m
	Lining	150 mm thick fibrecrrete lined (with concrete-lined base)
	Dimensions (lined)	9 m height × 9 m width ('D'-shaped)
	Maximum discharge	1,270 m ³ /s (both tunnels combined)
	Maximum velocity	8.8 m/s
Residual flow tunnel	Length	310 m
	Lining	Initial support – 50 mm shotcrete or 120 mm fibrecrrete Permanent lining – 250 mm thick reinforced concrete

Element	Key parameter	New Values
	Dimensions (lined)	Upstream of valves Clear dimension – 4 m wide × 4 m high (D-shaped) Valve chamber Clear dimension – 8 m wide × 10 m high (D-shaped) Downstream of valves Clear dimension – 4 m wide × 5.5 m high (D-shaped)
	Normal discharge	Assumed to be 50 m ³ /s
	Normal velocity	3.5 m/s
	Vertical rise length	180 m
	Vertical rise diameter	Clear dimension – 7.5 m
Lower intake tunnel	Length	180 m with bifurcation
	Lining	Initial support – 50 mm shotcrete Permanent lining – 250 mm thick reinforced concrete
	Dimensions (lined)	Clear dimension – 7.1 m wide × 7.1 m high (D-shaped)
	Maximum discharge	Varies
	Maximum velocity	Varies
	Vertical rise length	62 m
	Vertical rise diameter	Clear dimension – 10 m
Conveyance tunnels	Number	2
	Length	~1,050 m each
	Lining	Initial support – 50 mm shotcrete or 120 mm fibrecrete Permanent lining - 250 mm thick reinforced concrete
	Dimensions (lined)	Clear dimension – 7.1 m wide × ~7.1 m high (D-shaped)
	Normal discharge	Maximum generation flow – 320 m ³ /s
	Normal velocity	Maximum generation flow – 3–4 m/s
	Surge chamber length	2 × 120 m
	Surge chamber diameter	Clear dimension – 12 m
	Power shaft length	2 × (65 m + 45 m) = 220 m
	Power shaft diameter	Clear dimension – 7.1 m
Main embankment	Crest elevation	RL 238.5 m
	Crest length	747 m
	Crest width	12 m
	Maximum height (crest to toe)	190.5 m
	Maximum reservoir area	128 Mm ² at maximum PMF level (RL 232.4 m)
	Fill volume	29.66 Mm ³
	Foundation excavation depth	5 m
	Construction materials	Quarried rockfill, crushed rockfill and asphalt
	Upstream slope	1:2 (V:H)
	Downstream slope	1:1.8 (V:H) inter-bench and 1:2 (V:H) crown
	Embankment cut-off	1.7 m wide asphalt core tapered to width of 1.5 m
	Foundation cut-off	15–65 m deep, 1.5–2.3 m wide plastic concrete cut-off wall and fault grouting
Operating levels	Minimum operating level	RL 199.4 m
	Level at which power cannot be supplied to the export grid	RL 204.4 m
	Maximum operating level	RL 226.1 m with spillway gates closed
	Upper intake invert level	RL 185.6 m

Element	Key parameter	New Values
	Lower intake invert level	RL 143.3 m
	Residual flow tunnel intake invert level	RL 70 m
	Diversion tunnel intake invert level	RL 56 m
	Maximum PMF level (3 out of 4 spillway gates operational)	RL 232.4 m
Tailings and waste rock deposition	Maximum tailings and waste storage level	RL 159.4 m
	Maximum available storage capacity (at RL 159.4 m)	3.3 Bm ³
	Tailings	Pumped and deposited subaqueously
	Waste	Barge dumped
	Total storage requirement	2.17 Bm ³
Power generation	Normal maximum water level	RL 226.14 m
	Turbine centreline level	RL 45.6 m
	Maximum static head	186.4 m
	Large unit number and rating	8 × 69.2 MW
	Small unit number and rating	2 × 19.3 MW
	Installed capacity	592 MW
	Peak power demand at HV transformer terminals at peak FRCGP demand	Total = 381 MW (FRCGP = 277 MW and export grid = 104 MW)
	Peak power demand at HV transformer terminals at peak export demand	Total = 409 MW (FRCGP = 181 MW and export grid = 228 MW)
	Maximum annual generation to end users	2775 GWh/a
	Powerhouse size	196 m × 35 m
Turbine type	Francis	
Spillway	Type	Ogee crest on right abutment spillway with radial spillway gates
	Crest level	RL 212.4 m. Crest level for spillway four gates 7.5 m (W) × 16.2 m (H) to achieve spillway discharge required in a PMF event
	Top of gates	RL 228.6 m–RL 233.78 m
	Ogee crest length	30 m
	Energy dissipation	Flip bucket
	Spillway length (from ogee crest to edge beam)	745 m
	Gate type	Radial
	Maximum outflow during PMF conditions	5,100 m ³ /s
Roads	Permanent road length	3,1 km
	Permanent road width	7 m
	Temporary civil equipment road length	14.8 km
	Temporary civil equipment road width	13 m
	Temporary quarry equipment road length	12.7 km
	Temporary quarry equipment road width	22 m
Xstrata 2010–2011 Geotechnical Investigations	Drillholes - all	29 holes totalling ~2,400 m
SRK Geotechnical Investigations (Stage 1 and 2)	Drillholes - quarry	9 holes totalling 950 m
	Drillholes - embankment and associated infrastructure	47 holes totalling 4,395 m
	Downhole permeability testing	Carried out in 16 holes

Element	Key parameter	New Values
	Downhole televiewer survey	Completed in 9 holes
	Extensometers	Installed in 2 holes on the left abutment
	Vibrating wire piezometers	Installed in 1 hole on the left abutment
	Laboratory testing	UCS, elastic properties, direct shear of joints, slake durability, LA abrasion, PSD, Atterberg limits, Emerson dispersion testing
	Geophysical survey	Two seismic refraction traverses: 1,000 m on left abutment; 200 m on eastern riverbank

Table of Contents

Executive Summary	ii
Disclaimer.....	xliii
List of Abbreviations	xliv
1 Introduction and Background	1
1.1 Climate	2
1.2 Project history	2
1.3 Export grid power supply	3
1.4 Site selection.....	3
1.5 Project benchmarking	4
1.6 Embankment optimisation.....	5
1.6.1 Benchmarking	6
1.6.2 Seismicity	7
1.6.3 Rainfall	9
1.6.4 Hydroelectric power generation	9
2 Basis of Design	11
2.1 Objectives	11
2.1.1 Development	11
2.1.2 Operations.....	11
2.1.3 Closure	12
2.2 Hydroelectric power generation	12
2.2.1 Power demand based on May 2018 loads.....	12
2.2.2 Reliability	13
2.2.3 Early power	15
2.3 Tailings and waste rock deposition	17
2.3.1 Production	17
2.3.2 Properties.....	18
2.3.3 Deposition strategy.....	22
2.3.4 Storage capacity.....	22
2.4 Design framework	26
2.4.1 Standards	26
2.4.2 Dam classification and design criteria.....	27
2.4.3 Embankment height	28
2.5 Geotechnical and civil	28
2.5.1 Topography	28
2.5.2 Seismicity	29
2.5.3 Stability.....	36
2.5.4 Seepage	36

2.5.5	Rock properties	36
2.5.6	Tunnels and ground support	37
2.5.7	Roads	37
2.5.8	Spillway bridge	37
2.6	Water management.....	37
2.6.1	Hydrology baseline.....	37
2.6.2	Design flows for construction	39
2.6.3	Design flows for operations.....	40
2.6.4	Water management for closure.....	41
2.7	Wave size modelling	41
2.8	Quarry	42
2.9	Environment and social.....	42
2.9.1	Environmental	42
2.9.2	Limnology	44
2.9.3	Sedimentation	45
2.9.4	Social.....	45
3	Geotechnical Characterisation and Geohazard Assessment.....	46
3.1	FRHEP geotechnical characterisation study	46
3.1.1	Objectives.....	46
3.1.2	Work program.....	47
3.1.3	Regional geological setting	52
3.1.4	Site conditions	53
3.1.5	Site investigations	62
3.1.6	Geotechnical domains.....	74
3.1.7	Geotechnical properties – laboratory testing.....	90
3.1.8	Geotechnical properties – drill core logging results	100
3.1.9	Structural fabric – core logging and televiewer	107
3.1.10	Major structures.....	113
3.1.11	Hydrogeological characterisation	127
3.1.12	Geotechnical design inputs – embankment	139
3.1.13	Construction materials.....	144
3.1.14	Geotechnical design inputs – quarry limits and spoil dumps	146
3.1.15	Slope stability assessments – design of quarry and spillway slopes.....	152
3.1.16	Potential landslide upstream from embankment.....	153
3.1.17	Tunnel design assessments.....	153
3.2	Stage 2 Landslide Geohazard and Georisk Assessment	154
3.2.1	Objectives.....	154
3.2.2	Tasks	155
3.2.3	Site conditions	155
3.2.4	Geohazard assessment – background and process.....	162
3.2.5	Geohazard inventory	165

3.2.6	Geohazard assessment inputs.....	169
3.2.7	Areas of concern	173
3.2.8	Summary	179
4	Hydrology.....	181
4.1	Monitoring data	181
4.1.1	Precipitation data.....	181
4.1.2	Stream gauge data.....	182
4.2	Discharge rating review	183
4.3	Design flood hydrographs	185
4.3.1	Objectives.....	185
4.3.2	Approach	185
4.3.3	Design rainfall.....	186
4.3.4	Rainfall-runoff model	189
4.3.5	Design flood hydrographs	192
4.3.6	Probable maximum flood hydrographs	194
4.3.7	Long duration flood hydrographs	196
4.4	Generated streamflow series	197
4.4.1	Objectives.....	197
4.4.2	Approach	197
4.4.3	Generated inflow series.....	198
4.4.4	Hydrology for hydropower generation.....	203
4.5	Tailwater rating curves	205
4.5.1	Objectives.....	205
4.5.2	Approach	206
4.5.3	Calibration	206
4.5.4	Results	207
5	Power Demand	210
5.1	Power supply reliability standards.....	210
5.1.1	FRCGP reliability criteria	210
5.1.2	Export grid reliability criteria	210
5.1.3	Summary of reliability targets.....	210
5.2	Maximum electrical loads.....	211
5.2.1	Electrical loads provided by FRL in January 2018.....	211
5.2.2	Electrical loads provided by FRL in May 2018.....	214
5.3	Net electrical loads.....	217
5.4	Electrical load changes from the project sizing study	217
6	Water Balance, Limnology and Load Balance	219
6.1	Water balance	219
6.1.1	Water balance model	221
6.1.2	Water balance results.....	224

6.1.3	Conclusions and limitations.....	227
6.2	Limnology.....	227
6.2.1	Model description	229
6.2.2	Model set-up.....	229
6.2.3	Results	232
6.2.4	Summary and recommendations	237
6.3	Load balance (water quality assessment)	238
6.3.1	Tailings and waste rock geochemistry	238
6.3.2	Solute source term derivations.....	242
6.3.3	Results	250
6.3.4	Conclusions.....	259
7	Hydroelectric Power Water Balance and Energy Model	261
7.1	Models.....	261
7.2	Hydroelectric power measured flow hydrology.....	261
7.3	Hydroelectric power synthetic flow hydrology.....	266
7.4	Residual flow requirements.....	269
7.5	Tailwater level	270
7.6	Water balance	270
7.7	Implications of early power generation	271
7.7.1	Lower intake	271
7.7.2	Early filling	271
7.7.3	Storm buffer volume required during early filling	273
7.7.4	Combined delay and storm volume assessment	274
7.7.5	Impact of early filling and lower intake on time to first power generation	277
7.7.6	Early filling findings.....	278
7.8	Powerstation bypass valves.....	278
7.8.1	River transport flow requirements	279
7.9	Residual flow valve	280
8	Embankment.....	282
8.1	Design features	284
8.2	Foundation preparation	284
8.3	Seepage control	288
8.4	Embankment plinth sizing	291
8.5	Embankment plinth design.....	293
8.6	Filter/ transition zones	301
8.7	Toe drain.....	303
8.8	Zoned rockfill shell	304
8.9	Seepage analysis.....	304
8.10	Embankment failure modes	311
8.11	Embankment stability and deformation analysis.....	315

8.11.1	Design background	315
8.11.2	Input for deformation analyses	315
8.11.3	Constitutive models	316
8.11.4	Modelling strategy	316
8.11.5	Geotechnical units	317
8.11.6	Material parameters	317
8.11.7	Selection of ground motions	317
8.11.8	2D analyses	318
8.11.9	Material parameters	318
8.11.10	Initial stresses	319
8.11.11	Groundwater conditions	319
8.11.12	Boundary conditions for dynamic analyses	319
8.11.13	Construction stages	319
8.11.14	Procedure for reporting seismic displacements	320
8.11.15	Displacements during construction	322
8.11.16	Factor of Safety analyses	323
8.11.17	Displacements after seismic loading	324
8.11.18	Evaluation of the asphalt core bending strains	328
8.11.19	Conclusions	331
8.12	Integrated embankment design summary	332
9	Tunnels.....	334
9.1	Geotechnical design assessments	334
9.1.1	Preliminary ground support design	335
9.1.2	Tunnel spacing assessment.....	340
10	Water Management Structures.....	351
10.1	Diversion system sizing	351
10.1.1	Inputs and assumptions	352
10.1.2	Tunnel size	353
10.1.3	Tunnel flow operation	354
10.1.4	Flood routing	355
10.1.5	Long-term flow routing.....	356
10.1.6	Upstream cofferdam.....	358
10.1.7	Downstream cofferdam	358
10.1.8	Diversion dam	358
10.1.9	Diversion tunnel inlets and outlets	359
10.1.10	Diversion tunnel portals	360
10.1.11	Diversion tunnels	361
10.1.12	Plug.....	361
10.2	Upstream cofferdam	362
10.3	Downstream cofferdam	362

10.4	Diversion dam	363
10.5	Spillway	363
10.5.1	Spillway sizing	363
10.5.2	Spillway design.....	370
10.5.3	Spillway gates	373
10.5.4	Slope stability assessments for design of spillway and quarry slopes.....	376
11	Landslides.....	393
11.1	Aerial landslide risk	393
11.1.1	Characterisation	398
11.1.2	Landslide assessment.....	403
11.1.3	Subaqueous landslides	404
12	Roads	406
13	Embankment Instrumentation	408
14	Sediment and Surface Water Management	411
14.1	Temporary diversions	411
14.1.1	Runoff within the foundation excavation	412
14.1.2	Sediment erosion	413
14.1.3	Spoil dumps.....	414
14.1.4	Stilling basins	416
14.1.5	Sedimentation ponds.....	416
14.2	Permanent water management structures.....	419
14.2.1	Stormwater diversion channels	419
14.2.2	Roads	420
14.3	Spoil dump stability assessment.....	423
14.3.1	Design considerations	424
14.3.2	Slope stability assessment.....	424
14.3.3	Geotechnical strength parameters	424
14.3.4	Water	426
14.3.5	Modelling scenarios.....	426
14.3.6	Results and interpretation	427
14.3.7	Construction and development	428
15	Hydroelectric Power Configuration	430
15.1	Intake structure arrangement.....	430
15.2	Configuration of the conveyance system.....	431
15.3	Surge analysis of conveyance system.....	432
15.3.1	Introduction.....	432
15.3.2	Model inputs and assumptions.....	433
15.3.3	Summary of analysis.....	435
15.3.4	Results	436
15.3.5	Selection of PSS/E power systems model	441

15.3.6	Model parameter selection	442
15.3.7	Governor parameters	442
15.3.8	Power system study results	443
15.4	Numbers of generating units and generation reliability.....	447
15.4.1	Factors affecting turbine generator reliability	447
15.4.2	Cost optimisation of the number of units required	450
15.4.3	Reliability of recommended plant configuration and timing of unit installation.....	451
15.5	FRHEP arrangement	457
16	Hydroelectric Component Design.....	460
16.1.1	Liquefaction and lateral spreading risk.....	460
16.1.2	Spectral acceleration curves	460
16.1.3	Design events.....	462
16.1.4	Seismic loads on mechanical and electrical equipment.....	463
16.1.5	Design ground accelerations.....	464
16.1.6	Basis of future work.....	464
16.2	Residual flow system	464
16.3	Intake structures.....	465
16.3.1	Levels	466
16.3.2	Lower intake structure	466
16.3.3	Upper intake structure	468
16.3.4	Intake control buildings.....	470
16.3.5	Details of intake gates, valves and spillway gates	471
16.4	Conveyance system.....	472
16.4.1	General.....	472
16.4.2	Conveyance system optimisation.....	472
16.4.3	Conveyance system velocities	473
16.4.4	Conveyance system long section.....	474
16.4.5	Transient analysis	475
16.4.6	Tunnel and shaft sizes	475
16.4.7	Tunnelling conditions.....	475
16.4.8	Shaft construction.....	477
16.4.9	Penstock size and arrangement.....	477
16.4.10	Penstock material selection	478
16.5	Powerhouse bypass/ drain valve	479
16.6	Powerhouse	481
16.6.1	Building foundations.....	482
16.6.2	Building structure – flood protection.....	483
16.6.3	Building structure – general arrangement.....	483
16.6.4	Powerstation tailrace.....	484
16.7	Powerhouse equipment	485
16.7.1	Turbine generators	485

16.7.2	Powerhouse mechanical systems	489
16.7.3	Electrical equipment	491
16.7.4	Load bank	492
16.7.5	Equipment transport dimensions and weights	492
16.8	Substation and transmission	493
17	Early Filling/ First Power	496
17.1	Time to first power to FRCGP and export grid	496
18	Energy Production	499
18.1	Power supply reliability (16 year measured flow series)	499
18.1.1	Water balance and energy model	501
18.2	Energy production (200 × 38 year synthetic flow series)	504
19	Operations and Closure	512
19.1	Operations	512
19.1.1	Stewardship	512
19.1.2	Dam safety program	512
19.1.3	Corporate systems	514
19.1.4	Proposed role definitions	515
19.2	Tailings and waste rock disposal	516
19.2.1	Objectives	517
19.2.2	Limnology and geochemistry	519
19.2.3	Capacity	520
19.2.4	Mound failure and landslides	521
19.2.5	Deposition strategy	522
19.2.6	Tailings deposition	527
19.2.7	Waste rock deposition	527
19.2.8	Operations and maintenance	529
19.2.9	Summary	530
19.3	Hydroelectric power operation and control philosophy	530
19.3.1	Embankment and reservoir operating rules	531
19.3.2	Spillway gates	532
19.3.3	Governor control modes	533
19.3.4	Generator reactive power and voltage control	535
19.3.5	Recommended control settings for FRHEP generating plant	536
19.3.6	Control system architecture and function	537
19.4	Facility closure	540
19.4.1	Temporary suspension	541
19.4.2	Planned permanent closure	542
19.4.3	Early permanent closure	543
19.4.4	Closure during construction	543
19.5	Post-closure surface water management	543

19.6 Post-closure maintenance and monitoring	543
----------------------------------------------------	-----

List of Tables

Table 1-1: Power generation potential of other hydroelectric power dams.....	5
Table 1-4: Peak ground accelerations of notable earthquakes.....	8
Table 2-1: Power and energy demand for mining operations	12
Table 2-2: Reliability of power generation and water supply using the measured and synthetic inflow series	14
Table 2-3: Effect of early filling and lower intake on time to first power	16
Table 2-4: Time to first power - measured vs synthetic flow series	16
Table 2-5: LOM tailings and waste production.....	17
Table 2-6: Key assumptions – tailings geotechnical properties	18
Table 2-7: Tailings material properties	18
Table 2-8: Tailings undrained settling test results.....	19
Table 2-9: Key assumptions – waste rock geotechnical properties	20
Table 2-10: Waste rock material properties	20
Table 2-11: Waste rock – undrained settling test results	21
Table 2-12: Design dry density - sediment.....	23
Table 2-13: FRHEP reservoir storage capacities.....	24
Table 2-14: Consequence category	28
Table 2-15: Interpreted correlation of P-wave velocities with geotechnical horizons	34
Table 2-16: FRHEP infrastructure design ground accelerations.....	35
Table 2-17: Minimum factors of safety (ANCOLD, 2012)	36
Table 2-18: Rock properties	36
Table 2-19: Details of precipitation gauges ²¹	38
Table 2-20: Details of stream gauges ²¹	39
Table 2-21: Return periods for stormwater and sediment management infrastructure	40
Table 2-22: ANCOLD fallback flood capacity.....	40
Table 2-23: Operating water management requirements	41
Table 2-24: IFC guidelines for effluent water quality levels	43
Table 2-25: Data from meteorological stations and application to the limnological model	45
Table 2-26: Sedimentation predictions.....	45
Table 3-1: Summary of Stage 1 and 2 geotechnical investigations	49
Table 3-2: Geotechnical drill holes in the Stage 1 drilling campaign	62
Table 3-3: Geotechnical drill holes in the Stage 2 drilling campaign	62
Table 3-4: Interval weathering descriptions	65
Table 3-5: Field estimates of uniaxial compressive strength	65
Table 3-6: Field estimates of soil consistency.....	66
Table 3-7: Summary of televiewer survey intervals and structure counts.....	66
Table 3-8: Summary of laboratory testing undertaken	67

Table 3-9:	Summary of permeability tests.....	68
Table 3-10:	Summary of piezometers installed.....	69
Table 3-11:	Interpreted correlation of Vp with geotechnical horizons.....	70
Table 3-12:	Summary of geotechnical domains identified in each drill hole.....	88
Table 3-13:	Summary of laboratory testing undertaken.....	90
Table 3-14:	PSD and Atterberg limit results.....	90
Table 3-15:	Results of Emerson test.....	93
Table 3-16:	Summary of UCS test results.....	94
Table 3-17:	Summary of elastic properties.....	96
Table 3-18:	Summary of wet density.....	96
Table 3-19:	Summary of direct shear test results.....	96
Table 3-20:	Summary of sawcut shear test results.....	98
Table 3-21:	Slake durability testing results.....	98
Table 3-22:	LA abrasion testing results.....	98
Table 3-23:	Count of the different structure types – from logging.....	108
Table 3-24:	Count of the different structure types – from televiewer.....	108
Table 3-25:	Classification of fault structures.....	114
Table 3-26:	Classification of faults.....	117
Table 3-27:	Fault planes interpreted at the FRHEP site.....	118
Table 3-28:	Summary of permeability testing results.....	127
Table 3-29:	Groundwater levels.....	132
Table 3-30:	Material properties used for embankment design analyses.....	140
Table 3-31:	Peak friction angle for each layer as a function of depth.....	142
Table 3-32:	Input parameters for Plaxis modelling.....	143
Table 3-33:	Assessment of spoil material from quarry and spillway drill holes.....	149
Table 3-34:	Summary of geotechnical properties.....	152
Table 3-35:	Geohazard rating – geology.....	170
Table 3-36:	Geohazard rating - structural geology.....	170
Table 3-37:	Geohazard rating –slope angle.....	171
Table 3-38:	Geohazard rating – instability.....	171
Table 3-39:	Geohazard rating – hydrology – flooding and liquefaction.....	172
Table 3-40:	Geohazard rating – hydrology – stream ranking.....	173
Table 3-41:	Geohazard rating – overall.....	173
Table 4-1:	Precipitation gauges.....	182
Table 4-2:	Stream gauges.....	183
Table 4-3:	Design storm precipitation depths.....	186
Table 4-4:	PMP estimates for the FRHEP catchment.....	186
Table 4-5:	Spatial distributions.....	189
Table 4-6:	Calibrated model parameters.....	191
Table 4-7:	Model calibration results.....	191
Table 4-8:	Monitoring stations in the FRHEP catchment.....	203

Table 4-9:	PMP estimates for the Frieda River basin	205
Table 4-10:	Catchment hydrology of Frieda Basin.....	205
Table 4-11:	Tailwater rating curve table	208
Table 5-1:	Export grid Loss of Load Expectation - allowable departures.....	210
Table 5-2:	(a) Power demand scenario Years 1–17: January electrical loads	212
Table 5-3:	(b) Power demand scenario Years 18–34: January electrical loads	213
Table 5-4:	(a) Power demand scenario Years 1–16: May electrical loads.....	215
Table 5-5:	(b) Power demand scenario Years 17–33: May electrical loads.....	216
Table 6-1:	Details of assessment point locations.....	219
Table 6-2:	Waste rock and tailings particle properties	232
Table 6-3:	Summary table of sediment in downstream release water	236
Table 6-4:	Samples selected for column testing	239
Table 6-5:	Summary of kinetic test leachate properties	239
Table 6-6:	Waste rock classification criteria	240
Table 6-7:	Summary of waste rock production schedule and classification	240
Table 6-8:	Summary of average groundwater inflow quality.....	243
Table 6-9:	Assumed treated water quality (dissolved concentrations).....	245
Table 6-10:	Summary of tailings water quality	245
Table 6-11:	Summary of waste rock production by hardness.....	247
Table 6-12:	Assumed particle size distributions for fines fraction of waste rock.....	248
Table 6-13:	Estimated total metal content of natural suspended solids.....	249
Table 6-14:	Base case – summary of predicted average total metal concentrations (average flow conditions; treatment throughout operations)	256
Table 6-15:	Calculated complexed copper species for mean operational solute concentrations.....	257
Table 6-16:	Revised placement schedule to limit deposition rates in near-field zones	258
Table 7-1:	Days per month for which measured flow data is available.....	262
Table 7-2:	Days per month for which flow data are available - modified	264
Table 7-3:	Monthly mean inflows.....	265
Table 7-4:	Magnitude of inflow events of different durations	267
Table 7-5:	Residual flow assessment based on measured flows	269
Table 7-6:	Generation potential at the lower intake reservoir level - January electrical loads.....	271
Table 7-7:	Generation potential at the lower intake reservoir level - May electrical loads.....	271
Table 7-8:	Effect of early filling and low intake on time to first power	278
Table 7-10:	Bypass valve capacity at different water levels	279
Table 7-11:	Residual flow valve operation	281
Table 8-1:	Plinth widths across sections	292
Table 8-2:	Comparison of material grading for different zones of various asphalt core embankment	302
Table 8-3:	Maximum measured seepage rates from comparable ACRDs	305
Table 8-4:	Material permeabilities	305
Table 8-5:	Assumed asphalt core permeability based on various conditions	306

Table 8-6:	Seepage at toe with/ without plastic cut-off wall or concrete plinth (homogeneous and isotropic conditions)	308
Table 8-7:	Seepage at toe with/ without plastic cut-off wall with a higher permeability in cemented colluvium and alluvium material (non-homogenous and anisotropic conditions).....	308
Table 8-8:	Estimated hydraulic gradients for different conditions in each section	309
Table 8-9:	Total seepage results due to change in asphalt core permeability.....	309
Table 8-10:	Total seepage rates induced by potential shearing zones within the core	309
Table 8-11:	Exit gradient at downstream toe	310
Table 8-12:	Material properties selected to assess static stability of large haul road benches	314
Table 8-13:	Summary of material parameters.....	317
Table 8-14:	Ground motions for the seismic analysis	318
Table 8-15:	Coordinates of reference nodes.....	320
Table 8-16:	Factor of safety for different scenarios.....	323
Table 9-1:	Summary of FRHEP tunnels	334
Table 9-2:	Preliminary empirical ground support assessment	340
Table 9-3:	Material properties used for the model analyses	343
Table 9-4:	Applied in situ stress	345
Table 10-1:	Diversion flood routing results.....	355
Table 10-2:	Diversion flood routing results.....	366
Table 10-3:	Conditions at flip bucket lip at design discharge (3,000 m ³ /s)	369
Table 10-4:	Maximum controlled gate discharge	374
Table 10-5:	Spillway flows and discharges during PMF events using spillway only	375
Table 10-6:	Potential revised maximum operating water levels (bypass valves used to pass flood flows)	376
Table 10-7:	Rockmass Rating Classes	377
Table 10-8:	Orientations of main joint sets identified	379
Table 10-9:	Results of toppling failure analysis.....	380
Table 10-10:	Results of planar failure analysis	381
Table 10-11:	Summary friction angle values for the RH side of the gorge	382
Table 10-12:	HTA empirical methodology to derive friction angles from defect characteristics	382
Table 10-13:	Summary friction values from HTA empirical approach for right abutment area	383
Table 10-14:	Structural set characteristics	383
Table 10-15:	Results of spill berm width optimisation analysis.....	384
Table 10-16:	Rockmass properties used in <i>Slide</i> slope stability analyses.....	387
Table 10-17:	Summary of fault properties	388
Table 10-18:	Revised slope design parameters.....	390
Table 10-19:	Summary of results of slope stability analyses for the revised cut slope profiles	391
Table 10-20:	Slide results and sensitivity assessments for the natural slope profile.....	392
Table 11-1:	Wave amplitudes generated by landslides	396
Table 13-1:	Proposed monitoring data and instrumentation	408
Table 13-2:	Types of instrumentation for monitoring.....	409
Table 14-1:	Key diversion channels for construction sediment and stormwater.....	412

Table 14-2:	Surface water diversion channel profiles (refer to Table 14-1)	413
Table 14-3:	Design criteria for sedimentation ponds	418
Table 14-4:	Sedimentation pond dimensions	418
Table 14-5:	Sedimentation pond spillway characteristics	418
Table 14-6:	FRHEP permanent stormwater diversion channels	420
Table 14-7:	Crossing characteristics	421
Table 14-8:	Crossing design criteria	422
Table 14-9:	Catchment areas and design flows for bridges	423
Table 14-10:	Culvert sizing	423
Table 14-11:	Summary of geotechnical properties	426
Table 14-12:	Results of stability assessment – critical sections	427
Table 15-2:	Properties of water	433
Table 15-3:	Colebrook-White roughness	433
Table 15-4:	Wave speed (celerity)	434
Table 15-5:	Surge chamber parameters	434
Table 15-6:	Turbine parameters	435
Table 15-7:	Tunnel parameters	435
Table 15-8:	Surge chamber results	437
Table 15-9:	Combined reliability of unit configurations at RL 171.2 m reservoir level	453
Table 15-10:	Combined reliability of unit configurations at RL 204.39 m reservoir level	454
Table 15-11:	Combined reliability of unit configurations (normal operating levels, Years 2 to 10)	455
Table 15-12:	Combined reliability of unit configurations (normal operating levels, Years 11–33)	456
Table 16-1:	FRHEP structures design ground accelerations	464
Table 16-2:	Intake levels	466
Table 16-3:	Details of intake gates, spillway gates and valves	471
Table 16-4:	Conveyance system velocities and estimate of time operating at that velocity	474
Table 16-5:	Tunnel component sizes	475
Table 16-6:	Assumed initial support classification	476
Table 16-7:	Key turbine generator and auxiliary plant design details	485
Table 16-8:	Turbine generator data (normal running loads and flows) equalised penstock flow	487
Table 16-9:	Turbine generator data (peak running loads flows) equalised penstock flow	488
Table 16-10:	Turbine generator data (peak running loads) maximum flow through a single penstock	489
Table 16-11:	Critical equipment weights	492
Table 17-1:	Time to first power to FRCGP and export grid (January 2018 electrical load)	496
Table 17-2:	Comparison of time to first power based on the January and May electrical load profiles	498
Table 17-3:	Required dam crest height and time available to complete from start of filling	498
Table 18-1:	Optimised FRHEP generation for embankment crest height of RL238.5 m	499
Table 18-2:	Power supply reliability from FRHEP based on January electrical load profile	500
Table 18-3:	Power supply reliability from FRHEP based on May electrical load profile	500
Table 18-4:	Comparison of energy production (varying loads and flow series)	504

Table 18-5: Reliability of generation using the measured and synthetic flow series (January electrical load)	507
Table 18-6: Comparison of reliability in meeting the January and May electrical load profiles	507
Table 18-7: Predicted generation from the measured and synthetic flow series (January loads)	509
Table 19-1: Dam safety guidance documents	513
Table 19-2: Water management operating rules	531
Table 19-3: Spillway gate key parameters	532
Table 19-4: Closure scenarios	540

List of Figures

Figure 1-1: Location of the Frieda River Hydroelectric Project	1
Figure 1-2: Embankment site	4
Figure 1-3: Embankment height of other asphalt core rockfill dams compared to FRHEP	6
Figure 1-4: Embankment height of other tailings dams compared to FRHEP	6
Figure 1-5: Construction durations for other hydroelectric dams with comparable embankment heights	7
Figure 1-6: PGA regions of various dams	7
Figure 1-7: Operating Basis Earthquake (OBE) peak ground accelerations for other large tailings dam sites	8
Figure 1-8: Annual average rainfall of other dams compared to FRHEP	9
Figure 1-9: Rating vs operating life of hydroelectric power plants in the Asia-Pacific region	10
Figure 2-1: Mine power and energy demand	13
Figure 2-2: Tailings particle size distribution	18
Figure 2-3: Predicted dry density variation with depth within the tailings deposit	19
Figure 2-4: Particle size distributions – waste rock samples	20
Figure 2-5: Predicted dry density variation with depth of waste rock deposition	21
Figure 2-6: Tailings, sediment and waste rock volumes generated over the LOM (years)	23
Figure 2-7: FRHEP storage capacity curve	24
Figure 2-8: Footprints of the three compartments within the FRHEP	25
Figure 2-9: Extent of LiDAR survey (black lines)	29
Figure 2-10: Major geological elements of South East Asia and Australia	30
Figure 2-11: Comparison of FRHEP distance to the Nena ISF embankment locations	32
Figure 2-12: Regional geology of the Nena ISF site	33
Figure 2-13: Estimated shear-wave velocities for the subsurface layers at the Nena ISF	34
Figure 2-14: Horizontal and vertical design spectra for the MCE scenario on Zone 15 (35–75 km) for V_{S30} of 1,150 m/s	35
Figure 2-15: Locations of rain gauges	39
Figure 2-16: Locations of stream gauges	39
Figure 2-17: Meteorological stations	44
Figure 3-1: FRHEP geotechnical investigation	51
Figure 3-2: Geological setting of the FRHEP site and surrounds	52

Figure 3-3:	Diagrammatic N–S geology cross-section	53
Figure 3-4:	Plan view of modelled streams, drainage divide and topographic ridges	54
Figure 3-5:	Cemented colluvial material forming steep river banks	55
Figure 3-6:	Slope (left hand side) and aspect (right hand side) of the FRHEP site	55
Figure 3-7:	SSW–NNE diagrammatic cross-section looking west	56
Figure 3-8:	An example of intense weathering in wall rock of upper dunite bedrock	57
Figure 3-9:	A: Semi-brittle deformation and part development of shear bands; B: Brittle deformation and chlorite and serpentinisation; C: Semi-brittle and cataclastic deformation	57
Figure 3-10:	Drill core showing previously sheared and now serpentinised and deteriorating dunite, as shown in drill hole PH2 (above) and Q6 (below).....	58
Figure 3-11:	An example of third order fault conditions.....	60
Figure 3-12:	A small (fourth order) fault with gouge in good quality dunite.....	60
Figure 3-13:	WNW–ESE section (looking north) across the valley at the FRHEP site, just upstream of the proposed embankment centreline (Northing = 9486700)	61
Figure 3-14:	Positions of seismic refraction survey lines in plan view, with reference to contours and drill hole collar positions from various phases of investigation	71
Figure 3-15:	Combined section view (fence diagram) along Line 1 (left) and Line 2 (right), looking west, showing the Vp contours	72
Figure 3-16:	Isometric view of the Line1 and 2 contoured Vp sections and nearby drill holes, looking west.....	73
Figure 3-17:	Section view along Line 3, looking north.....	73
Figure 3-18:	Photograph of the steep right abutment, looking southeast, showing drill pads.....	74
Figure 3-19:	Diagrammatic cross-section through the right abutment, looking north	75
Figure 3-20:	Selected WNW – ESE sections (looking north) across the valley of the FRHEP site, showing the geotechnical model (above) slightly upstream of the proposed embankment centreline (Northing = 9486700), and (below) the approximate position of the hydroelectric powerhouse downstream (Northing = 9487200)	76
Figure 3-21:	3 m of soil-like colluvium in drill hole SW5	77
Figure 3-22:	Bedrock at surface in drill hole SW6	77
Figure 3-23:	Cemented colluvium in drill hole RH6: large subangular to angular boulders with an oxidised matrix	78
Figure 3-24:	Cemented alluvium in RH6: cobble- and pebble-sized, rounded clasts in an unoxidised matrix (zone of poor cementation apparent below 23.7 m)	78
Figure 3-25:	Partially weathered boulders, clast supported in an oxidised soil-like colluvial matrix	78
Figure 3-26:	Isometric view of the Leapfrog model (from above) showing the interpreted large landslide zone on the left abutment and potential smaller zone on the right abutment.....	79
Figure 3-27:	Core photograph showing variability of zones of highly fractured and oxidised rock with deteriorating matrix and/or soil-like infill in drill hole LH3 (66–80 m)	80
Figure 3-28:	Downhole OTV image in drill hole LH7 showing potential landslide materials below 70 m depth downhole.....	81
Figure 3-29:	Core photograph from drill hole LH3 showing base of potentially unstable ‘landslide’ zone (102.8–106.7 m).....	81
Figure 3-30:	Core photograph showing soil-like overburden material immediately above highly fractured rock in drill hole LH7 (6.4–10 m).....	82
Figure 3-31:	Drill hole SW4 showing boulder overburden material over the bedrock (17.5–19.9 m)	82
Figure 3-32:	Moderately to slightly weathered bedrock with thick joint infills	83

Figure 3-33: Slightly weathered to unweathered bedrock with joint infills of variable thickness (left), shown in acoustic televiewer survey image (right)	83
Figure 3-34: Examples of serpentinised bedrock in varying stages of deterioration.....	84
Figure 3-35: Examples of good-quality bedrock: strong and moderately to sparsely fractured	84
Figure 3-36: An example of third order fault conditions – highly fractured and sheared rock.....	85
Figure 3-37: Examples of fourth order faults: (A) discrete zone of fault gouge; (B) fractured, oxidised rock with gouge zone; and (C) discrete fault with gouge and slickensided surface, examples of fault zones in acoustic survey image.....	86
Figure 3-38: Isometric cross-section looking north, showing the interpreted fault plane and the permeabilities measured at drill hole intersection.....	87
Figure 3-39: Particle size distribution	91
Figure 3-40: Plasticity chart.....	91
Figure 3-41: Fines versus plasticity index	92
Figure 3-42: Natural moisture content versus plastic limit	92
Figure 3-43: Flow chart for interpretation of Emerson test results	93
Figure 3-44: UCS test histograms	95
Figure 3-45: Plot of direct shear test results.....	97
Figure 3-46: Logged strength distributions per domain.....	100
Figure 3-47: RQD distributions per domain.....	101
Figure 3-48: Joint spacing distributions per domain.....	102
Figure 3-49: Small-scale roughness distributions per domain	103
Figure 3-50: Infill distributions per domain	104
Figure 3-51: GSI distributions per domain.....	105
Figure 3-52: Laubscher RMR distributions per domain.....	106
Figure 3-53: Q distributions per domain	107
Figure 3-54: Stereonet showing orientation of all logged structures	108
Figure 3-55: Stereonet showing orientation of all identified structures from the televiewer.....	109
Figure 3-56: Stereonet showing orientation of structures logged – left abutment zone.....	109
Figure 3-57: Stereonet showing orientation of structures identified from televiewer – left abutment zone.....	110
Figure 3-58: Stereonet showing orientation of structures logged – RHN abutment zone.....	110
Figure 3-59: Stereonet showing orientation of structures logged – RHs abutment zone.....	111
Figure 3-60: Stereonet showing orientation of structures identified from televiewer – RHS abutment zone.....	111
Figure 3-61: Stereonet showing orientation of structures logged – QN zone	112
Figure 3-62: Stereonet showing orientation of structures logged – QS zone.....	112
Figure 3-63: Stereonet showing orientation of structures identified from the televiewer – QS zone	113
Figure 3-64: Stereonet showing orientation of structures logged – valley floor zone	113
Figure 3-65: Band of mylonite in drill hole F4 that offsets partially oxidised fractures/ joints.....	116
Figure 3-66: Illustrations of Fault 1 (Set A) interpretation in the left hillside: (above) isometric view looking NW showing the drill hole and seismic refraction traverse intersections; and (below) fault intersected in hole LH3.....	119
Figure 3-67: Illustrations of Set B fault interpretations in the right abutment: (above, from top to bottom) Fault 2, 3, 4 and 5 plane intersections with drill holes showing poor ground,	

	looking north; and (below) intersection pattern of Faults 2 (left) and 3 (right with the topography in the right abutment), in section view looking north.....	120
Figure 3-68:	Core photos illustrating the nature and variability of conditions along Fault 2 in the right abutment: (above) very thin gouge zone with oxidisation of surrounding joints in hole RH1; (middle) oxidised fracture zone with localised gouge in hole SW5; and (bottom) fractured, oxidised zone in hole SW6	121
Figure 3-69:	Fault 6 (main picture) interpretation with respect to topography and right abutment spillway in plan view; (inset) isometric view looking west showing topography and embankment	122
Figure 3-70:	Core photographs from the right hillside in hole PH1	123
Figure 3-71:	Fault 7 isometric view looking east showing the interpreted fault plane, quarry and embankment	123
Figure 3-72:	Core photographs of possible intersection in the south quarry area in hole Q6.....	124
Figure 3-73:	Isometric view looking west of Faults 8 and 9 (Set D) in the left hillside, relative to the poor ground in drill holes and the embayments in seismic refraction traverses 1 and 2.....	124
Figure 3-74:	Stereonet presenting joint sets patterns for the left side of the gorge: (left) from core logging; and (right) from televiewer survey	124
Figure 3-75:	Stereonet presenting joint sets patterns for the right side of the gorge	125
Figure 3-76:	Riedel shear sets for strike slip movement on the NNW–SSE striking Saniap Fault (dextral movement in this case, hence the diagram is reversed)	126
Figure 3-77:	Drill hole summary for hole DT2 (right abutment).....	129
Figure 3-78:	Drill hole summary for hole SW6 (right abutment).....	130
Figure 3-79:	Drill hole summary for hole RH6 (valley floor)	130
Figure 3-80:	Drill hole summary for hole LH6 (lower left abutment).....	131
Figure 3-81:	Drill hole summary for hole LH5 (left abutment)	131
Figure 3-82:	Section (looking north) showing the interpreted groundwater profile roughly along the centreline of the FRHEP embankment	133
Figure 3-83:	Positions of key drill holes that show moderately high to high permeability zones (plan view with north at bottom)	134
Figure 3-84:	Comparison of high k intervals and RQD/ fault intersections in hole LH5 (isometric view, looking north)	134
Figure 3-85:	Comparison of high k intervals and RQD/ fault intersections in hole LH6 (isometric view, looking north)	135
Figure 3-86:	Isometric views looking north, showing (above) comparison of high k intervals and RQD/ fault intersections in hole SW6; (below) drill hole position relative to proposed spillway cut.....	136
Figure 3-87:	Comparison of high k intervals and RQD/ fault intersections in hole RH1 (isometric view, looking north)	137
Figure 3-88:	Comparison of high k intervals and RQD/ fault intersections in hole LH5 (isometric view, looking north)	138
Figure 3-89:	Shear-normal stress curves developed for the rockfill (Zone 3A and Zone 3B) embankment construction materials	140
Figure 3-90:	Shear strength envelopes for the Ok Binai embankment (SRK, 2011) – for comparison	141
Figure 3-91:	Variation of friction angle in each rockfill zone.....	141
Figure 3-92:	Adopted friction angle compared to Barton & Kjaernsli (1981), Indraratna (1993), and Leps (1970)	142
Figure 3-93:	P-wave velocity contours of the subsurface materials in the vicinity of the proposed powerhouse site (section view, looking north).....	144

Figure 3-94: Locations of gravel and sand materials on the Frieda River near the FRHEP site (highlighted by red dashed zones).....	146
Figure 3-95: Examples of drill core from the northern part of the quarry	147
Figure 3-96: Examples of poor quality drill core from the southern part of the quarry	148
Figure 3-97: Significant fault through the quarry: conditions encountered in drill core of hole Q5.....	148
Figure 3-98: Plan views showing (above) original quarry and spillway design, with new southern limit based on drilling investigations; and (below) re-designed quarry merging with the spillway cut.....	150
Figure 3-99: Plan view showing the quarry and spillway design (Rev N) on the right side of the river (relative to the embankment position).....	151
Figure 3-100: Isometric view looking south showing location of the hypothesised failure mechanism relative to the embankment site	153
Figure 3-101: Plan of Frieda River catchment with extent of data coverage shown.....	155
Figure 3-102: Geology of the FRHRP area	158
Figure 3-103: Failure in the epicentral area triggered by 25 February 2018 earthquake.....	160
Figure 3-104: Risk assessment flow diagram	163
Figure 3-105: Geohazard process showing relationship between inputs and overall geohazard rating.....	165
Figure 3-106: Geohazard input layers and equation used for overall geohazard rating	165
Figure 3-107: Landslide classification	166
Figure 3-108: Various landslide types	167
Figure 3-109: Landslide failure examples, characteristics (Hunt, 1984) and cross-sectional profiles	168
Figure 3-110: Histogram of geohazard rating across the catchment	174
Figure 3-111: Spatial distribution of geohazard ratings across the catchment	175
Figure 3-112: Detail of geohazard rating around reservoir	176
Figure 3-113: Location of embankment with landslides outlined in red (dashed lines).....	177
Figure 3-114: Zones of High risk geology	179
Figure 4-1: Precipitation gauge map	181
Figure 4-2: Stream gauge map.....	182
Figure 4-3: Stream gauge data from GS105450	183
Figure 4-4: GS105450 rating curve and RQ-30 data	184
Figure 4-5: Storm duration distribution for higher intensity storms (higher 10%).....	187
Figure 4-6: Storm duration distribution for higher precipitation storms (higher 10%).....	188
Figure 4-7: FRHEP basin model.....	189
Figure 4-8: Inverse distance weighting example (values shown represent total pp in mm).....	190
Figure 4-9: Example model calibration of observed and modelled results for Event 1 (February 2009)	192
Figure 4-10: Observed versus designed flood peaks for all storm durations	193
Figure 4-11: Rare to very rare design flood hydrographs.....	193
Figure 4-12: PMF hydrograph for 72-hour storm – temporal distribution pattern A and spatial distribution S4	194
Figure 4-13: Observed versus designed flood peaks including PMF.....	195
Figure 4-14: Discharge variation with catchment area for maximum floods recorded globally (ICOLD B-156)	195

Figure 4-15: 1 in 100-year AEP, 2-day and 3-day inflow hydrographs	196
Figure 4-16: 1 in 100-year AEP, 5-day and 10-day inflow hydrographs	196
Figure 4-17: 1 in 100-year AEP, 30-day and 60-day inflow hydrographs	197
Figure 4-18: Yearly variability – annual runoff/ mean annual runoff.....	198
Figure 4-19: Projected mean annual flow for 50 scenarios	199
Figure 4-20: Comparison of observed versus simulated average flow for different durations for the 50 scenarios and the first 20 years of information	200
Figure 4-21: Comparison of observed versus simulated average flow for different durations for the 50 scenarios and 200 years of information	201
Figure 4-22: Flow duration curve – mean daily flow (log scale)	202
Figure 4-23: Flow duration curve – mean daily flow (normal scale).....	202
Figure 4-24: Locations of Frieda River gauging stations.....	204
Figure 4-25: Monthly rainfall distribution in the catchment area.....	204
Figure 4-26: Locations of tailwater rating curves.....	205
Figure 4-27: Model mesh and boundary conditions	206
Figure 4-28: Model calibration compares to tailwater rating curve at GS105450 (blue line)	207
Figure 4-29: Tailwater rating curves	207
Figure 4-30: HEC-RAS model results.....	209
Figure 5-1: Comparison of FRCGP loads for the Optimisation Study and SPS phase of project.....	217
Figure 5-2: Breakdown of May 2018 electrical loads	218
Figure 6-1: Locations of assessment points and FRHEP infrastructure	220
Figure 6-2: Schematic layout of water balance during operations	222
Figure 6-3: Schematic layout of water balance post closure of the FRCGP	222
Figure 6-4: Base case groundwater recharge to the open pits	224
Figure 6-5: Modelled range of flows at the assessment points – pre-embankment scenario	225
Figure 6-6: Daily average flow statistics at assessment points during mine operations (Years 1–33)	225
Figure 6-7: Reservoir outflows – operational period.....	226
Figure 6-8: Reservoir water levels – operational period.....	227
Figure 6-9: Footprint of reservoir illustrating proposed waste rock (coloured in green) and tailings (coloured in brown) storage areas	228
Figure 6-10: Model grid bathymetry with 200 × 200 m horizontal resolution	230
Figure 6-11: Location of modelled inflows	231
Figure 6-12: Simulation showing temperature profile over time at the embankment during the filling	233
Figure 6-13: Model output from Nena River headwaters (on the left) to the embankment (on the right) on 01/07/2009 showing tracer concentrations from the Nena River as an intrusion across the reservoir	234
Figure 6-14: Model output from Henumai River headwaters (on the left) to the embankment (on the right) on 01/07/2009 showing tracer concentrations from the Henumai River as an intrusion across the reservoir	234
Figure 6-15: Simulated concentration of 4-micron particles from catchment loads at the embankment during filling	235
Figure 6-16: Simulated concentration of TSS from catchment loads at the embankment during filling	235

Figure 6-17	Simulated concentrations of fine waste rock sediments and TSS in the intake water during continuous barge disposition (18 barges per day) at 1 km (top), 2 km (middle) and 4 km up the Nena arm (bottom) from the embankment.....	237
Figure 6-18:	Cumulative placement schedule within each zone	249
Figure 6-19:	Base case – sulphate concentrations in the ISF impoundment, outflow and downstream of the mine (average flow conditions)	251
Figure 6-20:	Base case – dissolved copper concentrations (average flow conditions)	252
Figure 6-21:	Base case – TSS concentrations.....	254
Figure 6-22:	Base case – total copper concentrations (treatment throughout operations).....	255
Figure 6-23:	Comparison between base case and restricted barge dumping in the 1–2 km and 2–4 km zones.....	259
Figure 7-1:	Correlation between monthly flows at GS105310and GS105450	263
Figure 7-2:	Regression analysis of daily mean flows - GS105310and GS105450	264
Figure 7-3:	Comparison of flow duration curves for synthetic and measured flows.....	266
Figure 7-4:	Close-up of flow duration curves for synthetic and measured flows.....	266
Figure 7-5:	Comparison of maximum inflow events for synthetic and measured flows	268
Figure 7-6:	Comparison of minimum inflow events for synthetic and measured flows	268
Figure 7-7:	Tailwater curve – powerhouse and spillway sites.....	270
Figure 7-8:	Ratio of the storm inflow event to the 72-hour PMF	273
Figure 7-9:	Relationship between the required Storm Buffer Volume and the storm event.....	274
Figure 7-10:	Critical dam crest and water levels during early filling – water levels are based on generation meeting budget	276
Figure 7-11:	Critical dam crest and water levels during early filling – water levels are based on no generation	276
Figure 7-12:	Variation in Storm Buffer Volume with time from start of filling.....	277
Figure 7-13:	Possible barge transport for major plant along the Frieda River	280
Figure 8-1:	Critical elevations for FRHEP operations.....	283
Figure 8-2:	Recommended depth of excavation	284
Figure 8-3:	Core photos from holes RH4 and RH6 – Frieda River riverbed representative of foundation level (~5 m)	285
Figure 8-4:	Core photos from holes RH7 and F4 – the Frieda River riverbed representative of foundation level (~5 m)	286
Figure 8-5:	Groundwater levels (blue) below surface level (brown) at the centreline of the embankment.	287
Figure 8-6:	Plinth sizing base width vs pressure head.....	292
Figure 8-7:	W–E cross-section through the FRHEP site (looking north) illustrating the locations of the material types.....	295
Figure 8-8:	Logged field estimated strengths per material type	295
Figure 8-9:	Logged GSI per material type	296
Figure 8-10:	Typical core from the Frieda River valley floor showing uncemented (2b) material.....	297
Figure 8-11:	View of a river bar in the Frieda River valley floor	297
Figure 8-12:	Correlation of RMR with gradient shown in a table (above) and graph (below) for a plinth design with internal slab	298
Figure 8-13:	Elastic finite element model	299

Figure 8-14: Settlement profile along the alluvium/ colluvium interface	300
Figure 8-15: Incremental change in deformation and rotation along the alluvium/ colluvium interface	301
Figure 8-16: Embankment cross-section detailing various components/ zones	304
Figure 8-17: Sections 1 and 2 along long section of embankment considered in seepage assessment	306
Figure 8-18: (a) Typical plinth profile at Section 1 and (b) 12 m concrete plinth at Section 2.....	307
Figure 8-19: Modelled crack sections illustrating displacement-induced cracks.....	307
Figure 8-20: Total vertical stress due to self-weight of embankment and seepage-induced uplift pressure	310
Figure 8-21: Total head contour diagram showing maximum phreatic level in Section 1 when asphalt core sheared at 60 m from embankment crest	311
Figure 8-22: Total head contour diagram showing maximum phreatic level in Section 2 when asphalt core sheared at 60 m from embankment crest	311
Figure 8-23: Total head contour diagram showing maximum phreatic level in Section 1 when asphalt core sheared at 60 m from embankment crest with no toe drain.....	311
Figure 8-24: Shaking table tests on typical asphalt core model.....	313
Figure 8-25: Permanent strain in the core and transition zones after dynamic loading	313
Figure 8-26: Static stability analysis for downstream slope assuming movement of large haul trucks (minimum FoS = 1.53).....	314
Figure 8-27: Detail of geometry and mesh – 2D model.....	318
Figure 8-28: Pore pressure contours at the last construction stage.....	319
Figure 8-29: Reference levels for each construction stage	320
Figure 8-30: Plaxis modelling of construction stages	321
Figure 8-31: Vertical centrelines selected to measure displacement.....	322
Figure 8-32: Mean horizontal and vertical displacements at centreline	322
Figure 8-33: Dam settlements compared with reference information from other dams	323
Figure 8-34: Failure surface obtained from FoS evaluation – Case A: Dam at RL 238.5 m, water at RL 232.4 m.....	324
Figure 8-35: Failure surface obtained from FoS evaluation – Case B: Dam at RL 238.5 m, water at RL 226.1 m, tailings at RL 159.4 m.....	324
Figure 8-36: Failure surface obtained from FoS evaluation – Case C: Dam at RL 238.5 m, water at RL 226.1 m, core cracked from RL 168 m to RL 181 m	324
Figure 8-37: Residual settlements at RL 230 m	325
Figure 8-38: Residual settlements at RL 215 m	325
Figure 8-39: True scale deformed shape of the crest of the embankment for the most unfavourable earthquake (FF_02)	326
Figure 8-40: Vertical residual displacements for Frieda Fault ground earthquake scaled to PGA 1.09g	326
Figure 8-41: Horizontal residual displacements for Frieda Fault earthquake scaled to PGA 1.09g	327
Figure 8-42: Vertical residual displacements for Zone 15 earthquake scaled to PGA 1.09g.....	327
Figure 8-43: Horizontal residual displacements for Zone 15 earthquake scaled to PGA 1.09g	328
Figure 8-44: Vertical (left) and horizontal (right) residual displacements for OBE ground motion	328
Figure 8-45: Horizontal residual displacements of the asphalt core	329
Figure 8-46: EQ_FF_02 – comparison between analysis with elastic and elastoplastic plate (left); mesh comparison between the original and refined model (right).....	330

Figure 8-47: Normal and shear residual stresses at the asphalt core interfaces between RL 190 m and RL 238.5 m - EQ_FF_02.....	331
Figure 8-48: Interpreted residual shear forces at the asphalt core between RL 205 m and RL 238.5 m (left); envelope of shear forces obtained from Plaxis (right) - EQ_FF_02	331
Figure 9-1: Cross-sectional design for each diversion tunnel	336
Figure 9-2: Distribution of Q data for diversion tunnels for (left) $J_w=0.33$ and (right) $J_w=0.5$	337
Figure 9-3: Distribution of Q data for conveyance tunnels for (left) $J_w=0.33$ and (right) $J_w=0.5$	338
Figure 9-4: Indicative support requirements.....	339
Figure 9-5: Plan view showing the locations of sections selected for <i>Phase2</i> analysis.....	341
Figure 9-6: Tunnel cross-sections: a) diversion tunnel; b) conveyance tunnel.....	341
Figure 9-7: Analysis sections for diversion tunnels: a) Section 1; b) Section 2	342
Figure 9-8: Analysis sections for conveyance tunnels: a) Section 3; b) Section 4.....	343
Figure 9-9: Plan view showing in situ stress regime orientation relative to tunnel alignment.....	344
Figure 9-10: Results plots for Section 1	346
Figure 9-11: Results plots for Section 2	346
Figure 9-12: Results plots for Section 3 (tunnel excavation after spillway cut).....	347
Figure 9-13: Results plots for Section 4 (tunnel excavation after spillway cut).....	347
Figure 9-14: Results plots for Section 1 (uniform vs non-uniform stress for lower bound general rockmass properties – diversion tunnels)	348
Figure 9-15: Results plots for Section 3 (uniform vs non-uniform stress for lower bound general rockmass properties – conveyance tunnels).....	348
Figure 9-16: Results plots for Section 1 (static vs seismic conditions for lower bound general rockmass properties – diversion tunnels)	349
Figure 9-17: Results plots for Section 3 (tunnel excavation before spillway cut – diversion tunnels).....	349
Figure 9-18: Results plots for Section 4 (tunnel excavation before spillway cut).....	350
Figure 10-1: Diversion tunnel tailwater curve	352
Figure 10-2: Reservoir storage curve for the diversion tunnel sizing	352
Figure 10-3: Typical diversion tunnel cross-section	353
Figure 10-4: Single diversion tunnel rating curve	353
Figure 10-5: Tunnel flow conditions.....	355
Figure 10-6: 24-hour, 1 in 100 AEP flood routing.....	356
Figure 10-7: Long term flood routing	357
Figure 10-8: February 2009 flood routing through diversion	358
Figure 10-9: Wheeled gate diversion structure	360
Figure 10-10: Spillway tailwater curve.....	364
Figure 10-11: Reservoir storage curve for the spillway sizing.....	364
Figure 10-12: Spillway rating curve	365
Figure 10-13: 24-hour PMF routing	367
Figure 10-14: 72-hour PMF flood routing	368
Figure 10-15: Summary hydraulics for design discharge (3,000 m ³ /s)	369
Figure 10-16: Jet trajectory for design discharge (3,000 m ³ /s) – flip bucket at 10°.....	369
Figure 10-17: Summary hydraulics for maximum discharge (5,100 m ³ /s)	370

Figure 10-18: Jet trajectory for maximum discharge (5,100 m ³ /s) – flip bucket at 10°	370
Figure 10-19: Ogee crest design	371
Figure 10-20: Suggested aerator locations	372
Figure 10-21: Slope design geometry terminology.....	376
Figure 10-22: Stereonet of the structures encountered on the RH side of the gorge, with identified dominant structural sets.....	378
Figure 10-23: Stereographic analysis of toppling failure for slope azimuth 300°	379
Figure 10-24: Stereographic analysis of planar failure for slope azimuth 280°	380
Figure 10-25: Plan view showing positions of analysis sections relative to the initial quarry and spillway design	386
Figure 10-26: Example section looking north showing groundwater surface adjusted to the quarry profile.....	388
Figure 10-27: Illustration of the previous and revised spillway and quarry designs, with comparison sections (looking north) of cut slope profiles.....	390
Figure 11-1: Geohazard ranking.....	393
Figure 11-2: High geohazard risks at the headwaters of the reservoir	394
Figure 11-3: High geohazard risk opposite the embankment	394
Figure 11-4: High geohazard risk at the embankment	395
Figure 11-5: High geohazard risk downstream of the embankment	395
Figure 11-6: Plan view of surface conditions at the embankment site	397
Figure 11-7: Plan view of potential unstable zone (in green) and drillhole locations in the right abutment	398
Figure 11-8: Section A of the potential unstable zone (in green)	399
Figure 11-9: Drillhole SW4 from 17.5 to 19.9 m, showing boulder overburden material over the bedrock	399
Figure 11-10: Plan view indicating approximate extent of the potential unstable zone on the left-hand abutment, with reference to the drillhole collar positions.....	401
Figure 11-11: Core photograph showing soil-like overburden material immediately above highly fractured rock in drillhole LH7, from 6.4 m to 10 m depth.....	401
Figure 11-12: Core photographs showing variability of zones of highly fractured and oxidised rock with deteriorating matrix and/ or soil-like infill in drillhole LH3, from 66 m to 80 m depth.....	402
Figure 11-13: Core photograph from 102.8 m to 106.7 m depth from drillhole LH3, showing the base of the potentially unstable 'landslide' zone.....	403
Figure 11-14: Cross-section through left abutment mass	404
Figure 14-1: Embankment sediment management catchments.....	413
Figure 14-2: Bio-engineering of erosion-prone slopes (photos taken in Minas Gerais, Brazil).....	414
Figure 14-3: Spoil dump catchments.....	415
Figure 14-4: Stilling basin/ outlet configuration concept.....	416
Figure 14-5: Typical sedimentation pond schematic of features.....	417
Figure 14-6: FRHEP stormwater catchments.....	419
Figure 14-7: Example arch culvert stream crossing photo (Source: www.ail.ca).....	421
Figure 14-8: Catchments for road crossings	422
Figure 14-9: Case 1 section	427
Figure 14-10: Slide output – Case 1.....	427

Figure 14-11: Slide output – Case 2.....	428
Figure 15-1: Intake arrangement.....	430
Figure 15-2: 3D models of intake structures (aerial view, inset underground view)	431
Figure 15-8: Tunnel 2 current long section.....	435
Figure 15-9: Surge chamber water level following a simultaneous full load rejection at maximum HWL....	437
Figure 15-10: Lower penstock pressure following a simultaneous full load rejection at maximum HWL	438
Figure 15-11: Hydraulic grade envelope following a simultaneous full load rejection at maximum HWL	438
Figure 15-12: Surge chamber water level following a simultaneous full load rejection at RL 204 m HWL....	439
Figure 15-13: Lower penstock pressure following a simultaneous full load rejection at RL 204 m HWL	439
Figure 15-14: Hydraulic grade envelope following a simultaneous full load rejection at RL 204 m HWL	440
Figure 15-15: Surge chamber water level following a single unit full load acceptance at minimum HWL	440
Figure 15-16: Lower penstock pressure following a single unit full load acceptance at minimum HWL.....	441
Figure 15-17: Hydraulic grade envelope following a single unit full load acceptance at minimum HWL	441
Figure 15-18: Transfer function illustration	442
Figure 15-19: System response to the loss of one unit at low water levels (additional unit operating)	444
Figure 15-20: System response to the loss of one unit at low water levels (spinning reserve unit operating)	444
Figure 15-21: System response, loss of one unit at low water levels (spinning reserve unit, peak mine load)	445
Figure 15-22: System Response, loss of one unit at low water levels (without a spinning reserve operating, peak mine load)	445
Figure 15-23: Variation in the total suspended solids discharging from the FRHEP reservoir	448
Figure 15-24: Breakdown of suspended solids	448
Figure 15-25: Suspended solid level by component	449
Figure 15-26: Timing of running repairs and the effect of sediment concentration.....	450
Figure 15-27: FRHEP aerial view from upstream (no embankment)	458
Figure 15-28: FRHEP aerial view from downstream (no embankment).....	459
Figure 15-29: FRHEP underground view of the conveyance.....	459
Figure 16-1: Horizontal seismic spectra (760 m/s).....	461
Figure 16-2: Horizontal seismic spectra (1,150 m/s).....	461
Figure 16-3: Intake arrangement (plan view)	465
Figure 16-4: Lower intake structure.....	467
Figure 16-5: Upper intake structure.....	468
Figure 16-6: Example of screen cleaner	469
Figure 16-7: Conveyance long section.....	474
Figure 16-8: Tunnel, shaft and surge chamber sections	476
Figure 16-9: Bifurcation of a 2-unit section.....	477
Figure 16-10: Bypass valve arrangements.....	479
Figure 16-11: Fixed cone dispersion valve.....	480
Figure 16-12: Powerhouse layout (plan view).....	481
Figure 16-13: Building long section	483
Figure 16-14: Tailrace configuration.....	484

Figure 16-15: 132 kV GIS configuration	495
Figure 16-16: 132 kV GIS configuration options	495
Figure 17-1: Distribution of time to first power - FRCGP and export grid.....	497
Figure 17-2: Dam crest and water levels during the filling of the reservoir	497
Figure 18-1: Reservoir level variation for most reliable sequence – Years -1–33	502
Figure 18-2: Reservoir water level and power generation for most reliable sequence – Years -1–33	502
Figure 18-3: Reservoir level variation for least reliable sequence – Years -1–33.....	503
Figure 18-4: Reservoir water levels and power generation for least reliable sequence – Years -1–33.....	503
Figure 18-5: Generation reliability in different years.....	506
Figure 18-6: Very long term inflows to the reservoir in the measured and synthetic flow series	508
Figure 18-7: Generation reliability, inflow and spill.....	510
Figure 18-8: Potential additional generation by reducing spill in wet years	510
Figure 18-9: Comparison of total generation potential and mean inflow.....	511
Figure 18-10: Peak hourly and daily spillway flows over the 33 years modelled	511
Figure 19-1: Components of a typical dam safety program	514
Figure 19-2: Organisation chart for FRHEP stewardship.....	516
Figure 19-3: Rates of reservoir water level rise during early filling	519
Figure 19-4: Stratification within the reservoir	520
Figure 19-5: Tailings and waste deposition layout assuming a waste density of 1.5 t/m ³	523
Figure 19-6: Deposition sequence.....	524
Figure 19-7: Proposed location of barge-loading facility	528
Figure 19-8: Barge latching system.....	528
Figure 19-9: Powerhouse generation control system.....	538
Figure 19-10: Bypass valve control system.....	538
Figure 19-11: Intake gates, spillway gates and residual flow valve control system	539

List of Appendices

Appendix 1: Drawings (SRK and Stantec)

Appendix 2: Artist's Impression

Disclaimer

The opinions expressed in this Report have been based on the information supplied to SRK Consulting (Australasia) Pty Ltd (SRK) by Frieda River Limited (FRL). The opinions in this Report are provided in response to a specific request from FRL to do so. SRK has exercised all due care in reviewing the supplied information. While SRK has compared key supplied data with expected values, the accuracy of the results and conclusions from the review are entirely reliant on the accuracy and completeness of the supplied data. SRK does not accept responsibility for any errors or omissions in the supplied information and does not accept any consequential liability arising from commercial decisions or actions resulting from them. Opinions presented in this Report apply to the site conditions and features as they existed at the time of SRK's investigations, and those reasonably foreseeable. These opinions do not necessarily apply to conditions and features that may arise after the date of this Report, about which SRK had no prior knowledge nor had the opportunity to evaluate.

List of Abbreviations

AC	alternating current
ACRD	asphalt core rockfill dam
AEP	annual exceedance probability
ANC	acid neutralising capacity
ANCOLD	Australian National Committee on Large Dams
AP	acid potential
ARI	average recurrence interval
BCM	bank cubic metre
Bm ³	billion metres cubed
BoD	Basis of Design
Bt	billion tonnes
CAPEX	capital expenditure
CDA	Canadian Dam Association
CFRD	concrete faced rockfill dam
DPS	Definition Phase Study
DSHA	deterministic seismic hazard assessment
EMP	Environmental Management Plan
ERP	Emergency Response Plan
FEL	front-end loading
FML	Freida Mountain Lake
FoS	factor of safety
FRCGP	Frieda River Copper-Gold Project
FRHEP	Frieda River Hydroelectric Project
FRL	Frieda River Limited
g	g-unit (force)
GHD	GHD Pty Ltd
GWh	gigawatt hour
GWh/a	gigawatt hour per annum
H	height
HDS	High Density Sludge
HEP	hydroelectric power
HV	high voltage
ICOLD	International Commission on Large Dams
IFC	International Finance Corporation
IFO	intermediate fuel oil
IPP	Independent Power Producers
IPS	Investigation Phase Study
ISF	integrated storage facility
kg/m ³	kilograms per cubic metre
km	kilometre
km ²	square kilometres
L	litres
L/s	litres per second
LCM	loose cubic metres
LiDAR	Light Detection and Ranging (remote sensing)
LOM	life of mine
M	million
m	metre

m ²	square metres
m ³	cubic metres
m ³ /s	cubic metres per second
MAA	Multiple Accounts Analysis
MCE	maximum credible earthquake
ML	million litres
mm	millimetres
Mm ³	million cubic metres
MPA	maximum potential acidity
MPa	megapascals
Mt	million tonnes
MTO	material take-off
MVA	megavolt amperes
MW	megawatts
MWh	megawatt hours
NAF	non-acid forming
NPV	net present value
OPEX	operational expenditure
PAF	potentially acid forming
PGA	peak ground acceleration
PMF	probable maximum flood
PMP	probable maximum precipitation
PNG	Papua New Guinea
PNGFP	PNG Forestry Products
PPA	Power Purchase Agreements
PPL	PNG Power Limited
PSD	particle size distribution
PSHA	probabilistic seismic hazard assessment
REL	Robinson Energy Limited
RH	right hand
RL	reduced level
SDP	Sepik Development Project
Sinohydro	Sinohydro Corporation Ltd of China
SKMPS	SKM, Pöyry and SMEC
SPS	Selection Phase Study
SRK	SRK Consulting (Australasia) Pty Ltd
Stantec	Stantec New Zealand Ltd
t/m ³	kilogram per cubic metre
TIRP	Tailings Independent Review Panel
TSF	tailings storage facility
TWh	terawatt hours
V:H	vertical: horizontal
W	width
WBS	work breakdown structure

1 Introduction and Background

Frieda River Limited (FRL) is evaluating the development of a combined Frieda River Hydroelectric Project (FRHEP) and the Frieda River Copper-Gold Project (FRCGP) in Papua New Guinea (PNG). FRL commissioned SRK Consulting (Australasia) Pty Ltd (SRK) to undertake a Selection Phase Study (SPS) design of the FRHEP. The FRHEP has two functions: to produce economic and renewable electricity and to provide permanent, safe and stable storage of tailings and waste rock from the FRCGP. The FRHEP will be the sole producer of power for the FRCGP. Excess power will be distributed to the export grid.

The SPS is a further development to the previously completed study phase of the FRHEP that identifies the preferred option for each major project component and develops basic designs to a level that is adequate to support cost estimates.

The FRHEP is located in the Sandaun Province of northwest PNG (Figure 1-1). The site is in the remote northern slopes of the Thurnwald Range, in mountainous and rugged terrain with dense rainforest. There is no road access or power. Elevations in the range extend from 60 m above sea level (masl) at the embankment toe to 2,800 masl. The embankment is 20 km from the proposed FRCGP and approximately 40 km south of the confluence with the regional Sepik River which runs from the central mountain range to the Bismarck Sea.



Figure 1-1: Location of the Frieda River Hydroelectric Project

This report presents the SPS design and summarises the studies and work packages completed during the SPS. SRK teamed with Robinson Energy Limited (REL) and Stantec who provided the engineering and design of the power generation components, and HydroNumerics Pty Limited (HydroNumerics) who investigated the limnology of the FRHEP reservoir. Additional specialists were engaged, as required, during execution of the SPS to provide expert advice for specialist work packages of the FRHEP.

1.1 Climate

The Frieda River is a tributary of the Sepik River, which originates in the central mountain ranges in the area of Telefomin. The Frieda River catchment conveys runoff through the Frieda River valley and past the proposed embankment location to the lower plains of the Sepik River, commonly referred to as the 'lowlands'.

The region is described as tropical rainforest – Köppen-Geiger climate classification of Af, which is defined as temperatures above 18 °C during the coldest month and precipitation in excess of 60 mm during the driest month².

The average annual rainfall in the surrounding mountainous areas is in the order of 8,000 mm. Because of the mountainous terrain, the climate is dominated by local weather effects rather than by synoptic-scale monsoonal effects. One of these is the lack of movement of the inter-tropical convergence zone, so the rainfall pattern exhibits very weak seasonality.

Local factors, including orographic effects, topographic features creating preferred paths and barriers for moisture feeds and storms, and constraints imposed by variable dewpoints, which would decrease with increasing altitude, may also be important influences on the spatial variability of rainfall. Rainfalls can vary significantly over short distances, depending on the relative importance of these factors; obvious patterns of rainfall variability are not distinguishable.

1.2 Project history

Prior studies to investigate the development of a combined hydroelectric power generation and tailings storage facility in the Frieda River area have been carried out. A feasibility-level design was undertaken in 2011 by SKM, Pöyry and SMEC (collectively SKMPS), which was followed by completion of an extended pre-feasibility design review by GHD Pty Ltd (GHD). The SKMPS study included a field and laboratory testing program, with extensive LiDAR topography and imagery capture, geohazard/ georisk studies, seismic hazard assessment, regional geology, hydrology, geochemistry and vegetation surveys. The 2011 study was based on a specific embankment location referred to as the SKMPS Frieda Mountain Lake (FML) site. The findings of the SKMPS study proposed that the valley embankment, its spillway and associated hydroelectric infrastructure would be positioned in the Frieda River valley. Tailings and waste rock would be stored in a separate facility located in the Ok Binai valley, within the FML catchment.

During 2015 and 2016, SRK developed further studies to investigate an alternative location for an integrated storage facility (ISF) in the Nena River (a tributary of the Frieda River). SRK developed the design of the Nena ISF for storage of tailings and waste rock and hydroelectric power generation to an FEL (front-end loading) 2 level.

FRL subsequently appointed Sinohydro Corporation Ltd of China (Sinohydro) to undertake an IPS for the FRHEP, including defining the site hydrology, geology and geotechnical conditions, and an embankment site selection study. These were to be followed by an IPS-level design of the temporary river diversion structures. The embankment site selection study report was completed in March 2017. However, the Sinohydro contract was suspended prior to completion of the full scope of work. The Sinohydro selection study report focused on three potential sites, all of which are positioned near the original FML site determined by SKMPS.

² Peel, M, Finlayson, B & McMahon, T, 2007. Updates world map of the Köppen-Geiger climate classification, *Hydrological Earth System Sciences*, pp.1633–1644.

SRK was subsequently appointed by FRL to develop concept and IPS-level designs for the FRHEP using all available and relevant information. SRK's study focused on identification of potential fatal flaws, power generation capabilities, and strategies for disposal of tailings and waste rock. SRK worked with FRL to narrow down the options and select a preferred go-forward option for development to the next design phase, the SPS.

The IPS resulted in the selection of an embankment with a crest elevation at RL 235 m designed for a maximum peak power demand of 386 MW and storage of a combined total of 2.2 Bm³ of tailings, waste rock and sediment over a 25-year LOM. The preferred embankment location was approximately 100 m north of the SKMPS embankment location.

After completion of the IPS, FRL appointed SRK to undertake the SPS, which is the subject of this report. The SPS included a comprehensive field geotechnical investigation and characterisation campaign.

1.3 Export grid power supply

PNG Power Limited (PPL) is PNG's state-owned power utility which currently manages the export grid – approximately 300 MW of generation assets across the country. This includes numerous large hydroelectric power schemes including the Rouna River cascade near Port Moresby and Yonki Dam in the Central Highlands.

New hydroelectric power projects typically have long lead times and require significant upfront investment. As a result, development of private schemes, such as the FRHEP is promoted. There are currently several large IPP schemes at various stages of design for which Power Purchase Agreements (PPAs) with PPL are being developed. These include, but are not limited to the following:

- 180 MW Ramu II scheme in the Central Highlands – recently tendered and it is understood that a PPA is in place
- 80 MW Naoro Brown scheme – detailed design stage
- 50 MW Edevu project – developed by PNG Hydro Development Ltd, a Chinese-led consortia (understood to be under construction)
- Hawaii Falls Hydro scheme – under development by an Israeli agricultural firm
- 1,800 MW Karimui scheme in Simbu – construction started in 2017 and to be completed by 2023
- 2,000 MW Purari project – progressed by Origin Energy over a number of years for interconnection with Australia, but currently in abeyance due to uncertainties over access to carbon credits for offshore electricity generation.

At present, there is only one IPP selling power to PPL – the 15 MW Baiune scheme located 50 km southwest of Lae. The scheme, which is owned and operated by PNG Forestry Products (PNGFP), was constructed in stages since the 1920s and previously served as a mining operation. PNGFP is proposing an additional 11 MW hydroelectric power scheme on the Baime River catchment. A draft PPA with PPL is understood to be in place, and PNGFP is currently progressing a procurement process to assess economic viability.

1.4 Site selection

The initial site selection, driven by the topography and hydrology, was an embankment location approximately 1,500 m downstream of the confluence between the Frieda and Ok Binai rivers. Beyond this stretch of river, the valley widens and a significantly large embankment volume would be required. The site's location in a short, narrow stretch of the Frieda River has lower construction volumes.

Studies by SKMPS, Sinohydro and SRK previously considered this stretch of river. At the start of the SPS, SRK performed a Multiple Accounts Analysis (MAA), a formal risk-based options analysis, in consultation with FRL to identify the most favourable of three embankment location options³. The options considered the geology and geotechnical characteristics, economics, topography and spatial requirements of the site layouts for key components of the FRHEP. The preferred site (Figure 1-2) between the SKMPS FML and the Sinohydro 'Midstream' sites was chosen as it had the most favourable alignment relative to areas of geotechnical concern and a stormwater gully of the left hand bank.

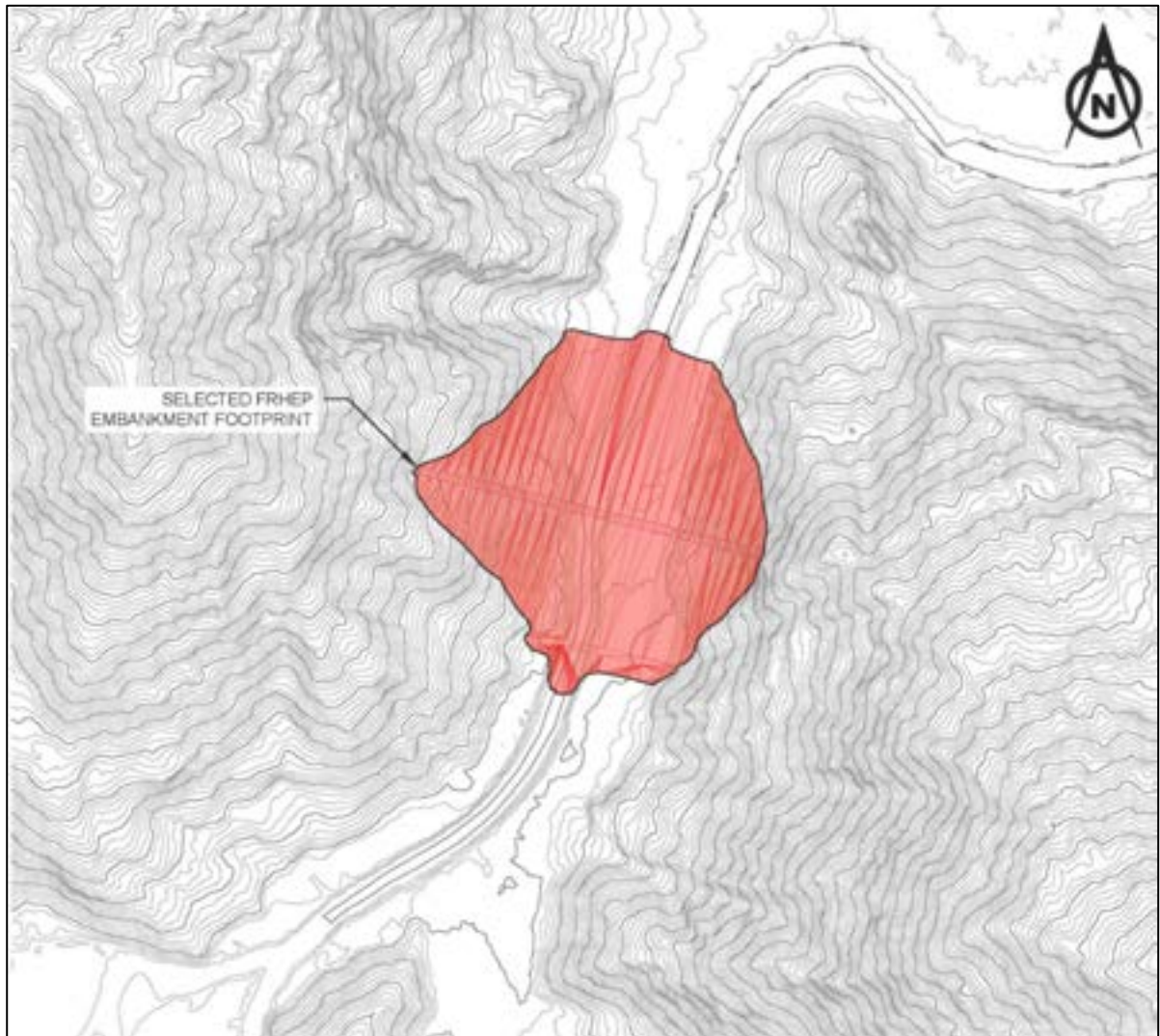


Figure 1-2: Embankment site

1.5 Project benchmarking

The benchmarking process considered the site's unique aspects – rainfall and seismicity – and embankment height. Table 1-1 summarises the power generation potential of other hydroelectric dams which are comparable – asphalt core rockfill dam (ACRD) type or embankment height lower than 200 m for concrete faced rockfill dam (CFRD) type – to the proposed FRHEP facility. Typically, installed capacity for comparable ACRD and CFRD hydroelectric dams is observed to vary between 130 MW and 760 MW, although some CFRD dams can generate more power, such as Tianshengqiao-

³ SRK 2018, Frieda River HEP Selection Phase Study – Options Analysis, PNA009_Frieda River HEP SPS Design - Options Analysis_Rev0

1 (1,200 MW, 178 m high) or Bakan (2400 MW, 222 m high). The FRHEP will have installed capacity of 593 MW, based on the large catchment area and reservoir capacity.

Although there are comparable hydroelectric schemes in operation, none are required to have the combined tailings and waste rock storage capabilities of the FRHEP. Integration of waste disposal with hydroelectric power generation at this scale appears to be unique.

Table 1-1: Power generation potential of other hydroelectric power dams

Dam Name	Location	Embankment height (m)	Seepage cut-off option	Installed capacity (MW)	Total energy (GWh/a)	Total capacity (Mm ³)	Catchment (km ²)
FRHEP ⁴	<i>Frieda River – PNG</i>	190.5	ACRD	593	2,790	9,600	1,033
Nena ISF ⁴	Nena River – PNG	171	ACRD	134	467–800	1,300	258
Quxue	China	164	ACRD	246	N/A	136.6	N/A
Cetin	Turkey	145	ACRD	420	1,100	610	N/A
Storglomvatn	Norway	128	ACRD	N/A	N/A	3,468	51.9
Storvatn	Norway	90	ACRD	N/A	4,500	3,100	49.1
Los Caracoles	Argentina	136	CFRD	130	N/A	560	N/A
Zipingpu	Sichuan, China	156	CFRD	760	N/A	1,120	N/A
Tianshengqiao-1	China	178	CFRD	1,200	N/A	10,257	50,139
Nam Ngum 2	Lao PDR	185	CFRD	615	2,220	4,200	5,640
Aguamilpa	Mexico	187	CFRD	960	2,131	6,950	73,800
Sogamoso	Colombia	190	CFRD	820	5,056	4,800	70
Kárahnjúkar	Iceland	193	CFRD	690	4,600	209.7	2.1

1.6 Embankment optimisation

REL and Stantec⁵ completed an earlier study of power scheme and embankment height optimisation, in conjunction with FRL. This study drew upon the design developed during the earlier IPS, and was updated to consider the revised FRCGP power loads (provided by FRL) and information regarding PMF magnitudes.

Based on the results of the Project Evaluation Model, FRL determined in December 2017 that the FRHEP should be progressed on the following basis:

- The waste rock will be transported to the reservoir by barge.
- The target FRHEP dam crest elevation is RL 235 m, corresponding to an embankment height of 187 m. This has been increased further to RL238.5m following the detailed analysis of the embankment.

⁵ SRK 2018, Frieda River HEP Selection Phase Study – Options Analysis, PNA009_Frieda River HEP SPS Design - Options Analysis_Rev0

⁵ SRK 2018, Frieda River HEP Selection Phase Study – Options Analysis, PNA009_Frieda River HEP SPS Design - Options Analysis_Rev0

1.6.1 Benchmarking

A benchmarking study comparing embankment height only indicated that while there are globally more than 87 water dams with embankment heights that exceed 190.5 m (i.e. the embankment height at the FRHEP), there are few tailings storage facilities (TSFs) with an embankment greater than this height. Most of these dams used a rockfill construction method, either with concrete facing (CFRD) or with an asphalt core. Figure 1-3 compares the heights of large ACRDs to the proposed FRHEP embankment height. Figure 1-4 compares other tailings dams of a similar height to the FRHEP and Figure 1-5 compares the construction durations of other hydroelectric rockfill dams globally.

Construction durations for embankment heights above 120 m typically vary between four years and eight years.

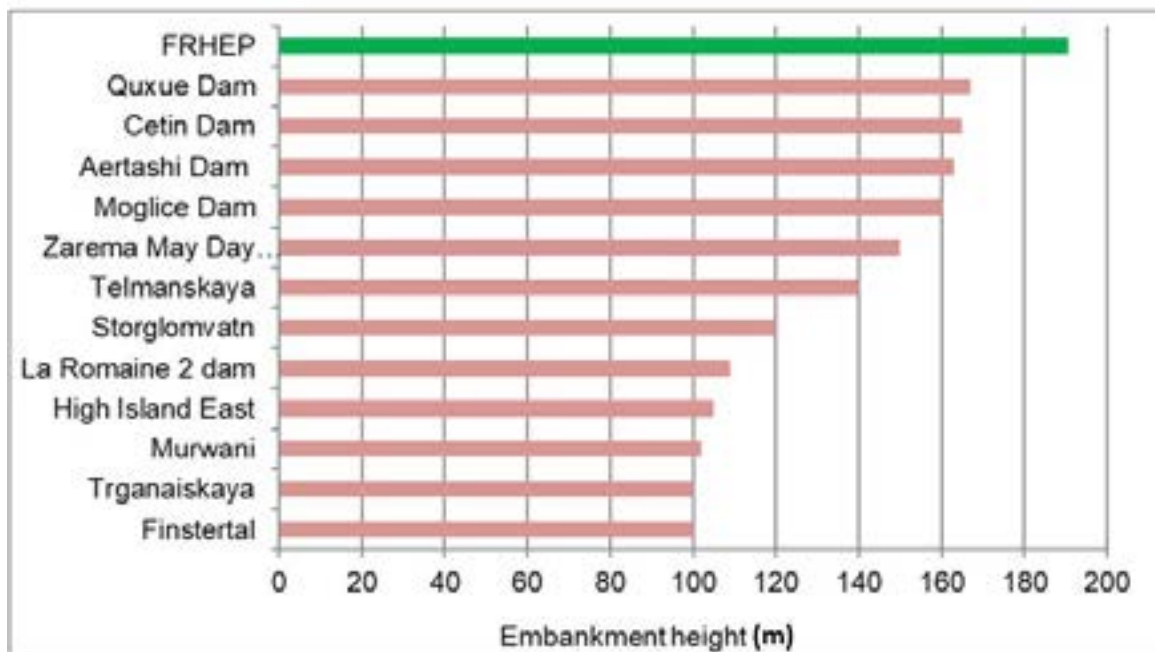


Figure 1-3: Embankment height of other asphalt core rockfill dams compared to FRHEP

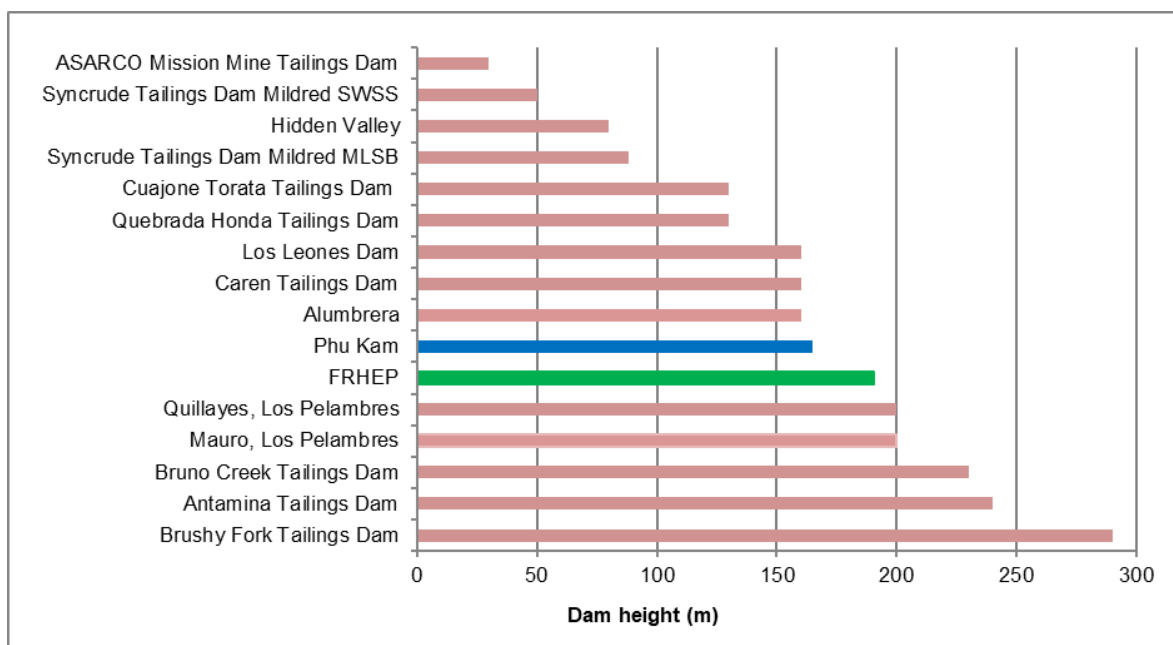


Figure 1-4: Embankment height of other tailings dams compared to FRHEP

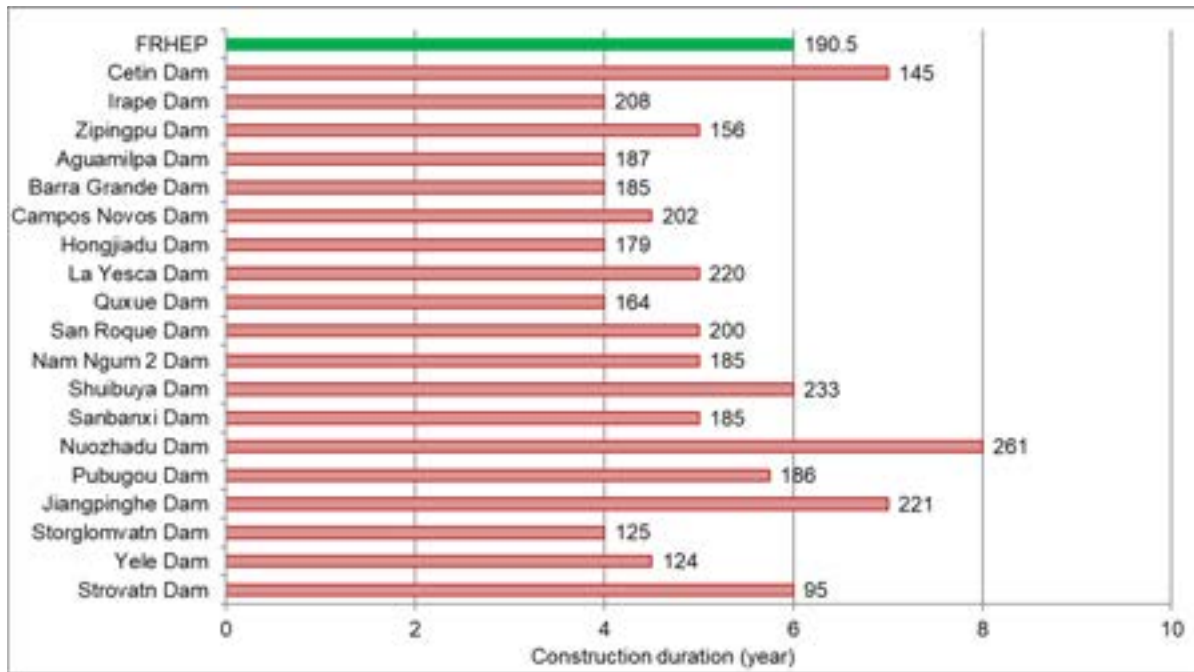


Figure 1-5: Construction durations for other hydroelectric dams with comparable embankment heights

Note: Embankment height is shown in metres at the end of each bar.

1.6.2 Seismicity

The Global Seismic Hazard Assessment Program (GSHAP) identifies the area of the FRHEP as a Moderate hazard with peak ground accelerations (PGAs) between 1.6 m/s² and 2.4 m/s² for a return period of 475 years. Figure 1-6 shows seismicity in locations of similar dams.

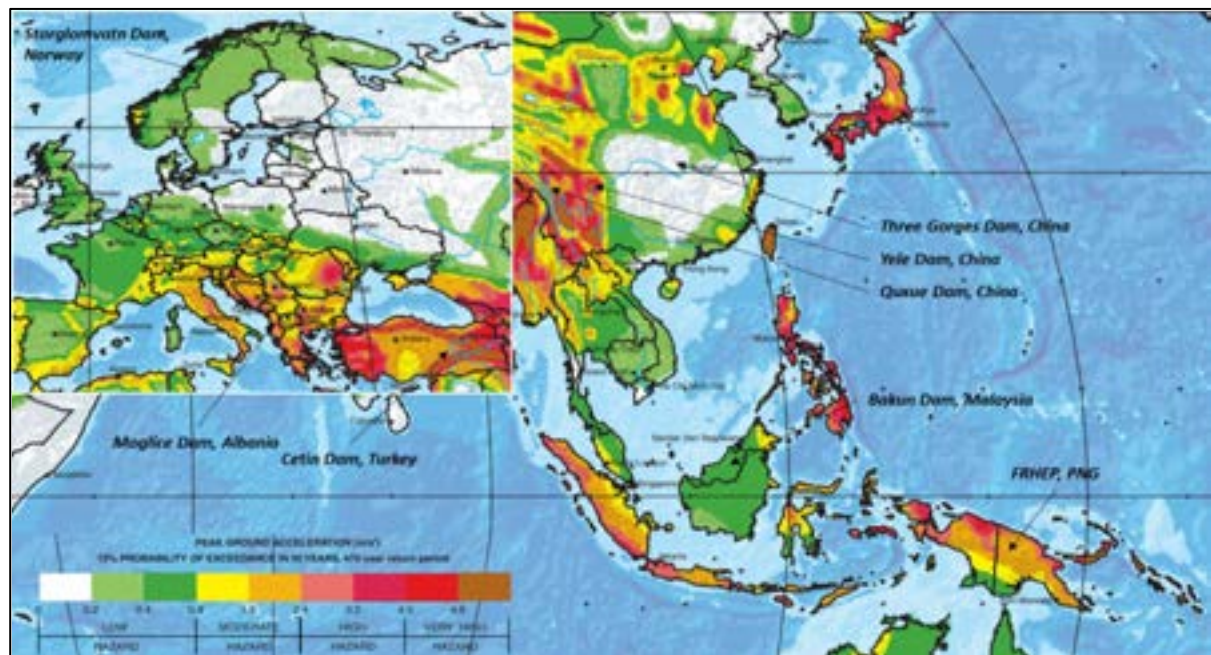


Figure 1-6: PGA regions of various dams

Source: Global Seismic Hazard Assessment Program.

Figure 1-7 compares regional seismic hazard PGAs at the Frieda River site to those at other large tailings dams. Most of the dams in high seismic zones are in South America in relatively arid environments.

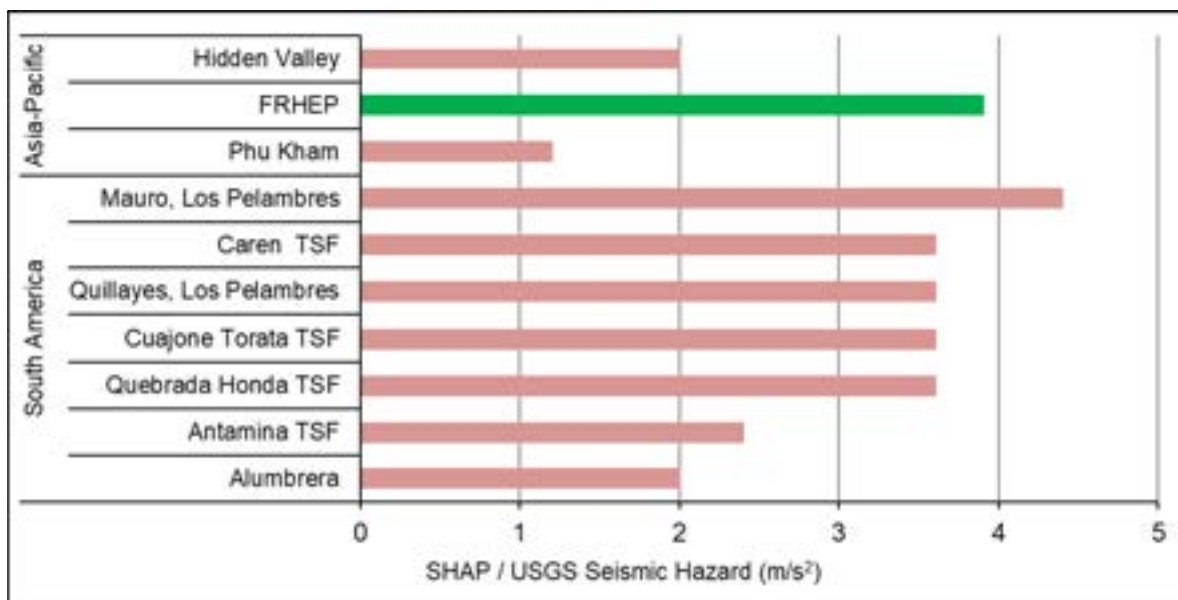


Figure 1-7: Operating Basis Earthquake (OBE) peak ground accelerations for other large tailings dam sites

Table 1-4 shows the proposed design MCE PGA (1.09g) for the FRHEP embankment benchmarked against actual PGAs of notable earthquakes.

Table 1-2: Peak ground accelerations of notable earthquakes⁶

PGA (g) single direction (maximum recorded)	PGA (g) vector sum (H1, H2, V) (maximum recorded)	Magnitude (Richter scale)	Depth (km)	Earthquake
3.2	N/A	7.5	N/A	2018 Papua New Guinea earthquake ⁷
2.70	2.99	9.0	30	2011 Tōhoku earthquake and tsunami
2.20	N/A	6.3	5	February 2011 Christchurch earthquake
2.13	N/A	6.4	6	June 2011 Christchurch earthquake
N/A	4.36	6.9/7.2	8	2008 Iwate-Miyagi Nairiku earthquake
1.70	N/A	6.7	19	1994 Los Angeles earthquake
N/A	1.47	7.1	42	April 2011 Miyagi earthquake
1.26	N/A	7.1	10	2010 Canterbury earthquake
1.01	N/A	6.6	10	2007 Chūetsu offshore earthquake
1.01	N/A	7.3	8	1999 Jiji earthquake
1.00	N/A	6.0	8	December 2011 Christchurch earthquake
0.80	N/A	6.8	16	1995 Kobe earthquake
0.78	N/A	8.8	23	2010 Chile earthquake
0.60	N/A	6.0	10	1999 Athens earthquake
0.51	N/A	6.4	N/A	2005 Zarand earthquake
0.50	N/A	7.0	13	2010 Haiti earthquake

⁶Source: https://en.wikipedia.org/wiki/Peak_ground_acceleration#Notable_earthquakes

⁷Source: https://reliefweb.int/sites/reliefweb.int/files/resources/poster_0.pdf

PGA (g) single direction (maximum recorded)	PGA (g) vector sum (H1, H2, V) (maximum recorded)	Magnitude (Richter scale)	Depth (km)	Earthquake
0.44	N/A	7.7	44	1978 Miyagi earthquake (Sendai)
0.40	N/A	5.7	8	2016 Christchurch earthquake
0.37	N/A	5.2	1	2011 Lorca earthquake
0.25–0.30	N/A	9.5	33	1960 Valdivia earthquake
0.24	N/A	6.4	N/A	2004 Morocco earthquake
0.18	N/A	9.2	23	1964 Alaska earthquake

1.6.3 Rainfall

Figure 1-8 compares the annual average rainfall at the Frieda River site to other tailings and water dams. The tailings dam with the highest rainfall is the Hidden Valley operation, also in PNG, with almost 3,000 mm per annum.

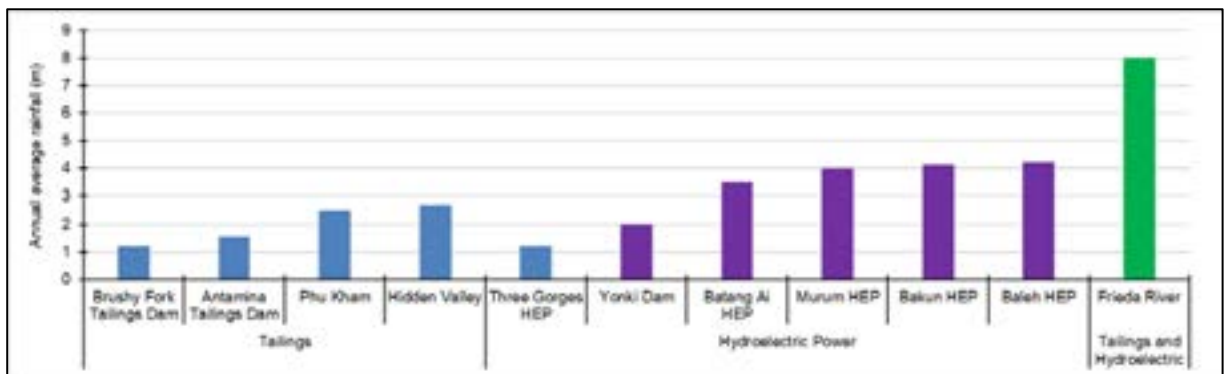


Figure 1-8: Annual average rainfall of other dams compared to FRHEP

1.6.4 Hydroelectric power generation

Hydroelectric power is a widely accepted renewable energy source, ranging from the smallest household schemes to the 22,500 MW Three Gorges Dams in China. By contrast, the FRHEP will produce approximately 2,763 GWh/a.

The generating facility is rated at 8 × 69.2 MW (large units) + 2 × 19.3 MW (small units), or 592 MW in total. Figure 1-9 illustrates the number of plants constructed in the Asia-Pacific region, with their rating (vertical axis) and relative age in years (horizontal axis). The FRHEP lies in the diagram as shown by the yellow circle.

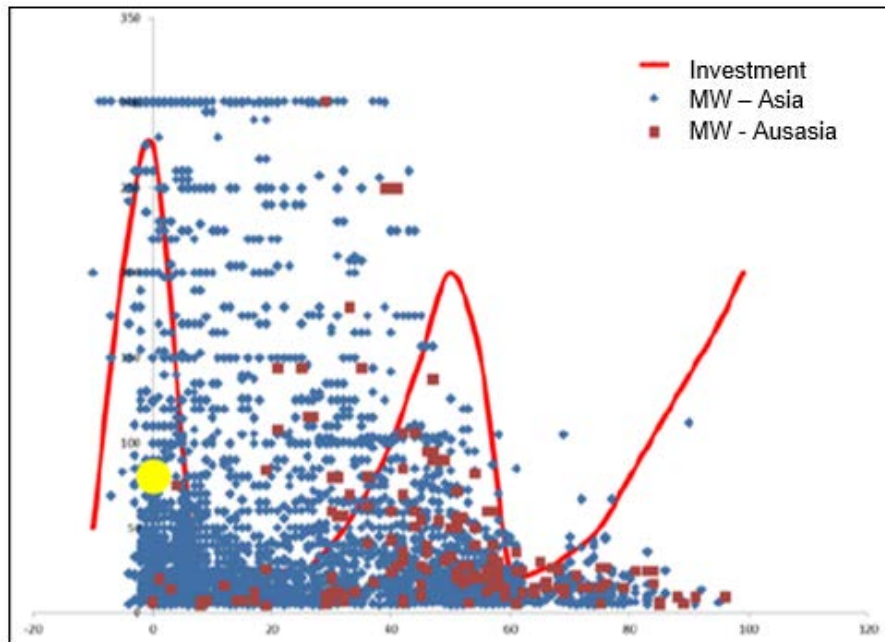


Figure 1-9: Rating vs operating life of hydroelectric power plants in the Asia-Pacific region

2 Basis of Design

The design criteria for the FRHEP have been determined from a number of sources – FRL criteria, criteria defined during previous design studies, including those completed for Xstrata; applicable national and international design standards; and assumptions based on SRK's experience.

2.1 Objectives

The primary function of the FRHEP is generation of hydroelectric power to supply the needs of the FRCGP, and secondly, to store tailings and waste rock. The design life of the FRHEP has been assumed to be in the order of 200 years.

The tailings and waste rock disposal strategy is sufficient for LOM production without sterilising opportunities for future expansion. The FRHEP was developed in accordance with international standards, while aligning with FRL's operating philosophy and stewardship requirements.

The FRHEP is designed to be constructible under local conditions – limited access, high seismicity and rainfall, and an eroding environment.

Specific objectives related to development, operations and closure are detailed in the following subsections.

2.1.1 Development

Although the FRHEP's target commissioning date has not been highlighted as a key project objective, FRL aims to have the FRHEP generating electricity to commission operations at the FRCGP. A temporary lower intake will be required should filling of the reservoir commence prior to the completion of the embankment and spillway. This will result in power being generated before the normal operating level in the reservoir is reached.

The proposed plan is to construct diversion tunnels to divert the Frieda River around the proposed embankment site, followed by construction of the cofferdam to allow the main embankment to be constructed. Materials and equipment will be barged to the site on the Frieda River in the first 18 months of construction; thereafter, access roads will be provided concurrent with development of the FRCGP.

Difficult construction conditions include the steep jungle covered terrain, high precipitation, weathered tropical soils, remote location and accessibility issues. Fugitive sediment from the site will require to be managed. Dedicated spoil stockpiles have been designed and sediment management methods will be implemented to limit and contain sediment generation.

2.1.2 Operations

Relevant density values for the 'as placed' tailings and waste rock will be adopted in determining the total storage capacity requirements, and ensuring sufficient storage capacity to attenuate and then discharge storms, while maximising hydroelectric generation potential.

Being a flow-through facility, discharge water must meet end-of-pipe discharge standards. This requires that oxidation of the tailings and waste rock must be limited prior to subaqueous disposal. Contaminated water inflows must be controlled or treated. Once inundated, the water cover will provide an oxidation barrier to inhibit further reaction.

To achieve operational objectives, the following will be required:

- The placement of tailings and waste will need to be done in a manner that minimises sediment release and the potential for sediment re-entrainment during high flood inflows. In general, if the water quality meets environmental standards, the water should be satisfactory for hydroelectric power generation without causing wear to the turbines.
- Extremely large floods may give rise to very high sediment levels. Depending on the particle sizes and the amount of sediment suspended in the water, hydroelectric power generation may need to be halted temporarily until sediment concentrations drop to acceptable levels.

2.1.3 Closure

The embankment landform will be required to maintain stable in perpetuity, in order to keep the tailings and waste saturated.

At closure, the reservoir level will be reduced as much as possible, while maintaining the water cover over the tailings and waste rock. It is expected that the reservoir will continue to fill with sediment, so that a layer of sediment will progressively form a cover over the tailings and waste rock.

The closure timeframes could vary because the length of continued hydroelectric power demand is yet to be determined. SRK has used a power generation lifespan of 200 years; however, the FRHEP has been designed for closure, irrespective of its succession potential.

2.2 Hydroelectric power generation

2.2.1 Power demand based on May 2018 loads

The FRHEP must be able to supply sufficient power to meet the FRCGP's power demand, taking the range of power demand scenarios under consideration into account.

FRL selected barging as the method of deposition for waste rock and provided a load projection for the 33-year LOM plus a commissioning year. The initial FRCGP demand is 165 MW but this increases slowly until there is a significant step change in Year 8. During peak production years, demand from the FRCGP is approximately 277 MW peak demand with energy requirements of 2,159 GWh/a. Details of the FRCGP power and energy demand are set out in Table 2-1 and displayed in graph form in Figure 2-1.

The FRHEP must also be able to provide power to the export grid. The potential to export power was optimised based on a preferred embankment height of RL 238.5 m. This is based on maximising the generation from the scheme at all times. The result is that in the first year of export sales 245MW and 1,658 GWh/a of power is available for export. This eases back to 1,420 GWh/a through to Year 7 when it drops to 652 GWh/a as the FRCGP load ramps up.

Table 2-1: Power and energy demand for mining operations⁸

Scenario	Power (MW)	Energy (GWh/a)
Revised hydroelectric power demand (barge-based deposition system)	Years 1 to 7: 165 to 181 Years 8 to 33: 277	Year 1 to 7: 1,139 to 1,369 Years 8 to 33: 2,122 to 2,159
PNG Grid - demand	Years 1 to 7: 235 to 219 Years 8 to 33: 100 to 107	Year 1 to 7: 1,658 to 1,420 Years 8 to 33: 630 to 657

⁸ Email – Power demand supplied by FRL, 10/10/2017

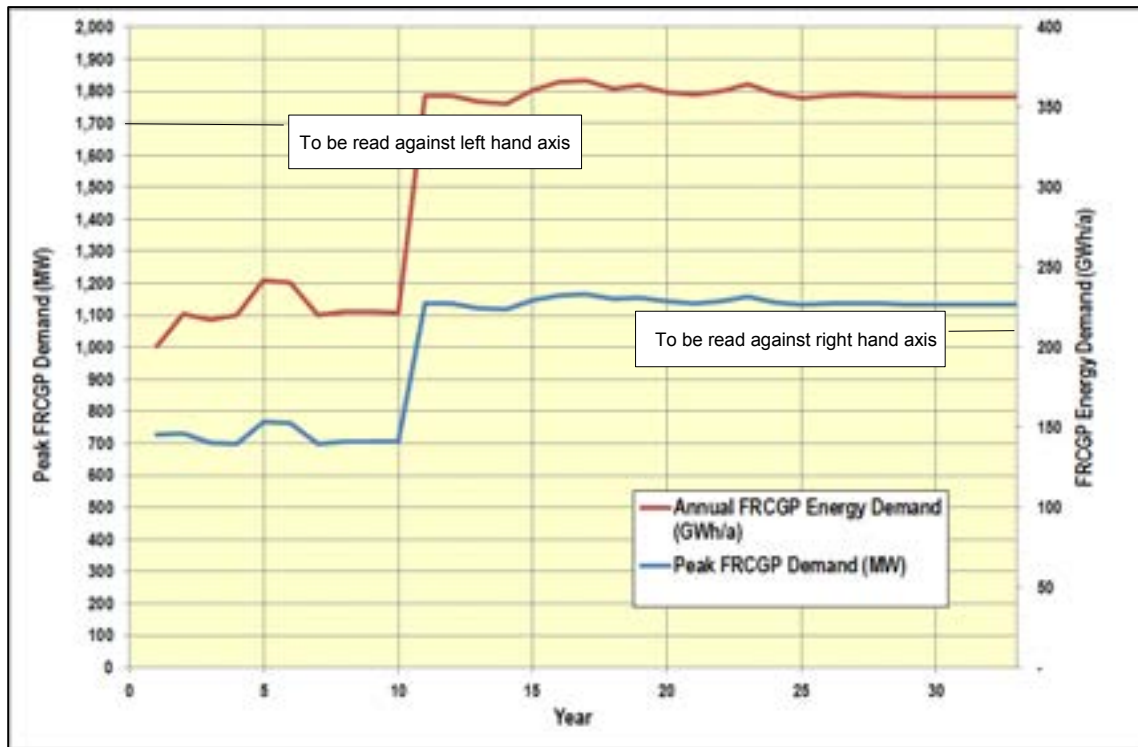


Figure 2-1: Mine power and energy demand

FRL provided four electrical demand profiles for the FRCGP:

- The first two profiles were provided in October 2017 and represented the power demand for two different tailings disposal options. These options were used in the Embankment Height Optimisation Study.
- A revised power demand for the FRCGP was provided in January 2018 based on the low demand (barging disposal) option. This provided the basis for the work set out in the draft versions of this SPS report to Revision C, which was provided to the TIRP for review. These are referred to as the January 2018 loads within this report.
- A final set of FRCGP loads was provided on 31 May 2018 which are approximately 15% greater than the January 2018 loads. A limited edit of the report to include this option has been carried out. However, analysis has been limited to the measured flow series with no work being carried out using the synthetic flow series. These are referred to as the May 2018 loads in this report and superseded the January 2018 loads.

This report is based for the most part on the January 2018 electrical loads as this was the data available at the time of design development. Where possible, values pertaining to the May 2018 loads have been provided and have been labelled clearly. Where no clear labelling is provided, the data is related to the January 2018 electrical load profiles.

2.2.2 Reliability

The reliability of supply to the FRCGP and export grid is governed by the following requirements:

- The power supply to the FRCGP (i.e. combined reliability of the generating plant and water supply) must achieve 99.73% reliability. This is equivalent to the FRHEP being unavailable one day per year.
- The export grid aims for 99.5% supply reliability in the short term, which is equivalent to the required generating plant reliability.

- The system frequency must be controlled to ± 2 Hz even during extreme events. This requires the plant to operate reliably, including during unit trips, transmission line trips and trips and start-ups of the major loads.
- The FRHEP must be able to maintain reliable supply, even during periods of prolonged maintenance on the generating units, substation and conveyance system.

A Water Balance and Energy Model over the various phases of the project was developed. Throughout this section the term 'flow sequence' describes a continuous set of flows covering reservoir filling and 33 years of supply to the FRCGP and the export grid.

The model uses two different inflow datasets to assess the water supply reliability:

- The first is a series of daily measured flows covering 16 years. This dataset is repeated to produce a full sequence of inflows to be modelled covering 33 years of FRCGP operations plus reservoir filling. Using each year of measured data to initiate the sequence, a total of 16 sequences were run.
- Using the hidden Markov model, SRK developed a synthetic dataset that accounts for the possibility of more extreme inflows (both high and low flows) occurring. The result is 200 sequences with up to 38 years of data, to yield a total of 7,600 years of synthetic data.

The resulting generating plant reliability and water supply reliability over all years, including years of peak demand, are set out in Table 2-2 based on the January 2018 electrical load data.

Table 2-2: Reliability of power generation and water supply using the measured and synthetic inflow series

Flow sequence	Measured series - reliability over 16 sequences	Synthetic series - reliability over 200 sequences	Measured series - reliability over 16 sequences	Synthetic series - reliability over 200 sequences
Water supply reliability	Years 1–33 (All years)		Years 11–33 (Peak demand years)	
Average of all sequences	99.58%	98.52%	99.97%	98.06%
Worst sequence	98.99%	94.13%	99.81%	92.30%
Reliability of supply to the FRCGP	100.00%	100.00%	100.00%	100.00%
Generation reliability				
Generating plant reliability at peak load + one spinning reserve unit	99.98%		98.71%	
Generating plant reliability at normal load + one spinning reserve unit	100.00%		99.98%	
Overall plant reliability at all loads + one spinning reserve unit	100.00%		99.96%	

For both datasets, the measured and synthetic flow series, the required water supply and generating plant reliabilities are achieved. The water supply reliability is 100%, while the average generation reliability using the average synthetic flow series in Years 11–33 is 98.06%. The FRCGP reliability remains 100% which means that the 5.4% shortfall (54 GWh/a) is absorbed by the power made available to the export grid.

The water supply reliability using the synthetic flow series is on average 2% less than the measured flow series during the peak demand years (98.06% versus 99.97%). However, in the worst sequence

(i.e. lowest flows), the synthetic flow series produces 5%–7% less power than the measured flow series (92.30% versus 99.81%).

To ensure a robust and reliable power supply, the following are included in the current FRHEP design:

- Two 7.1 m diameter conveyance systems consisting of tunnels, steel penstocks, and surge chamber supply the powerstation are included, so that if one system is being drained, the second system can maintain full supply to the FRCGP. In this situation, the spinning reserve unit will not be available and supply to the export grid will be restricted.
- The power system has been designed to cope with units and transmission lines tripping without leading to cascading outages. A transient surge analysis of the conveyance system was undertaken and the results used to develop the governor settings for input to the Power Systems Study (undertaken by GHD). This confirmed that the proposed power system configuration is satisfactory under all contingent cases investigated.
- A less common 3-bus system has been recommended for the powerhouse substation, because this has the following advantages:
 - It enables power to be supplied to the FRCGP from one bus and to the remote export grid from a separate bus. This allows the governors in units supplying the FRCGP to be set to control frequency and those supplying the export grid to be set to a fixed output and only support the frequency of the export grid in the event of a significant frequency excursion.
 - If the two loads were supplied from a common bus, it would not possible to limit the demand from the export grid except by tripping the transmission lines, which could have negative consequences for end users. The Power System Study determined that from a power system strength standpoint, it is desirable to have the two loads interconnected. However, this does not take the need to for separate management of the loads and water supply into account. Effectively, the operators will allocate water to meet the long-term requirements of the FRCGP and export grid separately, taking the expected inflow and reservoir levels into account.
 - The third bus is a reserve bus that enables the generators to liven the very large transformers at the FRCGP and in the export grid that cannot be livened any other way. The 80 MVA load bank is also connected to this bus. The load bank is used to commission the generating plant prior to the FRCGP operations commencing and to test units after maintenance to boost availability in the longer term.

2.2.3 Early power

Considering the rate of inflow, coupled with the requirement for maintain residual flows, it is likely to take several years to fill the reservoir to Full Supply Level (FSL). To meet the FRCGP's initial power requirements, there is likely to be pressure to complete construction of the embankment and power generation infrastructure. In addition, geotechnical or logistical issues may lead to embankment construction delays. To address the delay in power generation, the FRHEP design enables early power to be provided prior to full completion of the embankment construction by throttling or closing the diversion tunnels, allowing the reservoir to commence filling earlier.

There are two strategies for achieving the earliest possible date of first power generation:

- Provide a lower intake to meet the low initial demand from the FRCGP
- Commence filling the reservoir before the embankment construction is complete or the spillway is commissioned.

The lower intake accelerates the time to first power. Table 2-3 details the following four cases:

- Time to normal minimum operating level with upper intake
- Time to normal minimum operating level with upper intake plus early filling – this case has the same timings as the previous case because both cases require the full embankment height to be reached before filling can commence (i.e. the upper intake offers no benefit in terms of first power)
- Time to normal minimum operating level with lower intake
- Time to normal minimum operating level with lower intake plus early filling.

The provision of the lower intake reduces the time to first power to FRCGP by an average of 473 days and the early filling reduces it by a further 47 days, i.e. the combined total benefit is 520 days. The first power to the export grid is reduced by an average of 149 days and in combination with early filling, it is reduced by a further 47 days, i.e. the total combined benefit is 196 days.

Table 2-3: Effect of early filling and lower intake on time to first power

Filling case	Time to normal minimum operating level with upper intake (days)	Time to normal minimum operating level with upper intake plus early filling (days)	Time to normal minimum operating level with lower intake (days)	Time to normal minimum operating level with lower intake plus early filling (days)
First power to FRCGP				
Average	757	757	284	237
Earliest	680	680	227	180
Latest	853	853	422	375
First power to export grid				
Average	940	940	791	744
Earliest	808	808	636	589
Latest	1,085	1,085	954	907

Table 2-4 shows that the synthetic flow series and measured flow series produce very similar average time to first power (FRCGP and export grid).

Table 2-4: Time to first power - measured vs synthetic flow series

Time to first power	Supply to FRCGP (days)		Supply to export grid (days)	
	Measured flow series	Synthetic flow series	Measured flow series	Synthetic flow series
Average	237	246	744	773
Earliest	180	172	589	583
Longest	375	441	907	1,329
Standard deviation	52	48	82	134

Based on this analysis, the following conclusions are drawn:

- The two strategies for achieving early power are complementary.
- To protect against overtopping during early filling, a storm buffer volume of almost 1,100 Mm³ is required. This is almost equivalent to the 48-hour PMF volume of 1,130 Mm³ and is 79% of the 72-hour PMF inflow volume of 1,386 Mm³.
- The storm buffer volume and bypass valve capacity have been calculated using the 7,600 years of synthetic data to identify the worst-case inflows. An 8-day event was identified as the design case.

- The dam crest must reach RL 151.5 m before filling can commence to ensure the storm buffer volume is available and that a 6-month construction delay can be absorbed.
- A bypass valve capacity of 498 m³/s is required. This is provided by four Howell-Bunger bypass valves (2.3 m diameter) located at the powerhouse, installed in pairs connected to each conveyance system.
- The lower intake reduces time to first power at FRCGP by an average of ~15 months, while early filling expedites time to first power by an average of 7 weeks. The assumptions concerning the embankment height prior to commencement of filling may be found to be too conservative in the next phase of the project. If this is the case, or if the embankment construction is significantly delayed, the benefits of early filling could be substantially greater.

Alternatives to the use of bypass valves were considered, but were eliminated following the MAA. The bypass valves are not impeded by sediment and tailings potentially blocking the intake, and have several functions:

- They provide protection against overtopping during early filling.
- They allow high flows to be passed once the water level has reached the lower intake to allow large items for construction purposes to be transported up the river.
- During the next phase of the project, it may be determined that the bypass valves can act as pressure limiting valves. This allows the wicket gates of the turbines to move faster and a faster load response at lower water levels, reducing the need to apply load shedding in the event of unit trips.
- The valves can supplement the spillway. At the dam's maximum operating level, the valves can pass 704 m³/s compared with 800 m³/s through a single spillway gate. The bypass valves improve the reliability of the spillway. The valves can also be used to pass lower flows, which may reduce operating costs.
- The valves can assist in lowering the water level in the event of seismic damage to one or all of the spillway gates, a major spillway blockage, or if the reservoir level needs to be dropped to below the spillway crest. This is a significant advantage.

2.3 Tailings and waste rock deposition

The tailings will be deposited subaqueously from pipelines floating on the reservoir surface. The waste rock will be dumped via barges trafficking on the reservoir surface.

2.3.1 Production

FRL supplied tailings and waste rock tonnages for the LOM listed in Table 2-5. The waste disposal strategy accommodates the tailings and waste rock production without sterilising opportunities for future expansion, and without contributing to slumping caused by waves that could affect the embankment.

Table 2-5: LOM tailings and waste production

Criteria	Value	Source
LOM tailings tonnage	1.49 Bt (1.09 Bm ³)	Tonnage: Mine Schedule, 19 January 2018 Volume: FRHEP stage capacity RevG-1.5
LOM waste tonnage	1.56 Bt (1.04 Bm ³)	
LOM period	33 years	Mine Schedule, 19 January 2018

2.3.2 Properties

Tailings geotechnical properties

Tailings geotechnical properties assumed for the FRHEP design are summarised in Table 2-6. The tailings has a low liquid limit and low plasticity index and classifies as low plasticity silt (ML), as shown in Figure 2-2 and Table 2-7.

Table 2-6: Key assumptions – tailings geotechnical properties

Criteria	Value	Source/ comment
Dry density		Overall average densities estimated from testing undertaken as part of SRK 2011
Years 1–2	1.1 t/m ³	
Year 3	1.2 t/m ³	
Year 4	1.3 t/m ³	
Years 5–33	1.4 t/m ³	
Permeability	1 × 10 ⁻⁷ m/s	
Beach slope (subaqueous)	1%	Assumed
Discharge solids concentration (end-of-pipe discharge) (Thickened)	55%–60% w/w	FRL ⁹ - SRK selected 55%
Particle size distribution (PSD)	As in Figure 2-2	SRK 2011

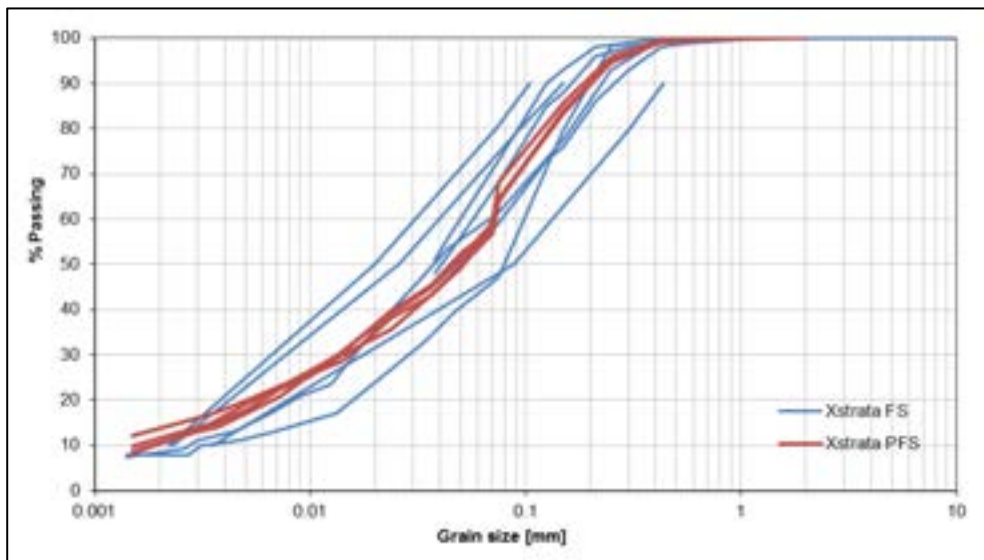


Figure 2-2: Tailings particle size distribution

Table 2-7: Tailings material properties

Tailings sample	Specific gravity (SG)	Atterberg Limits			USCS*
		Liquid Limit (LL)	Plastic Limit (PL)	Plasticity Index (PI)	
Primary Final Tails P-8	2.77	21	18	3	ML
Primary Final Tails P-13&14	2.82	21	18	3	ML
Primary Final Tails P-16	2.79	22	18	4	ML
Primary Final Tails Composite	2.84	22	18	4	ML

*USCS = Unified Soil Classification System

⁹ Email – FRL (Mick Hawkins) 08/05/2018

Falling head permeability testing was conducted on the tailings samples compacted to 1.5 t/m³. The hydraulic conductivity of the material varied from 4.3 × 10⁻⁸ m/s to 1.5 × 10⁻⁷ m/s, with an average of 1.0 × 10⁻⁷ m/s. Results of the undrained settling tests for tailings are shown in Table 2-8.

Table 2-8: Tailings undrained settling test results

Material	SG	Solids (% w/w)	Slurry dry density (t/m ³)	Final moisture (%w/w)	Dry density (t/m ³)
Primary Final Tails P-8	2.77	60.10	0.97	38.60%	1.32
Primary Final Tails P-13&14	2.82	46.50	0.66	45.70%	1.2
Primary Final Tails P-16	2.79	42.60	0.6	44.50%	1.12
Primary Final Tails Composite	2.84	57.40	0.91	38.60%	1.35

Consolidation testing and both drained and undrained settling tests were performed on the tailings samples. To calculate the average consolidated dry density, the average stress applied to achieve a certain void ratio/ dry density was related to a depth within the deposited tailings using the calculated saturated density. A graph of the results is shown in Figure 2-3.

An average tailings dry density of 1.1 t/m³ was selected as input to volume calculations for the first two years of production, with a gradual increase (by Year 5) to 1.4 t/m³. The lower density for the initial period was adopted to allow for the effect of higher rates of rise on consolidation.

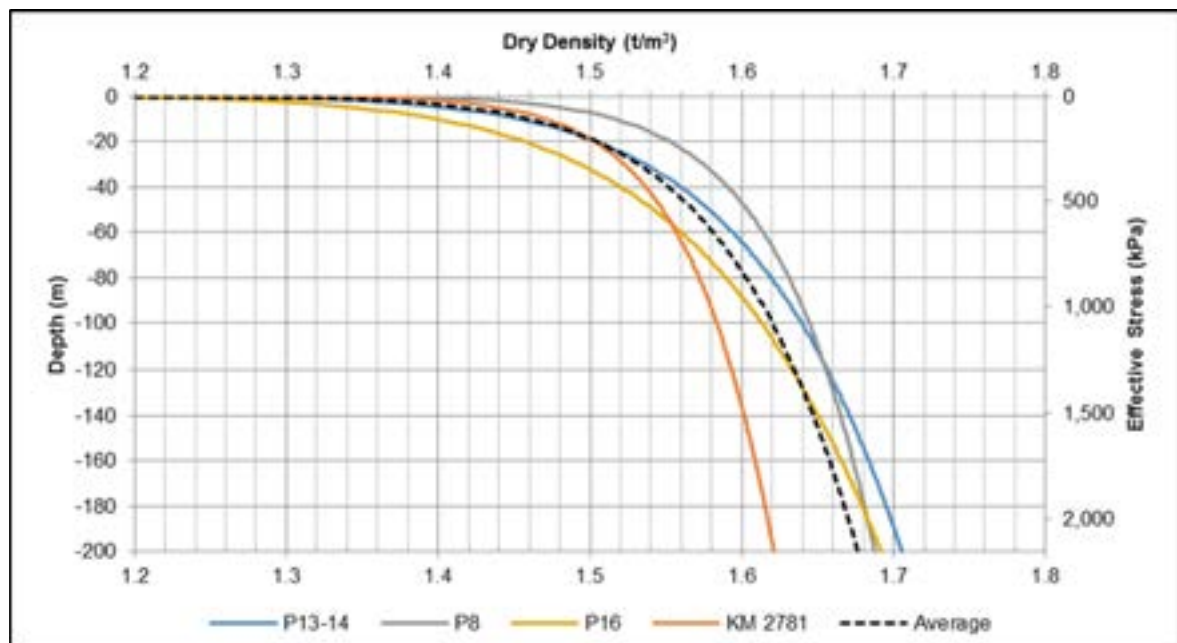


Figure 2-3: Predicted dry density variation with depth within the tailings deposit

Waste rock geotechnical properties

Once the water level reaches the headwaters of the reservoir and the barge facility is operational, the waste rock will be barge-dumped into the reservoir. The waste rock material will be crushed and transported by trucks or a conveyor to a barge loader, then dumped from the barges. This deposition method could result in relatively low bulk density, especially in the initial soft, soil-like waste.

The waste rock geotechnical properties assumed for the FRHEP design are shown in Table 2-9.

Table 2-9: Key assumptions – waste rock geotechnical properties

Criteria	Value	Source/ comment
Dry density: Years 0–33	1.5 t/m ³	Average consolidated density estimated from testing undertaken as part of SRK 2011
SG	2.6	FRL ¹⁰
Subaqueous beach slope	0.1%–10%	Assumed – average 5%
PSD	As in Figure 2-4	SRK 2011

The PSD and material properties of the waste rock samples tested are summarised in Figure 2-4 and Table 2-10. PSDs are not representative of the waste to be dumped in the reservoir as the material would only undergo primary crushing, resulting in material sizes of up to 300 mm. The PSD of this material has not been supplied to SRK.

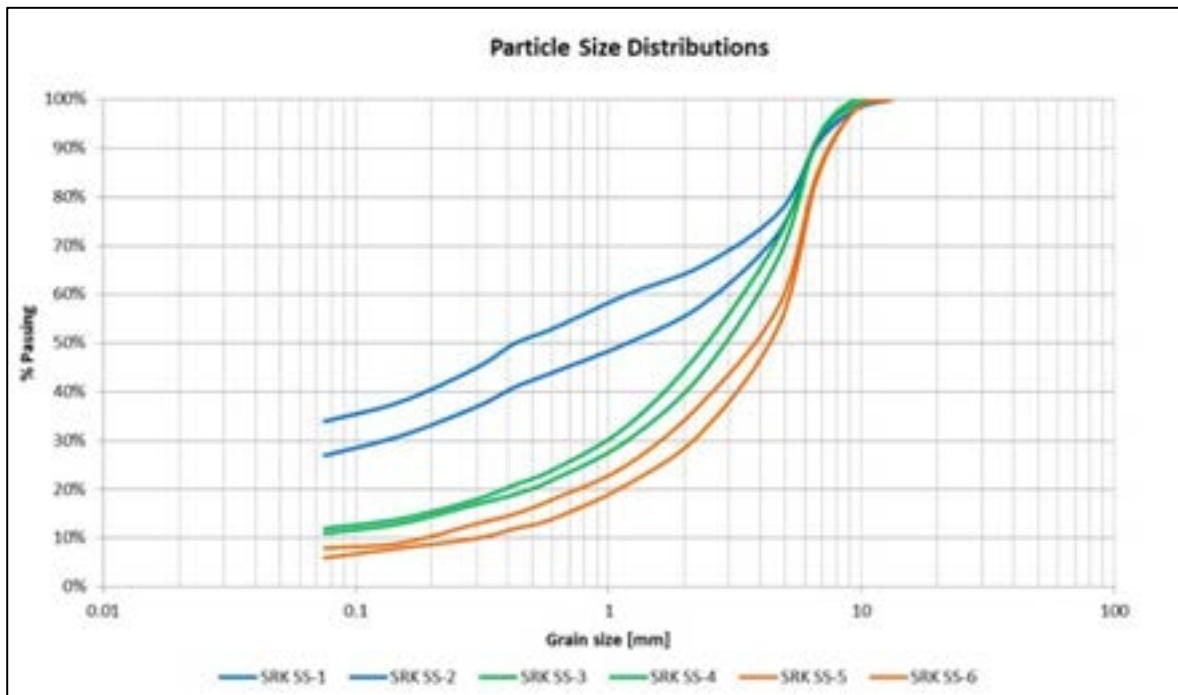


Figure 2-4: Particle size distributions – waste rock samples

Table 2-10: Waste rock material properties

Waste rock sample	Material type	SG	Atterberg Limits		
			LL	PL	PI
SRK SS-1	Soil/ gravel	2.77	32	26	6
SRK SS-2		2.75	33	26	7
SRK SS-3	High fracture/ low durability rock	2.8	23	19	4
SRK SS-4		2.88	23	18	5
SRK SS-5	Low fracture/ higher durability rock	2.85	20	17	3
SRK SS-6		2.84	21	17	4

The results of the settling tests indicate the initial settled densities shown in Table 2-11. Rowe cell testing results are shown in Figure 2-5. Using the average depth of the waste rock, an average

¹⁰ Email – FRL (Edward Chong) 03/11/2017

consolidated dry density of 1.5 t/m³ was estimated. The actual consolidated density may be higher if the Rowe cell testing was affected by the small particle size of the crushed waste rock. For volume calculations, an average design dry density of 1.5 t/m³ for the waste rock was used.

Table 2-11: Waste rock – undrained settling test results

Sample ID	SG	Deposition 1			Deposition 2		
		Dry density (t/m ³)	Void ratio, e	Moisture content, ω	Dry density (t/m ³)	Void ratio, e	Moisture content, ω
SRK SS-1	2.77	1.06	1.61	0.58	1.25	1.22	0.44
SRK SS-2	2.75	1.02	1.70	0.62	1.14	1.41	0.51
SRK SS-3	2.8	1.24	1.26	0.45	1.33	1.11	0.39
SRK SS-4	2.88	1.22	1.36	0.47	1.34	1.15	0.40
SRK SS-5	2.85	1.32	1.16	0.41	1.37	1.08	0.38
SRK SS-6	2.84	1.33	1.14	0.40	1.39	1.04	0.37

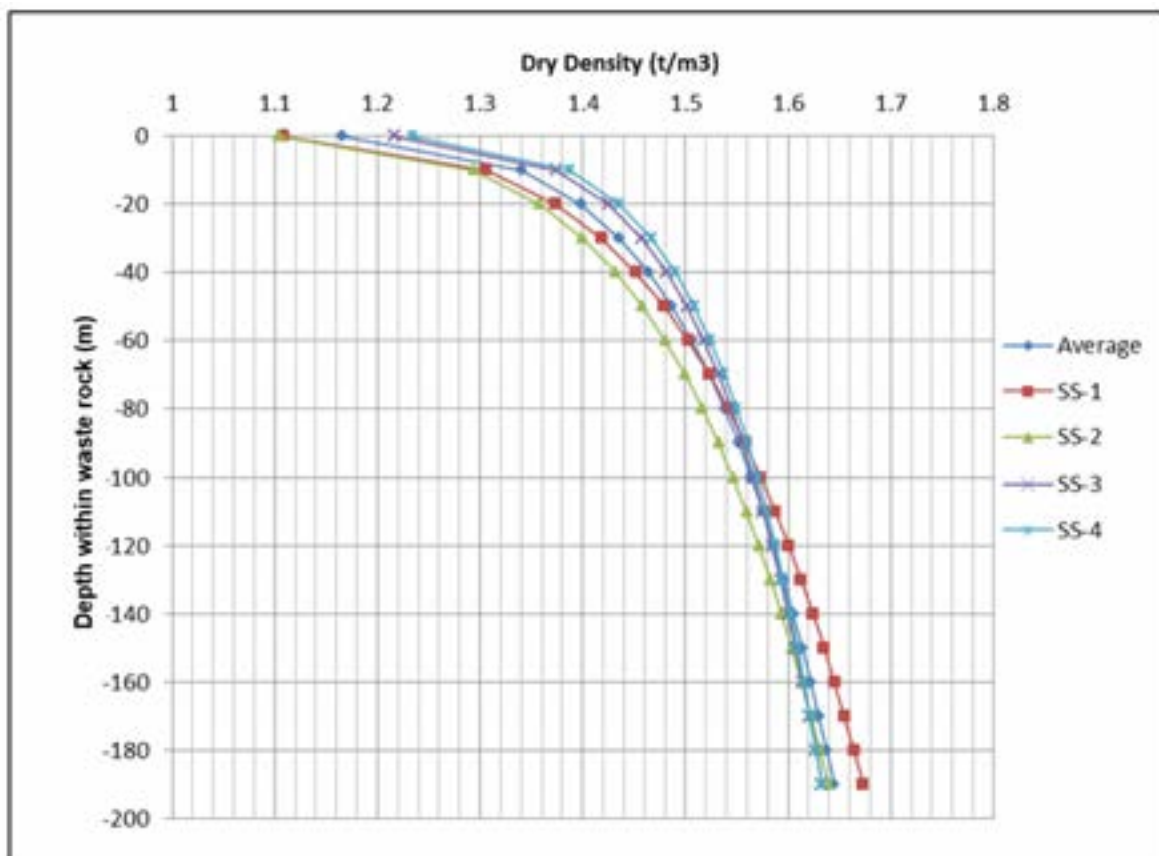


Figure 2-5: Predicted dry density variation with depth of waste rock deposition

Tailings geochemistry

Static testing of combined tailings has consistently shown the tailings to be potentially acid forming (PAF). Kinetic tests for samples of combined tailings from the metallurgical pilot plant indicated that drying of the combined tailings could lead to mildly acidic conditions and release of elevated copper concentrations. The lag time for the onset of acid generation is 12–19 weeks. However, copper could commence leaching at significant concentrations in as little as seven weeks, and the onset of even mildly acidic conditions leads to release of elevated concentrations of copper and other metals.

The results of geochemical testing indicates that deposition of the combined tailings and/ or the formation of tailings beaches in the air could lead to significant release of metals which supports the subaqueous disposal strategy.

Waste rock geochemistry

The static testing of representative waste rock samples shows that the vast majority of the waste rock is expected to have elevated sulphide mineralisation and would be PAF. Kinetic testing indicated short lag times, with some samples generating acidic leachates at the start of testing, whereas other samples exhibited a lag time of 4–6 weeks. The acidic leachates contained elevated concentrations of metals – in particular aluminium, copper and iron. The waste rock classification developed for the mined materials indicates that more than 69% of the material will classify as PAF and fall in the High Red category (based on a sulphur content of > 3%) and will exhibit very short, if any, lag time to the onset of acid generation.

The strongly acid-generating nature of the waste rock means that oxidation should be prevented to the extent possible. Subaqueous waste disposal and storage is the only proven method for meeting this objective.

2.3.3 Deposition strategy

The objective of the tailings and waste rock deposition strategy is to deposit as close to the process plant as possible, without introducing significant environmental risks.

Significant underwater slopes could fail under static or dynamic (earthquake) conditions, with the resulting material displacement causing a collapse slump and associated water displacement (wave). Tailings and waste rock disposal will require careful management so that large underwater slopes do not form.

2.3.4 Storage capacity

The volumes for storage of tailings, waste rock and sediment generated over the LOM are shown in Figure 2-6. These estimates were developed using the 19 January 2018 waste rock and ore processing schedules provided by FRL, and the design dry densities shown in Table 2-12, Table 2-6 and Table 2-9. The total estimated storage volume is 2.17 Bm³ (1.09 Bm³ of tailings, 1.04 Bm³ of waste rock and 39.7 Mm³ of sediment). The storage capacity of 3.3 Bm³ available below the recommended maximum tailings and waste rock storage level was determined by the findings of the limnology study. However, only part of this storage capacity should be used to minimise remobilisation of sediments.

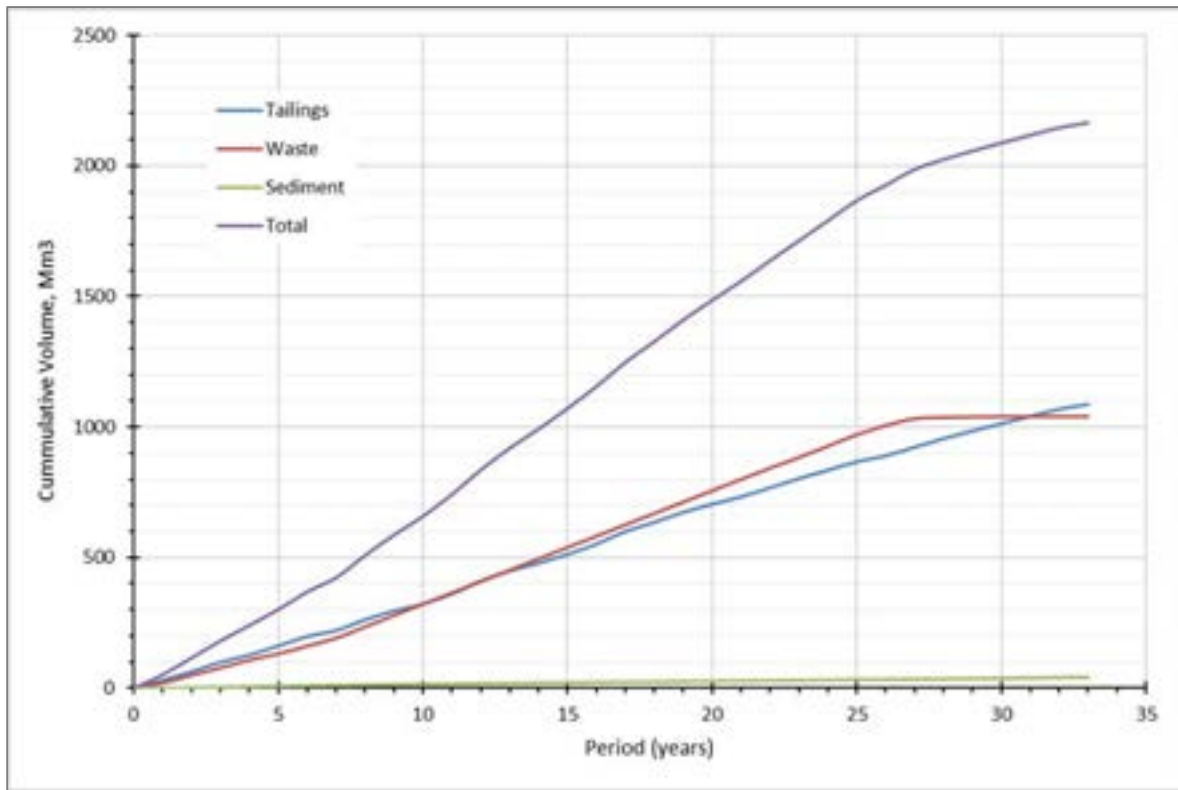


Figure 2-6: Tailings, sediment and waste rock volumes generated over the LOM (years)

Table 2-12: Design dry density - sediment

Material	Value	Units	Year
Sediment	1.1	t/m ³	Average

A storage capacity curve was developed using Rift TD software and LiDAR site topography at a 10 m digital elevation model (DEM) survey grid. Figure 2-7 illustrates the cumulative capacity and surface area of the FRHEP reservoir up to RL 300 m.

Storage in the FRHEP reservoir is broadly divided into three compartments: the upper Ok Binai compartment, the Nena/ Lower Ok Binai compartment and the Frieda compartment. Storage capacities for each of these compartments and the combined total storage at a crest elevation of RL 238.5 m are shown in Table 2-13 and correlate to the footprints within the reservoir shown in Figure 2-8.

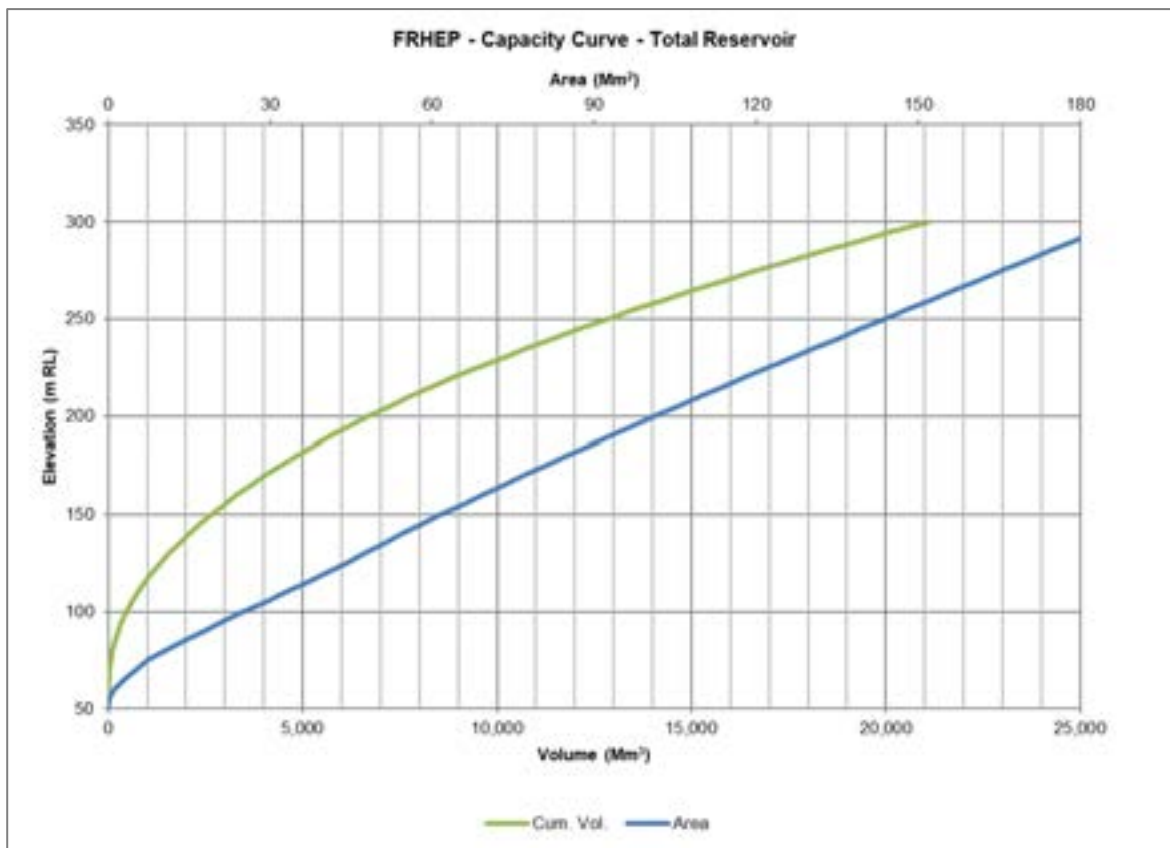


Figure 2-7: FRHEP storage capacity curve

Table 2-13: FRHEP reservoir storage capacities

Compartment	Approximate capacity at MOL of RL 226.1 m (Bm³)
Upper Ok Binai	0.8
Nena/ Lower Ok Binai	2.0
Frieda	6.8
Combined total FRHEP reservoir	9.6

MOL = maximum operating level

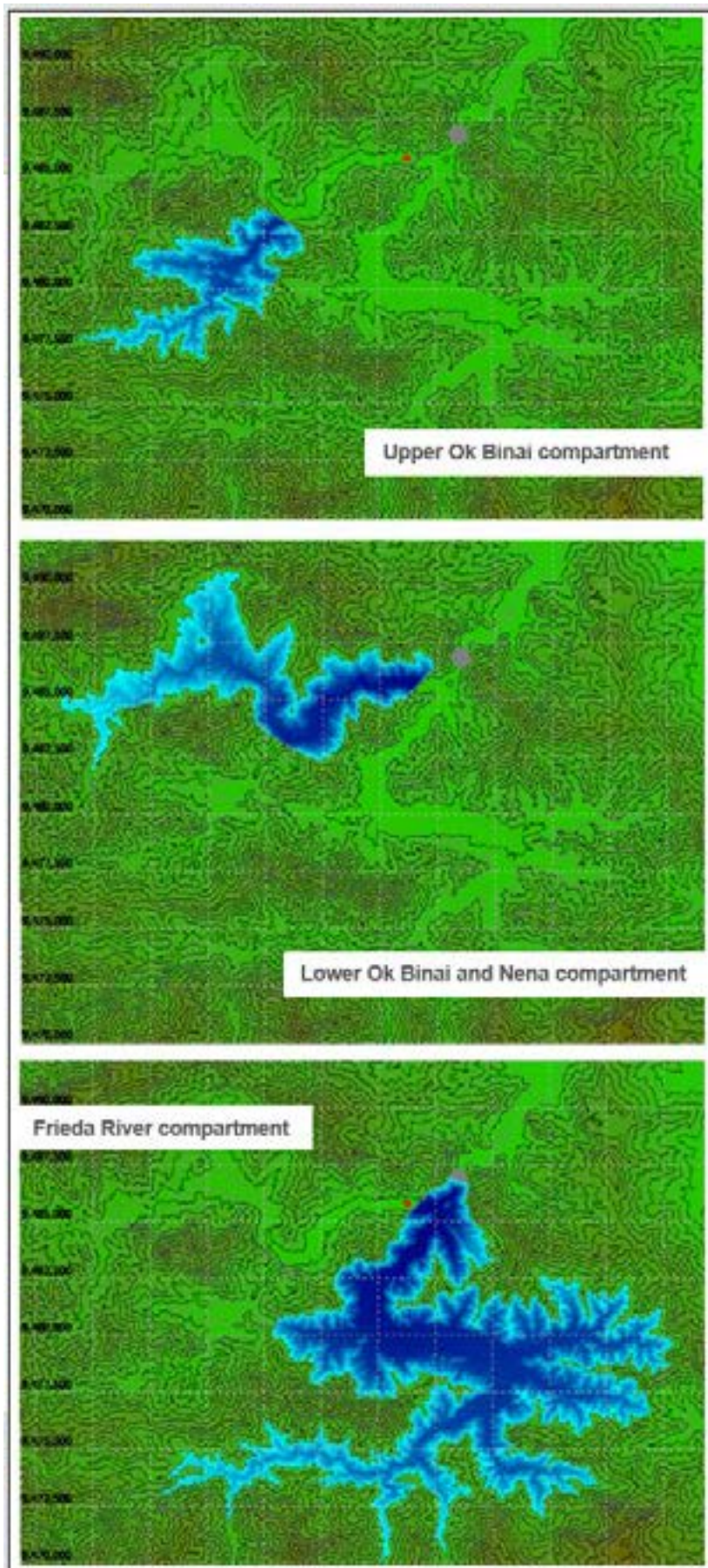


Figure 2-8: Footprints of the three compartments within the FRHEP

2.4 Design framework

2.4.1 Standards

The codes, standards and guidelines applicable to the FRHEP SPS design include, but are not limited to, the following:

- PNG Acts and Regulations:
 - *PNG Environmental Act (2000)*
 - *PNG Environmental Permits and Transitions Regulation (2002)*
 - *PNG Environmental Prescribed Activities Regulation (2002)*
 - *PNG Environmental Water Quality Criteria Regulation (2002)*.
- ANCOLD Guidelines:
 - Guideline for Design of Dams for Earthquakes (August 1998)
 - Guidelines on Tailings Dams – Planning, Design, Construction, Operation and Closure (May 2012)
 - Guidelines on Selection of Acceptable Flood Capacity for Dams (March 2000)
 - Guidelines on the Consequence Categories for Dams (October 2012)
 - Guidelines on the Environmental Management of Dams (January 2001)
 - Guidelines on Dam Safety Management (August 2003)
 - Guidelines on Risk Assessment (October 2003).
- ICOLD Guidelines:
 - Bulletin 156-2010: Integrated Flood Risk Management
 - Bulletin 151-2009: Tropical Residual Soils as Dam Foundation and Fill Material
 - Bulletin 150-2009: Cut-offs for Large Dams
 - Bulletin 148-2010: Selecting Seismic Parameters for Large Dams
 - Bulletin 147-2009: Sedimentation and Sustainable Use of Reservoirs and River Systems
 - Bulletin 141-2010: Concrete Face Rockfill Dams – Concepts of Design and Construction
 - Bulletin 140-2007: Mathematical Modelling of Sediment Transport and Deposition in Reservoirs
 - Bulletin 139-2011: Improving Tailings Dams safety
 - Bulletin 135-2010: Geomembrane Sealing Systems for Dams
 - Bulletin 130-2005: Risk Assessment in Dam Safety Management. A reconnaissance of Benefits. Methods and Current Applications
 - Bulletin 129-2005: Dam Foundations. Geologic considerations. Investigation methods. Treatment. Monitoring
 - Bulletin 125-2003: Dams and Floods – Guidelines and Case Examples
 - Bulletin 124-2002: Reservoir landslides: investigation and management – Guidelines and case histories
 - Bulletin 123-2002: Seismic design and evaluation of structures appurtenant to dams
 - Bulletin 121-2001: Tailings dams risk of dangerous occurrences – Lessons learnt from practical experiences
 - Bulletin 120-2001: Design features of dams to resist seismic ground motion
 - Bulletin 111-1998: Dam Break flood analysis – Review and recommendations

- Bulletin 106-1996: A guide to Tailings Dams and impoundments – Design, construction, use and rehabilitation
- Bulletin 098-1995: Tailings Dams and Seismicity – Review and Recommendations
- Bulletin 095-1994: Embankment dams – Granular filters and drains
- Bulletin 092-1993: Rock materials for rockfill dams – Review and recommendations
- Bulletin 084-1992: Bituminous cores for fill dams
- Bulletin 082-1992: Selection of design flood – Current methods
- Bulletin 078-1991: Watertight geomembranes for dams – State of the art
- Bulletin 072-1989: Selecting seismic parameters for large dams – Guidelines
- Bulletin 056-1986: Quality control for fill dams
- Bulletin 055-1986: Geotextiles as filters and transitions in fill dams
- Bulletin 048-1986: River control during dam construction.
- Canadian Dam Association (CDA) Guidelines:
 - Dam Safety Guidelines (2007)
 - Application of Dam Safety Guidelines to Mining Dams (2014).
- International Finance Corporation:
 - Environment, Health and Safety Guidelines for Mining (December 2007).
- United States Army Corp of Engineers (USACE) Engineering documents
 - ER 1110-2-1806: Earthquake Design and Evaluation for Civil Works Projects
 - ER 1110-2-1150: Engineering and Design for Civil Works Projects
 - EM 1110-2-2100: Stability Analysis of Concrete Structures
 - EM 1110-2-2104: Strength Design for Reinforced Concrete Hydraulic Structures
 - ETL 1110-2-584: Design of Hydraulic Steel Structures
 - EM 1110-2-2400: Structural Design and Evaluation of Outlet Works
 - EM 1110-2-6050: Response Spectra and Seismic Analysis for Concrete Hydraulic Structures
 - EM 1110-2-6053: Earthquake Design and Evaluation of Concrete Hydraulic Structures
- American Society of Mechanical Engineers
 - ASME B31.3 Process Pressure Piping
- Institute of Electrical and Electronics Engineers (IEEE)
 - All electrical components, and mechanical as appropriate, to be designed in accordance with IEEE standards.

2.4.2 Dam classification and design criteria

Dam consequence categories are derived from the potential failure modes of the facility and the resulting consequences to the business, social and natural environment, and the potential for loss of life, as shown in Table 2-14 (reproduced from ANCOLD, 2012¹¹). The classification has implications on selection of the design storm storage allowance and water management structures, as well as types and frequencies of monitoring and inspections required.

SRK¹² undertook a dam break analysis to inform the design in terms of risks associated with the FRHEP, develop inundation maps of potential flood extents and estimate flow at critical locations

¹¹ ANCOLD 2012, Guidelines on the Consequence Categories for Dams

¹² SRK 2018, Frieda River Hydroelectric Project Dam Break Analysis

downstream of the FRHEP in the event of an embankment failure. The results indicated that the consequences of a dam break are potentially catastrophic.

The FRHEP is assigned an 'Extreme' consequence category as shown in Table 2-14.

Table 2-14: Consequence category

Population at Risk	Severity of Damage and Loss			
	Minor	Medium	Major	Catastrophic
<1	Very Low	Low	Significant	High C
≥1 to <10	Significant	Significant	High C	High B
≥10 to <100	High C	High C	High B	High A
≥100 to <1,000	-	High B	High A	Extreme
≥1,000	-	-	Extreme	Extreme

Source: ANCOLD, 2012. Guidelines on the Consequence Categories for Dams.

2.4.3 Embankment height

The ICOLD (July 2011) definition for dam height is defined as the height between the lowest general foundation and the embankment crest on the downstream side of the embankment. The embankment crest will be at an elevation of RL 238.5 m. The elevation of the lowest level in the riverbed at the downstream toe of the embankment is assumed to be RL 48 m, resulting in an embankment height of 190.5 m.

2.5 Geotechnical and civil

2.5.1 Topography

The topographical survey data was sourced from a LiDAR survey carried out at an elevation of ~RL 240 m (Figure 2-9). The LiDAR was obtained in 2008 by AAMHatch and authenticated by geodetic survey in 2009 by Quickclose Pty Ltd. Any topography beyond this elevation was sourced from SRTM (Shuttle Radar Topography Mission).

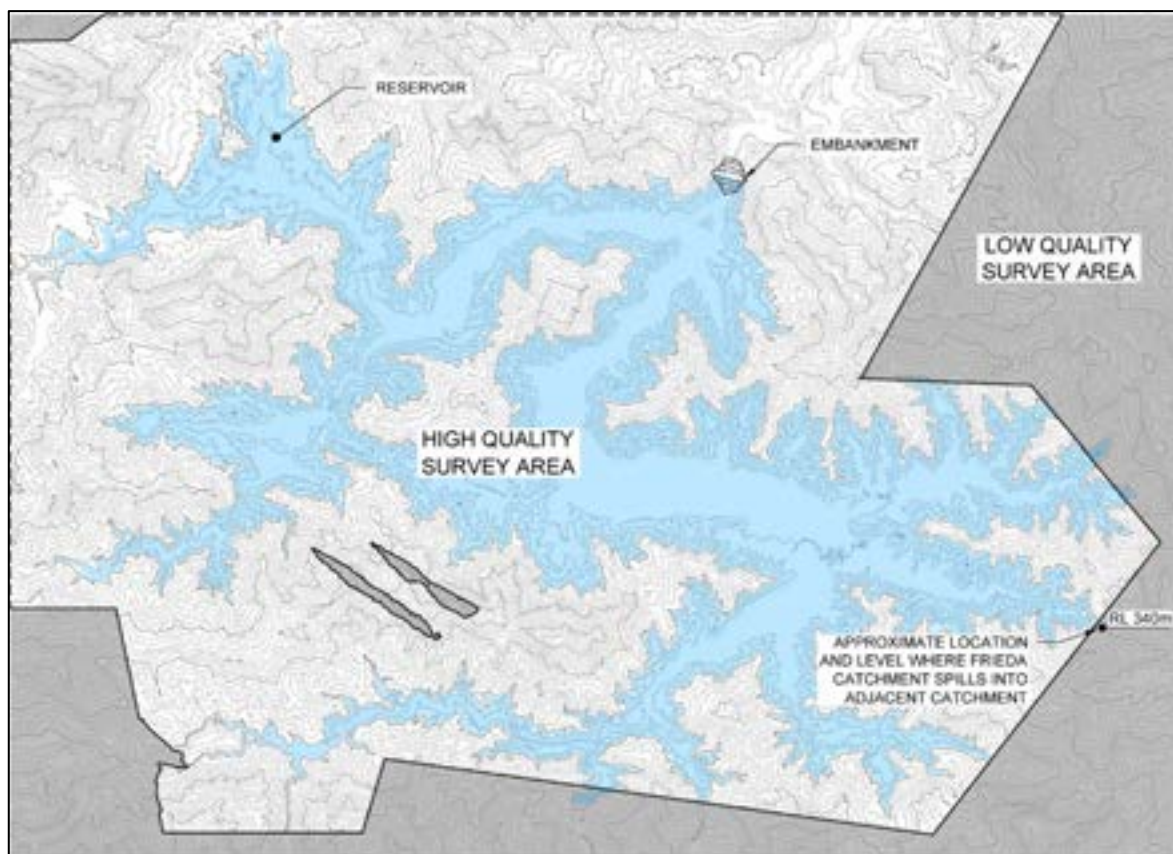


Figure 2-9: Extent of LiDAR survey (black lines)

2.5.2 Seismicity

Regional tectonic setting and seismicity

Papua New Guinea is located on the Pacific 'Rim of Fire' and is influenced by the interactive tectonic boundary between the Indo-Australian Plate to the south and the oceanic Pacific Plate to the north as shown in Figure 2-10. This tectonic boundary occurs as a complex arrangement of active subduction zones and associated island arcs extending east and south through the Solomon Islands, Vanuatu and Fiji to New Zealand, and west into Indonesia, the Philippines and Japan¹³.

¹³ Williamson and Hancock, 2005. The geology and mineral potential of Papua New Guinea: Papua New Guinea Department of Mining

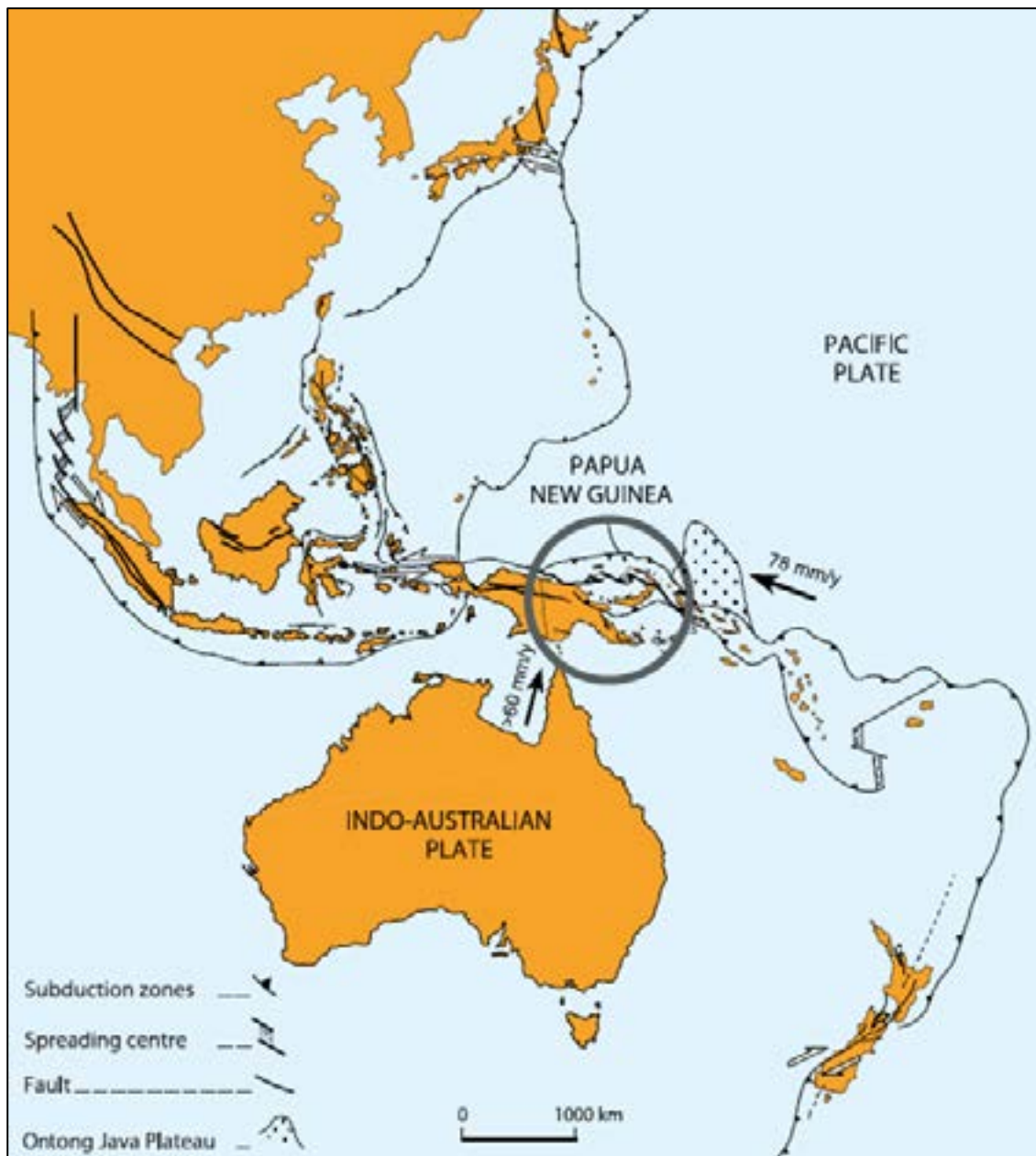


Figure 2-10: Major geological elements of South East Asia and Australia¹³

Western PNG is divided into four tectonic regions; from north to south, these are:

- 1 The belt of former island arcs, which is the northern rim of PNG including the Bewani-Torricelli and Finisterre Terrane.
- 2 New Guinea Thrust Belt, which includes low-angle thrusting, left-lateral strike-slip structures, and some Cretaceous active volcanism. The FRHEP is in this belt, adjacent to the southern boundary.
- 3 Papuan Fold Belt, which comprises the Australian continental crust deformed into fold and thrust structures.
- 4 Fly Platform/ Stable Plate/ foreland basin, which is the northern continuation of Australian continental crust.

Major fault zones separate the provinces described above. The Ramu-Markham Fault separates the Bewani-Torricelli and Finisterre Terrane from the New Guinea Thrust Belt; the New Guinea Thrust splits the New Guinea Thrust Belt from the Papuan Fold Belt; and the Papuan Thrust divides the Papuan Fold Belt from the Fly Platform.

A major subduction zone, the New Guinea Trench (NGT) underlies the western part of PNG. Most authors suggest this is a southwest dipping structure¹⁴. Recent studies on the seismic tomography for the subduction plate associated with the NGT indicated a dip angle between 10° and 30° to the southwest¹⁵.

PNG is in a very active seismic region; each year between 10 and 12 earthquakes with magnitude 6 or more and one of magnitude 7 or more occur¹⁶. A total of eight earthquakes with a magnitude of 7 or greater have occurred in the country since 1998¹⁷.

The Frieda River area is dominated by a series of E–W to ENE–WSW oriented fault systems. From north to south, these are the Saniap Fault, the Frieda Fault, the Fiak-Leonard Schultz (Fiak) Fault, and the Trangiso, Stolle and Figi faults. The latter three are sometimes grouped together as the Lagaip Fault¹³. These faults are all part of the New Guinea Thrust Fault Zone.

Design seismic parameters - Embankment

For an 'Extreme' consequence dam, both the ANCOLD and CDA guidelines recommend the use of the MCE as the design basis. Seismic parameters for use in simulating MCE effects were estimated for the location of the Nena River ISF in 2016, and Ok Binai in 2011. Both locations are shown in Figure 2-12.

During the Nena ISF project in 2016, SRK commissioned Al Atik & Gregor to update the design seismic parameters, including:

- Updating the probabilistic seismic hazard analysis (PSHA) for the Nena ISF using the British Columbia (BC) Hydro Ground Motion Prediction Equations (GMPEs) to determine subduction zone seismic contribution
- Undertaking a deterministic seismic hazard analysis for the Nena ISF site including adding the Frieda Fault, a south dipping thrust fault (Figure 2-12), and using the NGA-West2 GMPEs to determine the seismic contribution of crustal faults
- Using site-specific estimated shear wave velocity (V_{S30}) of 760 m/s and 1,150 m/s for the foundations.

The design location for the FRHEP is further from the Frieda Fault than the two previous locations, but closer to the Saniap Fault (Figure 2-11). However, it was agreed between FRL and SRK that the results of the seismic study performed for the Nena ISF would be applied to the new site in this SPS. The assumption was that any differences would be small enough to obtain a design within the SPS cost accuracy required by FRL. This assumption and the underlying seismic design parameters will need to be confirmed in later stages of engineering design.

¹⁴ Bechtel Australia Pty Ltd, 2010. Probabilistic Seismic Hazard Analysis and Development of Design Spectra; Document Number 25534-0FS-30R-K01-00001, November 1, 2010.

¹⁵ Tregoning and Gorbatov, 2004. Evidence for active subduction at the New Guinea Trench, *Geophysical Research Letters*, Vol 31, L13608, pp. 1-4.

¹⁶ SKM, Pöyry, SMEC, 2010. Seismotectonics of Papua New Guinea and in the Project Area, part of Frieda River Power Generation Extended Pre-Feasibility Study, Document No: FRP02-2200-EC-RP-0003, 11 Feb 2010.

¹⁷ USGS National Earthquake Information Center, 2011. Historic Earthquake Locations – Papua New Guinea, website: http://neic.usgs.gov/neis/eq_depot/2002/eq_020908/neic_ivay_h.html

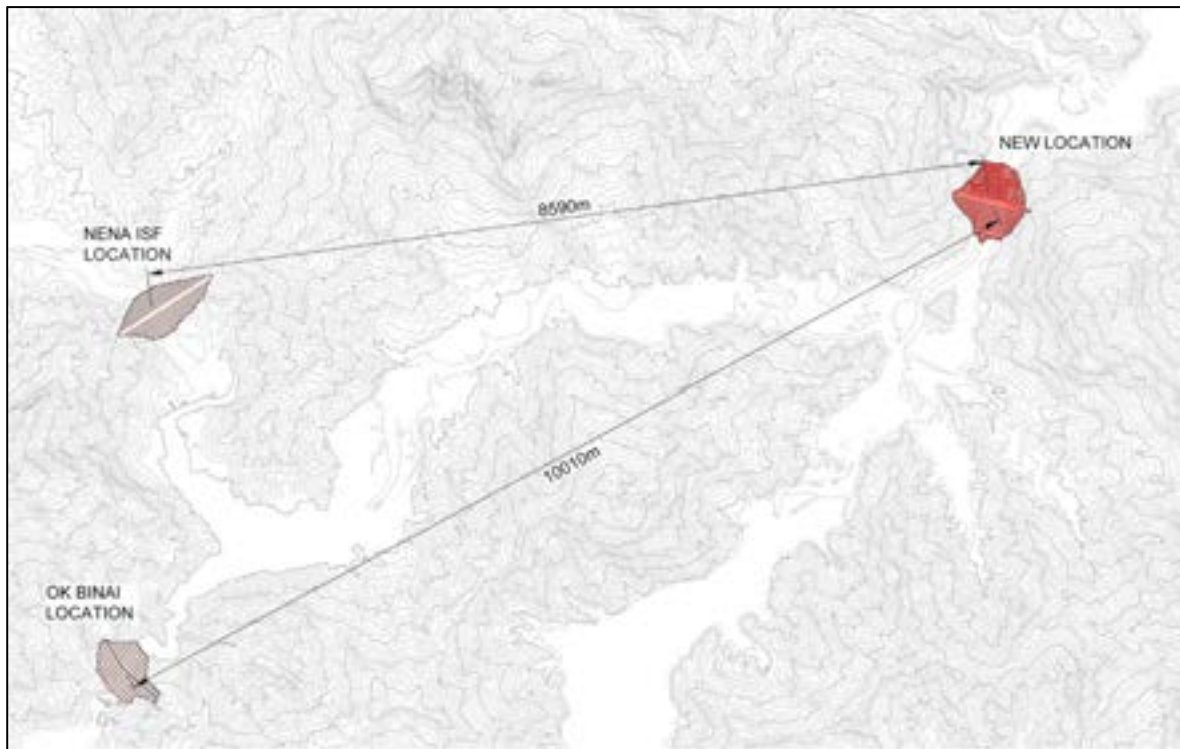


Figure 2-11: Comparison of FRHEP distance to the Nena ISF embankment locations

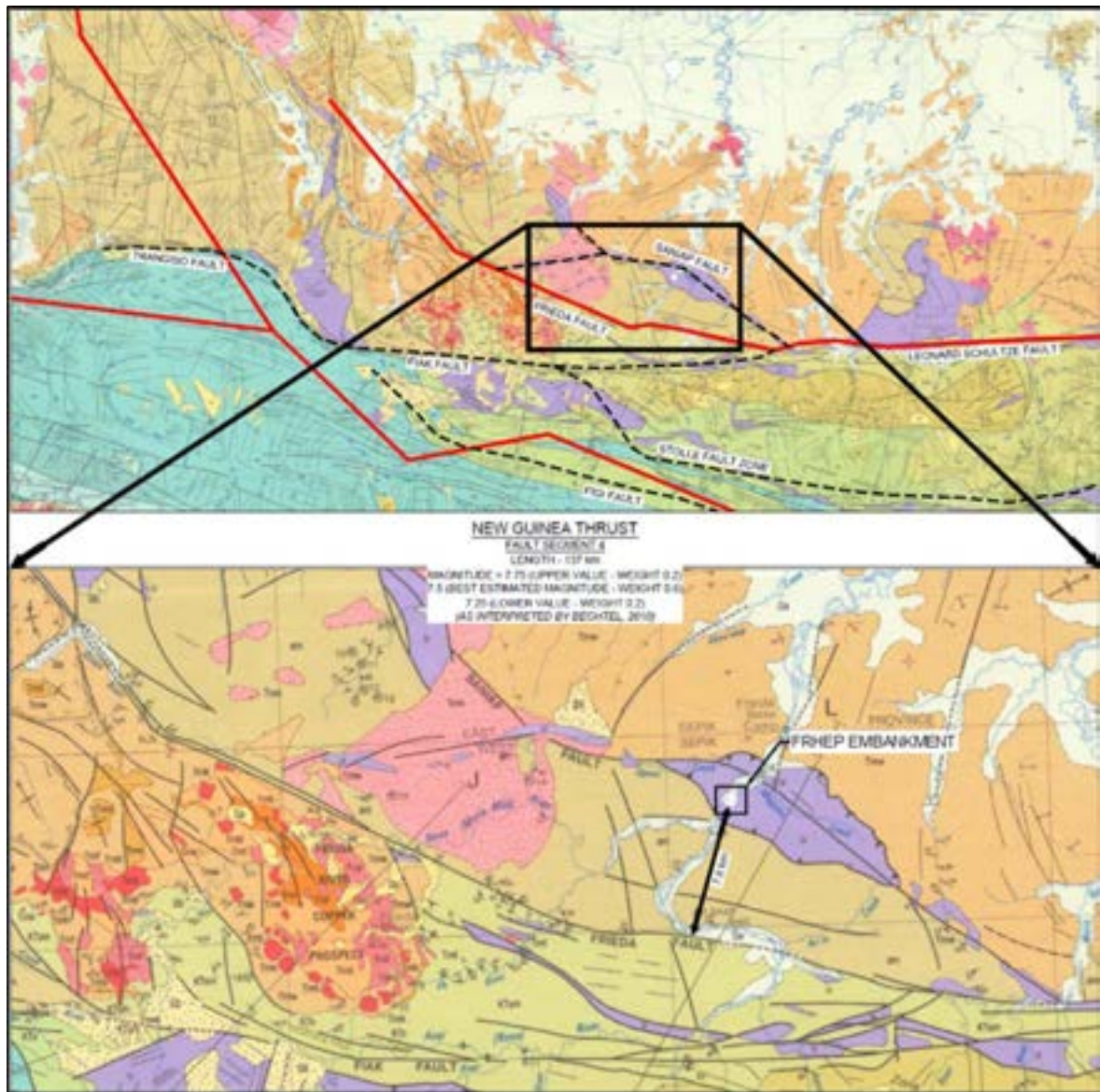


Figure 2-12: Regional geology of the Nena ISF site

SRK assessed the subsurface site conditions at the foundation level of the embankment based on a review of geophysical surveys (P-wave seismic refraction) and geotechnical investigation undertaken at the site. A summary of the P-wave velocities (V_p) for the various subsurface materials is given in Table 2-15. Shear-wave velocities (V_s) were estimated from P-wave velocities (V_p) using published relationships (Brocher 2005, Castagna et al., 1985) as shown in Figure 2-13. These relationships show good agreement in the estimated V_s values for the different subsurface layers. The seismic hazard study for the Nena ISF site was performed for V_{s30} of 1,150 m/s which corresponds to a V_p of 2,700 m/s; this velocity concurs with the range obtained for cemented colluvium and alluvium found at the foundation of the Frieda River site.

Table 2-15: Interpreted correlation of P-wave velocities with geotechnical horizons

Material	Approximate Vp range
Valley floor colluvium and alluvium (cemented)	2,500–4,000
Soil-like colluvium	0–1,500
Colluvium with boulders	1,500–3,000
Weathered rock with oxidised, infilled joints to layer of 'bedrock'	3,000–4,300
Strong to very strong SW and UW rock	>4,300
Potential landslide (unstable) zone – sheared and oxidised rock	<3,900

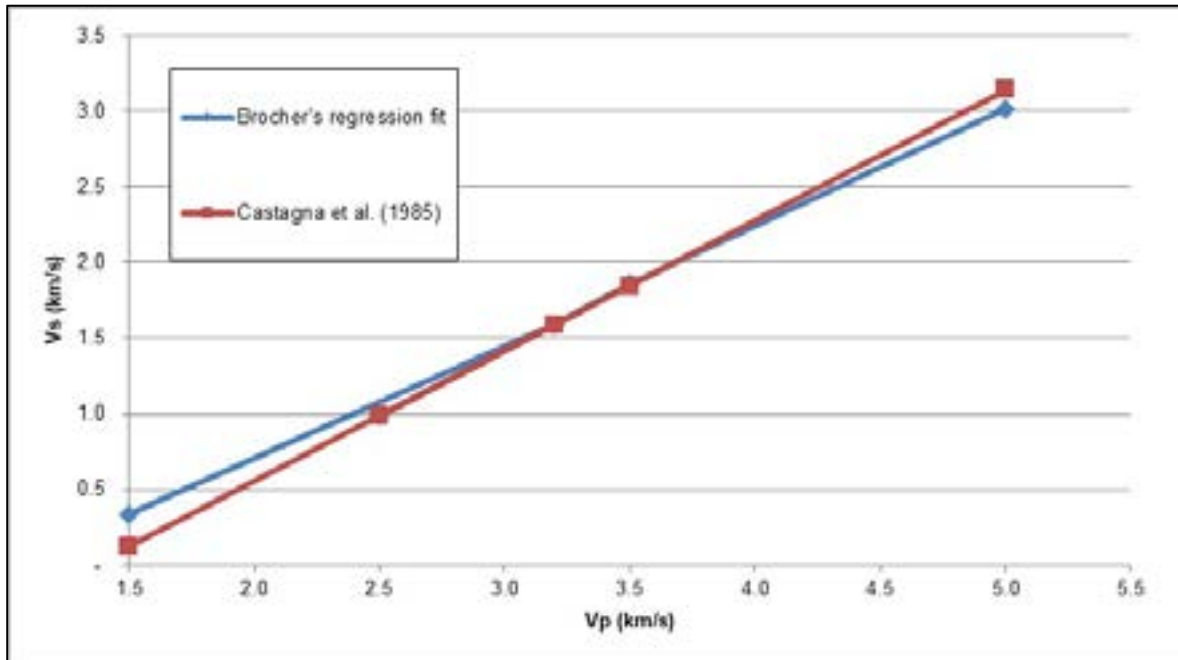


Figure 2-13: Estimated shear-wave velocities for the subsurface layers at the Nena ISF

Al Atik & Gregor (2016) evaluated the seismic source zones based on the spatial pattern of observed seismicity and tectonic considerations spanning the entire region of interest for the FRHEP. As a result, seismic source zones were defined for four depth ranges to account for the observed strong depth-dependent seismicity pattern in the PNG region: shallow <35 km and 35–75 km, intermediate 75–120 km, and deep 120–20 km.

Al Atik & Gregor (2016) updated the ground-motion characterisation model using the latest empirically based models appropriate for the tectonic environment and information from past studies. Given the lack of region-specific GMPEs for the PNG region, Al Atik & Gregor (2016) created ground-motion models developed from global ground-motion datasets for similar tectonic environments to that of the PNG region.

Al Atik & Gregor (2016) developed a series of PSHA curves and then de-aggregated the mean hazard at the site. They also calculated median and 84th percentile deterministic response spectra for the MCE scenarios on the Frieda Fault and the set of seven crustal faults using the five equally weighted NGA-West2 GMPEs. Past studies on the FRHEP recommended a design PGA of 1.09g and this has been adopted for the SPS, and the GMPEs were therefore scaled to match this.

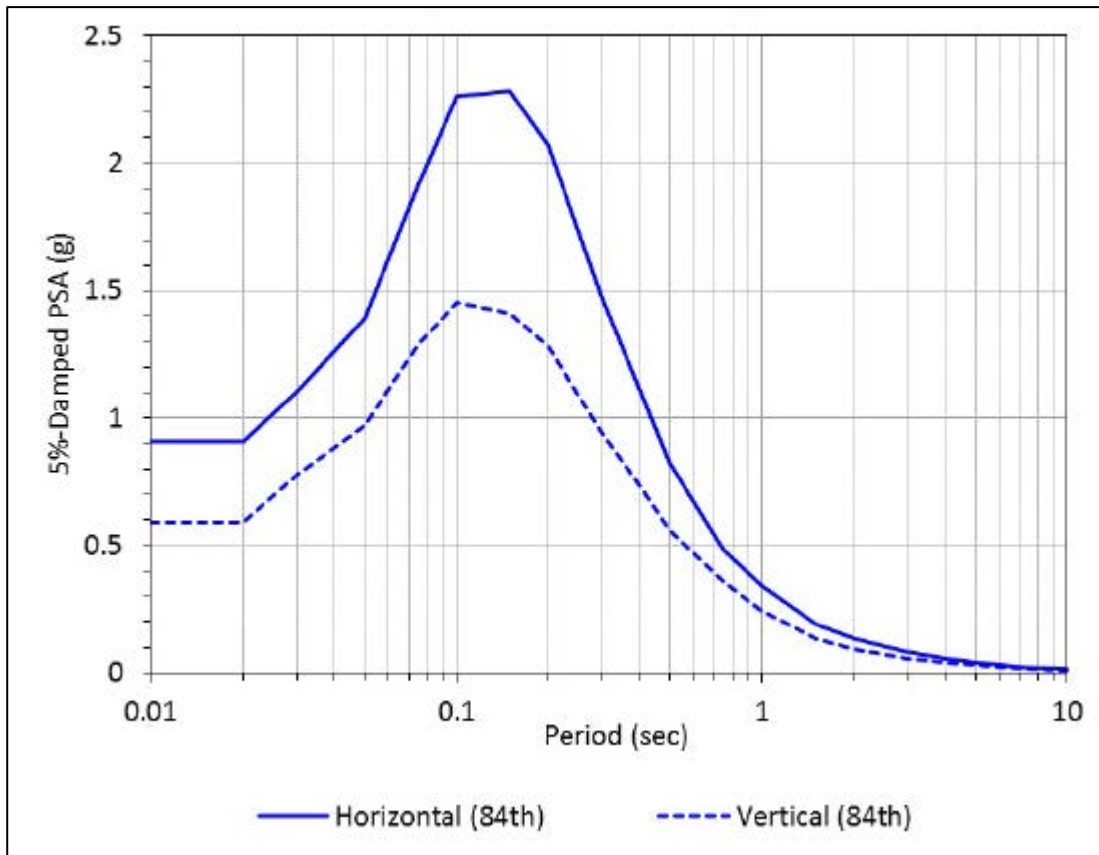


Figure 2-14: Horizontal and vertical design spectra for the MCE scenario on Zone 15 (35–75 km) for V_{S30} of 1,150 m/s

Design seismic parameters – Hydroelectric power infrastructure

The design seismic parameters shown in Table 2-16 have been adopted for the power generation infrastructure elements (intakes and powerhouse), and are based on the following design earthquakes:

- Safety Evaluation Earthquake (SEE) = MCE = deterministic PGA for Zone 15 84th percentile, as given in Atik & Gregor, 2016
- Operational Basis Earthquake (OBE) = 1 in 475-year event, as given in given in Atik & Gregor, 2016.

It is assumed that all components of FRHEP infrastructure are ‘Critical’ as defined by the USACE documents listed in Section 2.4.1.

Table 2-16: FRHEP infrastructure design ground accelerations

Structure	Period (seconds)	OBE acceleration (g)	SEE acceleration (g)
Powerhouse ($V_{S30} = 760$ m/s)	PGA	0.458	0.983
	0.2	1.034	2.386
	1	0.323	0.431
Intake structures ($V_{S30} = 1,150$ m/s)	PGA	0.407	0.908
	0.2	0.867	2.070
	1	0.178	0.343
Embankment	PGA	N/A	1.09

In accordance with USACE ETL 1110-2-584, all control gates are to consider an MCE event in addition to an OBE event as the earthquake load in an additional Extreme I load case with the spillway gates closed.

2.5.3 Stability

In accordance with ANCOLD (2012) guidelines, embankments will be designed to provide an acceptable factor of safety (FoS) against instability. Minimum FoS values are given in Table 2-17. ANCOLD (2012) recommends a range of post-seismic FoS from 1.0 to 1.2, depending on the confidence in selection of residual shear strength. An FoS of 1.2 was adopted for the SPS for post-seismic conditions as the actual strength properties are yet to be tested.

Table 2-17: Minimum factors of safety (ANCOLD, 2012)

Area	Loading Condition	Minimum FoS
Embankment	Long-term drained	1.5
	Post-seismic	1.2
Spoil dumps	Undrained	1.3
Spillway and quarry	Static	1.5
	Static with pseudo-static loading of 0.4g	1.1

Estimated deformations must be within serviceability limits. As recommended by ANCOLD (2012), 'deformations should not reduce freeboards to unacceptable levels or result in the potential disruption of the filter with large shear movements'. The embankment must be designed to withstand (i.e. not fail) under the MCE loading, but it may require subsequent maintenance.

2.5.4 Seepage

Being a hydroelectric power facility, any seepage results in lost revenue. The facility must therefore meet seepage loss criteria. In addition, seepage controls are often critical for maintaining stability and reducing the risk of foundation piping. The energy modelling is based on a total assumed water loss of 1,100 L/s. In combination with seepage cut-off infrastructure in the foundation and abutments, an impermeable zone has been designed to prevent water seeping through the embankment.

2.5.5 Rock properties

Key parameters related to the properties of rock materials on site and implemented in the SPS are shown in Table 2-18.

Table 2-18: Rock properties

Criteria	Value	Source/ comment
Minimum assumed wastage (Quarry - North Ridge)	16%	Calculated by SRK; 10% based on available core results and 6% due to handling
Minimum assumed wastage (Spillway)	18%	Calculated by SRK; 10% based on available core results and 8% due to handling
Minimum assumed wastage (smaller excavations including roads)	50%	Calculated by SRK; based on available core results
Swell factor (uncompacted)	1.25	PNA007 – FRL ISF FEL2 Design, dated October 2016 ¹⁸ – BCM to LCM

¹⁸ SRK 2016, Frieda River Project Integrated Storage Facility FEL2 Design, October 2016

Criteria	Value	Source/ comment
Swell factor (compacted)	1.15	Estimated by SRK – BCM to CCM (compacted cubic metres)

2.5.6 Tunnels and ground support

The minimum tunnel size considered constructible is 5 × 5 m (FRL¹⁹).

The preliminary design for ground support within the conveyance tunnels and diversion tunnels at this SPS level of study is based on a commonly used empirical method, whereby the rockmass conditions are defined using Barton's Q tunnelling index system (1974) and NGI (2015) and representative values/ ranges identified for the different rockmass conditions are then plotted on the ground support design chart of Grimstad & Barton²⁰. This chart provides indicative designs for bolt spacings and lengths, and thicknesses of shotcrete (external)/ fibrecrete (internal).

An excavation support ratio (ESR) of 1.3 (Class D) was used for the ground support design assessment of the conveyance tunnels, and an ESR of 1.6 (Class C) was used for the diversion tunnels.

2.5.7 Roads

For trafficability, the following minimum road widths have been adopted for access during the construction period; these values represent the total width of the wearing course surface, including road shoulders:

- Diversion dam embankment: 7 m
- Cofferdam embankment: 12 m
- Main embankment: 7 m
- Spillway inlet bridge: 12 m
- Civil construction haul roads: 13 m
- Large equipment haul roads for transporting quarry materials: 22 m.

2.5.8 Spillway bridge

The maximum weight lift needed on the spillway bridge is 30 t (gate sections and stoplogs).

2.6 Water management

2.6.1 Hydrology baseline

A hydrology baseline assessment was completed by SRK 2018²¹ and included the following:

- Design flood hydrographs for various locations in the FRHEP catchment for use in design of the spillway, cofferdam sizing and water quality assessments. Inflow hydrographs to the FRHEP and at various sub-catchment outlets were developed for the following flood events:
 - Average recurrence interval (ARI): 10 to 1,000 years plus the probable maximum precipitation (PMP)

¹⁹ Email – FRL (E Chong), 28/06/15

²⁰ Grimstad & Barton 1993, Updating of the Q-System for NMT. Proc. Int. Symp. on Sprayed Concrete - Modern Use of Wet Mix Sprayed Concrete for Underground Support, Fagernes

²¹ SRK 2018, Memorandum - Hydrology for FRHEP design, Document number PNA009_MEMO_Hydrology FRHEP_Rev3.docx.

- Duration: 6 hrs to 60 days
- Synthetic long-term flows series at the embankment location for use in modelling of the hydroelectric scheme and represents the energy source for power generation. Two full-record series were generated using a similar methodology: 50 scenarios of 200 years and 200 scenarios of 38 years
- Tailwater rating curves.

The hydrology baseline was developed using global, regional and local sources of data. Locations of the precipitation gauges located in the FRHEP catchment are shown in Figure 2-15 and the available period of record for each gauge is listed in Table 2-19. Data is generally available from 1995–1999 and 2008–2017.

Table 2-19: Details of precipitation gauges²¹

Station #	Location	Elevation (RL m)	Years of record
105200	Waste Dump Creek	425	12.3
105300	Upper Nena	635	11.0
105310	Lower Nena	190	13.7
105320	Ok Binai	110	11.8
05440	Frieda River downstream of Wabia Gorge	361	5.2
105450	Upper Frieda	100	11.9
105R03	Waste Dump Creek Top	1062	8.2
105R06	Mt Stolle	2240	9.3
105R07	Middle Stolle	850	9.2
105R10	Ok Binai Madang Ridge	627	8.5

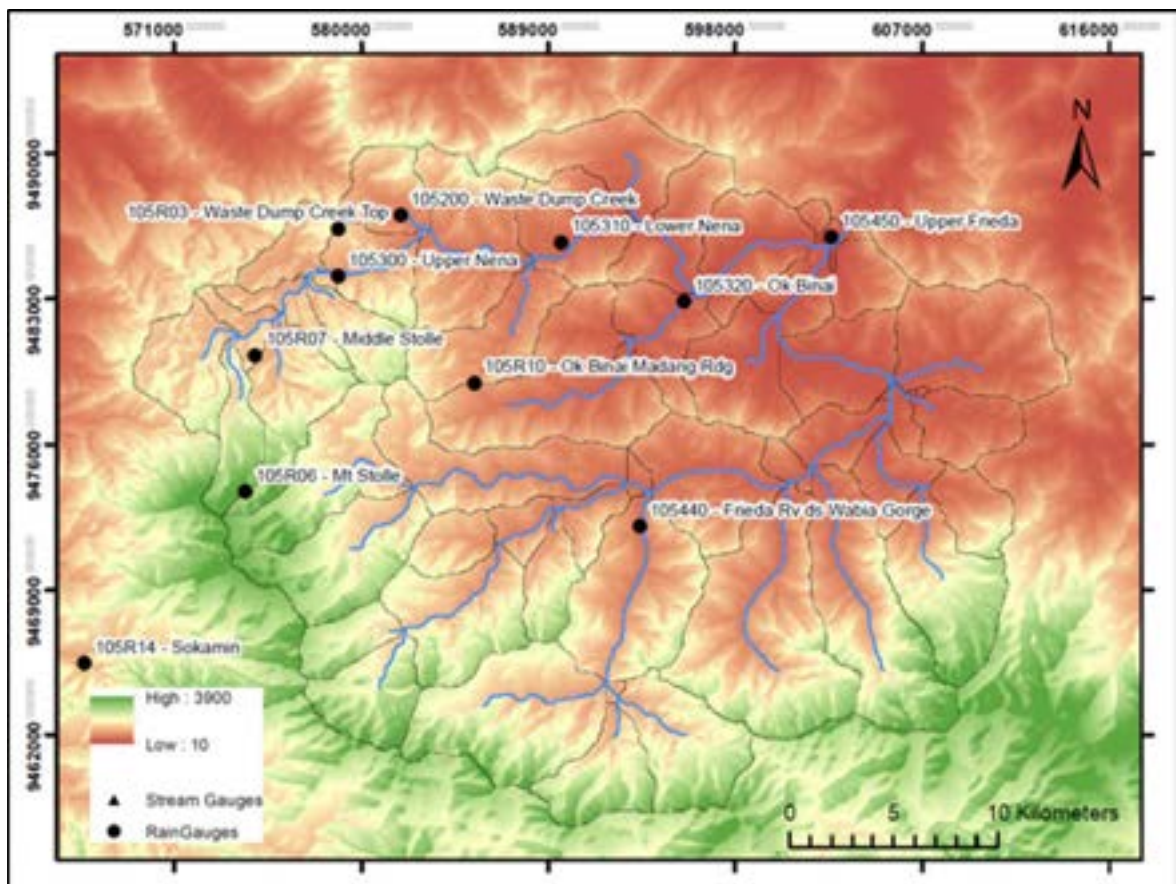


Figure 2-15: Locations of rain gauges

The locations of the stream gauges in the FRHEP catchment are shown in Figure 2-16 and the available period of record for each gauge is listed in Table 2-20. The ‘Upper Frieda River’ stream gauge (GS105450), which is located close to the FRHEP site, has been monitored since 1981. The other stream gauges have generally been recorded from 1995–1999 and 2008–2017.

Table 2-20: Details of stream gauges²¹

Station	Location	Elevation (RL m)	Catchment area (km ²)	Years of record
105100	Ekwai Creek Pit Area	750	3	5
105200	Waste Dump Creek	425	1	14
105300	Nena River upstream of Gorge	635	97	13
105310	Nena River downstream of Mine Site	190	205	12
105320	Ok Binai River upstream of Tailings Dam Site	110	69	8
105440	Frieda River downstream of Wabia Gorge	361	129	2
105450	Upper Frieda River	100	1,033	20

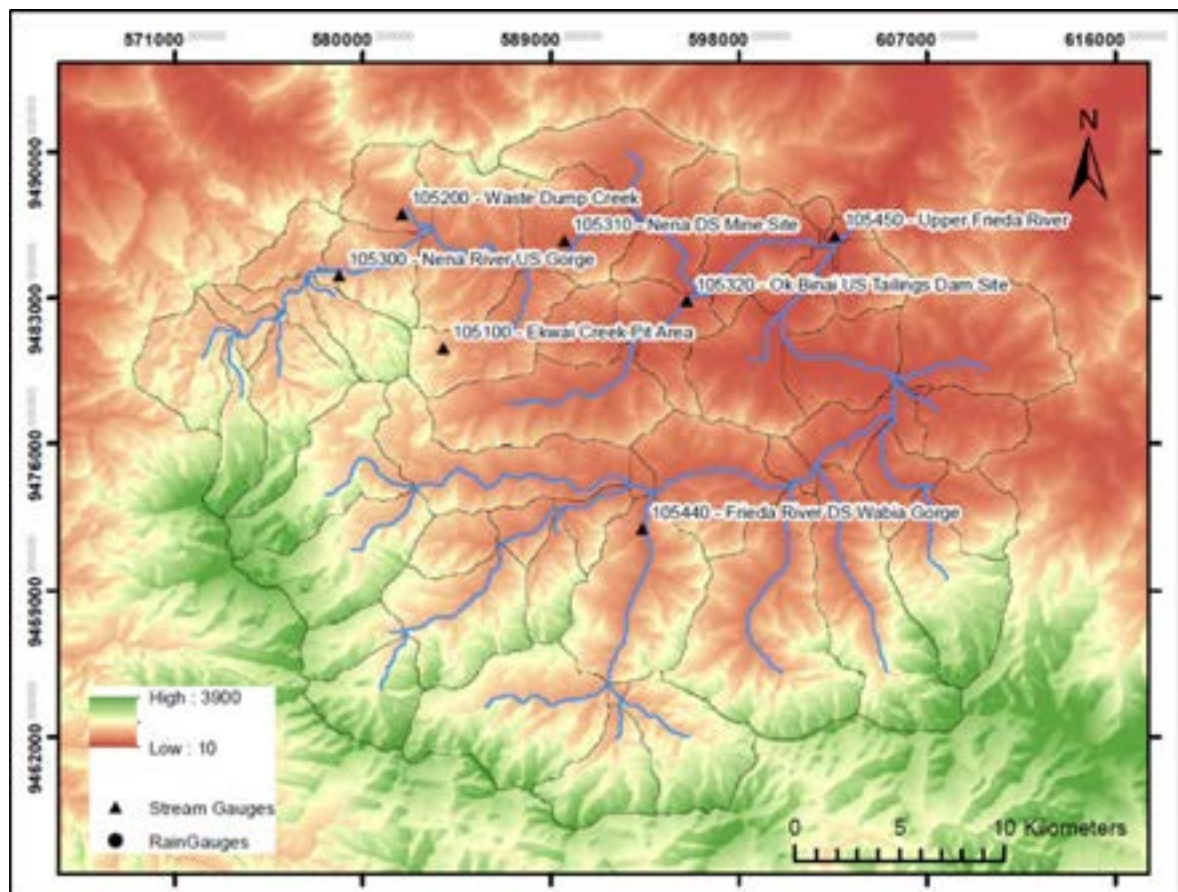


Figure 2-16: Locations of stream gauges

2.6.2 Design flows for construction

The design minimum flood capacity required during construction and for key temporary works is a 1 in 100-year annual exceedance probability (AEP) peak flow event as recommended by the TIRP for the Nena ISF design in 2015. The design flood volumes will be diverted and managed by the diversion tunnels and a cofferdam arrangement.

A temporary diversion dam will be constructed to facilitate construction of the upstream cofferdam. The diversion dam will be constructed to the level of the major bench in the river bank and has no specific storm event design criterion.

During early filling, the main embankment must provide flood capacity for the PMF plus 6 months as a contingency for construction delay (estimated discharge allowance of 500 m³/s to pass the PMF).

The design criteria for less critical stormwater management and sediment control infrastructure based on the design storms is shown in Table 2-21. Sediment retention particle size for the sedimentation ponds is >0.075 mm as determined by FRL (M Haywood, email 19/04/2018).

Table 2-21: Return periods for stormwater and sediment management infrastructure

Design Criteria	Value	Comment
Diversion and road drainage		
Permanent diversions	1 in 100-year AEP	Recommended by SRK
Temporary diversions	1 in 25-year AEP	Recommended by SRK
Permanent crossings	1 in 100-year AEP	Recommended by SRK
Temporary crossings	1 in 25-year AEP	Recommended by SRK
Sedimentation ponds		
Sediment retention storm	0.5 × 1 in 1-year AEP	IECA 2016
Spillway design storm	1 in 25-year AEP	Assumed

2.6.3 Design flows for operations

As recommended by ANCOLD (Table 2-22) for the 'Extreme' Dam Consequence Category, the PMF was adopted as the design flood. ANCOLD defines the pre-flood reservoir level to be the Full Supply Level (FSL). The embankment will have an open channel spillway to pass the design flood. The spillway operations for passing the PMF will be evaluated for a worst-case scenario of one spillway gate in four not working.

Table 2-22: ANCOLD fallback flood capacity²²

Consequence Category	Flood AEP
Extreme	PMF
High A	PMP Design Flood
High B	10 ⁻⁴ to PMP Design Flood or 10 ⁻⁶
High C	10 ⁻⁴ to PMP Design Flood or 10 ⁻⁵
Significant	10 ⁻³ to 10 ⁻⁴
Low/ Very Low	10 ⁻² to 10 ⁻³

The minimum water depths to be maintained above the tailings and waste rock during operations, including other relevant water management parameters, are summarised in Table 2-23. Water level fluctuations should be minimised to promote operability of barges; however, no maximum fluctuation range has been specified.

²² ANCOLD 2000, Guidelines on Selection of Acceptable Flood Capacity for Dams

Table 2-23: Operating water management requirements

Item	Value	Comment
Minimum operating water depth (barge)	10 m	FRL ²³
Absolute minimum water depth	8 m	
Minimum reservoir above tailings/ waste for hydroelectric power operations (worst case)	18 m	Comprises 5 m above the tailings to the invert of the intake, intake height, and submergence required for the intake velocity to prevent vortex formation
Freeboard	Allowance for wave run-up, earthquake settlement, landslide risk, underwater embankment failure, and 1 non-operational spillway gate	Defined by SRK and based on ANCOLD guidelines
Embankment and spillway flood capacity	PMF (n-1 spillway gates operational)	Defined based on the results of fault tree analysis
Powerhouse and other hydraulic structures	1 in 500 AEP flood and evaluated for a 1 in 1,000 AEP flood	Defined by SRK

The option of entirely draining the reservoir to perform maintenance is ruled out because the tailings and waste rock in the reservoir must be kept permanently under cover of water. This limitation has been considered in the design.

2.6.4 Water management for closure

To inhibit oxidation of tailings and waste rock in the reservoir, a minimum water depth of 2 m above the tailings and waste was assumed to be required for closure. The PMF will remain the design flood.

2.7 Wave size modelling

Subaqueous or subaerial landslides can cause large waves due to the resulting displacement when it occurs in, or into, a body of water such as the FRHEP reservoir. The site's environmental conditions, such as steep terrain, high rainfall and seismic activity is conducive to development of subaerial landslides.

Seismic activity or uncontrolled deposition of tailings and waste rock below the surface of the reservoir may result in subaqueous slope failures. The maximum height of tailings and waste rock deposition is 111 m (RL 159.4 m) and subaqueous slope failures under these conditions may result in development of waves that could have a material impact on the embankment and the operation.

The geohazard assessment (Section 3.2) identified risks due to geological hazards or landslides induced by reservoir filling that may also have a material impact.

Although predictions of wave height development due to either subaerial or subaqueous failure are particularly challenging due to the number of variables – seismicity, geology, geotechnics, topography and hydrodynamics, SRK undertook an assessment of predicted wave amplitude to understand the associated risks and identify mitigation measures, including freeboard requirements.

²³ FRL, Waste Rock Barges – 4000 DWT General Arrangement, document FRP03-0254-ESO-DG-D2-0001_C

Based on the assessment, SRK concludes the following:

- Based on various published studies on waves generated by subaqueous and subaerial landslides, two models developed by leading experts were used in this study, and correlated against the FRHEP.
- The subaqueous landslides model is different to the model used during IPS. The new model is more refined, and the results produce slightly smaller waves. A sensitivity analysis has shown that the shape of the landslides has a minimal effect on the calculated wave amplitude compared to the effect of the bed slope angle.
- Wave development due to subaerial and subaqueous landslides will occur; the amplitude of the waves must be considered in determining the required freeboard.
- The maximum subaqueous landslide wave height of 5.4 m has been estimated at the location of the embankment. Under these conditions, the waste rock and tailings are deposited to a maximum height of 111 m, at RL 159.4 m, with the reservoir's bottom level at RL 48 m.
- Wave amplitudes due to subaerial landslides were assessed using three landslide sizes based on the geohazard and georisk studies performed by Scott Wilson.
- The expected wave heights that can occur at the lowest water depth vary between 3.4 m for 1,000 m³ landslides and 43.3 m for 1,000,000 m³ landslides. Based on the assessments undertaken, landslides of 1,000,000 m³ will cause overtopping of the embankment. The probability of occurrence and associated impact must be established, based on the latest geohazard study to evaluate this project-specific risk.
- The results are conservative and the actual wave height may be lower as the model assumes a rigid body of material and expected deformation during failure will reduce the effect. As the subaerial landslide assessment model is sensitive to changes in input parameters, the assessment for this study was based on conservative parameters.

2.8 Quarry

Safety protocols in line with PNG regulatory requirements will be implemented for quarrying activities. Quarries have inherent safety risks to people and property due to the variable nature of the environment, blasting and flyrock, potentially unstable ground conditions and interactions with plant. The safety of construction personnel is a key project objective and will require significant effort to ensure safety performance targets are met.

Wastage in the quarry has been estimated as 18% from the spillway excavation and 16% from the quarry excavation. The wastage allowance, in excess of the 10% (as identified from core recovery), has been added for additional wastage generated due to handling.

2.9 Environment and social

2.9.1 Environmental

A surface water quality assessment was completed as described in the water and load balance assessment (Section 6.3). The outcomes of impact assessment have been utilised in the EIS to assess impacts on water quality (Coffey, 2018) considering the following regulatory requirements in PNG, as well as other guidelines and standards for guidance:

- PNG regulatory requirements, including PNG Ambient Water Quality Standards and the PNG Drinking Water Guidelines.
- Environmental Code of Practice for the Papua New Guinea Mining Industry.

- International Finance Corporation (IFC) effluent discharge guidelines (Table 2-24).
- International guidelines including the WHO guidelines for drinking water quality (WHO, 2017) and the Australian and New Zealand guidelines for fresh and marine water quality (ANZECC/ARMCANZ, 2000) for protection of aquatic ecosystems.

Compliance with the PNG ambient and drinking water regulatory criteria is not expected to provide adequate protection for aquatic ecosystems or human health based on the current state of knowledge of toxicant exposure to biota and people. As such, the ANZECC/ARMCANZ (2000) trigger values for 95% aquatic ecosystem protection were adopted for contaminants of concern and were used to indicate the need to undertake further action mitigate impacts from mining.

Table 2-24: IFC guidelines for effluent water quality levels

Parameter	Unit	Guideline value
TSS	mg/L	A maximum of: a) 50 b) background concentration in the Frieda River as measured upstream of the ISF above the raw water intake + 50 mg/L
pH	S.U.	6–9
COD	mg/L	150
BOD5	mg/L	50
Oil and Grease	mg/L	10
Arsenic	mg/L	0.1
Cadmium	mg/L	0.05
Chromium (VI)	mg/L	0.1
Copper	mg/L	0.3
Cyanide	mg/L	1
Cyanide Free	mg/L	0.1
Cyanide WAD (weak acid dissociable)	mg/L	0.5
Iron (total)	mg/L	2.0
Lead	mg/L	0.2
Mercury	mg/L	0.002
Nickel	mg/L	0.5
Phenols	mg/l	0.5
Zinc	mg/L	0.5
Temperature	°C	<3° differential

A minimum discharge from the FRHEP must be maintained at all times during construction and after commissioning. This provision will be to mitigate any potential negative impacts to the environment and downstream water users. A second objective would be to maintain barge trafficking up the river. Until FRL has defined the minimum flow requirements, an allowance of 50 m³/s has been assumed.

All trees, topsoil and vegetation stripped will be disposed in the designated spoil dump. No salvage or re-use is intended. An area to volume ratio of 1 m³ of stockpiled trees and vegetation per square metre of area stripped has been estimated and will be applied in order to establish storage requirements for all trees and vegetation to be stripped in the FRHEP working areas.

2.9.2 Limnology

A limnology study was performed to understand the characteristics of the water and the effects of resuspension of particles in the reservoir during filling, operation and closure. The variables that affect the characteristics of water in the reservoir are largely related to meteorology and topographic characteristics of the lake. For this reason, the meteorological data collected on site was used in the limnology study.

Meteorological data for the study area is available at 15-minute intervals from the Nena, Moraupi and Iniok weather stations (Figure 2-17). The data used for the FRHEP limnological modelling study includes air temperature (AT), relative humidity (RH), solar radiation (SR), and wind speed (WS) and direction (WD). Observations from Nena AWS (automatic weather station) are used as the basis for continuous time series required by the limnological model. Data collected over a 6-year period from January 2009 to December 2014 contains an almost complete time series of all data variables. To ensure a continuous modelling time series, data from the Moraupi AWS was used to fill the gaps in data from the Nena AWS.

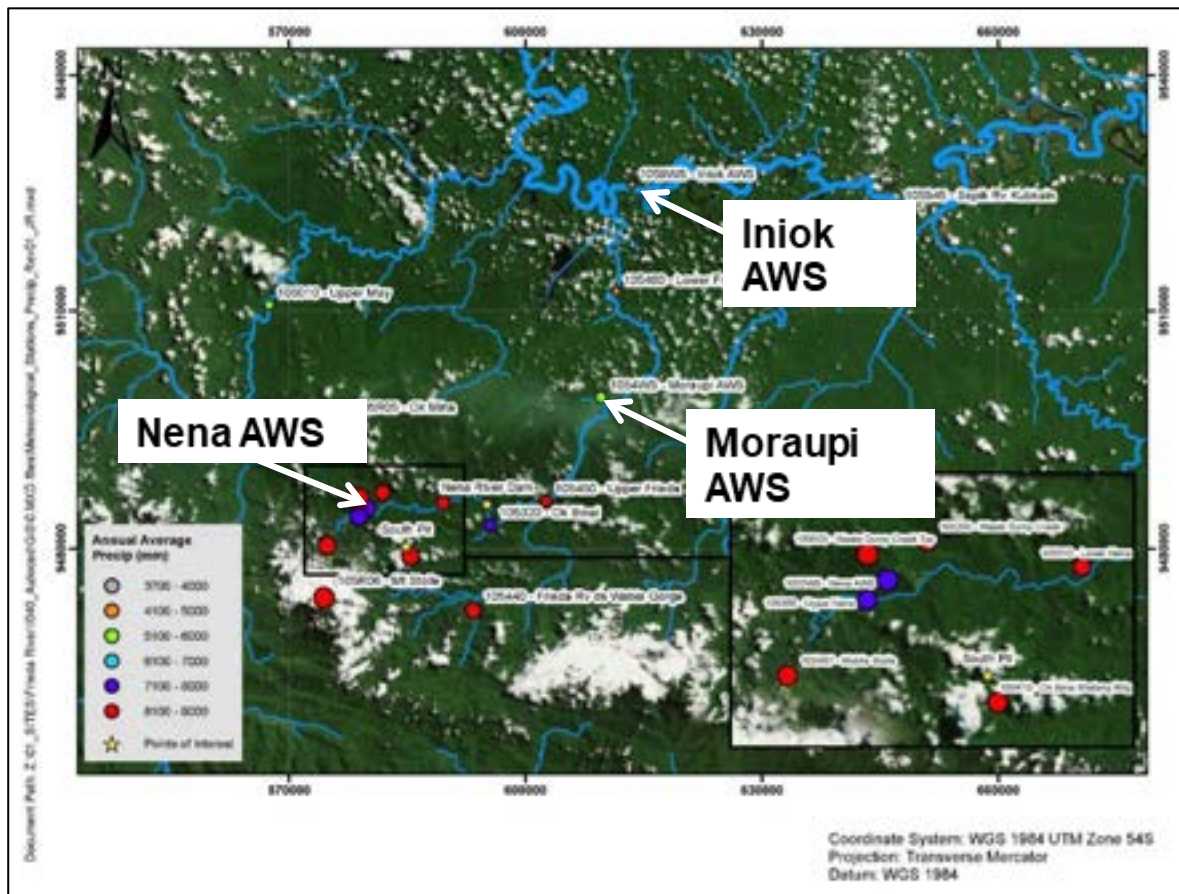


Figure 2-17: Meteorological stations

Table 2-25 summarises the data available for each of the monitoring stations.

Table 2-25: Data from meteorological stations and application to the limnological model²⁴

Met Station	Periods of Data	Application
Nena AWS	1994–1999 (WD, SR only) 2008–2017 (significant data gaps from 2015 onwards)	2009–2014 (6 years): AT, RH, SR, WS, WD WS for 2015–2016 used to fill data gaps
Moraupi AWS	2009–2017 (significant data gaps from 2014 onwards)	AT, RH, SR, WD for Nena data gaps (see notes above)
Iniook AWS	2008–2015 (significant data gaps from 2013 onwards)	Not used at this stage

2.9.3 Sedimentation

Table 2-26 summarises the sediment contribution to the reservoir over the 33-year LOM, which were extracted from the sedimentation calculation sheet developed by Golder Associates.

Table 2-26: Sedimentation predictions

Sediment load (Mt)	Dry density (t/m ³)	Volume (Mm ³)
43.6	1.1	39.7

2.9.4 Social

The FRHEP impoundment will flood two villages, and FRL has indicated that the two villages will be relocated. A downstream village within 5 km of the embankment will also be relocated.

The study activities related to the relocation is excluded from the SPS scope of works, and will be considered further by FRL.

²⁴ Email - Peter Yeates, dated 5/12/2017

3 Geotechnical Characterisation and Geohazard Assessment

This chapter presents the geotechnical assessments conducted for the FRHEP, as well as the landslide geohazard and georisk evaluation conducted for the wider Frieda River catchment area.

The assessments for the FRHEP are based on the information from recent geotechnical investigations that were undertaken in mid-2017 and late 2017 through early 2018, as well as earlier investigations conducted for Xstrata in 2010 and 2011. The chapter provides:

- Characterisation of the subsurface conditions at the site of the embankment and associated infrastructure as well as the quarry for construction materials
- Geotechnical design inputs to inform the SPS design.

This geohazard and georisk evaluation presents an update to relevant parts of the earlier geohazard assessment by SRK (2015), and geohazard study by Scott Wilson (2011), as well as the engineering geological assessment of the original site infrastructure by Douglas Partners (2011)²⁵. The recent phase of work has reviewed the geohazards identified in the earlier work and provides an updated inventory of previous and newly identified hazards for the wider Frieda River catchment area.

3.1 FRHEP geotechnical characterisation study

3.1.1 Objectives

As part of the SPS, SRK provided oversight of two stages of site drilling investigation and completed soil and rockmass characterisations to provide information for the embankment and powerhouse founding conditions, for the diversion and conveyance tunnel design, and for the spillway and quarry design. The aim of the investigative work was to provide:

- A characterisation of the ground conditions within the footprint of the proposed embankment (and associated development), including:
 - Nature and thickness of unconsolidated/ weak transported and residual materials
 - Depth and nature of weathered bedrock
 - Depth and nature of generally unweathered bedrock
- An overview of the geological conditions within the embankment development and surrounding area, including the following:
 - Description and distribution of major rock types
 - Characterisation of the rockmass fabric
 - Presence and nature of faults
- Characterisation of the abutment areas in terms of in situ permeability and the variability thereof
- Delineation and characterisation of a source of quarry materials suitable for embankment construction
- Recommendations for a geotechnical forward works program.

²⁵ Douglas Partners, February 2011, Frieda River Extended Interim Geotechnical Program. Field Report on Frieda Infrastructure Ok Binai WSG and TSF.

3.1.2 Work program

The geotechnical characterisation of the FRHEP site has been progressively developed in mid to late 2016, mid to late 2017, and early 2018 – as described in the subsections below.

High level site review: site comparison study

An evaluation of information from previous studies was performed in mid to late 2016 as part of the site comparison study, during which a high-level evaluation of the potential hazards and risks associated with the FRHEP site was developed (as described in SRK's memo, Frieda Mountain Lake Review, PNA007-SO003, August 2016)²⁶. The evaluations were based primarily on the following information:

- Scott Wilson, June 2011, Frieda River Copper-Gold Project, Papua New Guinea – Geohazard and Georisk Feasibility Study
- SKM, Pöyry & SMEC (SKMPS), September 2011²⁷, Appendix I-2 - 25534-000-V02-MG00-00014 - Geological and Geotechnical Report
- Douglas Partners, February 2011, Frieda River Extended Interim Geotechnical Program. Field Report on Frieda Infrastructure Ok Binai WSG and TSF.

Fatal flaw assessment

Based on a site visit, available literature and public datasets, a preliminary structural assessment of the FRHEP site was carried out, as described in SRK's memo, FML Fatal Flaw Assessment, PNA007-SO007, December 2016²⁸. The following actions were carried out:

- Regional lineament mapping of topographic (LiDAR) and satellite imagery data
- Appraisal of available drill data and drill core
- Limited site mapping
- Review of available geohazard assessments and other technical studies
- Review and interpretation of available aeromagnetic data.

Stage 1 Geotechnical investigations

Carried out in late May and early June 2017, the Stage 1 investigations were specifically designed to address gaps or concerns identified during the site comparison review and fatal flaw assessment. The Stage 1 geotechnical investigations are summarised as follows:

- Eight diamond-cored, oriented holes (100–180 m in length) were drilled within the FRHEP site and surrounds.
- One hole was drilled on a spur in the Frieda River valley some 9 km south of the embankment site (near the Ok Isai village) to investigate the potential for a large volume landslide, as indicated in the 2011 Scott Wilson Geohazard Report.
- Limited downhole permeability (packer and falling head) testing was carried out to attempt to characterise zones of potential high permeability and to identify the general rockmass permeability.

²⁶ SRK memorandum, 2016. Frieda Mountain Lake Review. Project number PNA007-SO003, August 2016.

²⁷ SKM, Pöyry & SMEC, September 2011, Appendix I-2 - 25534-000-V02-MG00-00014 - Geological and Geotechnical Report.

²⁸ SRK memorandum, 2016. FML Fatal Flaw Assessment. Project number PNA007-SO007, December 2016.

The Stage 1 drill holes include holes LH1 and LH2, holes RH1– RH5, hole Q5 and hole OE1. and are summarised in Table 3-1.

Stage 2 Geotechnical investigations

The Stage 2 investigations commenced in late September 2017 and were designed to bring the site characterisation to a feasibility level of understanding. The investigations are summarised as follows:

- 44 diamond-cored drill holes (25–350 m in length) were originally designed. Three holes were cancelled, and 36 were completed. Three holes were in progress (i.e. were incomplete) and two had not yet commenced at the premature termination of the investigation, due to issues on site.
- Permeability (packer and/ or falling head) testing was carried out in 10 selected holes.
- Vibrating wire piezometers (VWPs) were installed in only two holes, although these were also intended for installation in a further three holes that were not able to be completed. However, both completed installations were in holes on the left abutment of the proposed embankment. In one of these holes, the VWPs were damaged during the removal of drill rods immediately after installation.
- Televiewer downhole survey was intended in 11 holes, but was carried out in nine holes.
- Extensometers for measurement of slope creep were installed in two holes in the left abutment.
- Standard penetration testing (SPT) was intended in nine selected holes, but was not possible due to presence of bedrock or boulders near the surface.
- Laboratory testing was carried out for five (out of an intended seven) batches shipped during the program. Testing included the following:
 - Unconfined compressive strength (UCS) – rock
 - Young’s modulus and Poisson’s ratio – rock
 - Direct shear of joints – rock
 - Direct shear testing on saw-cut surfaces – rock
 - Slake durability – rock
 - Los Angeles (LA) Abrasion – rock
 - Particle size distribution and Atterberg limits – soil, joint infill and fault gouge
 - Emerson (Crumb) dispersion testing – soil.

A summary of the Stage 2 drill holes is provided in Table 3-1. The design collar positions of these drill holes, as well as drill holes from the previous phases of investigation, are shown with reference to the embankment, quarry and infrastructure designs in Figure 3-1.

Two seismic refraction traverses were completed: one of approximately 1,000 m length (performed as two lines) across the left abutment of the proposed embankment; and one of approximately 200 m in the vicinity of the proposed powerhouse location to the east of the Frieda River. The designed positions of these traverses are shown in Figure 3-1.

Selection Phase Study

The geotechnical study activities for the SPS were conducted over the following periods:

- Drilling, sampling and in situ testing – Stage 1: mid-May to mid-June 2017
- Drilling, sampling and in situ testing – Stage 2: late September 2017 to late March 2018
- Laboratory testing: November 2017 to April 2018
- Seismic refraction survey: late February to early March 2018

- Data collation: June and July 2017, and October 2017 through to April 2018
- Data interpretation, analysis and site characterisation: June and July 2017, and November 2017 through to May 2018
- Technical reporting: Early April 2018 through late June 2018.

Table 3-1: Summary of Stage 1 and 2 geotechnical investigations

Element	Sub-element	Drill hole	Status	Design length (m)	ATV completed	Permeability testing	Extensometer installation	VWP transducers	
Embankment	Right abutment	RH1	Completed	125		Y		1 at 125 m	
		RH2	Completed	175		Y		1 at 50 m	
		RH3	Completed	170					
		RH4	Completed	100					
		RH5	Completed	100		Y			
		RH6	Completed	100		Y			
		RH7	Completed	100		Y			
		RH8	Not commenced	75					
	Left abutment	LH1	Completed	125			Y		1 at 123 m
		LH2	Completed	175			Y		
		LH3	Completed	120			Y		
		LH4	Completed	75				Y	
		LH5	Completed	150	Y	Y			75 m & 150 m (both damaged)
		LH6	Completed	75			Y		1 at 75 m
LH7		Completed	150	Y	Y	Y			
Spillway	SW1	Completed	50						
	SW2	Cancelled							
	SW3	Completed	100						
	SW4	Completed	100						
	SW5	Completed	100						
	SW6	Completed	150	Y	Y				
Diversion tunnel	Alignment	DT1	Completed	125					
		DT2	Completed	250	Y	Y			
		DT3	Completed	320					
		DT4	Incomplete	350					
		DT5	Cancelled						
	Portals	DTP1	Completed	50					
		DTP2	Completed	80					
		DTP3	Completed	25					
DTP4		Completed	50						
Conveyance tunnel	Alignment	HT1	Completed	150	Y	Y			
		HT2	Incomplete	250					
	Portals	HTP1	Cancelled						
		HTP2	Completed	50					
		HTP3	Completed	25					
		HTP4	Completed	50					

Element	Sub-element	Drill hole	Status	Design length (m)	ATV completed	Permeability testing	Extensometer installation	VWP transducers
	Intake	HT11	Completed	180				
	Surge chamber	SC1	Completed	200	Y			
Powerhouse	PH1		Incomplete	50				
	PH2		Completed	50				
	PH3		Completed	40				
	PH4		Not commenced	40				
Quarry	Q5		Completed	100				
	Q6		Completed	150	Y			
	Q7		Completed	80				
	Q8		Completed	100				
	Q9		Completed	170	Y			
	Q10		Completed	75				
	Q11		Completed	50				
	Q12		Completed	75				
Q13		Completed	150					
Ok Isai landslide hazard	OE1		Completed	100				

Note: Y = yes

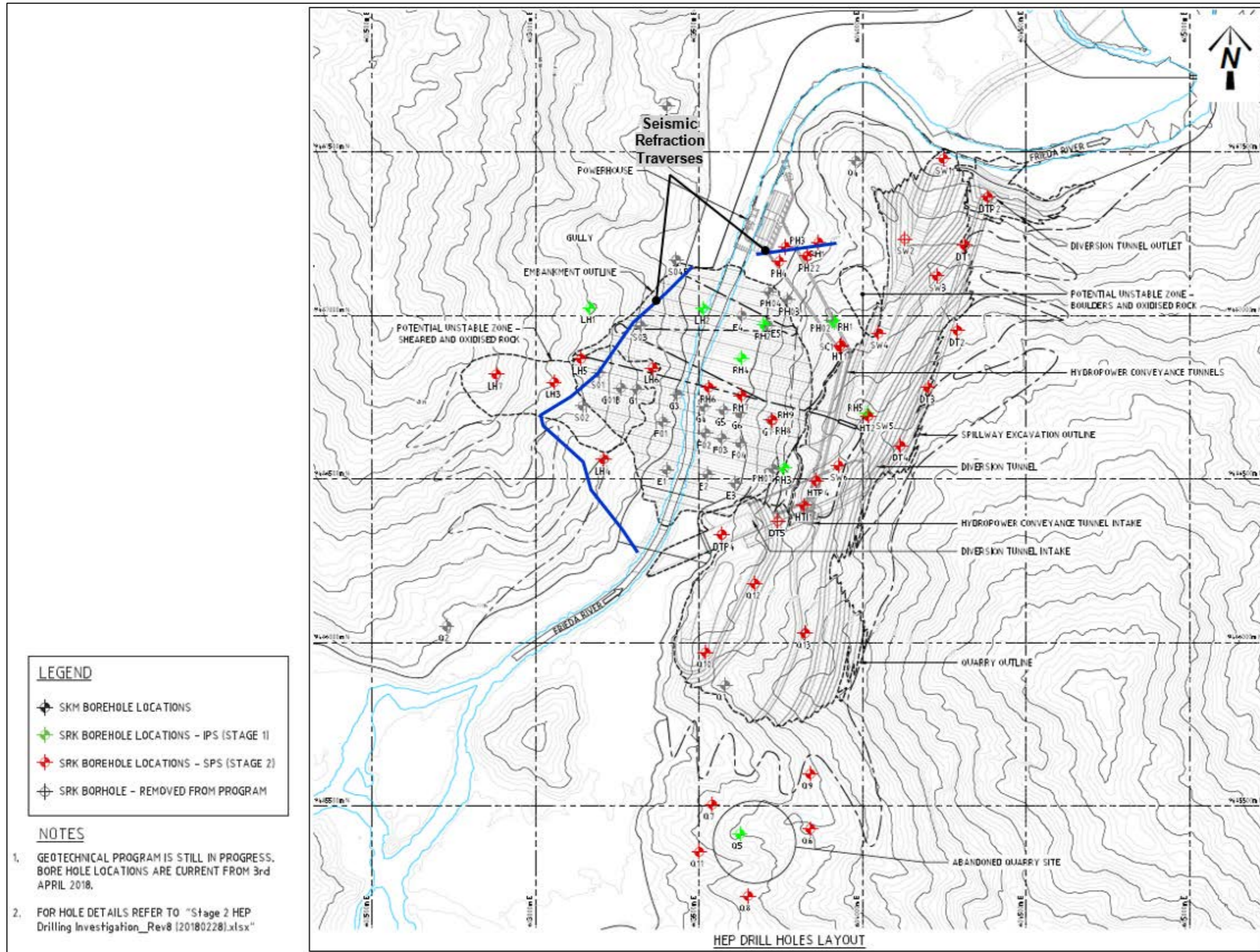


Figure 3-1: FRHEP geotechnical investigation

3.1.3 Regional geological setting

The FRCGP is located on the northern part of the Indo-Australian Plate, situated on the north flank of the Central Highlands. The FRHEP site is situated on EL1212, in an area dominated by three major WNW-ESE to NW-SE, northward-dipping thrust faults (Figure 3-2). These faults are splays of the Leonard Schulze fault, which lies approximately 100 km to the east. The major thrust splays, from south to north, are the Fiak, Frieda and Saniap faults. The Saniap fault forms the boundary between the rocks of the Wogamush Formation to the north and Ok Binai Phyllites to the south. Approximately 13 km to the southeast of the FRHEP site, a small moment magnitude (Mw) 4.2 earthquake occurred at a depth of 43 km on the Saniap fault in 2015.

The oldest rocks in the area are the Jurassic to middle Eocene aged Ok Binai Phyllite, which grades into the equivalent of the Wabia beds and Wahagi Group slate. The sequences comprise phyllitic mudstone, sandstone and volcanolithic rocks. The overlying Wogamush Formation consists of volcanogenic sequences and forms part of the late Oligocene to Miocene Maramuni Igneous complex. The sequences consist of andesite to basaltic volcanics, volcanolithic sandstone, mudstone and limestone and has, in places, been intruded by numerous plutons.

Major slices of April Ophiolites have been thrust over the Ok Binai and Wogamush sequences (Figure 3-3, with exaggerated vertical scale). The April Ophiolite is of Paleogene age and consists of undifferentiated ultrabasic and basic igneous rocks of basalt, gabbro and peridotite. These rocks represent the erosional remnants of a once more extensive thrust sheet of oceanic crust. They are variously serpentinised, and comprise layered to massive cumulate dunite (the bedrock at the FRHEP site), harzburgite and wehrlite.

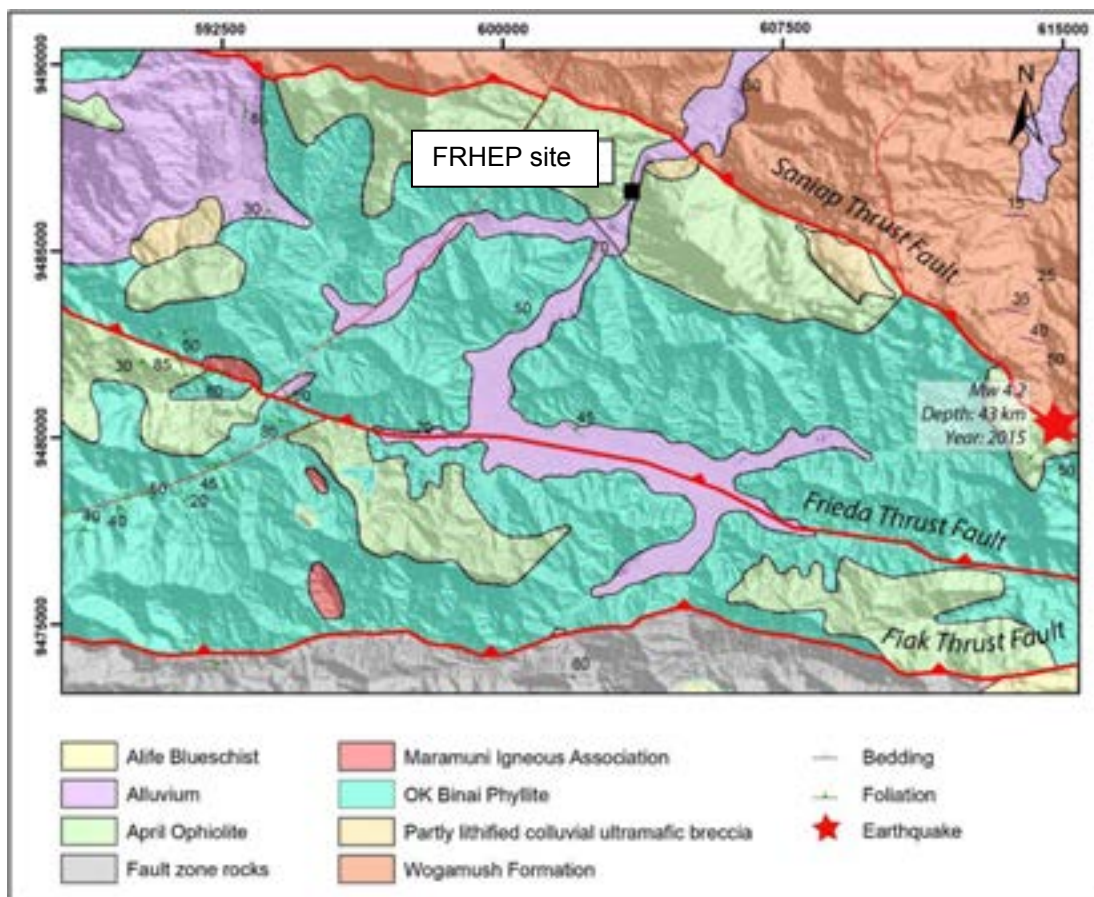


Figure 3-2: Geological setting of the FRHEP site and surrounds

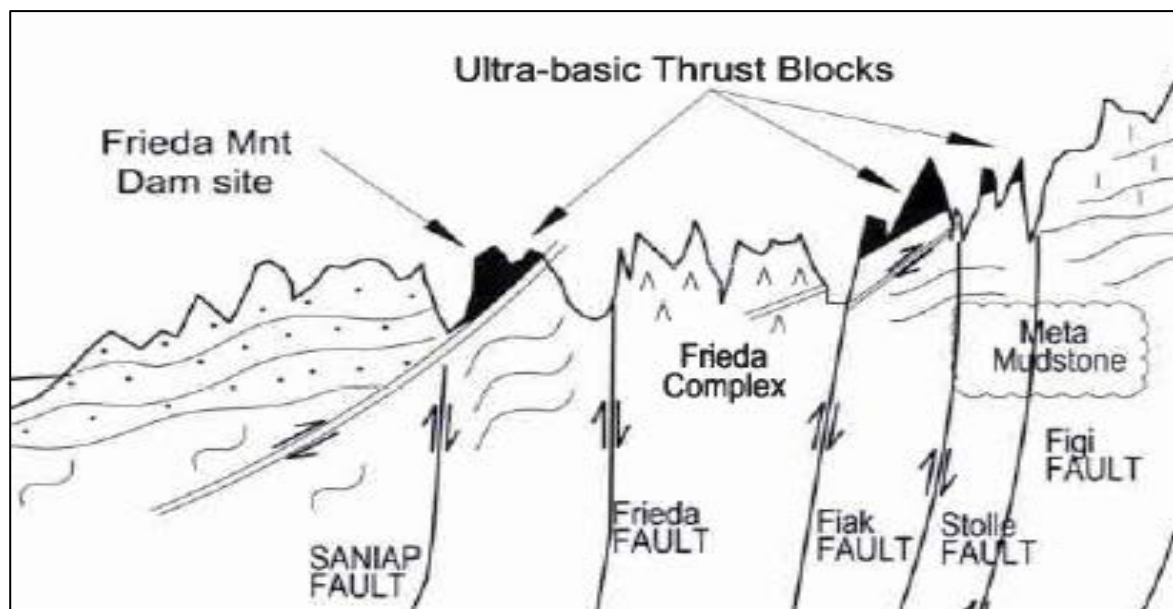


Figure 3-3: Diagrammatic N-S geology cross-section

Source: After Douglas Partners Extended Scoping Study (2009).

Note: North is to the left, and there is vertical exaggeration.

3.1.4 Site conditions

Geomorphology

The geomorphology of the site and surrounds is a strong reflection of active tectonics. The drainage divides have a general EW to WNW–ESE orientation. Topographic ridges are orthogonal to the main drainage divides. This is shown in Figure 3-4.

Streams have been modelled using the LiDAR dataset with ArcGIS software. This shows that the Frieda River has a sinistral offset of approximately 5 km to the west, before turning NE where it is joined by the Nena River, and enters the gorge, at the proposed FRHEP site.

The inset lineaments rose diagram in Figure 3-4 shows two main trends, namely: 1) NNE–SSW and 2) WNW–ESE. These mostly represent structural trends. The WNW–ESE peak shows the main trend of thrusting, e.g. the Saniap thrust, while the NNE–SSW trend includes the FRHEP site gorge. There are many NNE–SSW to NE–SW faults in the regional vicinity (e.g. as shown on the regional Mianmin Geological Map Sheet SB54-3 Papua New Guinea 1:250,000 Geological Series²⁹). The low sinuosity of the Frieda River over a stretch of about 2 km within the deep gorge suggests that its development has been controlled by faulting and fluvial incision from combined bed flow of the Frieda and Nena rivers.

The embankment site lies within a straight, V-shaped gorge. The slopes on the western (left hand) side of the gorge are of up to 450 m in height, and are generally at a 35°–40° angle, but the slopes are locally steeper on the flanks of old landslides in the northern part, where bedrock is very close to the surface. The slopes of the eastern (right hand) side of the gorge are generally steeper; between 40° and 60°, and up to 600 m in height.

Both banks and slopes are heavily vegetated with primary rainforest. At the proposed embankment site, the riverbank rises at approximately 65° to relatively flat terraces comprising cemented colluvial

²⁹ Mianmin Geological Map (Sheet SB54-3, 1:250,000 scale, Geological Survey of Papua New Guinea) and Accompanying Notes.

debris at 10–15 m above the river level (a waterfall over this riverbank material is shown in Figure 3-5). The terraces are between 20 m and 100 m wide and occur on both sides of the river.

In the central part of the gorge (at the position of the proposed FRHEP embankment), the river course lies closer to the western side of the valley, with wide and thick colluvial deposits accumulated on the right-hand bank; however, in the northern part of the gorge the river course is in the centre of the valley.

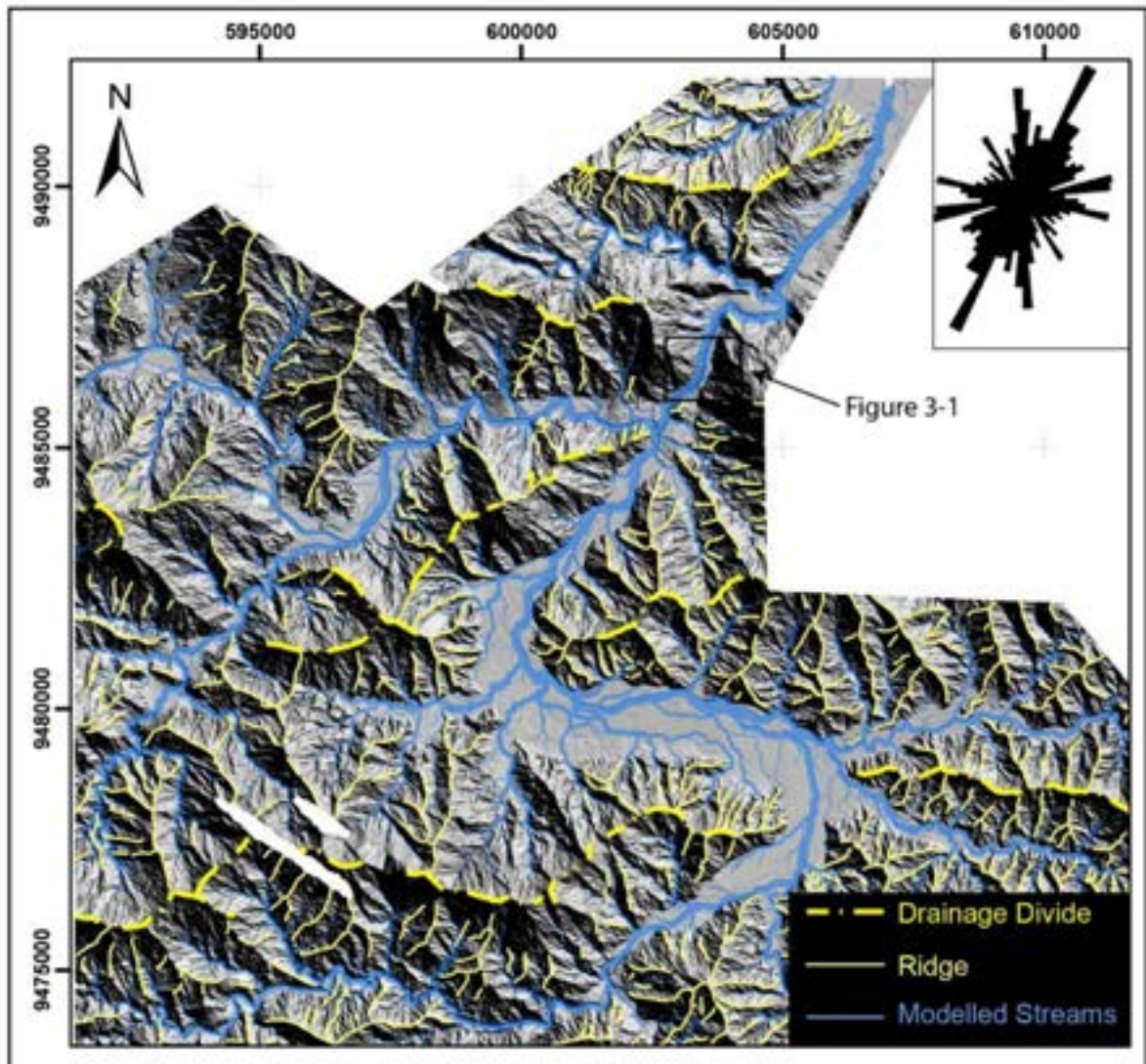


Figure 3-4: Plan view of modelled streams, drainage divide and topographic ridges

Note: Inset shows rose diagram with a dominant NNE–SSW trend reflecting the primary orientation of major ridges that are orthogonal to drainage divides.



Figure 3-5: Cemented colluvial material forming steep river banks

Figure 3-6 is a plan view topographic image of the FRHEP site showing river banks, valley floors, topographic ridges, and interfluvies. Previously identified landslides (Scott Wilson, 2011) have been completely re-vegetated, indicating that landslides occurred quite some time ago. Figure 3-6 also shows the slope aspect of the embankment gorge over a length scale of 5 m (LiDAR resolution).

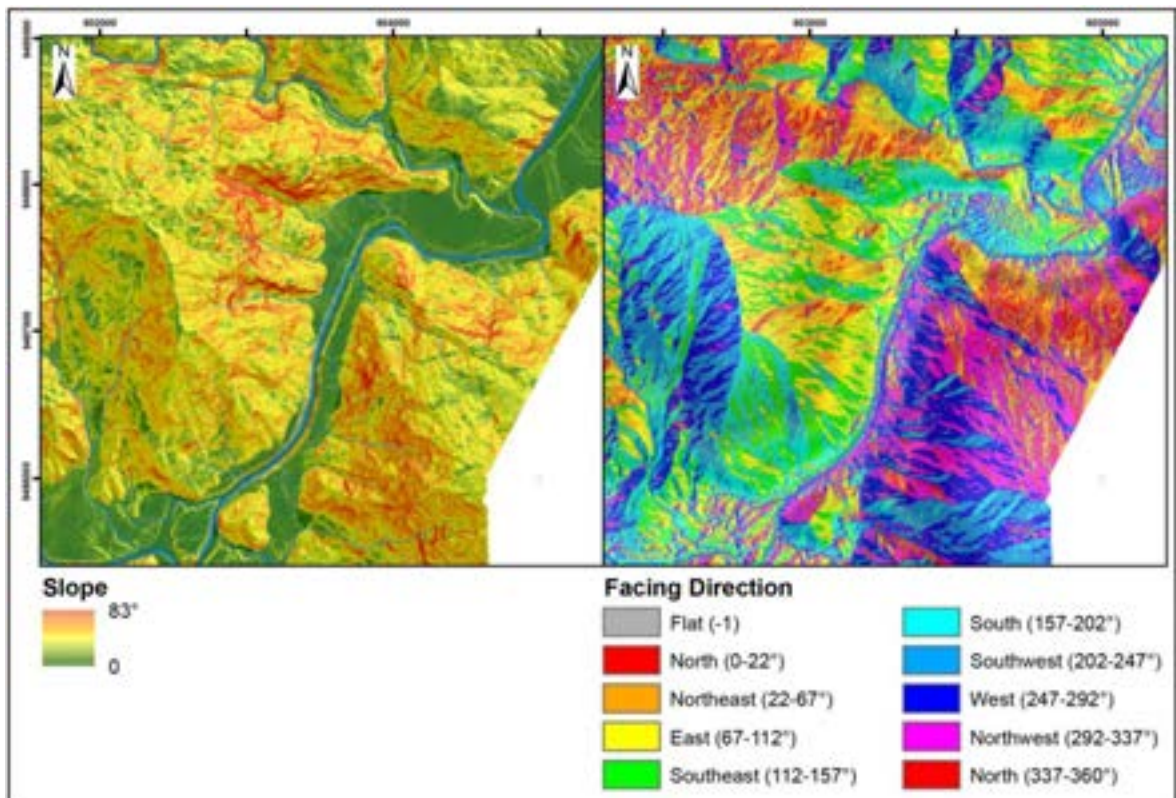


Figure 3-6: Slope (left hand side) and aspect (right hand side) of the FRHEP site

Geology

The FRHEP embankment site is situated within a klippe of April Ophiolite, separated from the underlying Ok Binai phyllite (to the south) and the underlying sedimentary Wogamush Formation (to the north) by a low-angle thrust fault (Figure 3-7). Drilling and mapping investigations have shown that the site is largely underlain by dunite, a relatively coarse-grained, massive, ultramafic igneous rock consisting largely of the mineral olivine ($Mg_2SiO_4 - Fe_2SiO_4$). A pale yellow-greenish variation, with limited distribution, is believed to be monticellite ($CaMgSiO_4$). Patchy alteration of chlorite, sericite and serpentine occurs locally, and some joint surfaces exhibit these materials. Drilling in the valley floor (exceeding 200 m in depth) has not encountered the old thrust contact, i.e. has not passed through into Ok Binai Phyllite or Wogamush Formation rocks – all holes have terminated within dunite.

As shown in Figure 3-2, EL1212 falls within a region transected by several WNW–ESE striking regional-scale thrust faults, the most notable of which are the Frieda Fault (7 km to the south of the FRHEP site), and the Saniap Fault (approximately 2 km north of the site). The Frieda Fault has been mapped and drilled within EL1212 and has been identified from carbon dating of organic fault debris to have been active within approximately the last 200 years. The Saniap Fault has been less well investigated, but based on carbon dating, is also interpreted to have been recently active. These faults should be considered as potential seismic sources for the FRHEP embankment and other appurtenant structure designs.

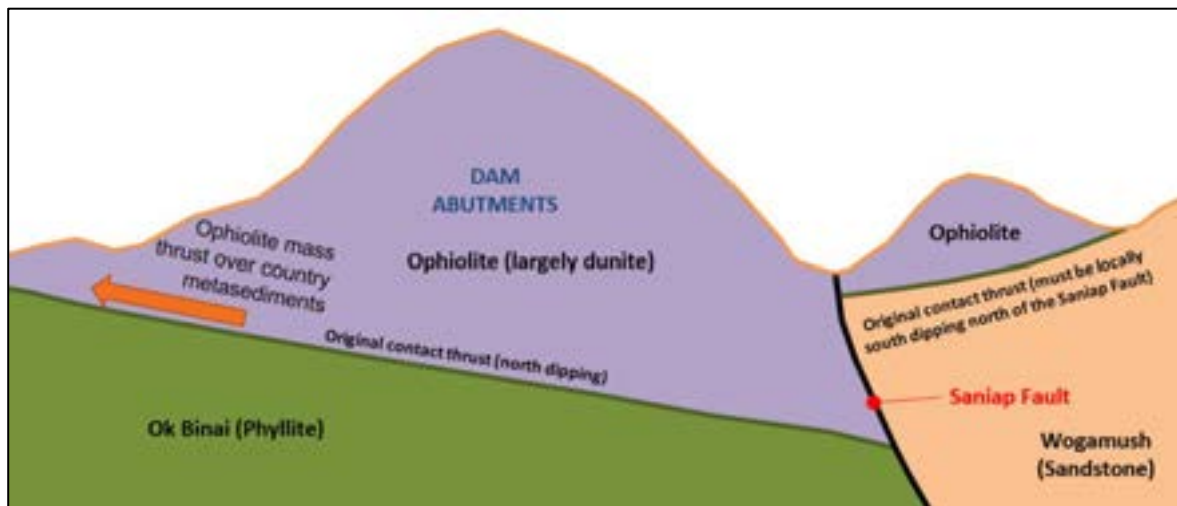


Figure 3-7: SSW–NNE diagrammatic cross-section looking west

Bedrock

The hillsides on both sides of the river are relatively steep and a thick in situ weathering profile has not developed. The upper bedrock consists of slightly weathered (SW) to moderately weathered (MW) rock, often displaying considerable weathering on the surfaces of structures, with underlying unweathered (UW) to SW rock. The dunite bedrock is generally moderately to sparsely fractured, and is strong to very strong, good quality rock. However, even within the generally UW bedrock, significant joint oxidation is present in discrete zones that likely form conduits for groundwater; an example of this is shown in Figure 3-8. Core drilling and early mapping indicates that the bedrock has colluvial infill in its upper part, indicating probable dilation of the near-surface rockmass, prior to the progressive mass wasting (in localised sliding and toppling mechanisms) over the long term.



Figure 3-8: An example of intense weathering in wall rock of upper dunite bedrock

A significant amount of the good quality, strong bedrock exhibits previous structural deformation and re-healing (Figure 3-9 shows examples of this). This is a tectonic overprint as an early deformation of the massive rock, and is observed as numerous, fine and often parallel, healed ‘cracks’ and/ or breccia texture. The matrix consists largely of cryptocrystalline olivine. In places, the olivine has been altered to serpentine, and locally this matrix is deteriorating – presenting weak, sheared rockmass conditions in parts of some drill holes. This is illustrated in Figure 3-10.

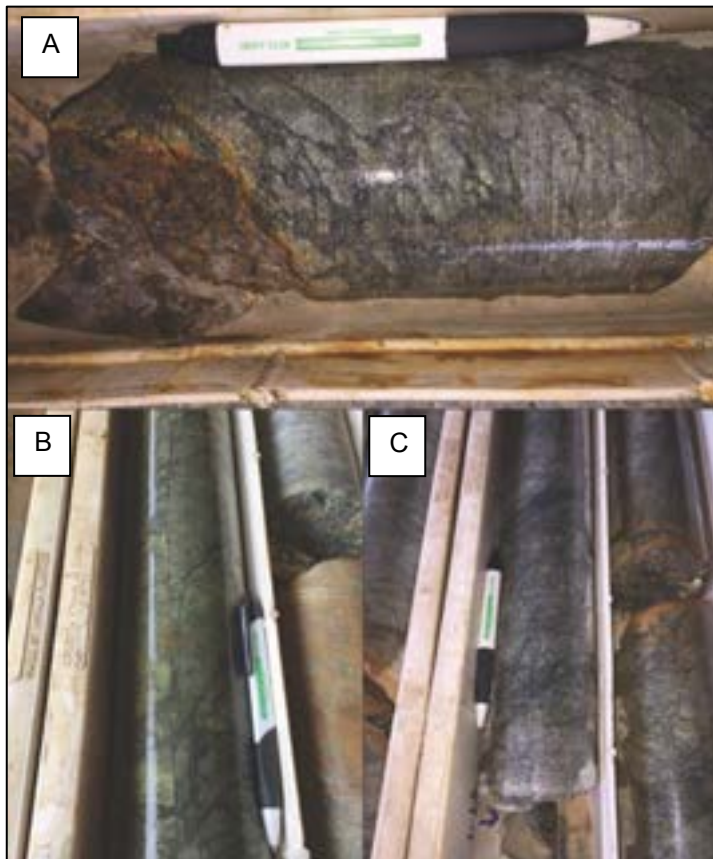


Figure 3-9: A: Semi-brittle deformation and part development of shear bands; B: Brittle deformation and chlorite and serpentinisation; C: Semi-brittle and cataclastic deformation

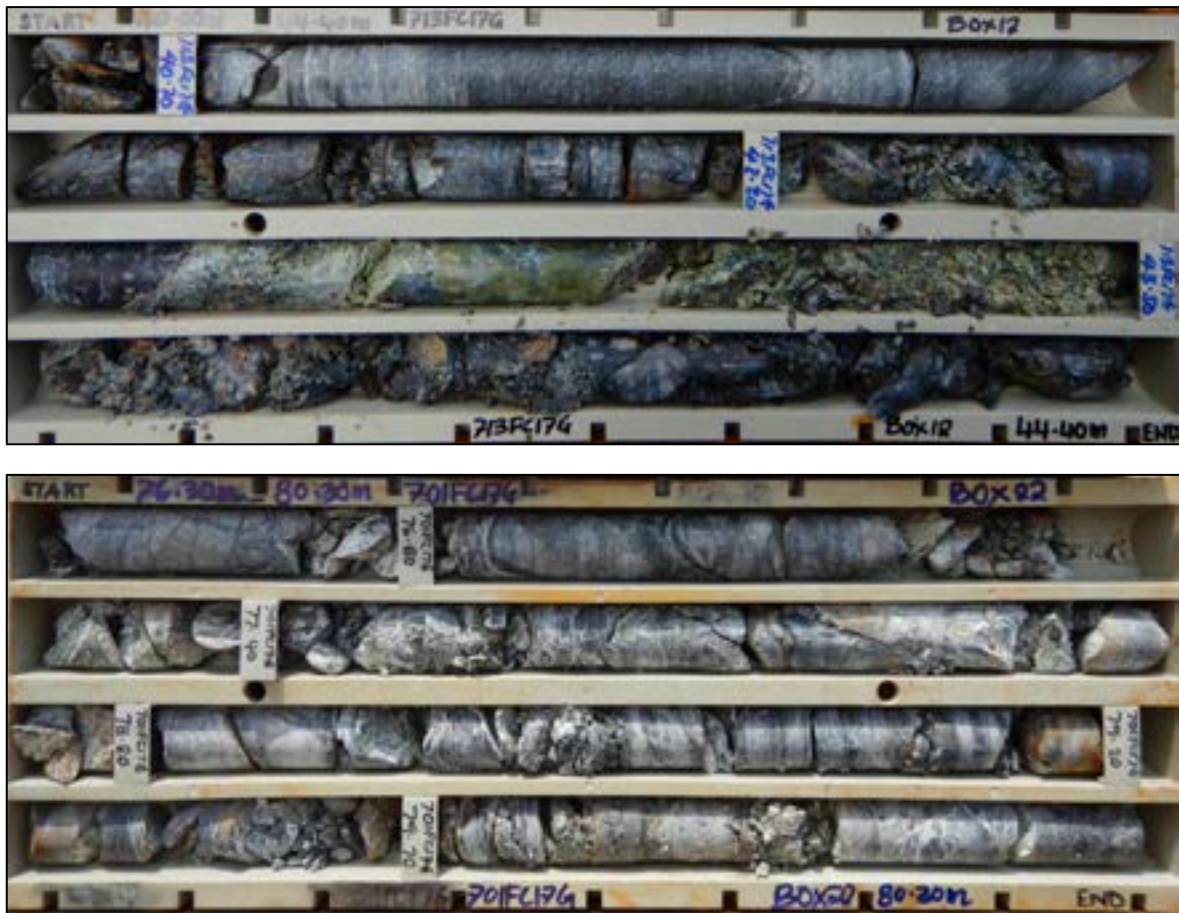


Figure 3-10: Drill core showing previously sheared and now serpentinised and deteriorating dunite, as shown in drill hole PH2 (above) and Q6 (below)

Surficial deposits

Colluvial material, in the form of soil-like material (gravelly-clayey silt or clayey-silty sand) and/ or boulders, forms only a very thin layer over the bedrock on the hillsides (generally between 1 m and 5 m in thickness, except where breaks in slope or local landslide debris result in locally thicker accumulations of boulders in particular).

In the valley bottom, colluvial materials are composed of a very large component (60%–80%) of coarse irregular fragments of dunite of varying sizes (some very large) in a cemented matrix, directly overlying dunite bedrock. Almost no completely weathered or highly weathered material is present; the overburden consists almost entirely of transported material. The colluvium forms terraces 10–20 m above the river on both sides, which present a nearly horizontal surface, sloping very gently downstream. A thin layer of fine-grained recent alluvial flood deposits is found in places on top of the terraces, more predominantly on the eastern side of the river.

The Scott Wilson (URS) Hazard Assessment report (2011) attributes the upper layers of the river terraces between a point just upstream of the Nena confluence and the sharp bend downstream of the proposed embankment site as part of the Frieda River Diamicton. The diamicton is the flow of a massive landslide event (or series of events) having occurred approximately 38,000 years ago. A number of alternative scenarios for the formation of this diamicton have been postulated. However, because all the coarse clasts in the diamicton consist of local dunite, it is likely that at this location they are the result of large landslides in the April Ophiolite klippe in the immediate vicinity, and of mass wasting from the steep slopes over time.

True alluvial material is constrained mainly to the actual river channel and beneath it, mainly on the western side of the valley bottom (but more in the centre of the valley in the north of the gorge). These alluvial materials are generally very coarse (boulders, cobbles, gravel and sand), and are loose in the upper ~25–40 m below surface and sometimes compacted/ cemented below this. At its margin, the alluvial materials are interfingering with the cemented colluvium.

Colluvial and alluvial material in the valley bottom presents a combined thickness of up to 70 m in places.

A section through the gorge geology at the approximate position of the FRHEP embankment is shown in Figure 3-13.

Structure

Faulting at the FRHEP site is described in detail in Section 3.1.10, and structural fabric of the rockmass (jointing) is described in Section 3.1.9.

A classification describing four orders of faults is applicable for EL1212. The first order structures in the vicinity of the FRHEP site include the regional scale thrust faults: the Saniap Fault (and likely fault splays) and the Frieda Fault, as described in Section 3.1.4. Several large NNE–SSW striking transfer fault zones (second order structures) have been included in previous geological interpretations of the region, with one of these faults indicated to pass roughly 1–2 km to the west of the FRHEP site.

Third order faults are significant faults that may have had movement to accommodate stress in between major thrusts and transfer faults. Such structures would include significant damage zones up to a few metres in width (or wider disturbed zones of general disturbance perhaps tens of metres in overall width), possibly multiple phases of movement and re-healing. Fault breccia/ gouge with re-healing and current smaller shears with gouge or mylonitisation may be present. Few of these structures have been identified at the FRHEP site; however, an example is shown in Figure 3-11.

Fourth order faults are common at the FRHEP site; these are networks of smaller faults and shears that may present small zones of breccia or gouge a few tens of centimetres wide, or highly fractured rockmass (not breccia) up to a few metres in width (though usually less than a metre in width). An example of a typical fourth order fault is shown in Figure 3-12.

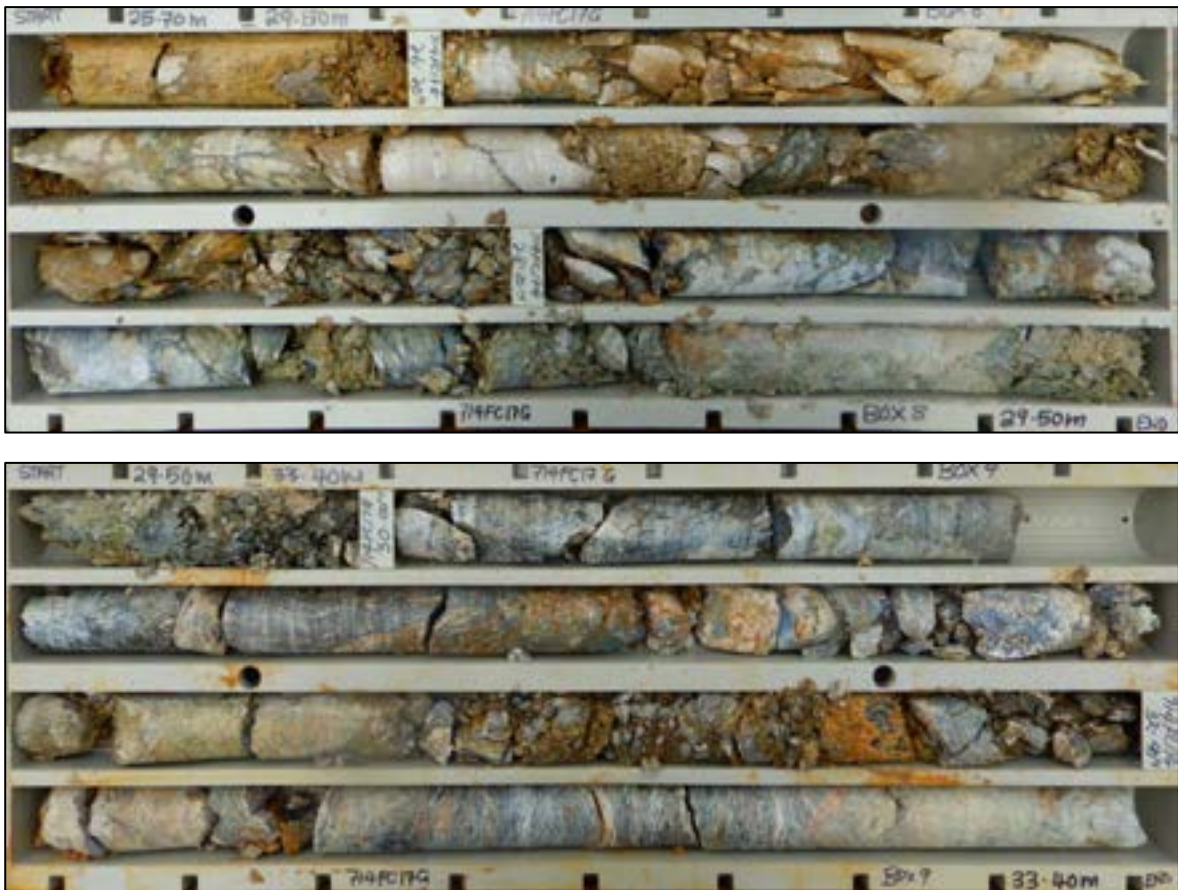


Figure 3-11: An example of third order fault conditions



Figure 3-12: A small (fourth order) fault with gouge in good quality dunite

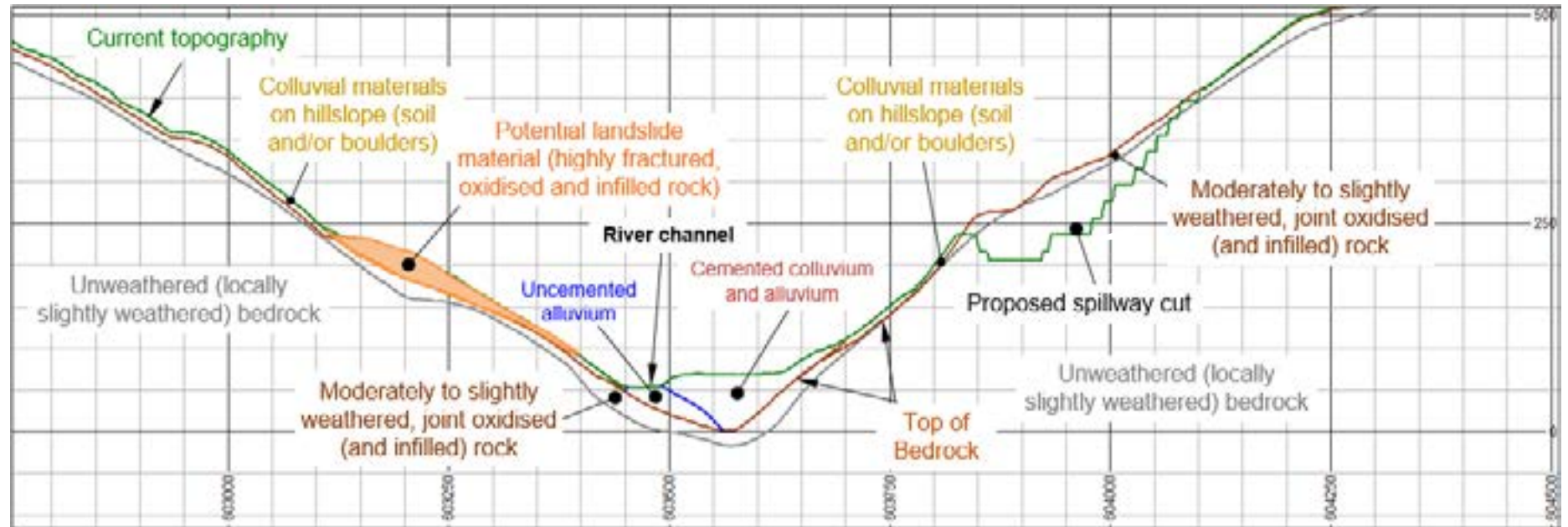


Figure 3-13: WNW–ESE section (looking north) across the valley at the FRHEP site, just upstream of the proposed embankment centreline (Northing = 9486700)

Note: This shows the typical profile of the colluvial material, weathered rock and unweathered rock, as well as a zone of highly fractured and oxidised, potentially unstable material on the left abutment at this location (not typical of the whole gorge).

3.1.5 Site investigations

Drilling program design and completion

The drill holes designed and completed in the Stage 1 and Stage 2 investigations are listed in Table 3-2 and Table 3-3 respectively.

A total of nine holes with a total length of 1207 m were completed in the Stage 1 investigations.

A total of 39 holes were drilled in the Stage 2 investigations, totalling 4,138 m of drilling. Three holes were incomplete. Two designed holes were not commenced – therefore 512 m of intended drilling was not completed. Three other holes from the original investigation plan were cancelled.

The earlier investigations completed at the site for Xstrata in 2010–2011 included 29 drill holes totalling ~2,400 m of drilling; therefore 76 holes and ~7,750 m of drilling have been completed for the site in total.

Table 3-2: Geotechnical drill holes in the Stage 1 drilling campaign

FRL drill hole number	Planned number	Easting (m)	Northing (m)	RL (m)	Dip (°)	Azimuth (°)	Depth (m)
685FC17G	LH1	603166	9487023	252	80	270	125
680FC17G	LH2	603513	9487021	59	60	105	180
688FC17G	Q5	603625	9485415	200	80	90	100
682FC17G	RH1	603913	9486980	213	65	90	147
681FC17G	RH2	603698	9486973	65	65	285	175
683FC17G	RH3	603761	9486533	165	55	315	170
686FC17G	RH4	603630	9486870	65	65	90	100
687FC17G	RH5	604013	9486700	365	75	300	110
684FC17G	OE1	598651	9478802	272	70	180	100

Table 3-3: Geotechnical drill holes in the Stage 2 drilling campaign

FRL drill hole number	Planned number	Easting (m)	Northing (m)	RL (m)	Dip (°)	Azimuth (°)	Depth (m)
697FC17G	DT1	604312	9487215	210	75	150	125
716FC17G	DT2	604290	9486954	305	82	285	250
696FC17G	DT3	604200	9486780	380	75	30	320
717FC17G	DT4	604116	9486602	420	90	0	170 of 350 Not complete
708FC17G	DTP1	604383	9487362	115	90	0	50
706FC17G	DTP2	604383	9487362	115	50	200	80
709FC17G	DTP3	603570	9486330	85	90	0	25
707FC17G	DTP4	603570	9486330	85	50	60	50
715FC17G	HT1	603934	9486910	250	75	135	150
Not listed	HT2	604017	9486692	365	70	250	66 of 250 Not complete
724FC17G	HTI1	603821	9486419	240	80	50	180
712FC17G	HTP2	603831	9487181	90	50	170	50
711FC17G	HTP3	603858	9486495	260	90	0	25

FRL drill hole number	Planned number	Easting (m)	Northing (m)	RL (m)	Dip (°)	Azimuth (°)	Depth (m)
710FC17G	HTP4	603858	9486495	260	50	90	50
699FC17G	LH3	603057	9486796	315	70	110	120
722FC17G	LH4	603208	9486560	160	75	270	75
720FC17G	LH5	603139	9486868	240	70	290	150
700FC17G	LH6	603358	9486840	115	75	110	75
729FC17G	LH7	602880	9486820	400	70	110	150
Not listed	PH1	603865	9487223	85	90	0	17 of 50 Not complete
713FC17G	PH2	603831	9487181	90	90	0	50
714FC17G	PH3	603765	9487210	65	90	0	40
Not drilled	PH4	603745	9487165	65	90	0	40 Not drilled
701FC17G	Q06	603840	9485430	250	65	160	150
690FC17G	Q07	603540	9485505	165	90	0	80
689FC17G	Q08	603650	9485225	195	60	0	100
702FC17G	Q09	603840	9485598	250	65	30	170
691FC17G	Q10	603520	9485970	180	90	0	75
692FC17G	Q11	603500	9485360	135	60	135	50
727FC17G	Q12	603670	9486180	170	90	0	75
728FC17G	Q13	603824	9486029	310	80	290	150
704FC17G	RH6	603530	9486780	70	90	0	100
723FC17G	RH7	603630	9486755	70	75	90	100
Not drilled	RH8	603725	9486680	130	75	170	75 Not drilled
698FC17G	RH9	603725	9486680	130	70	50	120
718FC17G	SC1	603935	9486850	270	90	0	240
705FC17G	SW1	604247	9487479	75	90	0	50
693FC17G	SW3	604227	9487121	265	70	270	100
695FC17G	SW4	604049	9486946	230	60	290	100
694FC17G	SW5	604017	9486692	365	60	120	100
703FC17G	SW6	603926	9486541	290	65	315	150

Geotechnical core logging

Drill run logging and structural logging was conducted at the drill rig during dayshift only. Geotechnical logging was undertaken at the core shed on completion of each hole. Geotechnical information was recorded into SRK data collection spreadsheets as summarised below:

- Drill run log: data collected for each drill run:
 - Core recovery, core loss and RQD for the run
 - Drill method (PQ, HQ, SPT, Shelby tube)
 - Confidence in orientation line

- Geotechnical log: data recorded per geotechnical interval:
 - Depth (from and to) of interval
 - Core recovery, core loss and RQD for the interval
 - Rock type
 - Weathering
 - Field estimated strength (FES)
 - Count of natural, open defects: joints and foliation counted separately; joints counted separately for three groups with alpha angles 0–30°, 30–60° and 60–90° to allow for more accurate joint spacing calculation
 - Representative structure roughness and infill for each set
 - Number of joint sets (Jn, a component of the Barton Q classification system)
 - Comments for additional description
- Structural log: data recorded for each structure (point data):
 - Depth of structure
 - Structure type
 - Alpha and beta angles (the latter only recorded if the core run was oriented)
 - Micro and macro roughness of each open structure
 - Infill type, thickness, and wall rock alteration.

The geotechnical rock logging information was used to calculate rockmass ratings for each interval. Rockmass ratings (RMR) were calculated according to the Bieniawski (1989)³⁰ system and the Laubscher (1990)³¹ mining rockmass rating (MRMR) system. The Q index value for the Barton (2002)³² classification system was also calculated. The SRK spreadsheets contain automatic calculations for different rockmass rating systems so that the results can be checked during the logging process.

The SRK spreadsheets also provide automatic calculation of dip and dip direction from the alpha and beta angle structural data, using the planned design or downhole survey results for each drill hole.

Weathering

Weathering was logged for each geotechnical interval based on the standard ISRM (2007)³³ descriptions in Table 3-4.

³⁰ Bieniawski, Z T, 1989. Engineering Rock Mass Classifications, 251 p (Wiley: New York).

³¹ Laubscher, D H, 1990. A geomechanics classification system for the rating of rock mass in mine design. Journal of the South African Institute of Mining and Metallurgy, Vol 90 (10): 257-273.

³² Barton, N, 2002. Some new Q-value correlations to assist in site characterisation and tunnel design. International Journal of Rock Mechanics and Mining Sciences, 39: 185-216.

³³ ISRM, 2014. The ISRM Suggested Methods for Rock Characterization, Testing and Monitoring: 2007-2014. Editor Reşat Ulusay. Springer August 2014.

Table 3-4: Interval weathering descriptions

Term	Abbreviation	Description
Unweathered (Fresh)	UW	No visible signs of weathering
Slightly weathered	SW	Partial (<5%) staining or discolouration of rock substance, usually by limonite. Colour and texture of the fresh rock is recognisable. No discernible effect on strength properties of the parent rock type.
Moderately weathered	MW	Staining or discolouration extends throughout all rock substance. Original colour of the fresh rock is no longer recognisable.
Highly weathered	HW	Limonite staining or bleaching affects all rock substance and other signs of chemical or physical decomposition are evident. Colour and strength of the fresh rock are no longer recognisable.
Completely weathered	CW	Rock has soil properties, i.e. it can be remoulded and classified according to the Unified Soil Classification System (USCS), although the texture of the original rock can still be recognised.

Source: ISRM, 2007.

It is normal for there to be variation between successive geotechnical intervals; change in weathering grade is one of the main determinants for geotechnical interval delineation (along with change in rock type, strength or fracture frequency). Where appropriate during later interpretation, adjacent intervals have been combined. For example, intervals of SW and HW rock may be present in a zone of predominantly MW rock.

Strength

Strength was assessed in the field during logging (called the field estimated strength or FES) and by laboratory UCS testing and point load testing.

The FES of the intact rock was estimated using the standard ISRM grades provided in Table 3-5 (rock) and Table 3-6 (soil).

Table 3-5: Field estimates of uniaxial compressive strength

ISRM grade	Term	UCS (MPa)	Tactile test
R6	Extremely strong	>250	Rock material only chipped under repeated blows, rings when struck.
R5	Very strong	100–250	Requires many blows of a geological hammer to break intact rock.
R4	Strong	50–100	Handheld specimens broken by a single blow of a geological hammer.
R3	Medium strong	25–50	Firm blow with geological pick indents rock to 5 mm, knife just scrapes surface.
R2	Weak	5–25	Knife cuts material but it is too hard to shape.
R1	Very weak	1–5	Material crumbles under firm blow of geological pick, can be shaped with a knife.
R0	Extremely weak	0.25–1	Indented by thumbnail.

Source: ISRM, 2007.

Table 3-6: Field estimates of soil consistency

Grade	Consistency	Approximate strength (kPa)	SPT N-value	Tactile test
S6	Hard	>400	>32	Indented by thumbnail with effort.
S5	Very stiff	200–400	16–32	Readily indented by thumbnail.
S4	Stiff	100–200	8–16	Indented by thumb.
S3	Firm	50–100	4–8	Penetrated by thumb with moderately effort.
S2	Soft	25–50	2–4	Easily penetrated 5 cm by thumb.
S1	Very soft	<25	<2	Easily penetrated 5 cm by fist.

Source: ISRM, 2007.

Downhole televiewer

Acoustic and optical televiewer surveys were undertaken in nine of the geotechnical investigation drill holes. The upper limits of the televiewer survey intervals are constrained by the depth of PQ drilling and casing installation, which was typically advanced to a depth of approximately 30 m. The lower limits of the televiewer survey intervals are defined either by the bottom of the drill hole, or by blockage of the hole in unstable ground.

Table 3-7 summarises the interval depths for optical and acoustic televiewer (ATV/ OTV) surveys, the total count of discontinuities picked in each hole, and the average number of discontinuities picked per metre.

Table 3-7: Summary of televiewer survey intervals and structure counts

Planned hole number	FRL hole number	OTV		ATV		Structures picked	Structures per metre (m ⁻¹)
		From (m)	To (m)	From (m)	To (m)		
Q6	701FC17G	32.5	41.8	41.8	149.3	322	2.8
Q9	702FC17G			38.4	121.8	310	3.7
RH9	698FC17G			13.4	119.6	271	2.6
DT2	716FC17G	35.7	108.4	108.4	248.8	165	0.8
LH7	729FC17G	44	119.8			219	2.9
HT1	715FC17G	26.7	116.6	116.6	149.7	185	1.5
SC1	718FC17G	29	134.5	134.5	199.8	232	1.4
LH5	720FC17G			65.6	149.6	264	3.1
LH4	722FC17G	17.7	67.5			340	6.8
SW6	703FC17G	23.2	54.5	54.5	56.6	81	2.4

Approximately 1,055 m of televiewer survey data were collected, with 2,389 discontinuities manually identified.

Sampling for laboratory testing

Core samples were taken from all drill holes for laboratory testing of geotechnical properties. More samples were collected than were planned to be tested to allow for possible sample breakage during transit to the laboratory and to ensure adequate coverage of material types and spatial distribution.

Testing for both soil and rock materials was undertaken at Trilab in Brisbane.

The aim of the testing was to identify the strength, durability and elastic/ plastic properties of soils and rocks to form part of the FRHEP embankment foundations and be used as construction materials for the embankment. The testing program is summarised in Table 3-8 and included the following:

- Particle size distribution (PSD) determination, including sieving and hydrometer, to identify the soil components and fines content of the soil materials
- Atterberg limits (liquid limit, plastic limit and shrinkage limit) testing to determine the plastic properties of soil materials
- Emerson Crumb testing to determine dispersivity characteristics of the soil materials
- UCS testing, including Young's modulus and Poisson's ratio determination on selected samples, to assess the compressive strength and elastic behaviour of rocks
- Direct shear testing (DST) of joint planes to assess defect shear strength
- Shear test on saw-cut core sticks to assess the base friction angle of the rock
- Slake durability testing to evaluate the potential for rock decomposition (in the short term) on exposure to the elements (wetting and drying)
- Los Angeles (LA) abrasion testing to assess aggregate toughness and abrasion characteristics.

Table 3-8: Summary of laboratory testing undertaken

Test	Number of tests
Unconfined compressive strength	81
Elastic properties Young's modulus and Poisson's ratio	29
Direct shear testing on natural discontinuities	27
Saw-cut shear box test	5
Particle size distribution & Atterberg limits	14
Emerson Crumb	4
Slake durability	29
LA abrasion	13

Details of tests and test results are provided in Section 3.1.7.

Permeability testing

Hydrogeological testing of permeability (hydraulic conductivity) was conducted for characterising the permeability (in m/s) of the rockmass below/ adjacent to the embankment foundations. Testing methods included Lugeon (packer) testing and falling head testing.

Lugeon testing was undertaken using the pneumatic, single-packer system. The original intent was to conduct packer testing at intervals of 40–50 m downhole. Tests were run over intervals ranging from 5 m to 70 m, according to the following constraints:

- Hole diameter: HQ diameter packer testing was conducted only.
- Ground conditions: packer testing was commenced only from depths at which the rock was of sufficient quality that a good packer seal could be confidently achieved and at which there was a low risk of damage to the packer. This generally included slight or moderate weathered rock that was not highly fractured or fragmented.
- Hydraulic conductivity: in zones of very high permeability it was impossible to build up pressure in the hole in order to conduct the packer testing.

Lugeon tests were conducted at a range of pressures (often 100, 200 and 300 kPa, but less in zones of high permeability (k) or weak rock). Results were plotted, and hydraulic conductivity was interpreted based on the distribution of flow at different pressures, as per standard practice.

Falling head testing was conducted where packer testing was not possible due to the constraints listed above. In general, falling head testing provides lower confidence results, but these simple tests can be run in soil and weathered rock profiles where packer testing cannot be conducted. Care was taken that falling head testing was not conducted over intervals that straddled the groundwater level and/ or the PQ/ HQ drilling diameter changeover depth.

The compilation table provides a summary of the testing to date on the FRHEP site, as well as comments on specific tests that were judged to have been 'failed' tests (for various reasons) or 'suspect high k' zones. It is important not to exclude the suspect tests from the program dataset, as often in packer testing very high k zones can produce test results that appear to be erroneous but are simply beyond the measuring capability of the test equipment. Therefore, each of these suspect test zones was compared to core and the geology model to establish if it was a failed test or a test exceeding the k testing ability. Those considered to be high k test zones have been included in the assessment.

Table 3-9: Summary of permeability tests

Drill hole number	Drilling Stage	Number of tests
F1	2011	5
F2	2011	2
F3	2011	1
S1	2011	3
S2	2011	1
S4B	2011	1
LH1	Stage 1	3
LH2	Stage 1	3
RH1	Stage 1	3
RH2	Stage 1	2
RH4	Stage 1	3
RH5	Stage 1	2
DT2	Stage 2	4
DT4	Stage 2	2
HT1	Stage 2	6
LH3	Stage 2	4
LH5	Stage 2	7
LH6	Stage 2	4
PH2	Stage 2	1
RH6	Stage 2	6
RH7	Stage 2	10
RH9	Stage 2	8
SW6	Stage 2	6

Piezometer installation

Vibrating wire piezometers (VWPs) were installed in two drill holes on the FRHEP left abutment; however, on installation the VWPs were damaged when the drill rods were removed. The VWPs were intended for installation in a further three holes that were unable to be completed. The holes were fully grouted after VWP installation. The aim of VWP installation was to be able to obtain a record of groundwater level and pore water pressure (pwp) within the embankment footprints prior to embankment construction.

Table 3-10: Summary of piezometers installed

Drill hole number	Depth of piezometer	Comment
LH5	75 m and 150 m	Damaged by drill crew
LH6	75 m	Successfully installed
RH8	75 m	Not installed due to program termination
DT4	200 m and 350 m	Not installed due to program termination
HT2	150 m and 250 m	Not installed due to program termination

Extensometer installation

Two 80 m long extensometers, with anchors at depths of 10, 20, 35, 50, 65 and 80 m, were installed in the left abutment to measure slope movement in the potential landslide zone (described in Section 3.1.4). The extensometers were installed in drill holes LH7 and LH5.

Groundwater depths

Standing water levels were measured in numerous drill holes across the site. These were used to help establish the groundwater levels across the site. The measured water levels are listed in Section 3.1.5, together with a description of the groundwater surface across the FRHEP gorge.

Geophysical survey

Draig Geoscience Pty Ltd (Draig) carried out a geophysical survey in the form of seismic refraction traverses. The detailed methodology and results of this geophysical investigation are presented in the Draig draft report, 'Geophysical Investigation Seismic Refraction, PanAust Frieda River Copper-Gold Project', report number DG1508SRK, dated 28 April 2018.

Seismic refraction survey was carried out along three traverse lines: two lines (Lines 1 and 2) effectively forming a continuous traverse across the left abutment, and a short traverse (Line 3) along the original proposed footprint of the powerhouse on the river terrace on the eastern bank of the river (downstream from the embankment footprint). The lines were modified slightly from the design during field investigations to be able to deal with locally very difficult conditions (terrain and vegetation).

The alignment of the powerhouse has subsequently been changed; however, Line 3 passes through the southern end of the new proposed footprint and provides a good insight into the subsurface profile of the river terrace in this vicinity.

A diagram showing the positions of these traverses is provided in Figure 3-14. A traverse similar to the one on the left abutment was not carried out on the right abutment as it was impractical in the very steep terrain; it was also thought to be largely unnecessary due to the very shallow depth to the bedrock, although future traverses over limited sections may be considered.

Draig produced sections along each traverse line showing the contoured P-wave velocity (V_p) in m/s. These velocities can be used to infer material type and quality – velocities are lower in low density materials such as soil, highly weathered rock and highly fractured/ fragmented rock (fault zones), and higher in good quality, strong bedrock. The contoured V_p sections for Lines 1 and 2 on the left

abutment are shown in Figure 3-15, and a 3D (isometric) view of these two sections is shown in Figure 3-16. The contoured Vp sections for Lines 3 on the eastern side of the river is shown in Figure 3-17.

From the results of the seismic refraction surveys and drilling data, SRK has interpreted an approximate general range of correlation of Vp with several of the main geotechnical domains identified from the drilling investigation. The interpreted approximate correlations with Vp are listed in Table 3-11.

It is important to note that, as mentioned in Draig's report, correlations of Vp with weathering/ rock hardness are variable along each traverse line and within each drill hole. The correlations summarised in the table represent an attempt to provide some general guidelines to assist with the extrapolation/ interpolation of interpreted geotechnical conditions at the FRHEP site.

Table 3-11: Interpreted correlation of Vp with geotechnical horizons

Material	Approximate Vp range
Valley floor colluvium and alluvium (cemented)	2,500–4,000
Soil-like colluvium	0–1,500
Colluvium with boulders	1,500–3,000
Weathered rock with oxidised, infilled joints top layer of 'bedrock'	3,000–4,300
Strong to very strong SW and UW rock	>4,300
Potential landslide (unstable) zone – sheared and oxidised rock	<3,900

The Vp data allows for a more detailed and confident interpretation of the positions of fault zones to be made. Fault zones can be interpreted within obvious zones where low Vp values extend to greater depth, although such zones of low Vp are not exclusively indicative of faulting, therefore topographical assessment and/ or drill hole data have been used to attempt to confirm fault zones. Faults can also be interpreted in narrow Vp anomalies (lows), or on the margins of wider lows, especially where apparent bedrock depth falls away sharply.

The Vp contour patterns for Lines 1 and 2 show the significant depth of relatively poor material (Vp is less than 2,000 m/s and then between 2,000 m/s and 3,900 m/s) in the upper part of the traverses where they have crossed the ridge on the left abutment on which the potential landslide materials have been encountered. Two embayments are evident – one in each traverse at similar levels (RL 150 m), presenting evidence of a shallow-dipping fault dipping back into the hillside (described in Section 3.1.10). The Vp contour patterns on the lower (left hand) side of Line 1 show a greater depth of bedrock and thicker colluvial materials on the lower hillside of the western side of the gorge, upstream of the embankment.

Line 3 shows relatively high Vp values (2,500 m/s and greater) from the surface in the river terrace on the right hand side of the river, near the proposed powerhouse. Vp values above 3,500 m/s are encountered from a 20 m depth or less. These patterns illustrate the relatively dense, strong nature of cemented colluvial and alluvial materials. A fault (oblique to the section) interpreted near hole PH1 may be responsible for the lower Vp values to a greater depth in the eastern part of the traverse, or this could be the result of a locally thicker accumulation of loose colluvial material at the toe of the slope.

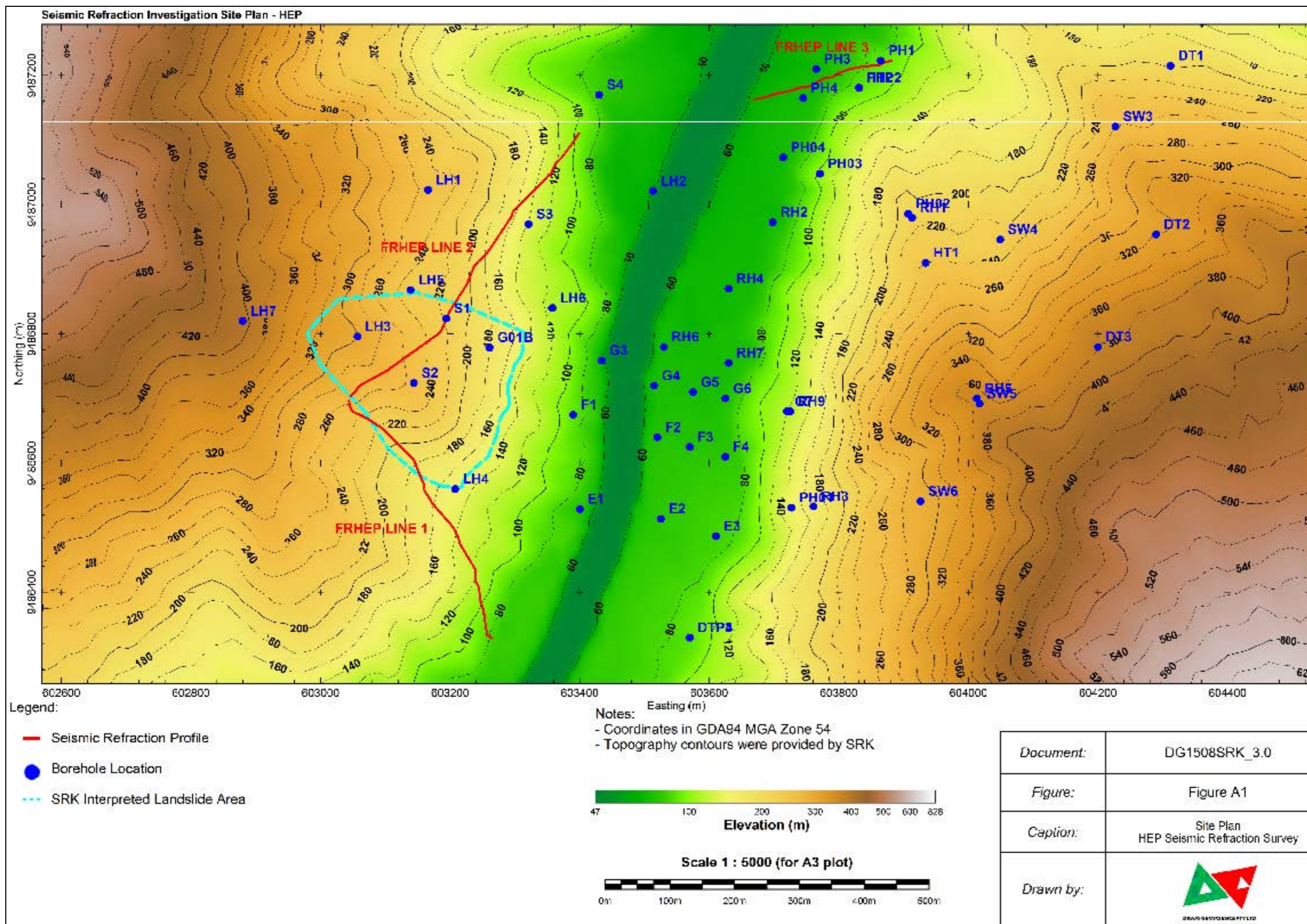


Figure 3-14: Positions of seismic refraction survey lines in plan view, with reference to contours and drill hole collar positions from various phases of investigation

Source: Draig, April 2018.

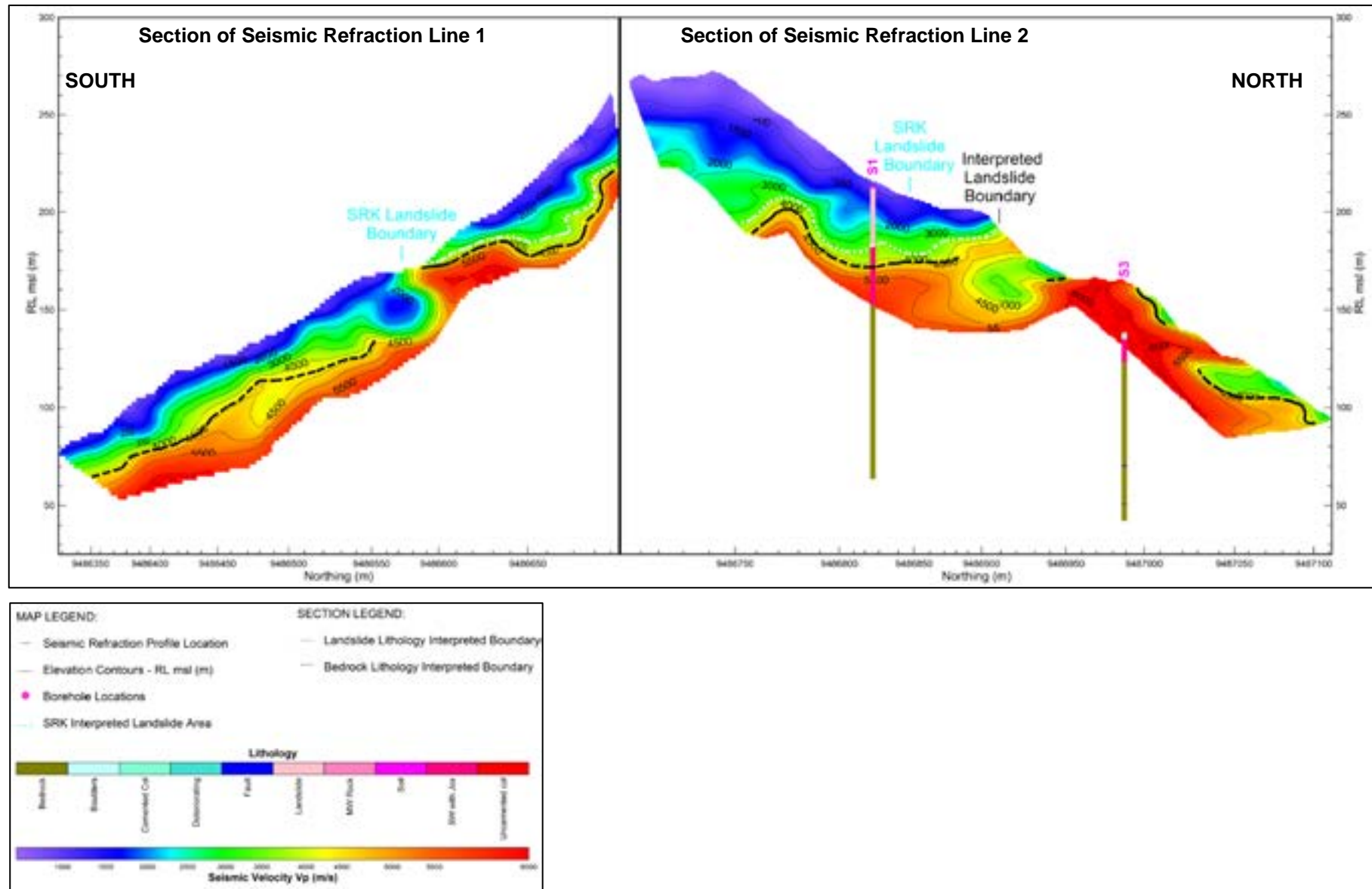


Figure 3-15: Combined section view (fence diagram) along Line 1 (left) and Line 2 (right), looking west, showing the V_p contours

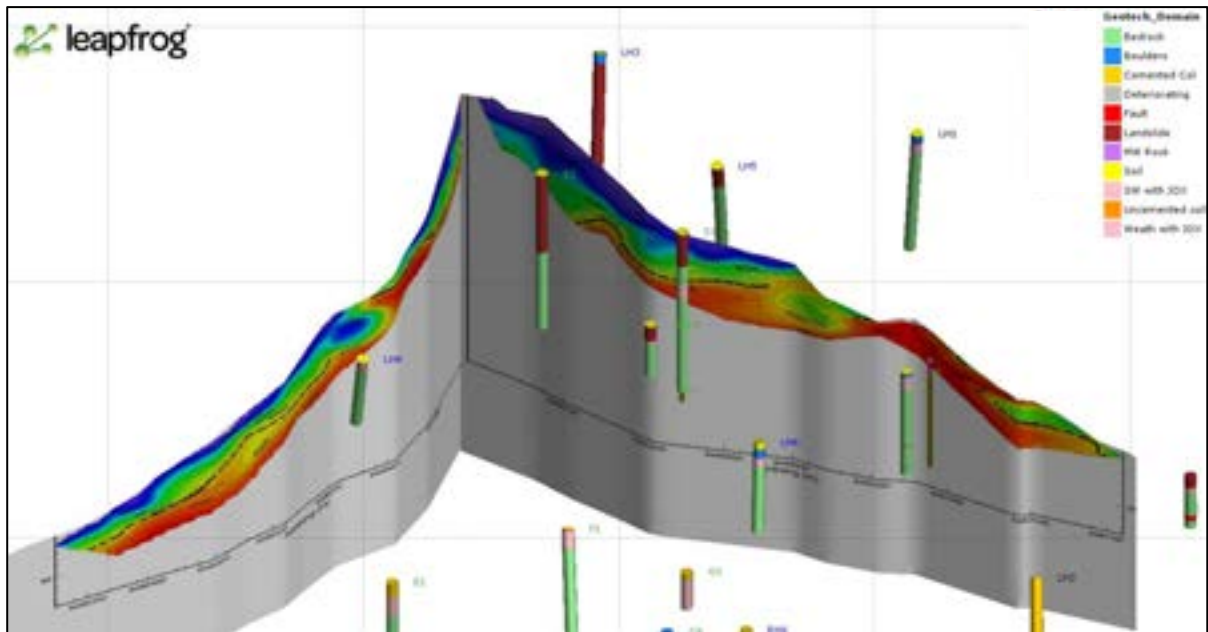


Figure 3-16: Isometric view of the Line1 and 2 contoured Vp sections and nearby drill holes, looking west

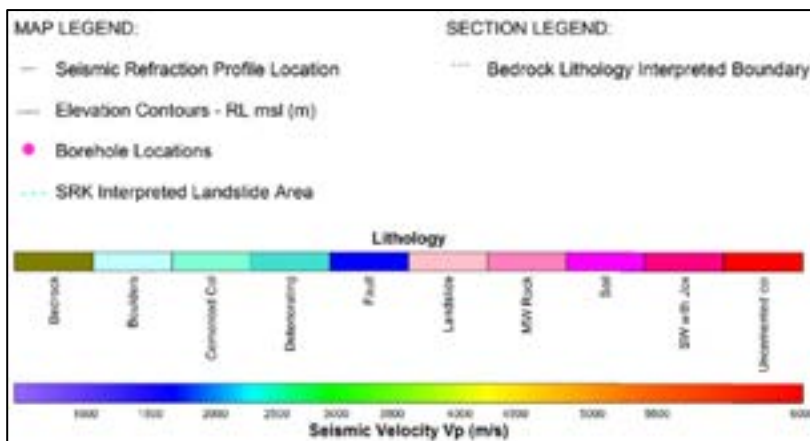
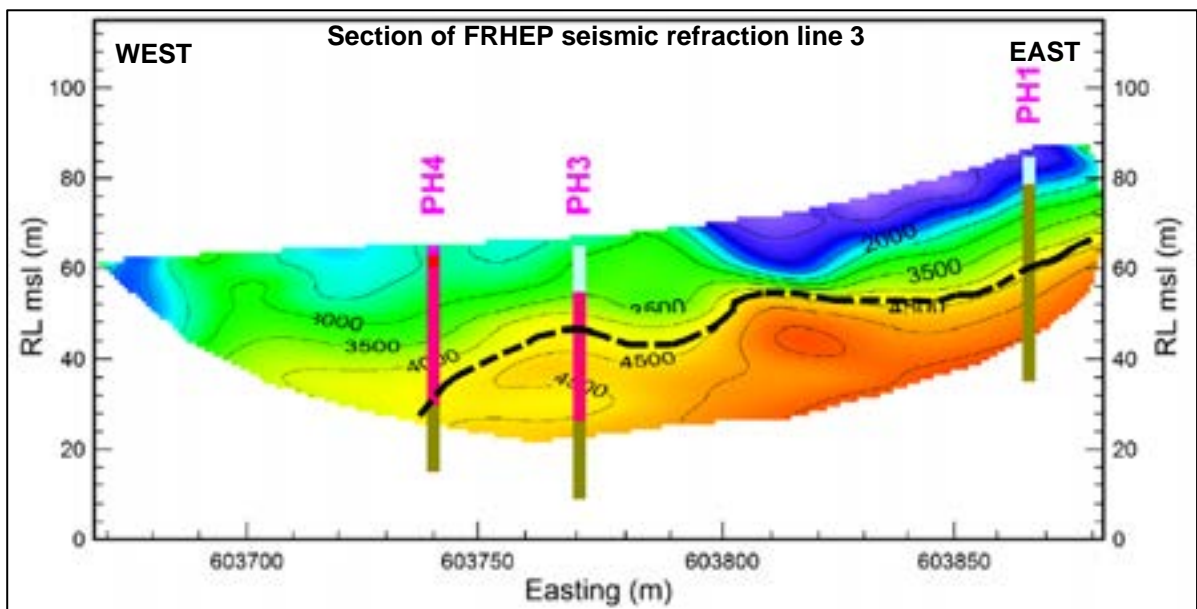


Figure 3-17: Section view along Line 3, looking north

3.1.6 Geotechnical domains

The nature of the dunite and the steep nature of the topography (particularly on the right abutment – as shown in Figure 3-18) have resulted in a very thin colluvial and weathering profile: bedrock is usually encountered within 1–5 m from the surface. A very thin layer of soil-like colluvium is present, with boulders in zones where lower angle slopes have allowed for their accumulation. The upper part of the bedrock consists of moderately to slightly weathered rock with strong joint oxidation and infill down to a variable depth – often less than 15 m in thickness, but sometimes of thickness up to ~30 m, particularly below the valley floor colluvial and alluvial materials. On steep hillsides it appears that the joints have dilated and been infilled with soil-like colluvium. The underlying rock is generally unweathered, but contains localised zones of pervasive oxidation along fractures. This is represented diagrammatically in Figure 3-19.

Relatively small faults have been encountered during drilling, presenting zones of highly fractured rock and/ or fault gouge 0.2–2 m in width. Permeability in these zones can be moderate to high (10^{-7} to 10^{-5} m/s); however, overall rockmass permeability is low to moderate (10^{-9} to 10^{-7} m/s). Localised zones of highly veined, serpentinised, weaker (deteriorating) rockmass have been encountered locally within drill holes; however, overall, the rockmass quality is good with strong rock and relatively low fracture frequency.



Figure 3-18: Photograph of the steep right abutment, looking southeast, showing drill pads

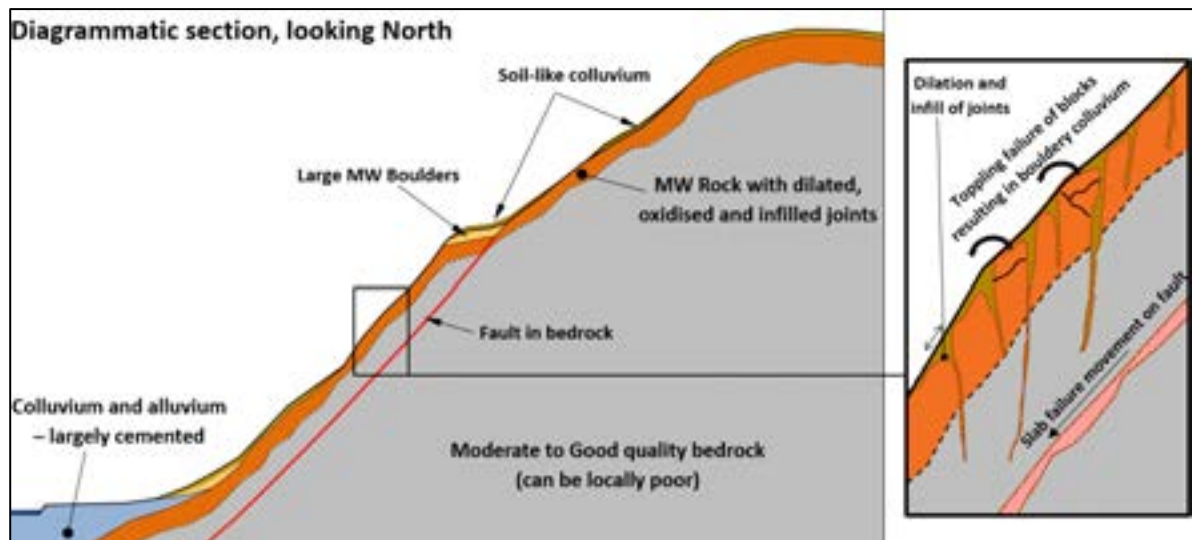


Figure 3-19: Diagrammatic cross-section through the right abutment, looking north

From the field investigations, 14 types of subsurface conditions were initially identified. These have been rationalised and simplified into eight main types:

- 1 Soil-like colluvial cover
- 2 Cemented (2a) (and locally uncemented – 2b) colluvium and alluvium in the valley floor
- 3 Large boulders (highly weathered (HW) to SW, usually MW) clast-supported in a colluvial matrix
- 4 Potential landslide zones – highly fractured rock with shear zones, oxidised and/ or deteriorated rock, and soil-like joint infills
- 5 MW to SW (occasionally HW) rock, with dilated, oxidised, infilled joints
- 6 Significantly deteriorated poor quality serpentinite bedrock
- 7 Moderate to good (locally poor) quality bedrock
- 8 Fault zones (three types: close fracturing, numerous small individual faults, fragments and gouge).

A 3D model of the distribution of the geotechnical material types has been constructed in Leapfrog software³⁴. Two cross-sections through the model, illustrating the positions of the materials types, are shown in Figure 3-20.

³⁴ Leapfrog (Geo) Version 4.1, 2018, www.leapfrog3d.com, ARANZ Geo Ltd.

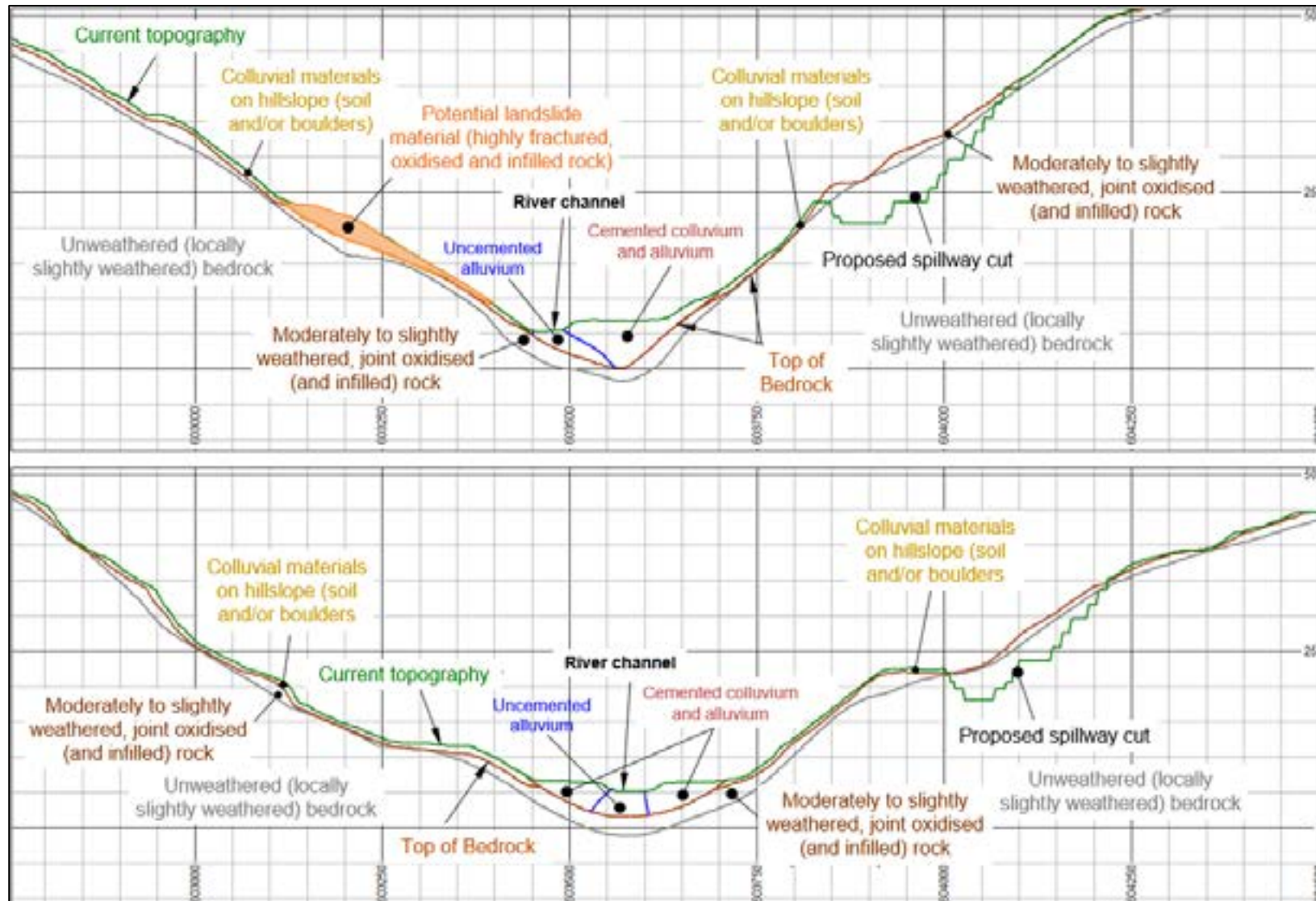


Figure 3-20: Selected WNW – ESE sections (looking north) across the valley of the FRHEP site, showing the geotechnical model (above) slightly upstream of the proposed embankment centreline (Northing = 9486700), and (below) the approximate position of the hydroelectric powerhouse downstream (Northing = 9487200)

Soil-like colluvial cover

Soil-like colluvial cover is generally less than 3 m in thickness; examples of variations in the thickness of the soil-like colluvial cover are shown in Figure 3-21 and Figure 3-22. As such, the material will be completely excavated from beneath the FRHEP embankment, therefore, no attempt has been made to characterise it in detail for input into infrastructure design assessments.

Laboratory testing indicates that the colluvium is a gravelly-clayey silt or clayey-silty sand. Logging indicates varying amounts of subrounded to subangular gravel and cobbles. The fines component classifies as MH (silt of high plasticity).



Figure 3-21: 3 m of soil-like colluvium in drill hole SW5



Figure 3-22: Bedrock at surface in drill hole SW6

Valley floor colluvium and alluvium

The valley floor colluvium and alluvium (both cemented and uncemented) is up to 70 m in thickness in the centre of the valley.

The cemented colluvium consists of coarse irregular fragments of dunite of varying sizes (some very large) in a cemented matrix. The material is largely clast-supported with localised matrix-supported material (Figure 3-23). The matrix is generally of 2–10 MPa in strength (from logging and laboratory testing), and is often, but not always, oxidised. The cemented matrix is shown to have locally deteriorated in parts of some drill holes, presenting softer material. The cemented alluvium, generally found beneath the river channel at depths greater than ~25 m, has similar properties; however, the matrix is generally not oxidised and the clasts are smaller (cobble-sized and small boulder-sized) and rounded to subrounded (Figure 3-24).

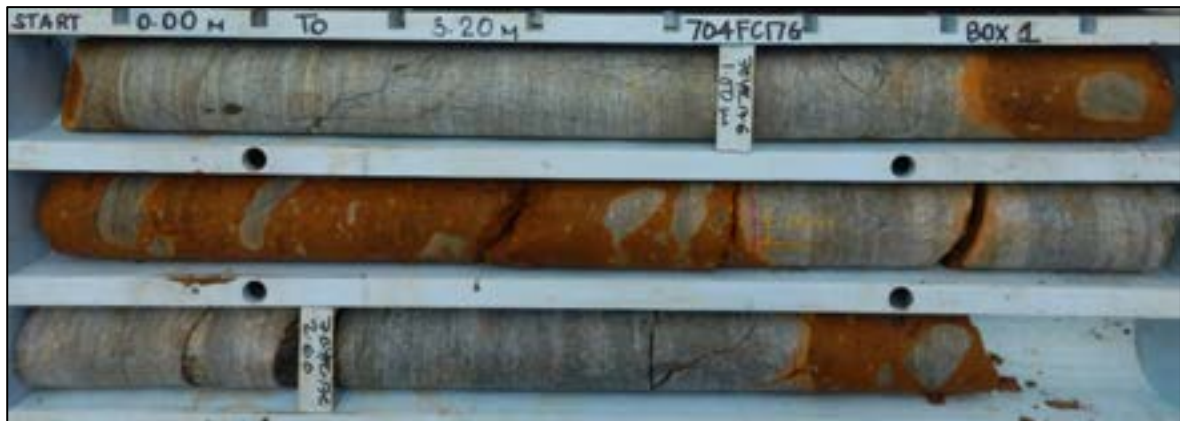


Figure 3-23: Cemented colluvium in drill hole RH6: large subangular to angular boulders with an oxidised matrix

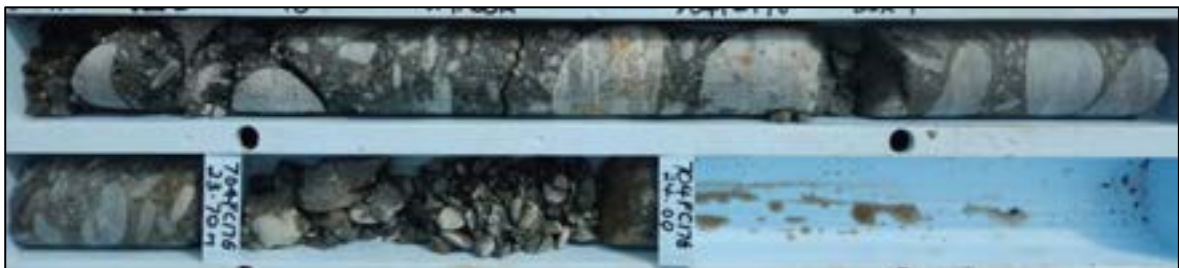


Figure 3-24: Cemented alluvium in RH6: cobble- and pebble-sized, rounded clasts in an unoxidised matrix (zone of poor cementation apparent below 23.7 m)

Large boulders (hillside colluvium)

Large boulders are found as part of the colluvial material in localised areas on the slopes – usually in areas of less steep topography (side ravines, breaks in the slope, and at the slope toe). An example of such material is shown in Figure 3-25. It can sometimes be difficult in drill core to distinguish between large boulders with small volumes of soil-like matrix and bedrock with open, oxidised, infilled joints.

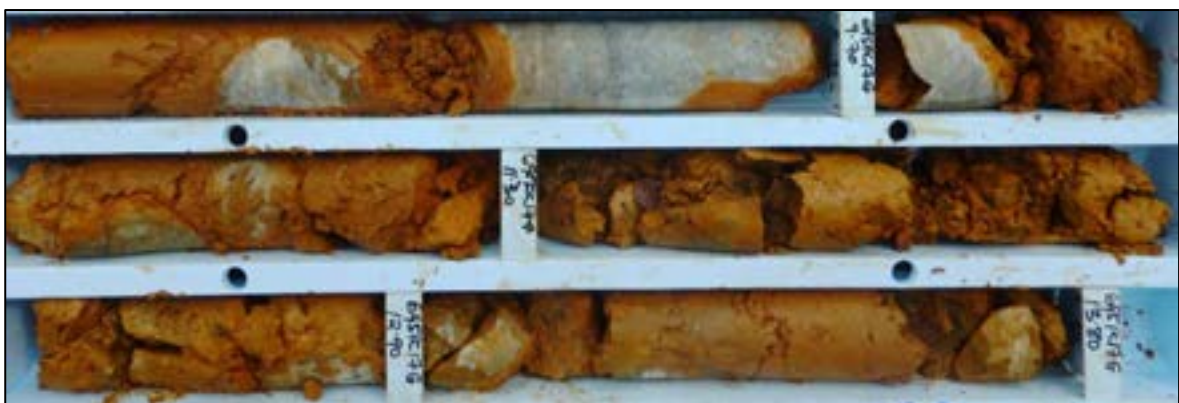


Figure 3-25: Partially weathered boulders, clast supported in an oxidised soil-like colluvial matrix

Potential landslide zones

In places with a matrix breakdown of previously recemented and oxidised breccia, a large zone of highly fractured/ oxidised rock has been identified on the left abutment, slightly upstream from the centreline of the proposed embankment. Significant thicknesses of such materials (up to 115 m of

drilled thickness; ~75 m normal to the slope) were encountered in drill holes S02 (an old 2011 investigation hole), LH3 and LH7. Lesser thicknesses of such materials were encountered in LH5 and S01, which are on the northern margin of the zone, and the zone is not present at all in LH4 which was drilled to the south. In LH6, downslope to the east, a more regular profile of bouldery colluvium nearer to the toe of the slope is encountered.

The material is probably less 'bouldery' than it appears in the drill core, and will likely be more 'slabby' (large slabs of rock with poor quality shear areas in between) overall. The nature of the material, in terms of potentially locally high permeability and the stability risk it presents during construction and maintenance of the embankment and associated infrastructure (especially where undercut at the toe), means that it will require to be removed prior to embankment construction. The large volumes of relatively intact rock in much of the zone indicate that it will likely require blasting for excavation and removal. Figure 3-27 and Figure 11-13 show an example of this material from drill hole LH3. OTV imagery of this material in LH7 is shown in Figure 3-28. This zone has been encountered in several drill holes and can therefore be delineated with a degree of accuracy; however, its precise upslope extent has not been delineated with confidence. The overburden material above the landslide zone is soil-like colluvium, in places with boulders having similar characteristics to the overburden material in the right abutment (Figure 3-30).

An additional potential zone (although much smaller in thickness and extent) has been identified down to a 26 m depth in drill hole SW4 in the right abutment, downstream of the embankment (near the proposed powerhouse). This zone comprises colluvial boulders of thickness greater than usual (Figure 3-31), with an underlying zone of fractured, oxidised and infilled rock below. It represents colluvial material collected in the lower angle slopes of the ravine in this area, and it has been identified in a single drill hole only; a conservative interpretation of its possible extent, based on the topography, has been provided in the Leapfrog model. However, it is necessary to flag the potential for less stable hillside material in this zone. It may be possible to use this material to form part of the upper slope in the western side of the spillway cut. The extent of the interpreted zones on the left and right abutments are shown in Figure 3-26.

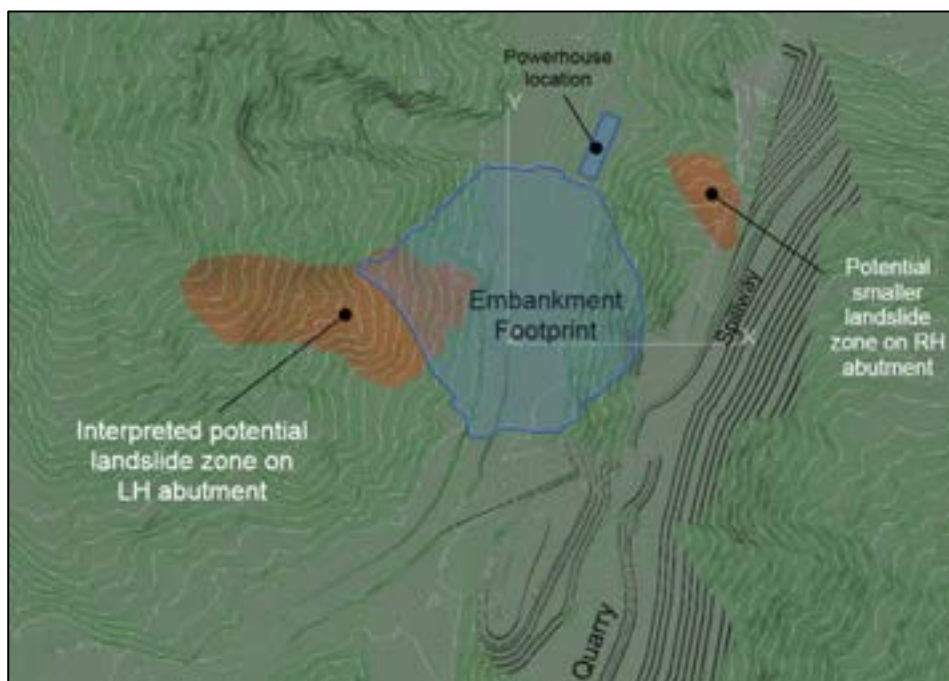


Figure 3-26: Isometric view of the Leapfrog model (from above) showing the interpreted large landslide zone on the left abutment and potential smaller zone on the right abutment



Figure 3-27: Core photograph showing variability of zones of highly fractured and oxidised rock with deteriorating matrix and/or soil-like infill in drill hole LH3 (66–80 m)



Figure 3-28: Downhole OTV image in drill hole LH7 showing potential landslide materials below 70 m depth downhole

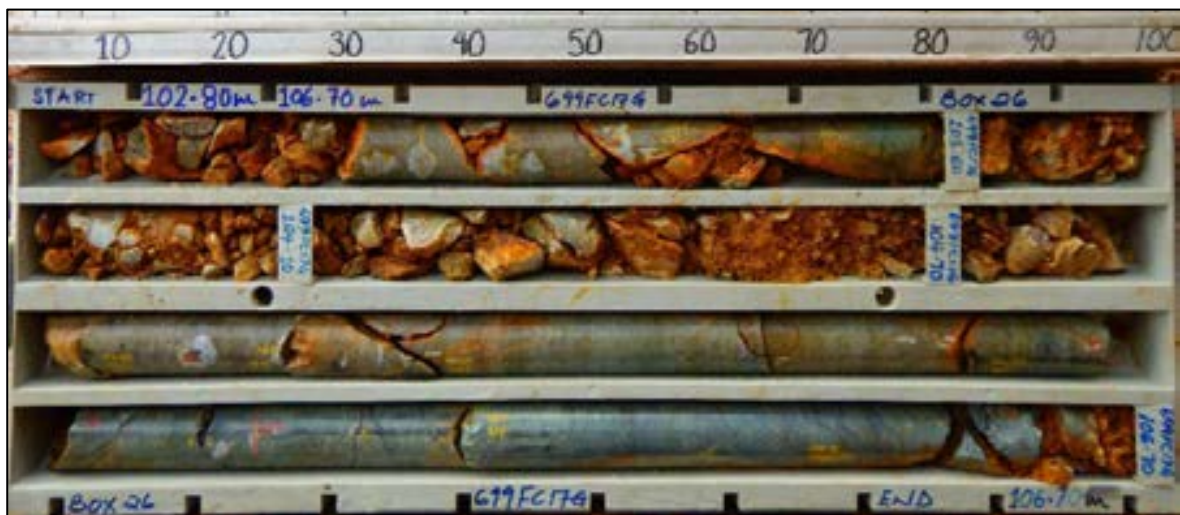


Figure 3-29: Core photograph from drill hole LH3 showing base of potentially unstable 'landslide' zone (102.8–106.7 m)



Figure 3-30: Core photograph showing soil-like overburden material immediately above highly fractured rock in drill hole LH7 (6.4–10 m)



Figure 3-31: Drill hole SW4 showing boulder overburden material over the bedrock (17.5–19.9 m)

Weathered rock with oxidised, infilled joints

The upper part of the bedrock consists of moderately to slightly weathered rock with strong joint oxidation and infill down to a variable depth – often less than 15 m thick, but sometimes up to ~30 m, particularly below the valley floor colluvial and alluvial materials. On steep hillsides it appears that the joints have dilated and been infilled with soil-like colluvium (and/ or highly oxidised thick joint infill). This material is illustrated diagrammatically in Figure 3-19. Examples are shown in Figure 3-32 and Figure 3-33.



Figure 3-32: Moderately to slightly weathered bedrock with thick joint infills



Figure 3-33: Slightly weathered to unweathered bedrock with joint infills of variable thickness (left), shown in acoustic televiwer survey image (right)

Deteriorated serpentinised bedrock

Deteriorated serpentinised material was encountered in seemingly irregular zones within the bedrock, where deterioration of a serpentinite matrix of previously brecciated and re-healed rock has occurred. It was encountered in the 2011 quarry investigation holes Q3 and Q4 (far to the north of the embankment), in holes SW3 and DT1 (on the eastern side of the spillway cut, to the northeast of the embankment), and in holes Q5, Q6, Q8 and Q11 in the south of the original quarry target area. Examples of deteriorated serpentinised rock in hole Q6 are shown in Figure 3-34.

This material occurs only in very localised zones in the abutment areas, which are very difficult to delineate, with the possible exception of an area near the spillway and diversion tunnels in the region of holes SW3 and DT1, although deterioration is not intense over significant areas. This material is encountered in extensive zones in the south part of the original quarry target area – resulting in this area being discounted as a potential source of construction material.

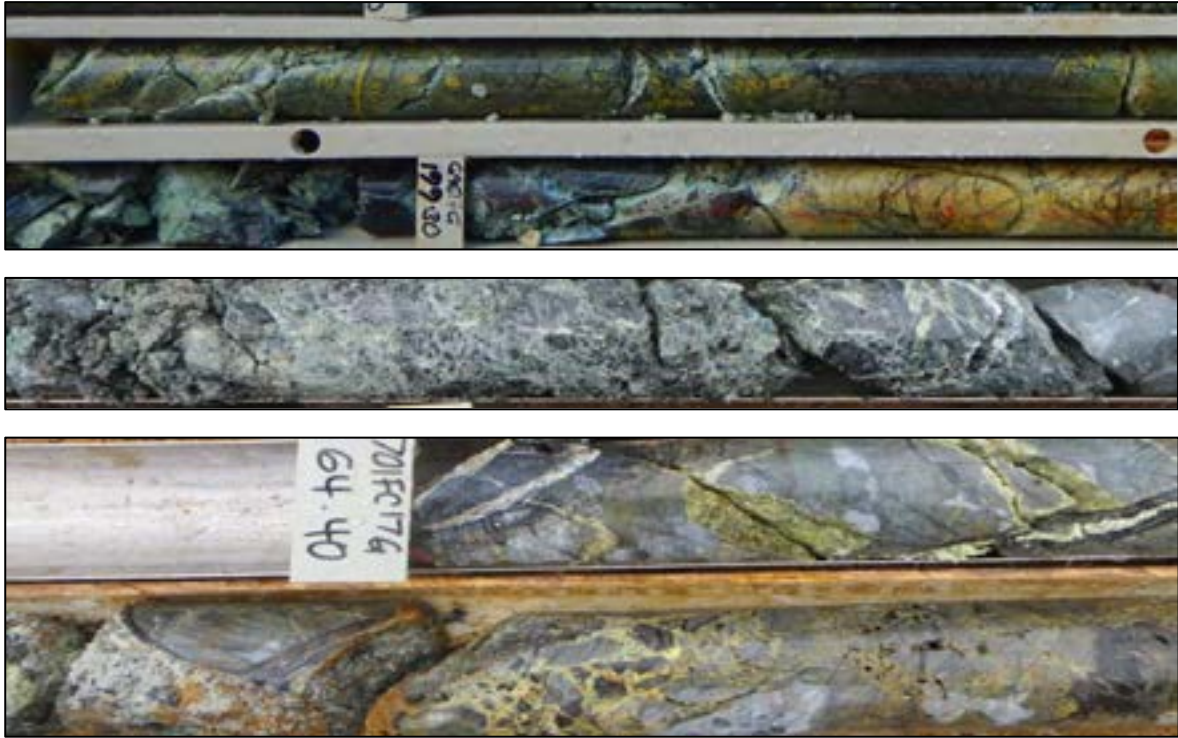


Figure 3-34: Examples of serpentinised bedrock in varying stages of deterioration

Moderate to good quality bedrock

The bedrock below the weathered zone is generally of good quality (moderately to sparsely fractured rock of high strength (50–100MPa). An example of good-quality dunite bedrock is shown in Figure 3-35. Calcite and quartz veins and old healed breccia textures (with cryptocrystalline olivine cement and intense veining) are often present. However, in places the bedrock can be of variable quality, with localised zones of moderately to highly fractured bedrock with oxidised joints, or local serpentinisation.

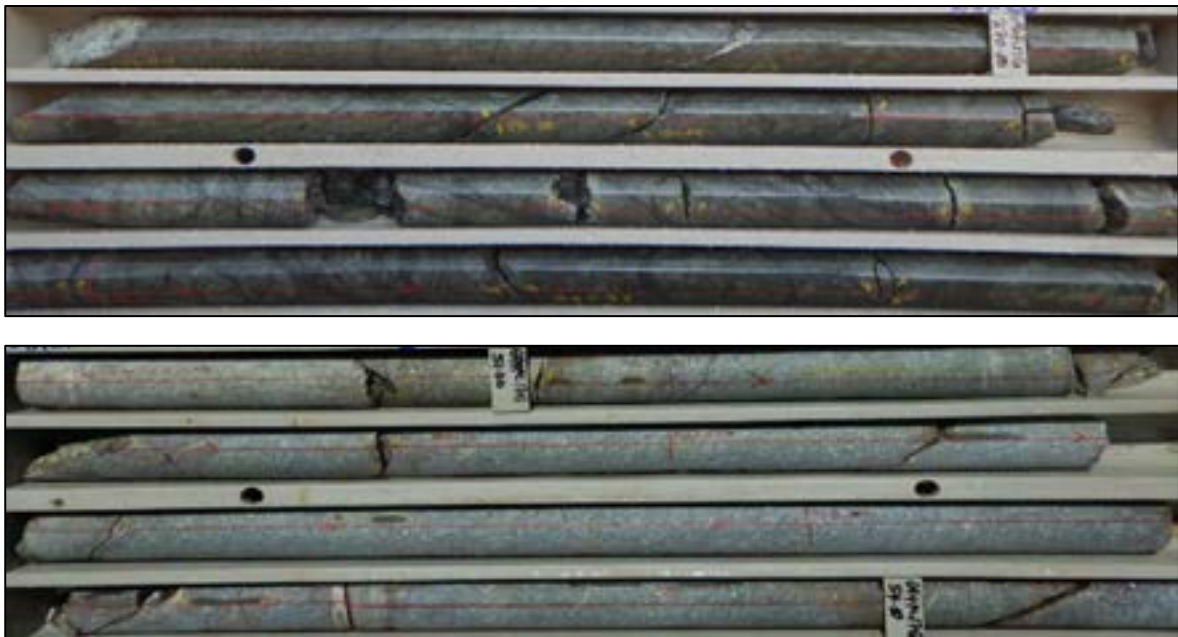


Figure 3-35: Examples of good-quality bedrock: strong and moderately to sparsely fractured

Fault/ shear zones

Faulting at the FRHEP site is described in detail in Section 3.1.10. A classification describing four orders of faults is applicable for the FRHEP site. The larger, regional first and second order structures are not encountered in the FRHEP gorge. Third order faults include significant damage zones up to a few metres in width (or wider disturbed zones of general disturbance with serpentinite – often with close fracturing, with or without oxidation) and tens of metres in overall width. Fault breccia/ gouge with re-healing and current smaller shears with gouge or mylonitisation may be present. Few of these structures have been identified at the FRHEP site. An example is shown in Figure 3-36.

Fourth order faults are common at the FRHEP site; these are networks of smaller faults and shears that may present small zones of breccia or gouge a few tens of centimetres wide, or highly fractured rockmass (not breccia) up to a few metres, though usually less than 1 m, wide. Examples of typical fourth order faults are shown in Figure 3-37.



Figure 3-36: An example of third order fault conditions – highly fractured and sheared rock

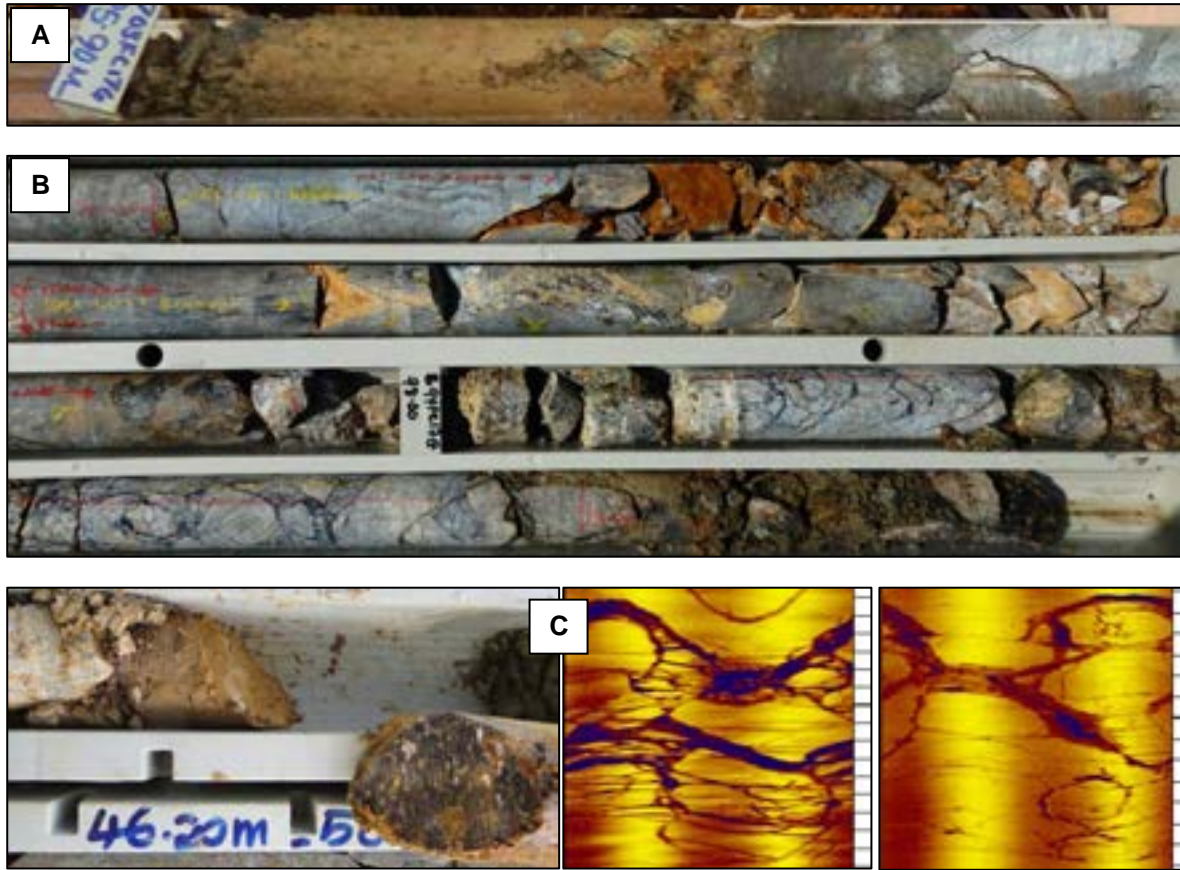


Figure 3-37: Examples of fourth order faults: (A) discrete zone of fault gouge; (B) fractured, oxidised rock with gouge zone; and (C) discrete fault with gouge and slickensided surface, examples of fault zones in acoustic survey image

Fault planes have been interpreted from drill core logging, televiewer imaging, permeability testing and topographical assessment (Section 3.1.10). An example of an interpreted fourth order fault plane is shown in Figure 3-38. The photographs show the character of the fault is different in the various locations in which it is intersected.

Faults are not strictly 'geotechnical domains', but cut across the other geotechnical domains described in Sections 3.1.6 through 3.1.10.

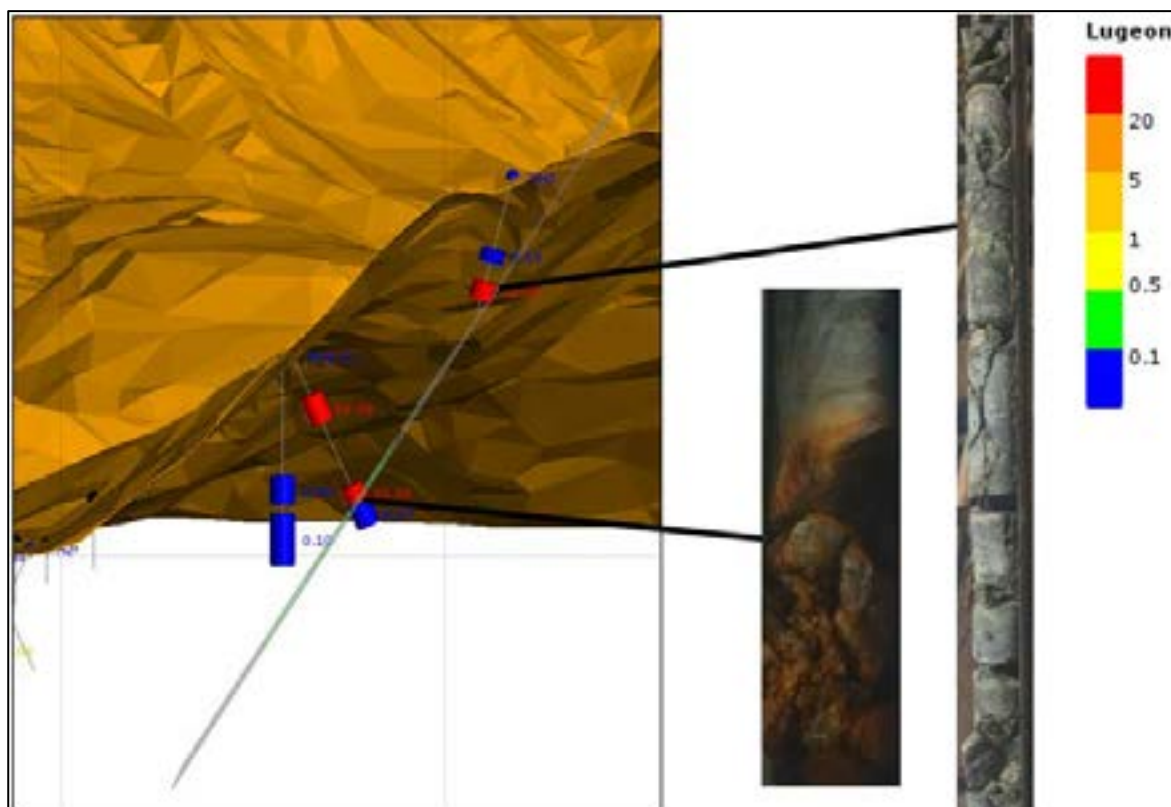


Figure 3-38: Isometric cross-section looking north, showing the interpreted fault plane and the permeabilities measured at drill hole intersection

Note: Core photographs shown the nature of the fault at these intersections.

Geotechnical domain summary

Table 3-12 provides a summary of the geotechnical domains as identified within each drill hole.

A Leapfrog geotechnical model has been constructed to provide a wireframe surface for the following:

- Topography
- Top of the bedrock, i.e. the interface between soil-like colluvium and/ or boulders and moderately to slightly weathered rock in the hillsides
- Interface between weathered rock (with oxidised, infilled joints) and (generally) unweathered rock
- Boundaries of cemented colluvium/ alluvium and uncemented alluvium in the valley floor
- Base of the potential landslide zones on the left and right hillsides
- Key interpreted faults, as described in Section 3.1.10
- Interpretation of the natural groundwater surface.

Table 3-12: Summary of geotechnical domains identified in each drill hole

Zone	Planned hole number	Drilled hole number	Soil-like cover		Uncemented colluvium or alluvium		Cemented colluvium or alluvium		Large boulders		Potential landslide – highly fractured with shear zones, oxidised rock and joint infills		HW to MW rock, with dilated, oxidised, infilled joints		SW rock, with dilated, oxidised, infilled joints		Significantly deteriorated poor-quality serpentinised bedrock		Moderate or good-quality bedrock	
			From (m)	To (m)	From (m)	To (m)	From (m)	To (m)	From (m)	To (m)	From (m)	To (m)	From (m)	To (m)	From (m)	To (m)	From (m)	To (m)	From (m)	To (m)
Left abutment - upper	LH1	685FC17G	0	0.5					0.5	9					9	18.9			18.9	125
	LH3	699FC17G	0	0.5					0.5	8.5	8.5	114.5							114.5	120
	LH4	722FC17G	0	1.1											1.1	12			12	75
	LH5	720FC17G	0	1.5							1.5	23.4							23.4	150
	LH6	700FC17G	0	5.6					5.6	13.05					13.05	20.3			20.3	75.1
	LH7	729FC17G	0	9.3							9.3	78			78	131			131	150
Right abutment - outflow	SW1	705FC17G	0	1.2											1.2	2.2			2.2	50.1
	DTP1	708FC17G	0	4.6											4.6	9.4			9.4	50.2
	DTP2	706FC17G	0	3.8											3.8	5.3			5.3	80.2
Right abutment - upper	DT1	697FC17G	0	1											1	3	3	125.3		
	SW3	693FC17G	0	1.3											1.3	15	15	101		
	DT2	716FC17G	0	0.3											0.3	22			22	250.2
	DT3	696FC17G	0	0.6					0.6	4.5					4.5	17.5			17.5	320.4
	RH5	687FC17G	0	1.6					1.5	5.5					5.5	20.5			20.5	110.3
	SW5	694FC17G	0	3.2									3.2	8.8					8.8	100
	HTP3	711FC17G	0	0.2											0.2	25.4				
	HTP4	710FC17G													0	14.2			14.2	50.7
	HTI1	724FC17G													0	25.2			25.2	180
SW6	703FC17G	0	0.3											0.3	13			13	150	
Right abutment - mid	RH1	682FC17G	0	2.9											2.9	39.1			39.1	147.2
	RH3	683FC17G							0	12					12	16			16	170.3
	RH9	698FC17G							0	6					6	17			17	120
	SW4	695FC17G	0	1					1	13.5	13.5	26.6			26.6	30			30	100
	SC1	718FC17G	0	3.7					3.7	6					6	20			20	200.2

Zone	Planned hole number	Drilled hole number	Soil-like cover		Uncemented colluvium or alluvium		Cemented colluvium or alluvium		Large boulders		Potential landslide – highly fractured with shear zones, oxidised rock and joint infills		HW to MW rock, with dilated, oxidised, infilled joints		SW rock, with dilated, oxidised, infilled joints		Significantly deteriorated poor-quality serpentinised bedrock		Moderate or good-quality bedrock		
			From (m)	To (m)	From (m)	To (m)	From (m)	To (m)	From (m)	To (m)	From (m)	To (m)	From (m)	To (m)	From (m)	To (m)	From (m)	To (m)	From (m)	To (m)	
	HT1	715FC17G	0	4											4	23			23	150	
Right abutment - intakes	DTP3	709FC17G	0	3.4			3.4	11.9							11.9	14.6			14.6	50.2	
	DTP4	707FC17G	0	3.6			3.6	10.7							10.7	15.6			15.6	50	
River valley	LH2	680FC17G	0	0.5			0.5	49.5							49.5	65.5			65.5	179.9	
	RH2	681FC17G					0	12.5							12.5	32.5			32.5	175.3	
	RH4	686FC17G					0	25.5							25.5	38			38	100	
	RH6	704FC17G			23.5	51.5	0	23.5											51.5	103.9	
	RH7	723FC17G					0	16							16	33.1			33.1	102.2	
Powerhouse	PH2	713FC17G	0	3.1					3.1	14.7								14.7	50.2		
	PH3	714FC17G	0	1			1	23.5										23.5	40		
	HTP2	712FC17G	0	1					1	7.2										7.2	50
Quarry North and Central	Q9	702FC17G	0	4									4	25.1				25.1	48.5	48.5	170
	Q1	Q1	0	1.8											1.8	30			30	70.8	
	Q10	691FC17G	0	0.5											0.5	49.8			49.8	75	
	Q12	727FC17G	0	1.5									1.5	2.2	2.2	24					
	Q13	728FC17G	0	2.2									2.2	7.3	7.3	15.5			15.5	122.3	
Quarry South	Q11	692FC17G	0	4							4	11						11	38	38	50.5
	Q5	688FC17G	0	1.5							1.5	75.2						75.2	94.5		
	Q6	701FC17G	0	5.3							5.3	46						46	150		
	Q7	690FC17G	0	5.5					5.5	67.8								67.8	77		
	Q8	689FC17G	0	0.2					0.2	12								12	100		

3.1.7 Geotechnical properties – laboratory testing

The laboratory testing completed for the FRHEP is summarised in Table 3-13. Further testing was planned but not carried out due to the drilling program being terminated in February 2018.

Table 3-13: Summary of laboratory testing undertaken

Test	Number of samples tested in FRHEP SPS Stage 1 and 2 investigations	Number of tests from SKM (2011) study
Unconfined compressive strength	81	29
Elastic properties Young's modulus and Poisson's ratio	29	29
Direct shear testing on natural discontinuities	27	0
Saw-cut shear box test	5	0
Particle size distribution & Atterberg limits	14	0
Emerson Crumb	4	0
Slake durability	29	0
LA abrasion	13	0

Testing of soil-like materials

The soils profile at the current FRHEP site consists of thin colluvium (often containing boulders) with a rapid transition into slightly weathered rock and fresh rock. The weathered material is of rock strength, and triaxial testing was thus not appropriate. It was difficult to obtain intact samples of colluvium and uncemented alluvium, and the amount of gravel and boulders in these materials meant that triaxial test results would not be representative of overall strength. No soils triaxial tests were undertaken.

Grading and Atterberg limits

Grading (using the USCS) and Atterberg limits determination was undertaken for colluvium, uncemented alluvium, fault gouge and landslide materials matrix. Results are given in Table 3-14 and Figure 3-39, and have been plotted on the plasticity chart to classify the fine proportion of the soils in Figure 3-40.

Table 3-14: PSD and Atterberg limit results

Hole ID	Depth (m)	Description	Gravel	Sand	Silt	Clay	LL	PL	PI	LS	W
SW5	5.2	Colluvium	37	34	16	13	81	54	27	12	37
DTP2	0.6	Colluvium	17	31	32	20	53	38	15	5	58
PH3	0.5	Colluvium	36	42	17	5	48	17	31	14	39
LH2	15.3	Cemented colluvium	2	45	29	24	87	45	42	16	69
LH2	18.9	Cemented colluvium	1	65	34			82	51	31	12
RH2	5.1	Cemented colluvium	17	44	39			76	34	42	15
RH2	11.2	Cemented colluvium	2	62	25	11	96	71	25	8	74
RH4	19.1	Cemented colluvium	0	29	71			85	49	36	13
DTP3	3.0	Cemented colluvium	15	41	26	18	80	44	36	16	43
PH3	4.6	Cemented colluvium	22	26	33	19	74	44	30	11	12
SW4	8.2	Landslide	3	49	36	12	83	67	16	6	66
LH3	63.0	Landslide	36	24	40			67	35	32	15

Hole ID	Depth (m)	Description	Gravel	Sand	Silt	Clay	LL	PL	PI	LS	W
LH3	96.0	Landslide	55	31	14		66	50	16	5	
LH2	62.3	Shear zone	0	77	23		148	82	66	23	
LH2	93.5	Fault gouge	23	45	32						
SW3	13.6	Fault zone	12	78	10		59	43	16	7	

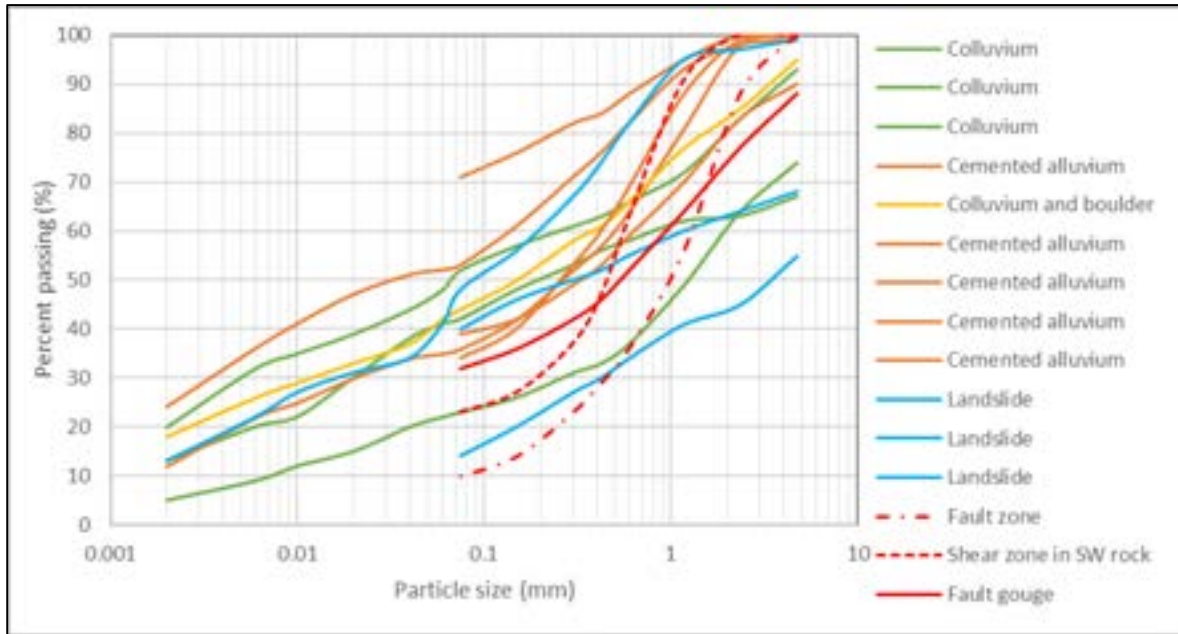


Figure 3-39: Particle size distribution

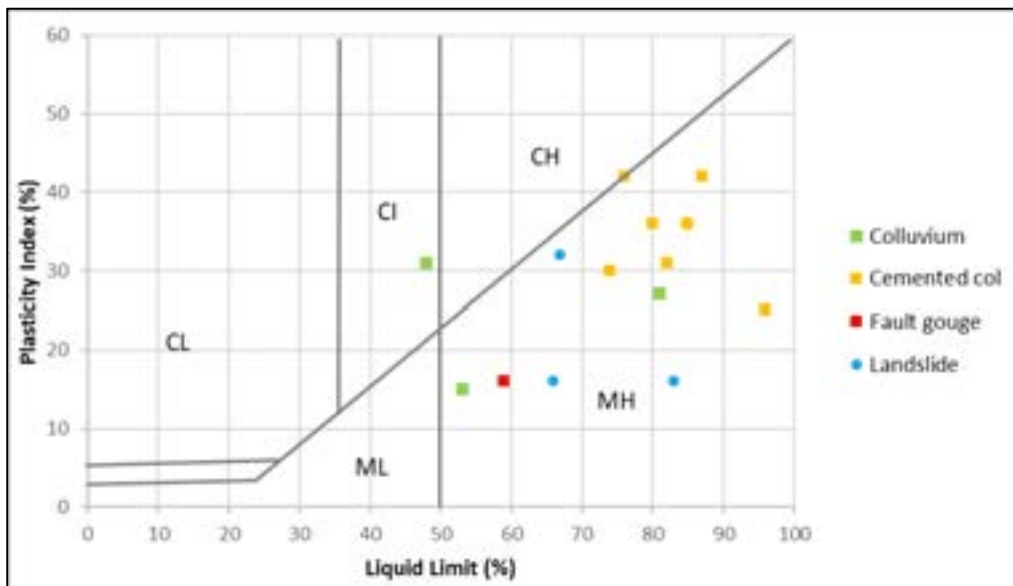


Figure 3-40: Plasticity chart

All materials show a wide range in particle size distribution, but all plot over the same range. The fines components plot in the MH category (silt of high plasticity). The fault gouge showed a low percent of clay and lower plasticity than the other samples.

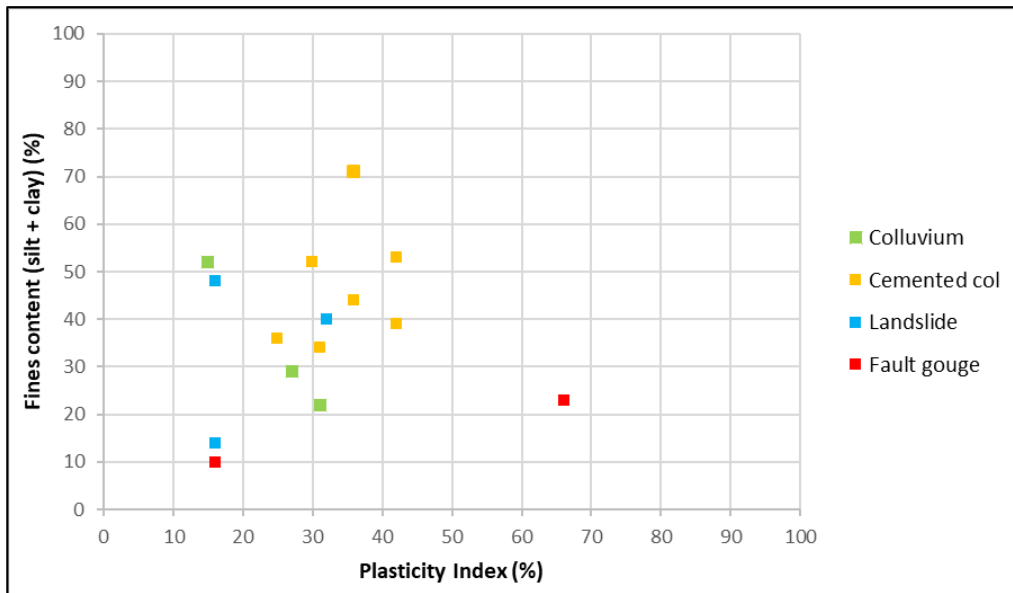


Figure 3-41: Fines versus plasticity index

Moisture content

The natural moisture content (NMC, or W) of samples was measured using the oven-drying technique.

W (%) for each soil sample was determined using the following equation:

$$W = \frac{W_w}{W_s} \times 100\%$$

Where Ww =Weight of water (g) and Ws = Weight of solids (g).

This property is expressed as the weight of water against the weight of dry solids. Therefore, in substances with a higher weight of water to solids, the moisture content will exceed 100%.

Natural moisture contents of the materials tested vary from 12% to 74%. Several samples show NMC greater than the plastic limit, indicating these materials may be difficult to work with and compact. This is not seen as an issue as the colluvium and landslip materials are not intended to be used as construction materials. NMC and plastic limits have been plotted in Figure 3-42.

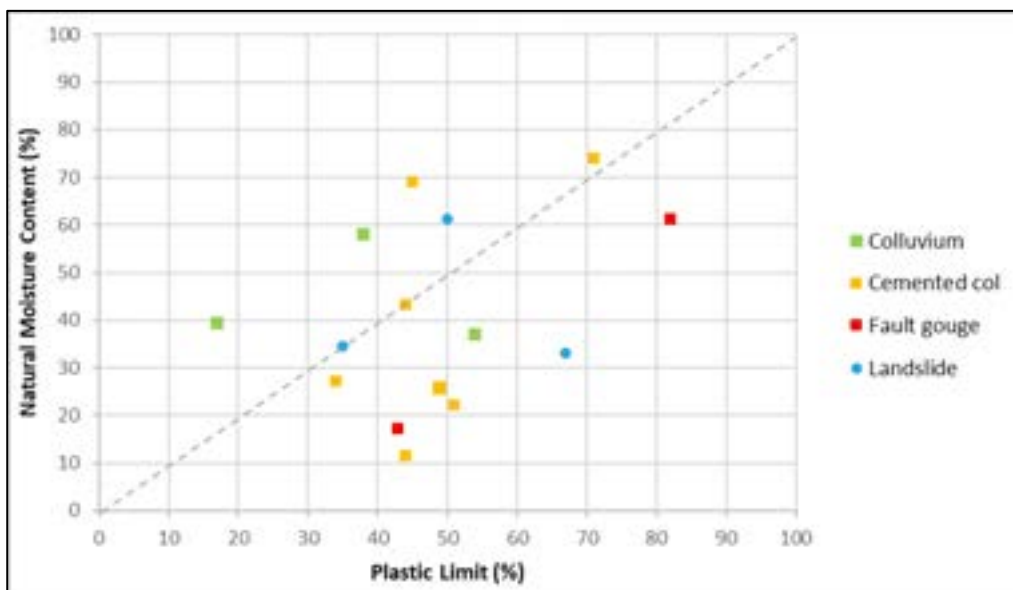


Figure 3-42: Natural moisture content versus plastic limit

Emerson dispersion test

The Emerson test is used to assess if dispersive soil conditions are present. Dispersion is a phenomenon associated with sodic soils where the clay fraction deflocculates and goes into suspension even in still water. Dispersive soils are prone to erosion and piping, especially if not carefully compacted. The results of the four Emerson tests undertaken on both colluvium and landslip material gave results in Class 5 or Class 6. A description of the classes is given in Figure 3-43. Both classes are considered non-dispersive, showing no signs of dispersion when air dried or when remoulded blocks of soil are immersed in water.

Table 3-15: Results of Emerson test

Planned hole number	Hole number	Depth (m)	Material	Description	Emerson Class
DTP4	706FC17G	0.0–2.8	Colluvium	Gravelly clay	6
DTP3	709FC17G	0.0–1.0	Colluvium	Sandy clay	6
PH3	714FC17G	2.65–2.85	Colluvium	Gravelly clay	5
LH7	729FC17G	5.2–5.4	Landslide	Gravelly clay	6

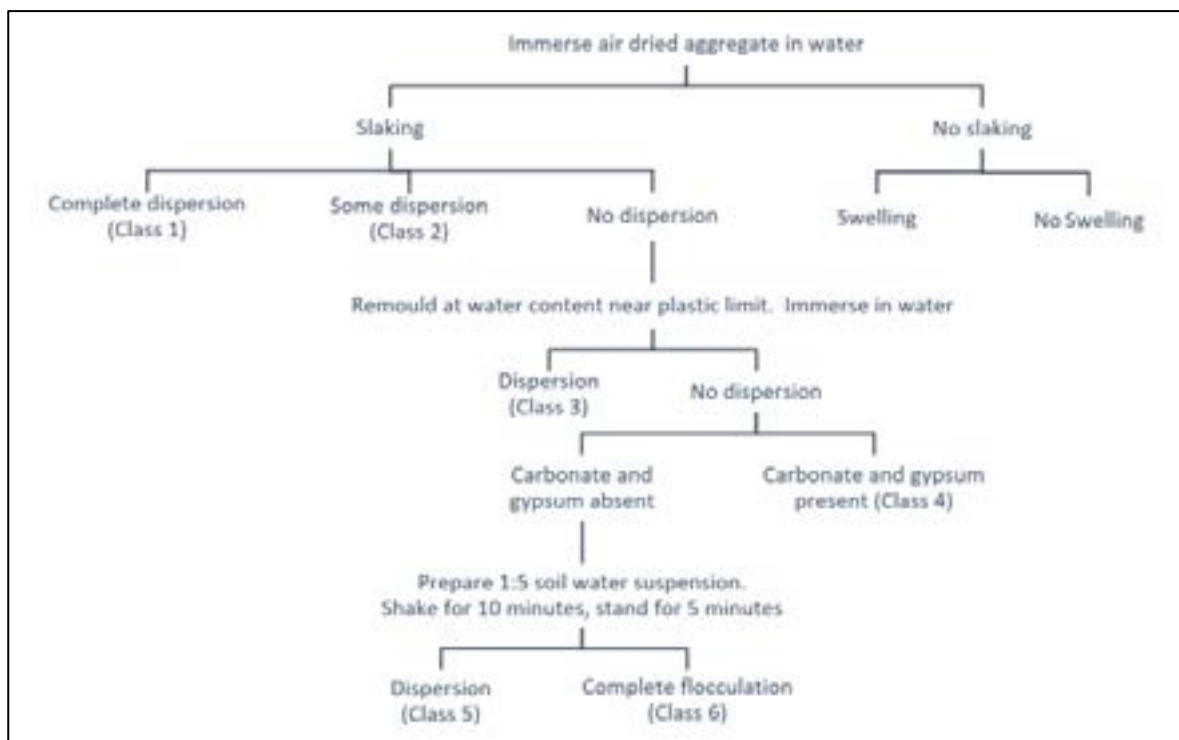


Figure 3-43: Flow chart for interpretation of Emerson test results

Unconfined compressive strength

The results of the UCS testing are summarised in Table 3-16 and Figure 3-44. Results from laboratory testing undertaken in 2011, as part of the Douglas Partners study, have been incorporated into the dataset.

Statistics provided include mean, standard deviation, minimum and maximum values. Tests with invalid failure modes (for example tests which had failed along pre-existing structures with very low UCS values) were excluded from the statistics.

Table 3-16: Summary of UCS test results

Area	Description	Number of valid tests	Number of invalid tests	Avg (MPa)	Std Dev (MPa)	Min. (MPa)	25 th percentile	50 th percentile	75 th percentile	Max. (MPa)
Right abutment	SW and UW dunite	65	6	59	22	29	45	53	68	166
Right abutment	Altered, deteriorating dunite	6	2	31	23	3	12	33	46	62
Left abutment	SW and UW dunite	28	6	55	21	21	38	54	71	96
Quarry	SW and UW dunite	15	3	80	21	50	62	79	95	117
Landslide		4	1	22	8	11	18	23	26	29
Cemented alluvium		2	0	5.9		1.61				10.2

The UCS tests from slightly weathered and unweathered rock showed very similar results, and the results were combined and assessed together. The UCS testing from the Douglas Partners (2011) report also plotted in the same range and the results were used in this assessment. Results from the right abutment, left abutment and quarry area were assessed separately. The right and left abutments showed similar range and average values; the quarry showed slightly stronger rock. UCS tests from the two holes on the right abutment with more altered or deteriorating rock were also assessed separately. These showed lower average and ranges than the surrounding dunite.

Samples did not exhibit anisotropic behaviour. A small number of samples did break along pre-existing veinlets/ cemented joints.

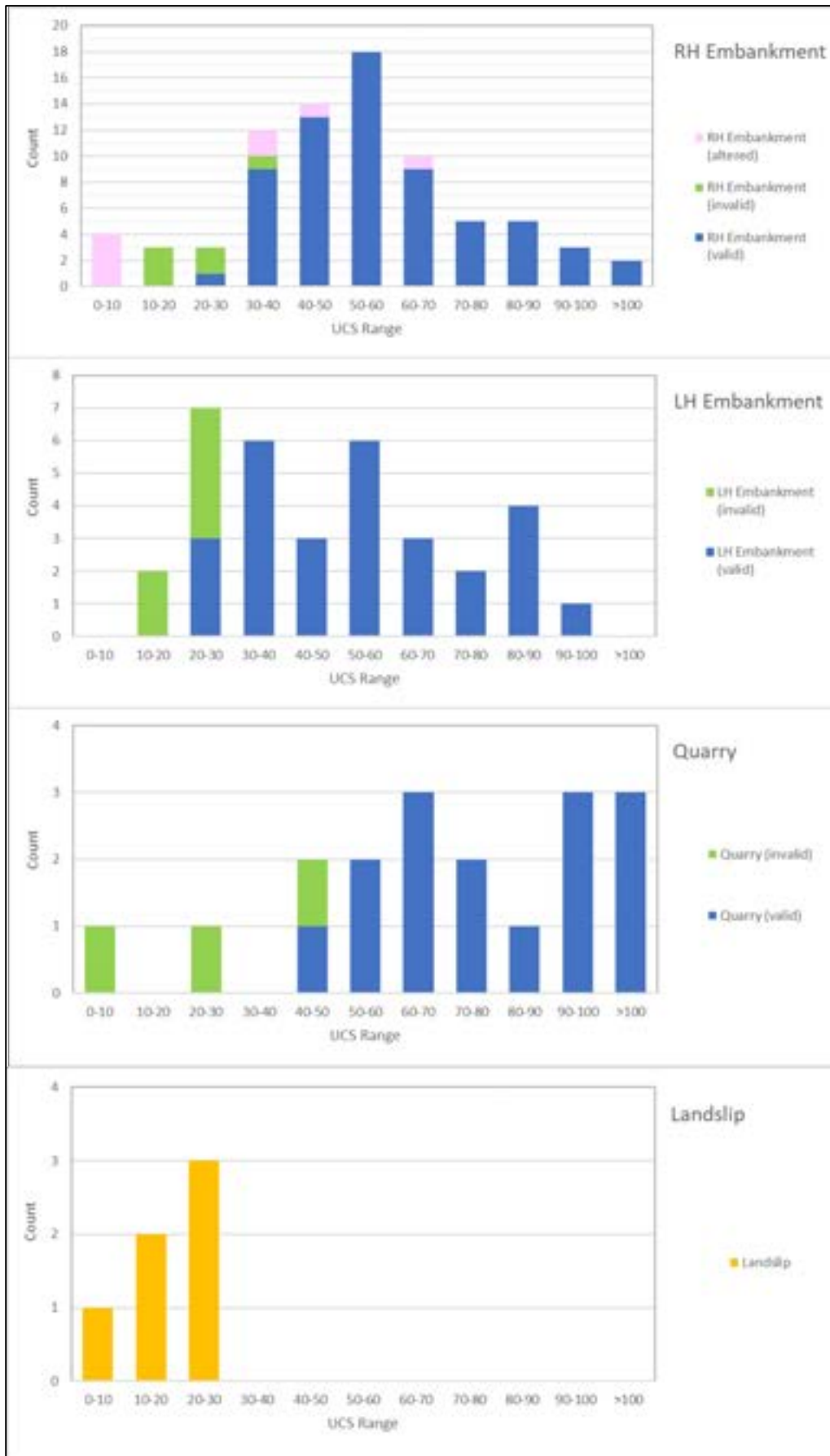


Figure 3-44: UCS test histograms

Young's modulus and Poisson's ratio

The results of the testing for elastic properties Young's modulus and Poisson's ratio are summarised in Table 3-17.

Table 3-17: Summary of elastic properties

Area	Description	Young's modulus E (GPa)					Poisson's ratio		
		Min.	25 th percentile	50 th percentile	75 th percentile	Max.	Avg	Min.	Max.
Right abutment	SW and UW dunite	46	102	112	159	187	0.25	0.23	0.26
Right abutment	Altered dunite	17	28	40	46	52	0.3		
Left abutment	SW and UW dunite	41	81	106	155	247	0.25	0.21	0.28
Quarry	SW and UW dunite	42	83	109	116	135	-		
Landslide				33			-		

Note: *Poisson's ratio testing generally gave low reliability results; only results considered valid are reported.

Density

Density was measured as part of the UCS testing. The moisture content was also measured, and typically varied between 0.1% and 0.4%. Average, standard deviation, minimum, maximum and 25th, 50th and 75th percentile values are given in Table 3-18.

Table 3-18: Summary of wet density

Area	Description	Number of tests	Average (MPa)	Std Dev (MPa)	Min. (MPa)	25 th percentile (MPa)	50 th percentile (MPa)	75 th percentile (MPa)	Max. (MPa)
Right abutment	SW and UW dunite	71	3.15	0.17	2.80	3.08	3.18	3.25	3.96
Right abutment	Altered, deteriorating dunite	8	2.61	0.26	2.19	2.49	2.60	2.71	3.10
Left abutment	SW and UW dunite	34	3.18	0.09	2.97	3.11	3.22	3.26	3.29
Quarry	SW and UW dunite	18	3.10	0.13	2.81	3.06	3.12	3.18	3.29
Landslide		5	2.75	0.1	2.63	2.65	2.78	2.84	2.84
Cemented alluvium		2			1.79				3.00

Discontinuity shear strength

The results of direct shear testing completed on foliation and joint planes are given in Table 3-19 and Figure 3-45. Friction angles are variable, likely depending on roughness and infill.

Table 3-19: Summary of direct shear test results

Planned hole number	FRL hole number	Depth (m)	Residual strength		Peak strength	
			Friction angle (°)	Cohesion (kPa)	Friction angle (°)	Cohesion (kPa)
RH1	682FC17G	20.1	23	81	23	34
RH1	682FC17G	47.2	27	2	31	0
RH5	687FC17G	83.3	36	45	17	26
RH6	704FC17G	70.2	25	0	28	0
RH7	723FC17G	96.9	26	8	30	0
RH9	698FC17G	75.0	28	104	32	25

Planned hole number	FRL hole number	Depth (m)	Residual strength		Peak strength	
			Friction angle (°)	Cohesion (kPa)	Friction angle (°)	Cohesion (kPa)
SW3	693FC17G	60.9	34	93	36	227
SW3	693FC17G	57.6	30	74	32	67
SW4	695FC17G	67.5	24	106	31	166
SW5	694FC17G	30.1	30	38	30	44
DT1	697FC17G	105.0	42	0	35	129
DT3	696FC17G	291.8	19	3	18	0
DTP3	709FC17G	34.11	24	8	25	9
DTP4	707FC17G	32.35	30	0	34	7
HTP2	712FC17G	45.0	26	0	28	6
LH1	685FC17G	66.4	40	123	43	245
LH2	680FC17G	54.5	20	9	25	2
LH3	699FC17G	117.6	26	13	23	0
Q7	690FC17G	55.4	39	129	45	162
Q9	702FC17G	109.9	28	3	39	186
Q11	692FC17G	25.9	27	20	29	7
Q10	691FC17G	37.9	24	1	24	11

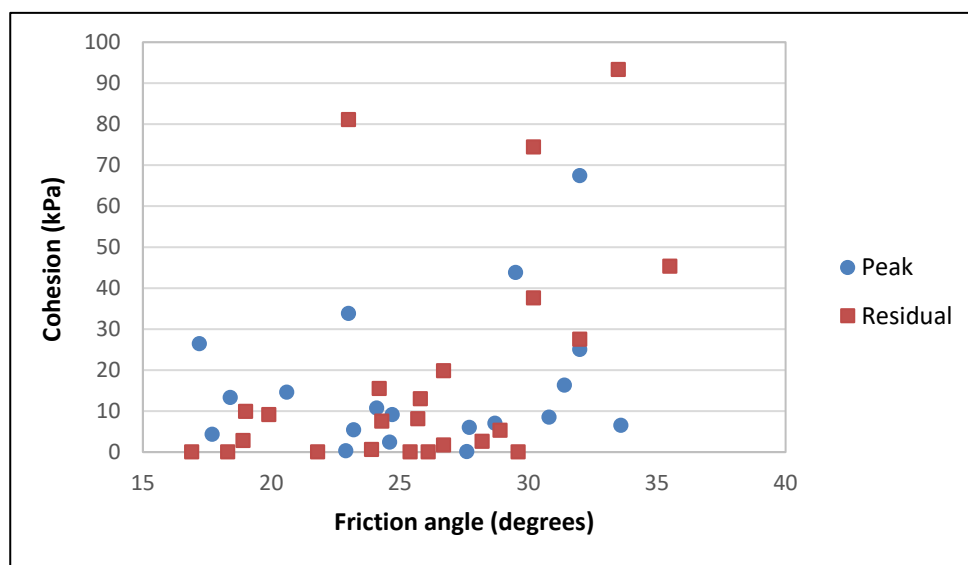


Figure 3-45: Plot of direct shear test results

Saw-cut shear strength

The results of shear testing completed on saw-cut planes are given in Table 3-20. The unweathered dunite showed base friction angles between 27° and 31°, and the altered (serpentinised) dunite showed a significantly lower angle of 22°.

Table 3-20: Summary of sawcut shear test results

Planned hole number	FRL hole number	Depth (m)	Base friction angle (°)	Cohesion (kPa)	Description
Q10	691FC17G	52.5	27.7	0	Bedrock (UW Dunite)
Q9	702FC17G	109.88	31.3	0	Bedrock (UW Dunite)
Q9	702FC17G	67.73	31.1	0	Bedrock (UW Dunite)
SW6	703FC17G	54.55	21.7	0	Deteriorating altered rock

Slake durability

Slake durability testing assesses rock resistance to short-term weathering caused by repeated wetting and drying. The potential for slaking behaviour is present in weathered, weak and clay-bearing rocks. The results can be used to assess mineral content, durability and likely decomposition of rock. The results of the slake durability testing for the FRHEP site are presented in Table 3-21.

Table 3-21: Slake durability testing results

Area	Description	Number of tests	Minimum (%)	Maximum (%)
Right abutment	Bedrock	12	99.5	99.8
Right abutment	Deteriorating altered rock	2	99.8	99.9
Left abutment	Potential Landslide	2	93.4	99.6
Quarry	Bedrock	10	98.8	99.9

All samples tested showed excellent durability with almost no loss of mass over the duration of the tests. The altered (serpentinised) dunite did not show any more tendency to slake than the unaltered rock.

Los Angeles abrasion

The Los Angeles (LA) abrasion test is a common test used to indicate aggregate toughness and abrasion characteristics. Rock core is broken to coarse aggregate size. The sample is subject to abrasion, impact and grinding in a rotating steel drum with steel balls. Following this, the weight of aggregate passing the 1.7 mm sieve is determined as a percentage of the original sample weight. The test is used to assess if aggregate is hard and tough enough to resist crushing, degradation and disintegration. Lower LA abrasion values indicate that an aggregate is tougher and more resistant to abrasion. Results are given in Table 3-22.

Table 3-22: LA abrasion testing results

Planned hole number	FRL hole number	Depth (m)	LA value (loss, %)	Selected test grading
SW3	693FC17G	57.6	14	K
SW4	695FC17G	97.0	24	B
SW6	703FC17G	14.0	20	B
SW6	703FC17G	9.8	27	B
SW5	694FC17G	34.2	19	B
Q7	690FC17G	54.4	17	K
Q8	689FC17G	45.2	19	B
Q8	689FC17G	78.8	17	B

Planned hole number	FRL hole number	Depth (m)	LA value (loss, %)	Selected test grading
Q9	702FC17G	55.2	23	B
Q9	702FC17G	145.4	27	B
Q10	691FC17G	51.2	18	B
Q11	692FC17G	22.3	17	B
Q11	692FC17G	46.3	10	B

There is no standard LA abrasion specification for pavement design; specifications are typically established by state or local agencies. Typically, US state specifications limit the abrasion of coarse aggregate to a maximum ranging from 25% to 55%, with most states using a specification of 40% or 45%. Requirements for Portland Cement Concrete tend to be similar, while requirements for specialised mixes such as Stone Matrix Asphalt tend to be lower at 30% (LA Abrasion, 2011)³⁵.

All samples tested for the FRHEP are well in excess of these specifications.

³⁵ Los Angeles Abrasion, 21 April 2011. Available from <<http://www.pavementinteractive.org>>. Accessed 22 June 2015.

3.1.8 Geotechnical properties – drill core logging results

Rockmass properties

The distribution of rock properties logged strength, RQD and joint spacing are provided in Figure 3-46, Figure 3-47 and Figure 3-48.

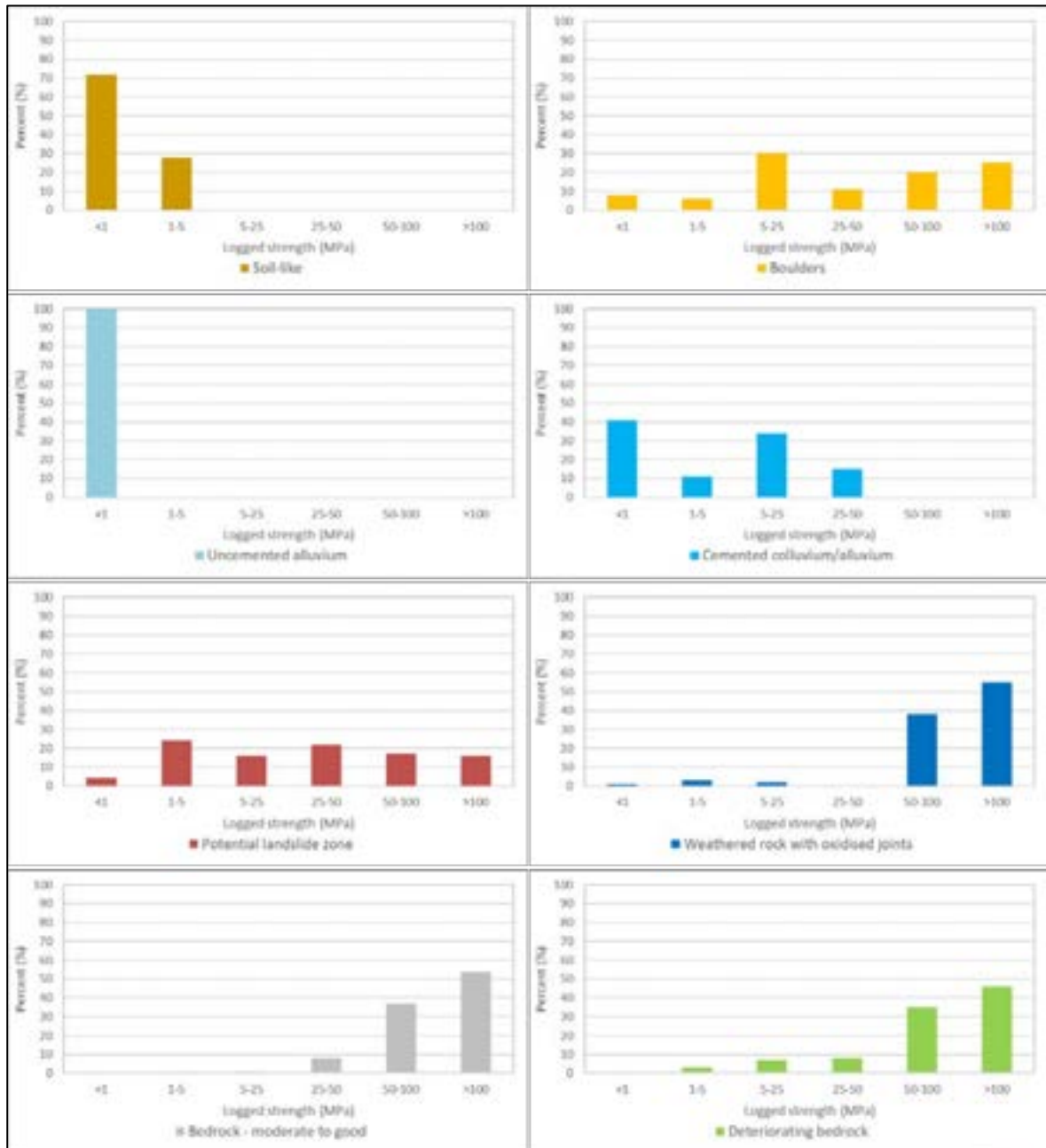


Figure 3-46: Logged strength distributions per domain

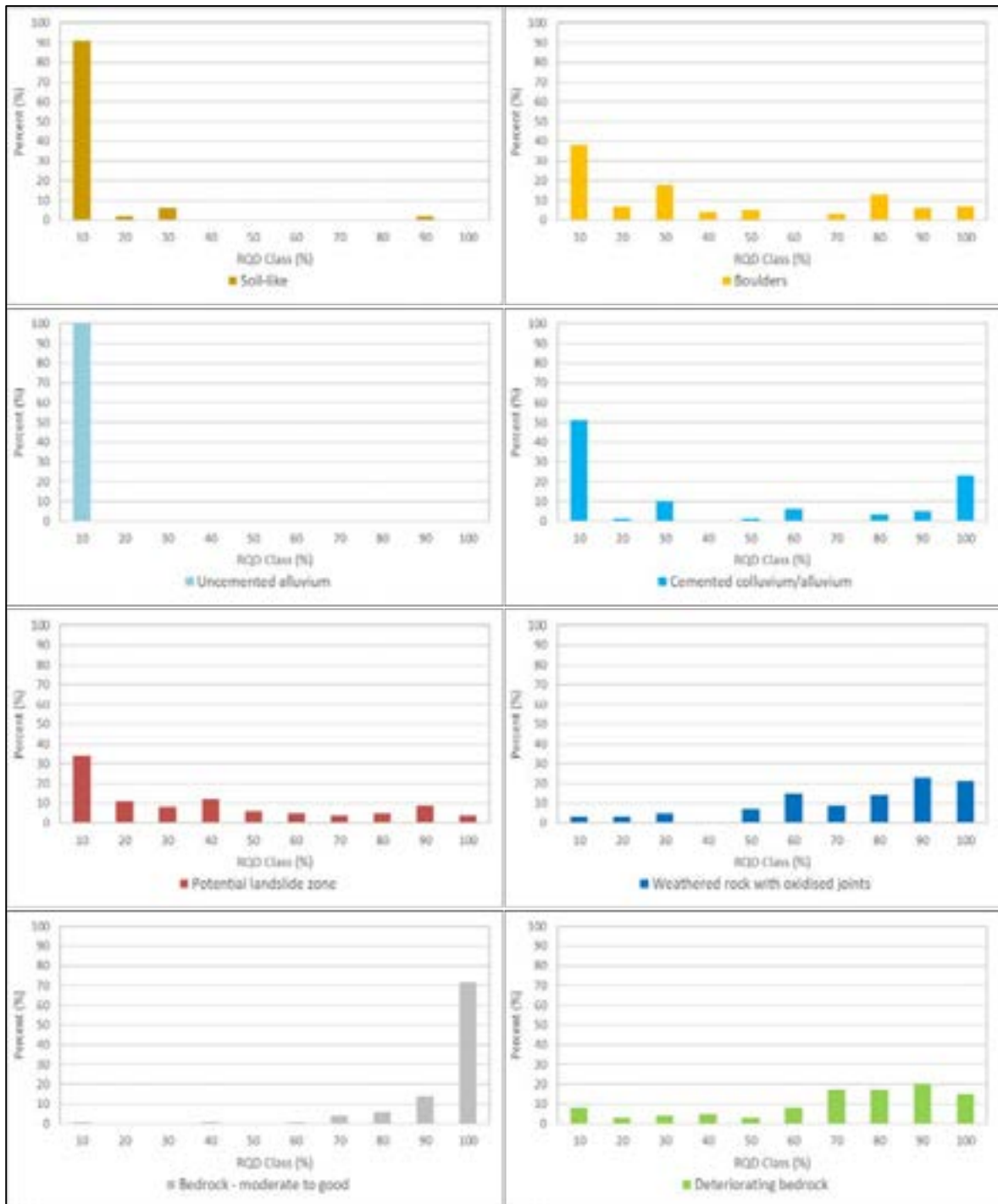


Figure 3-47: RQD distributions per domain



Figure 3-48: Joint spacing distributions per domain

Structural properties

Structural logging was undertaken to record the depth, orientation (where possible), roughness and infill of all structures. Histograms showing roughness and infill distributions are given in Figure 3-49 and Figure 3-50, respectively. The infill of faults was largely rock fragments (RF) or rock fragments and clay (RFC). Serpentinite and talc infills were found predominantly in the deteriorating, serpentinite-altered bedrock. Infills in the weathered rock and good-quality bedrock domains were similar (clay, iron straining or clean).

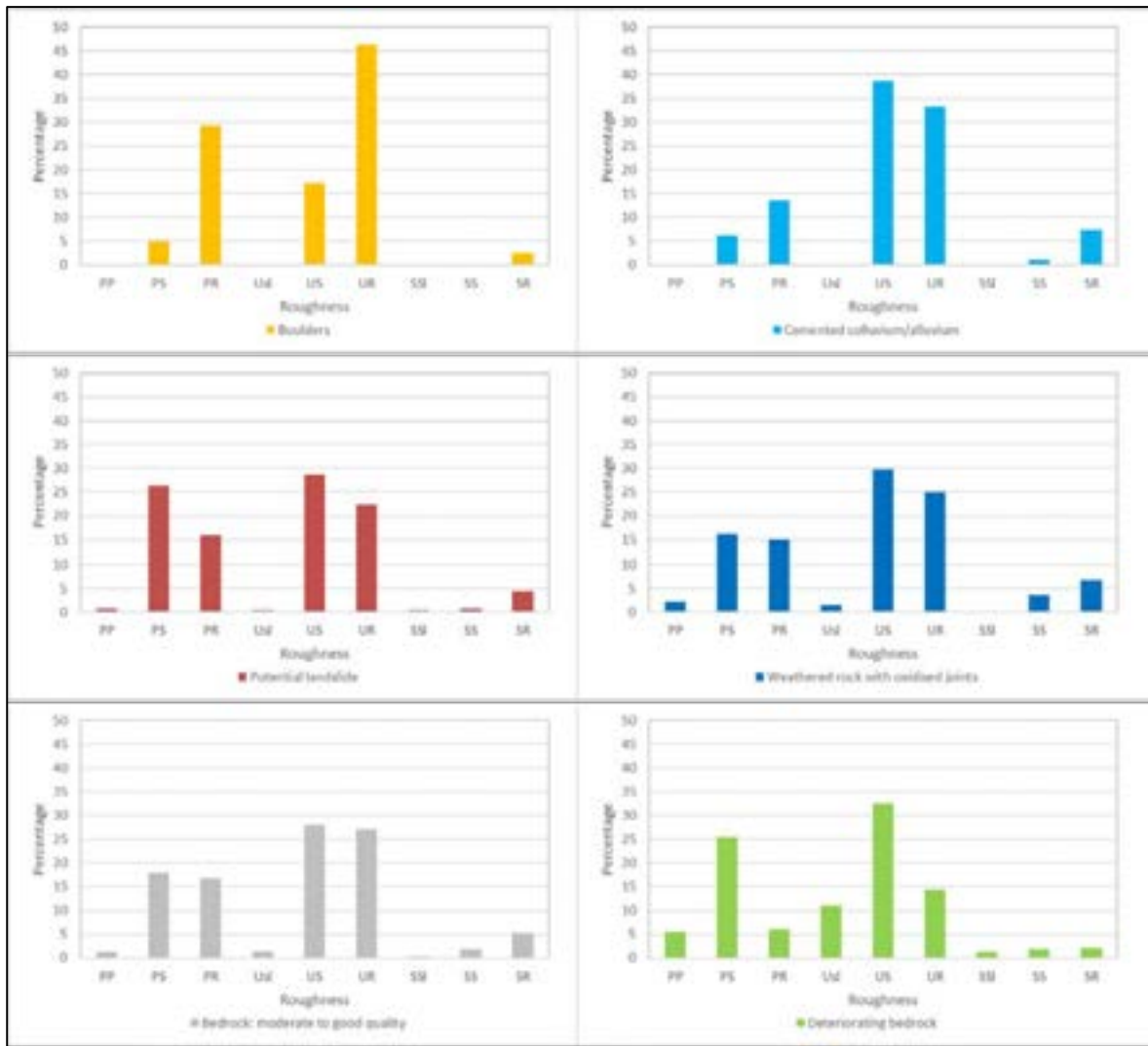


Figure 3-49: Small-scale roughness distributions per domain

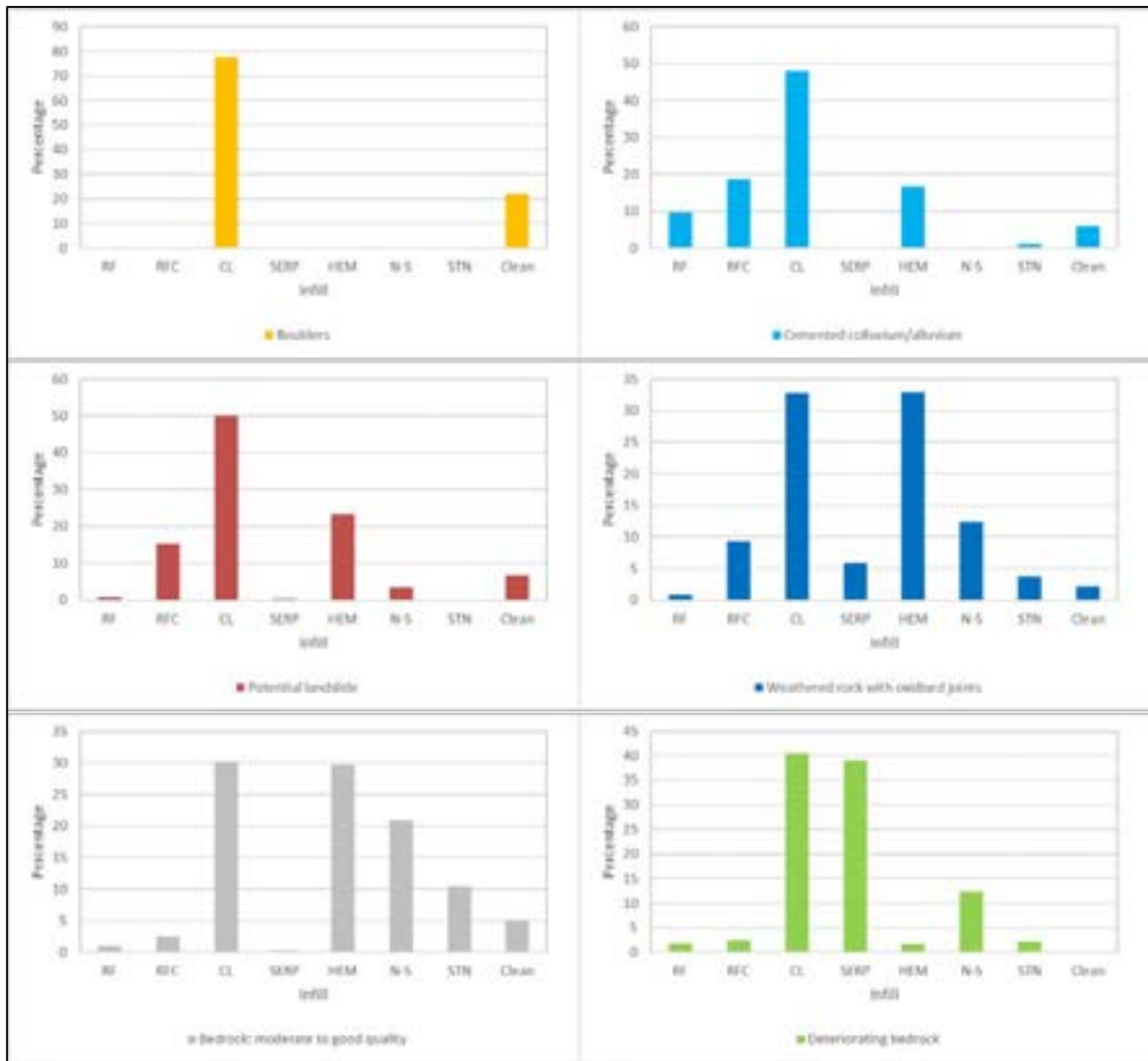


Figure 3-50: Infill distributions per domain

Calculated rock mass ratings

Rock mass ratings calculated using the Geological Strength index (GSI), Laubscher RMR and Q systems are given in Figure 3-51, Figure 3-52 and Figure 3-53 respectively.

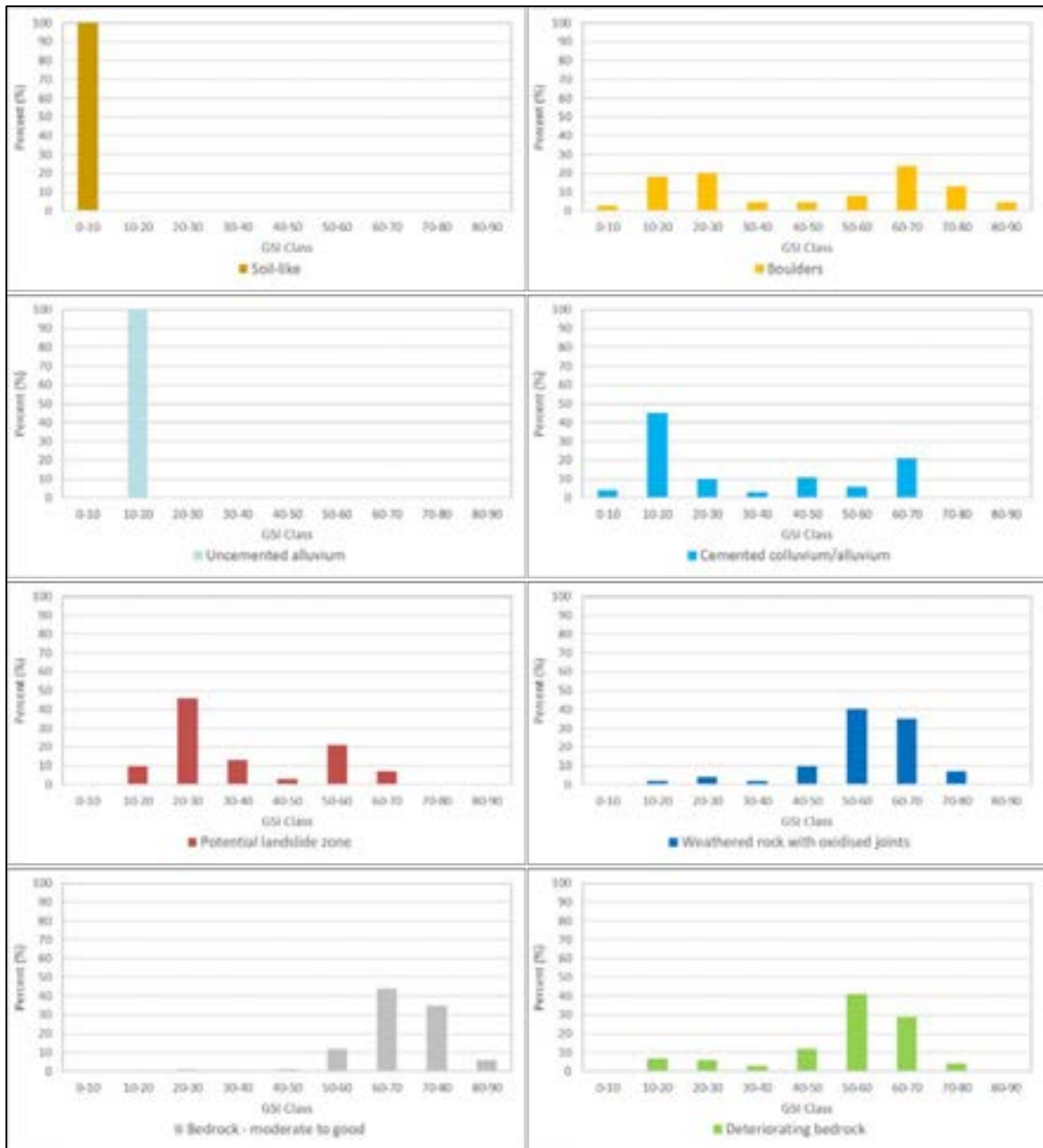


Figure 3-51: GSI distributions per domain



Figure 3-52: Laubscher RMR distributions per domain



Figure 3-53: Q distributions per domain

3.1.9 Structural fabric – core logging and televiewer

Oriented fabric data was obtained using conventional core orientation, but only 30% of the total logged structures could be oriented. Table 3-23 and Table 3-24 show the amount of each structure type from logging and from televiewer data respectively.

Table 3-23: Count of the different structure types – from logging

Structure Type	Description	Count
DEC	CW, HW, Altered	1
CJ	Lightly cemented joint	28
CT	Contact	6
DFR	Drill fragmented core	6
FA/FLT	Fault	20
FLTG	Fault Gouge	1
FOL	Foliation	1
J	Joint	1,954
SH	Shear	24
VN	Vein	32

Table 3-24: Count of the different structure types – from televiewer

Structure Type	Description	Count
CON	Contact	7
FLT	Fault	5
JN	Joint	1,657
SHR	Shear	586
VN	Vein	134

Structural data has been analysed for the following zones: Left Hand (LH) abutment, Right Hand North (RHN) abutment, Right Hand South (RHS) abutment, Valley Floor (VF), Quarry North (QN), Quarry South (QS).

Figure 3-54 shows the orientation of all logged structures and Figure 3-55 shows the orientation of all identified structures from the televiewer.

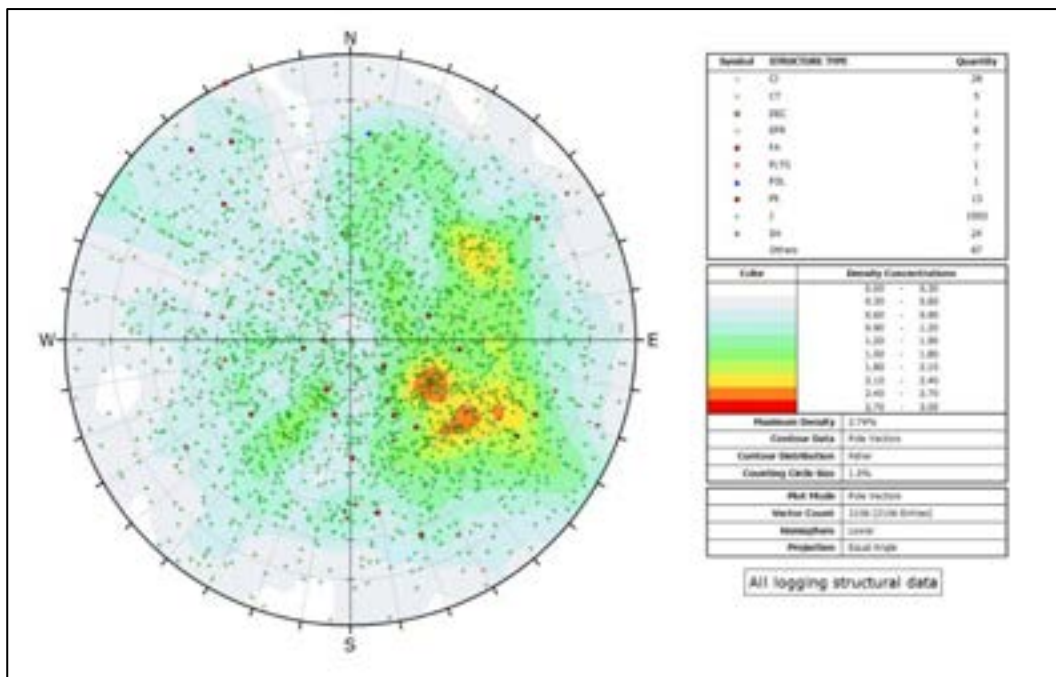


Figure 3-54: Stereonet showing orientation of all logged structures

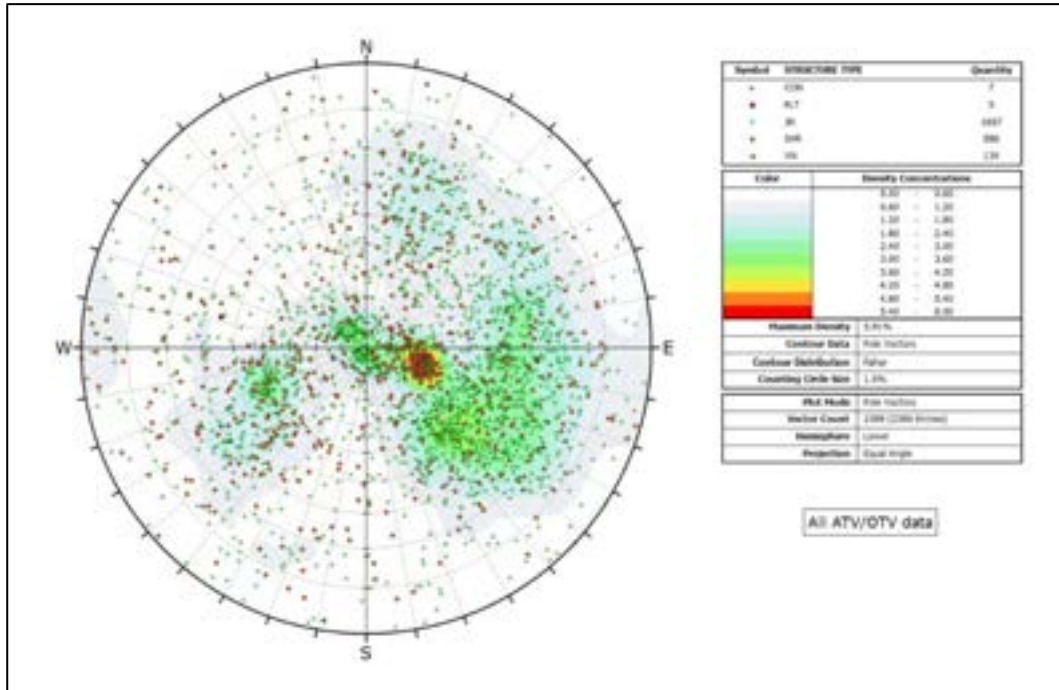


Figure 3-55: Stereonet showing orientation of all identified structures from the televiewer

Left abutment

Stereonet in Figure 3-56 and Figure 3-57 show the orientation of the structures observed in the left abutment zone from logging and ATV respectively.

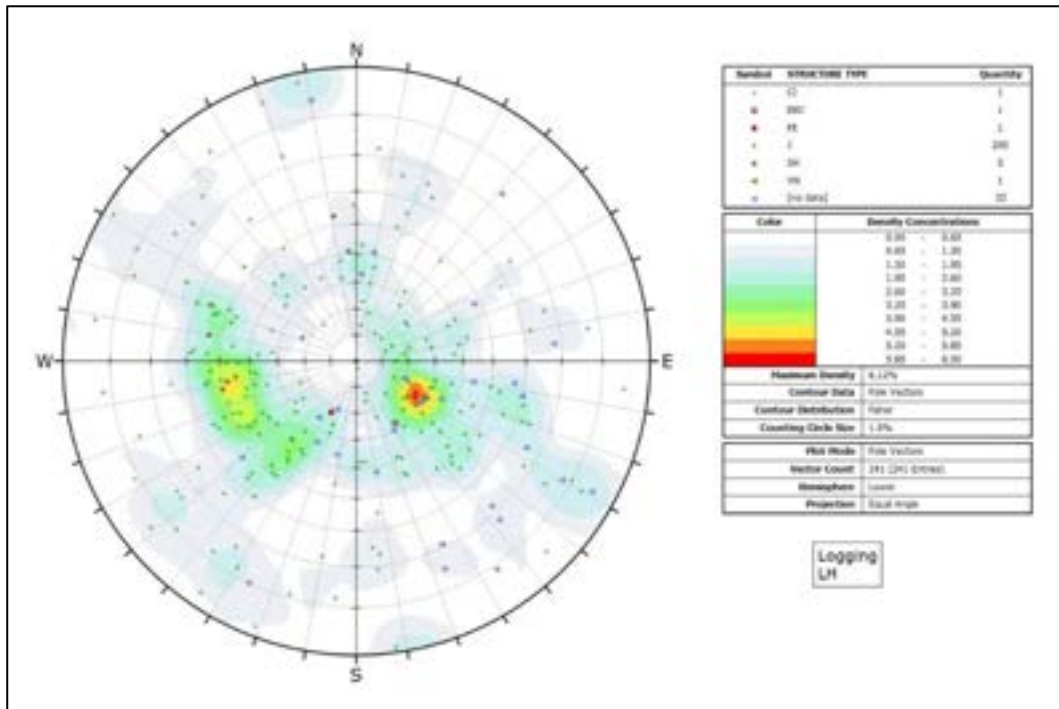


Figure 3-56: Stereonet showing orientation of structures logged – left abutment zone

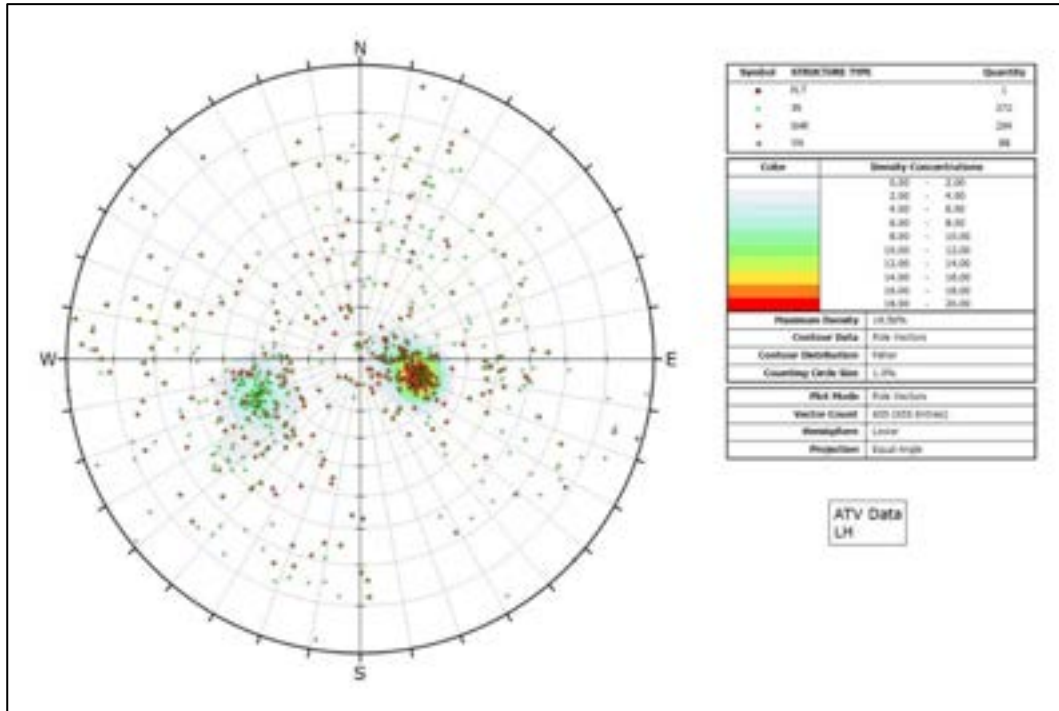


Figure 3-57: Stereonet showing orientation of structures identified from televiewer – left abutment zone

Right abutment

Stereonet plots in Figure 3-58 through Figure 3-60 show the orientation of the structures observed in the right abutment zone subdivided into North and South, from logging and ATV respectively. No televiewer surveys were undertaken in the RHN abutment zone.

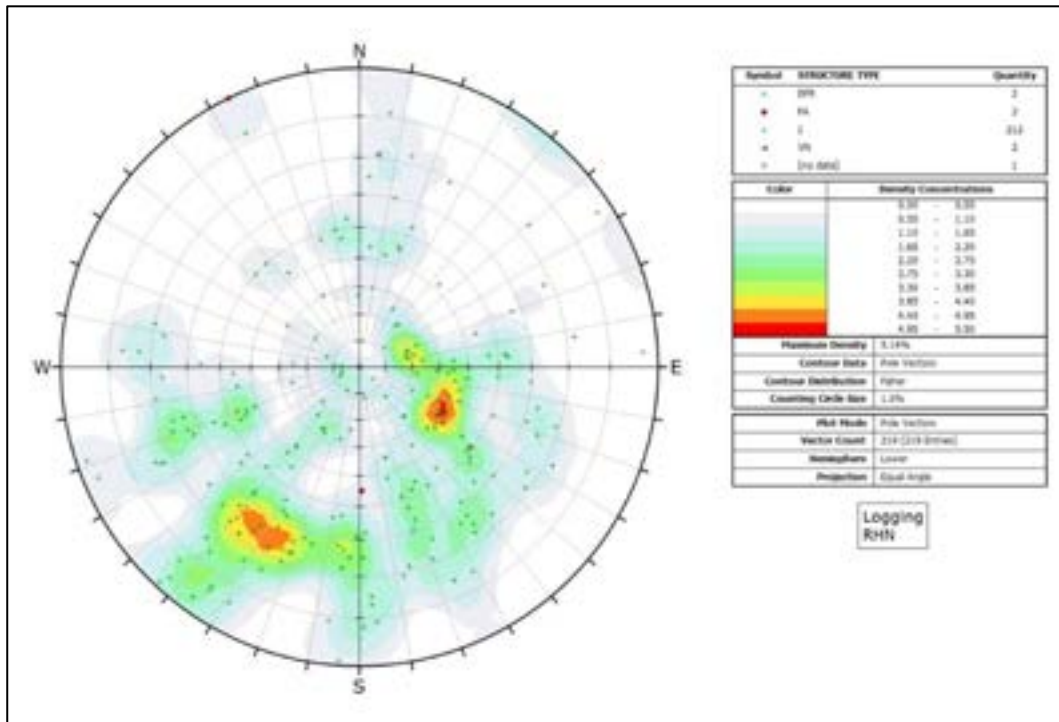


Figure 3-58: Stereonet showing orientation of structures logged – RHN abutment zone

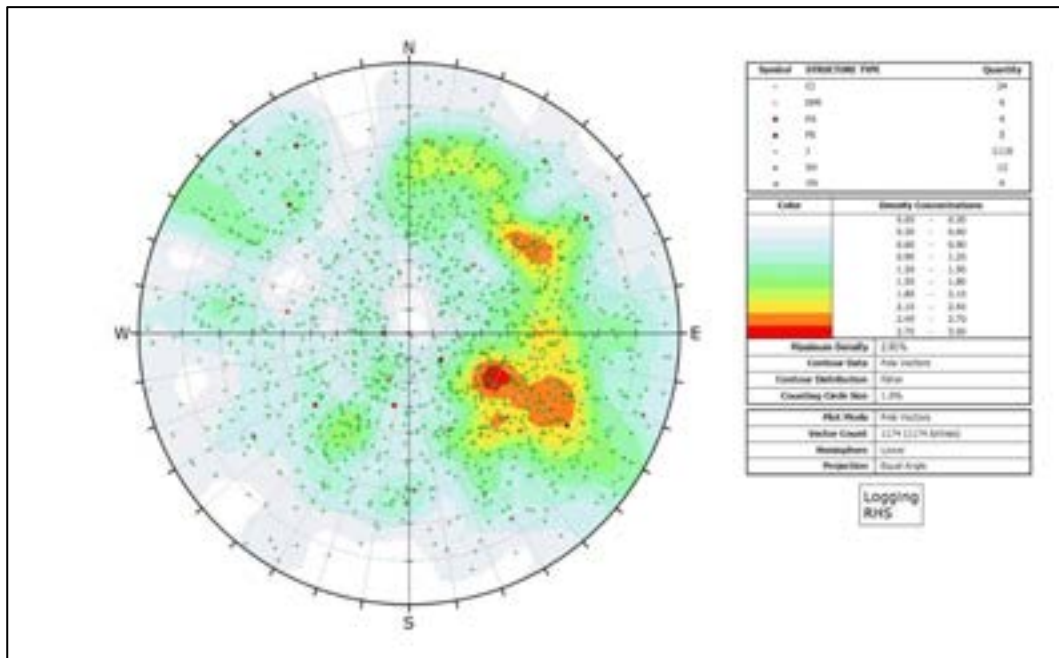


Figure 3-59: Stereonet showing orientation of structures logged – RHS abutment zone

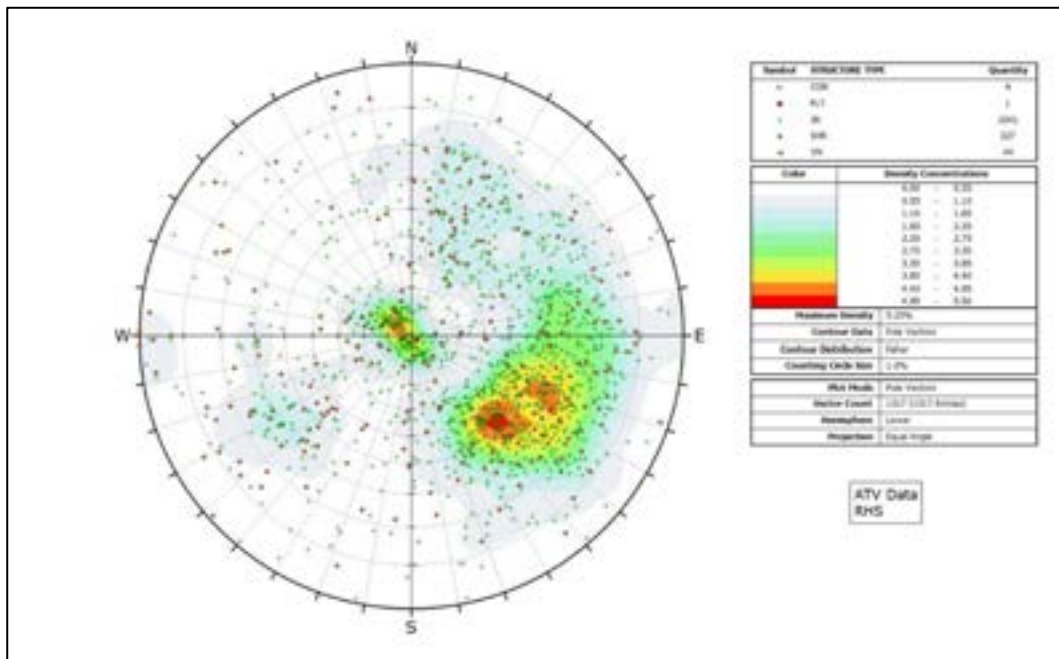


Figure 3-60: Stereonet showing orientation of structures identified from televiewer – RHS abutment zone

Quarry

Stereonet in Figure 3-61 through Figure 3-63 show the orientation of the structures observed in the quarry zone subdivided into North and South, from logging and ATV respectively. No televiewer surveys were undertaken in the QN zone.

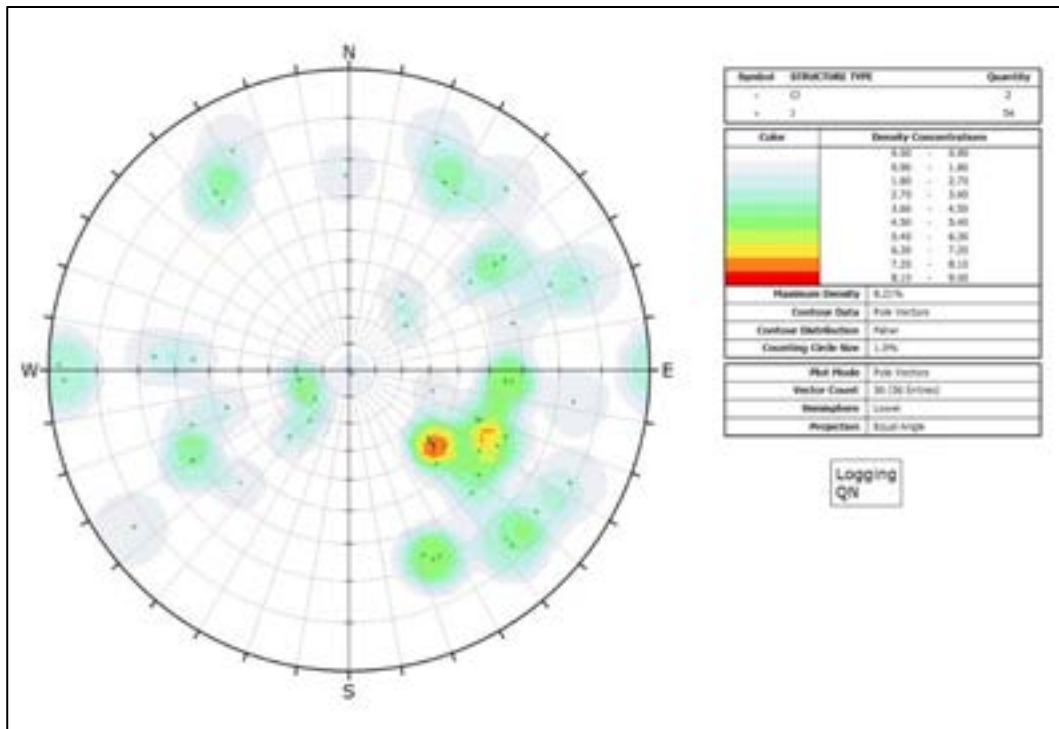


Figure 3-61: Stereonet showing orientation of structures logged – QN zone

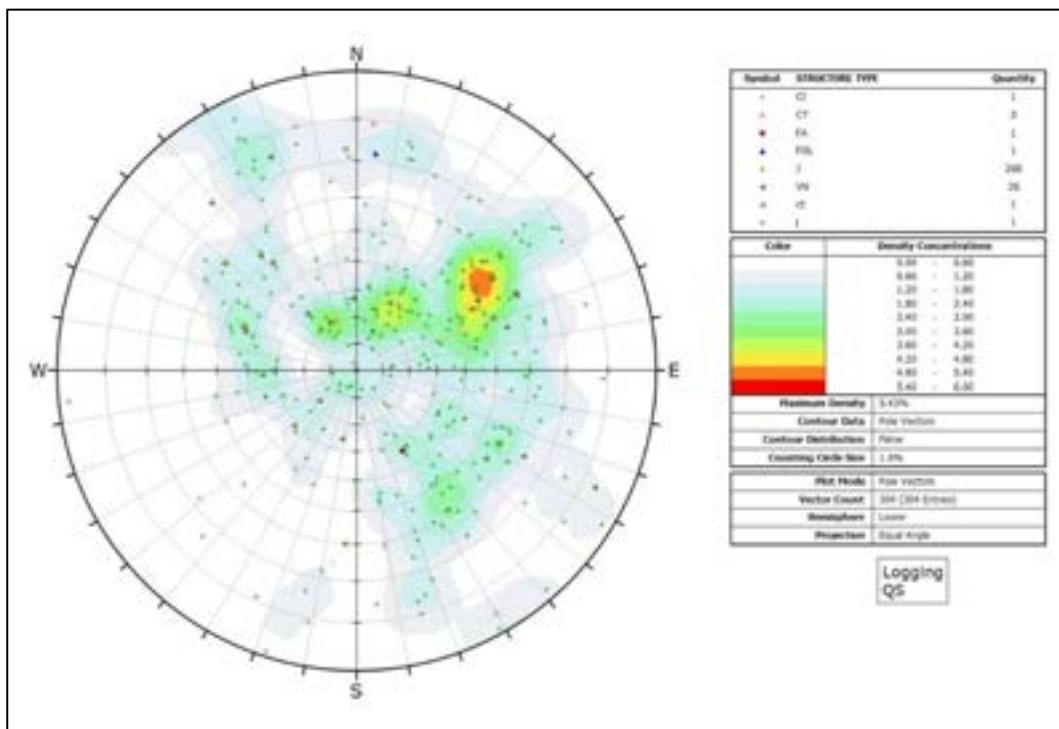


Figure 3-62: Stereonet showing orientation of structures logged – QS zone

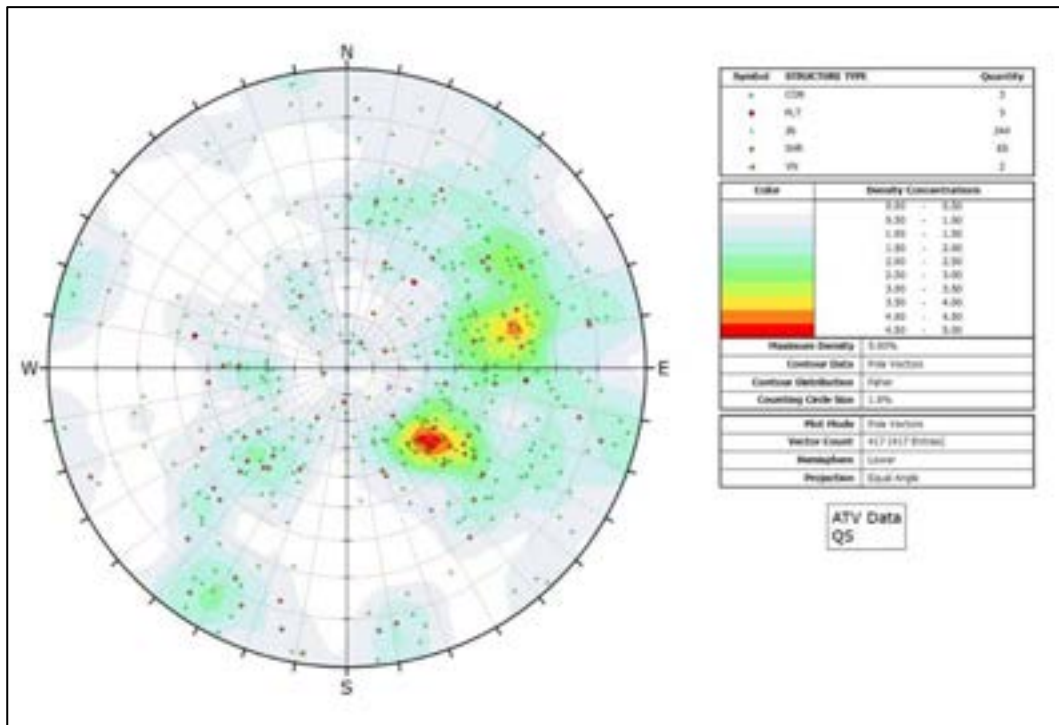


Figure 3-63: Stereonet showing orientation of structures identified from the televiewer – QS zone

Valley floor

Figure 3-64 shows the orientation of the structures logged in the valley floor zone. No televiewer surveys were undertaken in this zone.

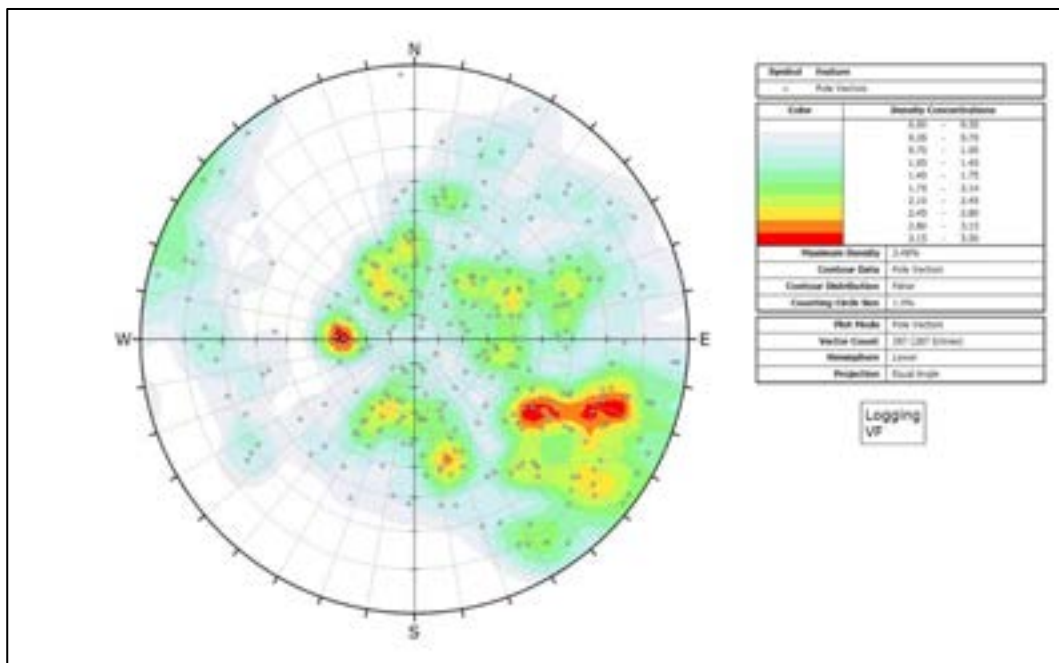


Figure 3-64: Stereonet showing orientation of structures logged – valley floor zone

3.1.10 Major structures

During the 2015 studies for an ISF (location of which was to the southwest of the FRHEP site in the valley of the Nena River), a preliminary classification of fault structures within EL1212 was suggested. This classification describing four orders of faults (the first order faults being the largest) was based

on regional geology information as well as field observations, where applicable. The classification has been simplified and adapted for the FRHEP site, as presented in in Table 3-25.

Table 3-25: Classification of fault structures

Ranking	Faults	Type	Description	Recently active	Confidence in position and orientation
First order	Frieda	Thrust fault with later normal and/ or strike slip movement	Major damage zones many tens of metres wide with multiple phases of movement and re-healing. Fault breccia/ gouge with quartz re-healing, current breccia and gouge with soil-like properties, oxidation	Yes	High
	Saniap	Thrust fault with later normal and/ or strike slip movement		Yes	High
Second order	Major Transfer Structures	No detailed investigation knowledge. Generally expected to have a NNE–SSW strike, a relatively steep dip, large continuity and damage zones of significant width		Possibly	Low
Third order	Large faults encountered in drill holes	Significant faults with strike-slip or other movement to accommodate stress in between major thrusts and transfer faults	Significant damage zones up to a few tens of metres wide with multiple phases of movement and re-healing. Fault breccia/ gouge with re-healing and current smaller shears with gouge or mylonitisation	Possibly, but possibly insignificant	Dependent on drilling information at FRHEP site – interpretations are of medium confidence
Fourth order	Numerous smaller faults encountered in drill holes	Network of smaller faults/ shear zones	May present small zones of breccia or gouge a few tens of cm wide, or highly fractured rockmass (not breccia) up to a few tens of metres across.	Probably insignificant	

First order structures

The Saniap Fault and likely fault splays lie close (1.5–2 km) to the north of the embankment site. This fault has been interpreted in previous studies (Scott Wilson, 2011) to be recently active (within the last 200–300 years). The Frieda Fault, located approximately 9 km to the south of the site, has been interpreted to be active within the last 200 years. Therefore, the embankment design will need to account for potentially high seismic ground accelerations. Re-evaluations of the seismicity of the area were conducted by Linda Al Atik and Nick Gregor in September 2016³⁶, as detailed in the report, ‘Seismic Hazard Assessment for the Frieda River Tailings and Waste Integrated Storage Facility, Papua New Guinea’. This assessment indicated a peak ground acceleration (PGA) for a maximum credible earthquake (MCE) of 1.09, based on earthquake scenarios on the Frieda Fault (it could be argued that the Saniap Fault might present a similar scenario) and a set of seven crustal faults. Regardless of potential seismicity issues, neither of these structures will directly affect the site of the FRHEP embankment and appurtenant infrastructure.

³⁶ Al Atik, L and Gregor, N, 2016. Seismic Hazard Assessment for the Frieda River Tailings and Waste Integrated Storage Facility, Papua New Guinea.

Potential second order structures

During the high-level site review and fatal flaw studies carried out in mid to late 2016, concern was expressed over the potential presence of large faults within the gorge in which the FRHEP embankment is to be situated. The gorge is distinctly straight, and it was assumed that it had been formed along a significant fault plane. It was considered that a fault that was responsible for the formation of the gorge could be a second order structure (large transfer fault).

The Scott Wilson (2011) report presented the opinion that a fault in the gorge would likely be limited to the klippe of April Ophiolite, and its short length and probable limited depth is not likely to be capable of generating a significant earthquake or primary surface rupture. However, the possibility of minor secondary displacements associated with a future large earthquake on the Frieda or Saniap faults was not precluded.

Although the FRHEP site gorge has an orientation roughly in line with what is expected for second order structures, previous geotechnical drilling investigations in 2010/ 2011 failed to encounter any faults of the magnitude that would be expected for a second order structure. The information suggested that the gorge may have been formed by a NNE–SSW striking, east dipping thrust fault the plane of which might govern the angle of the 30° dipping western slopes of the gorge. The large zone of highly fractured oxidised rock on the LH (western) slope of the gorge indicated that such a fault may be present. However, the low angle of the potential fault plane(s) is not easily reconcilable with the expected nature of second order structures, and a corresponding fault zone of large thickness has not been encountered dipping eastwards beneath the slopes on the right side of the gorge. Also, some structural observations taken within the gorge indicate that a major fault within the gorge may have a normal, rather than a reverse (thrust), sense of shear. It is possible that different shear senses have developed as the stress regime in the area has altered with different events over time, and that movement on different faults or sets of faults has occurred as these have been activated or re-activated; evidence is not conclusive.

One of the aims of the Stage 1 and 2 site investigations in 2017/ 2018 was to attempt to confirm or rule out the presence and position of large fault structures in the gorge, and this was considered in the drilling design. The investigations have confirmed that although numerous smaller faults (of third or fourth order) are present within the bedrock, no major faults of greater size have been identified.

Previous deformation

A significant amount of the good quality, strong dunite bedrock exhibits previous structural deformation and re-healing, with the matrix consisting largely of cryptocrystalline olivine. It is likely that this deformation occurred at a relatively early time, possibly related to the thrusting of the ophiolite package up over the terrestrial units (locally the Ok Binai and Wogamush units), and that it has little to do with the more recent stresses and fault patterns within EL1212. The re-healing of the material has rendered it good-quality rock; however, in places this olivine matrix has been serpentinised and the rockmass is deteriorating. This occurs only in localised zones, and the mechanism facilitating the deterioration has not been determined to the point of allowing for prediction and accurate delineation of the positions of such zones of rock.

Thin mylonite banding has been observed in some drill holes, although this is not easy to distinguish from the cryptocrystalline olivine that forms the re-healing matrix. In a few places this has been observed to offset partially oxidised joints by small amounts (Figure 3-65), indicating relatively young fault movement, although the timing of most recent movement is not known. Intense compressional force would have been required to pulverise the rock and then fuse it into a hardened mylonite band.



Figure 3-65: Band of mylonite in drill hole F4 that offsets partially oxidised fractures/ joints

Third and fourth order structures

The previous and current drilling investigations have encountered several fault zones of limited size; however, the drilling has not identified a single large fault damage zone beneath the gorge that appears to be trending parallel to it. The presence of major structures has therefore not played a critical role in the selection of the embankment site within the gorge. However, the presence of third or fourth order faults is likely to have played a role in defining the geomorphology of the FRHEP site, and may have an influence on slope stability and permeability through the abutments.

Using the drilling geotechnical and structural data, televiewer data and core photographs, an identification and characterisation of faults in the FRHEP site gorge has been conducted.

Fault characterisation

Fault/ fault zone intersections within each drill hole were recorded according to the following:

- Downhole depth of their upper and lower margins
- Geotechnical domain in which they were encountered
- Description of the material(s) within the fault zone
- Ranking according to the proportion of solid (fractured rock) and matrix (rock fragments, gouge, and soil-like materials) of the fault zone – classified according to Table 3-26
- Ranking according to the thickness of the fault zone and the rockmass conditions therein – classified according to Table 3-26.

Table 3-26: Classification of faults

Proportions of solid and matrix	
A	Solid > matrix
B	Solid = matrix
C	Mostly matrix: variable fragment size 2-15 cm
D	Mostly matrix: fragment size 3-5 cm
E	Mostly matrix: fragment size <3 cm

Ranking according to thickness and rockmass conditions	
0	Modelled fault zone has little obvious impact on drillhole core locally
1	Narrow zone (10-50 cm) with poor to fair rockmass conditions (30<RMR<50)
2	Narrow zone (10-50 cm) with very poor to poor rockmass conditions (0<RMR<30)
3	Fault zone of width 0.5-2 m, with poor to fair rockmass conditions (30<RMR<50)
4	Fault zone of width 0.5-2 m, with very poor to poor rockmass conditions (0<RMR<30)
5	Wide fault zone of width >2m, with poor to fair rockmass conditions (30<RMR<50)
6	Wide fault zone of width >2m, with very poor to poor rockmass conditions (0<RMR<30)

Interpretation of fault planes

By rationalising the fault characterisation, assessing the permeabilities measured downhole, and assessing the topography, a number of third and fourth order faults have been interpreted, for which approximate planes have been defined using Leapfrog software.

The interpreted faults summarised in Table 3-27 do not represent all structures that may be present at the FRHEP site. The following must be noted:

- The relatively narrow width (generally less than 2 m) and variable nature of the fault zones encountered in the drill holes makes direct correlation of faults between drill holes very difficult.
- The fault planes identified therefore represent tentative interpretations in terms of their precise orientation and position along their strike length; however, there is a fair degree of confidence that faults of this orientation ('set') are present. Faults in a set may be present in an anastomosing (braid-like) pattern – which would present a degree of large-scale waviness and/ or a limit to the persistence of individual structures, especially fourth order structures.
- The permeability testing results indicate that permeability along individual fault planes or sets can be locally variable depending on the local conditions (highly fractured, oxidised rock that is or has been transmissive or fault gouge which may inhibit flow etc.). It is not certain that any of the interpreted fault planes have moderate or high permeability along their entire length, even if high permeability may have been measured locally.
- The relatively narrow width and nature of the fault zones indicates that their large-scale shear strength properties may not be very low, due to large-scale waviness and/ or the presence of hard fractured rock or rock fragments within the fault zone.
- There is very little evidence from drill hole plods, core logging, televiewer images and core photos to suggest that any significant solution enhancement along fault structures (or joints) has occurred.

The faults identified have four main orientations:

- Shallow east dipping, N–S striking structures, roughly parallel to the slopes of the left (western) side of the gorge – Set A
- Moderate west dipping, N–S striking structures, roughly parallel to the steeper slopes on the right (eastern) side of the gorge – Set B
- E–W striking, moderately to steeply south dipping structures orientated across the gorge – Set C
- Shallow west dipping, N–S striking structures dipping into the left hillsides of the gorge – Set D.

Table 3-27: Fault planes interpreted at the FRHEP site

Fault ID	Approximate average orientation		Fault 'set'	Descriptive comments	Fault order	Ramifications
	Dip (°)	Dip azimuth (°)				
1	26	105	A	N–S striking, east dipping, low angle fault that generally forms the lower bound of the potential landslide zone on the left abutment. Appears to be one of a series of parallel structures in this set that has resulted in this zone. Faults of this set may have been terminated (or offset) by Set B faults, and are therefore not easily identifiable in the right abutment.	3 (4 for others in the set)	Presents poor-quality rockmass that will need to be excavated to prevent slope instability in the left abutment and passage of water around the embankment.
2	40–45	285	B	A series of sub-parallel, N–S striking, west dipping, moderate angle faults with relatively narrow damage zones that have largely defined the angle and shape of the right abutment slopes. It is possible that the Set A structures terminate against the Set B structures.	4	May present or exacerbate slope instability issues in the spillway and quarry cut slopes. Unfavourable (acute) angle of intersection with conveyance and diversion tunnels may result in local wedge instabilities and/ or overbreak in tunnel roofs. May present zones of locally high permeability for transmission of water through the abutment, around the embankment.
3						
4						
5						
6	60	180	C	E–W striking, steeply south dipping fault situated north of the embankment near the powerhouse. Forms the steep north margin of an old slope failure valley on the left side of the gorge, and the notch in the spur on the right side of the gorge.	3	Will result in poor rockmass conditions in the conveyance tunnel near/ at the outfall portal. May result in poor rockmass conditions in the diversion tunnel and spillway cut (but obtuse angle of intersection is favourable).
7	~80	205	C?	E–W striking, likely steeply south dipping fault that forms a valley in the right side of the gorge, upstream from the embankment. Defines the southern constraint of the potential quarry area.	3	Poor rockmass conditions in the fault and to the south of it have constrained the southern extension of the quarry.
8	14	275	D	N–S striking, west dipping, low angle faults that dip into the left abutment. Identified from P-wave velocity patterns in the seismic refraction profiles.	4	These faults appear to have exacerbated the poor quality rockmass in the potential landslide zone on the left abutment.
9	17	265				

The interpreted approximations of the fault planes are illustrated in Figure 3-66 through Figure 3-73.

It is important to note that the fault plane interpretations are indicative. The faults are unlikely to be as simple, planar and persistent as the plane interpretations make them appear. The faults may represent several near-parallel or overlapping structures which involve rock bridges and significant variability in terms of width, nature, infill and permeability along the fault zones.

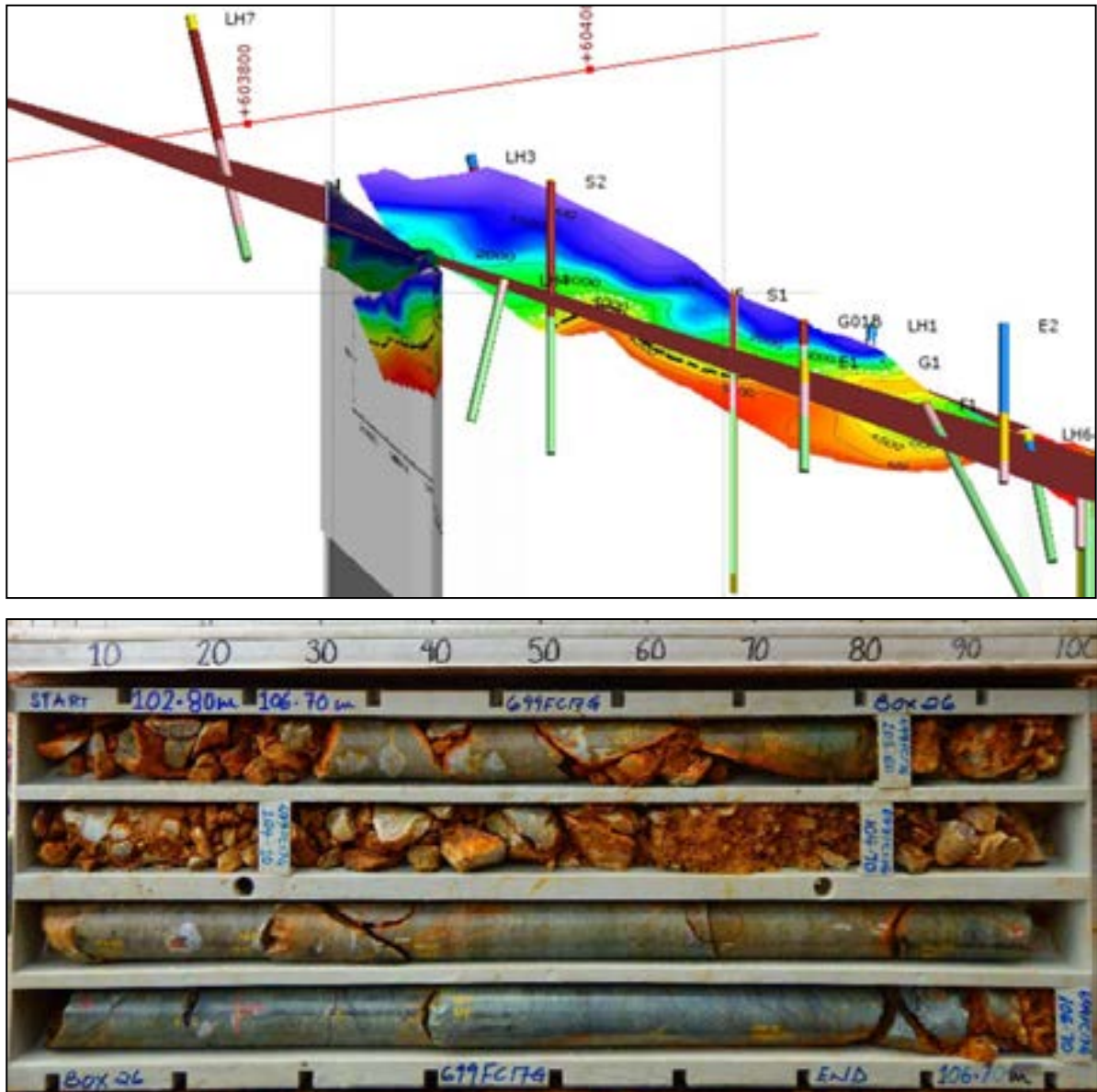


Figure 3-66: Illustrations of Fault 1 (Set A) interpretation in the left hillside: (above) isometric view looking NW showing the drill hole and seismic refraction traverse intersections; and (below) fault intersected in hole LH3

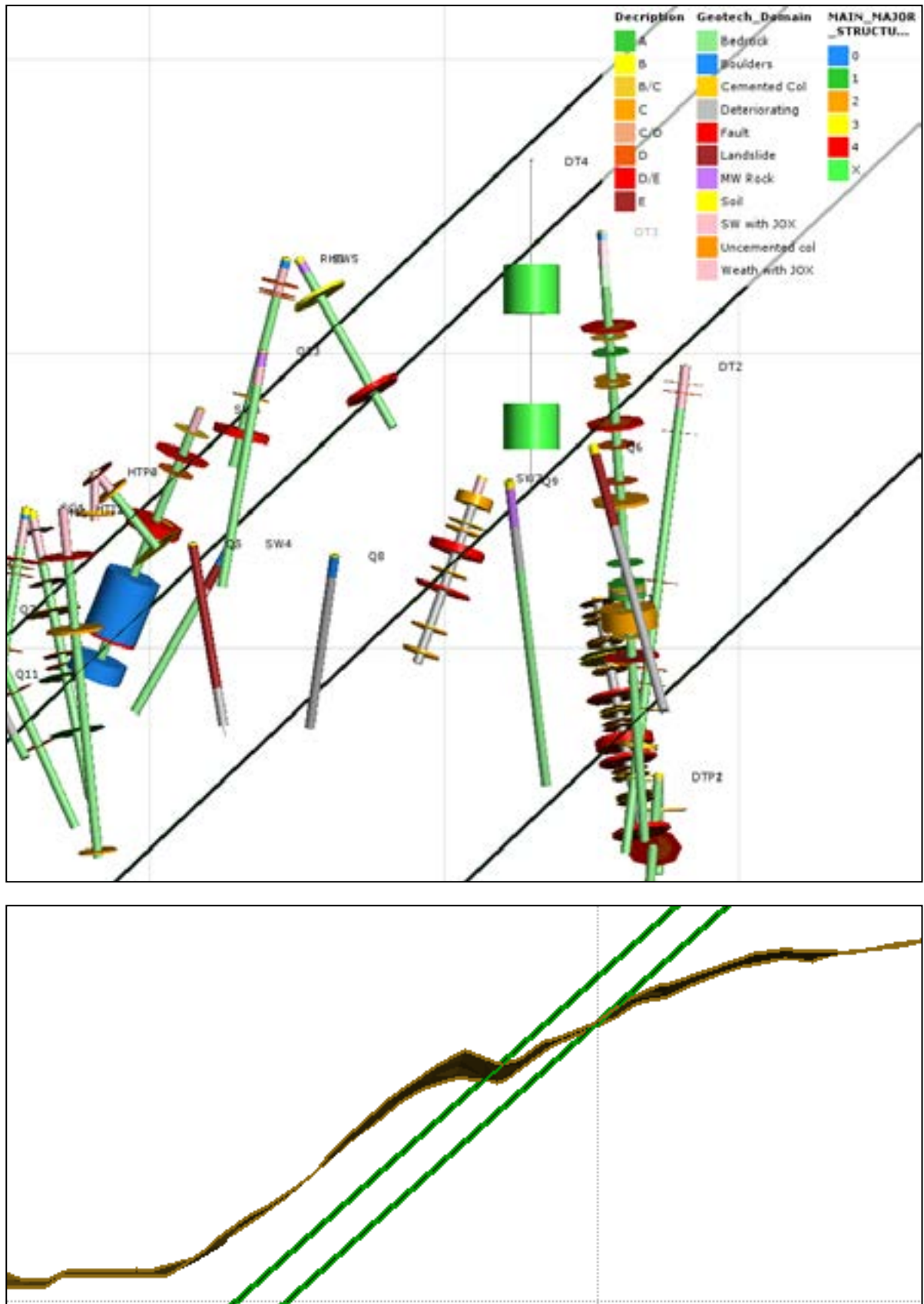


Figure 3-67: Illustrations of Set B fault interpretations in the right abutment: (above, from top to bottom) Fault 2, 3, 4 and 5 plane intersections with drill holes showing poor ground, looking north; and (below) intersection pattern of Faults 2 (left) and 3 (right with the topography in the right abutment), in section view looking north



Figure 3-68: Core photos illustrating the nature and variability of conditions along Fault 2 in the right abutment: (above) very thin gouge zone with oxidisation of surrounding joints in hole RH1; (middle) oxidised fracture zone with localised gouge in hole SW5; and (bottom) fractured, oxidised zone in hole SW6

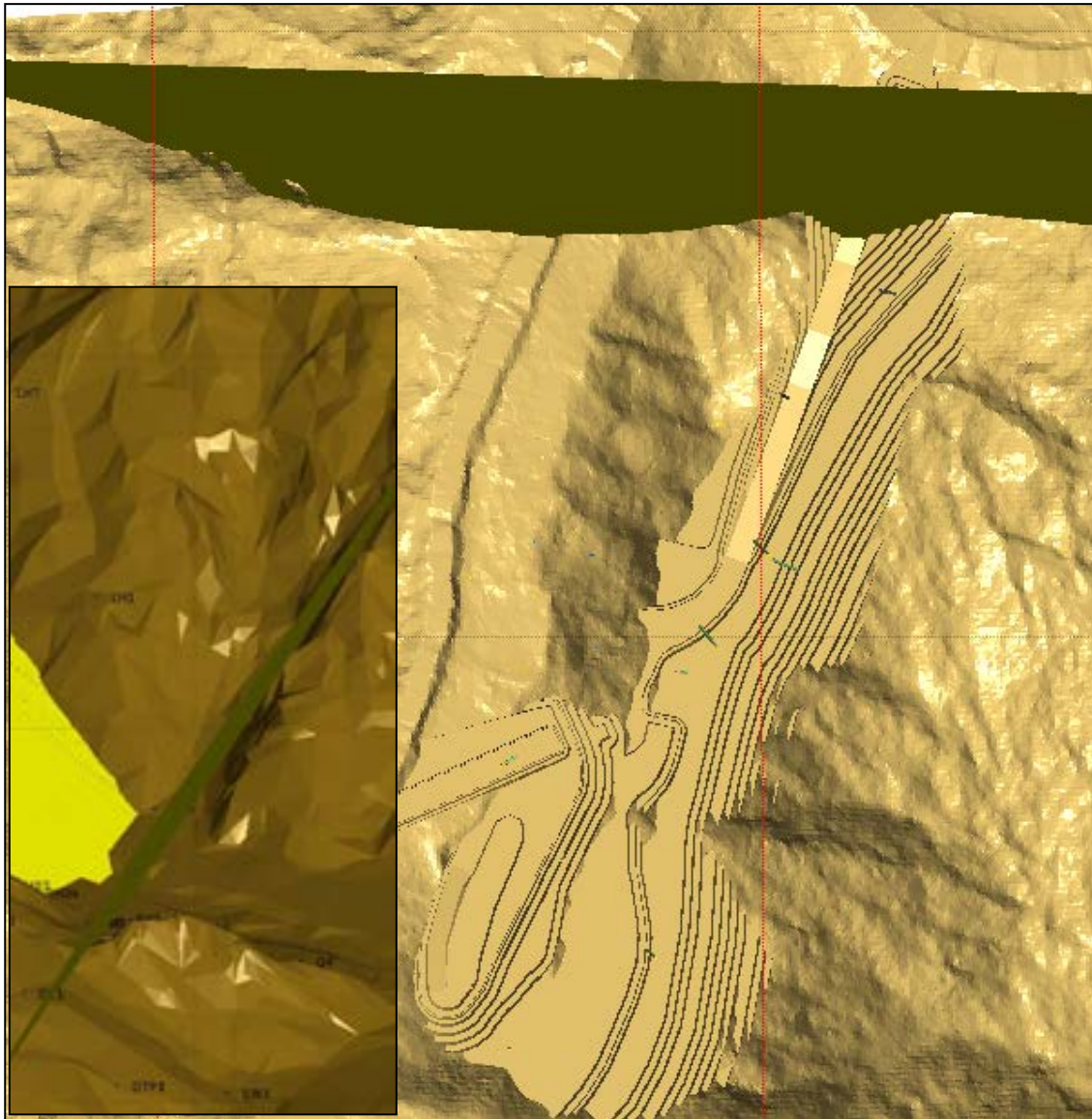


Figure 3-69: Fault 6 (main picture) interpretation with respect to topography and right abutment spillway in plan view; (inset) isometric view looking west showing topography and embankment



Figure 3-70: Core photographs from the right hillside in hole PH1

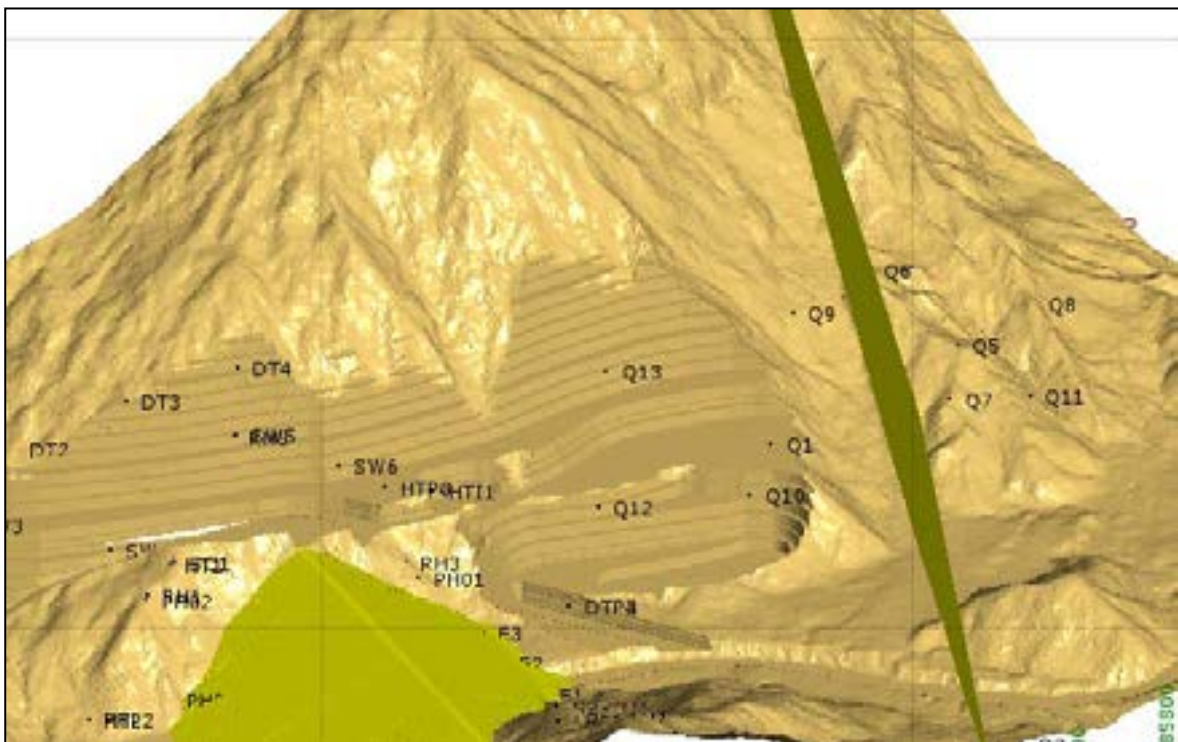


Figure 3-71: Fault 7 isometric view looking east showing the interpreted fault plane, quarry and embankment



Figure 3-72: Core photographs of possible intersection in the south quarry area in hole Q6

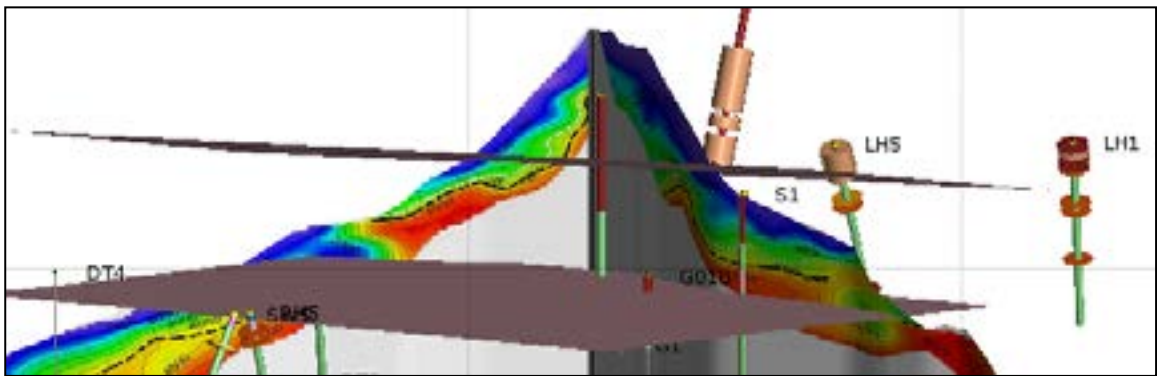


Figure 3-73: Isometric view looking west of Faults 8 and 9 (Set D) in the left hillside, relative to the poor ground in drill holes and the embayments in seismic refraction traverses 1 and 2

For comparison with fault orientations, the structural (joint set) patterns for the left and right hillsides of the gorge (represented as pole plots on stereonet) are shown in Figure 3-74 and Figure 3-75, respectively.

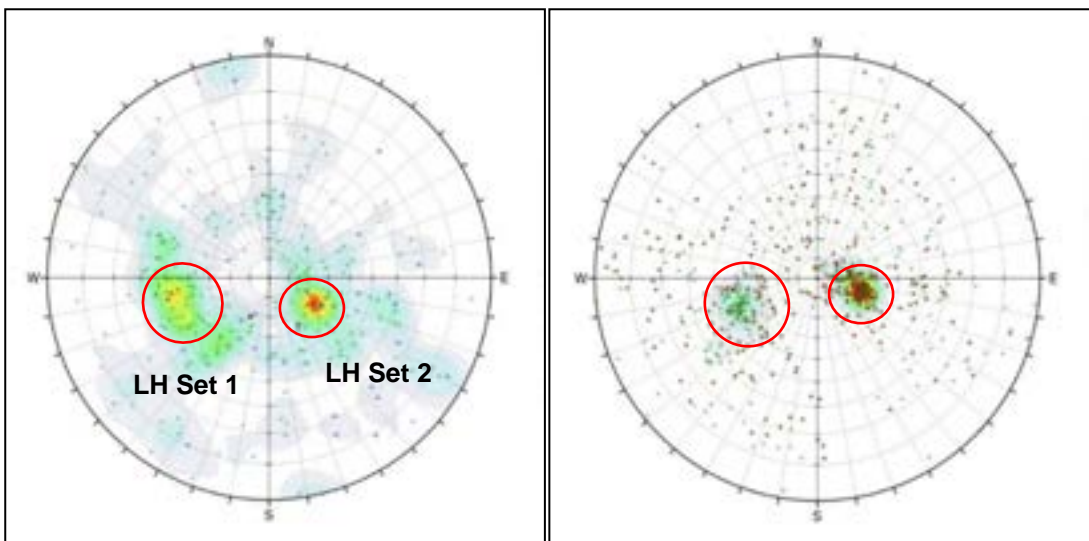


Figure 3-74: Stereonets presenting joint sets patterns for the left side of the gorge: (left) from core logging; and (right) from televiewer survey

Note: The core logging and televiewer results show good correlation, indicating two predominant joint sets.

On the left side of the gorge, the two predominant joint sets identified are (dip/dip direction):

- LH Set 1: 40°/ 080° (roughly equivalent but a little steeper than Fault Set A – Fault 1)
- LH Set 2: 20°/ 280° (equivalent to Fault Set D – Faults 8 and 9).

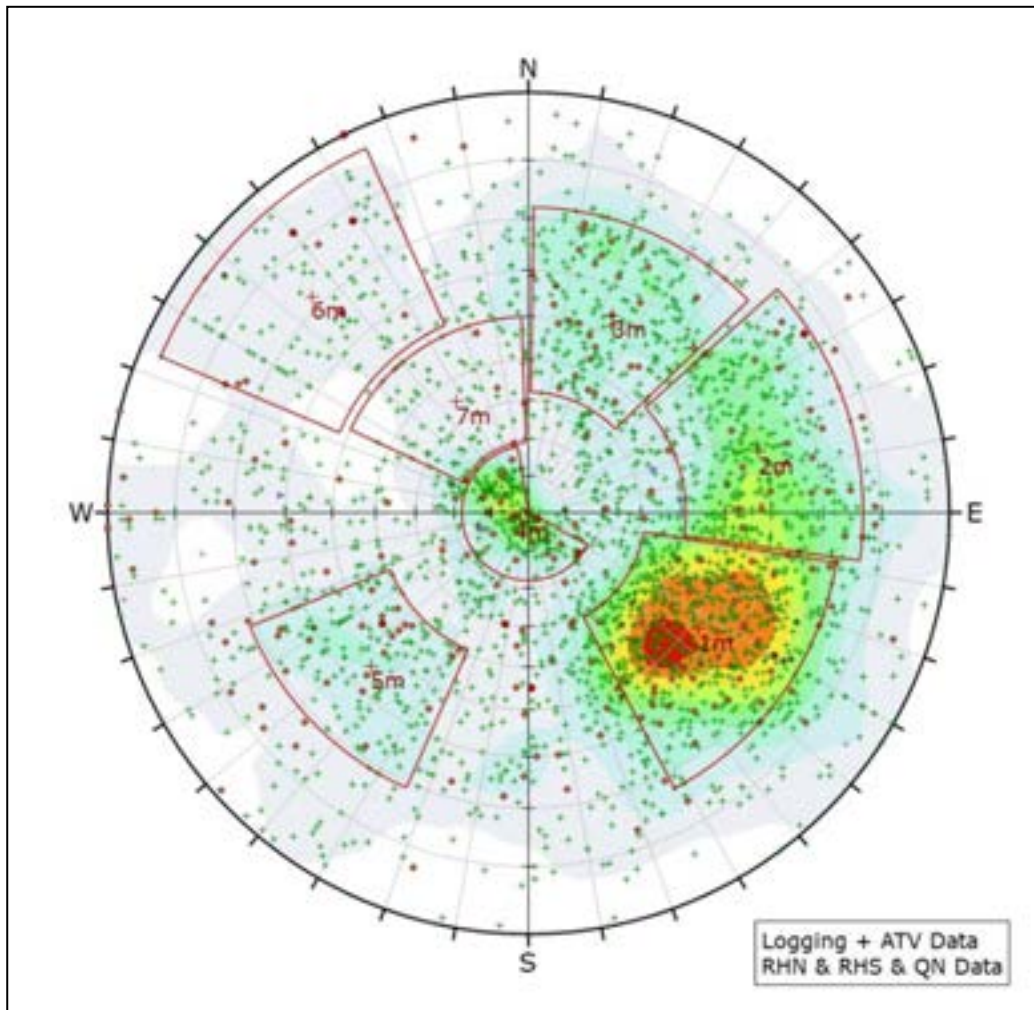


Figure 3-75: Stereonet presenting joint sets patterns for the right side of the gorge

On the right side of the gorge, the predominant joint sets identified are (dip/ dip direction):

- LH Set 1: 50°/ 305°
- LH Set 2: 60°/ 255°
- LH Set 3: 55°/ 205°
- LH Set 4: 05°/ 075°
- LH Set 5: 55°/ 045°
- LH Set 6: 70°/ 135°
- LH Set 7: 35°/ 145°.

Joint set 4 indicates the presence of shallow east dipping structures. Joint sets 1 and 2 indicate the presence of relatively strong sets of moderately west dipping structures (roughly in alignment with Fault Set B on the right hillside).

Figure 3-76 presents the predicted Riedel shear sets (at top left) for dextral strike slip movement on the NW–SE striking Saniap Fault, with major principal stress direction orientated approximately N–S, as expected. These can be compared with the rose diagram of the lineaments in the gorge and

surrounding areas (at top right). The dextral movement of the Saniap Fault is indicated by the eastwards offset of the topography to the north of the fault, as shown at the bottom of the figure.

The Set B faults and Joints sets 1 and 2 are loosely comparable to the R' and R shear sets (and the strongest, NNE–SSW and N–S trending sets on the rose diagram). The Set C faults, and the Set 3 (and to a lesser degree Set 5) joints are loosely comparable to the P shear set.

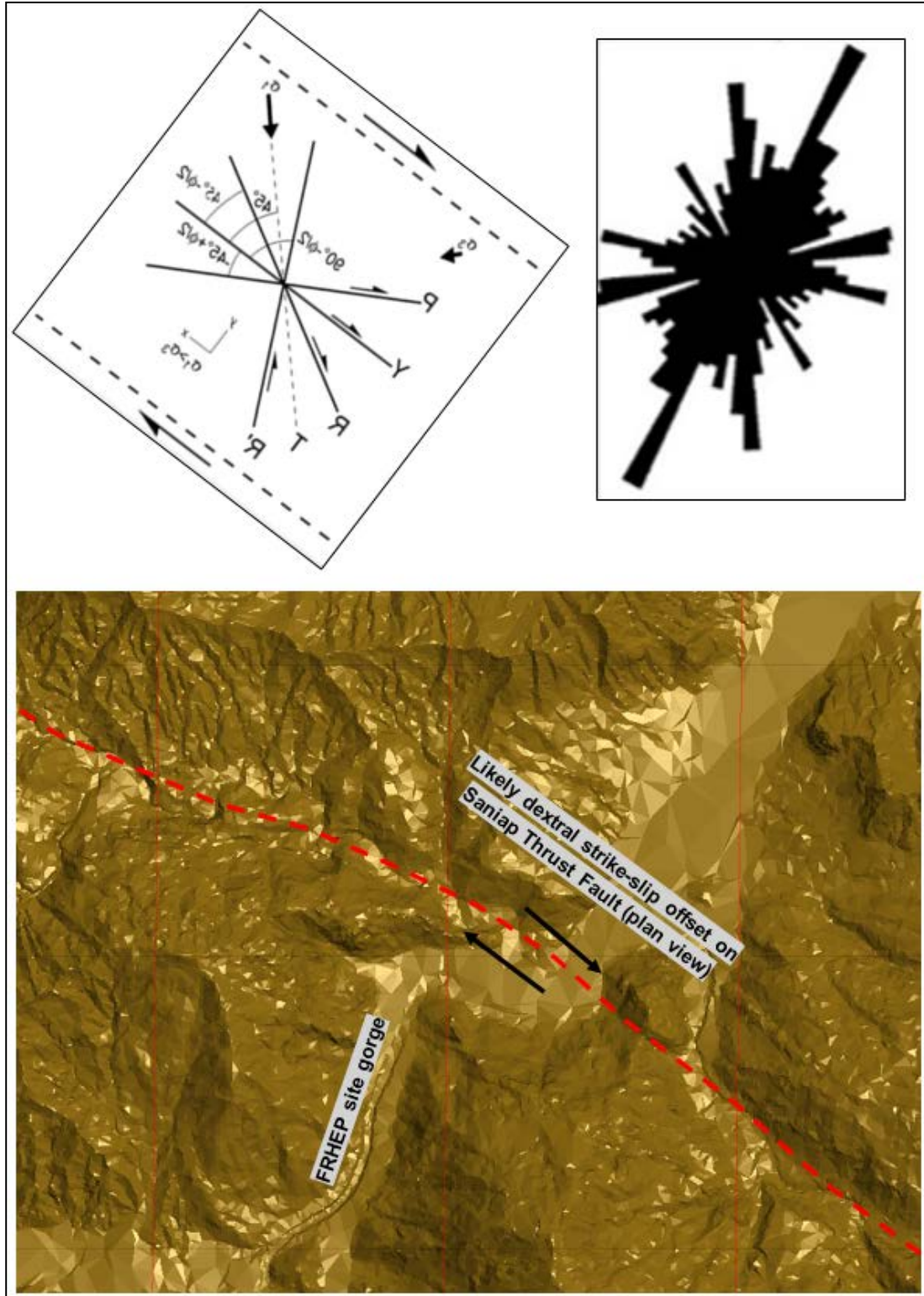


Figure 3-76: Riedel shear sets for strike slip movement on the NNW–SSE striking Saniap Fault (dextral movement in this case, hence the diagram is reversed)

3.1.11 Hydrogeological characterisation

Rockmass permeability testing results

Permeability testing (packer testing in bedrock and falling head testing in overlying or very poor quality materials) has been carried out in numerous drill holes within the valley floor and abutments at the FRHEP site.

A total of 79 permeability tests (68 with good or fair reliability of results) were performed in 17 geotechnical holes across the FRHEP site during the Stage 1 and 2 investigations. The finalised permeability testing results, as well as some results from earlier studies prior to SRK’s involvement, are summarised in Table 3-28.

Table 3-28: Summary of permeability testing results

k ranges (m/s)		Ranges Lugeon	Category
> 1E-05	5.00E-05	>50	High
5.00E-05	5.00E-06	10–50	Mod to high
5.00E-06	5.00E-07	5–10	Moderate
5.00E-07	5.00E-08	1–5	Mod to low
5.00E-08	> 1E-09	<1	Low

Area	Drill hole	Depth (m)	Permeability (k)		Test quality	k range
			m/s	Lugeon		
Left abutment - upper	LH1	33–53	6E-07	4	Good	Moderate
		74–99	1E-07	1	Good	Mod to low
		99–125	2E-07	2	Good	Mod to low
	LH3	80–120	3E-08	0.2	Good	Low
		110–120	2E-08	0.1	Good	Low
	LH5	47–76	2E-08	0.2	Fair	Low
		74–76	1E-05	-	FH test	Mod to high
		74–101	2E-07	1.4	Good	Mod to low
		89–101	2E-07	1.1	Good	Mod to low
		102–126	-	-	Suspect high k	High
		117–126	-	-	Suspect high k	High
		118–150	2E-07	1.7	Good	Mod to low
	133–150	1E-07	0.8	Good	Mod to low	
	S1	140–144		8	Historical DH	Moderate
		144–147		14	Historical DH	Mod to high
147–151			2	Historical DH	Mod to low	
S2	142–145		2	Historical DH	Mod to low	
Left abutment - lower	LH6	30–41	1E-07		Good	Mod to low
		40–41	1E-06		Fair	Moderate
		42–75	-	-	Suspect high k	High
		58–75	4E-08		Good	Low
		64–75	5E-08		Good	Low
	S4B	34–39		0.1	Historical DH	Low

Area	Drill hole	Depth (m)	Permeability (k)		Test quality	k range
			m/s	Lugeon		
River valley floor	LH2	68–105	1E-07	1	Good	Mod to low
		107–147	7E-09	0.05	Good	Low
		140–180	1E-08	0.08	Good	Low
	RH2	77–97	1E-07	1	Good	Mod to low
		104–166	6E-08	0.5	Good	Mod to low
	F1	51–70		0.5	Historical DH	Low
		100–108		4	Historical DH	Mod to low
		174–179		0.5	Historical DH	Low
		222–234		7	Historical DH	Moderate
		272–280		0.2	Historical DH	Low
	F2	69–75		0.1	Historical DH	Low
		75–81		0.1	Historical DH	Low
	F3	55–81		0.1	Historical DH	Low
	RH4	27–75	1E-07	0.7	Good	Mod to low
		55–75	4E-08	0.3	Good	Low
		75–100	7E-08	0.6	Good	Mod to low
	RH6	24–27	3E-07	-	Good, FH test	Mod to low
		35–38	9E-05	-	Good, FH test	High
		56–86	4E-07	3	Good	Mod to low
		74–86	8E-07	6	Good	Moderate
		86–104	5E-07	3	Good	Mod to low
	RH7	30–68	2E-08	0.2	Good	Low
		47–68	6E-09	0.03	Good	Low
		34–102	2E-07	1.5	Good	Mod to low
		67–102	5E-07	4	Good	Moderate
		85–102	9E-07	7	Good	Moderate
	Right abutment - upper	RH5	59–70	2E-08	0.1	Good
85–100			5E-07	3	Fair	Mod to low
DT2		149–163	1E-09		Fair	Low
		142–221	7E-09		Good	Low
		191–221	3E-09		Good	Low
		230–250	4E-08		Good	Low
DT4		53–78	6E-07		-	Moderate
		68–78	6E-07		Good	Moderate
		124–147	3E-07		Good	Mod to low
SW6		25–30	1E-05	29	Good	Mod to high
		52–77	7E-07		Good	Moderate
		94–127	-	-	Suspect high k	High
		141–150	-	-	Suspect high k	High

Area	Drill hole	Depth (m)	Permeability (k)		Test quality	k range
			m/s	Lugeon		
Right abutment - mid	RH1	34-57	-	-	Suspect high k	High
		112-126	-	-	Suspect high k	High
		112-147	-	-	Suspect high k	High
		127-147	1E-08	0.1	Good	Low
	PH02	90-160		0.1		Low
	HT1	31-69	6E-08		Fair	Mod to low
		46-69	6E-08		Fair	Mod to low
		84-120	2E-07		Good	Mod to low
		99-120	2E-07		Quest.	Mod to low
		124-150	2E-07		Good	Mod to low
140-150		6E-07		Good	Moderate	
Right abutment - lower	RH9	18-45	2E-08	0.2	Good	Low
		30-45	1E-08	0.08	Good	Low
		44-120	6E-09	0.15	Good	Low
		83-120	4E-09	0.03	Good	Low

Summary results from key drill holes are presented in Figure 3-77 through Figure 3-81 to illustrate the permeabilities measured in comparison with the rockmass conditions encountered.

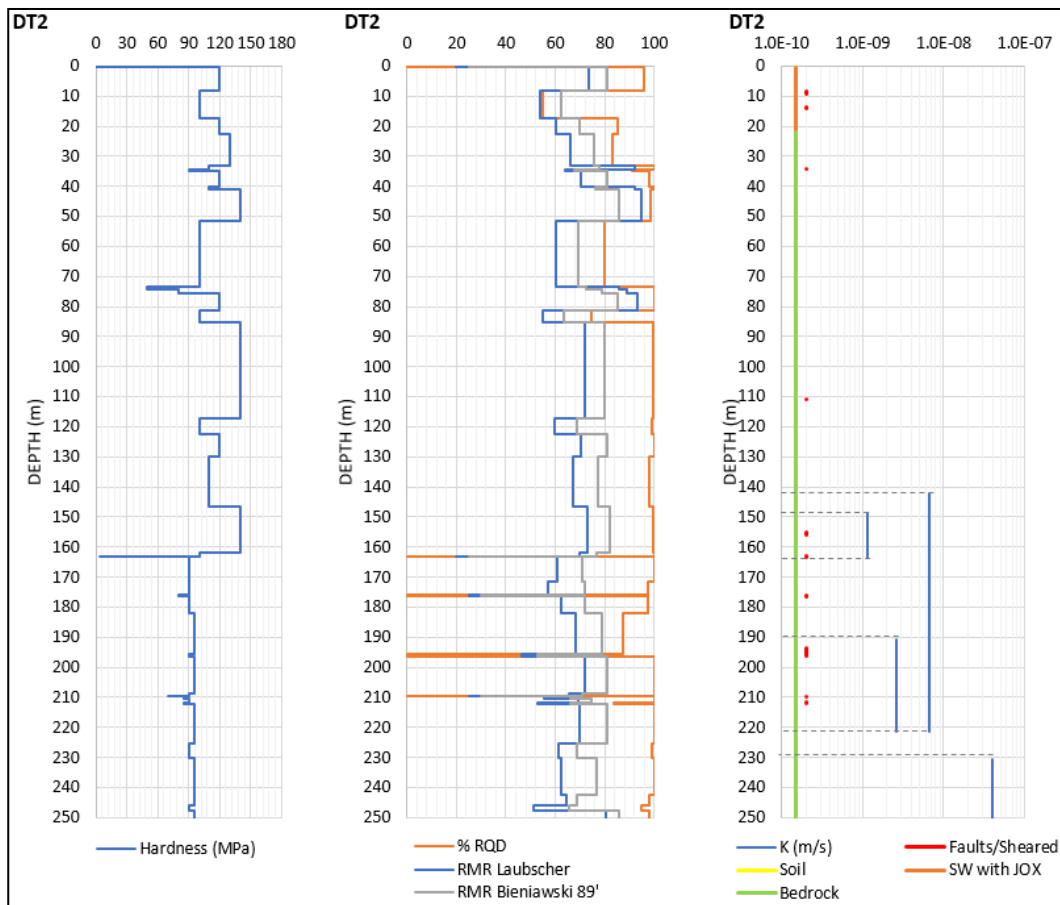


Figure 3-77: Drill hole summary for hole DT2 (right abutment)

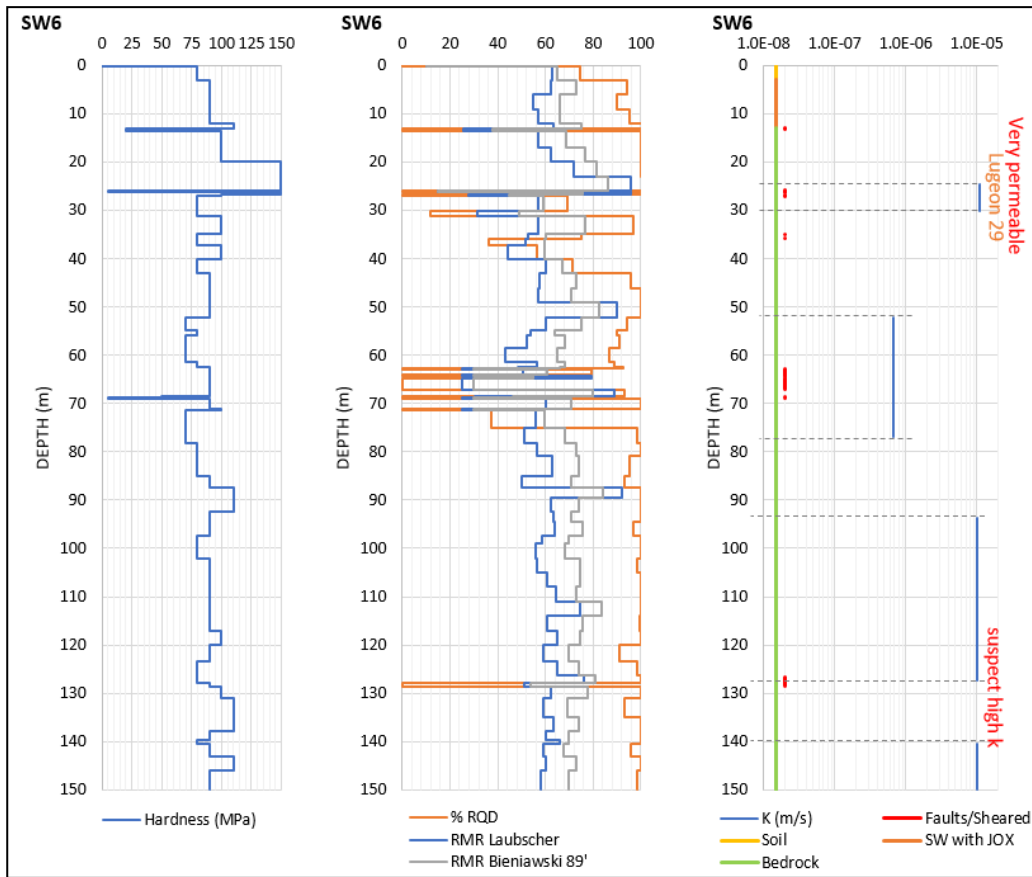


Figure 3-78: Drill hole summary for hole SW6 (right abutment)

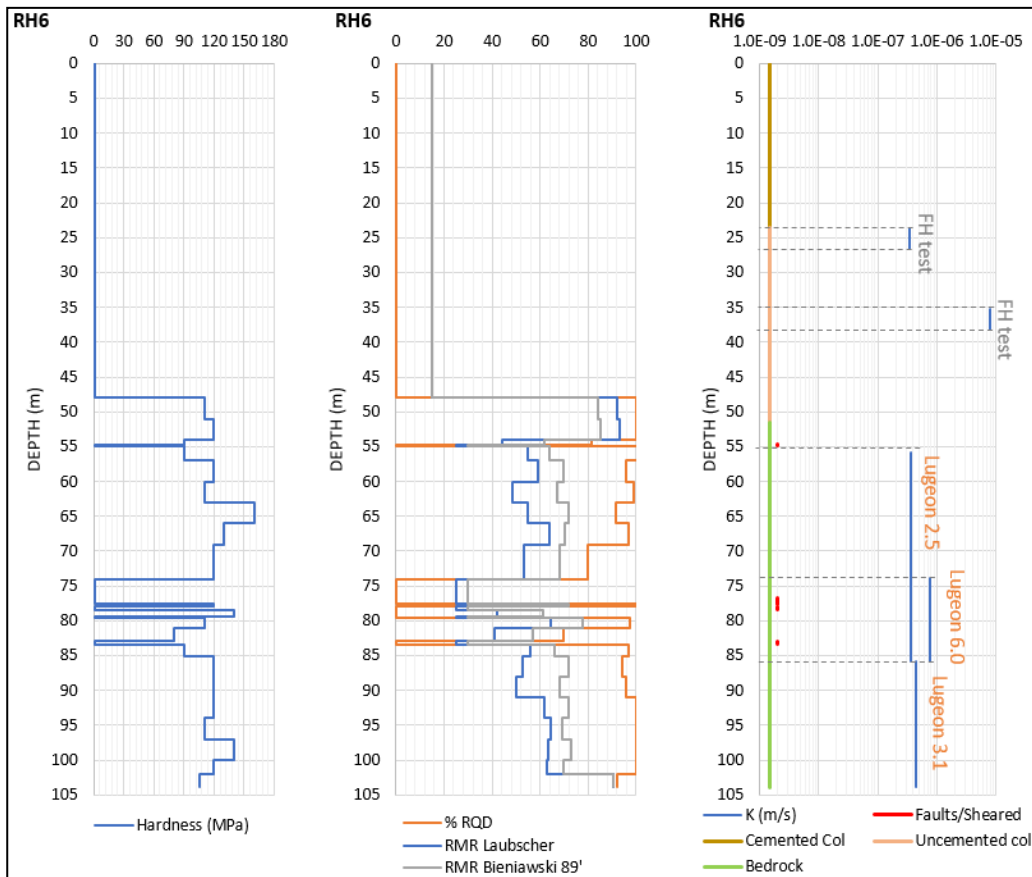


Figure 3-79: Drill hole summary for hole RH6 (valley floor)

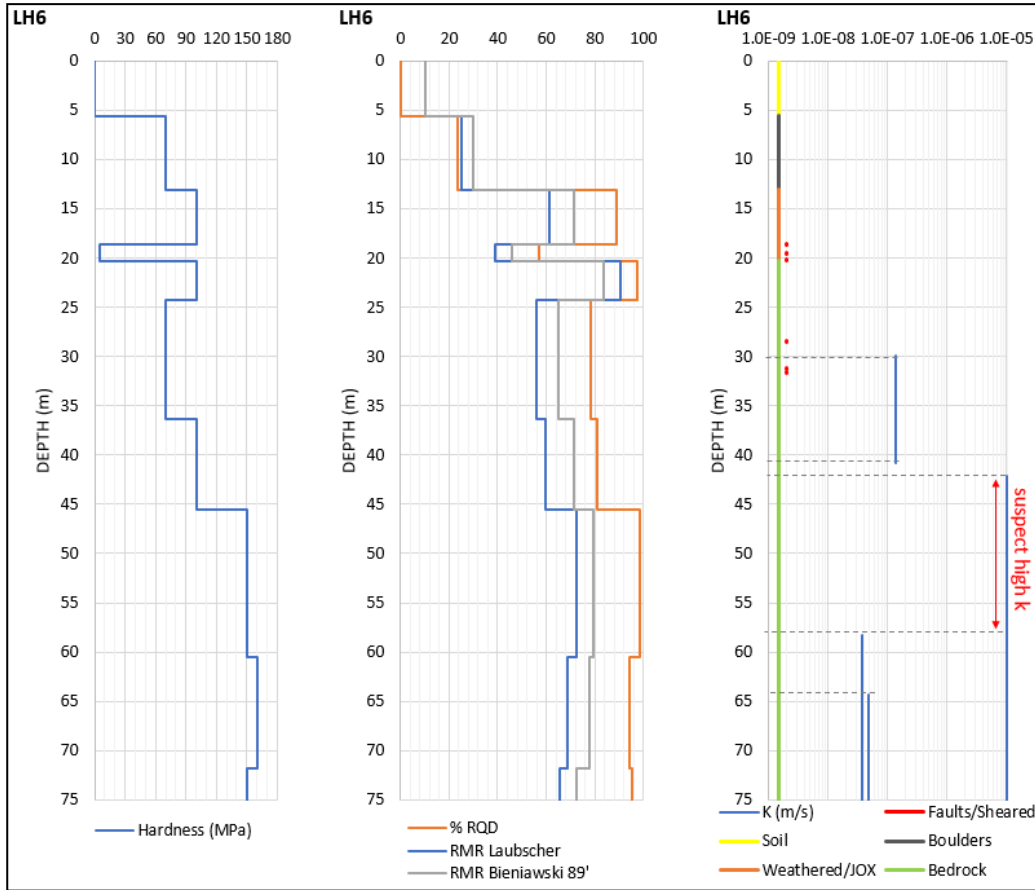


Figure 3-80: Drill hole summary for hole LH6 (lower left abutment)

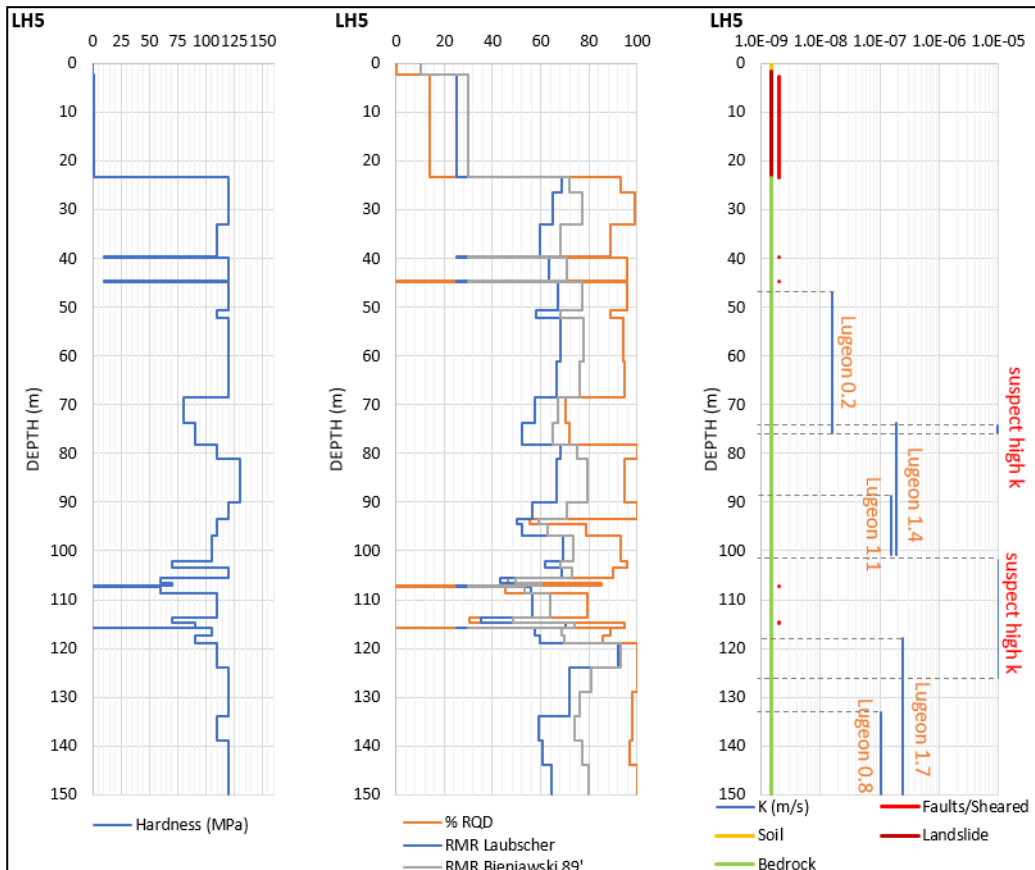


Figure 3-81: Drill hole summary for hole LH5 (left abutment)

Groundwater levels

The groundwater levels measured in the investigation drill holes are summarised in Table 3-29. Groundwater levels interpreted in the 2011 SKMPS study were also incorporated into the dataset. Some holes exhibited significant variability in the water levels for tests at different depths.

Table 3-29: Groundwater levels

Planned hole number	Drill hole number	Collar RL (m)	GWL (mbgl)	GWL RL (m)	Range in groundwater levels measured downhole (m)
LH1	685FC17G	251.8	37.6	214.2	35.9–39.8
LH2	680FC17G	59.1	8.9	50.2	9.1–11.5
LH3	699FC17G	299.2	94.0	205.2	100
LH5	720FC17G	232.6	31.3	201.3	31.8–90.0
LH6	700FC17G	120.1	17.3	102.8	17.9–56.8
RH1	682FC17G	213.1	54.4	158.7	57–100
RH2	681FC17G	64.6	1.7	62.9	1.1–2.7
RH4	686FC17G	65.2	4.0	61.3	4.4
RH5	687FC17G	366.2	62.6	303.6	39.2–90.5
RH6	704FC17G	66.5	16.0	50.5	16.0
RH7	723FC17G	67.0	6.1	60.9	3.8–8.0
RH9	698FC17G	120.7	10.3	110.4	7.3–14.7
SW6	703FC17G	287.0	44.9	242.2	49.5–91.4
DT2	716FC17G	315.4	103.0	212.5	96.0–110.8
DT4	717FC17G	414.6	65.3	349.3	65.3–65.3
HT1	715FC17G	239.1	57.8	181.4	59.6–59.6
E1	E1	73.3	17.4	55.9	
E2	E2	71.8	14.3	57.5	
E3	E3	78.2	15.2	63.0	
E4	E4	63.3	0.3	63.0	
E5	E5	67.4	4.3	63.1	
F2	F2	69.6	13.6	56.0	

The groundwater surface across the FRHEP gorge has been interpreted using Leapfrog. The software uses the measured downhole groundwater levels and the topographical patterns to interpolate/extrapolate a likely representative groundwater surface. Groundwater levels were very close to surface in the valley floor, 20–30 mbgl in the lower to mid hillside slopes, and 30–100 mbgl in the upper hillside slopes. An example of the interpreted groundwater level is shown in section in Figure 3-82.

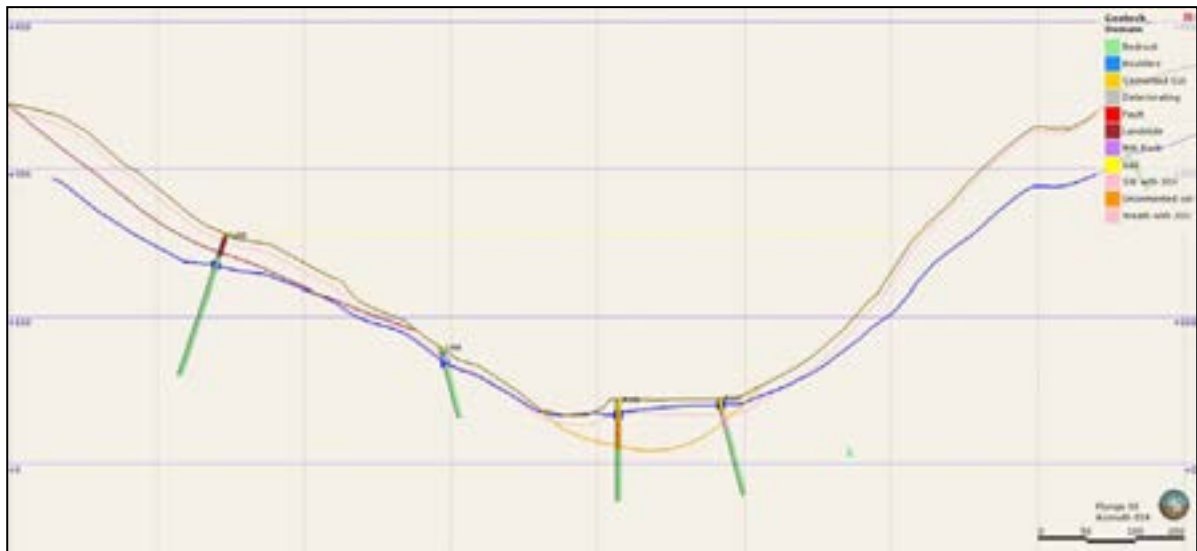


Figure 3-82: Section (looking north) showing the interpreted groundwater profile roughly along the centreline of the FRHEP embankment

For cut slope excavations, the effects of natural drainage and installation of 20–25 m long drainholes (in the spillway area) have led to the assumption of groundwater pushback to ~15–20 m behind the cut slope face. This does not represent significant depressurisation and will not significantly mitigate the risk of large-scale slope failures. To more accurately assess the requirements for and effectiveness of depressurisation measures on slope stability, seepage modelling should be done as part of future studies.

Conceptual understanding/ interpretation of abutment permeability

Hydrogeological conditions were assessed with respect to geological and geotechnical conditions in the holes tested and compared to untested holes in the embankment abutments. An attempt was made to correlate hydraulic conductivity values from the tests to features such as known and inferred major faults and areas of varying RQD, fractures per metre etc. to see whether high conductivity zones in parts of the abutment not directly tested could be identified or inferred.

In general, rockmass permeability within the embankment abutments can be characterised as low to moderate 1×10^{-9} m/s (<1 Lugeon) to 5×10^{-7} m/s (~5 Lugeons).

Drill holes that show high to moderately high permeability (k) zones, including ‘suspect high k tests’ are LH5, LH6, RH1, RH6 and SW6; the locations of these holes are shown in Figure 3-83. The holes are briefly described in the following sections, with comments on the expected controls on these zones provided. A comparison of high k intervals and RQD/ fault intersections in these holes is shown in Figure 3-84 to Figure 3-88.

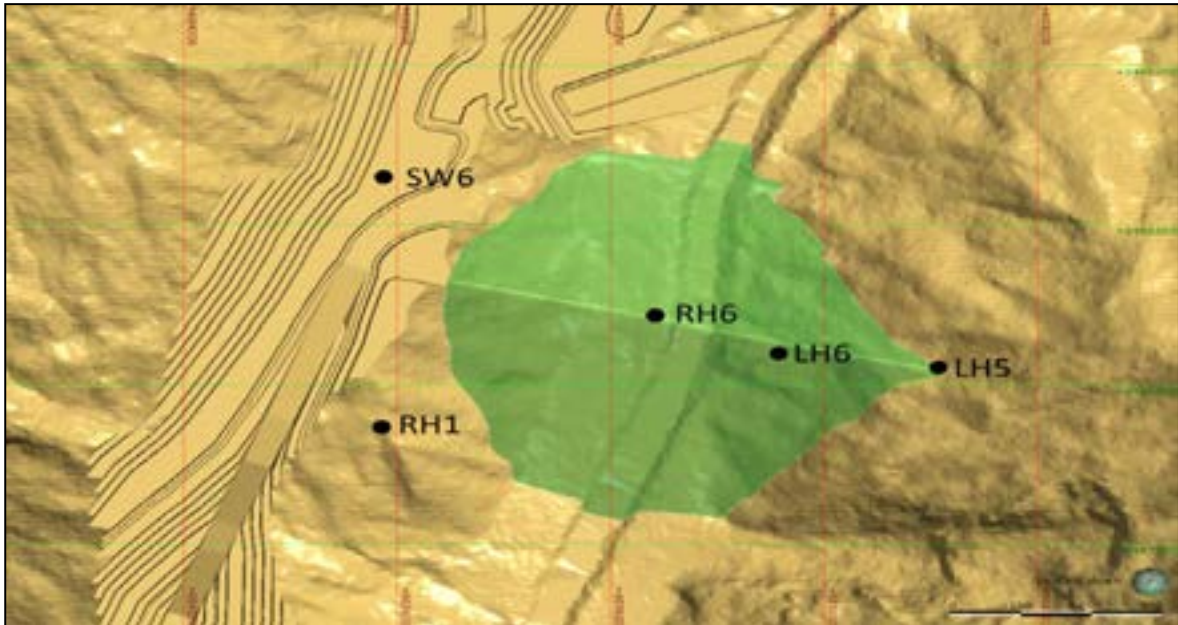


Figure 3-83: Positions of key drill holes that show moderately high to high permeability zones (plan view with north at bottom)

LH5 (embankment centreline; collar at embankment crest in left abutment)

- Large fracture zone is present from 101.9–125.9 metres down hole (madh). Pressure would not build during injection. Zone is suspect, but considered to be high k.
- RQD over this interval is variable (zero in places); appears to be related to Fault 8.

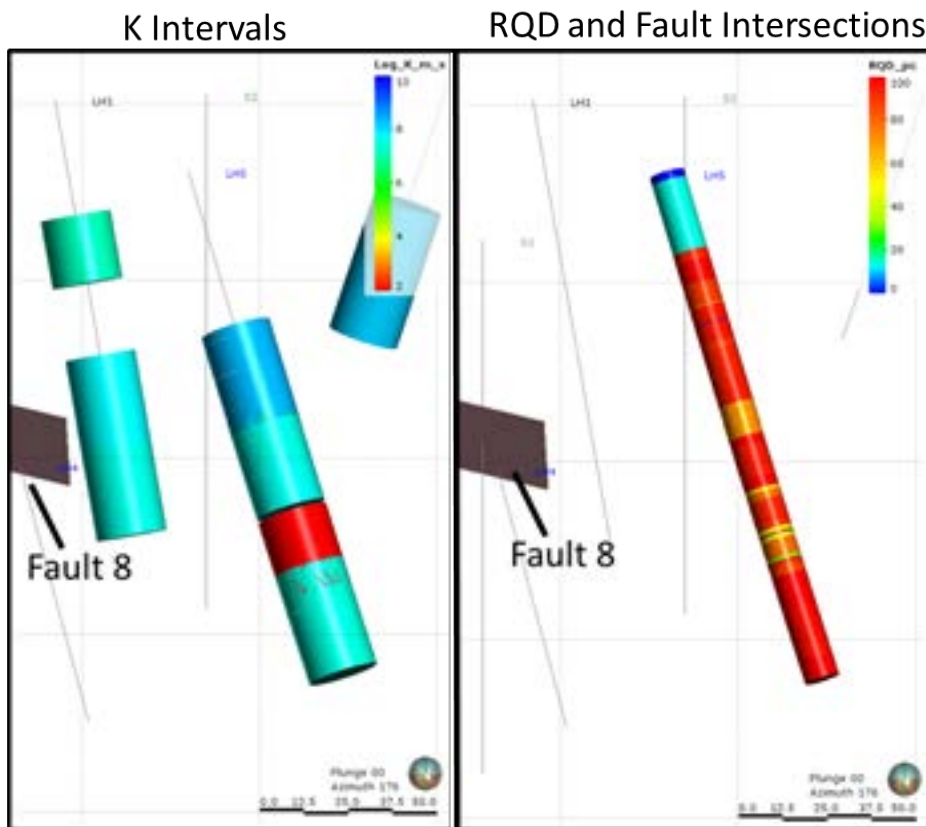


Figure 3-84: Comparison of high k intervals and RQD/ fault intersections in hole LH5 (isometric view, looking north)

LH6 (embankment centreline; collar low in left abutment)

- RQD is generally high in the high k interval, except for 1 m of core loss; however, little oxidation is evident. The zone of core loss may be associated with an additional discrete structure or splay below the interpreted Fault 1.

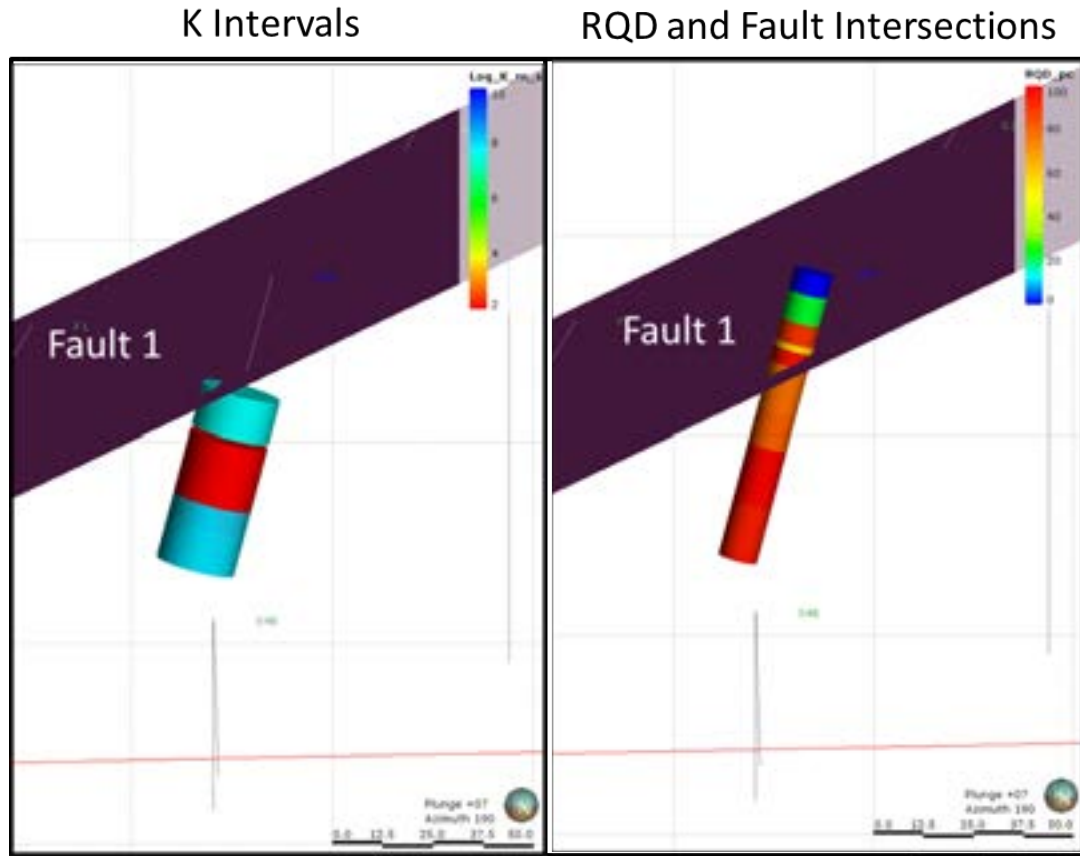


Figure 3-85: Comparison of high k intervals and RQD/ fault intersections in hole LH6 (isometric view, looking north)

SW6 (right abutment; collar ~60 m above embankment crest and to the south of centreline)

- High k (1.1×10^{-5} m/s) was measured near surface (24.6–30.0 metres downhole (madh)). This section will be removed during excavation of the spillway.
- In the lower two high k intervals, the test summary indicates no transducer data could be gathered, and high k is suspected.
- SW6 intersects both Fault 2 and Fault 3. RQD is low near Fault 3 from 127.8–128.62 madh, potentially causing the two high k intervals.

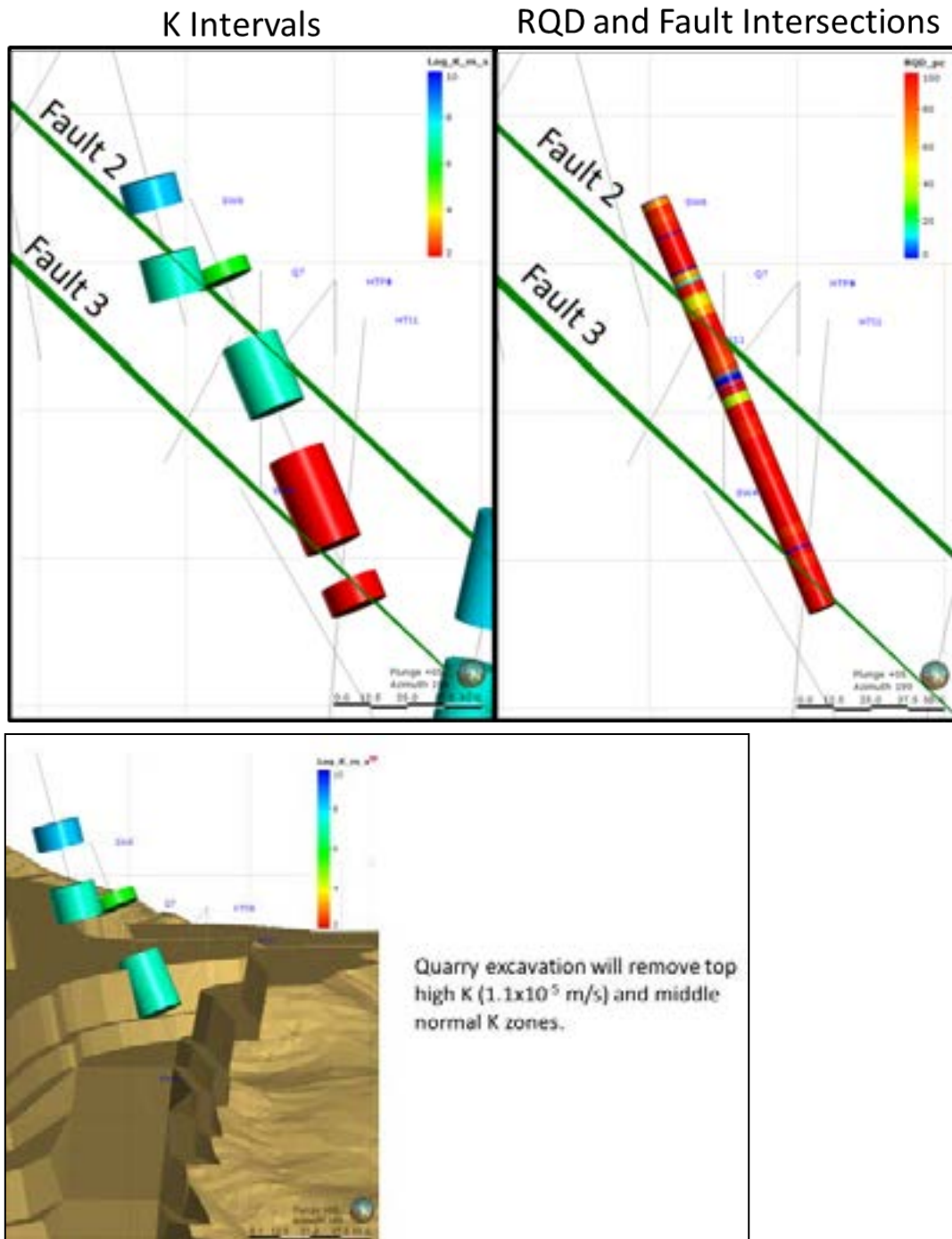


Figure 3-86: Isometric views looking north, showing (above) comparison of high k intervals and RQD/ fault intersections in hole SW6; (below) drill hole position relative to proposed spillway cut

RH1 (right abutment; collar at level of embankment crest and to the north of centreline)

- In upper and lower suspect high k intervals, no pressure build-up was observed despite injecting at 150 L/min for 45 minutes.
- Upper high k interval coincides with low RQD and Fault 2.

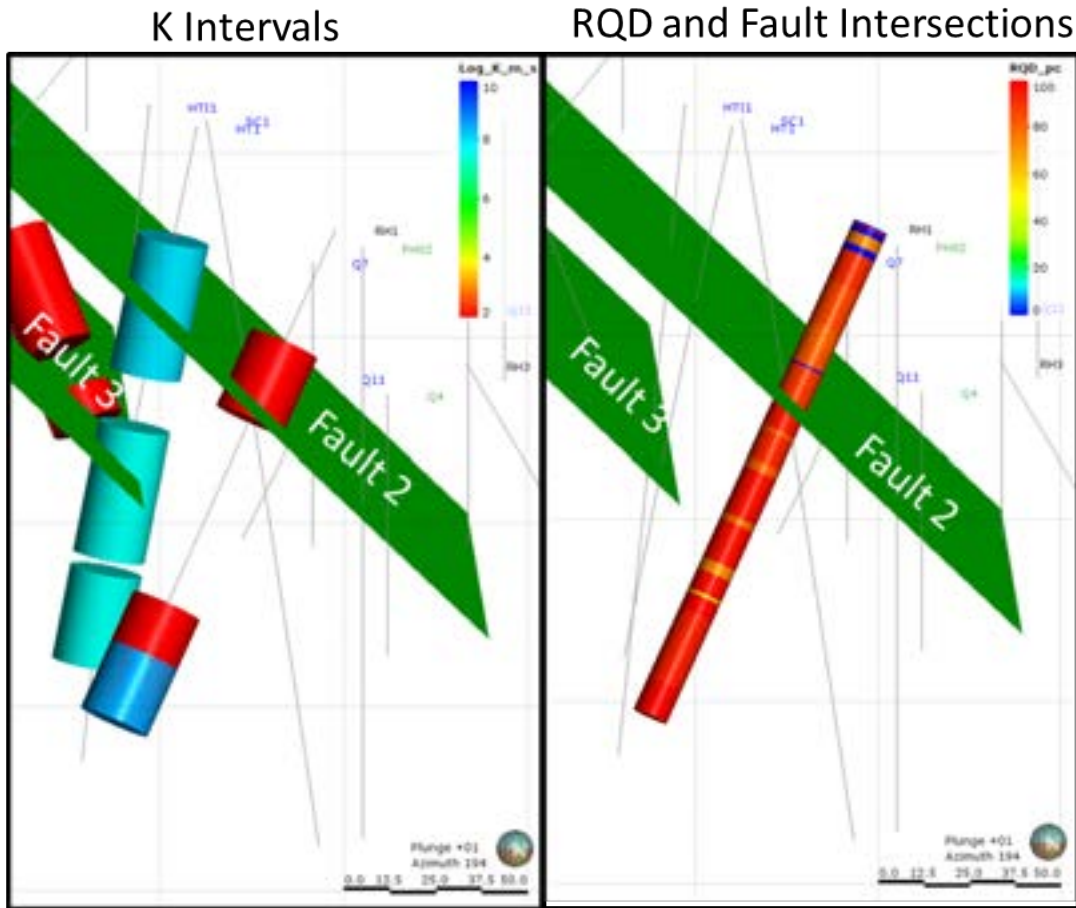


Figure 3-87: Comparison of high k intervals and RQD/ fault intersections in hole RH1 (isometric view, looking north)

RH6 (embankment centreline; collar in valley floor on alluvial terrace adjacent to river)

- A high k (8.5×10^{-5} m/s) interval was measured midway down RH6.
- This coincides with a large interval of low RQD. It is potentially related to Fault 1; however, it is likely that Fault 1 pre-dates the deposition of most of the valley sediments and therefore does not extend through them. The high k interval was measured in the uncemented colluvium approximately 40 m directly below the centreline of the embankment, and will be blocked by the cut-off wall.

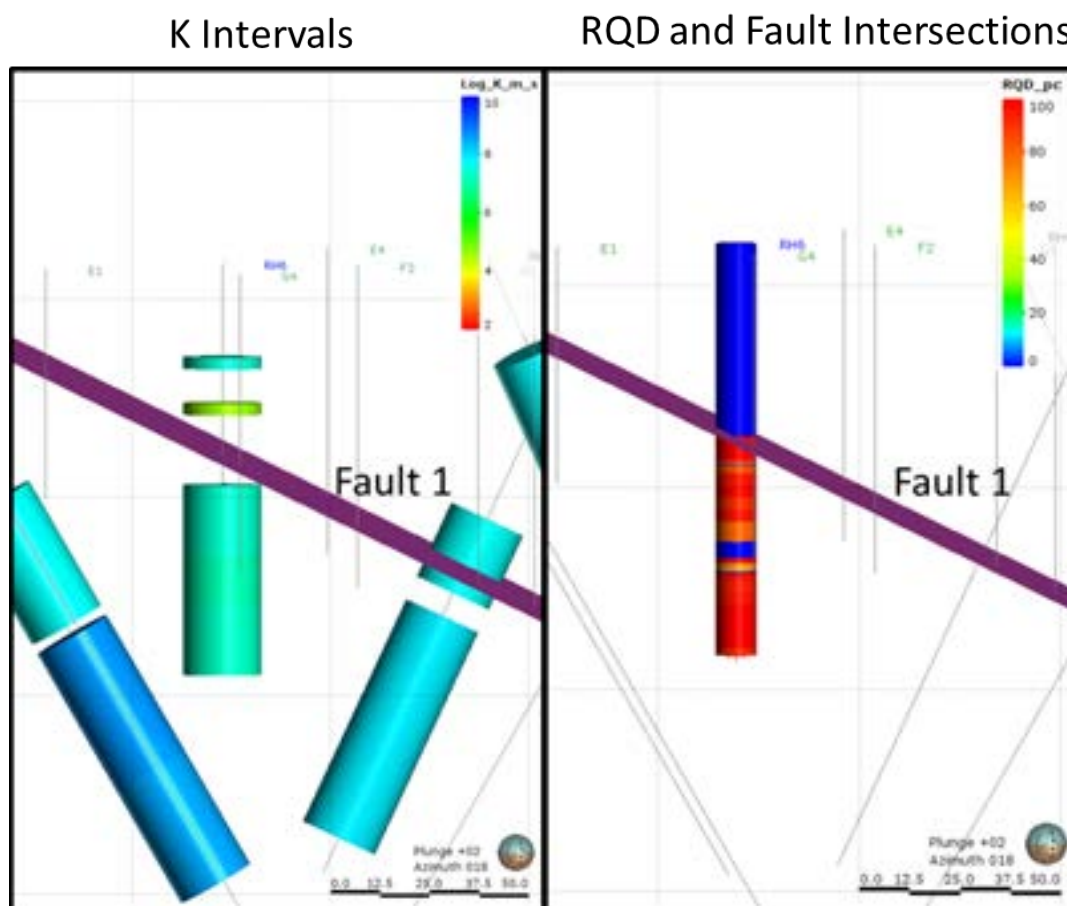


Figure 3-88: Comparison of high k intervals and RQD/ fault intersections in hole LH5 (isometric view, looking north)

The high to moderate k zones appear to be correlated to the narrow zone of uncemented alluvium below the embankment and the mapped or inferred structure. However, it was noted that tests along the same fault did not produce consistently high k zones, so the structures appear to have variable hydraulic conductivity along the feature. This could be due to variations in brittle damage zones, gouge infilling, or later weathering processes.

The faults in the abutment and foundation suggest potential flow paths that could present significant leakage through the embankment abutments, but only if they are continuous. If the faults are well identified/ delineated (difficult to achieve due to the potential complexity of their patterns) and targeted by drilling and grouting programs, it may be possible to seal the faults prior to reservoir filling and creation of a significant gradient across the feature. The issue may be in the length and number of drill holes required to access fault zones deep within the abutments.

The uncemented alluvial materials will be partially excavated during embankment foundation stripping and/ or mitigated by flow control measures consisting of dental grouting and a cut-off wall.

To date, strong correlations of all testing results with RQD, fracture frequency, fracture orientation and zones of joint oxidation have not been found. RQD and fracture frequency do not typically correlate well with permeability. However, because it is often controlled by the major structures, fracture orientation should be assessed carefully in any future drilling, with drill angles planned to cross the expected orientation for additional injection testing.

3.1.12 Geotechnical design inputs – embankment

The main embankment will be constructed in a single phase and will incorporate the main upstream cofferdam. Following completion of the diversion tunnels and cofferdams, the main embankment will be constructed as a rockfill embankment with a thick central asphalt core. Filter and transition zones will be constructed upstream and downstream of the central asphalt core. The crest of the embankment will be at an elevation of RL 238.5 m.

The main embankment wall will be constructed with engineered rockfill material. The foundation for the embankment will be excavated to bedrock, typically to a depth of about 5 m, except in the central portion of the valley. Rockfill, filter and drain material will be sourced from the quarry. Drain material will be crushed to specifications and supplemented with river alluvial materials if/ where possible. Bitumen for the asphalt core will be brought to site.

Embankment foundation seepage will be managed by installation of a plastic cement cut-off wall, to provide a ductile low permeability barrier, and a dental grout curtain to a depth of 20 m. Where geotechnical structures have been identified beneath and in the abutments of the embankment, fault grouting will be carried out to limit seepage through the plinth and through the abutments.

Properties for embankment stability modelling

To undertake 2D and 3D analyses for stability assessment of the proposed embankment design in Plaxis software, material mass properties were developed for the geotechnical material types (domains) described in Section 3.1.6. Properties for Domain 1 (colluvium) and Domain 3 (boulders) were not developed, as these relatively thin material layers will be removed from beneath foundations and from major slope cuts.

The material properties developed for the remaining natural and constructed materials are listed in Table 3-30. The Barton-Kjaernsli criterion (Barton & Kjaernsli, 1981; Barton, 2008)³⁷ was used to characterise the embankment rockfill considering a non-linear shear strength. The criterion takes the following relationship and parameters into consideration:

$$\tau = \sigma_n \tan(R \log \frac{S}{\sigma_n} + \text{Phi}_r)$$

where:

σ_n = effective normal stress

R = equivalent roughness, which is a function of the particle roundness and the porosity (n) of the dumped waste

S = size-dependent equivalent strength of the blasted particles, based on the UCS and the typical rock waste particle size at 50% passing (D_{50})

Phi_r = residual friction angle on the sawn surface of the rock.

³⁷ Barton, N and Kjaernsli, B, 1981. Shear Strength of Rockfill. Journal of the Geotechnical Engineering Division. Vol 107 No GT7.

Two rockfill zones were defined – Zone 3A is highly compacted material that will be placed adjacent to the asphalt core, i.e. represents the most internal zone of the embankment, and Zone 3B is compacted material that represents the external zone.

Table 3-30: Material properties used for embankment design analyses

Material	Unit Weight	Mohr-Coulomb Failure Criterion			Hoek-Brown Failure Criterion				Poisson's Ratio	Youngs Modulus (intact) E_i (GPa)	Youngs Modulus (rock mass) E_m (GPa)
		Cohesion	Friction Angle	GSI	UCS (MPa)	Material constant m_i	Disturbance factor D	ν			
		c' (kPa)	ϕ' (°)					(-)			
2A	Uncemented alluvium	20	0	35					0.25		0.15
2B	Cemented colluvium and alluvium	22	100	35	30	2	6	0	0.25	0.4	0.3
4	Potential Landslide	25	110 (100-150)	27 (25-30)	30	5	10	0	0.25	4	0.33
5	Weathered and oxidised dunite	29			57	40	12	0	0.3	18	8
6	Deteriorating, serpentinised dunite	31.5			45	30	12	0	0.3	40	9
7	SW-UW dunite	31.5			65	60	20	0	0.25	75	47
8	Faults	25	100	25					0.28		2.5
	Rockfill Type 3A	25	see graph						0.25		
	Rockfill Type 3B	25	see graph						0.25		
	Tailings	14	0	34							

Figure 3-89 shows the normal-shear stress curves obtained for the materials in the embankment zones (3A and 3B).

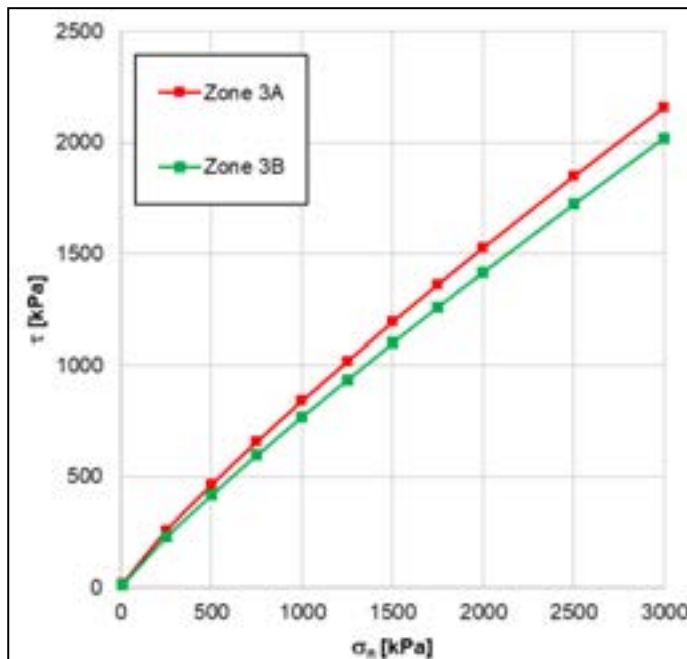


Figure 3-89: Shear-normal stress curves developed for the rockfill (Zone 3A and Zone 3B) embankment construction materials

These curves are comparable with the curves obtained for rockfill used for the Ok Binai embankment (also using April Ophiolite ultramafics) during the 2011 feasibility studies conducted for Xstrata (Figure 3-90). These envelopes were presented in SRK’s memorandum, ‘Frieda River Feasibility Study – Material Properties for Dams Design’, XST014, August 2011.

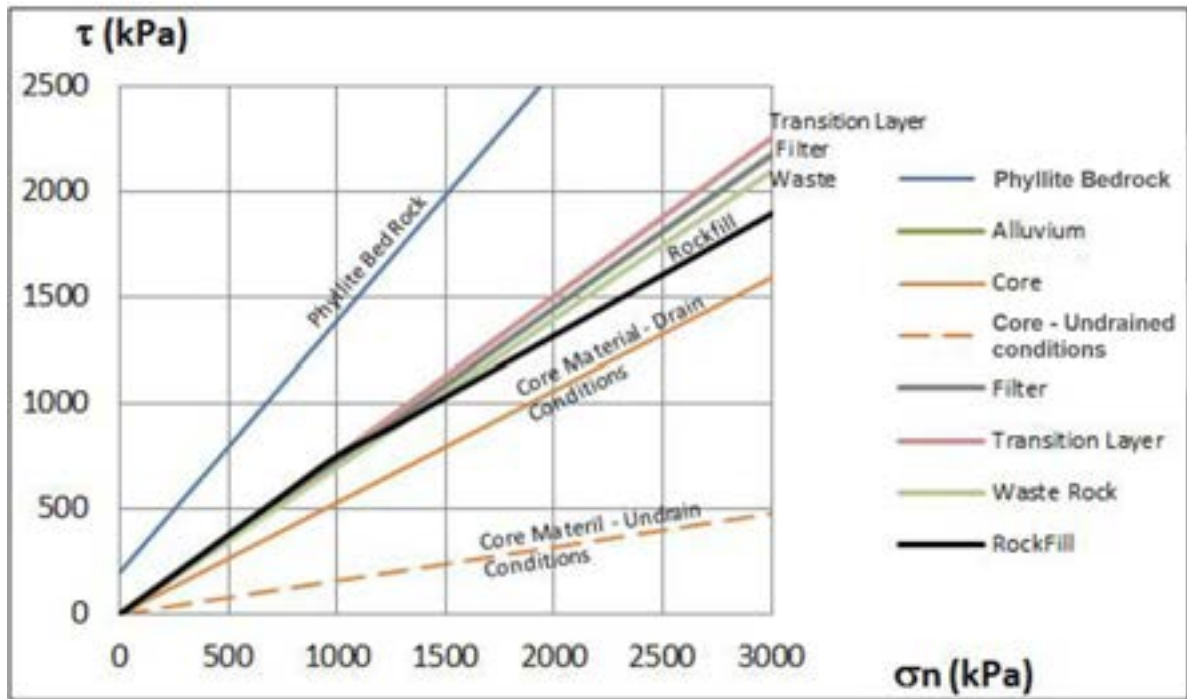


Figure 3-90: Shear strength envelopes for the Ok Binai embankment (SRK, 2011) – for comparison

Based on the information provided, and using relevant engineering expertise and experience, SRK further developed the material properties for the Plaxis models.

None of the constitutive models incorporate a shear strength envelope with a stress-dependent friction angle. To accommodate this, rockfill zones 3A and 3B were each divided in three layers, with different constant friction angles (Figure 3-91). The results are shown in Table 3-31 where ϕ_{adopt} is the adopted value.

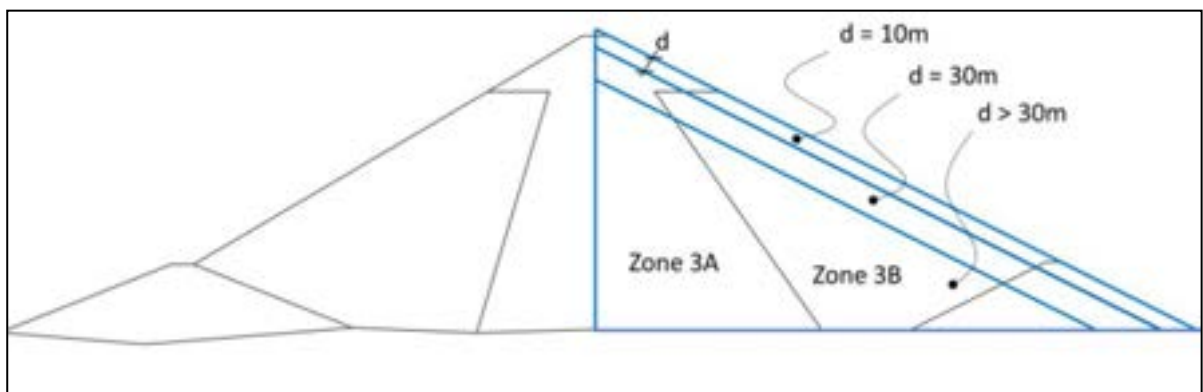


Figure 3-91: Variation of friction angle in each rockfill zone

Table 3-31: Peak friction angle for each layer as a function of depth

Rockfill	Depth [m]	ϕ_{tc} [°]	ϕ_{adopt} [°]
Zone 3A	1 – 10	53	56
	10 – 30	45	48
	>30	41	44
Zone 3B	1 – 10	48	51
	10 – 30	41	44
	>30	41	44

A comparison with Barton & Kjaernsli (in purple lines), Leps (as dots) and Indraratna (in black dashed lines) curves was performed with $\sigma_n \approx \sigma_3$ as shown in Figure 3-92. Adopted friction angles are marked with a red line for Zone 3A and with a green dashed line for Zone 3B.

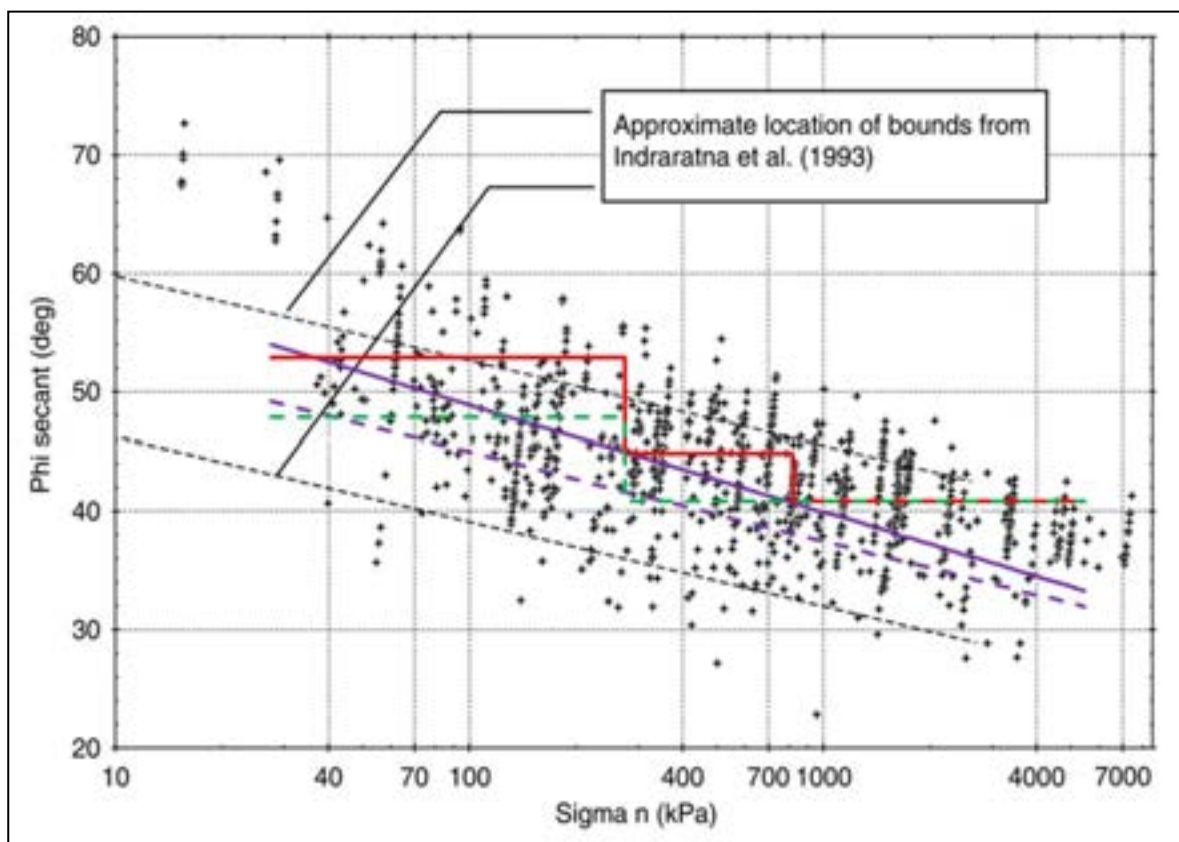


Figure 3-92: Adopted friction angle compared to Barton & Kjaernsli (1981), Indraratna (1993), and Leps (1970)

The final rockfill input parameters developed and adopted for the Plaxis models are summarised in Table 3-32.

Table 3-32: Input parameters for Plaxis modelling

Rockfill	Symbol	Unit	Values	
			Zone 3A	Zone 3B
Constitutive model	-	-	HSS	HSS
Unit weight	γ	kN/m ³	28.0	28.0
Equivalent cohesion	c	kPa	5	5
Triaxial friction angle	ϕ_{te}	°	53 45 41	48 41 41
Plane strain friction angle	ϕ_{ps}	°	56 48 44	51 44 44
Dilatancy angle	ψ	°	10 5 2	10 5 2
Initial shear modulus	G_0^{ref}	MPa	220	180
Reference shear strain	$\gamma_{0.7}$	-	1.0E-04	1.0E-04
Unload stiffness at 100 kPa	E_{ur}^{ref}	MPa	110	90
Secant stiffness at 100 kPa	E_{50}^{ref}	MPa	35	30
Oedometric stiffness 100 kPa	E_{oed}^{ref}	MPa	35	30
Stress exponent	m	-	0.5	0.5
Poisson ratio for uni/rel	ν_{ur}	-	0.2	0.2
Rayleigh damping parameters (D = 0.1% at f = 1 Hz & 5 Hz)	α	1/s	0.05236	0.05236
	β	1/s	2.65E-04	2.65E-04

Abutment stability

Drilling has indicated that bedrock is encountered at a very shallow depth in the relatively steep slopes of the right abutment. Landslides occurring on this abutment will likely be in the form of small superficial slides of limited extent that could occur after heavy rain, although very few of these are currently evident at the site. From time to time toppling failures of individual blocks of slightly weathered dunite may occur, but these would happen at widely-spaced intervals over geological time and present a low risk. Larger-scale failures within the rock, either along localised, adversely-orientated sheared/ serpentised zones, or resulting from large seismic events, may occur very infrequently – the risk is considered low.

The lower to middle part of the left slope has relatively shallow bedrock overlain by colluvium – indicating relatively good conditions apart from the likelihood of soil creep or risk of landslide within the colluvium. However, the variability in bedrock conditions in the mid-upper western left abutment is indicated by the region of highly fractured (likely sheared) zone. This material will need to be removed prior to embankment construction. Apart from this area, drilling has indicated that the bedrock is encountered at shallow to moderate depth and that the bedrock is generally of relatively good quality, as encountered on the right abutment. However, it cannot be ruled out that other areas of highly fractured rock could be encountered locally, particularly in spurs within the slope on the left abutment.

The risk of abutment instability will be highest during construction, before the embankment is of sufficient height to buttress the slopes. There is ongoing risk of instability affecting tunnel portals and blocking the spillway.

Powerhouse foundation

The material properties for the cemented colluvium and alluvium (Zone 2B) that will be encountered beneath the proposed powerhouse foundation are shown in Table 3-30. The cemented colluvium consists of coarse irregular fragments of dunite of varying sizes (some very large) in a cemented matrix. The material is largely clast-supported and locally matrix-supported with matrix strength

generally 2–10 MPa. The cemented matrix is shown in parts of some drill holes to have locally deteriorated, presenting softer material; this is more common in the uppermost 5–10 m of material, which is less dense. The relative density of the subsurface materials in the vicinity of the proposed powerhouse is indicated by the P-wave velocity contours in Figure 3-93. Moderately dense materials indicated by velocities of >2,000 m/s are encountered from surface, with velocities increasing to >4,000 m/s by 20 m depth, indicating dense, moderately strong rock-like material.

Excavation or piling through these materials could be challenging due to the large contrast and variations in strength/ hardness between the matrix and boulders, and the very large size (2–5 m) of some of the strong rock boulders.

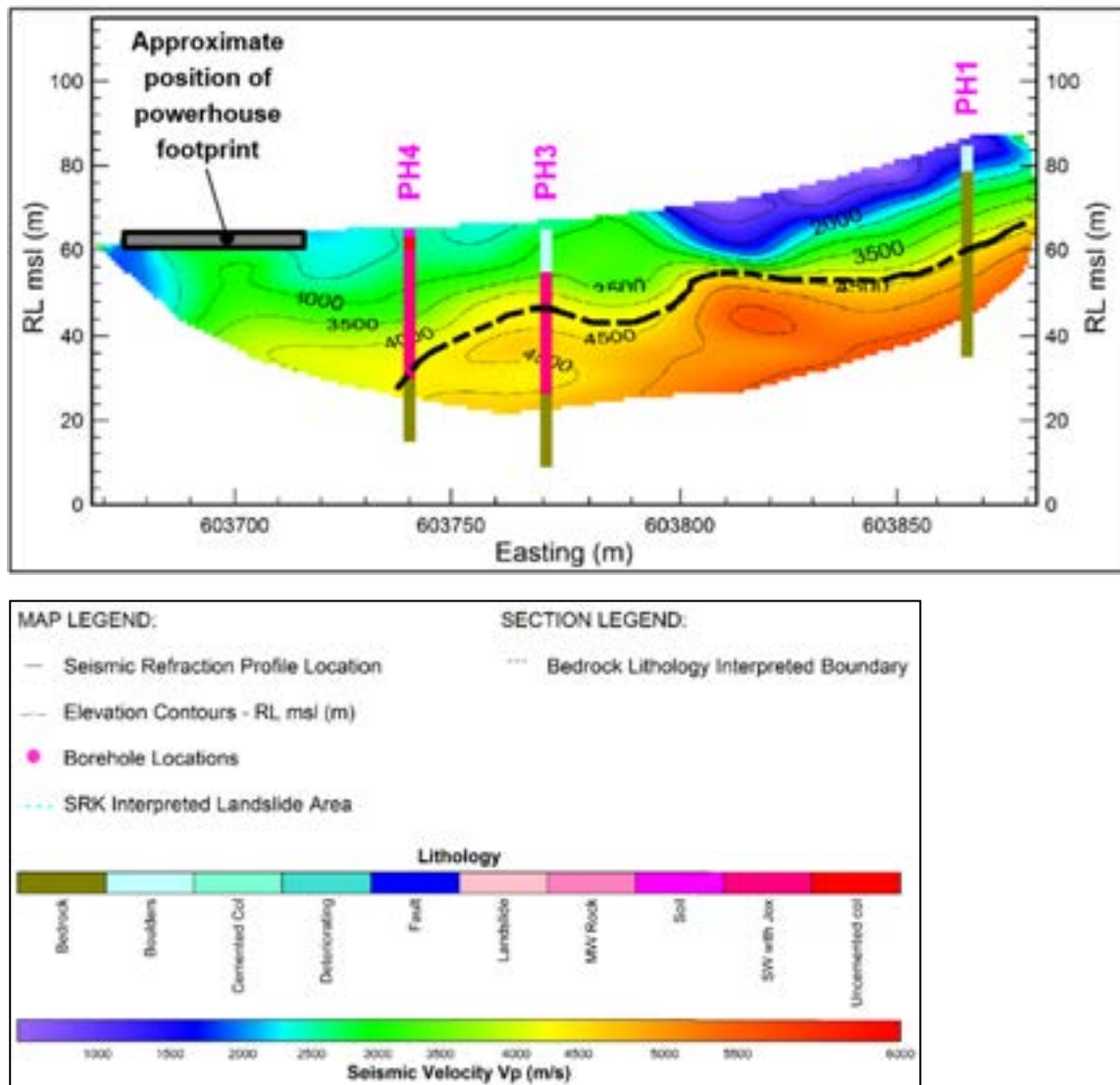


Figure 3-93: P-wave velocity contours of the subsurface materials in the vicinity of the proposed powerhouse site (section view, looking north)

3.1.13 Construction materials

Rockfill

Rockfill will be sourced from the quarry, situated on the right side of the Frieda River valley, upstream and to the south of the embankment position. The source material is unweathered, strong rock dunite. The right abutment spillway excavations will also provide dunite for rockfill. The rockfill properties are described in Section 3.1.3, and delineation of the quarry is described in Section 3.1.4.

Los Angeles abrasion test results

There is no standard LA abrasion specification for pavement design; specifications are usually established by state or local agencies. Typically, US state specifications limit the abrasion of coarse aggregate to a maximum ranging from 25% to 55%, with most states using a specification of 40% or 45%. The requirements for Portland Cement Concrete tend to be similar, while requirements for specialised mixes such as Stone Matrix Asphalt tend to be lower at 30% (LA Abrasion, 2011).

All samples tested are well in excess of these specifications:

- All samples (13 in total) displayed abrasion loss of <30%
- 8 out of 13 samples displayed abrasion loss of <20%.

Slake durability

In terms of slake durability, all 26 samples tested showed excellent durability with almost no loss of mass over the test duration. The altered (serpentinised) dunite did not show significantly more tendency to slake than the unaltered rock.

UCS

All valid UCS tests (i.e. tests that did not fail by invalid means, often along incipient structures within the sample) on samples taken from the quarry drill holes displayed a UCS >40 MPa. Two thirds of tests (80% of valid tests) displayed UCS >60 MPa. Of all valid UCS tests from the right abutment drilling (including the spillway), 87% displayed UCS >40 MPa.

Sand and gravel for filter systems

Several 'beaches' on the Frieda River, both upstream and downstream of the FRHEP embankment, have been identified as potential sources of sand and gravel to be used as construction materials. Due to the rounded shapes of the alluvial gravels and sands, variability in material type, and complexity of performing geotechnical and geochemical characterisation, the materials are not currently considered suitable for filter and transition layer construction purposes. The locations of these sand and gravel sources were observed during previous site visits and approximations of their position is shown on SRK Drawing PNA009-0020 (Figure 3-94).

No geotechnical investigations have been carried out on any of these potential sources and the geotechnical and geochemical characteristics are currently unknown. It is recommended that such geotechnical investigations, including tests to determine the alkali-silica reactivity of the materials, be done during future studies. For the purposes of the SPS, SRK has assumed that the filter and transition layer materials will be sourced from the quarry and crushed as needed.

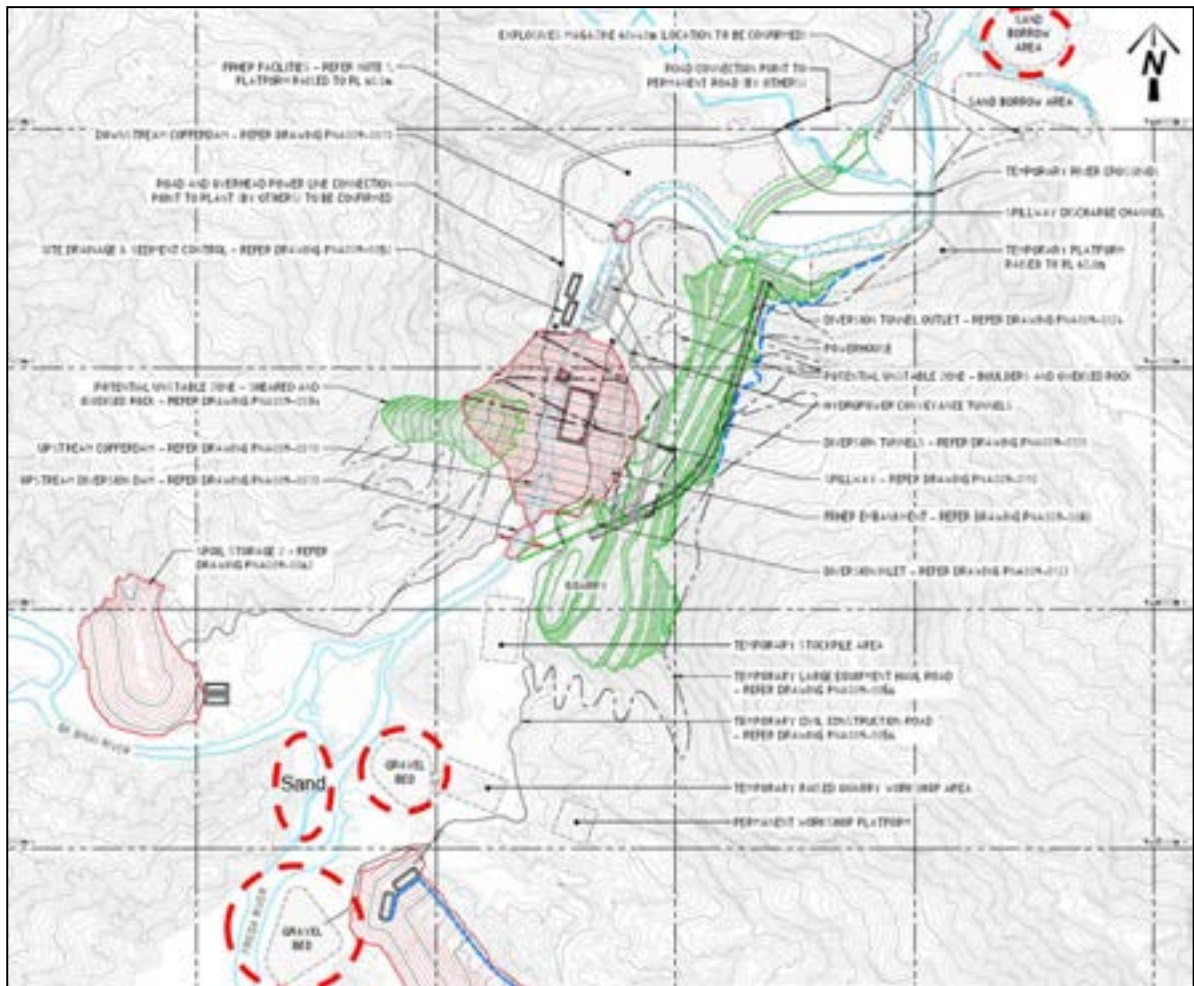


Figure 3-94: Locations of gravel and sand materials on the Frieda River near the FRHEP site (highlighted by red dashed zones)

3.1.14 Geotechnical design inputs – quarry limits and spoil dumps

Quarry and spillway position and delineation

A potential site for the quarry has been identified immediately south of the embankment on the right side of the Frieda River. The purpose of the quarry is to provide construction materials for the proposed FRHEP embankment, i.e. dunite of good quality. The quarry is situated favourably in terms of accessibility and is relatively close to the embankment site.

A gated spillway is included in the design. The spillway will comprise a nominally 30 m long ogee crest on the right abutment, with a reinforced concrete lined chute. Rock sourced from the spillway excavation will also be used in the embankment construction.

Core from holes Q1 (2011 drilling) and Q10, Q12 and Q13 (recent drilling) in the prominent ridge that forms the northern part of the area originally designated for the quarry shows the rock quality is generally good and will be suitable for use as embankment rockfill, and which is common on the right [abutment. Examples of this material are shown in Figure 3-95.



Figure 3-95: Examples of drill core from the northern part of the quarry

Of the holes drilled in the southern part of the quarry, core from Q5 and Q6 is mostly poor quality. The core from holes Q7, Q9 and Q10 also has significant zones of poor rock. The core shows old brecciation texture (possibly as a result of the original upthrust of the April Ophiolites over the Ok Binai Phyllites) that has since been recemented. Although some of this core presents material that may be suitable for rockfill, significant portions of the core have groundmass (matrix) exhibiting deterioration. This is in the form of serpentinisation/ chloritisation, which deteriorates further into softer, sandy/ silty 'material' containing the original breccia pieces. There are also numerous strongly oxidised zones and faults which contribute to the break-up and compartmentalisation of the rockmass and its oxidation and deterioration. Examples of poor quality material from holes in this area are shown in Figure 3-96.



Figure 3-96: Examples of poor quality drill core from the southern part of the quarry

A fault of significant size has been interpreted to transect the quarry, dividing it into northern and southern zones. The poor quality materials are generally encountered to the south of this fault. Conditions within the fault (from Q5) are illustrated in Figure 3-97. The position of this fault is shown in Figure 3-98.



Figure 3-97: Significant fault through the quarry: conditions encountered in drill core of hole Q5

Based on the available drill core photos and logging data, a preliminary assessment of likely spoil shows that ~50% of material in the southern quarry may be spoiled, compared with only ~10% in the northern quarry and spillway areas (Table 3-33).

Table 3-33: Assessment of spoil material from quarry and spillway drill holes

Drillhole	Drilled length of spoil (m)							Total length assessed	Approx. % spoil of total length drilled	Best Estimate of overall spoil
	Colluvium	Boulders	Weathered rock	Possible Landslip	Deteriorating	Faults	Total			
Spillway										
SW1	1.2		1				2.2	50.1	4	Approx. 10%
SW3	1.3		7		3	2.5	13.8	100.1	14	
SW4	1	8		5			14	100	14	
SW5	3.2		5.6			5	13.8	100	14	
SW6	0					6	6	150	4	
Quarry - South Zone										
Q5	1.5	8		14	20	23	66.5	94.5	70	Around 50%
Q6	5			34	2		41	62	66	
Q7	5.5	18		17		2	42.5	75	57	
Q8	0.15				7	2.5	9.65	100	10	
Q9	4				17		21	87.2	24	
Q11	4				10		14	50	28	
Quarry - North Zone										
Q1	1.8					2	3.8	70.8	5	Around 10%
Q10	0.5	3.5				6	10	75	13	
Q12	1.5		7			0.7	9.2	75	12	
Q13	2.2		5			5	12.2	122.3	10	

This assessment resulted in the compartmentalisation of the original quarry area into northern and southern zones, with the southern zone being discounted as potential rockfill material – necessitating a re-design of the quarry extending further to the north to merge with the spillway (Figure 3-98). The full quarry and spillway cut design is shown in Figure 3-99. Following detailed slope stability analyses (described in Section 3.1.5) and further assessment of practical design for the spillway and quarry cut slopes, the designs for the quarry and spillway have been amended from those shown in Figure 3-98 and Figure 3-99. This is explained and illustrated in Section 3.1.5.

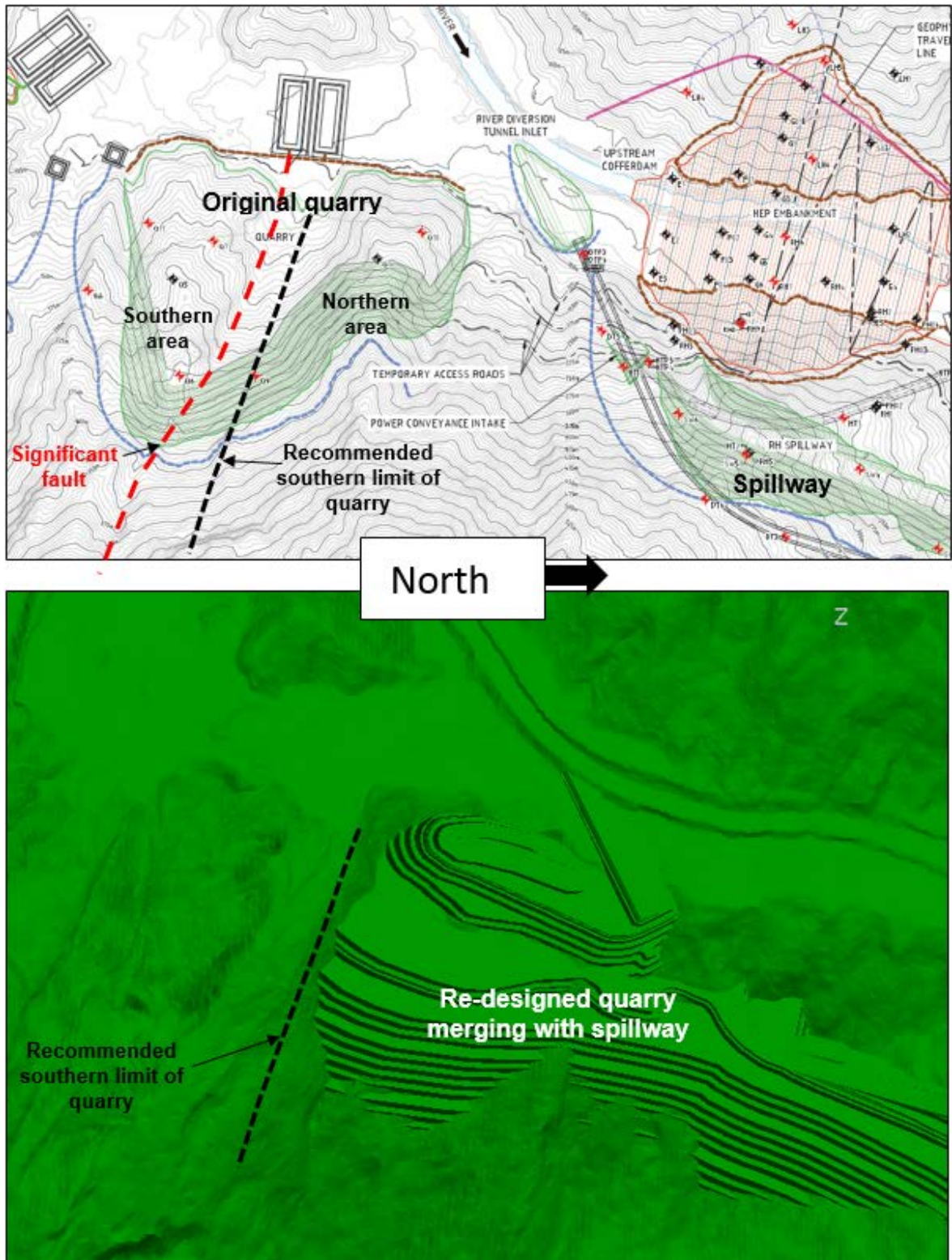


Figure 3-98: Plan views showing (above) original quarry and spillway design, with new southern limit based on drilling investigations; and (below) re-designed quarry merging with the spillway cut

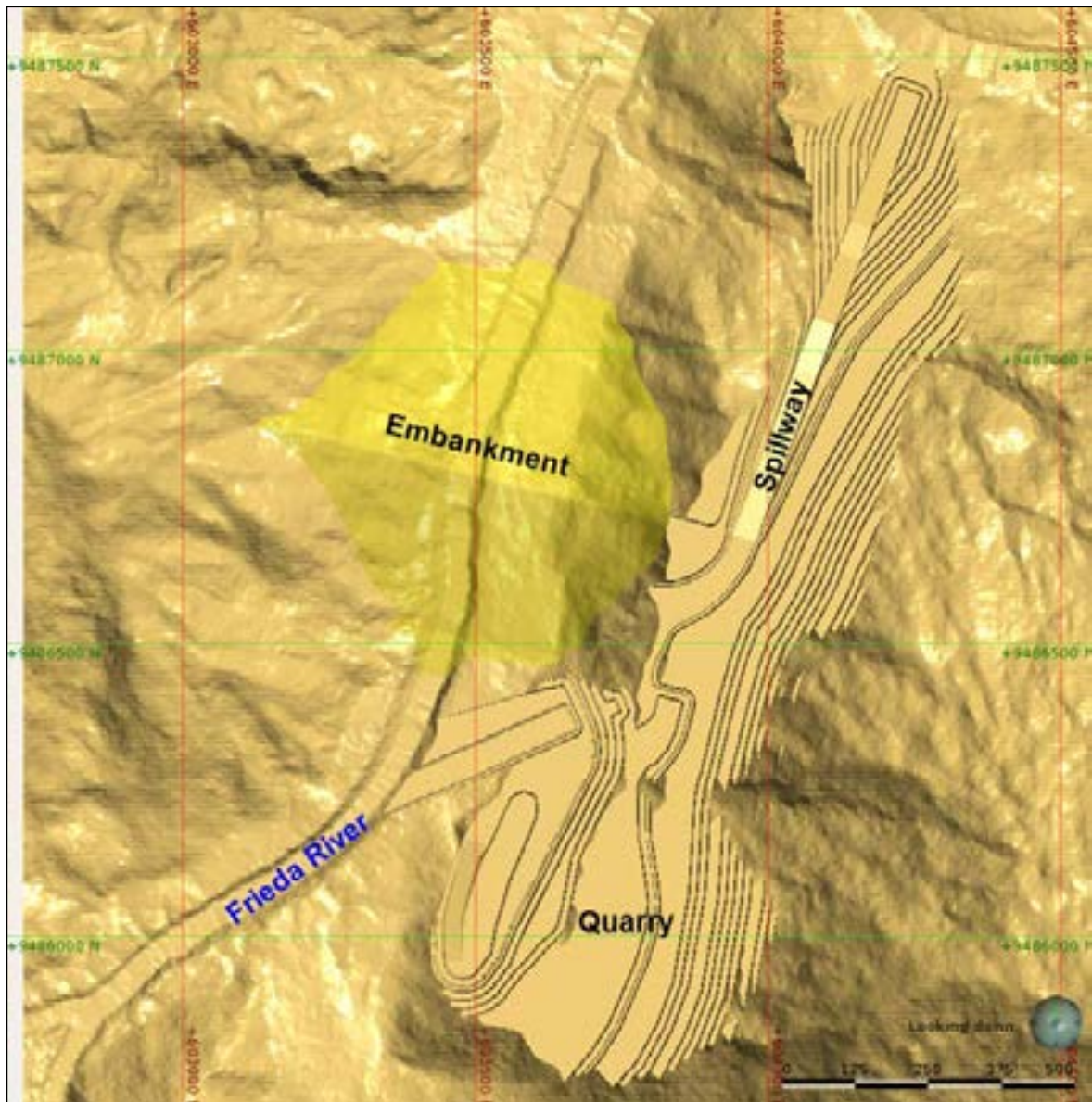


Figure 3-99: Plan view showing the quarry and spillway design (Rev N) on the right side of the river (relative to the embankment position)

Spoil dump – spoil storage south

Spoil material from foundation excavations, quarry development and slope stabilisation will be disposed of at the upstream spoil areas, together with sediment generated from the road slopes and other areas exposed during construction. All vegetation and organic material stripped from the construction areas will also be stored in the spoil dumps. The spoil dumps will be located upstream of the embankment on the left and right sides of the river, to facilitate construction on either side prior to damming with the cofferdam.

Both spoil dumps, including the ~110 m high dump located to the south of the embankment (spoil storage south), are located in the inundated footprint of the reservoir and will be completely submerged following the filling of the lake. In addition to risk of harm to personnel and damage to equipment as a result of a spoil dump failure, there is likely to be significant sediment discharge to the embankment and beyond. The spoil dumps therefore need to be engineered to safely contain all spoil material generated by the FRHEP construction, and diligent operational control will be required. No geotechnical investigations have been performed across the proposed spoil storage south

footprint. According to the geological maps, the foundation material in the location of the spoil dump is Ok Binai Phyllite. To assess the stability of the spoil storage, the foundation characteristics have therefore been assumed to be similar to the right abutment of the Nena ISF embankment, which is also located on phyllite, and in similar terrain.

Site characterisation for the Nena ISF embankment (as detailed in SRK's report, 'Frieda River ISF and Quarry Investigation Phase Two (Rev2), PNA005, October 2015) included delineation of the following key horizons within the weathered profile and identification of characteristic properties for these horizons:

- A. Extremely weak (<1 MPa) soil-like materials, including Colluvium and completely weathered (CW) materials – from 0 m to 10 m depth
- B. Very weak (1–10MPa) rock, including highly weathered (HW), and locally CW or moderately weathered (MW) rock – from 10 m to 20 m depth
- C. Weak (10–25MPa) rock, including HW and MW rock – from 20 m to 25 m depth
- D. Moderately strong (25–50 MPa) rock, including MW and slightly weathered (SW) rock (the effective start of 'bedrock') – from 25 m to 35 m depth
- E. Strong to very strong (>50 MPa) rock, including SW and unweathered (UW) rock – below 35 m depth.

Table 3-34: Summary of geotechnical properties

Material	Unit weight, γ (kN/m ³)	Cohesion, c' (kPa)	Friction angle, ϕ' (°)	Hoek-Brown			
				GSI	UCS (MPa)	m_i	D
Horizon A	19	10	30				
Horizon B	22.7			30	5	6	0
Horizon C	25.4			40	10	7	0
Horizon D	25.4			45	25	7	0
Horizon E	27.4			55	50	10	0

2D limit equilibrium stability analyses were carried out for assessment and design of the spoil dump slopes. While the analyses do not form part of the scope of the geotechnical characterisation work, details are provided in SRK's memorandum, 'Frieda River FRHEP Spoil Storage South Design', 15 March 2018.

3.1.15 Slope stability assessments – design of quarry and spillway slopes

On completion of the geotechnical investigations and collation of the geotechnical model, assessment of the slope stability for the final quarry and spillway design was carried out by means of the following:

- Preliminary empirical assessment of bench stack angles
- Kinematic (structural) failure analysis to assess the design at a bench-berm scale
- 2D stability analyses of the overall slopes for the quarry and spillway cut designs, with the intent to assess the slope stability in terms of the FoS.

These analyses and results are described in detail in Section 10.5.4.

3.1.16 Potential landslide upstream from embankment

The geological hazard assessment conducted by Scott Wilson (2011) identified a possible instability of April Ophiolite on a spur of the Frieda Valley, 9 km upstream of, and in a direct line to, the embankment site (Figure 3-100).

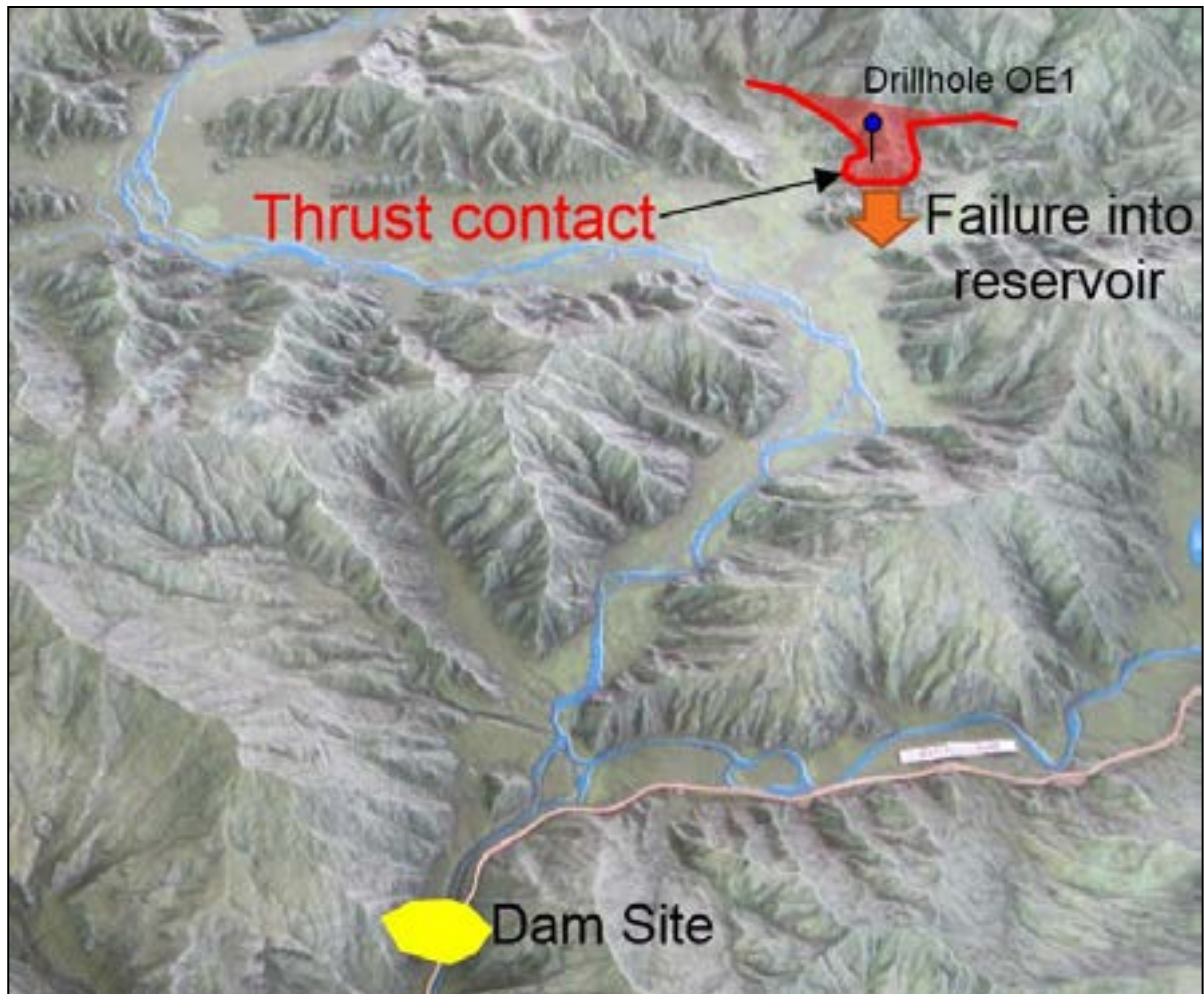


Figure 3-100: Isometric view looking south showing location of the hypothesised failure mechanism relative to the embankment site

The ophiolite is indicated to overlie a thrust fault that coincides with the approximate proposed reservoir water level. It was considered that the possibility of reservoir filling and/ or wave erosion may affect the stability of this rock mass above the thrust, resulting in a significant volume of material failure sliding into the reservoir, generating a wave that could impact or overtop the embankment.

Hole OE1, drilled during the Stage 1 investigations, showed that the geological map is incorrect – this spur is composed of phyllite which is present below the thrust fault. Therefore, the thrust contact will be above the reservoir level, and the mechanism of failure proposed by Scott Wilson is considered very unlikely to occur.

3.1.17 Tunnel design assessments

Geotechnical design assessments for the diversion tunnels and conveyance tunnels involved evaluating preliminary ground support design and spacing of the twin tunnels. These assessments and the resulting recommendations are described in Section 9.1.

3.2 Stage 2 Landslide Geohazard and Georisk Assessment

3.2.1 Objectives

SRK conducted a geohazard assessment of proposed FRHEP infrastructure and surrounding catchment using data provided by FRL. This assessment covers the wider Frieda River catchment to consider all geohazards that may affect the reservoir. The analysis was carried out in two phases:

- Phase 1 – desktop review of all data available to date and post processing to create a series of geomorphological, engineering and geotechnical models
- Phase 2 – incorporation of observations by SRK personnel familiar with the Frieda River geomorphology from involvement in site investigations, which made it possible to confirm or dismiss hypotheses and theories.

The Phase 1 desktop review was based on the interpretation of LiDAR data at a 5 m resolution supplied by FRL. The landslide assessment was extended to include the entire Frieda River catchment and areas of instability that, in the event of failure, may subsequently flow into the reservoir and potentially affect FRHEP infrastructure. The catchment was digitised from the basin model included in the Hydrology Baseline Report (SRK, 2016). Where 5 m resolution LiDAR data was not available, 30 m resolution SRTM data was used, as shown in Figure 3-101. Interpretation of the LiDAR and SRTM data resulted in identification of numerous instability features; however, due to the lower resolution of STRM data, there is lower confidence in the identification of instabilities in the area covered by STRM data. Most of the landslides are highly complex, multi-stage, reactivated instabilities that are likely to have been active over a significant period of time and have led to significant alteration of the landscape.

A fundamental understanding of the following key parameters and their interactions is required to interpret, understand and manage geohazards in PNG and to assess the risks associated with them:

- Correct planning and implementation of site or ground investigations to allow optimisation of the design and minimise maintenance requirements
- The previous morphological history of the mine site and surrounding area
- Seismicity affects the entire region to a similar degree and is therefore taken to be a constant for the FRHEP area; it will not be differentiated for the purpose of this assessment
- The effect of hydrolysis on the slopes and preferential weathering
- Storm events and rapid saturation of the upper layers inducing shallow, often small-scale rotational instabilities; these have potential to propagate up slope or regressively down slope (decreasing the overall slope angle and enlarging the area of failed toe material)
- Over-steepening and loss of toe weight or support, potentially leading to small-scale failures that can propagate or regress
- Significant or dramatic rise in groundwater resulting in creation of new spring lines and saturation, which causes instability and can be seen by the filling of the reservoir
- The geohazard assessment considers human activity in the FRHEP area; however, the effects of de-vegetation and deforestation require investigation on a local scale to understand the potential impact on slope stability.

3.2.2 Tasks

The scope of work was divided into a series of sequential tasks; the principal tasks are listed below:

- Review of available data
- Development of the landslide inventory
- Identification of individual element criteria
- Geohazard assessment classification
- Geohazard and georisk assessment reporting.

The development of the landslide inventory and the geohazard analysis required a good degree of expertise in engineering geology and judgement developed from undertaking geohazard assessments for earlier stages of the Project, inputs for regional exploration and working on mine development programs in similar tropical terrain. SRK's experience was complemented by a review undertaken by Dr Phil Flentje, a recognised expert in landslide hazard identification.

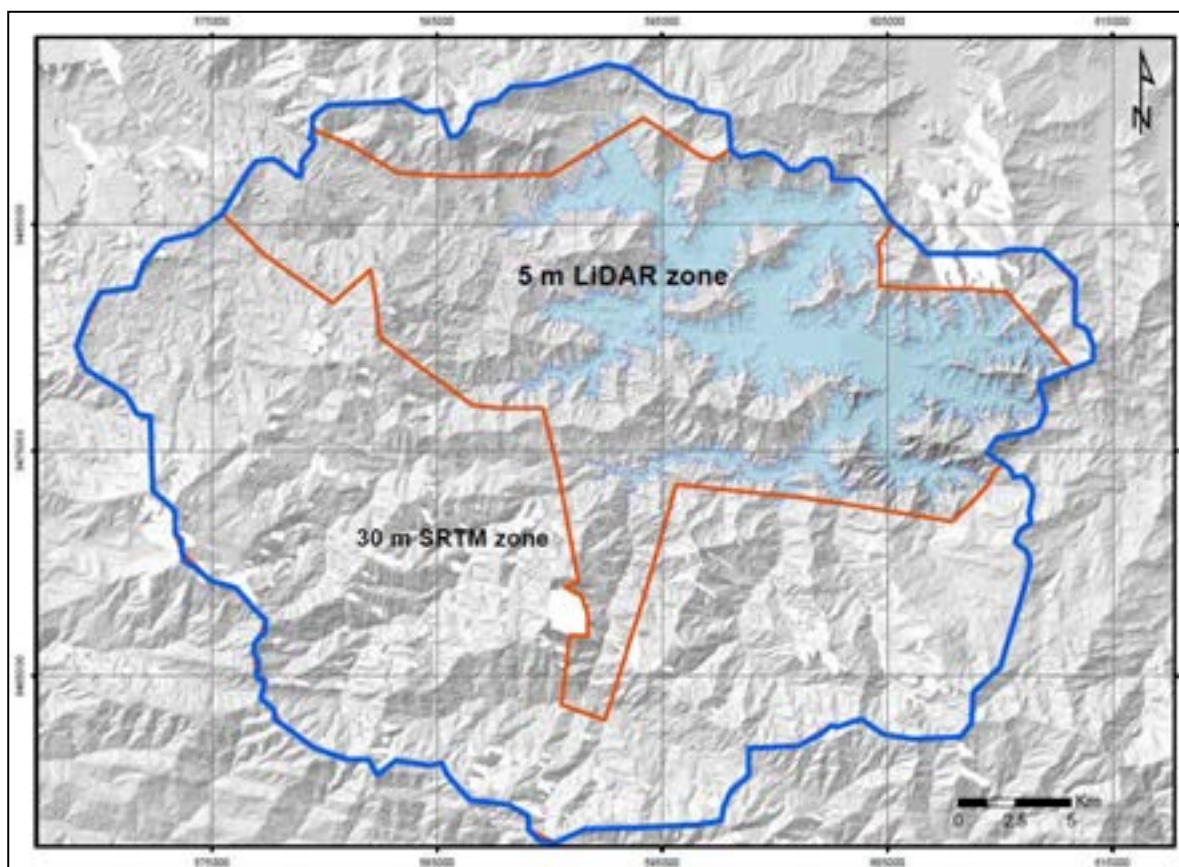


Figure 3-101: Plan of Frieda River catchment with extent of data coverage shown

3.2.3 Site conditions

The site is located in remote terrain at elevations up to 800 m and is ~200 km south of the PNG coastline in the foothills of the Schattenberg Range, some 70 km from the Sepik River.

The Lower Ranges consist of a north dipping thrust stack of deformed low-grade metasediment (Ok Binai Phyllite), ultrabasic rocks and un-metamorphosed sediment and volcanics (Wogamush Formation). These have been intruded by diorites. The Frieda Complex comprises mineralised porphyritic diorites; elsewhere the diorites are essentially unmineralised. All rock types may have a degree of pyrite mineralisation along joints.

The river valleys are generally underlain by a significant thickness of loose to medium density sand and gravel with a surface layer of very soft silt and clay (generally 1–5 m thick away from the current river channels). The depth of profound weathering (saprolite development) of the rock is 3–5 m in some of the Wogamush and ultrabasic rocks; 10–15 m (up to 30 m in places) in the Ok Binai Phyllites; and up to 30 m or more in diorites away from the Frieda Complex orebody. Within the orebody, or along major structures, profound weathering and hydrothermal alteration extends to depths of more than 50 m. To the north, the Sepik Basin (Sepik River Floodplain) stretches for approximately 60 km to Kubkain village and the proposed port facility. The floodplain is essentially a flat-lying, jungle-covered swamp with peat to depths between 14 m and 30 m overlying clay, silt and sand. In areas of ancient landslides, weakly reconsolidated to more competent, partially lithified debris flows have been identified and drilled to depths that locally exceed 30 m.

To the south and southwest of the site, in the greater catchment area, the Fiak Fault has an almost E–W strike. Fault zone rocks, including contorted and sheared material from nearby units, are associated with this major regional thrust. Historical landslide material is present in the southwest of the catchment, interpreted as partially lithified ultramafic breccia.

The Sepik Basin and the floor of the alluvial valleys are characterised by a high groundwater level controlled by the river level. In the Lower Ranges, the groundwater has been measured at generally 20–30 m depths under ridges and close to ground level in the alluvial valley areas, emerging as springs and forming incised creeks on side slopes. Perched groundwater is often a feature of the colluvial soils on the lower slopes.

Climate and geography

The site is located approximately 250 km from Wewak and is accessible via fixed-wing aircraft and helicopter. The area around the FRHEP site and approximately 40 km to the northeast is characterised by a dense jungle canopy which drapes steep mountains (Lower Ranges) that are incised by rivers and streams.

Rainfall is one of the main contributing factors in triggering landslides. The region is in a hot and humid rainforest environment with high rainfall (quantity and intensity). Average annual rainfall in the upland areas around the Horse-Ivaal deposit is reported to be between 7,000 mm and 8,200 mm, with no clear seasonal changes. Rainfall data from the lower Sepik Plains shows average annual rainfalls being between 3,500 mm and 4,600 mm, with a dry season from May to October and wet season from November to April.

Geology

The project geology is shown in Figure 3-102 and is generally described by Hill et al., (2002)³⁸. The basement close to the site comprises metavolcanics and metasediments from the Ok Binai Phyllite which unconformably underlie the Middle Miocene Wogamush Formation. The geological sequence also comprises Palaeogene igneous rocks belonging to the April Ophiolite and the Nena Diorite. The geohazard assessment includes surficial deposits of alluvium and colluvium.

Ok Binai Phyllite (KT a/c/am/sm/t)

The Ok Binai phyllite is the most prevalent rock type in the area and occupies the central part of the site. The rock generally appears as a dark-coloured, fine-grained phyllite, pelitic schist and greenschist. In outcrops, subtypes of phyllite have been differentiated by the intensity/ nature of

³⁸ Hill, K C, Kendrick, R D, Crowhurst, P V and Gow, P A, 2002. Copper-gold mineralisation in New Guinea: tectonics, lineaments, thermochronology and structure. Australian Journal of Earth Science. 49, 737–752.

foliation and by the presence of quartz banding and porphyroblasts due to contact metamorphism near large intrusive bodies. Numerous slides identified within the Ok Binai Phyllite may be movement down foliation planes.

Wogamush Sandstone (Tmw)

The Wogamush Formation forms a dark-coloured, medium- to fine-grained arenaceous or greywacke sandstone with a basal volcanolithic conglomerate. The basal conglomerate is discontinuous and is overlain by dark-coloured, fine limestone which transitions rapidly to a turbidite sequence of mudstone, siltstone and sandstone. Close to igneous margins there is baking or fusing of the fabric due to contact metamorphism. The unit occurs outside of the catchment, near the airstrip and beyond, as well as near the pit.

Nena Diorite (Tmn)

The Nena Diorite occurs typically north of the Frieda Fault and is a fine- to medium-grained quartz diorite, granodiorite and monzodiorite. The finer-grained texture tends to be associated with dykes and sills which form offshoots from the main intrusion and appear to be associated, in at least some cases, with thrust contacts or faults. The unit is of similar age to the main Frieda Complex and exhibits deep weathering and some association with large flows and slides.

April Ophiolite (U)

The April Ophiolite is an ultrabasic ophiolitic unit which is found in association with the Frieda Fault and pre-dates the main Frieda Complex. The unit comprises dunite and basalt with some gabbro. It is reported as being well jointed and prone to sliding and toppling failures. It typically forms a capping on elevated positions where it overlies the Ok Binai Phyllite.

Wabia Beds (K-Pw)

The Wabia Beds are present in the southern portion of the catchment, south of the Fiak Fault, and comprise the main component of the southern slopes. The unit comprises green volcanolithic sandstone, conglomerate and slate. Micrite limestone is present along the thrust contact. Common slides and flows are identified within this unit, likely in association with bedding planes and shears.

Fault Zone Rocks (Tfz)

Highly metamorphosed and contorted rocks from other units have been affected by the Fiak Fault (sometimes referred to as the Fiak-Leonard Shultze Thrust), which separates the southern Wabia Beds and Maril and Chim formations and the northern Ok Binai Phyllite. This highly structured zone is associated with historical instabilities, and due to association with the active major fault and splays, carries a high risk of remobilisation and triggering new landslides.

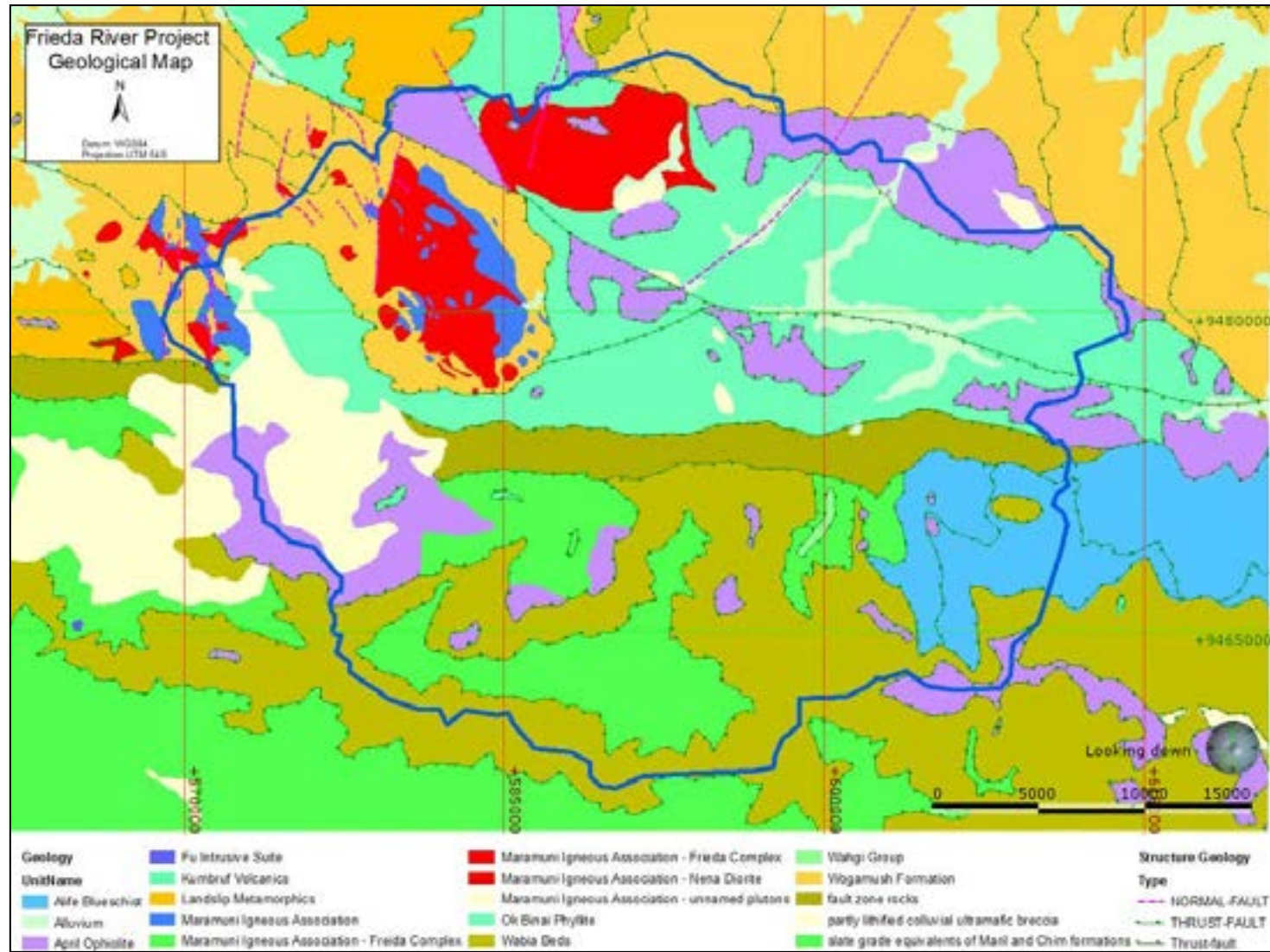


Figure 3-102: Geology of the FRHRP area

Source: PNG Geological Survey.

Geological structures

The FRHEP is located in the New Guinea Mobile Belt and is represented by a zone of distinct and complex faulting and folding. The following faults are the most significant major structures identified within the region:

- Transfer Faults – a series of north-northeast (NNE) trending extension faults that were strongly inverted during the late Miocene-Pliocene orogeny. These can be displaced by 50 km in some areas, indicating large-scale ground movements with zones of highly fractured and broken materials. Transfer faults have been mapped in the regional geological map and can also be seen in lineaments and geomorphological trends in the LiDAR/ SRTM data, often delineated by valleys and river alignment. It has been interpreted that the Frieda River flows along a valley formed by a transfer fault trace.
- Saniap Fault – a significant thrust fault located approximately 10 km north of the mine area, separating the Wogamush Formation in the north from the Ok Binai Phyllite in the south. This thrust fault forms the northern catchment boundary.
- Frieda Fault – a major regional thrust fault located approximately 4 km north of the mine area and forming a separation between two previous geological unit nomenclatures – the Ambunti Metamorphics (KTA/am) and the Salumei Formation (KTsm) – that are now collectively known as the Ok Binai Phyllite.
- Fiak Fault (Fiak-Leonard Shultz Thrust) – a major regional thrust fault located in the middle of the catchment, approximately 5 km south of the pit. This structure splits the catchment, separating the Ok Binai Phyllite to the north from the Wabia Beds in the south.

Continuing to the south of the catchment, other major faults are present such as the Stolle Fault Zone and the Figi Fault. At a regional scale, other structures include the New Guinea Thrust Fault and the New Guinea Trench. These regional structures have widths of tens to hundreds of metres, and can be laterally persistent for hundreds of kilometres, indicating a high stress environment with potential for large magnitude seismicity.

Scott Wilson (2011) identified that some of the faults (in particular, the Frieda Fault) were considered to be active. Current information does not strongly indicate active faults, although the river channel is inferred, in places, to be strongly structurally controlled and the landslide inventory developed for the catchment demonstrates the spatial distribution of instabilities, commonly along structural corridors, indicating the strong relationship between failures and proximity to faults.

As recently as 25 February 2018, a magnitude 7.5 earthquake occurred approximately 200 km southeast of the Frieda River camp. Closer to the epicentre, significant landslides occurred (Figure 3-103), with failures reported at the Ok Tedi mine, roughly 210 km west of the epicentre, as well as fatalities in nearby villages (Petley, 2018). While no known failures were reported at Frieda River, the February 2018 event demonstrates the seismically active nature of the Papua New Guinean highlands and the potential for earthquake-induced geohazards that are a risk to life and mine operations.

The Tumbi Quarry landslide that occurred in January 2012 is another example of a landslide impacting mining operations and causing loss of life. The location of this landslide is ~178 km southwest of the Frieda River site, some 30 km north of the location of the February 2018 event. Although considered a moderate landslide event, the associated human casualties and infrastructure damage

indicates the serious consequences of geohazards (Robbins et al., 2013)³⁹. It was considered that the main trigger for this failure was the elevated rainfall experienced in the region, demonstrating another major factor contributing to slope instability.

Surficial deposits

Three main surficial deposits have been identified from the investigations – alluvium, colluvium and diamictite. Alluvium and colluvium are highly susceptible to seismic loading and liquefaction given the low strength, normally consolidated nature of the deposits. The diamictite is a stronger and more mature deposit (Scott Wilson dated it at circa 50,000 years) that is generally less susceptible to the influence of dynamic loading.

Alluvium

The alluvium has been classified by Douglas Partners (2011) as belonging to a flood deposit or to a swamp deposit; the former is laid down beyond levee banks and comprises laterally grading or transgressional deposits of decreasing grain size from sand to clay. These deposits are typically underlain by peats and clays. The swamp deposits are widespread in flat-lying areas, typically comprising recent sediments and peat deposited over silts and sands. Testing has identified these units to be more than 30 m deep in places.



Figure 3-103: Failure in the epicentral area triggered by 25 February 2018 earthquake

Source: Petley, 2018.

Colluvium

Recent slope instability has led to the movement of weathered materials downslope. The colluvium is typically of granular or cohesive composition. The granular deposits tend to comprise sand, gravel, cobbles and boulders and are closer to the source areas of the failure, whereas the cohesive deposits

³⁹ Robbins, J C, Pettersen, M G, Mylne, K and Espi, J O, 2013. *Tumbi Landslide, Papua New Guinea: rainfall induced?* Landslides. 10, 673–684.

comprise predominantly finer materials – silts and clays with varying amounts of sand which have travelled further distances from the source along water courses.

Diamictite

As in the 2015 geohazard assessment, a distinction has been made to include diamictite in the landslide debris category. In some areas, colluvium has been developed to depths of at least 50 m, and some of the debris appears partially lithified (compacted and or cemented), suggesting older deposits (compared to the less lithified colluvium) were triggered by major seismic events along the nearby Fiak Fault. Diamictite typically contains a poorly sorted, granular mass supported by a finer matrix, and is often associated with highly mobile avalanches and flows as identified at Ekwai Debom. This has been adopted following drilling within some debris fans as part of the ISF quarry and embankment investigation.

Groundwater

The elevation range across the site terrain and the variation in the topography results in significant variation in the groundwater level. In general, groundwater is encountered within ~30 m of the ground surface on the ridges and close to ground level in the valleys. In the less weathered rock mass, the groundwater flow is controlled by fractures (jointing and foliation or faults). In more weathered or altered material, flow tends to be inter-granular and is controlled by the grain size and composition of the deposit.

Surface water

Surface water drainage across the project site is typically classified into three different domains, which are consistent with the Scott Wilson (2011) work: upland headwaters, middle reaches and lowland swamps.

URS defined the upland area as the area generally above an elevation of RL 50 m, with incised river valleys representing an area of sediment supply rather than deposition. This is reflected in the stream ranking, with lower ranked streams being of lower energy and having less erosion potential than the higher ranked streams found at lower elevations. The middle reaches are identified as the zone between RL 150 m and RL 50 m, where the river channel is increasingly braided and there is limited floodplain development. The lowland swamps lie below RL 50 m. The floodplain over this region is well developed, with a meandering and anabranching river channel. The zone is one of sediment deposition and relates to the region downstream of the existing air strip.

The FRHEP reservoir, with a maximum operating level of RL 224 m, will alter the surface water pattern. Once the reservoir is filled, the headwaters zone of lower ranked streams and sediment supply will become the only remaining surface water domain.

Seismicity

On the basis of SRK's earlier TSF design program (SRK, 2011) and confirmed through subsequent work completed to date (SRK, 2016), the most significant seismic influences would be exerted by the Frieda Fault and Zone 15 (Subduction/ Intraslab). A design horizontal PGA of 0.908g was obtained from a deterministic seismic hazard assessment as part of the updated seismic review (Al Atik & Gregor, 2016), which corresponds to the 84th percentile response spectra for the MCE scenario (MCE on Zone15). The probabilistic hazard assessment determined a horizontal PGA of 1.111g for a return period of 10,000 years.

3.2.4 Geohazard assessment – background and process

A geohazard is defined as ‘a condition with the potential for causing an undesirable consequence’.

Geohazard assessments are undertaken in the geotechnical engineering, engineering and construction industries to identify areas or locations of variable levels of hazard or risk from mass movement or instability (AGS, 2000⁴⁰, 2007a, b⁴¹; ANCOLD, 2003⁴²; Cruden and Varnes, 1996⁴³; Fell et al., 2005⁴⁴; Hearn, 2011⁴⁵; IAEG, 1990⁴⁶; Lee and Jones, 2004⁴⁷, 2014⁴⁸; McInnes and Jakeways, 2002⁴⁹; Varnes, 1984⁵⁰).

Fundamental to this is the knowledge and understanding of the GeoHazard (GeoH) base data; if this is low, the qualitative analysis should be undertaken until the knowledge and understanding increase to a point where quantitative values can be assigned. These are generally undertaken through definitive frameworks such as those proposed by AGS (2000, 2007a, b), Fell et al., (2008)⁵¹ (Figure 3-104) and Lee (2003)⁵², and through failure modes, effects and criticality analysis (FMECA) typically used in the dam industry (Hughes et al., 2000)⁵³.

⁴⁰ AGS (Australian Geomechanics Society), 2000. Landslide risk management concepts and guidelines. *Australian Geomechanics*. 35, 49–52.

⁴¹ AGS, 2007a. Guideline for landslide susceptibility, hazard and risk zoning for land use management. Australian Geomechanics Society landslide taskforce landslide zoning working group. *Australian Geomechanics*. 42 (1), 13–36.

AGS. 2007b. Commentary on Guideline for landslide susceptibility, hazard and risk zoning for land use management. Australian Geomechanics Society landslide taskforce landslide zoning working group. *Australian Geomechanics*. 42 (1), 37–62.

⁴² ANCOLD (Australian National Committee on Large Dams), 2003. *Guidelines on risk assessment*. Assessment National Committee on Large Dams Incorporated, Melbourne.

⁴³ Cruden, D M and Varnes, D J, 1996. Landslide types processes. In: *Landslides: Investigation and Mitigation* (Eds A K Turner, R L Schuster). Transportation Research Board, Special Report 247, National Research Council, National Academy Press, Washington DC, 36–75

⁴⁴ Fell, R, Ho, K K S, Lacasse, S, Leroi, E, 2005. A framework for landslide risk assessment and management. In: *Landslide Risk Management* (Eds. O Hungr, R Fell, R Couture, E Eberhardt). Balkema, Rotterdam, 3–26.

⁴⁵ Hearn, G J, 2011. Slope Engineering for Mountain Roads. Geological Society Engineering Geology Special Publication No. 24.

⁴⁶ International Association of Engineering Geology (IAEG) Commission on Landslides, 1990. Suggested nomenclature for landslides. *Bulletin of the International Association of Engineering Geology*. 41, 13–16.

⁴⁷ Lee, E M and Jones, D K C, 2004. *Landslide Risk Assessment*. Thomas Telford.

⁴⁸ Lee, E M and Jones, D K C, 2014. *Landslide Risk Assessment*. 2nd Edition. ICE publications.

⁴⁹ McInnes, R and Jakeways, J, 2002. *Instability: Planning and management*. Thomas Telford.

⁵⁰ Varnes, D J, 1984. *Landslide Hazard Zonation: A Review of Principles and Practice*. Engineering Geology Commission on Landslides and other Mass Movements on Slopes. UNESCO, Paris.

⁵¹ Fell, R, Corominas, J, Bonnard, C, Cascini, L, Leroi, E, Savage, W Z, 2008. Commentary on ‘Guidelines for landslide susceptibility, hazard and risk zoning for land-use planning’ on behalf of the JTC-1 Joint Technical Committee on Landslides and Engineered Slopes. *Engineering Geology*. 102, 99–111.

⁵² Lee, E M, 2003. *Coastal Change and Cliff Instability: Development of a Framework for Risk Assessment and Management*. Unpublished PhD thesis, University of Newcastle upon Tyne.

⁵³ Hughes, A, Hewlett, H, Samuels, P G, Morris, M, Sayers, P, Moffat, I, Hardings, A, Tedd, P, 2000. *Risk management for UK reservoirs*. Construction Industry Research and Information Association. (CIRIA) C542. London.

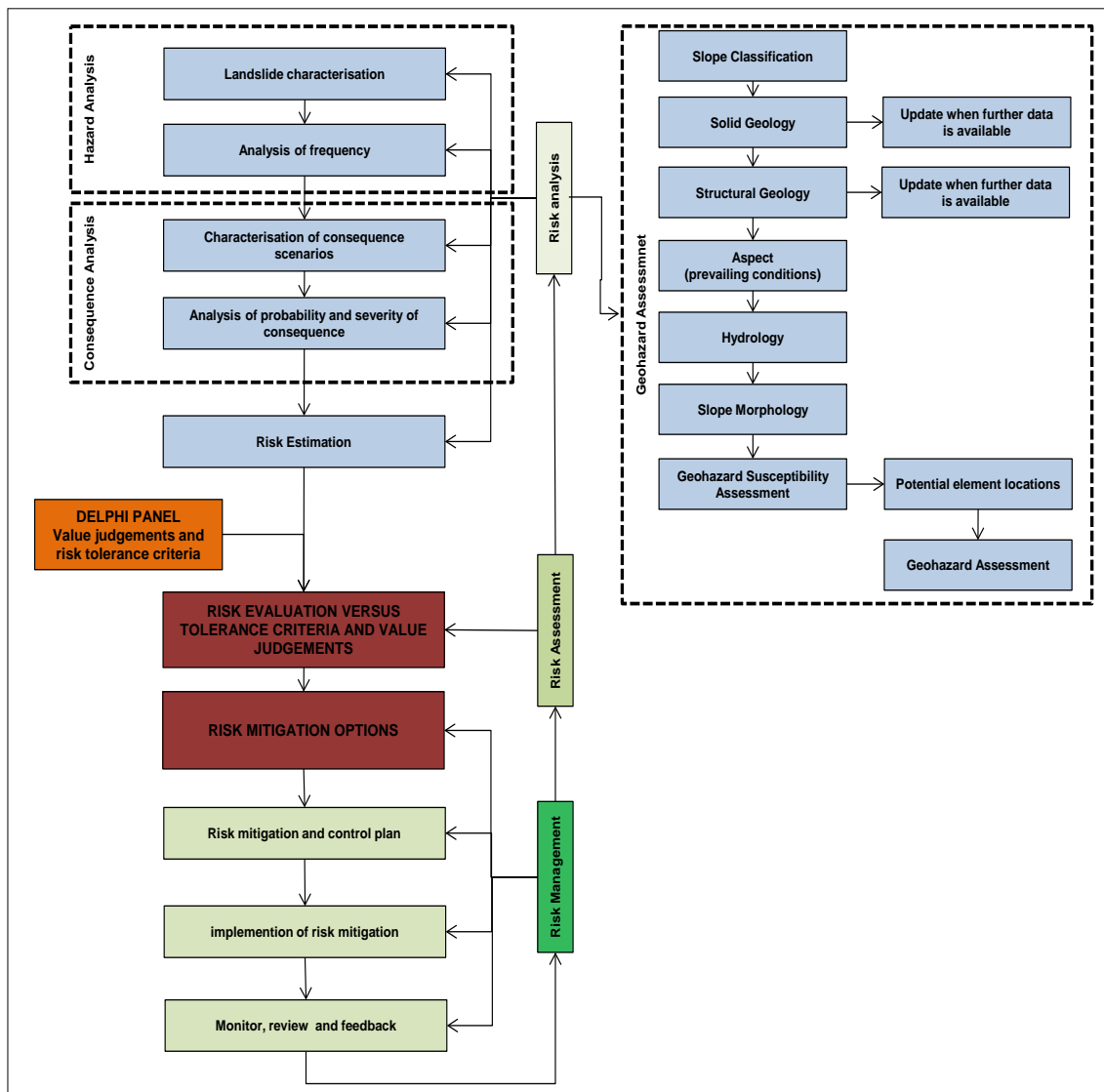


Figure 3-104: Risk assessment flow diagram

Source: After Fell et al., (2008).

Data gathering generally involves a linear sequence of events, starting with desktop studies, then field investigations and laboratory testing, through to the detailed analysis in 2D, 3D and potentially 4D, followed by reporting. The use of criteria based on spatial analysis using GIS packages is becoming more common for the rapid assimilation of data covering significant areas or volumes (Carrara et al., 1999⁵⁴; Flentje et al., 2011⁵⁵, Soeters and van Western, 1996⁵⁶; van Western, 2004⁵⁷; Guzzetti et al.,

⁵⁴ Carrara, A, Guzzetti, F, Cardinali, M, Reichenbach, P, 1999. Use of GIS technology in the prediction and monitoring of landslide hazard. *Natural Hazards*. 20(3), 117–135.

⁵⁵ Flentje, P, Stirling, D and Chowdhury, R N, 2011. Landslide Inventory, Susceptibility, Frequency and Hazard zoning in the Wollongong and wider Sydney Basin Area. Landslide Risk Management Roadshow 2011 National Seminar Series, Australian Geomechanics Journal, Vol. 46, No 2: 41–49.

⁵⁶ Soeters, R and van Western, C J, 1996. Slope instability recognition, analysis and zonation. In: *Landslides: Investigation and Mitigation* (Eds A K Turner and R L Schuster). National Research Council, National Academy Press, Washington, DC. 127–177. Transportation Research Board, Special Report 247.

⁵⁷ Van Western, C J, 2004. Geo-information tools for landslide risk assessment – an overview of recent developments. In: *Landslides, Evaluation and Stabilization*. Proceedings of the 9th

1999⁵⁸, 2006⁵⁹; Wu et al., 2014⁶⁰). This can be undertaken descriptively (qualitatively) or through the use of numerical methods, with the descriptions requiring a numerical rank prior to addition or multiplication in GIS, as has been conducted in this assessment. Conclusions can then be applied to the larger area through benchmarking of parameters (Aleotti and Chowdhury, 1999⁶¹; Carrara et al., 1998⁶²; Hearn, 2011⁶³).

The desktop geohazard assessment at Frieda River has been carried out principally in two phases:

- Phase 1: review of previous reports and documents
- Phase 2: geohazard assessment, including hazard categorisation and the development of landslide inventory, following by development of a geohazard map and reporting.

Phase 1 – Historical geohazard review

The purpose of SRK's geohazard analysis was to consolidate and enhance the understanding of the physical material properties in relation to slope instability in the Frieda River catchment. Previous assessments reviewed include SRK (2015), URS (2011), Douglas Partners (2011) and SRK (2011).

Phase 2 – Geohazard assessment

Phase 2 forms the basis for a digital qualitative geohazard assessment matrix, where hazards are evaluated based on assigned hazard ranking conditions assessed through a spatial calculation of layers in GIS. The criteria have been selected through a Delphi Panel process involving specialists in each field.

Figure 3-105 outlines the geohazard inputs and shows the critical input layers required for the assessment. These layers are then analysed to establish design criteria which rank or provide semi-quantitative values that can be applied in GIS multiplication (Figure 3-106). The values for the layers and weightings (outlined in Section 5) were input into the following formula:

$$GeoH = (layer\ rating_1(layer\ weighting_1) + layer\ rating_2(layer\ weighting_2) \dots)$$

It is important to note that this is a qualitative georisk assessment. With the incorporation of high confidence site data, and input parameters discussed and selected in a Delphi Panel forum, it is possible that a quantitative georisk assessment can be completed for selected areas of the catchment.

International Symposium on Landslides (Lacerda W, Ehrlich M, Fontoura S, Sayao A (eds)), Rio de Janeiro, pp 39–56.

⁵⁸ Guzzetti, F, Carrara, A, Cardinali, M, Reichenbach, P, 1999. Landslide hazard evaluation: a review of current techniques and their application in a multi-scale study, Central Italy. *Geomorphology*. 31 (1-4), 181–216.

⁵⁹ Guzzetti, F, Galli, M, Reichenbach, P, Ardizzone, F, Cardinali, M, 2006. Landslide hazard assessment in the Callozone area, Umbria, Central Italy. *Natural Hazards and Earth Systems Sciences*. 6, 115–131.

⁶⁰ Wu, Y Chen, L, Cheng, C, Yin, K, Torok, A, 2014. GIS-based landslide hazard predicting system and its real-time test during a typhoon, Zhejiang Province, Southeast China. *Engineering Geology*. 175, 9–21.

⁶¹ Aleotti, P and Chowdhury, R, 1999. Landslide hazard assessment: summary review and new perspectives. *Bulletin of Engineering Geology and Environment*. 58 (1), 21–44.

⁶² Carrara, A, Guzzetti, F, Cardinali, M, Reichenbach, P, 1998. Current limitations in modelling landslide hazard. *Proceedings of IAMG '98*. (Eds: A Buccianti, G Nardi and R Potenza), pp 195–203.

⁶³ Hearn, G J, 2011. Slope Engineering for Mountain Roads. Geological Society Engineering Geology Special Publication No.24.

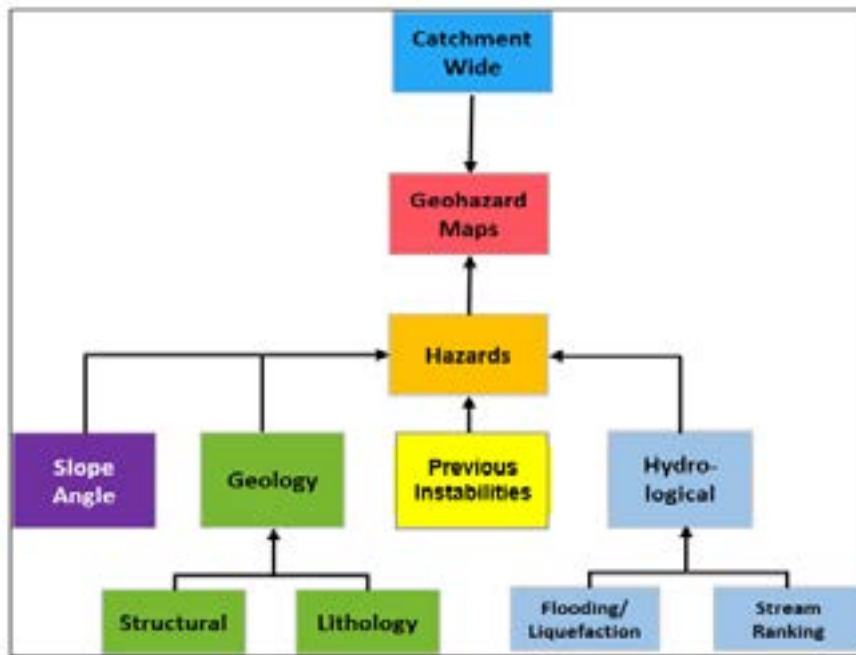


Figure 3-105: Geohazard process showing relationship between inputs and overall geohazard rating

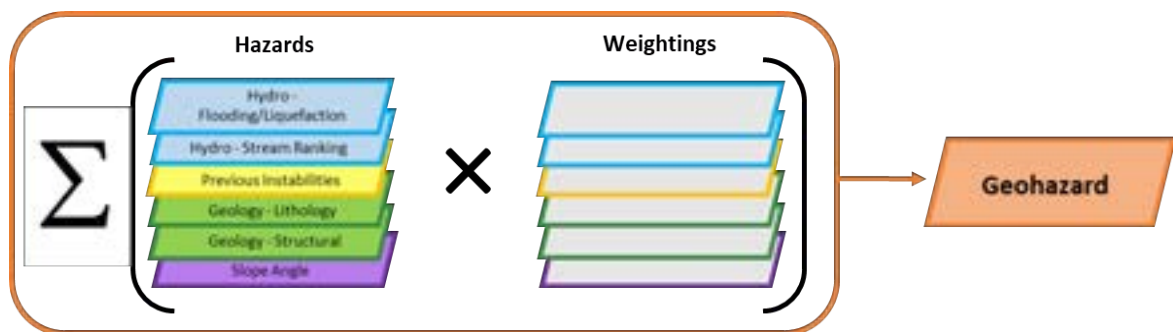


Figure 3-106: Geohazard input layers and equation used for overall geohazard rating

3.2.5 Geohazard inventory

A geohazard or landslide inventory was created to establish the mechanisms of slope instability and provide a qualitative understanding of the hill shade data, which is generated in GIS using the LiDAR and SRTM data based on changing the light direction in 45° increments. The basic morphology of a landslide and associated terminology defined by Varnes (1984) is shown in Figure 3-107.

A diagram of various landslide types is shown in Figure 3-108. The morphology of the schematic instability mechanisms was used to identify areas of instability in the LiDAR/ SRTM dataset for the Frieda River catchment.

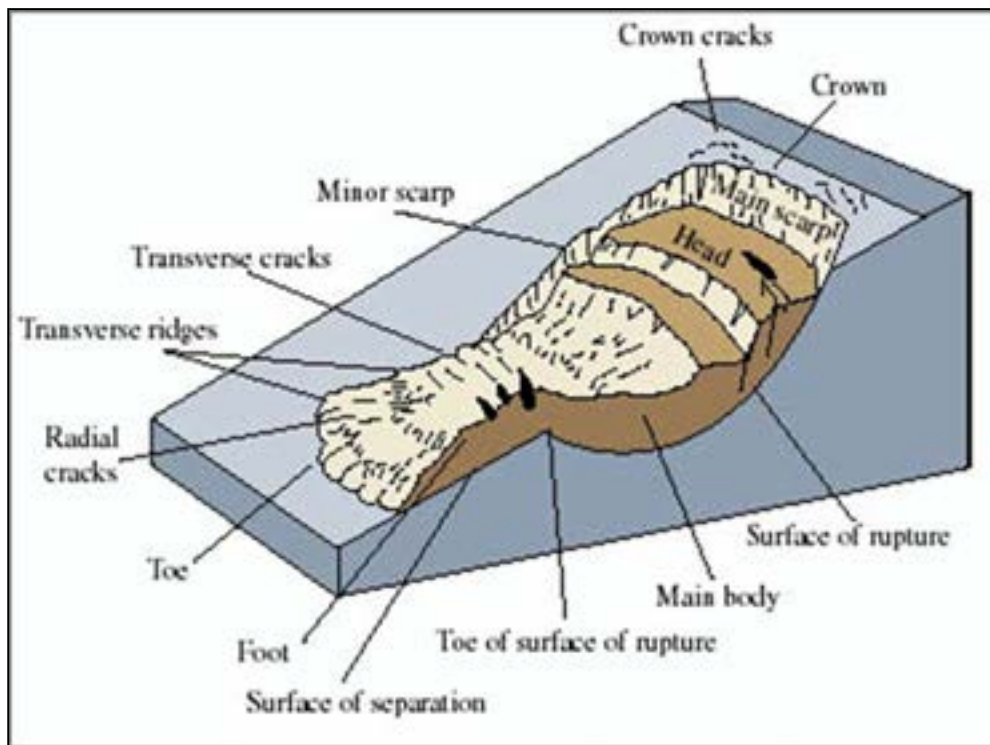


Figure 3-107: Landslide classification

Source: Varnes, 1984.

Although incomplete, the landslide inventory provides evidence of many of the failure types and areas that can be expected in the region. The landslides in the inventory have been identified based on their interpreted failure mechanism and confidence in their identification. Generally, landslides in the 30 m resolution SRTM dataset are of lower confidence than landslides in the 5 m resolution LiDAR dataset. The inventory shows that larger-scale landslides can typically be identified from the 30 m resolution DEM (digital elevation model) and that small-scale areas of instability may be overlooked due to the low resolution of the data.

As the landslides are identified based on the 2D geomorphological signatures, the area of the instability can be calculated; however, the volume of the material is unknown, unless site investigation data available provides information on thickness. SRK incorporated areas of instability identified in previous studies in the current landslide inventory. In some cases, landslides have been revised in size or type, or removed altogether, based on different interpretation and for consistency across the inventory. This geohazard assessment has refined the landslide inventory types to the four primary failure mechanisms: fall, flow, slide and debris fan. Examples of the failure types and characteristics, presented in plan and cross-sectional views are shown in Figure 3-109. Most failures are complex and comprise a combination of the four failure types.

The landslide inventory should be updated with results of ongoing work in the study area.

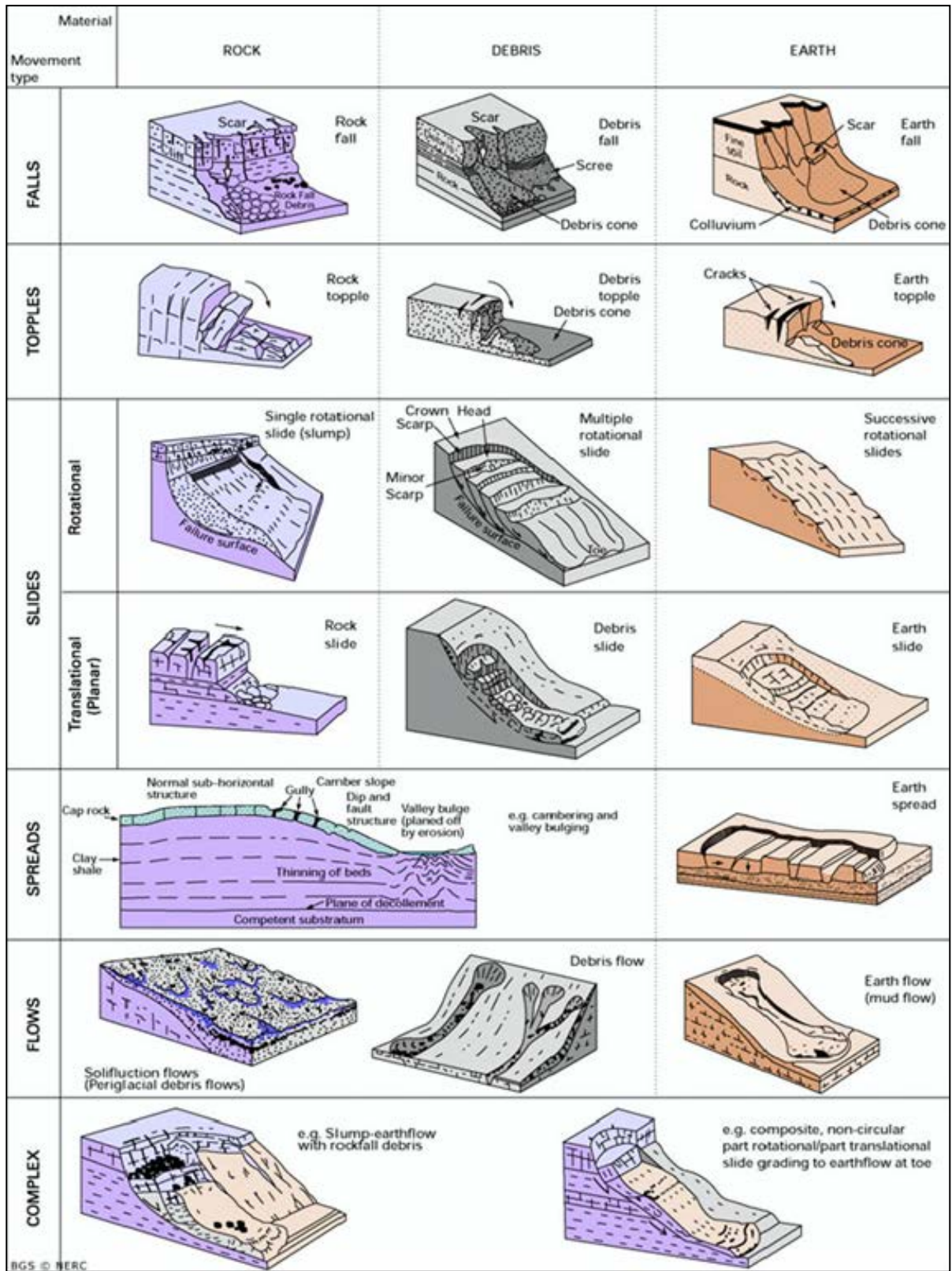


Figure 3-108: Various landslide types

Source: After Cruden and Varnes, 1996.

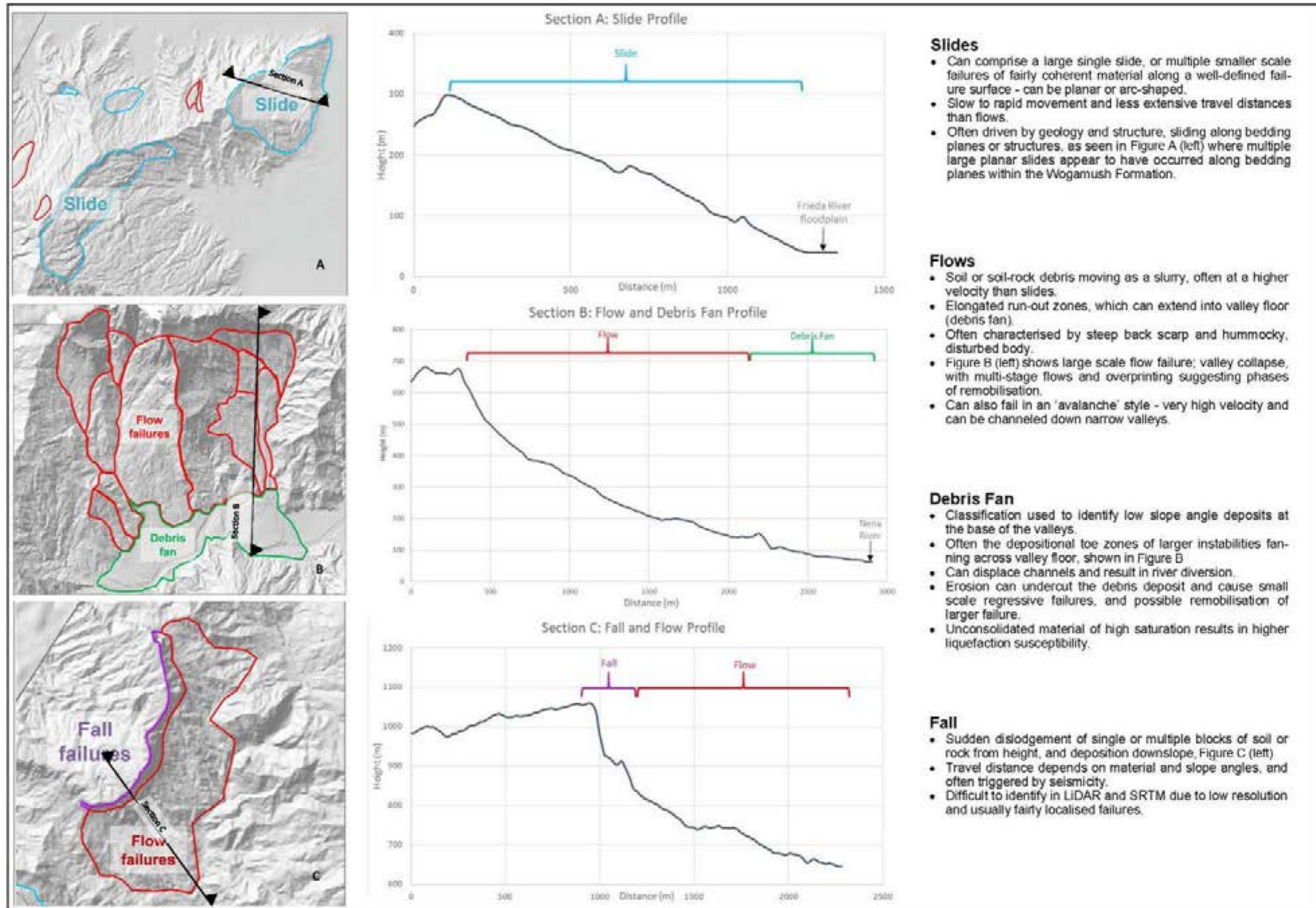


Figure 3-109: Landslide failure examples, characteristics (Hunt, 1984) and cross-sectional profiles

3.2.6 Geohazard assessment inputs

The methodology described in Section 3.2.5 was used for the qualitative geohazard assessment for the Frieda River catchment. This methodology involved multiplication of a series of different GIS layers to understand the spatial variability of the resulting overall geohazard layer. The principal components are the following:

- 1 Geology: superficial deposits and rock units
- 2 Structural geology: faults, thrusts and lineaments
- 3 Slope angle: the steepness or shallowness of the slopes
- 4 Previous instabilities: landslide inventory
- 5 Hydrology: areas impacted by flooding and liquefaction potential
- 6 Hydrology: stream ranking.

All assessment criteria were qualitatively ranked on a scale of 1 to 10. Where it was deemed necessary, these factors were weighted in the analysis based on the importance in the geohazard process. Weightings are based on the current understanding of the geohazard's influence on the slope processes and the expected impact on an element.

Geology – rock type

The underlying rock type is a fundamental control on the level of geohazard exposure. More competent, or solid, geological units typically present a lower level of expected hazard, compared to recent, or transported deposits such as alluvium and colluvium. The solid geology for the Project area was based on geological mapping by Hall et al., (1990)⁶⁴ and the regional geological map (1: 250,000 Mianmin Geological Map – Sheet SB54-3, Papua New Guinea). While rock mass quality and discontinuity characteristics are very important factors in slope stability, these have not been considered in this assessment as the data is not available across the catchment.

Table 3-35 outlines the hazard ratings that have been applied to the various geological units identified, as well as surficial deposits of alluvium and colluvium.

⁶⁴ Hall, R J, Britten, R M and Henry, D D, 1990. Frieda River copper-gold deposits: in Hughes F E (Ed.), 1990 Geology of the Mineral Deposits of Australia & Papua New Guinea. The AusIMM, Melbourne Mono 14, v2, pp. 1709–1715.

Table 3-35: Geohazard rating – geology

Rating	Geological Formation	Rock type
1		
2		
3	Maramuni Igneous Association, Kumbruf Volcanics	Metabasic rocks, gabbro, quartz diorite porphyry, basaltic dykes
4		
5	Alife Blueschist, April Ophiolite	Metabasic rocks, knotted pelitic schists
6	Wahgi Group, Wabia Beds, Maril and Chim formations, Ok Binai Phyllite, Wogamush Formation	Low-grade metabasic and metasandstones, phyllites, slate, minor quartzite, mudstone, interbedded micaceous siltstone, sandstone and conglomerate
7	Alluvium	Unconsolidated sediments
8	Partially lithified colluvium	Diamictite: compositionally variable dependent on source rocks, clast to matrix supported; thicknesses of 50 m are possible
9	Fault Zone Rocks, Colluvium	Schistose serpentine along fault zones, failed landslide material
10	Landslide Metamorphics	Schists, marble, gneiss, amphibolite

Geology – structural features

The 1: 100,000 and 1: 250,000 geological maps were combined and digitised for this study to understand the scale and rank of each structural feature. Major thrust faults, such as the Frieda, Fiak and Saniap thrusts and the Transfer Faults and the bifurcation of these features, were ranked the highest. Hill et al. (2002) and other literature indicates these features are highly persistent, with a large throw and width. Intermediate structures, and the intersection of structures have been included in the assessment and rated accordingly. Each structure was assigned an area of influence or 'buffer' that was determined by the structural continuity and type. The analogy is that structures with highest persistence contain the largest width component and pose the highest geohazard potential, as shown in Table 3-36.

Table 3-36: Geohazard rating - structural geology

Rating	Geological structure	Buffer (m)
1	No identified structure at catchment scale	
2		
3		
4		
5	Intermediate structures: lower persistence, identified as lineaments	200
6	Intersection of intermediate and major structures	
7		
8		
9		
10	Major regional structures: Frieda Fault, Fiak Fault, Saniap Fault, Transfer Faults	500

Slope angle

Slope hazard has been classified by the slope angle based on the LiDAR/ SRTM data. Slope angle is a major contributor to instability, with gravity and weather processes also being important factors. Generally, the steeper the slope, the higher the geohazard rating; however, the low slope angle zones also give an indication of areas of landslide deposition and 'hummocky' disturbed ground, which assists in the identification of historical instabilities. While slope curvature was considered, it has not

been included in the geohazard assessment, as the data provided by the slope angle gives sufficient information on the slope geometry.

Table 3-37 lists the hazard ratings and values assigned to the various slope angle categories.

Table 3-37: Geohazard rating –slope angle

Rating	Slope angle (°)	Slope type
1	0–2.5	Flat/ horizontal
1.5	2.5–10	
2	10–20	
4	20–30	
5	30–40	
6	40–50	
8	50–60	
10	65+	Extremely steep

Historical instabilities – landslide inventory

The terrain has been assessed using hill shade maps, slope angles, consideration of geology and proximity to structures to identify geomorphological features interpreted as areas of instability. The classification of the landslide types has been simplified into four failure mechanisms: fall, flow and slide, with debris fan included to differentiate the low angle, valley floor deposits. This classification systems have been simplified based on the LiDAR/ SRTM data resolution and the unknown material composition of all landslides. Identifying the instability and its general failure mechanism is considered sufficient to calculate the resultant geohazard risk.

Landslides identified in previous geohazard investigations (SRK, 2015; URS, 2011; Douglas Partners 2011) have been included in the current landslide inventory, but have been reclassified according to the current system and revised based on footprint, confidence level and, in some classes, removed from the inventory. Desktop observations must be validated in the field to understand the physical nature of the feature and materials.

Table 3-38 outlines the types of inferred slope failures that have been identified, as well as the confidence in their identification. Instabilities with a higher rating pose a higher geohazard risk.

Table 3-38: Geohazard rating – instability

Rating	Failure type
1	No instability identified on slope
4	Fall
	Debris fan
5	Slide – low confidence
6	Flow – low confidence
7	Slide – medium confidence
	Flow – medium confidence
9	Slide – high confidence
10	Flow – high confidence

Hydrology – flooding and liquefiable material

As part of the revised location for the FRHEP embankment, the resultant larger reservoir is expected to reach a maximum operating level of RL 224 m. A significant number of identified instabilities will be completely or partially submerged by the reservoir, and this will increase the risk of remobilisation. Where not completely submerged, erosion of toe material of landslides can destabilise and initiate failure into the reservoir.

Although it is unlikely the maximum reservoir level will exceed an elevation of RL 224 m, a 20 m buffer has been applied to the reservoir footprint to consider the impacts of a higher water table, suction and higher water content in the soil and rock surrounding the reservoir.

The site’s vulnerability to seismic loading is most pronounced for alluvium, which is susceptible to liquefaction and consolidation, or collapse. Alluvium is present along the river valleys within the catchment; however, when the reservoir has reached the maximum operating level, most alluvial deposits will be submerged. During filling, areas of alluvial deposits should be considered highly susceptible to liquefaction and an elevated geohazard risk applied.

Table 3-39 lists the ratings applied to the flooding and liquefiable materials in the geohazard assessment.

Table 3-39: Geohazard rating – hydrology – flooding and liquefaction

Rating	Hydrology – flooding and liquefaction
1	No flooding or liquefiable material expected
5	Within 20 m reservoir buffer zone
	Alluvium – liquefiable material
10	Flooded by reservoir (<RL 224 m)

Hydrology – stream ranking

Streamflow analysis was performed on the LiDAR/ SRTM dataset to understand drainage patterns within the catchment. The qualitative understanding of the catchment area and number of combined channels leads to an understanding of the relative velocity of water and potential for flash flooding (which is also heavily dependent of slope gradient and channel geometry). Stream ranking informs the potential for erosion at higher elevations within a catchment. The basic principle is that the potential hazard is directly related to the number of channels that join prior to coalescing into a larger channel. While not an explicit or definitive criterion, the approach provides an indication of catchment size, water velocity and erodibility.

A buffer was applied to each stream order to reflect the width of the stream and the potential for upslope inundation and scouring potential during heavier rainfall events. This was selected based on hill shade interpretation and site observations.

After filling of the reservoir to the maximum level of RL 224 m, most of the higher ranked streams will be submerged and smaller, lower ranked streams feeding into the flooded reservoir will remain at higher elevations. This assessment only considers streams outside of the reservoir footprint.

Table 3-40 lists the ratings applied to the stream ranking in the geohazard assessment.

Table 3-40: Geohazard rating – hydrology – stream ranking

Rating	Stream ranking	Buffer width (m)	Stream characteristics
0	Number of streams		No streams
1	1	5	Multiple streams: low energy environment
2	2	7.5	
3	3	10	
4	4	17.5	
5	5	25	
6	6	30	Single stream: high energy environment, i.e. Frieda River

Overall geohazard classification

The geohazard classification presents a qualitative assessment of SRK's current understanding of the FRHEP. This is a qualitative system to rank overall geohazards and provide an initial framework for further development as more data becomes available. The current overall geohazard assessment was calculated using a multiplication method, with some input parameters weighted to reflect the importance of that parameter. The results were validated with known conditions on site; SRK recommends that areas of high geohazard risk be ground-truthed to confirm or review the geohazard rating. Classification should be undertaken in consultation with all parties, including consultant designers, engineers and FRL, to understand the complex interrelationships between geohazard, probability, consequence and loss (or cost to project). The overall geohazard ratings are presented in Table 3-41. Specific areas of concern are discussed in Section 3.2.7.

Table 3-41: Geohazard rating – overall

Class	Geohazard
1	Very Low
2	
3	Low
4	
5	Moderate
6	
7	High
8	
9	Very High
10	Extreme

3.2.7 Areas of concern

Across the catchment, the geohazard has been assessed to range from Very Low to Extremely High, with the occurrence of the ratings shown in Figure 3-110 and the spatial distribution in Figure 3-111. The higher-rated hazards are generally focused at smaller, or local, scales. The modal hazard rating has been evaluated to be Low, followed by High – mainly coincident with major structures. Areas of concern which have High to Extremely High ratings were considered in further detail.

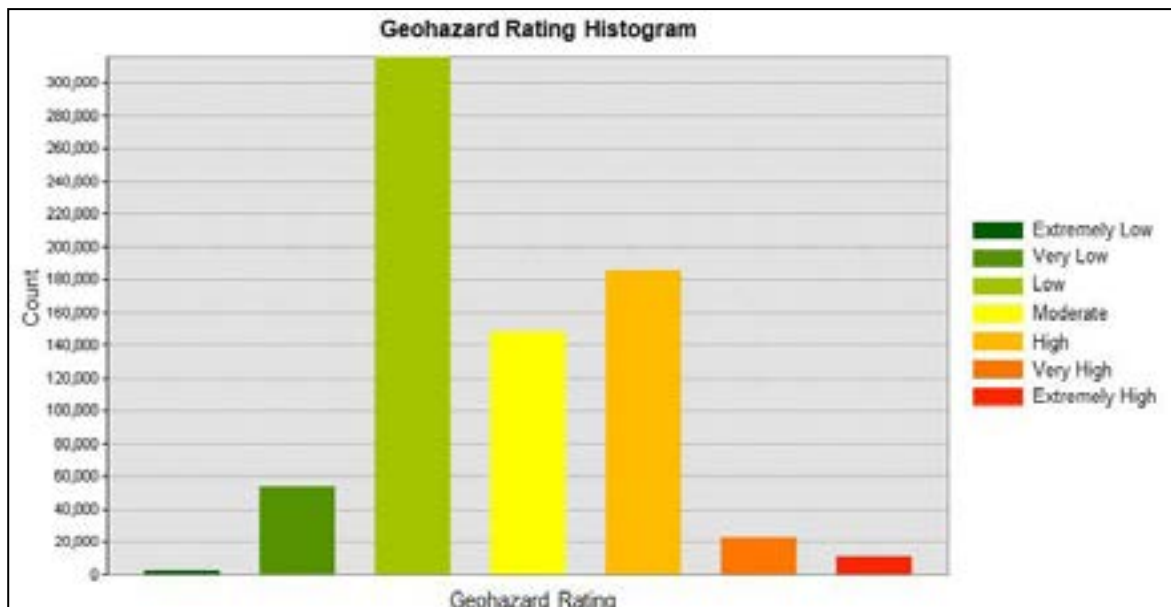


Figure 3-110: Histogram of geohazard rating across the catchment

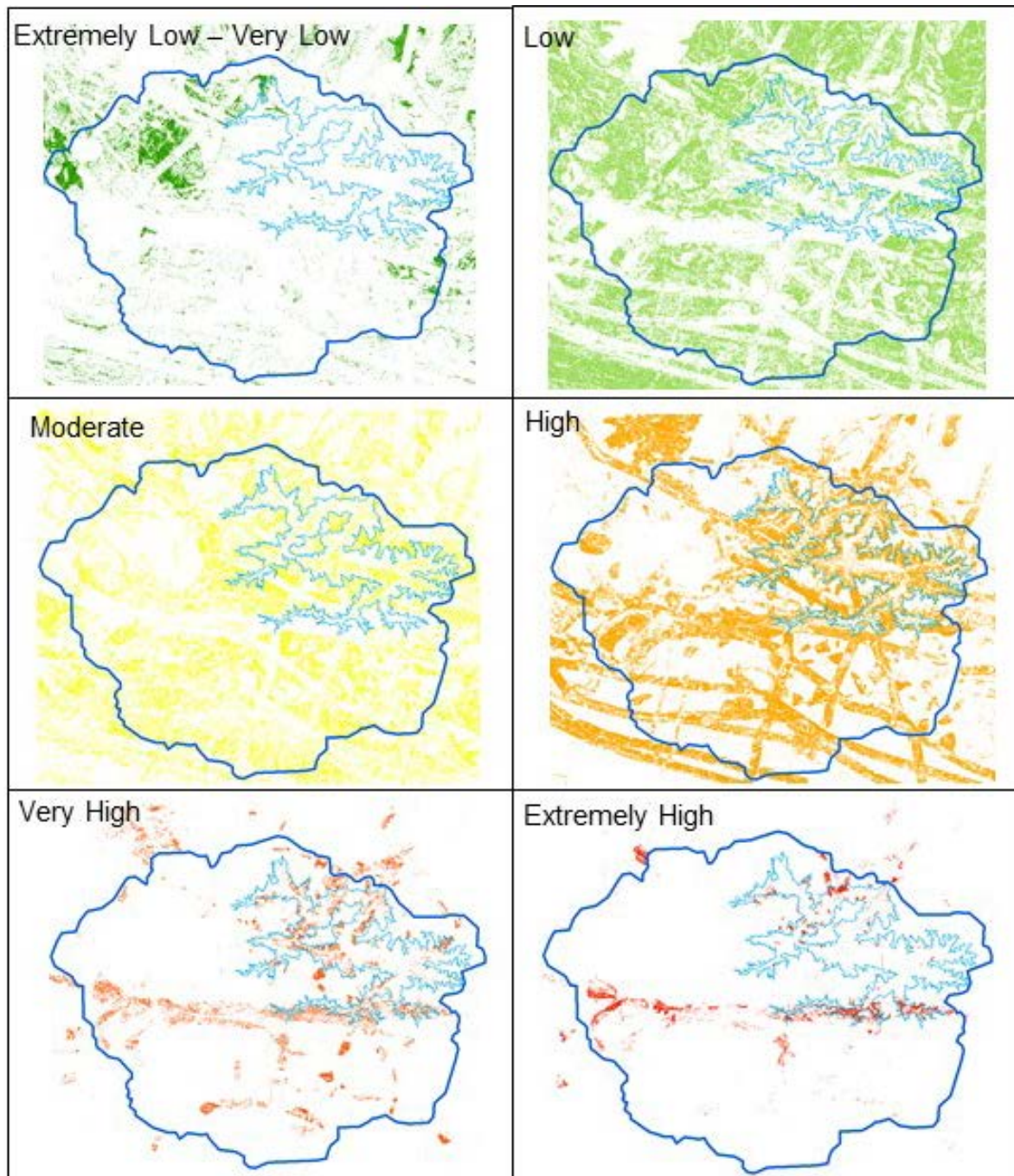


Figure 3-111: Spatial distribution of geohazard ratings across the catchment

Flooded areas

Geohazard rating: High to Extremely High

- The area within the footprint reservoir has a High geohazard rating (shown in Figure 3-112) because the introduction of water to weak material or historical instabilities reduces the material shear strength and the area is therefore at an elevated risk of failure.
- Periods of higher vulnerability will occur during water level fluctuations when the elevated pore pressure reaches equilibrium in the low strength or poor quality soil or rock mass.
- High confidence landslides within the reservoir footprint are rated Very High to Extremely High.

- Where major structures are present within the reservoir footprint, particularly on steep slopes, the rating is High. This can be seen along the Fiak Fault, Frieda Fault and the NNE trending Transfer Faults.
- The hazard rating along the Fiak Fault is elevated due to the combined effect of structural controls, steep slopes, problematic fault zone rocks and historical instabilities – all of which will be partially submerged by the reservoir.
- As this assessment has been completed based on the maximum operating level of the reservoir, the area affected by the reservoir should be observed and closely monitored during filling. Where movement is observed, appropriate mitigation methods should be applied. The potential scope and design of necessary mitigation should be investigated prior to the embankment construction, so the measures are available to be implemented when required.

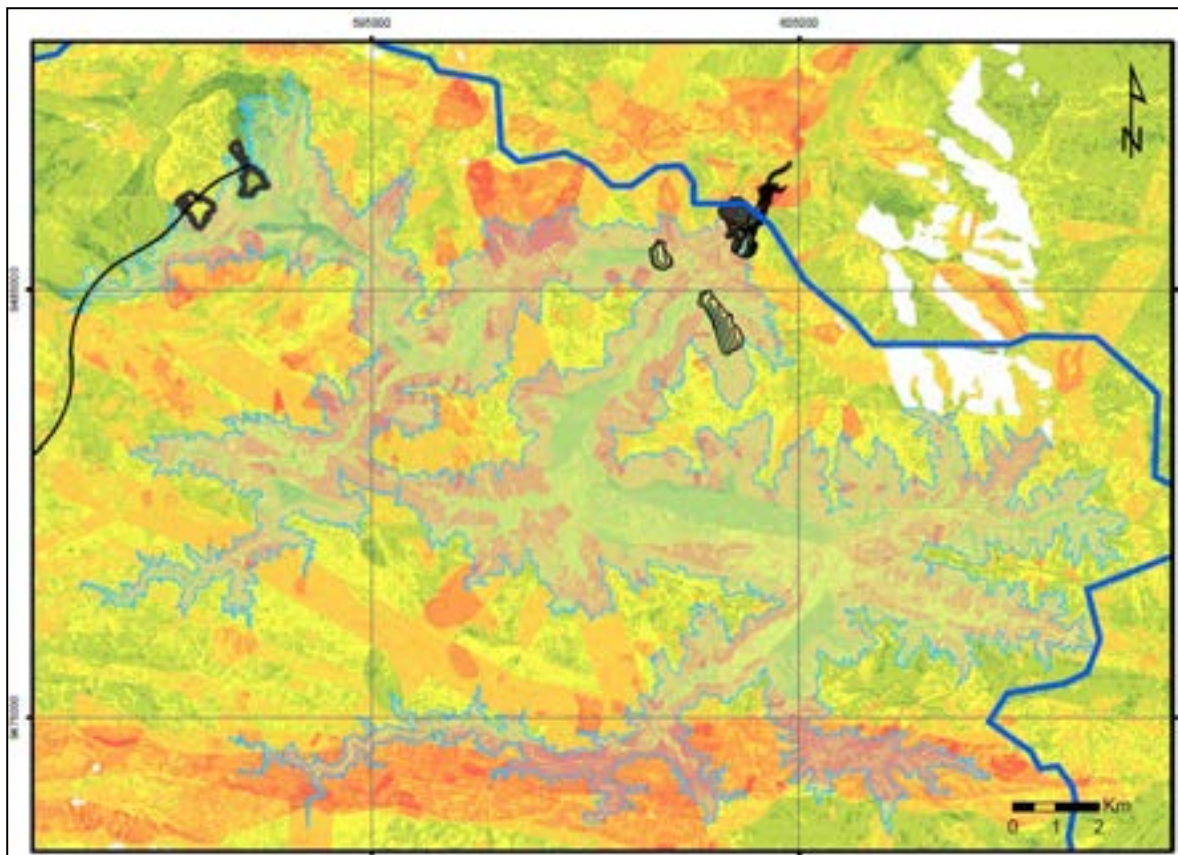


Figure 3-112: Detail of geohazard rating around reservoir

Infrastructure downstream of embankment

Geohazard rating: High to Extremely High

- Several medium and high confidence slides, flows and debris fans have been identified in the valleys downstream of the FRHEP site (Figure 3-113).
- Alluvium in the valley floor with a high liquefaction susceptibility, and partially lithified colluvium from historical instabilities in the eastern abutment valley wall represent geology with a High geohazard rating.
- The valley walls are composed of April Ophiolite, which has a Moderate geological hazard rating, but the valley is very steep ($>40^\circ$), which is considered to be the main control on instabilities.
- Additionally, the linear nature of the valley that the embankment is likely to have formed along the trace of a Transfer Fault (and splay of the Sepik Fault further downstream), with the sharp diversion

to the east downstream, demonstrates the structural controls in the area. The interaction of these structures increases the possibility of seismicity, which has been considered in the assessment.

- The geohazard rating downstream of the FRHEP embankment is High to Extremely High, as the occurrence of large landslides into the Frieda River valley could have major impacts on the powerhouse, spillway and the embankment structure. If downstream flow from the embankment is obstructed by landslide debris, water could pool behind the landslide material and back-up towards the embankment. Water accumulated downstream of the embankment could adversely impact the dam foundations/ structure.

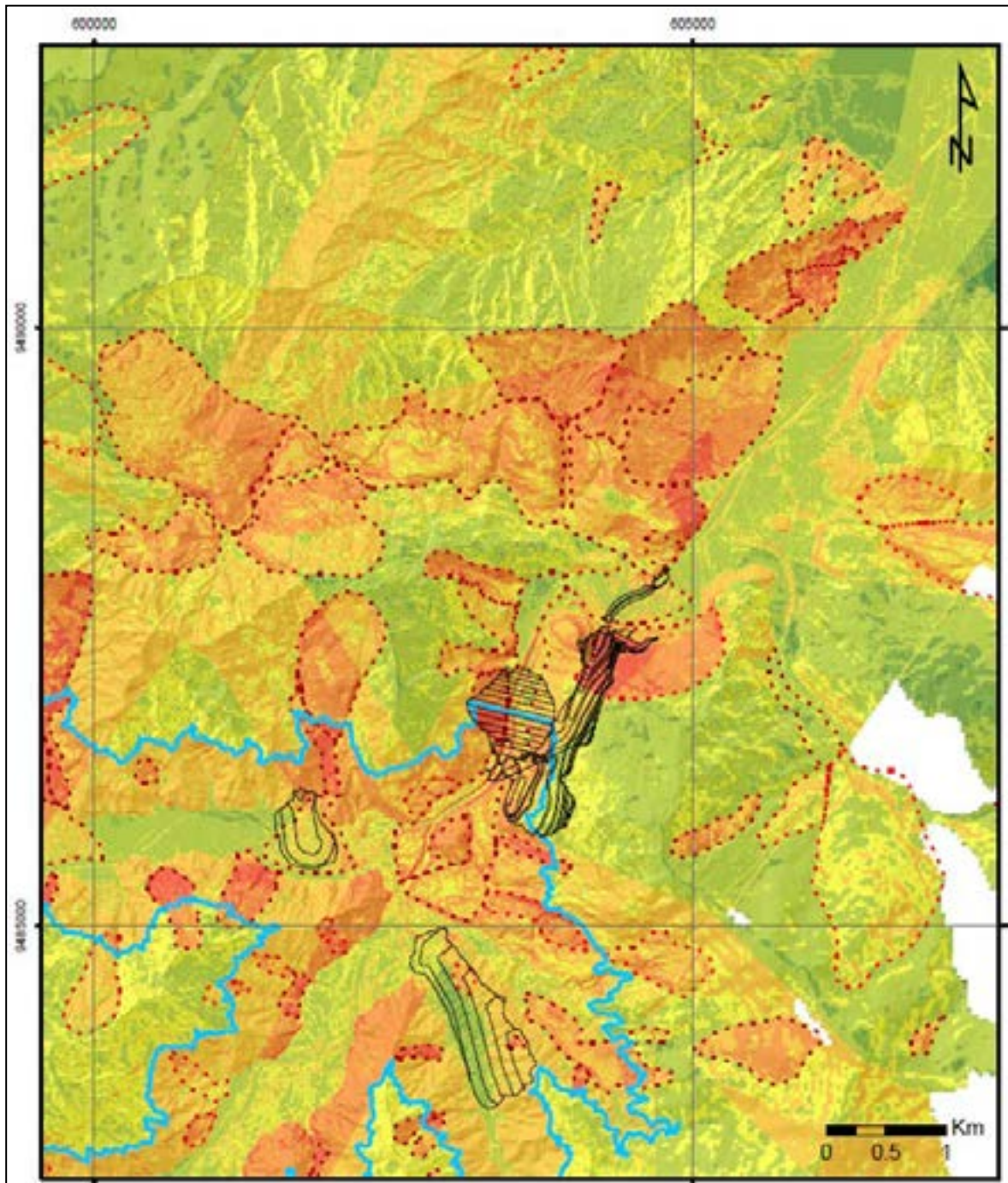


Figure 3-113: Location of embankment with landslides outlined in red (dashed lines)

- While drilling has been undertaken in the embankment abutments, not all slopes near the embankment site have been investigated. It is recommended the northwestern slopes be ground-truthed to confirm or reject areas of instability that have been identified. The removal of landslides from the landslide inventory following site inspections will lower the geohazard rating. Additionally, it is possible that some of the 'problematic' material, such as colluvium and alluvium, may be removed as part of the construction earthworks, which will also lower the geohazard rating.

High risk geology

Geohazard rating: High to Extremely High

Zones of high geology risk are coincident with major structures and high slope angles, as shown in Figure 3-114 and outlined below:

- **Fiak Fault**

The terrain along the Fiak Fault with problematic fault zone geology is a High to Extremely High geohazard zone, particularly where historical instabilities have been identified and where submerged by the reservoir. The presence of instabilities is likely due to heightened seismic risk along the Fiak Fault. The occurrence of landslides may pose a wave generation risk. While such waves would not be in the direct flow path of the embankment, they could travel along the reservoir.

- **Historical slides – northeast catchment**

The zone of high confidence flows in the northeastern quadrant of the catchment has a High to Extremely High geohazard rating. This is largely due to the high slope angles at the head scarps, and saturation at the toe due to the reservoir. The body of these flows has a relatively low slope angle, and is therefore not considered a high risk; however, the toe material should be monitored when filling the reservoir because toe erosion and saturation may cause regressive failures that can trigger larger-scale movement. If failure occurs at high velocity, there is risk of wave generation; however, waves would not be in the direct flow path of embankment.

- **Partially lithified colluvium**

Further to the west of the catchment, large areas of partially lithified colluvium from major historical landslides associated with seismic events along the Fiak Fault have been mapped – this zone is of High to Extremely High geohazard risk. The major failure deposits are High risk due to the weak composition within existing internal failure planes, and possible perched water tables within the colluvium. Although the slope angles are not particularly high, proximity to major faults may cause remobilisation of the material during seismic events. This zone is close to the Horse-Ivaal-Trukai (HIT) pit and the crusher site of the FRCGP; however, based on the topography and slope directions, any reactivation of this zone of colluvium is unlikely to travel in the direction of the mine.

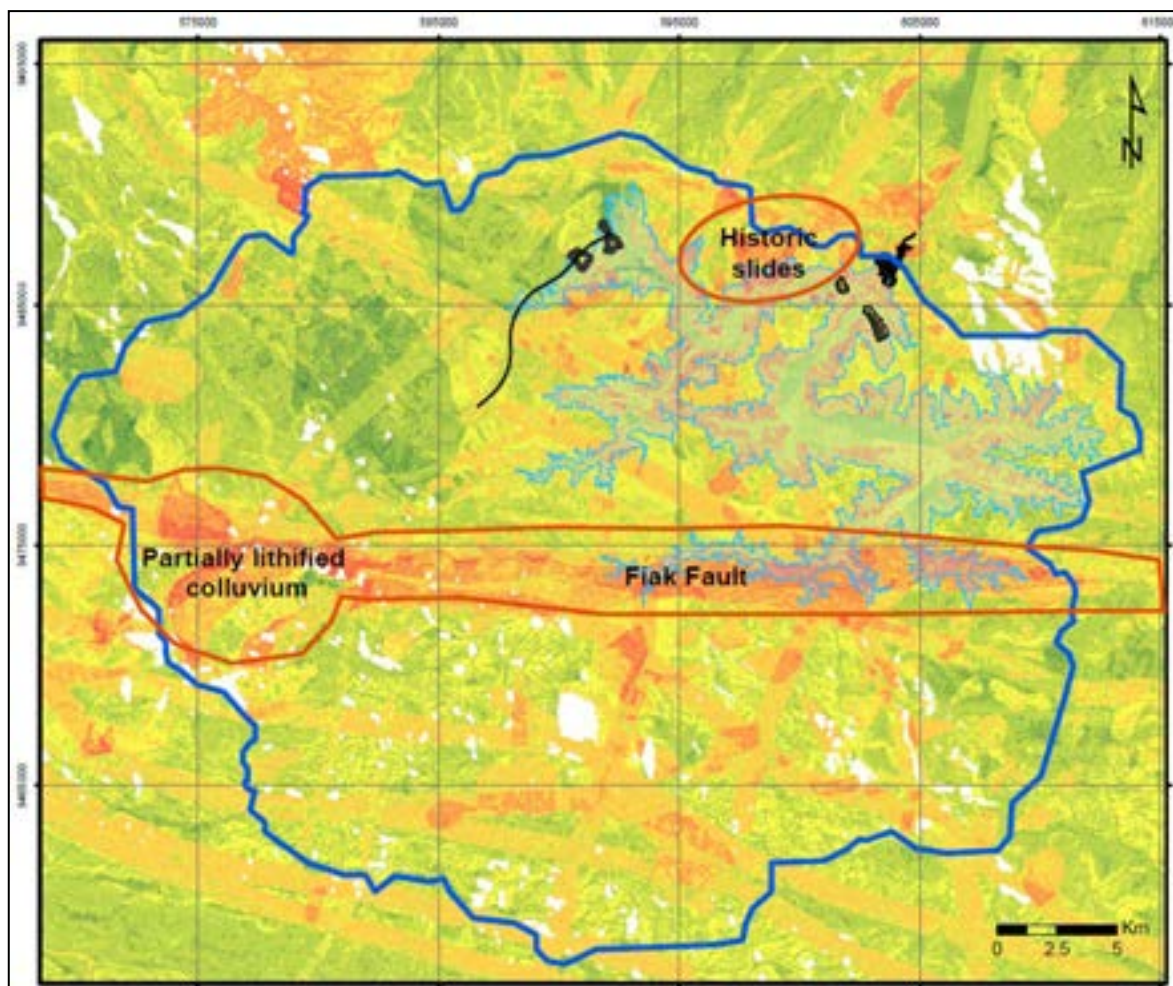


Figure 3-114: Zones of High risk geology

3.2.8 Summary

The following presents a summary of the main points of the geohazard analysis for the Frieda River catchment that includes the FRHEP site:

- The geohazard analysis highlights the relative hazards within the region when sections are correlated together. Geohazard evaluations can be combined with probability and loss figures to form a quantitative risk assessment for the region, if required.
- The location of high confidence historical landslides demonstrates that most instabilities are mainly a function of geology and steep slope angles. This relationship is also strongly influenced by the proximity to major geological structures.
- There is a strong correlation between historical instabilities and flooding caused by reservoir filling. It is likely that saturation of the failed material during reservoir filling will cause some failures. Areas with geohazard ratings of High or greater should be monitored to determine slope behaviour at the maximum operating capacity and during water level fluctuations.
- The geohazard assessment should be a 'live' document that is continuously updated using available data and information from ground-truthing. Validation of the parameters, logic and geohazard rankings will improve confidence in the study.

Recommendations

Areas of High geohazard rating identified during this qualitative geohazard assessment require validation to confirm the spatial extent, location and the significance of the hazard to the FRHEP.

This will allow the input parameters and weightings to be refined, resulting in reduced geotechnical uncertainty and higher confidence in the outcomes of the geohazard assessment.

As part of an ongoing work program, a commitment to continue assessing the geohazard risks by improving the geohazard assessment in the short and long terms should be made. Some of the recommendations are outlined below:

- Undertake ground-truthing in areas identified as High or greater geohazard risk in locations that pose a risk to mine infrastructure in order to validate the results. This may involve a site walk-over to inspect areas identified as experiencing instability, and refine the geohazard input parameters as more detailed data is collected and interpreted. Where the input parameters can be confirmed, rejected or simply reviewed, the resultant geohazard rating may be reduced. This is particularly relevant where the presence of historical landslides can be validated. This can be conducted through site walk-over or by site investigation techniques such as hand augers and dynamic cone penetrometer (DCP) testing to confirm the presence of colluvium. Where not accessible on foot, aerial inspection (from helicopter) may be useful in confirming or rejecting zones identified as High risk, such as the SRTM zone which has been assessed based on lower resolution data.
- Consider collection of higher resolution LiDAR data across the catchment. This would enhance the definition of the terrain and allow for higher confidence and accuracy when identifying areas of geohazard potential. This is strongly recommended for at least the greater catchment area currently only covered by 30 m resolution SRTM data, which represents 60% of the catchment area and 23% of the total landslides identified. Of this 23%, 57% of the landslides are considered low confidence, compared to 22% of the LiDAR landslide dataset. Consideration should also be given to capturing the entire catchment at very high resolution, say 1 m LiDAR (or 0.5 m pixel resolution DEM), which would provide greater accuracy in the dataset, and allow for the review or removal of low confidence landslides within the zone of 30 m resolution SRTM data.
- Establish long-term monitoring of landslides and major structures that may impact mine infrastructure and operations, particularly during reservoir filling. This could be general displacement monitoring through ongoing review of ground-based LiDAR data, robotic reflector surveys or satellite-based InSAR data, which could be provided by a network of reflector/ target installation at specific high risk points. Precision Partners, CGG or TRE Altamira are some of the providers which FRL could consider. This would provide deformation measurements with an accuracy of <100 mm that could be incorporated in a geohazard monitoring system with established trigger levels alerting movement. This will be valuable for tracking landslide activation for risk management and developing an understanding of the nature of movement during construction and for LOM operations.

4 Hydrology

The hydrological study for the SPS design of the FRHEP involved developing design flood hydrographs and synthetic long-term series of reservoir inflows that are adequate for use in the embankment design, appurtenant structures and hydroelectric power yield estimates. The proposed location of the FRHEP has a catchment area of approximately 1,033 km². The mean annual precipitation is 8 m and the discharge rate is approximately 220 m³/s.

Climate and meteorological information used for the hydrological study was extracted from SRK's 'Hydrology Baseline Report'⁶⁵, and the 'Estimation of Probable Maximum Precipitation' Report from the Australian Government Bureau of Meteorology (BoM)⁶⁶. These reports provide additional detail on the climate of the site, data sources, data processing and analyses.

Previous hydrological studies were developed by SKMPS (2011) for the Frieda River Feasibility Study and by SRK¹⁸ for an embankment lower than the FRHEP and located more than 8 km upstream from the current site.

4.1 Monitoring data

4.1.1 Precipitation data

The precipitation gauges located in the FRHEP catchment are shown in Figure 4-1 and the available period of record for each gauge is summarised in Table 4-1. Data is generally available across two periods – 1995–1999 and 2008–2017.

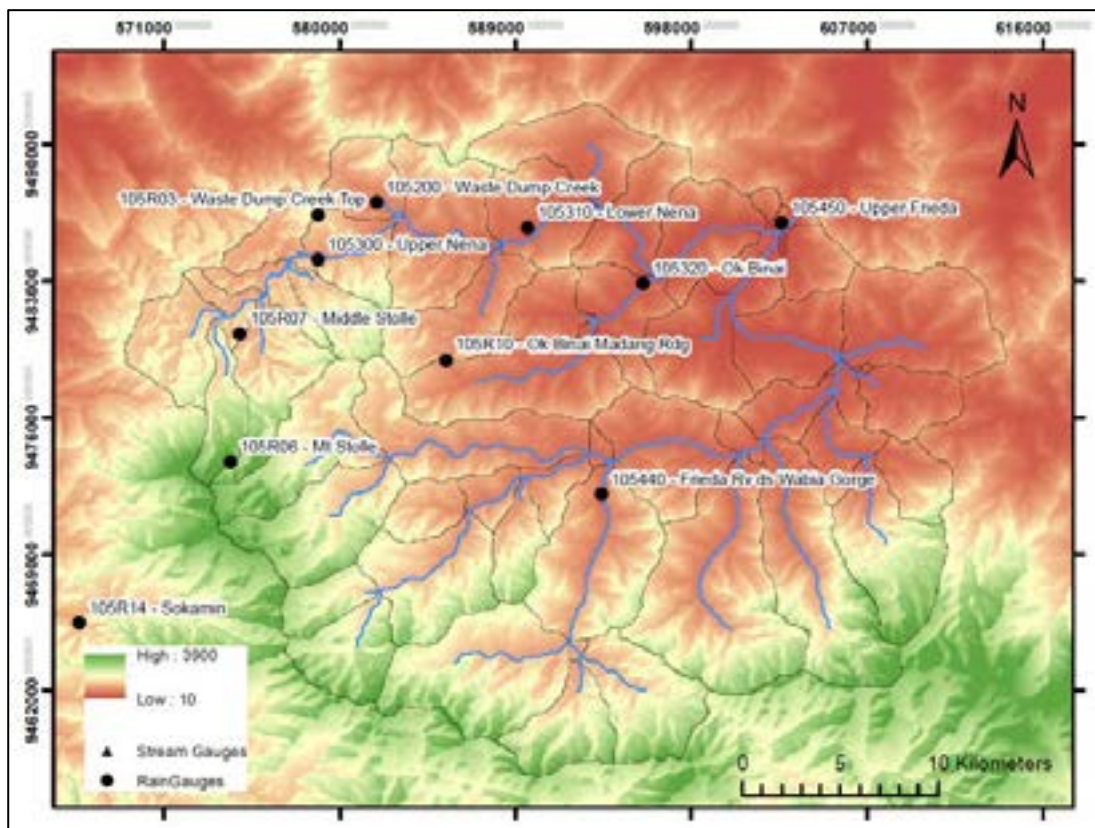


Figure 4-1: Precipitation gauge map

⁶⁵ SRK 2016, Hydrology Baseline Report.

⁶⁶ Australian Government Bureau of Meteorology 2011, Estimation of Probable Maximum Precipitation.

Table 4-1: Precipitation gauges

Station #	Location	Elevation (RL m)	Years of record
105200	Waste Dump Creek	425	12.3
105300	Upper Nena	635	11.0
105310	Lower Nena	190	13.7
105320	Ok Binai	110	11.8
105440	Frieda River downstream of Wabia Gorge	361	5.2
105450	Upper Frieda	100	11.9
105R03	Waste Dump Creek Top	1062	8.2
105R06	Mt Stolle	2240	9.3
105R07	Middle Stolle	850	9.2
105R10	Ok Binai Madang Ridge	627	8.5

4.1.2 Stream gauge data

The stream gauges located in the FRHEP catchment are shown in Figure 4-2 and the available period of record for each gauge is summarised in Table 4-2. The ‘Upper Frieda River’ stream gauge (GS105450), located close to the FRHEP site, has been monitored since 1981 (with gaps), as shown in Figure 4-3. The other stream gauges have been generally recorded across two periods – 1995–1999 and 2008–2017.

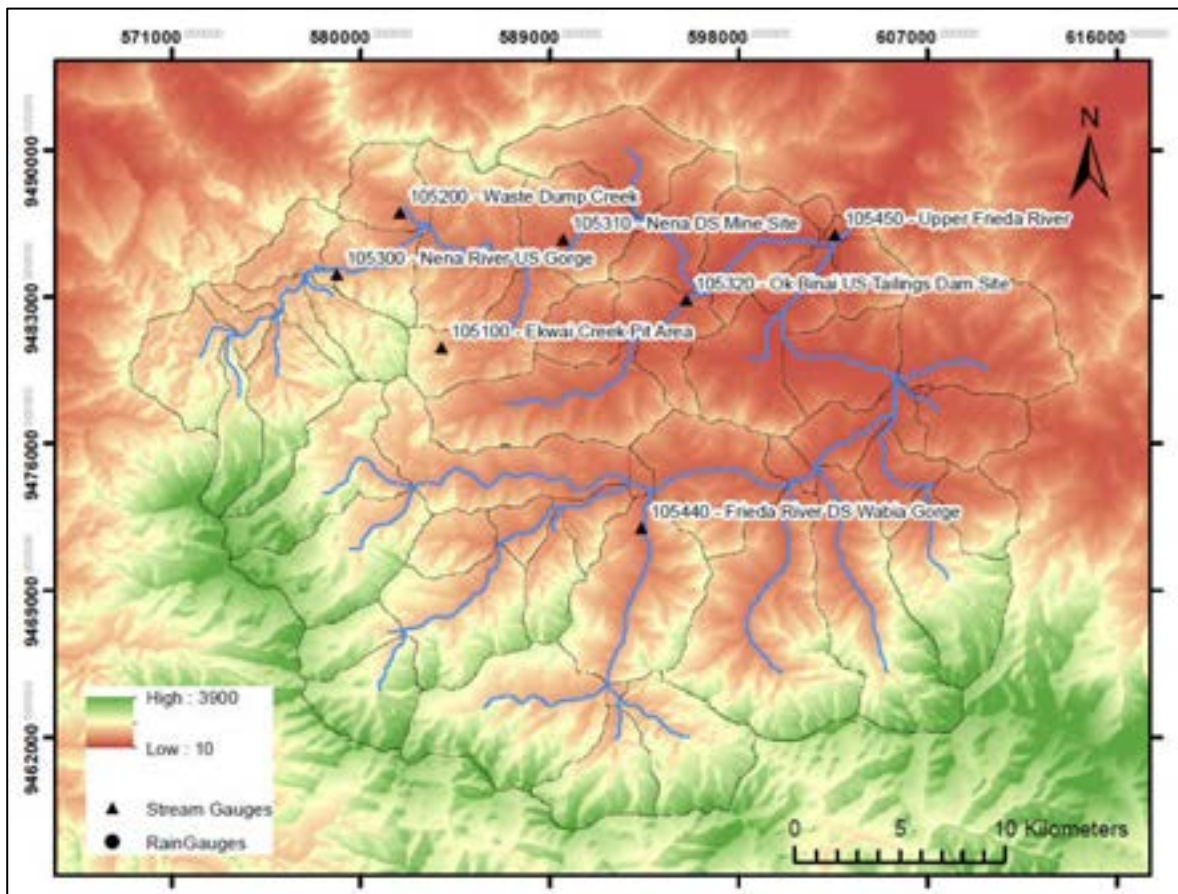


Figure 4-2: Stream gauge map

Table 4-2: Stream gauges

Station #	Location	Elevation (RL m)	Catchment area (km ²)	Years of record
105100	Ekwai Creek Pit Area	750	3	5
105200	Waste Dump Creek	425	1	14
105300	Nena River upstream of Gorge	635	97	13
105310	Nena downstream of Mine Site	190	205	12
105320	Ok Binai upstream of Embankment Site	110	69	8
105440	Frieda River downstream of Wabia Gorge	361	129	2
105450	Upper Frieda River	100	1,033	20

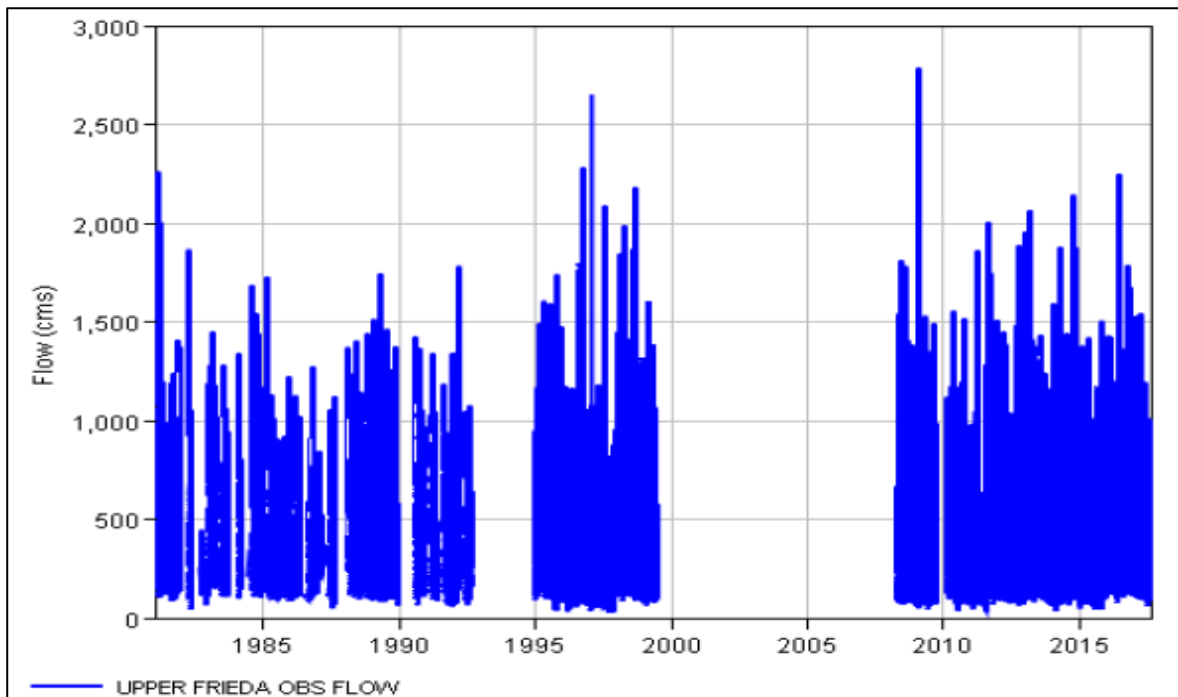


Figure 4-3: Stream gauge data from GS105450

4.2 Discharge rating review

The discharge data reported at each stream gauging station is calculated using the rating curve, i.e. relationship between water level and discharge, and water level measurements. Some level of error in the flow dataset is expected, depending on the ‘accuracy’ of the rating curve. This error is likely to be greater at higher discharge levels where the rating curve has been extrapolated.

The current rating curve for GS105450, last updated in October 2015, is based on 159 spot measurements taken since 2008. The current rating curve is shown in Figure 4-4 – the rating curve is shown in green and spot measurements are shown in orange.

Recent measurements taken with a velocity radar sensor (RQ-30) installed in January 2017 indicate that the rating curve may overestimate the low flows (approximately to the 575 m³/s discharge mark) and underestimate exponentially to the highest level recorded. A hysteresis effect is also indicated. The RQ-30 data is shown in Figure 4-4 (in blue).

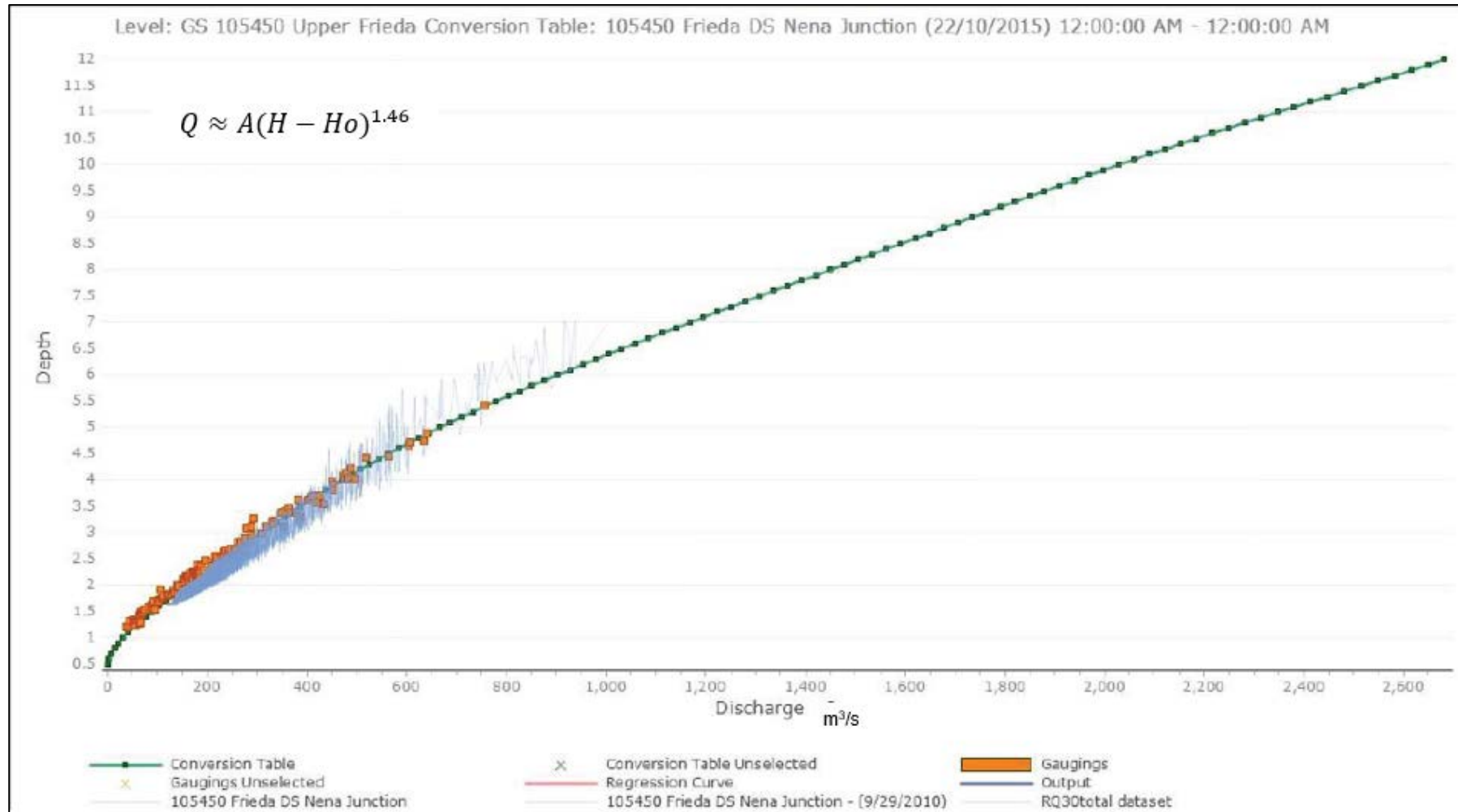


Figure 4-4: GS105450 rating curve and RQ-30 data

An Acoustic Doppler Current Profiler (ADCP) transducer was used to check the RQ-30 flow computations. The ADCP gauging indicated that the RQ-30 sensor was overestimating velocity as the river showed significant variations in velocity across the cross-section. Velocities were consistently higher on the left bank (towards the location of the RQ-30 sensor), such that the RQ-30 sensor was considered to be overestimating the average velocity resulting in higher flows being recorded.

Sentinel Pty Ltd suggested no further adjustment to the current rating curve, but recommended additional monitoring to reduce the uncertainty associated with the rating curve, particularly where data is extrapolated to higher flows.

4.3 Design flood hydrographs

4.3.1 Objectives

Design flood hydrographs were undertaken for various locations in the FRHEP catchment for use in design, i.e. spillway design and cofferdam sizing, and water quality assessments. Inflow hydrographs to the FRHEP and at various sub-catchment outlets were developed for the following flood events:

- Average recurrence interval (ARI):
 - 10 years
 - 25 years
 - 50 years
 - 100 years
 - 500 years
 - 1,000 years
 - Probable maximum precipitation (PMP).
- Duration:
 - 6 hrs
 - 12 hrs
 - 24 hrs
 - 36 hrs
 - 48 hrs
 - 72 hrs
 - 5 days
 - 10 days
 - 30 days
 - 60 days.

4.3.2 Approach

The Hydrologic Engineering Center – Hydrologic Modelling System (HEC-HMS) rainfall-runoff model was used to estimate inflows resulting from the design storm rainfall events. The HEC-HMS model provides options for simulating the different hydrological processes in a catchment based on conceptual representations of physical processes.

The model was calibrated using the recorded data from 10 large rainfall events selected from the complete record, and verified using the continuous record, i.e. all events).

To generate the design storm hydrographs, the HEC-HMS model was adjusted to account for future conditions in which the basin will be partially flooded due to the reservoir.

4.3.3 Design rainfall

Rainfall depths

The design precipitation depths (pp) for each frequency (2-year, 10-year and 100-year ARI) and duration (24 hours) for the precipitation gauges were obtained from the Hydrology Baseline Report⁶⁵ and are shown in Table 4-3. The precipitation depths were also calculated for all stations, for all durations and ARIs listed in Section 4.3.1 .

Table 4-3: Design storm precipitation depths

Station	Site Location	UTM WGS 84 Zone 54M (m)		Elevation (RL m)	pp 24 hr/ 2 year (mm)	pp 24 hr/ 10 year (mm)	pp 24 hr/ 100 year (mm)
		Easting	Northing				
105200	Waste Dump Creek	581856	9487016	425	186	206	215
105300	Upper Nena	578858	9484081	635	171	264	427
105310	Lower Nena	589619	9485727	190	192	240	307
105320	Ok Binai	595494	9482874	110	166	197	225
105440	Frieda River downstream of Wabia Gorge	593374	9472027	361	136	146	155
105450	Upper Frieda	602597	9485957	100	196	237	278
105R03	Waste Dump Creek Top	578860	9486369	1062	189	207	220
105R06	Mt Stolle	574411	9473706	2240	145	161	174
105R07	Middle Stolle	574861	9480276	850	183	200	217
105R10	Ok Binai Madang Ridge	585396	9478946	627	164	184	209

The PMP estimation report⁶⁶ provides pp estimates for the FRHEP catchment for different duration PMP events (Table 4-4). The spatial distribution of precipitation shows variability over the catchment, as discussed later in this section.

Table 4-4: PMP estimates for the FRHEP catchment

Duration (hrs)	pp (mm)
1	230
3	450
6	580
12	670
24	790
36	980
48	1130
72	1350

Storm duration patterns

The variability of the storm duration was assessed using the hourly site records. A storm was defined as the period between no precipitation and precipitation lower than 0.1 mm/hr. Higher intensity storms (i.e. intensities >90% of the complete set recorded at each station) were identified. Figure 4-5 shows

that 50% of the storms are shorter than 5 hours in duration at Waste Dump Creek and Ok Binai GS, or 2 hours in duration at the other sites. The Ok Binai GS and Waste Dump Creek stations record longer duration storms (but none exceeding 24 hours); however, almost all are less than 12 hours long.

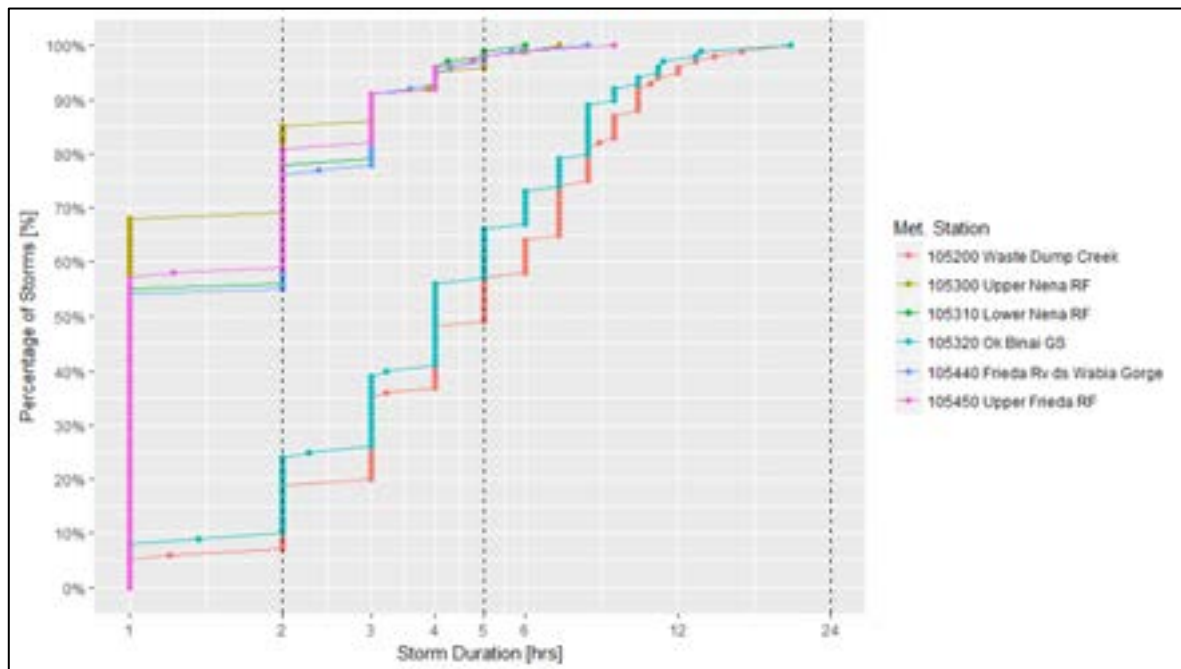


Figure 4-5: Storm duration distribution for higher intensity storms (higher 10%)

Higher total precipitation storms (i.e. total precipitation >90% of the complete set recorded at each station) were identified. Figure 4-6 shows that 50% of the storms are shorter than 12 hours at Ok Binai GS and Waste Dump Creek or 12 hours at all other sites. The Ok Binai GS and Waste Dump Creek stations record longer duration storms; however, almost all are less than 24 hours long.

This review indicates that most of the significant large storms (that have high precipitation or intensity) have a duration of less than 6 hours at Ok Binai GS and Waste Dump Creek and 12 hours at all other sites.

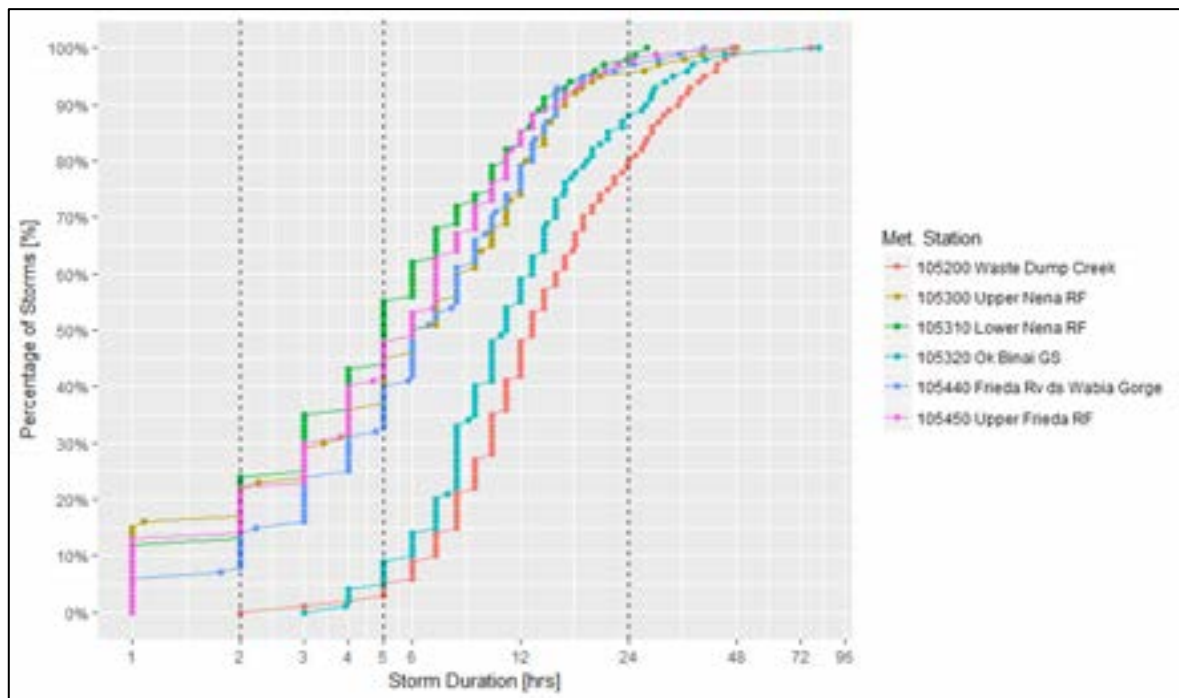


Figure 4-6: Storm duration distribution for higher precipitation storms (higher 10%)

Temporal patterns

Three different methods were used to estimate the temporal distribution of rainfall over the duration of each storm event. The first two methods (Huff method and Block method) are detailed in the Hydrology Baseline Report²⁴. The third method is detailed in the PMP estimation report (BoM⁶⁶).

- Huff: over 50,000 storm events were identified in the site monitoring data and the top 1% were analysed to determine the percentage of rainfall that falls in each percentage of storm duration.
- Block: the alternating block method assumes that peak storms of any duration incorporate all shorter duration peak storms. For example, the 10-year, 24-hour storm is assumed to incorporate the 6-minute, 12-minute, 30-minute, 1-hour, 2-hour, 3-hour, 6-hour and 12-hour events.
- BoM: the PMP estimation report⁶⁶ presents three different temporal distributions for each duration event – referred to as A, B and C in this report. These distributions were determined by averaging catchment data from selected historical storms. While these would constitute ‘design temporal distributions of PMP’ in terms of BoM, they are representative of storms observed at the site. It is therefore appropriate to use these distributions to represent the 10- to 1,000-year ARI design storms which are more likely than the more extreme PMP to behave similarly to the observed events.

Geoscience Australia’s Australian Runoff and Rainfall (ARR)⁶⁷ recommends the use of an ensemble of 10 temporal patterns representative of the catchment location and rainfall event frequency and duration for design floods up to the Probable Maximum Precipitation Flood (PMPF) (which is different to the PMF). The most critical duration should be determined and the average of the peak flows for that duration selected for use in the design⁶⁷. In the absence of the ARR-recommended temporal

⁶⁷ Ball, J, Babister, M, Nathan, R, Weeks, W, Weinmann, E, Retallick, M, Testoni, I, (Editors), 2016. Australian Rainfall and Runoff: A Guide to Flood Estimation, Commonwealth of Australia (Geoscience Australia).

patterns for the site, the BoM temporal patterns are considered most similar to the ARR approach. Long duration temporal patterns

The PMP estimation report (BoM)⁶⁶ only provides temporal patterns for short duration events. SRK therefore developed design long duration temporal patterns based on selected events having the highest average flows over the design storm duration. Temporal patterns were then determined by averaging rainfall data from the catchment for the selected events. Two temporal patterns, referred to as A (2-day event) and B (10 day-event) in this report, and one temporal pattern for the 30-day and 60-day events (C), were adopted.

Spatial distributions

The PMP estimation report (BoM)⁶⁶ provides the isohyetal analysis for the 24 hr and 48 hr storms (Table 4-5), and recommends that the February and July 2009 events be trialled for both durations and the one that gives the most critical PMF be adopted.

Table 4-5: Spatial distributions

Spatial distribution	Event	Duration (hours)
S1	Feb-2009	24
S2	Feb-2009	48
S3	Jul-2009	24
S4	Jul-2009	48

4.3.4 Rainfall-runoff model

Basin model

The FRHEP catchment was divided into 48 sub-catchments each with an average area of 21 km², as shown in Figure 4-7. ArcGIS provided the characteristics of each catchment, including slope areas, reach lengths, maximum and minimum elevations and longest paths.

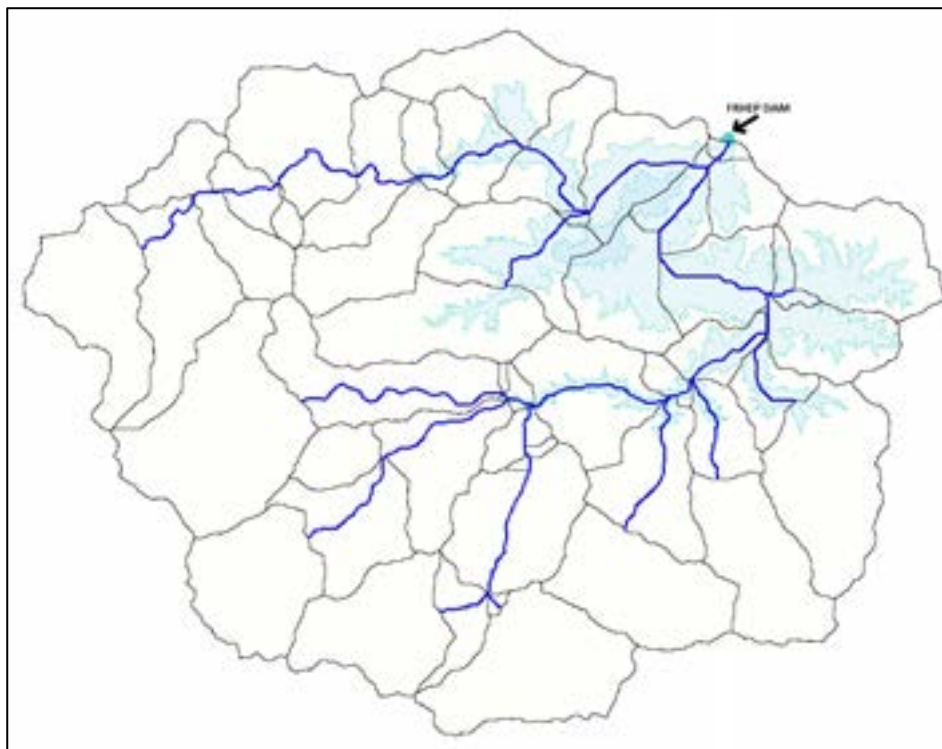


Figure 4-7: FRHEP basin model

Meteorologic model

The inverse distance weighting method was used to apply the precipitation to the catchment, as shown in Figure 4-8. The location of each precipitation gauge was used to determine the weighted precipitation to be applied to each sub-catchment. The model can switch from the use of proximal gauges to more distant gauges when there is no data for the proximal gauges.

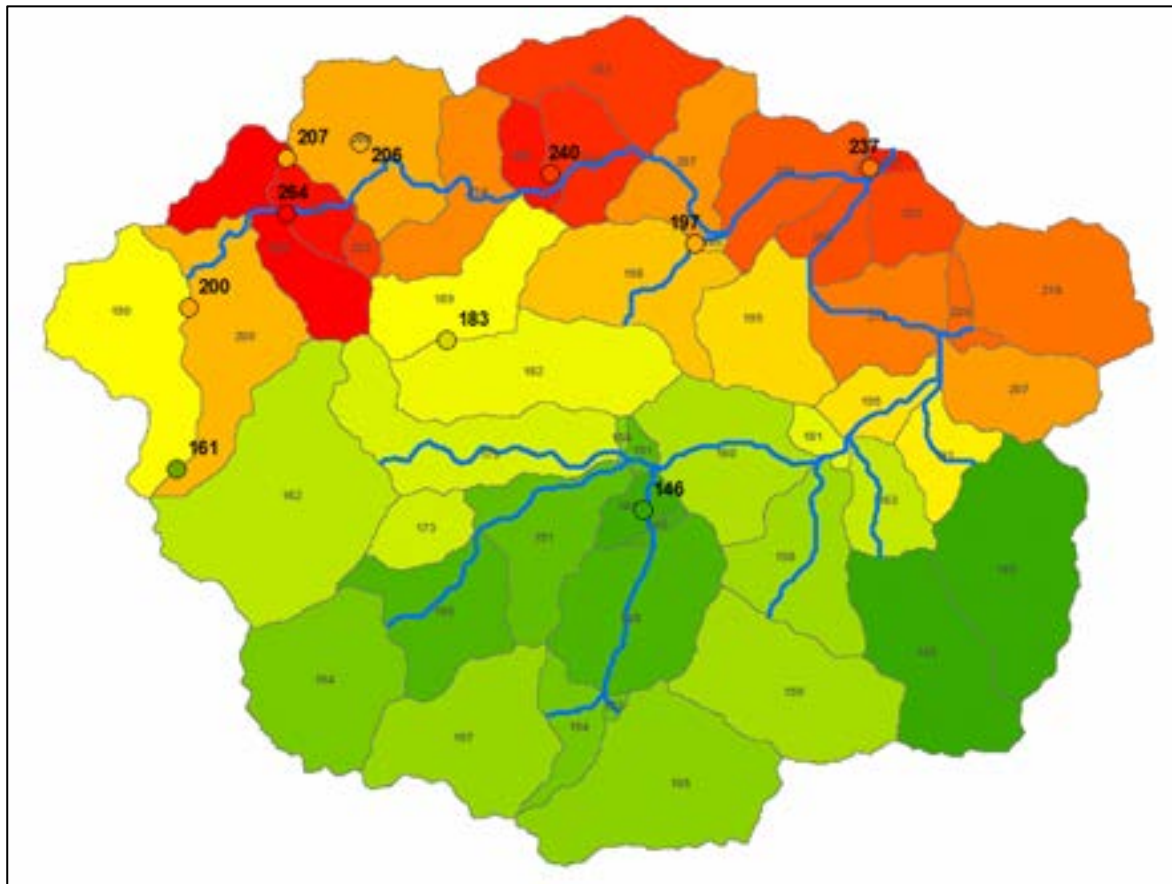


Figure 4-8: Inverse distance weighting example (values shown represent total pp in mm)

Hydrological model parameters

The following methods were used to simulate different hydrological processes in the catchment:

- Loss – soil moisture accounting
- Transform – SCS unit hydrograph with lag time estimated from catchment characteristics
- Baseflow – recession
- Routing – Muskingum-Cunge.

The calibrated model parameters are summarised in Table 4-6.

Table 4-6: Calibrated model parameters

Model component	Parameter	Value
Loss (soil moisture accounting)	Soil initial saturation	85%
	Maximum infiltration	30 mm/hr
	Percent impervious	0% (current state)
	Soil storage	200 mm
	Tension storage	75 mm
	Soil percolation	1 mm/hr
	Groundwater storage	None
Baseflow (recession)	Initial discharge	0.16 m ³ /s/km ²
	Recession constant	0.7
	Threshold flow	0.33 m ³ /s/km ²
Routing (Muskingum-Cunge)	Manning's n	0.2
	Channel width	30 m (estimated)
	Channel side slope	1V:4H (estimated)

Model calibration

To calibrate the model, SRK used the 10 largest rainfall events recorded at GS105450. The initial conditions of the catchment (initial saturation and initial discharge) were varied to achieve a good fit to the recorded data. The results of the model calibration are summarised in Table 4-7. An example hydrograph for the February 2009 event is shown in Figure 4-9 – blue line shows the modelled discharge and the black line shows the observed flows.

The model calibration results show the model is sensitive to the initial conditions assumed, where the initial saturation ranges from 47% to 90% and the initial discharge ranges from 0.12 m³/s/km² to 0.35 m³/s/km². The design therefore adopted conservative values of initial conditions – 85% initial saturation and initial discharge of 0.16 m³/s/km².

Table 4-7: Model calibration results

Parameter	Results	Event									
		1	2	3	4	5	6	7	8	9	10
		Feb-2009	Apr-2014	Sep-1996	Jun-2008	Oct-2014	Jan-2013	Jul-1997	Mar-2013	Aug-2011	Jul-2008
Initial conditions (m ³ /s/km ²)	Saturation	72%	90%	70%	50%	47%	84%	82%	75%	85%	70%
	Discharge	0.18	0.13	0.25	0.16	0.16	0.35	0.3	0.12	0.16	0.25
Peak discharge (m/s)	Observed	2,784	1,870	2,283	1,807	2,139	1,947	2,078	2,060	2,004	1,779
	Modelled	2,807	1,892	2,322	1,833	2,113	1,979	2,073	2,053	1,990	1,806
	Difference	1%	1%	2%	1%	-1%	2%	0%	0%	-1%	2%
Runoff volume (mm)	Observed	148	71	85	104	68	139	93	89	73	92
	Modelled	143	94	99	105	74	127	102	102	79	91
	Difference	-3%	33%	16%	1%	9%	-9%	10%	15%	8%	-1%

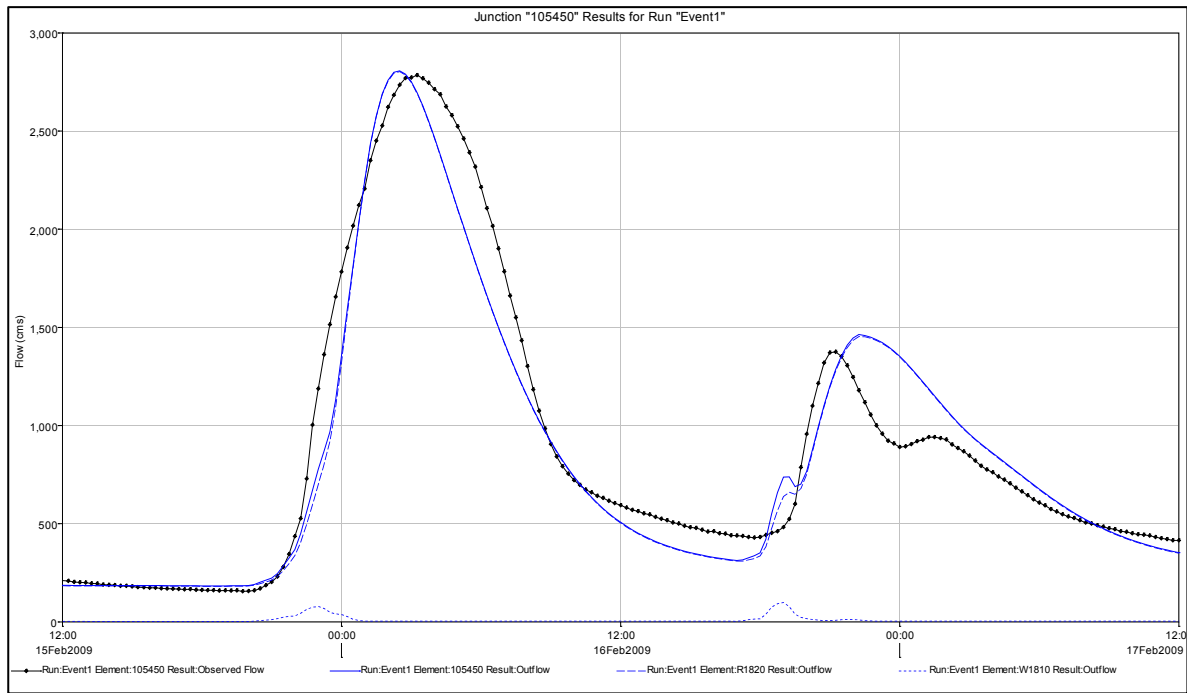


Figure 4-9: Example model calibration of observed and modelled results for Event 1 (February 2009)

4.3.5 Design flood hydrographs

Although the model was calibrated for the historical (baseline) basin condition, the purpose of this study is to estimate inflows to the future reservoir. The basin model was adjusted to reflect full reservoir conditions (13% of the catchment area to be covered by the reservoir was represented as impervious). Furthermore, the model shows design flows at the FRHEP location, which is approximately 1 km downstream from GS105450 and has a ~2 km² larger catchment.

The flood peaks from the hydrographs generated are plotted on the flood frequency curve shown in Figure 4-10, which shows that the hydrographs conservatively lie above the observed flood frequency curve. Some of the temporal distributions (i.e. block for all durations and BoM_C for the 24-hour storms) generate very large peak flows, and are likely to be over-conservative.

The 12-hour storms are typically the most critical, i.e. result in the highest peak flows. The BoM_C temporal patterns represent the median peak flows for the 6- and 24-hour storms, while the BoM_B patterns represent the median peak flows for the 12-hour storms. The hydrographs for the 12-hour storms generated using the BoM_B temporal patterns shown in Figure 4-11 are recommended for design.

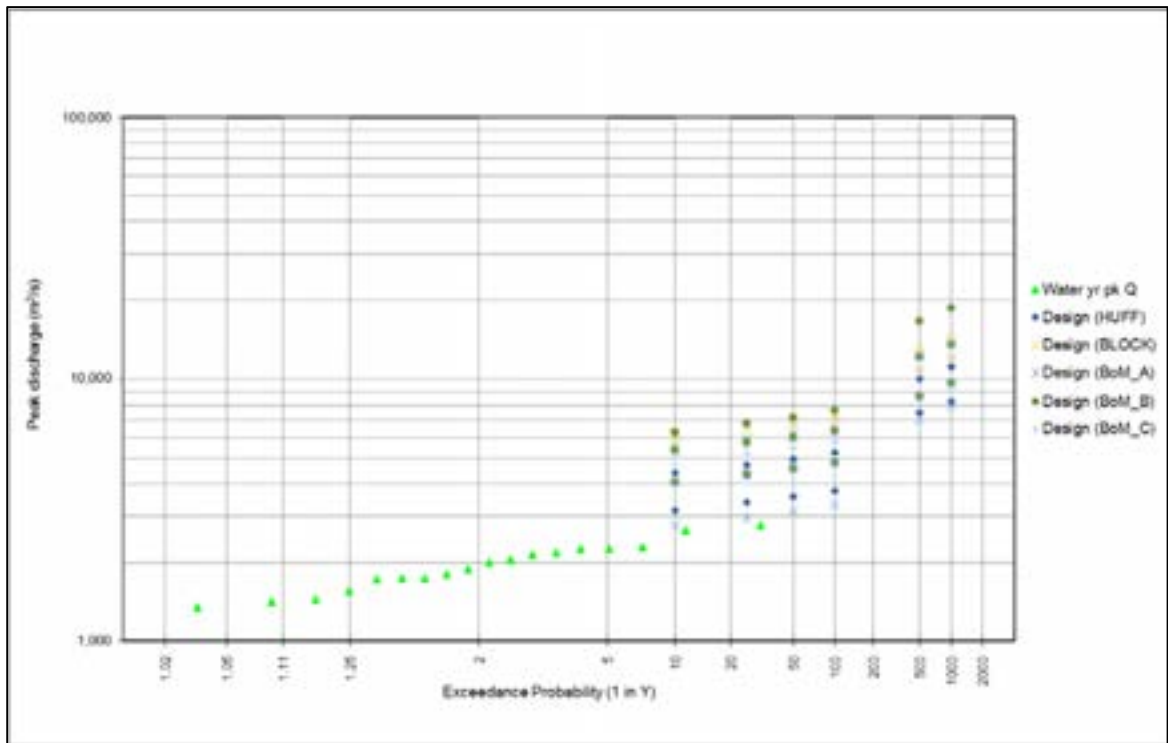


Figure 4-10: Observed versus designed flood peaks for all storm durations

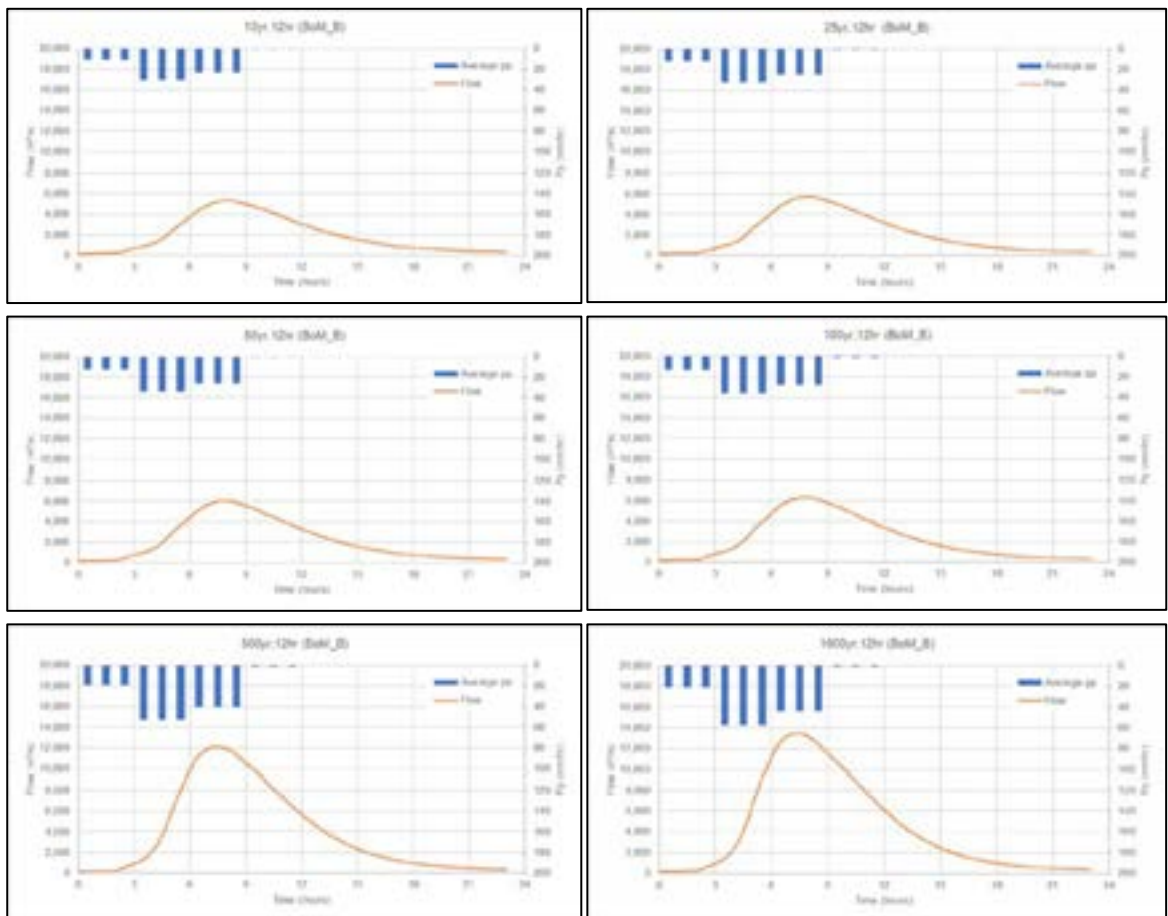


Figure 4-11: Rare to very rare design flood hydrographs

4.3.6 Probable maximum flood hydrographs

The generated probable maximum flood (PMF) hydrographs for design temporal distributions A, B and C and spatial distribution (S1, S2, S3 and S4) show all scenarios yielded similar peak flows in a range of 22,000–30,000 m³/s.

The critical scenario that yields the PMF with the largest peak – 30,000 m³/s – is the 72-hour storm with end-dominated temporal distribution (A) and S4 spatial distribution (Figure 4-12).

Figure 4-13 shows the flood peaks from the design hydrographs, including the PMF, plotted on the flood frequency curve. All the hydrographs generated conservatively lie above the observed flood frequency curve. The PMF uses an AEP of 10⁻⁶ based on ARR (2016) recommendations for a catchment area of approximately 1,000 km².

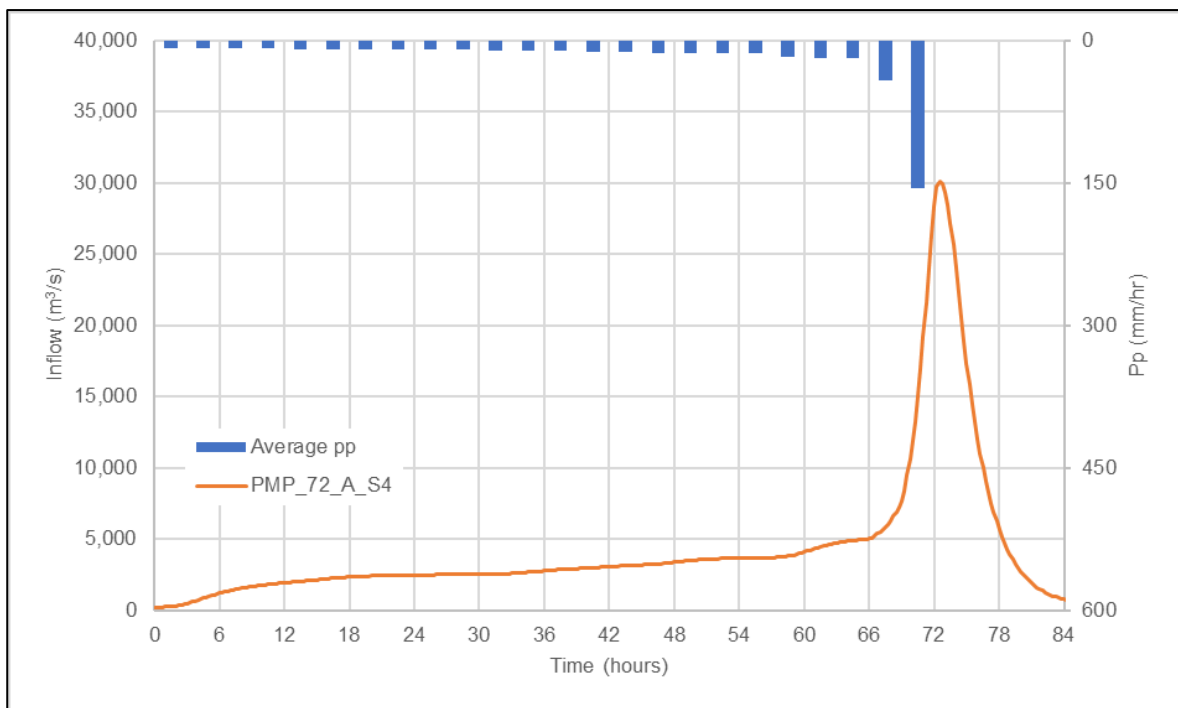


Figure 4-12: PMF hydrograph for 72-hour storm – temporal distribution pattern A and spatial distribution S4

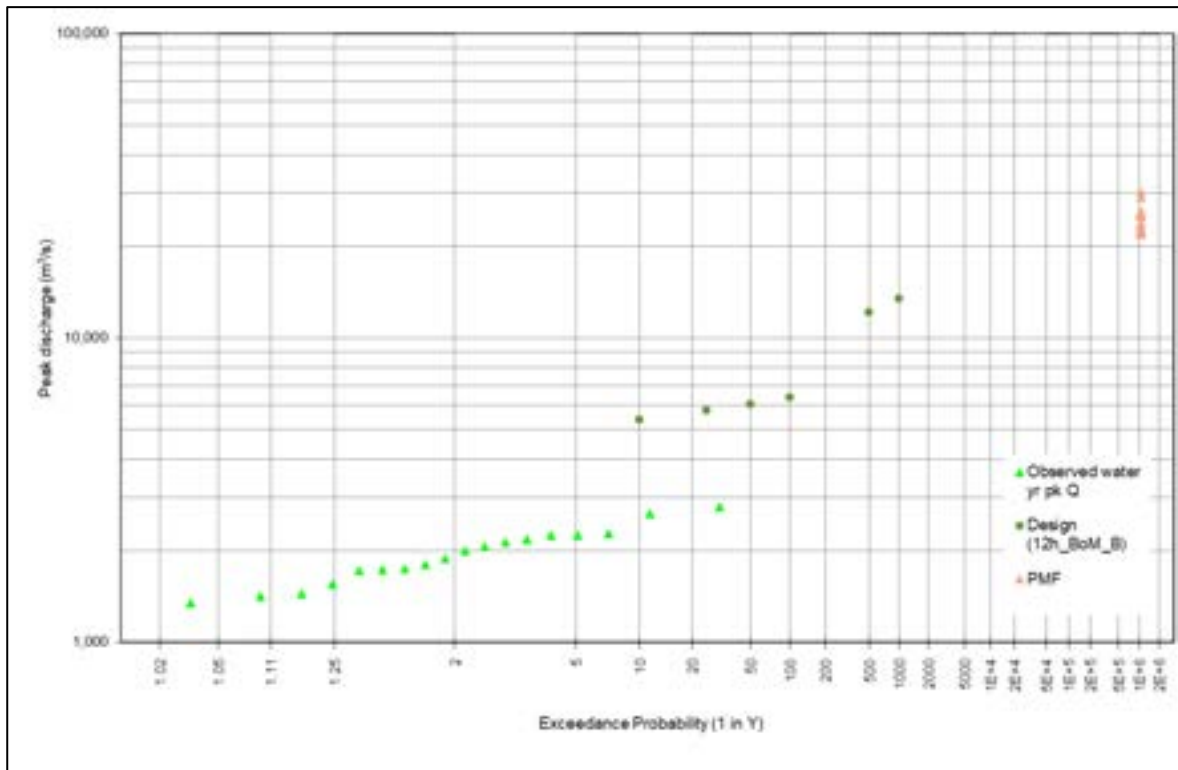


Figure 4-13: Observed versus designed flood peaks including PMF

To benchmark the PMF generated, the relationship between largest recorded floods globally and the FRHEP catchment was assessed. Figure 4-14 shows the generated PMF peak flow as an orange square and the FRHEP catchment area is shown as a blue line.

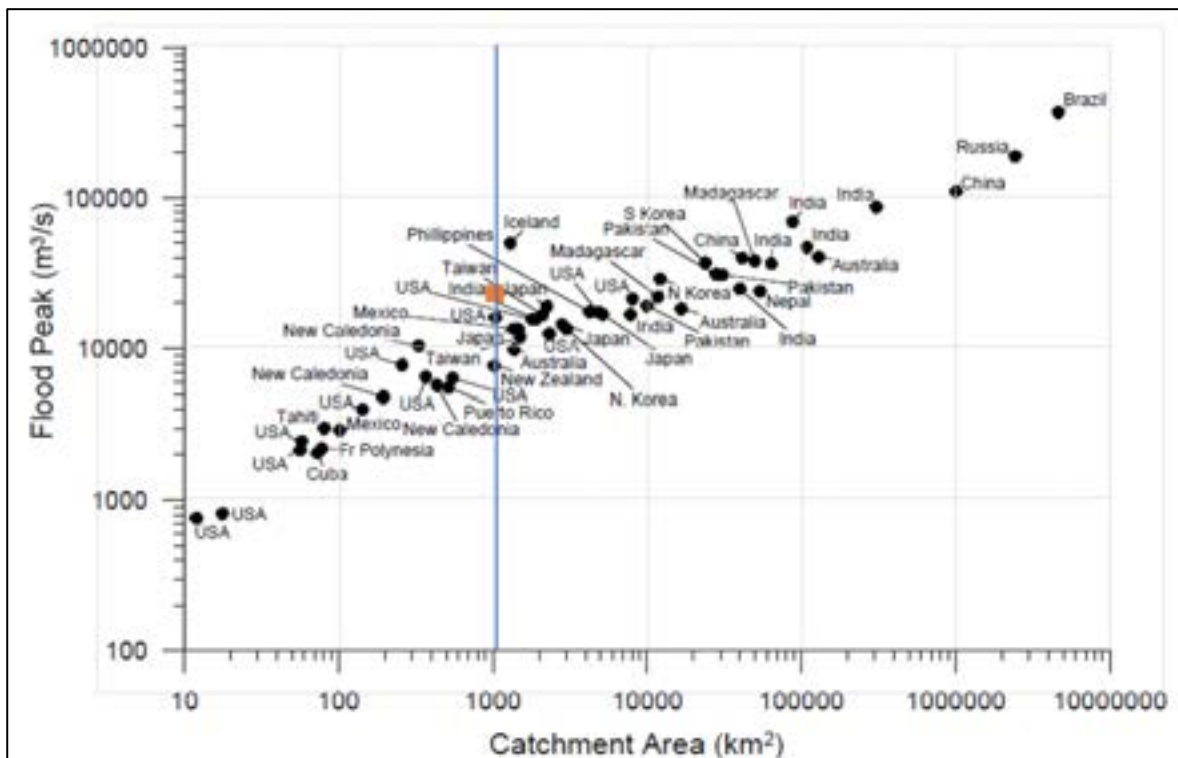


Figure 4-14: Discharge variation with catchment area for maximum floods recorded globally (ICOLD B-156)

4.3.7 Long duration flood hydrographs

The hydrographs generated for the long duration 1 in 100-year AEP storms are shown in Figure 4-15, Figure 4-16 and Figure 4-17 for two design temporal distributions (A and B) with 2, 3, 5 and 10-day inflows.

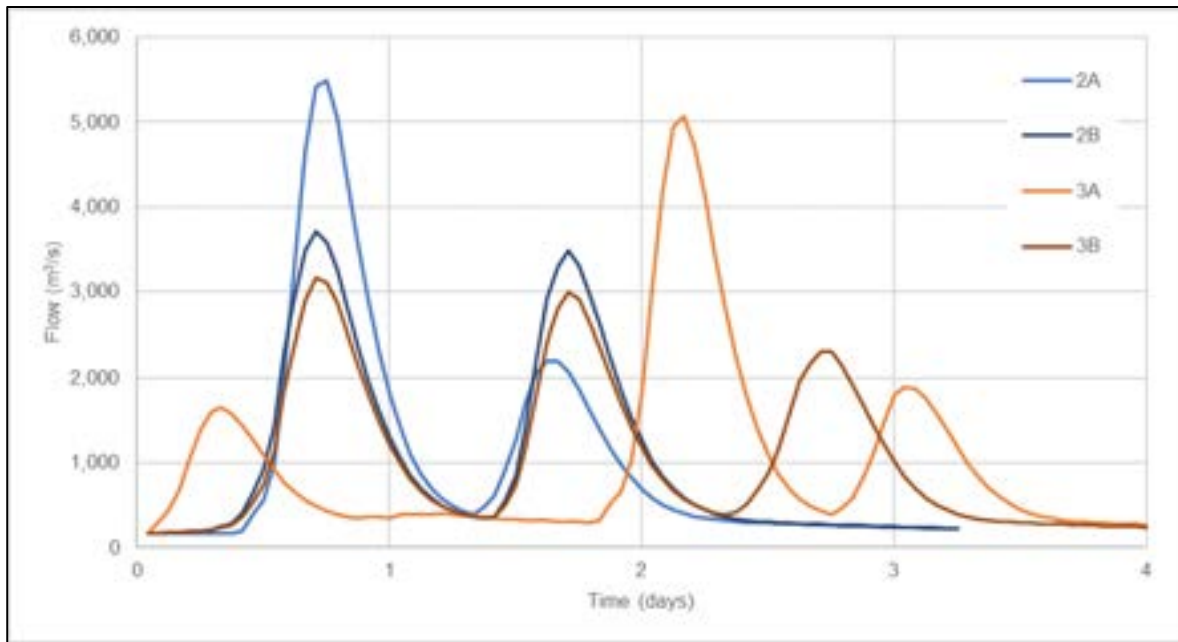


Figure 4-15: 1 in 100-year AEP, 2-day and 3-day inflow hydrographs

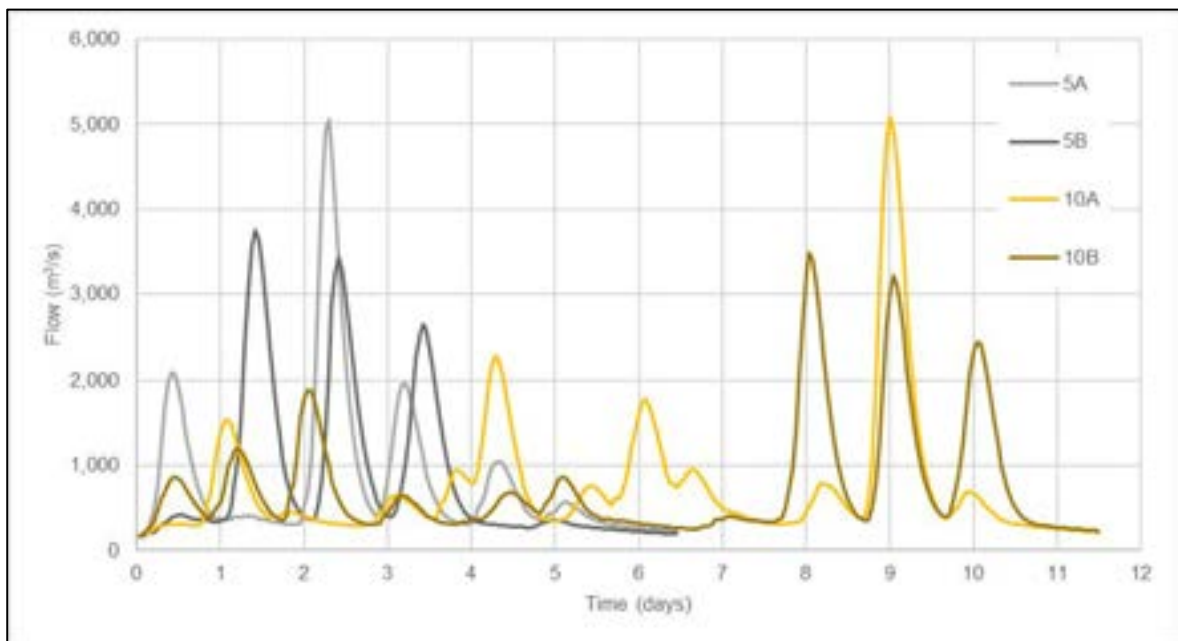


Figure 4-16: 1 in 100-year AEP, 5-day and 10-day inflow hydrographs

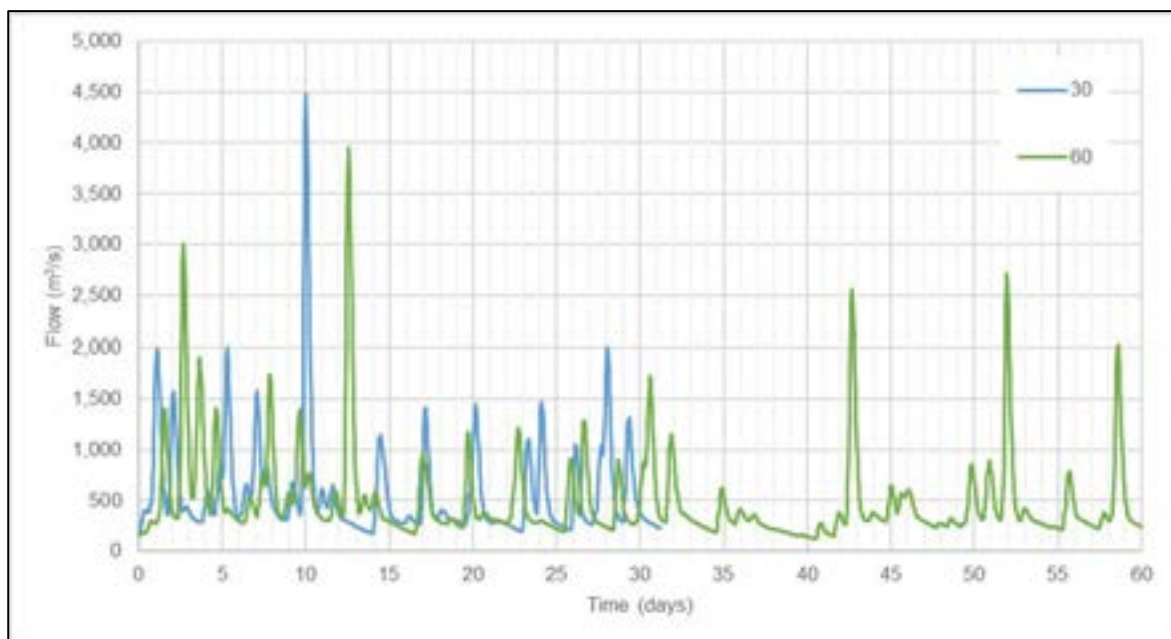


Figure 4-17: 1 in 100-year AEP, 30-day and 60-day inflow hydrographs

4.4 Generated streamflow series

4.4.1 Objectives

Several equally likely alternative realizations of 200 years of daily streamflow data at GS105450 have been generated as input to calculations of hydroelectric power yield. The use of an alternative time series allows the risk and uncertainty with respect to the yield estimates to be assessed. In contrast, a deterministic model with a single historical time series produces a single result, the uncertainty of which is difficult to assess.

4.4.2 Approach

A hidden Markov model was used to stochastically model daily streamflow data based on the historical flow gauging data, as presented in Pender et al.⁶⁸, Xu et al.⁶⁹ and Szilagyi et al.⁷⁰.

An alternative approach commonly used is to generate stochastic representations of precipitation and use a calibrated rainfall-runoff model to estimate the discharge from the catchment. This approach was not used for this study as the period of streamflow record is significantly longer than the precipitation record. The use of a rainfall-runoff model to generate flows introduces more steps and sources of potential error, i.e. generating stochastic precipitation, calibrating the rainfall model, then running the model. Furthermore, the significant spatial variation of precipitation over the catchment is not adequately represented by the existing precipitation gauges.

⁶⁸ Pender, D, Patidar, S, Pender, G and Haynes, H, 2016. Stochastic simulation of daily streamflow sequences using a hidden Markov model, *Hydrology Research* 47/1.

⁶⁹ Xu, Z, Schumann, A, Li, J, 2003. Markov cross-correlation pulse model for daily streamflow generation at multiple sites, *Advances in Water Resources* 26: 325–335.

⁷⁰ Szilagyi, J, Balint, G and Andras, C, 2006. Hybrid, Markov Chain-Based Model for Daily Streamflow Generation at Multiple Catchment Sites, *Journal of Hydrologic Engineering ASCE* - May/June 2006.

The following approach to generating the synthetic streamflow series was used:

- 1 Compile the input dataset: The GS105450 data obtained from the previous Hydrology Baseline Report⁶⁵, was 'patched' using appropriate values from other stations to complete the missing values. The dataset was also updated to include additional data received in November 2017.
- 2 Account for non-stationarity: The daily data was de-seasonalised by month, then a Box-Cox transformation was completed using a lambda (λ) value of -0.05 obtained from an optimisation process.
- 3 Apply the hidden Markov model: The use of the hidden Markov model resulted in a 200-year time series. The higher quartile of the observed data (99th and higher) was adjusted to a Pearson Type III distribution.
- 4 Account for non-stationarity: The time series was transformed back with the Box-Cox transformation ($\lambda=-0.05$) and seasonalised back.
- 5 Account for yearly variability: Observed annual flows at GS105450 were estimated – a representative average annual flow was considered when more than 10 months of data was available in a calendar year. The annual flows defined were adjusted to a log Pearson III distribution, which is one of the best fits for the available data. The lower tail of the distribution suggests minimum annual flows close to 0.6 times the mean record. It was determined that the minimum regional annual precipitation under ENSO (El Niño-Southern Oscillation) conditions was 0.6 to 0.8 times the mean annual precipitation (MAP). Figure 4-18 is a histogram showing the information measured at GS105450 in red and the log Pearson III distribution is shown in green.
- 6 Adjust yearly variability: Yearly variability was adjusted with quantile mapping using a smoothing spline between the log Pearson III distribution, and the 200-year time series raw estimations from the hidden Markov model after Box-Cox back-transformation.

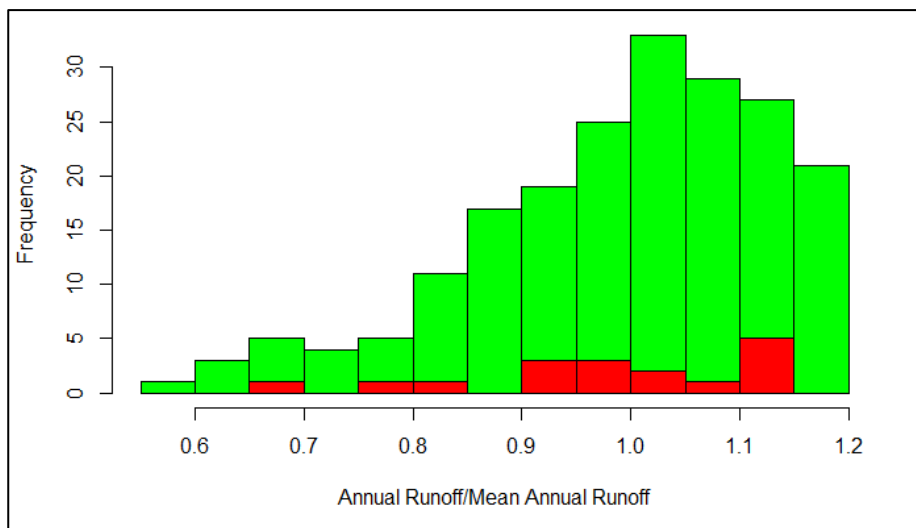


Figure 4-18: Yearly variability – annual runoff/ mean annual runoff

Note: Green bars show the log Pearson III distribution; red bars show actual information from GS105450.

4.4.3 Generated inflow series

Two full record synthetic series were generated using a similar methodology: 50 scenarios of 200 years and 200 scenarios of 38 years. Only the 50 scenarios of 200 years of daily flows has been described below due to the mathematical similarities between the two time series. only one will be described (50 scenarios of 200 years of daily flows). The 200 scenarios of 38 years was subsequently used for hydroelectric power yield estimates

Figure 4-19 shows a comparison of the results – the scenarios are compiled in groups of 10, black lines highlight the maximum, mean and minimum annual flow based on GS105450, and the minimum regional annual flow is shown as a dotted line. All scenarios show wider variability than the actual records, and the minimum annual flows are close to the minimum regional annual flow of 0.6 times the mean recorded.

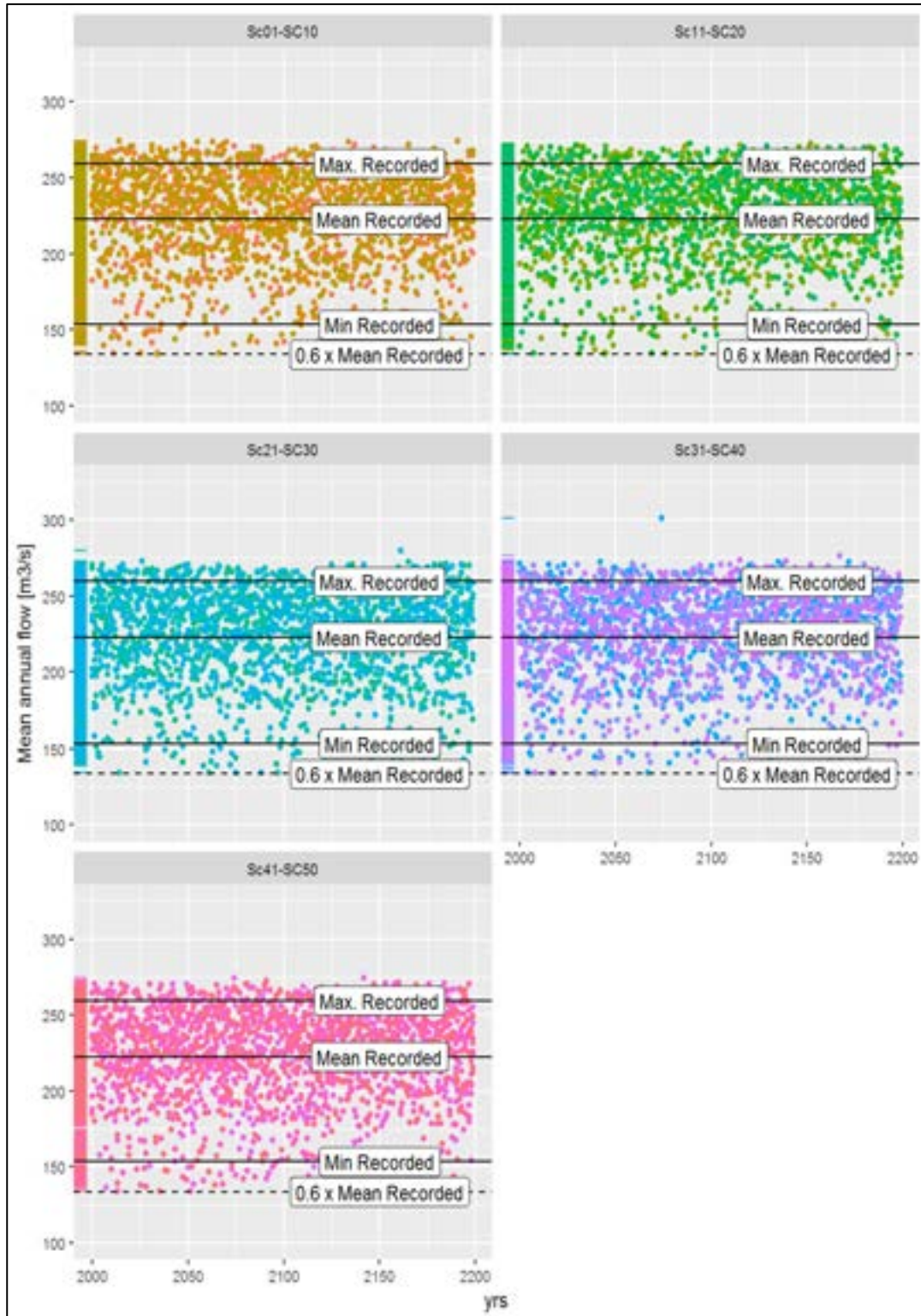


Figure 4-19: Projected mean annual flow for 50 scenarios

Note: Each graph presents 10 scenarios. Maximum, mean and minimum flows recorded at GS105450 is shown as a black line. The dotted line represents 0.6 times the mean flow recorded, which is considered the minimum based on regional flow analysis.

Figure 4-20 and Figure 4-21 are quantile-quantile plots (Q-Q plots) for different durations from 1 day to 365 days, showing a comparison of the recorded flows on the Y-axis and the modelled flows on the X-axis. Figure 4-20 shows the first 20 years of information, which is similar to the actual 16 years of records available at GS105450. While the graph shows there is significant variability, the values tend to lie around the red line, which corresponds to the Y=X line, and these overall values consequently tend to be around the actual measured flow records. Figure 4-21 shows the data in Figure 4-20 extended to 200 years of modelled flows. In this case, there is less variability and the values tend to follow the red line.

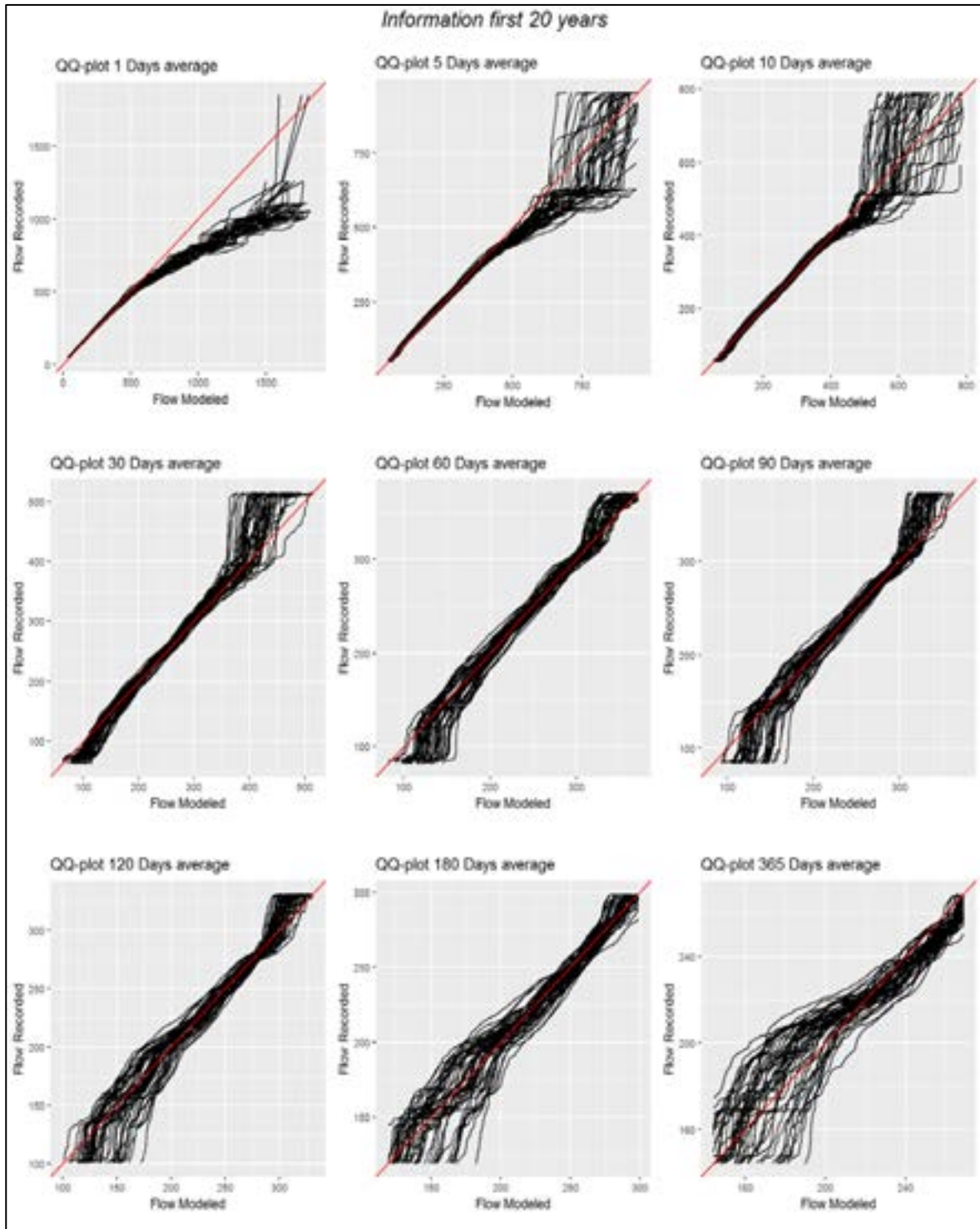


Figure 4-20: Comparison of observed versus simulated average flow for different durations for the 50 scenarios and the first 20 years of information

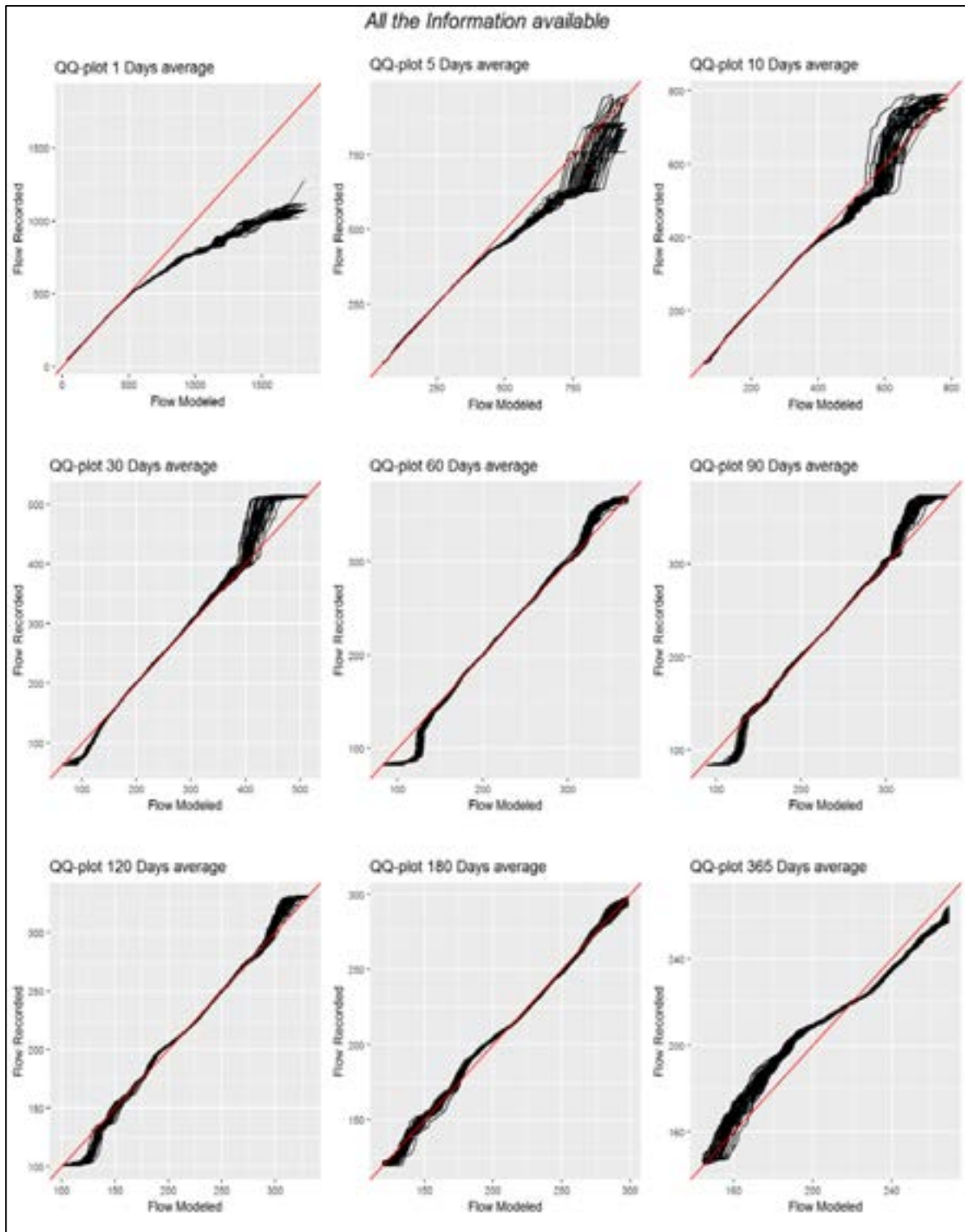


Figure 4-21: Comparison of observed versus simulated average flow for different durations for the 50 scenarios and 200 years of information

Flow duration curves comparing the observed and simulated flow series are shown in Figure 4-22 and Figure 4-23 (mean daily flows), on log and normal scales, respectively. All simulations tend to be described by similar curves with scenario lines superimposed. Flow values between exceedances of 5% and 70% are well represented by all scenarios; the extreme values in the higher and lower range, are extended beyond actual measurements.

The results indicate that the model is an adequate reproduction of the statistical parameters of the historical record, and the generated time series are therefore fit to use in reservoir design and analysis.

While the generated time series are considered appropriate for power generation design, they should be considered a stochastic tool to understand variability; it is recommended they be used in parallel with actual historical measurements. Additional baseline information should be used to refine and improve the understanding of daily/ monthly and annual variability. Therefore, additional flow records should improve the assumptions and time series presented.

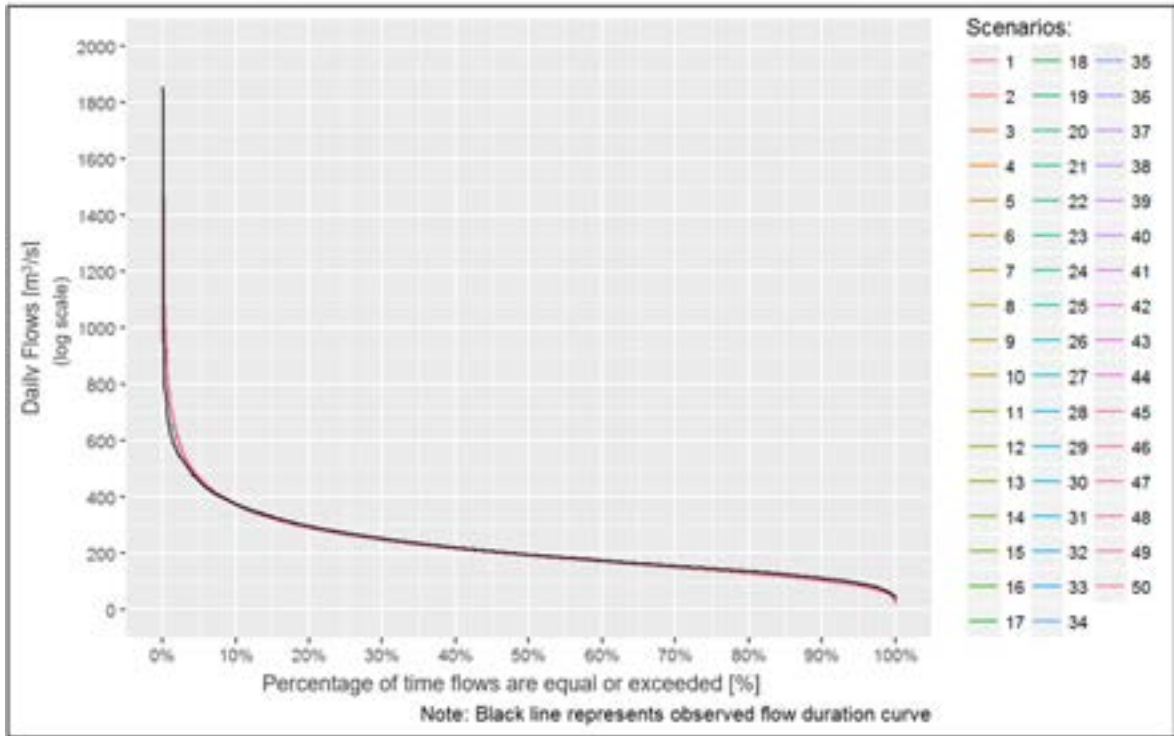


Figure 4-22: Flow duration curve – mean daily flow (log scale)

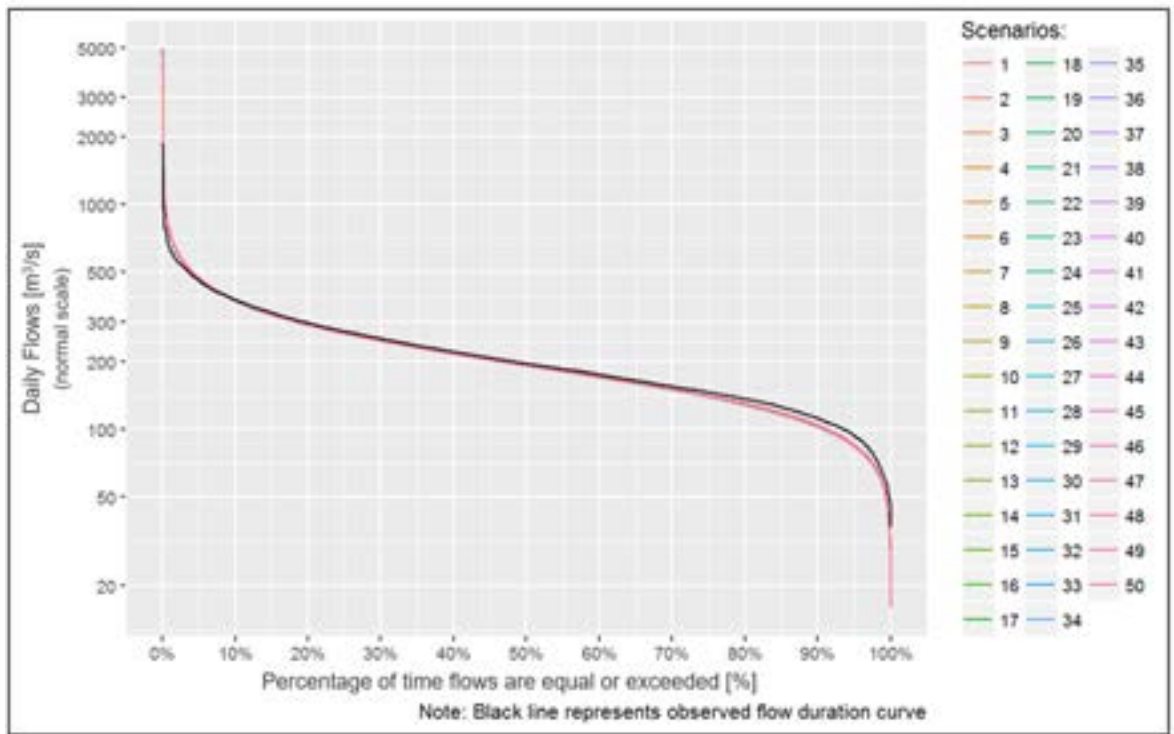


Figure 4-23: Flow duration curve – mean daily flow (normal scale)

4.4.4 Hydrology for hydropower generation

A hydrology study was undertaken between 2011 and 2016 for the SPS (Section 4). The hydrological assessments used to support the design for hydroelectric power generation have used the earlier dataset derived for the previous study phase due to its availability, but with additional data included to the end of 2016.

The following section provides a brief overview of the hydrology data utilised for hydroelectric power design.

Monitoring stations

The gauging stations used in the SKMPS analysis included the following:

- 2 temperature stations
- 4 evaporation stations
- 8 precipitation stations (4 within the Frieda River catchment)
- 14 flow gauging stations (5 within the Frieda River catchment).

Table 4-8 and Figure 4-24 provide details of the five monitoring stations within the Frieda River catchment only.

Table 4-8: Monitoring stations in the FRHEP catchment

Station	Location	UTM coordinates		Elevation (RL m)	Catchment (km ²)
		Easting	Northing		
105200	Waste Dump Creek	581856	9487016	425	N/A
105320	Ok Binai	595494	9482874	110	N/A
105300	Upper Nena	578858	9484081	635	97
105310	Lower Nena	589619	9485727	190	205
105450	Upper Frieda	602597	9485957	100	1,033



Figure 4-24: Locations of Frieda River gauging stations

Precipitation

The rainfall data collected between the periods 1995–1999 and 2008–2010 are reflected as a monthly rainfall distribution (Figure 4-25).

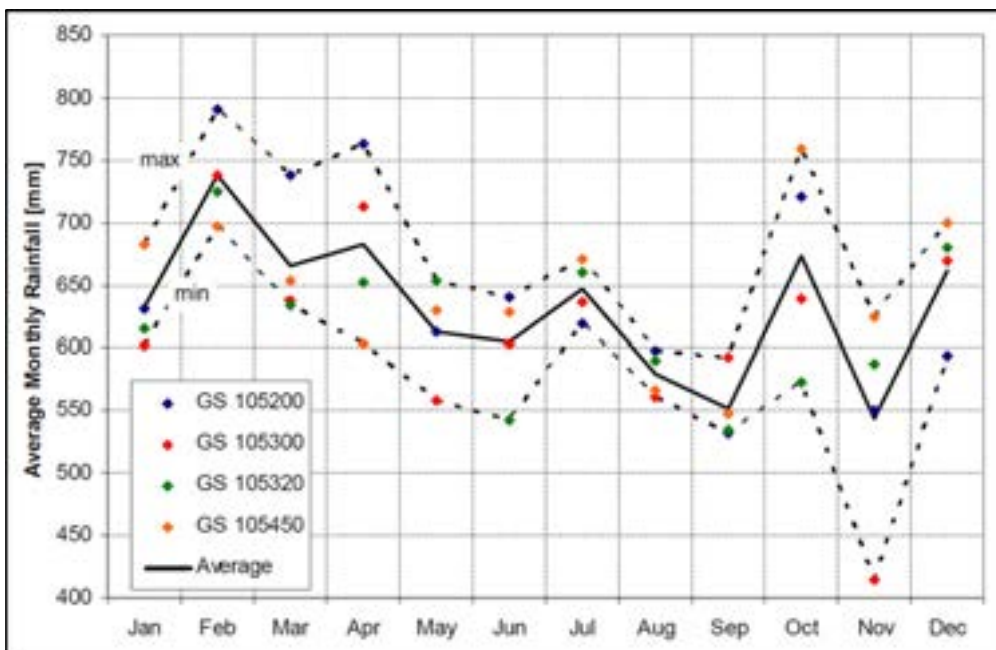


Figure 4-25: Monthly rainfall distribution in the catchment area

Source: Frieda River Feasibility Study, 2011.

The PMP estimates for the Frieda River basin listed in Table 4-9 were used in the embankment height optimisation. The total precipitation is unchanged from SKMPS study for 48-hour duration events and below. However, the peak inflows and hydrographs have changed. At this time, hydrographs are not available for durations longer than the 72-hour PMF events.

Table 4-9: PMP estimates for the Frieda River basin

	12 hours	24 hours	36 hours	48 hours	72 hours
BoM PMP (mm)	670	790	980	1130	1,386
Peak inflow (m ³ /s)	26,958	27,052	27,420	27,416	30,081

The key features of the Frieda River catchment are summarised in Table 4-10.

Table 4-10: Catchment hydrology of Frieda Basin

Mean annual discharge	Catchment area	Total precipitation	PMF
223 m ³ /s	1,033 km ²	7,600 mm/year	30,081 m ³ /s

Source: Frieda River Feasibility Study, 2011

4.5 Tailwater rating curves

4.5.1 Objectives

Tailwater rating curves were developed for four locations near the FRHEP embankment for use in design, i.e. powerhouse design and cofferdam sizing (Figure 4-26).

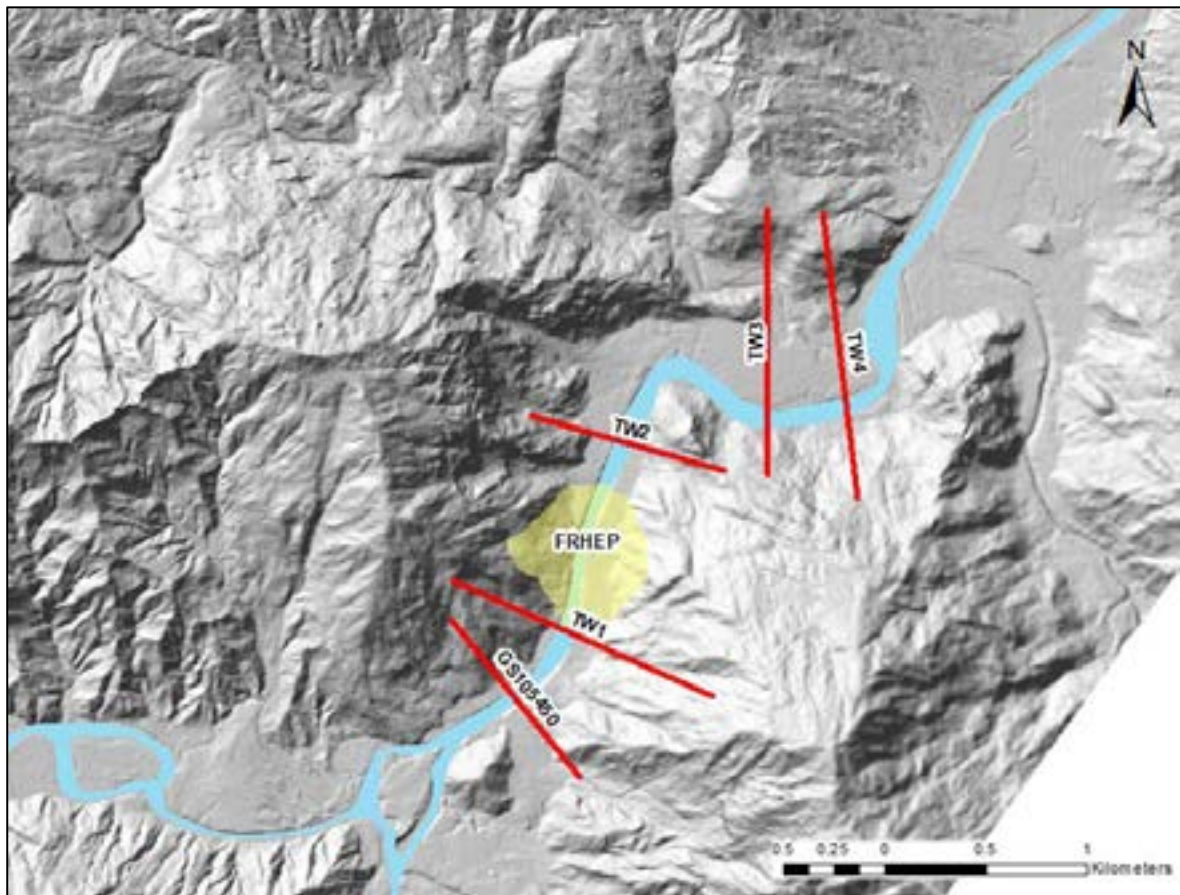


Figure 4-26: Locations of tailwater rating curves

4.5.2 Approach

The tailwater rating curves were developed using a two-dimensional HEC-RAS v5.0.3 hydraulic model based on the available LiDAR topographical survey. .

The HEC-RAS model was developed using the following assumptions and inputs:

- A Manning's 'n' roughness value of 0.04 was used for the channel of the river and the surrounding floodplain.
- The downstream boundary was modelled as a normal depth boundary condition, with a friction slope angle of 0.13% (the approximate average slope angle of the river channel). The model was extended approximately 5.5 km downstream of the embankment, such that the downstream boundary condition had minimal impact on the water surface profiles and rating curves.
- The upstream boundary was modelled as a stage hydrograph with varying inflow rates.
- The model mesh was developed with a spacing of approximately 30 m (Figure 4-27). Break lines were placed at each of the tailwater curve locations and along the banks of the main river channel.
- The model was run with a 1 minute timestep, which provided numerically stable and accurate solutions for the mesh size and the maximum velocities modelled.
- An initial condition ramp-up time of 48 hours was used to ramp up the surface from dry to wet initial conditions.

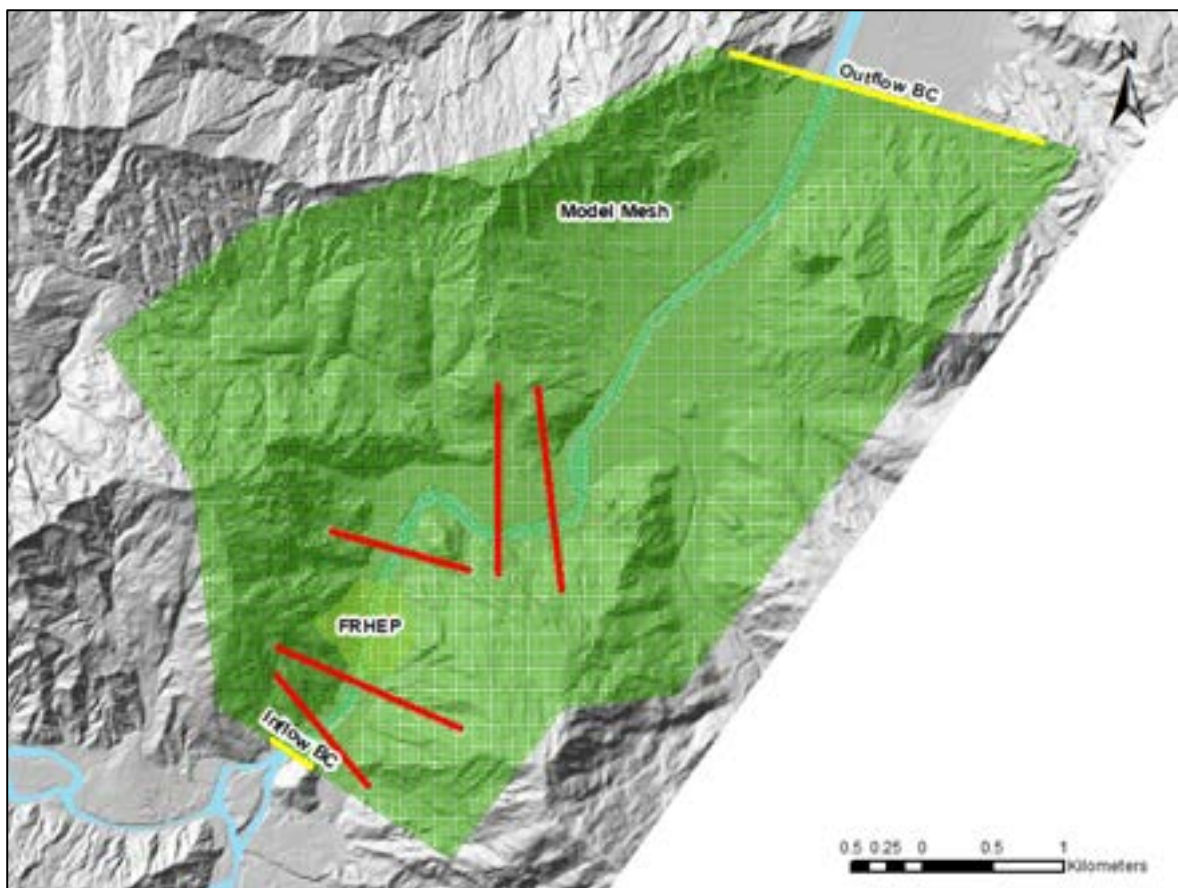


Figure 4-27: Model mesh and boundary conditions

4.5.3 Calibration

The HEC-RAS model was calibrated using the GS105450 tailwater rating curve. The modelled depths were reduced by 1.5 m to account for the difference in depth between the base of the river channel and the LiDAR survey.

The results of the model calibration shown in Figure 4-28 indicate that the model calibrates relatively well in the middle range; however, underpredicts the depth in the upper ranges of flow. Discrepancies in the upper flow range are possibly due to errors in the topography, the adjustment for the bathymetry and/ or the extrapolation of the GS105450 tailwater rating curve (the maximum flow measured to date is 1,000 m³/s). The accuracy of the model calibration and resulting tailwater rating curves could be improved by undertaking a bathymetric survey of the Frieda River around the proposed embankment, cofferdam, tunnel inlets and outlets and spillway discharge outlet.

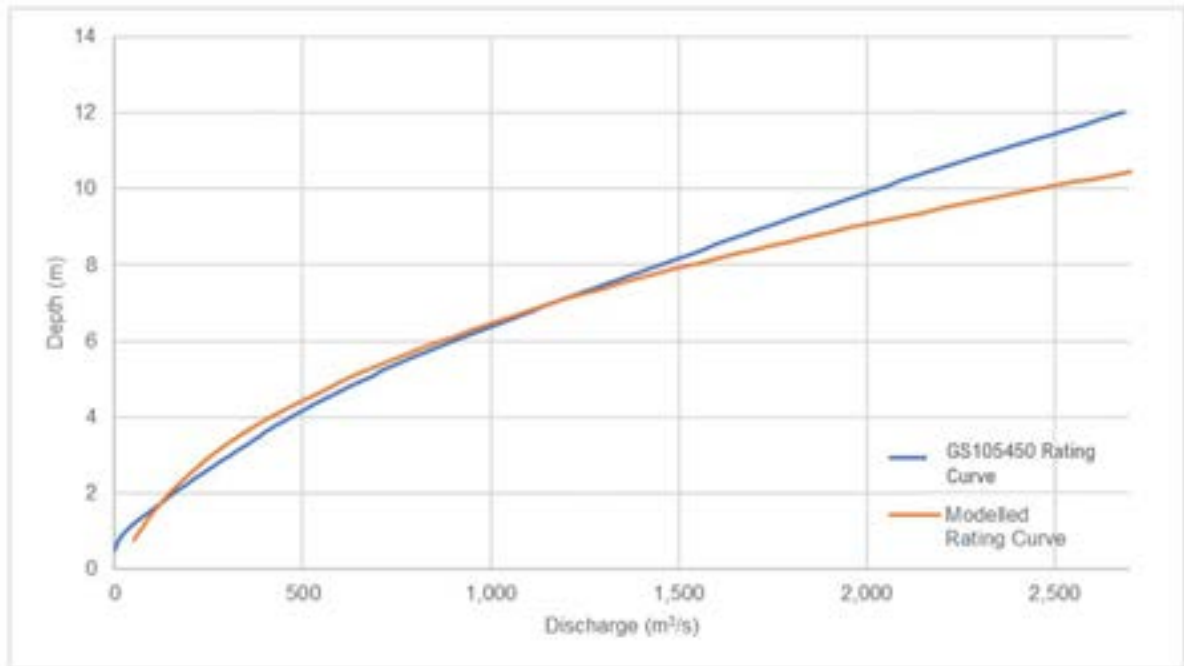


Figure 4-28: Model calibration compares to tailwater rating curve at GS105450 (blue line)

4.5.4 Results

The modelled tailwater rating curves are presented in Figure 4-29 and Table 4-11.

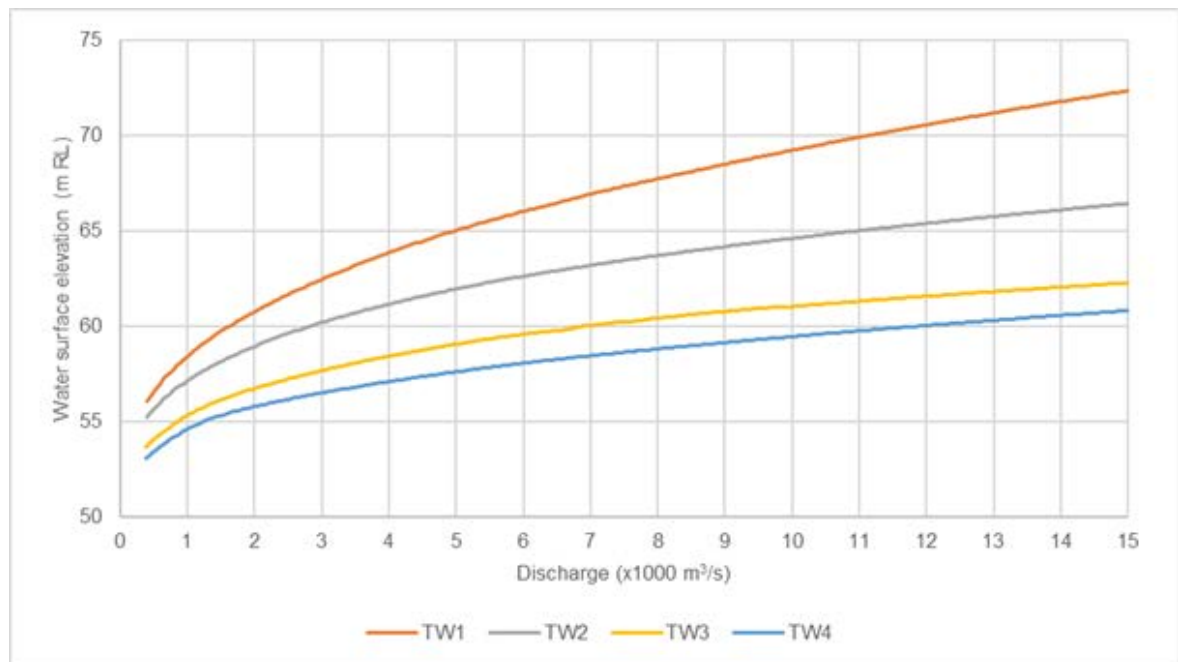
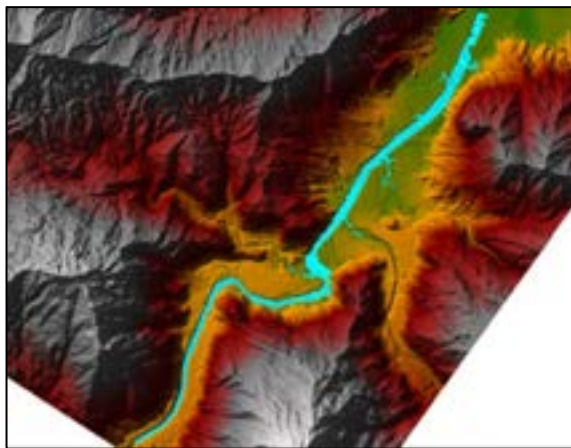


Figure 4-29: Tailwater rating curves

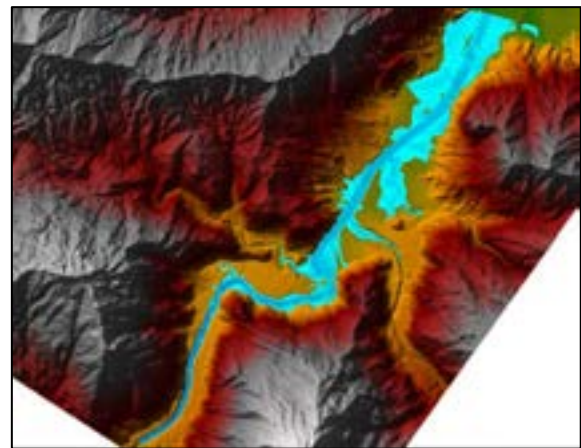
Table 4-11: Tailwater rating curve table

Flow (m ³ /s)	Water surface elevation (RL m)			
	TW1	TW2	TW3	TW4
400	56.1	55.3	53.7	53.1
600	57.0	56.0	54.4	53.7
800	57.8	56.6	54.9	54.2
1,000	58.4	57.1	55.3	54.6
2,000	60.8	59.0	56.7	55.8
4,000	63.9	61.2	58.4	57.1
6,000	66.0	62.6	59.6	58.1
8,000	67.7	63.7	60.4	58.8
10,000	69.2	64.6	61.0	59.5
12,000	70.6	65.4	61.6	60.0
14,000	71.8	66.1	62.0	60.6
15,000	72.3	66.4	62.3	60.8

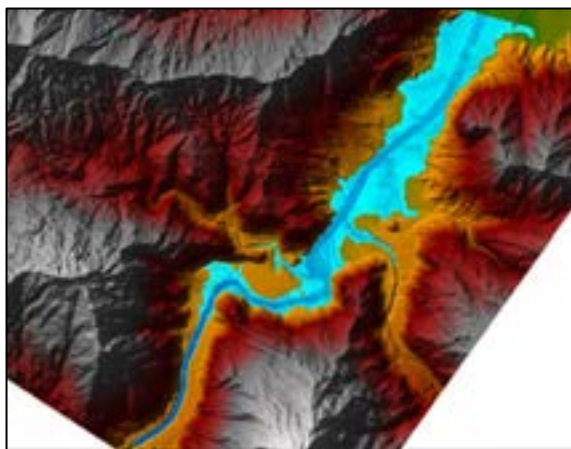
Graphical outputs of the model at various levels of discharge are shown in Figure 4-30. The tailwater rating curves have not been adjusted due to the lack of recent bathymetric survey data. As a result, the water surface elevation for all levels of discharge will be overestimated, which is considered conservative in most scenarios. It may be prudent to subtract the flow in the river channel beneath the LiDAR survey (estimated to be in the range of 200–300 m³/s) from the design level of discharge, before applying the tailwater rating curve to adjust for the lack of inclusion of a bathymetric survey. However, this is likely to have minimal impact, particularly in the middle to upper discharge ranges.



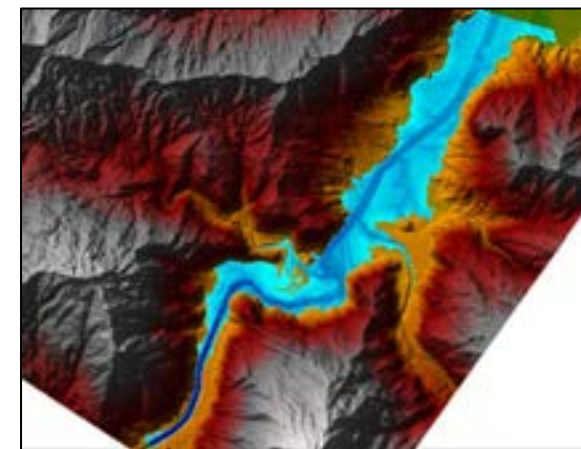
50 m³/s discharge



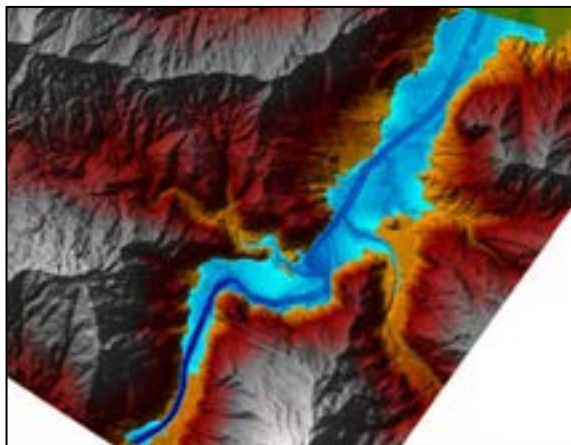
1,000 m³/s discharge



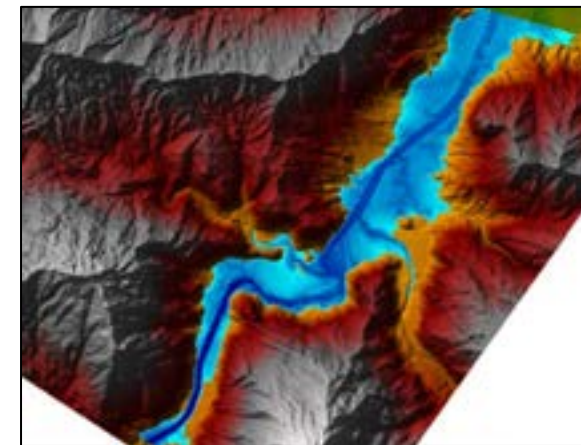
2,000 m³/s discharge



5,000 m³/s discharge



10,000 m³/s discharge



15,000 m³/s discharge

Figure 4-30: HEC-RAS model results

5 Power Demand

The FRHEP must be able to supply sufficient power to meet the FRCGP’s power demand, taking the range of scenarios for power demand and the required reliability standards into account.

5.1 Power supply reliability standards

5.1.1 FRCGP reliability criteria

FRL has set the following reliability targets:

- 1 day’s lost power per annum = 99.73%
- Loss of Load Expectation (LOLE) = 0.27%
- Expected Unserved Energy (EUE) = 0.27%.

Because of the very high reliability targets, the FRHEP will require to have one turbine unit as a spare and one turbine unit as a spinning reserve.

The 99.73% reliability target applies to the FRHEP’s total energy demand and includes allowance for shutdowns.

5.1.2 Export grid reliability criteria

The export grid has set reliability targets for the power generation system as a whole, not for the individual plant. The key points are:

- Loss of Load Expectation (LOLE) <2 days per year
- Expected Unserved Energy (EUE) <0.5%
- Reserve Capacity (N-2) must be available to operate at any time

These targets are close to those typically used in developed countries world targets. It may be difficult to achieve the N-2 reserve capacity requirement if large units are used.

Allowable departures from export grid’s LOLE Targets are listed in Table 5-1.

Table 5-1: Export grid Loss of Load Expectation - allowable departures

Case	Number of days per year	Percentage outage
Target LOLE	2	0.55%
Departure - 1 year	4	1.10%
Departure - 2 consecutive years	3	0.82%
Other cases	2.5	0.68%

5.1.3 Summary of reliability targets

Based on the reliability requirements, the combined generating plant and water supply reliability targets for the FRHEP are:

- FRCGP reliability target = 99.73%
- Export power to export grid = 99.5% (strictly this applies to planned generation at short term notice of 24–48 hours).

5.2 Maximum electrical loads

FRL provided two electrical demand profiles for the FRCGP:

- Electrical loads for the FRCGP were provided in January 2018. These loads have been applied in the analysis of the measured flow series and the synthetic flow series.
- A final set of loads was provided on 31 May 2018. However, the use of these loads has been limited to the measured flow series and no work has been carried out using these loads for the synthetic flow series.

5.2.1 Electrical loads provided by FRL in January 2018

During peak production, the FRCGP demand is approximately 1,004 GWh/a, increases to 1,834 GWh/a in Year 11 and then stabilises at 1,781 GWh/a in the later years. Details of the power demand in Years 1–33 are set out in Table 5-2 and Table 5-3.

The FRHEP must also be able to provide power to the remote export grid. This potential has been assessed taking the following into account:

- The maximum generation potential of the FRHEP with an embankment crest height of RL 238.5 m: This requires the maximum operating level and minimum operating level to be optimised and the generating plant configuration and efficiency variation with flow and head must also be accounted for. The maximum energy supply is estimated to be 2,790 GWh/a, based on the measured data.
- The freeboard required for PMF events and tsunami events caused by landslides.
- The FRCGP power demand provided by FRL: This is assumed to be provided at 100% reliability across the 16 years of measured data used in the energy simulations.
- The amount of energy available to the export grid is the difference between the total energy production potential of the scheme and the FRCGP demand, taking the required efficiency of supply to the export grid into account.

These are referred to as the January electrical loads in this report.

Table 5-2: (a) Power demand scenario Years 1–17: January electrical loads

Year	1	2	3	4	5	6	7	8	9	10	11	12	13	14	15	16	17
FRCGP operational																	
Maximum Load (MW)	145.71	145.89	140.60	139.72	153.72	152.66	139.98	141.26	141.01	140.79	227.08	227.16	224.78	223.95	229.42	232.62	233.36
Hours/a	160	160	160	160	160	160	160	160	160	160	160	160	160	160	160	160	160
GWh/a	23	23	22	22	25	24	22	23	23	23	36	36	36	36	37	37	37
Running Load (MW)	135.71	135.87	130.94	130.13	143.16	142.17	130.37	131.55	131.32	131.12	211.48	211.56	209.34	208.57	213.66	216.64	217.33
Hours/a	7,111	7,899	8,074	8,250	8,250	8,250	8,250	8,250	8,250	8,250	8,250	8,250	8,250	8,250	8,250	8,250	8,250
GWh/a	965	1,073	1,057	1,074	1,181	1,173	1,075	1,085	1,083	1,082	1,745	1,745	1,727	1,721	1,763	1,787	1,793
Non-Operational Load (MW)	10.84	10.84	10.84	10.84	10.84	10.84	10.84	10.84	10.84	10.84	10.84	10.84	10.84	10.84	10.84	10.84	10.84
Hours/a	1,489	701	526	350	350	350	350	350	350	350	350	350	350	350	350	350	350
GWh/a	16.14	7.59	5.70	3.80	3.80	3.80	3.80	3.80	3.80	3.80	3.80	3.80	3.80	3.80	3.80	3.80	3.80
Total GWh/a	1,004	1,104	1,085	1,100	1,209	1,201	1,102	1,112	1,110	1,108	1,785	1,785	1,767	1,760	1,803	1,828	1,834
Average Load	114.66	126.05	123.91	125.53	138.06	137.11	125.76	126.90	126.68	126.48	203.74	203.81	201.69	200.94	205.84	208.70	209.36
Hours	8,760	8,760	8,760	8,760	8,760	8,760	8,760	8,760	8,760	8,760	8,760	8,760	8,760	8,760	8,760	8,760	8,760
PNG Loads																	
PNG Peak Load (MW)	175.0	175.0	175.0	175.0	175.0	175.0	175.0	175.0	175.0	175.0	175.0	175.0	175.0	175.0	175.0	175.0	175.0
PNG Average Load (MW)	112.6	112.6	112.6	112.6	112.6	112.6	112.6	112.6	112.6	112.6	112.6	112.6	112.6	112.6	112.6	112.6	112.6
Hours/a	8,760	8,760	8,760	8,760	8,760	8,760	8,760	8,760	8,760	8,760	8,760	8,760	8,760	8,760	8,760	8,760	8,760
Total Energy Use (GWh/a)	996	996	996	996	996	996	996	996	996	996	996	996	996	996	996	996	996
FRCGP + PNG Load																	
Maximum Load (MW)	320.7	320.9	315.6	314.7	328.7	327.7	315.0	316.3	316.0	315.8	405.3	405.3	434.8	434.8	434.8	434.8	434.8
Operating Load (MW)	248.3	248.5	243.5	242.7	255.8	254.8	243.0	244.2	243.9	243.7	329.6	329.6	357.1	357.1	357.1	357.1	357.1
Total Energy Use (GWh/a)	2,001	2,101	2,082	2,096	2,206	2,198	2,098	2,108	2,106	2,104	2,851	2,851	3,082	3,082	3,082	3,082	3,082

Table 5-3: (b) Power demand scenario Years 18–34: January electrical loads

Year	18	19	20	21	22	23	24	25	26	27	28	29	30	31	32	33	34
FRCGP operations																	
Maximum Load (MW)	229.91	231.15	228.58	227.68	228.95	231.79	228.24	226.42	227.24	227.53	227.08	226.87	226.86	226.92	226.67	226.56	-
Hours/a	160	160	160	160	160	160	160	160	160	160	160	160	160	160	160	160	-
GWh/a	37	37	37	36	37	37	37	36	36	36	36	36	36	36	36	36	-
Running Load (MW)	214.11	215.27	212.88	212.04	213.22	215.87	212.56	210.87	211.64	211.90	211.48	211.29	211.28	211.33	211.10	210.99	-
Hours/a	8,250	8,250	8,250	8,250	8,250	8,250	8,250	8,250	8,250	8,250	8,250	8,250	8,250	8,250	8,250	8,250	-
GWh/a	1,766	1,776	1,756	1,749	1,759	1,781	1,754	1,740	1,746	1,748	1,745	1,743	1,743	1,743	1,741	1,741	-
Non-Operational Load (MW)	10.84	10.84	10.84	10.84	10.84	10.84	10.84	10.84	10.84	10.84	10.84	10.84	10.84	10.84	10.84	10.84	-
Hours/a	350	350	350	350	350	350	350	350	350	350	350	350	350	350	350	350	8,760
GWh/a	3.80	3.80	3.80	3.80	3.80	3.80	3.80	3.80	3.80	3.80	3.80	3.80	3.80	3.80	3.80	3.80	-
Total GWh/a	1,807	1,817	1,797	1,789	1,799	1,822	1,794	1,780	1,786	1,788	1,785	1,783	1,783	1,784	1,782	1,781	-
Average Load	206.27	207.38	205.09	204.28	205.41	207.96	204.78	203.15	203.89	204.14	203.74	203.56	203.55	203.60	203.37	203.27	-
Hours	8,760	8,760	8,760	8,760	8,760	8,760	8,760	8,760	8,760	8,760	8,760	8,760	8,760	8,760	8,760	8,760	8,760
Export grid load																	
PNG Peak Load (MW)	175.0	175.0	175.0	175.0	175.0	175.0	175.0	175.0	175.0	175.0	175.0	175.0	175.0	175.0	175.0	175.0	175.0
PNG Average Load (MW)	112.6	112.6	112.6	112.6	112.6	112.6	112.6	112.6	112.6	112.6	112.6	112.6	112.6	112.6	112.6	112.6	112.6
Hours/a	8,760	8,760	8,760	8,760	8,760	8,760	8,760	8,760	8,760	8,760	8,760	8,760	8,760	8,760	8,760	8,760	8,760
Total Energy Use (GWh/a)	996	996	996	996	996	996	996	996	996	996	996	996	996	996	996	996	996
FRCGP operations + Export grid load																	
Maximum Load (MW)	404.9	406.1	403.6	402.7	403.9	406.8	403.2	401.4	402.2	402.5	402.1	401.9	401.9	401.9	401.7	401.6	175.0
Operating Load (MW)	326.7	327.9	325.5	324.7	325.8	328.5	325.2	323.5	324.2	324.5	324.1	323.9	323.9	323.9	323.7	323.6	112.6
Total Energy Use (GWh/a)	2,803	2,813	2,793	2,786	2,796	2,818	2,790	2,776	2,783	2,785	2,781	2,780	2,780	2,780	2,778	2,777	986

5.2.2 Electrical loads provided by FRL in May 2018

During peak production, the FRCGP demand starts at approximately 1,131 GWh/a, increases to 2,132 GWh/a in Year 8, peaks at 2,159 GWh/a and then settles to 2,116 GWh/a in the later years. Details of the electrical load in Years -1–16 are set out in Table 5-4 and electrical load in Years 17–33 is shown in Table 5-5.

The FRHEP must also be able to supply power to the export grid. The potential for this to be achieved has been assessed, taking the following into account:

- The electrical loads include a 6-month commissioning year referred to as Year-1.
- Starting in Year 8, a second processing line is commissioned. While the processing plant is continuously operating, there will be periods when only one processing line is operating. This is referred to as 'Part Load running' in the tables. After Year 8, there is no minimum load case.
- The maximum generation potential of the FRHEP with a dam crest height of RL 238.5 m requires the maximum operating level and minimum operating level to be optimised. The generating plant configuration and efficiency variation with flow and head must also be accounted for. The maximum energy has been levelled to 2,789 GWh/a, based on modelling using the measured flow data across all years of operation.
- Initially, the export potential from the FRHEP is 1,658 GWh/a, but it soon drops to 1,420 GWh/a. In Year 8, the export potential proposed by FRL reduces to 657 GWh/a.
- All other criteria used for the January electrical loads are applicable.

These are referred to as the May Loads within this report.

Table 5-4: (a) Power demand scenario Years 1–16: May electrical loads

Year	-1	1	2	3	4	5	6	7	8	9	10	11	12	13	14	15	16
FRCGP operations																	
Maximum Load (MW)	165.16	165.16	169.60	171.58	171.58	180.56	180.98	180.98	276.80	276.80	277.21	277.21	277.21	277.21	277.21	277.21	277.21
Hours/a	160	160	160	160	160	160	160	160	160	160	160	160	160	160	160	160	160
GWh/a	26	26	27	27	27	29	29	29	44	44	44	44	44	44	44	44	44
Running Load (MW)	151.66	151.66	153.70	155.50	155.28	164.09	164.54	164.55	249.59	249.60	250.04	250.05	250.06	250.06	250.07	250.08	250.09
Hours/a	2,270	7,067	7,899	7,978	8,074	8,074	8,074	8,074	7,899	7,899	7,899	7,899	7,899	7,899	7,899	7,899	7,899
GWh/a	344	1,072	1,214	1,241	1,254	1,325	1,329	1,329	1,972	1,972	1,975	1,975	1,975	1,975	1,975	1,975	1,976
Part Load (MW)	-	-	-	-	-	-	-	-	166.40	166.40	166.69	166.70	166.70	166.71	166.72	166.72	166.73
Hours/a	-	-	-	-	-	-	-	-	701	701	701	701	701	701	701	701	701
GWh/a	-	-	-	-	-	-	-	-	117	117	117	117	117	117	117	117	117
Non-Operational Load (MW)	21.25	21.25	21.25	21.25	21.25	21.25	21.25	21.25									
Hours/a	1,986	1,533	701	622	526	526	526	526	-	-	-	-	-	-	-	-	-
GWh/a	42	33	15	13	11	11	11	11	-	-	-	-	-	-	-	-	-
Total GWh/a	413	1,131	1,256	1,281	1,292	1,365	1,369	1,369	2,132	2,133	2,136	2,136	2,136	2,136	2,137	2,137	2,137
Average Load	93.50	129.08	143.39	146.26	147.54	155.82	156.25	156.25	243.44	243.44	243.87	243.88	243.88	243.89	243.90	243.91	243.92
Hours	4,416	8,760	8,760	8,760	8,760	8,760	8,760	8,760	8,760	8,760	8,760	8,760	8,760	8,760	8,760	8,760	8,760
PNG Loads																	
PNG Peak Load (MW)	-	234.8	230.4	228.4	228.4	219.4	228.4	228.4	104.5	104.5	103.9	103.9	103.9	103.9	103.9	103.9	103.9
PNG Average Load (MW)	-	188.4	174.0	171.1	169.8	161.5	160.9	160.9	74.4	74.4	74.0	74.0	73.9	73.9	73.9	73.9	73.9
Hours/a	-	8,760	8,760	8,760	8,760	8,760	8,760	8,760	8,760	8,760	8,760	8,760	8,760	8,760	8,760	8,760	8,760
Total Energy Use (GWh/a)	-	1,658	1,533	1,508	1,497	1,424	1,420	1,420	657	656	653	653	653	653	652	652	652
FRCGP + PNG Load																	
Maximum Load (MW)	165.16	400.0	400.0	400.0	400.0	400.0	409.4	409.4	381.3	381.3	381.1	381.1	381.1	381.1	381.1	381.1	381.1
Operating Load (MW)	151.66	340.1	327.7	326.6	325.1	325.6	325.4	325.4	324.0	324.0	324.0	324.0	324.0	324.0	324.0	324.0	324.0
Total Energy Use (GWh/a)	413	2,789	2,789	2,789	2,789	2,789	2,789	2,789	2,789	2,789	2,789	2,789	2,789	2,789	2,789	2,789	2,789

Table 5-5: (b) Power demand scenario Years 17–33: May electrical loads

Year	17	18	19	20	21	22	23	24	25	26	27	28	29	30	31	32	33
FRCGP operations																	
Maximum Load (MW)	277.21	277.21	277.21	277.21	277.21	277.21	277.21	277.21	277.21	277.21	277.21	277.21	277.21	277.21	277.21	277.21	277.21
Hours/a	160	160	160	160	160	160	160	160	160	160	160	160	160	160	160	160	160
GWh/a	44	44	44	44	44	44	44	44	44	44	44	44	44	44	44	44	44
Running Load (MW)	250.10	252.13	252.73	248.73	248.32	249.31	250.25	248.98	249.48	248.50	249.44	251.47	249.26	248.85	248.51	247.64	247.66
Hours/a	7,899	7,899	7,899	7,899	7,899	7,899	7,899	7,899	7,899	7,899	7,899	7,899	7,899	7,899	7,899	7,899	7,899
GWh/a	1,976	1,992	1,996	1,965	1,962	1,969	1,977	1,967	1,971	1,963	1,970	1,986	1,969	1,966	1,963	1,956	1,956
Part Load (MW)	166.73	168.09	168.48	165.82	165.55	166.21	166.83	165.99	166.32	165.67	166.29	167.65	166.17	165.90	165.67	165.09	165.11
Hours/a	701	701	701	701	701	701	701	701	701	701	701	701	701	701	701	701	701
GWh/a	117	118	118	116	116	116	117	116	117	116	117	117	116	116	116	116	116
Non-Operational Load (MW)																	
Hours/a	-	-	-	-	-	-	-	-	-	-	-	-	-	-	-	-	-
GWh/a	-	-	-	-	-	-	-	-	-	-	-	-	-	-	-	-	-
Total GWh/a	2,137	2,154	2,159	2,125	2,122	2,130	2,138	2,127	2,132	2,123	2,131	2,148	2,130	2,126	2,123	2,116	2,116
Average Load	243.93	245.87	246.44	242.62	242.22	243.18	244.07	242.86	243.33	242.40	243.30	245.23	243.12	242.74	242.41	241.58	241.60
Hours	8,760	8,760	8,760	8,760	8,760	8,760	8,760	8,760	8,760	8,760	8,760	8,760	8,760	8,760	8,760	8,760	8,760
Export grid load																	
PNG Peak Load (MW)	103.9	100.9	100.0	105.9	106.6	105.1	103.8	105.6	104.9	106.4	105.0	102.1	105.3	106.0	106.5	107.8	107.8
PNG Average Load (MW)	73.9	72.0	71.4	75.2	75.6	74.6	73.8	75.0	74.5	75.4	74.5	72.6	74.7	75.1	75.4	76.2	76.2
Hours/a	8,760	8,760	8,760	8,760	8,760	8,760	8,760	8,760	8,760	8,760	8,760	8,760	8,760	8,760	8,760	8,760	8,760
Total Energy Use (GWh/a)	652	635	630	664	667	659	651	662	657	666	658	641	659	663	666	673	673
FRCGP operations + Export grid load																	
Maximum Load (MW)	381.1	378.1	377.3	383.1	383.8	382.3	381.0	382.8	382.1	383.6	382.2	379.3	382.5	383.2	383.7	385.0	385.0
Operating Load (MW)	324.0	324.1	324.1	323.9	323.9	324.0	324.0	323.9	324.0	323.9	324.0	324.1	324.0	323.9	323.9	323.9	323.9
Total Energy Use (GWh/a)	2,789	2,789	2,789	2,789	2,789	2,789	2,789	2,789	2,789	2,789	2,789	2,789	2,789	2,789	2,789	2,789	2,789

5.3 Net electrical loads

The loads at the FRCGP and the export grid do not provide for the losses in the transmission system. Details of transmission losses are set out in Section 18 (Table 18-1). For the purposes of this study, it is assumed that the very low losses of 0.2% to supply the FRCGP and 1.5%–5.0% (depending on load) to supply the export grid are absorbed by the uncertainty of the load estimates.

5.4 Electrical load changes from the project sizing study

The January electrical loads being used for the SPS investigations for the FRCGP are slightly less than for Optimisation Study, as shown in Figure 5-1.

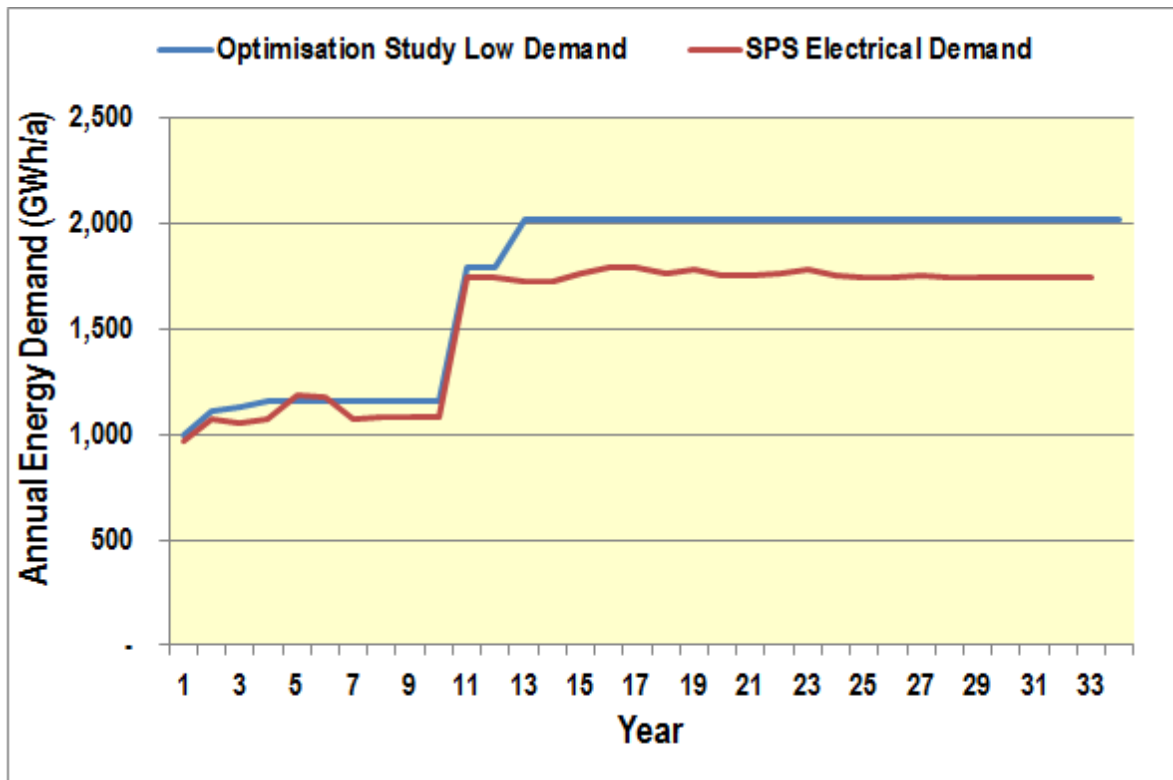


Figure 5-1: Comparison of FRCGP loads for the Optimisation Study and SPS phase of project

Figure 5-2 shows the May electrical loads for the FRCGP are over 15% more than the January electrical loads. The export grid demand also rises substantially in the early years in line with the demand on the FRHEP.

The implications of the increased May electrical loads for the FRCGP are considered in Section 18.

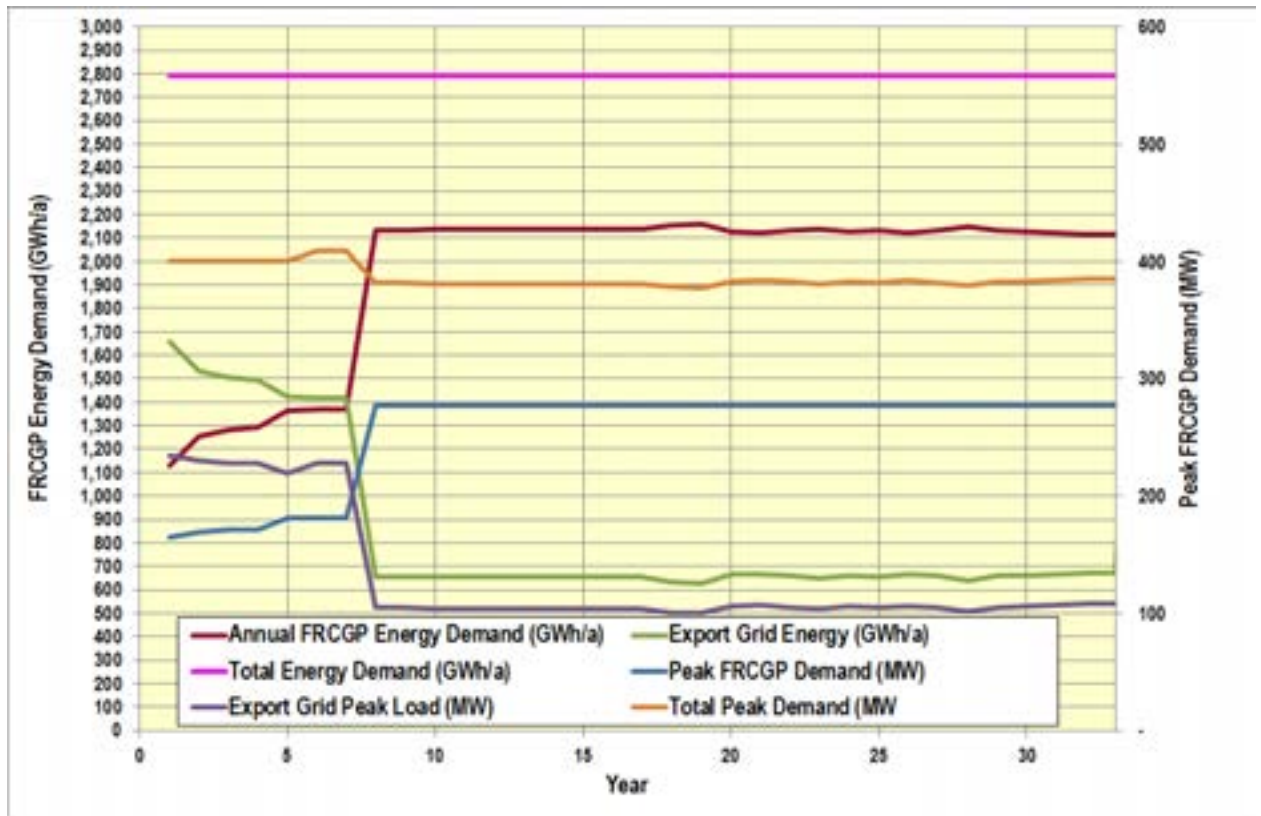


Figure 5-2: Breakdown of May 2018 electrical loads

6 Water Balance, Limnology and Load Balance

This chapter summarises the basis of, and outcomes from, supporting investigations completed to assess the following:

- i) Water balance for the FRCGP upstream of the FRHEP reservoir, the FRHEP reservoir and receiving environment downstream of the embankment to evaluate the filling and operation of the FRHEP and assess changes in flows downstream of the embankment, and to provide input to the evaluation of suspended solids release from the site (completed by Golder Associates)
- ii) Limnology of the FRHEP reservoir to evaluate the effects of tailings and waste rock disposal on the stability of the lake and sediment transport through the reservoir from these and natural upstream sources
- iii) Water quality impacts from the FRCGP mining activities upstream of the FRHEP reservoir, and mine tailings and waste rock disposal in the ISF, as well as downstream of the FRHEP embankment.

The outcomes from these studies also supported the development of the Environmental Impact Statement (EIS) for the FRCGP and the FRHEP.

6.1 Water balance

Since the water balance was developed to also support the EIS, flows were determined for a number of key locations within the upper catchments as well as downstream of the FRHEP embankment extending to the Sepik River (AP13) at Kubkain. The extent of the area covered by the current phase of water and load balance modelling is presented in Figure 6-1 and described in Table 6-1.

Table 6-1: Details of assessment point locations

Assessment point	Description	Justification	Easting	Northing	Catchment (km ²)
AP1	Ubai Creek U/S Nena River	Downstream of pits	587573	9482676	20
AP2	Ubai Creek U/S Nena River	Downstream of pits	586686	9484334	6
AP3	Nena River U/S Uba Creek	As reference site	585756	9485363	151
AP4	FRHEP northern arm	In reservoir (Nena)	600888	9485937	195
AP5	FRHEP southern arm	In reservoir (Niar)	601723	9483812	845
AP6	Downstream of FRHEP Embankment	ISF discharge	603751	9487432	1,040
AP7	Frieda River (Airstrip)	Downstream of FRHEP	606698	9490214	1,047
AP8	Frieda River U/S Kaugumi Creek	Downstream of FRHEP	609703	9498016	1,092
AP9	Frieda River (Frieda Mountain)	Downstream of FRHEP	613056	9500190	1,210
AP10	Frieda River (Lower Frieda River GS)	Downstream of FRHEP	612331	9509042	1,345
AP11	Frieda River U/S Sepik River	Downstream of FRHEP	611840	9521775	1,466
AP12	Sepik River (Iniok GS)	First impact in Sepik FRHEP	613145	9525695	25,200
AP13	Sepik River (Kubkain GS)		649377	9525394	29,500

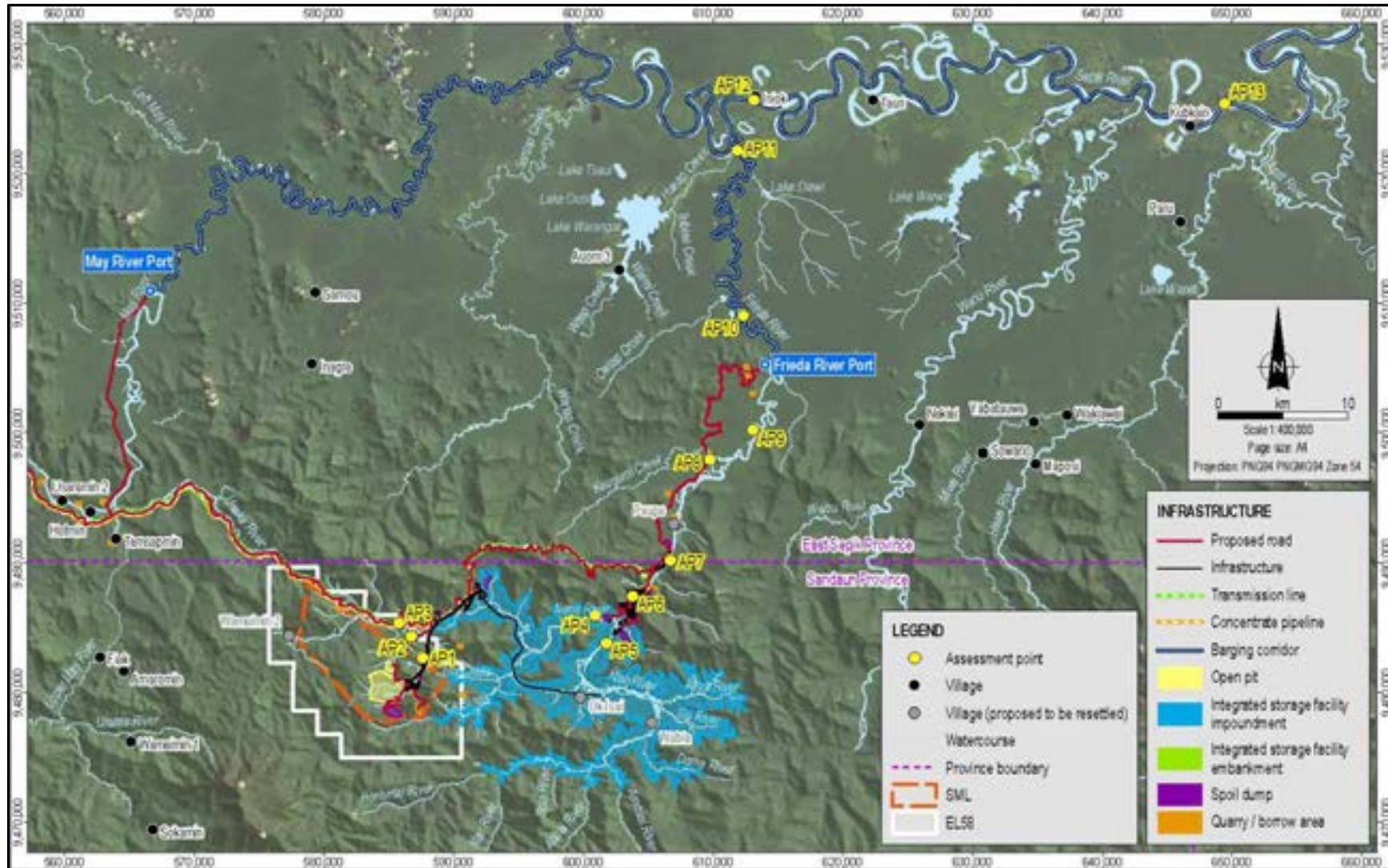


Figure 6-1: Locations of assessment points and FRHEP infrastructure

Source: Coffey MXD Reference: 11575B_21_GIS001_v01_1.

Most of the FRCGP and the FRHEP infrastructure will be located within the catchments of the Nena, Niar and Frieda rivers, all of which drain into the Sepik River. At 1,100 km in length, the Sepik River is one of the longest rivers in Papua New Guinea.

The FRCGP and the FRHEP are located in a region that has a tropical rainforest climate. The climate is influenced seasonally by location relative to the mountain ranges. Climatic conditions in this area may be separated into two zones – the uplands and the lowlands. For the purposes of this study, the approximate boundary between the regions is the Frieda River Airstrip (AP7), with the area upstream of this assessment point classed as uplands.

Analysis of climatic data from the FRCGP and FRHEP region has been carried out (Section 4.1) and is not repeated here. The analysis indicated that the mean annual precipitation (MAP) values for the uplands region range from 7,700 mm/yr to 8,600 mm/yr, and for the lowlands region range from 3,700 mm/yr to 6,000 mm/yr. Monthly average relative humidity is consistently above 80%.

Seasonal variability in precipitation is typically higher in the lowlands than the uplands; however, in both regions the higher precipitation months are February to April, with a peak in March, and the lower precipitation months are May to August.

The HIT (Horse-Ivaal-Trukai) and Ekwai open pit areas are within the Ubai Creek catchment and the Koki open pit is in the Uba Creek catchment. Both the Ubai and Uba creeks flow directly into the Nena River. The upper catchments flow through steep incised valleys and are characterised by relatively narrow channels with steep banks and rocky beds containing large boulders. Flows are characteristically high energy and velocity due to the frequent rainfall events and, typically, build-up of loose sediment or vegetation in the stream beds is minimal.

Further downstream, the valley terrain remains relatively steep throughout the mid-catchment area where channels are typically wide, with straight to partly meandering channels containing cobble/gravel beds and banks. AP7 and AP8 are located in this mid-catchment area on the Frieda River.

From around location AP9 (Frieda Mountain), the Frieda River enters the lower gradient lowland plains and meanders through the Sepik River floodplain. In the floodplain area, river dynamics have created a series of oxbow lakes and main channels are commonly wide with highly braided sections.

6.1.1 Water balance model

The site-wide water balance model was constructed using the GoldSim modelling platform. A simplified schematic diagram showing the water balance flows during operations is provided in Figure 6-2. During operations, diversions around the open pit areas will be established, and tailings and waste rock will be deposited into the ISF. Water from the open pits will be treated and discharged to the ISF. After cessation of the FRCGP operations, the open pits will be flooded.

The post-embankment scenario was developed primarily to assess water levels in the reservoir during the operational and FRCGP closure phases, and to assess the capacity of storages, develop estimates of contact and non-contact water volumes, inform water treatment requirements and assess potential impacts to receiving water bodies.

Modelling was performed using daily time steps for a 55-year period, to estimate flows and volumes throughout the embankment construction period, the 33-year FRCGP mine life, and post-closure of the FRCGP. The 55-year period provided by FRL is based on 2 years pre-mining, 33 years mining and 20 years after closure.

The following sub-sections briefly summarise development of the water balance model and modelling results.

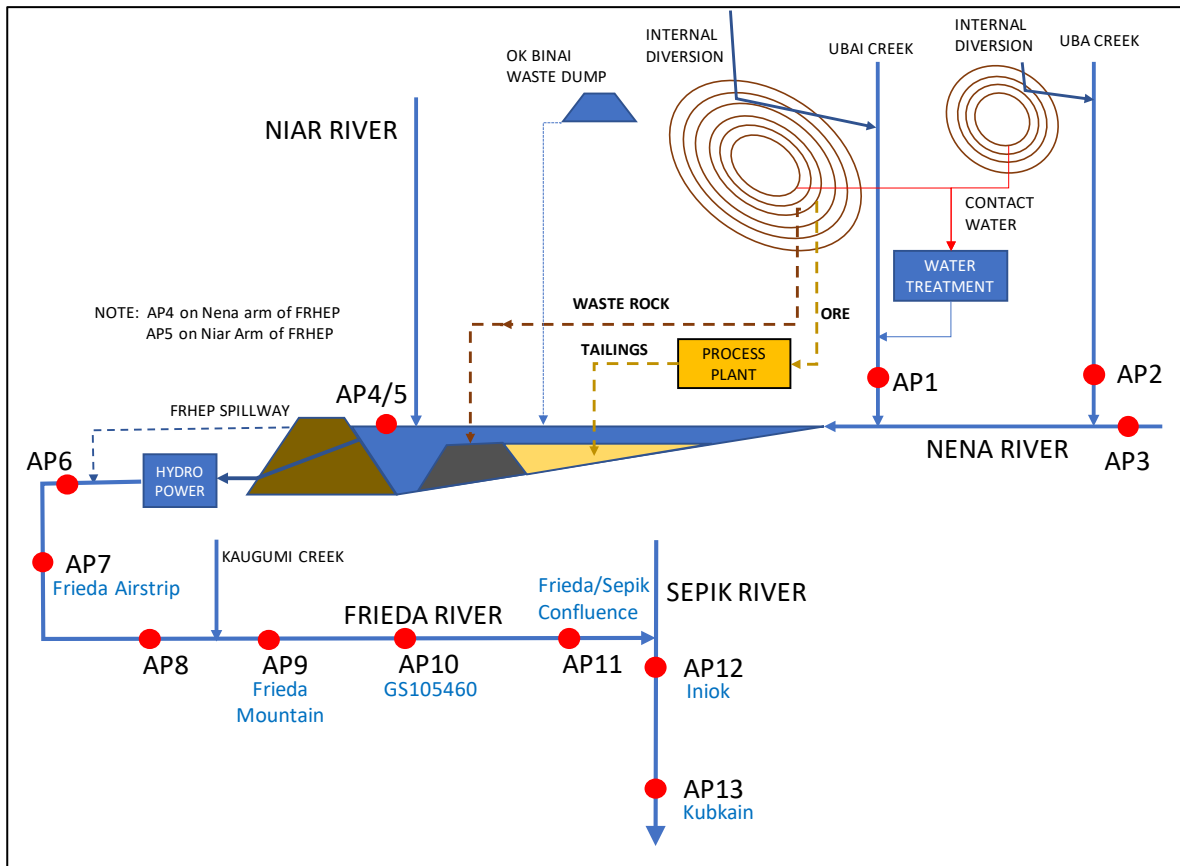


Figure 6-2: Schematic layout of water balance during operations

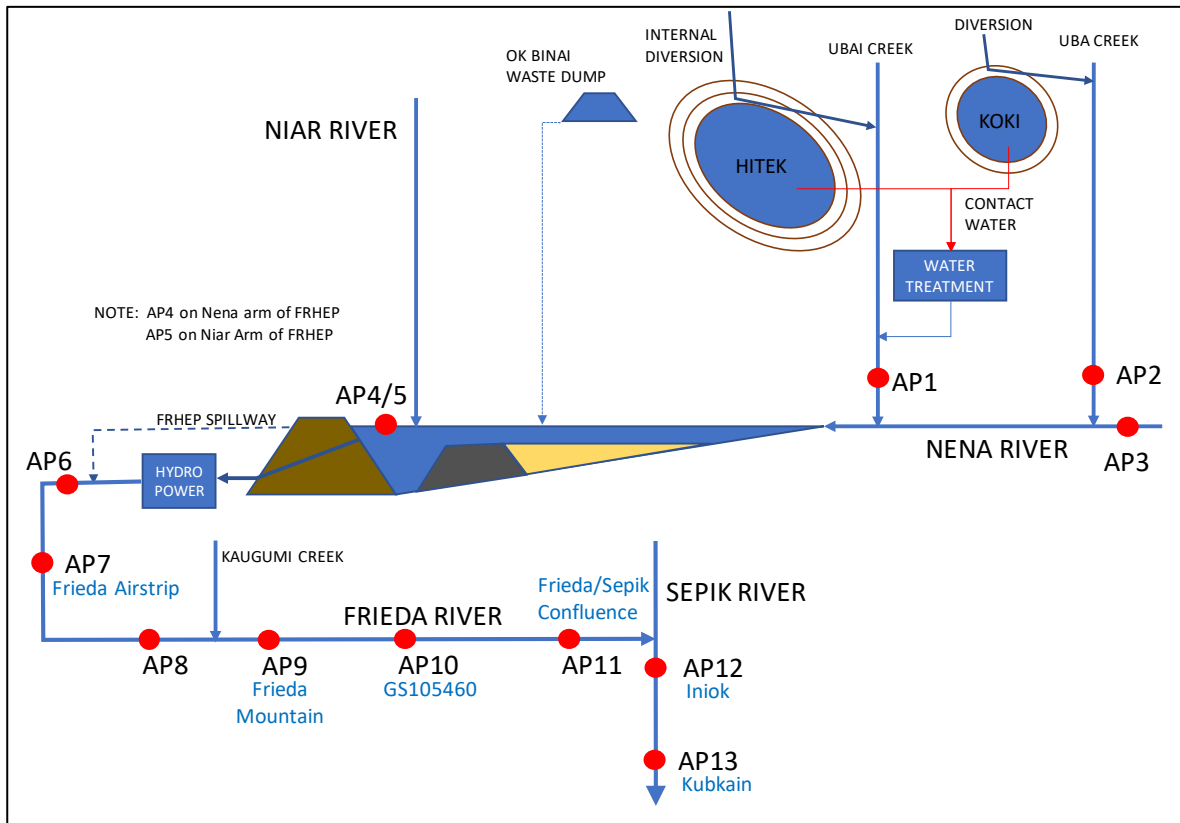


Figure 6-3: Schematic layout of water balance post closure of the FRCGP

Precipitation - stochastic assessment

Two stochastic rainfall modules were developed to generate a wide range of climate sequences for the uplands and lowlands regions respectively. Data indicated that the lowlands region is around 40% drier than the uplands area. The stochastic modules generated precipitation sequences that showed the same seasonality and statistical characteristics as the historical datasets.

Although the historical dataset used to create the stochastic precipitation patterns covered a relatively short period, it includes the 1997–1998 El Niño period and a short La Niña period in 2008–2009. Therefore, the variability related to the El Niño Southern Oscillation (ENSO) is likely to have been at least partly captured in the stochastic variability.

Evaporation and evapotranspiration

Evaporation and evapotranspiration (ET) were modelled based on the Nena AWS monitoring data. Modelled ET values were used directly for losses from the land surface and vegetation for the uplands, and modelled ET values were multiplied by 1.25 for the lowlands, based on information for differences in evaporation due to altitude in the region, as presented in the handbook *Climate of Papua New Guinea* (McAlpine et al., 1983).

Catchment runoff

An Australian Water Balance Model (AWBM) module (Boughton, 2004) was incorporated into the GoldSim model to estimate runoff from natural catchment areas. The AWBM input parameters for the uplands area (i.e. AP1–AP7 catchments) were calibrated to the flow data developed as part of a hydrology analysis of the Frieda River Basin presented in SRK (2018b).

The AWBM method was used for all catchment areas, except for the open pit walls. For open pit wall surface sub-catchments, a runoff coefficient of 0.95 was used in conjunction with a zero storage capacity assumption for the wall rocks.

Open pit water management

The water management plan established for the open pits comprises three discrete stages in the mine life – Phases 1–3, Phases 4–7 and Phases 8–11, which correspond to pit development stages at mining operational Year 7, Year 18 and Year 33 respectively. Diversion structures are considered to be in place to divert non-contact water around the pits where possible, and contact water to central collection points (SRK, 2018c). Water management will include diversion around the pit crest, diversion of upstream flows through sections of the pit using bench drains, and pumping water from sumps at the base of the open pits. Furthermore, contact water will be directed along benches to side-drains where it will be collected and, together with the contact water pumped from the base of the pit, will be transferred to the water treatment collection and transfer locations. The treated effluent will be discharged into Ubai Creek upstream of location AP1.

The Year 33 footprint areas were maintained for the closure period and assumes that the diversions will remain in place (except for the period that water would be diverted to the pit to accelerate flooding).

Groundwater inflow

All groundwater inflow to the open pits is assumed to report to the pit sumps at the base of the respective pits, where it will be collected along with runoff from the lower open pit walls. The estimated base case groundwater inflows to the open pits are illustrated in Figure 6-4. Note that recharge into the pits continues at the same rate after mine closure.

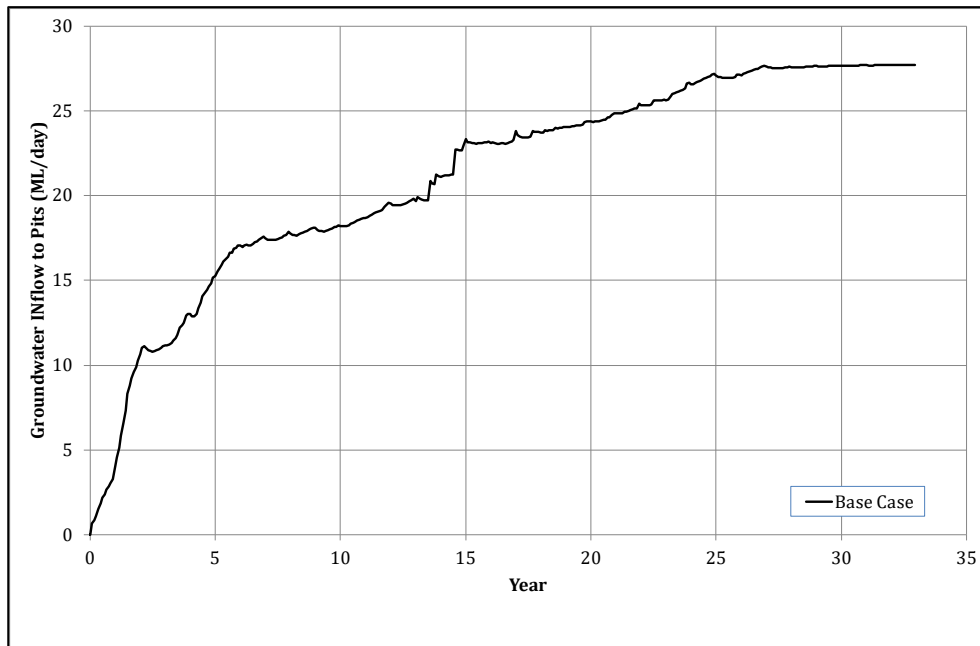


Figure 6-4: Base case groundwater recharge to the open pits

Source: AGE, 2018

FRHEP reservoir

The FRHEP reservoir is a major component of the water balance. The ISF basin will accumulate tailings, waste rock and natural sediment. The water inflows will comprise tailings water, runoff and rain falling directly on the pond surface. Discharges will comprise evaporation from the pond surface, minor seepage through the embankment and into natural ground, outflow through the hydroelectric power system and outflow through the spillway.

Reservoir capacity as a function of water elevation was estimated from the basin topography and embankment location. To account for the deposition of solids, the reservoir volume was reduced at each time-step by the volume equivalent to tailings, waste rock and sediment deposition that had occurred. This was based on the production schedule for tailings and waste rock provided by FRL. The sediment loads for the operations and post-closure periods were estimated from modelling data provided by Golder Associates. Hydroelectric water demand was modelled for the facility and a series of operating rules developed by Robinson Energy Ltd were adopted. A minimum residual flow of 50 m³/s was maintained for the construction, flooding and operational periods. After closure of the FRCGP operation, the FRHEP will continue to operate.

6.1.2 Water balance results

The water balance model was used to process 100 realizations of the stochastic climate data, each with two different stochastic precipitation patterns (upland and lowland). Two primary scenarios were developed – a pre-embankment and post-embankment model. The pre-embankment scenario was developed to provide flow data for use in sediment load and limnological studies. The post-embankment scenario was developed to assess water levels in the reservoir during the operational and closure phases, and to support solute and suspended transport modelling for the AP locations shown in Figure 6-1.

Stochastic modelling results indicate that flows at the AP sites will typically range over at least one order of magnitude; however, the range between the 10th (i.e. 'dry' rainfall) and 90th (i.e. 'wet' rainfall) percentiles is significantly smaller, as shown in Figure 6-5. The results provide pre-mining estimates of flows for a modelled period of 55 years.

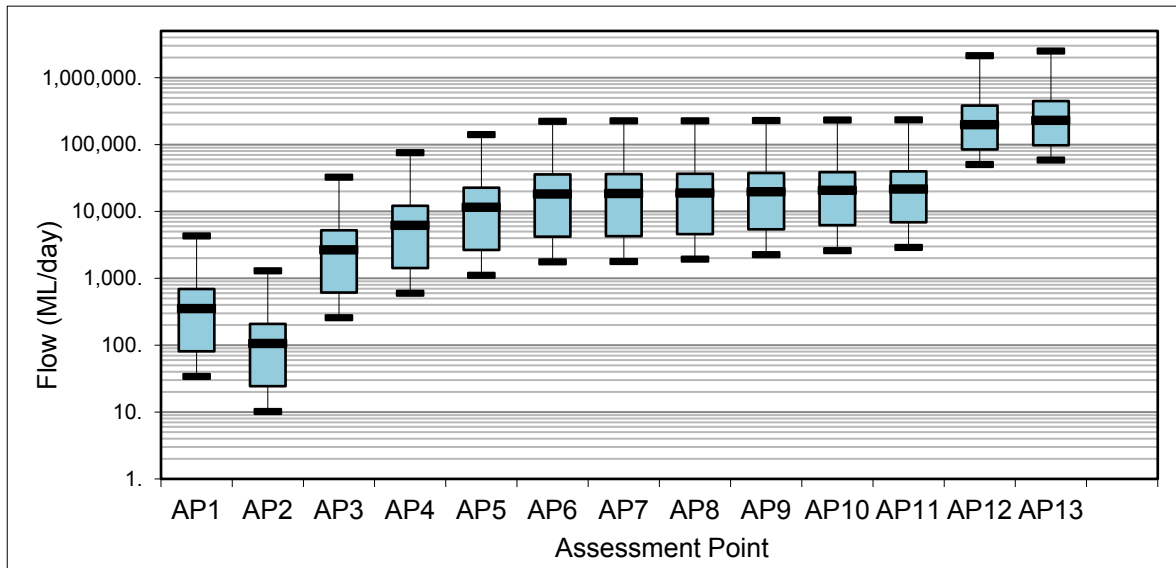


Figure 6-5: Modelled range of flows at the assessment points – pre-embankment scenario

Note: The plot shows mean and 10th/ 90th percentile values (box) along with minimum and maximum (whiskers).

The post-embankment scenario was developed primarily to assess water levels in the reservoir during the operational and FRCGP closure phases, and to assess the capacity of storages, develop estimates of contact and non-contact water volumes, inform water treatment requirements and assess potential impacts to receiving water bodies.

During the operational period, flows into the reservoir are influenced by mine operations and outflows from the reservoir are dominated by hydroelectric power generation demands.

A statistical summary of flows for the operational period is provided in Figure 6-6. Flows for AP4 and AP5 are not included as these locations are within the lake (calculated flows were used for assessment of lake water quality only).

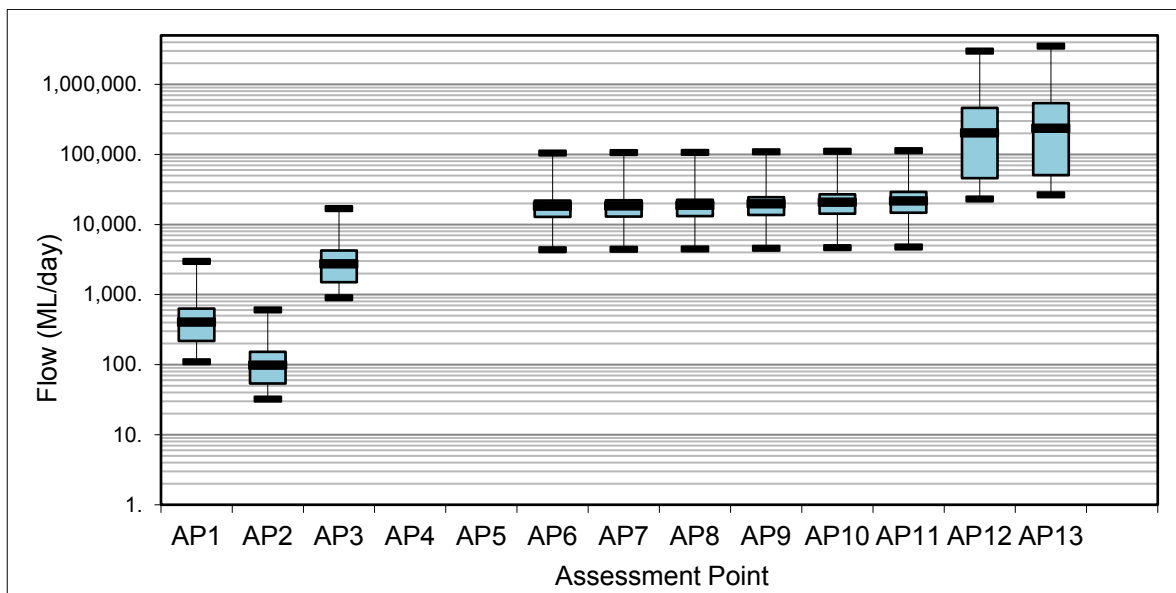


Figure 6-6: Daily average flow statistics at assessment points during mine operations (Years 1-33)

Note: The plot shows mean and 10th/ 90th percentile values (box) along with minimum and maximum (whiskers).

As indicated in the plot (Figure 6-6), flows downstream of the reservoir embankment show less variability between minimum and maximum values, and 10th and 90th percentile values in comparison with the pre-embankment scenario (Figure 6-5). There are also increases in average and 10th percentile flows, which are the result of the regulation of flows due to the FRHEP. The effects of the altered flow regime extend along the entire Frieda River system. Flows modelled in the Sepik River AP locations (AP12 and AP13) do not change significantly during operations. While maximum flows appear to have increased in the Sepik River, this is likely due to a single realization, and is not reflective of the overall system.

Average (mean for all realizations) modelled hydroelectric water demand is provided in Figure 6-7, inclusive of all water losses from the reservoir other than spillway flow. Mean hydroelectric water demand is consistent for periods based on a water demand schedule provided by Robinson (2018) and is the dominant outflow from the reservoir during operations.

Water levels in the reservoir may not be sufficient to enable full hydroelectric power production during low precipitation realizations (typically below the 20th percentile), particularly during periods of high demand (~Years 11–33, inclusive).

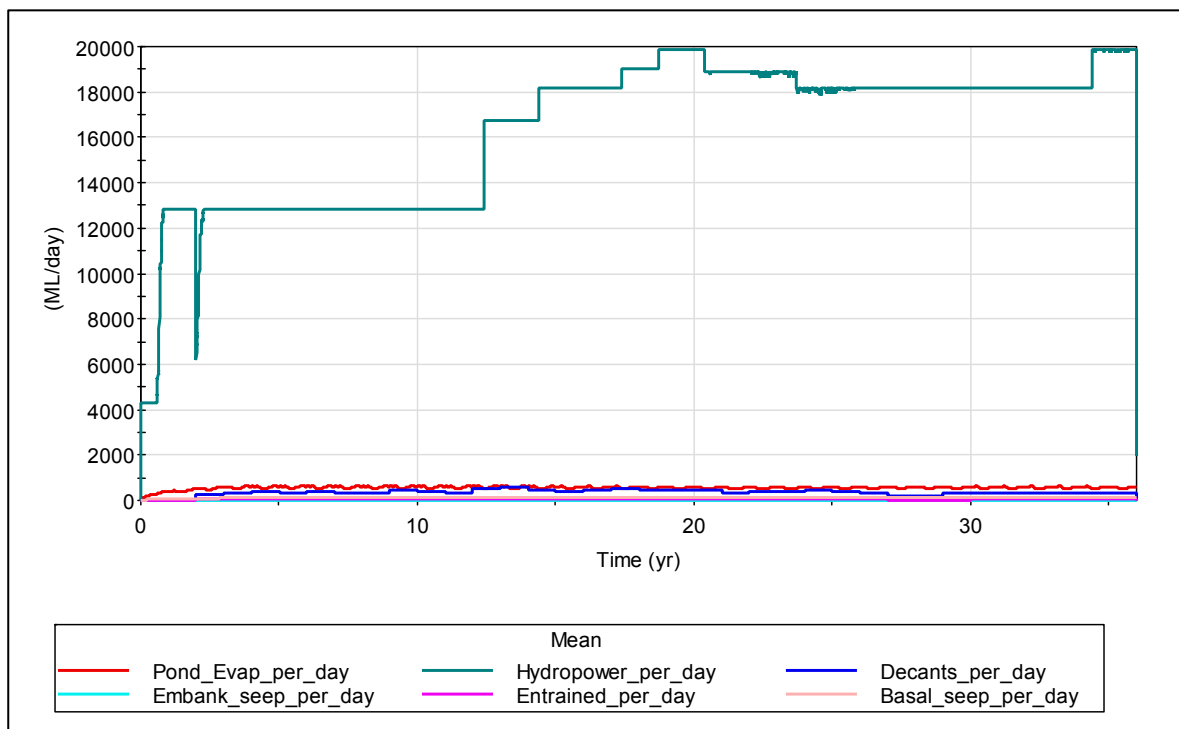


Figure 6-7: Reservoir outflows – operational period

Note: Mean flow data for all model realizations.

Water levels in the FRHEP reservoir (Figure 6-8) are regulated by the spillway invert (upper limit) and partially regulated by the minimum operating water level of the hydroelectric facility (RL 199.4 m), although minimum flows of 50 m³/s are maintained at all times. When water levels fall below the minimum operating level, hydroelectric power demand generation will cease and flows through the embankment will reduce to maintain the minimum residual flows in the Frieda River (50 m³/s). Hydroelectric power production will recommence once water levels recover above the minimum operating level (RL 199.4 m). The results of the stochastic modelling suggest that in the dry (i.e. 10th percentile) rainfall scenario, generation of hydroelectric power may be disrupted due to low water levels in the FRHEP reservoir.

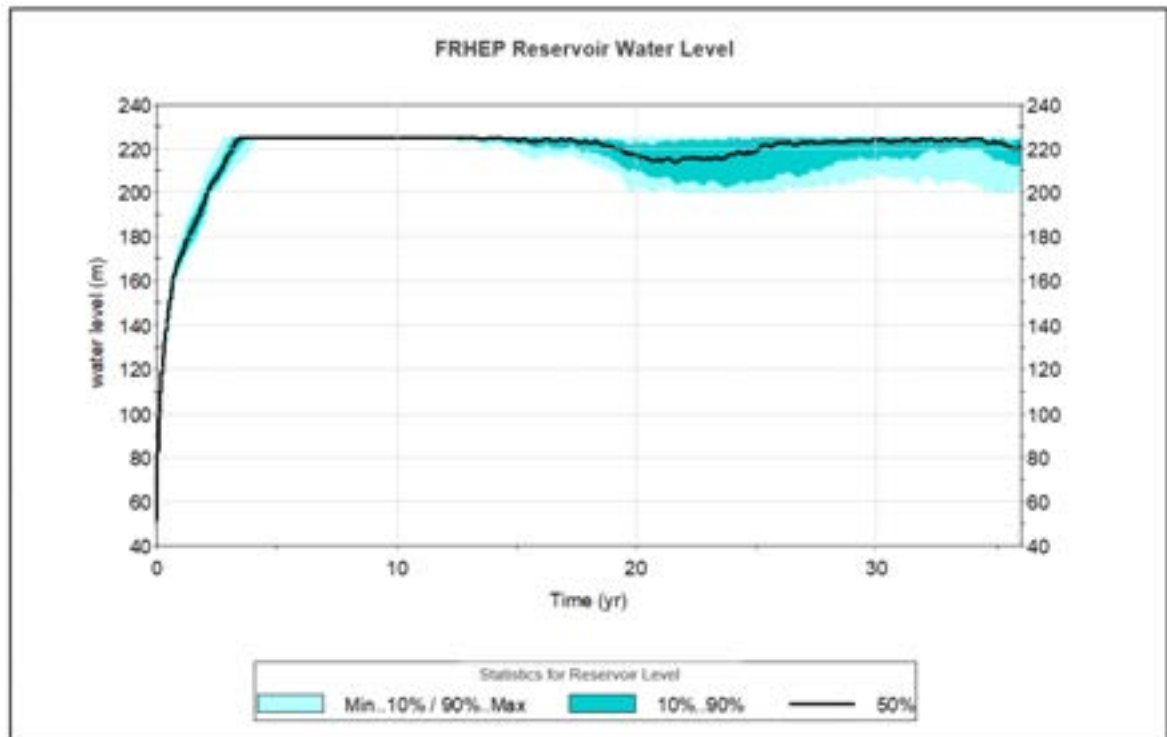


Figure 6-8: Reservoir water levels – operational period

Note: The plot shows median (black line) and 10th/ 90th percentile ranges of values (blue area).

6.1.3 Conclusions and limitations

During operations, flows downstream of the reservoir embankment show less variability between minimum and maximum values, and between 10th and 90th percentile values due to the regulation of flows from the FRHEP. The altered flow regime extends along the entire Frieda River to its confluence with the Sepik River; however, no significant changes are predicted to occur within the flow regime of the Sepik River.

The modelling results further suggest that water levels in the reservoir may not be sufficient to support the planned hydroelectric power production during extended dry periods, with interruptions to operations possible during extended low rainfall periods (typically below the 10th percentile) – particularly during periods of high water demand for hydroelectric power generation.

The water balance model has been developed using generally conservative methods and assumptions; however, the model has limitations/ uncertainties. First, flow conditions for the natural catchment areas have been estimated using the AWBM, which is designed for long-term water balance purposes and is suitable for assessing the effects on the hydrologic system, but produces results that may not represent low and high flow conditions. Second, results for outflows from the FRHEP are dependent on assumptions regarding operations for the site and, in some cases, information provided by third parties. These assumptions may not reflect the actual operation of the FRHEP.

6.2 Limnology

The limnological assessment was completed by HydroNumerics (HydroNumerics, 2018). The reservoir will inundate three major river courses that form the primary reservoir branches – the Nena to the west of the embankment; the Ok Binai, which flows from the southwest and converges midway along the Nena branch; and the Niar (Upper Frieda), which carries converged flow from numerous dendritic sub-branches that flow up from the south towards the embankment (Figure 6-9).

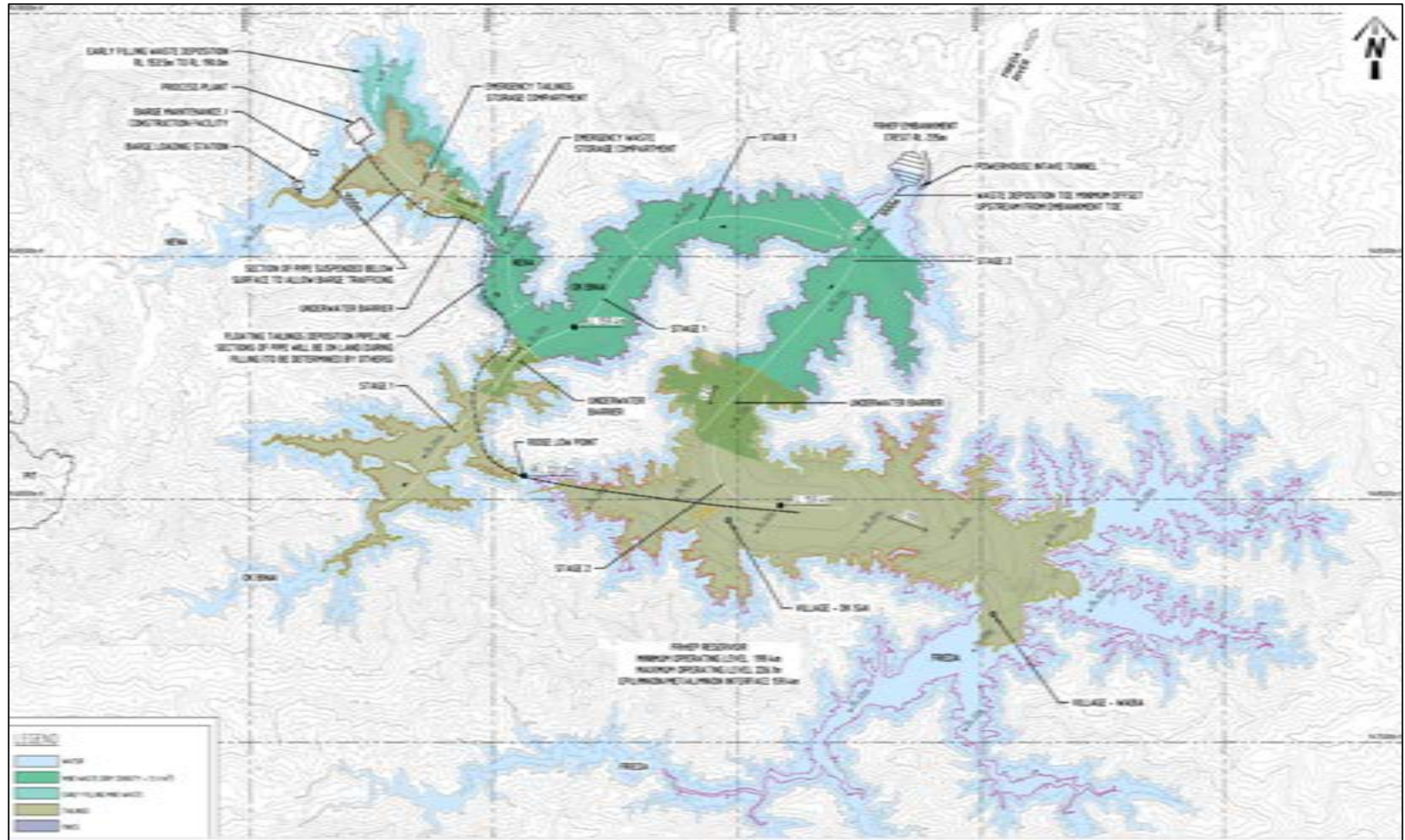


Figure 6-9: Footprint of reservoir illustrating proposed waste rock (coloured in green) and tailings (coloured in brown) storage areas

Source: SRK, 2018.

With respect to the FRHEP's secondary function of storing waste rock and tailings, waste rock generated by the FRCGP will be deposited into the reservoir via barges, and tailings will be deposited at the bottom of the reservoir via a floating pipeline, a series of floating pontoons and tremie pipe system. The purpose of the tremie pipe system is to minimise suspension of the tailings.

6.2.1 Model description

The 3D Aquatic Ecosystem Model (AEM3D) was used to simulate the hydrodynamics and sediment transport in the FRHEP reservoir. The transport equations in AEM3D are unsteady Reynolds-averaged Navier-Stokes equations and scalar transport equations with the Boussinesq approximation with no non-hydrostatic pressure terms. The free-surface evolution is governed by an evolution equation developed by a vertical integration of the continuity equation applied to the Reynolds-averaged kinematic boundary condition.

AEM3D is a deterministic model based on generic algorithms that describe observed physical processes with mathematic form and coefficients (generally for efficiency of processes such as mixing rates) that are known (within an acceptable range) from laboratory work presented in the literature. The model does not rely on empirical derivations and does not require extensive calibration of parameters to tune the hydrodynamics.

AEM3D computes solutions to the following processes (in the order shown) at time steps in the order of minutes:

- Surface heating/ cooling in the surface layer
- Mixing of scalar concentrations (i.e. dissolved and suspended constituents) and momentum using a mixed-layer turbulent kinetic energy model
- Introducing wind energy as a momentum source in the surface mixed-layer
- Solving the free-surface (water level) evolution and velocity field
- Applying horizontal diffusion of momentum
- Advection of scalars in the velocity field
- Horizontal diffusion of scalars.

Sediment dynamics in AEM3D are modelled concurrently with the hydrodynamics. Sediments are treated as a concentration of inert particles with user-prescribed diameter and density. The particles are introduced within terrestrial flow or resuspended from an initialised bed load and undergo settling based on a Stokes settling derivation. Resuspension rates are determined for each particle size based on the particle density, bottom shear stress (above a critical shear stress) and a user-defined erosion rate. Bottom shear is determined from currents resolved by the hydrodynamic solver, AEM3D, in response to winds, tides, river inputs and internal waves. The resuspension and deposition of the sediments changes the bottom morphology.

AEM3D is a recent update (released in 2016) of ELCOM-CAEDYM that was previously developed by the Centre for Water Research, University of Western Australia, and has been extensively published in peer-reviewed scientific literature (Trolle et al., 2012).

6.2.2 Model set-up

Simulation periods

The simulation time periods coincided with the rainfall and runoff realisations. The time series of total suspended solids (TSS) inputs into the model takes estimates of catchment runoff and contributions from project activities upstream of the reservoir that were provided by Golder Associates (2018) into account.

The model was configured to simulate three separate periods:

- **Filling** – a 10-year period that starts with filling of the reservoir. In this baseline simulation, no waste rock and tailings are stored in the reservoir to assess the behaviour of the reservoir and the downstream release of sediments during the filling and construction phase and continuing through to the operational phase.
- **Operations** – a 10-year period starting at operational water level (RL 225 m) and includes the final storage plan for waste rock and tailings. This simulation has been designed to assess the impact of the waste rock and tailings storage in the reservoir.
- **FRHEP closure** – this simulation is an extension of the operations simulation to assess the change in limnology after the FRHEP operations cease.

Bathymetry

LiDAR data with a 10 × 10 m horizontal resolution was used to generate two sets of orthogonal model grids with 100 × 100 m and 200 × 200m horizontal resolution. The vertical resolution for both was set to 2 m. The cell structure of the 200 × 200 m resolution bathymetry is illustrated in Figure 6-10.

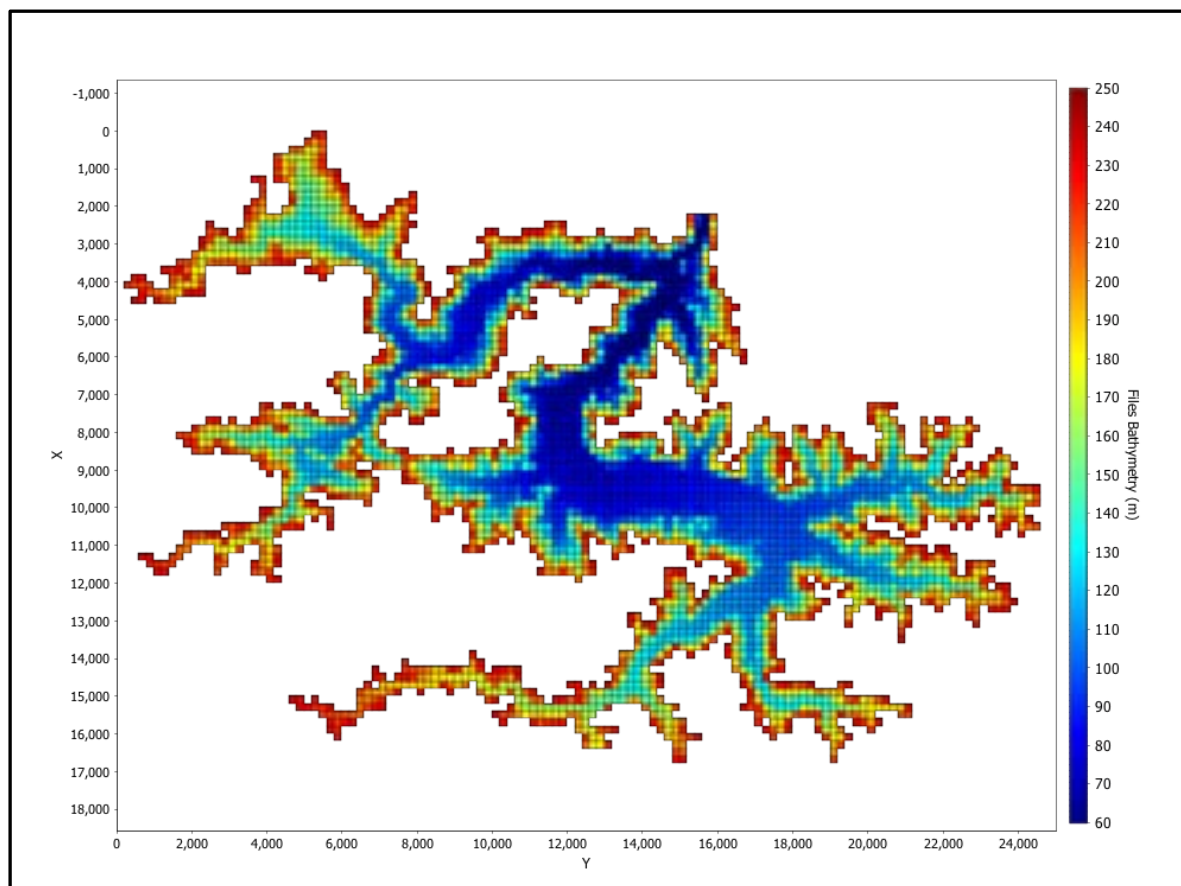


Figure 6-10: Model grid bathymetry with 200 × 200 m horizontal resolution

Note: Horizontal axes and vertical scale are in metres.

Meteorology

Meteorological data recorded at 15-minute intervals at the Nena, Moraupi and Inioke AWS was used for the FRHEP reservoir model. Nena AWS temperature (AT), relative humidity (RH), solar radiation (SR), and wind speed (WS) and direction (WD) data from January 2009 to December 2014 were used to develop a time series for the model. Data from the Moraupi AWS was used to fill gaps in the Nena AWS record, allowing the model's requirement for a continuous time series to be met.

Daily average cloud cover was approximated by comparing solar radiation records at the Nena AWS to theoretical estimates of clear-sky incoming solar radiation at the edge of the Earth’s atmosphere. Synthesised rainfall data for the lower Frieda River catchment was provided by SRK (2017c, realisation #88) and applied as precipitation on the reservoir surface. The temperature of the rainfall was set to the temperature of the reservoir surface.

Inflows and outflows

The model was configured to account for 16 inflow entry points into the FRHEP reservoir (Figure 6-11), with flow rates and sediment concentrations consistent with the sediment transport provided by Golder Associates (using daily flow rates for each tributary based on flow realisation #88). Daily inflow rates were compressed into 6-hour hydrographs, and the shape of each daily hydrograph was extracted from the peak flow assessments.

The temperature of the inflows was assigned using a relationship between streamflow temperature and air temperature derived from the limnology assessment, given by $T_{inflow} = 0.232T_{air} + 14.21$. This relationship was derived using a least-squares fit between water temperature recorded in the Upper Nena River and air temperature at the Nena AWS during 2008. The calculated inflow temperatures include a diurnal variation that follows air temperature and range between 20.1 °C and 23.5 °C (mean of 21.4 °C).

The TSS in each inflow consist of four particle size groups derived by Golder Associates. A specific gravity of 2.65 was assigned to each group.

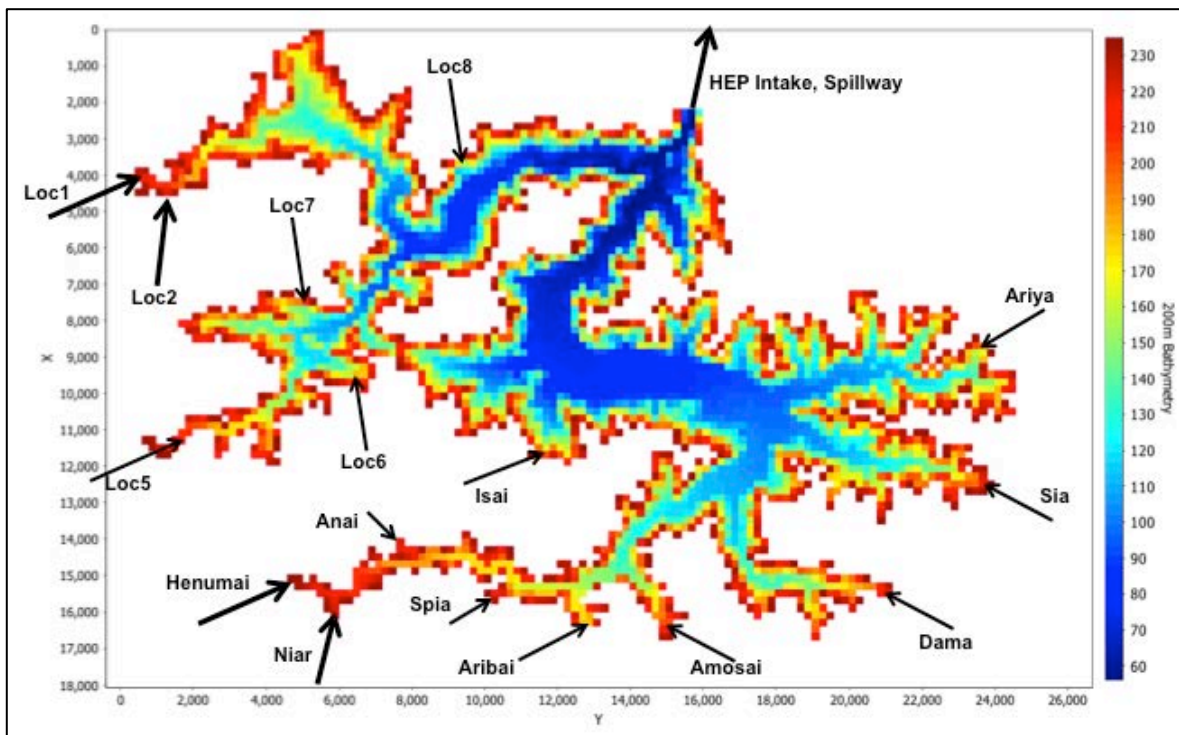


Figure 6-11: Location of modelled inflows

The outflow sequence is based on the modelled water level, with the following embankment operations:

- Extraction of 50 m³/s occurs via the residual flow tunnel for 8 months until the water level reaches RL 171.2 m.
- Extraction then transitions to a lower intake (at RL 143.3 m), with extraction rates following a time series which increases from 50 m³/s to 148.3 m³/s the first few months.
- Extraction switches from the lower intake to the upper intake at RL 185.6 m with intake rates between 148.3 m³/s and 229.9 m³/s.

Assessment of sediment transport

The assessment of the mobility of stored waste rock and tailings is based on the final in-filled storage condition (Figure 6-9). The waste rock and tailings particle size distributions were discretised as per Table 6-2 based on the particle size distribution curves for waste rock and tailings.

Settling rates of resuspended waste rock and tailings are determined in the model from Stokes settling velocity for singular particles without flocculation.

Table 6-2: Waste rock and tailings particle properties

Sediment origin	Size (microns)	Distribution	Critical shear stress (Pa)	Erosion rate (g/m ² /day)
Tailings	1.6	12.1%	1.1E-02	2.0E+07
Tailings	5.4	7.7%	2.4E-02	8.9E+06
Tailings	14.8	11.4%	4.7E-02	4.6E+06
Tailings	50	68.8%	1.0E-01	2.1E+06
Waste rock	1.6	0.44%	1.1E-02	2.0E+07
Waste rock	5.4	0.12%	2.4E-02	8.9E+06
Waste rock	14.8	4.43%	4.7E-02	4.6E+06
Waste rock	40	5%	9.0E-02	2.4E+06
Waste rock	300	10%	2.0E-01	1.1E+06
Waste rock	1000	20%	5.8E-01	3.7E+05
Waste rock	3000	60%	2.2E+00	9.9E+04

6.2.3 Results

Filling

The 10-year simulation with no waste rock and tailings stored in the reservoir was undertaken to assess the behaviour of the reservoir and the downstream release of catchment sediments during the filling and construction phase and continuing through to an operational phase.

Calculated temperature at the embankment (Figure 6-12) illustrates a filling period of approximately 3 years and 4 months over which time a thermal stratification develops and persists for the remainder of the simulation. Temperatures are predicted to reach 26 °C to 32 °C in the surface layer of about 10 m, separated from cooler waters beneath (22 °C to 24 °C) characterised by a strong temperature gradient from 10 m to 30 m deep that weakens below 30 m. The temperatures of the inflows control the temperature of the underlying waters during the filling stage.

The height of the FRHEP intake affects the temperature profiles as indicated when the lower intake at RL 143.3 m ceases and FRHEP intake changes to RL 185.6 m. When operating at a water level of RL 226 m, and after a period of adjustment over 4 years, the stratification consists of a warm, mixed

epilimnion above approximately RL 215 m. Underneath the epilimnion, the upper portion of the metalimnion is defined by gradients from RL 215 m down to RL 185 m that weaken in the lower metalimnion from RL 185 m down to RL 160 m, before reaching the hypolimnion where temperature gradients are weak and near linear.

There are fluctuations in simulated epilimnion temperatures over time as the surface waters equilibrate to warm and cool weather. While the epilimnion and upper metalimnion temperatures and temperature gradients decrease during cooler periods, the model results suggest that this process alone is insufficient to induce significant mixing and the stratification remains intact.

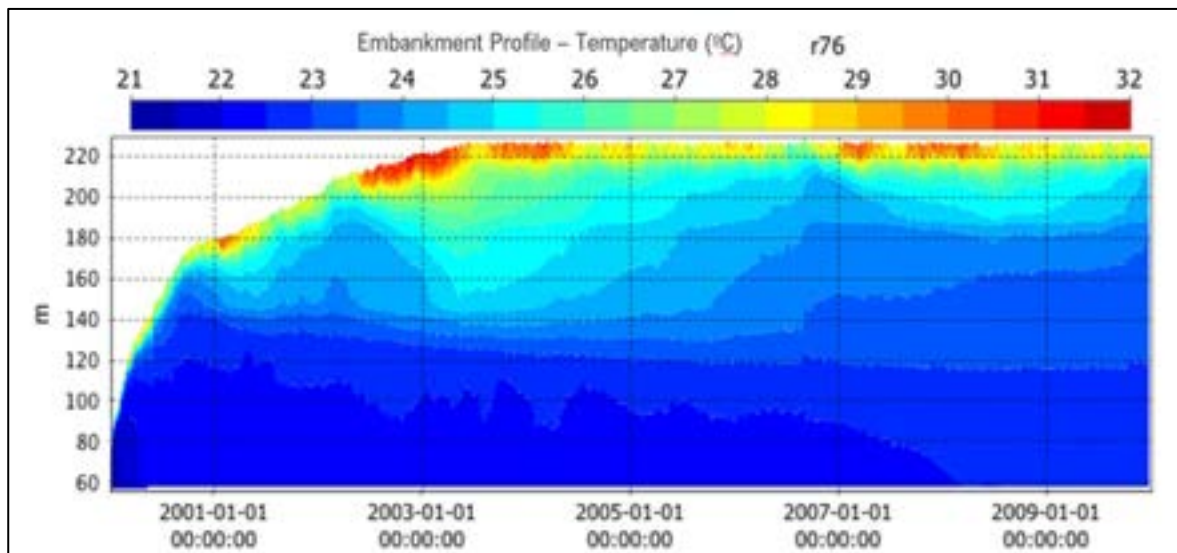


Figure 6-12: Simulation showing temperature profile over time at the embankment during the filling

Overall, the model results suggest that under conditions of median flow (used for the simulations) and over the available range of observed meteorological conditions, the reservoir is likely to be persistently stratified with no regular periods of significant vertical mixing.

The model results also show that inflows to the reservoir traverse the upper reaches as underflows that entrain warmer ambient water before peeling off the reservoir bed as lateral intrusions at a depth of neutral buoyancy within the thermal structure. The depth of the FRHEP extraction within the stratified metalimnion leads to a thinned selective withdrawal layer. Examples of intrusions are shown in Figure 6-13 and Figure 6-14.

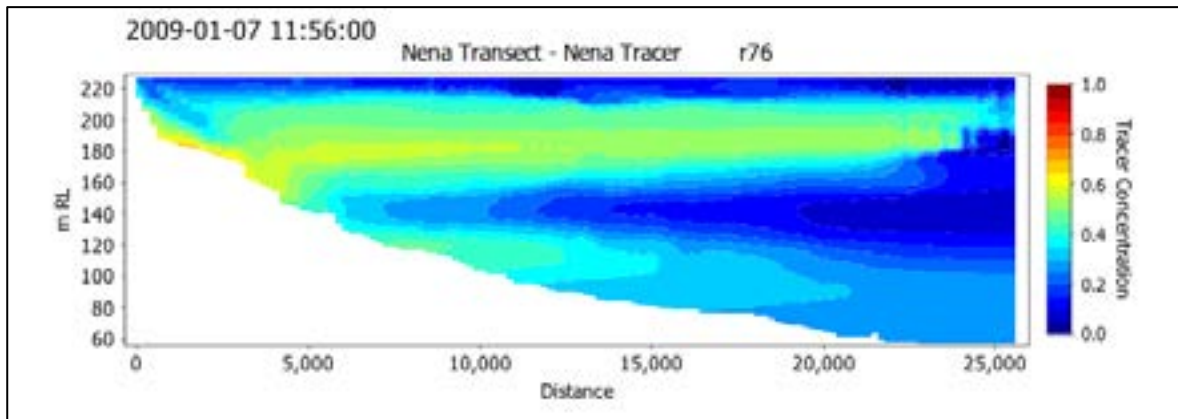


Figure 6-13: Model output from Nena River headwaters (on the left) to the embankment (on the right) on 01/07/2009 showing tracer concentrations from the Nena River as an intrusion across the reservoir

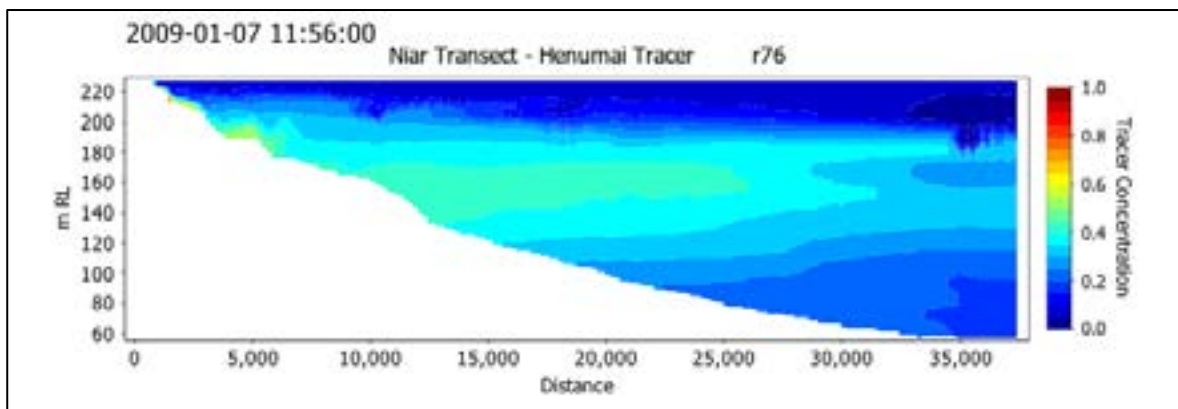


Figure 6-14: Model output from Henumai River headwaters (on the left) to the embankment (on the right) on 01/07/2009 showing tracer concentrations from the Henumai River as an intrusion across the reservoir

Suspended sediments entering the reservoir from the tributaries follow the trajectory of the inflow as described above; however, as the particles settle over time, the extent over which the concentrations are elevated thickens (downwards) as shown in Figure 6-15 and Figure 6-16. The attributes of the particles dictate settling velocity; the 2-micron particles take approximately 12 months to settle from the metalimnion to the bed once they reach the embankment (a vertical travel distance of 120 m). Larger particles (4-micron)) settle significantly faster (in approximately 3–4 months). The TSS in the reservoir therefore comprise mostly the finest particle fractions that remain in suspension longer.

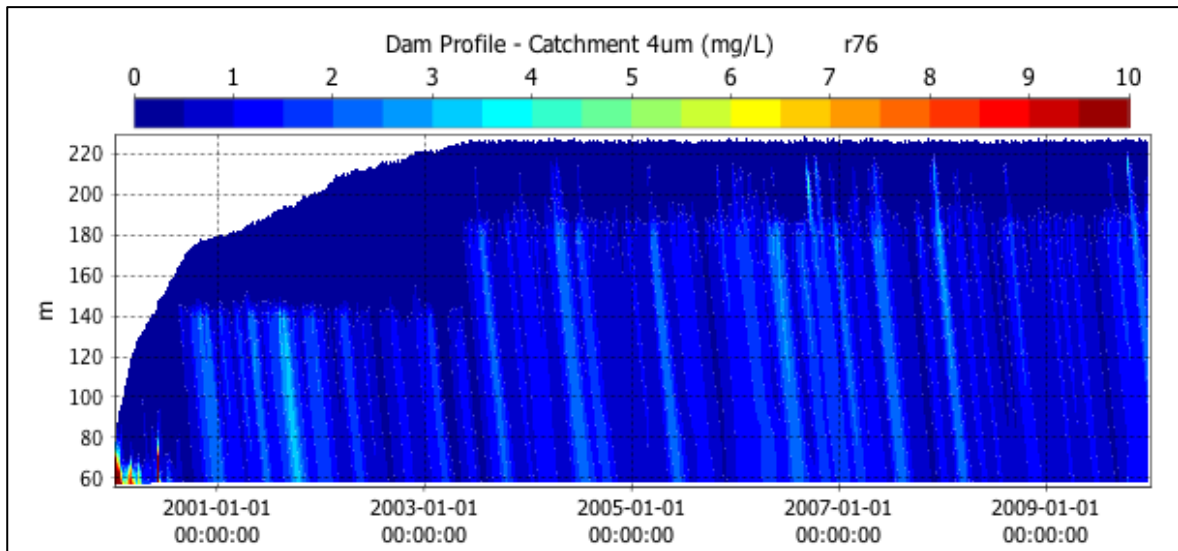


Figure 6-15: Simulated concentration of 4-micron particles from catchment loads at the embankment during filling

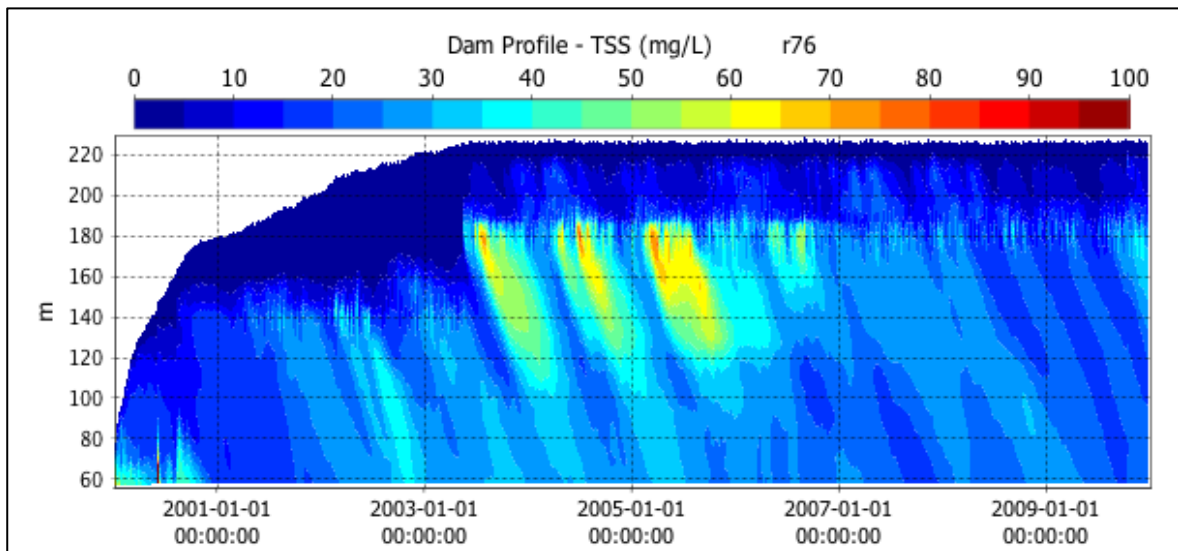


Figure 6-16: Simulated concentration of TSS from catchment loads at the embankment during filling

A summary table of sediment concentrations in the downstream release water is provided in Table 6-3. The results show that during the filling simulation less than 7% of the incoming catchment sediments, which includes sediment contribution from FRCGP activities upstream of the reservoir, would be released from the embankment. Average concentrations are predicted to be highest at approximately 50 mg/L during operation of the residual flow tunnel, reducing to an average release concentration of approximately 16 mg/L (combined hydroelectric power and spillway) when the upper intake is operating. A large majority of the released sediment is the finest 2-micron size fraction.

Table 6-3: Summary table of sediment in downstream release water

Simulation	Percentage of incoming sediments released downstream		Average concentrations	
	TSS (%)	Catchment 2-micron (%)	TSS (mg/L)	2-micron catchment (mg/L)
Filling simulation				
Residual flow tunnel	5.5	16.5	49.4	40.0
Lower intake	4.6	15.3	17.4	16.7
Operations hydroelectric power	6.2	19.9	22.1	21.3
Spillway	0.7	2.2	4.1	4.0
Operations hydroelectric power + spillway	6.9	22.1	16.4	15.8
Operations simulation – equal mobility – hydroelectric power open				
Operations hydroelectric power	7.0	23.0	12.8	12.0
Spillway	0.2	0.6	2.5 m	2.4
Operations hydroelectric power + spillway	7.2	23.6	12.0	11.2
Operations simulation – derived mobility – hydroelectric power open				
Operations hydroelectric power	7.1	23.1	12.9	12.1
Spillway	0.2	0.6	2.5	2.5
Operations hydroelectric power + spillway	7.3	23.7	12.0	11.3
Hydroelectric power –equal mobility – closure simulation				
Spillway	4.7	15.3	7.0	6.6
Hydroelectric power – closure simulation – derived mobility				
Spillway	4.7	15.3	6.9	6.6

Barge deposition

The impact of barge deposition of waste rock was assessed by applying a continuous deposition of 18 × 5,000 t barges per day at sites 1 km, 2 km and 4 km upstream of the embankment in the Nena arm. The results in Figure 6-17 show a clear reduction in waste rock contribution to TSS in the intake waters as the barge deposition location moves upstream from the embankment. There is also a shift in the particle size distribution of waste rock material reaching the embankment. When barge deposition occurs at 1 km from the embankment, the TSS contribution from barged waste rock material in the intake water is dominated by a contribution of 14.6-micron particles – the TSS in the intake water may reach 300 mg/L. When barging takes place at distances further from the embankment, the overall TSS and waste rock material contribution is increasingly dominated by the finer fractions that settle more slowly. For barge deposition 4 km upstream, the results indicate that the catchment contributions (and not the contributions from waste rock material) dominate TSS concentrations in the intake water.

For each scenario, and aside from diurnal fluctuations (in response to the 6-hour hydrograph), the results also show there is a relatively steady-state contribution from waste rock sediment to the intake TSS when the deposition rate and location are constant. While there is a period of increase in TSS in the intake water at the beginning of the simulation and some lower-frequency changes (in response to the hydrodynamics) thereafter, the model does not suggest an upward trend in waste rock contribution to the TSS in the intake water over the period of the simulation. It is therefore likely that the TSS contribution from waste rock material in the intake waters will adjust to the proposed barge deposition schedule to reach a steady state that is dependent on the location and rate of deposition (frequency of barge dumping at any given location). A rapid return to background conditions is likely at the end of the barge deposition period.

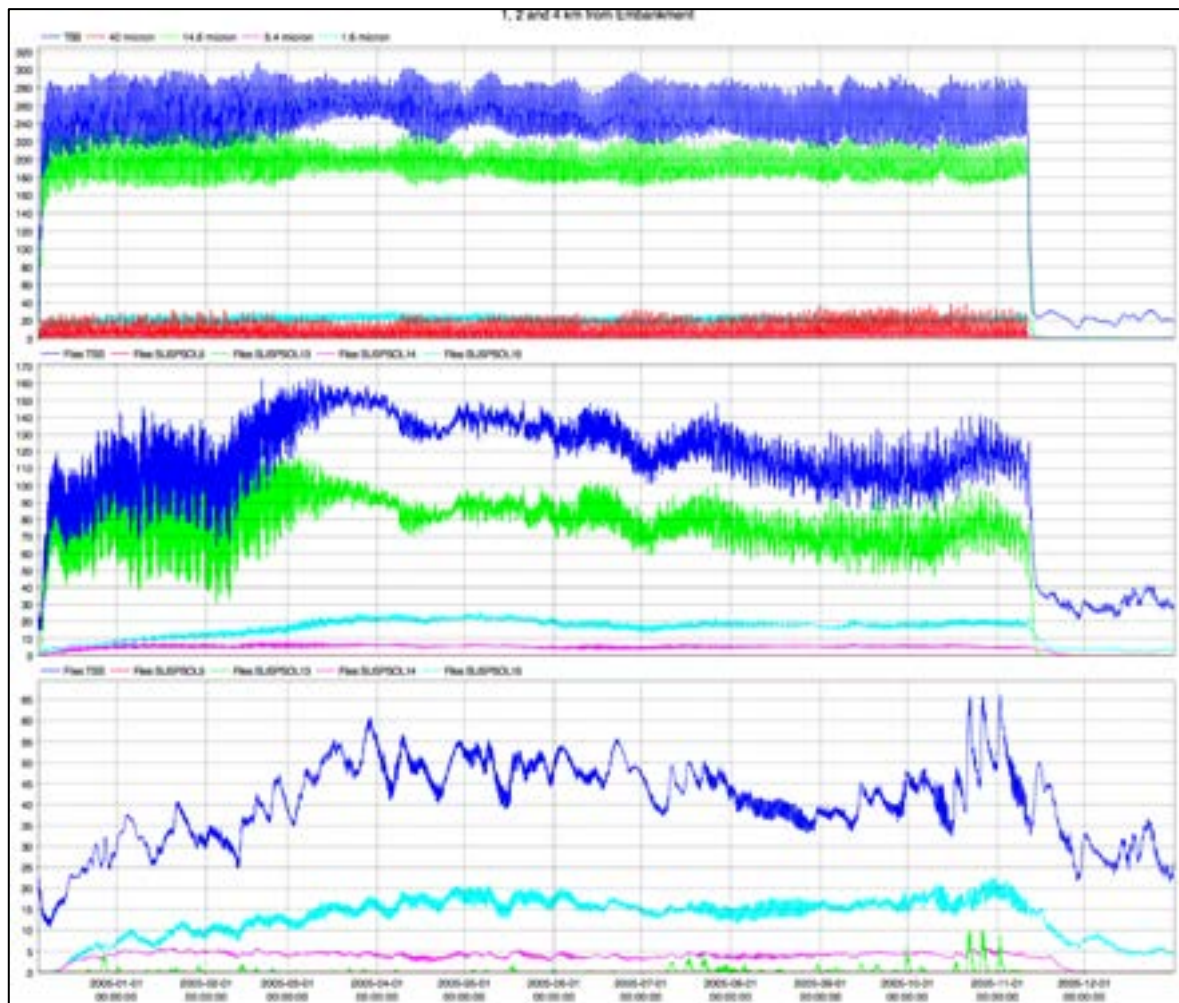


Figure 6-17 Simulated concentrations of fine waste rock sediments and TSS in the intake water during continuous barge disposition (18 barges per day) at 1 km (top), 2 km (middle) and 4 km up the Nena arm (bottom) from the embankment

6.2.4 Summary and recommendations

The model results suggest that the FRHEP reservoir is likely to be stratified at all times, with no regular periods of complete mixing, and that deposition of waste rock and tailings beneath the epilimnion is unlikely to alter the top-down stratification structure. Modelled inflows from the major rivers form intrusions through the reservoir at a depth of neutral buoyancy following an initial plunge near their headwaters. In addition to the inflows, the FRHEP intake rate and depth play an important role in shaping the stratification and promoting short-circuiting of inflow waters through the reservoir.

Despite preferential flow paths of the catchment inflows (which carry high sediment loads), a large portion of the natural catchment sediments is predicted to settle at the bottom during the time it takes for the inflows to travel through the body of the reservoir. The settled material falls into the deeper waters of the reservoir that are beneath the FRHEP intake and accumulate on the bed. While some degree of resuspension of the settled catchment material may occur, this is likely to occur only periodically in the upstream reaches when flow events of sufficient size create enough bed stress to mobilise the settled material. Bed stress declines in deeper areas away from the headwaters and mobilisation after settling at locations away from the headwaters decreases.

The modelling indicates that deposition near the embankment (1–2 km) at high deposition rates is likely to have a significant impact on TSS concentrations at the embankment (and inflow into the FRHEP intakes) due to the slow settling rate of the fine fraction of the barged waste rock material.

There is uncertainty associated with all elements of this study phase given that the model cannot be calibrated and validated; however, some uncertainties can potentially be addressed. The first is to investigate the critical shear stress at which the waste rock and tailings mobilise and the resultant rate of erosion. There are uncertainties associated with the mobility of the waste rock and tailings that are stored in the reservoir; addressing these uncertainties will require additional information about the potential mobility of the waste rock and tailings particles (from laboratory analysis) and re-simulation of their mobility in the FRHEP reservoir using the additional information under a range of environmental conditions (such as high flows and storms).

Future modelling works should also consider additional scenarios to assess the potential in-lake and downstream impact of a failure of the tailings deposition pipes. The extent of the impact will depend on the size and location of the failure in the reservoir – most critically the distance from the embankment – and the depth of the failure.

Long-term changes (i.e. up to 100 years) in the limnological behaviour that occur in response to changes in flow and meteorology have not been considered, but should form part of future investigations.

Consideration should also be given to the operational rules of the FRHEP reservoir to avoid large and frequent fluctuations in water levels that would put strain on littoral habitats and potentially reduce the likelihood of establishing a lake with good water quality.

6.3 Load balance (water quality assessment)

The FRCGP comprises a large-scale conventional open pit mine operation, including the development of two open pits and production of ~1.56 Bt of waste rock and ~1.1 Bt of tailings that will be deposited in the reservoir.

The objective of the load balance model is to provide information for site-wide water management and generate predictions of potential water qualities associated with the open pits, discharge from the ISF and a range of AP locations downstream of the embankment.

A solute load balance was set up to assess the potential impacts of mining operations, and tailings and waste disposal in the reservoir on water quality in the impoundment and in downstream watercourses. The load balance was developed based on the results from the water balance described in Section 6.1.

The approach and assumptions to estimate the solute concentrations in the discharge from the ISF and at downstream assessment points are described in the following sections. The water and load balance is reported in SRK (2018d).

The assessment relied on results from historical geochemical characterisation programs to support solute release calculations. The geochemical properties of the waste rock and tailings are summarised in Section 6.3.1.

6.3.1 Tailings and waste rock geochemistry

Waste rock geochemistry

Several geochemical testing programs for ore and waste rock from the HITEK deposit have been undertaken. Static and kinetic testing of the major lithological units indicated that acid generation from waste rock is likely to be a significant risk (EGi, 1996, 2011). In general, the results indicate that the lithological units differ little in terms of acid generating properties within the limits of the final pit shell. The maximum potential acidity (MPA) values, calculated from the total sulphur content, exceed the generally low acid neutralisation capacity (ANC) values.

The results further suggest that the quantity of non-acid forming (NAF) materials that may be present in the waste rock would be small.

Kinetic testing was completed to assess the rate of oxidation and estimate solute release rates from the various waste rock types. The testing program, comprising a total of nine column tests, was completed by EGi (2011). Descriptions of the samples and their acid generation properties are provided in Table 6-4.

Table 6-4: Samples selected for column testing

Column ID	Sample Description	Total S (%)	MPA	ANC
Column HIT WR-1	DVP (Argillic alteration)	6.19	190	0
Column HIT WR-2	DVP (silica-alunite alteration)	2.68	82	0
Column HIT WR-3	HMD (Argillic alteration)	3.66	112	0
Column HIT WR-4	HMD (Potassic alteration)	2.81	86	14
Column HIT WR-5	HMD (Phyllic alteration)	3.38	104	1
Column HIT WR-6	LW (Potassic alteration)	2.12	65	9
Column HIT WR-7	FDP (Propylitic alteration)	2.72	83	10
Column HIT WR-8	FDP (Phyllic alteration)	1.35	41	12
Column HIT WR-9	HMD (Phyllic alteration)	5.41	166	0

The results showed that all samples were net acid generating and the kinetic tests generated acidic leachates in the longer term. While some of the samples had some available ANC, it was rapidly consumed. The concentrations of some key parameters are listed in Table 6-5.

Table 6-5: Summary of kinetic test leachate properties

Parameter	Units	Leachate concentrations	
		Reactive materials Tests 1, 2, 3, 5, 7 and 9	Less reactive materials Tests 4, 6 and 8
Leachate pH		<3	6–4
SO ₄	mg/L	1200–7,000	100–200
Fe	mg/L	200–7,000	0.1–10
Al	mg/L	150–1000	0.01–1
Cu	mg/L	2–2000	0.01–1
Zn	mg/L	0.5–200	0.01–1
Mn	mg/L	0.1–40	0.1–10
Co	mg/L	0.4–7	0.01–0.1
Ni	mg/L	0.3–10	0.001–0.1
As	mg/L	0.01–2	<0.001
Cr	mg/L	0.02–1	<0.001
Cd	mg/L	0.001–1	0.0001–0.01

As indicated by the elevated sulphate (SO₄) concentrations in Table 6-5, high rates of oxidation are expected for most of the waste rock materials. The absence of ANC further indicates that the waste rock materials would likely become acidic rapidly, with short lag times expected unless oxidation is limited. The leachate chemistries further indicate that elevated concentrations of metals (in particular copper, iron and aluminium) would be expected from the waste rock when exposed to oxidising conditions. The results further indicated that the oxidation rates and metal release rates are more closely correlated to the alteration type rather than the lithological description.

Waste rock classification

FRL developed a waste rock classification strategy that primarily uses the sulphur content to classify the waste rock into four different categories – Green, Amber, Red and High Red (Table 6-6). The quantities of waste rock that will be produced each year, the waste rock classification and average sulphur content are summarised in Table 6-7.

The waste rock in the Green category is considered to have a low risk of acid generation and metal leaching. The risk of acid generation and metal leaching increases significantly with increasing sulphur content for the Amber, Red and High Red categories. During the initial two years, more waste rock would be classified in the Green category, which is expected to have a lower risk of acid generation. In subsequent years, the proportion of waste rock with higher sulphur grades will increase significantly accompanied by a proportionate increase in risk of acid generation. Overall, only approximately 14% of the waste rock would be classified as Green, with the majority classified as net acid generating, and 69% falling within the highest risk category (High Red).

Table 6-6: Waste rock classification criteria

Waste rock category	Average S (%)	Maximum S (%)
Green	0.18	0.47
Amber	0.73	0.97
Red	1.99	2.96
High Red	5.27	11.5

Table 6-7: Summary of waste rock production schedule and classification ⁷¹

Year	Waste rock category (t)					Total waste rock (t)
	Organic	Green*	Amber	Red	High Red	
-1	480,558	3,446,293	197,714	2,231,007	714,882	6,589,896
1	953,905	13,665,489	1,798,383	5,017,966	3,489,267	23,971,106
2	1,232,827	16,544,076	4,041,437	16,864,643	7,549,843	45,000,000
3	990,421	16,378,879	2,747,295	11,202,591	11,221,249	41,550,014
4	840,893	16,251,467	2,564,279	10,070,204	16,114,050	45,000,000
5	1,371,384	21,203,510	2,422,675	6,596,386	5,697,129	35,919,700
6	1,186,103	20,010,748	1,832,940	9,706,271	13,450,041	45,000,000
7	783,266	15,263,884	1,837,918	10,770,344	17,127,854	45,000,000
8	1,021,972	15,249,914	3,742,002	14,542,851	31,465,234	65,000,000
9	805,165	11,595,475	1,356,446	14,428,978	37,619,101	65,000,000
10	279,050	4,775,593	657,436	13,041,092	46,525,879	65,000,000
11	821,520	7,623,383	970,996	9,224,475	47,181,146	65,000,000
12	650,535	11,255,514	1,186,785	5,609,729	46,947,973	65,000,000
13	428,990	7,925,587	1,693,420	12,466,658	42,914,336	65,000,000
14	312,306	3,316,062	1,318,694	8,251,232	52,114,012	65,000,000
15	168,100	1,746,487	441,688	2,948,731	59,863,094	65,000,000
16	137,827	2,601,328	504,170	6,575,831	55,318,672	65,000,000
17	31,111	420,578	186,581	8,931,494	55,461,346	65,000,000

⁷¹ FRL_HITEK_V2b_OPTv4_phase_1604v1_Sch1e_Final_ARD

Year	Waste rock category (t)					Total waste rock (t)
	Organic	Green*	Amber	Red	High Red	
18	48,247	1,123,907	396,781	2,303,543	61,175,769	65,000,000
19	393,652	5,838,677	1,826,707	3,559,852	53,774,764	65,000,000
20	233,714	4,348,106	1,697,149	5,300,263	53,654,483	65,000,000
21	212,788	1,836,649	905,047	6,673,985	55,584,318	65,000,000
22	261,843	6,449,305	1,223,202	4,934,344	52,393,150	65,000,000
23	139,424	1,545,943	372,354	7,155,633	51,457,334	60,531,264
24	266,442	4,180,773	1,313,382	7,962,456	51,543,389	65,000,000
25	171,117	2,285,076	713,221	6,878,230	55,123,472	65,000,000
26	56,520	670,409	446,708	4,975,826	46,600,140	52,693,082
27	-	94,571	557,455	3,176,196	35,941,861	39,770,084
28	-	0	494,609	946,832	5,262,396	6,703,837
29	-	24,861	328,466	716,453	1,668,241	2,738,021
30	-	0	66,185	647,335	1,152,414	1,865,933
31	-	0	0	362,851	464,103	826,954
32	-	0	0	0	0	0
33	-	0	0	0	51,290	51,290
Total	(14,279,680)	217,672,541	39,842,127	224,074,283	1,076,622,231	1,558,211,182
Distribution	(1%)	14%	3%	14%	69%	100%

Note: * Mass reported for Green waste rock includes Organic waste.

Implications for waste rock management

The absence of significant ANC in any of the waste rock means that oxidation should be precluded as soon as possible after the rock is mined. Subaqueous waste disposal and storage is the only proven method to meet this objective.

The proposed strategy for waste placement is barge dumping, i.e. the waste rock will be flushed with lake water as it sinks to the bottom of the ISF. All solutes generated from oxidation prior to deposition in the ISF are expected to be released from the waste rock when deposited.

Depending on the mining schedule and methodology, the duration of exposure prior to subaqueous deposition may be relatively short; however, as noted above, some materials have a very short lag time to acidification. Solute release may therefore be significant for materials with a high sulphide content and deposition of these materials should be prioritised to keep exposure times as short as possible before inundation. Secondary mitigation strategies to limit solute release may include blending of limestone or lime with the waste rock to neutralise acidity and precipitate metals to prevent mobilisation when deposited in the ISF.

Tailings geochemistry

Initial testing by EGi (EGi, 2011) indicated that tailings with a sulphur content as low as 0.23% sulphide sulphur (MPA of 7 kg H₂SO₄/t) may potentially be acid generating (NAG testing – NAG-pH of 4.1).

Initial column tests completed on the high sulphur (1.53% S) and low sulphur (0.23% S) tailings samples indicated that the lag time for acid generation from the high sulphur tailings would be in the order of 12–14 weeks. The leachate from the low sulphur sample remained circum-neutral in pH until about week 68 after which the pH decreased to below 5. The leachate pH decreased below 4 after about 77 weeks.

The results further indicated that should the tailings oxidise, the tailings would leach metals at concentrations that may potentially be of environmental significance, including copper (above 40 mg/L), cobalt (0.16 mg/L), manganese (1.4 mg/L) and nickel (0.12 mg/L). As the tailings become more acidic, the concentrations of these and other metals would be expected to increase.

The static and kinetic test results indicate that the tailings are likely to be net acid forming unless disposed of subaqueously. The kinetic test results show the lag time for tailings may be as short as 12 weeks (3 months) before a decrease in pH can be expected. These outcomes indicate that subaerial tailings deposition and formation of tailings beaches could lead to the release of metals. Therefore, the preferred disposal strategy for tailings is subaqueous deposition.

6.3.2 Solute source term derivations

The solute and suspended sediment sources that may contribute to the water quality in the FRHEP reservoir include:

- Upstream and downstream background flows, including creeks upstream of the HITEK pits, the Niar River and the Nena River upstream of the FRHEP, and associated tributary creeks and natural runoff downstream of the FRHEP
- Wall rocks in the open pits and/ or treated discharge water
- Ok Binai valley failing organic waste spoil dump
- Waste rock deposited in the reservoir by barge
- Process tailings and associated discharge water
- Runoff from quarries and other earthworks
- Cut and fill for construction of haul and access roads
- Foundations and pads at the process plant, FRCGP and site accommodation village
- Temporary low grade ore stockpiles.

Shorter term sources that would occur during the construction phase only may also contribute solute loadings to the downstream environment. These sources – quarry for embankment construction fill material and temporary stockpiles of mineralised material associated with the construction – will generally be inundated as the level of the FRHEP reservoir rises and are unlikely to be significant in the context of the current assessment.

Many of these sources will also release TSS upstream of, and directly to, the FRHEP, and downstream of the FRHEP. The TSS released from these sources have been determined by Golder Associates (2018) and transport within the FRHEP has been assessed in Section 6.2. The outcomes of these calculations have been incorporated in the water quality estimates presented herein.

The following sections briefly describe the approaches adopted for each of the key sources that contribute solutes to the reservoir and FRHEP discharge water quality.

Background loadings

Background solute loadings for all inflows and downstream tributaries were obtained from water quality monitoring undertaken from 2007 to early 2013.

Open pit wall rock runoff

Wall rocks will be exposed following blasting and removal of the broken material. Depending on the mining efficiency, broken rock may remain on the walls (as a result of blast damage) and on the benches (as uncleared rubble). Considering the high rainfall environment, it is likely that erosion of the pit walls will occur, resulting in accumulation of talus on the benches. The talus would contain

coarse and fine particle sized materials from the walls; these accumulations would represent shallow 'waste rock deposits', having geochemical properties similar to the materials contained in the batter wall rock. The shallow nature of the material accumulation (compared to full-scale waste rock dumps) means it would be relatively oxygenated and could therefore react at the maximum rates of oxidation measured for corresponding materials.

In contrast, oxygen ingress to the fractured or blast damaged wall rocks could, depending on the severity of the fracturing, be limited to diffusion-controlled flux. Competent wall rocks with narrow fractures would therefore react more slowly, but as a result, are expected to react over a much longer timeframe before the sulphide minerals are depleted. Therefore, contaminants reporting to the open pit sump could come from two sources:

- Oxidation of the accumulated talus on the open pit benches
- Oxidation of the fractured wall rock on the batters and benches.

The general approach adopted to estimate solute generation rates was as follows:

- 1 Calculate wall rock exposure by material reactivity category [Green, Amber, Red, High Red (EGi, 2016)] based on the open pit development sequence and block modelling outcomes.
- 2 Estimate mass equivalents of reactive materials based on talus and wall rock exposure.
- 3 Assign solute generation rates based on average steady-state kinetic test release rates. (Due to the high rainfall environment, it was assumed that most of the solutes generated would be flushed, except where solubility controls may apply.)

FRL developed the surface areas exposed by material category and incorporated these directly into the calculations. The exposure schedule comprises a series of pit development phases that coincide with the open pit development over time. This material is conservatively assumed to be fully oxygenated – the sulphate and metal release rates can therefore be estimated from the kinetic testwork previously completed as part of the tailings and waste geochemical characterisation programs.

Solute release from intact wall rock may depend on several factors including the degree of fracturing, depth of fracture damaged zone, reactivity of the exposed wall rock and depth of oxygenation. Since there are no standard methods or models to assess solute release from wall rocks, a simplified approach based on the potential for oxygen diffusion into the wall rock was used.

The last step in the calculations is to assign solute release rates to each material type. These were obtained from the kinetic testing results as reported in EGi (2016). The steady-state solute release rates for each material type as reported by EGi were adopted for the calculations.

Groundwater inflows

Groundwater inflows to the open pits will also contribute to the solute loadings reporting to the open pit sumps. The groundwater quality parameters adopted for the analysis are summarised in Table 6-8. Flow volumes are as described in the Section 6.1.2.

Table 6-8: Summary of average groundwater inflow quality

Parameter	Units	Average	Maximum
pH	s.u.	6.3	7.8
EC	µS/cm	1002	2260
TDS	mg/L	651	1470
Total Hardness	mg/L	577	1520
Bromide (Br)	mg/L	0.02	0.05
Bicarbonate Alkalinity	mg/L	29	77

Parameter	Units	Average	Maximum
Total Alkalinity	mg/L	29	77
Sulphate (SO ₄)	mg/L	533	1460
Chloride (Cl)	mg/L	1.3	5.0
Calcium (Ca)	mg/L	226	599
Magnesium (Mg)	mg/L	3.3	8.0
Sodium (Na)	mg/L	8.0	23.0
Potassium (K)	mg/L	1.6	3.0
Aluminium (Al)	mg/L	0.30	2.2
Arsenic (As)	mg/L	0.0022	0.015
Beryllium (Be)	mg/L	0.0005	0.0005
Barium (Ba)	mg/L	0.019	0.065
Cadmium (Cd)	mg/L	0.00006	0.00020
Chromium (Cr)	mg/L	<0.0005	<0.0005
Cobalt (Co)	mg/L	0.002	0.007
Copper (Cu)	mg/L	0.026	0.507
Lead (Pb)	mg/L	<0.0005	<0.0005
Manganese (Mn)	mg/L	0.287	0.944
Molybdenum (Mo)	mg/L	0.0006	0.002
Nickel (Ni)	mg/L	0.0018	0.006
Selenium (Se)	mg/L	<0.005	<0.005
Strontium (Sr)	mg/L	2.2	5.6
Vanadium (V)	mg/L	<0.005	<0.005
Zinc (Zn)	mg/L	0.015	0.063
Boron (B)	mg/L	0.025	0.025
Iron (Fe)	mg/L	1.2	17
Mercury (Hg)	mg/L	<0.00005	<0.00005
Silicon as SiO ₂	mg/L	32	55
Fluoride (F)	mg/L	0.140	0.500

Source: AGE 2016; detection limits used where results were below detection limits.

Treated discharge water quality

All contact water collected from the open pits, including haul roads adjacent to the open pits, will be treated in the water treatment plant. The treatment plant is to be located close to the HIT pit, and treated water will be discharged to Ubai Creek (upstream of AP1) and will flow into the FRHEP. The proposed treatment process will comprise a high density sludge (HDS) lime treatment system. The water treatment solids (sludge of metalliferous precipitates) will be piped to the process plant, discharged to the tailings launder and deposited with the tailings in the FRHEP reservoir.

The assumed solute concentrations in the treated water, based on geochemical speciation modelling (using PHREEQC) and benchmarked against operating HDS systems (e.g. GARD Guide, 2016), are given in Table 6-9. The range represents variability in water quality that may result from treatment of influent water quality within the range of that predicted for the open pits. While treatment criteria have not yet been established, targeting the higher end of the pH range would generally result in lower dissolved metal concentrations. Conservatively, however, the higher concentration values in the given range have been adopted, other than for alkalinity and pH.

Table 6-9: Assumed treated water quality (dissolved concentrations)

Parameter	Units	Range	
pH	s.u.	9.5	9.0
Total Alkalinity	mgCaCO ₃ /L	200	100
Silver (Ag)	mg/L	0.001	0.001
Aluminium (Al)	mg/L	0.077	1.0
Arsenic (As)	mg/L	0.044	0.001
Barium (Ba)	mg/L	0.004	0.001
Calcium (Ca)	mg/L	499	600
Cadmium (Cd)	mg/L	0.004	0.004
Cobalt (Co)	mg/L	0.090	0.09
Chromium (Cr)	mg/L	0.002	0.02
Copper (Cu)	mg/L	0.020	0.05
Iron (Fe)	mg/L	0.026	0.5
Nickel (Ni)	mg/L	0.060	0.2
Lead (Pb)	mg/L	0.010	0.001
Selenium (Se)	mg/L	0.010	0.04
Sulphate (SO ₄)	mg/L	2106	1400
Zinc (Zn)	mg/L	0.020	0.07

Tailings water quality

With tailings being deposited subaqueously, no beaches will form. Since the submerged tailings would not be expected to oxidise after inundation, no further solute release is expected to occur from the tailings solids, other than the expulsion of porewater after deposition and settling of the tailings solids. The solute contribution from the tailings is therefore the solutes present in the process water at the time of deposition. The process water quality adopted for the load balance is shown in Table 6-10.

Table 6-10: Summary of tailings water quality

Parameter	Units	Average
pH	s.u.	7.7
Alkalinity, Total (as CaCO ₃)	mg/L	28
Ammonia as N	mg/L	0.164
Total Nitrogen	mg/L	0.488
Total Phosphate as P	mg/L	0.073
Sulphate (SO ₄)	mg/L	1600
Dissolved Metals		
Aluminium (Al)-	mg/L	0.313
Antimony (Sb)-	mg/L	0.001
Arsenic (As)-	mg/L	0.001
Barium (Ba)-	mg/L	0.030
Cadmium (Cd)-	mg/L	<0.00025
Cobalt (Co)-	mg/L	0.002
Copper (Cu)-	mg/L	0.031
Iron (Fe)-	mg/L	<0.030

Parameter	Units	Average
Lead (Pb)-	mg/L	0.005
Manganese (Mn)-	mg/L	0.032
Mercury (Hg)	mg/L	<0.000010
Molybdenum (Mo)-	mg/L	0.055
Nickel (Ni)-	mg/L	0.008
Selenium (Se)-	mg/L	0.033
Silicon (Si)-	mg/L	1.048
Silver (Ag)-	mg/L	<0.000050
Strontium (Sr)-	mg/L	3.014
Uranium (U)-	mg/L	0.0002
Zinc (Zn)-	mg/L	<0.015

Source: G&T Metallurgical Services Ltd (G&TMS) Canada as referenced in EGi, 2016.

Waste rock

Only organic waste (classed as green or non-reactive waste) will be placed in the failing organic waste spoil dump located at the head of the Ok Binai valley. The organic waste will comprise primarily soils and pre-strip generated at development of the open pit, and then during subsequent pushbacks, and is expected to contain little or no sulphide mineralisation. The materials will therefore not be a source of acid generation and metal leaching, and no solute source term was generated for the waste spoil dump. However, the dump will continually fail and will result in the transport of TSS to the Ok Binai River which will then be carried to the FRHEP in a relatively isolated zone of the reservoir.

The balance of the waste rock will be deposited in the ISF by barge dumping. The waste rock production schedule is provided in Table 6-6. The waste rock will be generated when fractured by blasting and will then be crushed and transported to the FRHEP for deposition. While the time between blasting and transport is expected to be 4–6 weeks, the wall rock will remain in place in some areas for much longer and will be a function of the staging of mining the open pit (i.e. there may be periods of several years before a pushback is mined, during which time the wall rock and talus will have continued to oxidise). Therefore, at times the waste rock will be relatively fresh when mined, and at other times it may have been exposed for an extended period and may have accumulated solutes that will be released when placed in the FRHEP.

On average however, waste rock will be blasted, mined, crushed and transported for deposition within a few weeks. Therefore, for the purposes of calculating solute generation rates, it was assumed that the waste rock will typically be exposed for up to 12 weeks (i.e. 3 months) before being deposited in the FRHEP by barge.

The humidity cell test results were used to estimate the rate of solute release from waste rock based on the assumed exposure times. It was then assumed that all soluble solutes generated from the oxidation of the waste rock will be released to the water column in the ISF.

Blast residues

Blasting of the waste rock will employ an ammonium nitrate fuel oil (ANFO) emulsion explosive. Missed rounds and spillage will lead to release of ammonium nitrate. The ammonium and nitrate levels that are expected to be released from the blasted waste rock were estimated based on an average powder factor of 0.098 kg/t rock (as provided by FRL) with an assumed loss of 1% (ORICA advised that a loss of between 0.6% and 1.3% is typical for large-scale operations). All the ammonium nitrate thus released was assumed to report to i) the process water in the tailings (from ore), and, ii)

the water column when the waste rock is deposited in the ISF. Total loadings were established based on the ore and waste rock production rates.

Total suspended solids

Background TSS concentrations and suspended solids release and transport from construction activities were generated by Golder Associates. The estimates of TSS loadings produced by Golder for the catchments upstream of the FRHEP were then used to assess the natural sediment loadings into the FRHEP, and incorporated into the limnological modelling.

The waste production modelling undertaken by FRL indicated that the waste rock that will be produced can be classed in three categories of hardness as shown in Table 6-11. In general, crushed hard rock will be expected to have a lower fines fraction than soft rock, with the soils and overburden type materials likely to contain the highest fraction of fines. The assumed particle size distributions for the hard and soft waste rock are shown in Table 6-12.

Initial modelling completed by HydroNumerics indicated that deposition of finer materials such as soils within 1 km of the FRHEP embankment would result in very high TSS concentrations since the retention time within the FRHEP would be too short to allow the fines to settle to an elevation below the hydroelectric power intake.

To negate this, the barge deposition was scheduled based on the following assumptions:

- Only hard rock waste will be deposited within the distance range of 1–2 km from the embankment in either the Niar or Nena River arms, and daily deposition rates within this zone will not exceed 90,000 tonnes per day;
- Only soft and/or hard rock waste will be deposited within 2–4 km from the embankment, and deposition rates will not exceed 100,000 tonnes per day within this zone; and,
- All remaining waste (i.e. soft rock comprising soils and overburden type materials) will be deposited 4 km or more from the embankment, irrespective of deposition rates.

FRL also required that early deposition of waste rock be as close as possible to the process plant facility (i.e. >4 km from the embankment). A preliminary deposition schedule based on these requirements is shown in Figure 6-18. The plot shows the cumulative placement within each the waste zones.

To apply these calculations to the placement schedule shown in Figure 6-18, the steady-state TSS values for each zone were corrected by multiplying the concentration with the ratio of the scheduled production rate to the modelled production rate, and then summing the TSS concentrations for all zones. Based on the TSS capture assessment for the FRHEP completed by HydroNumerics, the fines associated with tailings deposition will be attenuated within the FRHEP (i.e. TSS reporting downstream of the ISF mostly represent fine material from waste rock deposition).

Table 6-11: Summary of waste rock production by hardness

Period	Soil+Clay (t)	Soft (t)	Hard (t)
1	3,231,409	3,336,852	21,635
2	10,573,853	12,339,444	1,057,810
3	12,218,968	29,381,733	3,399,299
4	10,945,338	29,344,064	1,260,611
5	11,703,669	26,693,149	6,603,182
6	13,377,295	21,520,059	1,022,346
7	15,632,644	24,118,072	5,249,284
8	13,980,796	26,420,234	4,598,970

Period	Soil+Clay (t)	Soft (t)	Hard (t)
9	13,845,657	39,854,525	11,299,818
10	10,506,517	50,191,657	4,301,826
11	4,705,312	56,046,602	4,248,086
12	7,057,614	41,109,670	16,832,715
13	10,760,989	31,927,389	22,311,622
14	7,333,021	44,796,979	12,869,999
15	2,816,176	41,495,639	20,688,185
16	1,694,860	41,909,100	21,396,040
17	2,587,210	43,605,318	18,807,472
18	414,661	52,474,356	12,110,983
19	1,034,645	51,101,571	12,863,783
20	5,168,785	26,200,934	33,630,282
21	3,498,944	27,150,464	34,350,592
22	1,400,833	35,194,504	28,404,664
23	5,093,291	43,035,808	16,870,902
24	1,379,030	35,323,441	23,828,793
25	3,190,028	38,822,614	22,987,358
26	2,064,122	44,221,104	18,714,774
27	545,041	21,409,247	30,738,795
28		5,164,156	34,605,928
29		168,026	6,535,811
30			2,738,021
31			1,865,933
32			826,954
33			51,290
Total	176,760,708	944,356,712	437,093,762

Table 6-12: Assumed particle size distributions for fines fraction of waste rock

Screen size (mm)	Soft rock and soils (10% passing 40 um)		Hard rock (5% passing 40 um)	
	Fraction passing	Fraction retained	Fraction passing	Fraction retained
0.0373	0.100	0.0000	0.050	0.0000
0.0242	0.0817	0.0183	0.0408	0.0092
0.0148	0.0346	0.0471	0.0173	0.0235
0.0108	0.0113	0.0233	0.0057	0.0117
0.0076	0.0104	0.0009	0.0052	0.0005
0.0054	0.0100	0.0005	0.0050	0.0002
0.0038	0.0088	0.0011	0.0044	0.0006
0.0031	0.0081	0.0007	0.0041	0.0003
0.0016	0.0077	0.0005	0.0038	0.0002

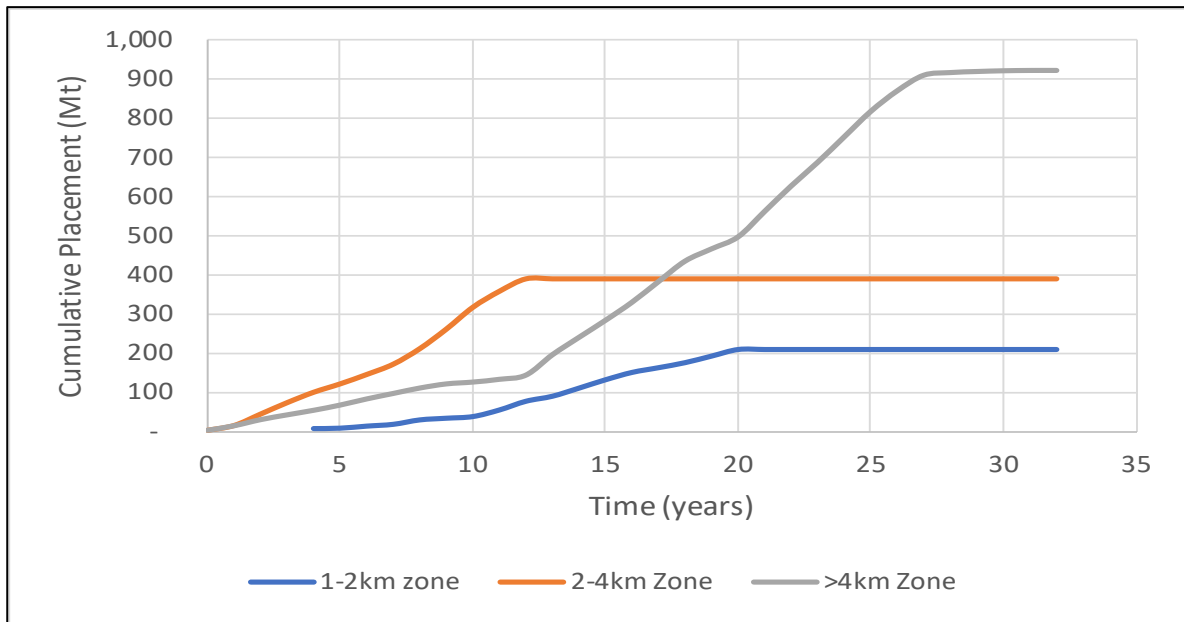


Figure 6-18: Cumulative placement schedule within each zone

Effect of TSS on total metal concentrations

The majority of the TSS that will be released from the FRHEP will comprise fines from the waste rock. No information is available for the fractional analysis of the fines (i.e. composition for individual size fractions) that may be generated during crushing of the waste rock since actual run-of-mine crushed rock has not yet been produced. However, the waste rock generally will be sourced from outside the ore deposit and therefore would be expected to be similar to the country rock that is currently being eroded and generating TSS in the natural streams.

The contribution of suspended solids released from the FRHEP to total metal concentrations were therefore estimated from the baseline water quality monitoring data to estimate the natural suspended solids metal content as shown in Table 6-13.

Table 6-13: Estimated total metal content of natural suspended solids

Parameter	TSS content (mg/kg)
Aluminium (Al)	13,000
Antimony (Sb)	9
Arsenic (As)	5
Cadmium (Cd)	0.3
Chromium (Cr)	15
Cobalt (Co)	3
Copper (Cu)	650
Iron (Fe)	22,000
Lead (Pb)	160
Manganese (Mn)	630
Nickel (Ni)	32
Selenium (Se)	23
Silver (Ag)	2
Zinc (Zn)	480

Stockpiles

Temporary stockpiles of both waste rock and ore will be established at the site. The waste rock will require temporary storage during the transportation process to accommodate loading of the barges. Ore stockpiles will be required to facilitate scheduling at the process plant. FRL has indicated that both stockpiles will be covered. It is further anticipated that these facilities will be bunded, and sumps will be installed to collect any seepage or runoff that may occur. This should afford the opportunity to treat the water before it is released.

In the case of the waste rock, any solutes generated during the transport process and during storage is accounted for within the allowance of the 12-week period that has been adopted for the calculations. Therefore, no additional source term is required for the waste rock stockpiles.

In the case of the ore, solutes generated within the stockpile will be introduced to the process plant and will be captured in the tailings water.

Limitations and exclusions

The load balance calculations did not include the following:

- Source solute loadings from any quarries that may expose mineralised wall rocks; the majority of the quarries will be located within the FRHEP basin (source of material for embankment construction) and will be inundated soon after completion of the embankment and therefore would not represent a significant ongoing source of solutes. (Note that TSS loadings from quarries have been captured in the Golder Associates estimates and are carried through the current analysis.)
- Source solute loadings (other than TSS) from the process plant site due to cut and fill operations for foundations; the geochemical analysis of foundation materials sampled during geotechnical investigations indicated that the materials that are likely to be subject to cut-and-fill are not mineralised (<0.02% S) and will not represent a significant source of solutes.
- Any solute loadings from the proposed airport site and/or other site works that may be undertaken on the floodplains along the Frieda or the Sepik rivers. These earthworks will occur primarily in floodplain sediments that are considered to be non-mineralised.
- Allowance for the risk that fine particulate sulphide minerals, which are naturally hydrophobic, may float to the surface during the deposition of the waste rock. Since crushed waste rock representative of the run-of-mine material is not available, the potential for this to occur could not be assessed. However, it is considered a residual risk that will need to be evaluated in the forward works program.

6.3.3 Results

Base case assessment

Water quality estimates for the pit contact water indicated that it would become acidic and contain elevated concentrations of solutes, including aluminium, copper and iron, which if released would adversely impact receiving water quality and may lead to exceedances of water quality trigger value. Therefore, the base case operational strategy is to treat all contact water that will be accumulated in the open pits. The treated water will be released to Ubai Creek and will flow into the ISF. The treatment sludge will be discharged to the tailings launder and will be deposited with the tailings in the ISF. Furthermore, for the base case, the waste rock will be blasted, crushed and then deposited in the ISF within an average exposure period of 12 weeks. The base case considers average flow conditions.

For the base case assessment, pH conditions are predicted to not deviate from baseline conditions. The predicted sulphate concentrations within the ISF pond and in the outflow, as well as downstream

of the embankment, are shown in Figure 6-19. As shown, sulphate concentrations are predicted to increase to a maximum between 70 mg/L and 80 mg/L in the ISF (Nena arm) and to a maximum just above 60 mg/L in the outflow (AP6). In the downstream reaches of the Frieda River, the sulphate concentrations are predicted to generally decrease from the maximum outflow value for consecutive assessment points. Only a marginal increase in sulphate concentrations is indicated for the Sepik River when compared to background concentrations, with predicted average concentrations of ~10 mg/L for the operational period.

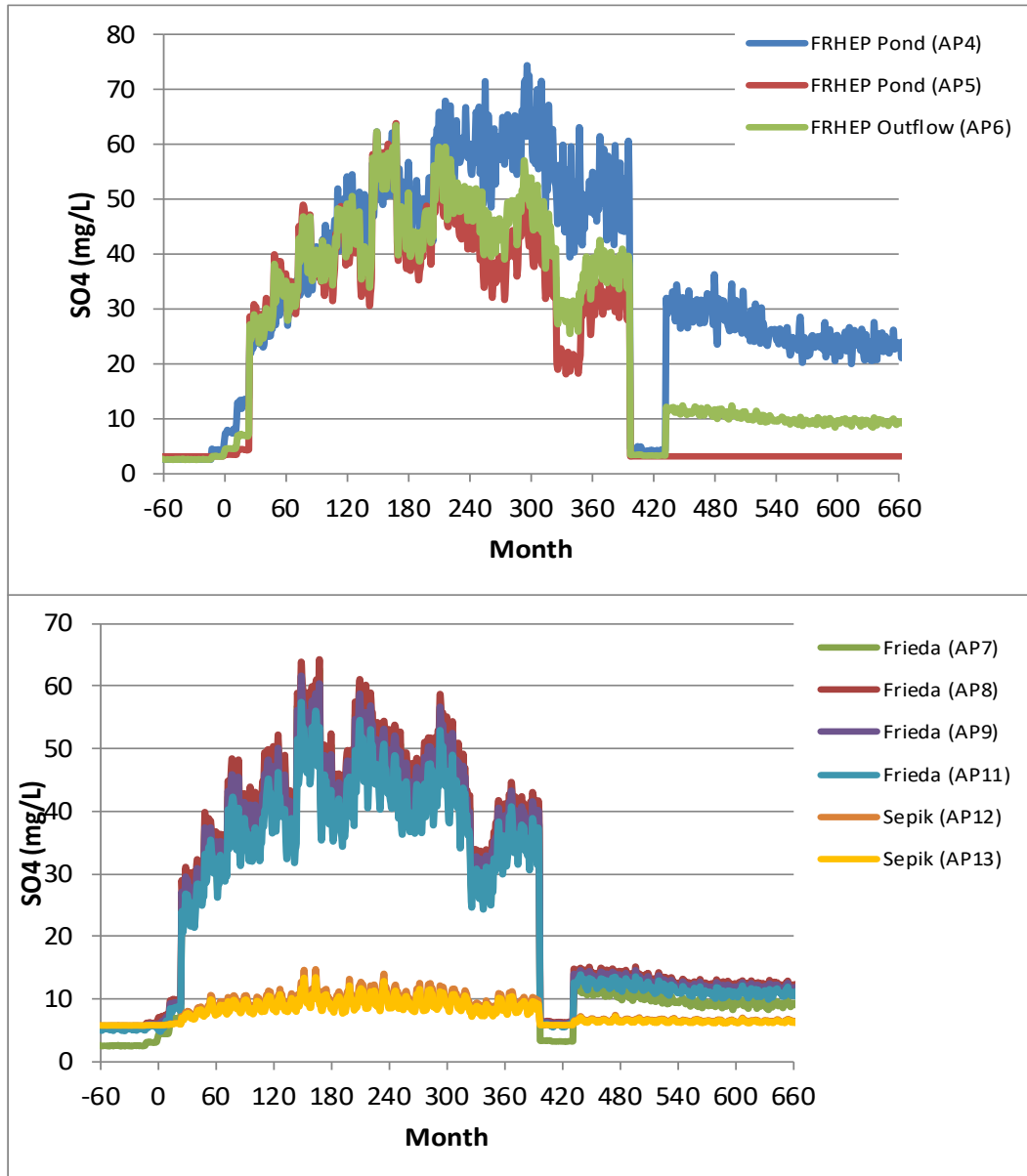


Figure 6-19: Base case – sulphate concentrations in the ISF impoundment, outflow and downstream of the mine (average flow conditions)

Maximum dissolved metal concentrations are predicted to occur during the middle years of operations when the waste rock production rates will be at a maximum. As an example, Figure 6-20 shows the copper concentrations in the ISF and in the discharge, and downstream of the embankment. As shown, within the ISF, the maximum copper concentration will occur in the Nena arm (AP4) with a value of about 0.0356 mg/L; the corresponding maximum concentration in the outflow of 0.0174 mg/L (AP6). Within the reaches of the Frieda River, the concentration is predicted to increase to

~0.016 mg/L. Within the Sepik River at AP13, the dissolved copper concentration may increase fractionally to ~0.003 mg/L.

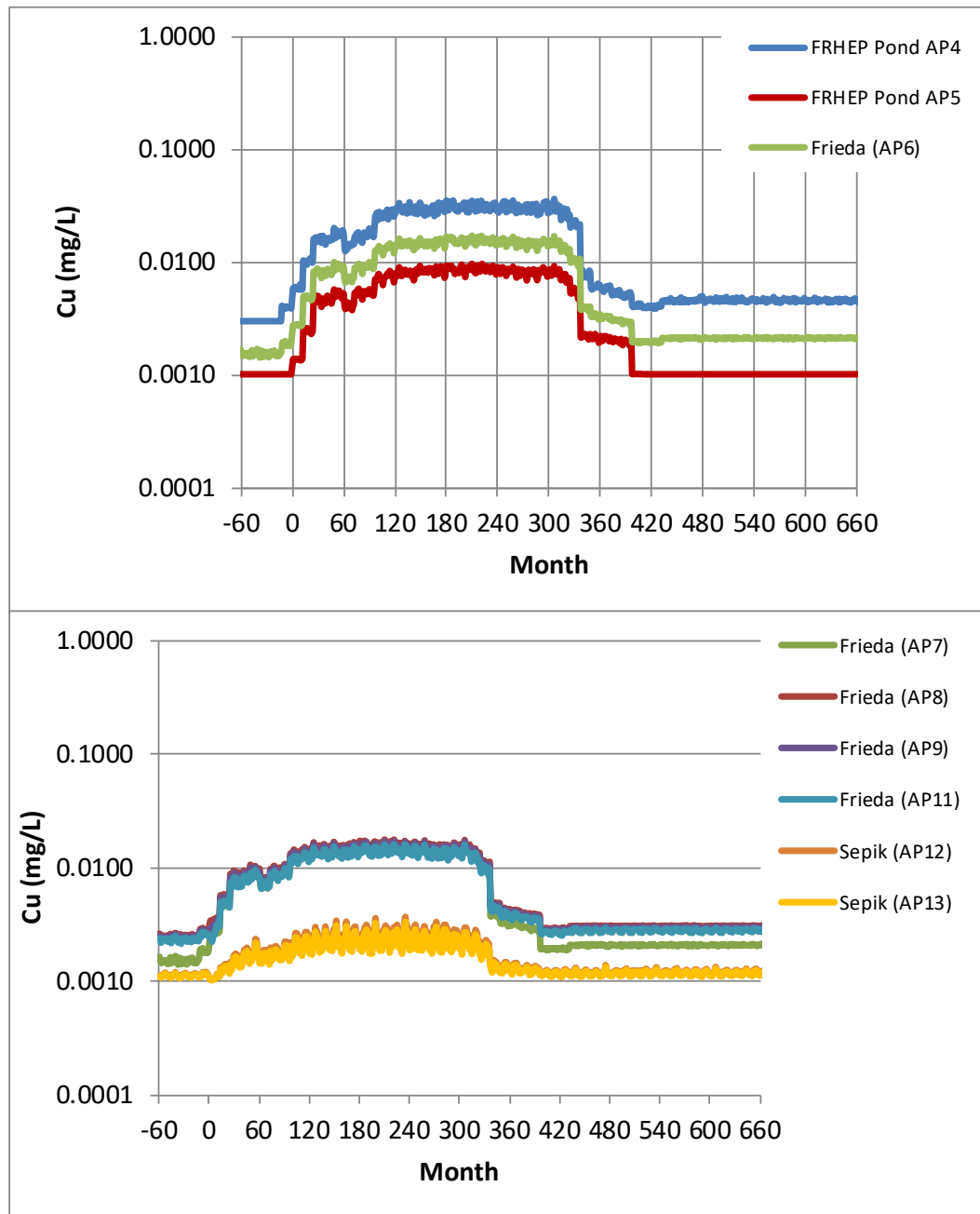


Figure 6-20: Base case – dissolved copper concentrations (average flow conditions)

Average predicted dissolved metal concentrations are predicted to meet IFC effluent guidelines for all parameters at the ISF discharge (AP6). Within the reaches of the Frieda River (down to AP11) the predicted concentrations for aluminium, chromium, cadmium, copper and zinc are likely to exceed the ANZECC water quality guidelines for 95% protection of freshwater aquatic life. It should however be noted that the background concentrations for chromium were below detection at all locations, and the background concentration was set to 80% of the analytical detection limit (the detection limit coincides with the water quality guideline). Typically, the incremental chromium concentration is less than the guideline. Within the reaches of the Frieda River, the predicted average copper concentration is typically about 7 to 8 times the ANZECC guideline, whereas the predicted aluminium concentration is about three times the guideline, and the zinc concentration is about twice the guideline value.

The predicted cadmium concentration is only fractionally above the guideline. Dissolved concentrations at all locations meet PNG Schedule 1 ambient water quality criteria.

Within the Sepik River, only copper is predicted to exceed the ANZECC guideline due to background concentrations. On average the copper concentration is predicted to exceed the guideline by a factor of about 1.4 to 1.5. It should be noted that a proportion of the dissolved copper (and zinc) would be complexed by dissolved organic carbon, which would reduce its bioavailability.

The total metal concentrations are a function of the TSS concentrations. TSS concentrations within the ISF will be highly variable and will be a function of the location of active deposition. The deposition strategy has identified the zone from the embankment to approximately 1 km upstream of the embankment as a 'no-go' zone; i.e. no deposition will occur within this area. This area will therefore represent a settling basin for TSS removal from the water column. Based on the deposition strategy, the TSS release can be regulated within specific zones so that the TSS in the outflow can be estimated.

The predicted TSS concentrations for the base case are illustrated in Figure 6-21, together with the TSS concentrations in the downstream environment. As shown, the TSS concentrations in the ISF outflow are predicted to range up to 250 mg/L for average flow conditions, originating predominantly (> 95%) from mine waste deposition by barge. The ISF discharge TSS concentration would exceed the IFC discharge limit of 50 mg/L; however, it should be noted that the median baseline (background) TSS concentration in the Frieda River at AP7 is well above 100 mg/L (and is highly variable). Due to high baseloads of TSS in the Frieda River and the Sepik River, the discharge of TSS concentrations in flows from the ISF during mining operations (i.e. active waste rock disposal in the ISF) is not expected to result in significant deviations from baseline conditions. Towards the end of the mining operations, the TSS is expected to decrease below the median baseline condition, and after mining ceases, the TSS will be consistently and significantly lower than median baseline conditions in the Frieda River. The resulting reduced TSS loading to the Sepik River is relatively minor but will still result in overall lower TSS concentrations at AP12 and AP13 as shown in the plots.

The total copper concentration profiles are shown in Figure 6-22. As shown, total copper concentrations are predicted to decrease below baseline conditions within the reaches of the Frieda River due to the lower TSS concentrations. However, total concentrations within the Sepik River are not expected to show a significant change. Generally, total copper concentrations in the Sepik River will remain comparable to background concentrations.

A summary of maximum total metal concentrations for key parameters is provided in Table 6-14 and are compared to WHO (2011) drinking water guidelines. Total concentrations of aluminium and iron are predicted to be elevated at all locations, and concentrations of lead are predicted to be marginally elevated above the drinking water quality guidelines (WHO, 2011). As discussed for copper, these metals are naturally elevated in the Nena, Frieda and Sepik rivers due to existing suspended solids loadings in the background waters.

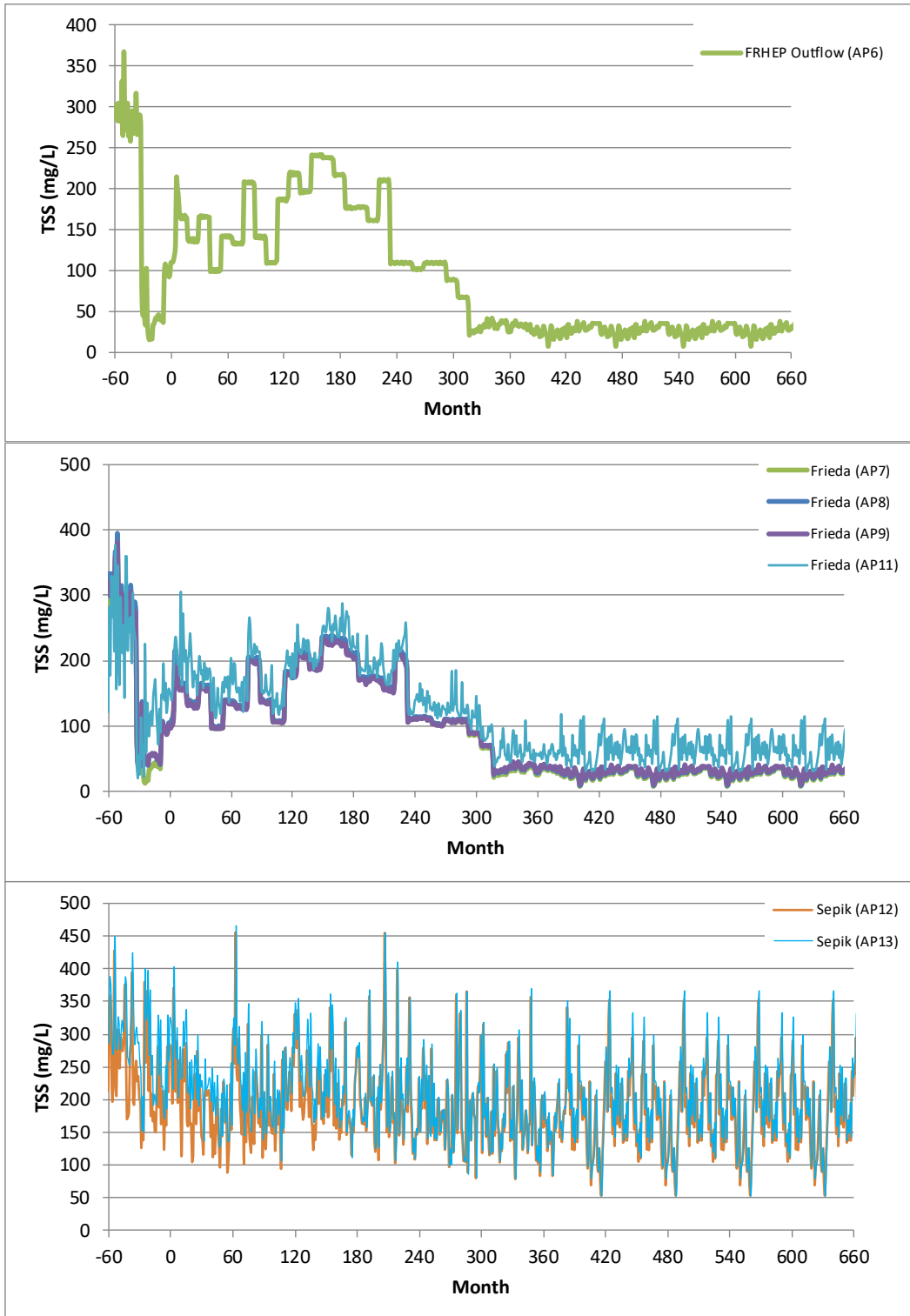


Figure 6-21: Base case – TSS concentrations

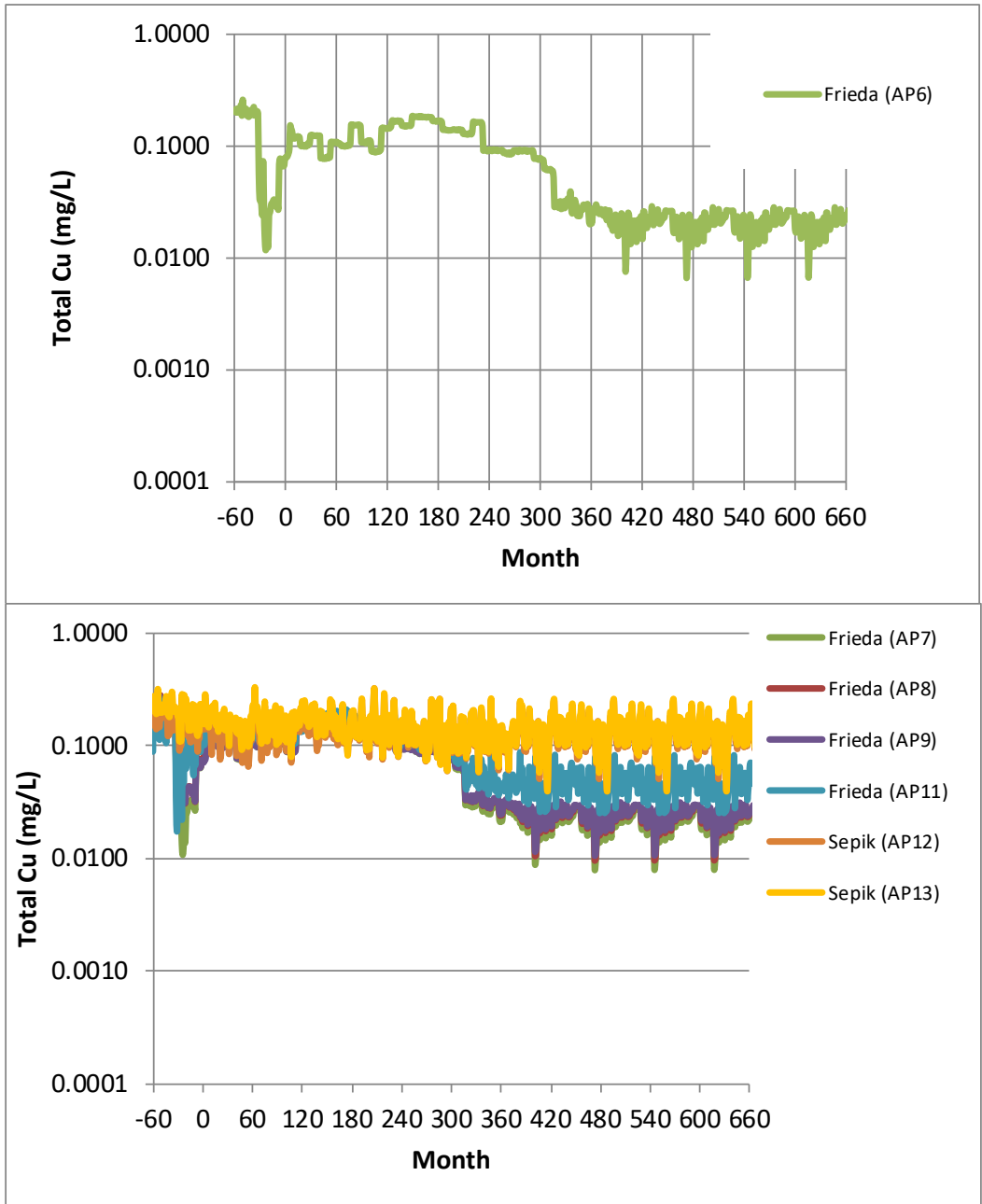


Figure 6-22: Base case – total copper concentrations (treatment throughout operations)

Table 6-14: Base case – summary of predicted average total metal concentrations (average flow conditions; treatment throughout operations)

Location		Al (mg/L)	As (mg/L)	Cd (mg/L)	Cr (mg/L)	Cu (mg/L)	Fe (mg/L)	Pb (mg/L)	Mn (mg/L)	Ni (mg/L)	Zn (mg/L)
ISF Discharge	AP6	4.5	0.0023	0.00071	0.0054	0.10	4.66	0.009	5.3	0.011	0.074
Frieda River U/S Kaugumi Creek	AP7	4.4	0.0023	0.00070	0.0054	0.10	4.60	0.009	5.3	0.011	0.073
Frieda River (Frieda Mountain)	AP8	4.5	0.0032	0.00081	0.0062	0.10	4.72	0.010	8.7	0.012	0.079
Frieda River (Lower Frieda River GS)	AP9	4.4	0.0032	0.00078	0.0061	0.10	4.60	0.009	8.5	0.012	0.077
Frieda River U/S Sepik River	AP11	5.3	0.0033	0.00088	0.0069	0.12	5.58	0.011	8.5	0.014	0.091
Sepik River (Iniok GS)	AP12	6.5	0.0026	0.00089	0.0074	0.14	6.92	0.012	5.5	0.014	0.101
Sepik River (Kubkain GS)	AP13	7.0	0.0026	0.0010	0.0080	0.15	7.47	0.013	5.6	0.015	0.109
Water Quality Guidelines											
WHO (2011) drinking water		0.2	0.01	0.003	0.05	1	0.3	0.01		0.07	3

Note: Bold values indicate above drinking water quality guidelines.

Predictions were also compared for high flow (90th percentile) and low flow (10th percentile) conditions. In general, higher flow conditions result in lower solute concentrations whereas low flow conditions generally result in an increase in solute concentrations. At low flow conditions, the predicted concentrations for aluminium, cadmium, chromium, copper and zinc are likely to exceed the ANZECC water quality guidelines within the reaches of the Frieda River. Within the Sepik River, the predicted average aluminium, chromium, copper and zinc concentrations would exceed the ANZECC guidelines (95% protection). The implications of these solute concentrations are discussed in the Environmental Impact Statement (Coffey 2018).

Dissolved metal complexation

Metal-humate interactions in aqueous and terrestrial ecosystems control the speciation of metals and, as a result, influence the bioavailability and toxicity of the metals. Humic acids are widely distributed natural organic substances present on almost every segment of the terrestrial aquatic environment.

Dissolved metal aqueous speciation is dependent, amongst other things, on DOC, pH and the concentrations of competing ions (such as Ca, Fe aqueous species). The MINTEQA2 model incorporating the Stockholm Humic Model (SHM) was used to estimate the complexing of the copper together with all the calculated dissolved metals that are likely to interact with the DOC. The results in general show that the organic carbon complexes primarily with iron (10%–17% of the DOC) and calcium (8%–10% of the DOC). The copper results for average operational concentrations are summarised in Table 6-15. The results show that the labile copper concentrations are likely to range from ~0.0025 mg/L to 0.0037 mg/L within the Frieda River, and from 0.0002 mg/L to 0.0003 mg/L in the Sepik River.

Table 6-15: Calculated complexed copper species for mean operational solute concentrations

Location	Hardness (as CaCO ₃)	pH	Total organic carbon	Dissolved copper (mg/L)	Dissolved copper complexed (%)	Dissolved copper complexed (mg/L)	Labile copper species (mg/L)
AP4	58	7.5	2.1	0.022	71.2	0.0156	0.0063
AP5	72	7.6	1.5	0.006	71.1	0.0044	0.0018
AP6	67	7.6	1.7	0.011	77.9	0.0087	0.0025
AP7	67	7.6	1.7	0.011	70.4	0.0078	0.0033
AP8	98	7.6	2.6	0.012	68.8	0.0082	0.0037
AP9	95	7.5	2.6	0.011	69.9	0.0079	0.0034
AP10	92	7.5	2.6	0.011	69.9	0.0076	0.0033
AP11	90	7.5	2.6	0.010	70.8	0.0074	0.0031
AP12	64	7.2	3.0	0.0021	87.3	0.0018	0.0003
AP13	63	7.2	3.0	0.0019	87.3	0.0017	0.0002

The results also showed that chromium is likely to be strongly complexed (typically > 90%), with zinc cadmium and aluminium less so. Based on these results, the labile chromium concentration should be well below the ANZECC receiving water quality guideline.

TSS sensitivity to barge deposition strategy

The base case assessment addressed a possible barge dumping strategy based on waste rock production rates. An alternate deposition strategy was derived to reduce the rates of deposition in the near-field zones to a minimum, with the following operating constraints in place:

- Zone 1–2 km: Maximum of five barge depositions per day (i.e. deposition restricted to a maximum of 25,000 tpd); deposition commences only at the beginning of Year 5.

- Zone 2–4 km: Maximum of eight barge depositions per day (i.e. deposition rate restricted to a maximum of 40,000 tpd); deposition commences from Year 1 in the Niar Arm to contain tailings deposition upstream from this area; deposition in the Nena Arm will coincide with requirements to contain emergency tailings deposition in the area near the process plant.
- Zone >4 km: Accommodates all material that cannot be placed in the other zones at any given time.

Under these constraints, the time to fill the 1 to 2 km zone would be increased to about 30 years, and to fill the 2–4 km zone, about 32 years. The revised schedule of deposition is shown in Table 6-16 and corresponding predicted TSS concentrations in the outflow from each of the zones together with the combined TSS release is illustrated in Figure 6-23. The figure includes the plot for the base case TSS concentrations for comparison. As shown, by limiting the rate of deposition within each of the zones, it would be possible to reduce the TSS concentrations in the ISF outflows.

Table 6-16: Revised placement schedule to limit deposition rates in near-field zones

Year	Zone: 1–2 km		Zone: 2–4 km		Zone: >4 km	
	Total placed (t)	Rate (tpd)	Total placed (t)	Rate (tpd)	Total placed (t)	Rate (tpd)
1	-	-	6,589,896	18,055	-	-
2	-	-	21,189,896	40,000	9,371,107	25,674
3	-	-	35,789,896	40,000	39,771,107	83,288
4	9,125,000	25,000	50,389,896	40,000	57,596,120	48,836
5	18,250,000	25,000	64,989,896	40,000	78,871,120	58,288
6	27,375,000	25,000	79,589,896	40,000	91,065,820	33,410
7	36,500,000	25,000	94,189,896	40,000	112,340,820	58,288
8	45,625,000	25,000	108,789,896	40,000	133,615,820	58,288
9	54,750,000	25,000	123,389,896	40,000	174,890,820	113,082
10	63,875,000	25,000	137,989,896	40,000	216,165,820	113,082
11	73,000,000	25,000	152,589,896	40,000	257,440,820	113,082
12	82,125,000	25,000	167,189,896	40,000	298,715,819	113,082
13	91,250,000	25,000	181,789,896	40,000	339,990,819	113,082
14	100,375,000	25,000	196,389,896	40,000	381,265,818	113,082
15	109,500,000	25,000	210,989,896	40,000	422,540,818	113,082
16	118,625,000	25,000	225,589,896	40,000	463,815,818	113,082
17	127,750,000	25,000	240,189,896	40,000	505,090,818	113,082
18	136,875,000	25,000	254,789,896	40,000	546,365,818	113,082
19	146,000,000	25,000	269,389,896	40,000	587,640,817	113,082
20	155,125,000	25,000	283,989,896	40,000	628,915,818	113,082
21	164,250,000	25,000	298,589,896	40,000	670,190,818	113,082
22	173,375,000	25,000	313,189,896	40,000	711,465,819	113,082
23	182,500,000	25,000	327,789,896	40,000	752,740,820	113,082
24	191,625,000	25,000	342,389,896	40,000	789,547,084	100,839
25	200,750,000	25,000	356,989,896	40,000	830,822,084	113,082
26	209,875,000	25,000	371,589,896	40,000	872,097,084	113,082
27	219,000,000	25,000	386,189,896	40,000	901,065,167	79,365
28	228,125,000	25,000	400,789,896	40,000	917,110,251	43,959
29	234,828,837	18,367	400,789,896	-	917,110,251	-
30	237,566,858	7,501	400,789,896	-	917,110,251	-
31	239,139,749	4,309	401,082,939	803	917,110,251	-
32	239,139,749	-	401,909,893	2,266	917,110,251	-
33	239,139,749	-	401,961,183	141	917,110,251	-

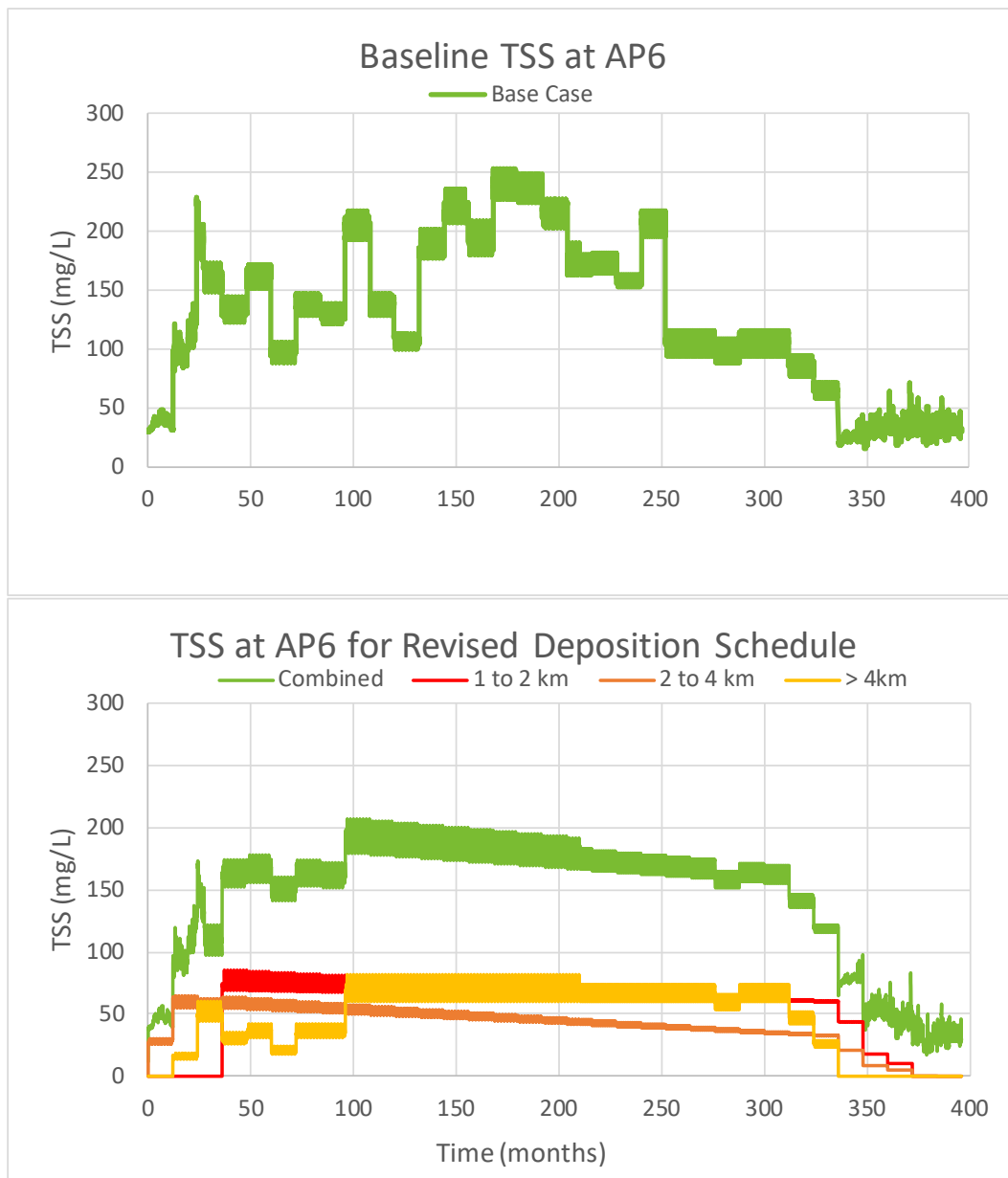


Figure 6-23: Comparison between base case and restricted barge dumping in the 1–2 km and 2–4 km zones

6.3.4 Conclusions

Results of the water and load balance modelling indicate the following:

- Construction of the embankment will equalise flows downstream of the facility in the reaches of the Frieda River only (i.e. no changes in flows within the Sepik River will occur) during operations and post closure.
- Contact water quality for the open pits is predicted to become acidic early on during operations and remain acidic after flooding of the open pits at closure. Water treatment prior to discharge is proposed to be undertaken throughout operations.
- FRHEP outflows are predicted to result in increases in solute concentrations in the Frieda River (AP6 to AP11), and may lead to exceedance of corresponding ANZECC receiving water quality trigger values. The predicted increases will vary depending on the flow conditions, stage of operations and deposition strategy. Copper concentrations in the Sepik River are predicted to remain comparable to background levels.

- Dissolved organic carbon species are expected to complex copper and other metals to various degrees which would reduce the labile metals concentrations and reduce toxicity. Copper speciation calculations indicate that on average between 68 and 87 % of the dissolved copper may be complexed by organic species. This would decrease the labile copper concentrations in the reaches of the Frieda River to about 0.003 mg/L. Adsorption to suspended particulate matter may also reduce bioavailable metals concentrations.
- The mean TSS concentrations downstream of the embankment at AP6 are predicted to be about 130 mg/L, with a 90th percentile concentration of 215 mg/L during the operational period of the FRCGP. The TSS concentrations at AP6 are predicted to decrease from the pre-project (existing) conditions (mean TSS concentration of 191 mg/L, and 90th percentile concentration of 338 mg/L).
- TSS concentrations in the ISF outflow may further be reduced by scheduling and selective placement of waste rock during operations. Assessment of an alternate scheduling strategy indicated that the maximum TSS concentration may be reduced to about 200 mg/L, (as compared to a 90th percentile concentration of 338 mg/L); i.e. the maximum predicted concentration will be about the same as the average background concentration at AP6.
- Post closure, water treatment will be required to mitigate against the release of contact water from the open pits.
- The FRHEP will also act as a large scale settling basin for natural sediments from upstream sources so that the TSS release downstream will be reduced significantly when compared to pre-project concentrations.
- The water quality assessment indicated that the discharge from the open pit will have an unacceptable impact on the downstream receiving water quality. An engineered water treatment system will be installed to treat the water collected from the open pit before it is discharged.
- Treatment of the open-pit water will continue for a period of approximately 50 years or until closure criteria are met.

With the implementation of the proposed water treatment and other control measures, the site is predicted to remain in compliance with the PNG Environment (Water Quality) Regulations (2002) and PNG Drinking water guidelines downstream of the proposed mixing zone during operations and post-closure of the FRCGP.

The water balance model and water quality assessment have been developed using generally conservative methods and assumptions. Remaining model limitations or uncertainties that have been identified as potentially significant include the following:

- Solute source terms are based on best available data and information. Gaps in available information necessitated adoption of assumed (and conservative) values for some parameters.
- The extent of oxidation and duration of waste rock exposure prior to deposition in the ISF may significantly impact the solute loading to the receiving environment. More detailed planning and scheduling prior to project implementation may reduce the uncertainty associated with the current conservative assumption of 12 weeks average waste rock exposure.
- Uncertainty remains in the assumptions adopted for the operational and post closure pit wall rock conditions with respect to talus accumulation, depth of fracture damage, and overall rates of oxidation. These can be refined once mining commences and actual rates of solute generation can be measured.

7 Hydroelectric Power Water Balance and Energy Model

A detailed description of the hydrology of the site is presented in Hydro in Section 4.

7.1 Models

Two versions of the Water Balance and Energy Model – using measured and synthetic flow data – have been used for the SPS.

Version 1 – Measured flow data

This is the standard model that has been used throughout the different phases of the FRHEP project and the FRHEP investigations. The model uses 16 years of measured flow data in the simulations. The number of years used is limited by the requirement to have a continuous record with equal numbers of each month of the year being modelled. To cover the 33 to 37 years needed to simulate the FRHEP inflows, the years are re-cycled. To prevent distortion resulting from high or low flow in the first year of the simulation, a separate sequence was run with the simulation commencing with each of the 16 years. To expedite run time and avoid iterative calculations, some minor simplifications have been made.

Version 2 – Synthetic flow data

This version uses the same basic equations as Version 1 throughout all aspects of the analysis. The model uses the large synthetic flow data series that was developed to extend the data available for the analysis of the energy output. In total, 200 × 38-year series have been developed – providing the 24-hour mean flow for 7,600 individual years. The minor simplifications used in Version 1 to significantly decrease the model run time, by avoiding a large number of iterative calculations, have not been made. The net result is a more accurate simulation and slight improvement in water utilisation. The downside of Version 2 is that several major parameters use the results of Version 1 model. These include the performance of spillway gates, freeboard, maximum and minimum water levels and the turbine size.

In the development of the Energy Model, the hydrology data is used in a different way to the design of the dam and spillways for 'floods'. In general, the 'low flow' hydrology is more important to the energy from the scheme than the large floods that are spilled from the facility. Therefore, some interrogation of the base data and use of different methods to fill in missing data have been undertaken.

7.2 Hydroelectric power measured flow hydrology

The FRHEP catchment area is 1,033 km². A runoff coefficient of 0.786 was used for the FRHEP energy modelling.

Full-year measured data is preferred as it allows annual water balance simulations and generation simulations to be carried out, without relying on synthetic data. Monitoring of flows commenced in 1980 and results are available to August 2017. Readings within the raw flow data are frequently intermittent, and there are long gaps of days or even months. The records are intermittent from 1981 to 1994. As a result, there are only six years which have complete annual flow records – 1995, 1998, 2012, 2013, 2014 and 2015.

During previous phases of the project, it was found that flow data processed and received from others used flow data from a single reading to fill in gaps in the previous reading. This led to distortions in the recorded flow, which subsequently could not be compared with the rainfall records or other gauging station data. This has led to differences in the flow series being used for flood assessments and

energy production. The same raw data forms the basis, and while the data sparsity in some years does not prevent the data being used for flood assessment work, it is not useful for assessing the energy production potential.

Table 7-1 shows the number of days in each month for which measured data is available. Data gaps on any day were addressed by using the reading for the following day, i.e. the infilled data for all missing days is not based on standard application of the same value. This resulted in whole days of data for various years within the table. The highlighted rows indicate years for which complete datasets exist.

Table 7-1: Days per month for which measured flow data is available

Year	Month												Total days
	Jan	Feb	Mar	Apr	May	Jun	Jul	Aug	Sep	Oct	Nov	Dec	
1981	31	28	31	30	31	30	31	31	30	31	30	12	346
1982	0	0	4	30	6	0	3	31	30	17	14	31	166
1983	31	28	31	3	0	30	31	31	24	0	0	0	209
1984	8	21	0	0	24	24	6	31	30	31	30	9	214
1985	0	10	30	30	31	30	31	31	30	31	30	31	315
1986	31	19	31	30	15	0	0	11	30	31	30	30	258
1987	31	10	0	0	6	29	24	19	0	0	0	0	119
1988	0	13	31	30	31	30	23	0	17	31	30	31	267
1989	31	28	31	30	31	30	31	31	30	31	30	17	351
1990	0	0	0	0	0	0	14	31	30	31	19	0	125
1991	0	17	31	30	14	0	0	19	30	31	30	31	233
1992	31	29	24	0	6	30	31	31	29	31	29	28	299
1993	29	26	31	17	29	24	22	30	24	26	28	27	313
1994	1	0	0	0	0	0	0	0	0	0	0	12	13
1995	31	28	31	30	31	30	31	31	30	31	30	31	365
1996	31	29	31	30	28	0	21	29	16	31	30	31	307
1997	19	22	31	30	31	30	31	31	30	31	30	31	347
1998	31	28	31	30	31	30	31	31	30	31	30	31	365
1999	31	28	31	30	31	26	0	0	0	0	0	0	177
2008	0	0	0	11	31	30	31	31	30	31	29	30	254
2009	31	28	31	30	31	30	31	31	30	1	0	0	274
2010	0	16	31	30	31	30	31	31	30	31	30	31	322
2011	31	28	31	30	23	0	16	31	30	31	30	31	312
2012	31	29	31	30	31	30	31	31	30	31	30	31	366
2013	31	28	31	30	31	30	31	31	30	31	30	31	365
2014	31	28	31	30	31	30	31	31	30	31	30	31	365
2015	31	28	31	30	31	30	31	31	30	31	30	31	365
2016	31	29	31	12	17	30	31	31	30	31	30	31	334

Since the previous studies, more data covering the periods from 1981 through to May 1999 (from GS105450) and May 2008 to 31 December 2016 has been received.

This data was analysed to ensure that whole days of measured data were extracted for comparison with the flow records for GS105310 (Lower Nena gauging station). The results of the comparison of monthly flows are plotted in Figure 7-1, which shows there are whole months of measured data at both

gauging stations. Where one or the other station has incomplete days in each month, the data has not been used. The result is a simple linear relationship with a slope of 0.172 and a regression coefficient of 0.81. The GS105310 catchment is 19.8% of the area of GS105450, but produces 17.2% of the flow.

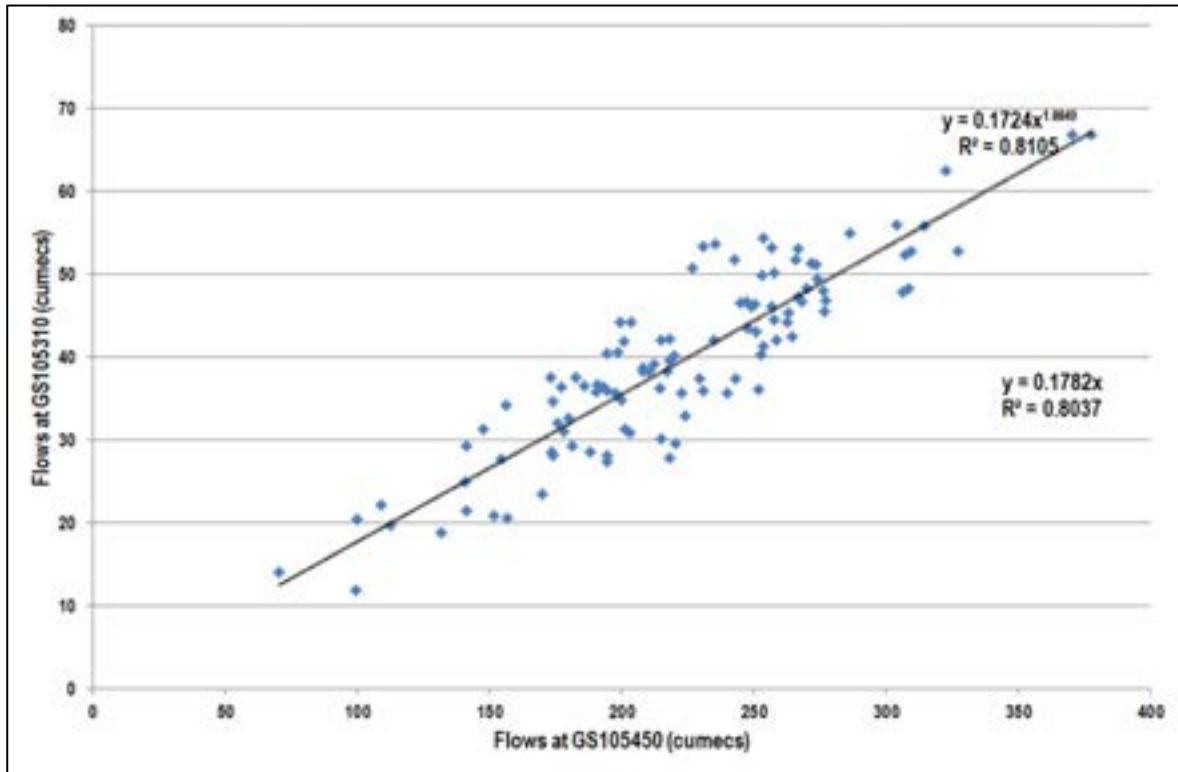


Figure 7-1: Correlation between monthly flows at GS105310 and GS105450

The comparison on a daily basis (Figure 7-2) shows considerable scatter, which is to be expected. Nevertheless, the linear relationship slope is 0.17 and the regression coefficient is 0.72.

This analysis shows a relatively close relationship between the flows at the two gauging stations. Therefore, using data from the Frieda River gauging station to fill in gaps in the Lower Nena River gauging station data can be done without skewing or distorting the flow series information.

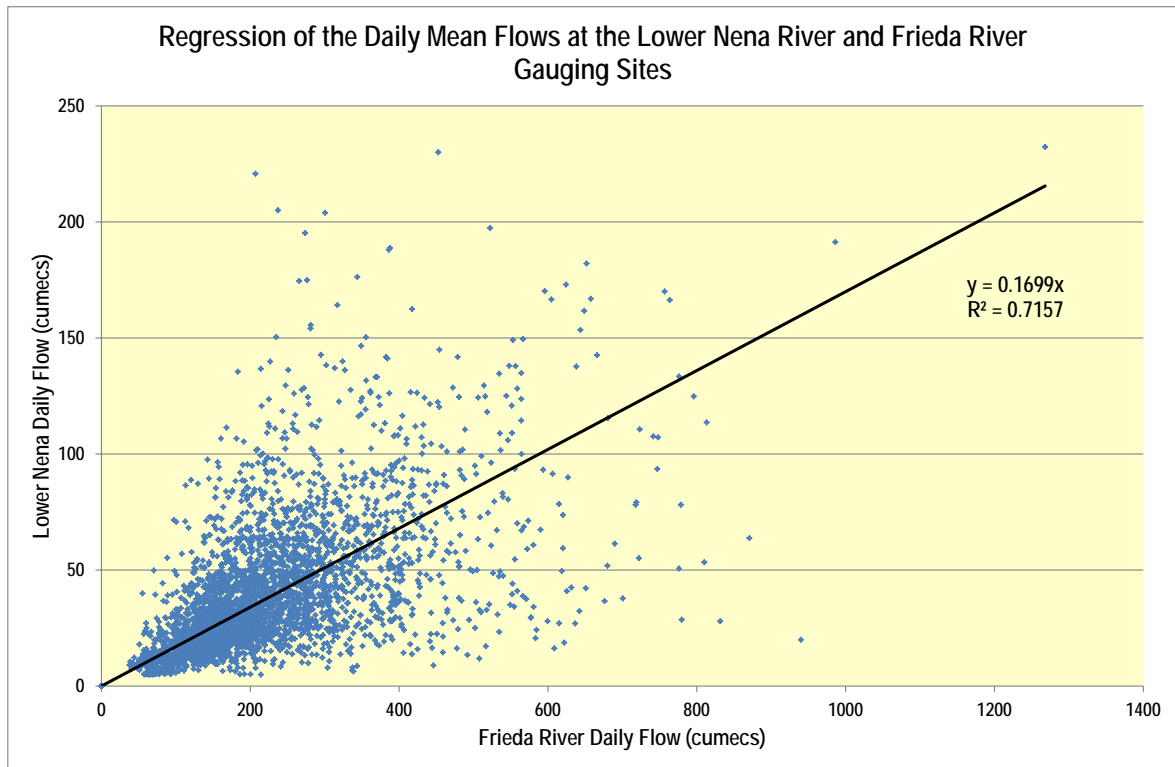


Figure 7-2: Regression analysis of daily mean flows - GS105310 and GS105450

The result is a significant number of additional years can be used in the flow series for analysing the hydroelectric power potential by patching the missing data with correlations to the Nena River catchment. To expand data to the Frieda River catchment, two further compromises were made:

- 1985 is complete other than the first two months and 1986 has complete data for these periods; the mean flows for which data is available are very similar in both years. As a result, the data from the first two months of 1986 has been added to the 1985 data to create a full year of data.
- Complete data was available for the first half of 1999 and the second half 2008. These two years have been merged to create a single year of data.

In total, there are 16 years of ‘patched’ data available. The resulting modified dataset in Table 7-2 shows eight of the years are incomplete, but data missing in any of these years is between 6 and 31 days. This has been completed using data averaged for all years. Importantly, full data is available for some of the more significant events such as the low inflow periods of 1996/97 and also in 2015. The net result is the mean flow of the measured data being used for energy modelling is 220.4 m³/s. The mean measured flow across all measured data is 222.3 m³/s. The dataset being used for analysis has data for each day of the year in the dataset. The measured data has more missing data in December, January and February which may slightly distort the dataset.

Table 7-2: Days per month for which flow data are available - modified

Year	Month												Total days
	Jan	Feb	Mar	Apr	May	Jun	Jul	Aug	Sep	Oct	Nov	Dec	
1981	31	28	31	30	31	30	31	31	30	31	30	12	346
1985	31	19	31	30	31	30	31	31	30	31	30	31	356
1989	31	28	31	30	31	30	31	31	30	31	30	17	351
1995	31	28	31	30	31	30	31	31	30	31	30	31	365
1996	31	29	31	30	31	24	21	29	19	31	30	31	337

Year	Month												Total days
	Jan	Feb	Mar	Apr	May	Jun	Jul	Aug	Sep	Oct	Nov	Dec	
1997	19	22	31	30	31	30	31	31	30	31	30	31	347
1998	31	28	31	30	31	30	31	31	30	31	30	31	365
2008	31	28	31	30	31	30	31	31	30	31	30	31	365
2009	31	28	31	30	31	30	31	31	30	31	30	31	365
2010	31	28	31	30	31	30	31	31	30	31	30	31	365
2011	31	28	31	30	31	30	20	31	30	31	30	31	354
2012	31	29	31	30	31	30	31	31	30	31	30	31	366
2013	31	28	31	30	31	30	31	31	30	31	30	31	365
2014	31	28	31	30	31	30	31	31	30	31	30	31	365
2015	31	28	31	30	31	30	31	31	30	31	30	31	365
2016	31	29	31	12	17	30	31	31	30	31	30	31	334

The monthly mean flows are shown in Table 7-3. A review of the data shows that the mean flow in the FRHEP area is 220.4 m³/s. In addition, the following extreme periods have occurred (shown as green in Table 7-3):

- The wettest period is the first months of 2008.
- The driest periods are the middle months 1997 and July to September 2015.
- The wettest years are 2013, which is complete, and 1981, which has 20 days of missing data in December.

Table 7-3: Monthly mean inflows

Year	Month (mm)												Annual average
	Jan	Feb	Mar	Apr	May	Jun	Jul	Aug	Sep	Oct	Nov	Dec	
1981	292.0	250.6	326.1	326.2	218.7	230.9	236.5	179.8	221.6	230.2	272.7	285.1	254.2
1985	207.6	245.6	220.4	206.3	205.9	192.0	164.2	218.7	218.4	254.8	190.6	168.8	206.6
1989	237.0	185.2	222.1	175.7	196.8	181.8	202.7	189.5	195.2	209.0	250.3	121.8	200.3
1995	246.7	293.0	302.0	270.6	216.2	226.1	239.6	200.4	156.3	228.2	198.0	262.3	236.4
1996	206.4	244.1	156.0	235.4	268.8	281.1	230.5	205.8	271.6	281.0	142.1	166.8	221.3
1997	103.7	253.4	121.5	167.3	163.6	85.0	256.4	108.6	70.5	99.3	140.6	230.5	149.4
1998	273.3	314.1	192.7	370.0	262.2	252.4	222.3	202.8	254.4	256.8	214.6	214.7	251.8
2008	178.2	249.5	377.3	275.8	207.8	265.9	248.3	264.7	209.9	204.0	249.0	184.4	242.8
2009	147.6	322.7	234.9	220.0	154.4	177.1	203.4	218.0	185.7	193.1	196.3	140.5	198.5
2010	230.6	309.4	286.4	266.6	276.5	173.6	117.2	222.8	244.9	208.3	170.0	194.4	224.5
2011	141.2	194.3	309.9	182.1	149.1	176.1	334.6	327.3	256.5	258.0	218.0	277.4	233.0
2012	273.5	188.2	249.0	247.7	231.0	179.9	173.7	269.8	308.3	197.8	250.9	174.1	228.7
2013	267.9	257.4	307.2	303.8	229.6	266.8	306.0	243.2	253.2	199.4	190.8	212.4	253.1
2014	242.7	210.4	190.5	194.3	201.3	217.8	199.7	181.3	256.6	252.5	264.3	263.1	222.9
2015	140.6	258.4	194.6	220.2	215.0	251.8	131.7	151.9	156.7	101.0	111.8	218.8	178.7
2016	208.0	176.2	142.4	113.1	168.2	255.5	233.4	227.7	251.7	311.9	278.7	234.2	224.5
Monthly average	215.0	246.7	239.6	240.7	211.5	212.5	215.8	213.3	218.2	217.8	208.7	208.9	220.5

7.3 Hydroelectric power synthetic flow hydrology

The derivation of the synthetic 200 × 38 year flow series using the hidden Markov model is described in Section 4.2. The synthetic data has been analysed below to determine how it extends the measured dataset to cover events for which other data is not available.

Figure 7-3 and Figure 7-4 compare the flow duration curves for the synthetic and measured flow series. As can be seen they are very similar except the synthetic series has more extreme low flows and maximum flows.

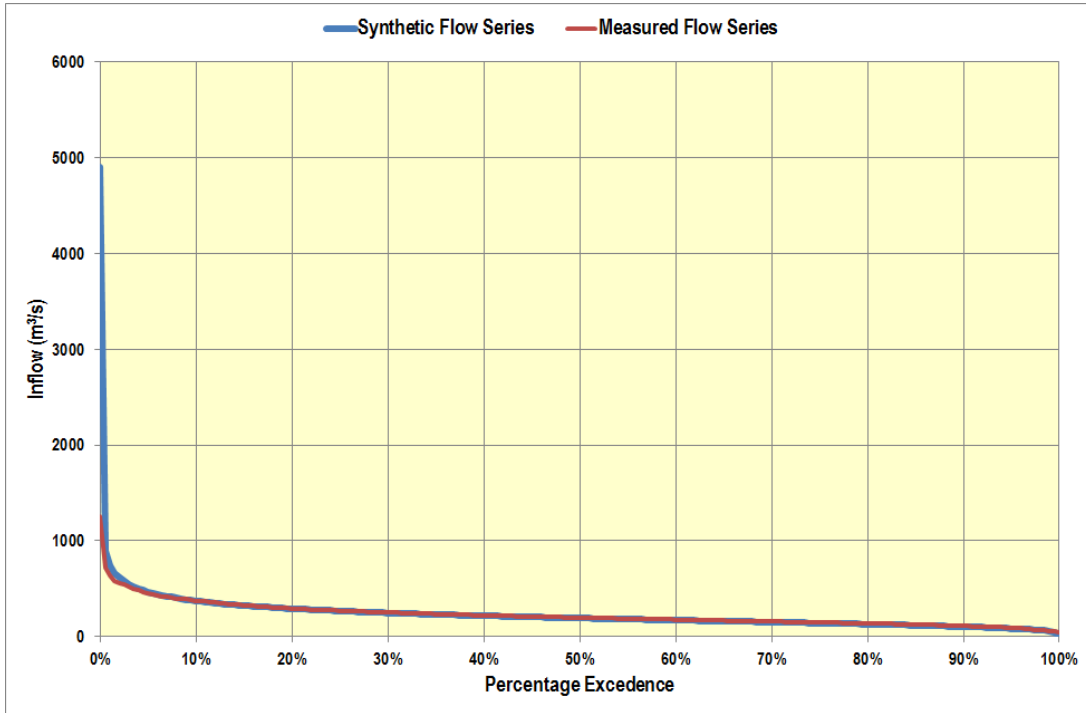


Figure 7-3: Comparison of flow duration curves for synthetic and measured flows

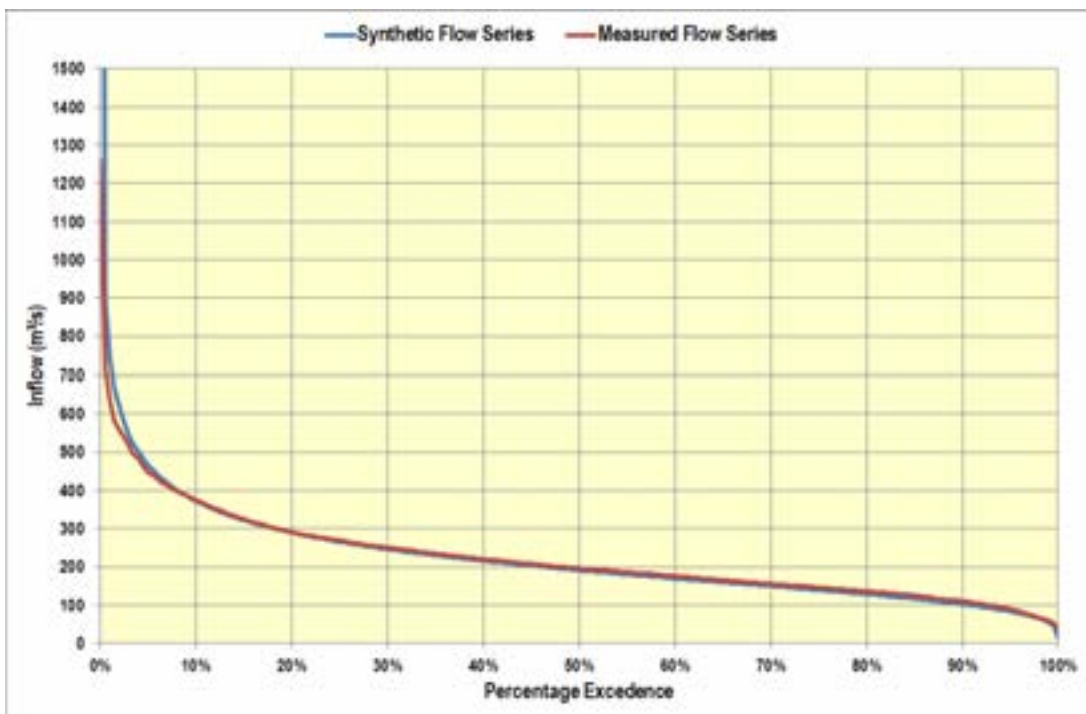


Figure 7-4: Close-up of flow duration curves for synthetic and measured flows

The more extreme inflow events have been reviewed in more detail. Figure 7-5 and Figure 7-6 compare the average daily inflow for a wide range of events from one day to one year. In this instance, 16 years data of measured flows is being compared with 7,600 years of synthetic flows. Figure 7-5 shows the comparison for the maximum inflows and Figure 7-6 for the lowest inflow events. The data for the synthetic data is very much more extreme than in the measured series.

The data for the events is detailed in Table 7-4.

Table 7-4: Magnitude of inflow events of different durations

Inflow event (days)	Maximum		Minimum	
	Synthetic flow series (m ³ /s)	Measured flow series (m ³ /s)	Synthetic flow series (m ³ /s)	Measured flow series (m ³ /s)
1	4,909	1,260	12	37
2	2,965	892	15	39
3	2,237	725	18	41
4	1,819	626	19	44
5	1,563	590	21	49
6	1,415	562	24	49
7	1,361	548	25	49
8	1,274	528	27	50
9	1,184	502	28	54
10	1,100	485	29	55
14	872	487	30	56
21	740	418	34	57
25	677	394	40	59
30	610	386	41	63
35	571	371	47	72
40	540	361	47	75
45	509	362	50	77
50	488	360	51	76
55	462	352	52	79
60	449	350	53	81
90	397	310	58	84
180	359	290	69	119
365	302	270	81	145

It should be noted that the highest measured flow is 1,784 m³/s. It occurs in a year of very limited data and as a result has not been included in the measured dataset used for energy modelling.

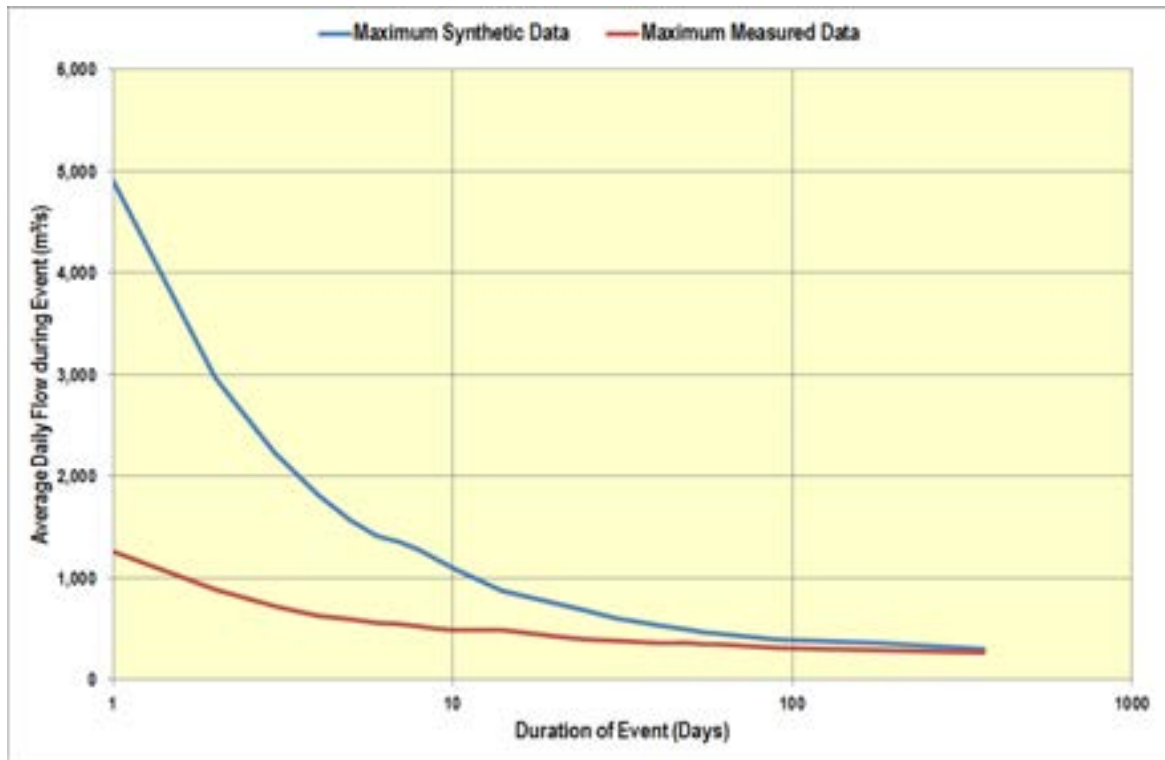


Figure 7-5: Comparison of maximum inflow events for synthetic and measured flows

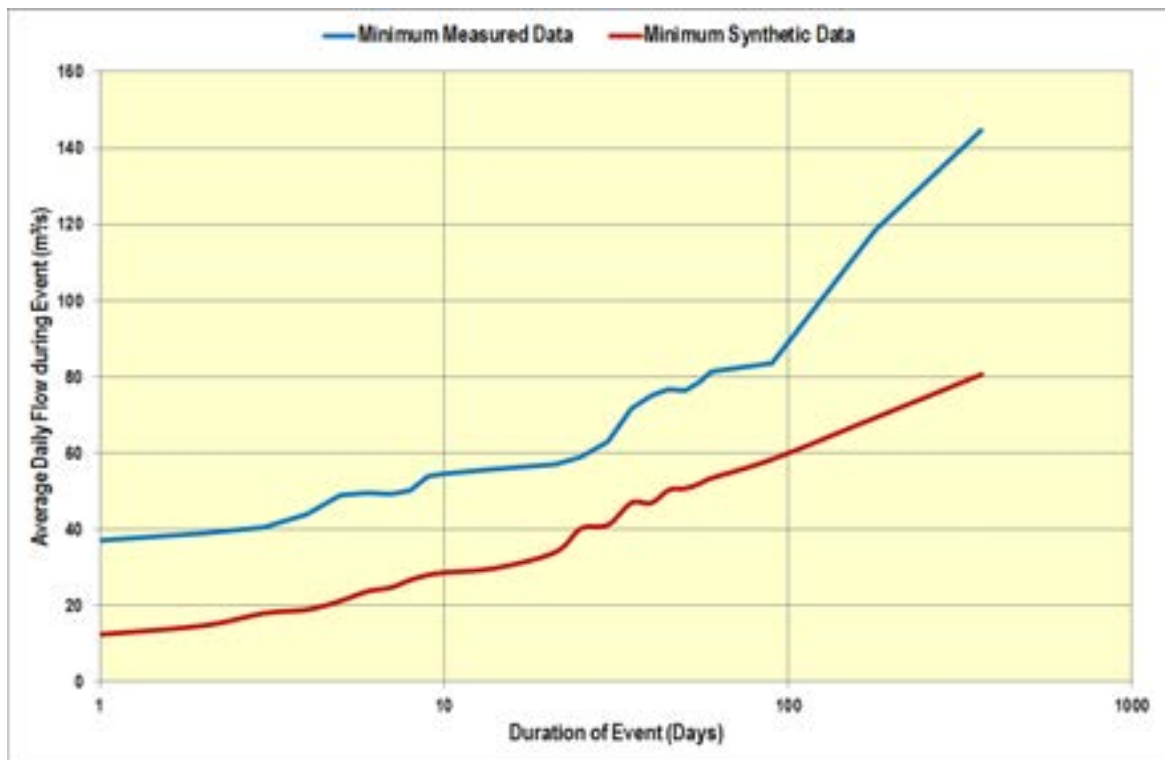


Figure 7-6: Comparison of minimum inflow events for synthetic and measured flows

The following overall conclusions in relation to comparison between the measured and synthetic flow series were drawn:

- The flow duration curves are very similar.
- The extreme events are in line with expectations. The highest 24-hour flow in the synthetic flow series aligns with the assessment of the 1,000-year 24-hour flood.
- The average flow of all the measured data is 222 m³/s but the average for the 16 years used for energy modelling is 220 m³/s and 223 m³/s across all measured data. The synthetic series average is 223 m³/s, as well. The average flows of the 200 × 38 years synthetic series vary over a wide range from 210 m³/s to 234 m³/s.
- The synthetic series low flows are extremely low and last for very much longer than those in the measured flow series. One possible reason for this may be the effect of El Nino. Using the NAOO index there is evidence that if the index is high in the latter half of the year it leads to low rainfall, while if it is high in the first half of the year it is somewhat more likely to be associated with high rainfall. This pattern is seen in the low flow years of 1997 and 2015 in the measured flows series where they are followed by relatively high inflows. It is possible that this synthetic series does not reflect this.
- The measured series low inflows occur over a period of 4–6 months, twice in 16 years of data (1996/97 and 2015). However, it is known that the dataset contains data from the two years of lowest flow since 1980. In other words, the reservoir is effectively buffering low inflow events that occur typically once every 10–20 years. Meeting the demand at times of low water levels sets the operating range of the reservoir.
- The representativeness the measured flow dataset has been investigated further as part of the main SPS. The lowest inflow year in the measured record is 1997 with a 147 m³/s average flow, which is only 66% of the long term average. It has been found that based on the NOAA assessment of the southern oscillation (El Nino/ La Nina), 1997 is the worst year since the records began in 1871. However, since 1960 a number of years have approached 1997 in intensity.
- As a result, it is possible that 1997 was the lowest inflow year in 130 years and may be a century event. However, going forward it is possible that it is an event that is increasingly likely with a return period of 20 years or so.
- Overall, the synthetic series provides a basis for extending the generation projections. It is may be conservative in terms of the long periods of very low flows. The projection of an average flow over a twelve month period seems very conservative and can be compared with worst case of 144 m³ in the measured series. The maximum twelve month flow in the synthetic series is 302 m³/s compared with 270 m³/s in the measured series.

7.4 Residual flow requirements

The minimum flows that need to be maintained during the reservoir filling were investigated. In the absence of a detailed environmental assessment, several different methods can be used to assess minimum flows. The lowest value has been used, based on the minimum 7-day average flow, which is 50 m³/s (Table 7-5).

Table 7-5: Residual flow assessment based on measured flows

Assessment basis	Value	Unit
Residual flow selected	50.00	m ³ /s
10 th percentile flow	98.52	m ³ /s
Minimum 7-day average flow	49.27	m ³ /s
10% 7-day average	130.67	m ³ /s

7.5 Tailwater level

The tailwater curve is based on three sources of information:

- A series of water level rise projections between 400 m³/s and 6,000 m³/s
- Calibration data for the flow gauging site to cover the level change with flow up to 400 m³/s
- Average daily flow from the LiDAR survey in September 2009 was 186 m³/s, while the daily flows varied from 87 m³/s to 482 m³/s. During the survey, the best estimate of the water level at the powerstation site is RL 49.96 m.

Together, these three sources of information provide a tailwater curve for use in the energy modelling by assuming the mean monthly flow during the LiDAR survey. The resulting curves for the powerhouse and spillway sites are shown in Figure 7-7. The tailwater to the powerhouse is the highest level set by the discharge at the powerstation and the backwater from the discharge of the spillway plus powerhouse flows.

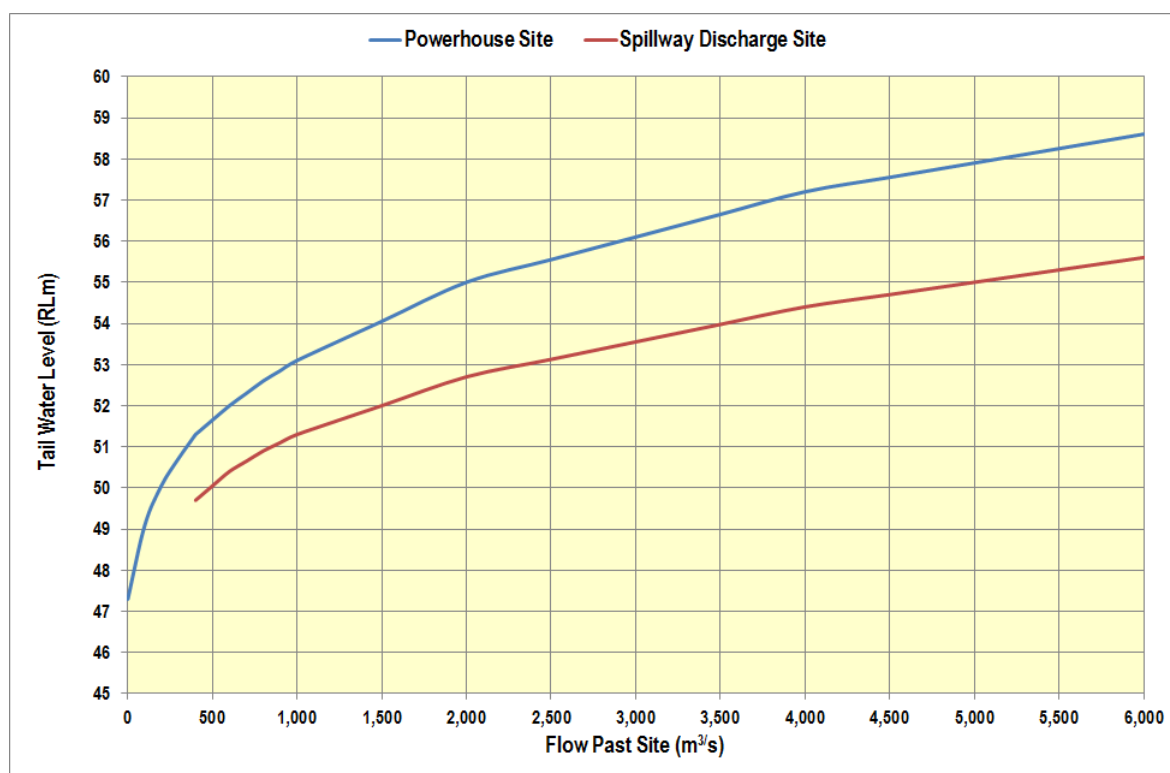


Figure 7-7: Tailwater curve – powerhouse and spillway sites

7.6 Water balance

Based on the design of the FRHEP, reservoir operating rules have been prepared for the Frieda reservoir using a water balance model. The water balance model takes account of the following:

- Inflows as described in Sections 7.2 and 7.3.
- Seepage losses from the dam and reservoir – the permeability of the embankment is assumed to be 1×10^{-8} m/s in the absence of the basal seepage assessment. This value will be revised once the design is developed further. The sensitivity of the generation potential to this assumption has been included in this study.
- Evaporation from the reservoir surface
- The higher yield of rainfall that falls directly on the reservoir: Analysis of the rainfall and flows indicates that 78.6% of the rainfall is recovered as flows into the river on average. The net result

is that the correction for this direct rainfall more than compensates for the evaporation losses from the reservoir.

- An allowance for spillway discharges has been included in the model and is calculated on an hourly basis to prevent instability in the model when high flows are encountered.

Full details are set out in the FRHEP water management operating rules (Section 19.3.1).

7.7 Implications of early power generation

There are two ways of achieving early power at FRHEP:

- To provide a lower intake that allows the generation to commence before the normal operating range is reached. This works because the demand is low in the first few years of operation when only the FRCGP is supplied. The correct level for the intake is determined by ensuring the flow required for full power is significantly less than the mean river flow so that the reservoir can continue to fill, albeit at a reduced rate, once generation commences.
- To commence filling the reservoir before the embankment is complete and the spillway is commissioned. This has been referred to as 'Early Filling' in this investigation.

These strategies can be implemented separately or together. Implementing both strategies will result in soonest achievement of early power.

7.7.1 Lower intake

Considerable modelling has been undertaken to determine the optimum level of the lower intake that can be used at the FRHEP. The net result is set out in Table 7-6 and Table 7-7 for the January and May electrical demand profiles respectively.

Table 7-6: Generation potential at the lower intake reservoir level - January electrical loads

Parameter	Unit Performance	Station Performance
Minimum operating level (RL m)	157.65	157.65
Maximum achievable flow (m ³ /s)	44.5	178.0
Maximum achievable output (MW)	36.5	146.0

Table 7-7: Generation potential at the lower intake reservoir level - May electrical loads

Parameter	Unit Performance	Station Performance
Minimum operating level (RL m)	166.20	166.20
Maximum achievable flow (m ³ /s)	46.8	187.3
Maximum achievable output (MW)	41.3	165.2

7.7.2 Early filling

The adoption of an early filling strategy has some risk compared with reliance on the completed embankment and commissioned spillway. Before early filling can commence there are a number of prerequisites:

- The embankment should be protected from overtopping in events with a return period of up to 10,000 years. In absence of a spillway the freeboard needs to be significantly greater during filling compared with normal operation.
- In the event of high inflows, it must be possible to drain the reservoir back to the target water level for a given embankment height.

There are three ways water can be drained from the reservoir during filling:

- Using the residual flow valves which have a capacity of 50 m³/s
- Using the spillway once the level is high enough
- Using a dedicated set of valves or gates. This is discussed in detail in Sections 7.8 and 15.2.

The methodology used to estimate the Storm Buffer Volume and embankment freeboard during early reservoir filling based on data from the synthetic flow series in the absence of other information was endorsed by the TIRP at the June 2018 review meeting. However, they suggested that less conservative assumptions would be acceptable to allow earlier filling of the reservoir. The updated list of prerequisites required for early filling are given below. Before early filling can commence there are a number of prerequisites:

- 1 Both of the conveyance systems must be complete in all respects.
- 2 The intakes must be complete, and the gates installed and dry commissioned on the lower intake and preferably the upper intake as well.
- 3 The four powerstation bypass valves and their respective guard valves must be dry commissioned and fully operational, other than the fact that they have not been wet commissioned.
- 4 All 10 turbine generator inlet valves must be in place. The valves should be blanked off if the turbine generator is not connected to them and the water passage installation complete. Ideally, their service and maintenance seals will be operational to ensure the valves are also sealed.
- 5 The embankment must be built to a height that allows a major storm to be buffered before the bypass valves can drain the water. The need for a 6-month delay in construction, which was the basis of the previous Storm Buffer Volume has been removed on the grounds that the long-term embankment safety in the event of any delay relies on the integrity of the bypass valves. Instead three further assumptions have made:
 - a. It would take 2 months to repair a routine issue that is identified affecting all of the bypass valves. This is extremely unlikely and a full Fault Tree Analysis during future studies is necessary to confirm this allowance. However, a volume equivalent to the greatest 2-month inflow has been included in the synthetic flow series, less the residual valve flow over this period at 50 m³/s. This is a delay volume of 2,096 Mm³.
 - b. An additional Storm Buffer Volume is required which can rely on the bypass valves to protect the dam. It can be seen from the analysis in this section that a Storm Buffer Volume of 715 Mm³ is required. Four 2.3 m diameter fixed cone valves are required. These valves can pass 500 m³/s when all valves are operational, and the reservoir is over RL 160 m. This increases to almost 700 m³/s when the reservoir reaches the normal maximum operating reservoir level.
 - c. The dam must be safe even if no advantage is taken of the early filling. This is significant as once the power generation commences the rate of level rise of the reservoir reduces significantly. If power generation does not commence at the planned rate, the water level rise in the reservoir could be greater than expected. This situation could arise if early filling commences and operation of the FRCGP transmission line to the mine or the FRHEP generating plant is delayed.
- 6 The spillway and spillway crest must be in place before the water level can be increased over RL 181 m. The gates do not need to be operational, but they must be able to be dogged in the fully open position
- 7 The Storm Buffer Volume assumes that a level rise equivalent to 25% of the buffer volume is required before the valves commence to open.

7.7.3 Storm buffer volume required during early filling

The determination of the required Storm Buffer Volume can only be completed to a preliminary level at this time. The ideal methodology would involve analysing a range of long duration events up to perhaps 30 days or more with return periods of 1,000 to 10,000 years as suggested by the TIRP. It would be desirable to review longer period events as well with return period of 100,000 and 1,000,000 years to allow the safety margins to be established.

There is no hydrograph information available for long duration events. In the absence of this information the synthetic data series which consists of 200 series of 38 years has been used. It provides daily average flows for each day in the 7,600 years. This data is described in more detail in Figure 7-8. Using this series, the total inflows for a range of long duration storms has been derived. These are large scale events and bring in more water in most cases than the design 72-hour PMF which sizes the spillway on the completed embankment. It can be seen that an 8-day storm is regarded as the design storm for the early filling buffer and the total inflow over the eight days is equivalent to 0.89 times the water from the 72-hour PMF event. The required buffer volume to allow the bypass valves to drain the reservoir to restore the freeboard is 0.52 times the water volume from the 72-hour PMF event.

It should be noted that not only the duration of the event and total water volume flowing into the reservoir determines the required storm buffer volume. It is also determined by the capacity of the bypass valves.

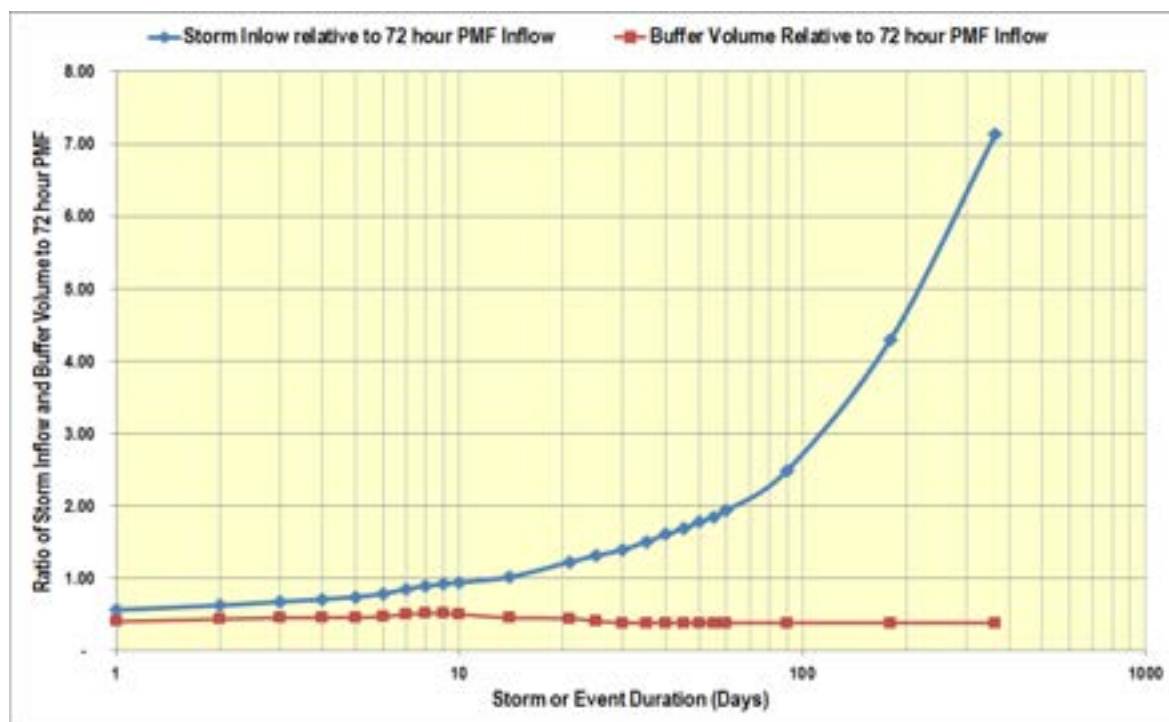


Figure 7-8: Ratio of the storm inflow event to the 72-hour PMF

The sizing of the bypass valves involves a number of considerations:

- The larger the bypass valve capacity, the higher the cost and the higher the velocity in the conveyance system.
- Initially all of the flow from the bypass valves must pass through the single lower intake. This is the design case for the sizing of the intake screens.
- The greater the required discharge through the bypass valve, the greater the submergence (or driving head) required on the bypass valves.

Through a process of trial and error, it was found that the optimum valve configuration is four Howell-Bunger valves 2.3 m in diameter (90 inch), each with its own butterfly guard valve. These valves can pass 498 m³ at the minimum operating level. This is not a large flow in comparison with the inflows that can occur and hence the long duration events are important in determining the Storm Buffer Volume.

A second issue is to decide how the Storm Buffer Volume will be utilised. The problem is how to distinguish at the outset between a high inflow event which is filling the reservoir more rapidly than a few days earlier, or a major event the requires water release. At this time the strategy adopted is to assume that the operators will have sufficient data available to them that will allow them to characterise high inflow events when monitoring inflows. A management system that provides this data will be required. Once a threshold level is exceeded, the bypass valves will commence operation. At this time, the level set for the valves to open is half the buffer volume.

The result of modelling the inflows is shown in Figure 7-9. This shows the following information:

- The average inflow over the duration of the event
- Total inflow volume over the event
- Required Storm Buffer Volume
- Days to drain the Storm Buffer Volume using the bypass valves.

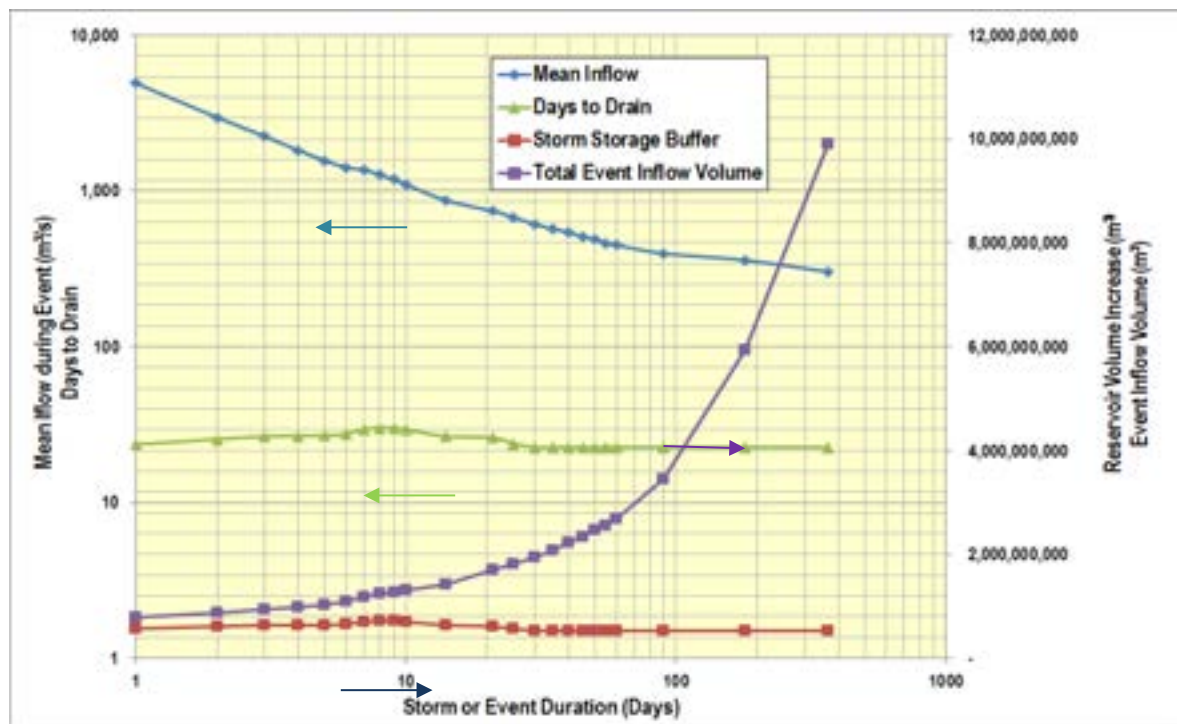


Figure 7-9: Relationship between the required Storm Buffer Volume and the storm event

7.7.4 Combined delay and storm volume assessment

Analysis of the storms considering these new criteria has confirmed the 8-day event set out in the previous section is still the critical event. Figure 7-10 and Figure 7-11 show the following information:

- The fastest (maximum) water level that occurs during early filling assuming generation commences as soon as possible
- The average water level that occurs during early filling assuming generation commences as soon as possible

- The slowest (minimum) water level that occurs during early filling assuming generation commences as soon as possible
- The required dam crest level including a 3.5 m freeboard to cope with the maximum water level that can occur assuming generation commences
- The required dam crest level including a 3.5 m freeboard to cope with the maximum water level that can occur assuming generation commences and assuming a 2-month delay in valve operation
- The required dam crest level including a 3.5 m freeboard to cope with the maximum water level that can occur assuming generation does not commence and assuming a 2-month delay in valve operation with the water ultimately spilling down the spillway when the crest height is reached
- The required dam crest level including a 3.5 m freeboard to cope with the maximum water level that can occur assuming generation does not commence – in this case no allowance has been made for a Delay Buffer to cope with the outage of the valves
- The required dam crest level including a 3.5 m freeboard to cope with the maximum water level that can occur assuming generation commences and assuming a 2-month delay in valve operation. In this case an allowance has been made for a Delay Buffer to cope with the outage of the valve. This is assessed based on the measured flow data only.
- The required dam crest level including a 3.5 m freeboard to cope with the maximum water level that can occur assuming generation does not commence and assuming a 2-month delay in valve operation. In this case an allowance has been made for a Delay Buffer to cope with the outage of the valve. This is assessed based on the measured flow data only.
- The required dam crest level including a 3.5 m freeboard to cope with the maximum water level that can occur assuming generation commences and assuming a 2-month delay in valve operation. In this case an allowance has been made for a Delay Buffer to cope with the outage of the valve. This is assessed based on the synthetic flow data.
- The required dam crest level including a 3.5 m freeboard to cope with the maximum water level that can occur assuming generation does not commence and assuming a 2-month delay in valve operation. In this case an allowance has been made for a Delay Buffer to cope with the outage of the valve. This is assessed based on the synthetic flow data.

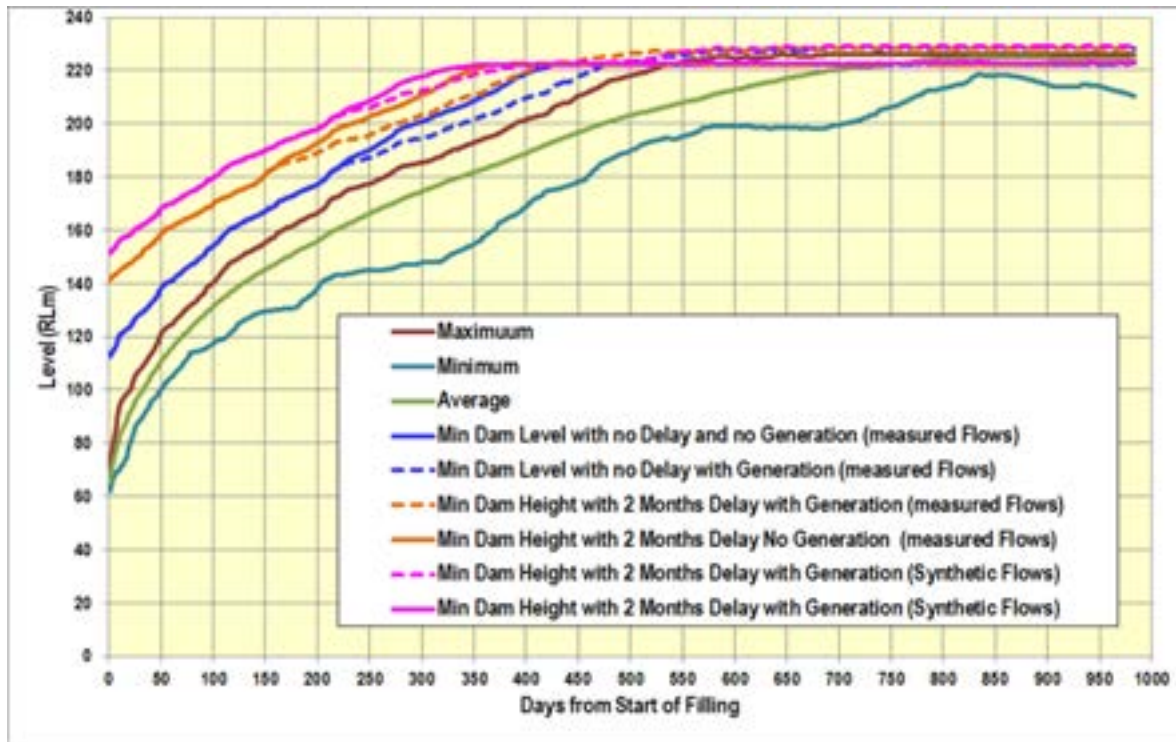


Figure 7-10: Critical dam crest and water levels during early filling – water levels are based on generation meeting budget

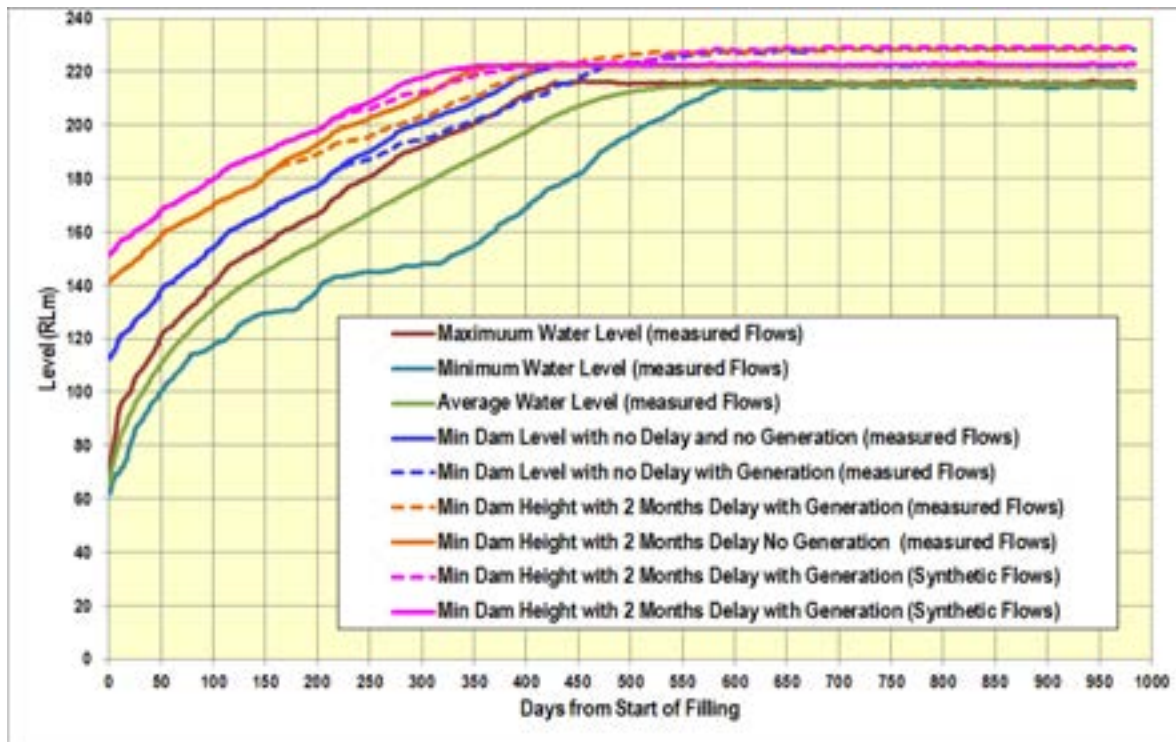


Figure 7-11: Critical dam crest and water levels during early filling – water levels are based on no generation

As can be seen the various methods of assessing the Delay Buffer and Storm Buffer Volume result in significantly different embankment heights. The most conservative option has been selected which requires an embankment height of RL 151.48 m for early filling to commence and an embankment height of RL 201.69 m by the time the water level reaches a level for generation to commence.

This reduces the embankment volume that is required to be in place for filling to commence to 66% of the total volume. Further analysis of the embankment construction rates is required to confirm that full advantage can be taken of the early filling, with all intermediate heights having the required freeboard. This will need to be reviewed substantially during the next phase of the project. A Fault Tree Analysis approach to confirming the adequacy or otherwise of the 2-month delay allowance for bypass valve repairs is required.

Figure 7-12 shows the required Storm Buffer Volume as the reservoir is filled. It varies based on the bypass valve capacity at different reservoir levels and once the spillway crest is reached. The initial Storm and Delay Buffer is initially 2,536 Mm³ and it stabilises at 360 Mm³ to 390 Mm³.

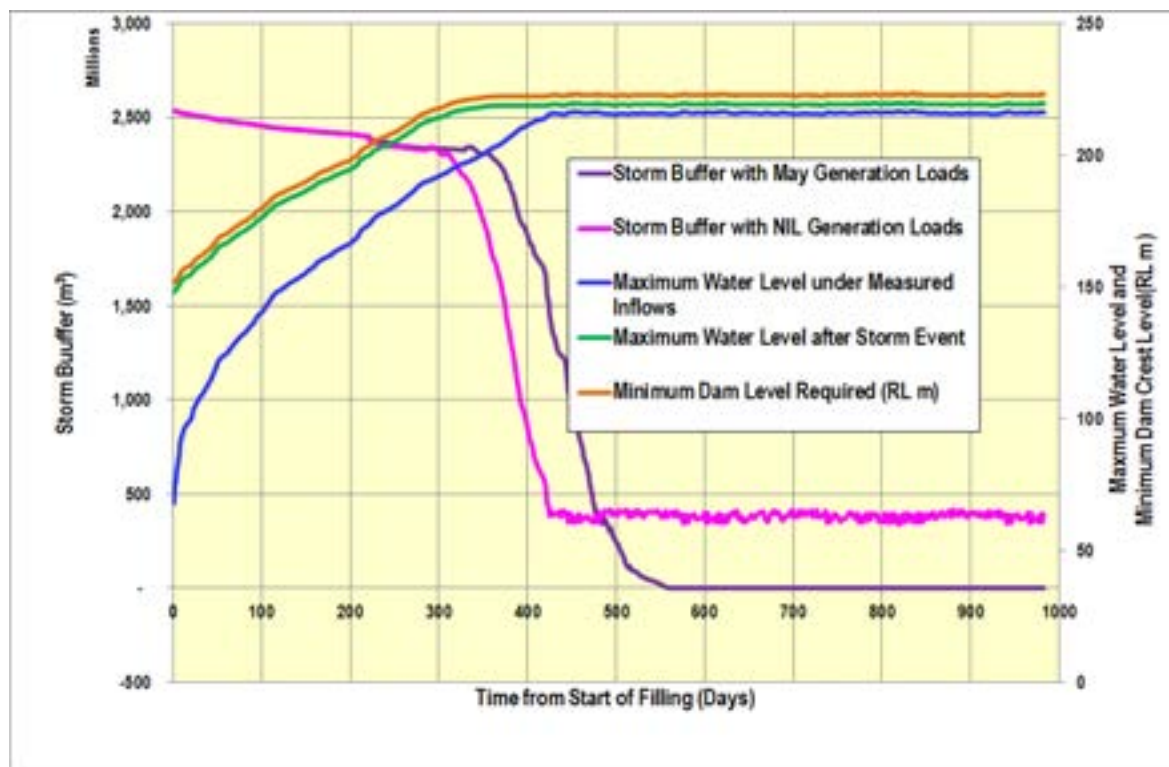


Figure 7-12: Variation in Storm Buffer Volume with time from start of filling

7.7.5 Impact of early filling and lower intake on time to first power generation

Provision of the lower intake at the level proposed above accelerates the time to first power generation as detailed in Table 7-8, for the following four cases:

- Time to normal minimum operating level with upper intake
- Time to normal minimum operating level with upper intake plus early filling. It should be noted that this case has the same timings as the previous case. The reason is that the dam needs to be to full height before this option can commence filling and hence it offers no benefit.
- Time to normal minimum operating level with lower intake
- Time to normal minimum operating level with lower intake plus early filling.

All cases have a common base date. Some of the time difference relates to the time that the dam embankment takes to construct the embankment to the level needed to allow filling to commence. Adjustments to the construction time assume even placement of material as the dam is constructed. A 28-month embankment construction time is assumed to construct the embankment to full height.

The use of the lower intake reduces the time to first power to FRCGP by an average of 200 days and the early filling reduces time to first power by a further 292 days, i.e. a total benefit of 492 days on

average. The first power to the export grid is increased by an average of 64 days owing to the low intake. The increase is caused by the fact that more water is discharged through the powerstation decreasing the amount of water retained in the reservoir. Early filling reduces it by 292 days giving a total benefit is 228 days on average.

Table 7-8: Effect of early filling and low intake on time to first power

Filling Case	Time to normal minimum operating level with upper intake (days)	Time to normal minimum operating level with upper intake plus early filling (days)	Time to normal minimum operating level with lower intake (days)	Time to normal minimum operating level with lower intake plus early filling (days)
Embankment volume in place for filling to commence	100%	99%	100%	66%
Time to first power to FRCGP				
Average	767	753	567	275
Earliest	689	675	779	212
Latest	867	848	699	407
Time to first power to Export grid				
Average	937	937	1,001	709
Earliest	805	791	852	560
Latest	1,075	1,061	1,165	873

7.7.6 Early filling findings

Based on this analysis, the following conclusions are drawn:

- The required Storm Buffer Volume is almost 715 Mm³. This is 52% of the 72-hour PMF inflow volume of 1,386 Mm³. A Delay Storage Buffer of 2,096 Mm³.
- A bypass valve capacity of 498 m³/s is required when the reservoir level exceeds RL 160 m. This is provided by four 2.3 m diameter Howell-Bunger valves located at the powerstation.
- The lower intake reduces construction times by 200 days while early filling improves matters by an average of 292 days. The combined benefit is 492 days (16 months). It should be noted that the assumptions concerning the level of embankment prior to filling commencing may be found to be too conservative at the next phase of the project. If this is the case, or if the embankment construction is delayed, the benefits could be significantly greater.

7.8 Powerstation bypass valves

The powerstation bypass valves have the following primary functions:

- To drain the reservoir to a normal level following a major storm event or high inflow event during early filling operations. The valves have been sized at 498 m³/s for this purpose as described in Section 7.7.3.
- To provide sufficient water to allow the river barges to operate. No bathymetric survey of the river downstream of the FRHEP to allow an accurate assessment of the flows required for river transport is currently available. The limited known information related to the flow requirements for barge operation is set out in Section 7.8.1.

The performance of the bypass valves under different conditions is set out in Table 7-10.

Table 7-9: Bypass valve capacity at different water levels

Case	Maximum PMF water level	Maximum normal operating level	Minimum level to obtain full flow	Minimum level to obtain full flow
Number of intakes in use	1	2	1	2
Intake	Upper	Upper	Upper	Lower
Water level (RL m)	231.5	226.1	201.10	161.23
Flow (m ³ /s)	705.1	693.9	634.0	497.7
Velocity at bell mouth (m/s)	2.61	2.57	2.35	3.69
Submergence (m)	4.73	4.65	4.25	6.68

7.8.1 River transport flow requirements


There is little information available concerning the flow requirements for barging. Figure 7-13 shows details of an existing barge on the Frieda River which can transport 380 tonnes. This is sufficient for a generator rotor and stator in a single load. The maximum draught is approximately 2.1 m, if the barge transport terminates at an area similar in width to where the spillway is located, a river flow of 250–500 m³/s will be required to allow the barge to access the area. Information from 16 August 2016 shows the barge portrayed could not travel up river when flows were varied between 100 m³/s and 200 m³/s for the previous fortnight. It is known that the barge did travel up river in February and March 2017 when the river flows varied between 200 m³/s and 400 m³/s. The required draft for the load being carried is not known.

The only conclusion possible at this time is that to maintain navigation while the dam is filling and in the early years of generation, releases of 250–500 m³/s will be required for several days to allow a large barge to navigate the river. This flow is not available from the residual flow valve, which is sized for flows of 50 m³/s. Once generation commences, the turbine flows will vary between 15 m³/s and 50 m³/s over the first few months and then increase to between 140 m³/s and 160 m³/s. This is also unlikely to be sufficient for navigation purposes and will require supplementing with additional flows.

At this time there is insufficient information concerning the river depth required, and hence flows required, to allow definitive conclusions to be drawn. There is no bathymetric survey of the barge route and port site to allow the relationship between flow and depth to be confirmed. As a result, the information in this section is somewhat speculative.

The conclusion is that bypass valves sized to pass major storms during early filling at 498 m³/s should be adequate for allowing navigation of the river to be maintained with the 380 tonne deadweight barge used at present to access the Frieda River region.

The wider impact on existing river users of decreased downstream river flows during and after construction of the project will have to be addressed in the Environmental Study to be undertaken during future studies.




P.O. Box 750 Lae, Papua New Guinea
Phone: (675) 4721990 Fax: 4726025

P.O. Box 1824, Port Moresby, PNG
Phone: (675) 3201013 Fax: 3213135

[Email: bismark@online.net.pg](mailto:bismark@online.net.pg)

MV FRIEDA RIVER



Type:	Twin Screw Landing Craft
Classification:	NMSA/PNG Gov
Year Built:	1979
Flag:	PNG
Port of Registry:	Port Moresby
Official No.:	001290
IMO:	7923811
Call Sign:	P2V5442
Length Overall:	47.43
Breadth:	10.40m
Depth:	2.7m
Draft Maximum:	2.1m
Gross Registered Tonnage:	473 Tonnes
Net Tonnage:	167 Tonnes
Available Deck Area:	380m ² approx..
Deadweight:	380 Tonnes approx..
Fresh Water Capacity:	100,000 Litres
Fuel Capacity:	300,000 Litres
Fuel Consumption:	140 Litres/Hour
Main Engine:	Two Caterpillar D379 at 500HP at 1225 rpm each
Generators:	1 x 120 KVA – Detroit 1x 100 KVA – Detroit
Speed:	8 knots
Accommodation:	11 men

Figure 7-13: Possible barge transport for major plant along the Frieda River

7.9 Residual flow valve

This study has therefore proceeded on the basis that a flow of 50 m³/s as set out in Section 7.4. It is stressed that the purpose of installing a residual flow valve is to pass residual flows only; it is not intended to pass storms, but the inclusion of a residual flow valve can contribute additional flow capacity.

When filling commences, the residual flow valves are opened and the diversion stoplogs installed.

This valve can be controlled hydraulically from surface. Hydraulic pipes will run from a control building at ground level, down the raised bore, to the residual flow valves and their guard valves. The valve installation consists of the two shrouded 1800 mm jet flow residual flow valves. An 1,800 mm butterfly guard valve will also be provided for each residual flow valve. The residual flow valve is sized to pass 50 m³/s once the water level reaches RL 80 m. If required, higher flows could be passed. The details are set out in the table below. This shows the required water level to allow the system to pass 50 m³/s, 75 m³/s and 100 m³/s. The time it takes the reservoir to reach the required level is also shown, based on the measured flow data series. The 100 m³/s row shows the maximum flow potential of the system. Above this the operation of the valves will be compromised by the water level rise in the downstream chamber.

Table 7-10: Residual flow valve operation

Flows (m ³ /s)	Required water level (RL m)	Time to achieve design flow (days)		
		Shortest	Average	Longest
50	80	6	10	21
75	100	22	34	51
100	128	69	92	139
121	162 ⁽¹⁾			

Note: (1) Level at which power generation can commence.

If a greater residual flow is required larger tunnels and valves will need to be installed to allow the valve to pass the required flow at low levels, which will mean a larger residual flow tunnel and a larger raised bore for access and valve installation.

8 Embankment

The selection of an embankment location and associated footprint was based on the results of a formal options analysis and optimisation assessment completed as part of the SPS. The final location is the most favourable site for geological, geotechnical and financial reasons, and its location in the narrow part of the Frieda River downstream from its confluence with the Ok Binai River, makes it suitable for hydroelectric power generation, as shown on SRK Drawing PNA009-0020.

The final design embankment height is RL 190.5 m, measured from the lowest level in the river at the downstream toe to the crest of the embankment at RL 238.5 m. The embankment will be constructed as a single raise rockfill embankment.

The results of the stability assessment and deformation numerical modelling detailed in Section 8.11 were used to inform the embankment design.

Raise strategy

The embankment will be designed to safely retain approximately 9.6 Bm³ of water at the maximum operating level to satisfy hydropower requirements, as well as ~2.17 Bm³ of tailings, waste and sediment over the life of the FRCGP. Sediment will continue to run off into the reservoir into perpetuity. The long-term sediment distribution throughout the reservoir was not modelled as part of the SPS, but should be carried out to validate the storage capacity for natural sediment contribution to the reservoir after closure of the FRCGP when continuous water supply for ongoing hydroelectric power generation will be needed. In SRK's opinion, available storage will be adequate, given the low forecast rate of natural sedimentation.

Early filling of the reservoir will commence once the diversion tunnels are sealed, at which stage the embankment crest will be constructed to a specified elevation. Construction of the embankment will continue throughout reservoir filling period. However, the elevations used in the following design were based a previous early filling strategy whereby filling would only commence once the embankment crest reaches an elevation of RL 181 m.

Power generation will commence once the embankment crest has reached approximately RL 201.7 m.

The construction of the embankment will be undertaken upstream and downstream of the asphalt core, to allow embankment fill to be continued while the cut-off wall and concrete plinth construction is in progress.

Key elevations

During the SPS, a number of critical elevations for operation of the FRHEP were defined (Figure 8-1). These elevations have been used as the basis for design.



Figure 8-1: Critical elevations for FRHEP operations

8.1 Design features

The embankment has been designed as a zoned rockfill embankment with an impermeable core. The embankment design includes the following main features:

- Foundation: excavation of unsuitable material from the foundation of the embankment
- Impermeable core: asphalt core zone slightly upstream of the centre of the embankment
- Filter/ transition layers: upstream and downstream of the core and partial horizontal filter and transition zones at the base of the downstream half of the embankment
- Embankment seepage cut-off: plastic concrete cut-off wall and grout curtain, including pressure grouting of fault structures
- Plinths: two plinth designs – for the valley plinth and the abutments plinths
- Toe drain
- Zoned rockfill shell.

8.2 Foundation preparation

Geotechnical investigations undertaken for the SPS (Section 3.1) indicated that the depth to competent material in the centre of the valley or river section is relatively shallow (~5 m), whereas the depth of weathering on the abutments are in places even less. Figure 8-2 shows a representation of the recommended foundation excavation depths (vertical) across the FRHEP footprint.

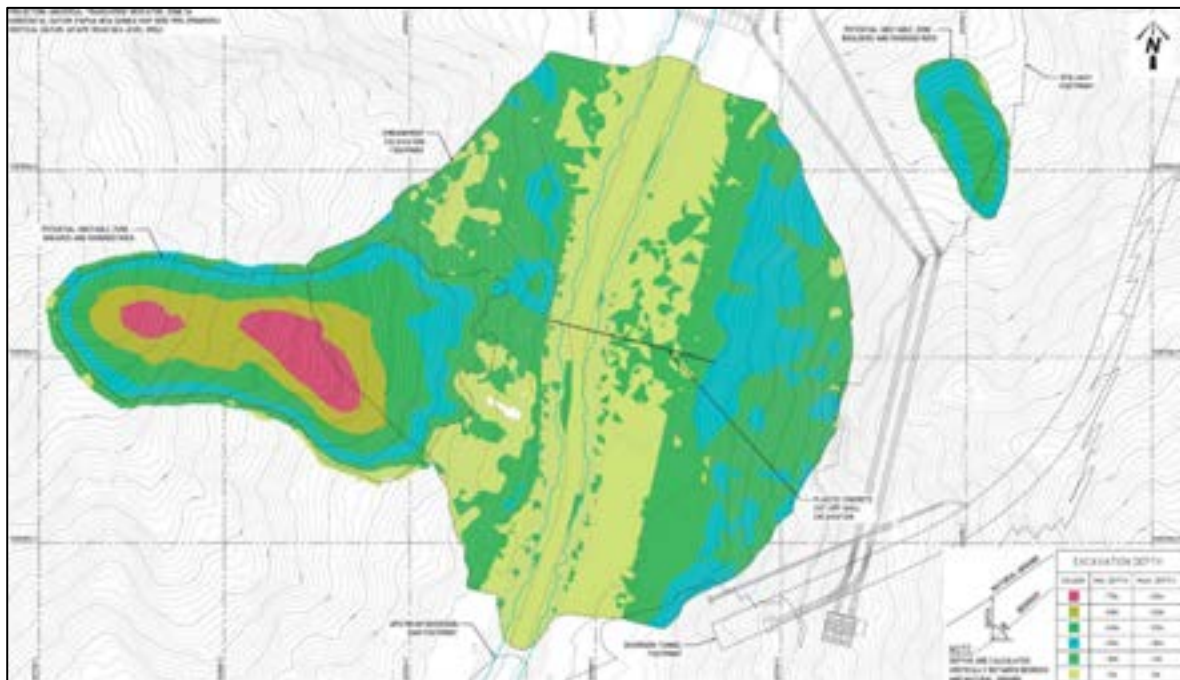


Figure 8-2: Recommended depth of excavation

Figure 8-3 and Figure 8-4 are core photos from holes F4, RH4, RH6 and RH7 drilled as part of the geotechnical investigation of the Frieda River riverbed that represent the typical geology of the founding level (~5 m).



Figure 8-3: Core photos from holes RH4 and RH6 – Frieda River riverbed representative of foundation level (~5 m)



Figure 8-4: Core photos from holes RH7 and F4 – the Frieda River riverbed representative of foundation level (~5 m)

The depth of material removed will be decided on site during construction and will depend on the depth at which the prescribed quality of material is encountered during stripping, and the local strength and saturation of the material.

The investigation indicated that there is a considerable depth of weathering on the left abutment. All weathered material in this zone must be removed as it is deemed unstable. The depths of excavation across the plinth alignment are shown in SRK Drawing PNA009-0084. Typical soil profiles are shown on SRK Drawings PNA009-0030 and PNA009-0032.

The properties of the material horizons including the embankment founding layer are summarised in Section 3.1 (Geotechnical Investigation).

The material in the river section is clast-supported alluvial/ colluvial material which will have larger settlement characteristics than the abutments. Settlement is likely to occur with a slight rotational movement with uncemented alluvium expected to present the most settlement.

Findings from the geotechnical investigation identified that the left and right abutment groundwater levels are below the maximum excavation depth for the embankment foundation and are therefore not likely to affect the foundation cut slopes (Figure 8-5). However, the potentially unstable weathered mass on the left abutment and spillway cut on the right abutment are likely to intersect groundwater and will require rock drainage. Groundwater levels become progressively shallower with proximity to the river and where excavations intersect the groundwater; sumps are to be installed to control seepage during construction. Collection and review of accurate groundwater data is recommended for ongoing assessment. In the absence of accurate data, the phreatic surface has been conservatively assumed; however, this should be refined in a later design stage.

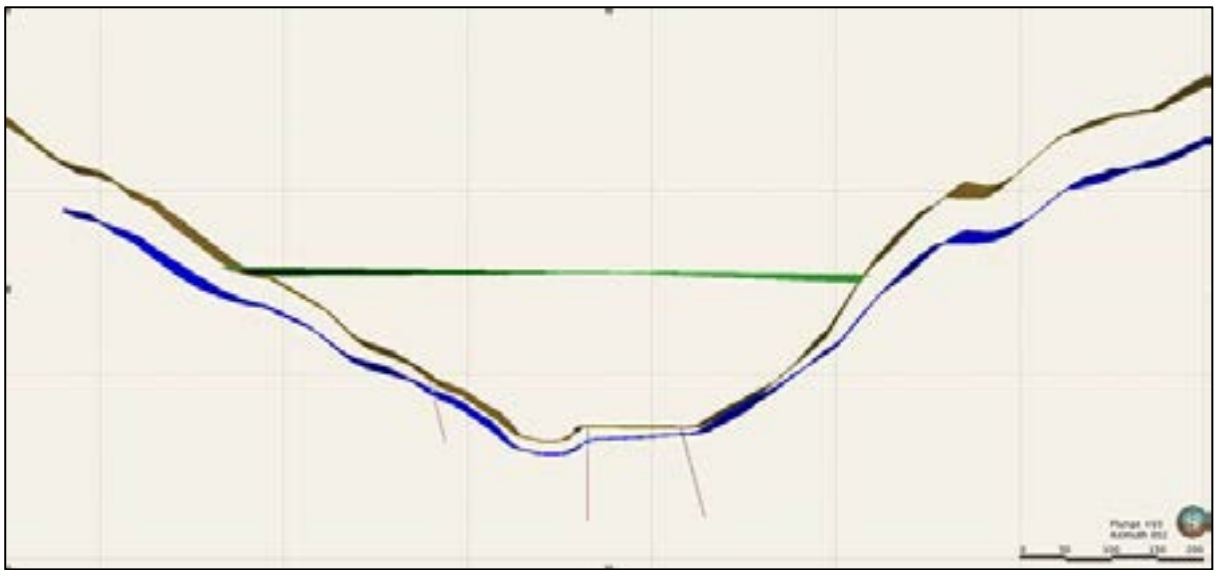


Figure 8-5: Groundwater levels (blue) below surface level (brown) at the centreline of the embankment.

Sudden grade changes in the foundation rock profile and angles steeper than 50° along the long section of the plinth must be avoided. SRK has identified areas that require foundation re-profiling, particularly on the right abutment, as shown on SRK Drawing PNA009-0084. Once the foundation has been cleared, the actual profiles should be re-assessed. This may require additional excavation to be undertaken.

Temporarily exposed foundation excavations at the base of the embankment may have steep slopes that require temporary rock supports. Such requirements will be assessed and considered during construction. Temporary excavations will have localised areas steeper than 1V:2H. Further analysis will be conducted after the SPS to confirm the stabilisation requirements for the foundation base excavations.

The excavation slope will extend to the natural surface or to a soil anchored wall. Soil anchored walls will be required where the foundation box-cut slope would otherwise intersect the haul road alignment, or where a considerable reduction in excavation volumes could be achieved. SRK has excluded the allowance for soil anchors from the current SPS.

8.3 Seepage control

Seepage measurement and control is an important consideration for the embankment design. The embankment has been designed with an asphalt core located slightly upstream of the centre. The following sections address the design and development of the asphalt core, concrete plinth, plastic concrete cut-off wall and grout curtain for embankment seepage control, and associated filter and transition layers. To avoid potential stability hazards, the design of the embankment allow the phreatic surface to exit at, or below, the downstream embankment toe in a controlled manner. High seepage rates above the downstream toe can lead to erosion and potential embankment instability. In addition, there is a requirement to prevent hydraulic uplift and to retain water for power generation.

The seepage barrier consists of an asphalt core with a cut-off wall and plinth positioned slightly upstream of the centre of the embankment. This alignment will be further evaluated during future studies. The cut-off under the plinth is comprised of a plastic concrete cut-off wall extending to bedrock and a concrete grout curtain to seal any high-permeability zones, including fractures or faults that may exist. The embankment cross-section of the asphalt core and plinth is shown on SRK Drawing PNA009-0082.

The design has considered normal operating conditions and more extreme, less likely conditions that the FRHEP may experience during operations and post closure.

Asphalt core

The use of an asphalt core has commonly been applied to rockfill embankments in regions of high seismicity and extreme rainfall. The simple and robust core is favourable for placement and compaction in these conditions. The asphalt core is ductile with viscoelastic-plastic properties that allows the core to sustain significant earthquake cyclic loads with no deterioration of material properties⁷². Additionally, an asphalt core exhibits self-healing properties especially under compressive stress conditions such that if any crack occurs, the crack can repair itself. Studies by Zhang et al., 2012⁷³ show that depending on the size, cracks on asphalt core seal comparatively quickly, and within five hours of cracking, the measured leakage reduces by 1–4 orders of magnitude depending on the compressive stress levels imposed. The asphalt core's low permeability ensures the embankment is watertight during operations and closure, as well as during static and earthquake loading conditions.

To reduce the amount of asphalt required, an asphalt core is typically tapered at the top where lower hydraulic gradients are expected, as shown on SRK Drawing PNA009-0082. SRK's benchmarking exercise revealed that the thickest asphalt core built to date is 1.5 m – at the 174 m high Quxue Dam in China.

Significant seismic activity is expected at the FRHEP site, which is likely to result in larger than normal displacements in the upper third of the embankment. Excessive post-seismic displacement may cause shearing of the asphalt core, resulting in a severed core and development of an open flow path. To accommodate post-seismic displacement, the design includes a 1.5 m thick asphalt core in the upper part of the embankment. The asphalt core gradually widens towards the base to a thickness of 1.7 m. Based on previous field measurements on three of the highest asphalt core dams built to date,

⁷² Höeg, K, 1993. Asphaltic concrete cores for embankment dams. Norwegian Geotechnical Institute Publication.

⁷³ Zhang, Y, Höeg, K, Wang, W and Zhu, Y, 2013. Watertightness, cracking resistance, and self-healing of asphalt concrete used as a water barrier in dams. Canadian Geotechnical Journal, 50(3): 275-287.

the maximum asphalt core displacements have been 0.15 m for Finstertal Dam⁷⁴ (149 m high), and 0.25 m for Storglomvatn Dam⁷⁵ (128 m high) and the Yele Dam⁷⁶ (125 m high). The embankment characteristics, including the filter and transition zones that provide lateral support to the core, result in the design bending strain at the FRHEP being acceptably small. The tolerable bending strain ranges from 2% to 8% in the literature where the estimated strain is 0.15% for an average thickness of 2.3 m at the top.

The numerical modelling established that the vertical shear forces are within acceptable limits and differential settlement between the upstream and downstream segments of the rockfill will likely cause shearing in the filter zone, as opposed to carrying sufficient load to the core that will result in shearing of the core. The acceptable shear stress is 0.43 MPa; the maximum estimated shear stress is 0.27 MPa which corresponds to the cross-section where the maximum stress was developed.

The foundation footing for the asphalt core is twice the width of the asphalt core immediately above the plinth. This provides a larger contact zone between the asphalt core and the foundation and this ratio is required across the entire asphalt core and plinth contact zone.

The design mix content of the asphalt core, including development of a suitable aggregate grading, should be evaluated in future studies. To promote ductility, higher than normal asphalt content may be considered so that larger deformations due to potential seismic loading can be accommodated. The core is supported laterally by a filter/ transition layer on either end, and raised at the same time as the construction of the asphalt core.

Plastic concrete cut-off wall

Although the cemented and uncemented alluvium and colluvium material directly below the embankment foundation has sufficient strength to support the embankment loads, this material will likely permit significant seepage through the foundation and along preferential flow paths. The alluvium and colluvium consist of varying sizes of material confined in a cemented and uncemented matrix, from small rocks up to boulders up to 5 m in diameter. The cemented infill between the boulders and rocks will make it difficult to install grouting.

A positive cut-off methodology using a trench-cut diaphragm wall has therefore been selected. The average 1.5 m wide wall will use plastic cement to provide a ductile, low permeability barrier. The specification of the diaphragm wall includes a permeability of approximately 1×10^{-9} m/s, although a lower value has been used in the seepage modelling to reflect the permeability likely to be achieved.

A concrete plinth connects the plastic cut-off wall and core in the riverbed section. The cut-off wall will also provide support for the core that would otherwise be founded on the alluvium and colluvium, where settlement is expected to be greater relative to the foundations on the abutments. The differential settlement across various parts of the valley would transmit unwanted loads to the core. Due to the expected differential settlement of the alluvium and colluvium in the riverbed section, and the potential for load transfer to the plastic cut-off wall, SRK recommends that the cut-off wall is 2.3 m at the top to accommodate the loads.

During the 2011 feasibility studies performed by SKMPS, Bauer was consulted to advise on a method for providing a cut-off to suit conditions on site. Bauer advised a similar methodology to earlier work.

⁷⁴ Pircher, W and Schwab, H, 1988. Design, construction and behaviour of the asphaltic concrete core wall of the Finstertal Dam. In Proceedings of the 16th Congress of the International Commission on Large Dams, San Francisco, Calif. ICOLD Press, Paris (Vol. 2: 901-924).

⁷⁵ Höeg, K, Valstad, T, Kjaernsli, B and Ruud, A M, 2007. Asphalt core embankment dams: recent case studies and research. International Journal on Hydroelectric power and Dams, 13(5): 112-119.

⁷⁶ Wang, W, Höeg, K and Zhang, Y, 2010. Design and performance of the Yele asphalt-core rockfill dam. Canadian Geotechnical Journal, 47(12): 1365-1381.

Further work performed by Bauer and Keller during the IPS confirmed the selected methodology; however, Keller recommended the use of various trench development techniques to accommodate variance in material types below the embankment. Pre-grouting has been identified as a method of solidifying the foundation matrix to promote a firm medium for cutting the trench and preventing unwanted movement of rocks.

The diaphragm wall will extend under the plinth to fresh bedrock as shown on the long section of the plinth line on SRK Drawing PNA009-0088. Typically, the depth of the diaphragm wall will range from 15 m to 65 m, and the average minimum wall width will be 1.5 m. The cut-off has been designed to ensure an adequate seal is achieved at the interface between the cut-off and the bedrock. For this reason, it is recommended that the wall be installed at least 3 m beyond the interface into bedrock.

As the invert of the deepest section of the river portion is approximately 16 m lower than the platform, the plastic concrete cut-off will be extended in this section to provide sufficient cut-off in this zone and to match the elevation of the top of the cut-off wall in the platform, as shown on SRK Drawing PNA009-0088. This section of the cut-off wall will be raised in conjunction with the embankment in this part of the valley. This configuration results in the cut-off and asphalt core interface being at a constant elevation across the valley.

Grouting

To reduce permeability, a two-line grout curtain below the plinth on the abutments is proposed. The grout curtain will also extend to fresh bedrock below the cut-off. A third grouting line is provided for grouting that specifically penetrates geological features and preferential flow paths. Although the fractured mass will be removed, the rock foundation surrounding the fractured rock zone may be of higher permeability and therefore requires additional grouting. Grouting in this area will require careful control to prevent further fracturing of the rock along the edge of the excavation and to prevent excessive loss of grout into the excavation.

The effectiveness of the grout and the likely grout take is determined by the permeability and the size of the fissures/ faults. The grout curtain will be installed through the external portion of the plinth which will act as the grout cap. It is proposed that a primary grouting campaign be undertaken with grout holes at 10 m spacing, followed by a secondary infill grouting campaign to achieve the minimum required permeability of 1×10^{-8} m/s. Further grouting may be needed post-commissioning to ensure the required level of cut-off has been achieved. Grouting from the embankment crest through the transition layer upstream of the core is expected to reach the required depths needed for post-commissioning grouting.

The geotechnical campaign indicated the presence of unfavourable geological features such as minor faults below the plinth. The location of these features in relation to the plinth is shown on SRK Drawing PNA009-0088.

Two faults have been identified on the right abutment in a zone where focused grouting will be required. A third fault further into the abutment may exist; however, this further requires confirmation.

Blanket grouting under the plinth to reduce the seepage and increase erosion resistance is required.

Development of preferential flow paths along the interface between the bottom of the plastic concrete cut-off wall and the bedrock should be restricted. To ensure a watertight cut-off, grouting of this interface is recommended to increase erosion resistance and close off any gaps due to misalignment between plastic concrete panels. The exact profile of the bedrock will be determined during construction to ensure the panels reach the required depths.

8.4 Embankment plinth sizing

A reinforced concrete plinth will extend across the top of the plastic concrete cut-off wall and abutment foundation to provide a watertight connection between the asphalt core and the cut-off wall, and the asphalt core and abutment foundations respectively. The plinth has the following purposes:

- It provides a cap for the plastic concrete cut-off wall and grout curtain.
- It provides a seepage cut-off at the embankment foundation.
- It serves as a footing for the asphalt core.

Asphalt mastic (resin) is typically used as the bonding and sealing agent between the footing of the asphalt core and the plinth. Laboratory tests have proven the mastic to be an effective sealing agent under expected significant hydrostatic pressures. Asphalt mastic has also been used as the bonding and sealing agent between the individual segments of the plinth.

Two embankment plinth designs were developed based on different grouting requirements; only the preferred option is discussed in this report. The second option is similar to the preferred, however, the core is offset against the cut-off wall to allow for a post-installation grouting.

Abutment plinth

The width of the plinth will depend on the quality of the rock foundation, the treatment of the foundation and the consolidation grouting of the rock to achieve an acceptable hydraulic gradient.

The plinth on the abutments will be installed on moderately weathered rock or fresh rock. By applying the Materón rock mass rating (RMR) method⁷⁷, the minimum plinth widths have been calculated based on the expected foundation conditions and the construction requirements for installation of the grout curtain. A rectangular plinth that provides a solid, even footing for the asphalt core, has been selected. The width of the upstream segment of the plinth is governed by the practicality of using the plinth as a grout cap — a 2.5 m width has been selected. This component of the plinth widens the overall plinth base and helps to lower the hydraulic gradient across the plinth. The maximum recommended hydraulic gradients are dependent on the RMR, which varies between 60 and 65.

The minimum plinth width selected is based on two different foundation conditions on site. Once the inferior material from the left abutment has been removed, it is expected that the upper layers of the remaining bedrock will have a slightly lower RMR. As the difference in foundation rock conditions is similar, the same plinth widths have been adopted across the left and right abutments (Figure 8-6).

The pressure head varies between 0 m and 183.5 m, resulting in a minimum plinth width requirement between 5 m and 12.2 m (Figure 8-6).

⁷⁷ ICOLD 2004, Concrete Face Rockfill Dams. Concepts for Design and Construction.

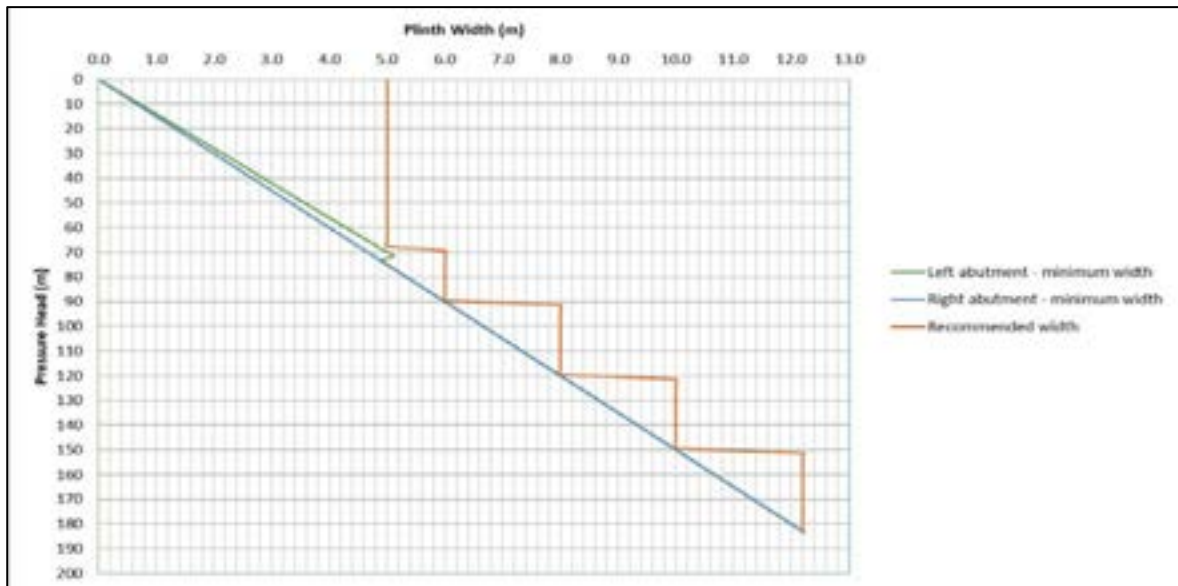


Figure 8-6: Plinth sizing base width vs pressure head

Different plinth widths to accommodate the design profiles are required (Table 8-1).

Table 8-1: Plinth widths across sections

Elevation (RL m)	Design width (m)
48–82	12.2
82–112	10.0
112–142	8.0
142–165	6.0
164–232	5.0

The plinth will be constructed in a series of panels with step-changes at each interval. Joint details consisting of waterstops and asphalt mastic infill will provide the required cut-off.

Plinth thicknesses typically vary between 0.9 m and 1 m for large dams (>120 m) reducing to 0.4–0.6 m with progression up the abutments. The slab thickness of the Barra Grande and Campos Novos dams was estimated using the following relationship:

- $T(m) = 0.3 + 0.002H$ ($H < 100$ m)
- $T(m) = 0.005H$ ($H > 100$ m).

Applying the same methodology, the required plinth thickness varies between 0.9 m and 0.3 m. A single plinth thickness of 1 m has been adopted across the length of the plinth to accommodate uneven rock profiles and to infill local gaps. The thickness can be optimised during future study work.

Foundation preparation requires re-profiling of areas steeper than 50° or sudden grade changes along the long section of the plinth (Section 8.1).

Foundation preparation requirements will depend on the extent of the weathering of the dunite. Once the foundation bedrock is cleared, the base will be prepared using two different methods. The method selected is dependent on the profile of the foundation in relation to the plinth base. Dental grout can be used to fill the potentially uneven rock foundation if the volume is less than 1 m³; alternatively, backfilling may be considered if the volume is more than 1 m³.

The concrete plinth will be reinforced and anchored to solid bedrock. Grout access holes for grouting of the underlying foundation are spaced to suit construction requirements.

Riverbed plinth

The conditions and requirements below the plinth in the riverbed differ from those against the abutments, resulting in a different plinth profile. Due to the estimated differential settlement within the alluvium and colluvium found in the riverbed section (Figure 8-15), the plinth will need to be articulated. Due to the estimated load transfer as a result of overburden pressure from the core, SRK recommends the upper part of the 1.5 m thick plastic concrete cut-off wall be widened. These parameters should be assessed as part of future studies. The plastic concrete cut-off has an average 1.5 m width at the interface between the plinth and the top of the cut-off wall, and a transition between the cut-off and the asphalt core with a 3.4 m wide footing is required. The reinforced concrete plinth provides the interface and transition.

An asphalt mastic layer will act as the seepage barrier between the asphalt core and the plinth; this is a proven methodology for preventing seepage through the interface⁷⁶. The design includes asphalt mastic, combined with a triple-layered waterstop arrangement to provide the required ductility while ensuring a watertight seal.

Transition

The plinth in the riverbed section has been profiled near the abutments such that there is a transition in plinth width between the two distinctly different plinth shapes –the 5.2 m plinth in the riverbed section and 12.55 m plinth at the abutments. This transition continues over a horizontal distance of 36 m.

8.5 Embankment plinth design

The embankment site consists of a relatively steep-sided valley characterised by weathered, slightly weathered and fresh rock overlain in areas by colluvium and landslide materials. On the valley floor, a thick sequence of cemented and uncemented colluvium/ alluvium forms the river bed.

It is proposed that a 1.5 m wide plastic concrete cut-off wall be installed through the colluvium/ alluvium and into the underlying rock. The RC plinth foundation will be founded approximately at the current river level on the cut-off wall with lateral support provided by the in situ colluvial/ alluvial material. The colluvium/ alluvium will be prone to settlement under the surcharge load of the full dam; therefore, the RC foundation design has been articulated to allow reasonable movement and deformation.

On the abutments, the weathered material will be stripped to competent rock to accept the incremental construction of RC foundation as the embankment construction progresses. The RC foundation will be keyed into the rock and held in place with rock bolts in the abutment areas.

A critical design aspect is the articulation of the RC foundation panels along the length of the colluvial/ alluvial valley floor and particularly at the interface with the rock on the flanks, as shown on the SRK Drawings (Appendix 1).

Geology, engineering geology and material properties

Geological and material properties were evaluated as part of the Geotechnical Investigation (Section 3.1). Key criteria for the basis of the plinth design are summarised below.

The typical geology is dunite bedrock directly overlain by transported colluvium that consists of soil-like material and/ or boulders. Weathering is minimal, with almost no completely weathered or highly weathered material present. The soil profile rapidly transitions from slightly weathered to fresh bedrock.

Colluvium on the steeper hillsides forms a thin (1–5 m) layer, except where breaks in slope or landslide debris cause thicker accumulations.

In the valley, the colluvium forms near-horizontal terraces (10–20) m above the river on both sides of the valley) that slope very gently downstream. The terraces are overlain by a thin layer of fine-grained recent alluvial flood deposits, predominantly on the eastern side. Valley floor colluvium typically comprises 60%–80% coarse irregular dunite fragments of varying sizes in a cemented matrix and is usually clast supported. The valley floor colluvium has been attributed to a massive landslide event (or series of events) that occurred approximately 38,000 years ago.

True alluvial material is constrained mainly to the actual river channel on the western side, but also in the centre of the valley in the north of the site. The alluvial material is generally very coarse (boulders, cobbles, gravel and sand), and loose in the upper ~25–40 m below surface and sometimes compacted/cemented at depths below ~25 m. At its margin, the alluvial material is interfingered with the cemented colluvium. The combined total thickness of the valley floor colluvium and alluvium (both cemented and uncemented) is up to 65 m in the centre of the valley.

The cemented colluvial matrix and compacted alluvial material have similar properties, generally 2–10 MPa in strength (from logging and laboratory testing), often, but not always, oxidised, and locally deteriorated. A section showing the local geology at the FRHEP site is shown in Figure 3-13.

Testing of soil-like material

No soils triaxial tests were undertaken due to a lack of weathered material and limitations with sampling the unconsolidated colluvium and larger particles. Particle size distribution and Atterberg limits were determined in colluvium, uncemented alluvium, fault gouge and landslide material. The results are presented in Section 3.1. All materials show a wide range in particle size distribution. The fines components plot in the silt high plasticity category. Fault gouge showed a lower clay percentage and lower plasticity than the other samples.

Geotechnical material types

From geotechnical field investigations, 14 types of subsurface conditions were identified and rationalised into eight main material types and their material properties are presented in Table 3-30:

- 1 Soil like colluvial cover
- 2 Cemented (2A) (and locally uncemented – 2B) colluvium and alluvium in the valley floor
- 3 Large boulders, highly weathered (HW) to slightly weathered (SW), usually moderately weathered (MW), clast-supported in a colluvial matrix
- 4 Potential landslide zones – highly fractured rock with shear zones, oxidised and/ or deteriorated rock, and joint infills
- 5 MW to SW (occasionally HW) rock, with dilated, oxidised, infilled joints
- 6 Significantly deteriorated poor quality serpentinite bedrock
- 7 Moderate to good (locally poor) quality bedrock
- 8 Fault zones (three types – close fracturing, numerous small individual faults, fragments and gouge).

A 3D model of the distribution of geotechnical material types has been constructed in Leapfrog software. A cross-section through the model illustrating the positions of the materials types is shown in Figure 8-7.

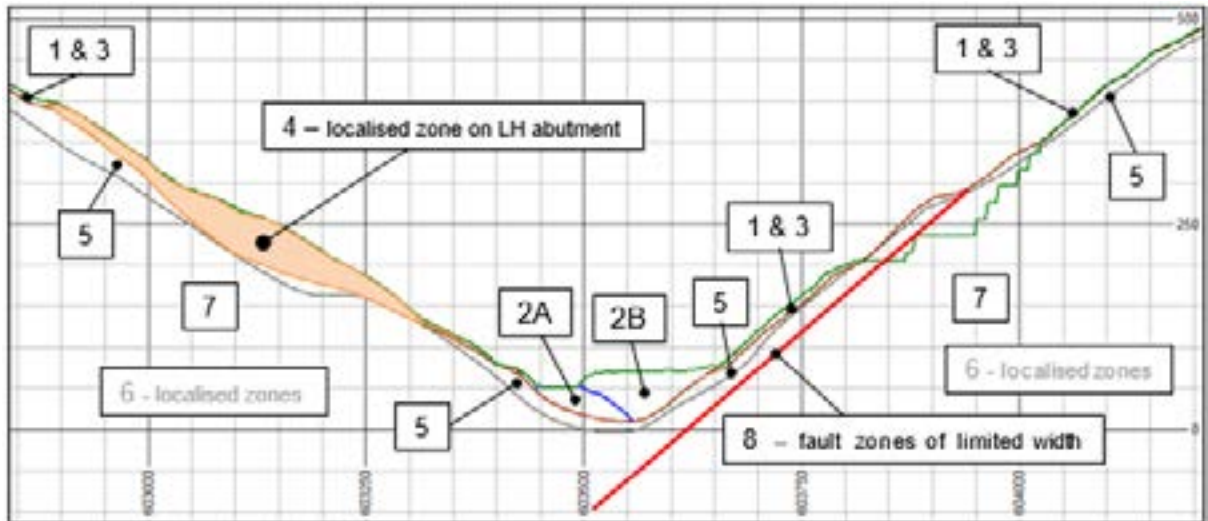


Figure 8-7: W-E cross-section through the FRHEP site (looking north) illustrating the locations of the material types

Field estimated strengths and Geological Strength Index (GSI) are shown in Figure 8-8 and Figure 8-9 respectively.

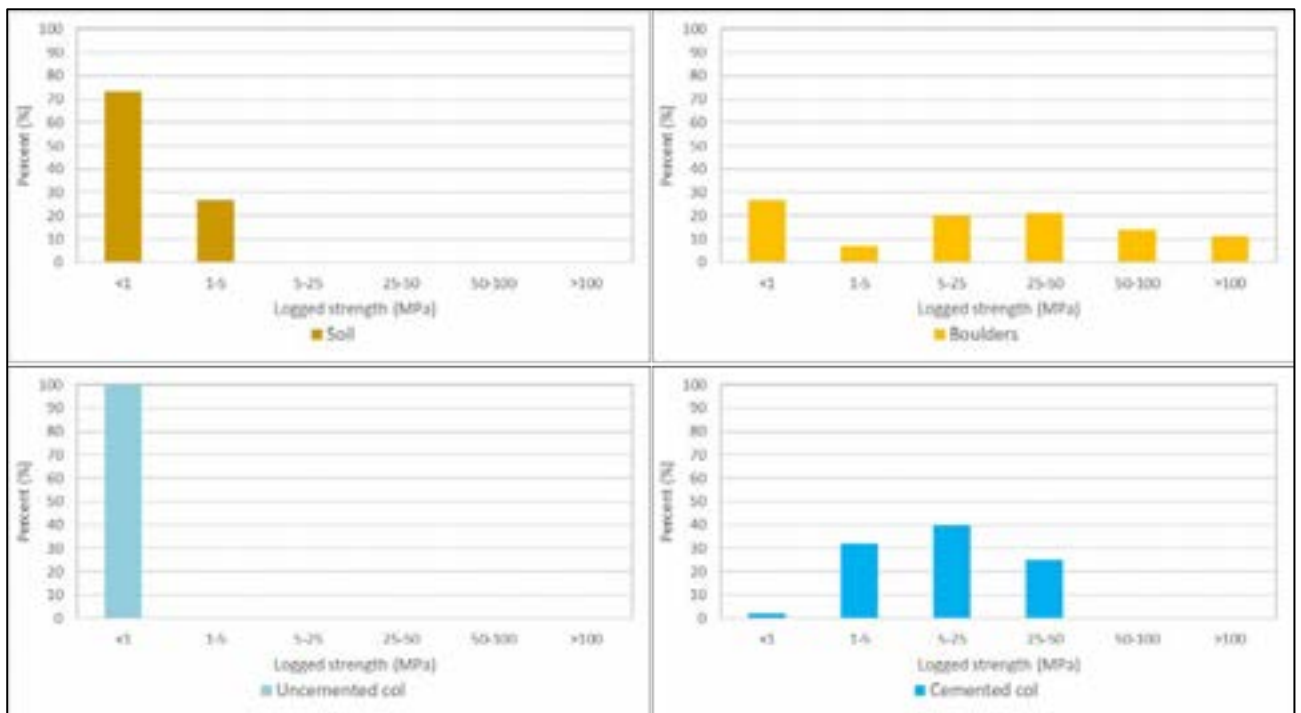


Figure 8-8: Logged field estimated strengths per material type

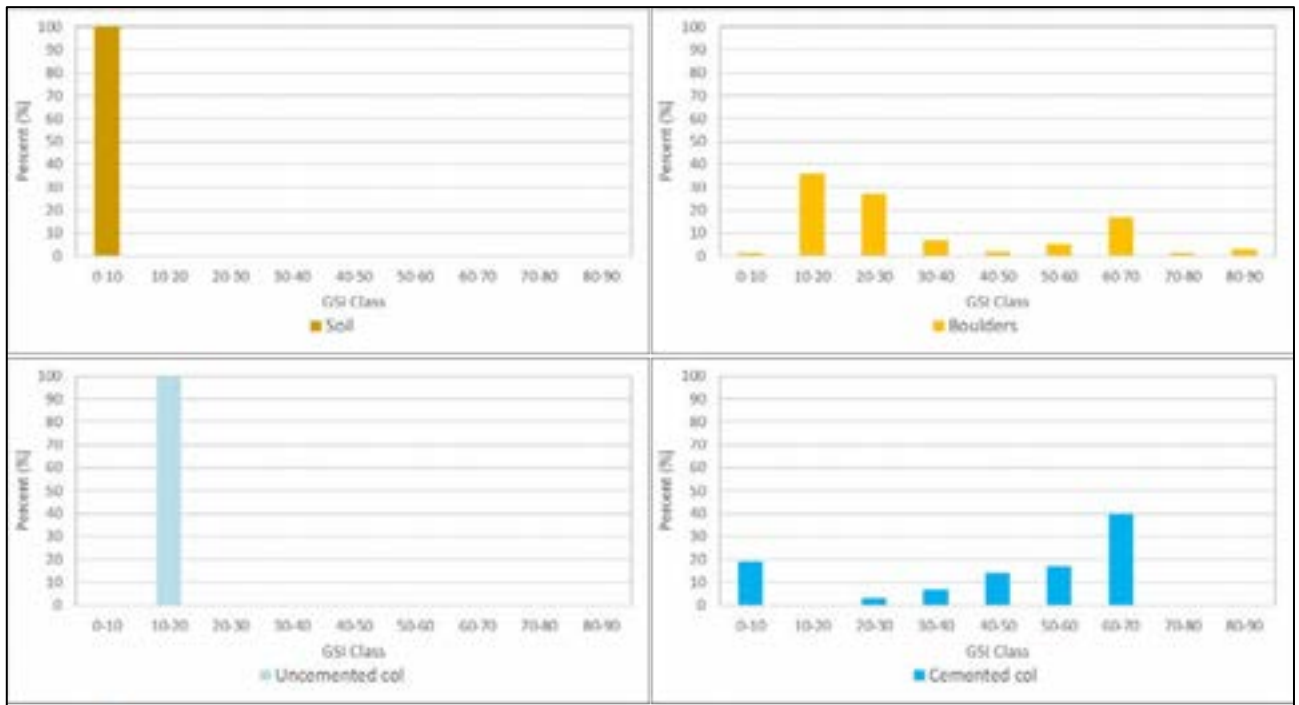


Figure 8-9: Logged GSI per material type

The material mass properties developed for embankment and abutment stability are shown in Table 3-30. Two rockfill zones were defined – Zone 3A, being highly compacted material that will form the most internal zone of the dam, and Zone 3B, being compacted material that will form the external zone. Properties for materials types 1 and 3 (colluvium and boulders) were not developed, as these are relatively thin layers beneath foundations and in major slope cuts that will be removed.

The photos in Figure 8-10 and Figure 8-11 illustrate the uncemented (2B) materials. They comprise largely sand/ gravel and large boulders, often clast supported rather than matrix supported and therefore may not be very compressible.

The estimated Young’s modulus (E) is 300 MPa for the cemented (2A) and 150 MPa for the uncemented alluvium/ colluvium (2B). There is no practical way of measuring this directly, therefore a conservative approach for the RC foundation design has been adopted. While E = 300 MPa is a reasonable assumption for the cemented material, the uncemented material has been described in soil terms as boulders within a sand matrix, and even though it might be clast supported, a value of E = 75 MPa has been adopted for differential settlement/ rotation assessment.



Figure 8-10: Typical core from the Frieda River valley floor showing uncemented (2b) material



Figure 8-11: View of a river bar in the Frieda River valley floor

Plastic concrete cut-off wall

The plastic concrete to be used in the cut-off wall has a strength of 2–4 MPa and is likely to have an E value between 500 MPa and 2000 MPa.

The assumption is that 500 MPa is a similar stiffness to the cemented 2a material, but considerably greater than the stiffness of the 2b (uncemented) material. This effectively means that foundation settlements will be distributed between the cut-off wall and the 2a material, with the cut-off wall ‘supporting’ the 2b foundation material, and therefore attracting more load due to its greater stiffness. This also means the stress on the cut-off wall will be much more than geostatic (vertical column) stress at the foundation level. Previous investigations of several failures of ‘rigid’ conveyance tunnels under

stockpiles indicate that the load on the tunnel is up to four times the geostatic load. In essence, this means the load is not derived from the vertical column of material above, but from a cone increasing in size upwards. The modular E ratio between the 2b and cut-off wall is potentially large (~75/500) and hence, for any significant depth of material, differential and load transfer issues will result. For this reason, the cut-off wall may need to be wider in the soft material.

Further assessment of these aspects during future studies is required.

RC foundation plinth design (abutments)

The average RMR of the rock on the abutments is approximately 60. For the purposes of the current design, a hydraulic gradient of 14 has been selected, as determined from the static head across the width of the plinth. The correlation of RMR and gradient is shown in Figure 8-12. This method assumes that the rock mass has not been grouted and the design is therefore conservative. During detailed design of the cut-off grouting, it is recommended that the RC foundation/ plinth design be revisited and optimised.

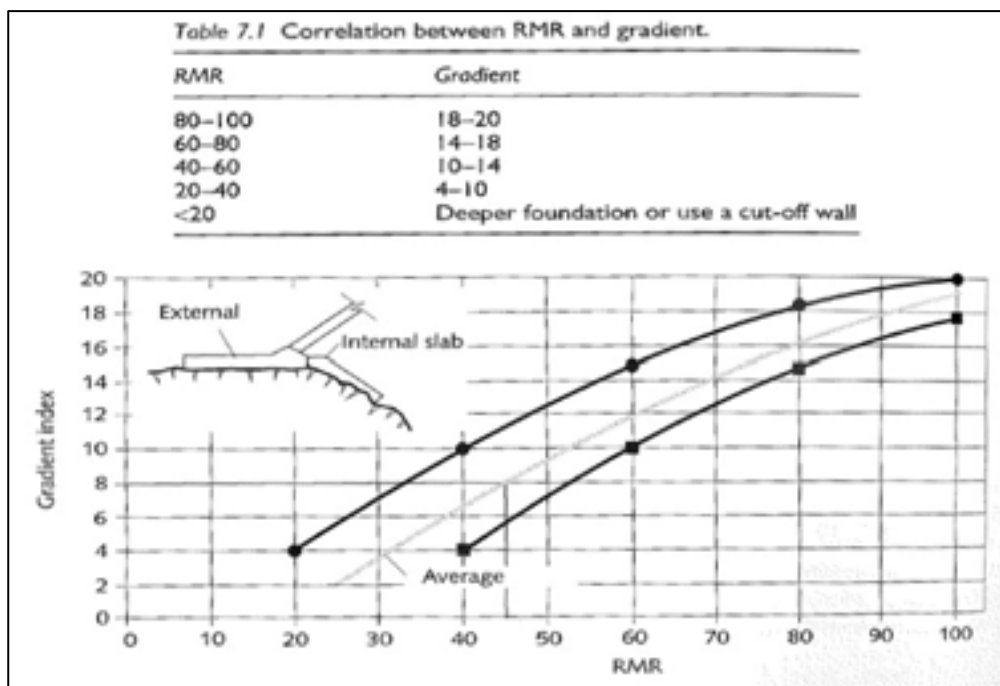


Figure 8-12: Correlation of RMR with gradient shown in a table (above) and graph (below) for a plinth design with internal slab⁷⁸

The structural design of the RC foundation follows an articulated pattern with individual blocks ranging in size to a maximum of 5 m (W) × 7 m (L). These blocks are nominally reinforced and held in place by rock bolts spaced at 750 mm centres both ways. For durability, a concrete strength of 35 MPa is recommended.

A recessed asphalt mastic infilled construction joint with a minimum of three waterstops per section has been specified between all panels to prevent the development of bending moments. Shear dowels are provided between panels on either side of the waterstops.

The provisional selection of waterstop is the Tricosal® FM 500 Elastomer from SIKA. This waterstop meets the requirements for a 100 mm joint as well as the rotational requirements (for the alluvium/

⁷⁸ Cruz, Materón and Frietas, 2009. Concrete Face Rockfill Dams, CRC Press, Netherlands, p. 194.

colluvium base panels, see below). A detailed waterstop specification will be drawn up during future studies. Alternative approved waterstops by other manufacturers according to specification can also be considered.

Plinth design (alluvium/ colluvium base)

Due to the cemented and uncemented alluvial/ colluvial deposits on the river floor, the main design consideration is the differential settlement and rotation of the articulated base panels. To determine a preliminary estimate of the magnitude of the settlements likely at the RC foundation plinth and alluvium/ colluvium level, an elastic finite element model has been prepared using the geotechnical information summarised above. The model has been developed in the RS² software (by Rocscience, Canada) and is shown in Figure 8-13. Note that the alluvium/ colluvium has been modelled as two separate materials (cemented and uncemented) with appropriate material properties as shown. The model embankment is incrementally ‘built’ to simulate the likely settlements and deformations with (construction) time.

An approximate model of the 67 m wide river channel is shown in Figure 8-13. While it is likely that stiffness will increase with depth, a constant stiffness has been used in this model.

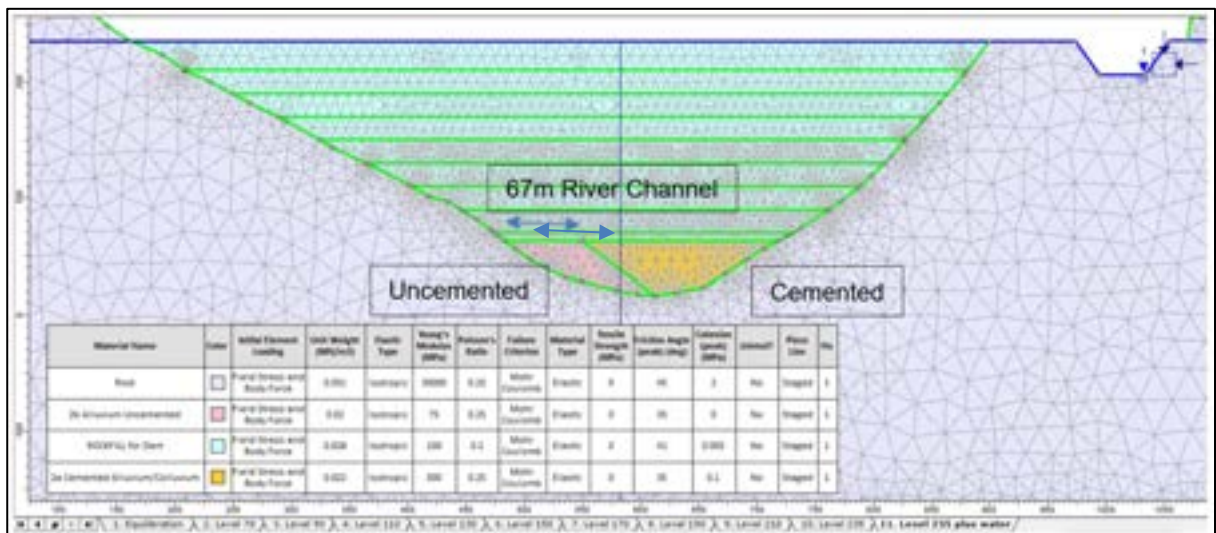


Figure 8-13: Elastic finite element model

Figure 8-14 shows the expected settlements with time along the interface. The left and right sides of the figure where little settlement is measured represent the rock flanks.

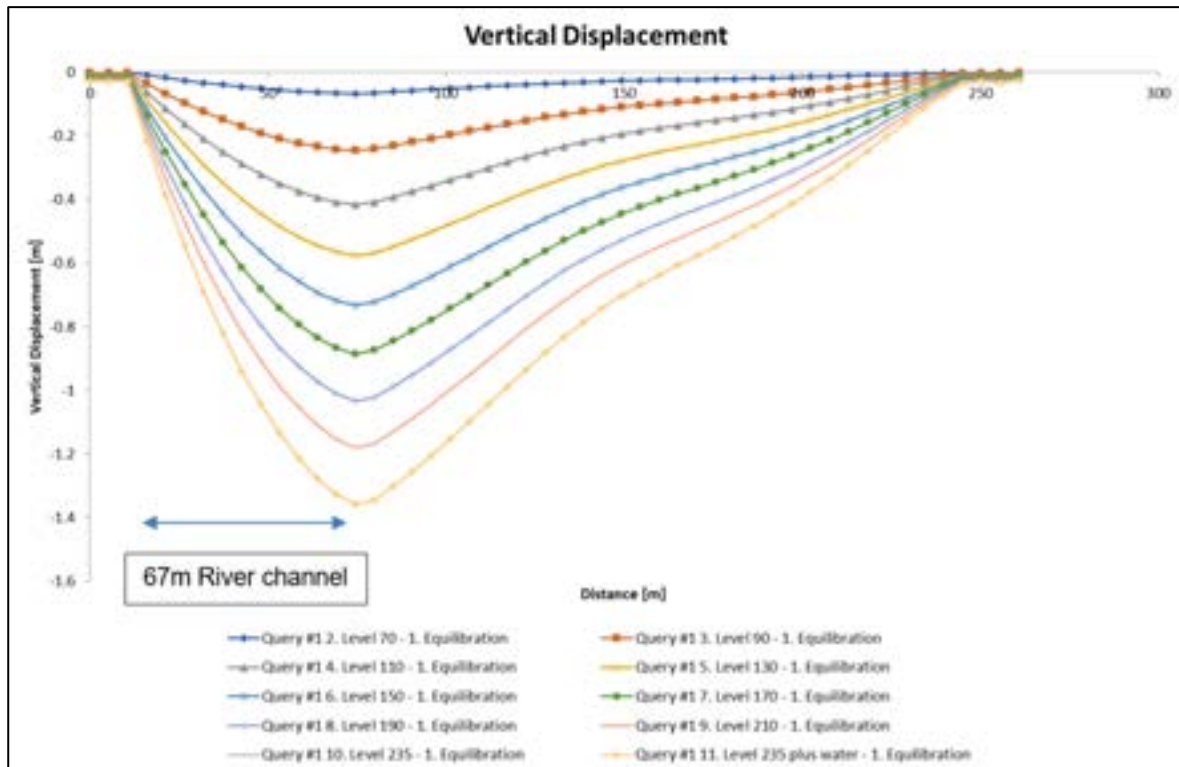


Figure 8-14: Settlement profile along the alluvium/ colluvium interface

Figure 8-15 shows the relative deformation along the interface in units of (i) mm/m and (ii) degrees, calculated over a length of 5 m.

This assessment shows that on the left bank, the rotation of one panel to the next can be in the order of 35 mm/m. This rotation decreases progressively across the river to about 10 mm/m at 80 m along the base, then stays reasonably constant at this value to the right bank. The panel sizes have therefore been shortened at the abutments to 2 m and increased to 5 m where differential displacement is minimal. The rotation angles and panel sizes relate directly to the flexibility of the joint materials and waterstop material to be used, which for this design has been limited to 75 mm or 25% strain in the waterstop per joint.

The joint movement is directly related to the stiffness and deformation characteristics of the uncemented alluvium/ colluvium (Figure 8-15). It is recommended that this be further investigated during future studies by physical geotechnical investigation and numerical modelling, which should include the contribution of the cut-off wall to the settlement/ rotation profile.

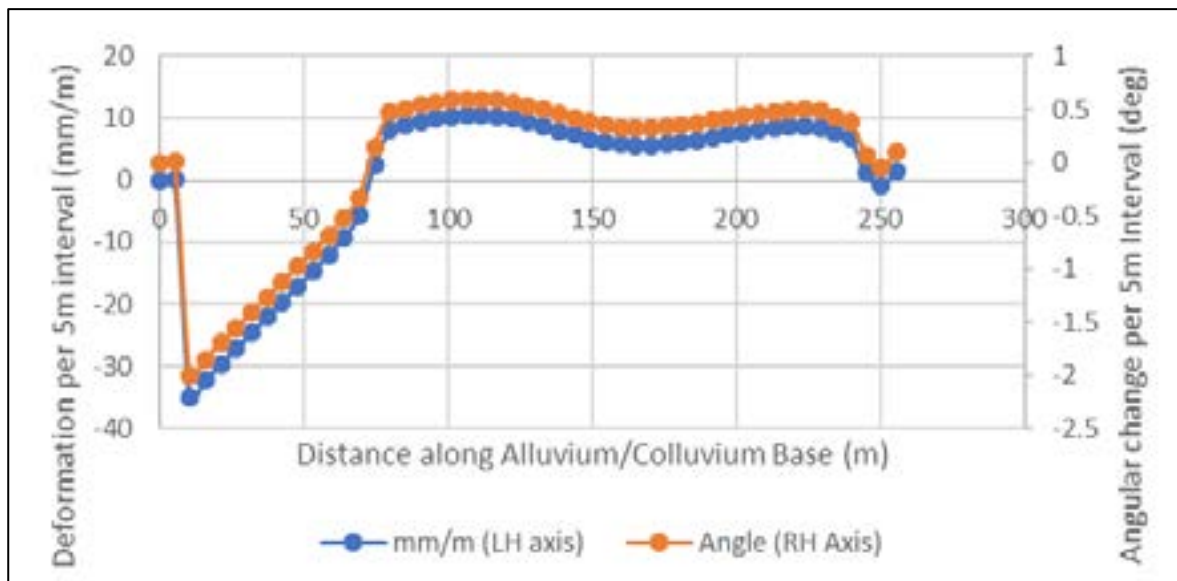


Figure 8-15: Incremental change in deformation and rotation along the alluvium/ colluvium interface

Cut-off wall width

The width of the cut-off wall is of concern mainly in the uncemented alluvium (2b) material on the left flank. The concern is related to the difference in E for the alluvium (mainly uncemented) and the plastic concrete. The stiffness of the uncemented alluvium has been estimated previously as $E = 150 \text{ MPa}$, but as it is described more as a soil, even though clast supported, it is possible that the stiffness could be $\sim 75 \text{ MPa}$ which has been used in the assessment of differential settlement. This is compared to a lower E for the cut-off wall plastic concrete, where E is likely to be in the range of 1-4 GPa or more than 10 times the alluvium E value. Under these conditions, the foundation/ plinth load transfer will be directly into the cut-off wall plastic concrete as the alluvium will preferentially deform rather than accept load. The stiffer material (the cut-off wall) will therefore absorb most of the load/ stress.

It is estimated that the foundation/ plinth (which is also stiff in the transverse direction) will draw more load to itself than just the geostatic load and will 'drive' the plinth onto the cut-off wall. This potential stress transfer must be addressed in conjunction with differential settlement and differential rotations in the transverse direction.

It is therefore recommended that the cut-off wall be widened and/ or a sounder stress transfer zone be provided immediately beneath the foundation. SRK recommends the cut-off wall is 2.3 m at the top to accommodate the stress transfer. It is also recommended that two extensions on both ends of the plinth be considered during future studies with the aim to serve as a cap that will contain any strain/ deformation to the cut-off wall. This interface should be optimised as part of future studies.

8.6 Filter/ transition zones

Material properties

The design of the embankment must cater for the long-term life of the facility after closure, short-term displacement associated with loads induced during construction, and impoundment – including potential displacement related to seismic events.

The transition/ filter zones on either side of the asphalt core are constructed simultaneously to the asphalt core and provide immediate lateral support for the hot, soft asphalt, eliminating the need for formwork. During reservoir impoundment and operation, the transition/ filter zones maintain even and

sturdy contact surfaces for the core. If severe cracking occurs in the top part of the core due to extreme seismic loading, the transition/ filter zones act as a filter layer to prevent internal erosion and migration of fine materials to the downstream embankment. A material with crack-stopping abilities is therefore recommended for the layer immediately upstream of the core.

Although tailings and waste rock are not intended to be deposited against the embankment, the design will accommodate such conditions. The filter/ transition layers, combined with the ability of the crack-stopping material, will therefore require grading to prevent migration of these fines.

To retain any fines and prevent piping through the foundation, a filter/ transition layer will be installed at the base of the downstream embankment in the valley section and partway up the abutments. The design of these layers will be optimised following development of a 3D seepage model.

Due to the requirement for lateral support, the particle sizes of the layers directly adjacent the core must be large enough to provide the shear strength required. The material sizes adopted for the various layers have been based on the size distributions of similar ACRDs, including the expected rock material sizes to be produced by the quarry as shown in Table 8-2.

Table 8-2: Comparison of material grading for different zones of various asphalt core embankment

Zones	Material sizes adopted for various layers (mm)				
	FRHEP (190.5 m)	Yele Dam ⁷⁶ (125 m)	Storglomvatn Dam (128 m)	Finstertal Dam ⁷⁴ (149 m)	Knezhevo Dam ⁷⁹ (75 m)
Filter layer (Zone 2A)	0–60	0–80	0–60	0–100	0–60
Transition layer (Zone 2B)	0–200	0–150	0–150	0–100	0–250
Rockfill (Zone 3A)	10–600	0–800	0–500	0–700	0–650
Rockfill (Zone 3B)	40–1000	0–800	0–1000	0–700	0–650

The exact grading curves, including the sizing of the toe drain and crack-stopping layer, need to be defined.

Filter zone sizing

The filter and transition thicknesses have been based on empirical methods, by considering typical widths of similar facilities. If cracking occurs in the embankment, similar cracking is expected in the filter/ transition zones. The filter/ transition material must control the flow and prevent the migration of tailings or upstream material to the downstream embankment. Therefore, a minimum filter layer thickness of 1.5 m has been selected for the downstream side to prevent erosion and potential increases in hydraulic gradient.

The required filter thickness, applying a FoS of 1.5, is calculated as:

- Static displacement (x): 0.35 m
- Earthquake displacement (x): 1 m
- Minimum filter width to be maintained: 1.5 m
- Total thickness required: 2.85 m
- Selected thickness: 4.75 m.

⁷⁹ Tanchev, L, 2014. Dams and appurtenant hydraulic structures. CRC Press.

The upstream filter zone is intended to function as a crack stopper, and a thickness of 1.5 m has therefore been selected.

Transition zone sizing

The required thickness for the downstream transition layer is expected to be in the order of 3 m to allow for optimal drainage, however it should also cater for potential displacements of the dam mass due to static and seismic deformation; from the deformation analyses there is a potential total displacement of 3 m. Considering a factor of safety of 1.5, the total downstream thickness should be 9 m in total. The upstream transition zone is intended to function as a crack stopper and a thickness of 3.5 m has therefore been selected.

Basal drainage

The proposed foundation preparation will extend to bedrock on the abutments and to competent alluvium and colluvium in the river valley section. It is expected that upward flows will occur at the embankment base in the river valley section, and localised flows will occur on the slopes.

A horizontal filter/ transition blanket has been designed to intercept basal drainage through these interfaces. The purpose of the filter/ transition system is to reduce the risk of particle migration and associated piping. The horizontal blanket drain will also extend partway up against the abutments as an inclined drain. The blanket will provide a flow path to the central filter/ transition section to collect upward foundation seepage and flow from the inclined drain. Particle migration originating from the foundation is not expected to be significant; however, localised zones of particle migration may be encountered once the entire footprint is exposed. The infill matrix will likely be the medium for particle mobility. It is assumed the finer fraction of the particles is a silty sand.

Additional filter/ transition features will be required for control of the flow of smaller streams which pass through the embankment footprint. Finger drains will be laid beneath the embankment to pass the flow from each stream to the central drainage/ transition blanket where it will exit at the downstream toe.

The footprint of the horizontal drainage/ transition blankets is shown on SRK Drawing PNA009-0080.

SRK evaluated the basal drainage relationship between the foundation and filter/ transition materials, and the proposed rockfill to develop criteria for horizontal blanket drainage. The primary concern relates to the compatibility of any foundation material that may be transported to the rockfill material (zones 3A, 3B and 3C - toe drain material). SRK considered the use of zones 2A and 2B as a horizontal filter/ transition blanket. Zone 3A has also been extended across the base to the edge of the embankment, across Zone 3B and the toe drain base to reduce the number of zones of interface.

Although it is not the primary means of seepage mitigation, the use of a horizontal drainage/ transition layer introduces risks. Compaction or blockages, caused by the load of the embankment overburden or over-compaction could result in reduced permeability. Crushing of the drainage/ transition layer particles may also occur due to excessive overburden stresses, leading to a finer material and reduced permeability. If drain permeability was to decrease, a larger drain would be required. A more accurate analysis of likely permeabilities of the drainage/ transition material is recommended as part of future studies.

8.7 Toe drain

A toe drain has been included in the downstream segment of the embankment and consists of larger grained material selected from quarry excavations. The toe drain will limit the risk of internal erosion and assist in controlling phreatic levels should the core be sheared and seepage into the downstream segment occurs. The impact of the toe drain once failure occurs is discussed in Section 8.9.

The inclusion of a toe drain provides a failsafe for an embankment that must remain functional into perpetuity.

8.8 Zoned rockfill shell

The rockfill material used to construct the embankment will be quarry material consisting largely of dunite for which PSD and UCS data are available. The minimum particle size will be restricted to 10 mm. Placement methodology and material properties are described in Section 8.11.

8.9 Seepage analysis

A seepage analysis was undertaken to evaluate the embankment performance and associated seepage cut-off system across different sections under various conditions. Justification for a seepage cut-off system is based on the comparison of the total seepage and internal hydraulic gradient below the embankment, both with and without the cut-off system. The performance of the embankment with the associated seepage cut-off system is evaluated by assessing the total seepage rates (in the case of a fully functional asphalt core and a potentially degraded asphalt core), hydraulic gradients at the toe of the embankment, hydraulic uplift due to pore water pressure and the maximum phreatic levels at any time. The analysis was based on a 2D steady-state seepage model using the finite element software, SEEP/W. Figure 8-16 shows the various components of the embankment incorporated in the seepage model.

The seepage model limitations should be considered when interpreting the results. Assumptions and estimates regarding the properties of materials have been made and some variation can therefore be expected. Seepage modelling is undertaken in a 2D space with isotropic permeability for each zone, and results in 3D space may be different. Exact seepage characteristics are difficult to determine as the surrounding geology is non-isotropic and non-homogenous.

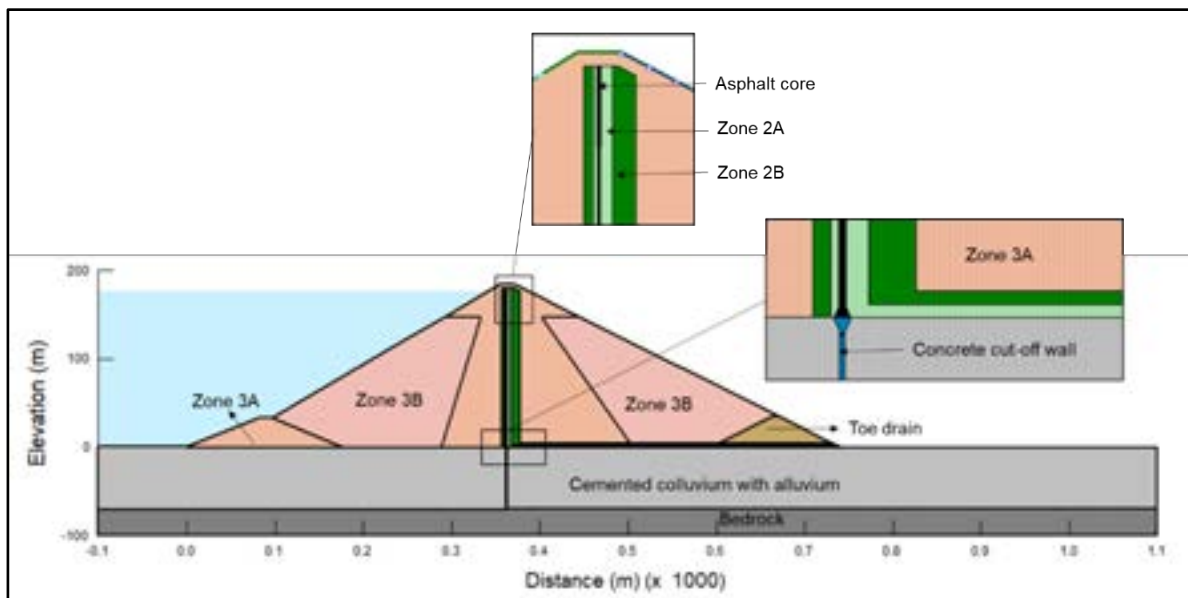


Figure 8-16: Embankment cross-section detailing various components/ zones

Seepage benchmarking

A benchmarking exercise was undertaken to establish reasonable measured seepage rates for similar rockfill dams. Table 8-3 shows the measured seepage rates from a selection of existing ACRDs. Dams with available measured field data were selected based on type, height and comparison against the embankment. At its full supply level, the maximum total seepage rate recorded at Yele Dam, which is most comparable with the FRHEP, was 358 L/s, and was less than the maximum estimated design

seepage rate of 500 L/s⁷⁶. Storvatn Dam recorded a seepage of 10.2 L/s with a difference of one order of magnitude less than Yele Dam. This difference is due to a higher seepage segment at Yele on the right abutment. After additional grouting was carried out and drainage wells installed, the seepage of the dam reduced to 277 L/s. Hence, the total seepage rate for ACRDs ranges between 358 L/s and 10.2 L/s.

Table 8-3: Maximum measured seepage rates from comparable ACRDs

Dam	Height (m)	Maximum measured seepage rate (L/s)	Reference
Yele	124.5	358	Wang et al., 2010 ⁷⁶
Storvatn	90	10.2	Höeg, 1993 ⁷²
Aqing	61	23.81	Zhou et al., 2015 ⁸⁰

Material properties

The permeabilities in Table 8-4 are based on the assumed particle sizes for the sub-components of the embankment and available geotechnical data for the underlying geology. The zones are also assumed to be isotropic; however, in practice, the zones will not be isotropic.

Table 8-4: Material permeabilities

Material Zone	Material	Permeability (m/s)	Source/ comment
	Cemented colluvium and alluvium – homogeneous and isotropic	1.0×10^{-7}	SRK and SKM Geotechnical investigation
	Grouted bedrock	1.0×10^{-8}	SRK and SKM Geotechnical investigation
3A	Highly compacted rockfill	5.0×10^{-4}	Estimated by SRK based on the particle sizes of possible materials
3B	Compacted rockfill	1.0×10^{-3}	
2B	Transition material	2.5×10^{-4}	
2A	Filter material	1.2×10^{-4}	
Toe drain	Large rocks	1.0×10^{-2}	Assumed by SRK
Cut-off wall	Plastic concrete cut-off	1.0×10^{-8}	SKMPS, 2011
Asphalt core	Asphalt	Varied	Höeg, 1993 ⁷² , SRK

Different levels of performance of the asphalt core were modelled. The parameters selected are shown in Table 8-5. The permeability of the asphalt core is variable; the ideal condition is assumed to be 1×10^{-10} m/s, with air porosity in the embankment core less than 3%⁷². SRK assumed a value for asphalt core permeability between 1×10^{-9} m/s and 1×10^{-8} m/s during operating conditions to consider possible defects during construction that may reduce the permeability of asphalt core. The performance of the asphalt core may degrade due to passage of time, temperature or even chemical exposure. To evaluate the possible consequences, SRK therefore modelled this degradation by increasing the permeability in the asphalt core to 1×10^{-7} m/s.

⁸⁰ Zhou, Q, Wang, X D and Wu, M X, 2015. Seepage analysis and control of asphalt core dam of Aqing hydroelectric power station, Rock and Soil Mechanics, 36(S2), pp.469-477.

Table 8-5: Assumed asphalt core permeability based on various conditions

Asphalt core permeability (m/s)	Conditions
1×10^{-9}	Expected operating condition
1×10^{-8}	
1×10^{-7}	Degrading condition

Modelled sections

The development of the seepage models was undertaken on two sections at the embankment (Section 1 and Section 2 in Figure 8-17). The sections were considered representative of the different foundation cut-offs and distinctly different foundation conditions below the embankment. The water level at each section was taken as RL 226.1 m, which is the maximum operating level, while the lowest section in the valley downstream of the embankment is at an elevation of RL 48 m.

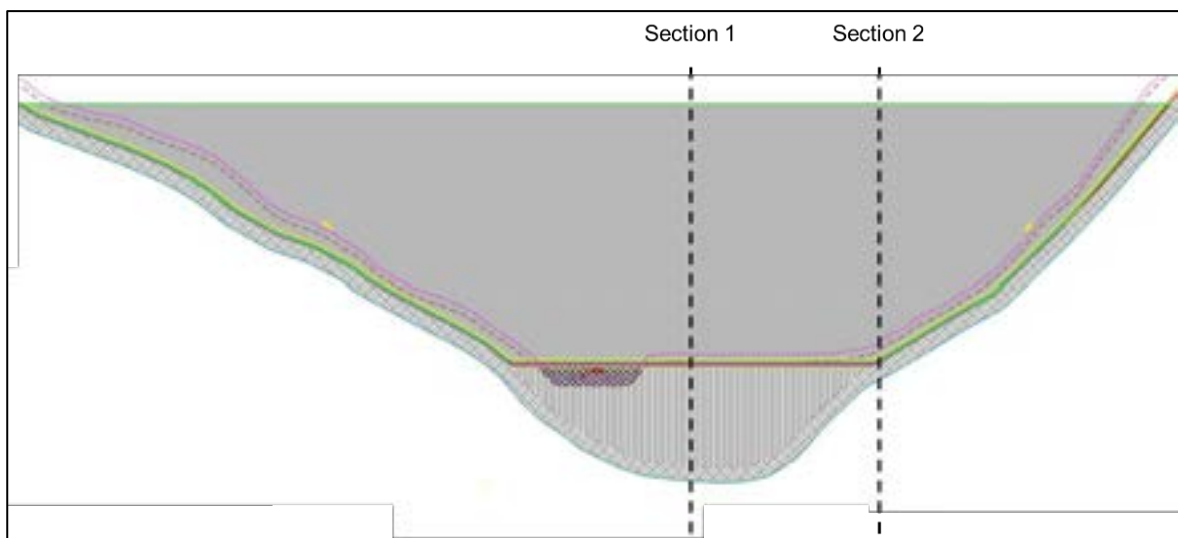


Figure 8-17: Sections 1 and 2 along long section of embankment considered in seepage assessment

Section 1 represents the foundation on the river section, comprised of cemented, uncemented colluvium and alluvium materials. Section 2 represents the section at the edge of the embankment, with the 12 m concrete plinth founded on bedrock. The typical plinth geometry for each section shown in Figure 8-18 is taken from the seepage model which is based on a working design. The plinth design has since been updated to the current design drawings, however the seepage model has not been updated as the updated geometry does not significantly change the seepage results.

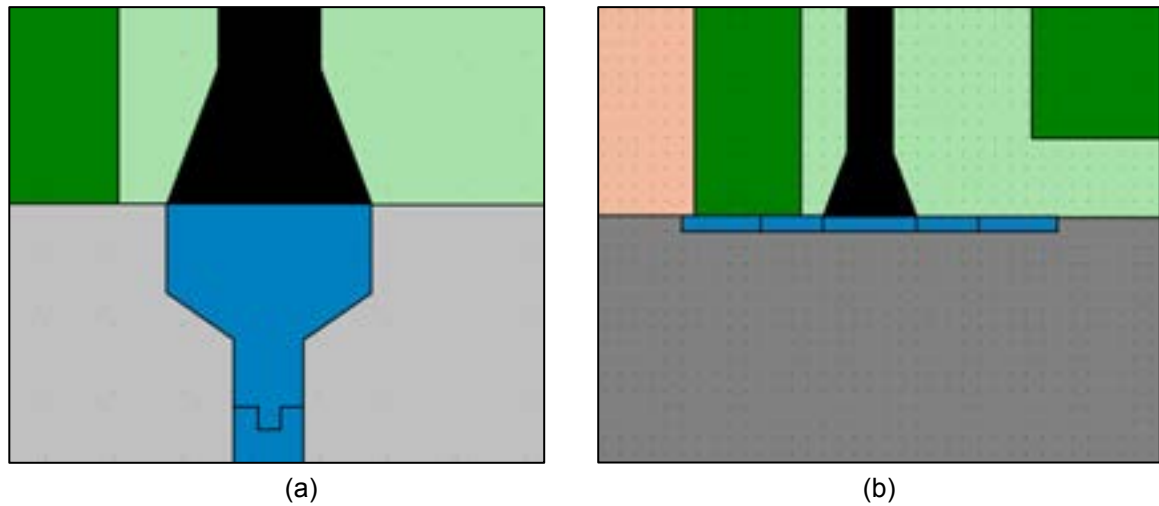


Figure 8-18: (a) Typical plinth profile at Section 1 and (b) 12 m concrete plinth at Section 2

Modelled shearing of the asphalt core

The core may be subjected to excessive displacement-induced cracking such that the asphalt core is sheared, resulting in an aperture allowing free flow conditions. SRK modelled the hypothetical shearing of the asphalt core by creating a 5 m highly permeable ($k = 1 \times 10^{-1}$ m/s) zone along the asphalt core to represent the shearing zone. If shearing occurs, it is most likely to occur within the top third of the asphalt core height, therefore the possible location of the aperture can vary from 0 m to 60 m from the embankment crest. The two locations selected for modelling were therefore at 35 m and 60 m from the embankment crest. The results are shown in Table 8-10.

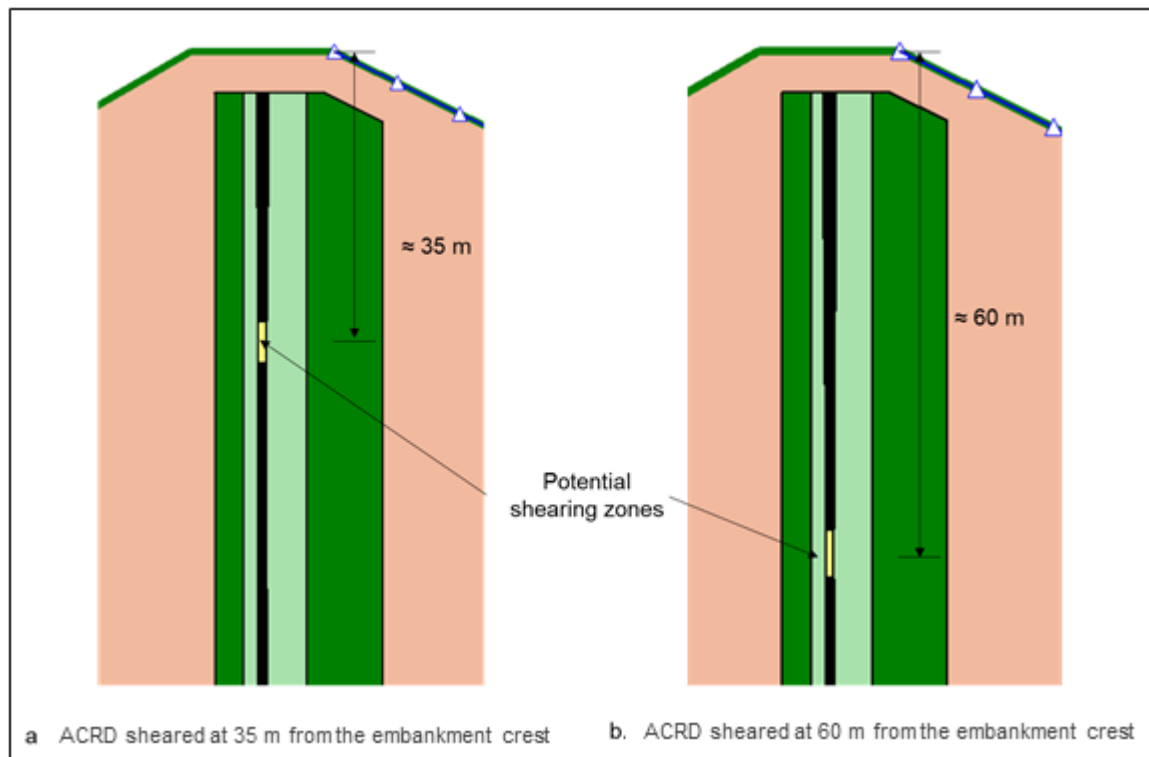


Figure 8-19: Modelled crack sections illustrating displacement-induced cracks

Seepage cut-off system

The foundation seepage cut-off system was analysed to compare the total seepage rate and the internal hydraulic gradient of the embankment with and without the cut-off system.

Total seepage rate

The total seepage rates per section are calculated by multiplying the unit rate of seepage per metre at the toe by the length of the interface between the embankment and cemented colluvium and alluvium material for Section 1, and the embankment and bedrock for Section 2. Table 8-6 shows minimal differences in seepage rates with and without the cut-off system below the embankment. However, these outcomes are based on the assumption that the foundation material is homogenous and isotropic. It is expected that actual conditions will include higher permeability zones in the foundation due to localised preferential flow paths created by the foundation infill matrix.

Table 8-7 shows the results of modelling the cemented colluvium and alluvium material which has a higher permeability of 1×10^{-5} m/s to evaluate the effect of localised preferential flow paths, compared to a permeability of 1×10^{-7} m/s. Section 1 without the plastic cut-off wall resulted in an increased seepage rate of 507 L/s, compared to a rate of 6 L/s with the cut-off system. This indicates that the plastic cut-off wall is necessary for preventing seepage rates through the foundation that are larger than acceptable.

Table 8-6: Seepage at toe with/ without plastic cut-off wall or concrete plinth (homogeneous and isotropic conditions)

Asphalt core permeability (m/s)	Seepage rate (L/s)			
	Section 1		Section 2	
	With plastic cut-off wall	Without plastic cut-off wall	With 12 m concrete plinth	Without 12 m concrete plinth
1×10^{-8}	5.5	6.9	14.1	14.2

Table 8-7: Seepage at toe with/ without plastic cut-off wall with a higher permeability in cemented colluvium and alluvium material (non-homogenous and anisotropic conditions)

Asphalt core permeability (m/s)	Seepage rate (L/s) – Section 1	
	With plastic cut-off wall	Without plastic cut-off wall
1×10^{-8}	6	507

Internal hydraulic gradient below embankment

Table 8-8 shows the hydraulic gradients estimated for different conditions in each section below the embankment. Without a cut-off system such as plastic cut-off wall and concrete plinth, the estimated hydraulic gradient is at least four times larger in Section 2 and 40 times larger in Section 1. The presence of the plastic cut-off wall and the 12 m concrete plinth lengthens the flow path and therefore reduces the hydraulic gradient.

Additionally, the seepage force underneath the embankment, being dependent on the hydraulic gradient, will increase if the flow path is short. The reduction in hydraulic gradient is necessary to prevent erosion and piping underneath the embankment.

Table 8-8: Estimated hydraulic gradients for different conditions in each section

Section	Conditions	Estimated hydraulic gradient (<i>i</i>)
Section 1	With plastic cut-off wall	1.5
	Without plastic cut-off wall	60
Section 2	With 12 m concrete plinth	14
	Without 12 m concrete plinth	60

Results

Total seepage

SRK calculated the seepage rates in operating conditions for the as-built asphalt core and where the core may degrade physically (e.g. displacement or cracking), or chemically (e.g. loss of viscosity).

The total seepage rates through the embankment are calculated by assuming the seepage rates for both sections. The seepage rate for each section is obtained by multiplying the seepage rate at the toe by the length of the interface between the embankment and cemented colluvium and alluvium material for Section 1, and the interface length between embankment and bedrock for Section 2.

Table 8-9 provides the maximum estimated seepage rates at the embankment toe for expected operating conditions. The estimated average seepage rate for the embankment varies between 2.2 L/s and 19.7 L/s, and is within the range of seepage rates of comparable ACRDs listed in Table 8-3. Under modelled conditions, the interface between the cut-off and bedrock is ideal and results in a good seal. In actual conditions, small imperfections exist at these interfaces, which may increase seepage rates. As part of these analyses, all preferential flow paths through the abutments are assumed to have been grouted and sealed.

Conversely, a seepage rate of 145 L/s is estimated when the potential degradation of asphalt core is modelled by increasing its permeability to 1×10^{-7} m/s. The results also highlight the sensitivity to change in asphalt core permeability.

Table 8-9: Total seepage results due to change in asphalt core permeability

Asphalt core permeability (m/s)	Total seepage rate (L/s)	Comments
1×10^{-9}	2.2	Expected operating conditions
1×10^{-8}	19.7	
1×10^{-7}	145	Degrading condition of asphalt core

In the event of significant shearing of the asphalt core, the shearing zone located at 60 m from the embankment crest induced a higher seepage rate of 491 L/s compared to the shearing zone at 35 m from the embankment crest, which induced a seepage rate of 271 L/s (Table 8-10). This observation seems to be consistent with the higher pressure head experienced by the lower shearing zone.

Table 8-10: Total seepage rates induced by potential shearing zones within the core

Distance of shearing zones from embankment crest (m)	Total seepage rate (L/s)	Comments
35	271	Distance is approximately 1/5 of embankment height
60	491	Distance is approximately 1/3 of embankment height

Hydraulic gradient at downstream toe

Table 8-11 shows the values of exit gradients estimated at the downstream toe for different asphalt core permeabilities at each section. The critical exit gradient for most soils is typically close to 1⁸¹. Based on modelling, all exit gradients calculated for different conditions in each section are less than 1. Hence, the risk of piping at the toe of the embankment is controlled, and therefore unlikely.

Table 8-11: Exit gradient at downstream toe

asphalt core permeability (m/s)	Hydraulic gradient at toe (m/m)	
	Section 1	Section 2
1×10^{-9}	0.79	0.33
1×10^{-8}	0.84	0.47

Uplift pressure due to water seeping below the embankment

Uplift may occur if the uplift forces underneath the embankment are greater than the self-weight of the embankment, and this may result in failure. The pore pressure underneath the embankment (from the centre of embankment to the toe drain) was determined using SEEP/W software. The total vertical stress of embankment due to self-weight is calculated by multiplying the average unit weight of material (assumed to be 20 kN/m³) by the height of the embankment. Figure 8-20 shows that the total vertical stress due to the embankment's self-weight is, for the most part, at least twice the uplift pressure due to pore water. Hence, risk to the embankment from seepage-induced uplift pressure is low.

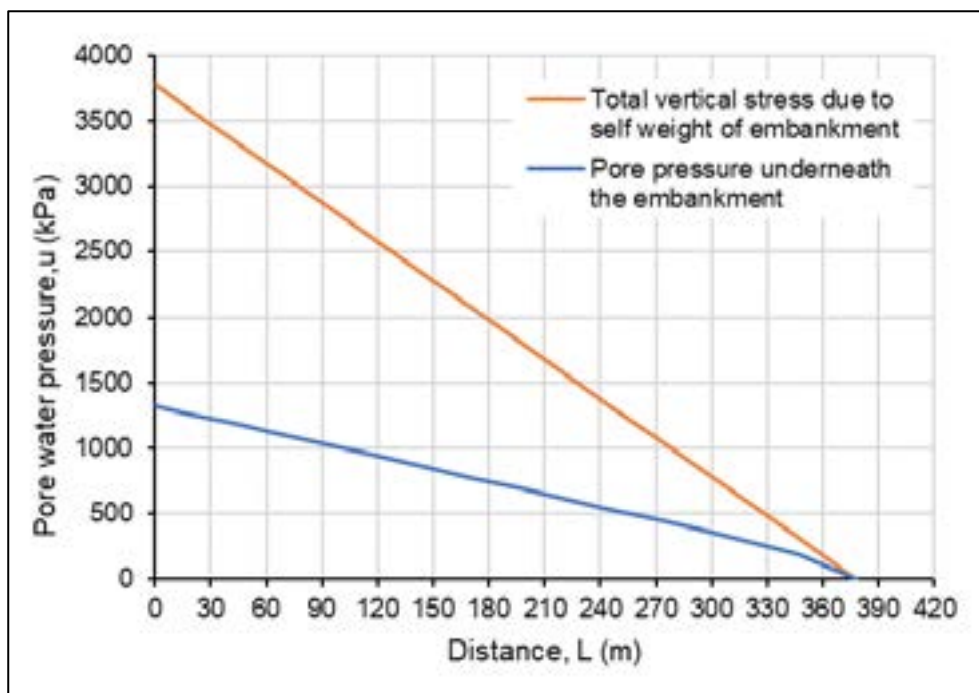


Figure 8-20: Total vertical stress due to self-weight of embankment and seepage-induced uplift pressure

Maximum phreatic levels

Phreatic levels for each section were determined to ensure levels are acceptable within, and at the downstream end of, the embankment. The asphalt core was assumed to be sheared to represent the worst-case scenario. Figure 8-21 and Figure 8-22 show the maximum phreatic level for both sections

⁸¹ Braja, M.D. 2008. Advanced soil mechanics. Taylor & Francis, 270, pp.170-180

maintained below the surface of the downstream embankment face. Figure 8-23 shows the phreatic level is above the toe and penetrates the embankment outer face if a toe drain is not installed. The results illustrate the importance of a toe drain at the base of the embankment, not only to minimise soil erosion at the downstream toe, but to manage the phreatic level. The more permeable Zone 3B further promotes phreatic level control during extreme conditions.

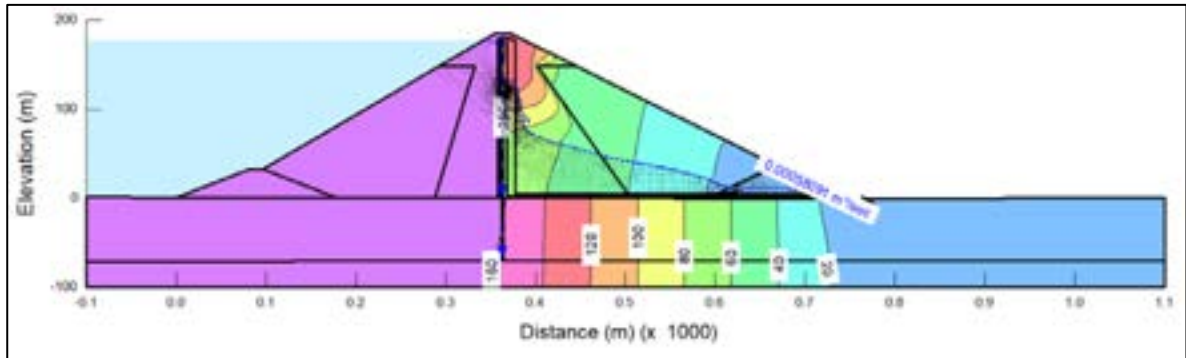


Figure 8-21: Total head contour diagram showing maximum phreatic level in Section 1 when asphalt core sheared at 60 m from embankment crest

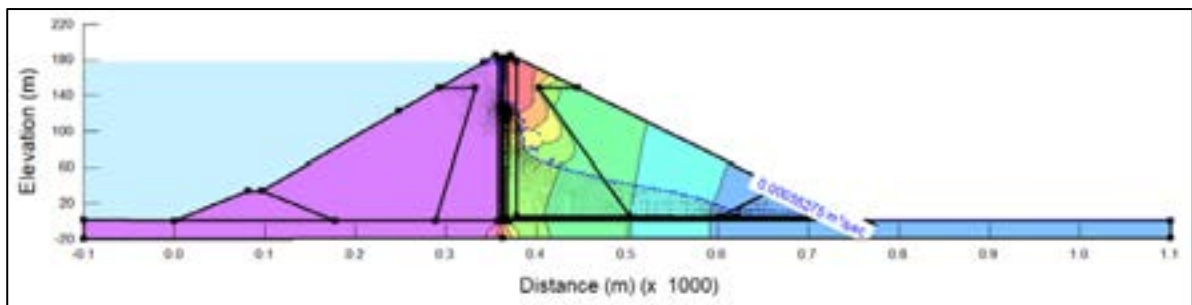


Figure 8-22: Total head contour diagram showing maximum phreatic level in Section 2 when asphalt core sheared at 60 m from embankment crest

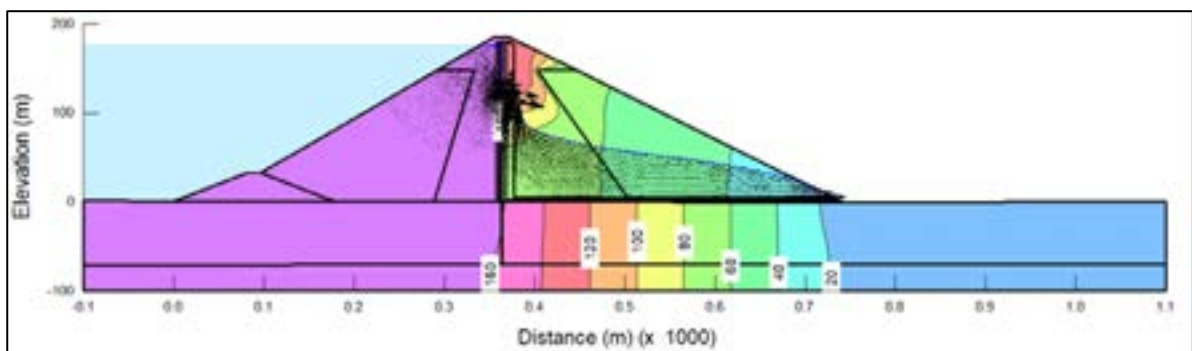


Figure 8-23: Total head contour diagram showing maximum phreatic level in Section 1 when asphalt core sheared at 60 m from embankment crest with no toe drain

8.10 Embankment failure modes

The following potential failure mechanisms were investigated and is further described below:

- Overtopping
- Bending and resultant failure of the core
- Shearing of the core
- Failure as a result of the impact of roads on the embankment outer profile.

Overtopping

Seismic analyses of the embankment indicated the maximum settlement experienced by the upstream side of the embankment would have the crest deformed down to RL 230 m.

Overtopping due to crest settlement could predominantly occur under two conditions; overtopping at the time of crest settlement and overtopping after settlement.

Once settlement has occurred, the embankment and potentially damaged asphalt core will need repair. If, while repairs are being carried out, the embankment is exposed to a maximum design storm event, immediate lowering of the maximum operating level to within acceptable limits until such time as the repair is complete, is required.

The maximum operating level of the FRHEP is set at elevation RL 226.1 m. If the maximum design storm and scaling the 24 hr, 1:1000 year to a 72 hr, 1:1000 year storm event are considered, the maximum water level rises to RL 230 m. This water elevation is below the final settled crest elevation of RL 230.7 m, and overtopping will therefore not constitute a failure, even if the operating level is not lowered as recommended before the onset of a large storm event.

Bending and resultant failure of the core

The maximum strain estimated in the core during an MCE is less or equal than 0.15%, whereas the tolerable strain ranges between 2% and 8%, and will therefore not constitute failure of the core. The deformation analysis showed that cracks preferentially occur on the downstream face than on the upstream face of the core.

However, should the core undergo severe cracking, the toe drain would arrest seepage exiting this aperture. A 2D seepage assessment by SRK has indicated the phreatic levels indicated in Figure 8-21 and Figure 8-23, with a maximum of 491 L/s assuming a 5 m aperture, 60 m from the crest. The phreatic level is unlikely to result in slope failure; however, repairs to the damaged core would have to be performed as soon after cracking is noted as possible.

Shearing forces of the core

The deformation analysis indicated differential settlement between the upstream and downstream faces of the core. The results of the modelling suggest that the deformation would promote a plastic failure through the finer filter and transition layers. More detailed modelling of the core and interface would be required during future studies.

Feizi-Khankandi et al. (2009) reported a seismic analysis conducted for an asphalt core dam, where the asphalt core mobilised only 0.5% of shear strain, with the majority of the strain absorbed by the transition layers (Figure 8-25). Shaking table tests confirmed that the core did not experience significant degradation under post-seismic conditions. The numerical modelling has indicated that settlement between upstream and downstream segments will be differential, while shaking table tests⁸² suggest that the relative settlement would be equal (Figure 8-24).

The numerical deformation analysis indicated that the estimated shear stresses on the core will be acceptable, with a maximum shear stress of 0.27 MPa developed during earthquakes, and the core having an available shear strength of 0.43 MPa (Section 8.11).

⁸² Feizi-Khankandi, S, Ghalandarzadeh, A, Mirghasemi, A A and Hoeg, K, 2009. Seismic analysis of the Garmrood embankment dam with asphaltic concrete core. *Soils and Foundations*, 49(2), pp.153-166.

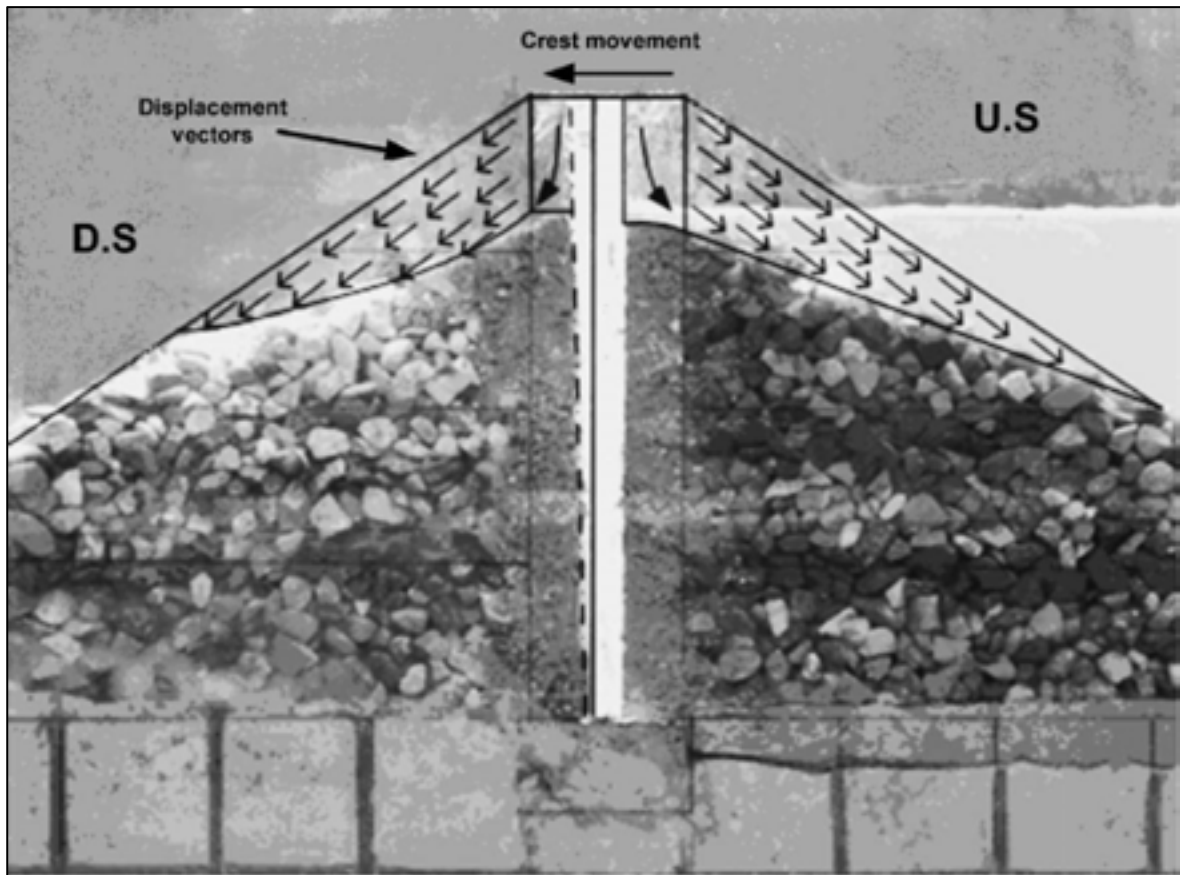


Figure 8-24: Shaking table tests on typical asphalt core model

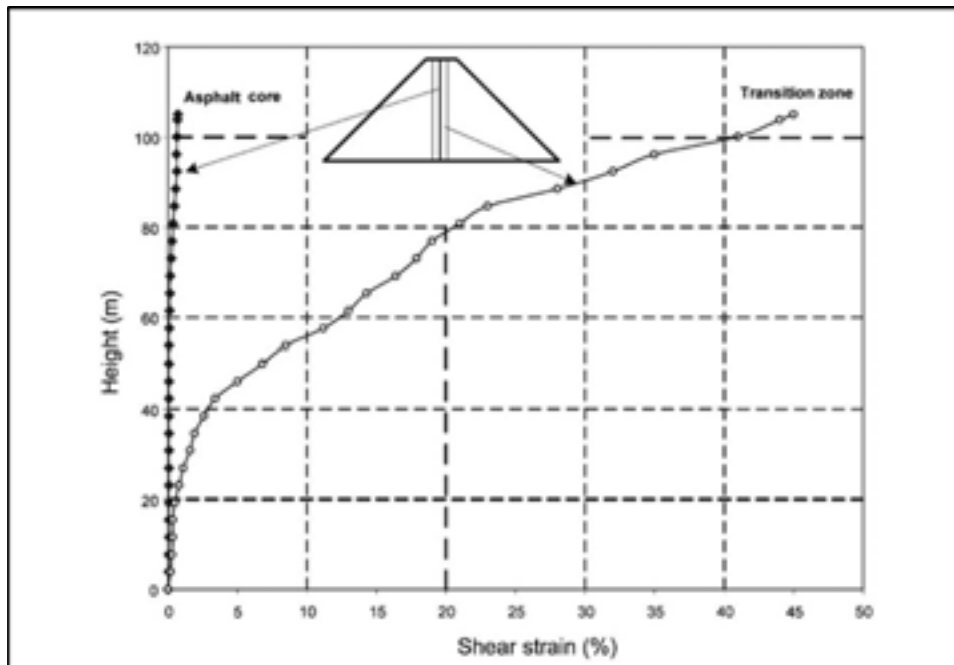


Figure 8-25: Permanent strain in the core and transition zones after dynamic loading

Failure as a result of the impact of roads on the embankment outer profile

SRK has assessed whether roads can be installed for temporary construction and long term operational reasons. Temporary roads (30 m wide) on the upstream and downstream slopes of the embankment will only be operational during construction. These roads will be used by heavy haul

trucks. The earthquake loading design requirements will be lower than the OBE due to the period of exposure, however, smaller ground motions were not available at the time of this study and the OBE acceleration has been used for the analysis.

The 12 m wide permanent roads used for the lifetime of the embankment require to be designed to satisfy serviceability requirements – the OBE acceleration has been used for the analysis. The permanent roads were assessed for dynamic loading, considering their period of exposure. Only the outer part of the lowest road bench would experience 20–60 cm of settlement, allowing vehicle access to be maintained (Section 8.11).

As the haul roads represent the worst-case profile, they were selected to represent static loading. The road section has also been simulated on the steeper inter-bench downstream embankment slope to simulate the worst case. Fully loaded large haul trucks would apply an instantaneous static load on the bench, assuming two trucks are crossing that particular location.

The material properties in Table 8-12 are based on Zone 3B material. The friction angles are reasonably conservative in comparison with friction angles expected on the final embankment. For simplicity, the embankment was modelled as homogenous zone, i.e. zones of varying strength were excluded.

Table 8-12: Material properties selected to assess static stability of large haul road benches

Unit weight (kN/m ³)	Strength type	Cohesion, c (kPa)	Friction angle, ϕ (°)
24	Mohr-Coulomb	5	44

The following analysis was performed:

- Vertical slices with Janbu simplified analysis
- For convergence options, 50 slices with tolerance of 0.005 up to maximum iteration of 75
- Haul truck loads with an expected final load of 390 tonnes were applied.

The static stability analysis results are shown in the model outputs (Figure 8-26). There is a higher concentration of slip surfaces on the slope below the bench than on the upper slope above the bench.

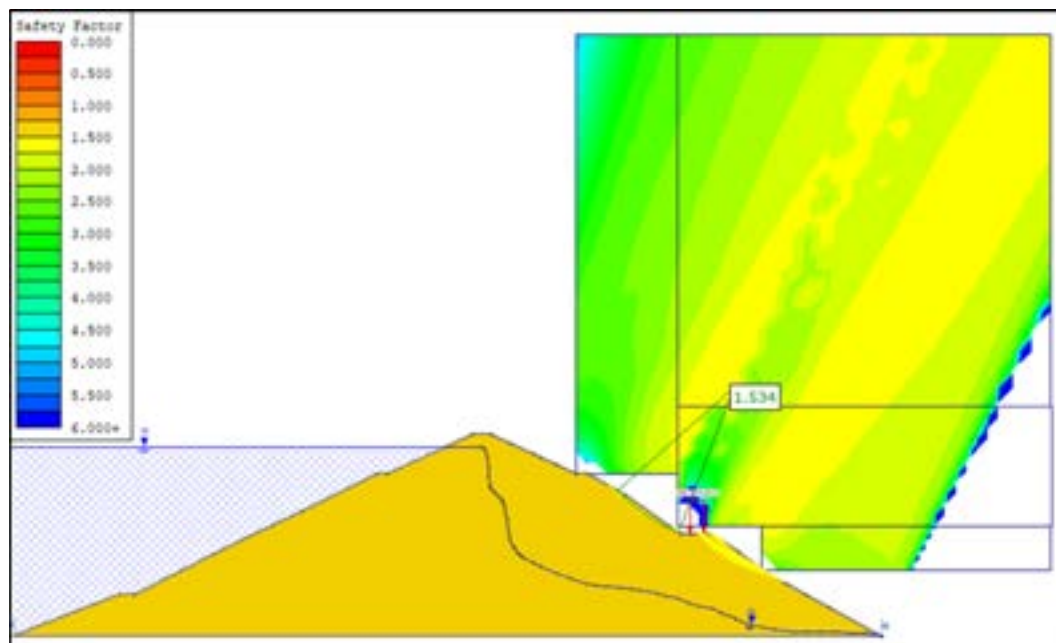


Figure 8-26: Static stability analysis for downstream slope assuming movement of large haul trucks (minimum FoS = 1.53)

All potential slip surfaces have a minimum FoS of 1.5.

8.11 Embankment stability and deformation analysis

Static and dynamic stability and deformation analyses for the FRHEP structures were undertaken. The results will be used to confirm suitability of the configuration of the embankment structure and determine its behaviour under plausible loading conditions is within expected ranges.

Numerical modelling, including 2D models in Plaxis for static and seismic (time-history) analyses, was carried out.

The 2D numerical model is an updated embankment configuration that incorporates road benches and ground motions from seismic hazard studies. The main aims are to evaluate static and dynamic deformations, failure mechanisms and FoS, and bending strains and shear stresses on the asphalt core.

8.11.1 Design background

Deformation analyses were previously done for four dam configurations. The dynamic analyses of Dams A, B and C were done using three ground motions sets, selected from an extensive database and scaled to the corresponding peak ground acceleration (PGA) and Arias intensity (AI). Dam D used ground motions scaled from SHA.

The dam geometries are summarised as follows:

Dam A: 17 m wide crest at RL 235 m; centrally positioned asphalt core. Upstream slope 2.0H: 1.0V and downstream slope 1.7H: 1.0V.

Dam B: 17 m wide crest at RL 235 m; asphalt core positioned 5 m towards upstream. Upstream slope 2.0H: 1.0V and downstream slope 1.8H: 1.0V. Four berms of 4.0 m width at RL 85 m, RL 135 m, RL 168 m and RL 198 m. Eleven geogrids starting at RL 198 m with a spacing of 3 m.

Dam C: 17 m wide crest at RL 235 m; asphalt core positioned 5 m towards upstream. Upstream slope 2.0H: 1.0V and downstream slope 1.8H: 1.0V below RL 198 m. Upstream and downstream slopes 2.2H: 1.0V above RL 198 m. One berm of 10.0 m width at RL 198 m.

Dam D: 17 m wide crest at RL 235 m; asphalt core positioned 5 m towards upstream. Upstream slope 2.0H: 1.0V and downstream slope 1.8H: 1.0V below RL 198 m. Upstream and downstream slopes 2.2H: 1.0V above RL 198 m. Three downstream road benches at RL 215 m, RL 147 m and RL 110 m.

The results indicated that there is an associated risk of partial loss of serviceability after an MCE event, which may require water operating levels to be lowered. To maintain full serviceability in such an event, an increased embankment height would be required. A new dam configuration (Dam E) with a crest elevation of RL 238.5 m was therefore considered.

8.11.2 Input for deformation analyses

Embankment cross-section

The configuration of the dam is as follows:

- Dam foundation: RL 50 m
- Dam crest: RL 238.5 m
- Crest width: 12 m
- Centrally positioned asphalt core
- Upstream slope: 2.0H:1.0V
- Downstream slope: 1.8H:1.0V below RL 198 m and 2.0H:1.0V above RL 198 m
- Three downstream road benches (12 m wide) at RL 219 m, RL 149 m and RL 112 m.

8.11.3 Constitutive models

The following constitutive models were employed:

- Linear elasticity (LE): For bedrock and cemented colluvium/ alluvium
- Mohr-Coulomb (MC): For material interfaces between the rockfill and the asphalt core
- Hardening Soil model with small strain stiffness (HSS) model: For rockfill and tailings and waste
 - this is an isotropic hardening model for materials undergoing plastic compression and consolidation, static and cyclic shear strains. The model properly accounts for:
 - increase in stiffness and shear strength (undrained and drained) with confining pressure
 - small-strain elasticity
 - pre-failure hardening plasticity with hyperbolic stress-strain response
 - hysteretic damping (no need to resource to Rayleigh damping)
 - compression plasticity allowing for the simulation of primary consolidation and compression stress-paths.

8.11.4 Modelling strategy

Software

Plaxis 2D, a finite element code widely used in the construction and infrastructure industries for soil–structure interaction, was used for the analyses (www.plaxis.com).

Analysis type

Standard finite-element analyses were performed. Full interaction between ground, construction materials and pore water was simulated by employing finite element technologies that simultaneously reproduce the behaviour of the solid and fluid phases of the various materials making up the body of the embankment and its foundation.

Drainage conditions

All models were performed under drained conditions. Changes in pore pressure due to external loading were assumed to occur at a rate slow enough for water to flow and achieve full dissipation of excess pore pressures. This is a valid approach for all static loading of dams and for seismic loading of coarse-grained materials, but not necessarily for tailings or waste rock deposition.

No flow through the asphalt core is assumed to exist, and the downstream face of the dam is therefore assumed to be dry. The study did not consider unsaturated soil behaviour including suction and collapse.

The modelling strategy is supported by the following facts:

- Zone 2A filters, connected to the toe drain, prevent the generation of a phreatic surface that might affect the behaviour of the downstream slope.
- Bedrock behaviour is largely elastic, with pore pressures not having a significant impact on stress conditions.

Tailings and rockfill clogging

Tailings were only considered for a single stage of FoS analysis. The design scenario corresponds to full water storage at its maximum operational level and without tailings.

Tailings materials might be in contact with the upstream slope; however, fines migration into the rockfill zones was not taken into account because tailings and waste rock will be deposited subaqueously, so there is insufficient hydraulic gradient to drive particles through the rockfill zones.

8.11.5 Geotechnical units

Geotechnical units are identified as follows:

- Rockfill – Zone 3A
- Rockfill – Zone 3B
- Bedrock
- Cemented colluvium & alluvium
- Tailings and waste rock.

8.11.6 Material parameters

The most relevant geotechnical parameters are summarised in Table 8-13.

Table 8-13: Summary of material parameters

Geotechnical Units	Constitutive model	$\gamma_h \gamma_{sat}$ (kN/m ³)	c (kPa)	ϕ_{ps} (°)	$E_{ref}^{50} E$ (MPa)
Rockfill – Zone 3A (0–10 m)	HSS	25 28	5	56	35
Rockfill – Zone 3A (10–30 m)	HSS	25 28	5	48	35
Rockfill – Zone 3A (>30 m)	HSS	25 28	5	44	35
Rockfill – Zone 3B (0–10 m)	HSS	24 26	5	51	30
Rockfill – Zone 3B (10–30 m)	HSS	24 26	5	44	30
Rockfill – Zone 3B (>30 m)	HSS	24 26	5	44	30
Bedrock	LE	31 31	-	-	12,000
Cemented colluvium & alluvium	LE	26 28	-	-	500
Tailings and waste rock	HSS	20 20	5	34	10

Note: Linear elasticity was employed for bedrock and cemented colluvium & alluvium. The value reported is the Young's modulus adopted for such units.

8.11.7 Selection of ground motions

A total of 11 ground motions were used for the seismic analysis of the dam; these were provided in a Seismic Hazard Assessment report (Al Atik & Gregor, 2016) prepared specifically for the region. Of these, 10 ground motions correspond to the MCE and one corresponds to the OBE.

The SHA report used the 84th percentile response spectra for the MCE scenarios on the deep intra-slab source Zone 15 and on the crustal Frieda Fault as the DSHA-based horizontal design spectra.

The MCE ground motions – five taken from the Frieda Fault and five from the Zone 15 – were scaled to the specified $PGA = 1.09 g$ ($10.69 m/s^2$), while the OBE ground motion was not scaled. The original and scaled ground motions are detailed in Table 8-14.

Table 8-14: Ground motions for the seismic analysis

ID	Description	Original record		Scaled record		
		PGA (m/s ²)	AI (m/s)	Scale Factor	PGA (m/s ²)	AI (m/s)
EQ_FF_01H	MCE – Frieda Fault source	5.59	0.90	1.91	10.69	3.28
EQ_FF_02H		5.17	6.27	2.07	10.69	26.86
EQ_FF_03H		5.31	3.19	2.01	10.69	12.95
EQ_FF_04H		5.57	2.11	1.92	10.69	7.76
EQ_FF_05H		5.55	3.50	1.93	10.69	13.00
EQ_Z15_01H	MCE – Zone 15 source	8.62	17.42	1.24	10.69	26.81
EQ_Z15_02H		8.03	11.26	1.33	10.69	19.97
EQ_Z15_03H		7.86	9.58	1.36	10.69	17.71
EQ_Z15_04H		8.62	10.95	1.24	10.69	16.85
EQ_Z15_05H		7.85	11.40	1.36	10.69	21.16
EQ_OBE_01H		3.82	2.74	1.02	3.88	2.83

8.11.8 2D analyses

Geometries and meshes

Figure 8-27 shows details of the geometry and mesh for the 2D model.

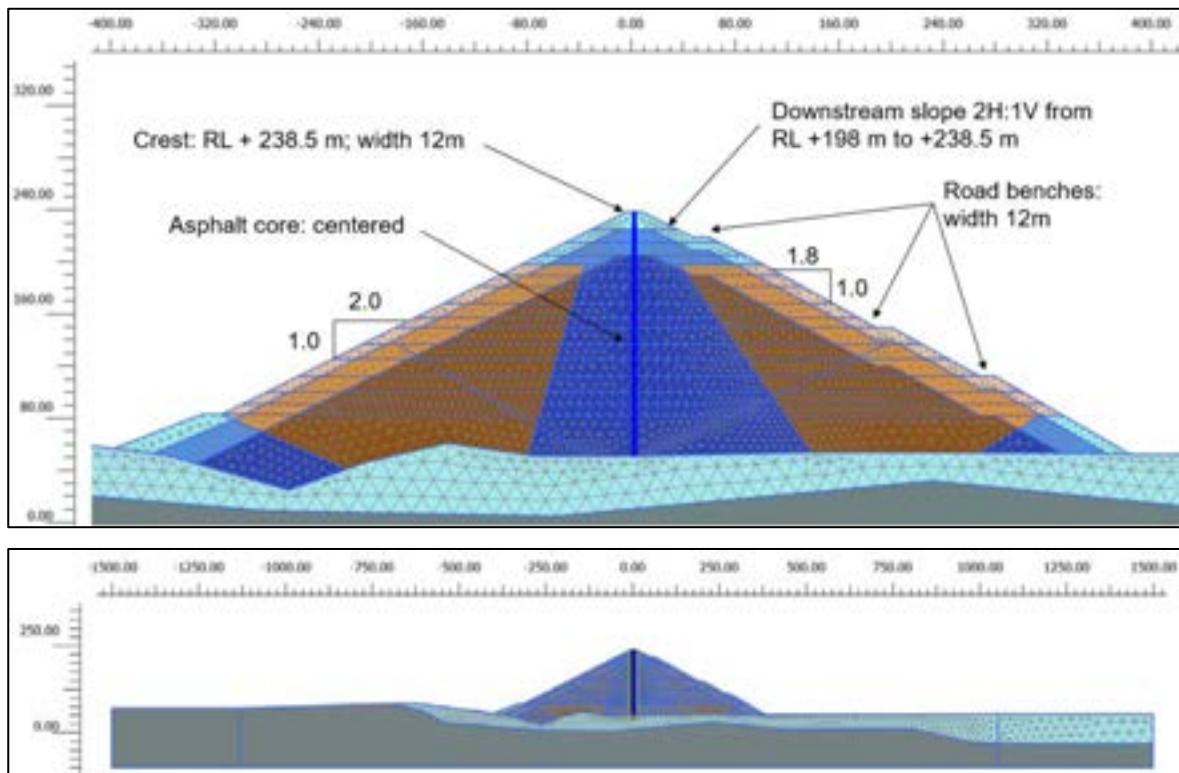


Figure 8-27: Detail of geometry and mesh – 2D model

8.11.9 Material parameters

Geotechnical units and relevant modelling parameters are indicated in Section 8.11.6.

The asphalt core was modelled as an elastoplastic plate with a thickness of 1.50 m, a Young’s modulus of 50 MPa and a Poisson’s ratio of 0.35. The Young’s modulus was increased to 1,000 MPa for

dynamic loading, based on experimental studies reported by Wang (2008) for an asphalt core used in the Yele Dam. A very low yield moment of 0.25 MNm/m was adopted to ensure that the flexural strength of the core does not contribute to dam stiffness.

The filter layers on both sides of the asphalt core were included in the deformation analysis by employing interface elements between the fill zones and the asphalt core. These interface elements were modelled as a Mohr-Coulomb material with $c' = 2 \text{ kPa}$ and $\phi' = 35^\circ$, which would mobilise a smaller shear strength than the rockfill itself.

8.11.10 Initial stresses

Initial stress state plays a minor role in the behaviour of the natural and man-made materials under the loadings produced by the construction of the embankment. In the absence of measured values, an initial stress ratio in the range $K_0 = 0.35|0.45$ was adopted for all materials.

8.11.11 Groundwater conditions

Hydrostatic pore water pressure distribution was adopted for the upstream side, while the downstream remains dry. Figure 8-28 shows the pore pressure distribution for the last construction stage. The modelling strategy comprised drained behaviour and steady-state flow, so the adopted value of soil permeability for each layer has no impact in the results.

8.11.12 Boundary conditions for dynamic analyses

Dynamic analyses were performed with a water level of RL 226.1 m. Viscous boundary conditions were used at the left and right ends of the model. For the bottom, a compliant base boundary condition was considered, where horizontal accelerations were input.

8.11.13 Construction stages

The simulation of the dam construction was done in discrete raises. For each raise, the dam is built in horizontal layers of compacted fill. The maximum dam height and reference levels for each construction stage are shown in Figure 8-29.

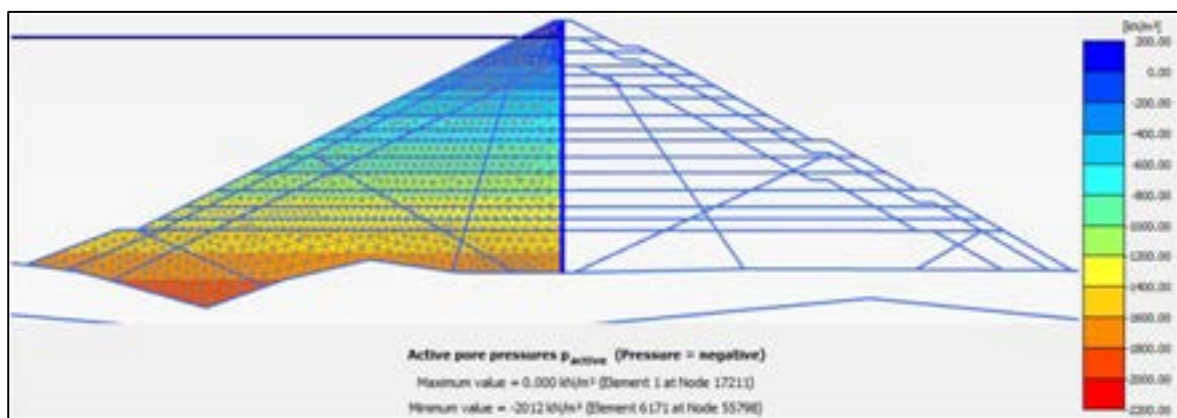


Figure 8-28: Pore pressure contours at the last construction stage

Construction stages are shown in Figure 8-30. The asphalt core was built progressively in tandem with the adjacent rockfill layers.

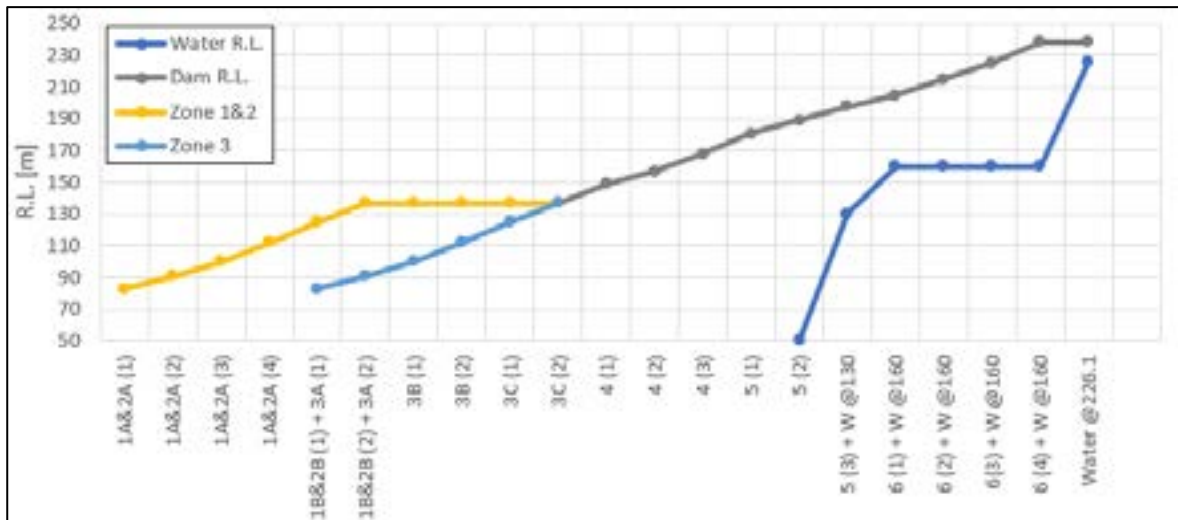


Figure 8-29: Reference levels for each construction stage

8.11.14 Procedure for reporting seismic displacements

Six nodes near the dam crest were selected to report the seismic performance of the dam. Nodes A, B and C are at RL 230 m; nodes D, E and F are at RL 215 m. Table 8-15 shows the coordinates of the nodes.

Table 8-15: Coordinates of reference nodes

Coordinate	Node A	Node B	Node C	Node D	Node E	Node F
X (m)	-5.0	0.0	5.0	-20.0	0.0	20.0
Y (m)	230.0	230.0	230.0	215.0	215.0	215.0

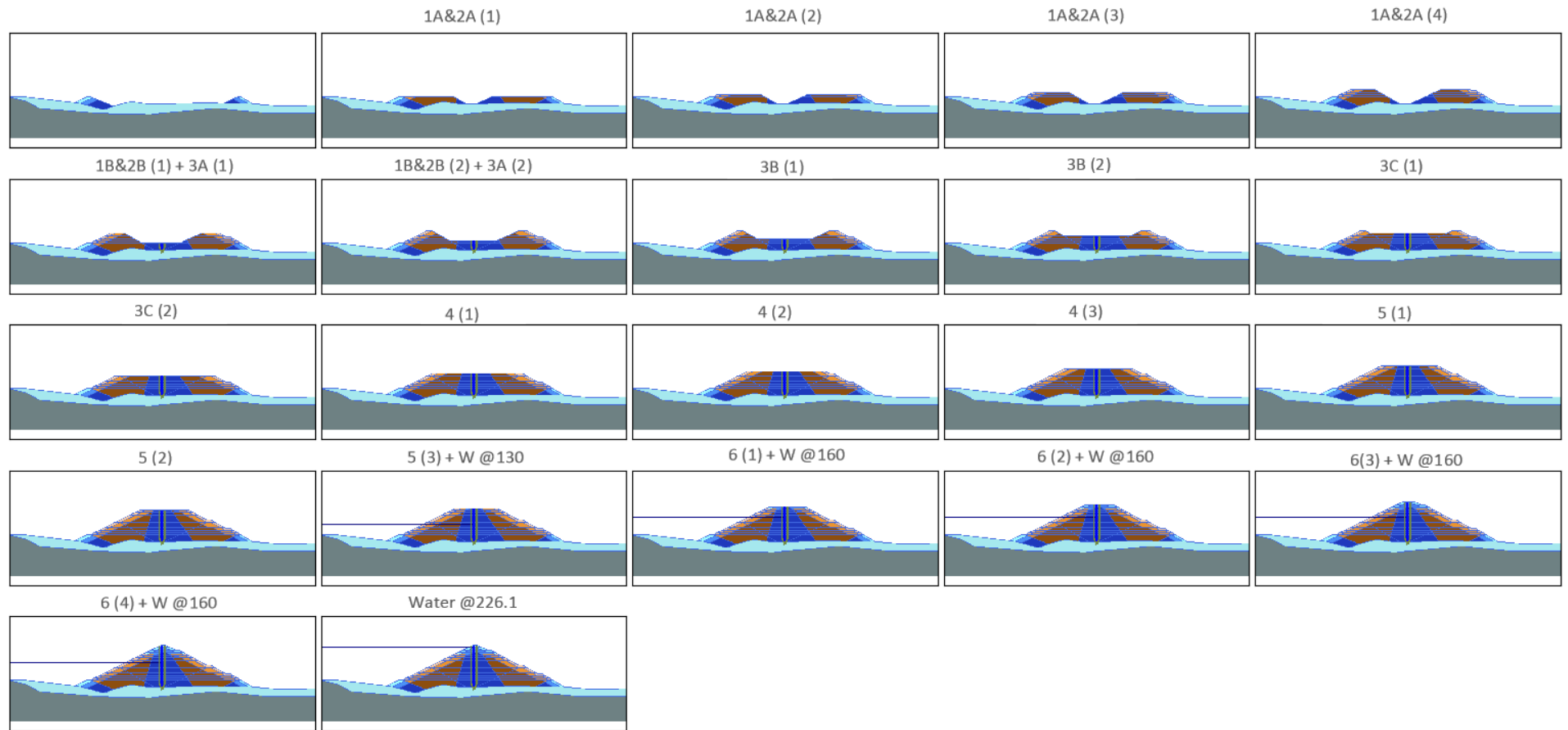


Figure 8-30: Plaxis modelling of construction stages

8.11.15 Displacements during construction

Displacements during construction are measured along the centreline of the final dam configuration (Figure 8-31, line A-A) in Figure 8-32. Displacement curves are calculated as the sum of the phase displacements of each stage. Positive values of horizontal displacements U_h indicate a displacement towards downstream. Negative vertical displacements U_v indicate settlements. Maximum mean values of vertical and horizontal displacements are -0.86 m and 0.33 m, respectively.

The effect of compaction was incorporated by introducing an intermediate stage where the weight of the fresh layer is doubled, and its friction angle is decreased to 30°. Figure 8-33 shows a comparison of calculated settlements measured at other dams.

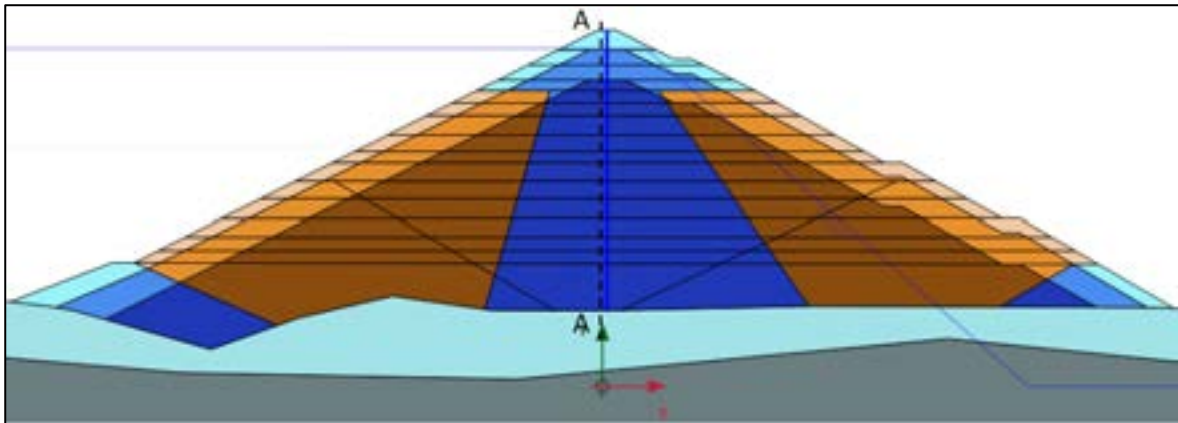


Figure 8-31: Vertical centrelines selected to measure displacement

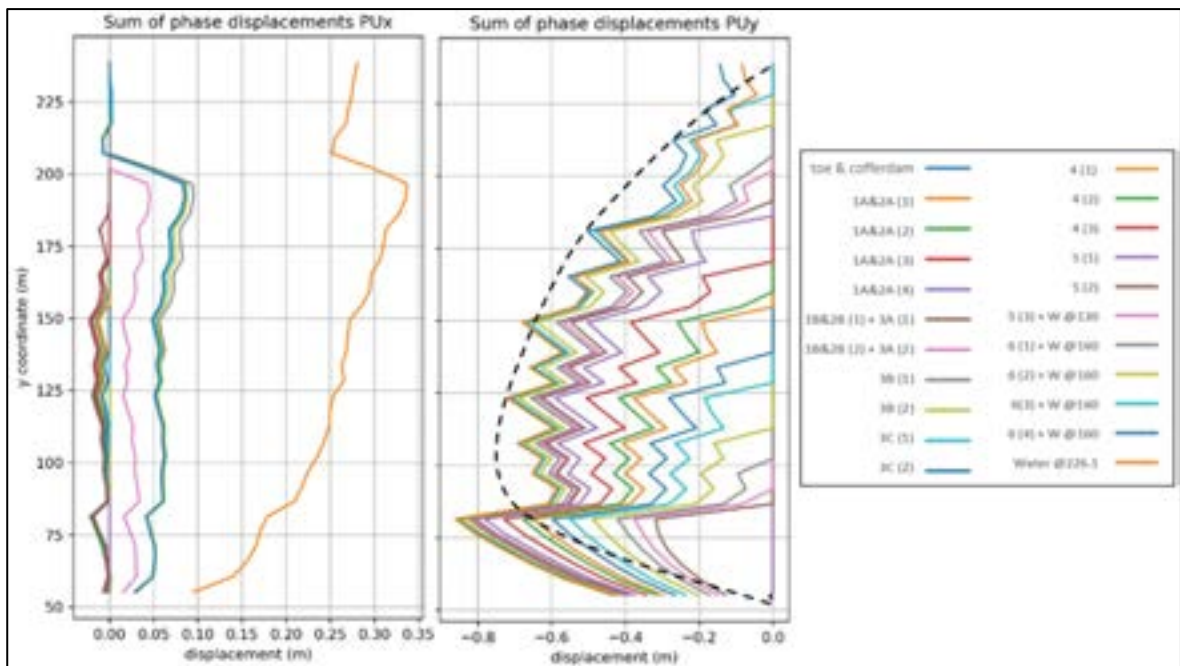


Figure 8-32: Mean horizontal and vertical displacements at centreline

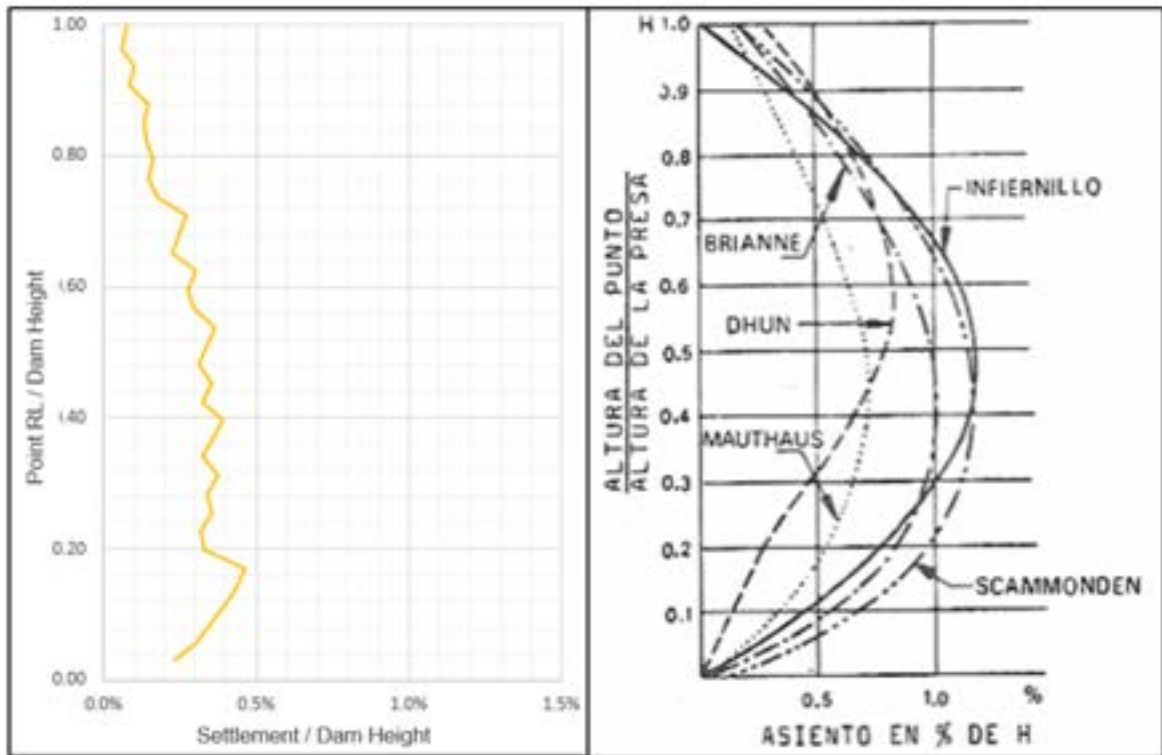


Figure 8-33: Dam settlements compared with reference information from other dams

8.11.16 Factor of Safety analyses

The FoS was evaluated using the strength reduction technique for the three different cases shown in Table 8-16

Case C corresponds to an extreme event in which the core cracks at two thirds of its height due to an earthquake. For this case, the steady-state groundwater flow is computed considering that the core is completely permeable between RL 168 m and RL 181 m and the water table downstream is at RL 50 m close to the toe drain. The soil hydraulic conductivities are: $1 \cdot 10^{-2} \text{ m/sec}$ for the toe drain; $5 \cdot 10^{-4} \text{ m/sec}$ for Zone 3A; $1 \cdot 10^{-3} \text{ m/sec}$ for Zone 3B; bedrock and asphalt core are considered impermeable.

Calculated values are shown in Table 8-16. Illustrations of the potential failure surfaces for each case are shown in Figure 8-34, Figure 8-35 and Figure 8-36. The FoS evaluated for all cases exceeded the values recommended by ANCOLD (2012) for various conditions.

Table 8-16: Factor of safety for different scenarios

Construction stage	FoS
Dam at RL 238.5 m, water at RL 232.4 m	1.96
Dam at RL 238.5 m, water at RL 226.1 m, tailings at RL 159.4 m	1.96
Dam at RL 238.5 m, water at RL 226.1 m, core cracked from RL 168 m to RL 181 m	1.76

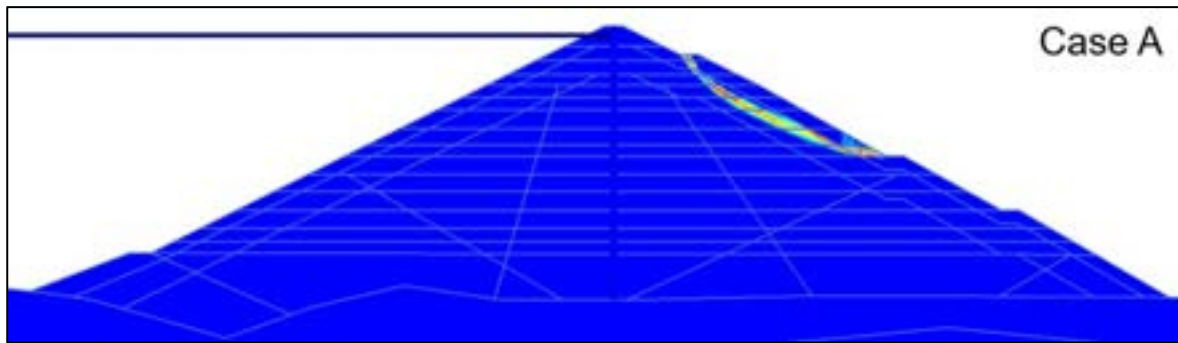


Figure 8-34: Failure surface obtained from FoS evaluation – Case A: Dam at RL 238.5 m, water at RL 232.4 m

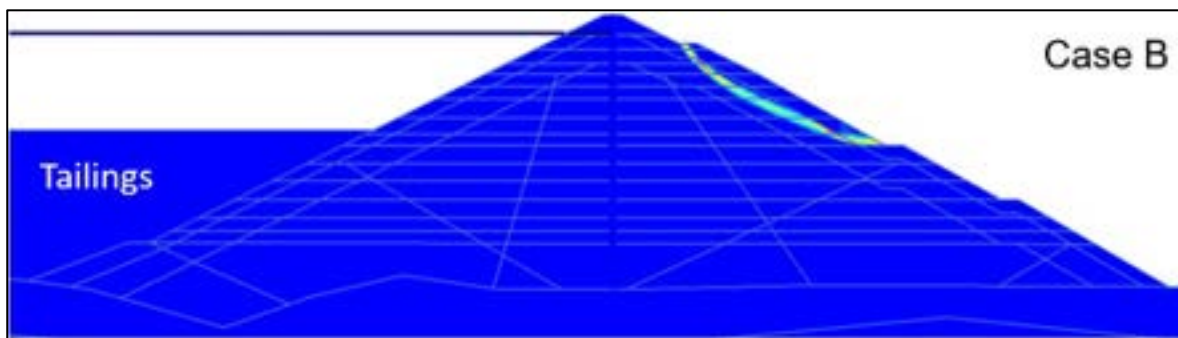


Figure 8-35: Failure surface obtained from FoS evaluation – Case B: Dam at RL 238.5 m, water at RL 226.1 m, tailings at RL 159.4 m

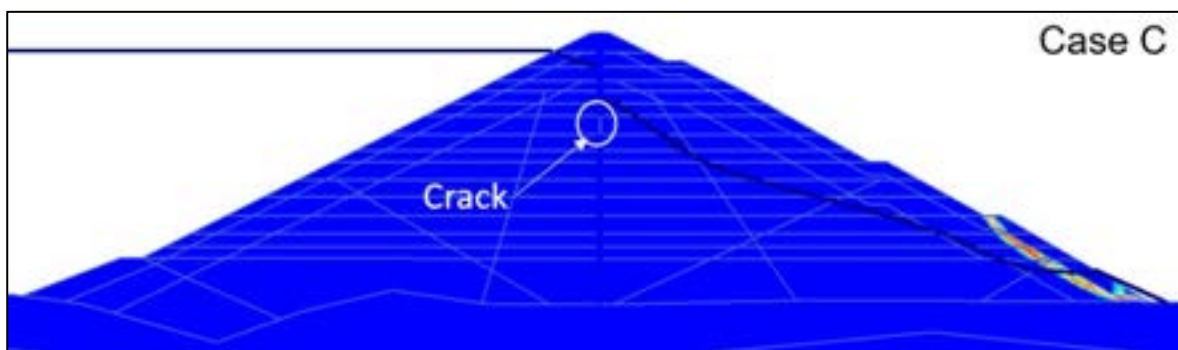


Figure 8-36: Failure surface obtained from FoS evaluation – Case C: Dam at RL 238.5 m, water at RL 226.1 m, core cracked from RL 168 m to RL 181 m

8.11.17 Displacements after seismic loading

Post-seismic residual settlements were obtained along two horizontal cross-sections. Figure 8-37 presents the settlement distribution at RL 230 m for all ground motions. Figure 8-38 presents the same information at RL 215 m.

Both plots show significant settlements of the wet slope and much smaller settlements on the dry slope. For RL 230 m, the maximum average upstream settlement is 4.00 m and the downstream settlement is 0.86 m. For RL 215 m, the corresponding values are 3.38 m and 0.28 m, respectively.

In addition to the cross-sections, continuous seismic displacements were recorded for each of the selected nodes.

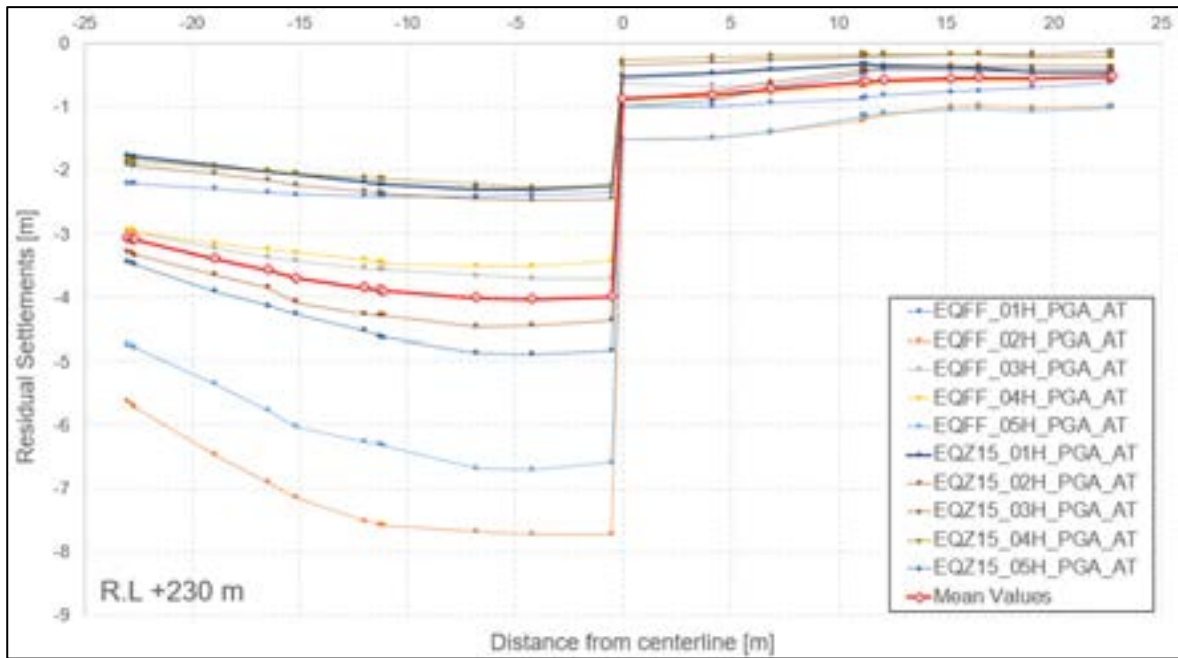


Figure 8-37: Residual settlements at RL 230 m

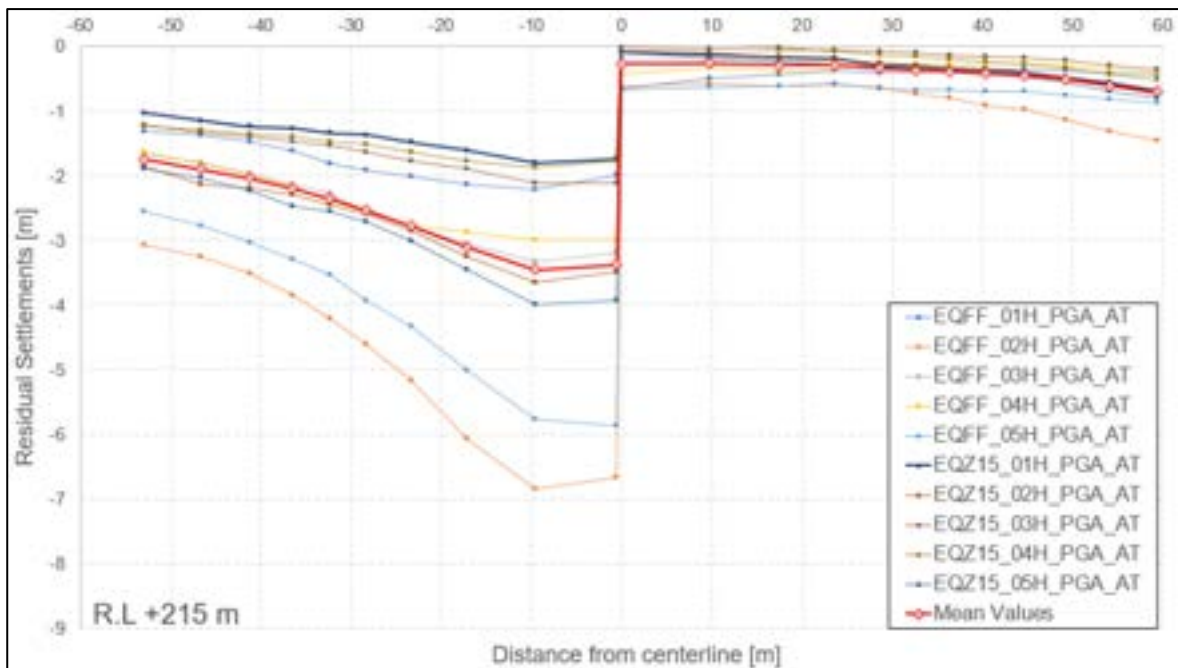


Figure 8-38: Residual settlements at RL 215 m

The deformed shape at true scale of the crest and the water level for normal operation is shown in Figure 8-39 after the most unfavourable earthquake occurs. The following conclusions can be drawn:

- The settlement of the upstream slope will probably result in exposure of the asphalt core (for the most extreme earthquake).
- The differential settlement between both sides of the dam – 6.0 m for the most unfavourable result – will produce an unbalanced horizontal load on the core that might cause cracking or, in the worst case, might cause the core to collapse towards the upstream side.

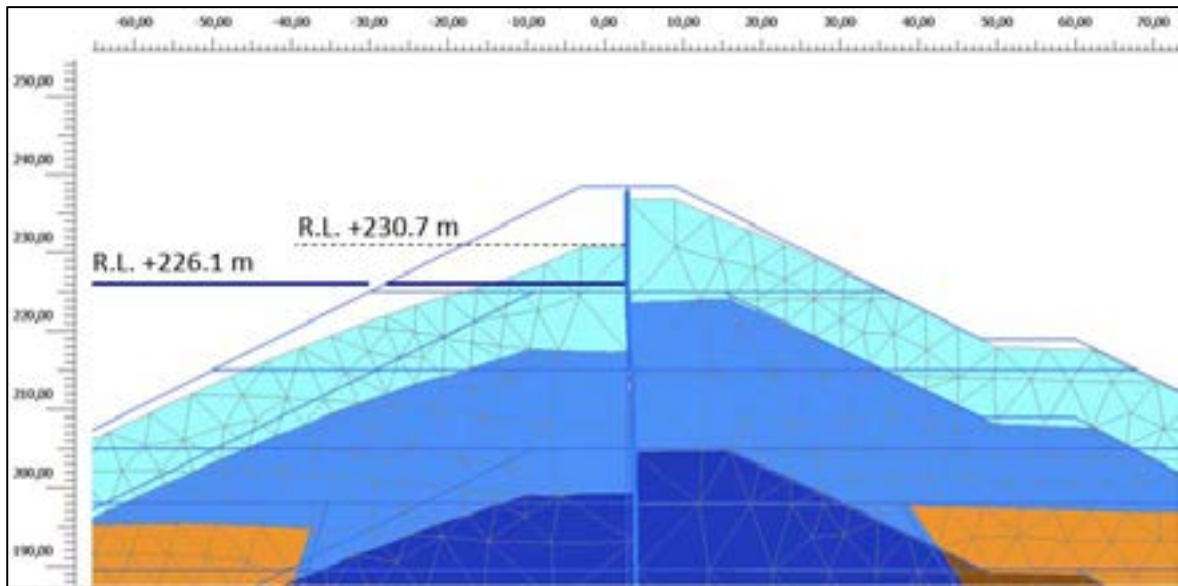


Figure 8-39: True scale deformed shape of the crest of the embankment for the most unfavourable earthquake (FF_02)

Figure 8-40 and Figure 8-41 show the residual settlement and horizontal displacement contours for Frieda Fault scaled ground motions. Figure 8-42 and Figure 8-43 show the same information for Zone 15 scaled ground motions. It can be observed that Set02 and Set05 are the worst ground motions in terms of vertical and horizontal displacements for Frieda Fault and Zone 15 source, respectively.

Figure 8-44 shows the residual settlement and horizontal displacement contours for the OBE ground motion. The maximum settlement of 0.56 m is located at the crest on the upstream (wet) side. The maximum horizontal displacement of 0.72 m is located near the cofferdam.

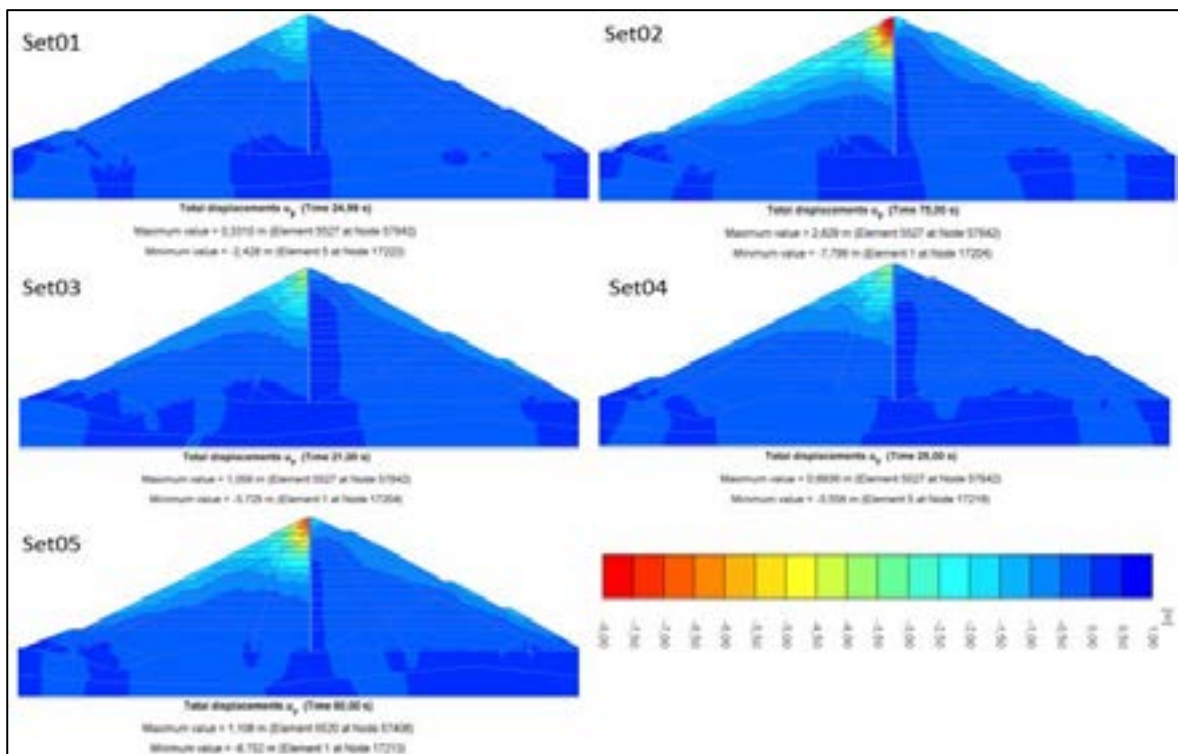


Figure 8-40: Vertical residual displacements for Frieda Fault ground earthquake scaled to PGA 1.09g

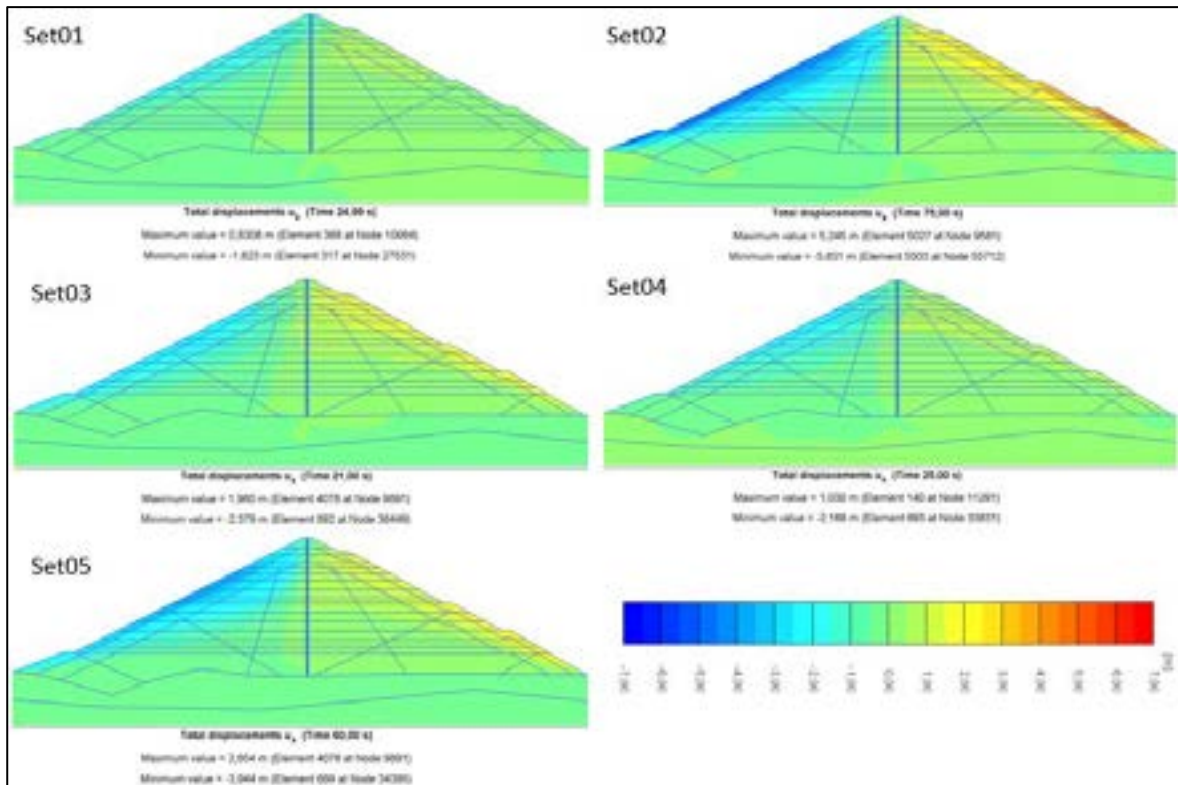


Figure 8-41: Horizontal residual displacements for Frieda Fault earthquake scaled to PGA 1.09g

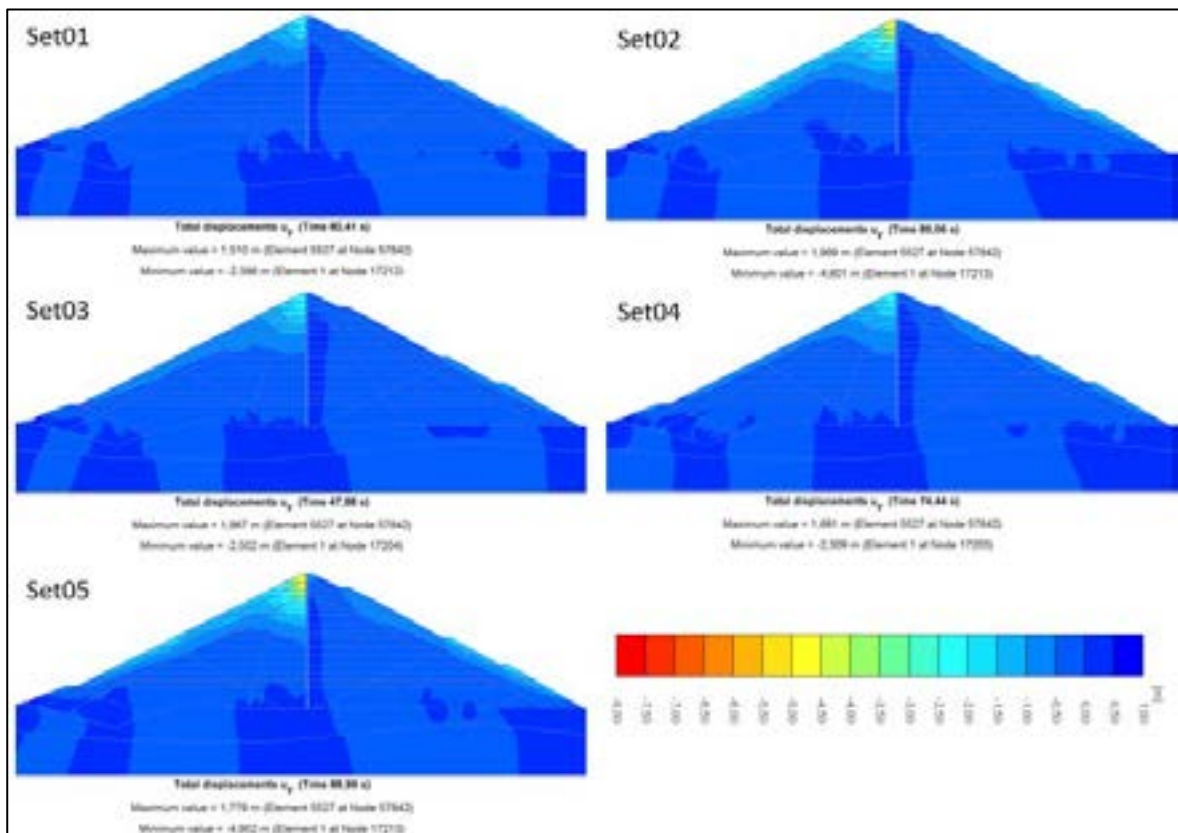


Figure 8-42: Vertical residual displacements for Zone 15 earthquake scaled to PGA 1.09g

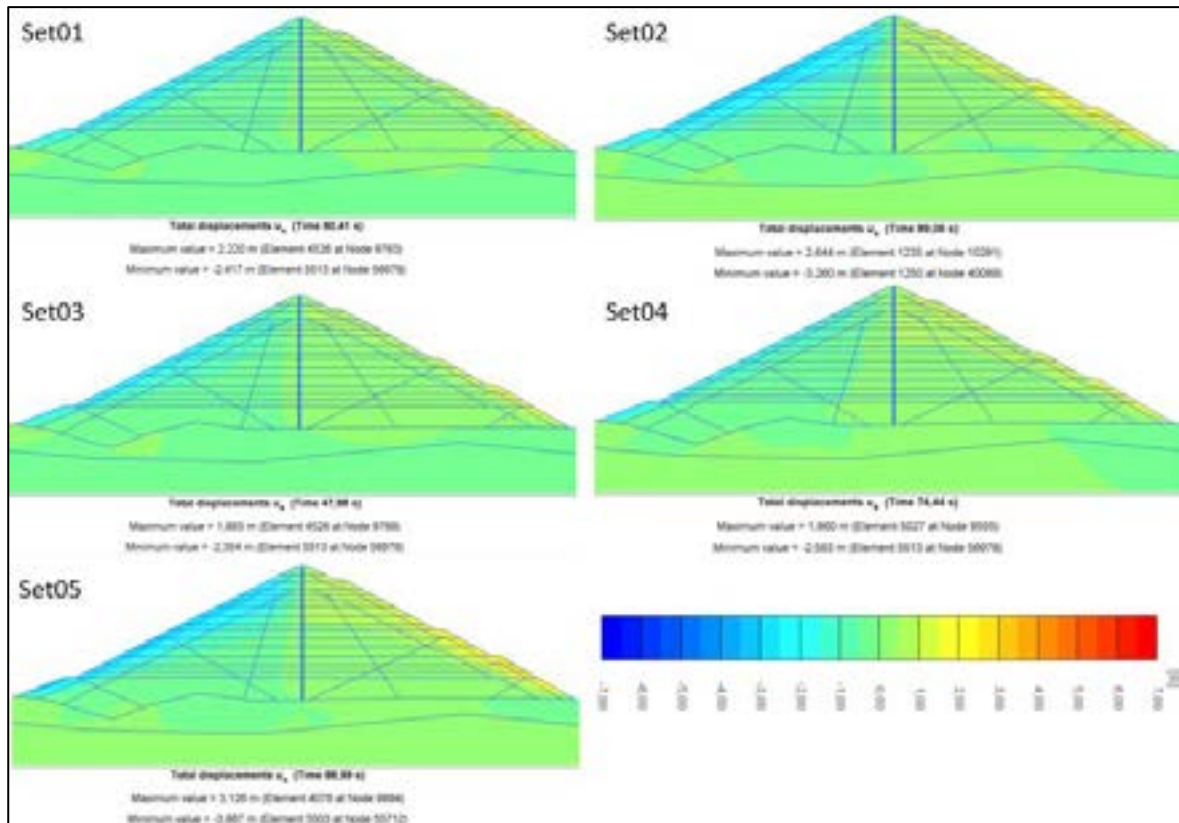


Figure 8-43: Horizontal residual displacements for Zone 15 earthquake scaled to PGA 1.09g

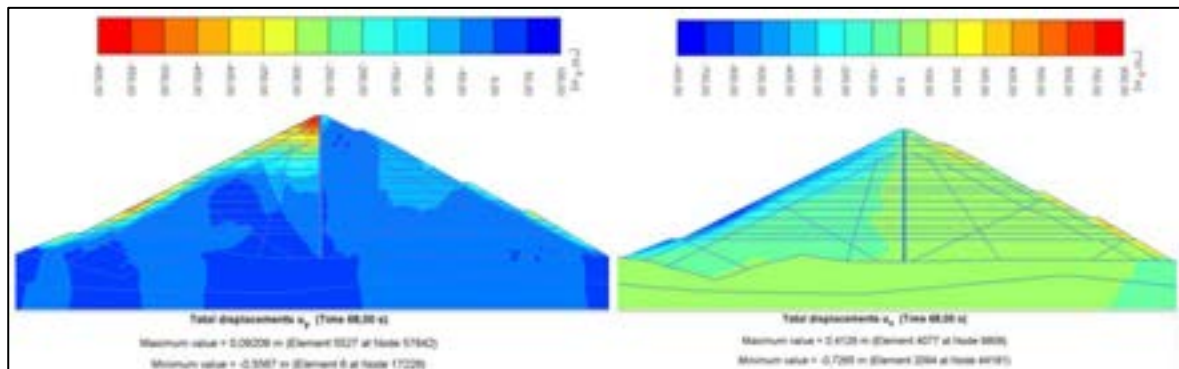


Figure 8-44: Vertical (left) and horizontal (right) residual displacements for OBE ground motion

8.11.18 Evaluation of the asphalt core bending strains

To evaluate whether the asphalt core bending strains are within an acceptable range, the horizontal residual displacements on the asphalt core interface were considered (Figure 8-45). According to Zhang (2013), the tolerable bending strain before the asphalt core cracks is in the range of 2%–8%, depending on the asphalt mix.

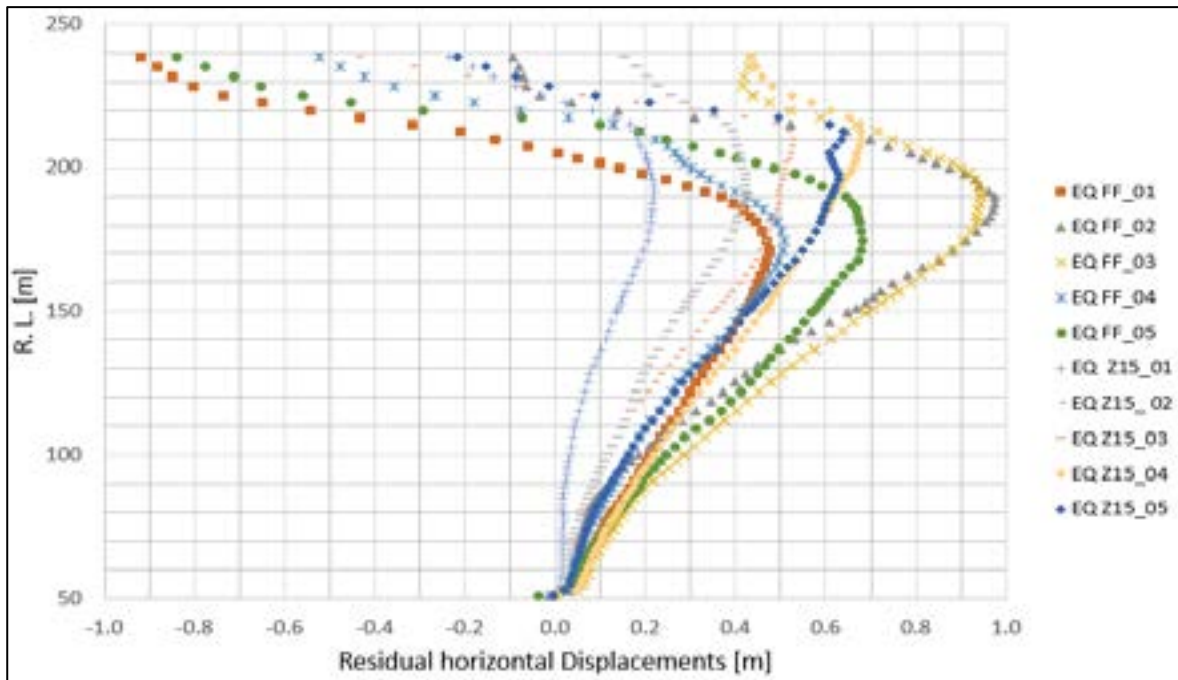


Figure 8-45: Horizontal residual displacements of the asphalt core

Some ground motions (such as EQ_Z15_05) result in rotation discontinuities. This is because the plate was modelled as an elastoplastic material to avoid unrealistic contributions to the dam stiffness, and so it apparently cracks for the plastification moment assumed. Therefore, an additional dynamic analysis was done for the most severe earthquake (EQ_FF_02) using an elastic plate and refining the mesh above RL 190 m to improve interface stresses accuracy.

Figure 8-46 shows a comparison between the horizontal residual displacements for the elastic and elastoplastic plate for EQ_FF_02. The displacement data was fitted for the elastic plate using the following two second grade polynomial functions (Figure 8-46):

- 1 Between RL 195 m and to RL 202 m:

$$\delta_x(z) = -8.58 \cdot 10^{-4} \cdot z^2 + 0.341 \cdot z - 32.77$$

the curvature was computed as the second derivative of $\delta_x(z)$:

$$k = -1.72 \cdot 10^{-3}$$

- 2 Between RL 215 m to RL 230 m:

$$\delta_x(z) = 1.02 \cdot 10^{-3} \cdot z^2 - 0.489 \cdot z + 58.57$$

the curvature was computed as the second derivative of $\delta_x(z)$:

$$k = 2.04 \cdot 10^{-3}$$

The bending strains are computed as:

$$\epsilon_b = k(z) \cdot \frac{h}{2}$$

Considering an asphalt core thickness of 1.5 m, the maximum bending strain is 0.15%, which is lower than the expected crack strain level. The maximum bending is located at RL 225 m to RL 237 m.

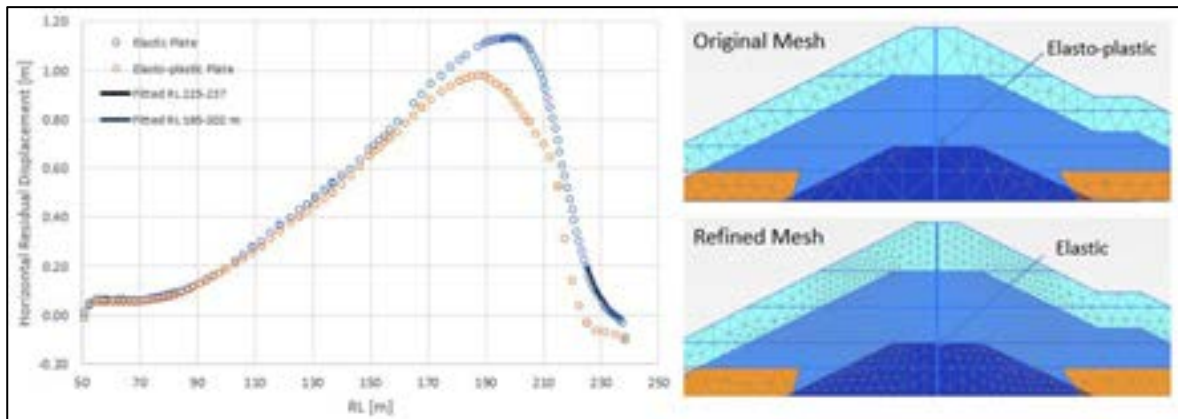


Figure 8-46: EQ_FF_02 – comparison between analysis with elastic and elastoplastic plate (left); mesh comparison between the original and refined model (right)

Evaluation of the asphalt core shear stresses

The evaluation of shear stresses on the asphalt core is done for the most severe earthquake (EQ_FF_02) using the results of the model with the elastic plate and refined mesh. The mesh densification entails a better approximation of strains, and so of stresses.

Figure 8-47 shows normal and shear stresses at the upstream and downstream interfaces between the asphalt core and the rockfill at the top 50 m of the dam (RL 190 m to RL 238.5 m) after the most unfavourable earthquake (EQ_FF_02).

The shear forces are computed as the integral between normal stress differences along depth and are plotted in Figure 8-48. The envelope of shear forces obtained from the Plaxis model are shown. There is an acceptable agreement between both approaches, but the integration gives the highest force, which is 408 kN/m, which is located at RL 215 m.

The maximum shear force of 408 kN/m corresponds to a shear stress of 0.27–0.41 MPa on the asphalt core, for a thickness of 1.0 m and 1.5 m, respectively. According to Wang & Hoeg (2016), the asphalt core deviatoric yield stress can be estimated as using the following equation:

$$(\sigma_1 - \sigma_3)_p = 2 \frac{c \cdot \cos \phi + \sigma_3 \cdot \sin \phi}{1 - \sin \phi}$$

where c and ϕ are the Mohr-Coulomb ‘cohesion’ intercept and friction angle, respectively. Based on triaxial test interpretations, the recommend values are $c = 0.12 - 0.17 \text{ MPa}$ and $\phi = 16^\circ$.

For simplicity, the confining pressure is computed as the overburden pressure where the highest shear force occurs (RL 215 m). The cohesive intercept is assumed to be 0.15 MPa. Therefore:

$$\tau_{max} = \frac{(\sigma_1 - \sigma_3)_p}{2} = \frac{c \cdot \cos \phi + (\gamma_{core} \cdot h) \cdot \sin \phi}{1 - \sin \phi}$$

$$\tau_{max} = \frac{0.15 \text{ MPa} \cdot \cos 16^\circ + 0.026 \frac{\text{MN}}{\text{m}^3} \cdot (238.5 \text{ m} - 215 \text{ m}) \sin 16^\circ}{1 - \sin 16^\circ} = 0.43 \text{ MPa}$$

Subsequently, the maximum shear stresses are lower than the shear strength of the asphalt material. In addition, it is expected that the shear stress will be reduced due to creep effects. In this case, the asphalt core thickness could be increased to 1.50 m.

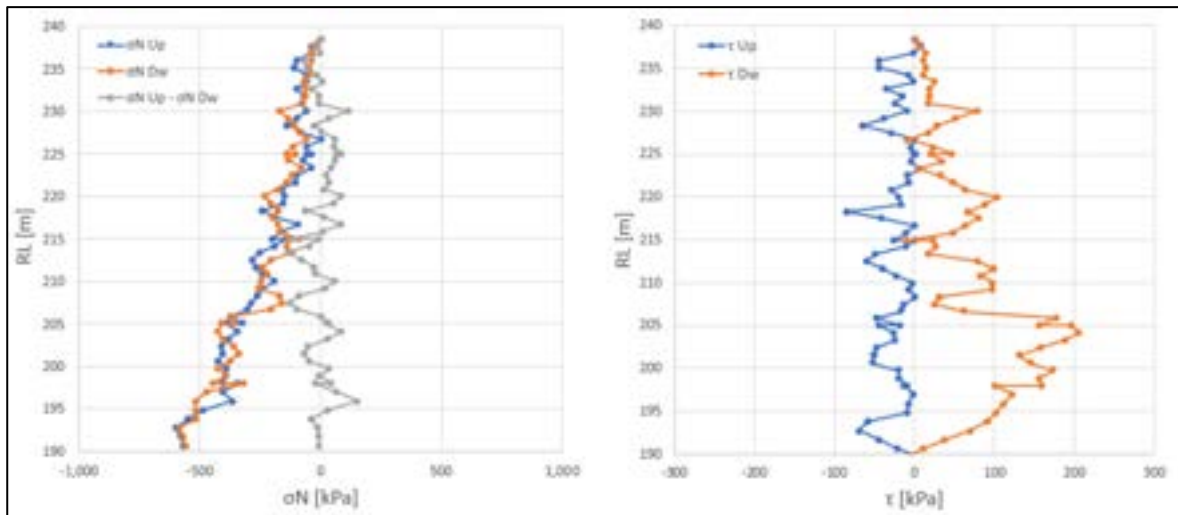


Figure 8-47: Normal and shear residual stresses at the asphalt core interfaces between RL 190 m and RL 238.5 m - EQ_FF_02

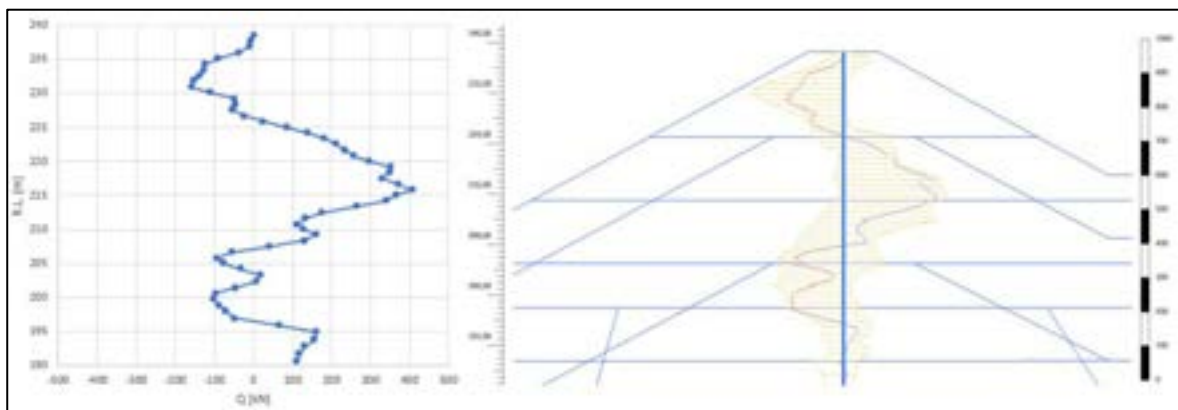


Figure 8-48: Interpreted residual shear forces at the asphalt core between RL 205 m and RL 238.5 m (left); envelope of shear forces obtained from Plaxis (right) - EQ_FF_02

8.11.19 Conclusions

The deformation analysis of embankment was undertaken by 2D finite element modelling in Plaxis. The configuration of the dam is 12 m wide crest at RL 238.5 m; centrally positioned asphalt core; upstream slope 2.0H:1.0V; downstream slope 1.8H:1.0V below RL 198 m and 2.0H:1.0V above RL 198 m; three road benches 12 m wide on the downstream slope at RL 219 m, RL 149 m and RL 112 m.

The simulation of the dam construction was done in stages, activating clusters to reproduce the embankment construction sequence. The effect of compaction of each layer was taken into account. Settlements during construction are in the range of 0.8 m to 0.9 m.

The FoS evaluation showed that potential failure surfaces would likely develop at the downstream slope for all cases and that the achieved FoS values are adequate and align with values recommended by ANCOLD (2012), for the three analyses.

A total of 11 ground motions were input to the seismic analysis (taken from the Seismic Hazard Assessment report). Of these, 10 correspond to the MCE, which were scaled to PGA = 1.09g, and one to the OBE, which was not scaled.

Post-seismic residual settlements on the upstream slope close to the crest show local failure with asphalt core exposure, with a minimum average settlement of 4.0 m and a maximum of 7.7 m. On the downstream side, the maximum average value reaches 0.86 m.

Bending strains on the asphalt core were evaluated – a maximum value of 0.15% was obtained corresponding to EQ FF_02 located at RL 225 m to RL 237 m. This value is below the maximum recommended values in the literature, which range between 2% and 8%.

asphalt core shear stresses were computed for EQ_02_FF using an elastic plate with a refined mesh at the upper part of the embankment. The values were compared with a yield criterion proposed by Wang & Hoeg (2016), and proved to be satisfactory. Nevertheless, the difference between both sides of the embankment – 6.0 m for the most unfavourable result – will produce an unbalanced horizontal load on the asphalt core that might cause cracking, in the worst case, may cause the core to collapse towards the upstream side.

8.12 Integrated embankment design summary

SRK concludes as follows:

- The embankment cut-off system consists of an asphalt core, plastic concrete cut-off wall, grout curtain and associated concrete plinth.
- The optimised embankment profile is 1:2 upstream and 1:1.8 downstream, with the asphalt core located in the centre of the embankment.
- The asphalt core varies in thickness from 1.7 m at the base to 1.5 m at the crest.
- Permanent shear strain of the asphalt core after large ground motion will be within allowable limits. Experience shows that the permanent shear strain of the asphalt core is approximately 0.5%, with most of the strain being absorbed by the transition layer.
- The plastic concrete cut-off wall is 2.3 m at the top, to be installed to a maximum depth of 65 m in the alluvium and colluvium layers below the foundation.
- The crest and permanent road widths be constructed on 12 m benches.
- The 30 m wide, large haul truck roads will be constructed temporarily and backfilled using the outer fill once no longer in use, to form the final embankment profile.
- The plastic concrete cut-off wall in the deepest section of the river will be raised during the development of the embankment foundation and will not be installed using the same conventional cutting technique.
- Two different concrete plinth details will be implemented at Section 1 and Section 2 (Figure 8-17). The plinth will need to be articulated to accommodate the large differential settlements expected in the riverbed section.
- Two options have been identified for the plinth design in the riverbed section; Option 1 has been selected and used for estimating purposes.
- Grout will be installed across the foundation as curtain grout, targeted grout and blanket grout. Grouting will be required to achieve the design requirements; post-commissioning grouting may also be required to ensure the design seepage rates are achieved.
- A benchmarking study has revealed that the measured seepage rates of ACRDs typically range between 10.2 L/s and 358 L/s.
- The seepage profile modelled might differ from the actual embankment due to the variability of foundation material parameters and the presence of preferential fractures and fissures.

- Analyses with and without the cut-off system have shown that the presence of the plastic concrete cut-off wall and concrete plinth are important in limiting the total seepage rate and hydraulic gradient underneath the embankment; a total seepage rate of 507 L/s was estimated for the embankment without the cut-off system, in comparison with a seepage rate of 6 L/s for the embankment with the cut-off system.
- The estimated hydraulic gradient for Section 1 is 1.5, and 14 for Section 2; without the use of a cut-off wall and concrete plinth, the hydraulic gradients in both sections have been estimated to be 60.
- Considering the potential variance in parameters across the embankment's sub-components, the estimated seepage rates for the embankment may vary between 2.2 L/s and 145 L/s; under normal operating conditions, seepage rates are expected to be between 2.2 L/s and 19.7 L/s.
- The exit gradients calculated at the toe drain in both sections under various conditions are below the critical hydraulic gradient of most soils, $i_{critical} = 1$; piping at the toe of embankment is unlikely to occur. Acceptable hydraulic gradients must be defined during further assessment of the hydraulic gradients.
- A roads strategy has been investigated for implementation.
- Maximum deformation of 7.8 m has been estimated for the upstream segment of the embankment. The RL 238.5 m crest will be able to accommodate and provide sufficient freeboard and flood protection in excess of the projected 1:1000-year storm (above the maximum operating level).
- Should shearing of the asphalt core occur, the toe drain will arrest any seepage such that static stability will be maintained.
- The embankment is not at risk of rupture, as the uplift pressure due to pore pressure underneath the embankment is less than the overburden pressure from self-weight of the embankment.
- The presence of the toe drain and Zone 3B is critical to reduce phreatic levels in the downstream segment of the embankment in the event of significant asphalt core failure.
- The total seepage rate is estimated to be approximately 491 L/s under worst-case scenario, significant asphalt core failure due to large deformation of embankment. A particle retention assessment is required to investigate the increased the risk of piping.
- Site-specific design modifications may be required during construction to accommodate actual conditions once the foundations are exposed.
- The deformation and stability analysis of the embankment was undertaken through a 2D finite element model run in Plaxis. The FoS evaluation showed that potential failure surfaces would likely develop at the downstream slope for all cases and that the achieved FoS values are adequate, i.e. are within the recommended ANCOLD (2012) values for the three analyses.

Predicted post-seismic residual settlements on the upstream slope near the crest indicate settlement resulting in exposure of the asphalt core. The minimum average settlement is 4.0 m and the maximum is 7.7 m. On the downstream side, the maximum average value reaches 0.86 m. Bending strains on the asphalt core were evaluated, a maximum value of 0.15% was obtained located at RL 225 m to RL 237 m. This is below maximum recommended values in the literature, which range between 2% and to 8%.

9 Tunnels

The facility will require various tunnels to support the FRHEP, not only during operation but also during construction. Table 9-1 provides a summary of the various tunnels and associated power shafts. The specifics of each tunnel system are detailed in Sections 10 and 16.

Table 9-1: Summary of FRHEP tunnels

Tunnel	Approximate length (m)	Internal diameter (m)	Tunnel shape
Diversion tunnels	1375	9 × 9 high	'D' shaped
Residual flow tunnel	245	4 × 4 high	'D' shaped
Residual flow valve chamber	16	8 × 10 high	'D' shaped
Residual flow dissipation chamber	60	4 × 5.5 high	'D' shaped
Residual flow tunnel outlet	50	4 × 4 high	'D' shaped
Residual flow valve shaft	165	7.5	Circular
Lower intake tunnel 1	150	7.1	'D' shaped
Lower intake tunnel 2	70	7.1	'D' shaped
Lower intake gate shaft	62	10	Circular
Conveyance tunnel 1	550	7 × 7 high	'D' shaped
Conveyance tunnel 2	600	7 × 7 high	'D' shaped
Conveyance tunnel 1 power shaft	100	7	Circular
Conveyance tunnel 1 power shaft	100	7	Circular
Conveyance tunnel 1 (steel-lined)	250	7 × 7 high	'D' shaped
Conveyance tunnel 2 (steel-lined)	250	7 × 7 high	'D' shaped
Surge chamber 1	120	12	Circular
Surge chamber 2	120	12	Circular

Although the final lining requirements may be different for the various tunnels, the support for stability requirements are similar. The quality of local rock has been identified as suitable for construction with some areas of weathering expected. To this end, two support specifications have been provided.

9.1 Geotechnical design assessments

Two diversion tunnels will be required to divert river flows from the Frieda River away from the construction area of the main embankment while providing protection against 1:100 storm events. The diversion tunnels, approximately 1,375 m long, will consist of two approximately 9 m × 9 m ('D' shaped) shotcrete-lined tunnels located within the eastern (RH) hillsides of the Frieda River.

Both the inlets and outlets of the tunnels will be located to avoid ongoing construction work areas. The inlet of the diversion tunnels will be upstream of the FRHEP diversion and cofferdam, and the outlet of the diversion tunnels will be downstream of the downstream coffer and sediment dams located further downstream of the main containment dam. Once the two tunnel ends are connected to the inlet and outlet works, the Frieda River will be diverted to flow into the diversion tunnels following the construction of the diversion dam and downstream coffer dam. The associated main cofferdam will then be completed.

9.1.1 Preliminary ground support design

Based on the drilling and testing information, the right abutment rockmass has been characterised according to the following:

- Barton's Q tunnelling index
- Uniaxial compressive strength (UCS)
- Geological Strength Index (GSI).

When assessing the data for ground support design and tunnel spacing assessment, it has been assumed that all colluvial and/ or highly weathered materials will be removed during the construction of inlet and outfall box cuts, so no characterisation for these materials has been considered. The tunnel inlets and outfalls will therefore be established in bedrock, either slightly to moderately weathered and joint oxidised rock, or unweathered rock.

It has been assumed that both sets of tunnels will transect predominantly good-quality, strong, unweathered to slightly weathered (locally joint oxidised) dunite (the 'general' bedrock), and the ground support assessments have been carried out accordingly. It is likely that the tunnels will locally pass through moderately weathered, joint oxidised rock (most likely near portals) or weak, serpentinised rock. Therefore, alternative ground support recommendations have been provided for the poorer rockmass conditions; however, exactly where these will be encountered is difficult to predict. Therefore, horizontal probe drilling along the tunnel alignments ahead of development is strongly recommended for advance preparation. It is estimated that poorer ground will be encountered along less than 10% of the tunnel lengths.

Appropriate ground support for both the diversion and conveyance tunnels has been determined using an empirical method. The distribution of values calculated for each interval of logging data according to the Barton's Q tunnelling index system (1974) and NGI (2015) have been assessed, and representative values/ ranges identified for the different rockmass conditions. These were then plotted on the ground support design chart of Grimstad & Barton 1993 (Figure 9-4).

The Q-system was developed for classification of rock mass for underground excavations. While the system was developed for use in underground mapping data, it has been successfully applied to geotechnically logged drill core as well. The Q-value describes the rock mass stability of jointed rock masses on a logarithmic scale. High Q-values indicate good stability and low values indicate poor stability. The Q-value is calculated from six parameters, as per the following equation:

$$Q = \frac{RQD}{J_n} \times \frac{J_r}{J_a} \times \frac{J_w}{SRF}$$

Where:

RQD	= Rock quality designation, indicative of jointing spacing
J _n	= Joint set number
J _r	= Joint roughness number
J _a	= Joint alteration or infill number
J _w	= Joint water reduction factor
SRF	= Stress Reduction Factor

RQD and J_n give an indication of the degree of jointing and block size, J_r and J_a give joint friction or inter-block shear strength and J_w and SRF give the active stress regime of the specific underground area.

The first two terms of the equation, i.e. (RQD/J_n) × (J_r/J_a), effectively describes the quality of the in situ rock mass, while the third term (J_w/SRF) represents the active stress coefficient (external

influences of stress and groundwater) that is applicable after excavation. For the FRHEP tunnels, two separate scenarios of J_w have been assessed in the context of the adjacent reservoir (the latter scenario is more conservative):

- Large inflow or high pressure in competent rock with unfilled joints ($J_w = 0.5$)
- Large inflow or high pressure with considerable outwash of joint fillings ($J_w = 0.33$).

Diversions tunnels

The diversion tunnels have been designed with an arched roof, and final dimensions are of 9 m width and 9.25 m height to the top of the arch (Figure 9-1). As these dimensions are post-installation of ground support and tunnel lining, SRK has assessed ground support for initial blasted tunnel dimensions of 9.5 m × 9.4 m.

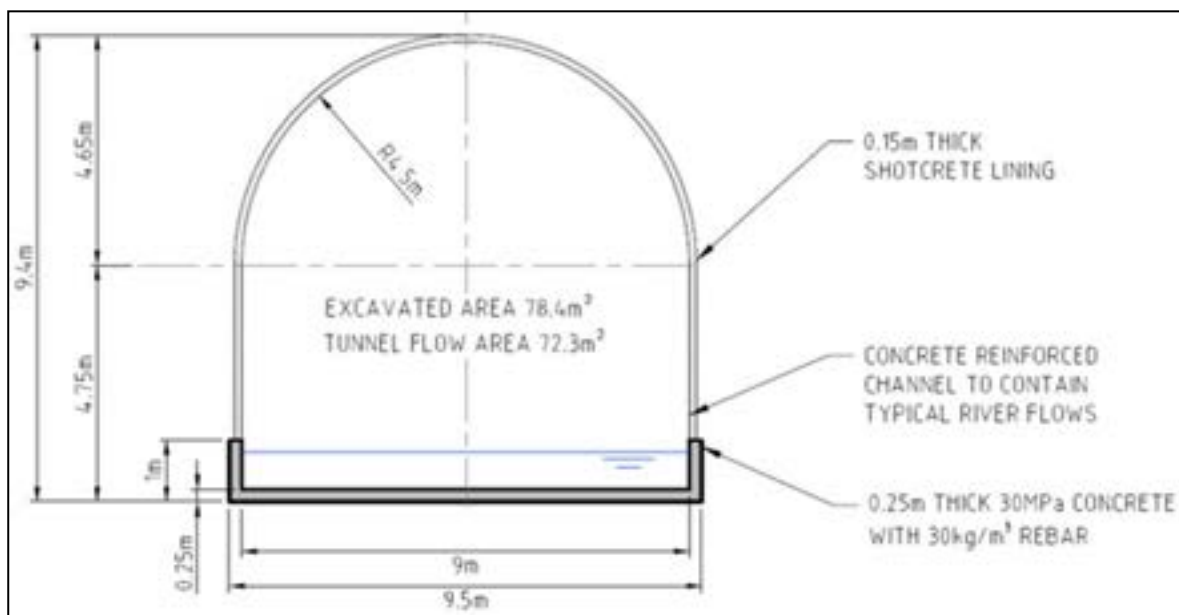


Figure 9-1: Cross-sectional design for each diversion tunnel

The support requirements for the diversion tunnel have been designed commensurate with the requirements for safety and permanence. The diversion tunnels are effectively temporary; they will be blocked and sealed once the embankment has been constructed. However, the risk profile is such that a conservative approach to ground support has been adopted in order to minimise risk of rockfall to present a safe working environment during the tunnel construction and to prevent collapse during its limited time of operation. An excavation support ratio (ESR) of 1.6 (Class C used for permanent mine openings and conveyance tunnels) was therefore used for the ground support design assessment for the diversion tunnels. The tunnel span/ ESR for the conveyance tunnels is therefore $9.5/1.6 = 5.9$.

The distribution of Q data for the diversion tunnels for weathered/ joint oxidised rock, unweathered rock and serpentinised rock is presented in Figure 9-2.

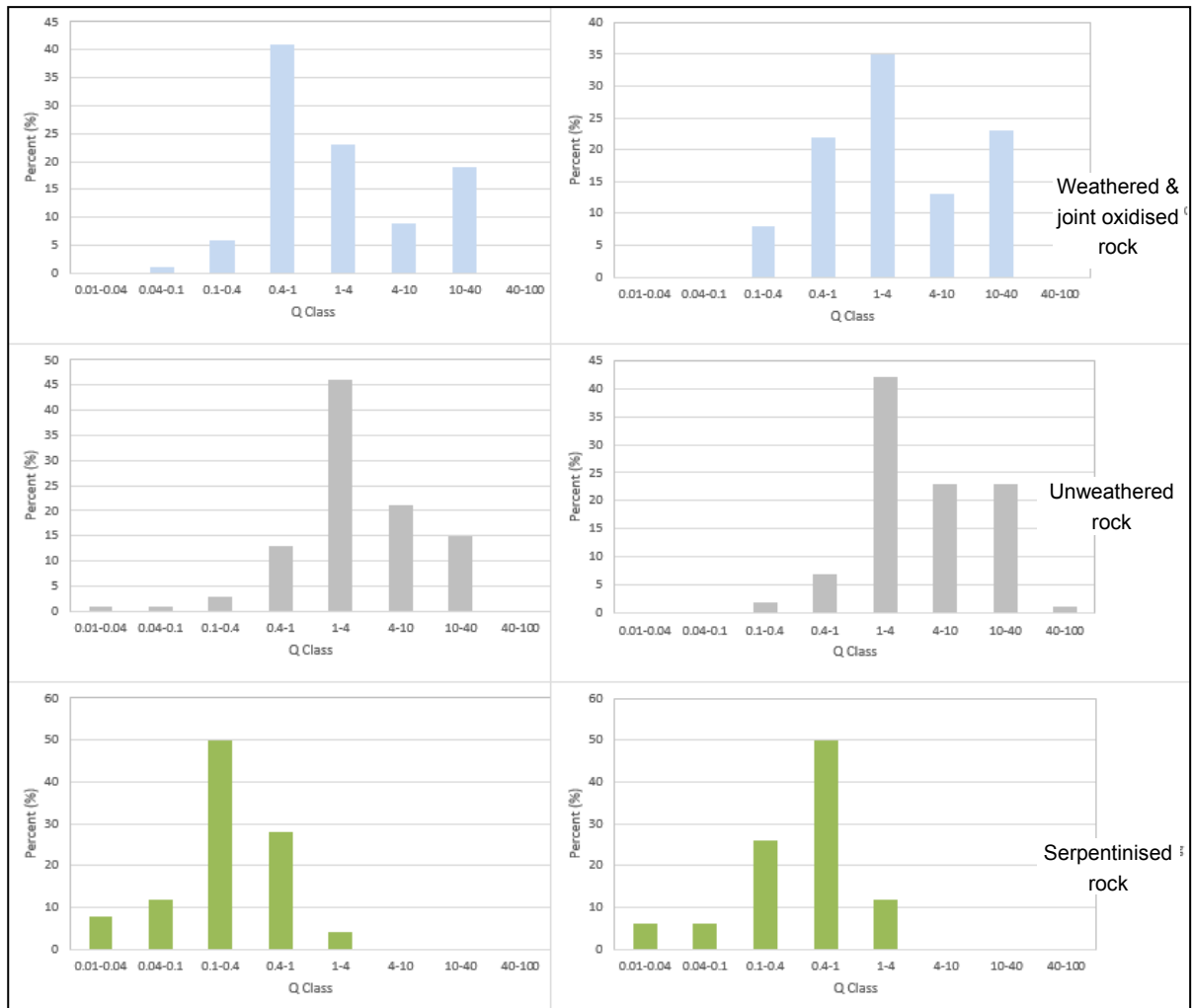


Figure 9-2: Distribution of Q data for diversion tunnels for (left) $J_w=0.33$ and (right) $J_w =0.5$

Conveyance tunnels

The conveyance tunnels have been designed with an arched roof, and final dimensions of a 7 m width and 7 m height to the top of the arch. As these dimensions are post-installation of ground support and tunnel lining, SRK have assumed initial blasted dimensions of approximately 7.5 m × 7.5 m.

It is understood that the conveyance tunnels will be concrete and/ or steel-lined. However, because the lining is likely to be installed well after tunnel excavation, and because much work will be conducted in the tunnel prior to the lining installation, the initial support requirements have been designed commensurate with the requirements for safety. An excavation support ratio (ESR) of 1.3 (Class D used for long term development – storage caverns, surge chambers, access tunnels) was therefore used for the ground support design assessment. The tunnel span/ ESR for the conveyance tunnels is therefore very similar to that for the diversion tunnels: $7.5/1.3 = 5.8$.

The distribution of Q data for the conveyance tunnels for weathered/ joint oxidised rock, unweathered rock and serpentinised rock is presented in Figure 9-3.

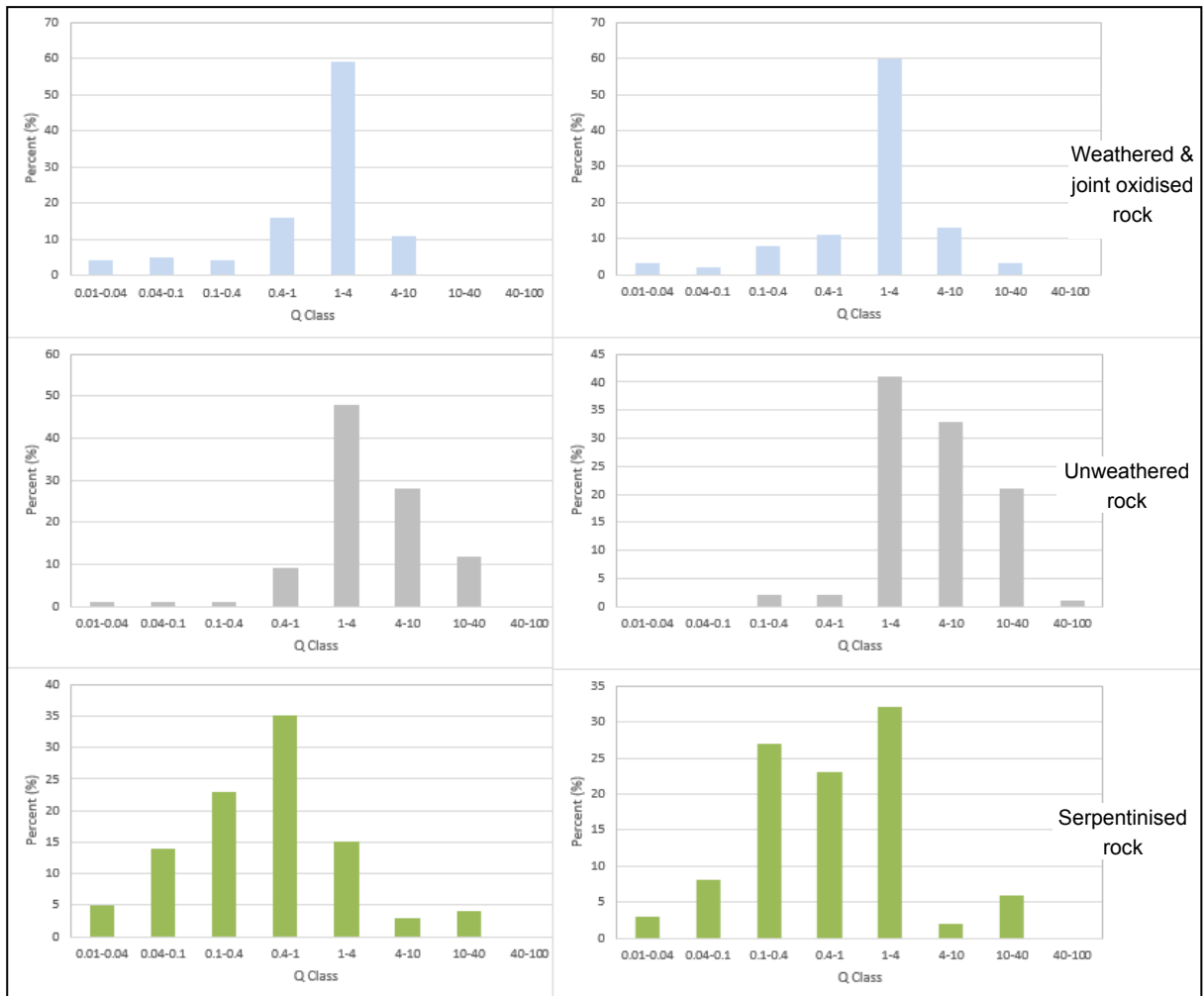


Figure 9-3: Distribution of Q data for conveyance tunnels for (left) $J_w=0.33$ and (right) $J_w=0.5$

Ground support recommendations

By assessing and comparing the distribution of Q data in Figure 9-2 and Figure 9-3, two main ranges of rock mass conditions have been identified (Figure 9-4) and therefore two types of ground support (support regimes A and B) have been identified for both the diversion and conveyance tunnels. The empirical ground support assessment has been supplemented with practical engineering experience to provide suitable preliminary recommendations for ground support design for each domain, as listed in Table 9-2, with supplementary recommendations also listed within the table.

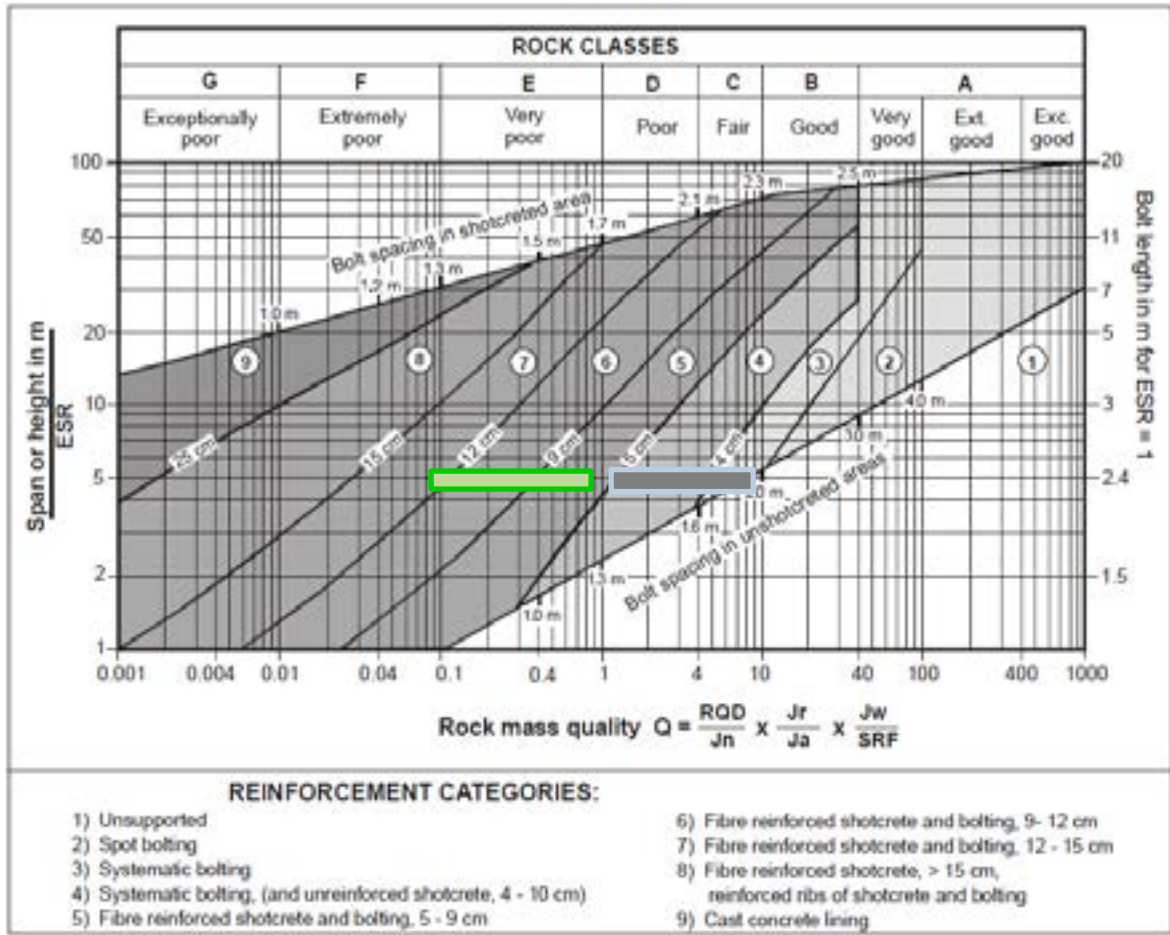


Figure 9-4: Indicative support requirements

Source: Grimstad & Barton, 1993.

Table 9-2: Preliminary empirical ground support assessment

Rockmass condition	Representative Q Index range	Recommended support
A – ‘General’ (majority of) bedrock Including slightly weathered, joint oxidised rock and unweathered rock	1–10 Fair to poor-quality rock, downgraded from good to fair-quality rock due to groundwater (Jw rating)	50 mm thick shotcrete <u>or</u> mesh on shoulders and roof Bolt length 2.4 m in walls, 3 m in roof Bolt spacing 2.0 m (ring spacing 1.5 m if mesh is used)
B – Localised poorer quality bedrock Including moderately weathered rock with significant joint infills, weaker deteriorating, serpentinised rock, and local fault/ shear zones of limited extent	0.1–1.0 (very poor rock)	120 mm thick fibrecrete lining walls and roof Bolt length 2.4 m in walls, 3 m in roof Bolt spacing 1.5 m Possible use of steel sets, lattice girders spiling and cable bolts near portals Possible use of cable bolts where large fault-controlled wedges are evident in tunnels Possible use of steel sets in zones of extremely poor-quality rock
<p>The following supplementary recommendations apply:</p> <ul style="list-style-type: none"> As it will form the final tunnel lining on the walls and roof during operation life, fibrecrete installed within the diversion tunnels should be of 150 mm thickness for all rockmass conditions. At portal entrances, spiling and/ or use of cable bolts should be considered within the brows to prevent kinematic wedge or slab failures. If poor rockmass conditions are encountered, steel sets or lattice girders may also be required. It is to be noted that relatively poor rockmass conditions have been identified in the bedrock of holes PH2 and PH3, in the vicinity of the conveyance tunnel outfalls near the powerhouse. These are interpreted to be associated with localised fault conditions. The use of cable bolts may be required if large fault-controlled wedges are evident in the tunnels, or if significant yielding zones develop in localised zones of poorer rockmass conditions (particularly in deteriorating serpentinised rock, as shown in the stress-strain plot for prediction of yielded ground around tunnels shown in the following sections). The additional use of steel sets or lattice girders may be necessary if zones of extremely poor-quality rock are encountered in fault zones. <p>It is expected that rockmass condition B (poorer ground) will be encountered along less than 10% of the tunnel lengths.</p>		

9.1.2 Tunnel spacing assessment

Numerical analyses were conducted to assess the possible interactions between the twin tunnels designed for both the diversion and conveyance tunnel systems. 2D (sectional) analyses were carried out using Rocscience *Phase2* finite element software. Four critical sections, two sections each for the diversion and conveyance tunnels, were selected for the 2D modelling by considering rockmass conditions and tunnel positions and orientations. The locations of the sections are shown in Figure 9-5.

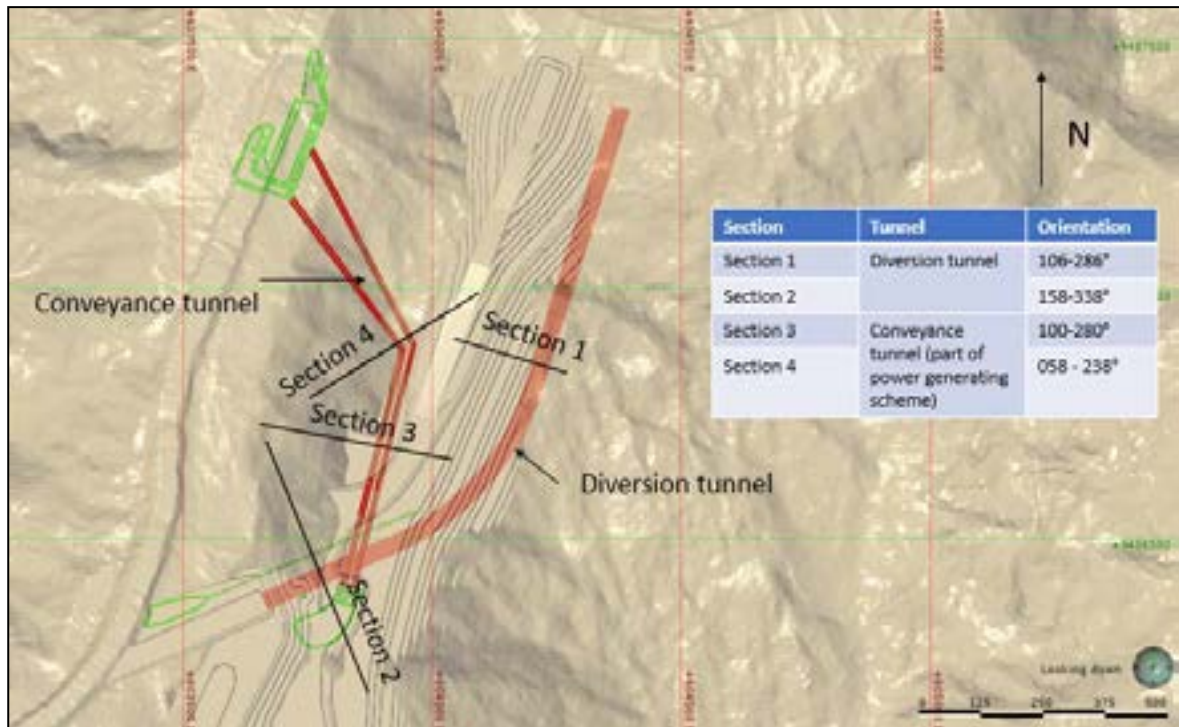


Figure 9-5: Plan view showing the locations of sections selected for Phase2 analysis

Proposed tunnel configurations and analysis sections

The cross-sectional dimensions for both the diversion and conveyance tunnels are shown in Figure 9-6. At their closest, the twin tunnels were approximately 18 m and 10.5 m apart for diversion and conveyance tunnel systems, respectively.

Analysis sections for diversion and conveyance tunnels are presented in Figure 9-7 and Figure 9-8, respectively. The diversion tunnels will be excavated before the excavation of the spillway/quarry has commenced, whereas the conveyance tunnels are expected to be excavated after or at the same time as spillway excavation. It is of note that the analyses did not consider any tunnel support, and a worst-case scenario was provided just after the tunnel excavation (i.e. before the installation of support). For the diversion tunnels, the interaction was therefore assessed before the excavation of the spillway, whereas for the conveyance tunnels, assessment was initially conducted after the spillway excavation and then before the spillway excavation as a sensitivity analysis.

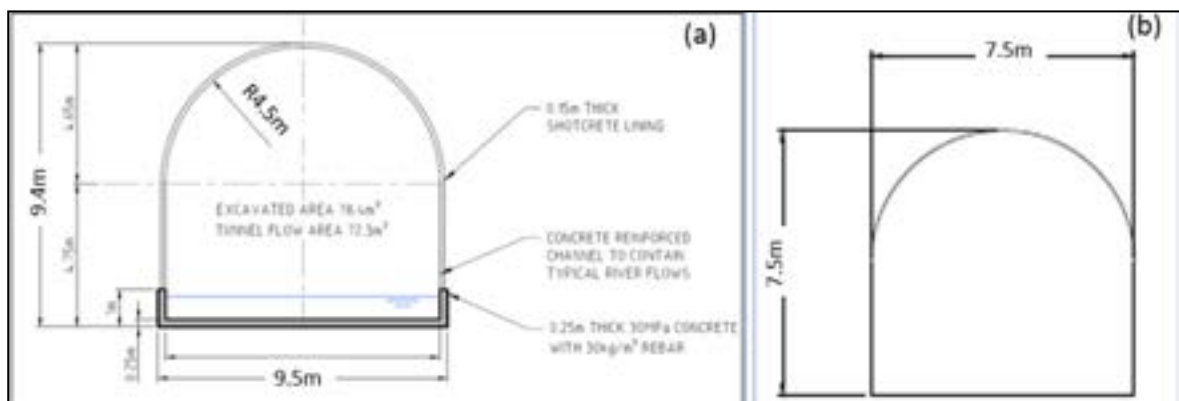


Figure 9-6: Tunnel cross-sections: a) diversion tunnel; b) conveyance tunnel

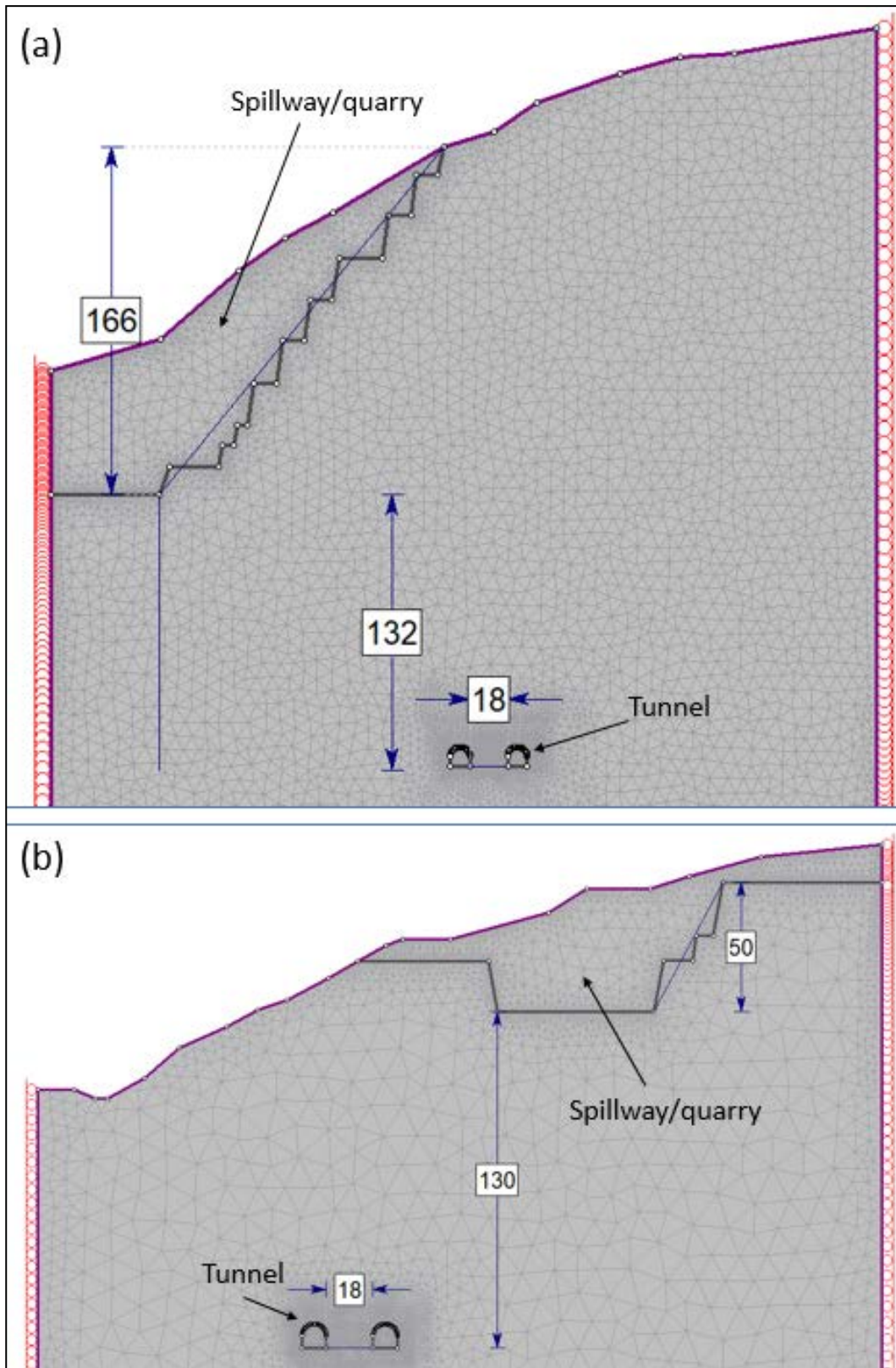


Figure 9-7: Analysis sections for diversion tunnels: a) Section 1; b) Section 2

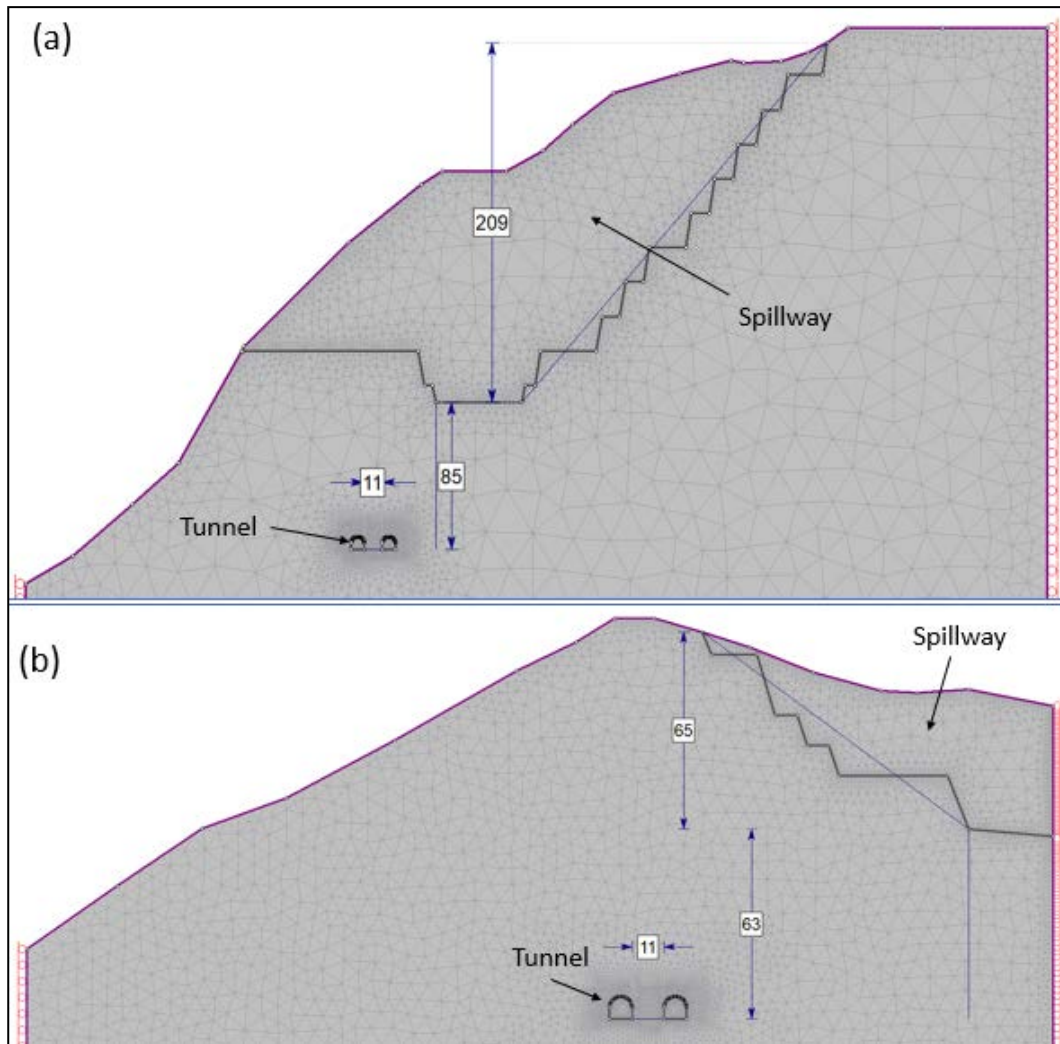


Figure 9-8: Analysis sections for conveyance tunnels: a) Section 3; b) Section 4

Material properties

The material properties used for the geotechnical materials types are listed in Table 9-3. The bedrock rockmass strength, expressed in terms of Geological Strength Index (GSI), was calculated from drill core logging information. The UCS was assessed from laboratory testing results. Average or 50th percentile values were identified, as well as ‘lower bound’ 30th percentile values.

These model analyses were based on lower bound material properties for the general bedrock as these represent the critical condition. Analyses were also conducted using alternative, weaker properties representing serpentinised dunite.

Table 9-3: Material properties used for the model analyses

Parameters	General bedrock (average values)	General bedrock (lower bound value)	Serpentinised dunite
GSI	60	55	50
UCS (MPa)	55	45	35
Poisson’s ratio	0.2	0.2	0.3
Young’s modulus (GPa)	95	82	40
<i>m_i</i>	20	20	13
Density (kN/m ³)	31	31	27

In situ stress field

Specific in situ stress measurements or studies have not been conducted at Frieda River. Therefore, the stress regime based on the work conducted at nearby OK Tedi mine was considered the most applicable for the site. The in situ stress regime used in the analyses (reported in the paper: 'Rock Stresses at Ok Tedi, Papua New Guinea', by Lee et al., 2014⁸³) is provided below (a directional illustration is shown in Figure 9-9).

$$\sigma_1 = \sim 1.4\sigma_{\text{vertical}} \text{ NNE-SSW } (\sim 030^\circ)$$

$$\sigma_2 = \sim 1.0\sigma_{\text{vertical}} \text{ Sub-vertical}$$

$$\sigma_3 = \sim 0.7\sigma_{\text{vertical}} \text{ WNW-ESE } (120^\circ)$$

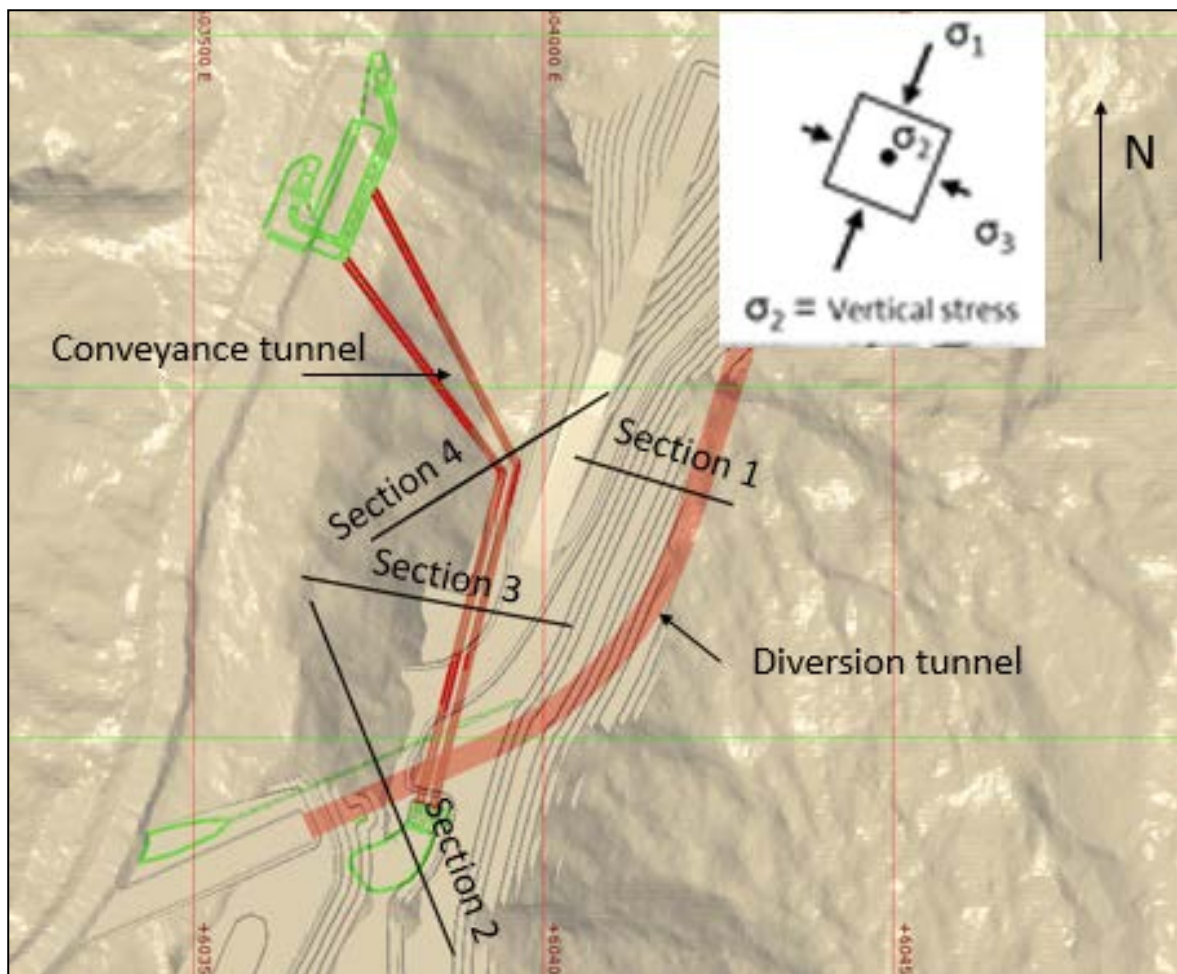


Figure 9-9: Plan view showing in situ stress regime orientation relative to tunnel alignment

As the analysis sections are two dimensional; the in-plane and out of plane stresses were calculated using stress rotation methods. The applied in-plane and out-of-plane stresses for each section are provided in Table 9-4. As a sensitivity analysis, a uniform stress regime was applied for Section 1 to understand the impact of the anisotropic stress regime.

⁸³ Lee et al, 2014. Rock Stresses at Ok Tedi, Papua New Guinea. Third Australasian Ground Control in Mining Conference (AusRock 2014), Sydney, 5-6 November 2014: 337-345.

Table 9-4: Applied in situ stress

Section	Section orientation (strike°)	In-plane stress/ vertical stress	Out of plane stress/ vertical stress
1	106-286	0.74	1.36
2	158-338	0.97	1.13
3	100-280	0.78	1.32
4	058-238	1.25	0.85

Analyses

The analyses were performed considering a homogeneous isotropic material under elastic and plastic conditions for comparison. *Phase²* (Version 8.0, Rocscience)⁸⁴, a 2D elastoplastic finite element stress-strain analysis software, was used for the analysis.

In the elastic analyses, Strength Factor (SF) was used to describe the potential disturbed zones within the rock mass around the tunnels, whereas in plastic analyses, yielded element plot was used for the same purpose. The SF represents the ratio of the material strength to the induced stress at a given point. Values lower than 1 indicate regions of probable instability/ disturbance. Dry groundwater conditions were considered in the analyses, as the tunnels would largely drain the rock mass in the immediate vicinity (i.e. in the rockmass under consideration).

Analyses were conducted for both lower bound general dunite bedrock properties and weaker serpentinitised dunite properties under appropriate in-plane and out-of-plane stress conditions for each section.

The analyses have not considered the influence of ground support to manage any deformation that may occur, or the effect of potential faults and proximity to tunnel portals.

Analysis results

The results plots are presented from Figure 9-10 through Figure 9-13 for Sections 1 through 4, respectively.

In the elastic analyses plots, red and dark orange zones indicate the region where strength factor is less than 1 (yielded zones – possible instability). In plastic analyses plots, the non-blue region indicates the yielded zones.

In general, the plastic analyses indicate zones of disturbance of somewhat larger extent compared with the elastic analyses. As expected, the tunnels within weaker serpentinitised dunite material show disturbed/ damaged zones of larger extent in comparison with general unaltered dunite bedrock.

Based on the analysis results of all the sections and methods, the twin tunnels in the divergence and conveyance tunnel systems are not expected to interact with each other at the current design spacings of 18 m and 10.5 m. The analyses indicate that the diversion tunnels could be spaced at a minimum of around 14 m, and the conveyance tunnels could be spaced at a minimum of around 8 m.

⁸⁴ Rocscience Inc., 2017. *Phase² 8.0 – 2D Finite Element Slope Stability Analysis Programme*. www.rocscience.com, Toronto, Ontario, Canada.

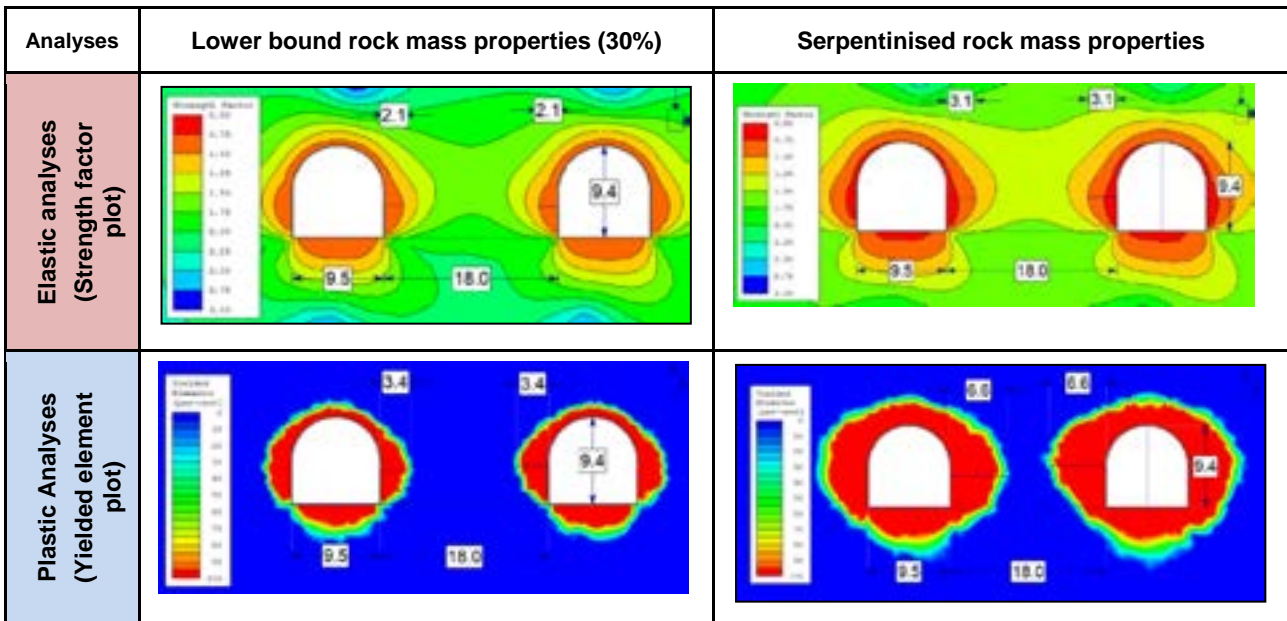


Figure 9-10: Results plots for Section 1

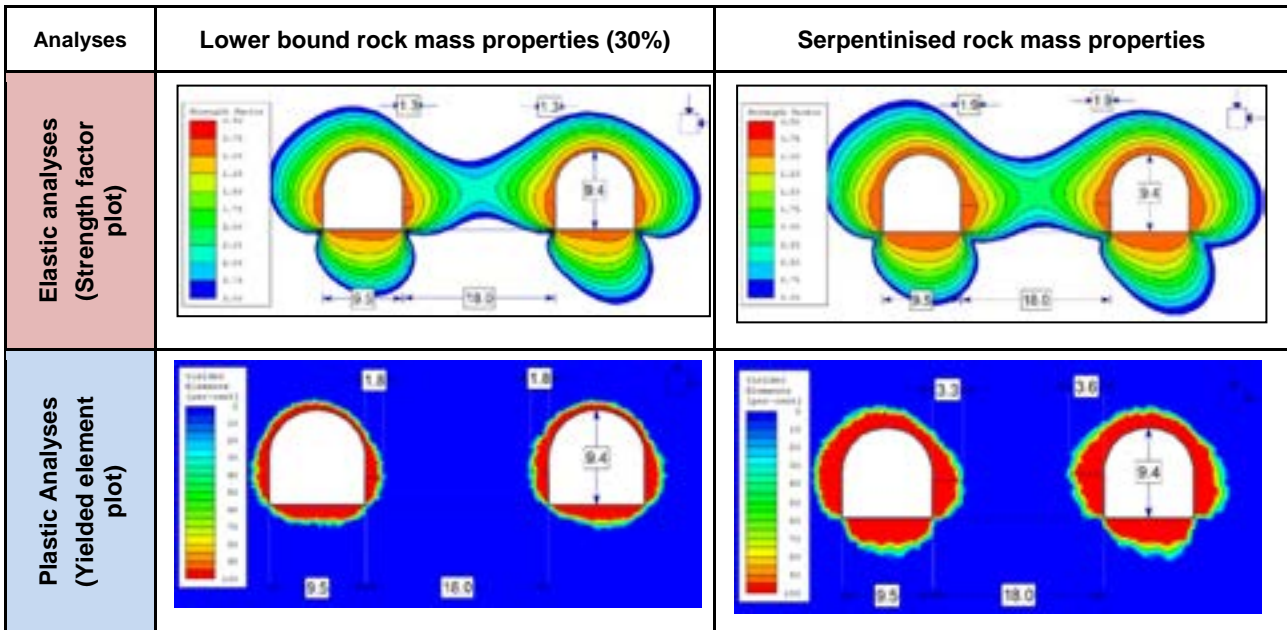


Figure 9-11: Results plots for Section 2

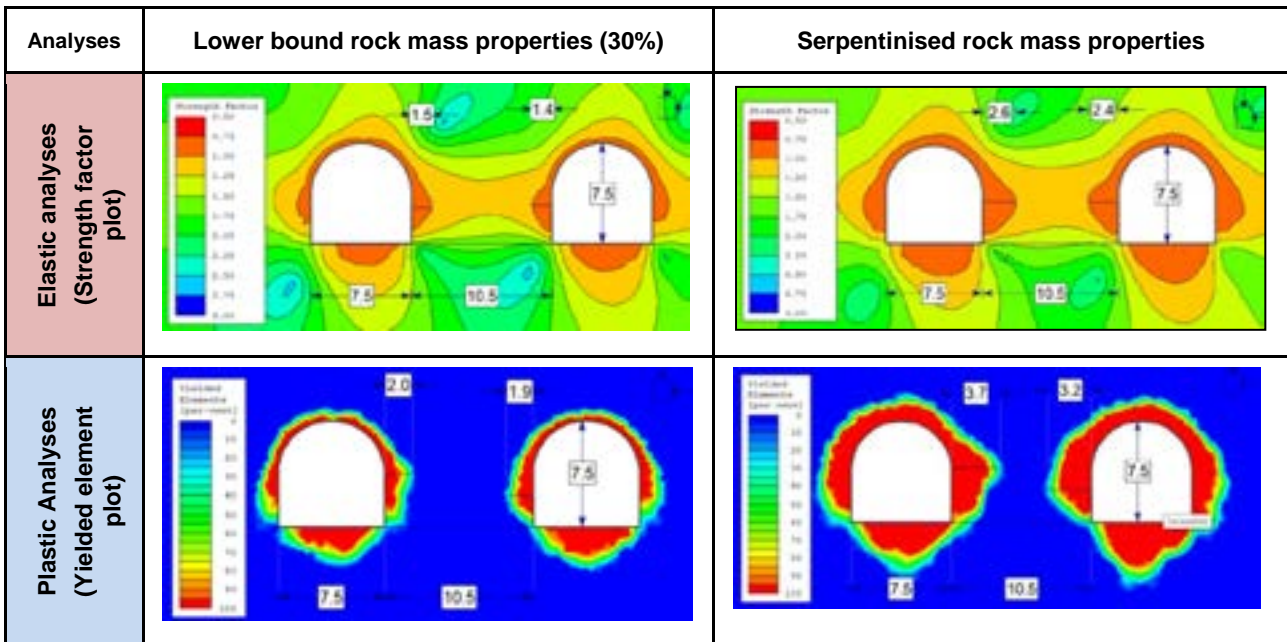


Figure 9-12: Results plots for Section 3 (tunnel excavation after spillway cut)

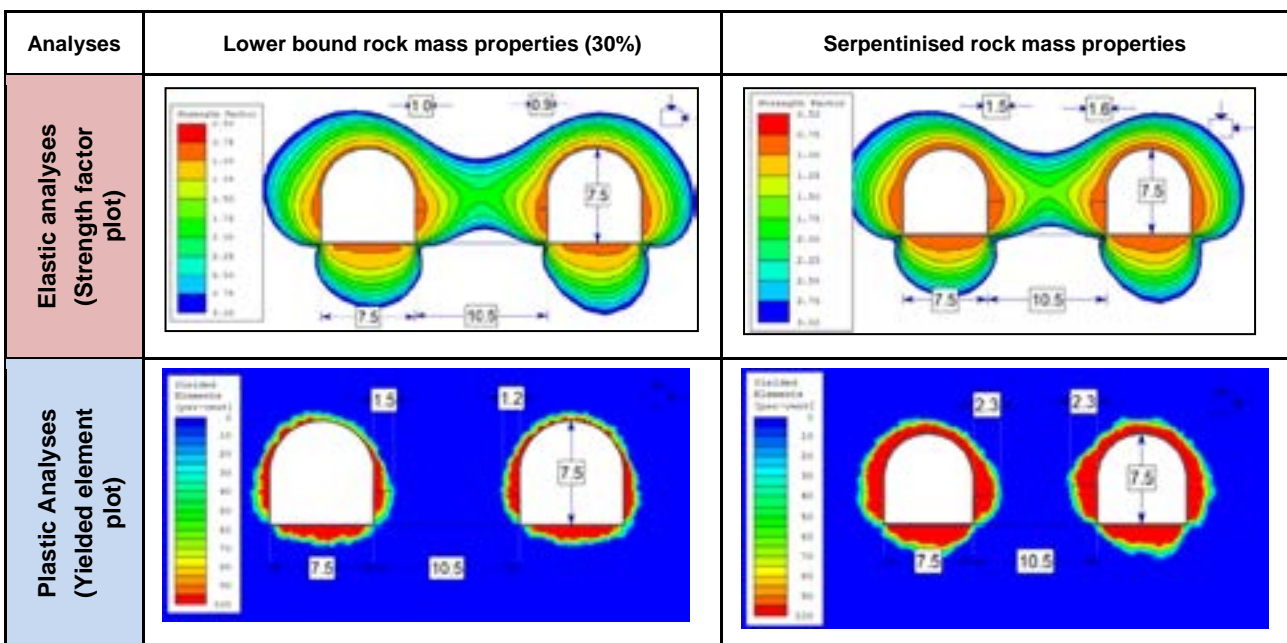


Figure 9-13: Results plots for Section 4 (tunnel excavation after spillway cut)

Sensitivity analyses

Sensitivity analyses were carried out for the following cases:

Uniform gravitational stress regime for Section 1 and Section 3, with lower bound properties

The results plots are shown in Figure 9-14 and Figure 9-15 for Section 1 and Section 3 respectively. For Section 1, the disturbed zone is slightly reduced when a uniform stress field is considered, whereas for Section 3, it is increased slightly. In general, the impact of the considered in situ stress fields on the tunnel interaction is considered minimal.

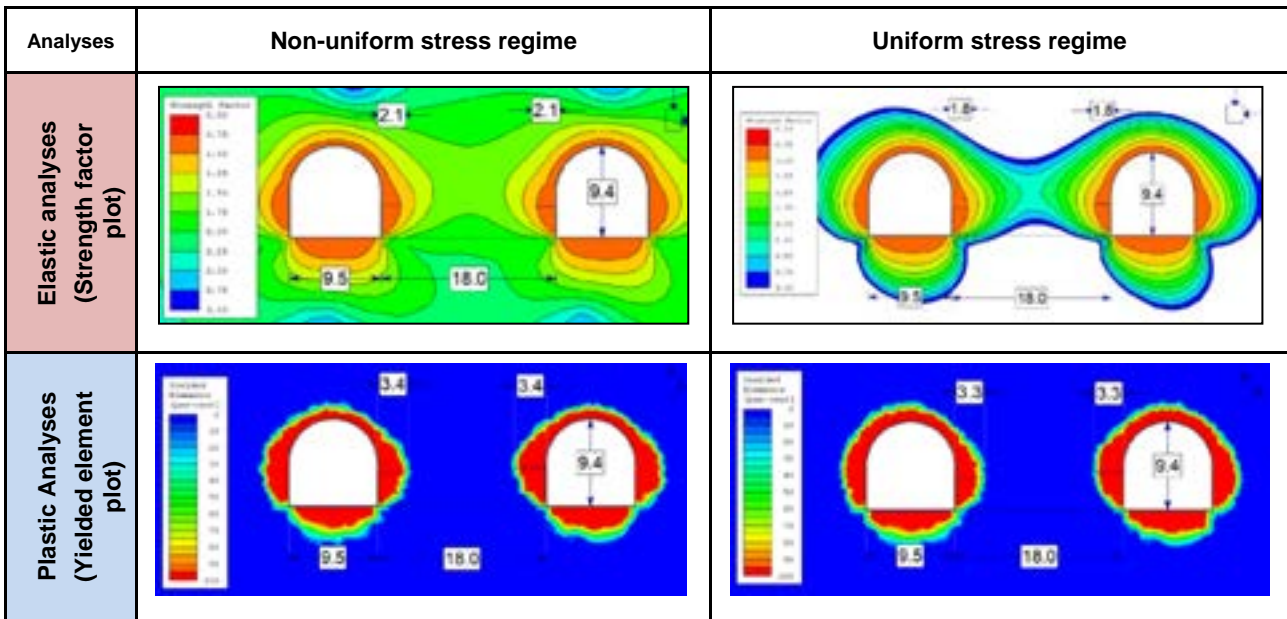


Figure 9-14: Results plots for Section 1 (uniform vs non-uniform stress for lower bound general rockmass properties – diversion tunnels)

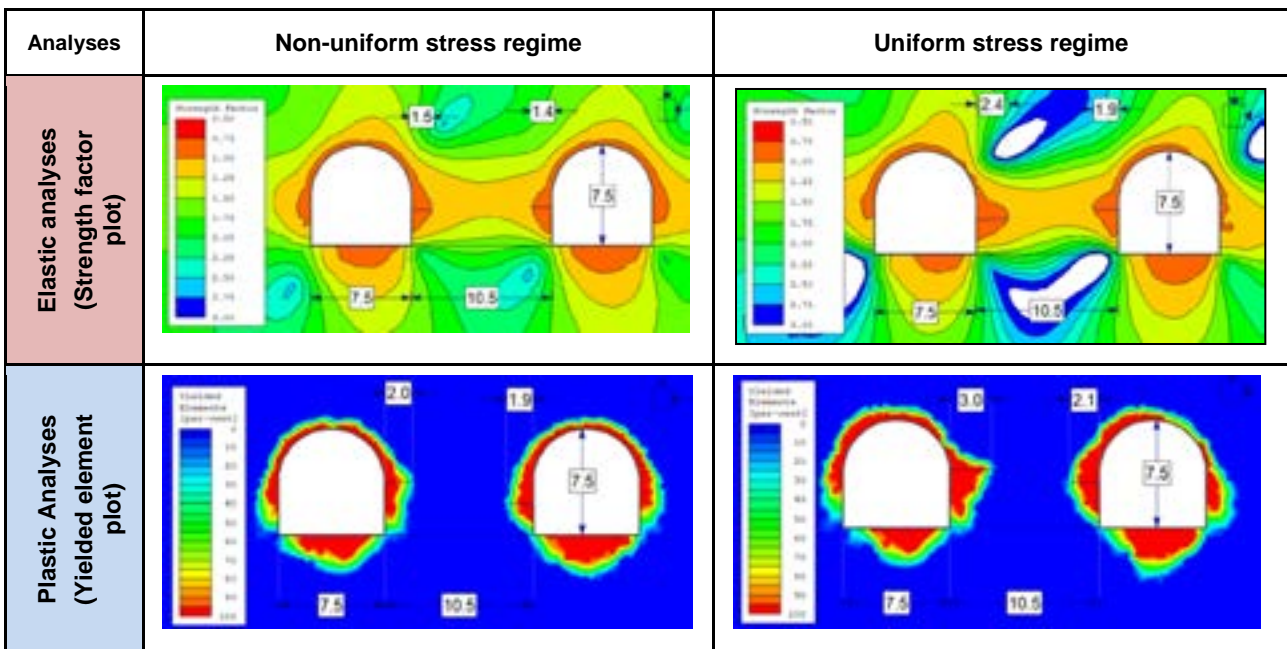


Figure 9-15: Results plots for Section 3 (uniform vs non-uniform stress for lower bound general rockmass properties – conveyance tunnels)

Pseudo static seismic loading of 0.2g for Section 1

Based on the analysis results (Figure 9-16), the effect of seismic loading on the tunnel interaction is considered to be insignificant.

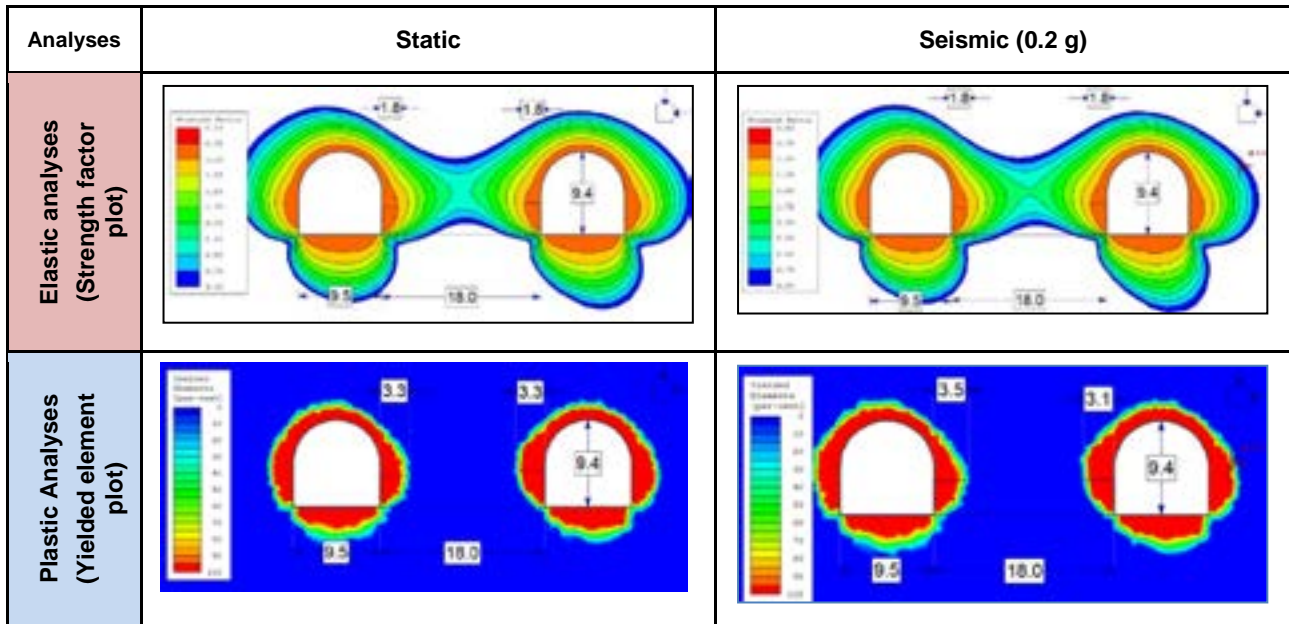


Figure 9-16: Results plots for Section 1 (static vs seismic conditions for lower bound general rockmass properties – diversion tunnels)

Tunnel excavation before spillway excavation for Section 3 and 4

The results plots are shown in Figure 9-17 and Figure 9-18 for Section 3 and 4, respectively. In comparing Figure 9-17 with Figure 9-12, the damaged region is significantly increased for Section 3 if the conveyance tunnel is excavated before the spillway. For poorer, serpentinised rock, the plastic analysis indicates that the conveyance tunnels at a current spacing of 10.5 m in Section 3 may be expected to interact each other (Figure 9-17). This represents a most conservative and least likely case, however. For Section 4, the impact is indicated to be insignificant (comparing Figure 9-13 with Figure 9-18).

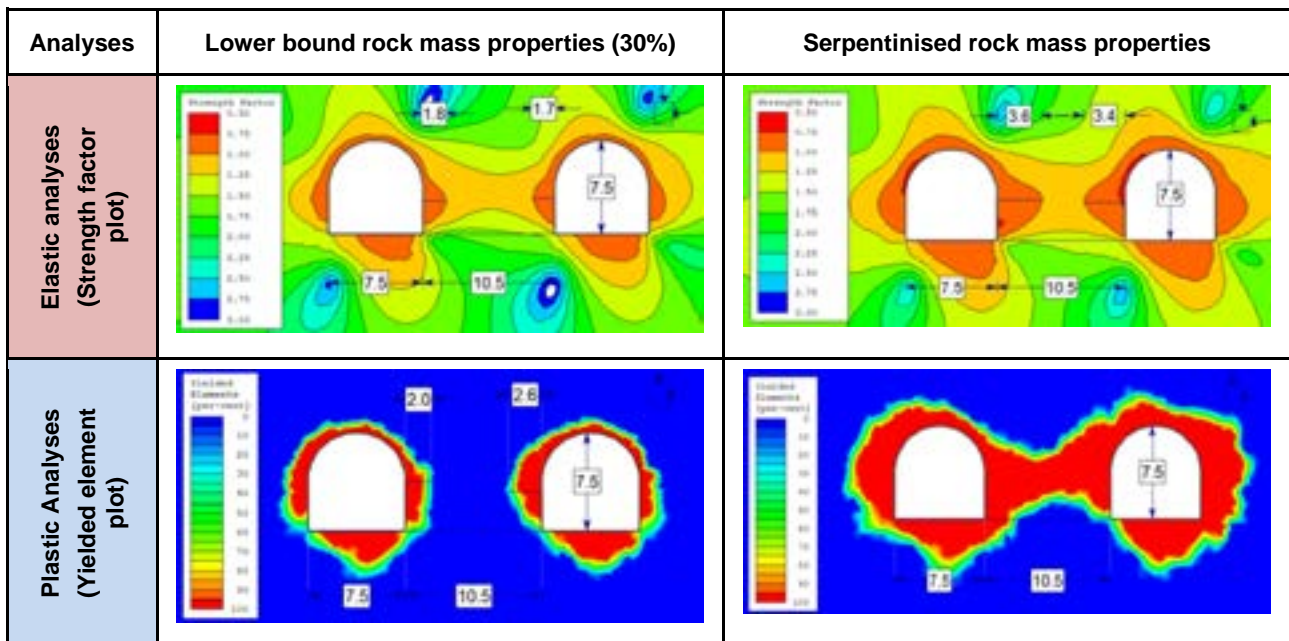


Figure 9-17: Results plots for Section 3 (tunnel excavation before spillway cut – diversion tunnels)

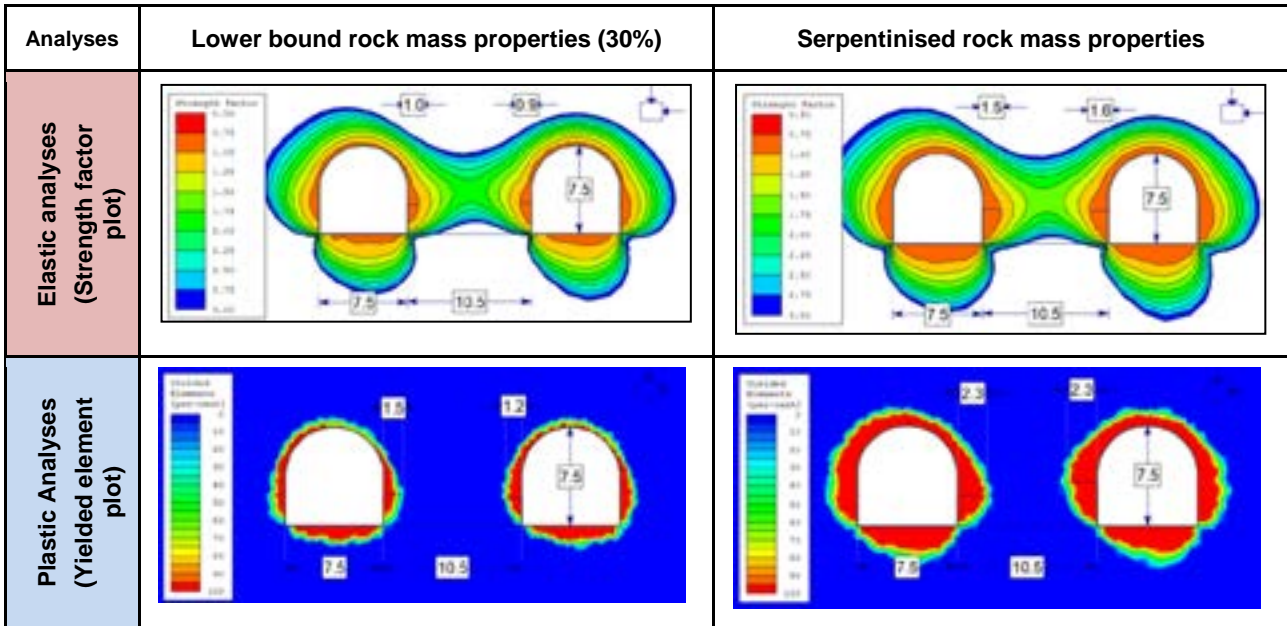


Figure 9-18: Results plots for Section 4 (tunnel excavation before spillway cut)

10 Water Management Structures

The FRHEP experiences significant streamflow and extensive water management works will be required. Management of the large runoff volumes require a robust system to assure stability of the FRHEP while limiting residual impact and allowing for closure of the facility. In addition, safety and access needs to be assured within design storm parameters to protect personnel constructing the embankment cut-off system, foundation stripping, and plinth development.

Water management structures have been designed to manage the upstream catchment runoff, precipitation falling on the facility, plus any tailings supernatant water, throughout the life of the facility including:

- Construction: A diversion dam, main cofferdam, downstream cofferdam, two diversion tunnels, a residual flow tunnel and associated power shaft
- Operation: Two conveyance tunnels with integrated lower and upper intakes and surge chambers, and a right abutment spillway
- Closure: Right abutment spillway.

The sizing assessment of the FRHEP water management structures focused on key project components that either present a significant risk to the project, or which may have significant cost implications. Early identification of preferred options minimises significant changes to the design during the future project phases.

10.1 Diversion system sizing

Water diversion infrastructure is required to create a dry construction zone for the main embankment and associated works close to the embankment. The diversion works consist of two diversion tunnels with associated inlet and outlet structures, an upstream diversion and cofferdam, and a downstream cofferdam. The layout of the diversion system is shown on SRK Drawings PNA009-0070, PNA009-0072, PNA009-0120, PNA009-0122 and PNA009-0124.

The first stage of diversion works is the diversion tunnel, with construction of the diversion dam once the diversion tunnel installation is complete. River flow will be routed through the tunnel system once in operation. After diversion of the river and construction of the diversion dam, construction of the components of the upstream cofferdam located within the continually flowing course of the river can commence.

During filling of the reservoir, residual flow will be reticulated through the diversion tunnels via a separate intake to maintain minimum residual flows.

No consideration was given during this capacity assessment for any residual or emergency discharge into the tunnel(s) during early filling (i.e. via the smaller third adit). Depending on the operating strategy, the tunnels may be able to be used to discharge flows at a higher head than the maximum design head presented in this memorandum. Once the operating strategy is confirmed, the tunnel hydraulics will be assessed for the full range of operating levels. SRK does not expect that this assessment will have any impact on the sizing of the tunnels; however, if the maximum design velocity increases significantly, additional lining and/ or dissipation measures may be required.

The tunnel inlet layout is shown on SRK Drawing PNA009-0122. The inlet inverts are located approximately 5 m above river level at RL 55 m. The inlets are located higher than river level to create a 0.45% tunnel grade, which increases the tunnel free flow discharge capacity such that the tunnels will operate partially full under the range of typical flows, and will only become submerged under relatively high flow conditions (~RL 70 m).

The location of the inlet inverts and size of boxcuts will determine the location of benches at higher elevations and requires investigation as part of further studies. Relocation of the inlet towards the river would result in a smaller boxcut, and would allow quicker access to the portal and limit rock stockpile requirements.

10.1.1 Inputs and assumptions

The following inputs and assumptions are relevant to the diversion sizing:

- Cofferdam design flood – 1 in 100 annual exceedance probability (AEP), 24-hour storm
- Shotcrete protection maximum velocity – 15–20 m/s
- Design flood hydrographs for the 1 in 100 AEP, 6-hour – 24-hour duration storms as sourced from the Hydrology Study (Section 4)
- Tailwater curve at the outlet of the diversion tunnels was also sourced from the Hydrology Study (Figure 10-1)
- Reservoir storage curve (Figure 10-2).

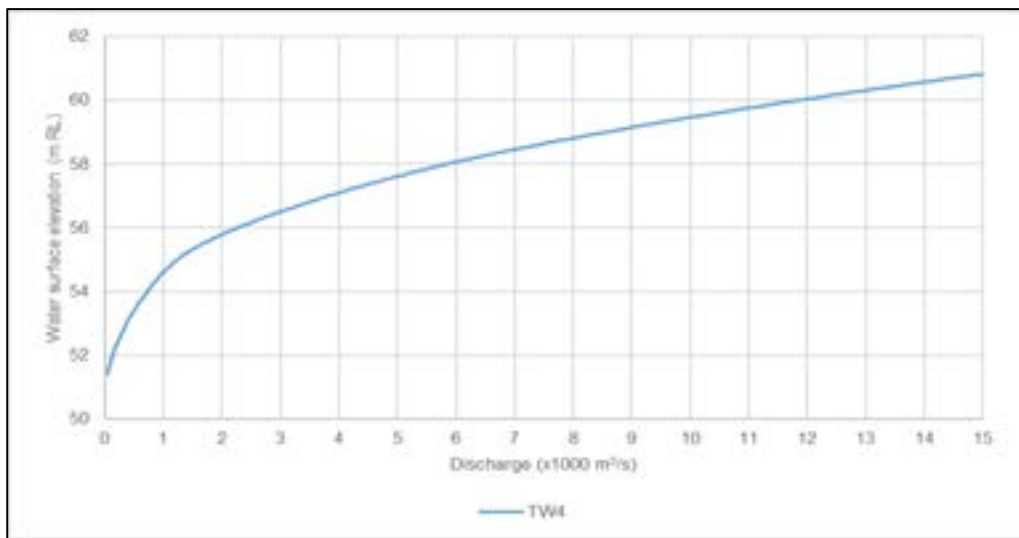


Figure 10-1: Diversion tunnel tailwater curve

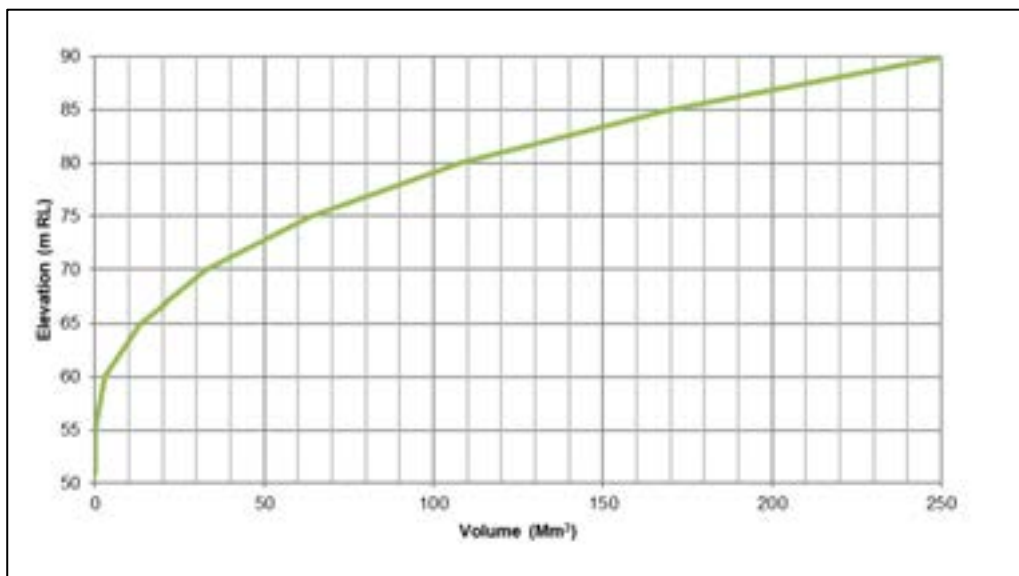


Figure 10-2: Reservoir storage curve for the diversion tunnel sizing

10.1.2 Tunnel size

Several combinations of tunnel size, inlet and outlet level, and lining options were assessed to determine the most optimal trade-off between tunnel size and cofferdam height. Flood routing for each scenario was completed using HEC-HMS 4.2.1 software.

A preferred tunnel configuration involving two 9 × 9 m (9.5 × 9.4 m excavated), 'D'-shaped tunnels, with shotcrete hanging walls and grades of 0.45% (inlet invert RL 56 m and outlet RL 49 m) was selected. A typical cross-section of the selected tunnel size is shown in Figure 10-3. The rating curve for a single tunnel has been estimated, as shown in Figure 10-4. This assumes entrance losses of $K_e = 0.2$, and tunnel lining roughness of $e_{\text{shotcrete}} = 100 \text{ mm}$ and $e_{\text{concrete}} = 2 \text{ mm}$.

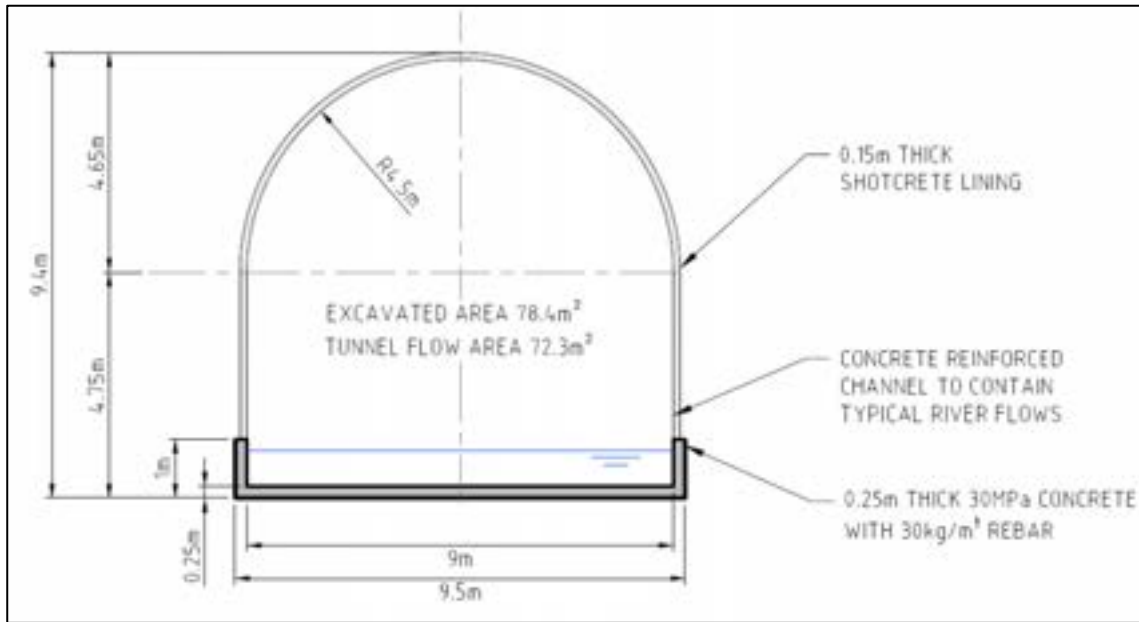


Figure 10-3: Typical diversion tunnel cross-section

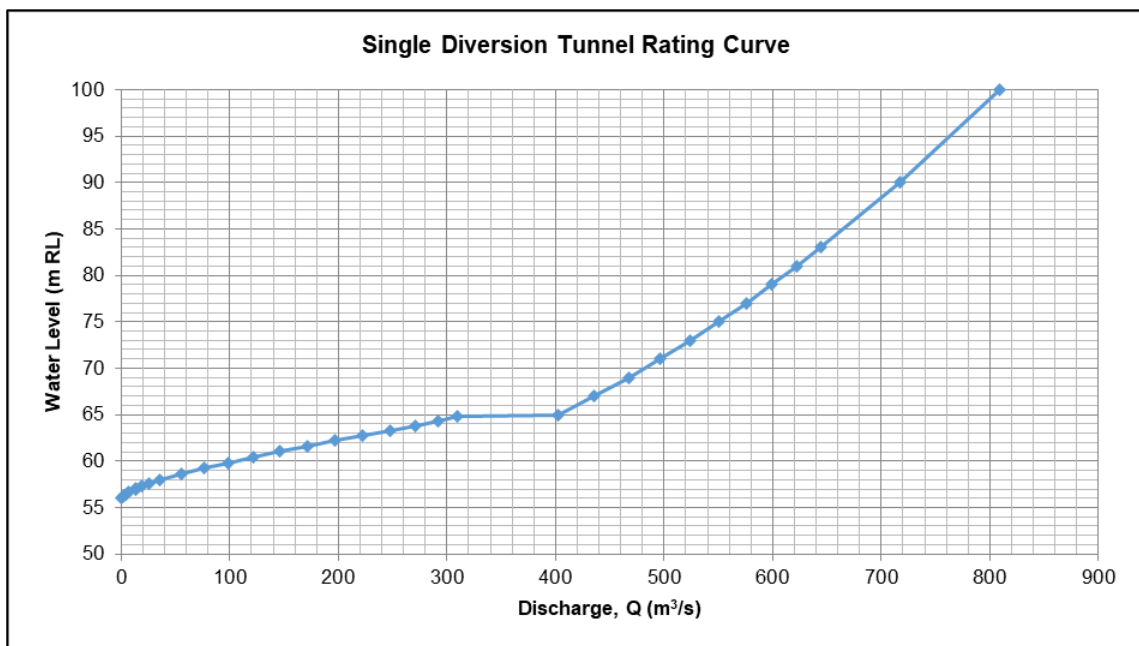


Figure 10-4: Single diversion tunnel rating curve

10.1.3 Tunnel flow operation

During average flows of 220 m³/s, the tunnels will be partially full – discharges in each tunnel will be in the order of 113 m³/s, with a water level of RL 60.2 m (i.e. ~4 m deep), and velocities of approximately 4 m/s. Daily inflows typically range between 100 m³/s and 600 m³/s, i.e. 50–300 m³/s per tunnel. Over the typical range, the tunnels will operate in one flow regime (partially full), and will only become submerged under relatively high flow conditions.

The tunnels will operate under increasingly full flow conditions as the upstream flow increases. As the tailwater level (TWL) will be low (<RL 55.1 m) across the full operating range of the tunnels and the outlet will always be unsubmerged, the headwater level (HWL) will control the flow through the tunnels.

The transition from partial flow to full flow will occur at a HWL of approximately RL 64 m. This transition is generally associated with air being taken in at the upstream end, and either travelling along the tunnel under open channel conditions or as pockets, or remaining in a single location of pockets to be later dragged out at the higher discharges. The tunnel construction (reinforced with external shotcrete, anchors/ rock bolts and concrete sections) is assumed to handle any transient loading due to air pockets, as tunnel flows are likely to be of low magnitude with flow velocities estimated to be less than 10 m/s through the tunnel. Air intake structures/pipes at the intake inlets could eliminate the formation of air pockets within the tunnels.

At a HWL of approximately RL 67 m to RL 69 m, i.e. 1.2–1.5 times the tunnel diameter, the intake of air is expected to occur only through vortices at the entrance, as the tunnels will be operating at close to full flow conditions at the inlet.

The estimated flow velocities and TWLs for the design range of HWLs is shown in Figure 10-5. It should be noted that the velocities shown are at the tunnel inlet. Outlet velocities will be slightly higher, but are predicted to remain below 9 m/s. The tunnels will operate at full flow conditions in the higher HWLs. The expected flow conditions are summarised as follows:

- HWL RL 65 m, TWL RL 54.2 m – tunnel flowing partially full throughout, V_{inlet} 5.6 m/s, V_{outlet} 7.5 m/s
- HWL RL 70 m, TWL RL 54.5 m – tunnel will flow full for approximately 45% of the length of the tunnel from the inlet, and partially full for the remainder of the downstream length, V_{inlet} 6.7 m/s, V_{outlet} 8 m/s
- HWL RL 80 m, TWL RL 54.5 m – tunnel will flow full for approximately 90% of the length of the tunnel from the inlet, and partially full for the remainder of the downstream length, V_{inlet} 8.4 m/s, V_{outlet} 9 m/s.

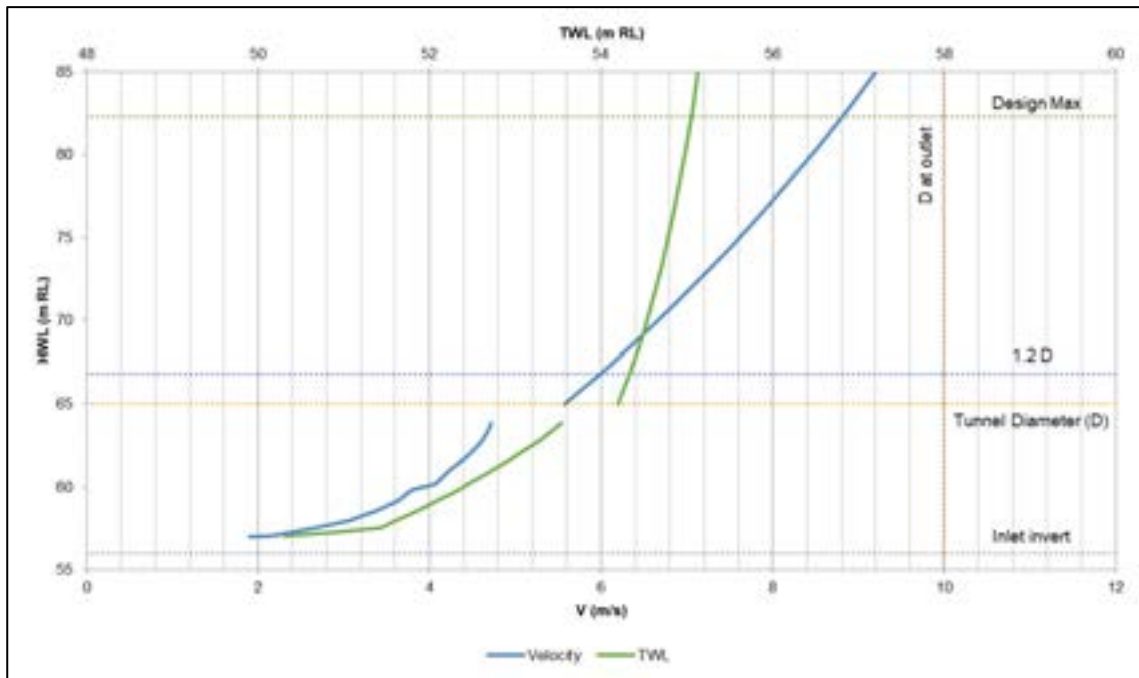


Figure 10-5: Tunnel flow conditions

10.1.4 Flood routing

The inflow flood hydrographs for the return interval of 6-hour to 60-day, 1 in 100 AEP flood events were used as a basis for routing flows through the diversion tunnels to estimate the maximum resultant water levels at the cofferdam. The initial water level was assumed to be RL 60.2 m, i.e. the water level at the average flow of 220 m³/s.

The results of the flood routing are summarised in Table 10-1. The highest maximum water level for the 1 in 100 AEP design flood is the 24-hour event, calculated to be RL 82.3 m. The 24-hour event therefore represents the Critical Storm Event.

Detailed results of the 24-hour, 1 in 100 AEP flood event routing is shown in Figure 10-6. During this flood event, water will flow through the tunnels at full capacity with peak discharges for the routed peak flow in each tunnel in the order of 635 m³/s (~1,270 m³/s through both tunnels) and maximum velocities of approximately 8.8 m/s. These velocities are well below the maximum allowable velocity for shotcrete of approximately 15–20 m/s.

Table 10-1: Diversion flood routing results

Duration (1 in 100 AEP)	Peak inflow (m ³ /s)	Peak outflow (m ³ /s)	Maximum water level (RL m)
6 hours	4,840	1,170	77.9
12 hours	6,380	1,260	81.6
24 hours	7,640	1,270	82.3
48 hours	5,490	1,230	80.4
3 days	5,070	1,220	79.7
5 days	3,760	1,240	80.9
10 days	5,080	1,240	80.3
30 days	4,480	1,210	79.4
60 days	3,950	1,170	77.7

Note: Grey shade represents the highest maximum water level, i.e. the critical storm event.

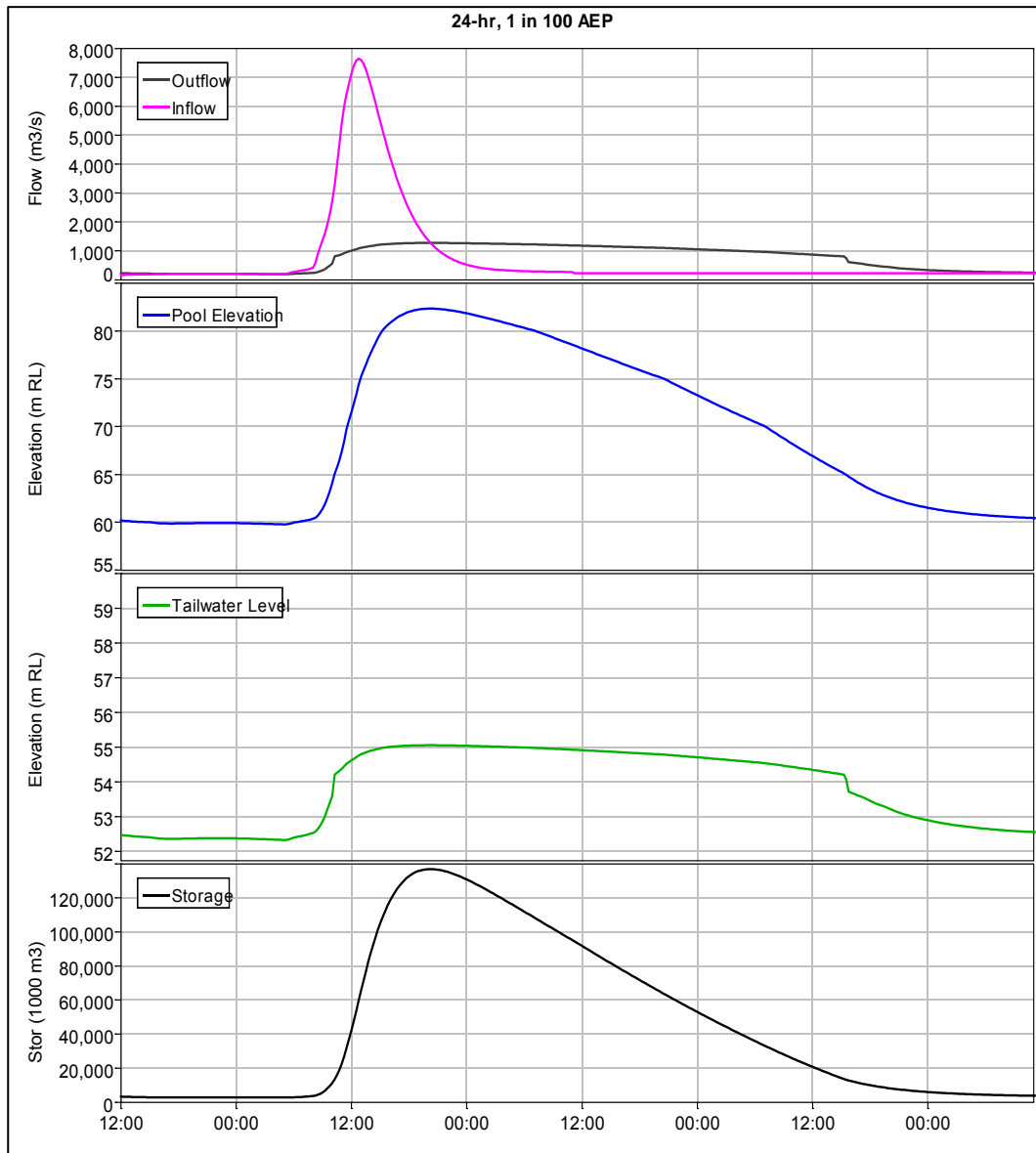


Figure 10-6: 24-hour, 1 in 100 AEP flood routing

10.1.5 Long-term flow routing

One year of historical flow data from the flow meter GS105450 was used to perform long-term deterministic routing to develop an idea of the range of typical operating levels during the diversion period. Flow data from August 2012–2013 were used, as they represent the highest average annual flow over the 12-month (complete) record. Six relatively large events with peak flows larger than 1,500 m³/s occurred over this period. The flows recorded between August 2012 and 2013 were routed through the diversion system and the results of the routing are shown in Figure 10-7. The water storage elevation ranges from a minimum of RL 57.9 m to a maximum of RL 70.1 m, with an average of RL 60.9 m. It should be noted that the operating levels in Figure 10-7 are significantly lower than that of the design flood, which is expected given that the design floods are conservative.

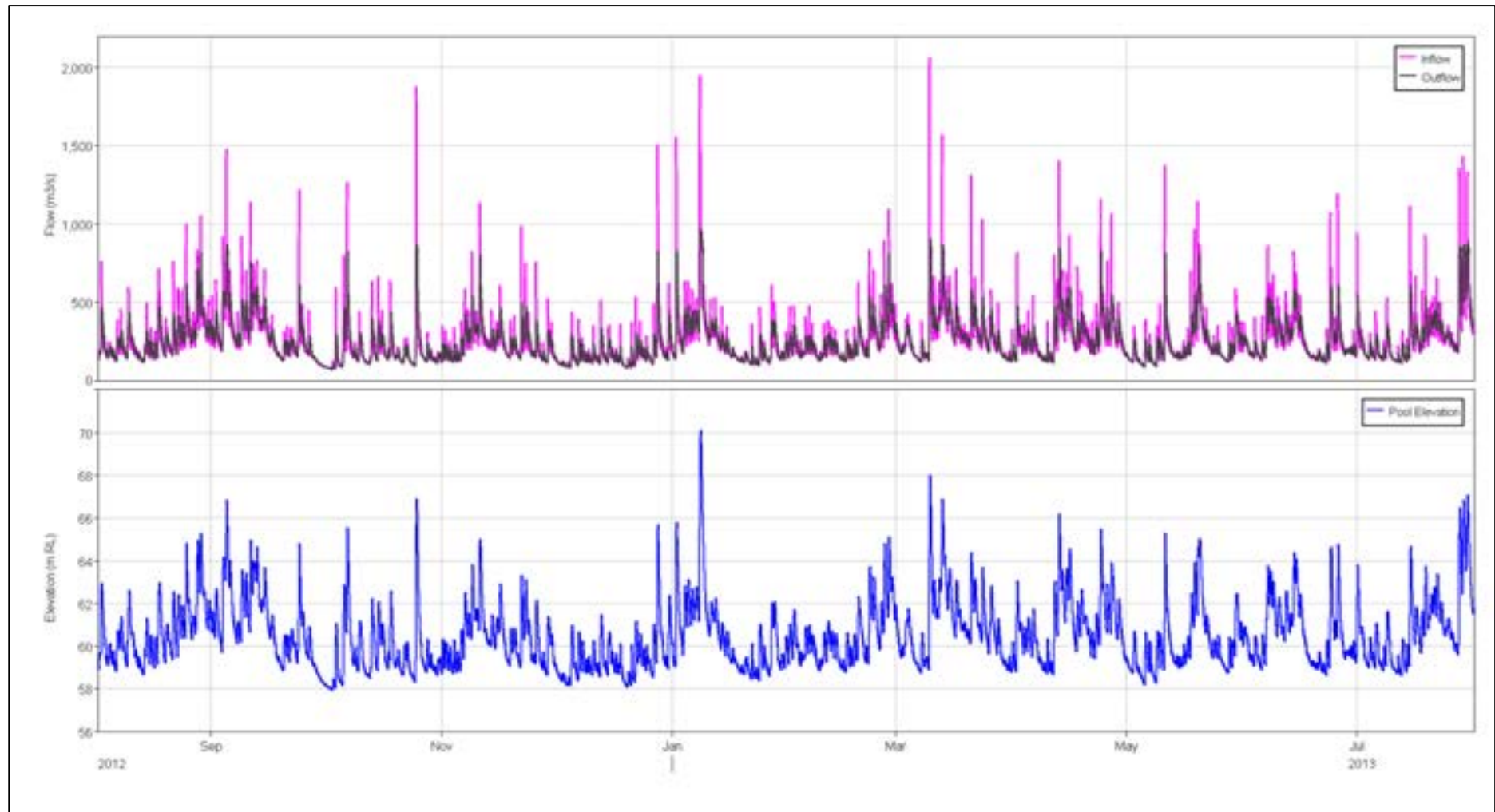


Figure 10-7: Long term flood routing

10.1.6 Upstream cofferdam

As the maximum water level of the critical 1 in 100 AEP design flood is RL 82.3 m (Table 10-1), a cofferdam crest level of RL 83 m, including a 0.7 m freeboard allowance, has been selected.

10.1.7 Downstream cofferdam

The maximum tailwater level during 1 in 100 AEP design flood is RL 55.1 m. As such, a cofferdam crest level of RL 55.5 m, including a 0.4 m freeboard allowance, has been selected.

10.1.8 Diversion dam

The diversion dam will be constructed to the level of the major bench in the river bank, with a corresponding crest level of approximately RL 74.5 m. With a freeboard allowance of 0.5 m, the diversion dam provides approximately 57.5 Mm³ of storage, and the maximum discharge capacity of the two tunnels in combination is 1,090 m³/s.

While there is no specific storm event design criterion for the diversion dam sizing, a high-level check of the capacity of the diversion dam was undertaken by routing the largest flood on record at GS105450 (February 2009) through the diversion system (Figure 10-8). The maximum water level in the diversion dam that would have been reached during the February 2009 event is RL 72.7 m, which is 1.8 m lower than the proposed crest of the diversion dam.

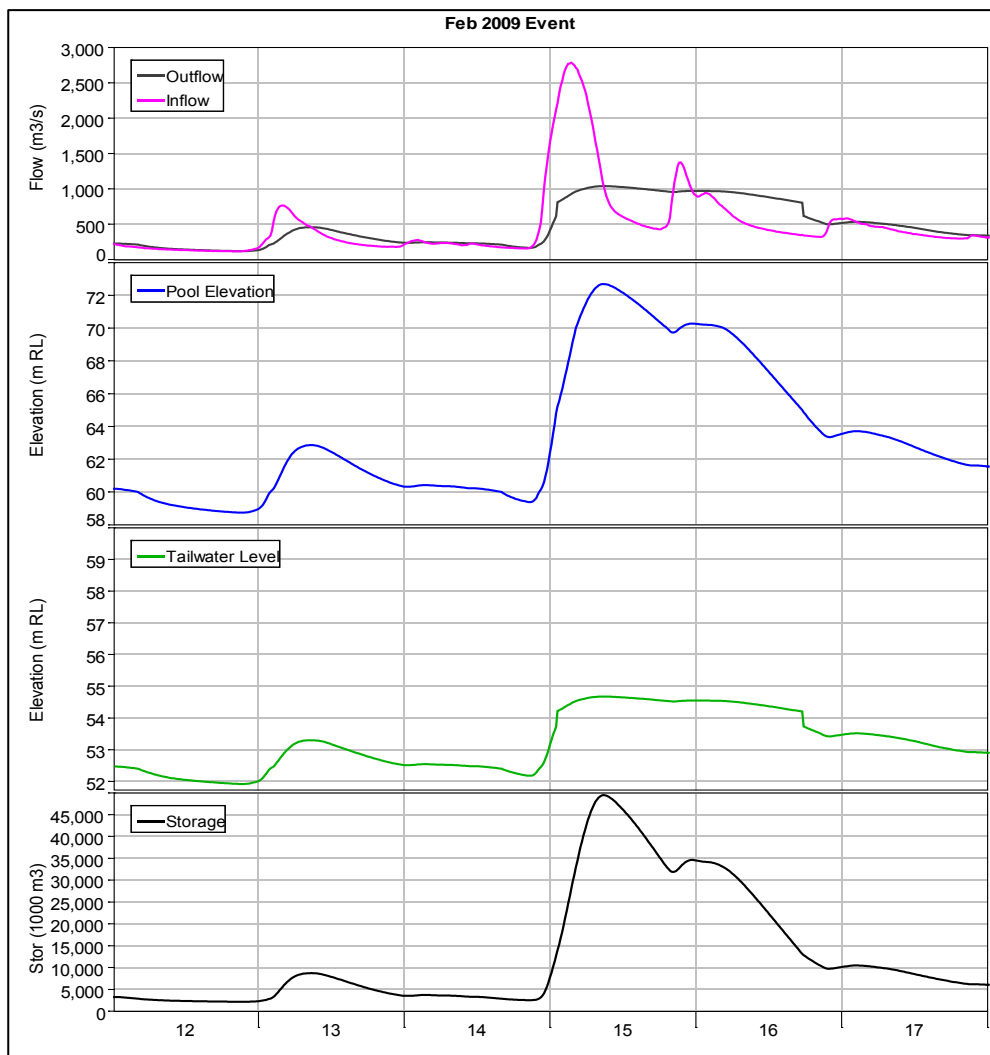


Figure 10-8: February 2009 flood routing through diversion

10.1.9 Diversion tunnel inlets and outlets

The FRHEP diversion tunnel requires robust hydraulic structures, capable of ensuring the smooth transition of entering flows and minimal disturbance to the foundation material at the tunnel outlet. The inlet and outlet hydraulic structures have been conceptually designed to achieve these desired outcomes.

The main design features included in the hydraulic structure design are:

- A winged entrance at each of the culvert inlets designed to provide the river flow with a smooth transition into the diversion tunnel
- Steel wheeled gates will be used to block the tunnel entrances and allow plugging to commence as soon as the diversion tunnels are closed during early filling, as shown in SRK Drawing PNA009-0122. As the water level will rise quickly during early filling, wheeled gate guides have been provided that can be operated using a crane from a bench at a higher elevation
- Although the flow velocities in the tunnels are not expected to be high and the discharge ends are constructed in solid rock, a reinforced headwall and wingwall arrangement has been designed to formalise the outlet and protect the portal. The requirement of wingwalls for erosion protection will be reviewed during further studies. Large rocks have also been provided to further reduce velocities before the diversion stream enters the river.

By ensuring the bench at higher elevation (used for crane access) is developed close to the entrance will minimise extension of the overreaching crane arm during construction of the inlet structures and operation of the wheeled gates. A smaller boxcut would also enable development of an access route between the quarry and the embankment during construction.

The inlet structures consist of rectangular bell-mouth entrances, which protrude as a box culvert approximately 13.5 m from the inlet box cut excavation. The box culverts transition to the 'D'-shaped tunnels over 7 m.

The inlets feature an entrance with slots to accommodate steel wheeled gates which can be lowered to allow work in the tunnel including installation of the engineered plugs for permanent closure once the construction period is complete. An example of a wheeled gate is shown in Figure 10-9.



Figure 10-9: Wheeled gate diversion structure⁸⁵

10.1.10 Diversion tunnel portals

The inlet portal will be developed as part of quarry development. Both the inlet and outlet portals are also expected to contain rock of a suitable quality for construction. Only a thin layer of overburden is found at these locations and will be removed, together with blasting of the box-cuts, using a top-down method (SRK Drawings PNA009-0122 and PNA009-0124). The tunnel portals will therefore be entirely developed in rock.

Stabilisation of the natural hill slope and surface water control should be undertaken at the earliest opportunity during box-cut construction as these are important in reducing geotechnical risks during tunnelling. Minimal disturbance of vegetation around the box-cut must be adhered to reduce risk of slope instability and surface erosion.

The box-cuts above the portals will be more than 100 m high and developed using a similar benching profile as the quarry. Additional rock supports and a shotcrete have been included to support the outside face of the box-cuts as required. Workings at lower levels will be protected by installation of catchfences.

The tunnel flow is released back into the natural riverbed approximately 1.2 km downstream of the main embankment to allow sufficient area for the construction laydown areas and downstream

⁸⁵ Hydro-Quebec/SEBJ, Eastmain 1 Project

cofferdam. The outlet invert elevation is at RL 49 m, which corresponds to the river bed elevation at this location.

No dedicated energy dissipation structures are expected to be required, as the maximum velocities of the discharge are estimated as 9 m/s at the tunnel outlet, which will decrease significantly as the flow exits the tunnel and enters the natural riverbed. Some competent tunnel spoil will be placed along the river bank directly opposite the outlet to prevent erosion.

10.1.11 Diversion tunnels

Due to the flat slope across the length of the diversion tunnels and difficulties experienced with optimisation of the hydraulic properties of the tunnel, a smoother tunnel lining is required than is typical to improve hydraulic flow. A temporary support of 150 mm thick (thicker than the minimum requirement for temporary support), mesh-reinforced shotcrete lining has been specified to enable undulations in the rock profile after blasting to be smoothed out. The mesh reinforcing will not only assist with providing a smoother surface for hydraulic purposes, but also provide additional strength to compensate for the hydraulic loads expected as a result of the trapped air during flow regime change. The final thickness will be achieved during a single installation by this method. The minimum temporary support requirements and the spacing for the tunnels is described in Section 3.1.

The floor and lower sidewalls of the tunnels will be concrete-lined to provide a lined-flat working base. The concrete floor is also provided to accommodate the higher flow velocities expected from the residual flow tunnel and further provide wear resistance due to sediment transport through the system. The height of the reinforced concrete lined floor is yet to be sized. The concrete lining will most likely be constructed using cast in situ methods and placed behind the advancing tunnel face.

Groundwater is expected during development of the tunnels, but volumes are not expected to be significant unless water carrying features are intersected.

10.1.12 Plug

Once operations have ceased, the tunnels will be permanently closed. An allowance has been made for a 50 m long concrete plug for each diversion tunnel. The design of the plugs has not been undertaken as part of the SPS. The following steps define the closure strategy:

- Once the inlet wheeled gates are installed the eastern tunnel can be closed off with a concrete plug from the downstream end of the tunnel. The stoplogs at the tunnel inlets are sized to accommodate a low water head pressure as the concrete plugs will be installed shortly after closing the inlets
- The rate of water level rise at the inlets following closure is expected to be quick, with water likely to enter the residual flow tunnel inlet within a few days
- To plug the western diversion tunnel, it is envisaged that a temporary, possibly prefabricated stoplog blocking arrangement (or plug) be installed upstream of the discharge point of the residual flow tunnel. This will prevent backwater from entering the area to be plugged
- Once the temporary plug/ stoplog is installed in the western tunnel and the residual flow tunnel is commissioned, a crosscut can be developed into the chamber of the western tunnel from the eastern tunnel. A permanent concrete plug can then be installed in the western tunnel.

10.2 Upstream cofferdam

A construction cofferdam will be required upstream of the main embankment works and will be integrated as part of the main embankment (SRK Drawing PNA009-0082). The cofferdam will be similar to the main embankment and founded 5 m below the river bed, following removal of the overburden material (SRK Drawings PNA009-0070 and PNA009-0072).

To ensure the downstream workings are kept dry, a composite lining system consisting mainly of a protected high-density polyethylene (HDPE) liner will be installed upstream of the embankment and raised with the raising of the embankment. The liner will be keyed in the riverbed, along the abutments and on the crest.

The cofferdam will consist of 3A material to ensure integration with the main embankment, and will have a final crest elevation of RL 83 m based on the FRHEP's flood protection requirements. The slopes of the cofferdam have been designed at 2.5:1 (H:V) and are slightly flatter than the outer slope of the main embankment.

Construction of the cofferdam will commence on the platform as soon as access to the area has been achieved and prior to installation of the diversion dam. The components of the cofferdam located within the continually flowing course of the river will be protected from the streamflow only once the diversion dam is constructed. A two-staged construction sequence is therefore required.

The main embankment will be keyed into the downstream embankment face by benching of the face which facilitates embankment construction.

10.3 Downstream cofferdam

A downstream cofferdam will be required between the diversion tunnel outlet and the hydroelectric power working area to protect the main working areas from flooding as a result of backwater build-up from diversion tunnel discharge (SRK Drawing PNA009-0020).

To ensure the workings upstream are kept dry, a lower permeability core will be compacted between two embankments (SRK Drawing PNA009-0072). The typical construction sequence involves three steps and can be seen on the drawing.

The cofferdam will consist of 2B type material to ensure adequate strength and maintain a grading that prevents internal erosion of the low permeability core. The low permeability core will contain enough clay content and will be compacted in layers to ensure an adequate seal is achieved. This material will be sourced from spoil removed during earlier excavations.

The embankment will have a final crest elevation of RL 55.5 m based on the FRHEP's flood protection requirements. The slopes of the cofferdam have been designed at 3:1 (H:V). These slopes have been designed to be reasonably flat, as quality control during construction will be difficult due to the submerged and wet conditions. The embankments will not have a drainage system which will result in phreatic level build-up on the upstream outer face. The low angle of the cofferdam slopes improves stability.

The construction of the cofferdam will commence after the installation of the upstream diversion and commissioning of the diversion tunnels.

The diversion dam will be removed later during construction when it is no longer required.

10.4 Diversion dam

A diversion dam will be required directly downstream of the diversion tunnel inlet to protect the main section of the cofferdam from flooding during completion of works, see SRK Drawing PNA009-0020.

The initial blocking of the river will need to be performed during normal flow conditions. To achieve this, an end-tipped embankment must be constructed once the diversion tunnels have been commissioned and the inlet channel to the diversion intake created. The material for the end-tipped embankment will consist of selected large rocks. Once the initial end tipped embankment has been created and raised to a level to provide vehicle access across the river, a finer grained material can be end-tipped from the upstream face of the embankment across the larger rocks. Both the large rocks and finer material can be sourced from spoil removed during earlier excavations. This process will continue until the seepage has adequately been sealed off, see SRK Drawing PNA009-0072.

The embankment of the diversion dam will have a final crest elevation of RL 74.5 m based on the FRHEP's flood protection requirements. The slopes of the diversion dam have been designed at 2.5:1 (H:V) and 3:1 (H:V). As with the downstream cofferdam, slopes have been designed to be reasonably flat. This is due to quality control issues during construction in submerged and wet conditions and phreatic level build-up on the upstream outer face of the embankment.

During construction, the remaining gap between the diversion dam and main cofferdam will behave as a collection sump for seepage and rainfall water. This must be backfilled on completion using spoil material to reduce haulage of spoil elsewhere.

The diversion dam will remain intact and submerged during filling of the reservoir.

10.5 Spillway

10.5.1 Spillway sizing

The spillway configuration selected for the FRHEP comprises an ogee crest control structure leading into a flip bucket/ plunge pool arrangement, with the plunge pool located at a sufficient distance from the downstream toe of the embankment to prevent interference.

Inputs and assumptions

The inputs and assumptions relevant to the spillway sizing include:

- Spillway design flood –PMF
- Design flood hydrographs for the PMF sourced from the Hydrology Study (Section 4)
- Tailwater curve at the outlet of the spillway sourced from the Hydrology Study (Section 4) (Figure 10-10)
- Reservoir storage curve (Figure 10-11)
- The reservoir is assumed ready to spill prior to the PMF storm, i.e. the starting water level is at the maximum hydroelectric power operating level (RL 226.1 m)
- No flows are passed through the diversion or conveyance tunnels, i.e. both storm and regular flows are passed through the spillway.

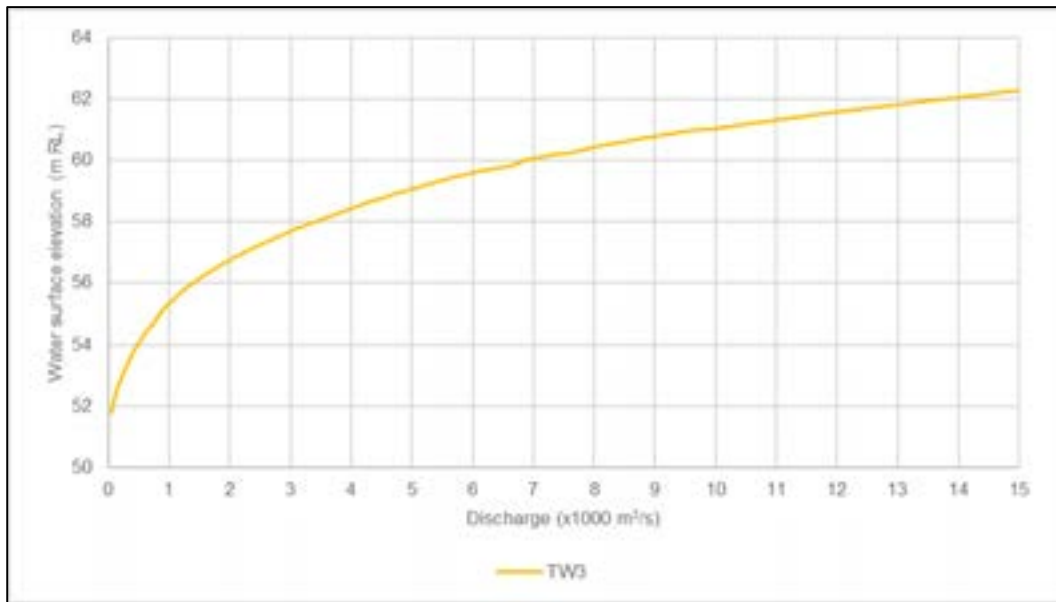


Figure 10-10: Spillway tailwater curve

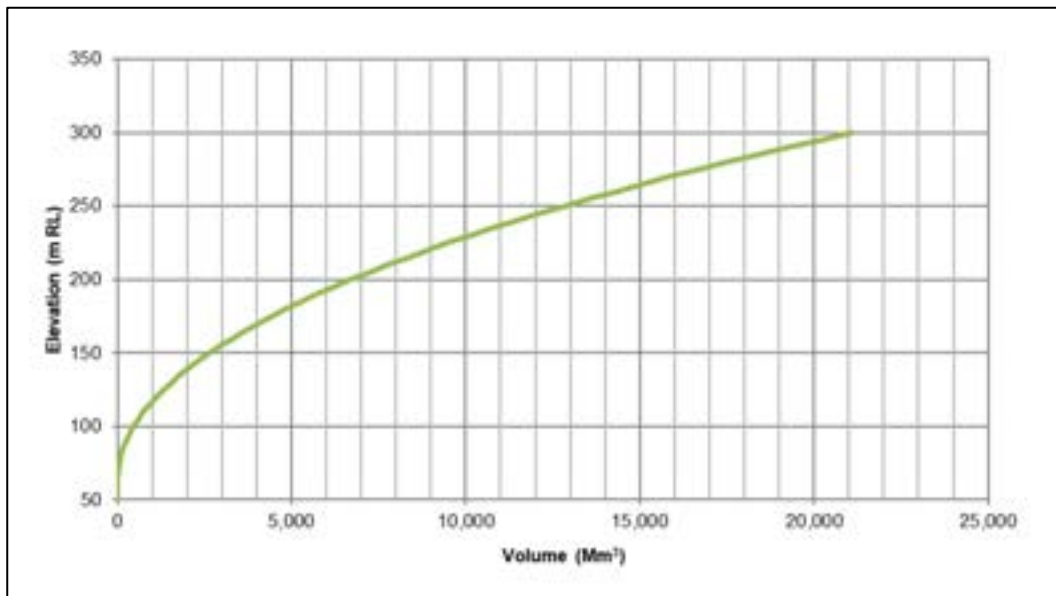


Figure 10-11: Reservoir storage curve for the spillway sizing

Rating curve

The spillway rating curve shown in Figure 10-12 is based on recommendations in the USBR guidelines⁸⁶ and the following inputs/ assumptions:

- Spillway crest level is RL 212.4 m
- Spillway crest length is 30 m
- Design head is 13.6 m (70% of maximum PMF head) – the design head equates to a discharge of approximately 3,000 m³/s
- Discharge coefficient is 2.10 at the design head (varies from 1.68 to 2.25, depending on head)

⁸⁶ United States Department of the Interior Bureau of Reclamation (USBR) 1987, Design of Small Dams

- Spillway operating rules – these rules have been assumed for the purposes of the designs, however the gates will open at a slower rate during operations, which will have minimal impact on the spillway sizing:
 - The spillway is gated with gates that open gradually once the water level reaches the maximum operating level of RL 226.1 m
 - The gates have been assumed to gradually open twice as fast as the water level rises, i.e. 0.2 m opening for each 0.1 m rise in water level
 - The gates lift clear once the water level rises 1.5 m above the maximum operating level (at RL 227.6 m).
- All four spillway gates are operational
- Discharge capacity has been reduced (assumed 10%) to account for expected loss of efficiency due to gates and piers.

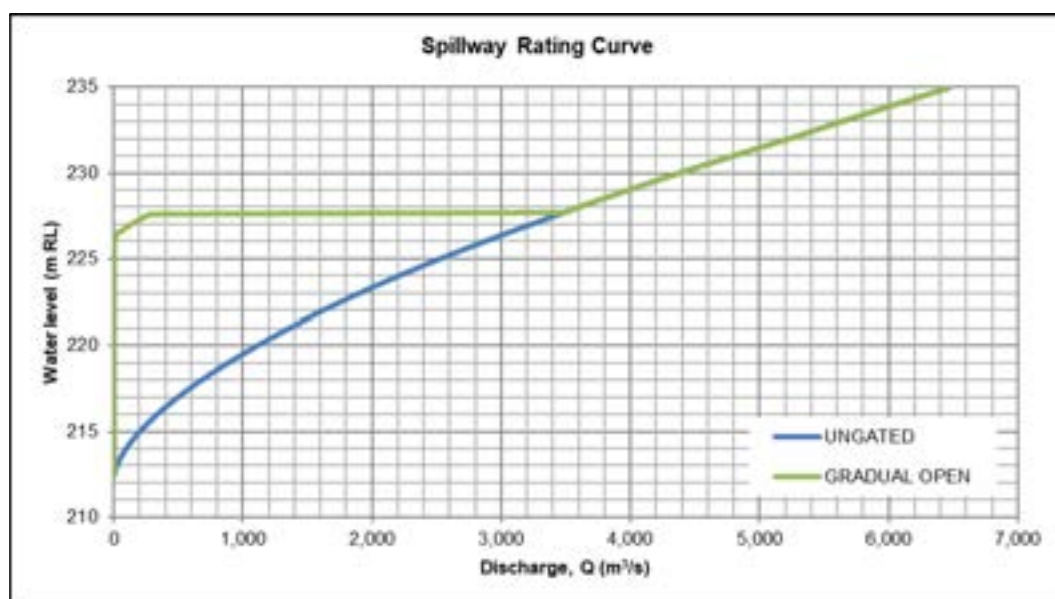


Figure 10-12: Spillway rating curve

Flood routing

The PMF inflow flood hydrographs with durations of 12–72-hours were routed through the reservoir and spillway to estimate the maximum resultant water levels. The initial water level was assumed to be the maximum operating level of RL 226.1 m.

The PMP estimation report (BoM, 2011) presents three different temporal distributions for each duration event (referred to as A, B and C in this report). These were determined by averaging catchment data from selected historical storms. While these were recommended by BoM as 'design temporal distributions of PMP', they are representative of storms observed at the site, and are appropriate to represent the 10 to 1,000-year ARI design storms, which are more likely to behave similarly to the observed events (than the more extreme PMP). Flood routing utilised three different temporal distributions provided by the Bureau of Meteorology (BoM)⁸⁷ for each duration event (A, B, and C). The results of the flood routing, summarised in Table 10-2, indicate that the highest maximum water level for the 24-hour, PMF design flood is RL 230.8 m. However, the 72-hour PMF has a slightly higher maximum water level of RL 231.8 m. It is noted that the maximum duration PMF developed to

⁸⁷ Bureau of Meteorology (BOM) 2011, Estimation of Probable Maximum Precipitation

date is the 72-hour event. PMFs of longer duration should be developed in future design stages to confirm that the 72-hour event is the most critical for spillway design.

Table 10-2 also shows the maximum water level for each of the events if only three of the four spillway gates are operational (i.e. spillway capacity is reduced by 25%). The highest maximum water level for the PMF for this scenario is RL 232.4 m for the 72-hour event.

The detailed results of the 24-hour and 72-hour PMF routing are shown in Figure 10-13 and Figure 10-14 respectively. The maximum peak outflow is approximately 5,100 m³/s, with a corresponding tailwater level of RL 59.1 m. The maximum water depth over the spillway crest is 19.4 m. It should be noted that the hydroelectric power platform is planned to be constructed at RL 65 m.

Table 10-2: Diversion flood routing results

PMF ID	Duration (hours)	Peak inflow (m ³ /s)	Peak outflow (m ³ /s)	Maximum water level (RL m)	
				Design	3 of 4 gates operational
PMP_12_A_S1	12	25,700	4,450	230.2	230.4
PMP_12_B_S1	12	22,400	4,330	229.9	230.2
PMP_12_C_S1	12	22,400	4,290	229.8	230.1
PMP_24_A_S1	24	25,500	4,710	230.8	231.1
PMP_24_B_S1	24	23,900	4,480	230.3	230.7
PMP_24_C_S1	24	22,200	4,280	229.8	230.2
PMP_36_A_S4	36	25,600	4,780	231	231.5
PMP_36_B_S4	36	23,700	4,670	230.7	231.2
PMP_36_C_S4	36	22,700	4,300	229.8	230.2
PMP_48_A_S4	48	25,600	4,790	231	231.8
PMP_48_B_S4	48	22,800	4,650	230.7	231.3
PMP_48_C_S4	48	22,700	4,300	229.8	230.5
PMP_72_A_S4	72	30,100	5,010	231.5	232.4
PMP_72_B_S4	72	25,900	4,410	230.1	230.6
PMP_72_C_S4	72	29,000	5,110	231.8	232.3

Note: Grey shade represents highest maximum water levels described in the text.

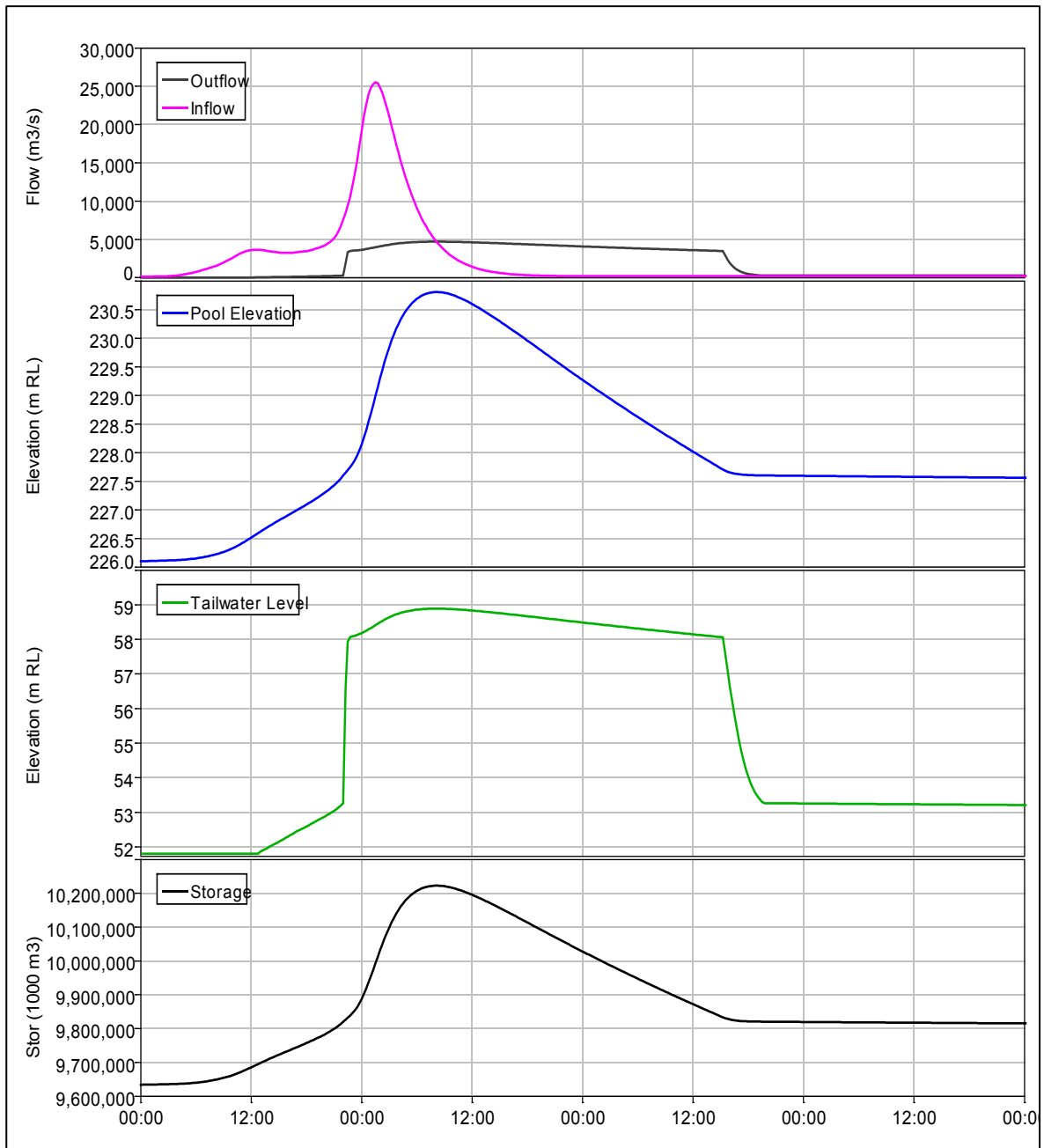


Figure 10-13: 24-hour PMF routing

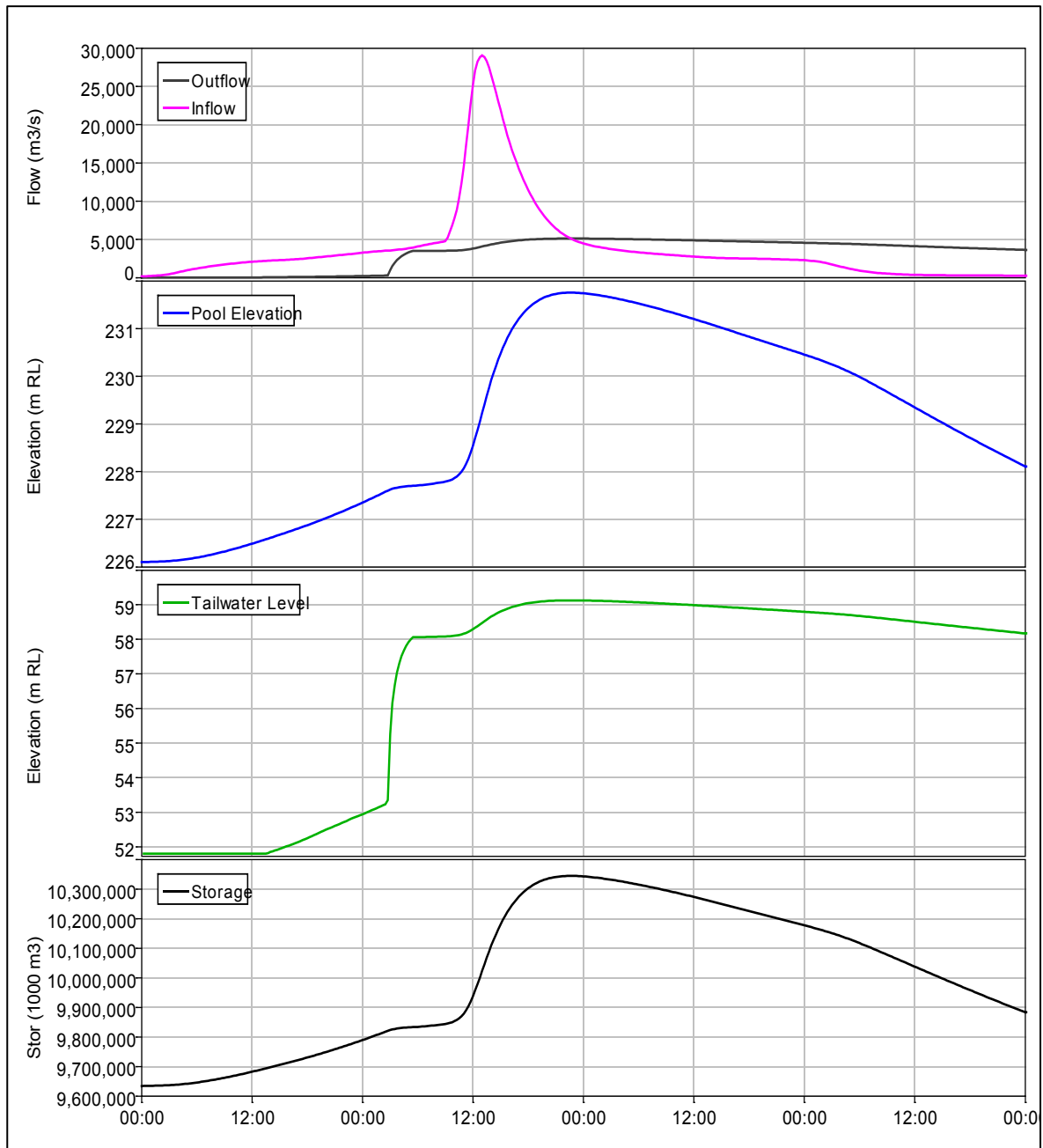


Figure 10-14: 72-hour PMF flood routing

Spillway hydraulics

The flow from the spillway crest to the flip bucket and beyond was calculated, taking into account the presence of a growing turbulent boundary layer and the effect on friction losses. Figure 10-15 summarises the conditions down the chute for the design discharge of 3,000 m³/s. The velocity reaches 30 m/s (the indicator of the first aerator location) at approximately 325 m from the crest.

Conditions at the flip bucket lip are summarised in Table 10-3. The velocity at the flip bucket exit is approximately 46 m/s, and the jet would follow the trajectory shown in Figure 10-16. The jet reaches RL 0.0 m at approximately 225 m (785 m – 560 m) from the flip bucket lip.

Corresponding results for the 5,100 m³/s maximum PMF discharge are shown in Figure 10-17 (summary hydraulics profiles) and Figure 10-18 (jet trajectory).

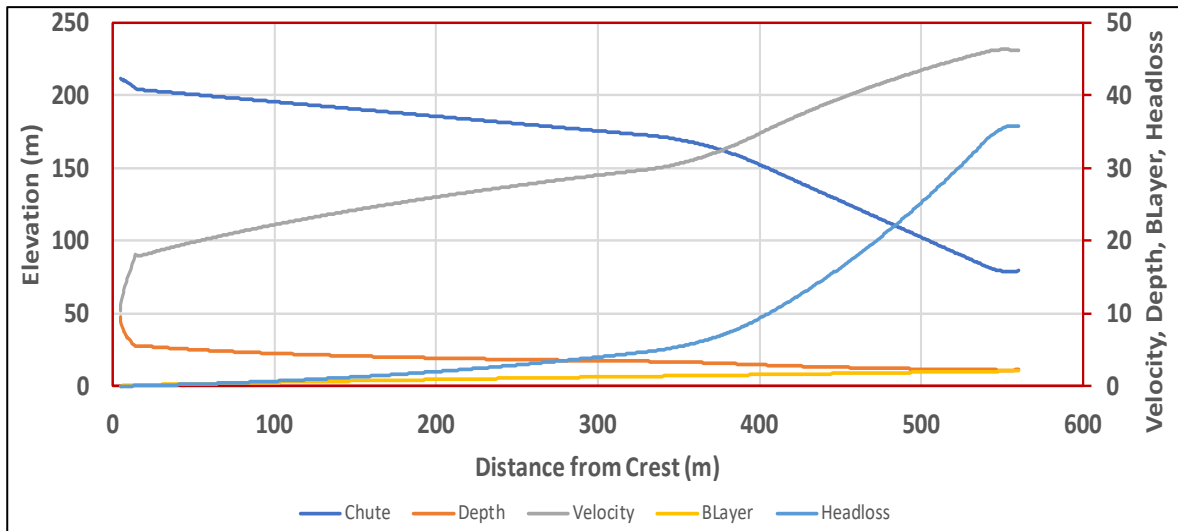


Figure 10-15: Summary hydraulics for design discharge (3,000 m³/s)

Table 10-3: Conditions at flip bucket lip at design discharge (3,000 m³/s)

Depth (m)	Boundary layer thickness (m)	Velocity (m/s)	Head loss (m)
2.17	2.12	46.1	35.8

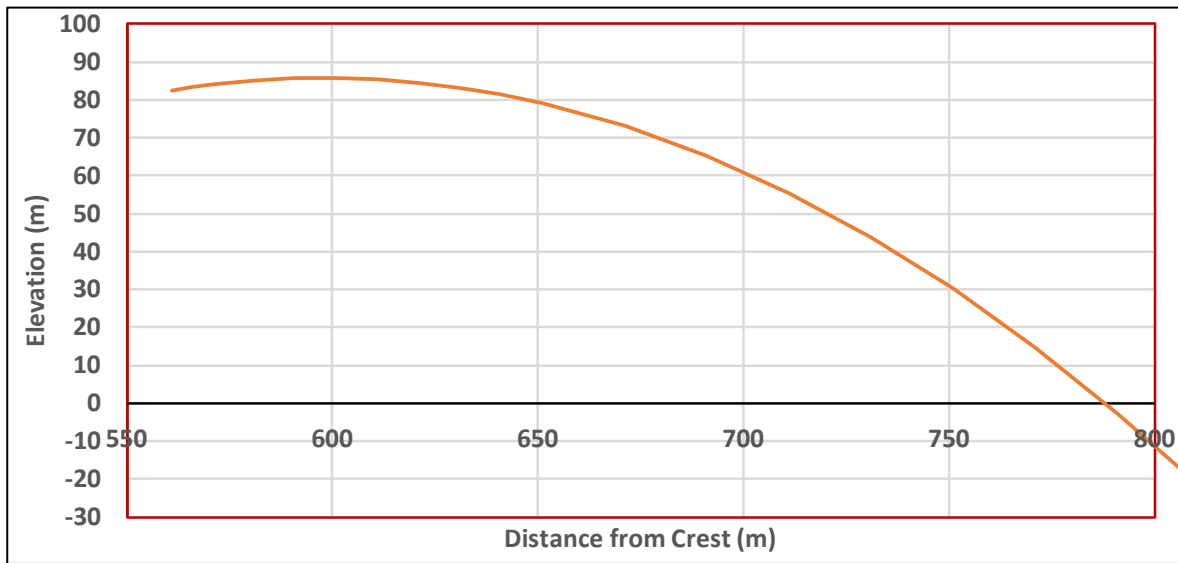


Figure 10-16: Jet trajectory for design discharge (3,000 m³/s) – flip bucket at 10°

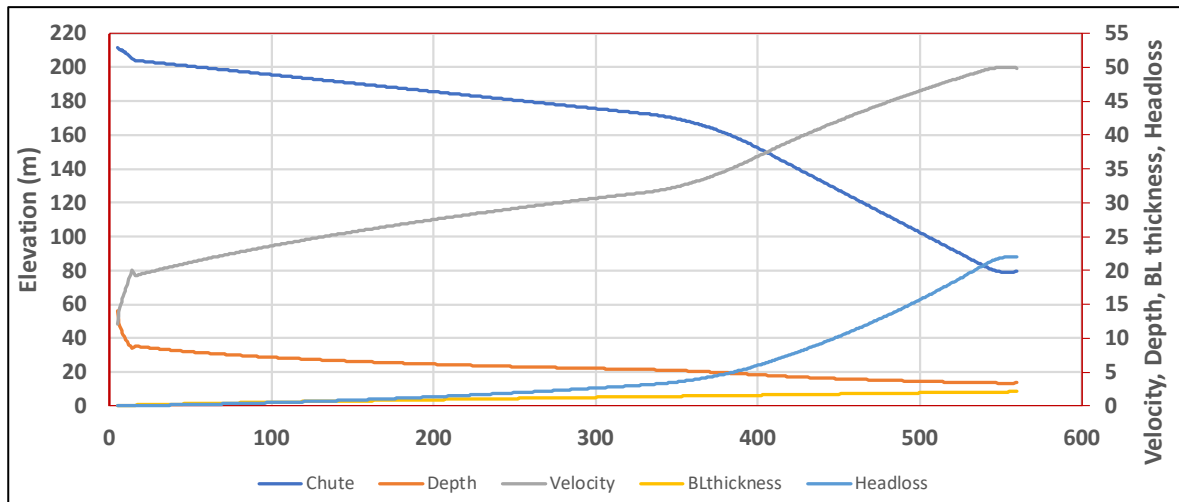


Figure 10-17: Summary hydraulics for maximum discharge (5,100 m³/s)

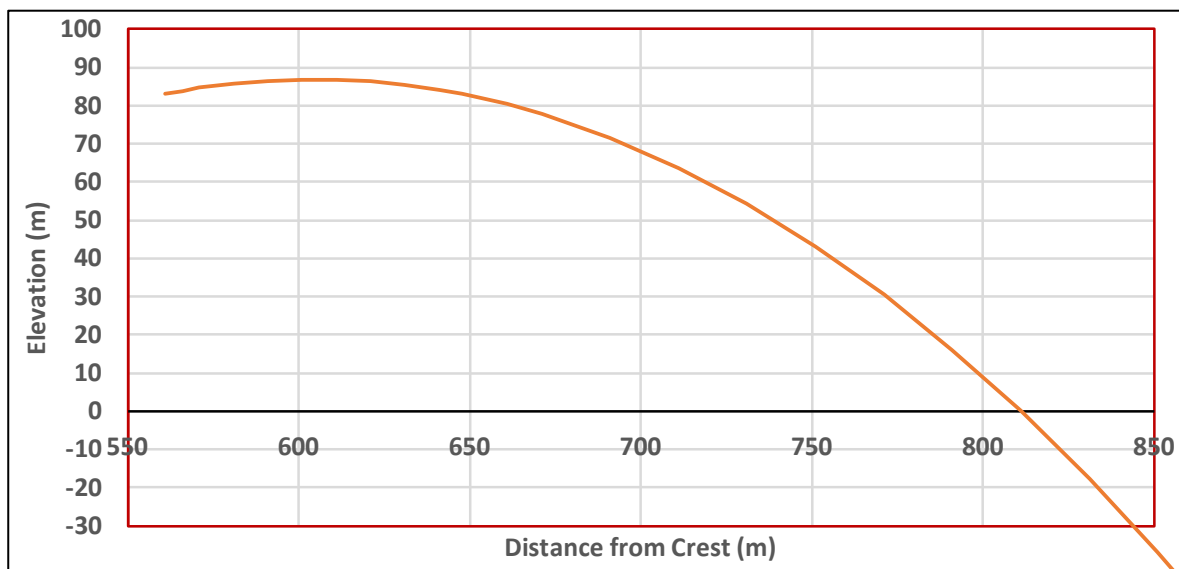


Figure 10-18: Jet trajectory for maximum discharge (5,100 m³/s) – flip bucket at 10°

10.5.2 Spillway design

The spillway design is shown in SRK Drawings PNA009-0110, PNA009-0112, PNA009-0114, PNA009-0116 and PNA009-0118, and incorporates the following features:

- The chute vertical sidewall heights will be tapered from the inlet going down the chute to accommodate the maximum flow depth needed to ensure the water is contained during PMF discharge conditions.
- Excavations will be benched as presented in the Geotechnical Design (Chapter 3) to ensure stability is maintained and to allow access during quarry development. The high cut slopes will require installation of catch fences during construction and rock drainage to drain water from the rock face to improve slope stability. The excavations of the spillway will form part of the quarry activities and is therefore an integrated unit. The quarry development team will be doing the bulk excavations, with more specific and accurate civil excavations to be undertaken by the civil construction team.
- At the interface with the fractured rock mass on the right abutment, larger excavations to produce lesser slopes may be required to mitigate the potential risk of slope failure.

- A vertical division wall located down the centre of the spillway chute to allow operational flexibility, whereby one channel can be closed for maintenance if required.
- Radial gates have been incorporated for operational requirements with stoplogs to safely isolate the gates for maintenance.
- A 10° flip bucket to produce a jet trajectory as shown Figure 10-16 and Figure 10-18. During high flow conditions this will dissipate the water stream as it enters the plunge pool. The flip bucket is anchored to accommodate high impact loads.
- The plunge pool location has been located in competent rock; otherwise, the discharge energy into the river section is expected to cause significant erosion. The final hydraulically controlled profile of the plunge pool will be determined during future study phases.
- A section of rock must be left in position between the river and plunge pool during construction to mitigate the effects of flooding. This feature can be removed once the spillway construction is completed.
- A bridge has been sized to accommodate mobile crane access for installation of gates and stoplogs during construction and operation. The gates and stoplogs can be dismantled into 30 t sections. It has been assumed that mobile cranes will be utilised for the required lifts.
- An edge beam at the end of the spillway apron to reduce the risk of erosive undercutting.
- The ogee crest profile as shown in Figure 10-19 was designed following the recommendations of USBR (1987)⁸⁸ for a design head of 13.6 m (70% of maximum PMF head). The crest equation is $y = 0.058 x^{1.832}$, where x is the distance from the crest and y the vertical height below the crest level. The Ogee profile has been selected to achieve optimal capacity and flow control.

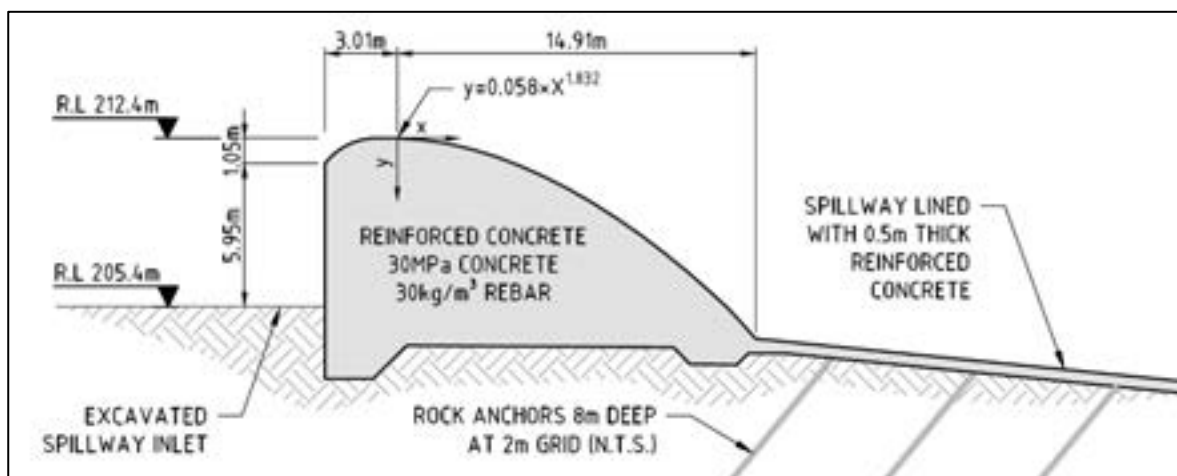


Figure 10-19: Ogee crest design

The spillway will also include the flowing key elements, which will be designed as part of the detailed design stage:

- Drains under the chute slab that feed out to catch drains outside the walls
- Anchors that hold the chute into the underlying rock – the chute concrete base has been anchored to the rock to accommodate possible uplift forces that may be as a result of joint penetration, drains not working or wave pressure effects. An underlying drainage system will supplement the requirements to limit uplift.

⁸⁸ United States Department of the Interior Bureau of Reclamation, 1987, Design of Small Dams

- The concrete sidewall has been structurally designed on the basis that the rock terraces will be supported by rock anchors. To this end, the concrete will act more as a façade and has not been designed to have retaining capabilities.
- Aerators strategically spaced to avoid cavitation damage to the chute concrete – based on the results of the velocity analysis at the design discharge (3,000 m³/s), three aerators are proposed in the locations shown in Figure 10-20; two different aerator geometries will be adopted, depending on the slope of the chute (i.e. Type A at 325 m and Type B at 400 m and 475 m), and the performance of the aerators will form part of the proposed hydraulic model studies for the spillway.

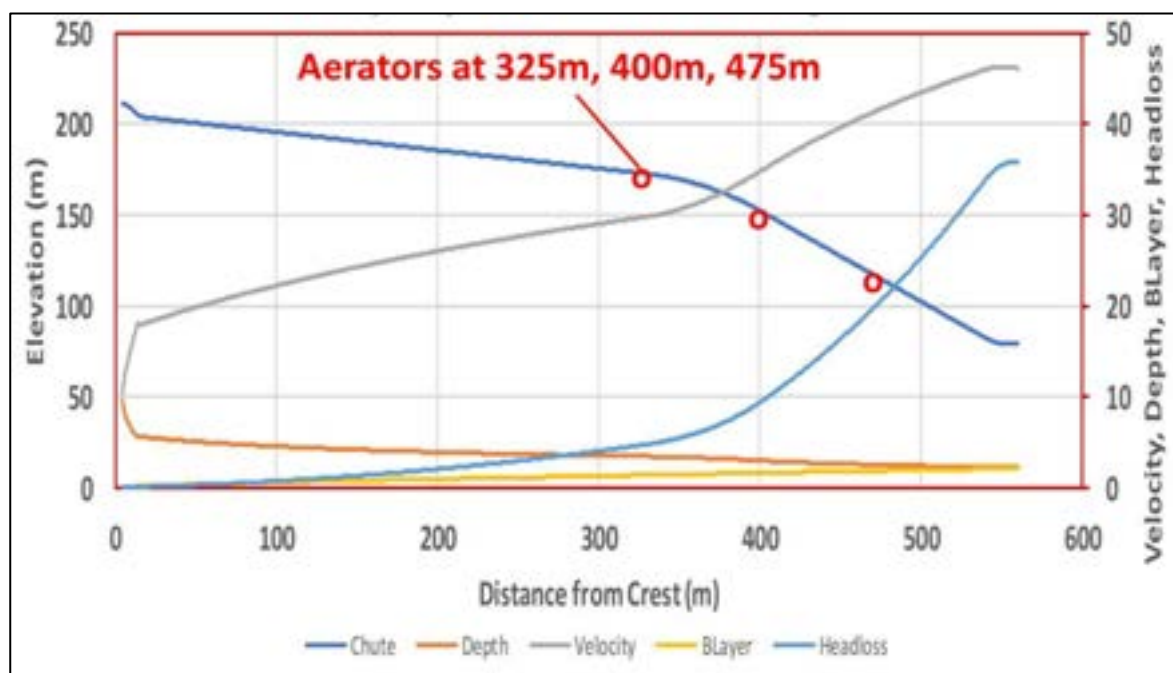


Figure 10-20: Suggested aerator locations

Joints will be provided with waterstops and slabs will be keyed to adjacent slabs. The construction must be such that the chute design thickness is accomplished, and the finished concrete joints are constructed to ensure that there are no projections of the downstream joint surface above the level of the upstream joint surface.

Spillway sizing summary

This report presents the sizing of the FRHEP spillway. A spillway crest width of 30 m results in the following maximum values during the critical design PMF event:

- Water level: RL 231.8 m (all spillway gates operate)
RL 232.4 m (if only 3 of the 4 spillway gates operate)
- Depth over the spillway crest: 19.4 m
- Outflow: 5,100 m³/s
- Tailwater level: RL 59.1 m.

The spillway rating curve should be refined considering the design of the gates and piers once developed, and any changes to the operating rules. The flood routing should then be repeated using the updated rating curve.

10.5.3 Spillway gates

The PMF routing is an important aspect of the optimisation work as it establishes the freeboard required between the top of the embankment filters and the maximum normal operating water level.

The dam freeboard is set by the following:

- Water level rise for PMF. It is found that retaining up to 65% of the PMF inflow produces a peak outflow that minimises the spillway size
- Water level rise owing to tsunami owing to landslides
- Seismic settlement – 7.8 m has been allowed for seismic settlement. The details of this rationale are set out in Section 8.11.
- The tsunami allowance and the PMF utilise the same freeboard. The allowance is not additive.
- The dam filters are at the maximum PMF water level of RL 237.5 m.

Radial gates on the spillway have been provided. To size the gates and determine the maximum reservoir operating level, a routing study for a range of PMF events was completed. The following should be noted:

- Increasing the spillway capacity further increases the excavation volume and cut slope heights. This can prevent surge chambers being installed where required.
- 4 radial gates to pass PMF.
- System can pass the PMF with acceptable level rise with only three gates operating (the level rises an additional 1 m when compared with 4 operational gates).
- Based on the consultant's experience from other projects, assuming 3 out of 4 gates operational improves the gate reliability by 5 or 10 times. This is significant in trying to achieve a very high level of reliability for protection against dam failure from all causes. A formal analysis of spillway options was prepared to consider the issue of gated versus ungated spillways³. The results concluded that there was a small advantage in considering the 3 gates out of 4 operating during a PMF event.

When the spillway gates are used, the flow can only be controlled by the gates while the gate tip is submerged in the flow. A value of 0.7 m submergence has been assumed to ensure there is no vibration of the lower skin plate of the gate. As the reservoir level increases, the gate will open further. It has been assumed that once the water level rises more than 1.5 m above the normal maximum operating level the gates will be lifted clear.

The gates can follow two alternative operating rules:

First Option

- The gates can be opened progressively to maintain a constant level in the reservoir. For this embankment height the maximum operating level is RL 226.14 m. Up to a discharge of 2,733 m³ the reservoir level will not change, and the outflow will be equal to the inflow less the generation flow.
- This can be done using a PID level control. This has the advantage that the gates automatically compensate for the mal-operation of one of the gates. They do not need to communicate between themselves, which causes complexity.
- When the opening corresponding to maintaining the minimum submergence of the gate tip is reached at a flow of 2,733 m³, the gate can follow the reservoir level rise to maintain the gate tip submergence.

- The gates continue to open while maintaining the minimum submergence. Once a set level, possibly 1.5 m above the normal operating level (RL 227.64 m) is reached and with a discharge of 3,243 m³, the gates should lift clear.
- The water will flow freely over the spillway and reach a maximum level of RL 231.8 m and a peak flow of 4,531 m³ with all four gates operating.
- Should one of the spillway gates fail to open the reservoir will reach a maximum level of RL 232.40 m and the peak spillway flow will be 3,770 m³.

This option will maximise the available storage to buffer a major storm.

Second Option

- Initially the gate will open linearly with level until a flow of 2,831 m³ is reached with the gate 0.3 m open.
- The gate will follow a different relationship above this such that the opening at a level 1.5 m above the discharge will be 3,243 m³ as above.
- At this point the gates will go fully open. The peak flows and levels will be similar to those under (Option 1) above.
- The gates need to communicate between themselves to compensate for the mal-operation of a gate. This is complex to achieve in practice since one has to determine what constitutes mal-operation when you may be unable to communicate with the defective device – is still working but not communicating.

Table 10-4 shows the maximum controlled flow through the gates with a 1.5 m rise in the reservoir water level and 0.7 m submergence of the gate tip. As can be seen, the maximum flow with four gates operating is 3,243 m³/s and with three gates operating the maximum flow is 2,485 m³/s. It should be noted that the four large bypass valves at the powerstation can also be used to pass a major flood. These valves add almost 700 m³ to the flood capacity to bring the total controlled discharge to 3,941 m³/s and 3,183 m³/s respectively with four and three gates operating. The impact of the bypass valves is almost sufficient to allow the capacity of three gates plus the valves to match the discharge from four gates.

Of particular importance is that the use of the bypass valves allows the dam to be lowered to approximately RL 190 m to allow control of the reservoir level should a major repair be required following an earthquake or tsunami on the reservoir.

Alternative arrangements are discussed below, and the comparison is presented in Table 10-6.

Table 10-4: Maximum controlled gate discharge

Number of gates operating	Unit	4 of 4 Gates	4 of 4 Gates	3 of 4 Gates	3 of 4 Gates
Gate raise	m	–	1.50	–	1.50
Opening fully level	RL m	226.14	227.64	226.14	227.64
Crest	RL m	212.44	212.44	212.44	212.44
Maximum opening above crest	m	10.22	11.34	10.22	11.34
Gate vertical lift	m	8.59	9.53	8.59	9.53
Gate opening across flow	m	9.52	10.64	9.52	10.64
Gate flows	m³/s	2,733	3,243	2,050	2,485
Bypass valve flow	m ³ /s	694	698	694	698
Combined flow	m³/s	3,427	3,941	2,744	3,183

The following points should be noted in reviewing the tables in this section:

- The values presented in this section differ from those in the attached Sizing Optimisation Study because they are based on the final developed design for the spillway gates.
- Radial gates due to their geometry. The gate opening used to determine the flow is the opening perpendicular to the flow, which is not the same as the vertical opening of the gate, although the two are related. The gate opening depends on the location of the gate on the crest, and the gate radius and the location of the trunnion bearings. Very small changes in the values can change the gate capacity by as much as 25%. The final gate sizing is four gates 16.4 m (H) × 7.5 m (W). The spillway crest level is RL 212.44 m.

Table 10-5 shows the information for the spillway operation using the spillway gates only, and for raising the gates fully once the reservoir level has increased by 1.5 m. As can be seen the peak spillway discharge with four gates operating is 4,531 m³/s and the maximum level is RL 230.86 m. With only three gates operational the peak spillway flow is 3,770 m³/s and the maximum level is RL 232.10 m, which is 0.60 m above the filters. The dam closure case with the gates removed has a peak flow of 1,829 m³/s and a peak level of RL 222.89 m.

Table 10-5: Spillway flows and discharges during PMF events using spillway only

PMF	Duration	12 hour	24 hour	36 hour	48 hour	72 hour
Peak Inflow	m ³ /s	26,958	27,052	27,420	27,416	30,081
Case	DAM CREST LEVEL RL235m 4 GATES OUT OF 4 OPERATING					
Peak Outflow	m ³ /s	4,057	4,142	4,277	4,428	4,531
Peak Level	RL m	229.63	229.86	230.21	230.60	230.86
Gate Open level	RL m	226.14	226.14	226.14	226.14	226.14
Level Rise	m	3.50	3.72	4.07	4.46	4.73
Case	DAM CREST LEVEL RL235m 3 GATES OUT OF 4 OPERATING					
Peak Outflow	m ³ /s	3,127	3,268	3,484	3,661	3,770
Peak Level	RL m	229.93	230.42	231.15	231.74	232.10
Gate Open level	RL m	226.14	226.14	226.14	226.14	226.14
Level Rise	m	3.79	4.28	5.02	5.61	5.96
Case	DAM CREST LEVEL RL212.4m UNGATED SPILLWAY (CLOSURE CASE)					
Peak Outflow	m ³ /s	666	879	1,188	1,463	1,829
Peak Level	RL m	218.00	219.05	220.42	221.53	222.89
Gate Open level	RL m	212.44	212.44	212.44	212.44	212.44
Level Rise	m	5.56	6.61	7.98	9.09	10.45

The maximum operating level of the scheme has been set at RL 226.14 m. This had to be done to allow a range of parallel activities that form part of the SPS to be carried out. There is an opportunity to increase the maximum operating level of the scheme. However, Table 10-6 indicates a decrease could be required. The table shows the maximum water levels that occur at different design operating regimes, changes to maximum reservoir water levels, when three or four gates are operating, and when the bypass valves are and are not used to increase the flood discharge.

Table 10-6: Potential revised maximum operating water levels (bypass valves used to pass flood flows)

Design Case	Selected maximum operating level (RL m)	4 gates out of 4 operational Maximum level during 72-hour PMF (RL m)	3 gates out of 4 operational Maximum level during 72 hour-PMF (RL m)
Gates with assistance from bypass valve	226.14	231.8	232.40
Gates with no assistance from bypass valve	226.86	231.50	232.54
Gates with assistance from bypass valve	227.35	231.50	232.26
Gates with no assistance from bypass valve	225.36	230.19	231.50
Gates with assistance from bypass valve	226.48	230.58	231.50
Gates with assistance from bypass valve	226.14	230.25	231.18

10.5.4 Slope stability assessments for design of spillway and quarry slopes

As a result of the re-definition of the quarry limits (described in Section 3.1.4), the quarry area was restricted in its southward extent and was extended further to the north and merged with the spillway cut. The same slope design parameters used for the spillway cut were extended into the quarry for practicality. The importance of the spillway cut being stable in the very long term is greater than for the quarry slopes.

Upon completion of the geotechnical investigations and collation of the geotechnical model, assessment of the slope stability for the final prepared spillway and quarry design was carried out by the following means:

- Empirical assessment to derive preliminary slope bench stack and inter-ramp angles
- Kinematic (structural) failure analysis to assess the design at a bench-berm scale
- 2D stability analyses of the overall slopes for the SRK quarry and spillway cut designs, with the intent to assess the slope stability in terms of the factor of safety (FoS).

Slope design geometry terminology is illustrated in Figure 10-21.

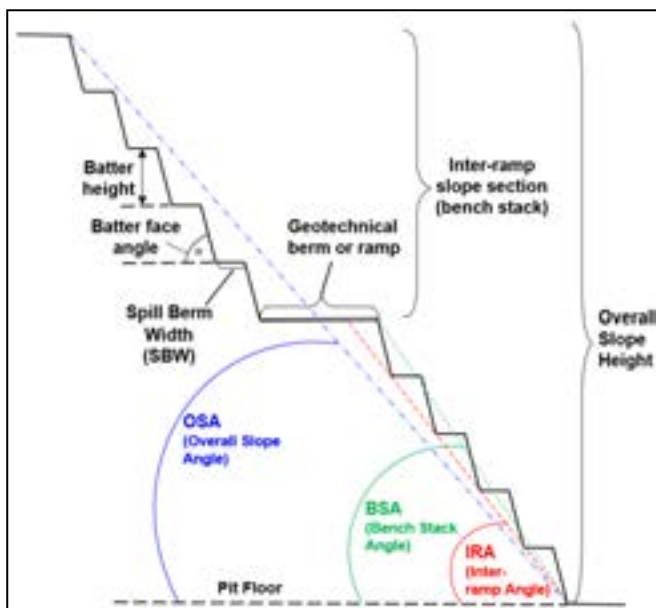


Figure 10-21: Slope design geometry terminology

Preliminary empirical assessment

Preliminary quarry design commenced while the geotechnical field investigations were still ongoing. Preliminary slope design inputs were provided for the design, using engineering judgement of the conditions observed, empirical assessment of the available data, and some preliminary, indicative slope stability assessments. The assessments took into account the expected slope cut heights. It must be noted that the slope design parameters were developed with practicality in mind, for the predominant (good-quality) rockmass conditions, as poor conditions within the right abutment are expected only locally and are difficult to predict in their extent.

Geotechnical core logging data forms the basis for empirical rockmass characterisation, using the Mining Rockmass Rating (MRMR) classification system of Laubscher (1990), in combination with the Haines and Terbrugge (1991)⁸⁹ empirical method for slope design. The results of the rockmass characterisation are used to provide mining rockmass ratings, which, in turn, are used to evaluate indicative bench stack angles (BSAs), and/ or provide indicative overall slope angles (OSA). Bench stacks within the overall slope are separated by ramps or wide geotechnical safety berms. The MRMR classification system is an extremely useful and robust method of utilising all of the relevant rockmass parameters to assist with preliminary slope design.

The in situ rockmass of the various material types can be classified based on their range of RMR calculated from the logged data, as indicated in Table 10-7.

Table 10-7: Rockmass Rating Classes

Material Type	100–80	80–60	60–40	40–20	20 – 0
Description	Very Good	Good	Fair	Poor	Very Poor

The representative Laubscher RMR value of 55 was assessed from the logging data for the bedrock, and was considered suitable for the preliminary analyses.

To simulate the response of the rockmass in an excavation environment, percentage adjustments are applied to RMR values to obtain MRMR values. These adjustments are made to account for the potential time-dependent deterioration of the rockmass upon exposure, the unfavourable orientation of discontinuities with respect to excavation stability, the stress environment, and damage induced by blasting. The MRMR value is calculated by multiplying the individual adjustment factors together to get the total adjustment and then multiplying the RMR value by this total adjustment.

A representative MRMR value of 48 was calculated from the Laubscher RMR using the following adjustments: Blasting 97% (pre-split blasting); Weathering 100% (little time dependant deterioration over most of the rock face); Orientation 95% (orientation of joints not necessarily favourable, but persistence is very limited); Stress 95% (stress is unlikely to have a significant influence on the shallow surface cuts).

Using the Haines and Terbrugge method, the MRMR value is used to determine a BSA or OSA for a given slope height.

It is important to note that the bench stack angle represents the actual slope angle of the bench stack (crest to toe), and is used for stability analysis. This angle will vary depending on the number of benches within the stack (i.e. changes in stack height). The inter-ramp angle (IRA) (crest to crest or toe to toe) is a useful alternative for describing the slope angle of a bench stack because it is not

⁸⁹ Haines, A. and Terbrugge, P. J. (1991). Preliminary estimation of rock slope stability using rock mass classification systems. 7th International Conference on Rock Mechanics Proceedings, Volume 2 pp 887 – 892. Aachen, Germany.

dependent on the number of benches within the stack and thus remains constant with changes in stack height).

The Haines and Terbrugge empirical method is indicative only, and was intended only to provide very preliminary design inputs. These have been used as a starting point for subsequent limit equilibrium stability modelling (using Rocscience *Slide* software) carried out to provide design inputs for the quarry and spillway slopes. These analyses were performed on sections through the quarry topography with initial cut slopes generated using the empirical assessment results.

Bench-berm kinematic analyses

Kinematic failure analyses were conducted to assess the potential for structurally-controlled failure within the benches (batters) constituting the quarry and spillway cut slopes. This included basic assessment of toppling and planar sliding failure, and a more comprehensive assessment of wedge failure.

Structural data from drill core structural logging and downhole televiewer survey within the bedrock was grouped for the quarry area and spillway area (right hand side of the gorge). The stereonet pole plot in Figure 10-22 shows the identified dominant structural sets.

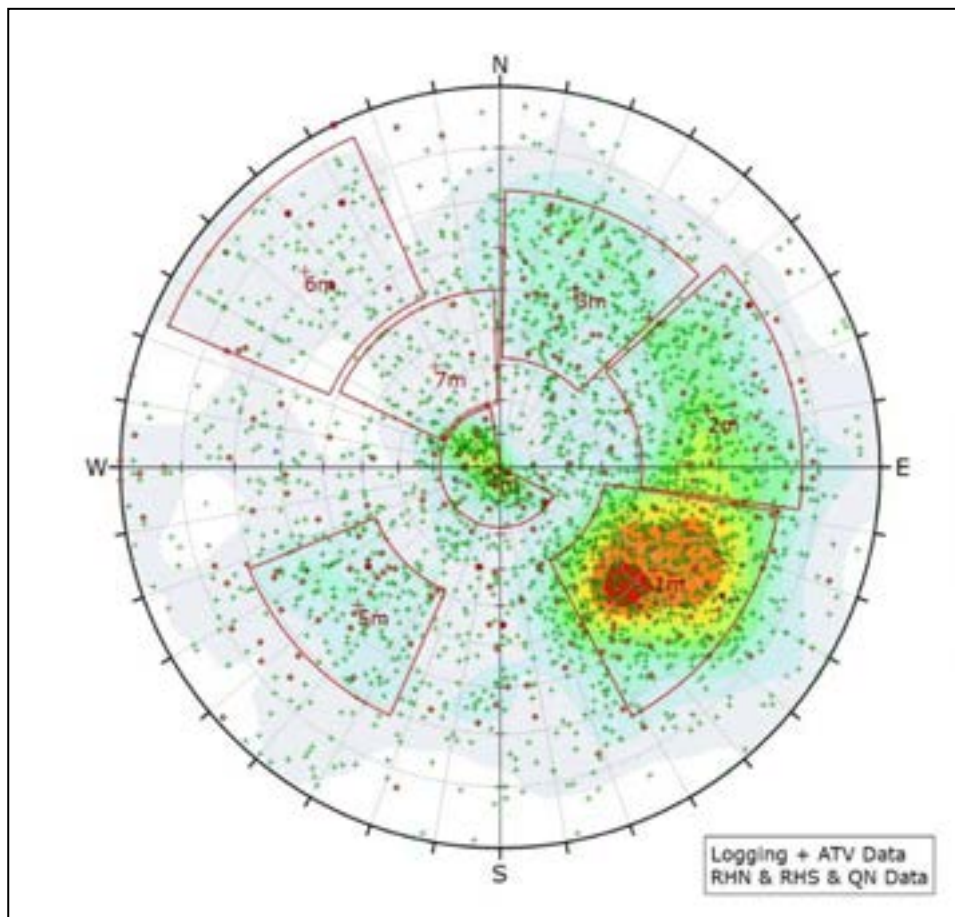


Figure 10-22: Stereonet of the structures encountered on the RH side of the gorge, with identified dominant structural sets

The main structural sets identified were used to assess batter-scale stability. The average orientations of the main structural sets are listed in Table 10-8.

Table 10-8: Orientations of main joint sets identified

Set	Set Orientation	
	Dip (°)	Dip Azimuth (°)
1	52	304
2	59	255
3	54	203
4	4	75
5	55	46
6	72	135
7	35	147

Four main slope orientations (dip azimuths) identified in the quarry and spillway cuts – 100°, 280°, 300° and 320° – were used in the analyses.

Stereographic analysis of toppling and sliding (planar) failure

Stereographic analysis of toppling failure was carried out for each main slope orientation, by plotting the expected failure envelope for toppling against the structural pole plots. An example of this, for slope azimuth 300°, is shown in Figure 10-23.

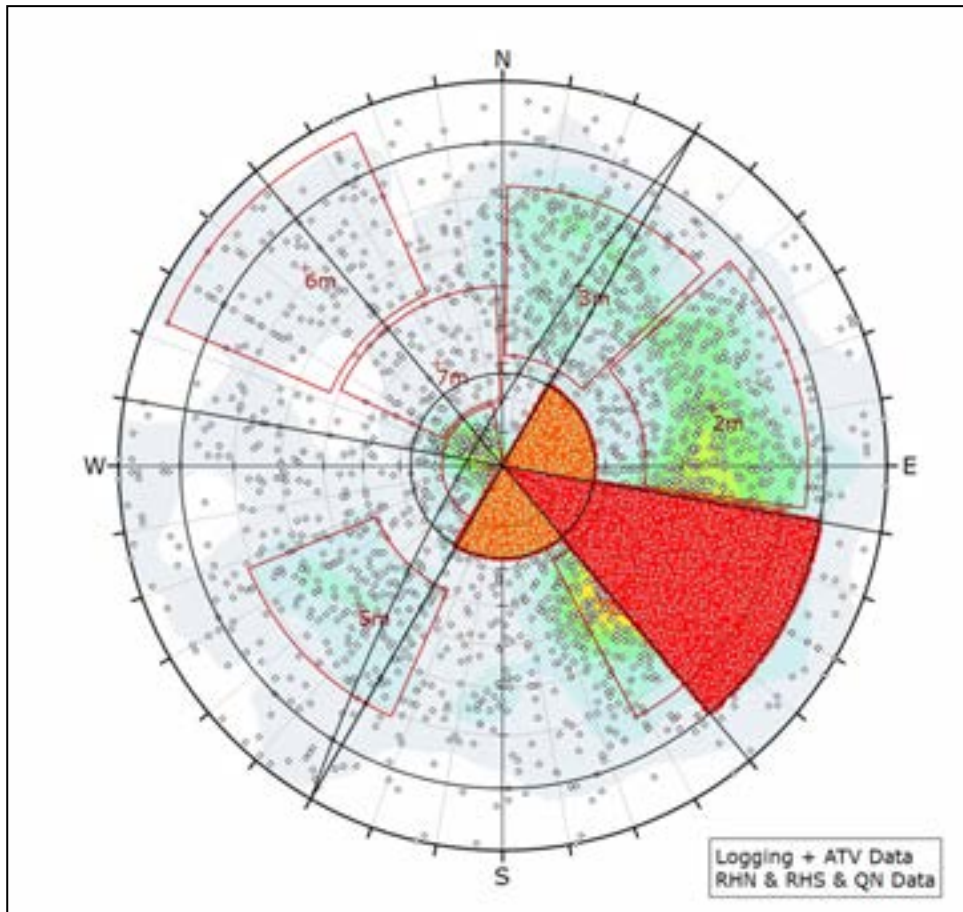


Figure 10-23: Stereographic analysis of toppling failure for slope azimuth 300°

The results of the toppling failure analysis are presented in Table 10-9.

Table 10-9: Results of toppling failure analysis

Wall dip azimuth (°)	BFA (°)	Assumed friction angle (°)	Probability of occurrence (%)
280	80	27	4
300	80	27	5
320	80	27	5
100	80	27	13

The results indicate that toppling in the batters of the eastern cut slopes will not represent a significant mode of failure. On the western cut slopes, the risk of toppling failures will be higher (due to the strong joint sets dipping moderately to steeply into the slope); however, the risk is within general batter-scale acceptance criteria (<20%).

Stereographic analysis of planar failure was also carried out for each main slope orientation, by plotting the expected planar failure envelope for sliding against the structural pole plots. An example of this, for slope azimuth 280°, is shown in Figure 10-24.

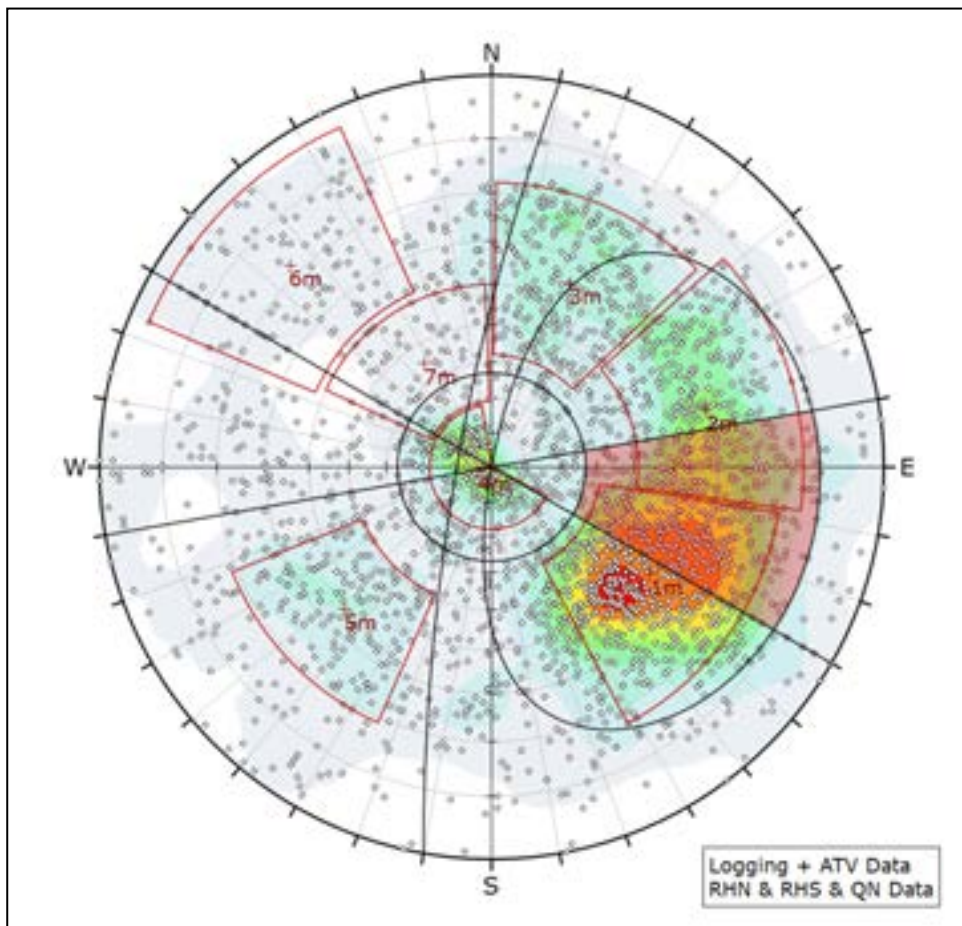


Figure 10-24: Stereographic analysis of planar failure for slope azimuth 280°

The results of the planar failure analysis are presented in Table 10-10.

Table 10-10: Results of planar failure analysis

Wall dip azimuth (°)	BFA (°)	Assumed friction angle (°)	Probability of occurrence (%)
280	80	27	19
300	80	27	22
320	80	27	19
100	80	27	4

The results indicate that planar failure in the batters of the eastern cut slopes does represent a significant mode of failure, due to the strong joint sets dipping moderately to steeply out of the batter faces. The risk is marginally within general batter-scale acceptance criteria (20%). However, it is expected that this will be mitigated by the likely limited persistence of joints. Planar failure is not a significant mode of failure in the western cut slopes.

Analysis of wedge failures

Wedge failure analysis is the primary means by which optimisation of pit slope geometries from a structural perspective is carried out. Wedges are only free to slide when they exist in combination with specific slope geometry, and the wedge failure will thus depend on the orientation and face angle of individual benches.

For this structural pit slope optimisation process, the following factors were considered:

- Structural characteristics of the rock mass, including:
 - Orientation of dominant structural sets
 - Persistence of discontinuities
 - Nature (friction and cohesion) of discontinuity surfaces
- Geometric considerations:
 - Orientation of pit walls
 - Bench face (batter) angle
 - Bench height
 - Spill berm width (SBW).

Deterministic and probabilistic wedge failure analysis was conducted using MWedg software (Gibson, 2013). MWedg can analyse multiple combinations of wedges generated by large numbers of discontinuity sets. It identifies all possible wedge geometries, their FoS, and the volumes and shapes of failed materials generated, and then calculates the SBWs required to contain the failed material (wedge failures of FoS ≤ 1.1), assuming a 38° average angle of repose for failed wedge material and a swell factor of 1.35.

Input structural characteristics

The availability of structural persistence data is limited by the reliance on drill core information. Very little mapping data in the immediate area was available for this study. Persistence values of 20 m (corresponding to recommended bench heights) were used for all the structural sets, although this is considered to be very conservative. Another set of analyses that assumed a 10 m persistence was therefore conducted.

Joint shear strength

Structures were assigned zero cohesion because it was assumed that, at the batter scale, cohesion would have been largely destroyed by blasting during pit excavation.

The results from direct shear laboratory testing of joints have been summarised in Table 10-11, according to the geotechnical domain from which the samples were taken.

Table 10-11: Summary friction angle values for the RH side of the gorge

Domain	Test count	Friction angle (°)		
		Minimum	Maximum	Average
Good-quality bedrock	14	17.2	33.6	25.1
Deteriorating bedrock	4	27.7	36.4	32.8
Weathered bedrock with oxidised joints	1	23	23	23.0
Total	19	17.2	36.4	26.6

For comparison, an empirical method was also used to calculate the friction angle of the defects. The empirical method used was developed by HTA Consultants (unpublished) and uses the defect roughness (micro and macro roughness) and infill type recorded in each geotechnical logging interval to estimate the friction angle, as detailed in Table 10-12.

Table 10-12: HTA empirical methodology to derive friction angles from defect characteristics

Macro roughness	Infill	Macro roughness and infill combined	Micro roughness								
			SI	SS	SP	UR	US	UP	PR	PS	PP
			9	8	7	6	5	4	3	2	1
I (5)	Nil – a	5-a	50	47.5	45	42.5	40	37.5	35	32.5	30
	Hard, partial fill - b	5-b	47.5	45	42.5	40	37.5	35	32.5	30	27.5
	Soft filled - c	5-c	20	20	20	20	20	20	20	20	20
S (4)	Nil – a	4-a	47.5	45	42.5	40	37.5	35	32.5	30	27.5
	Hard, partial fill - b	4-b	45	42.5	40	37.5	35	32.5	30	27.5	25
	Soft filled - c	4-c	20	20	20	20	20	20	20	20	20
C (3)	Nil – a	3-a	45	42.5	40	37.5	35	32.5	30	27.5	25
	Hard, partial fill - b	3-b	42.5	40	37.5	35	32.5	30	27.5	25	22.5
	Soft filled - c	3-c	20	20	20	20	20	20	20	20	20
U (2)	Nil – a	2-a	42.5	40	37.5	35	32.5	30	27.5	25	22.5
	Hard, partial fill - b	2-b	40	37.5	35	32.5	30	27.5	25	22.5	20
	Soft filled - c	2-c	20	20	20	20	20	20	20	20	20
P (1)	Nil - a	1-a	40	37.5	35	32.5	30	27.5	25	22.5	20
	Hard, partial fill – b	1-b	37.5	35	32.5	30	27.5	25	22.5	20	17.5
	Soft filled – c	1-c	20	20	20	20	20	20	20	20	20

Detailed histograms of the micro roughness, and Infill distributions per rock domain are provided in Section 3.1.8.

Table 10-13 summarises the friction angle values from the HTA empirical approach per main rock unit for the RH side of the gorge. It can be observed that the representative friction angle values are comparable with the average laboratory testing values.

Table 10-13: Summary friction values from HTA empirical approach for right abutment area

Domain	Reading count	Friction angle (°)			
		Min.	Max.	Average	Std Dev
LH landslide zone	10	17.5	27.5	22.8	3.2
Deteriorating bedrock	1,166	17.5	45	22.1	4.6
Weathered bedrock with oxidised joints	447	17.5	47.5	26.6	7.7
Good-quality bedrock	2,620	17.5	47.5	27.0	7.1
Total	4,316	17.5	50	25.6	7.0

Table 10-14 summarises the structural set properties that have been adopted for the wedge failure analysis. A friction angle of 27° was used for all the identified structural sets; this value corresponds to the average friction angle value of all the direct shear tests and to the value obtained from the HTA empirical approach for the good quality bedrock rock (which is predominant). A significantly lower friction angle value of 15° was also used for a set of sensitivity analyses.

Table 10-14: Structural set characteristics

Set	Orientation			Set weighting factor	Rock unit weight (kN/m ³)	Properties		
	Dip (°)	Dip direction (°)	Std Dev			Friction angle (°)	Std Dev	Cohesion (kPa)
1	52	304	20	1	27	27	3	0
2	59	255	20	1	27	27	3	0
3	54	203	20	0.75	27	27	3	0
4	4	75	30	0.75	27	27	3	0
5	55	46	20	0.75	27	27	3	0
6	72	135	20	0.5	27	27	3	0
7	35	147	25	0.5	27	27	3	0

Spill berm width optimisation analysis

A bench height of 20 m and batter face angle (BFA) of 80° have been analysed. The analyses were conducted to identify:

- The largest spill berm width (SBW) required to contain the volumes of failed material generated by the various common wedge failures (considering an FoS of ≤ 1.1) – identified by deterministic and methods
- The probability of failure (PoF) of wedges for FoS of ≤ 1.1 .

The results of the wedge failure analyses are presented in Table 10-15.

Table 10-15: Results of spill berm width optimisation analysis

Batter height (m)	Wall dip azimuth (°)	Friction angle (°)	Joint persistence (m)	BFA (°)	SBW required (m) (for FoS ≤ 1.1) Deterministic	PoF (%) (for FoS ≤ 1.1)
20	280	27 +/- 3	20	80	9.75	49.5
20	300		20	80	2.18	48.6
20	320		20	80	7.02	49.3
20	100		20	80	9.91	29.8
20	280	27 +/- 3	10	80	4.87	50.1
20	300		10	80	1.09	47.5
20	320		10	80	3.51	49.6
20	100		10	80	5.87	30.6
20	280	15 +/- 3	10	80	4.87	65.7
20	300		10	80	1.09	64.7
20	320		10	80	3.51	67.5
20	100		10	80	5.87	48.9
20	280	15 +/- 3	20	80	9.75	65.5
20	300		20	80	2.18	64.3
20	320		20	80	7.02	67.9
20	100		20	80	9.91	49.1

The results of the deterministic analyses for SBW optimisation indicate that the existing design of 10 m (for batter height 20 m and BFA of 80°) will be sufficient to contain the likely wedge failure volumes. For some scenarios, favourable face orientations relative to structural sets indicate that SBWs of significantly lesser width could be accommodated; however, these are not considered practical due to the following:

- They would result in unacceptable steep bench stack and overall slope angles
- According to the empirically-derived modified Ritchie equation (Ryan and Pryor, 2000⁹⁰), the minimum required SBW = (0.2 × batter height) + 4.5; therefore, SBWs of at least 8.5 m would be necessary for a 20 m high batter.

The calculated theoretical PoF for wedges are high: from ~30% to ~65% depending on the batter face orientation and the friction angle assumed. This is due to the predominant orientation of structures dipping at moderate angles, particularly out of the eastern cut slopes. This would normally be considered unacceptably high; however, it has not been used as a constraint on the batter-berm design because of the following:

- It is considered from drill core observation that the actual numbers and spacings of the joints in the various sets are actually relatively low within the generally good-quality rockmass, and likely with limited persistence; therefore, the actual spatial probability of occurrence of wedge failures is likely to be relatively low, and the wedge sizes are likely to be moderate to small
- The means of mitigating PoF is to significantly reduce the batter angles. Doing so without reducing the SBW would result in a reduction of the BSA/ IRA by as much as 10°. The impact of this would be to significantly increase the height of the cut slopes within the steep hillsides, which may

⁹⁰ Ryan, T.M. and Pryor P.R., 2000. Designing catch benches and interramp slopes. Slope Stability in Surface Mining pp 27-38 SME Colorado.

adversely impact overall slope stability. Therefore, it is not considered a practical solution in light of the risk (probably overstated by the analyses) posed by bench crest loss due to wedge failures.

Overall slope stability analyses

Method

2D limit equilibrium analyses for assessing the overall stability of the final SRK quarry and spillway cut slope design were undertaken using Rocscience *Slide* Version 7.0 software⁹¹. This utilised both circular and non-circular failure paths and the Morgenstern-Price analysis method. Generalised Hoek-Brown rockmass input properties were used, and the failure area was unrestricted. When assessing the impact of faults, the analyses were run using non-circular surfaces and block search mode associated with drawn polyline (and still using the Morgenstern Price method), to force the failure to go through the fault.

The type of stability analyses carried out are appropriate at this (SPS) level of study, with the associated timeframe. However, it is acknowledged that in places, due to the complexities of the steep terrain, a 3D model may have provided more accurate results locally. Also, more complex analyses using finite element or finite difference methods may also refine the stability assessment for the expected predominant rockmass conditions (relatively sparse jointing but with small scale faults). Such analyses can better incorporate probabilistic rockmass variability and can utilise dynamic seismic loading. Such analyses may be considered for the next phase of study; however, the results of the current analyses provide a reasonable indication of slope performance range at this time.

Three sections were selected and analysed to assess the stability of the quarry and spillway cut slopes, based on the latest SRK design. The positions of these are shown in Figure 10-25. Section 1 was positioned through the centre of the quarry slope, and Sections 2 and 3 were positioned through the spillway cut. It is important to note that, at the quarry site in particular, the relatively steep natural hillsides extending upwards from the crest of the cut slopes play a role in the performance of the slopes overall. The minimum factor of safety (FoS) slip circles identified included the entire cut slopes, and often extended into the natural slope above.

⁹¹ Rocscience Inc., 2016. *Slide Version 7.0 - 2D Limit Equilibrium Slope Stability Analysis*, www.rocscience.com, Toronto, Ontario, Canada.



Figure 10-25: Plan view showing positions of analysis sections relative to the initial quarry and spillway design

A range of sensitivity analyses was conducted to assess the impacts of various factors on the slope performance, as described in the following sections.

Material properties

Each section was assessed with input properties for ‘weathered rock’ (denoted ‘SW’ in the sections) in the upper part of the bedrock down to ~ 20 m depth. In the predominantly unweathered rock beneath this, alternative properties were assessed for good-quality ‘fresh’ rock (the predominant conditions) and alternatively for altered/ serpentinised rock. The thin (less than 5 m thick) layer of colluvial material was not included in the analysis sections because it will have no impact on overall slope stability of the cut slope sections, and it is accepted that localised superficial landslides of relatively small volume within this material can occur from time to time in the natural hillsides after periods of heavy rain. Such slips will have to be managed and contained as part of the slope maintenance and management processes developed for construction and operation.

Rockmass properties for fresh rock, deteriorating serpentinised rock and weathered rock used in the *Slide* models are presented in Table 10-16. The assessment of rock mass strength parameters for the slightly weathered and fresh material was carried out using the non-linear Hoek-Brown failure criterion (2002)⁹². The Hoek-Brown criterion relates the strength envelope to rock mass classification through the Geological Strength Index (GSI). Input values for uniaxial compressive strength (UCS),

⁹² Hoek, E, Carranza-Torres, C and Corkum, B, 2002. Hoek-Brown Failure Criterion – 2002 Edition. 5th North American Rock Mechanics Symposium and 17th Tunnelling Association of Canada Conference: NARMS-TAC, 2002, pp 267-271.

m_i , GSI (RMR89-5), vertical stress ($\sigma_{3 \max}$), and disturbance factor (D) were used to calculate σ'_n (kPa) and τ (kPa), entered in *Slide* as a shear/ normal function. The input values were obtained/ interpreted from rockmass classification and laboratory testing. The values for GSI and UCS were based on the statistics produced for each domain, complemented by engineering judgement. Note that there is some difference in the representative GSI and UCS properties for the fresh rock adopted for the quarry and spillway. The intact material constant (m_i) has been estimated based on engineering judgment and consideration of published values.

The disturbance factor for the rockmass, used in the Hoek-Brown criterion to account for blasting damage and dilation due to unloading of the rockmass during excavation, was varied. A D factor of 0.5 has been used for the first case, indicating little blast damage due to very good blasting with pre-splitting (which has been specified in order to minimise damage to the rock face), and very little unloading effect. However, as the analyses show that slope failure (should it occur) will likely be deeper-seated, blast damage is unlikely to affect the rock mass properties within the planes/ surfaces of instability. Dilation due to unloading is unlikely to be significant, as excavation will have taken place backwards into an existing hillside (i.e. the volumes of excavated material contributing to the unloading effect is relatively small). Therefore, a second case with D factor of zero has been analysed, and this less conservative approach is considered to be more representative.

Table 10-16: Rockmass properties used in *Slide* slope stability analyses

Parameter	Quarry (Section 1)			Spillway (Sections 2 and 3)		
	Fresh	Deteriorating	Weathered	Fresh	Deteriorating	Weathered
UCS (MPa)	80	40	40	60	40	40
Geological Strength Index (GSI)	62	50	50	65	50	50
Material constant, m_i	20	20	20	20	20	20
Disturbance Factor, D	Cases analysed for 0 and 0.5					
Unit weight (kN/m ³)	32	32	28	32	32	28

Influence of faults

A set of faults (Set B, as described in Section 3.1.10) have been modelled as four planar surfaces, some of which have been included in each Slide section. The faults are sub-parallel to the natural hillslopes in the right abutment (N-S striking, W-dipping, moderate angle), and have relatively narrow damage zones. Two faults are present in the near vicinity of the quarry east highwall and have been considered in the stability analyses for Sections 1 and 2. For sensitivity assessment, only one fault at a time was modelled. Stability analyses, including faults, have not been carried out for Section 3, as it was determined that the results for Section 2 would be more conservative in this regard and thus generally representative for the spillway.

The faults were modelled with a thickness of ~1 m, as observed in the core photographs. The fault zone properties were represented using a Mohr-Coulomb model, which requires friction and cohesion values as inputs. Table 10-17 lists the fault properties. The cohesion and friction angle values of 150 kPa and 30° were assumed based on the more typically fractured nature of the fault zone (i.e. faults contain fragmented rock or fragmented rock with minor clay, and thick clay or gouge was seldom logged), and the likely large-scale waviness of the structures over significant distances compared with the width of the fault zone – necessitating shearing of the rockmass asperities for mobilisation. The destabilising effects of faulting on large-scale slope instability may be significantly exaggerated in 2D analyses, due to the local variability of the terrain and the likelihood that the faults may not necessarily represent single continuous planes but rather anastomosing sets of structures

(as mentioned in Section 3.1.10). This would present a large degree of waviness and more constrained persistence.

Table 10-17: Summary of fault properties

Material	Cohesion c' (kPa)	Friction angle ϕ' (°)	Unit weight γ' (kN/m ³)
All faults – Set B	150	30	20

Seismic loading

The stability of the cut slopes was analysed for static conditions, and pseudo static analyses were also initially performed for a range of seismic loading peak ground acceleration (PGA) values, of 0.2g, 0.4g, 0.6g and 0.8g. In addition, the stability of the natural hillslopes (i.e. without excavation) were analysed under static conditions and with loadings of 0.2g and 0.4g.

Groundwater

A groundwater surface interpretation was created using Leapfrog software, by the means of an interpolation using the topography patterns and the downhole recorded water levels and piezometric values (described in Section 3.1.1). This surface was then adjusted to the quarry/ spillway profile using a 15–20 m pushback behind the slope and considering a reasonable drawdown shape. This pushback can likely be achieved using short (~25 m long) stab holes drilled at regular intervals into the face by production drill rigs during excavation of the quarry and spillway. Figure 10-26 shows the groundwater surface utilised for Section 1.

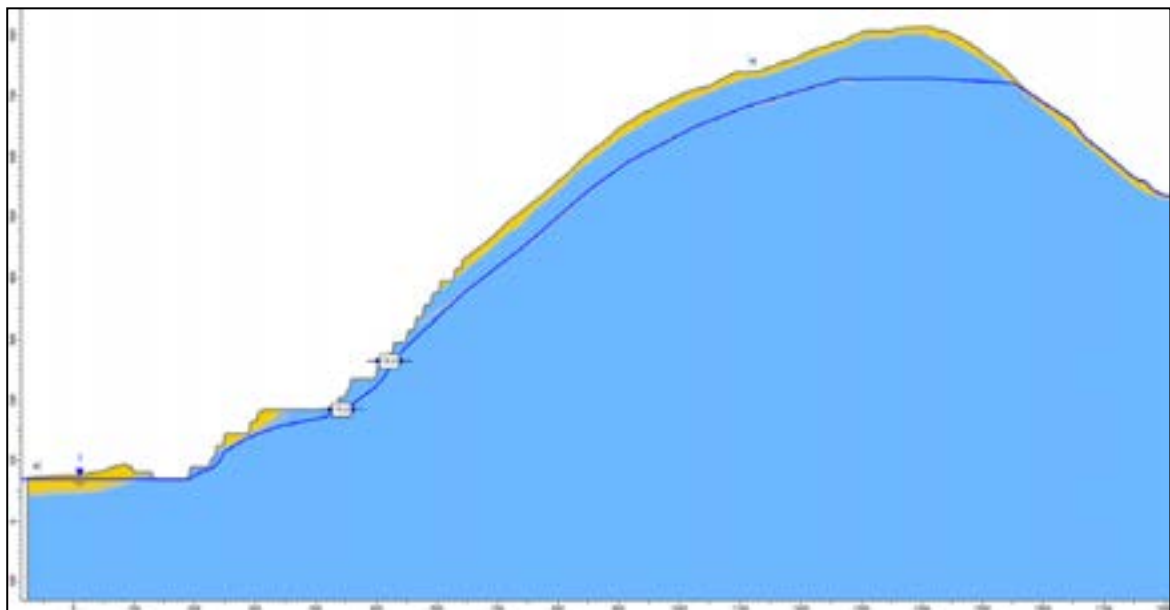


Figure 10-26: Example section looking north showing groundwater surface adjusted to the quarry profile

Basis of design – factor of safety and seismic loading

The long-term risk profile for the quarry is theoretically lower than for the spillway. Once the embankment has been completed, the quarrying operations have finished, and the reservoir is full, the immediate ongoing risk of quarry instability to on-site activities will be much reduced and the water will provide some degree of buoyant support to the lower section of the cut slopes/ hillsides. However, the risk and/ or impact of slope failures into the quarry and nearby construction activities during construction, and the potential effect of slope failures post construction and reservoir-filling (with resultant displacement of water nearby to the embankment) have resulted in a target FoS of 1.5 being

adopted for the quarry slopes under static conditions, and a target FoS of 1.1 under pseudo static loading.

The same FoS criteria have been adopted for the spillway, where the slopes will need to remain stable in the long-term post closure, once all operational tunnels have been blocked and the spillway gates have been removed. The seismic loading adopted as the basis of design would in theory need to be greater for the spillway, based on the risk profile in the long term (i.e. a higher loading corresponding to a longer return period should be adopted).

The basis of design (BoD) regarding pseudo static loading is not straightforward to define. There is almost no existing literature providing guidelines or obvious benchmarking on appropriate seismic loading PGA values for pseudo static stability analyses, specifically for spillway cut slopes, and appropriate values would depend on the long-term risk profile for the spillway and quarry. It could be argued that it is not allowable for a large-scale slope failure to block the spillway at any time before or after closure. Therefore, it could be suggested that a PGA for a return period of at least 10,000 years (i.e. a PGA corresponding to a maximum credible earthquake (MCE)) should be adopted as a basis for design for the spillway cut slopes – as it often is for spillway engineered structures. The PGA for an MCE at the FRHEP site has been determined as $\sim 1.1g$. It could be considered that an OBE earthquake event (475-year return period) would be suitable for the quarry slopes, with equivalent PGA of $\sim 0.5g$.

Seismic loading represented as a pseudo-static load is acknowledged to significantly overstate the actual loading effects. There is common acceptance in the mining industry that modelling of seismic loading (especially by pseudo-static means) significantly overestimates the likelihood of large-scale slope failure in strong rock masses. Smaller-scale failures of individual batters are far more likely, but these will not have a significant impact on the spillway. In the Guidelines for Open Pit Slope Design (Read & Stacey, 2009)⁹³, it is stated that horizontal PGA of half to one third of the basis for design value should be adopted for large-scale slope stability analysis if pseudo-static loading is used.

Therefore, it is considered reasonable that a horizontal PGA seismic loading coefficient of $\sim 0.4g$ be used as the basis of design in the analyses for the spillway slopes and a PGA seismic loading coefficient of $\sim 0.2g$ for the quarry slopes where seismic loading is represented as pseudo-static.

Initial analyses and revision of designs

Based on the results from an initial comprehensive set of stability analyses, significant re-design of the cut slopes in both the quarry and the spillway was assessed in conjunction with the SRK mining engineering team. This was done in order to meet the BoD acceptance criteria and improve the practicality of the design. The initial set of analyses had illustrated the impact of faults on the stability of the west-facing slopes, particularly under extreme seismic conditions, and numerous sensitivity analyses were conducted in order to understand the mechanisms of potential instability and to improve the design.

⁹³ Read, J and Stacey, P, 2009. Guidelines for Open Pit Slope Design, 496 p (CSIRO Publishing: Collingwood).

A series of new design profiles/ plans were considered and evaluated, resulting in design revision P3. This revision included:

- Significant reduction (approximately 10°) in overall slope angle for the spillway cut slopes
- Significant increase in slope height, with corresponding increase in quarried rockfill volume, for the spillway cut slopes
- Significant decrease in slope height and quarried rockfill volume for the quarry area
- Wider (35 m) working berms/ platforms for the cut/ quarrying activities, with bench stacks reduced from 100 m in height to 60 m in height.

The revised slope design parameters are presented in Table 10-18, and the revised spillway and quarry designs generated are illustrated in Figure 10-27.

Table 10-18: Revised slope design parameters

Parameter	Revised recommendation
Batter (bench) height	20 m
Batter angle	80°
Berm width	10 m
Inter-ramp angle (toe to toe)	52.2°
Bench stack angle (crest to toe)	60°
Geotechnical safety berm	35 m width every 60 m vertically

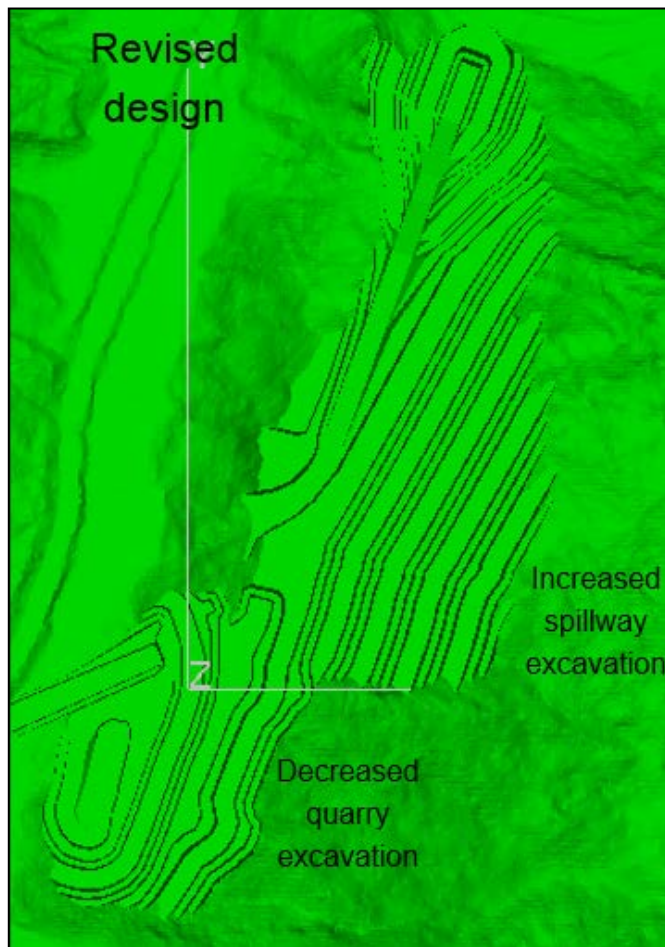


Figure 10-27: Illustration of the previous and revised spillway and quarry designs, with comparison sections (looking north) of cut slope profiles

Results of overall slope stability – assessment of revised cut slope designs

A summary of the results of the most relevant slope stability analyses for the revised cut slope design profiles is presented in Table 10-19. The results are expressed in terms of minimum FoS for slope instability. FoS below the target (BoD) are indicated in orange text, and FoS below 1 (theoretical slope failure) are indicated in red text.

Table 10-19: Summary of results of slope stability analyses for the revised cut slope profiles

Section	Fresh rock UCS (MPa)	Fresh rock GSI	Seismic load coefficient PGA (g)	Non-circular failure: block with polyline		
				FoS with discontinuous Fault 3	FoS with discontinuous Fault 4	
					Prior to reservoir filling	After reservoir filling (with buoyant support)
1 (Quarry area)	80	62	0	1.37	1.58	
	80	62	0.2 (OBE)	1.02	1.24	1.27
	80	62	0.4 (MCE)	0.92	0.88	0.88
2 (Spillway South area)	60	65	0	Fault 3 mined out	2.12	
	60	65	0.2 (OBE)		1.65	
	60	65	0.4 (MCE)		1.27	

The following main outcomes were from the set of detailed overall slope stability analyses carried out for the revised slope profiles:

1 Quarry slopes

- The stability analyses for the revised slope design in the quarry have indicated stable slopes under static conditions and under OBE earthquake conditions. Where fault structures are close to the face in the quarry slopes, however, slope stability is still highly sensitive to the persistence of fault structures, particularly under seismic conditions. FoS under OBE conditions are less than target (FoS of 1.1) where highly persistent faults are present, but are well over target if faults are discontinuous.
- Under MCE earthquake loading, quarry slopes are still indicated to fail, even though the height and angle of cut slope design has been much reduced – this is due to the nature of the very steep natural slopes above the quarry (even the natural slopes may be only marginally stable under such high seismic loading).
- Under very high seismic loading, even buoyant support from water-level rise in the reservoir does not provide any benefit. The rising water level also does not have any negative impact on the slope stability because the groundwater levels analysed assumed the faults in the lower slope to be wet (i.e. pressurised) even prior to water level rise.

The mitigation of slope failures might be achieved by effective slope depressurisation; however, it is likely that significant groundwater pushback would need to be achieved (which may not be possible).

2 Spillway slopes

The stability analyses for the revised slope design in the spillway have indicated stable slopes, with FoS above target, under static conditions and under OBE and MCE earthquake conditions.

During future study phases, the following analyses are recommended to provide better understanding of the risk of instability, and to further refine the design of cuts slopes (if necessary):

- 2D (or 3D if necessary) complex numerical modelling to more accurately assess the stability of the right abutment hillsides, particularly the slopes created after excavation of the quarry and spillway cuts, under dynamic seismic loading. Establish the impact of rapid drawdown and the effect it may have, particularly in conjunction with surrounding geological features, such as faults.
- Perform seepage analyses to assess the likely groundwater profiles upon excavation of the spillway and quarry cuts, to assess the potential pressurisation of faults of high hydraulic connectivity and persistence, and to assess the need for and effectiveness of passive drainage measures (drainholes).

Results of overall slope stability analyses - natural slope profile

For comparison, *Slide* analysis were also undertaken considering the natural slope profile, again using various sets of properties for the fresh material and also different seismic loading values. A summary of the results of the most relevant slope stability analyses for the natural slope profiles is presented in Table 10-20. FoS below the target (BoD) are indicated in orange text, and FoS below 1 (theoretical slope failure) are indicated in red text.

Table 10-20: Slide results and sensitivity assessments for the natural slope profile

Section	Fresh rock UCS (MPa)	Fresh rock GSI	Seismic load coefficient PGA (g)	Circular failure	Non-circular failure	Circular Failure	Non-circular failure: block with polyline	
				Without Faults			With Fault 3	With Fault 2
				FoS with D=0.5	FoS with D=0.5	FoS with D=0	FoS for straight, continuous fault	FoS for straight, continuous fault
1 (Quarry area)	80	62	0	2.24	2.27	2.6	1.97	
	80	62	0.4	1.16	1.15	1.34	1.24	
	80	62	1.09	0.43	0.43	0.49		
2 (Spillway South area)	60	65	0	2.6	2.51			1.38
	60	65	0.4	1.3	1.27	1.49		0.81
	60	65	1.09	0.5	0.51	0.57		

From the results of the analyses for the natural hillsides, the following key results are evident:

- Where the MCE of 1.09 g is used with no reduction for use of pseudo-static loading, the FoS for the natural hillslopes in the right abutment and hillsides are well below 1, indicating failure. This is considered to be a significant over-representation of seismic loading, however.
- If structures of great persistence are present in the quarry area, FoS for natural hillslopes under BoD seismic conditions and static conditions are well above 1.1 and 1.5 respectively.
- If structures of great persistence are present in the spillway area, FoS for natural hillslopes are somewhat below 1.5 under static conditions, and are less than 1 (indicating failure) under BoD seismic loading of 0.4 (for an MCE). This indicates that the natural hill slopes in the spillway area may be unstable in the event of an MCE due to the weakening effects of faults (if they are highly persistent).

11 Landslides

Landslides that have the potential to impact the FRHEP can develop from aerial or subaqueous sources. Aerial landslides occur due to failure of stability and mass movement of material from the slopes surrounding the FRHEP. Local conditions – steep terrain, high rainfall, seismic events and changes to river flows – all increase the risk of aerial landslides developing. Subaqueous landslides could result from the mass movement of material due to instability generated by tailings and waste rock deposited in the reservoir.

The impacts resulting from both landslide types can be direct due to the mass movement of material, or indirect from subsequent wave development. As part of the SPS, wave size modelling was undertaken to define the potential size of waves that may develop as a result of aerial or subaqueous landslides. Further assessments are required to assess potential impacts from landslides.

11.1 Aerial landslide risk

A desktop geohazard assessment was undertaken as part of the SPS to identify the landslide risk of areas within the FRHEP catchment (Section 3.2). Geohazard rankings of the FRHEP catchment were made following the use of geology, hydrology and slope stability inputs, and interpretation of LiDAR and STRM data. The geohazard ranking ranges from Very Low to Extreme (Figure 11-1).

Class	Range	Geohazard
1	0–20	Very Low
2		
3	20–28	Low
4		
5	28–30	Moderate
6		
7	30–38	High
8		
9	38–41	Very High
10	41–56.5	Extreme

Figure 11-1: Geohazard ranking

The area close to the FRHEP site is likely to experience small-scale slope failures within the thin layer of colluvial material overlying the bedrock on the steep abutments, most likely after heavy rains. For the purpose of the SPS, aerial landslides have only been considered for the following high risk areas identified during the geohazard assessment (Section 3.2):

- Headwaters of the reservoir (Figure 11-2) – high risk during early filling of the reservoir, operations and closure
- Close to the embankment (Figure 11-3 and Figure 11-4) – potential to impact the FRHEP during construction, operations and closure
- Immediately downstream of the embankment – may impact the FRHEP during construction, operations and closure.

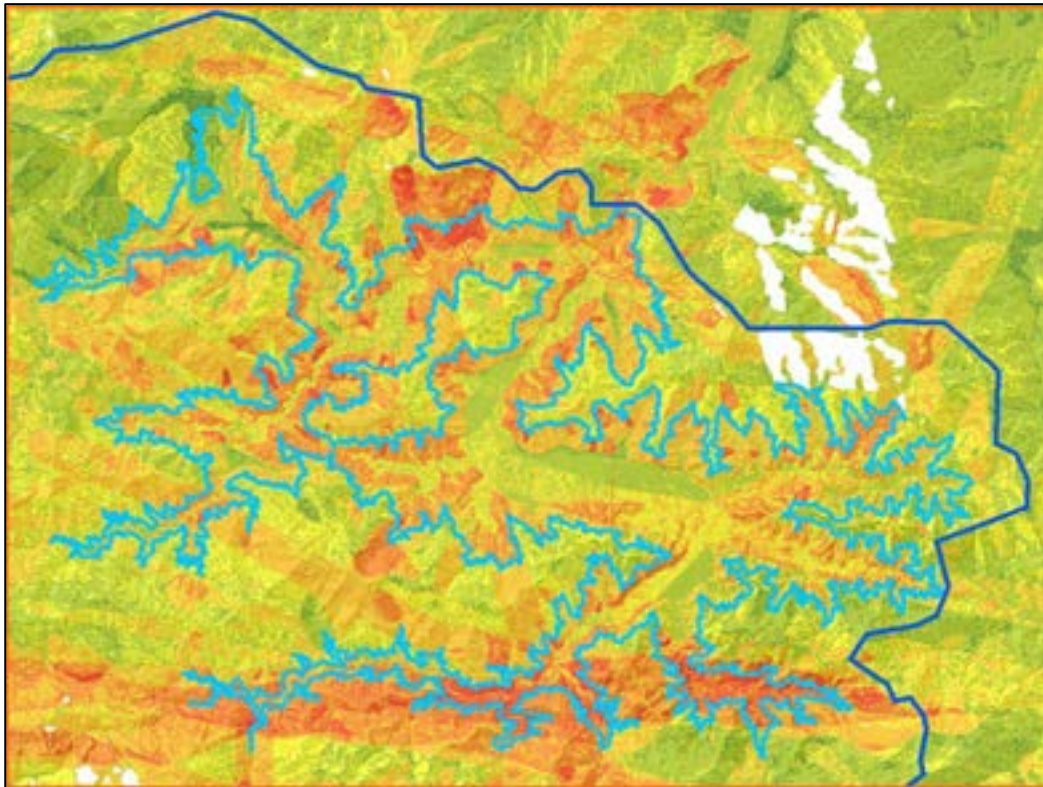


Figure 11-2: High geohazard risks at the headwaters of the reservoir

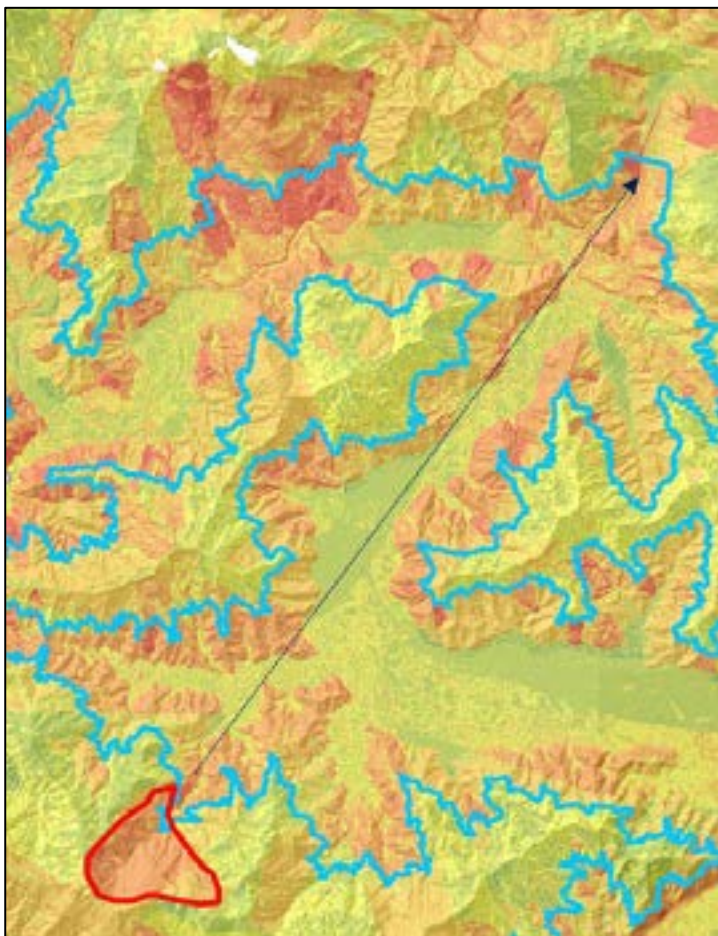


Figure 11-3: High geohazard risk opposite the embankment

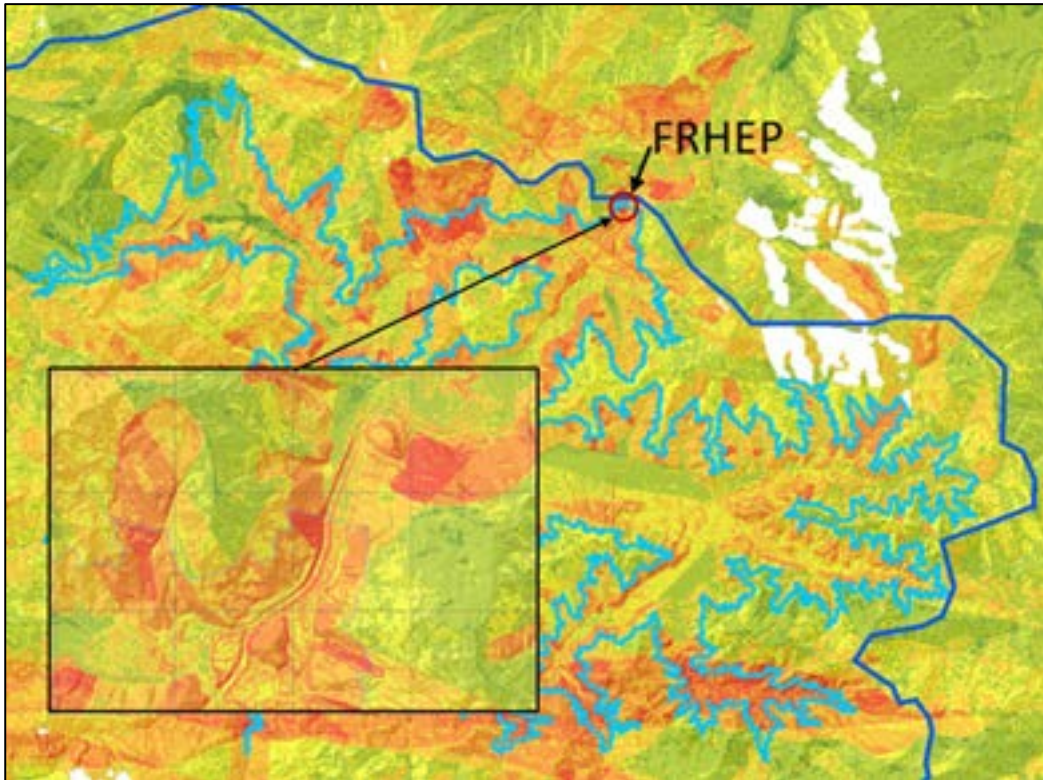


Figure 11-4: High geohazard risk at the embankment

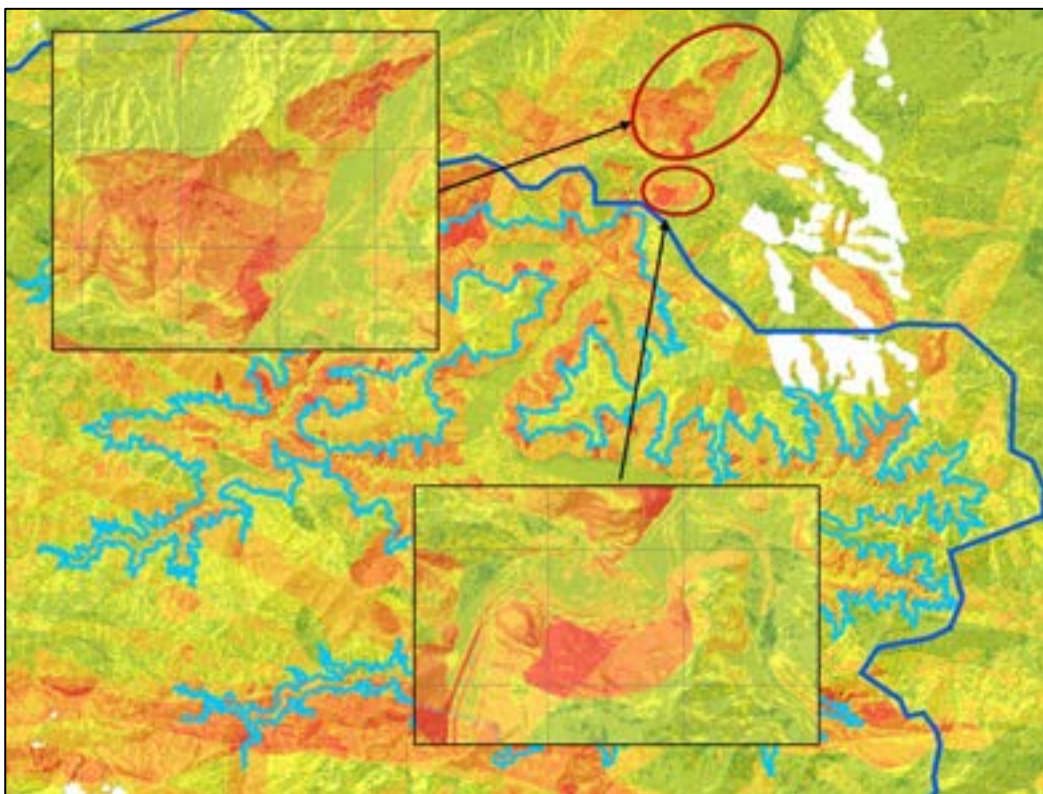


Figure 11-5: High geohazard risk downstream of the embankment

Areas around the reservoir (Figure 11-2) have an increased risk of landslide development during filling of the reservoir and due to fluctuating water levels during FRHEP operations. Large landslides could generate waves of a substantial size that have the potential to cause significant damage to FRHEP components, including equipment operating on the reservoir and at the reservoir margins. Various

scenarios related to wave size and proximity to the embankment have been analysed; Table 11-1 indicates wave sizes generated by landslides according to different material volumes and associated available freeboard at the closest proximity of the dam. Arbitrary landslide sizes were selected for investigation of potential wave impacts. Landslides with volumes between 10,000 m³ and 100,000 m³ would be expected to generate waves that, depending on the operating level at that time, may overtop the embankment. Other factors such as landslide mass velocity, location of landslide relative to the embankment etc. will affect the size of the wave being generated and the size of the wave when it reaches the embankment. The likelihood and risk of landslides needs to be further assessed during future studies.

Table 11-1: Wave amplitudes generated by landslides

Operation cases	Depth of reservoir water to RL 148 m (m)	Wave amplitude, a _m (m)			Available freeboard (m)
		V = 1,000 m ³	V = 10,000 m ³	V = 1,000,000 m ³	
Maximum operating level	78.1	3.1	6.9	39.9	12.4
No power to export grid	56.4	3.3	7.4	42.5	34.1
Minimum operating level	51.4	3.4	7.4	43.3	39.1

Note: V = landslide volume

A landslide generated from a zone previously identified directly opposite the embankment (Figure 11-3) would likely generate waves higher than those in Table 11-1. A conceptual assessment of landslide size revealed that this zone may be more than 100 Mm³ in size. Hole OE1, drilled during the Stage 1 investigations, showed that the geological map is incorrect – this spur is composed of phyllite which is present below the thrust fault. Therefore, the thrust contact will be above the reservoir level, and the mechanism of failure proposed by Scott Wilson is considered unlikely to occur. However, the position and nature of the topographical feature is such that a degree of associated geohazard risk remains

Zones with a high geohazard risk rating downstream of the embankment (Figure 11-5) may result in backwater build-up and associated flooding of the powerhouse or construction site due to a large landmass failure blocking the downstream valley. It appears that the downstream valley opens up a short distance beyond what has been indicated in the drawing, but this has to be confirmed. As recommended in the geohazard assessment, a field investigation would be required to further characterise this zone.

The embankment zones (Figure 11-4) have been investigated and are reasonably well understood.

Small-scale slope failures within the thin layer of colluvial material overlying the bedrock on the steep abutments at the FRHEP site are most likely to occur after heavy rain and be very limited in extent. The risk would be increased where vegetation cover is removed.

SRK's Geotechnical Investigation (Section 3.1) and earlier hazard mapping by Scott Wilson (2011) have both indicated the presence of larger volumes of material close to the embankment that may have undergone limited downslope movement or that may in the future present potential risk of landslides of greater volume. Two such areas (shown in Figure 11-6) are notable:

- 1 A large volume of highly fractured, oxidised material with deteriorating matrix and soil-like infills forming the crest of a spur on the left hand (LH) abutment within, above and slightly upstream from the embankment footprint. This zone has been encountered in several drillholes, and can be

delineated with a degree of accuracy; however, its precise upslope extent has not been delineated with confidence.

The feature on the left abutment has significant consequences to the surrounding embankment and associated infrastructure during construction, operations and closure, in terms of volume of material that will need to be removed, and the risk of slope instability.

- 2 A zone of colluvial boulders of greater thickness than usual, with an underlying zone of fractured, oxidised and infilled rock below. This zone is situated in a shallow ravine to the north of the embankment footprint in the right abutment, upslope from the proposed powerhouse location. This zone has been encountered in only a single drillhole, so its extent is not well understood but has been extrapolated using topographical observation. The thickness and lateral extent of this zone is far smaller than the zone on the left abutment.

Due to its position, failure or movement of this zone may affect the integrity of the spillway excavation in that particular location or impact the powerhouse located directly downstream. This feature will therefore present a risk not only during operation and closure, but also during construction.

Figure 11-6 presents an interpretation of the extent of the two zones.

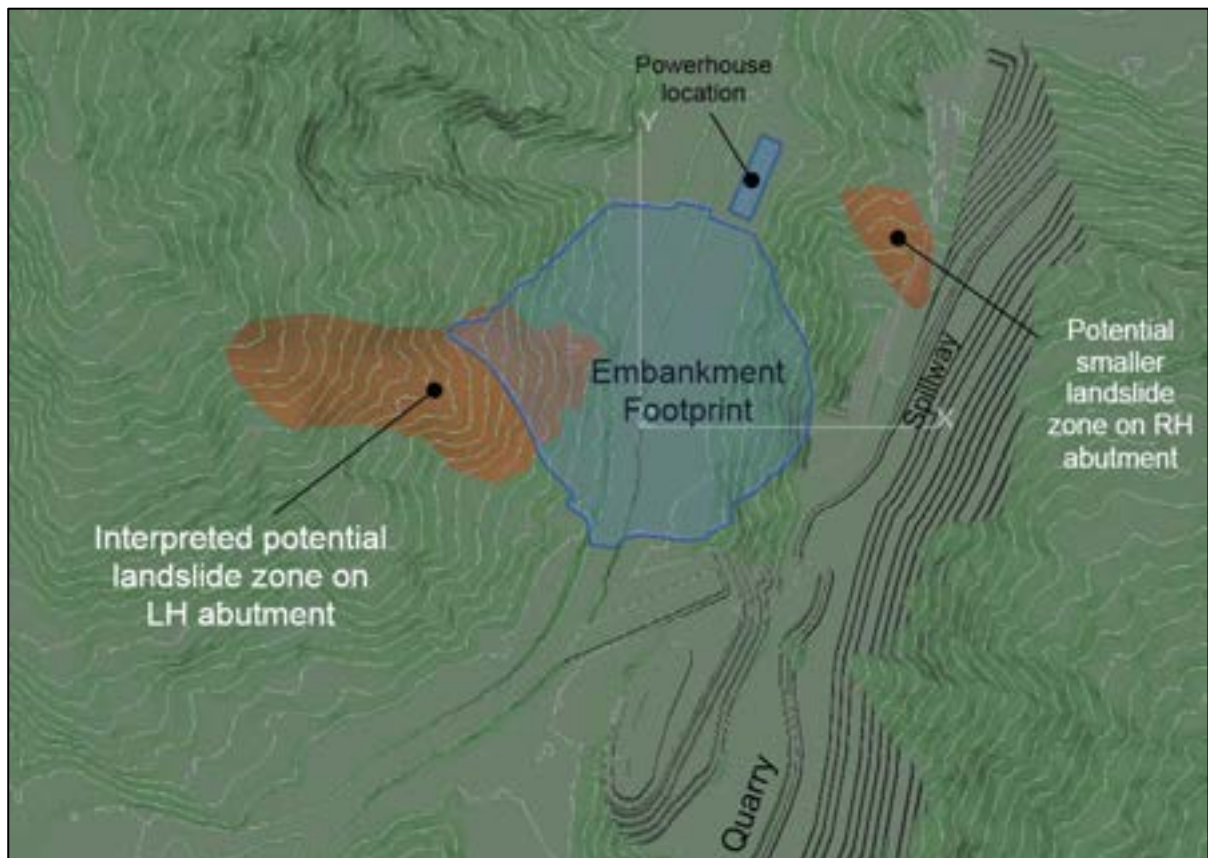


Figure 11-6: Plan view of surface conditions at the embankment site

The following section (Section 11.1.1 and 11.1.2) describes SRK's interpretation of the two features and the proposed method for managing each of them.

11.1.1 Characterisation

Right abutment feature

Figure 11-7 presents the potential unstable zone in the right abutment and the holes drilled close to this area. Figure 11-8 presents a cross-section of this feature. The estimated potential material volume is 63,000 m³.

The drilling campaign conducted by SRK included a few drillholes near this feature: HT1, SW3 and SW4. Only hole SW4 intersected the thicker zone (~20 m thick) of boulders, colluvium and oxidised rock, so its extent is not well understood but has been extrapolated using topographical observation. Figure 11-9 presents a typical core photograph of the material found in this zone.



Figure 11-7: Plan view of potential unstable zone (in green) and drillhole locations in the right abutment

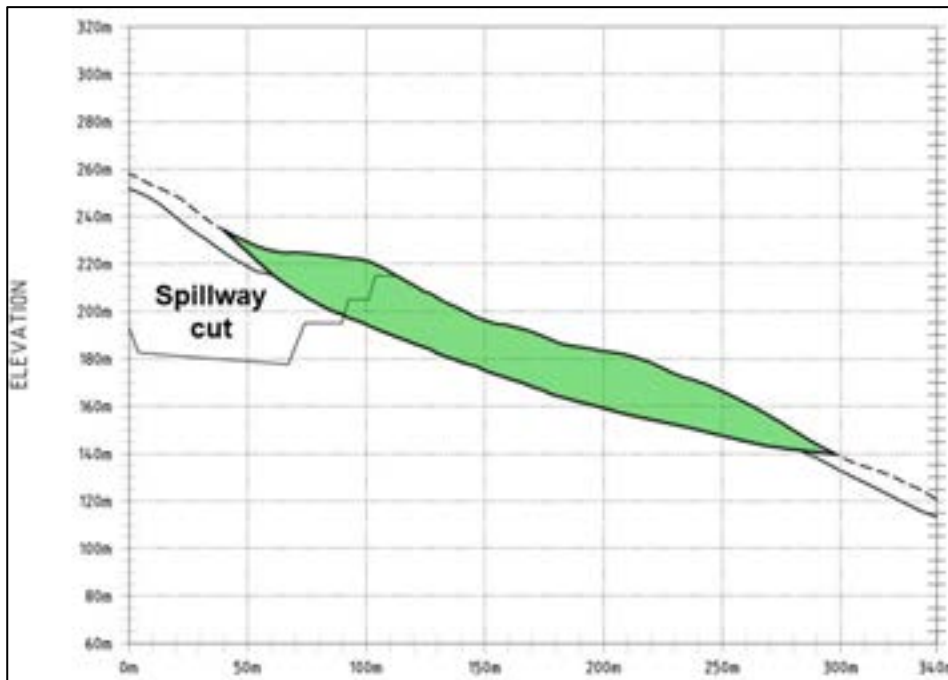


Figure 11-8: Section A of the potential unstable zone (in green)



Figure 11-9: Drillhole SW4 from 17.5 to 19.9 m, showing boulder overburden material over the bedrock

The overburden material consists almost entirely of transported material and is a mixture of cobbles and boulders embedded in a silty, clayey matrix. The proportion of cobbles and boulders (some in the order of 1 to 2 m in size) ranges from about 30 to 80% by volume, and are sub-angular. They are composed exclusively of fractured and slightly weathered dunite. The matrix consists of orange clayey silt of high plasticity. The underlying dunite bedrock has strong oxidised, infilled joints.

Left abutment feature

During the drilling campaign conducted by SKM in 2010/11⁹⁴, drillholes S1, S2 and G1B intersected and identified this feature (Figure 11-10). Hole G1 had to be abandoned at a depth of only 7 m, still within the colluvial material, due to sliding of the overburden material. Holes S1 and S2 encountered a thick sequence of poor quality overburden and highly fractured, oxidised rock; more than 30 m in S1 and more than 70 m in S2. However, G1B, approximately 60 m upslope above the abandoned G1 site, encountered only 14 m of overburden material. From the observation of these drillholes, SKM concluded that this area presents a dislocated, slightly creeping slope mass. Drillhole G1B was equipped with an inclinometer for monitoring; however, no information has been recorded from this hole by Xstrata or PanAust over the years, and its collar position needs to be re-established. SKM originally recommended that additional inclinometers be installed at S1 and S2 to inform future assessments and decisions, along with data from adjacent groundwater piezometers. However, the installations were never carried out.

The drilling campaign conducted by SRK in 2017 and 2018 included five drillholes near the feature: holes LH3, LH4, LH5, LH6 and LH7 (Figure 11-10). These holes, and a seismic refraction traverse conducted by Draig Geoscience Pty Ltd, were used to further define, explain and delineate this potentially unstable feature. This feature is described in the SRK Geotechnical Investigation (Section 3.1).

The overburden material is a soil-like colluvial, which in places has boulders with similar characteristics to the overburden material found in the right abutment. The underlying material consists of a large zone of highly fractured/ oxidised rock, in places with breakdown of matrix comprising previously re-cemented and oxidised breccia. The overburden and underlying highly fractured and oxidised rock together form the unstable zone. Significant thicknesses of this zone (up to 115 m of drilled thickness; ~75 m normal to the slope) were encountered in drillholes S02 (an old 2011 investigation hole), LH3 and LH7. Lesser thickness of such materials was encountered in LH5 and S01, which are on the northern margin of the zone; the zone is not present at all in LH4 drilled to the south. LH6, downslope to the east, encounters a more regular profile of bouldery colluvium nearer the toe of the slope.

The fractured rock material is most probably less 'bouldery' than it appears in the drill core, and will likely be more 'slabby' overall (large slabs of rock with poor quality shear areas). SRK interprets the feature to be the result of numerous parallel shear zones, dipping eastwards into the valley at a similar angle to the overall slope on the left abutment. The nature of the material in terms of locally high permeability, and the risk it presents during construction and maintenance of the embankment and associated infrastructure (especially where undercut at the toe), means that it will need to be removed prior to embankment construction. The large volumes of relatively intact rock within the zone indicate that it will require blasting for excavation and removal. Examples of the material in this potentially unstable feature are shown in Figure 11-11, Figure 11-12 and Figure 11-13.

⁹⁴ SKM 2011, Frieda River Feasibility Study. Power generation and transmission. Document Number FRP03-2200-EC-RP-0001_0_Geotech_Report

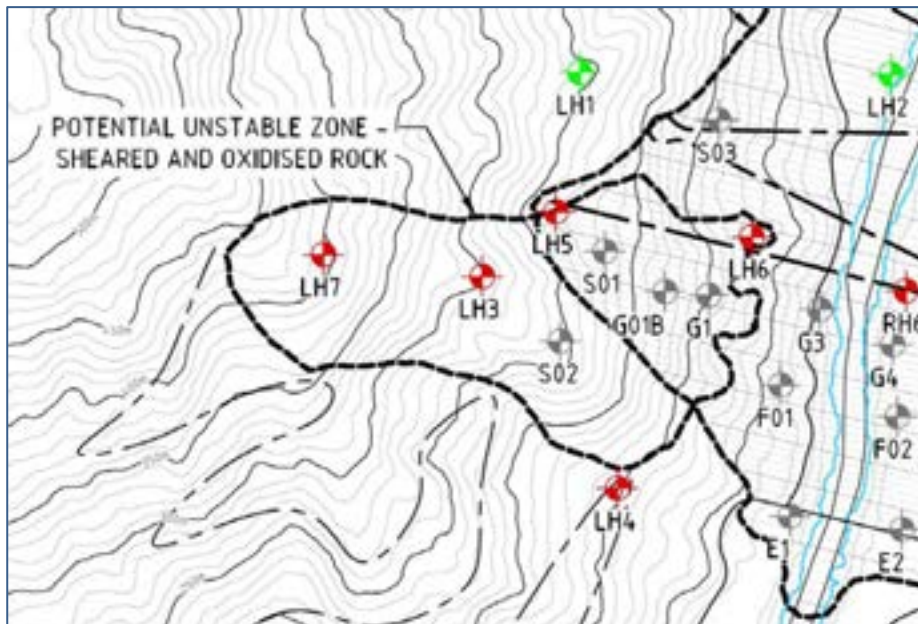


Figure 11-10: Plan view indicating approximate extent of the potential unstable zone on the left-hand abutment, with reference to the drillhole collar positions



Figure 11-11: Core photograph showing soil-like overburden material immediately above highly fractured rock in drillhole LH7, from 6.4 m to 10 m depth





Figure 11-12: Core photographs showing variability of zones of highly fractured and oxidised rock with deteriorating matrix and/ or soil-like infill in drillhole LH3, from 66 m to 80 m depth

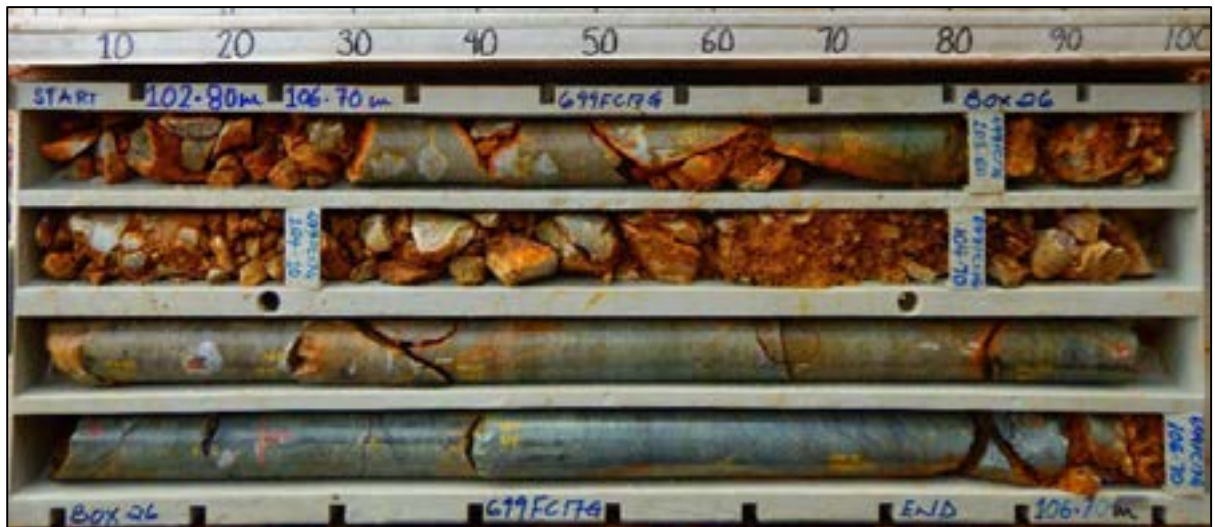


Figure 11-13: Core photograph from 102.8 m to 106.7 m depth from drillhole LH3, showing the base of the potentially unstable 'landslide' zone

11.1.2 Landslide assessment

Right abutment feature

It is estimated that the size of the feature in the right abutment may be up to 63,000 m³ (although this is poorly defined from surface interpretation as the feature has been intersected by only one drillhole), and is located partly across the footprint of the spillway. The powerhouse will also be located directly downhill from this mass.

Based on the findings of the geotechnical investigation, and considering the risks associated with this potentially unstable zone, the following should be considered:

- Locally adjust the spillway excavation slope profile to ensure stable slopes are maintained where intersection with this mass is projected. The exact extent of this zone will be established on site and the design may require minor adjustments during construction. Further assessment of the landmass characteristics, may however prove the need for this mass to be removed and will be determined during future studies.
- Limit disturbance of the toe and surface of the slope during construction and operation
- Protect the powerhouse and associated infrastructure from any potential failure run-out. The requirements would need to be assessed as part of future studies once there is a better understanding of the feature
- Monitor the landmass during construction, operations and closure to pre-empt movement or failure, and develop safe evacuation plans to support the monitoring program
- Removal or stabilisation activities of the zone.

Left abutment feature

Approximately 50% of the estimated 4 Mm³ of the identified feature is located above the crest of the embankment. Failure of the mass could result in significant damage to the embankment and surrounding infrastructure, including intakes opposite this feature, on the right abutment. Within the lower half of the mass, a portion could be supported by the embankment; however, the portion immediately south of the embankment will remain unsupported. This portion will also be submerged below the surface of the reservoir during filling.

The feature is located directly upstream of the main workings of the embankment, and failure during construction could have catastrophic consequences. Apart from the potential impact to personnel and equipment, the project would likely stop for extended periods before construction could recommence.

Predicting the exact behaviour of this feature is difficult; failure, even if pre-empted will have a significant impact on the FRHEP.

Leaving this feature in place as it is will make it difficult to extend the cut-off into it, and will also impede effective grouting of the area.

Having assessed the profile and characteristics of this zone, and as with SKM's previous recommendations, SRK recommends the complete removal (or removal of a very large percentage) of this feature during early construction.

Based on the findings of the geotechnical investigation and considering the risks associated with this feature, the following should be implemented:

- Remove most of the mass of the feature from the top down using various methods of excavation and maintaining a benched profile. It is noted that the benched profile cannot be used within the footprint of the embankment. This is illustrated in Figure 11-14.
- Refrain from disturbing large surface areas ahead of the bulk excavation
- Monitor the landmass during construction to pre-empt movement or failure, as construction activities will continue during the removal of the material mass, and develop safe evacuation plans to support the monitoring program
- Protect the workings located downstream of the feature from falling rocks and debris during construction by using appropriate techniques.

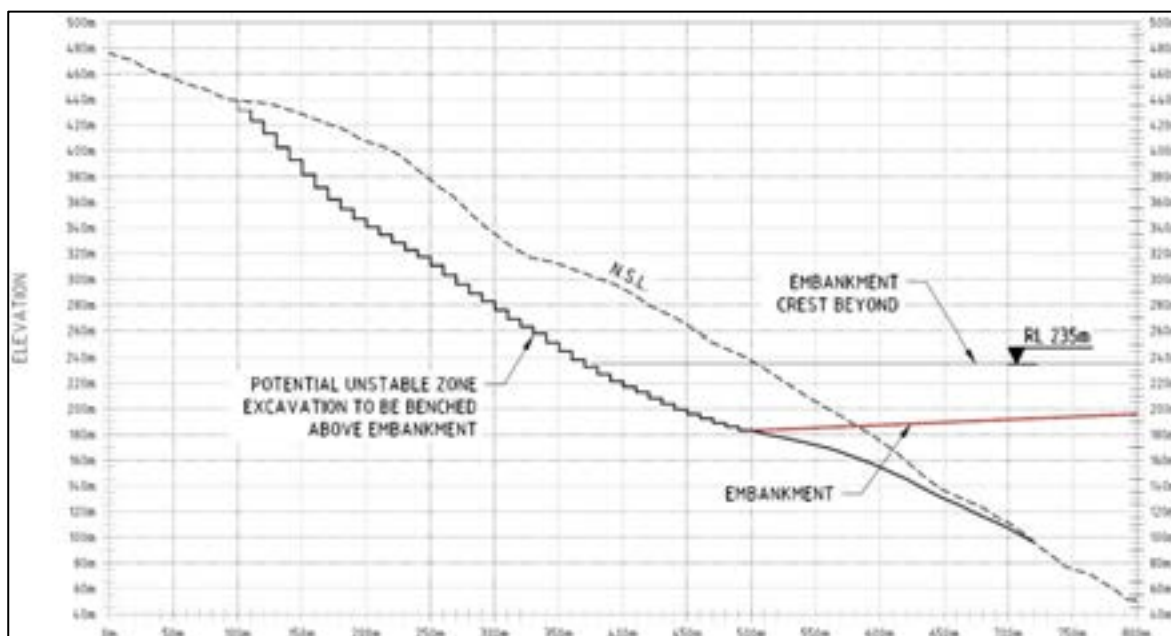


Figure 11-14: Cross-section through left abutment mass

11.1.3 Subaqueous landslides

Subaqueous landslides have the potential to develop from the instability of deposited tailings and waste rock within the reservoir. The risks and associated impacts have been discussed in the Operations and Closure (Section 19).

The wave size modelling assessment identified the maximum expected wave height generated by subaqueous landslides to be ~5.4 m. Under most operating conditions, a wave height of 6 m is not expected to overtop the embankment, but may overtop the gates. However, a 5.4 m high wave during PMF conditions may overtop the embankment. The impact of such a wave may damage some embankment infrastructure such as the gates and intake structures, but is not expected to incur significant damage. The surge due to a sudden increase in pressure could affect the hydroelectric power infrastructure.

Propagation of a large wave may also trigger landslides around the headwaters of the reservoir. Further assessment of the potential waves sizes and associated risks must be further investigated.

12 Roads

Site access for the delivery of equipment and construction material prior to completion of the main access road (by the mine, 18 months after site handover) will be via barge along the Frieda River. The barge facility is therefore important during the early phases of construction.

Roads will be required during construction and operations to connect the key infrastructure components. Small and large construction equipment will be separated to promote safety and efficiency. SRK has classified roads into five categories as listed below (SRK Drawing PNA009-0056):

- Permanent roads: to be used during operation of the FRHEP
- Temporary small vehicle haul roads across the Frieda River: to be used during construction by typical civil construction equipment
- Temporary large vehicle haul roads across the Frieda River: to be used by larger quarry equipment
- Temporary small vehicle haul roads constructed on the steep abutments: to be used by smaller civil construction equipment
- Temporary large vehicle haul roads constructed on the steep abutments: to be used by larger quarry equipment.

As agreed with FRL, the SPS has not performed 3D modelling of road profile and alignment. As a result, all estimates are based on typical sections and horizontal road alignments as shown in SRK Drawing PNA009-0058. SRK has sized the roads based on the equipment sizes expected to be utilised for the FRHEP, including the use of the CAT 785 dump truck for the quarry haul roads.

Removal of the weathered rock mass on the left abutment and quarry development must occur from the top down, requiring road development up the steep mountain terrain.

Most excavations on steeper ground will require blasting to remove solid rock; this will be expensive and time-consuming, and will require dedicated road-building teams during construction (especially during early pioneering to provide access to working areas) to ensure all working fronts are accessed in time. Any large vertical cuts created by the construction on the hillside of the road will require further rock supports. These requirements will need to be reassessed on site during development of the roads. Catchfences are also recommended to prevent smaller rock falls from landing on roads. Although the rock is of good quality there may be zones of weaker rock and the steep terrain and high rainfall increases the risk of rockfalls, especially when there is lots of construction activity in these areas. The rock bolts are preventative, however, should there be small scale failure or rock detaching from the surface, the drape mesh will guide the loose material and dissipate their energy.

Roads in the riverbed south and upstream of the embankment will endure flooding, especially once the diversion system has been commissioned and flows from further up the river are channelled downstream through the tunnels. SRK recommends that spoil material be utilised to raise the roads above these flood levels (SRK Drawing PNA009-0056). Construction of many of the FRHEP's key infrastructure components must be commenced as soon as possible, which will lead to the need for road fill material; raising of roads may therefore have to be done in stages as the construction schedule allows.

A comprehensive stormwater management system is essential to maintain driveable road conditions during construction (Section 14.2.2). Roads have been designed to be dual purpose with adjacent drainage channels and are therefore the main stormwater control infrastructure for the site. Stormwater entering the roads from the hillside will be conveyed in channels and piped underneath the roads to discharge downslope.

A few significant stormwater crossings will require either bridges or large culverts to accommodate the flood levels expected at the FRHEP. Two such crossings are directly north of the embankment and will provide initial access to the construction site. To reduce bridge construction time, it is recommended that the contractor procures the materials prior to establishing the site. Typical prefabricated steel girders can be installed requiring minimal in situ construction effort. Upfront road base development will also be required to raise the bridge to a suitable level. In addition, to allow quick access across the Frieda River, a pontoon or floating barge facility must be provided by the contractor during early construction prior to installation of any bridges.

Some of the roads will be developed inside the footprint of the final quarry and will therefore be removed during quarry development.

Permanent roads must be operational for the lifetime of the facility and be easy to repair and upgrade as required. SRK therefore recommends concrete block paving which is easy to place, rehabilitate, repair and remove, and which can accommodate large loads such as those on regular haul trucks. Not providing a durable surface (asphalt, concrete, paving) will in the long run cost more in terms of maintenance, especially considering the rainfall expected at Frieda. Of the three options, SRK selected interlocking block paving, as it is versatile, easy to install, long lasting and can be specified to take heavy axil load traffic. Asphalt will be difficult to maintain considering the remoteness of the site and availability of asphalt (following completion of the project). Concrete is a good alternative to paving, however has reinforcement can corrode where paving cannot. Concrete is also more difficult to repair than paving (which can be removed in smaller sections and replaced). The availability of paving may prove to be a concern but would have to be investigated going forward. Parts of the surfacing could perhaps be done at a later stage, but that would only delay capex and in fact be more expensive.

As roads are key infrastructure and of significant value, a detailed road study is recommended to optimise road requirements and refine the design. Road construction techniques must also be investigated with the support and expertise of a standard dam building contractor.

Temporary roads, backfilled once no longer in use has been allowed for the up and downstream face of the embankment and connects with the quarry roads at various nodes along the embankment face. These roads are further described in the embankment construction section of the Implementation report. The only noticeable cost involved in the development of these roads will be the rehandling of the fill portion that will be required to backfill the road cut.

13 Embankment Instrumentation

SRK has proposed a conceptual instrumentation and monitoring program for the entire FRHEP site to provide data to measure the embankment's performance and associated structures during construction, first filling of the reservoir, operations and closure. The types of data and instruments to be used are listed in Table 13-1.

Table 13-1: Proposed monitoring data and instrumentation

Data type	Instruments
Pore pressure and uplift pressure	Vibrating wire piezometers, stand pipe piezometers, total pressure cells, fibre optic sensors
Seepage and leakage	Seepage weirs and fibre optic sensors
Loading conditions	Total pressure cells
Surface movement and internal movement	Vertical settlement gauges with inclinometers, hydrostatic settlement cells, surface markers, extensometers, strain gauges, fibre optic sensors
Seismic loads due to earthquake	Strong-motion accelerometers

The measured data will allow for the following:

- Verification of design and analysis assumptions
- Evaluation of behaviour during construction, first filling, operation of the structure and closure
- Evaluation of the performance of specific design features, such as plastic concrete cut-off walls
- Observation of the performance of known geological and structural anomalies
- Evaluation of performance with respect to potential site-specific failure modes.

Table 13-2 lists instrumentation to be used (see SRK Drawing PNA009-0090 for layout of sections A-G) and possible locations for effective monitoring, such that the instruments will provide data representative of the entire embankment.

Other instruments required during construction of the FRHEP will be to monitor movement of the potentially unstable masses on the left and right abutments and evaluation of the phreatic surface in the spoil dumps using piezometers.

Surface markers to assess ground stability and movement are also recommended for the large spillway and quarry excavations.

Table 13-2: Types of instrumentation for monitoring

Instrumentation	Purpose	Embankment	Location	Section	Quantity	
					Number	Length (m)
Vertical settlement gauges with inclinometer tubing	To provide settlement and inclination measurements – inclinometer readings can be taken in two orthogonal directions, parallel to the embankment axis and normal to the embankment axis	Cofferdam	Installed at RL 75 m to foundation, RL 48 m	D	1	20
		Main embankment	Installed at RL 157 m to foundation, RL 48 m	A, C, D, F	4	109
Hydrostatic settlement cells	To monitor differential movements within the embankment body	Cofferdam	Installed horizontally at RL 75 m along inner rockfill zones	D	1	NA
		Main embankment	Installed horizontally at RL 75 m, RL 116 m, RL 157 m and RL 198 m along inner rockfill zones	All	59	NA
Total pressure cells	To determine the distribution, magnitude and directions of total stresses and contact pressures between individual rockfill zones	Cofferdam	Installed at RL 75 m and within the foundation	D	1	NA
		Main embankment	Installed at RL 75 m, RL 116 m, RL 157 m and RL 198 m in five or six different directions to determine the principal stresses	All	59	NA
Fixed embankment extensometers	To monitor horizontal displacement of rockfill material	Cofferdam	Installed at RL 75 m	D	1	NA
		Main embankment	Installed at RL 75 m, RL 116 m, RL 157 m and RL 198 m at a 50 m spacing	All	111	NA
Surface settlement markers	To measure movement of the embankment relative to a fixed location	Main embankment	Installed on the surface of downstream and upstream surface of the freeboard	All	59	NA
Fibre optic displacement monitoring	To detect leakage immediately downstream of the asphalt core, as the seepage temperature changes the wave length of fibre optics. Movement in the embankment induces changes in the strain, which then changes the wave length. This can then be used to determine displacement locations.	Cofferdam	NA	NA	NA	NA
		Main embankment	Installed underneath the plastic concrete cut-off, plinth and along the centre core at RL 45 m, RL 116 m, RL 157 m and RL 198 m	All	NA	>2,500

Instrumentation	Purpose	Embankment	Location	Section	Quantity	
					Number	Length (m)
Vibrating wire piezometers	To measure pore water pressures within the embankment foundation and adjacent to the grout curtain and plastic concrete cut-off walls. To monitor efficiency of grout curtain during impounding and to control the drainage system at the lower riverbed areas.	Cofferdam	Installed at RL 75 m and RL 47 m within the foundation	D	1	NA
		Main embankment	Installed at RL47 m, RL 75 m, RL 116 m, RL 157 m and RL 198 m. Additional piezometers will be grouted as part of grouting the plastic concrete cut-off walls	All	84	NA
Strong-motion accelerometers	To record seismic activity and resulting embankment movements	Main embankment	Main embankment crest and right abutment	D	2	NA
Seepage measuring weirs	To measure the amount of seepage and allow visual inspection and sampling to take place	Main embankment	Downstream toe at main embankment	D	1	NA
Open standpipe piezometers	To measure the groundwater levels around the abutments	Main embankment	Along the foundation abutment	NA	6	NA
Strain gauges	To monitor the perimeter joint movements and stress between construction joints at Sections C and E	Main embankment	Embedded in reinforced concrete plinth	C & E	3	NA
Switch box	To serve as a junction for instrumentation cables	Main embankment	An allowance for five data acquisition systems has been made. The construction methodology used will determine the final position of the systems.	Anywhere convenient	5	NA
Data acquisition system	To collate information recorded from each of the instrumentation devices and convert it into usable data. Data acquisition systems are to be housed inside transportable sheds for protection against adverse weather conditions.	Main embankment	An allowance for five data acquisition systems has been made. The construction methodology used will determine the final position of the systems.	Anywhere convenient	5	NA

14 Sediment and Surface Water Management

As a result of high regional rainfall and the erodible nature of the soils found on site, surface water and sediment generated during construction of the embankment will require diligent management. The objectives are to prevent contamination of the embankment transition and filter layers, including the foundation cut-off wall, prevent flooding and limit the volumes of fugitive sediment leaving the site.

The three main sediment generation areas are the spoil area, quarry and main embankment works area. Using the basic philosophy outlined below, SRK developed the conceptual plan shown on SRK Drawings PNA009-0052, PNA009-0060 and PNA009-0062:

- Manage, collect and contain sediment at source
- Limit soil disturbance
- Divert runoff away from embankment foundation excavations, quarry and spoil piles
- Manage runoff inside the foundation excavation and prevent filter and transition layer contamination
- Manage foundation excavation spoil
- Settle out eroded sediment in sedimentation ponds
- Remove sediment from settlement ponds as and when required for disposal at the spoil dumps.

The critical period for sediment management will be early on, during foundation stripping, spoil dump development and quarry overburden stripping operations. During this period, large areas of predominantly sandy soil will be exposed and susceptible to erosion. Therefore, it is important to set up the external diversions and sediment management infrastructure as early as possible to divert water away from work/excavation areas and minimise erosion.

Local stormwater and sediment management at the working front will be managed by the contractors and have not been included in this study. Contractor responsibilities typically include the following:

- Development and management of minor diversions around construction areas
- Supply and management of construction transfer sumps and pumps required during construction
- Local sediment prevention, collection and disposal.

The roads will be constructed with adjacent drainage channels and also used to divert stormwater away from key FRHEP infrastructure via strategic placement of culverts and discharge channels. The roads will therefore serve as supplementary stormwater management infrastructure for key construction areas such as the spillway, quarry and other areas. Water management for temporary and permanent roads is discussed in Section 14.2.2.

14.1 Temporary diversions

Diversion channels will be installed upstream of the roads, foundation cuts, spoil dumps, powerhouse and the quarry to prevent runoff entering the worksites, as shown on SRK Drawing PNA009-0052. The relevant catchments are shown in Figure 14-1. Once the quarry is established, the size of catchments PH1 and E3 will reduce.

The key diversions and their characteristics are presented in Table 14-1 and Table 14-2. SRK recommends that key diversions are lined with riprap in areas where erosion is likely to be significant.

Minor diversion channels will be constructed adjacent to work areas to collect any minor runoff. These will be smaller than the key diversions upstream, and active during short periods of

construction. Channels should be lined with either an HDPE liner or riprap if significant erosion is expected to occur. No design has been developed for these minor channels; however, for cost estimation purposes, an allowance for the excavation and HDPE liner has been made.

14.1.1 Runoff within the foundation excavation

External runoff entering the embankment excavation footprint will be negligible due to the installation of diversions; however, direct precipitation on the foundation excavation will require management to reduce sediment loads and protect the worksite, particularly during construction of the filter and transition layers.

Prior to stripping of the abutments, a sediment conveyance channel will be constructed near the valley floor on either side of the valley. Runoff during excavation of the abutments will flow down the valley slopes into the conveyance channels which discharge into the sedimentation ponds (SRK Drawing PNA009-0052).

Channels were sized using Manning's equation and the rational method, assuming a runoff coefficient of 1 and a conservative channel slope of 0.5%. FRHEP catchments during construction are shown in Figure 14-1. The characteristics of the channels shown in SRK Drawing PNA009-0052 are presented in Table 14-1 and Table 14-2.

Contact water from the excavation of the cut-off wall working platform will be pumped into the sediment conveyance channels via sumps. After stripping of the abutments and cut-off wall area, the conveyance channels will be removed as part of the stripping operations. Contact water will then be diverted into a sump at the riverbed for pumping into the sedimentation ponds.

Once foundation stripping is completed, temporary channels placed parallel to the riverbed near the bottom of each abutment will collect runoff from the abutments and discharge it into sumps. There would likely be one sump on each side of the footprint bed. The channels and sumps will be progressively relocated as the embankment fill rises. The relocation will be managed as required on site, and will be critical for protection of the transition and filter layers.

Table 14-1: Key diversion channels for construction sediment and stormwater

Diversion ID	Name	Channel type	Reports to
SC1	Embankment sediment channel 1	C	SC2
SC2	Embankment sediment channel 2	C	ESP1
SC3	Embankment sediment channel 3	B	SC4
SC4	Embankment sediment channel 4	B	ESP1
E1	Embankment diversion channel 1	C	E6
E2	Embankment diversion channel 2	B	SP2
E3	Embankment diversion channel 3	C	River
E4	Embankment diversion channel 4	D	PH1
PH1	Powerhouse diversion channel	Note 1	River
Q1	Quarry sediment channel 1	C	SC3
SP1	Embankment sedimentation pond outflow 1	B	SP2
SP2	Embankment sedimentation pond outflow 2	A	River
SD1	Spoil dump diversion channel 1	A	River

Note 1. Powerhouse diversion channel will be a concrete-lined permanent channel (Section 14.2.1).

Table 14-2: Surface water diversion channel profiles (refer to Table 14-1)

Type	Design freeboard (m)	Total depth (m)	Base width (m)	Side slope (V:H)
Channel A	0.30	3.70	1.5	1:2
Channel B	0.30	2.90	1.5	1:2
Channel C	0.30	2.30	1.5	1:2
Channel D	0.30	1.30	1	1:2

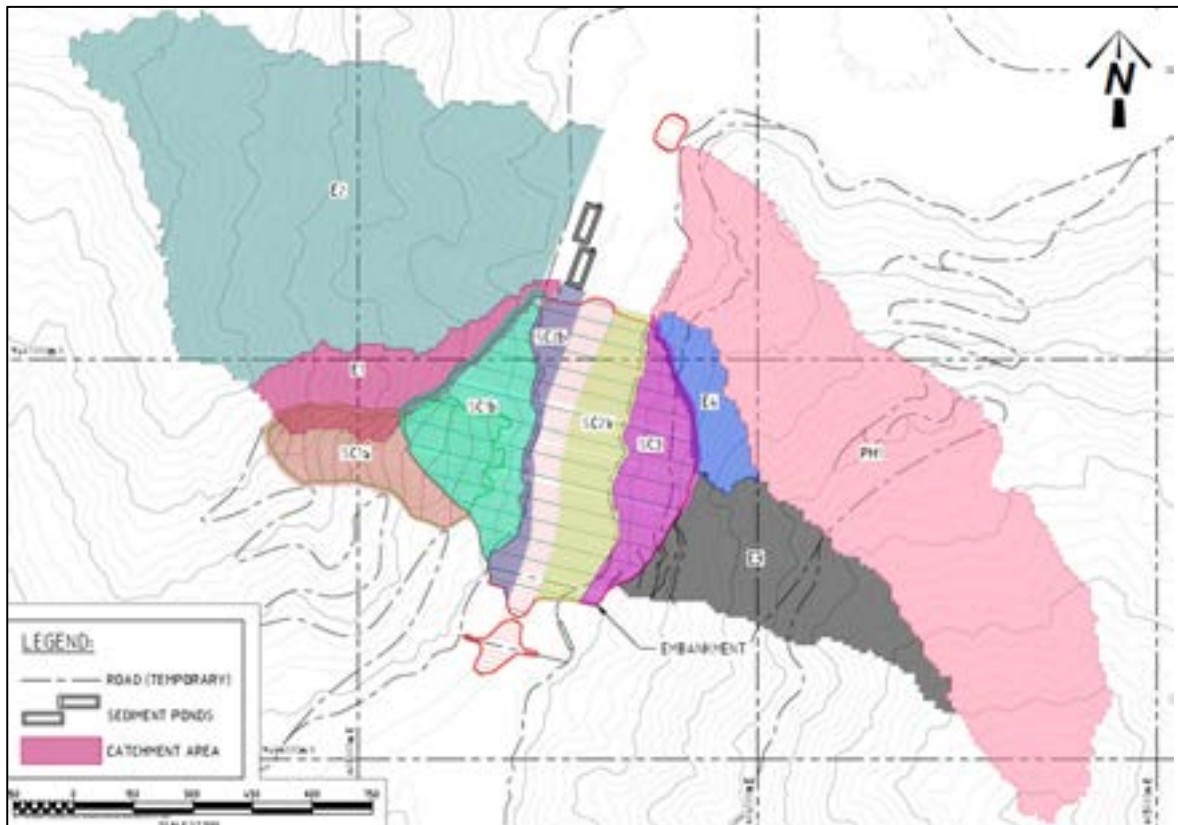


Figure 14-1: Embankment sediment management catchments

Note: Figure has been adjusted to suit final drawings, and calculations were based on working drawings.

14.1.2 Sediment erosion

The extent of progressive stripping of vegetation will be based on practicality and schedule considerations. It is reasonable to assume the embankment footprint will be stripped of vegetation in several stages in a top-down manner. After each stage of vegetation removal, the de-vegetated footprint will be excavated to its intended final depth. Erosion will be significantly reduced once the embankment footprint is excavated to the moderately weathered bedrock of the abutments, and cemented colluvium/ alluvium of the valley floor.

Erodible material at excavation cut slopes will be protected to reduce most of the eroded sediment movement. Placement of the protection covers will likely be carried out progressively in conjunction with stripping operations to minimise the soils' period of exposure. Erosion protection has not been considered as part of this study. Protection options include jute/ coir matting and other bio-engineered products, and the typical procedure is shown in Figure 14-2. The high rainfall at Frieda will exacerbate sediment generation and discharge from the site.

The embankment fill is erosion-resistant rockfill, which is more resistant than the in situ material. As a consequence, the level of erosion will decrease over the construction period as the embankment fill is raised.

For these reasons, the level of erosion from the embankment footprint is considered comparable to non-disturbed areas after excavation operations are completed.



Figure 14-2: Bio-engineering of erosion-prone slopes (photos taken in Minas Gerais, Brazil)

14.1.3 Spoil dumps

Spoil generated during construction of the FRHEP, including spoil from the foundation excavation, will be hauled and placed in two primary stockpiles upstream of the embankment, as shown on SRK Drawing PNA009-0020. The spoil dump design is presented in Section 14.3.

Sediment management procedures for the spoil dump include the following features, shown on SRK Drawings PNA009-0060 and PNA009-0062:

- Stormwater diversion channel at the toe
- Sedimentation ponds located on the spoil dump above the cofferdam design flood zone
- Sediment retention paddocks at the toe of the spoil dump for areas not captured by the main sedimentation ponds; bund is required on outside edge to prevent erosion during flooding
- Stormwater diversion channel at the toe
- Drop structures down the face of the spoil dump to convey contact water to the sedimentation pond; drop structures require dissipation features at benches
- Spoil dump benches to convey sediment to the drop structures
- Continuously developed/ maintained channel on the top of the dump to direct flow to the drop structures
- Compaction of the outer wall and key parts of the spoil dumps to improve stability and minimise erosion
- 'Zone 1' comprising 'best quality' spoil material selected to prevent erosion during the cofferdam design flood.

The northern spoil dump is smaller than the southern spoil dump and will primarily be used during early stages of construction, predominantly for spoil from the fractured rock mass. The design features of the northern spoil dump have been scaled from the southern spoil dump.

Sediment generated by the spoil dumps will be conveyed and collected in sedimentation ponds located downstream at each dump. The spoil dump sedimentation ponds are designed to allow retention of sediment and the release of excess water to the river, as discussed in Section 14.1.

The southern spoil dump will have a large upstream catchment of approximately 2.7 km²; therefore, a diversion channel has been conceptually designed to divert the runoff around the edge of the dump (SRK Drawing PNA009-0060). While the channel will have a critical function during short-duration storms, during long-duration storms it is likely that the channel will be inundated by the Frieda River.

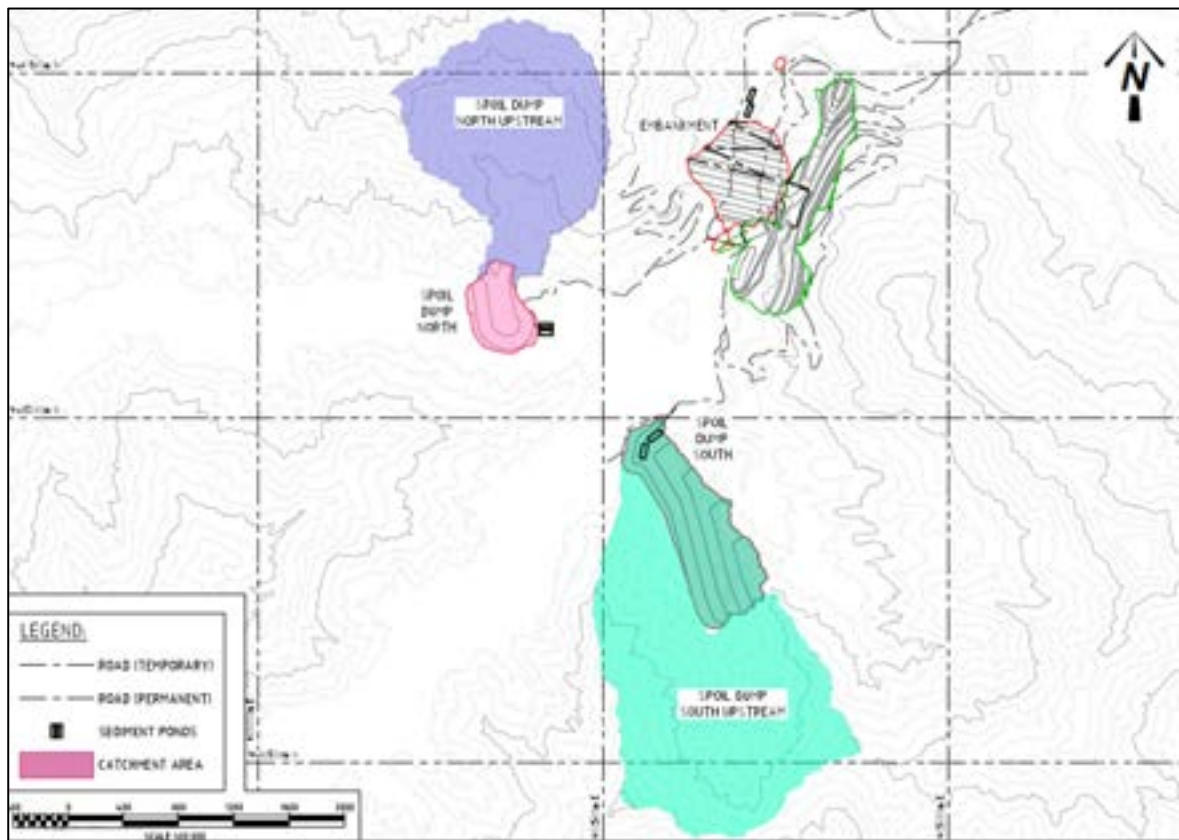


Figure 14-3: Spoil dump catchments

Note: Figure has been adjusted to suit final drawings, and calculations were based on working drawings.

The spoil dump sedimentation ponds will discharge into the tail end of the stormwater diversion channel, where a drift crossing is required to allow access to the proposed gravel pit to the west (SRK Drawing PNA009-0060). The width of this segment depends on trafficability requirements.

The paddocks will be located adjacent to the diversion system. Ponding in the paddocks during flood events will prevent movement of water from eroding the paddocks. After a flooding event, water would be pumped from the paddocks.

The drop structures will be progressively constructed and maintained as the dump develops. Alternative options for the drop structure arrangement include:

- Concrete-lined drop structures
- Geotextile-lined riprap channels (if competent/ durable larger rock is available, i.e. >300 mm)
- Reno mattress-lined channels with intermittent gabions (if only smaller rock is available)
- Combination of the above options, e.g. concrete or riprap base and bio-engineered side slopes.

For cost estimation purposes, SRK has assumed the geotextile-lined riprap channels will be adopted. However, the other alternatives should be considered during later design stages.

The drop structures may require a deep cut-off and/ or bunds installed along the bench crest. The drop structures cross-section need to be larger near the tail end where flow from the benches accumulates. For costing purposes, an average size over the length of the channel has been estimated using the

rational method and Manning's equation. The calculated size is 1.3 m (depth) × 1.0 m (base width), with channel slopes at 1:2 (V:H) and 0.3 m thick riprap lining.

14.1.4 Stilling basins

Stilling basins will be installed at channel outlets and drop structures to control flow velocity and prevent erosion. The proposed stilling basin consists of a trapezoid-shaped pond lined with riprap, and overflow from the outlet spills into the toe diversion channel or natural stream, as shown in Figure 14-4. An allowance for riprap volume has been included for costing purposes.

An alternative stilling basin may be constructed using reno mattresses and bio-engineering.

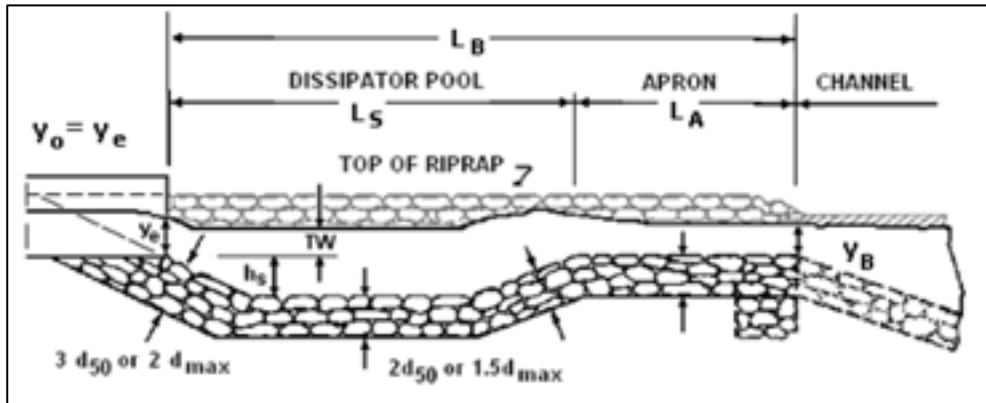


Figure 14-4: Stilling basin/ outlet configuration concept

14.1.5 Sedimentation ponds

Sedimentation ponds will be required downstream of the embankment and at the spoil dumps.

Two sedimentation ponds are required at each location to be used alternately, to allow sedimentation pond cleaning to be undertaken during operations. The pond layouts are shown on SRK Drawings PNA009-0052, PNA009-0060 and PNA009-0062. The following alternative sedimentation pond types could be considered:

- Wet basin: a sediment basin that is not free-draining and needs to be manually dewatered after a storm
- Dry basin: a sediment basin that is free-draining and begins to dewater soon after water enters the basin.

For costing purposes, it has been assumed that the basin will operate as a wet basin, which needs to be pumped out periodically to allow cleaning. Cleaning of sedimentation ponds can be done using conventional dredging, with the spoils stored into the spoil dump.

The features of the proposed sedimentation pond, shown in Figure 14-5, include the following:

- Excavated basin
- Forebay and level spreader
- Sediment storage zone
- Settlement zone
- Spillway
- Manual dewatering system
- Basal drains to promote dewatering of sediments to facilitate trafficability.
- Erosion-resistant diversion bunds along outside edges.

The sedimentation ponds have been located where they can remain functional throughout the entire construction period. Sediment generation will peak for a limited time during the early construction period, followed by lower volumes for the remainder of the construction period, predominantly generated from the spoil dump.

After bulk-stripping is completed, the embankment sedimentation ponds will be less critical. As discussed previously, limited erosion will occur from the embankment footprint. Similarly, limited erosion will occur from the spoil dump. Erosion protection has not been considered. Furthermore, limited erosion will occur from the quarry once the overburden is stripped because the disturbed area will consist of rocky material that is not susceptible to erosion.

Lining of the pond wall is unlikely to be required, and would not be practical as the liner may be damaged during cleaning operations. The pond walls should be constructed with a stable slope angle.

No design of the basal drainage system has been undertaken; however, for costing purposes an allowance for drainage material has been made.

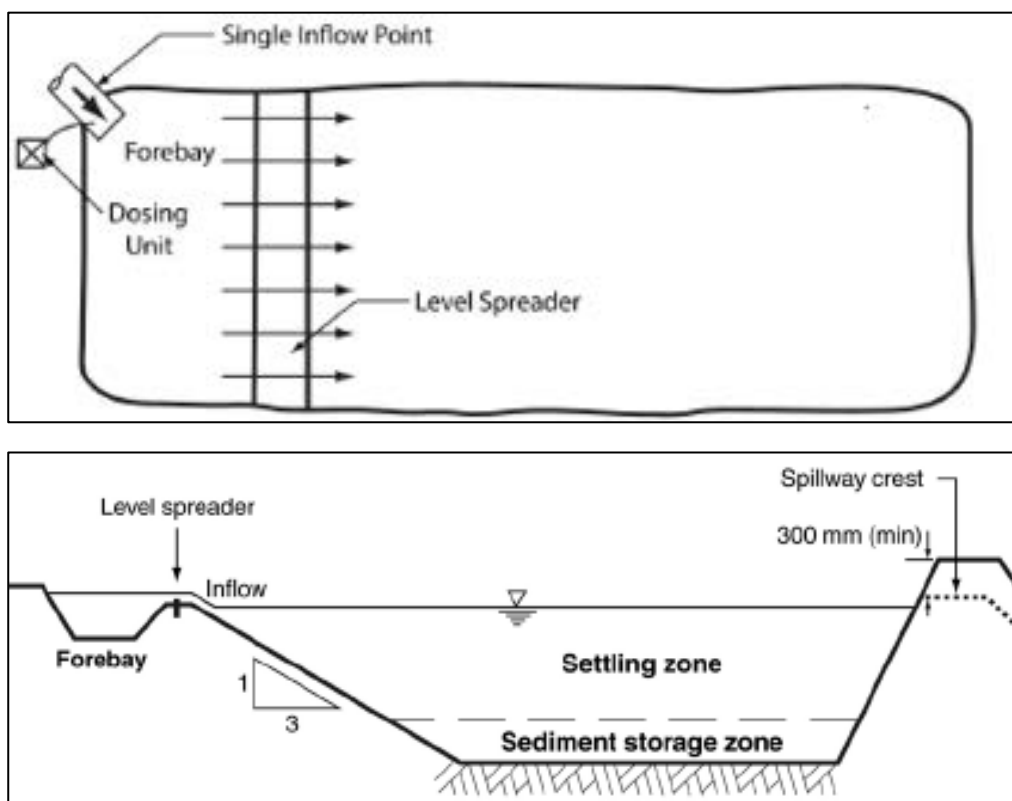


Figure 14-5: Typical sedimentation pond schematic of features

Source: IECA, 2016

Note: Flocculant dosing not required for proposed sedimentation ponds.

Sedimentation pond sizing

The sedimentation pond design criteria are presented in Table 14-3.

Table 14-3: Design criteria for sedimentation ponds

Design Criteria	Value	Comment
Sedimentation pond retention design storm	0.5 × 1 in 1-year AEP	IECA 2016 ⁹⁵
Sedimentation pond retention particle size	>0.075 mm	PanAust email on 19/04/2018 (M Haywood)
Sedimentation pond spillway design storm	1 in 25-year AEP	Assumed by SRK

The sedimentation pond and spillway design characteristics are presented in Table 14-4 and Table 14-5 respectively. Flows were calculated considering the contributing sediment conveyance channels shown in Table 14-1. Spillway dimensions were assessed using the broad crest weir equation and an assumed weir coefficient of 1.5. The length and width of the sedimentation pond were calculated using the method described in IECA⁹⁵ based on a typical particle settlement velocity.

The Revised Universal Soil Loss Equation (RUSLE) was used to estimate an order of magnitude volume of sediment from the disturbed areas during stripping operations. Based on estimated sediment volumes, the sedimentation ponds would need to be cleaned/ alternated frequently (i.e. monthly) during peak stripping operations. Based on the storage zone, the volume to be cleaned at each cycle would be approximately 6,000 m³.

Flocculant dosing would need to be considered to expedite particle settlement if the retention particle size criteria is less than 0.075 mm.

Table 14-4: Sedimentation pond dimensions

Sedimentation ponds	Length (m)	Width (m)	Sediment storage depth (m)	Settlement zone depth (m)	Total depth (including spillway) (m)
Embankment	100	40	2	0.7	4
Southern Spoil Dump	100	40	2	1	4
Northern Spoil Dump	100	40	2	1	4

Table 14-5: Sedimentation pond spillway characteristics

Spillway	Design freeboard (m)	Total depth (m)	Base width (m)	Side slope	Riprap depth (m)
Embankment	0.3	1.3	30	1V:2H	0.3
Southern Spoil Dump	0.3	1.0	15	1V:2H	0.3
Northern Spoil Dump	0.3	1.0	15	1V:2H	0.3

⁹⁵ International Erosion Control Association (IECA), 2016, Appendix B – Draft Document Revision December 2016

14.2 Permanent water management structures

14.2.1 Stormwater diversion channels

Four primary diversion features will be installed to manage stormwater at the embankment and powerhouse, and are shown on SRK Drawings PNA009-0052 and PNA009-0110:

- Concrete drop structures at the intersection of the abutment and the embankment
- Concrete diversion channels at the powerhouse facility
- Concrete diversion channels at the top of the spillway excavation and around the diversion tunnel outlet
- Stormwater diversion channels associated with the permanent roads.

The diversion channels have been designed to accommodate the 1:100-year AEP storm from the FRHEP catchments (Figure 14-6). The channel characteristics are presented in Table 14-6. Channel sizing was based on the rational method assuming a runoff coefficient of 1.

The powerhouse stormwater diversion channel will be installed prior to construction of the powerhouse as part of stormwater and sediment management features required during construction.

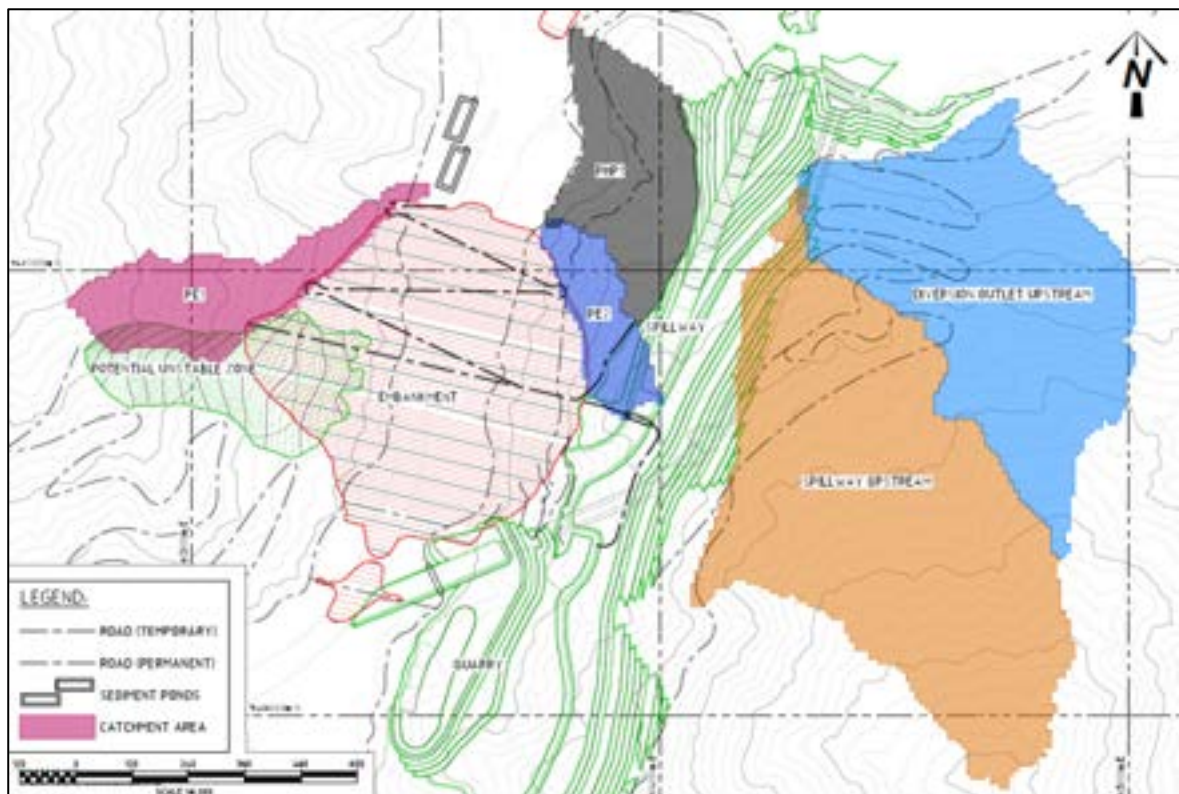


Figure 14-6: FRHEP stormwater catchments

Table 14-6: FRHEP permanent stormwater diversion channels

Structure ID	Name	Reports to	Design freeboard (m)	Total depth (m)	Base width (m)	Side slope (V:H)
PE1	Embankment permanent stormwater channel/ drop structure 1	River	0.3	1.0	1.0	1:2
PE2	Embankment permanent stormwater channel/ drop structure 2	PH1	0.3	1.0	1.0	1:2
PH1	Powerhouse diversion channel	River	0.3	2.0	1.0	1:2
SPP1	Spillway diversion channel	DOP1	0.3	2.0	1.0	1:2
DOP1	Diversion tunnel outlet diversion channel	River	0.3	2.5	1.5	1:2

14.2.2 Roads

Water management

The temporary and permanent roads and crossings will require the following surface water management features, which are shown on SRK Drawings PNA009-0056 and PNA009-0058:

- Channels at the road edges to convey runoff from upstream
- Minor crossings (culverts) to pass minor natural streams and discharge channel flows
- Large arch culverts to pass major natural streams (Figure 14-7)
- Bridges with piers to pass the Frieda River.

The road crossing characteristics are summarised in Table 14-7. The following should be noted:

- Road channel dimensions are nominal at this stage
- Minor crossing characteristics are indicative, being based on a representative catchment (indicated in Figure 14-8). While the exact locations of individual culverts have not been assessed, at a minimum, the catchments shown on Figure 14-8 will need to be passed.
- The lengths of pier bridges B2 and B3 were estimated to inform budget estimates; however, no design of bridge components has been undertaken, with the exception of the spillway bridge (B5), which has been designed for costing purposes
- Erosion protection has been assumed for costing purposes.

Table 14-7: Crossing characteristics

Crossing ID	Location	Lifespan	Type of crossing	Characteristic size	Erosion protection
B1	Pioneer road	Permanent	Open bottom arch	4 × 3.3 m radius	Gabions/ grouted riprap at inlet/outlet
B2	Frieda River	Construction period	Temporary bridge with piers	90 m long	Gabions/ grouted riprap at abutments
B3	Diversion tunnel inlet	Construction period	Temporary bridge with piers	80 m long	Gabions/ grouted riprap at abutments
B4	East of southern spoil dump	Construction period	Open bottom arch	3 × 3.3 m radius	Gabions/ grouted riprap at inlet/outlet
D1	Southern spoil dump	Construction period	Drift crossing	NA	Gabions/ grouted riprap at abutments
B5	Spillway	Permanent	Permanent bridge	52.4 m	Concrete-lined spillway
Minor crossings	All roads	Construction period or permanent	Culverts	6 × 1 m diameter typical (Note 1)	Headwall, riprap at inlet/ outlet

Note 1: Minor crossing characteristics are indicative only, based on a representative catchment (indicated in Figure 14-1). The exact locations of individual culverts have not been assessed; however, at a minimum, the catchments shown in Figure 14-1 will need to be passed.



Figure 14-7: Example arch culvert stream crossing photo (Source: www.ail.ca)

Note: Photo does not reflect size of proposed stream crossings

Crossing sizing

The crossing sizes are presented in Table 14-7. The design criteria for permanent and temporary crossings are shown in Table 14-8.

The following design factors were considered for each crossing location:

- The bridge opening area required to pass flow from the tributary stream
- The road elevation required to prevent flooding from the Frieda River as identified during evaluation of diversion sizing (Section 10.1)
- The elevation of the natural ground near the bridge
- The size of the natural stream near the bridge.

The rational method was used to estimate design flows for bridges B1 to B4 based on the catchments shown in Figure 14-8, with catchment areas reflected in Table 14-9. Bridge B2 and B3 convey run-off from the entire TSF catchment; the design flows were obtained from the hydrology study (Section 4). The flow area was determined using Manning’s equation, assuming a trapezoidal flow area with side slopes of 1:2 (V:H).

Drift crossing 1 (D1) will be a wide erosion-resistant channel that will allow flooding over the crossing area. During times of flooding, it will not be possible to access the gravel pit to the west of the southern spoil dump.

Culvert crossings were sized using the software HY-8 assuming a bed slope of 1.0%. The culvert summary characteristics are presented in Table 14-9.

Table 14-8: Crossing design criteria

Design Criteria	Value	Comment
Permanent crossings	1 in 100-year AEP	Assumed
Temporary (construction period) crossings	1 in 25-year AEP	Assumed

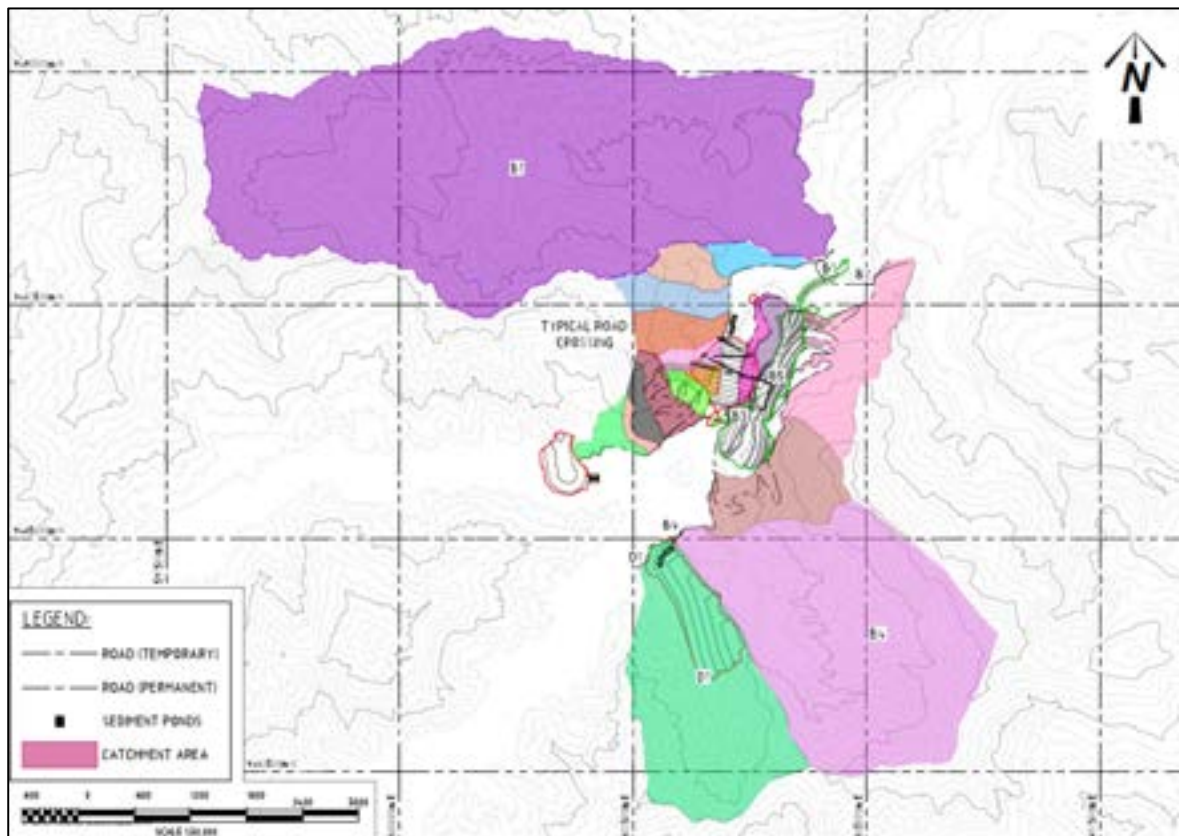


Figure 14-8: Catchments for road crossings

Note: The FRHEP catchment reports to B2 and B3 and has not been shown in the figure.

Table 14-9: Catchment areas and design flows for bridges

Crossing	Catchment area (km ²)	Design flow (m ³ /s)	Design flow source
B1	13.9	300	Rational method
B2	1,033 (FRHEP catchment)	2,750	SRK (Section 4)
B3	1,033 (FRHEP catchment)	2,750	
B4	6.13	170	Rational method
B5	3.46	100	

Table 14-10: Culvert sizing

Crossing	Type of crossing	Radius (m)	Number	Headwater depth (m)	Total base width (m)
B1	Open bottom arch with inlet mitred to conform to slope	3.3	4	5.1	40
B4	Open bottom arch with inlet mitred to conform to slope	3.3	3	4.1	30
Minor crossings	Concrete lined culvert with headwall	0.5	6	2	9.5

14.3 Spoil dump stability assessment

The FRHEP will generate approximately 33 Mm³ of material that will need to be safely disposed requiring two spoil storage facilities. 30 Mm³ will be disposed of in the spoil dumps with the difference being used for road construction and in forming terraces for laydowns and stockpile areas. Vegetation and related organic material, topsoil, weathered and fractured material, boulders and rocks (including sediment generated during the construction period) will be stored in two designated spoil dumps located to the south and southwest of the embankment. The sites were selected based on ease of access and minimising haulage distances.

Spoil material will be generated throughout the construction period with a ramping-up and ramping-down phase at each of the initial and final project phases respectively. Temporary stockpiling followed by later re-handling will be required to accommodate the volumes of spoil generated prior to the spoil dumps being established. Vegetation and topsoil will be cleared and removed as required to limit the size of disturbed areas, thereby reducing erosion and helping to maintain stability of the natural ground surface. Both spoil dumps are located to the south of the embankment in the footprint of the reservoir that will be partially inundated once the reservoir has been filled. This includes a ~120 m high spoil dump directly south of the quarry. An opportunity exists whereby some of the spoil material may potentially be disposed of in the lower parts once the quarry development in this area is complete.

The conversion of 0.5m³ (of processed vegetation) per square metre of stripped forest was applied during the volumetric calculations for the estimated spoil volume. This parameter should be further assessed and validated based on the processing method selected by FRL and the site-specific forest characteristics.

The spoil dumps will generate sediment while aerially exposed throughout the construction period. Any sediments released from the spoil dump site will be discharged into the construction works and potentially downstream of the embankment.

Failure of any spoil dump during development may have significant consequences due to the presence of construction personnel and equipment. Failure will likely also result in significant sediment

discharge to, and beyond, the embankment. Challenges related to the spoil dump design include limited space, wet environmental conditions, uncertainty related to the spoil material strength properties and the resultant impact of blending the various spoil types including fluctuating water levels during construction.

The facilities therefore need to be engineered to be capable of safely storing and containing all spoil material generated by the FRHEP.

The following section describes the stability assessment and resultant design requirements to ensure safe construction and operating conditions are maintained. Sediment management and stormwater control, an important part of the spoil dump development, are discussed in Section 14.1.3.

Only the design of the Southern spoil dump was undertaken as the same concept has been adopted for the cost estimation of the other spoil dump.

14.3.1 Design considerations

As defined by the Basis of Design, a FoS of 1.3 satisfies the static stability criteria for temporary structures based on ANCOLD (2012) for short term undrained loading condition with no potential loss of containment. Seismic loading has not been considered as part of this assessment and must be considered during future study phases.

Inter-bench stability was also not evaluated as part of this assessment.

SRK did not undertake sizing of the dumps to accommodate sediments originating from the upper parts of the catchments, outside the immediate FRHEP working area. SRK has assumed that any sediment transported to the embankment will remain in suspension and pass through the diversion tunnels, and that sediment generated in mining areas upstream of the construction site will be managed and contained at source as far as practicable.

The impact of decomposition of organic material within the spoil dump was also not considered.

The geotechnical parameters for the spoil dump foundation were selected based on SRK's review of available information. It has been assumed that the characteristics and parameters of the spoil storage footprint are similar to the Nena ISF embankment site, due to the similar geology.

Spoil material strength properties were based on findings from field investigations or literature research.

14.3.2 Slope stability assessment

SRK has undertaken a stability assessment using a representative cross-section through the spoil dump. The slope stability was evaluated using the Limit Equilibrium Method (LEM) to determine the FoS. The analyses were completed using Slide V6.0 software (Rocscience, 2010). Slip surfaces were evaluated using the GLE/ Morgenstern & Price method.

The stability assessment was performed assuming drained conditions.

SRK considered circular and non-circular failure surfaces to determine the probable failure mechanism. The sections below include the results of the stability assessment.

14.3.3 Geotechnical strength parameters

Foundation

No geotechnical investigations have been performed across the proposed spoil storage footprint. According to the geological maps, the foundation material in the location of the spoil dump is Ok Binai

phyllite. To assess the stability of the spoil storage, the foundation characteristics have therefore been assumed to be similar to the Nena ISF embankment; also located on phyllite.

The horizons within the weathered profile and identification of characteristic properties for these horizons as described below:

- A. Extremely weak (<1 MPa) soil-like materials, including Colluvium and Completely Weathered (CW) materials
- B. Very weak (1–10 MPa) rock, including Highly Weathered (HW), and locally CW or Moderately Weathered (MW) rock
- C. Weak (10–25 MPa) rock, including HW and MW rock
- D. Moderately strong (25–50 MPa) rock, including MW and Slightly Weathered (SW) rock (effectively the start of 'bedrock')
- E. Strong to very strong (>50 MPa) rock, including SW and Unweathered (UW) rock.

It is considered the presence of a 1 m thick layer of organic topsoil. According to the relevant literature^{96, 97}, consideration of a 15° internal friction angle and cohesion of 5 kPa is recommended.

Spoil

The engineering properties of materials expected to be stored within the dumps are difficult to predict, especially given their non-homogenous in situ nature, the wide spectrum of material types found across the site and resultant geotechnical properties of the blended composite.

A literature review on a mixture of materials deposited as an integrated medium (municipal solid waste landfill) and materials with high organic materials (fibrous peat) was completed to assess possible friction angles. The friction angles for municipal solid waste landfill varied from 15° to 22° for a landfill in China⁹⁸, whereas back-analysis of a slope failure of a landfill in the United States produced a friction angle of 35°⁹⁹. Most of the lower range friction angles between 3° and 25° are reported for tropical peat deposits such as Malaysia. The proposed friction angle of 18° for the assessment is likely to be slightly conservative, considering that the FRHEP environment is tropical and that seismicity was not assessed. Undrained analyses were not conducted for the SPS, as characterisation of the waste is not defined, and it has been assumed that the embankment will exhibit drained behaviour.

To improve prediction of the spoil dump behaviour and increase the overall stability, SRK proposes the dumps be developed in three zones using selected spoil of varying degrees of strength. Grouping the weaker, less well-understood organic material in separate compartments deep within the spoil dump will facilitate development of a more stable outer containment. SRK proposes the external fill (cover layer) be composed of a finer spoil and the base consist of the most competent rock and granular soil (spoil–colluvium). Table 14-11 summarises the geotechnical properties for the foundation and spoil materials. Figure 14-9 correlates with the material types presented in Table 14-11.

⁹⁶ Hertlen & Wolski 1996, *Embankments on Organic Soils*, 432 p, Elsevier: Amsterdam

⁹⁷ Thiyyakkandi & Annex 2011, *Effect of Organic Content on Geotechnical Properties of Kuttanad Clay*, *European Journal of Government and Economics*, 16: 1653–1663

⁹⁸ Feng et al. 2017, *Geotechnical properties of municipal solid waste at Laogang Landfill, China*, *Waste Management*, 63, 354–365

⁹⁹ Eid, Stark, Evans, & Sherry 2000, *Municipal solid waste slope failure. I: Waste and foundation soil properties*, *Journal of Geotechnical and Geoenvironmental Engineering*, 126, 397–407

Table 14-11: Summary of geotechnical properties

Material type	Legend	Unit weight, γ (kN/m ³)	Cohesion, 'c' (kPa)	Friction angle, ' ϕ ' (°)	Hoek-Brown			
					GSI ¹⁰⁰	UCS (MPa)	M(<i>i</i>)	D ¹⁰¹
Spoil cover		17	5	25				
Spoil colluvium		18	0	30				
Spoil		15	5	18				
Top soil		16	5	15				
Horizon A		19	10	30				
Horizon B		22.7			30	5	6	0
Horizon C		25.4			40	10	7	0
Horizon D		25.4			45	25	7	0
Horizon E		27.4			55	50	10	0

14.3.4 Water

A significant water influx is expected as a result of high daily rainfall and requires control measures to achieve dump stability.

Upon commissioning of the diversion tunnel, the water level is expected to rise to approximately RL 83 m during a 1:100-year rainfall event. This will result in partial submergence of the toe of the spoil dump. Some of the recorded rainfall events would have caused the water level to rise to peak levels and a return to normal levels over a period of several days. For this reason, any drainage system installed in the spoil dump would need to be installed at foundation level, using non return valves. It is therefore recommended that the water table in the dump be maintained at RL 83 m (to accommodate a 1:100-year rainfall event) because water build-up within the dump may rise to these levels.

It is further recommended that the spoil colluvium material be selected such that its permeability is similar to granular materials (1.0×10^{-6} m/s), allowing the phreatic level in the dump to draw down and a curved outer face profile to be maintained at all times (Figure 14-9).

14.3.5 Modelling scenarios

SRK modelled the stability of the dump considering a number of options to define the cross section that would provide adequate FoS. Using the selected cross section, two distinctive operating scenarios are presented below

Case 1: Topsoil removed and a spoil colluvium 'buttress' at the toe of the spoil dump. This buttress is 25 m high (crest at RL 90 m) to prevent submergence during flooding and is 100 m wide at the base (Figure 14-9). The topsoil layer is removed by creating a box-cut across the width of the buttress.

¹⁰⁰ Geological Strength Index

¹⁰¹ Disturbance factor

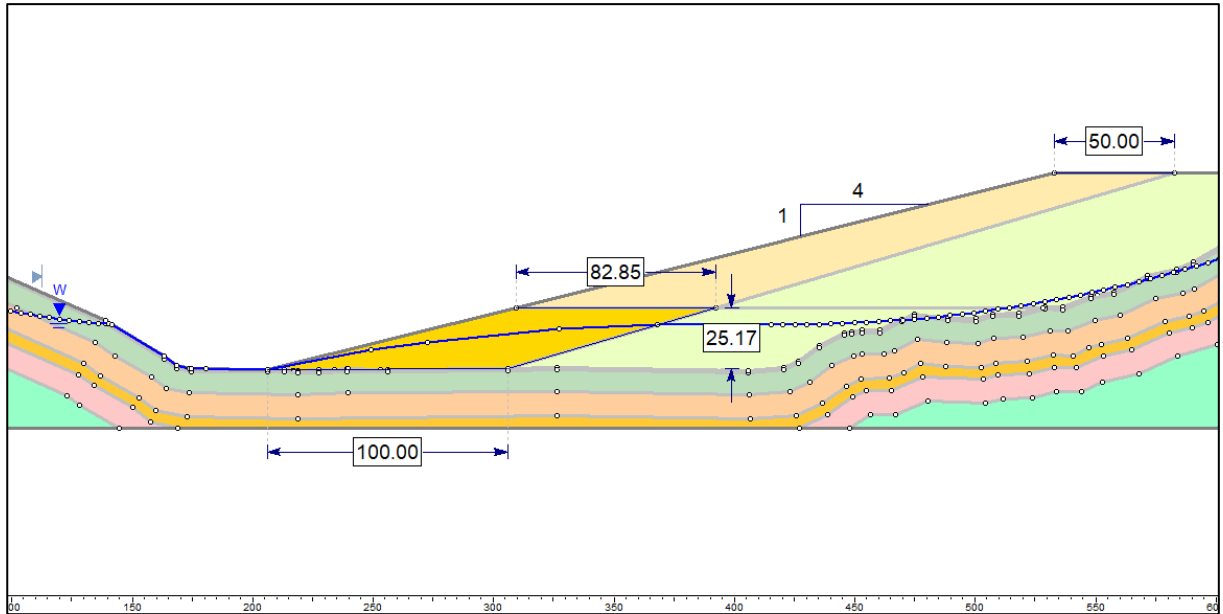


Figure 14-9: Case 1 section

Case 2: Same slope configuration, but includes ponding water at an elevated level (RL 155 m) that represents filling of the reservoir.

14.3.6 Results and interpretation

The results following the assessment are summarised in Table 14-12.

Table 14-12: Results of stability assessment – critical sections

Case	Required FoS	Achieved FoS
1	1.30	1.13
2	1.30	1.80

The Slide modelling outputs from the stability analyses are presented in Figure 14-10 to Figure 14-11.

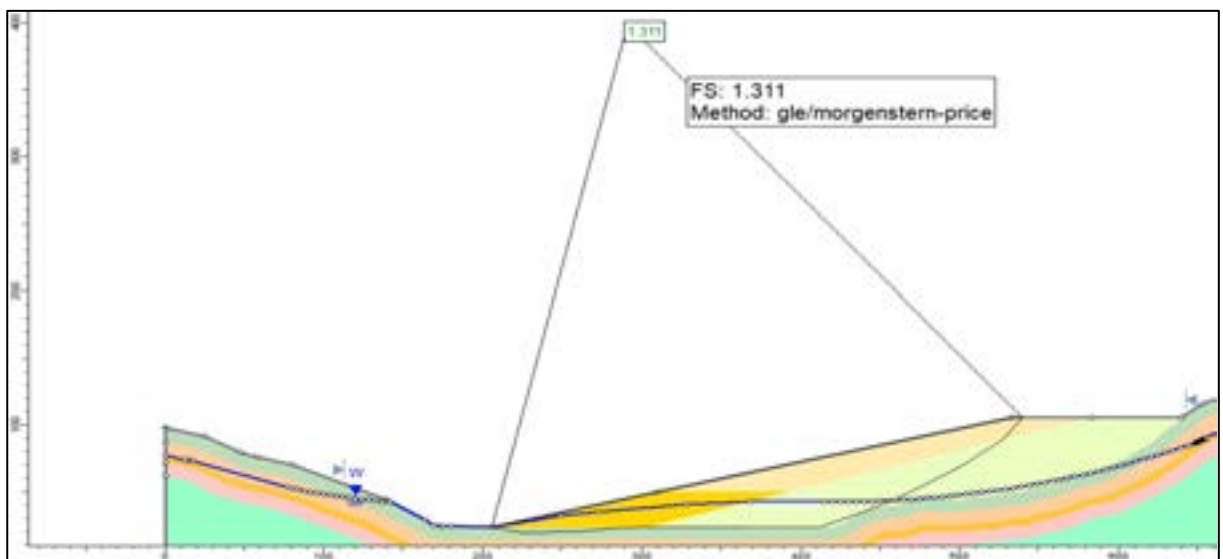


Figure 14-10: Slide output – Case 1

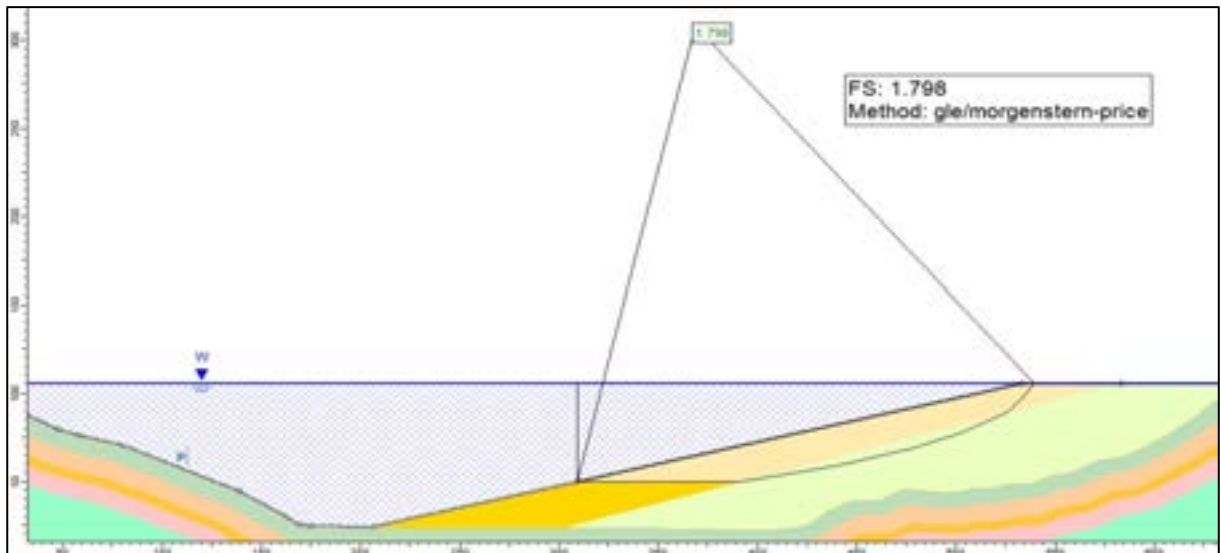


Figure 14-11: Slide output – Case 2

SRK has interpreted the results as follows:

- The embankment requires the inclusion of a buttress to maintain adequate safety
- The spoil dump would remain stable during filling of the reservoir; however, minor localised consolidation and resultant sloughing across the outer face may occur.
- An acceptable design FoS is achieved when granular material is placed as a buttress at the toe of the spoil dump and topsoil and organic soil cover is cleared. The practicality and availability of the coarser grained/ better suitable material must be further investigated during further studies.
- The presence of water within the dump significantly reduces the embankment strength due to the build-up of pore pressures, therefore limiting water ingress and pore pressure build-up is integral to maintaining stability.
- Large pockets of lower strength vegetation within the spoil dump will result in areas where large slip circles could be generated, which would compromise the overall dump stability.

14.3.7 Construction and development

Based on the above findings, SRK recommends the following design and construction methodology be implemented:

- Maintain the average minimum outer embankment slope of 1:4.
- Remove topsoil and any organic matter below the footprint of the spoil dump.
- Install and maintain a drainage system to convey stormwater around the spoil dump during development, thereby reducing water infiltration and erosion of the dump.
- Encapsulate the vegetation with soil in smaller compartments, or paddocks, similar to the development of landfill sites.
- Install an internal drainage system that would discharge water build-up within the spoil dump. The rate of rise must be investigated during further studies to assess whether the drainage system will function adequately.
- Develop the dump using a benched outer profile to prevent excessive erosion of the outer embankment face; protection of the outer slopes and promotion of vegetation growth will assist in minimising erosion.

- The practicality and availability of the courser grained/better suitable material must be further investigated during future design phases.
- Select material for the construction of the outer buttress such that this zone is sufficiently porous to prevent pore pressure building up on the outer surface of the dump.
- Compact the spoil dump I areas where the next stage of stability assessment indicates the need to ensure stability is maintained.
- The performance and associated stability will depend on sound operational procedures, including construction and monitoring.
- Sensitivity assessments must be performed during future design phases to investigate the impact of change in the variables that contribute to the strength of the overall dump.

15 Hydroelectric Power Configuration

15.1 Intake structure arrangement

Unlike a 'normal' hydroelectric plant, the operating range for the FRHEP in terms of water level is very large, due to the requirement to utilise the water through the FRHEP as soon as practical, to power the FRGCP. This need to generate early and from multiple intake levels has added to the complexity of the engineering structures across project.

It was determined that a 'multiple structure' option would be both the best engineering solution and also the most cost effective for the FRHEO. The following advantages of this solution are noted:

- It can fit into the required topography, without massive excavations and temporary support.
- There are no real restrictions as to the placement of tailings.
- Operation can be achieved over nearly all of the operating life of the reservoir, with short interruptions between levels changes.
- Access and maintenance is relatively straightforward.
- Seismic performance of the structure can be achieved.
- The solution is cost effective in comparison to the other options.

With an initial operating water level of RL 171.2 m, and a final minimum operating level of RL 199.4 m and maximum operating level of RL 204.4 m, it became apparent that having two structures was the optimal arrangement and shown in Figure 15-1.

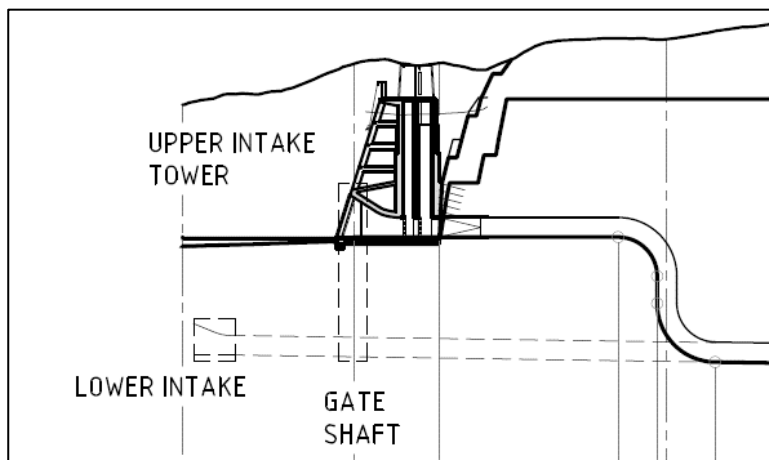


Figure 15-1: Intake arrangement

The final resulting arrangement of the intakes is also depicted in 3D diagrams (Figure 15-2).

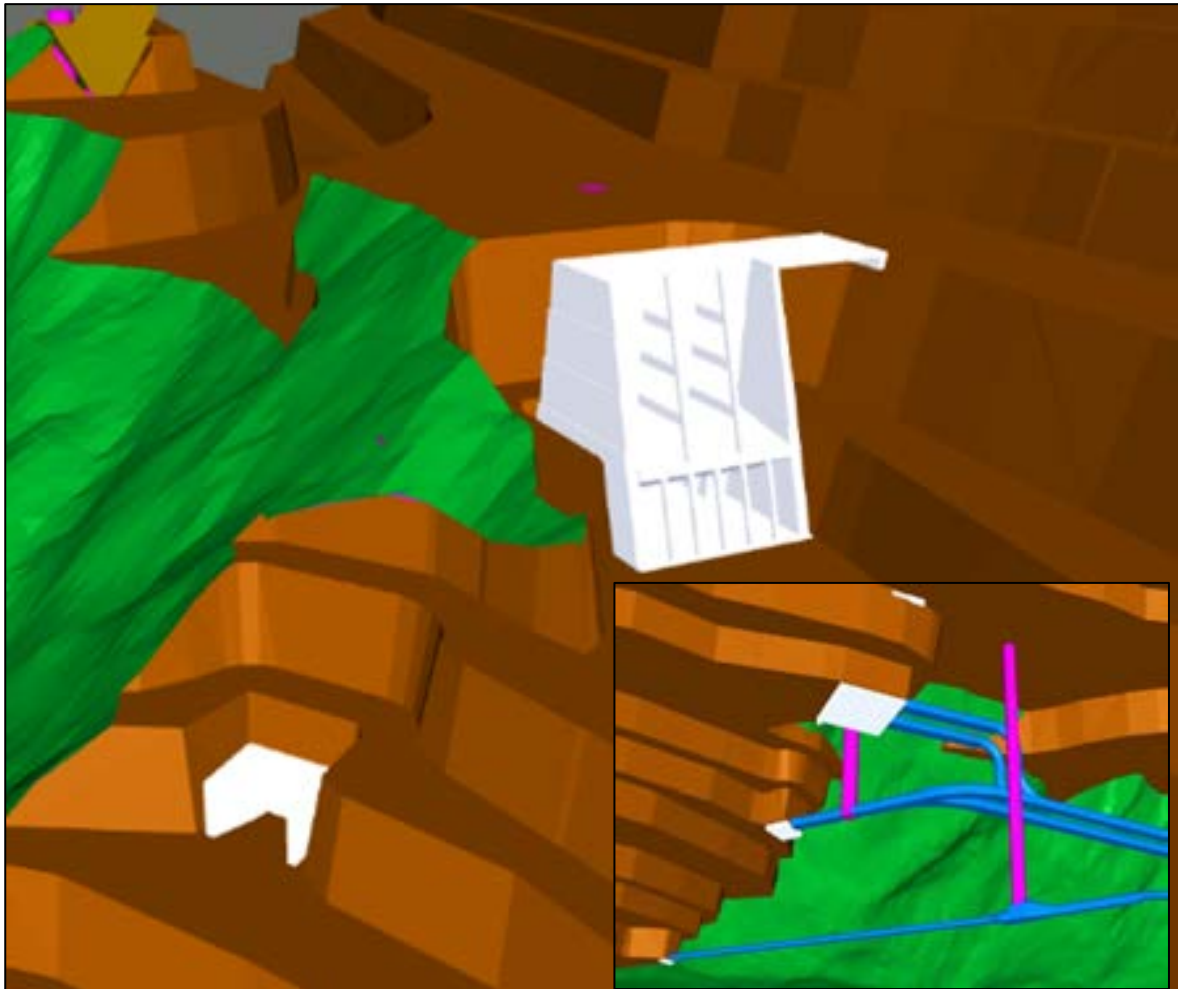


Figure 15-2: 3D models of intake structures (aerial view, inset underground view)

15.2 Configuration of the conveyance system

Configuration of the conveyance system for the FRHEP is dependent on several factors, primarily:

- 1 Flow
- 2 Turbine Unit Selection (and in particular the number)
- 3 Distance to Powerhouse
- 4 Ground Cover
- 5 Location of surge facilities
- 6 Geology
- 7 Ability to incorporate early filling
- 8 Ability to protect the dam construction from flooding
- 9 Provision of river navigation downstream of the powerhouse (for delivery of some equipment).

With these factors in mind, Stantec developed five primary general arrangements to incorporate all of these factors.

Within each of the five options identified, the primary function of delivering water to the turbine is shown via a twin tunnel arrangement, which is split at the powerhouse to feed each of the individual units. These were sized hydraulically in terms of the tunnels and shafts to suit the design flow.

The overall alignment of the tunnel was arranged to:

- 1 Provide a constant intake arrangement, for the main intake structure, and the 'early filling' lower intake
- 2 Avoid the geotechnical feature under the right abutment
- 3 Be located far enough from the assumed dam excavation footprint to ensure that no influence of the embankment/ tunnel interaction would affect the conveyance components
- 4 Arrange the downstream heading change to allow the surge chambers to daylight at the desired surface level, without the need for an extensive structure above ground.

These criteria resulted in the major remaining factors for the conveyance system related to the ability to:

- 1 Drain a flood from the dam during the end of construction, post the 'early filling' time
- 2 Pass the required flow to enable the river to remain navigable downstream of the powerhouse. While the actual design flow has not been determined (required to be studied in a future phase), a quantum of 500 m³ has been assessed to be a suitable flow for this stage of the project, based on some initial flow calculations, and anecdotal evidence about general river transportation, as discussed in Section 7.8.

15.3 Surge analysis of conveyance system

15.3.1 Introduction

A transient surge analysis of the power conveyance tunnels has been undertaken as part of the developed design of the hydroelectric power scheme. The analysis consisted of building and running a model of the conveyance system using specialised surge (transient analysis) software. The output of the transient analysis has been used to develop a model of the turbine governor operation. This is a major input to the Power System Study carried out by GHD for FRL. This study examined the ability of the governors to allow the turbines to maintain the system frequency during a range of events ranging from the trip of a hydro unit, trip and start-up of a Semi-Autogenous Grinding (SAG) mill and the trip of transmission lines.

This exercise helped determine optimum tunnel and surge chamber diameters and tested alternative options, such as eliminating the surge chamber and providing a Turbine Relief Valve (TRV). The model also tested various wicket gate timings (minimum allowable open and closing times) and also looked at the impact of HWL across the entire operating range and its impact on system response.

The results of the surge analysis provide a Hydraulic Grade Line (HGL) envelope, showing the minimum and maximum pressures developing along the tunnel following a surge event. The results also indicate the surge chamber level range, and how quickly the tunnel flow and pressure oscillations decay after an event.

The surge model extends from the tunnel intake to the tailrace. All hydraulic components in between are included, such as the upper and lower intakes, headrace and high conveyance pressure tunnels, surge chamber geometry, penstock and bifurcation, inlet valve, turbine and draft tube. In one case, a control valve (TRV) was modelled in parallel with each turbine.

The model included a single conveyance tunnel on the assumption that the hydraulic behaviour would be similar for both tunnels.

15.3.2 Model inputs and assumptions

Modelling software

The surge analysis was performed using a commercially available software package called KYPipe (2016), which uses the Wave Method of computation.

Table 15-2 gives the modelling assumptions for the properties of water.

Table 15-1: Properties of water

Property	Value
Specific gravity	1
Water temperature (°C)	20
Kinematic viscosity (m ² /s)	1.0e ⁻⁶

Steady-state pipe losses

The software uses a steady-state model to calculate friction loss based on the Darcy-Weisback equation and Colebrook-White formula for the friction factor.

Table 15-3 presents the Colebrook-White roughness assumed for the various sections of the conveyance system. The surge chamber throat is considered as steel-lined tunnel.

Table 15-2: Colebrook-White roughness

Conduit Section	Roughness, k (mm)
Tunnel – cement-lined section	2
Tunnel – steel-lined section	0.3
Steel penstock	0.3

Typical minor loss coefficients, resulting from bends, junctions, fittings and other flow disruptions were included, where appropriate. For example, the intersection between the surge chamber throat and the tunnel/ power shaft. Coefficients were obtained from data presented in 'Internal Flow Systems', 3rd Edition, Miller, D.S., based on experiments and studies conducted by the British Hydromechanics Research Association (BHRA).

Transient wave speed

The transient wave speed, otherwise known as celerity, is the speed at which a pressure wave is transmitted along the full pipeline from a point where a change in flow is initiated. The software package built-in calculator was used to calculate the transient wave speed for given pipe and tunnel materials.

For all types of lining within the tunnel, a wave speed of 1400 m/s was assumed. This is based on rock of high Young's modulus, such as quartz or granite, with thick surroundings (> 1 m diameter). The relationship between properties of the rock (Young's modulus, Poisson's ratio) and wave speed were taken from 'Fluid Transients in Pipeline Systems', 1st Edition, Thorley, A.R.D., 1991.

The buried penstock is assumed to be steel boiler plate of sufficient thickness for internal pressure and handling considerations.

The wave speeds in Table 15-4 were included in the current model.

Table 15-3: Wave speed (celerity)

Conduit Section	Diameter (m)	Wave speed (m/s)
Tunnel (cement and steel-lined)	All	1,400
Steel penstock	7.1	780
Steel pipe within manifold	5.5	780
Steel pipe to turbine inlet	3.9	1,000

Surge chamber

The surge chamber was modelled as a vertical, cylindrical chamber with an open water surface. A reduced diameter throat connects the surge chamber to the tunnel at the top of the power shaft. Losses associated with the throat geometry are included in the model, unique for each direction of flow (inflow to, or outflow from the chamber).

The current derived surge chamber dimensions are presented in Table 15-5.

Table 15-4: Surge chamber parameters

Parameter	Value
Top of surge chamber elevation (RL m)	255
Base of surge chamber elevation (RL m)	135
Connection of throat to tunnel elevation (RL m)	125
Surge chamber diameter (m)	12
Throat diameter (m)	7.1
Surge chamber inflow resistance ($m/(m^3/s)^2$)	0.00003
Surge chamber outflow resistance ($m/(m^3/s)^2$)	0.00002
Minor loss coefficient for throat/ tunnel connection, K	2

Inlet valve

The turbine inlet valve is included as head loss only. Emergency closing scenarios have not been considered in this point of the design. A ball valve with a flow resistance, R, of $0.0003 m/(m^3/s)^2$ is assumed. This equates to a head loss of 0.75 m with a flow of $50 m^3/s$ through the valve.

Francis turbine

The turbine was modelled as two separate components. Firstly, an actuated valve with a flow coefficient versus opening curve approximating a Francis turbine wicket gate characteristic. Secondly, a Turbine component to simulate the relationship between runner speed, flow and head loss.

The wicket gate position can be adjusted from one position to another in a set period of time in the model. For example, to simulate a trip, the wicket gate could be moved from 80% open to fully closed in 12 seconds.

The rotational inertia of the turbine-generator dictates the acceleration of the runner during a sudden load rejection (trip). This is important from a surge perspective as it determines how quickly the flow is throttled by the runner as it enters over-speed conditions. The minimum inertia generally provides a worst case during a trip.

The total inertia for the generating units was estimated based on an empirical equation developed by Westinghouse, 1959. The equation provides the 'Standard Inertia' for a generator of given megavolt amperes (MVA) and rated speed. Standard inertia is defined as the minimum inertia of a generator, without additional inertia (flywheel) being added for stability requirements. The standard inertia has

been calculated for the appropriate size units and used in the surge model. The turbine parameters for the current turbine selection (8 large units) are presented in Table 15-6.

Table 15-5: Turbine parameters

Parameter	Value
Rated speed (RPM)	300
Turbine rated power (MW)	69.2
Wicket gate flow resistance, R , 100% open ($m/(m^3/s)^2$)	0.009
Generator rated MVA (0.85 power factor)	81.7
Generator inertia, GD^2 (t.m ²)	1681
Generator inertia, wr^2 (N.m ²)	4.12e ⁶

15.3.3 Summary of analysis

The analysis evolved as the tunnel alignment and geometry was developed. This report presents the results for the final alignments, with high and low intakes and four main turbines per tunnel with the upper and lower tunnels connected mid-way by a power shaft and surge chamber. Figure 15-8 represents the current alignment of Tunnel 2. The upper intake is shown at the left, surge chamber in the centre and powerhouse at right.

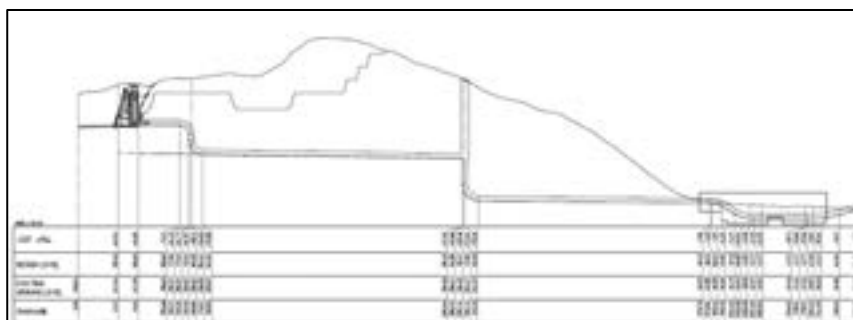


Figure 15-3: Tunnel 2 current long section

Geometry and parameters

The overall tunnel geometry and water levels are presented in Table 15-7.

Table 15-6: Tunnel parameters

Parameter	Surge chamber included
Maximum operating HWL (RL m)	226
Minimum operating HWL (RL m)	158
Conveyance system total length (m)	1,150
Headrace tunnel ('D' shaped) width (m)	7.08
Headrace tunnel equivalent diameter ¹ (m)	7.55
Circular tunnel diameter (m)	7.08
Tunnel liner and penstock diameter (m)	7.08
Surge chamber diameter (m)	12
Tunnel design flow (m ³ /s)	212
Maximum static head at turbine bifurcation (m)	184
Number of turbines per tunnel	4

Note: The head race 'equivalent diameter' is the diameter entered into the model to represent the true cross-sectional area of the 'D'-shaped tunnel. This is needed because the software allows input in diameter format only.

Surge scenarios

The following surge events were assumed to cause the worst case hydraulic transients during normal operation of the scheme:

- 1 Simultaneous full load rejection of all generating units
- 2 Full load acceptance of one unit while all other units continue to generate.

The full load rejection events were modelled at both Minimum and Maximum HWL to determine the minimum and maximum surge results.

The wicket gate timing is defined as the minimum time to move through a full stroke. This represents the fastest response available from the turbine to accept or reject load. This also has a large impact on the surge pressure rise during a load rejection and pressure fall during load acceptance. The optimum gate timing is determined through model runs to obtain the fastest response while limit the peak pressure and surge chamber level fluctuations.

For maximum HWL cases, the wicket gates are expected to be at a lower opening to produce the turbine rated power output. This is because less flow is required to produce the same power output with a higher net head. For example, for the gate timing, the wicket gates may be at approximately 80% open at maximum HWL, with a gate timing of 15 seconds. Therefore, the gates would close from 80% open in 12 seconds. This is accounted for in the modelled scenarios.

The turbine runner also creates a surge pressure rise during load rejection, because of the throttling effect during over-speed. Depending on the wicket gate timing, the runner effect can cause a significant rise in pressure. The runner accelerates quickly (a function of the machine rotating inertia) and is often responsible for the initial pressure rise during a load rejection.

Required hydraulic performance

Allowable surge chamber level

With the current tunnel alignment, the ground level above the surge chamber is RL 255 m. This sets a maximum surge chamber level of around RL 245 m, including a reasonable margin to prevent overtopping. The minimum water level sets the floor of the enlarged surge chamber, but must be above the tunnel soffit to prevent draining. A minimum level of RL 135 m is allowed.

Maximum penstock pressure

A penstock pressure rise of 30% above the static head at maximum operating HWL is considered an appropriate maximum for penstock and hydraulic machinery. The wicket gate timing has been selected to limit peak pressure to this maximum.

15.3.4 Results

The key results for design of the conveyance system are the water level range within the surge chamber and the maximum pressure developed at the turbine inlet. Rate of damping of pressure and flow oscillations after a surge event is also important.

In order to meet the requirements of the hydraulic performance (Section 15.3.3), a surge chamber diameter of 12 m and a wicket gate timing of 15 seconds was selected.

Three scenarios were tested, including a full load rejection at minimum and maximum levels for 'full output' operation, and a load acceptance at minimum operating level. Table 15-8 summarises the results.

Table 15-7: Surge chamber results

Scenario description	Full Load Rejection	Full Load Rejection	Load Acceptance
	4 units on a single penstock simultaneous full load rejection	4 units on a single penstock simultaneous full load rejection	3 units at full load on a single penstock, 4 th unit rapid load acceptance
Reservoir level (RL m)	226	204	154
Initial flow (m ³ /s)	187	212	141
Final flow (m ³ /s)	0	0	179
Wicket gate full stroke timing ¹ (s)	15	15	15
Initial gate position (%)	80	100	10
Final gate position (%)	0	0	100
Duration of wicket gate movement (s)	12	15	13.5
Peak pressure at bifurcation (m)	238	230	114
Peak pressure/ max. static pressure at bifurcation	1.29	1.25	0.62
Surge chamber max. level (RL m)	242	222	159
Surge chamber min. level (RL m)	214	191	153

Note: The wicket gate timing is the minimum time that the gates can move from 100% open to fully closed, or vice versa.

Full load rejection – reservoir level at RL 226 m

The following figures (Figure 15-9 to Figure 15-11) indicate the hydraulic behaviour in the conveyance system for a simultaneous trip of 4 turbines with wicket gates closing from 80% in 12 seconds and maximum head water level.

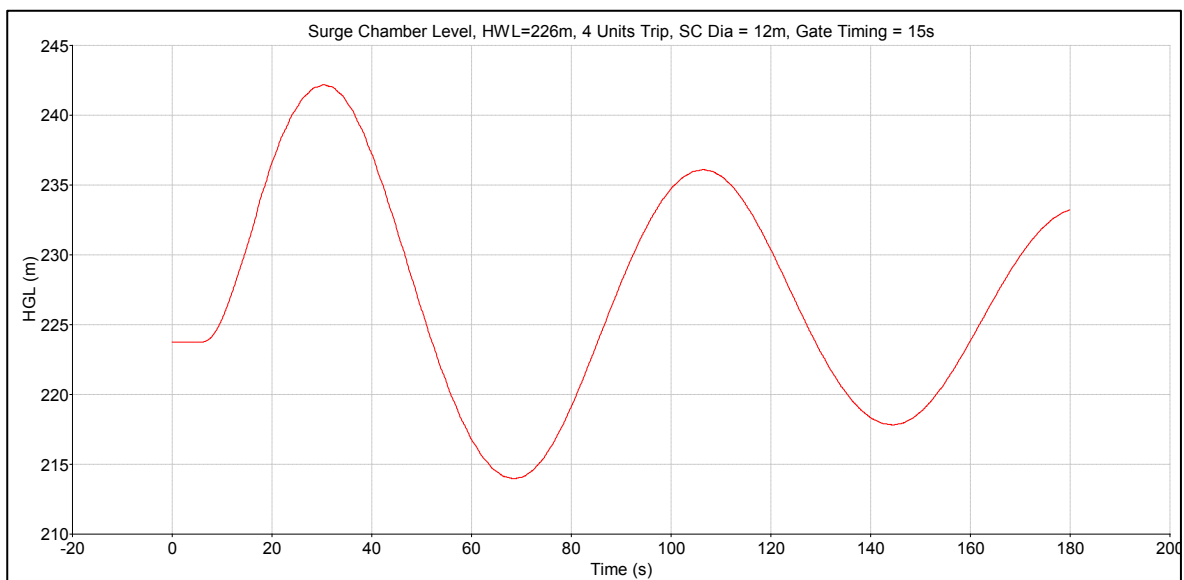


Figure 15-4: Surge chamber water level following a simultaneous full load rejection at maximum HWL

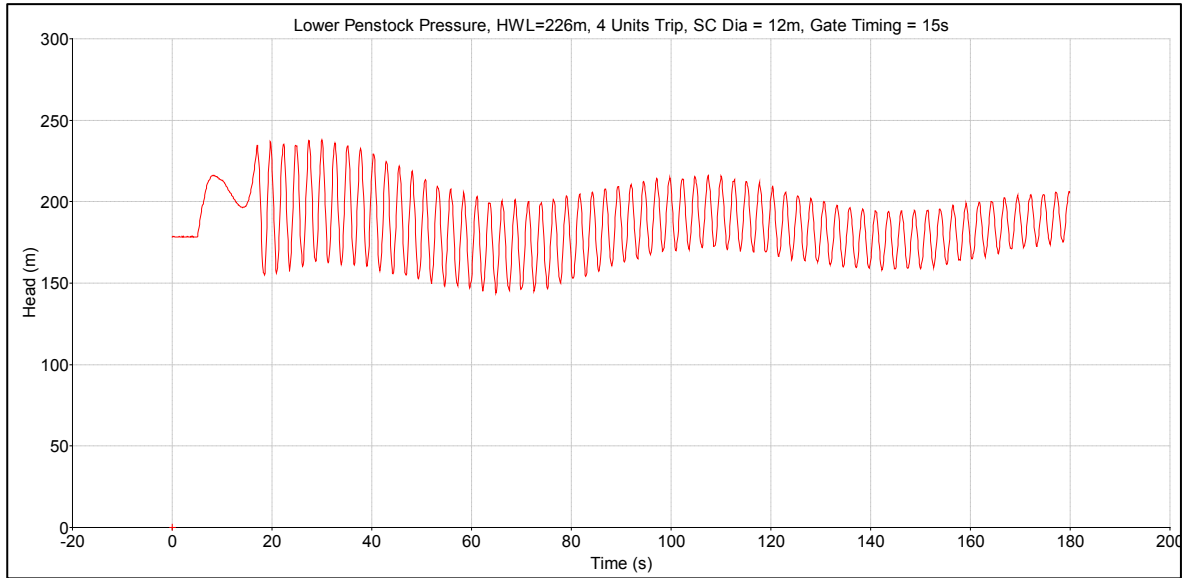


Figure 15-5: Lower penstock pressure following a simultaneous full load rejection at maximum HWL

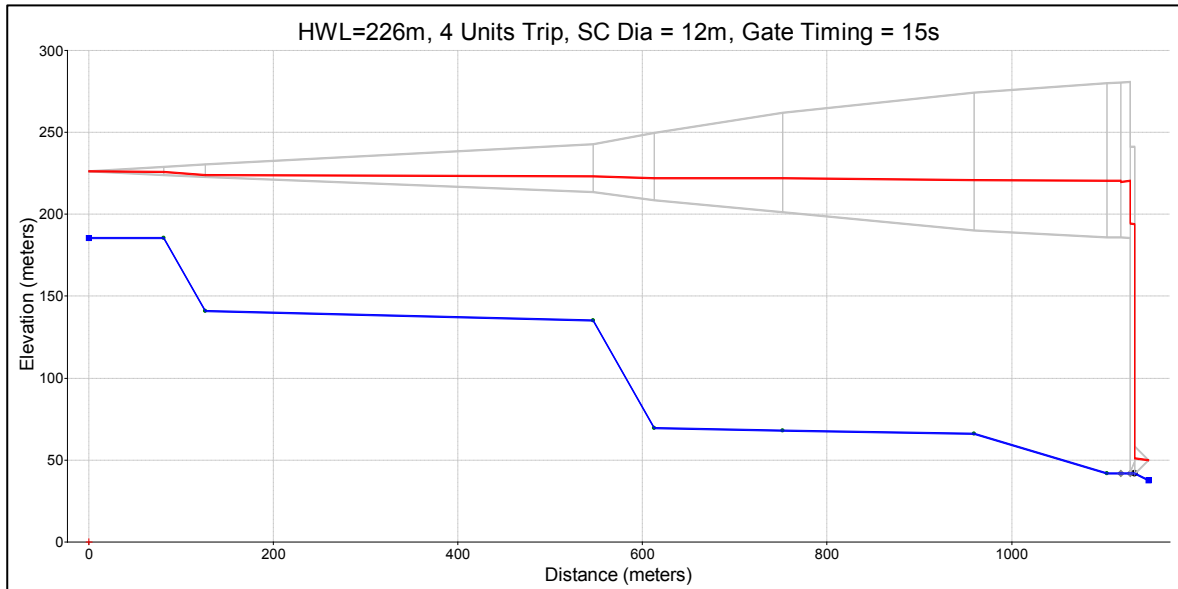


Figure 15-6: Hydraulic grade envelope following a simultaneous full load rejection at maximum HWL

In Figure 15-11, the blue line represents the tunnel profile (longitudinal section), the red line represents the steady-state HGL before the event, while the grey lines represents the envelope of maximum and minimum hydraulic grade that occurs along the tunnel following the event.

Full load rejection – reservoir level at RL 204 m

The following figures indicate the hydraulic behaviour in the conveyance system for a simultaneous trip of 4 turbines with wicket gates closing from 100% in 15 seconds. This case represents the largest reduction in flow rate, however the static head is somewhat lower than the maximum HWL case.

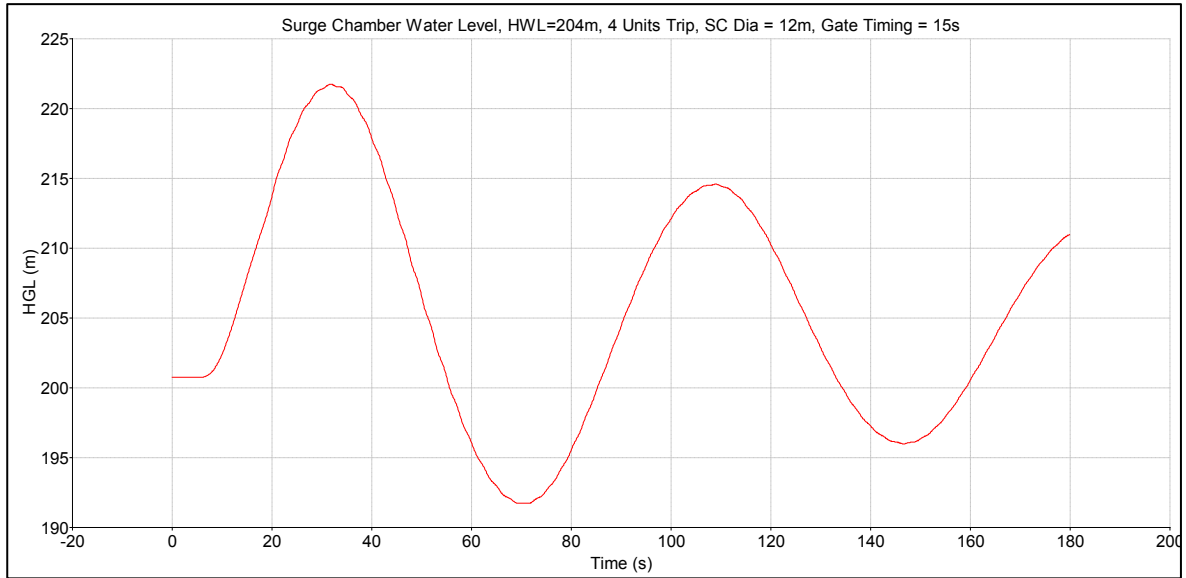


Figure 15-7: Surge chamber water level following a simultaneous full load rejection at RL 204 m HWL

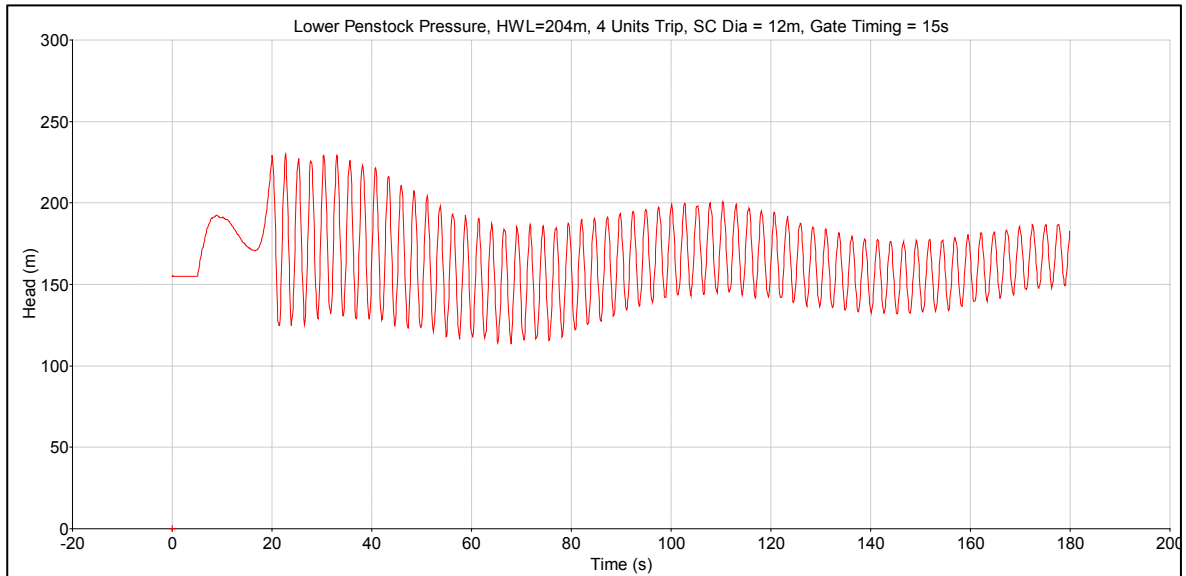


Figure 15-8: Lower penstock pressure following a simultaneous full load rejection at RL 204 m HWL

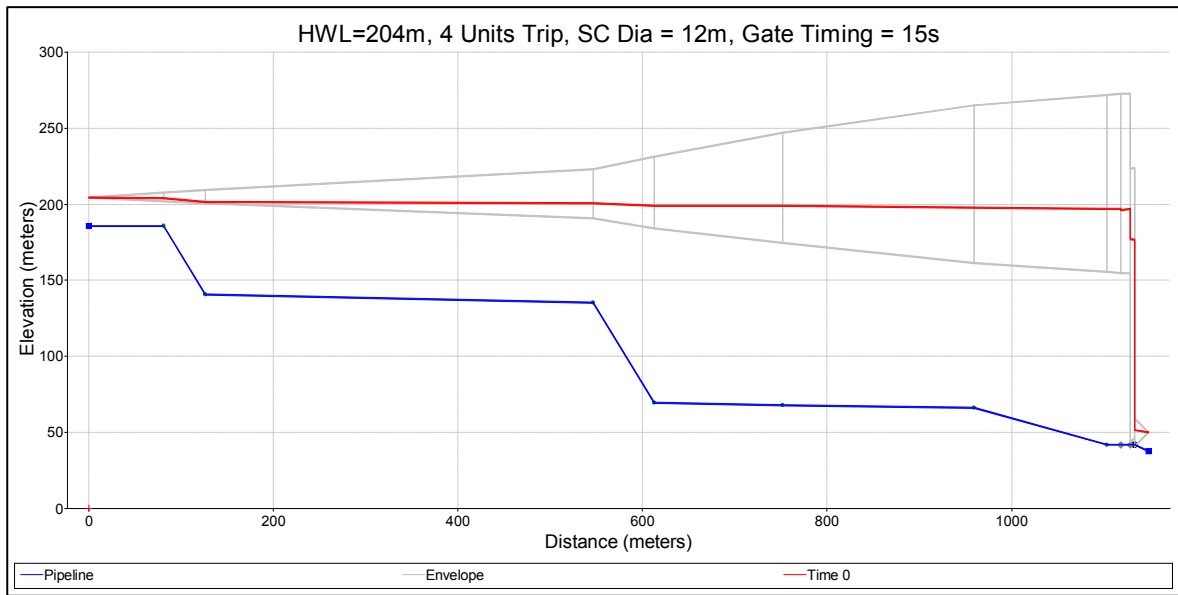


Figure 15-9: Hydraulic grade envelope following a simultaneous full load rejection at RL 204 m HWL

Load acceptance – reservoir level at RL 157 m

Figure 15-15 to Figure 15-17 indicate the hydraulic behaviour in the conveyance system for a full load acceptance of one turbine while all other turbines continue to generate.

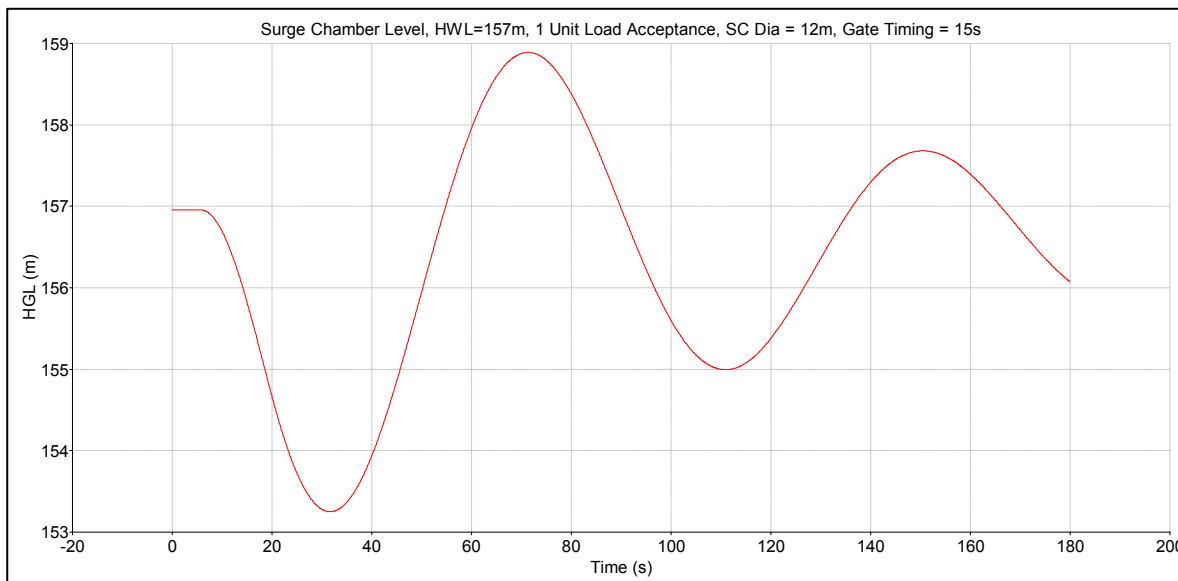


Figure 15-10: Surge chamber water level following a single unit full load acceptance at minimum HWL

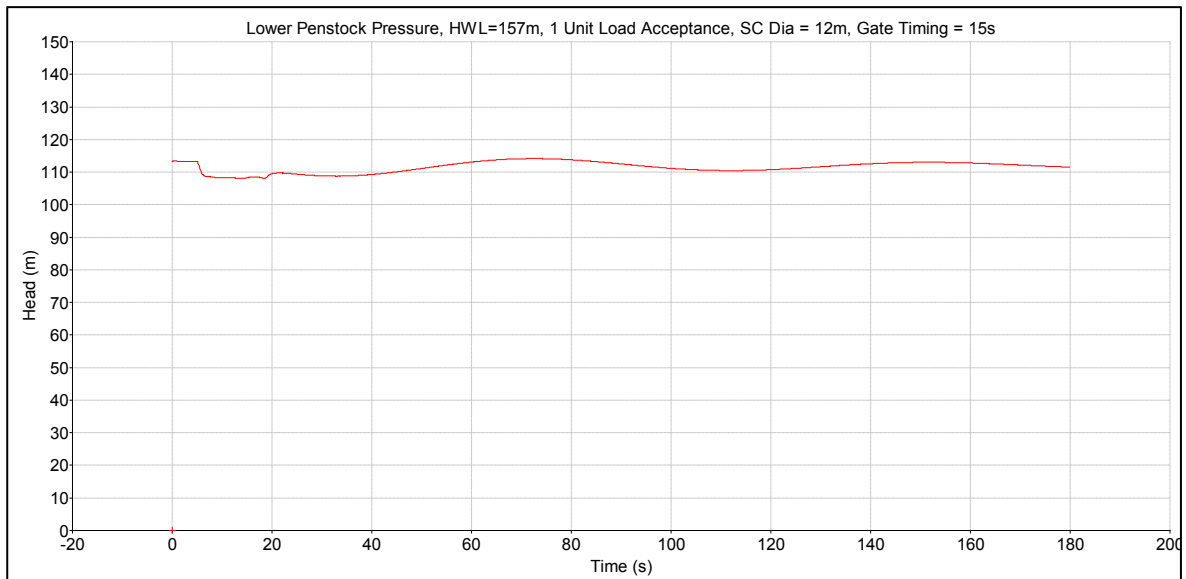


Figure 15-11: Lower penstock pressure following a single unit full load acceptance at minimum HWL

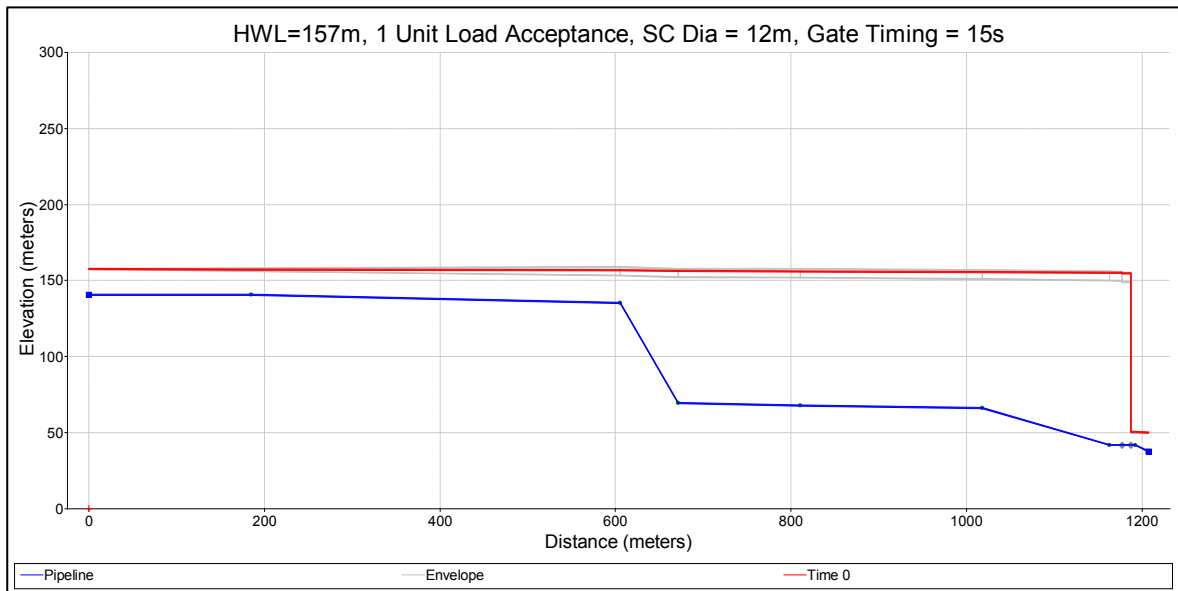


Figure 15-12: Hydraulic grade envelope following a single unit full load acceptance at minimum HWL

The current surge chamber design allows responsive load acceptance and rejection, while limiting the penstock pressure rise to an acceptable level. The surge chamber decreases the distance between the turbine and the nearest open water surface and therefore provides a lower T_w . This is an important parameter for governing stability. Governor response and the power system study

15.3.5 Selection of PSS/E power systems model

FRL commissioned GHD to undertake the modelling of the power system response to a variety of contingency events such as the response to unit trips, spinning reserve units starting, SAG mills stopping and starting and the tripping of transmission lines. An industry standard model was selected for this investigation. This section documents the PSS/E hydro model selection and the parameters developed for the selected model. The study team provided the governor, generator, excitation,

turbine and conveyance system parameters for inclusion in the PSS/E software model of the overall power systems.

15.3.6 Model parameter selection

PSS/E software has a range of modules for modelling the governor response of generating plant. The HYDGOVT model was selected for this project (as this incorporates an elastic wave) model for the penstock and tunnel. The wave model is selected owing to the concern that wave effects must be considered given the ratio or the wave travel time is of the order of 30% of the penstock water time and the fact that simple inelastic water column models are cautioned against where this ratio is greater than 25% (IEEE 1207 para 4.26 (IEEE, 2011)) Additionally, calculations indicate that the error in the head/ flow transfer function at the cross-over frequency could be approximately 20% to 30% if the simple inelastic water column model was used.

15.3.7 Governor parameters

The HYDGOVT model assumes an electro-hydraulic governor employing temporary droop. In assessing appropriate governor settings, the governor has been modelled as a PID unit, which it would be in practice, but with no derivative term ($K_d=0$). This is acceptable as a PI governor can be shown to be mathematically equivalent to a temporary droop governor noting the following equivalence:

- $r = \text{temporary droop} = 1/K_p$, where $K_p = \text{proportional gain}$
- $T_d = \text{governor time constant} = \text{dashpot time constant} = K_p/K_i$, where $K_i = \text{integral gain}$.

The governor parameters were set to achieve both stability in island running (given the system will not be connected to a large external grid) and a fast response to system load changes. However, these goals are not complementary, and a balance by not being overly conservative in the stability margin was sought.

In order to undertake the frequency response analysis, the mathematical transfer functions were set up as described in Figure 15-18 following.

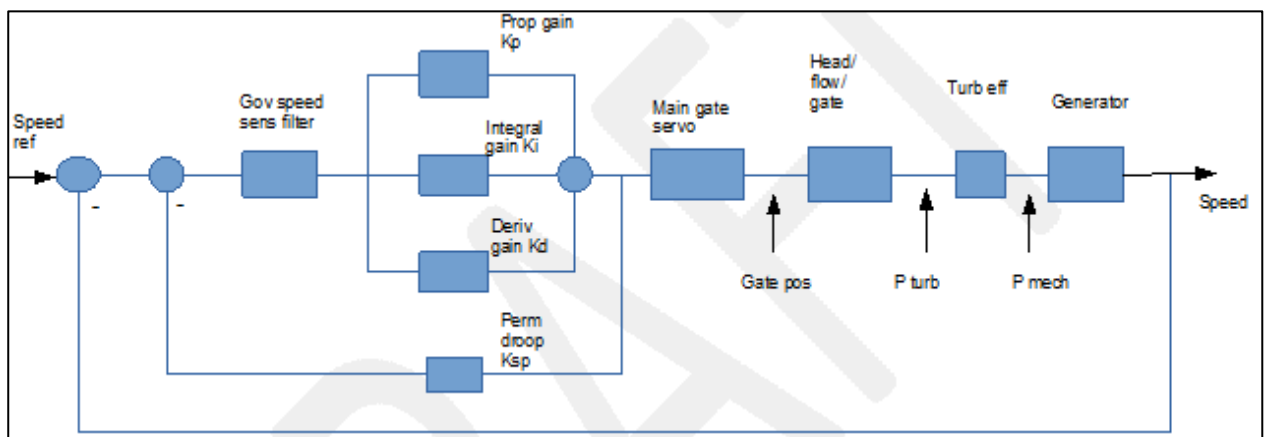


Figure 15-13: Transfer function illustration

Finite element analysis had shown the wave travelled the full penstock plus tunnel length – that is, the surge chamber did not provide a sufficient terminating interface for the pressure wave and, hence the long wave travel time.

In order to undertake the quasi-stationary frequency (domain) analysis, $Z_{p\text{tanhs}}(T_e)$ is linearised as a McLaurin series of order $n=1$.

The PSS/E software cannot determine the governor settings such as the proportional, integral and differential gains, permanent droop and temporary droop. These have been determined as part of the SPS study using in-house software that can cope with multiple turbines being connected to a single penstock. This software can handle a number of situations:

- It can model correctly the trip of a turbine which goes into over speed and which tries to throttle the water passing through the turbine owing to the closure of the wicket gates but also owing to the hydraulic characteristics of the turbine runner, which decreases the flow as the unit speeds up after the trip. This is important as the increase in pressure when the first unit trips causes the spinning reserve unit to load more rapidly improving the system response by 15 to 20% and reducing the magnitude of the frequency swing by 15% approximately, which is not insignificant.
- The in-house model overcomes the inherent weakness of the PSS/E software in modelling multiple units connected to a single penstock. PSS/E assumes each unit has a single penstock. In providing parameters for modelling the governor response to power system changes, the units must be grouped. To limit the number of cases to be analysed, the parameters provided assume the maximum number of units (4) connected to the single penstock. As a result, the water acceleration times are considerably higher than in the normal situation, which means the performance assessment from the PSS/E software is very pessimistic, compared the in-house software package in modelling the system frequency response. It will be inclined to overstate the voltage swings.
- The PSS/E package is better at modelling the power system response for matters such as load shedding, motor starting and stopping and voltage.

15.3.8 Power system study results

The Power Systems Study has analysed over 70 contingency cases at different loads and different operating water levels. The report concludes that the system response is acceptable in all cases investigated. In this section we have highlighted several of cases. The aim is not to summarise the Power Systems Study. It is to identify how the conveyance design and governor settings can influence the power system stability and response. It also aims to help identify issues that need to be investigated further during future phases of study.

A frequency change during a major disturbance of +/- 2.0 Hz is targeted.

Figure 15-19 shows the case of the station supplying the mine with a load of 100 MW shared between four units. When a single unit trips, the frequency drops an acceptable 3%, 1.5 Hz.

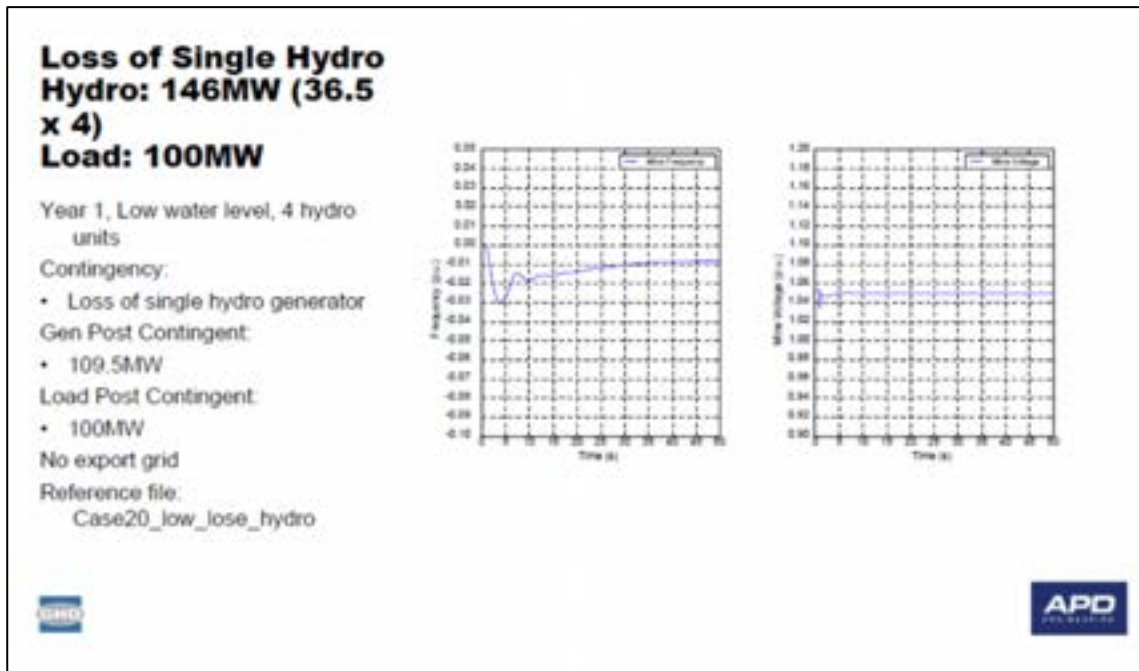


Figure 15-14: System response to the loss of one unit at low water levels (additional unit operating)

The example in Figure 15-20 is an extremely demanding case. Two units only are running on part load to supply the mine with a third unit on spinning reserve. When one unit trips, 50% of the operating capacity, the spinning reserve unit ramps up as does the other operating unit. The frequency drop is 8.8% or 4.4 Hz at a water level of RL 204.39 m and 8.0%, 4.0 Hz at RL 226.14 m. The frequency is outside the preferred range for less than 10 seconds. These values are without load shedding which shows the system is very responsive. With load shedding of the SAG mill, the frequency drop is an acceptable 1.7 to 2.0 Hz for the two water levels. This is the most extreme case in the Power Systems Study.

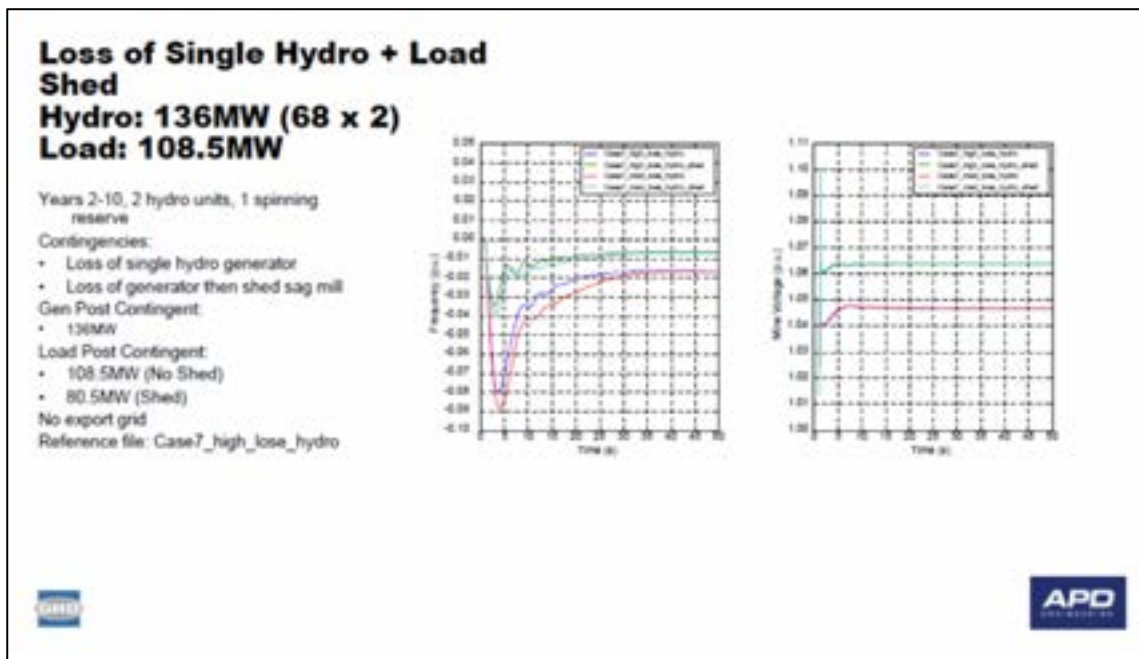


Figure 15-15: System response to the loss of one unit at low water levels (spinning reserve unit operating)

The final example included is shown in Figure 15-21. In this case the FRCGP is operating at peak load with four units operating and a fifth on spinning reserve. When one unit trips 25% of the operating capacity, the spinning reserve unit ramps up as do the other operating units. The frequency drop is 4.0% or 2.0 Hz at a water level of RL 204.39 m and 3.4%, 1.7 Hz at RL 226.14 m. These values are without load shedding which shows the system is very responsive. With load shedding of the SAG mill, the frequency drop is an acceptable 1.0 to 08 Hz for the two water levels. Even without the load shedding the response is acceptable.

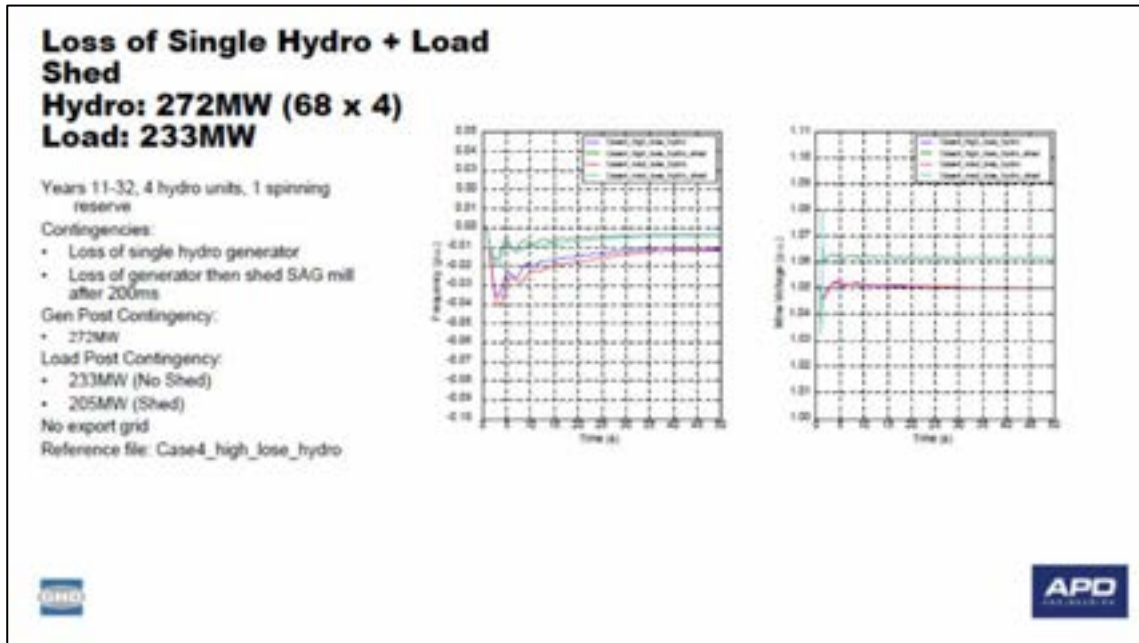


Figure 15-16: System response, loss of one unit at low water levels (spinning reserve unit, peak mine load)

The final example provided in Figure 15-22 is the same as the previous case, but without spinning reserve. Without load shedding the frequency drops 2.0 Hz but does not recover owing to a lack of capacity. With load shedding of the SAG mill the frequency drops 1.4 Hz, which is acceptable.

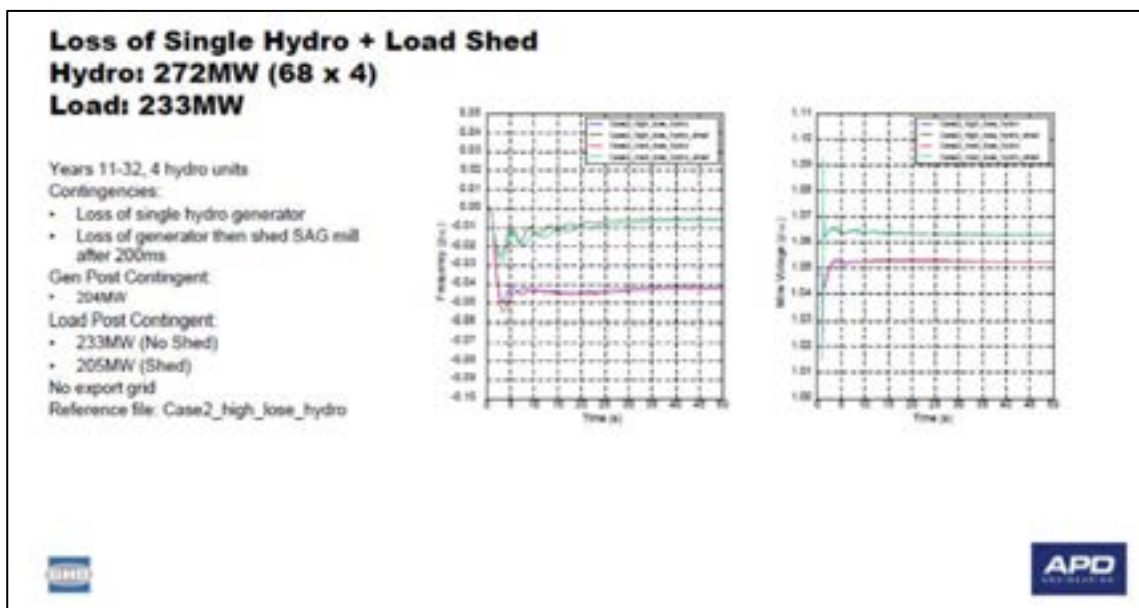


Figure 15-17: System Response, loss of one unit at low water levels (without a spinning reserve operating, peak mine load)

The key points from the Power Systems study were as follows:

- In all cases investigated the system response was acceptable. However, in some cases the SAG mill was required trip to keep the frequency in the required range. However, the inter-trip on the mill acted within 200 ms of the unit trip which does not provide time to confirm if the trip of the SAG mill was necessary
- As noted, the most onerous contingency is the loss of the SAG mill load. The loss of a fully loaded hydro unit would be more onerous except that this is tempered by the 20 MW automatic load shedding inter-trip.
- These results confirm that fundamental design of the unit configuration and sizing in combination with the two penstocks and tunnel systems is acceptable. Also, the choice of relatively high operating velocities to minimise the conveyance system diameters and costs has been confirmed as justified.

In reviewing the results several points emerge:

- The difference in response between the medium operating level and high operating level is the difference in wicket gate speed. At medium level it takes 15 seconds to load fully but at the high level it is only 12 seconds. This reduces the absolute frequency swing by around 10% but it has significantly greater impact on the time the frequency is outside the +/-2.0 Hz target range
- Work using the in-house model suggests that increasing the generator inertia from 1,681 Tm² to 2,200 Tm², which may be possible at negligible cost, coupled with more aggressive PID settings on the governor could reduce the frequency swing in all cases by approximately 25%, which is very significant
- The wicket gate timing may be able to be decreased. However, this will give rise to higher percentage pressure rises increasing the over speed on the generators following a trip. Using the station bypass valves to limit the over pressure percentage could control this problem but it will need an intelligent control system to achieve the desired result
- Two stage wicket gate closing may improve matters and should be investigated.
- Small changes to the temporary droop and possibly permanent droop may allow the hydro units to power the system when the load matches hydro output and to cope with the tripping of a hydro unit mill without the need to trip a SAG mill
- The power system analysis has shown that the proposed hydraulic design with a 15 second wicket gate time is acceptable. This also demonstrates that a surge chamber is an essential part of the scheme in order to achieve this closing rate
- Different wicket gate timings at different reservoir levels can be used to improve the system response
- An investigation into delaying the load shedding using the SAG mill is required to minimise the times that this is implemented
- FRCGP may be able to review the time that the plant can operate outside the desired frequency range to prevent the need to shed mine load in the event of the event of the trip of operating generating units.

15.4 Numbers of generating units and generation reliability

15.4.1 Factors affecting turbine generator reliability

There are three main factors that influence the reliability of the turbine generator plant. These are as follows:

- The Power Systems Study has demonstrated that a spinning reserve unit operating on tailwater depression is able to maintain the frequency of the system within allowable limits in the event of a wide range of contingencies including trip of a generating unit, trip of a transmission line, loss of a SAG mill and start-up of a SAG mill. Further this is achievable without the need for load shedding although the frequency swings are limited if load shedding is implemented. In other words, a spare unit is required at all times
- The FRHEP is extremely remote. A major repair that requires parts to be shipped to either South East Asia or Australia for repairs or accessing parts that are not available on site, could lead to a short outage becoming two weeks longer than at a more accessible site
- Throughout the earlier phases of this project there has been a concern about the potential for heavy wear on the turbine runner and wear parts. The Water, Limnology and Load Balance Study (Section 6) has now provided more reliable information, as discussed below.

Sedimentary flow impact on turbine runners

Turbines cope well with a certain level of sediment. In this instance, it is cost effective to ensure the specific speed is in the region of 140 to 150 which helps limit the velocities of water through the turbine water passages. If sediment levels were in excess of 300–500 g/m³, it could be expected that repairs will be required every second year. However, there is a view that the type of damage required to cause this level of damage requires particles in excess of 50 µm, whereas it is expected that the particles passing through the embankment will be smaller than 15 µm. It is understood that the more abrasive sediments such as quartz and feldspar are found in smaller quantities. A testing program is needed to assess the sediment properties for inclusion in the equipment purchase tender. However, initial estimates are now available.

Figure 15-23 shows the results of simulations which determine the estimated TSS at the reservoir discharge over forty years from the start of construction, through filling through to mine closure and beyond. The results are presented on daily basis. There is a spike in levels at the start of impoundment. As can be seen the levels rise to a peak 250 g/m³ after 15 to 17 years and then fall steadily. A breakdown of the material that makes up the suspended solids has been provided. This is shown in Figure 15-24. As can be seen the percentage of hard material increases over time. However, it is only less than 30% of the total solids when the TSS values peak.

The combined impact of the changing amount of TSS over time and its constituents are shown in Figure 15-25. As can be seen the level of hard material increases from less than 20 g/m³ to as high as 80 g/m³ before falling to approximately 30 g/m³. It should be noted that the only a percentage of the hard material is comprised of the most abrasive materials and the size is under 15 µm.

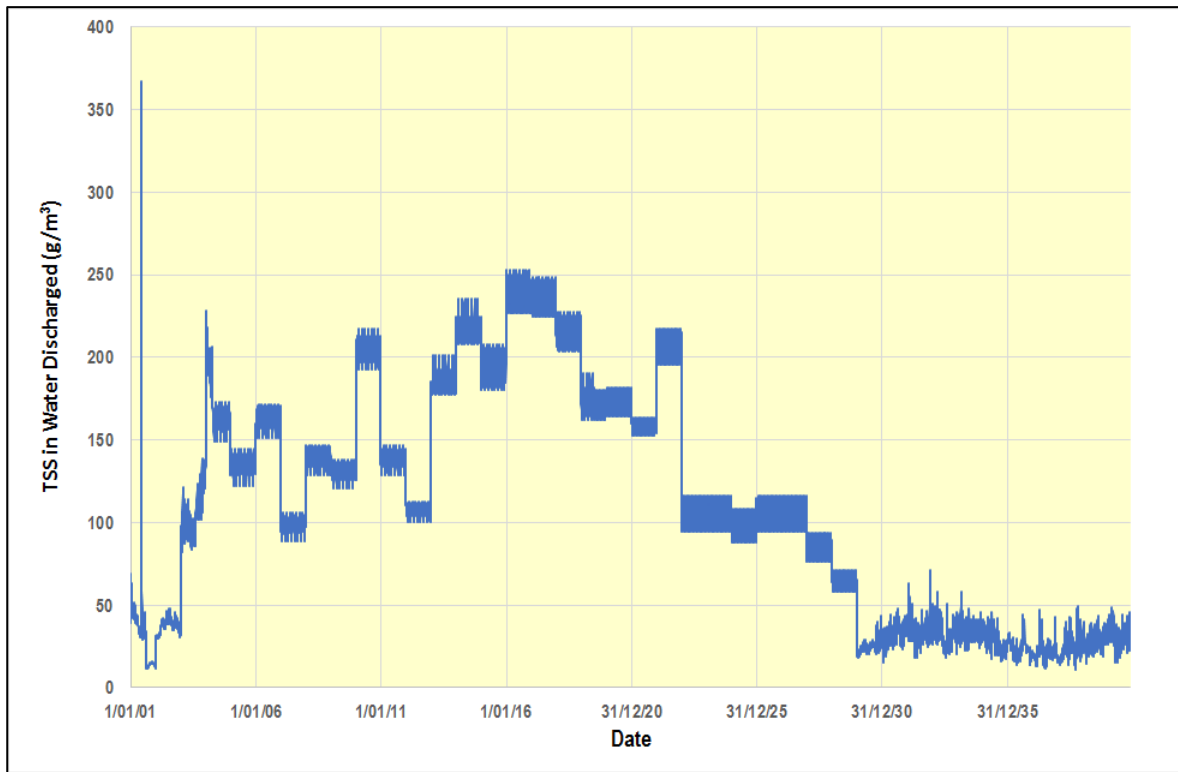


Figure 15-18: Variation in the total suspended solids discharging from the FRHEP reservoir

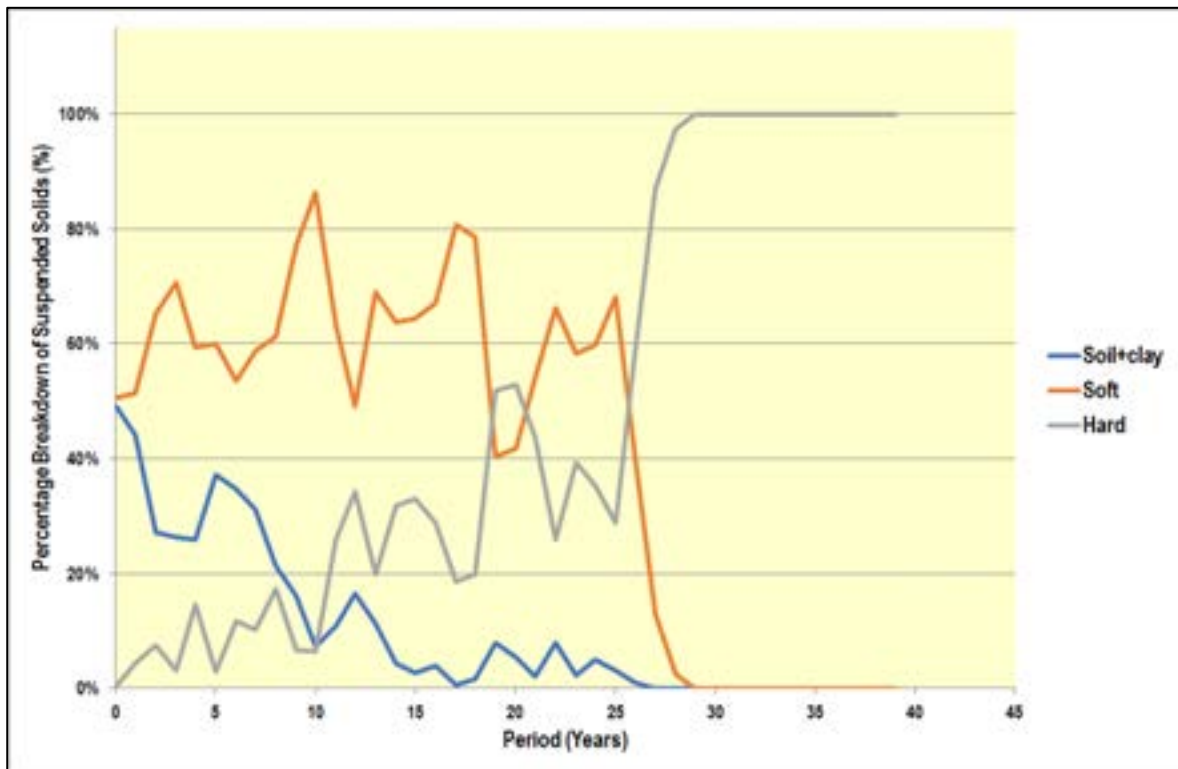


Figure 15-19: Breakdown of suspended solids

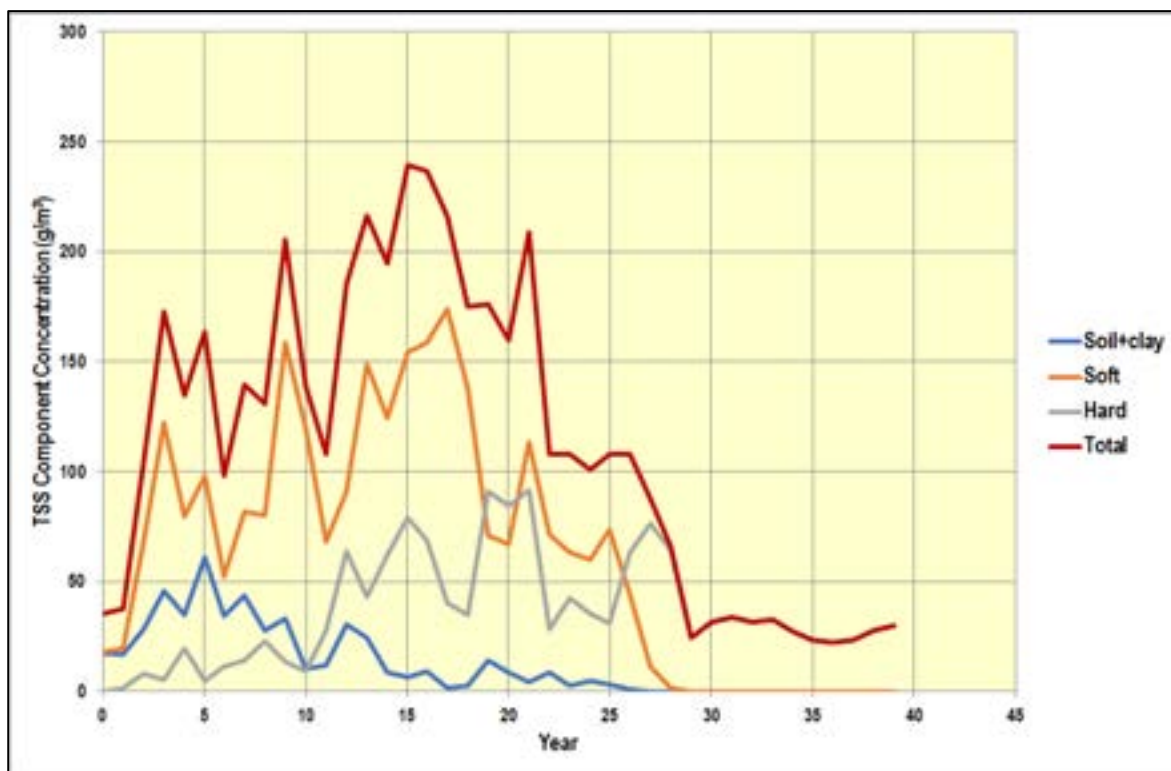


Figure 15-20: Suspended solid level by component

During large floods, the concentration of sediments entering the reservoir from the rivers could be in the range of 1,000–10,000 g/m³. These will be substantially attenuated by the reservoir with much of the material dropping out in the upper reaches of the reservoir.

While the sediment levels are significantly lower than thought previously, damage to runners is still expected, as well as to areas where sediment may accumulate, such as the seals. Similarly, the effect of the small particles on the potential cavitation damage in the machines is highly uncertain.

The turbines will have a tungsten carbide coating specified and this can extend the operating life significantly, up to fivefold. Some manufacturers reduce the guaranteed efficiency by ~1% if the coating is applied. Taking this into account, the repair time may be extended to four years or more. However, there is currently insufficient information to confirm this value.

Figure 15-26 provides an estimate of the time between runner repairs for a Francis turbine.¹⁰² The graph is based on uncoated runners. Based on an average TSS of 190 g/m³, of which the hard material is 50 g/m³, during the middle years of turbine operation, the mean time between repairs is likely to be around five years. With the coating it is hoped that this could be extended to 15 to 20 years. The runner life may be longer than the life of the mine. The net result is that sediment is not seen to be a major threat to the availability of the turbine generators, based on the information in Section 6.

In this investigation, the normal values for turbine generators have been adopted. These are a planned outage rate of 4.5% with a forced outage rate of 0.5% giving 5.0% total outage rate. There is potential for higher outage rates to occur either because of inadequate spares inventories leading to prolonged outages, heavy erosion owing to the sediment issues being greater than expected or cavitation issues owing to the sediment, which can be difficult to predict. The upper end of the outage rates that could be considered is a planned outage rate on average of 10% of the hours each year with the forced

¹⁰² Nozaki, T., 'Technical Report: Estimation of Repair Cycle of Turbine Due To Abrasion Caused By Suspended Sediment and Determination of Desilting Basin Capacity,' Japan International Cooperation Agency, 1990

outage rate being double the normal rate at 1.0% giving an 11.0% total outage rate. Both sets of planned and forced outage rate have been evaluated to demonstrate the sensitivity to the issue.

By comparison, alternative generation sources such as IFO engines are expected to have a long-term availability of 91% and need significant (50%) additional capacity to meet the reliability standard of the FRCGP.

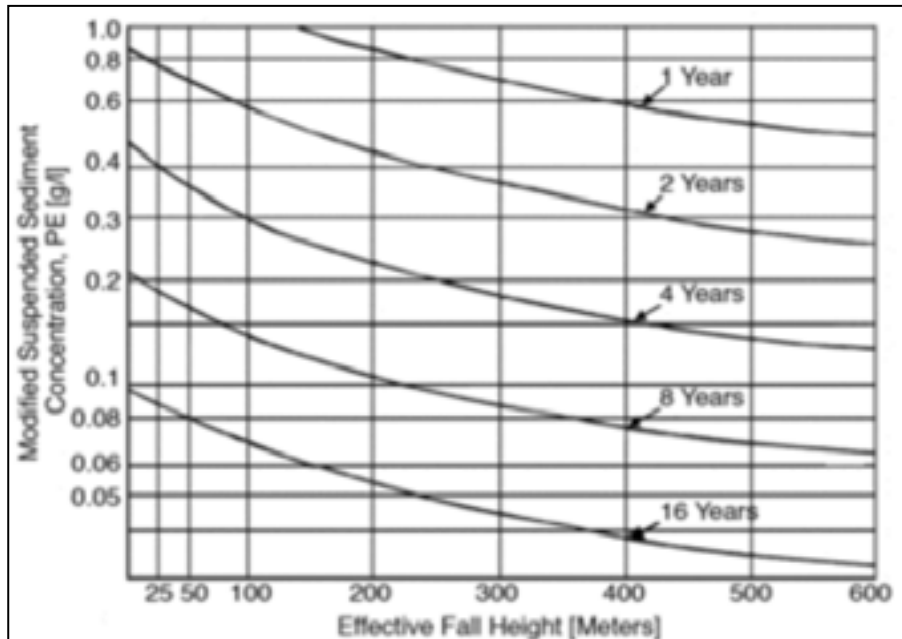


Figure 15-21: Timing of running repairs and the effect of sediment concentration

15.4.2 Cost optimisation of the number of units required

The number of units required has been optimised on a cost basis. It should be noted that all unit outputs quoted in this section are at the HV step-up transformer terminals.

There are several considerations:

- Two spare units are required to provide the mine with the required reliability level of 99.73%. One of the spare units will be spinning reserve and one may be out for planned maintenance.
- The output from the turbines varies with head and flow. Also, for a given runner size, the higher the head the greater the maximum flow that can be passed through the turbine. As shown in Section 16.7, where this matter is discussed further that it has been found that the turbines must pass sufficient water to allow full power from the units at a water level of RL 204.39 m. This is the minimum level for the RL 238.5 m embankment that can supply both the FRCGP and the export grid with full power. As the water level rises, the flow that can be passed increases allowing more power to be generated from the turbine because of the higher head and the higher maximum flow. To take advantage of this the generator needs to be uprated. However, the extra power is only available at higher reservoir levels. For this study, it is assumed that full power from a unit is the value achieved at the normal minimum water of RL 204.39 m. At higher water levels, the governor has to limit the wicket gate opening to restrict the power from the units to the generator capacity. Oversizing the generators would increase the cost of the generators and the powerhouse. The main advantage is that it would improve the generator reliability at high water levels but not sufficiently to allow one large generator to be deleted. The water level where generation starts is determined by the level at which the reduction in generator flow with lower head still allows the full FRCGP load of 146 MW in the first year to be met.

- In sizing units, it is important to check if they can be configured to supply the 175 MW to the export grid from a separate substation bus to the bus that supplies up to 234 MW to the mine plus having a single spinning reserve unit dedicated to the mine and provision being made for one unit on planned maintenance.
- When the mine is not operating, the minimum FRCGP load varies between 10.8 and 13 MW. The powerstation and dam auxiliaries will also use power. In addition, there are the no load losses of the transmission system. These factors could increase the minimum load at the FRCGP to between 12.5 and 15 MW. The difficulty is that any large turbine under consideration to meet the FRCGP and export grid loads is too large to meet these minimum loads without the probability of cavitation and as a result the large turbines will not be operated to meet this load. As a result, two small turbines are required with a rating of 15 to 20 MW to meet the minimum loads.

An exercise has been carried out to determine the cost of 3 to 6 main generating units plus 2 spare units sized to meet the of the FRCGP and export grid. The two small units have been sized to be the minimum of 15 MW or the capacity that is needed to allow one of the following, while retaining one spare unit while the export grid and FRCGP operate on independent buses at the substation.

The arrangements considered the allocation of sufficient large units to meet the FRCGP load plus a spinning reserve unit. The small units are sized to make up the 175 MW capacity required to supply the grid with the remaining large units and two small units operating at full load, while one unit is spare.

It was determined that the use of 8 large units has the lowest capital cost and smallest installed capacity. The powerhouse is narrower, but slightly longer for the 8-unit case, which has advantages on this site. Overall the recommendation is for:

- Eight large units with a rating of 69.2 MW, 81.4 MVA at the generator terminals (68.3 MW, 80.0 MVA) at the transformer HV terminals
- Two small units with a rating of 19.3 MW, 22.7 MVA, (19.1 MW, 22.5 MVA) at the transformer HV terminals.

15.4.3 Reliability of recommended plant configuration and timing of unit installation

In this section the timing of when units are required and the overall reliability of generation taking account of both the large and small units is considered. The analysis is based on the January electrical loads. The May electrical loads are very similar and as a result the reliability is extremely similar.

The load on the system increases in three major increments and with the effect of reservoir having to be considered as well. The following four load cases are considered:

- In Year 1 when the mine is fully commissioned the load is expected to be 146 MW. The initial water level could be as low as RL 171.2 m which limits the unit output to 36.5 MW. The results of the analysis are presented in Table 15-9.
- In Year 1 when the mine is fully commissioned the load is expected to be 146 MW. Once the reservoir level reaches RL 204.39 m, the full generator output of 68.3 MW will be available. It increases slightly until it is 154 MW in Year 5. The results of the analysis are presented in Table 15-10.
- Depending on the inflows, in Year 2 or Year 3, the reservoir will have reached a level that export of power to the remote grid can be considered. This could add anything between 20 MW and 175 MW to the FRHEP load depending on whether the remote load is a mine or is dependent on connecting to existing towns and existing electrical distribution infrastructure. The result is that in Year 5 the maximum load could be 328 MW. This case is modelled to cover Years 2 to 10. The results of the analysis are presented in Table 15-11.

- Finally, in Year 11 the FRCGP load is expected to increase to 227 MW and to increase slowly until it is 234 MW in Year 17. The peak combined load is 409 MW. This case is modelled to cover Years 11–33. The results of the analysis are presented in Table 15-12.

The overall combined reliability of different numbers of units for reliable operation at each of the three major load increments years has been assessed. From this unit installation schedule can be optimised. Note the configuration is eight large units and two small units. The effect of allowing for a spinning reserve unit is considered.

A review of Table 15-9 to Table 15-12 allows several conclusions to be drawn:

- The two small units must be commissioned first to provide power for dry commissioning. At the lowest operating water level, the power output is 10 MW per unit. This is sufficient for the dry commissioning of the process plant at the mine.
- When generation first commences for mine dry commissioning the loads are likely to be 10 to 20 MW and this situation could last for three months approximately. The initial load during wet commissioning of the process plant could be 60 to 80 MW and will ramp up to a running load of 126 MW with peaks of 146 MW during the year. At the initial water level, when the turbine output is constrained, six large units and two small units are required to meet the peak and running demand with a spare unit and spinning reserve giving a reliability from Table 15-9 of 99.3% (97.0% at the higher outage rates) which is slightly less than the target. However, during this period more units could potentially be commissioned and planned outages should not be required. If they were provided, installation could be co-ordinated with the mine commissioning. If only five units are provided there is still a single unit available for spinning reserve but no spare unit. The reliability of the generating plant is 99.5% (98.0% at the higher outage rates).
- Later in Year 1, when the water level reaches the minimum normal operating range of RL 204.39 m. Table 15-10 shows that four units yield a generation reliability of 99.77% (98.98% at the higher outage rates). With five units, generation reliability is 100.00% (99.97% at the higher outage rates). The conclusion is that five units at most are required in Year 1.
- The load increment for the export grid is likely to occur a year or possibly two years after power supply to the FRCGP commences – dependant on the inflows. Table 15-11 shows that seven units are required to achieve the target reliability. The table shows that the overall generation reliability is 99.97% (99.83% at the higher outage rates). At times of peak demand, the reliability is slightly less at 99.03% (95.84% at the higher outage rates).
- The final load increment is when the FRCGP load increases in Year 11. Table 15-12 shows that with the eighth large unit being installed, the overall generation reliability is 99.96% (99.75% at the higher outage rates). At times of peak demand, the reliability is slightly less at 98.71% (94.51% at the higher outage rates).

The final suggestion for commissioning dates is as follows:

- The two small units and four large units must be available for the start of Year 1.
- Two further large units should be installed during Year 1 and be available for the start of Year 2. The final unit could be installed at the same time to allow the export power to be maximised.

The installation of the final large unit could be delayed until Year 11 to defer capital expenditure if desired by FRL, when the FRCGP load increases, if the capacity for export grid power is limited to 175 MW up to that time. The final unit installation can be delayed even if the energy sales to the export grid are higher than 996 GWh/a, provided the peak demand does not exceed 175 MW.

Table 15-8: Combined reliability of unit configurations at RL 171.2 m reservoir level

Load Case Year 1 Water Level at RL 157.65 m	Hours/ annum	Load (MW)	Configuration 4.5% Planned Outage Rate 0.5% Forced Outage Rate				
			4 Large Units	5 Large Units	6 Large Units	7 Large Units	8 Large Units
			2 Small Units	2 Small Units	2 Small Units	2 Small Units	2 Small Units
Peak Running + Spinning Reserve	160	182	N/A	75.58%	99.30%	99.99%	100.00%
Normal Running + Spinning Reserve	7111	172	N/A	75.58%	99.30%	99.99%	100.00%
Non-Running + Spinning Reserve	1489	11	100.00%	100.00%	100.00%	100.00%	100.00%
Combined Peak Running and Normal Running Probability			N/A	79.73%	99.42%	99.99%	100.00%
Peak Running	160	146	80.37%	99.53%	99.99%	100.00%	100.00%
Normal Running	7111	136	80.37%	99.53%	99.99%	100.00%	100.00%
Non-Running	1489	11	100.00%	100.00%	100.00%	100.00%	100.00%
Combined Peak Running and Normal Running Probability			83.71%	99.61%	99.99%	100.00%	100.00%

Configuration 10.0% Planned Outage Rate 1.0% Forced Outage Rate				
4 Large Units	5 Large Units	6 Large Units	7 Large Units	8 Large Units
2 Small Units	2 Small Units	2 Small Units	2 Small Units	2 Small Units
N/A	47.55%	97.00%	99.90%	100.00%
N/A	47.55%	97.00%	99.90%	100.00%
100.00%	100.00%	100.00%	100.00%	100.00%
N/A	56.47%	97.51%	99.91%	100.00%
57.64%	97.98%	99.94%	100.00%	100.00%
57.64%	97.98%	99.94%	100.00%	100.00%
100.00%	100.00%	100.00%	100.00%	100.00%
64.84%	98.32%	99.95%	100.00%	100.00%

Table 15-9: Combined reliability of unit configurations at RL 204.39 m reservoir level

Load Case Year 1 Water to RL 204.39 m	Hours/ annum	Load (MW)	Configuration 4.5% Planned Outage Rate 0.5% Forced Outage Rate				
			4 Large Units	5 Large Units	6 Large Units	7 Large Units	8 Large Units
			2 Small Units	2 Small Units	2 Small Units	2 Small Units	2 Small Units
Peak Running + Spinning Reserve	160	214	99.67%	100.00%	100.00%	100.00%	100.00%
Normal Running + Spinning Reserve	7111	204	99.72%	100.00%	100.00%	100.00%	100.00%
Non-Running + Spinning Reserve	1489	11	100.00%	100.00%	100.00%	100.00%	100.00%
Combined Peak Running and Normal Running Probability			99.77%	100.00%	100.00%	100.00%	100.00%
Peak Running	160	146	100.00%	100.00%	100.00%	100.00%	100.00%
Normal Running	7111	136	100.00%	100.00%	100.00%	100.00%	100.00%
Non-Running	1489	11	100.00%	100.00%	100.00%	100.00%	100.00%
Combined Peak Running and Normal Running Probability			100.00%	100.00%	100.00%	100.00%	100.00%

Configuration 10.0% Planned Outage Rate 1.0% Forced Outage Rate				
4 Large Units	5 Large Units	6 Large Units	7 Large Units	8 Large Units
2 Small Units	2 Small Units	2 Small Units	2 Small Units	2 Small Units
98.28%	99.95%	100.00%	100.00%	100.00%
98.78%	99.97%	100.00%	100.00%	100.00%
100.00%	100.00%	100.00%	100.00%	100.00%
98.98%	99.97%	100.00%	100.00%	100.00%
99.97%	100.00%	100.00%	100.00%	100.00%
99.99%	100.00%	100.00%	100.00%	100.00%
100.00%	100.00%	100.00%	100.00%	100.00%
99.99%	100.00%	100.00%	100.00%	100.00%

Table 15-10: Combined reliability of unit configurations (normal operating levels, Years 2 to 10)

Load Case Year 2 to 10	Hours/ annum	Load (MW)	Configuration 4.5% Planned Outage Rate 0.5% Forced Outage Rate					Configuration 10.0% Planned Outage Rate 1.0% Forced Outage Rate				
			4 Large Units	5 Large Units	6 Large Units	7 Large Units	8 Large Units	4 Large Units	5 Large Units	6 Large Units	7 Large Units	8 Large Units
			2 Small Units	2 Small Units	2 Small Units	2 Small Units	2 Small Units	2 Small Units	2 Small Units	2 Small Units	2 Small Units	2 Small Units
Peak Running + Export grid + Spinning Reserve	160	397	N/A	N/A	70.84%	99.03%	99.98%	N/A	N/A	37.66%	95.84%	99.84%
Normal Running + Export grid + Spinning Reserve	8250	324	N/A	75.58%	99.30%	99.99%	100.00%	N/A	47.55%	97.00%	99.90%	100.00%
Non-Normal Running + Export grid + Spinning Reserve	350	123	100.00%	100.00%	100.00%	100.00%	100.00%	99.99%	100.00%	100.00%	100.00%	100.00%
Combined Peak Running and Normal Running Probability			N/A	N/A	98.81%	99.97%	100.00%	N/A	N/A	96.04%	99.83%	99.99%
Peak Running + Export grid	160	329	N/A	75.58%	99.30%	99.99%	100.00%	N/A	47.55%	97.00%	99.90%	100.00%
Normal Running + Export grid	8250	256	80.37%	99.53%	99.99%	100.00%	100.00%	57.64%	97.98%	99.94%	100.00%	100.00%
Non-Running + Export grid	350	123	100.00%	100.00%	100.00%	100.00%	100.00%	99.99%	100.00%	100.00%	100.00%	100.00%
Combined Peak Running and Normal Running Probability			N/A	99.12%	99.98%	100.00%	100.00%	N/A	97.14%	99.89%	100.00%	100.00%
Peak Running + Spinning Reserve	160	222	99.67%	100.00%	100.00%	100.00%	100.00%	98.28%	99.95%	100.00%	100.00%	100.00%
Normal Running + Spinning Reserve	8250	212	99.67%	100.00%	100.00%	100.00%	100.00%	98.28%	99.95%	100.00%	100.00%	100.00%
Non-Running + Spinning Reserve	350	11	100.00%	100.00%	100.00%	100.00%	100.00%	100.00%	100.00%	100.00%	100.00%	100.00%
Combined Peak Running and Normal Running Probability			99.68%	100.00%	100.00%	100.00%	100.00%	98.35%	99.95%	100.00%	100.00%	100.00%
Peak Running	160	154	100.00%	100.00%	100.00%	100.00%	100.00%	99.97%	100.00%	100.00%	100.00%	100.00%
Normal Running	8250	143	100.00%	100.00%	100.00%	100.00%	100.00%	99.97%	100.00%	100.00%	100.00%	100.00%
Non-Running	350	11	100.00%	100.00%	100.00%	100.00%	100.00%	100.00%	100.00%	100.00%	100.00%	100.00%
Combined Peak Running and Normal Running Probability			100.00%	100.00%	100.00%	100.00%	100.00%	99.97%	100.00%	100.00%	100.00%	100.00%

Table 15-11: Combined reliability of unit configurations (normal operating levels, Years 11–33)

Load Case Year 11–33	Hours/ annum	Load (MW)	Configuration 4.5% Planned Outage Rate 0.5% Forced Outage Rate					Configuration 10.0% Planned Outage Rate 1.0% Forced Outage Rate				
			4 Large Units	5 Large Units	6 Large Units	7 Large Units	8 Large Units	4 Large Units	5 Large Units	6 Large Units	7 Large Units	8 Large Units
			2 Small Units	2 Small Units	2 Small Units	2 Small Units	2 Small Units	2 Small Units	2 Small Units	2 Small Units	2 Small Units	2 Small Units
Peak Running + Export grid + Spinning Reserve	160	477	N/A	N/A	N/A	66.14%	98.71%	N/A	N/A	N/A	27.96%	94.51%
Normal Running + Export grid + Spinning Reserve	8250	398	N/A	N/A	70.84%	99.03%	99.98%	N/A	N/A	37.66%	95.84%	99.84%
Non-Normal Running + Export grid + Spinning Reserve	350	123	100.00%	100.00%	100.00%	100.00%	100.00%	99.99%	100.00%	100.00%	100.00%	100.00%
Combined Peak Running and Normal Running Probability			N/A	N/A	N/A	98.47%	99.96%	N/A	N/A	N/A	94.77%	99.75%
Peak Running + Export grid	160	408	N/A	N/A	70.84%	99.03%	99.98%	N/A	N/A	37.66%	95.84%	99.84%
Normal Running + Export grid	8250	330	N/A	75.58%	99.30%	99.99%	100.00%	N/A	47.55%	97.00%	99.90%	100.00%
Non-Running + Export grid	350	123	100.00%	100.00%	100.00%	100.00%	100.00%	99.99%	100.00%	100.00%	100.00%	100.00%
Combined Peak Running and Normal Running Probability			N/A	N/A	98.81%	99.97%	100.00%	N/A	N/A	96.04%	99.83%	99.99%
Peak Running + Spinning Reserve	160	302	72.54%	97.20%	99.93%	100.00%	100.00%	45.65%	87.50%	99.33%	99.98%	100.00%
Normal Running + Spinning Reserve	8250	286	80.17%	99.47%	99.99%	100.00%	100.00%	56.94%	97.37%	99.90%	100.00%	100.00%
Non-Running + Spinning Reserve	350	11	100.00%	100.00%	100.00%	100.00%	100.00%	100.00%	100.00%	100.00%	100.00%	100.00%
Combined Peak Running and Normal Running Probability			80.83%	99.45%	99.99%	100.00%	100.00%	58.45%	97.30%	99.90%	100.00%	100.00%
Peak Running	160	233	97.83%	99.95%	100.00%	100.00%	100.00%	90.22%	99.56%	99.99%	100.00%	100.00%
Normal Running	8250	217	99.67%	100.00%	100.00%	100.00%	100.00%	98.28%	99.95%	100.00%	100.00%	100.00%
Non-Running	350	11	100.00%	100.00%	100.00%	100.00%	100.00%	100.00%	100.00%	100.00%	100.00%	100.00%
Combined Peak Running and Normal Running Probability			99.65%	99.99%	100.00%	100.00%	100.00%	98.20%	99.94%	100.00%	100.00%	100.00%

15.5 FRHEP arrangement

The arrangement of the FRHEP can be summarised to consist of the following elements:

- A residual flow intake at a low level to provide river flow once the diversion tunnels are closed and plugged. The residual flow arrangement has an intake, tunnel, flow control valves, stilling chamber and connection to one of the diversion tunnels. Once the reservoir level reaches a suitable level above RL 200 m, and the bypass valves are operating correctly the residual flow intake can be plugged. The valves could be removed. A decision on plugging the raised bore would be required as well.
- A lower intake to provide the early operation of the power scheme, once filling of the reservoir commences. This low level arrangement also provides the initial access to the main conveyance tunnels, allowing construction to be undertaken from both ends. Once the upper intake is operating correctly, the low intake should be decommissioned and plugged. The lower intake is in use for short period of time – possibly only two years at most. To simplify the installation no screen cleaner is provided for the low intake. The two upper intakes will be fitted with a fully automated screen cleaner.
- An upper intake structure feeding a twin conveyance tunnel arrangement. This intake structure includes two sets of hydraulically controlled wheeled gates and stoplogs, a screen, an automated screen cleaner and an access bridge at RL 235 m.
- Twin 7.1 m diameter conveyance tunnels, including power shafts and surge chambers. Each tunnel will be concrete lined, with steel lining at the outlet end, connecting to the twin main penstocks.
- Twin 7.1 m diameter penstocks that connect the powerhouse to the conveyance tunnels. Each penstock is then split via a manifold to provide water to each turbine, and the bypass valves.
- A powerhouse containing the generating and switching equipment. The building itself is some 196 m long by 35 m wide, and is located on the original river bank of the Frieda River, just downstream of the embankment toe. The powerhouse has multiple levels to access the equipment, and a loading/ erection bay to allow installation (and future maintenance) of the equipment. On the river side of the powerhouse a submerged tailrace is provided to allow discharge of the water from the turbines to the river. The tailrace contains a series of flood protection stoplogs.
- Adjacent to the powerhouse are two other major structures, being the bypass valve flow chambers. Connected to each penstock are four large (2.3 m) cone valves, housed in a stilling/ anchor chamber. These bypass valves structures are required to bypass the flow around the powerhouse, and allow flows to enter into the Frieda River just below the dam to enable the river to remain navigable during the periods in the construction (and later during the operation should they be required).
- The powerhouse contains a series of 10 turbine generators units in total. Eight of these are rated at 69 MW, and two smaller units at 19 MW. Connection to each penstock/ conveyance tunnel is in a four large plus one small unit arrangement. The four large units on each penstock will generally be operated as follows:
 - 2 or 3 units available for generation
 - 1 unit available as spinning reserve one penstock only
 - 1 unit available to be out of service for maintenance
 - 1 small unit available to meet the local load.

- All major electrical equipment is located within the powerhouse, except for the load banks, which are located adjacent to the powerhouse.
- Various access roads are provided for both final operation and construction to all areas, many of these are provided as a by-product of 'the dam' and 'the quarry' earthworks.

The three dimensional layouts of the resulting arrangements are shown in Figure 15-27, Figure 15-28 and Figure 15-29.

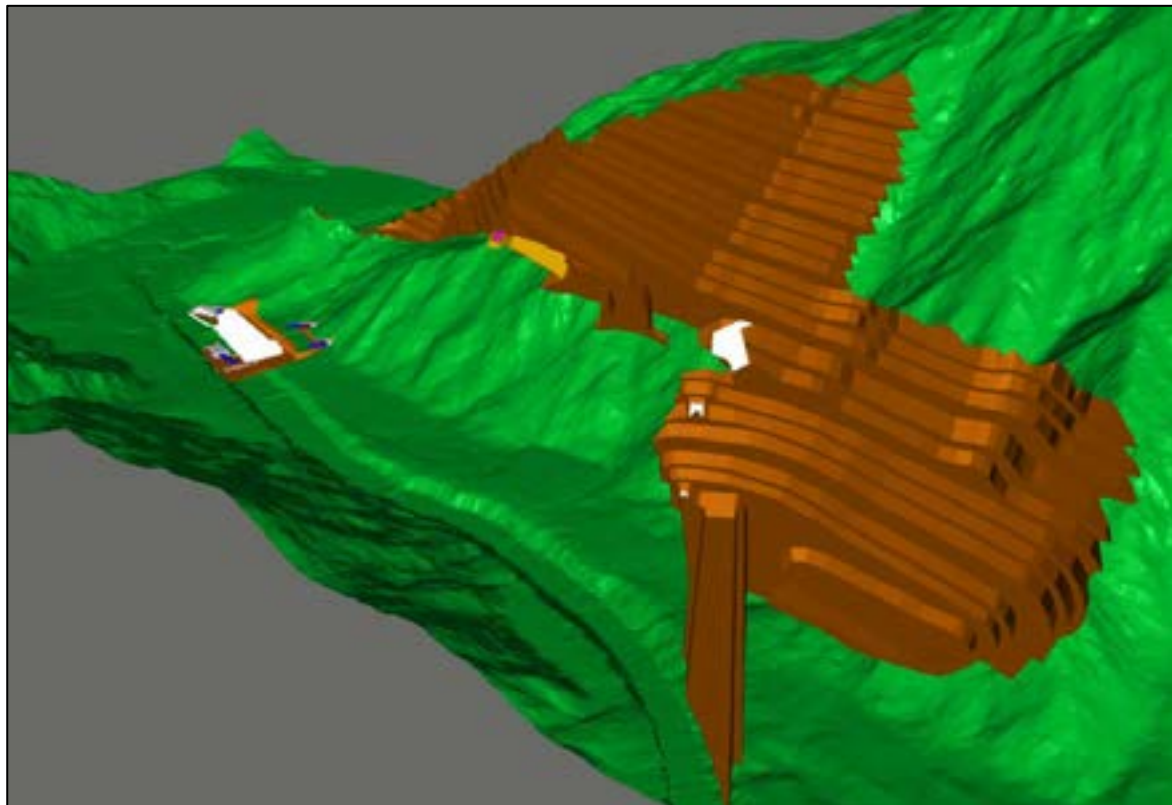


Figure 15-22: FRHEP aerial view from upstream (no embankment)

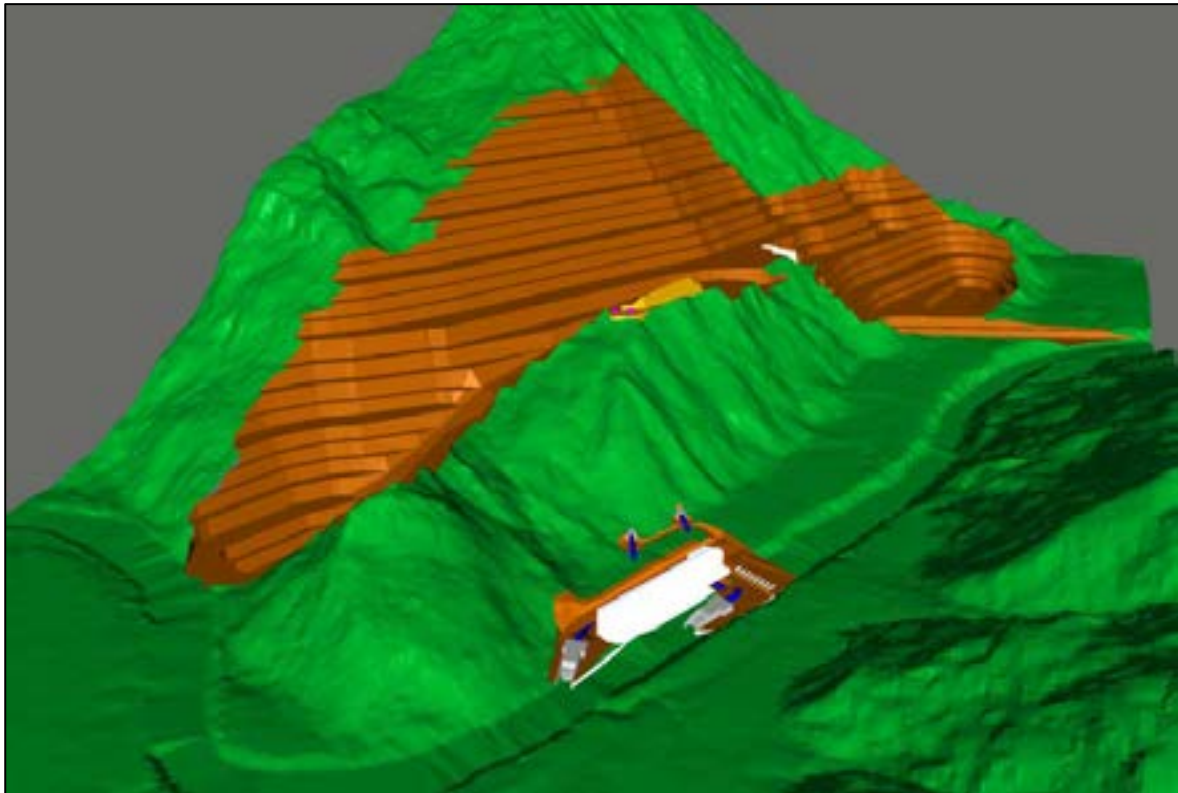


Figure 15-23: FRHEP aerial view from downstream (no embankment)

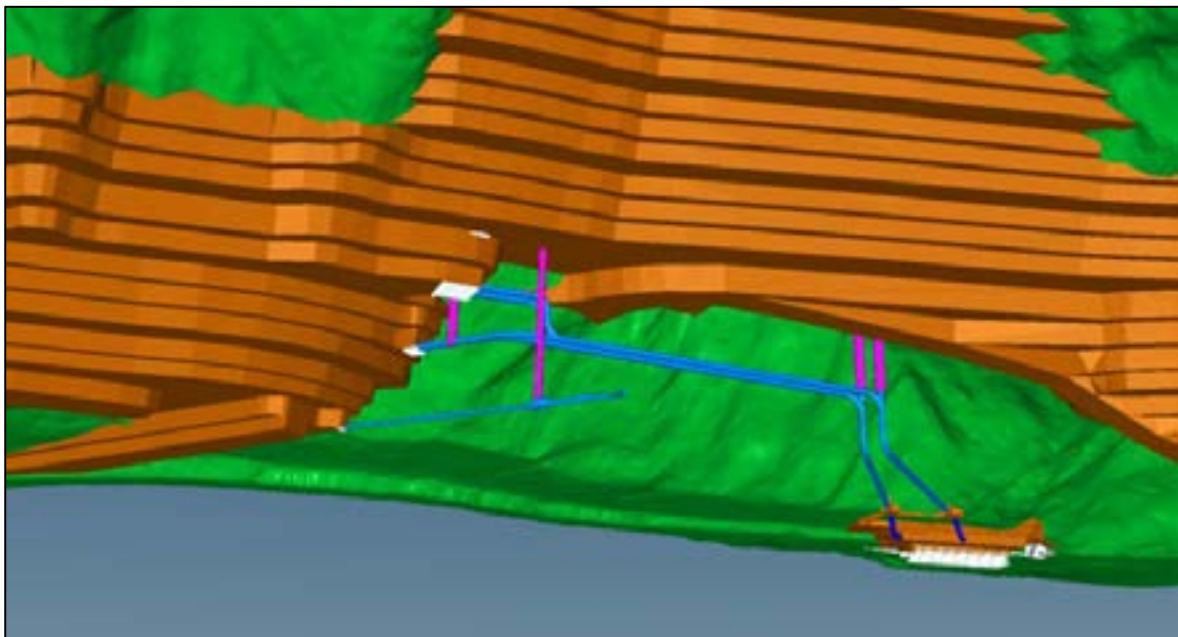


Figure 15-24: FRHEP underground view of the conveyance

16 Hydroelectric Component Design

Each hydroelectric power component has been developed to the power demand requirements (Section 5). This section describes the components and briefly addresses some overall design aspects as follows:

- 1 Residual Flow system
- 2 Intake Structures
- 3 Conveyance System
- 4 Powerhouse Bypass/ Drain Valves
- 5 Spillway Gates (refer to the Spillway design section 10)
- 6 Powerhouse
- 7 Powerhouse Equipment
- 8 Substation and Transmission.

16.1.1 Liquefaction and lateral spreading risk

There is little risk of liquefaction and lateral spreading at the site, as it is the same material used upstream as the foundation material for the embankment in the valley floor which is coarse clast supported. Seismic design

The seismic design completed to date has been in accordance with US Army Corp Engineering (USACE) Regulation No.1110-2-1806, and ICOLD Bulletin 148:2016, with modification to reflect practice within Australia and New Zealand.

16.1.2 Spectral acceleration curves

The seismic design undertaken to date is based on the September 2016 report by Atik and Gregor, 'Seismic Hazard Assessment for the Frieda River Tailings and Waste Integrated Storage Facility, Papua New Guinea'.

Atik and Gregor undertake a probabilistic analysis followed by a deterministic assessment. Stantec have adopted the deterministic PSA (g) 84th Percentile for Zone 15 for the SEE, as this provides the most conservative and governing deterministic spectra, while providing more realistic results than the corresponding probabilistic events. This approach is consistent with NZSOLD and ICOLD guidance.

The horizontal design spectra for the 5% damping for Frieda TSF site for differing shear wave velocities are provided in tables 7-1 and 7-2 of the Atik and Gregor report, (Figure 16-1 and Figure 16-2 below) (the zone 15 84th curve is shown in solid red). The recommended vertical to horizontal ratios are provided in Tables 7-4 and 7-5 of the Atik and Gregor report.

In advance of the final geotechnical reporting we have made the following assumptions regarding the V_{S30} shear wave velocities:

- $V_{S30} = 760$ m/s is close to a subsoil class C as defined in NZS1170.5 (V_{S30} for class C is between 360 to 760 m/s), which is reflective of the powerstation foundation material. Therefore, the spectra given in Figure 16-1 was adopted when considering the powerhouse structure.
- $V_{S30} = 1,150$ m/s is equivalent to a subsoil class B as defined in NZS1170.5 (V_{S30} for class B is greater than 760 m/s), which is reflective of the intake foundation material. Therefore, the spectra given in Figure 16-2 was adopted when considering the powerhouse structure.

It is stated in Section 3 of the Atik and Gregor report that the soil and CW material at the powerhouse is expected to have a $V_{S30} = 1,150$ m/s. If this is confirmed, there may be an opportunity to use the

less conservative spectra in the detailed design of the powerhouse, but at this stage we have adopted the more conservative approach.

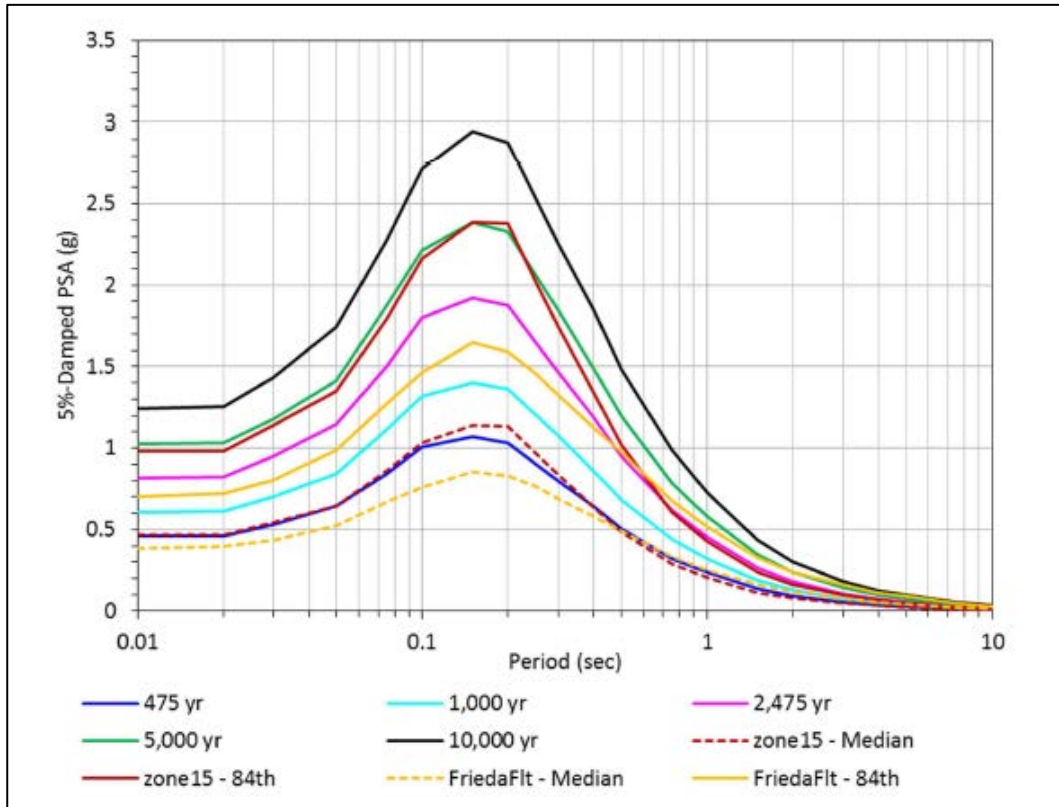


Figure 16-1: Horizontal seismic spectra (760 m/s)

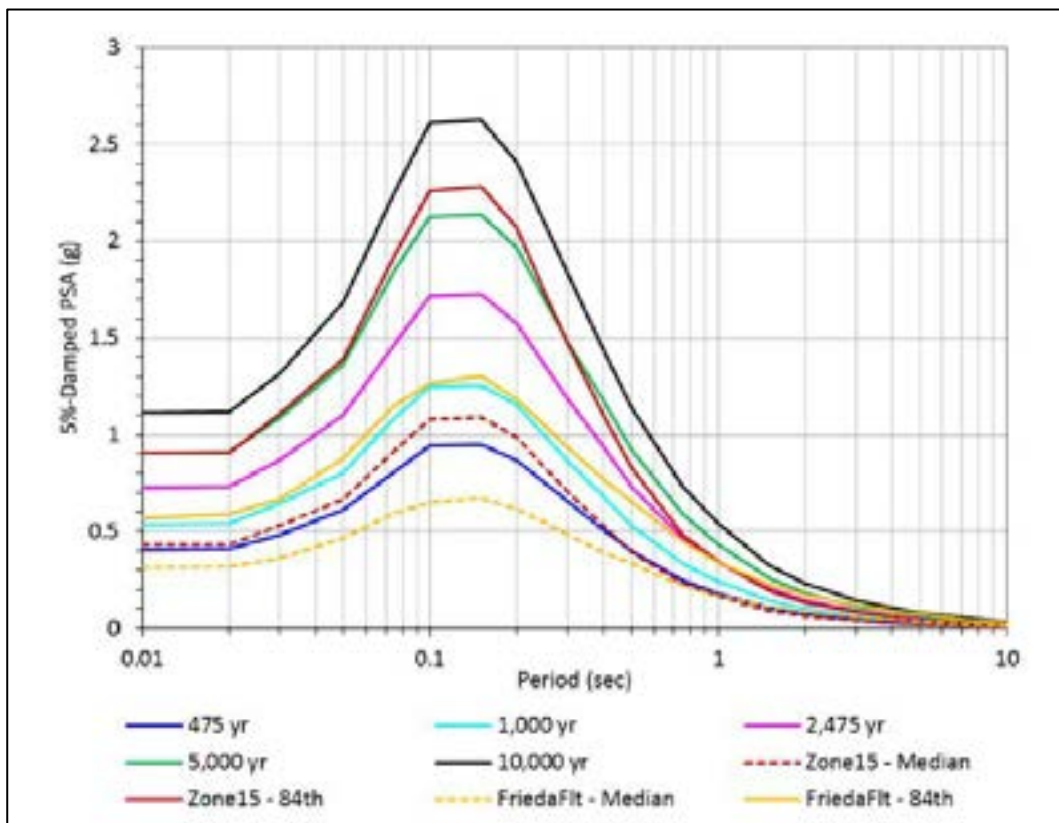


Figure 16-2: Horizontal seismic spectra (1,150 m/s)

16.1.3 Design events

Two level of design earthquake motion have been considered within the design to date. They are summarised below:

- Safety Evaluation Earthquake = Maximum Credible Earthquake = deterministic PGA for Zone 15 84th Percentile, as given in Figure 16-1 and Figure 16-2
- Operational Basis Earthquake = 1 in 475 UHS year event, as given in the figures above.

Further discussion regarding the adoption of these criteria is provided below.

Safety Evaluation Earthquake (SEE)

Given the stage of the project, and that the embankment design is currently still being developed, we have assumed that all FRHEP structural components are critical as defined by USACE ER 1110-2-1806 cl 6.a and USACE EM 1110-2-2400 cl4-6.a:

'Critical features are the engineering structures, natural site conditions or operating equipment and utilities at high hazard projects whose failure during or immediately following an earthquake could result in loss of life due to inundation. Such a loss of life could result directly from failure or indirectly from flooding damage to a lifeline facility. All other features are not critical features.'

'A critical intake tower is as described based on its capability to lower the reservoir. Damage to or failure of an intake tower located at a high-hazard project may result in a reduced ability to lower the pool following an earthquake. Lowering of the pool may be necessary to relieve pressure head on an embankment dam possibly damaged by earthquake ground motions, or to inspect and repair an embankment dam. In cases where the loss of capacity to lower the pool will result in downstream fatalities, the tower is a critical project feature. If these conditions do not jeopardize lives, the tower is not critical.'

Therefore, the Maximum Design Earthquake (MDE) is taken to be equal to the SEE defined above. USACE EM 1110-2-3001 for powerstations requires that the SEE is used for the MDE.

Within the next stage of the project it is recommended that this assumption be confirmed through a formalised whole-of-project strategy considering measures required to manage the reservoir level following a seismic event.

If the embankment design is sufficiently robust, and the spillway gates, piers and slopes are sufficiently robust, the intake maybe considered as not being critical to lowering the reservoir, and could be designed for a less severe seismic event, such as 1 in 2,500 years (approximating to 1 in 2,475 year event shown above).

Operational Basis Earthquake (OBE)

The OBE event is defined as being the level of ground motion for which the installation is expected to remain functional with little of damage. While this concept is focused on structural aspects, it has also been applied to the mechanical and electrical equipment as discussed below.

While the stated typical return period is 1 in 145 years within the USACE and ICOLD documentation, it is noted this is lower than Australian and New Zealand structural standards, as given in AS/NZS 1170.0, which requires an Importance Level 4 structure (post-earthquake function) with a 50-year design life to main operational continuity after a 1 in 500-year event. Therefore, a number of owners in Australia and New Zealand have chosen to adopt this higher standard, and this approach is proposed as a minimum level within the draft of the proposed ANCOLD Guidelines for Design of Dams and Appurtenant Structures for Earthquake.

We also note that for the design of upgrade works to extreme consequence category dams in Australia, an even higher OBE ground motion event of 1 in 1000 years is currently being adopted. While we have not adopted this higher standard at this time, it is recommended that it be considered after proper consideration within later stages of the project.

Therefore, for the purposes of this study, we have adopted the 1 in 475 year UHS event as the OBE ground motion for structural design of critical infrastructure and critical mechanical and electrical equipment. This closely approximates to the 1 in 500-year event discussed in ANZ standards, and is as recommended by proposed ANCOLD guidelines, but warrants confirmation with FRL prior to commencing further design stages.

16.1.4 Seismic loads on mechanical and electrical equipment

Given the current stage of design, we have limited consideration of seismic loads on equipment to reviewing current and proposed equipment supply specifications to ensure the high seismic loads can be accommodated within equipment meeting these specifications.

For electrical equipment we have reviewed the draft standard (IEEE P693:D17) in addition to the current standard (IEEE 693:2005). In both standards there are three seismic qualification levels (high, medium, low). The main difference between the two is that the draft document introduces two qualification approaches for these seismic levels:

- Performance level qualification approach (PLQA). This is a new to the draft standard.
- Design level qualification approach (DLQA). This is the implicit approach within the current standard.

The difference between the two qualification methods is that the PLQA requires physical testing of complete major components, while the DLQA method allows qualification predominantly through analysis (Finite Element, etc), with physical testing of smaller individual components informing the analysis. DLQA is therefore much easier and cheaper to complete.

Equipment specified to a 'high seismic performance level qualification' using the PLQA in accordance with the draft standard would be qualified to continue operating following events with a PGA of 1g, which is the level of motion expected within the switch room in the powerhouse during the OBE event. However, it is not certain that equipment meeting this standard will be available, given the high level of physical testing associated with it.

Equipment supplied in accordance with the DLQA would only have qualified performance of 0.5g, half that of the PLQA qualified equipment.

The current design standard, that is based on DLQA, assumes that the actual performance of the equipment will be greater than the level the equipment is qualified for, '*Projecting the performance beyond the qualification level (to the performance level) is justified if the dynamic response of the equipment is generally understood*', (cl 8.4, IEEE 693:2005). This difference between the qualified level and expected performance is suggested as being a factor of 2. Therefore, it is theoretically possible for equipment currently supplied using a DLQA to have a high seismic qualification, would be able to meet the higher PLQA, but it is not certain.

Further detailed discussions with electrical suppliers are required to confirm equipment availability to the draft standard, and if equipment is available, this issue may significantly limit the range of suitable suppliers.

16.1.5 Design ground accelerations

Based on the above considerations Table 16-1 provides the ground accelerations adopted for the main hydroelectric power structures.

Table 16-1: FRHEP structures design ground accelerations

Structure	Period (s)	OBE acceleration (g)	SEE acceleration (g)
Powerhouse ($V_{s30} = 760$ m/s)	PGA	0.458	0.983
	0.15	1.034	2.386
	1	0.323	0.431
Intake Structures ($V_{s30} = 1,150$ m/s)	PGA	0.407	0.908
	0.15	0.867	2.070
	1	0.178	0.343

16.1.6 Basis of future work

Within future stages of design work it is expected that the major FRHEP structures (intakes, powerhouse and drain valve structures) shall require analysis using finite element time history, either linear or non-linear, in 2D and possibly 3D for the powerhouse, depending on the assessment of its irregularity.

16.2 Residual flow system

The residual flow tunnel intake level is RL 70 m. The valve has been set to the centreline which allows the valves to discharge free in air. The chamber downstream from the valve is sized to allow the water to flow freely away from the valves and into the western diversion tunnel. The key to the safe operation is ensuring that the water in the residual flow chamber is above the water level at the diversion tunnel discharge into the Frieda River. The estimated tailwater level in the Frieda River at this point even during a PMF event is less than RL 55 m, which means the diversion tunnel will be filled partially with water but the residual flow valve chamber should be above the water level at all times. This is conservative given that residual flow valves may be decommissioned shortly after the spillway is commissioned.

The installation details are as follows:

- The residual flow tunnel is excavated from the upstream end. A stoplog will need to be available to keep water out of the excavation works if the river level starts to rise.
- The downstream chamber is also excavated.
- A raise bore 7.5 m in diameter is created to allow the jet flow and guard valves to be installed, the access ladders, pipework and instrumentation cabling to be installed. Normal access to the bottom of the chamber would be by man cage. The area where the residual flow valves are installed may be regarded a confined space even though free flow ventilation is available from the diversion tunnel and up the raise bore. Ventilation ductwork to supply fresh air may also be required.
- The valves will be installed and connected to a short section of steel liner with a bifurcation to split the flow to the two sets of valves.
- The mechanical and controls installation in the tunnel and the spillway gate control room will then be completed and the valves dry commissioned.
- Once the diversion system can operate safely using a single tunnel the final break through from the residual flow tunnel to the western diversion tunnel can take place. The timing of this is a sensitive issue. It should occur shortly before the filling is about to commence. The embankment

height must be sufficient to buffer the diversion works design flood event using a single diversion tunnel for drainage.

- The residual flow valves should be wet commissioned.
- Once the stoplogs are installed in the second diversion tunnel the residual flow valves will commence operation to maintain the required residual flow.
- If required, the residual flow valves can pass additional water during early filling operating in parallel with the powerstation bypass valves.
- Once it is no longer required, the residual flow tunnel can be plugged by pumping in concrete from above once the stoplog on the entrance is positioned by divers. The valves can be left in place or removed.

A screen over the residual flow intake will consist of a vertical bar screen, with spacing of the bars at approximately 200 mm. The purpose of the screen is to catch floating material in the reservoir and prevent entry into the remaining waterway, and more importantly through the flow control equipment.

Given the short duration of use, it is considered that the screen will not require cleaning, and therefore no provision has been made to do so.

16.3 Intake structures

The intake structure has been developed from several concepts to effectively be a single structure for the operation of the scheme over its life. However due to the requirement for 'early filling', an initial, more simple structure will also be installed. These are referred to as the 'upper' and 'lower' intake structures.

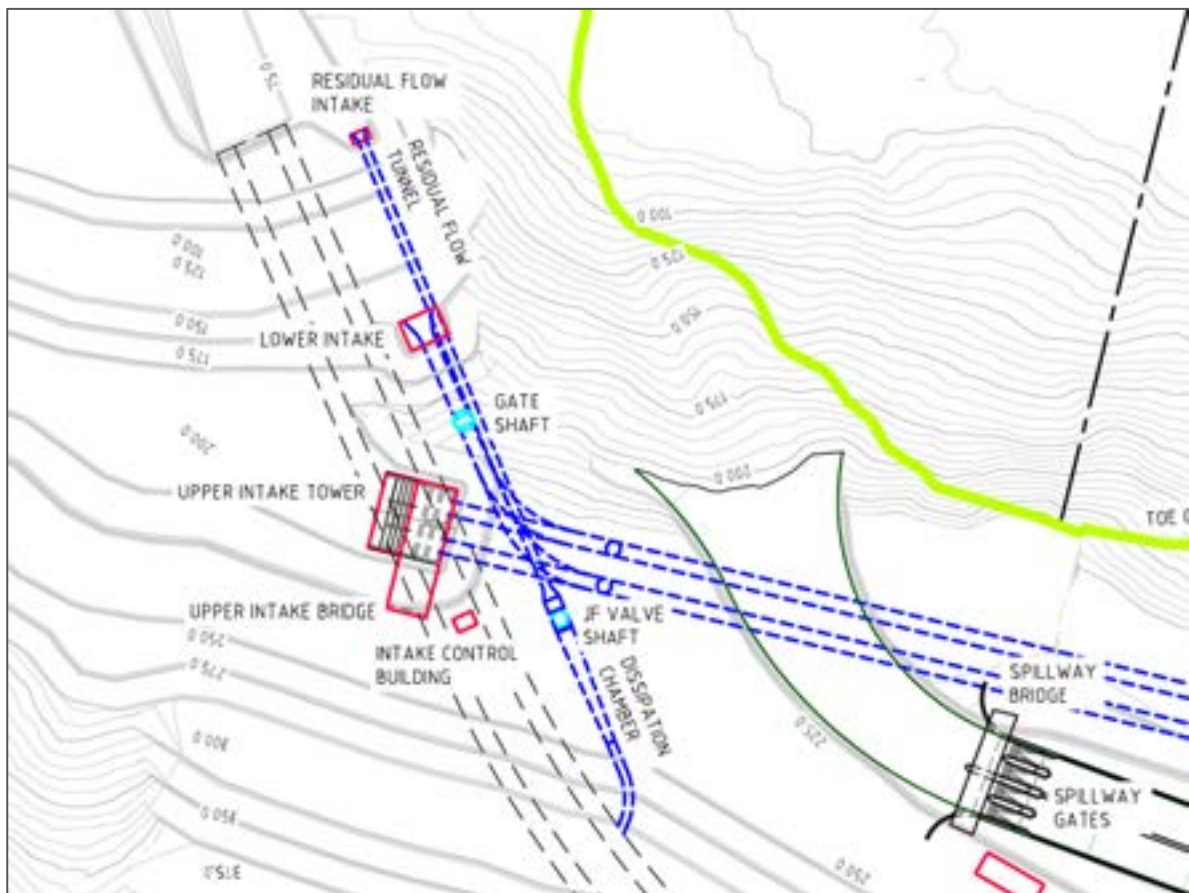


Figure 16-3: Intake arrangement (plan view)

Based on Figure 16-3, it can be seen that:

- The lower intake is significantly smaller than the upper intake.
- The lower intake structure is designed to operate during early filling, when only limited power is required, and it is likely that the entire powerhouse is not fully complete. Therefore, its flow capacity is significantly less than the upper, and effectively half the intake area is provided.
- The lower intake structure will only be required to operate over a limited time up to two years but probably less than one year, and as such mechanical screen cleaning equipment has not been provided as a cost saving measure.
- The lower intake structure feeds a single tunnel which is then split to form the two main conveyance tunnels. Within the single tunnel length, a sacrificial gate shaft is provided. When the lower intake has completed its service life, the gates within this shaft will be closed, and the tunnel plugged with concrete for permanent closure.
- The upper structure is a multi-chamber structure, housing screens, two hydraulically operated wheeled control gates and two maintenance stoplogs. It will have an automated mechanical screen cleaner, and permanent road access to the top of the completed structure.

16.3.1 Levels

Table 16-2 provides an assessment of the elevations for the intake structure.

Table 16-2: Intake levels

Level	Unit	Value
Dam crest	RL (m)	238.50
Upper intake platform	RL (m)	235.00
'Slumped Dam Crest'	RL (m)	231.50
PMF water level	RL (m)	231.80
Dam Level at time of first fill	RL (m)	151.50
Lower intake invert	RL (m)	143.30
Lower intake initial operation level	RL (m)	166.20
Lower intake final operation level	RL (m)	199.39
Upper intake invert	RL (m)	185.60
Upper intake initial (minimum) operation level	RL (m)	199.39
Upper intake normal operating level	RL (m)	204.39 to 226.14
Upper intake maximum operating level	RL (m)	231.50
Intake submergence above invert at full flow	m	14.50

Based on the assessment of the above table, the overall nominal height of the intake structure is approximately 49.4 m.

16.3.2 Lower intake structure

The layout of the lower structure is shown in Figure 16-4. This figure is a long section of the structure and associated gate shaft.

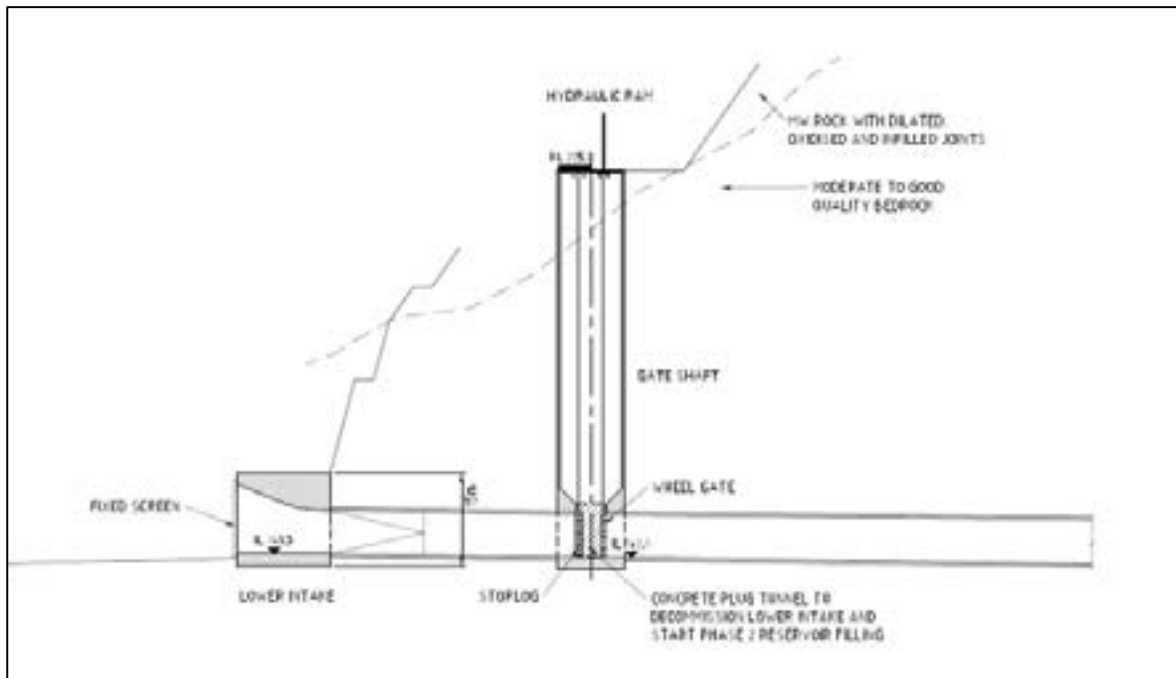


Figure 16-4: Lower intake structure

The lower structure is effectively a concrete 'box' structure, which supports the tunnel portal opening, and the fixed bar screen.

Intake equipment (gates and screens)

To control the flow of water through the conveyance system, the lower intake will include the following equipment:

- Intake screen (fixed bar screen)
- Gravity close emergency shut off gates (wheel gates)
- Stoplog/ concrete bulkhead.

Intake screen and cleaner

The screen over the upper intake will consist of a vertical bar screen, with spacing of the bars at around 75 mm. The purpose of the screen is to catch floating material in the reservoir and prevent entry into the remaining waterway, and more importantly through the turbine rotating equipment. The turbine equipment and tunnel traps will be designed to deal with the smaller suspended material that will enter the system through the screen.

Given the short duration of use, it is considered that the screen will not require cleaning, and therefore no provision has been made to do so.

Wheeled control gates

A steel gate is provided in the intake to control the flow through the waterway system. The proposed gate is a coated steel panel, placed in slots in the concrete structure, which have a wheel system to guide it into place. The wheel gate has rubber seals, which seal against the upstream face of the structure. The wheel gate is lifted by hydraulic rams and is effectively lowered under gravity, rolling down the guides.

The wheel gates have several functions:

- To close on emergency shutdown of the powerstations under full flow conditions, and will close in a fail-safe manner
- To close to isolate the tunnel
- To close to provide water from the specified inlet opening and level.

Stoplog

The stoplog is effectively a large steel and concrete block, which is placed to seal the waterway. The stoplog is generally placed when the waterway is to be closed, and accessed for maintenance, and provide a second level of isolation to the wheel gate, and hence a higher level of safety protection to people entering the closed waterway.

In this case, when the lower intake has completed its service life, the stoplog and control gate will both be lowered, and the gap between permanently plugged with concrete. Upon completion of this closure activity the reservoir level can be raised, and the gate shaft permanently flooded.

16.3.3 Upper intake structure

The layout of the upper structure is shown in Figure 16-5. This figure is an elevation and cross-section of the structure and its associated equipment.

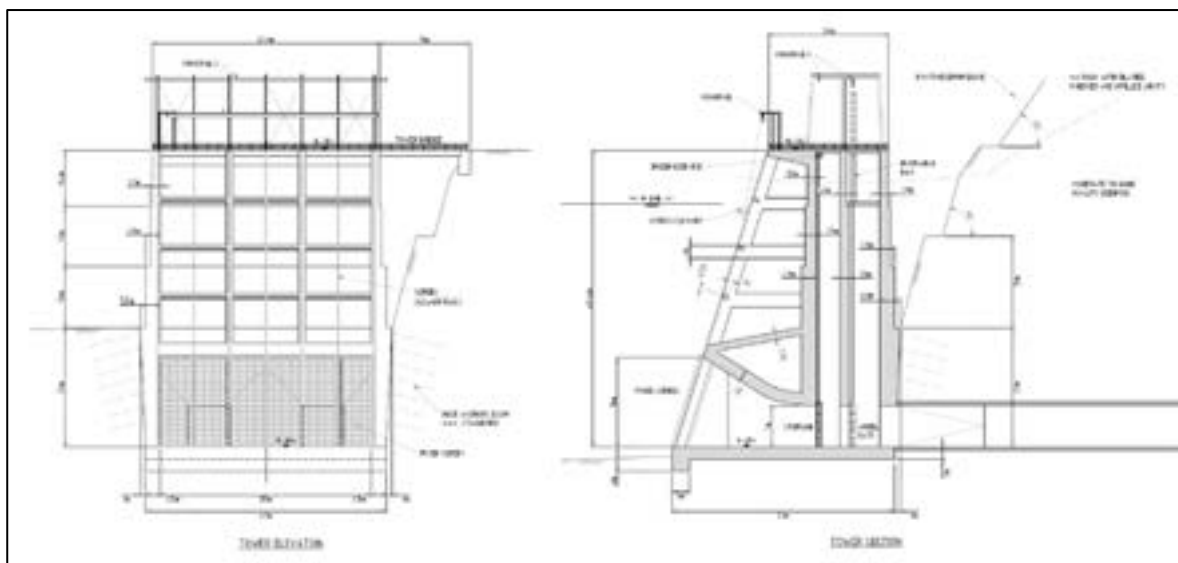


Figure 16-5: Upper intake structure

The upper intake structure is a significant structural concrete element. At approximately 50 m high, it has the equivalent dimensions of a 12 storey office building. Due to its required height, and the conditions of the surrounding rock, the structure is effectively vertically cantilevered over a significant portion of its height. With the high seismic design loads (as described above), this results in the structural thickness of the lower wall sections approximately 3.5 m in thickness.

Over its lower levels (the tunnel portal area) the structure is designed to support the portal earthworks, and will be pinned to the surrounding rock. The upper slopes of the excavation are cut back as self-supporting slopes, based on the geotechnical design parameters described above.

The bounds of the excavation also form the boundary of the quarry that supplies the embankment construction. The nominal foundation conditions upon which the structure is supported are very competent bedrock (good quality dunite).

Intake equipment (gates and screens)

To control the flow of water through the conveyance system, each tunnel intake will include the following equipment:

- Intake screen (fixed bar screen)
- Automated screen cleaner, able to rake the intake screen; facilities for grappling logs and also for dealing with floating surface material will also be provided
- Gravity close emergency shut off gates (wheel gates)
- Stoplogs/ concrete bulkheads.

Intake screen and cleaner

The screen over the upper intake will consist of a vertical bar screen, with spacing of the bars at around 75 mm. The purpose of the screen is to catch floating material in the reservoir and prevent entry into the remaining waterway, and more importantly through the turbine rotating equipment. The turbine equipment and tunnel traps will be designed to deal with the smaller suspended material that will enter the system through the screen.

A mechanical 'grab' type hydraulic screen cleaner will also be installed on the top of the upper intake structure. Guide rails down the intake structure face will guide the cleaner to each submerged screen to complete the cleaning function.

The process is therefore:

- Open cleaner grab descends to the screen.
- Grab closes and captures material (e.g. tree branches and logs).
- Grab is then raised up the rails to the surface.
- Grab releases the material into an awaiting truck or skip, which will take the material to an approved waste material site.

In addition to the process above, the cleaner will be fitted with an arm to grapple with larger logs and also facilities to deal with material floating on the surface. An example of such a cleaner is shown in Figure 16-6.



Figure 16-6: Example of screen cleaner

Operation of the cleaner will be automated, and pressure sensors both upstream and downstream of the screen will be placed to determine when the screen is blocked through measuring the pressure differential across the screen. At the designed set-point for pressure differential, the cleaner will operate to clear the screen and re-establish the 'unblocked' pressure readings.

Wheeled control gates

Steel gates are provided in the intakes to control the flow through the waterway system. The proposed gates are coated steel panels, placed in slots in the concrete structure, which have a wheel system to guide them into place. The wheel gates have rubber seals, which seal against the upstream face of the structure. The wheel gates are lifted by hydraulic rams, and are effectively lowered under gravity, rolling down the guides.

The wheel gates have several functions:

- To close on emergency shutdown of the powerstations, and will close in a fail-safe manner
- To close to isolate the waterway tunnel
- To close to provide water from the specified inlet opening and level.

Stoplogs

The stoplogs are effectively a large steel and concrete block, which is placed to seal the waterway. The stoplogs are generally placed when the waterway is to be closed, and accessed for maintenance, and provide a second level of isolation to the wheel gate, and hence a higher level of safety protection to people entering the closed waterway.

Miscellaneous equipment

Within the intake structure, the following equipment will also be provided:

- Tunnel filling valve - a smaller valve arrangement to fill the tunnel at a constant low flow, (after it has been dewatered)
- Overhead crane at the top of the structure to lift the stoplogs, and assist during maintenance, for the likes of a person cage
- Access hatches (which are removable by crane) at the top of the structure to allow access to the chambers.

16.3.4 Intake control buildings

There are extensive power supply, controls and hydraulic systems required for the various gates and valves. These will be housed near the intakes, with two buildings are provided for this purpose.

The first is the main Spillway Gate Control Building. Overall the control building will be 31 m × 12 m in plan.

This will house the following:

- Hydraulic power pack and the spillway gate control panels and Programmable Logic Controllers (PLC) for each gate. The equipment for each gate will be located in a separate fire compartment.
- Two standby generators will be provided at the intake. Each will be capable of meeting the entire electrical load of the intakes and spillway including gates, cranes, screen cleaners and lighting. Each generator will be in a separate fire compartment.
- Diesel storage for at least 1 week of operation will be provided.
- Dual 24 V DC systems for all controls and battery room

- 400 V system and dry type auxiliary transformer to allow power from the powerstation to be supplied to the intake
- Control room where all intake and spillway gates, screen cleaner and residual flow valves can be operated from
- The level sensor equipment would be terminated in the building.
- Temporary accommodation for operators in the event of a major storm will be provided at the building.
- Communications with the powerhouse and intake control building.

A second smaller (10 m × 7 m) building close to the intakes will be provided. It is located near the intake to minimise pipe run lengths. This will provide the following:

- Hydraulic power pack, control panels and PLC for each intake gate. The equipment for each gate will be located in a separate fire compartment.
- Residual flow controls (2 off)
- Tunnel filling valve controls (3 off)
- Dual DC systems and battery room
- All power supplies and communication links will come from the Spillway Gate Control Building.

To limit the length and cost of hydraulic control pipework and associated concrete ducting, this second control building maybe further split, with one building to control the upper and lower intakes, and a second building for the residual flow valves.

16.3.5 Details of intake gates, valves and spillway gates

Table 16-3 summarises the key dimensions and weights of all major gates and valves.

Table 16-3: Details of intake gates, spillway gates and valves

Description	Location	No.	Type	Actuation	Dimensions	Weight (t)
Lower intake gate	Lower intake	1	Wheel gate	Hydraulic	7.5 m (W) × 7.5 m (H)	100
Lower intake stoplog	Lower intake	1	Slide gate	Electric hoist	7.5 m (W) × 7.5 m (H)	64
Upper intake gate	Upper intake	2	Wheel gate	Hydraulic	7.5 m (W) × 7.5 m (H)	50
Upper intake stoplog	Upper intake	1	Slide gate	Electric hoist	7.5 m (W) × 7.5 m (H)	50
Spillway gates	Spillway crest	4	Radial	Hydraulic	7.5 m (W) × 16.2 m (H)	108
Spillway gate stoplog	Spillway crest	1	Segmented gate	Crane	7.5 m (W) × 16.2 m (H)	106
Residual flow control valve	Residual flow tunnel	2	Jet flow valve	Hydraulic	1.8 m diameter	15
Residual flow guard valve	Residual flow tunnel	2	Butterfly valve	Hydraulic	1.8 m diameter	25
Small unit tailrace gates	Powerhouse	2	Wheel gate	Hydraulic	3.9 m (W) × 4.6 m (H)	10
Small unit tailrace stoplog	Powerhouse	1	Slide gate	Electric hoist	3.9 m (W) × 4.6 m (H)	9

Description	Location	No.	Type	Actuation	Dimensions	Weight (t)
Large unit tailrace gates	Powerhouse	8	Wheel gate	Hydraulic	5.6 m (W) × 7.8 m (H)	26
Large unit tailrace stoplog	Powerhouse	1	Slide gate	Electric hoist	5.6 m (W) × 7.8 m (H)	26
Bypass flow control valve	Powerhouse tailrace	4	Cone valve	Hydraulic	2.3 m diameter	35
Bypass flow guard valve	Powerhouse tailrace	4	Butterfly valve	Hydraulic	2.3 m diameter	50

16.4 Conveyance system

16.4.1 General

The conveyance system is defined as the waterway components that connect the intakes to the inlet valve at the powerhouse and has the following components:

- Intake structure (described above)
- Low pressure conveyance tunnel, from the intake structure to the power shaft (vertical transition between low pressure and high pressure tunnels sections)
- Surge chamber
- High pressure conveyance tunnel
- Tunnel exit portal
- Buried penstock
- Bifurcations manifold and bends.

16.4.2 Conveyance system optimisation

The reasons for the use of a twin conveyance system at the FRHEP are listed below:

- It limits the size of each of the tunnels.
- It allows a single tunnel to be drained for inspection which means the full mine FRCGP load can be met and some power supplied to the export grid. The amount will depend in part on the water level but could be as high as 60 MW.
- With single tunnel systems the steel tunnel liner and buried penstock will require extremely thick walls. This will mean every weld will require post weld heat treatment to approximately 595°C. This is extremely difficult in a site installation situation and needs to be avoided.
- A second major point is that the conveyance system sizing is determined by considerations of response to the power system load, rather than by selecting the optimum diameters to achieve the optimum trade-off between head loss and energy output on a net present value basis.
- The ability of the generating plant to respond quickly to system load changes is essential if a reliable power system is to be provided. The key is to ensure that a cascade of failure of the supplies does not occur. If one generating unit trips it is essential that another unit can be loaded to meet the load before the system frequency drops to unacceptable levels. This is a system frequency of 48.0Hz ideally as a minimum but 47.5 Hz may be acceptable. Similarly, trips of transmission lines or major loads such as the SAG mills must not lead to high frequencies which in turn lead to the protection systems starting to trip load. To achieve this, the generating units require rapid loading and unloading rates. There are a number of criteria for ensuring the units are responsive and can control the systems frequency.

- The wicket gates must allow the units to load and unload between 100% and 0% in 15 seconds at most. The Power System Study demonstrates that this is the limit. The faster the gate timing the greater the pressure swing in response to a load change. The only way to reduce the magnitude of the pressure swing, and consequent frequency swing is to reduce the water velocity in the conveyance system by increasing the diameters of the conveyance system.
- It is essential that the inertia of the generating plant is at least double the momentum of the conveyance system water column. Without this it is not possible for generators to respond to a load change and to be able to damp out the subsequent oscillations of the system frequency. If the generator inertia is less than the water column inertia the oscillations in response to a change of load increase with time and the system is totally unstable.
- The inertia of the water column is measured by a parameter called the water acceleration time (T_w). This is directly proportional to the velocity in the conveyance system and inversely proportional to the head. A value of less than 2.0 seconds is ideal and less than 3.0 seconds is acceptable. If the acceleration time is longer, the period of the frequency oscillations becomes too long and the potential for trips at low or high frequency or for load shedding to commence increases. With the proposed design at Frieda the water acceleration time is 2.4 seconds and means the velocities in the conveyance system are quite aggressive.
- The higher the velocity in the conveyance system the higher the pressure rise and turbine over speed following a trip. The current design limits the over speed to 20% of synchronous speed, which is acceptable. Higher velocities would lead to higher over speed which impacts on the life of the generators.
- Overall, the lower the conveyance system velocity the better the response to changes of load in the power system. However, this comes at the cost of a very much more expensive power system. The current design has maximised the velocities in order to limit the capital cost while achieving an acceptable response to system changes and frequency control.

16.4.3 Conveyance system velocities

As noted above, relatively high conveyance system velocities have been selected, but this occurs in the less frequent cases only. This is illustrated in Table 16-4. Under the most common operating cases during normal generation the system velocities are in the normal range. However, it should be noted that the high velocities that can occur mean that the steel lined sections will require high quality internal coatings to prevent erosion/ corrosion action. Care will also be needed during initial flushing of the system to ensure the conveyance is cleaned to avoid erosion from the high velocities pushing debris through the system.

Table 16-4: Conveyance system velocities and estimate of time operating at that velocity

Parameter	Unit	Operating Mode					
		Normal medium level operation	Normal medium level operation (4 units, 1 intake)	Normal high level operation	Normal high level operation (4 units, 1 intake)	Bypass valve maximum flow (limited)	Bypass valve maximum flow (limited)
Percentage of time in the mode		15%	1%	83%	1%	1% but could be higher	If used in the event of a spillway gate failure
Flow	m ³	159.3	212.3	138.0	184.0	250.0	355.0
Peak output	Percentage of time	0.3%	0.0%	1.5%	0.0%	N/A	N/A
Concrete tunnel	m/s	3.56	4.75	3.08	4.11	5.59	7.93
Round tunnel, steel-lined tunnel and penstock	m/s	4.05	5.39	3.51	4.67	6.35	9.02
Normal output	Percentage of time	14.7%	1.0%	81.5%	1.0%	N/A	N/A
Concrete tunnel	m/s	2.85	3.80	2.47	3.29	5.59	7.93
Round tunnel, steel-lined tunnel and penstock	m/s	3.24	4.31	2.80	3.74	6.35	9.02

16.4.4 Conveyance system long section

The long section of the conveyance system is shown in Figure 16-7.

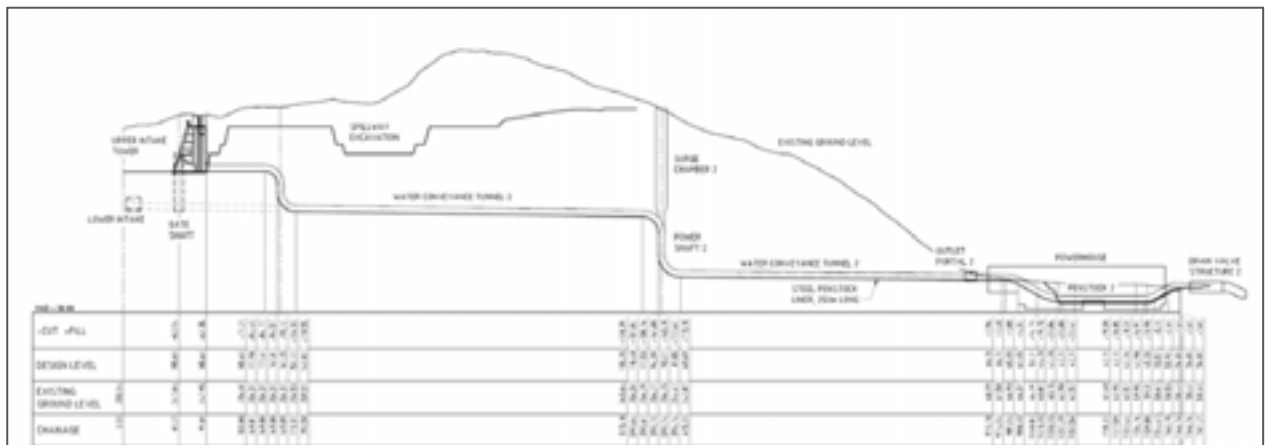


Figure 16-7: Conveyance long section

The conveyance system has been optimised in design to achieve the shortest length of tunnel between the intake and powerhouse. However, several key parameters have dictated the overall alignment and hence the sizing of some of the elements:

- The alignment is such that the excavation of the embankment itself and the potential for geotechnical features under the right abutment of the embankment means that a direct line between the intake and powerhouse could not be achieved. Instead the alignment was kinked at the power shaft to miss these features.
- The depth of excavation of the spillway also meant that the lower alignment of the low pressure section of the tunnel was the optimal location, and this is aligned to the level of the lower intake.

- The required elevation of the top of the surge chambers dictated their location. An elevation of RL 255 m was required to daylight the surge chambers, and the location is dependent on the topography. The final diameter allows alignment of the spillway and its associated excavation to remain on the original alignment without interference to the surge chamber construction or operation.
- For stability of the operating units and the required shutdown times, the surge chambers were required on the conveyance system. Ideally these would have been placed closer to the powerhouse, reducing their size, however this was not possible with the available topography.

16.4.5 Transient analysis

A detailed transient analysis was undertaken to determine the various hydraulic sizes of the conveyance elements. This study is described in Section 15.3.

16.4.6 Tunnel and shaft sizes

The diameters in Table 16-5 for each of the waterway components are based on the final sizing of the hydraulics. The nominal diameter for each component is converted to an inverted 'D' shape for the horizontal elements.

Table 16-5: Tunnel component sizes

Component	Shape	Diameter (m)	Final lining type
Low pressure tunnel	'D'	7.1 × 7.1	Concrete
Power shaft	Circular	7.1	Concrete
Surge chamber	Circular	12.0	Concrete
Surge chamber throat	Circular	7.1	Concrete
High pressure tunnel	'D'	7.1 × 7.1	Concrete/ Steel
Main penstock	Circular	7.1	Steel
Penstock branch to main units	Circular	3.9	Steel
Penstock branch to small units	Circular	2.0	Steel
Penstock branch to bypass valves	Circular	7.1	Steel

16.4.7 Tunnelling conditions

The support design from the diversion tunnels is considered the 'initial support' in terms of the permanent conveyance tunnels, and as such a 'final lining' is then placed over this initial support to form the final tunnel lining (Table 16-5). This final lining provides an allowance for the permanent condition, including high water pressure, hydraulic smoothness and possible negative pressures during dewatering. The initial support design is taken from 'Indicative support requirements, Grimstad & Barton, 1993'²⁰, and uses the 'Q' system for the rock mass condition.

Table 16-6: Assumed initial support classification

Rockmass condition	Representative Q Index range	Recommended support	Percentage of construction assumed
A – ‘General’ Majority of bedrock Including slightly weathered, joint oxidised rock and unweathered rock	1–10 fair quality rock, downgraded from good quality rock due to groundwater (Jw rating)	50 mm thick shotcrete or mesh on shoulders and roof Bolt length 2.4 m in walls, 3 m in roof Bolt spacing 2.0 m (ring spacing 1.5 m if mesh is used)	100% shafts 80% tunnel
B – ‘Localised’ Poorer quality bedrock Including moderately weathered rock with significant joint infills, weaker deteriorating, serpentinised rock, and local fault/shear zones of limited extent	0.1–1.0 very poor rock	120 mm thick fibrecrete on walls and roof Bolt length 2.4 m in walls, 3 m in roof Bolt spacing 1.5 m Possible use of steel sets, spiling and cable bolts near portals. Possible use of cable bolts where large fault-controlled wedges are evident in tunnels Possible use of steel sets in zones of extremely poor quality rock	20% tunnel

The resulting typical sections for construction of the tunnels and shafts are shown in Figure 6-18.

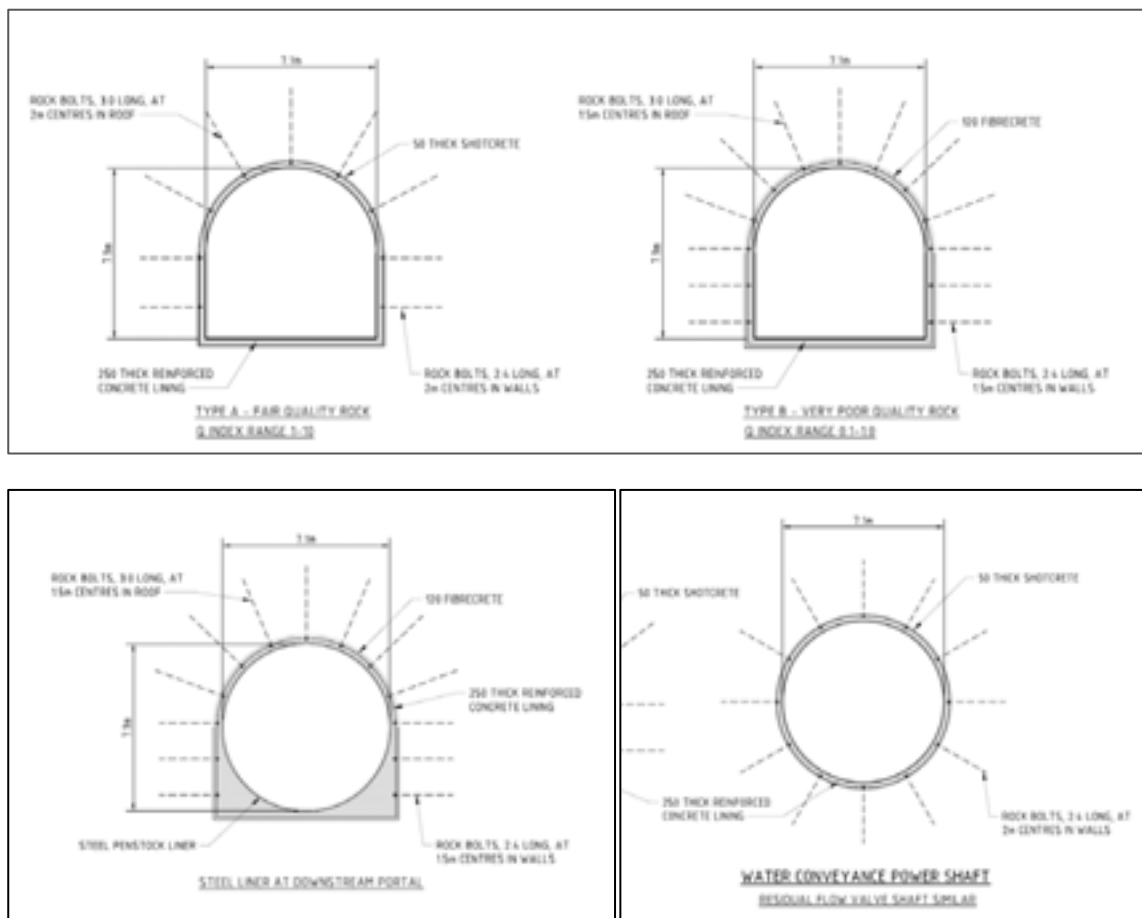


Figure 16-8: Tunnel, shaft and surge chamber sections

16.4.8 Shaft construction

The shafts will then be constructed using the following process:

- Establish the shaft collar using surface excavation and concrete works.
- Drill pilot hole for the excavated platform, down to the tunnel invert (noting that access adit at the higher level will be offset to the tunnel and connected later).
- Upon reaching the tunnel, a raise bore head will be fitted, and the raise boring process undertaken. In the lower section of the surge chamber, the cutter head will be changed to suit the ‘throat shaft’.
- Upon completion of the raiseboring, a top-down excavation will be undertaken to expand the initial diameter upper shaft to the final surge chamber diameter.
- The shafts will be progressively lined, as the excavation proceeds.

16.4.9 Penstock size and arrangement

The penstock pipeline connects the tunnel to the powerhouse. The overall arrangement is as follows:

- A steel lining is installed in the lower reach of the tunnel due to hydraulic pressures.
- The steel lining is the same diameter as the ‘penstock’ and effectively anchors the penstock to the tunnel.
- The penstock exits the tunnel, and is then a buried pipeline, where it then bifurcates to connect to each of the turbine inlet valves, via a manifold.
- The bifurcation section progressively reduces (Figure 16-9) in size as each unit is connected, to minimise the steel required for the pipeline, and keep the flow characteristics the same at each machine.



Figure 16-9: Bifurcation of a 2-unit section

The penstock itself is designed as a buried pipeline, and is therefore designed using a full stress analysis – it is actually designed as a ‘flexible’ pipe, thus not requiring specific anchor blocks. All of the applied forces are resolved in the stress design of the pipe; the result is that a large force is not applied to the powerhouse. This flexibility is gained by the use of the geometry of the system bends.

The use of a flexible connection, such as a thin walled steel penstock, provides an effective and efficient mitigation against the potential for differential settlement between:

- the tunnel outlet portal, which is expected to be founded in the good quality bedrock with a possible thin layer of cemented colluvium and alluvium, and
- the powerhouse, which is expected to be founded on thick layer (70 m+) cemented colluvium and alluvium.

The penstock can be fabricated in several ways; this will depend on the contractor at the time and could include:

- Supply of fully fabricated pipe sections to the site, site welded together
- Supply of plate steel, with the fabrication undertaken on site.

Either option will also require internal and external coatings as a corrosion protection to the penstock. The internal coating will be an epoxy system, and the external coating a thick, flexible wrap covered to protect the coating during backfilling, or an epoxy system where above ground.

16.4.10 Penstock material selection

The following steel plate materials, commonly used in the industry, were considered for the penstock cans: ASTM A516, A517 and A537. The different steel specifications have varying tensile strengths and would result in varying plate thickness and Post Weld Heat Treatment (PWHT) requirements. These materials are recognised by the ASME pressure vessel code (BPVC) and piping codes (B31) and the ASCE penstock design manual (MOP 79). Of these design codes, ASME B31.3 (Process Piping) and ASCE MOP 79 (Steel Penstocks) provide the highest basic allowable design stress and therefore result in lower plate thickness. Lower plate thickness is desirable for transportation.

PWHT is performed for stress relieving the steel after welding, to prevent cracking or tearing from built up stress during the weld process. It is also to remove trapped hydrogen gas that could cause subsequent cracking. The requirement is determined by the design codes, chiefly, ASME BPVC Section VIII. Generally, higher alloy content and greater plate thickness are factors influencing the requirement for PWHT. Performing PWHT adds complication and expense, especially for penstock welds in the field, due to the specialised equipment and process control involved. For example, for A517 specification steel of 38 mm plate thickness, the weld area would be heated to above 540°C and held for 1.5 hours. This would likely involve using induction or resistive heating elements wrapped around the pipe circumference with insulating blankets, performed in the pipe trench.

Through careful material selection, it may be possible to avoid PWHT requirements and the associated cost. It should be noted that PWHT will still be required at the site for the penstock bifurcation components because of the large wall thickness of the reinforcing plates. However, this would be done in the fabrication yard rather than the pipe trench.

A517 (all grades) have the highest tensile strengths of the materials considered and therefore provide the lowest plate thickness for the given design. For this material, Post Weld Heat Treatment (PWHT) is required for plate thickness over 32 mm according to ASME BPVC (Section VIII). Basic calculations suggest that the straight pipe wall thickness would be around 32 mm (including a small corrosion allowance). This is on the boundary for PWHT requirement.

A516 (all grades) and A537 (all classes) require PWHT on plate thickness above 38mm. Of these, A537 (Class 2) has the highest tensile strength. Basic calculations suggest that the straight pipe wall thickness for this material would be around 45mm (including a small corrosion allowance). The greater plate thickness, thicker welds and requirement for PWHT makes these materials a less favourable option.

GB 713, grade Q345R was also considered, being a commonly produced pressure plate in China. An ASME Code Case exists, allowing the use of this material with ASME VIII certified designs. Basic calculations suggest that the straight pipe wall thickness for this material would be around 51 mm (including a small corrosion allowance). The greater plate thickness, thicker welds and requirement for PWHT makes this material a less favourable option. Additionally, the thicker walled would be more adversely affected by any differential settlement between powerhouse and tunnel outlet portal, discussed in section above.

Other steel plate materials were investigated in an attempt to find a high strength plate that did not require PWHT at the design wall thicknesses. A group of materials were found with similar tensile strength to A517 but without mandatory PWHT requirement at the design wall thickness. These included A353, A543, A553 and A645. These materials are defined as Nickel Alloy steels, often used for low temperature service. These materials are assumed to be significantly higher cost compared to the common penstock steels and probably less commonly used in hydroelectric schemes.

In conclusion, A517 is the recommended penstock material. The final design would aim to eliminate the need for PWHT on the field welds by limiting the plate weld thickness to 32 mm.

16.5 Powerhouse bypass/ drain valve

At the powerhouse, two bypass and/ or drain structures are provided, and serve the following purposes:

- Provide a mechanism of bypassing the powerhouse should it be out of service (particularly at the early stages of operation before the spillway is completed)
- Provide a controlled flow into the river channel to provide the ability to maintain navigable flow in the lower reaches of the river (required to transport equipment to site)
- To protect the dam from overtopping if filling is commenced early. Some 500 m³/s of capacity is required ensure the dam is protected, which cannot be achieved using the powerhouse equipment.

Figure 16-10 provides a plan arrangement of the powerhouse area. The circled structures are the bypass valve facilities.

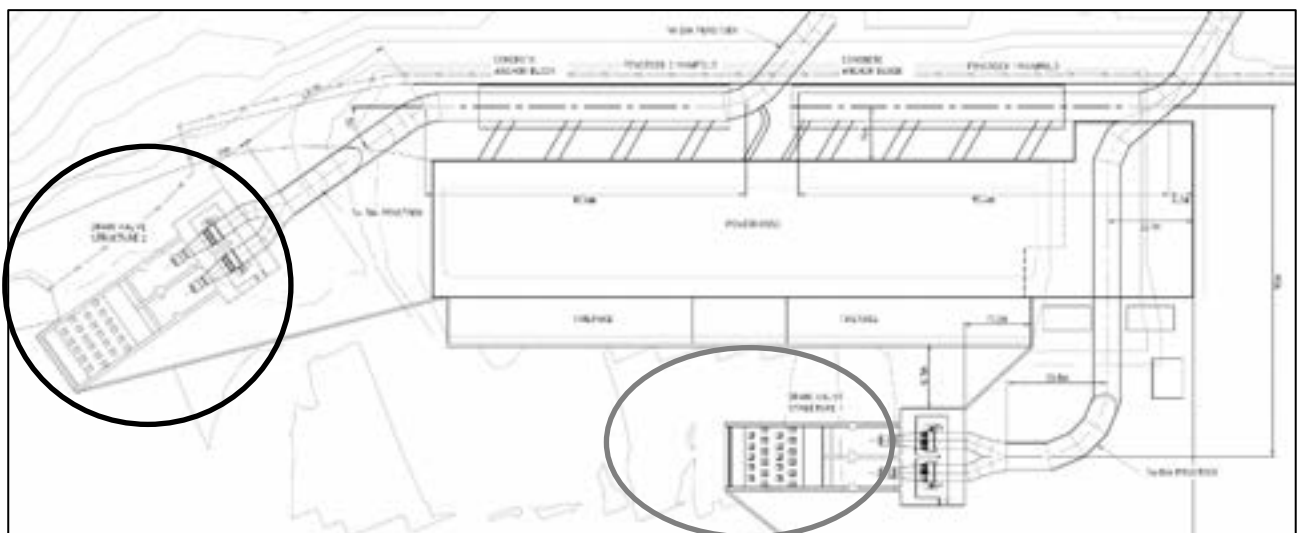


Figure 16-10: Bypass valve arrangements

The structures themselves contain the following:

- Connection to the main conveyance system
- Bifurcation of the penstock
- Fixed Cone Dispersion Valves (2 per structure) and the associated guard valve
- The piled structural chamber/ anchor facility
- An energy dissipation chamber allowing exit of the water into the existing river channel.

Figure 16-11 shows provides an example of a similar sized single valve installation, albeit at a relatively low flow. However, this valve has a shroud fitted to limit the dispersion of the spray. An unshrouded valve will spray water in at 45° to the valve centre line all around the valve creating an enormous amount of spray. At FRHEP a full energy dissipation chamber is provided to reduce the discharge velocity to less than 6 m/s.



Figure 16-11: Fixed cone dispersion valve

Four 2.3 m (90 inch) bypass valves are proposed. Two larger valves had been considered but this would require the largest Howell-Bunger valves made. Increasingly fewer manufacturers are making such large valves whereas a number make the smaller valves. Also, the dimensions and weights improve handling greatly.

There is a gravity close guard valve upstream of each Howell-Bunger valve. Butterfly guard valves have been chosen because their trunnions carry the friction load. A common alternative is to use knife gate valves but they have a reputation for sticking and being impossible to operate after they have been installed for a period of time.

Howell Bunger valves come in three versions:

- Unshrouded where the water sprays in a cone-shaped discharge pattern all around the valve circumference at an angle of 45°. The water will spray causing intense 'rain' over 30 to 8m from the valve, which is not practical. It would cover the powerstation and may cause access issues.
- The second option is to place a metal shroud to contain the water jet. This has a very low dispersion angle. However, the discharge velocity of potentially more than 40m/s. Depending on

the valve alignment this could throw 40 to 100 m but without the lateral dispersion spray as in the previous option.

- Construct a massive concrete energy dissipation structure downstream of the valve. There are many designs for this structure. A USBR design has been adopted for this project. This is expected to dissipate approximately 95% of the water jet energy (98% is the calculated figure). This reduces the velocity in the discharge from the energy dissipation structure to approximately 5.6 m/s compared with over 40 m/s at the valve.

The USBR energy dissipation design has been adopted for this project:

- It eliminates most spray during valve operation.
- It prevents high velocity water impinging on the river banks causing erosion.
- It ensures that there are no unstable flows and water levels in tailrace when the valves operate in parallel with the generation plant.

The Howell-Bunger valve hydraulic power packs and controls would be located in the powerhouse. Hydraulics are used for several reasons:

- It is easy to provide a duty and standby hydraulic pump, one driven with an electric motor and one driven by a diesel engine.
- The rate at which valves open and close can be adjusted readily. Different speeds for opening and closing are possible and it is possible to set up two speed operation as well. This may be important when the transient pressure surges that occur during valve operation are considered, especially when operating in parallel with the turbine generators to provide navigation flows in the Frieda River.

16.6 Powerhouse

The revised powerhouse provides a ten-unit station, comprising eight primary units and two smaller auxiliary units to meet the low load.

The overall powerhouse complex is shown in Figure 16-12.

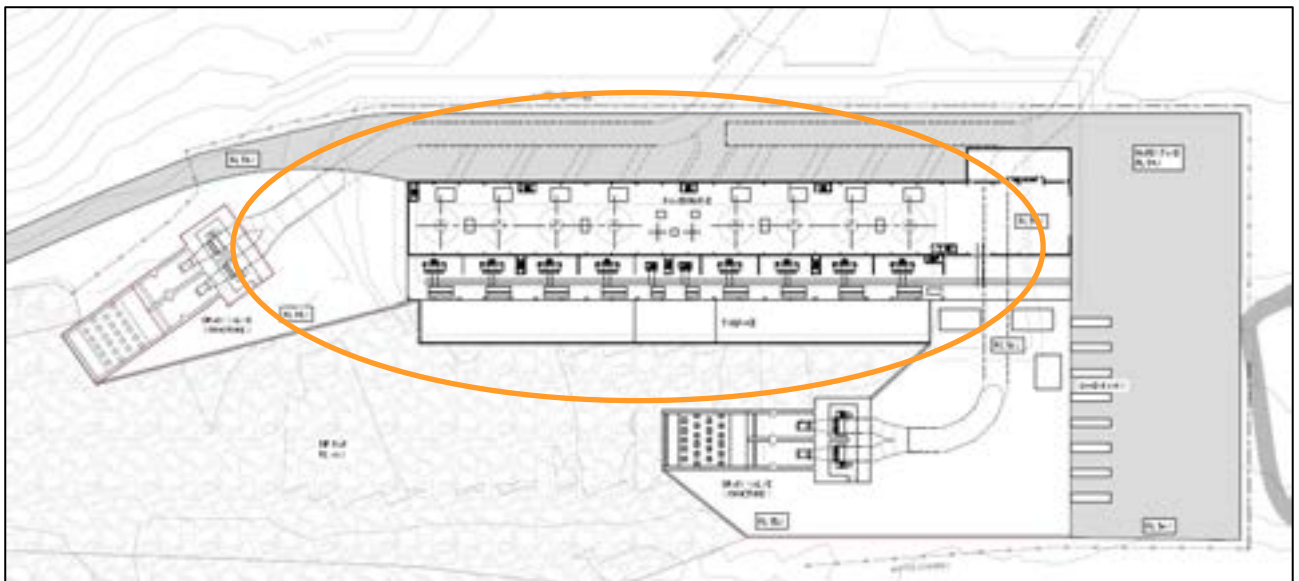


Figure 16-12: Powerhouse layout (plan view)

The major dimensions of the building are as follows:

- Machine Hall 160 × 22 m
- Transformer Bay 160 × 13 m
- Panel Rooms 160 × 9 m
- Tailrace 151 × 12 m
- Loading Bay 40 × 26 m
- Switchgear room 158 × 13 m.

The overall powerhouse complex (Figure 16-12) can be considered to include:

- The tunnel exit portals and penstocks
- The main turbine hall housing the generating equipment
- An erection/ loading bay and workshop are for assembling the equipment and for undertaking future maintenance to the equipment
- A local control room and office facilities
- Electrical equipment rooms
- An area to locate the step-up transformers, switchgear building
- A tailrace, discharging into the Frieda River.
- The bypass valve chambers (described above)
- Exterior laydown/ road/ access area at the toe of the dam, and at the rear of the building, which incorporates an area for the load banks.

The powerhouse location has been selected on the basis of:

- A preliminary assessment of the foundation conditions at the site, which appear to be good material, and located away from potential landslides, with the possible exception of a zone above the powerhouse near the spillway. This may need to be removed during construction.
- The river location allows for the construction to be within the area of river diversion required for the dam itself.
- A construction platform can be achieved at the toe of the dam, with the use of spoil from the initial earthworks at the sites.
- The river location provides for the larger equipment (generators and the like) to be transported directly to the site using the river for barging.

However, it is noted that access for construction (and the access to the completed facility) will require the construction of a significant length of road, and in some cases, require crossing the completed spillway, most likely via a bridge.

16.6.1 Building foundations

The powerhouse is predominately founded on the cemented colluvium and alluvium, which has a UCS of 2 MPa, so bearing under gravity loads is not considered an issue.

A preliminary pseudo-static analysis has indicated that the powerhouse fails in stability under both the SEE and OBE seismic events without piles, governed by sliding. This assessment includes an allowance for the passive pressure developed at the front of the structure in an SEE event (no movement is permitted in the OBE event, and therefore no passive pressure is developed). Therefore, piles have been included in the design and reflected in the MTO.

Stantec have allowed for 180 No. 1.5 m diameter, 20 m long, bored and placed in situ reinforced concrete piles on a nominal 6 × 5 m grid in the design. These will be designed as combined tension/shear members to also provide rotational stability to the powerhouse under horizontal seismic loads.

While it has been assumed that the cementation of the colluvium and alluvium under the powerhouse is reliable when considering the global action of the structure, it can vary locally. Therefore, the design has allowed a limited amount of drilling and consolidation grouting within the design to mitigate local issues.

It is considered that the overall foundation design of monolithic base slab, piles and limited localised consolidation grouting addresses the foundation risks identified to date. It is acknowledged that construction of the piles through the cemented colluvium/ alluvium could be difficult.

16.6.2 Building structure – flood protection

The building structure will be primarily constructed of in situ reinforced concrete. The lower levels of the structure will be waterproofed to protect the structure (and its contents) from river water flooding.

The building is to be protected against flooding during both the construction (via the cofferdam) and during operations, via both passive and active defence mechanisms.

These include:

- Passive: Designing of the concrete shell to be ‘waterproof’ to the desired levels; having fully sealed covers to any openings in the building below the flood level
- Active: Providing automated gate closure to the tailrace at the onset of a flood; providing an automated pumped drainage system within the powerhouse.

As designed, the building is protected against an estimated PMP flood routed through the spillway gates. The overall powerhouse stability is governed by seismic considerations, and the design is not unduly conservative for PMF protection.

16.6.3 Building structure – general arrangement

The layout of the powerhouse has been undertaken as an ‘elongated’ building (Figure 16-13) to fit into the natural contours of the site, having a low encroachment into the river channel, while providing for modest excavations behind the structure.

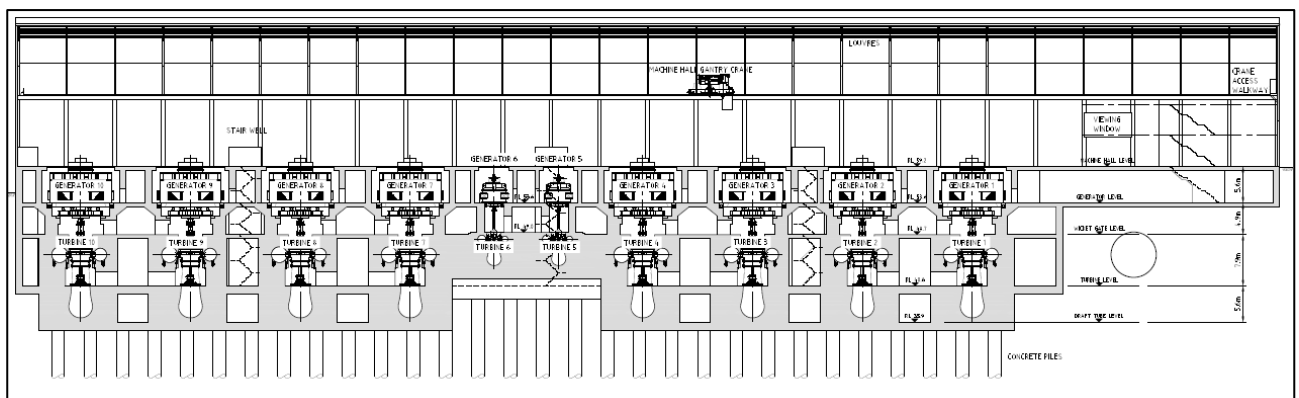


Figure 16-13: Building long section

The building will have several floor levels to provide access to the various components of the generating equipment.

The superstructure (above the machine hall level to the underside of the powerhouse crane) is also shown as a series of reinforced concrete columns, infilled with concrete precast (or in situ) wall panels.

Above the crane rails the structure will be a series of structural steel portal frames, clad with insulated panel roofing and wall cladding.

The lay down and other ancillary buildings will be constructed in a similar manner; however, some areas around the transformers will require explosion proof concrete walls. The laydown area has been sized to provide an area to fully disassemble two units at a time, and is serviced by the overhead crane. Hardened areas for assembling the stators and two holes for the rotor shaft assembly will be provided

The travelling overhead crane, is rated at 230T to suit the assembled generator stator/ rotor) as the largest components for lifting of the installed equipment. This can be a single crane or two cranes coupled together are commonly used. The crane span is 21 m. It is also possible that the generator stator could be delivered in two halves. The crane will be used both during construction, and for operations and maintenance. The arrangement also allows the main transformers to be railed into the building laydown area, where the crane can also be used to lift these

16.6.4 Powerstation tailrace

The tailrace from the powerhouse is where the water is discharged from the generating plant, back into the river system (Figure 16-14). The tailrace will be a reinforced concrete channel structure, directing the discharge water perpendicular to the building axis, and then down the original river channel. Earthworks and rock protection in the old river channel 'directs' the water downstream of the building.

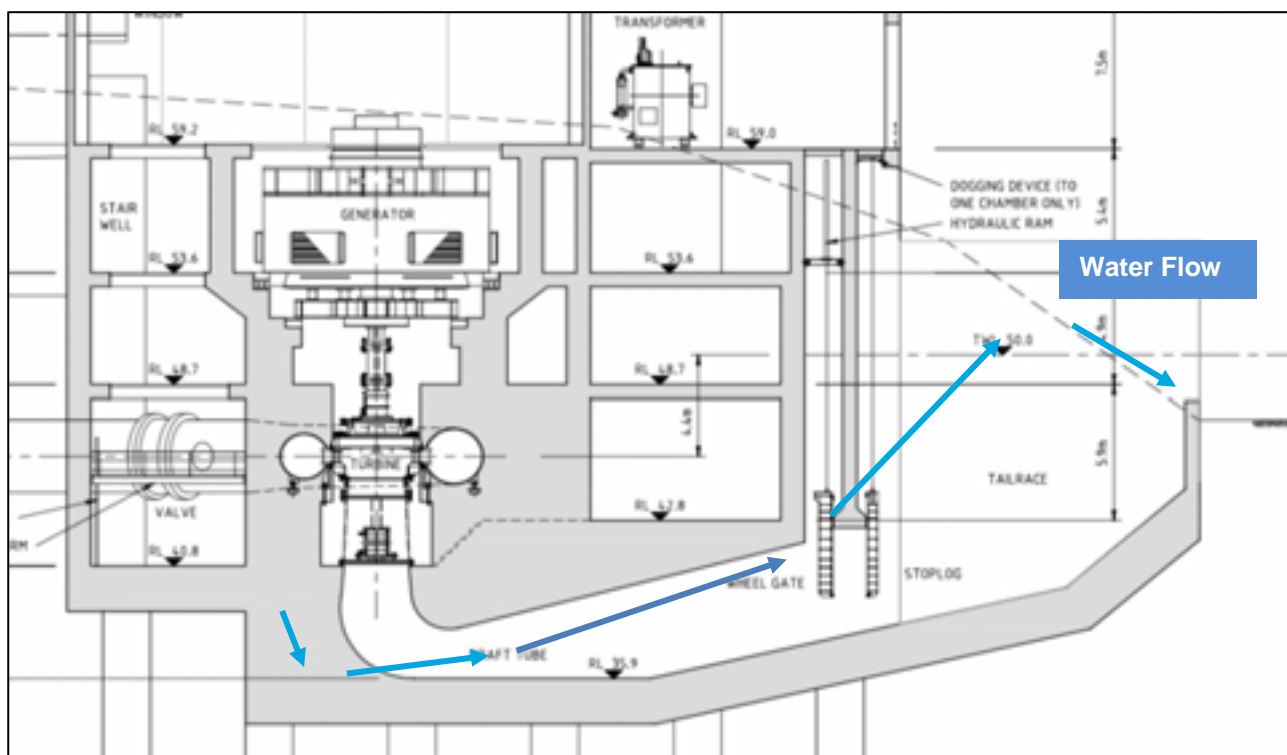


Figure 16-14: Tailrace configuration

Between the tailrace and draft tube, will be a series of double tailrace gates, which when closed, will enable to draft tubes to be dewatered, to allow access and maintenance. Double gates are provided to provide added safety when entering these below water level spaces. The gates are also used to protect the building from inundation in the case of severe river flooding (caused by backed up tailwater from the spillway discharge combined with the local catchment drainage flow).

16.7 Powerhouse equipment

This section discussed the powerstation generating plant and its auxiliaries.

16.7.1 Turbine generators

The optimum configuration of turbine generators is 8 large turbine generator units rated at 69.2 MW and two smaller units rated at 19.3 MW. Taking account of the flow and head, Francis turbines are the only possible turbine option.

In simplistic terms, the optimum synchronous speed for the large units is 272rpm (22 poles). This imposes restrictions on the winding of the stator and as a result this is not a favoured rotational speed. 300rpm has been selected as the economic optimum.

- It allows the top generator floor that supports the trust bearing to be at the building entry level which is well above the PMF flood level and without requiring a longer than normal generator shaft.
- The turbine runner setting is 4.6 m below the tailwater level.

In selecting the units several points should be noted.

- In normal operation the units should be dispatched to equalise the flows on the two penstocks to the greatest degree possible. This maximises the water to wire efficiency of the generating plant. In practice this means that three large units should be allocated to each penstock.
- The full rated output of the unit must be available when three large units are operating at full load on a single penstock over the full range of operating levels.
- 98% of the rated output of the unit must be available when three large units are operating at full load on a single penstock over the reservoir level range from RL 204.39 m and RL 231.50 m.
- The maximum mine demand of 233.4 MW must be met with four large units operating on a single penstock over the full range of operating levels.
- The design case is three large units operating on a single penstock with a reservoir level of RL 204.39 m. This is the level at which the supply of power to the export grid stops.

The key performance requirements for the Turbine Generator Plant are set out in Table 16-7.

Table 16-7: Key turbine generator and auxiliary plant design details

Turbine	Units	Large Unit	Small Unit
Number of units		8	2
Rated power output at generator terminals	MW	69.2	19.3
Rated generator output at generator terminals	MVA	81.4	22.7
Synchronous speed	rpm	300	500
Generator flywheel effect GD ²	T-m ²	1,750 (minimum) In excess of 2,250 preferred	130 (minimum) In excess of 160 preferred
Generator efficiency at peak output and unit power factor		98.5%	98.5%
Generator efficiency at peak output and 0,85 power factor		97.0%	97.0%
Transformer efficiency at rated output		99.3%	99.3%
Auxiliary power losses		<0.5% of station output	<0.5% of station output

Details of the design heads and flows are set out in Table 16-8 to Table 16-10.

Table 16-8 shows the following details for a range of load cases. In all cases the loads are the normal running load at the FRCGP and the typical load on the export grid. Further, the number of units connected to a single penstock has been minimised to reduce the head loss.

The tables show the following data:

- Intakes in use (lower or upper)
- Number of operating units
- Total flow to the powerstation
- Reservoir head water level
- Powerhouse tailwater level
- Maximum number of units connected to a single penstock
- Penstock flow
- Unit flow
- Penstock head loss
- Gross head
- Net head
- Power demand
- Generator efficiency assumed taking into account Power Factor. In general, a value of 97% has been used and this is very conservative. The generator efficiency at peak unit output and unity power factor should be in excess of 98.5%. Under normal running the power factor will be between 0.95 and unity.
- Required turbine efficiency to achieve the output
- Allowance for auxiliary losses. In reality it is expected that a value of half this amount will not be exceeded
- Step-up transformer efficiency.

The data is based on the January electrical Loads which were used to optimise the turbine generator design. Details are provided for a range of load cases that correspond to the full reservoir operating range of the plant and the different loads that correspond to the different operating reservoir levels. The last column provides the details for the normal running case at a common reservoir operating level of RL 224 m.

Table 16-8: Turbine generator data (normal running loads and flows) equalised penstock flow

Case		Normal first power at minimum level supplying FRCGP only	Normal running at minimum level supplying FRCGP only	Normal running at minimum level supplying FRCGP and export grid	Normal running at maximum level supplying FRCGP and export grid	Normal running at typical level supplying FRCGP and export grid
Intake in Use	Units	Low	High	High	High	High
Number of intakes	No.	1	2	2	2	2
Operating units	No.	4	4	5	5	5
Station flow	m ³ /s	158.36	167.43	251.42	222.81	230.57
HWL	RL m	157.65	199.39	204.39	226.14	224.00
TWL	RL m	49.72	49.79	50.34	50.16	54.92
Units per penstock	No	2	2	3	3	3
Penstock flow	m ³ /s	79.18	83.72	150.85	133.69	138.34
Unit flow	m ³ /s	39.59	41.86	50.28	44.56	46.11
Head loss	m	2.04	2.25	5.04	3.97	4.25
Gross head	m	107.93	149.60	154.05	175.98	169.08
Net head	M	105.89	147.35	149.00	172.01	164.83
Load	MW	135.7	217.3	329.9	329.9	329.9
Generator efficiency assumed taking power factor into account	%	97.0%	97.0%	97.0%	97.0%	97.0%
Required turbine efficiency	%	86.50%	94.15%	94.13%	92.01%	92.79%
Acceptable auxiliaries losses	%	0.50%	0.50%	0.50%	0.50%	0.50%
Transformer efficiency	%	99.30%	99.30%	99.30%	99.30%	99.30%

Table 16-9 shows similar information but with the FRCGP and export grid operating at peak load. In this instance a case is provided showing the operation of plant under a PMF condition. In all cases the flow on the two penstocks has been balanced to the greatest extent while minimising the number of units operating.

Table 16-9: Turbine generator data (peak running loads flows) equalised penstock flow

Case		Peak first power at minimum level supplying FRCGP only	Peak running at minimum level supplying FRCGP only	Peak running at minimum level supplying FRCGP and export grid	Peak running at maximum level supplying FRCGP and export grid	Peak running at typical level supplying FRCGP and export grid
Intake in Use	Units	Low	High	High	High	High
Number of intakes	No.	1	2	2	2	2
Operating units	No.	4	4	6	6	6
Station flow	m ³ /s	170.71	180.27	319.07	270.19	276.14
HWL	RL m	157.65	199.39	204.39	226.14	230.86
TWL	RL m	49.81	49.88	50.72	50.45	54.95
Units per penstock	No	2	2	3	3	3
Penstock flow	m ³ /s	85.36	90.13	159.54	135.10	138.07
Unit flow	m ³ /s	42.68	45.07	53.18	45.03	46.02
Head loss	m	2.37	2.61	5.64	4.05	3.45
Gross head	m	107.84	149.51	153.67	175.69	171.19
Net head	M	105.47	146.90	148.03	171.63	167.74
Load	MW	145.7	233.4	408.4	408.4	408.4
Generator efficiency assumed taking power factor into account	%	97.0%	97.0%	97.0%	97.0%	97.0%
Required turbine efficiency	%	86.50%	94.21%	92.43%	94.13%	94.25%
Acceptable auxiliaries losses	%	0.50%	0.50%	0.50%	0.50%	0.50%
Transformer efficiency	%	99.30%	99.30%	99.30%	99.30%	99.30%

Table 16-10 shows similar information to Table 16-9 but with the FRCGP and export grid operating at peak load. In this instance a case is provided showing the operation of plant under a PMF condition. In all cases the flow in the two penstocks is unbalanced and four units are operating on a single penstock. The plant must be able to operate under this condition. However, it is rare and occurs during the estimated 160 hours/ annum when the plant is at peak load and at the same time the outage of units means that the flow imbalance between the two penstocks cannot be minimised to flow the water to wire efficiency to be maximised.

Table 16-10: Turbine generator data (peak running loads) maximum flow through a single penstock

Case		Peak first power at minimum level supplying FRCGP only	Peak running at minimum level supplying FRCGP only	Peak running at minimum level supplying FRCGP and export grid	Peak running at maximum level supplying FRCGP and export grid	Peak running at typical level supplying FRCGP and export grid
Intake in Use	Units	Low	High	High	High	High
Number of intakes	No.	1	2	2	2	2
Operating units	No.	4	4	6	6	6
Station flow	m ³ /s	176.80	185.61	328.01	273.44	278.72
HWL	RL m	157.65	199.39	204.39	226.14	230.86
TWL	RL m	49.85	49.92	50.77	50.47	54.95
Units per penstock		4	4	4	4	4
Penstock flow		176.80	185.61	218.68	182.29	185.82
Unit flow		44.20	46.40	54.67	45.57	46.45
Head loss	m	5.96	6.43	8.90	6.20	5.03
Gross head	m	107.80	149.47	153.62	175.67	171.19
Net head	M	101.84	143.04	144.72	169.46	166.16
Load	MW	145.7	233.4	408.4	408.4	408.4
Generator efficiency assumed taking power factor into account	%	97.0%	97.0%	97.0%	97.0%	97.0%
Turbine efficiency	%	86.50%	93.97%	91.96%	94.21%	94.26%
Auxiliaries use	%	0.50%	0.50%	0.50%	0.50%	0.50%
Transformer efficiency	%	99.30%	99.30%	99.30%	99.30%	99.30%

16.7.2 Powerhouse mechanical systems

The powerhouse will have a full range of auxiliary systems. These include the following:

- 8 × large turbine generators rated at 69.2 MW, 81.4 MVA
- 2 × small turbine generators rated at 19.3 MW, 22.7MVA
- 10 × governor systems complete with dedicated hydraulic power packs with duty and standby pumps. A separate leakage pump, to supply the valve leakage should be provided if required. The governor should meet the requirements of IEC60308 for sizing accumulator oil and gas volumes.
- 10 × turbine inlet valves. It is proposed that spherical (plug or ball) valves are used rather than butterfly valves. The spherical valves provide steel seats for the maintenance and service seals. They can provide a drip tight shut off. Given that the inlet valves will be installed at the start early in the project, with the turbine generators following at a later date, the highest possible quality seal is required in this instance. This point is reinforced when the high sediment loads (as discussed in section 0) are also considered. A butterfly valve could be used but it has higher head losses and the seals are not as resilient. On the large units these valves could be 2.5 to 2.75 m in diameter and the small units the valves could be 1.3 to 1.5 m diameter. The valves would be hydraulically operated, each with a dedicated hydraulic power pack and a reservoir sized to allow three CLOSE, OPEN, CLOSE actions.

- 2 × compressed air system for the tailwater depression system. This will include duty and standby air compressor, and receivers at two locations to minimise the pipe length to the large units. Tailwater depression will only be provided for the large units. The air receivers and piping need to be sized to allow the water level to be pushed down to 2 m below the bottom of the runner in 30 seconds. Two units may be on spinning reserve at any time. The air receivers should be located in two banks in the middle of each group of four large units.
- Compressed air system for the all generator braking systems
- Dual 110 V DC systems with 24-hour battery life shall be provided for the operation of the control system and generator, substation switchgear and transformer protections systems. It also needs to provide back-up for the powerstation bypass valves.
- Dual standby generators are to be provided. At this stage the rating is taken to be 1 MW each. The final rating will be determined by the need to meet the demand for power during construction and commissioning when none of the hydro generators are available and without the need to connect in construction site temporary generators. The generators must meet the demand of the powerstation auxiliary systems, bypass valve auxiliaries, lighting, substation crane and powerhouse main crane.
- The main powerhouse overhead travelling crane will be rated at 230 tonne lifting capacity on the main hoist. An auxiliary hoist will need to be provided to lift the inlet valves. An alternative arrangement would be to provide two 120 tonne overhead travelling cranes with a lifting beam rated at 230 tonnes. This latter arrangement has advantages given the number of units.
- Substation 10 tonne travelling crane rated to lift all switchgear items. The crane shall be able to lift a concrete hatch in the floor of the switchgear room to allow the switchgear components to be lifted from ground level into the high level switch room.
- 10 × Cooling water systems for turbine generators (including capacity for generator step-up transformers).
- 10 × tailrace wheel gates. The wheel gates can be actuated by either an electric hoist or hydraulic ram. Wheel gates have been chosen at this time to ensure that the tailrace gates can be closed under all circumstances. It is possible that if the spillway flows or powerstation bypass valves flows are high, stoplogs could not be lowered. Consideration could be given to automating the tripping of the units and lowering the tailrace gates automatically in the event of high tailwater levels. These could occur suddenly if there is a landslide for some reason downstream of the powerhouse. In addition to the wheel gates, a single steel stoplog is provided to allow double isolation when people are working in the draft tube/ tailrace area of the unit. It also allows the wheel gate to be maintained.
- 1 × oil treatment system for generating units waste
- 1 × fire protection systems for generating units (including capacity for generator step-up transformers)
- 1 × overall powerhouse fire sprinkler system
- 1 × compressed air system for tailwater depression and generator braking
- 1 × powerhouse drainage system
- 2 × turbine dewatering system
- 1 × flood pump system to allow high inflows from surface water that enter the powerhouse to be pumped to the river
- Dedicated blanket fire protection system for HV switchgear rooms and also for control panel rooms

- Powerhouse ventilation system consisting of roof extract fans and a supply air systems to the lower floors
- Control room air conditioning
- Water supply, potable water system and waste water holding system for trucking by tanker to disposal network.

16.7.3 Electrical equipment

The electrically equipment will include:

- 8 × generators each rated at 81.4 MVA
- 2 × generators each rated at 22.7 MVA
- 10 excitation systems
- 8 × 13.8kV/ 132kV step-up transformers, each rated at 81.4 MVA
- 2 × 13.8kV/ 132kV step-up transformers, each rated at 22.7 MVA
- 10 × segregated phase bus ducts from the generators to the MV switchgear and transformers
- 10 × generator 13.8 kV switchgear
- 10 × unit HV 132 kV switchgear and associated integral disconnectors
- 4 × 132 kV outgoing switchgear
- 4 × 132 kV bus coupler switchgear
- 3 × GIS encapsulated buses with 3 phases in a single enclosure to provide dedicated buses for the FRCGP and export grid plus a separate bus for livening rid transformers and for use with the load bank
- 10 × electrical protection systems (including all duplicate type):
 - Turbine generator protection
 - Segregated phase bus protection
 - Circuit breaker failure protection
 - Generator step-up transformer protection
 - Local service transformer protection.
- Control and automation systems for the turbine generators and appurtenant facilities including:
 - 10 × turbine generator unit controller stations
 - 10 × turbine generator machine condition monitoring systems
 - 4 × powerstation bypass valves unit controllers
 - 1 × station services controller stations
 - 1 × intake services controller station
 - 1 × set HMI terminals and servers.
- Remote control and monitoring systems for the lower and upper intake, intake gates (3 offs), spillway gates (4 off) and residual flow and guard valves (2 off)
- Remote control and monitoring systems for the generator step-up transformers and 132 kV switchgear
- Remote monitoring systems for the 132 kV switchgear at the switchyard
- 1 × water level monitoring system
- 2 × local service alternating current (AC) power systems including two 13.8 kV to/ 400 V auxiliary transformers, rated at 1 MVA for turbine generator ancillary plant and for the powerhouse services

supply. Sufficient capacity shall be included for the powerhouse building services, generator step-up transformer ancillary loads, 132 kV switchyard, and HVAC systems.

- 1 × AC UPS (uninterruptible power supply) system
- 2 × standby diesel generator system at the powerhouse rated to supply the turbine generator and powerhouse essential services. These are sized at 1 MW each.
- Connections to the powerhouse grounding systems for the Plant.

16.7.4 Load bank

An electrical load bank rated at 69 MW, 82 MVA is to be provided. It is assumed that the unit will provide both resistive and inductive loads. The load bank will be a permanent installation and serve a range of functions:

- It will allow units to be tested and wet commissioned without the mine load being available.
- The governor control modes can be tested and proven.
- Load sharing between units can be tested with up to three units able to operate in conjunction with the load bank.
- The operation of the tailwater depression system and the spinning reserve unit can be fine-tuned and tested prior to operating with the mine load.
- Full drop load tests will be able to be carried out on each unit without disrupting the power supply to the mine.
- The transient response of the water system will be able to be tested without disrupting the mine. This will allow the wicket gate times and surge chamber heights to be confirmed and corrective action taken in a timely manner if required.
- All units will be wet commissioned using the load bank.
- Once all units are commissioned the load bank can be used to test units following maintenance. This will aim to improve reliability by addressing the fact that 90% of trips on hydro units occur after start-up following maintenance.

The load bank will be supplied through step down transformer identical to the generator step-up transformers on each unit. The load bank consists of 10 modules supplied at 13.8 kV. The step down transformer can be used as a spare transformer if there is a major fault with one of the unit transformers that takes a long time to correct.

16.7.5 Equipment transport dimensions and weights

Details of the indicative weights of the various items of equipment (for transportation purposes) are set out in Table 16-11.

Table 16-11: Critical equipment weights

Item	Location	Length (m)	Width (m)	Height (m)	Weight (t)
Power transformer	Powerhouse	6.0	3.5	4.0	70
Generator rotor	Powerhouse	10	4–6 diameter		150–180
Turbine runner	Powerhouse		2.4 diameter	2.0	15 plus 20 for the shaft
Generator stator frame (two sections)	Powerhouse		4–4.5	3.5	75
Generator stator frame (one piece)	Powerhouse		6.5–7.5	3.5	150

Item	Location	Length (m)	Width (m)	Height (m)	Weight (t)
Powerhouse crane girder	Powerhouse	21	1.5	3.0	30
Inlet valve	Powerhouse	3.0	3.0	4.0	60
Radial gates (four sections per gate)	Spillway	7.5	4.1	2.5	20–25 per section
Inlet gate	Upper intake	1.5	7.5	7.5	68
Inlet gate	Lower intake	1.5	7.5	7.5	100
Residual flow valve	Valve shaft	3.5	2.5	2.5	15
Residual flow guard valve	Valve shaft	1.5	3.5	5.5	25
Station bypass valves	Powerhouse	5.5	4.5	4.5	35
Station bypass guard valves	Powerhouse	2.5	4.5	7.0	50

The assembled rotor would be about 3–5 m in diameter and would weigh upwards of 200 t. There is a very considerable range of size and dimensions for generators and they depend in part on the required flywheel effect required. It would be normal to ship the rotor with the poles removed and with the rotor spider separate from the shaft. On site the spider would be shrunk fit onto the shaft, the rim laminations assembled & then the poles fitted. The rotor spider would probably be around 4 m in diameter – but would only weigh 15–20 tonnes. If the transport restrictions would not permit this diameter, then the manufacturers would reduce the rotor spider diameter to the maximum transport size & then increase the width of the rim laminations.

The generator upper bracket would have a similar diameter to the stator ~ 5–6 m and would probably be a 6 or 8 leg construction. The manufacturer could keep the width within transport requirements by having some of the legs site fitted (bolted or welded).

The turbine distributor would be cut into the largest sections possible that are consistent with the permitted transport dimensions.

There is some flexibility of how big some items are. However, reducing the size into sections greatly increases the onsite assembly time. It could add 4 months to the project timetable for each unit. There would also be some cost increase, potentially. Also, the potential for a significant delay owing to the amount of site assembly increases significantly.

16.8 Substation and transmission

As noted in the previous section, the powerstation will consist of eight primary turbine generators, each rated at 69.2 MW/ 81.4 MVA, and two secondary turbine generators each rated at 19.3 MW/ 22.7 MVA.

The generators will generate at a nominal voltage of 13.8 kV, with the final voltage being selected by the generator manufacturer.

Each generator will be provided with a 13.8 kV Generator Circuit Breaker (GCB) which will be used to provide protective isolation as well as during normal starting/ synchronising and stopping of the generator. It is possible that the 132 kV circuit breakers could be used for this duty and the need for the generator circuit breakers on the primary generators will be reassessed during detailed design. However, with the reduction in the cost of the low voltage breakers it has become more common to provide them as they are better suited to the synchronising function than the 132 kV breakers.

The output of each generator will be stepped up to the 132 kV transmission voltage by means of a three phase 13.8/ 132 kV generator step-up transformer.

The 13.8 kV generator connections from the generator terminals to the step-up transformer will use a phase isolated busbar for the primary units and either phase isolated busbar or cables for the secondary units.

Powerstation auxiliary 400 V services will be taken from the 13.8 kV side of the generator step-up transformers on two of the secondary units.

The 132 kV switchyard will utilise gas insulated switchgear (GIS) and will be located indoors within the powerstation complex at RL 66.5 m as shown on drawing G037. A three bus configuration is proposed, using three phase encapsulated equipment, where all three phases of one bus are housed in a single SF6 gas insulated enclosure. The GIS may require base isolation in order to address seismic loads.

The three bus configuration is adopted to provide full flexibility to permit each generator to supply either the FRCGP or the export grid. The third bus is provided for three reasons:

- As a backup to the 'FRCGP' and 'export grid' buses
- To permit connection of the generator to the load banks for testing and commissioning purposes. This allows full drop load tests to be carried out without affecting the operation of the export grid.
- To allow the FRHEP generators to be used to bring up the large remote transformers. This is an onerous duty and requires the units to bring up the system voltage slowly. This cannot be done by the main grid without risking a collapse of the voltage.

Bus tie circuit breakers are provided to permit load to be transferred between buses. These can be used to interconnect the FRCGP and export grid buses during operation if necessary. Similarly, they can be used to disconnect the two systems if paralleled.

'Black' energisation of one of the FRCGP transformers, or one of the export grid interconnection transformers, may create issues with the generating facility owing to the high inrush currents. It is therefore intended that such loads would be connected to the backup (reserve) bus. One turbine generator would then be started with the GCB closed and also connected to the backup bus. Once the turbine generator was up to speed, the generator excitation would gradually raise the generator and connected load voltage, preventing any initial inrush. Once the transformers and transmission lines are fully energised the backup bus would synchronise to the required bus (mine or PNG) and the relevant bus tie circuit breaker closed. The load disconnectors would then be reconfigured to connect the load to the correct bus, and the bus coupler breaker opened.

If during operation of the facility it is needed to parallel the FRCGP and Export grid buses, then this would be accomplished by using the bus tie breakers. These breakers will also include auto-synchronisers which will match the voltage, frequency and phase difference between the two busbars prior to permitting the breaker to be closed. Once the bus tie is closed the generators and loads can be reallocated by adjusting the disconnect switches, after which the bus coupler can be reopened to separate the two buses again.

The triple bus configuration envisaged would have the three busbar chambers located horizontally with the generator step-up transformers connected to the GIS switchyard by means of gas insulated bus as shown in Figure 16-15.

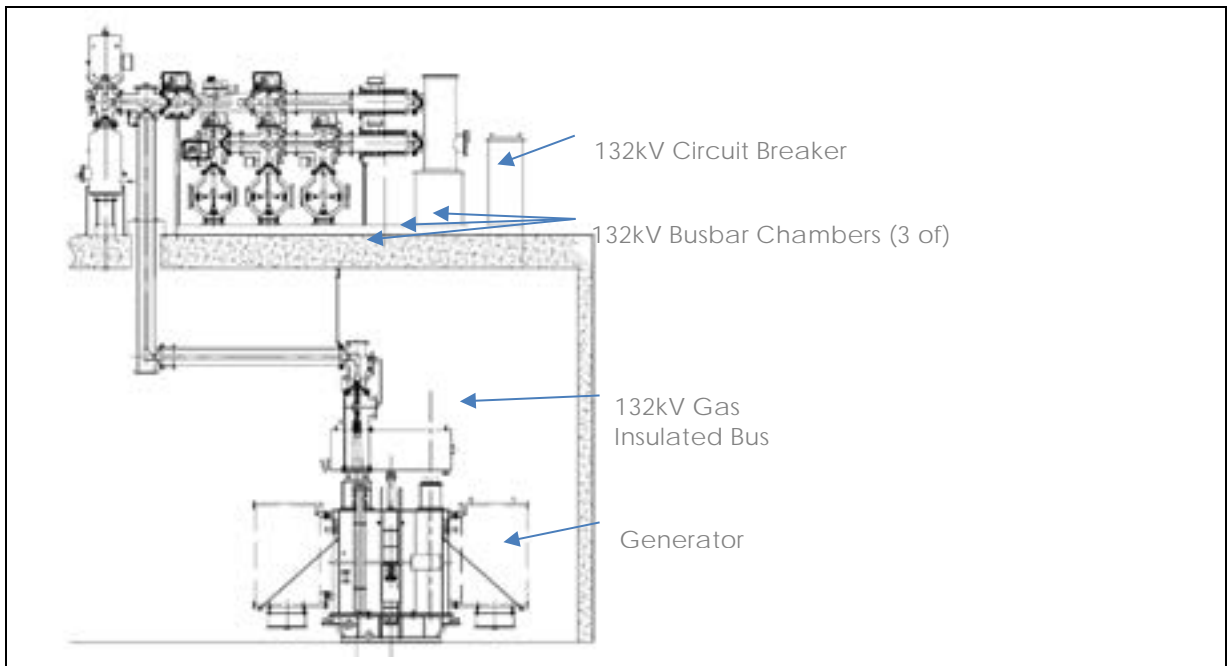


Figure 16-15: 132 kV GIS configuration

Each 132 kV circuit breaker bay will be approximately 3m wide and will be located on the same 13 m centres as the generators. Three phase encapsulated busbars will connect the bays to form a complete assembly.

It is noted that triple bus GIS configurations are relatively rare and it may prove necessary for some manufacturers to use two circuit breakers per bay to achieve the required bus configuration, in particular if they do not utilise a horizontal bus, three phase encapsulated, configuration in their standard designs.

A solution for such manufacturers could be to use standard two bus switchgear, but install two circuit breaker bays for each connected generator or transmission line. Manufacturers that use a vertical bus configuration or single phase encapsulated busbars may need to adopt this arrangement. Figure 16-16 shows both the proposed arrangement (Option 1) and the alternative (Option 2). Many Chinese GIS manufacturers use the horizontal bus configuration, whereas European suppliers tend to adopt the vertical bus configuration.

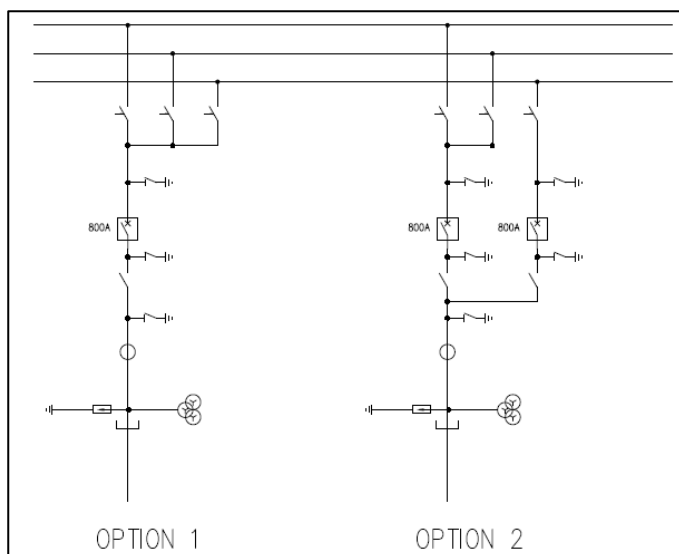


Figure 16-16: 132 kV GIS configuration options

17 Early Filling/ First Power

17.1 Time to first power to FRCGP and export grid

The time to first power is set out in Table 17-1. The table shows the results of the analysis based on the 16 sequences of 16 years of measured data and the 200 sequences of 38 years of synthetic data.

As can be seen, the mean time to first power from the start of filling is 237 and 246 days from the analysis of the measured flow and synthetic datasets. The most rapid filling estimate is 180 days and 172 days from the measured flow and synthetic datasets. Both these sets of values are extremely similar. The longest filling time is 375 and 441 days for measured flow and synthetic datasets. These are similar but the synthetic series is longer.

The time to first power to the export grid, when the reservoir level reaches RL 224.14 m, shows a similar pattern. The mean time to first power to the export grid from the start of filling is 744 and 773 days from the analysis of the measured flow and synthetic datasets. The most rapid filling estimate is 589 days and 583 days from the measured flow and synthetic datasets. Both these sets of values are extremely similar. The longest filling time is 907 and 1,329 days for measured flow and synthetic datasets. These are similar but the synthetic series is almost 50% longer.

Table 17-1: Time to first power to FRCGP and export grid (January 2018 electrical load)

Parameter	Supply to FRCGP (days)		Supply to export grid (days)	
	Measured data series	Synthetic data series	Measured data series	Synthetic data series
Average Time to First Power	237	246	744	773
Earliest Time to First Power	180	172	589	583
Longest Time to First Power	375	441	907	1,329
Standard Deviation	52	48	82	134

Figure 17-1 shows the distribution of the time to first power at the FRCGP and export grid from the synthetic flow series. It can be seen that the exceedance from the longest filling time from the measured flow series occurs at:

- 4% of occasions for the time to first power at the FRCGP
- 17% of occasions for the time to first power to the export grid.

Overall, there is good agreement between the Measured and Synthetic Flow series in predicting the average time it takes to fill the reservoir. From a risk mitigation standpoint, the close agreement between the earliest filling date using the two series adds some confidence to the dam safety proposals during early filling. The larger deviation in the projected longest date for filling the reservoir is not unexpected.

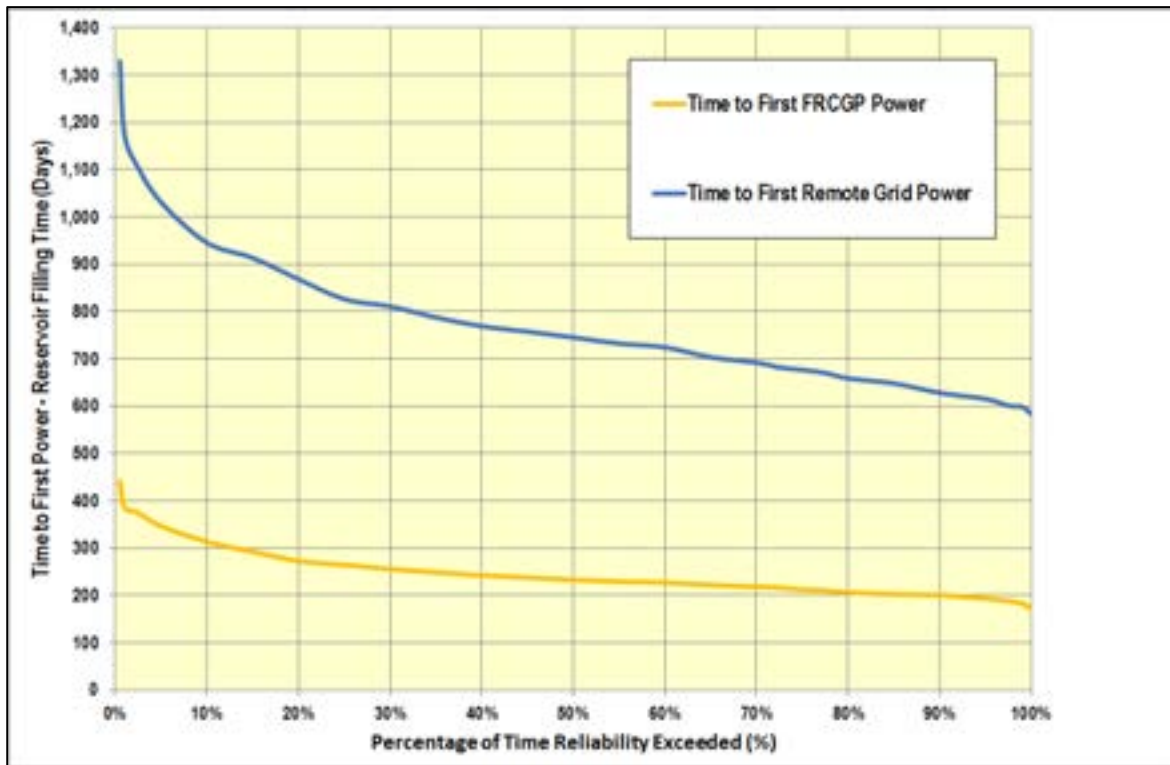


Figure 17-1: Distribution of time to first power - FRCGP and export grid

Figure 17-2 shows the filling rate variability for all sixteen measured inflow sequences. As can be seen the variations are quite significant, as also shown in Table 17-1.

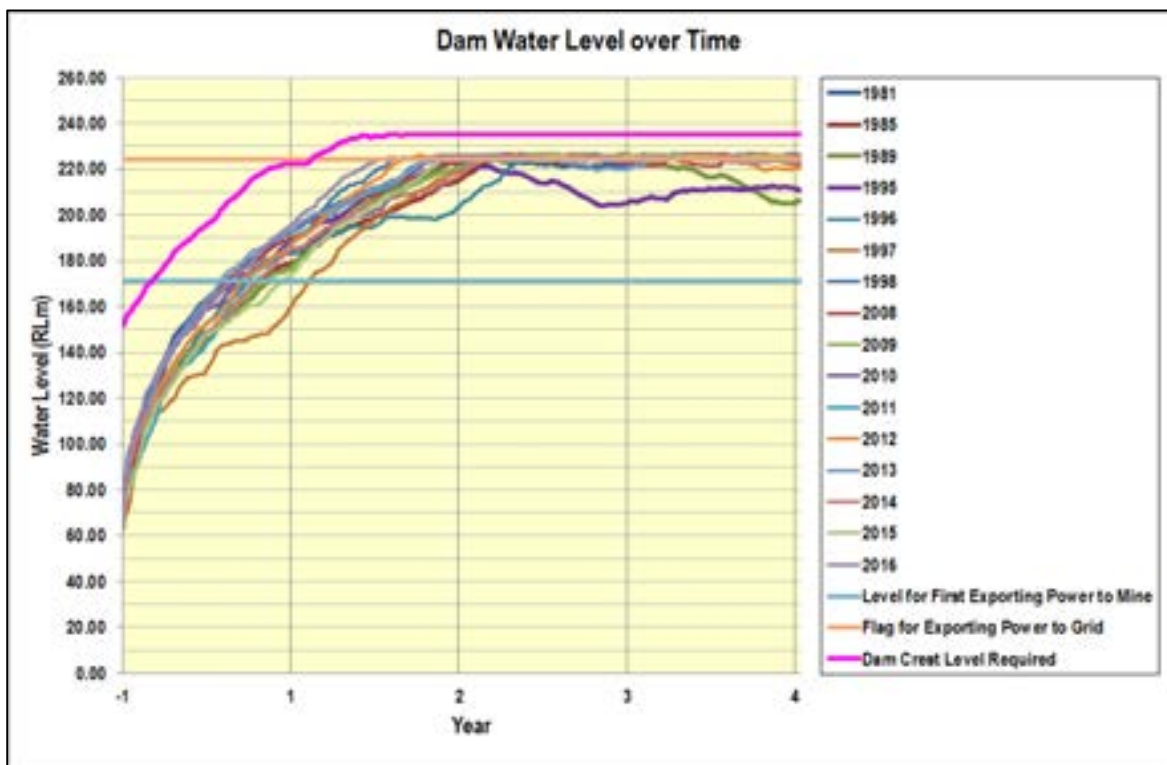


Figure 17-2: Dam crest and water levels during the filling of the reservoir

Table 17-2 compares the time to first power to the export grid and FRCGP based on the January 2018 electrical load profiles and the original early filling strategy with the May 2018 electrical load profiles

and the revised early filling strategy based on the June 2018 TIRP meeting outcomes. As can be seen the higher reservoir level before generation can start has some impact but is offset slightly by the earlier commencement of filling.

Table 17-2: Comparison of time to first power based on the January and May electrical load profiles

Parameter	Supply to FRCGP (days)		Supply to export grid (days)	
	January Electrical Loads with original early filling strategy	May Electrical Loads with revised early filling strategy following the TIRP review	January Electrical Loads with original early filling strategy	May Electrical Loads with revised early filling strategy following the TIRP review
	Measured Data Series	Measured Data Series	Measured Data Series	Measured Data Series
Average time to first power	237	275	744	709
Earliest time to first power	180	212	589	560
Longest time to first power	375	407	907	873
Standard Deviation	52	53	82	83

The required dam crest levels at different times during filling are detailed in Table 17-3 that follows. The information is based on the measured inflow data series. As can be seen there is 394 days available to bring the dam up to the final crest level and to commission the spillway.

Table 17-3: Required dam crest height and time available to complete from start of filling

Parameter	Units	January 2018 Electrical Loads with original early filling strategy	May 2018 Electrical Loads with revised Early Filling Strategy
Required embankment crest height at start of filling	RL m	180.69	151.48
Embankment volume to be placed for filling to commence		91%	66%
First power height - required embankment crest height at start of supply to FRCGP	RL m	204.65	201.69
Time available to construct embankment from start of filling to first power height	Days	180	212
Time available to construct embankment from start of filling to final height RL 238.5 m	Days	394	RL 370 m to RL 222 m RL 508 m to RL 235 m

It can be seen that the times are similar that the revised strategy for filling requires more rapid construction of the embankment if advantage is to be taken of the early filling. However, the amount of the embankment that must be constructed with the revised filling strategy may be excessive for the time available. In other words, filling can commence but the reservoir level may need to be held at one elevation for periods of time to allow construction targets to be achieved, which will introduce additional delays. The final capping off of the embankment can be delayed with the revised strategy by using the spillway with the gates dogged fully open in parallel with the bypass valves.

The embankment and reservoir operating rules are set out in Section 19.3.1.

18 Energy Production

Details of the optimised energy production are provided for the 16-year measured flow series and for the 200 × 38-year synthetic flow series.

18.1 Power supply reliability (16 year measured flow series)

The Water Balance and Energy Model (Section 7) has been used to maximise the generation potential from the FRHEP, while ensuring the FRCGP and export grid reliability targets are achieved.

The result is set out in Table 18-1 for Year 17, the year of peak demand at the FRCGP for the January and May 2018 Electrical loads.

Table 18-1: Optimised FRHEP generation for embankment crest height of RL238.5 m

Parameter	Units	January electrical load data	May electrical load data
FRCGP peak demand	MW	233.4	277.2
FRCGP energy demand	GWh/a	1,792.9	2,158.8
Indicative supply losses	%	0.2%	0.2%
Net FRCGP energy supply	GWh/a	1,788.9	2,154.5
Export grid peak demand	MW	175.0	100.0
Export grid energy demand	GWh/a	996.5	630.2
Supply losses	%	2.2%	1.5%
Net export grid energy supply	GWh/a	974.4	620.7
FRHEP peak demand	MW	408.4	377.2
FRHEP energy demand	GWh/a	2,789.4	2,789.0
Supply losses	%	0.9%	0.5%
Net FRHEP energy supply	GWh/a	2763.3	2,775.2

The reliability of the supply of power from the FRHEP has been assessed using 16 sequences with each of the measured years being treated as the first year. The results are presented in Table 18-2 and Table 18-3 that follow for the January and May electrical load profiles respectively.

These tables show a range of information:

- Overall power supply reliability over 33 years from the start of supply to the FRCGP and the export grid
- Overall power supply reliability from Years 11–33 to the FRCGP and the export grid. These years cover the period of maximum FRCGP and export grid demand.
- Total number of lost days in supplying the export grid. This occurs when the reservoir level falls to RL 204.39 m at which point only the FRCGP will be supplied.
- Total number of lost days in supplying the FRCGP. This occurs when the reservoir level falls to RL 199.39 m at which point the FRCGP will be unable to process ore. The non-operating loads will still be met.
- The spill from the reservoir as percentage of the total inflow over Years -1–33
- The spill from the reservoir as percentage of the total inflow over Years 11–33.

Table 18-2: Power supply reliability from FRHEP based on January electrical load profile

Measured Sequence Start Year	Supply reliability Years 1–33	Supply reliability Years 11–33	Export grid Loss of Load (days)	FRCGP Loss of Load (days)	Spill Years 1–33	Spill Years 11–33
1981	100.00%	100.00%	0	0	10.9%	6.4%
1985	100.00%	100.00%	0	0	10.8%	5.5%
1989	99.99%	99.99%	3	0	10.6%	4.4%
1995	99.94%	99.92%	17	0	10.6%	4.7%
1996	99.93%	99.90%	22	0	10.7%	4.5%
1997	99.83%	99.77%	52	0	10.8%	3.9%
1998	99.81%	99.74%	57	0	10.5%	3.3%
2008	100.00%	100.00%	0	0	10.6%	3.4%
2009	100.00%	100.00%	0	0	11.3%	4.9%
2010	100.00%	100.00%	0	0	11.2%	4.7%
2011	100.00%	100.00%	0	0	11.0%	4.3%
2012	100.00%	100.00%	0	0	11.2%	5.7%
2013	100.00%	100.00%	0	0	11.3%	6.3%
2014	100.00%	100.00%	0	0	11.4%	5.8%
2015	99.99%	99.99%	2	0	11.0%	5.5%
2016	99.99%	99.98%	4	0	10.6%	5.2%
Overall	99.97%	99.96%	10	0	10.9%	4.9%
Worst Sequence	99.81%	99.74%	57	0	11.4%	6.4%

Table 18-3: Power supply reliability from FRHEP based on May electrical load profile

Measured Sequence Start Year	Supply reliability Years 1–33	Supply reliability Years 11–33	Export grid Loss of Load (days)	FRCGP Loss of Load (days)	Spill Years 1–33	Spill Years 11–33
1981	100.00%	100.00%	0	0	3.9%	4.9%
1985	100.00%	100.00%	0	0	3.9%	4.9%
1989	100.00%	100.00%	0	0	3.9%	5.3%
1995	99.87%	100.00%	27	0	3.4%	5.0%
1996	99.98%	99.98%	8	0	6.2%	5.8%
1997	99.99%	99.99%	4	0	6.0%	5.8%
1998	100.00%	99.99%	2	0	5.6%	5.2%
2008	99.99%	99.99%	3	0	5.6%	4.4%
2009	99.98%	99.97%	12	0	5.5%	4.2%
2010	99.86%	99.82%	67	0	5.2%	4.3%
2011	99.91%	99.87%	47	0	4.9%	4.0%
2012	99.95%	99.93%	25	0	4.2%	3.5%
2013	99.99%	99.99%	4	0	4.0%	3.4%
2014	100.00%	100.00%	0	0	4.2%	3.7%
2015	100.00%	100.00%	0	0	3.9%	4.0%
2016	100.00%	100.00%	0	0	3.4%	4.0%
Overall	99.97%	99.97%	12	0	4.6%	4.5%
Worst Sequence	99.86%	99.82%	67	0	6.2%	5.8%

From Table 18-3, the following conclusions can be drawn:

- The overall power supply reliability over Years -1–33 from the start of supply from the FRHEP varies from 99.86% to 100.00% with an overall value of 99.97%.
- The overall power supply reliability from Years 11–33 from the FRHEP varies from 98.82% to 100.00%, with an overall value of 99.97%.
- Total number of partial lost days in supplying the export grid vary from 0 to 67 days over Years -1–33 with a mean value of 12 days.
- There is no loss of supply to the FRCGP in any of the 16 sequences of measured.
- The spill from the reservoir as percentage of the total inflow over Years -1–33 varies from 3.4% to 6.2% with an expected value of 4.6%.
- The spill from the reservoir as percentage of the total inflow over Years 11–33, when the loads are at the maximum, ranges from 3.4% to 5.8% with an average value of 4.5%.
- A comparison of the two tables for the January and May electrical loads shows that the higher firm power requirements for supplying the FRCGP loads results in a slightly lower reliability overall and a lower spill. However, 100% reliability of supply to the FRCGP is maintained. It will be seen that there is considerable variation in the amount of power available to the export grid when analysed using the synthetic flow data.

In assessing these results there are several points to note:

- The reliability for power supply to the FRCGP taking the combined generation reliability and water supply reliability values is achieved. From Section 15.4.3 (Table 15-11 and Table 15-12), it can be seen that the generation reliability during normal running, including providing a spinning reserve unit is 99.98%. At peak load this reduces to 98.71%; however, this load is expected to occur for less than 160 hours/annum. In combination with 100% water supply reliability, the overall reliability is 99.97%. This can be compared to the FRCGP's reliability requirement of 99.73%.
- The supply reliability for the export grid is likely to be in excess of 99.87% provided the generation commitments are kept in line with the available water supply. This is comparable to the target of 99.5%.
- Most of the loss of supply to the remote grid occurs during the first year of supply and the cause of this has not been confirmed. However, reliability improves significantly after the first year.
- The spill values after Year 11 indicate that perhaps an additional 50 to 80 GWh/a could be supplied to the export grid. This water would be dependent on the inflows and would not be at a high level of annual reliability. Nevertheless, it is saleable. The concern of a commitment of this power for sale is that there will be a tendency to assume it is available and to dispatch power to the export grid that in reality is not available. This would lead to cuts in power supply that may affect the FRCGP.

18.1.1 Water balance and energy model

Typical outputs of the Water Balance and Energy Model are provided in Figure 18-1 to Figure 18-4.

Points to note:

- The maximum spill from reservoir overall the sequences is 700 m³/s on a daily basis with a peak hourly flow of 990 m³/s. The bypass valves could pass nearly all of the spillway flow if it was thought that this would minimise operating costs
- It can be seen that the reservoir levels take years to recover from the extreme low flow year (1997) in the measured flow series. The generation flows increase significantly because of the low reservoir levels.

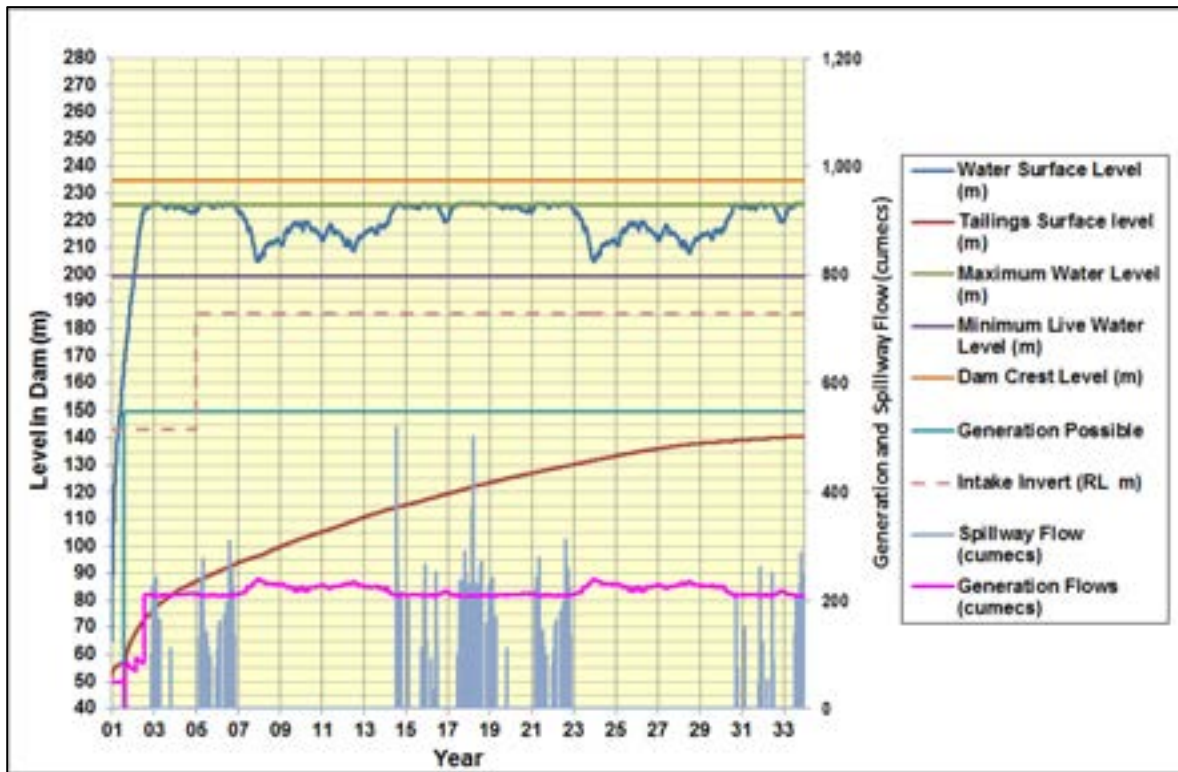


Figure 18-1: Reservoir level variation for most reliable sequence – Years -1–33

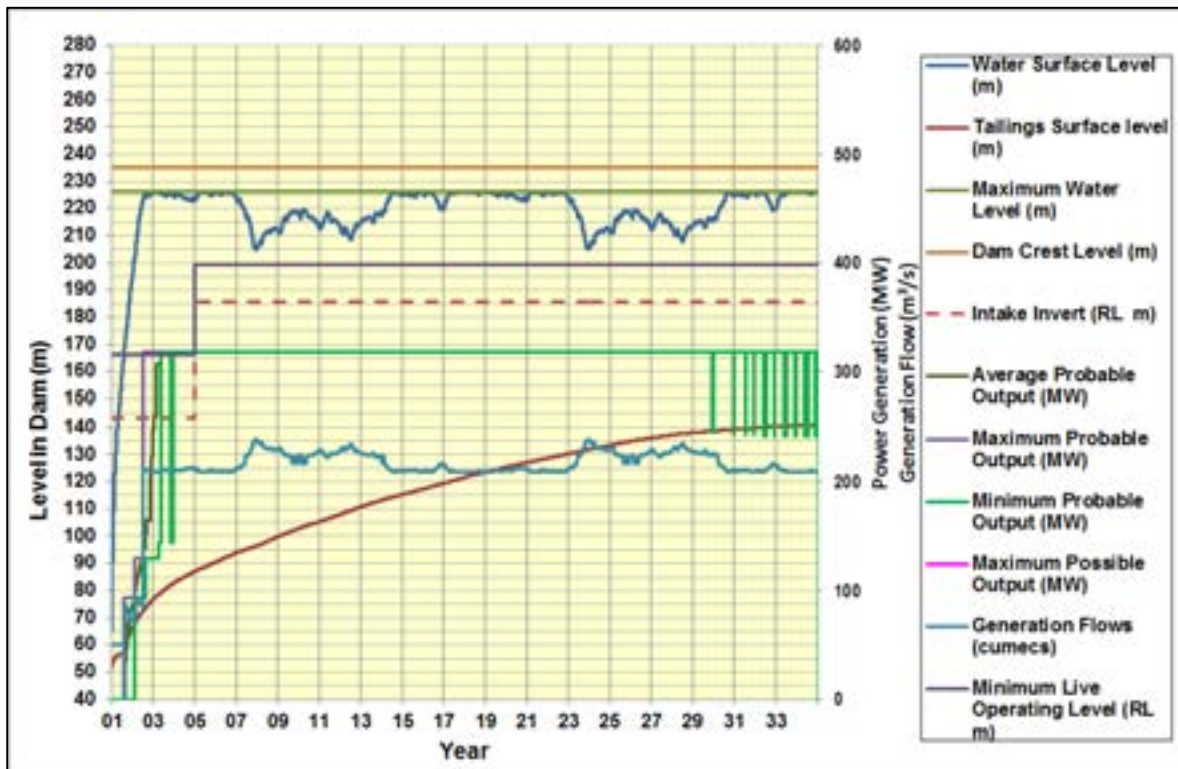


Figure 18-2: Reservoir water level and power generation for most reliable sequence – Years -1–33

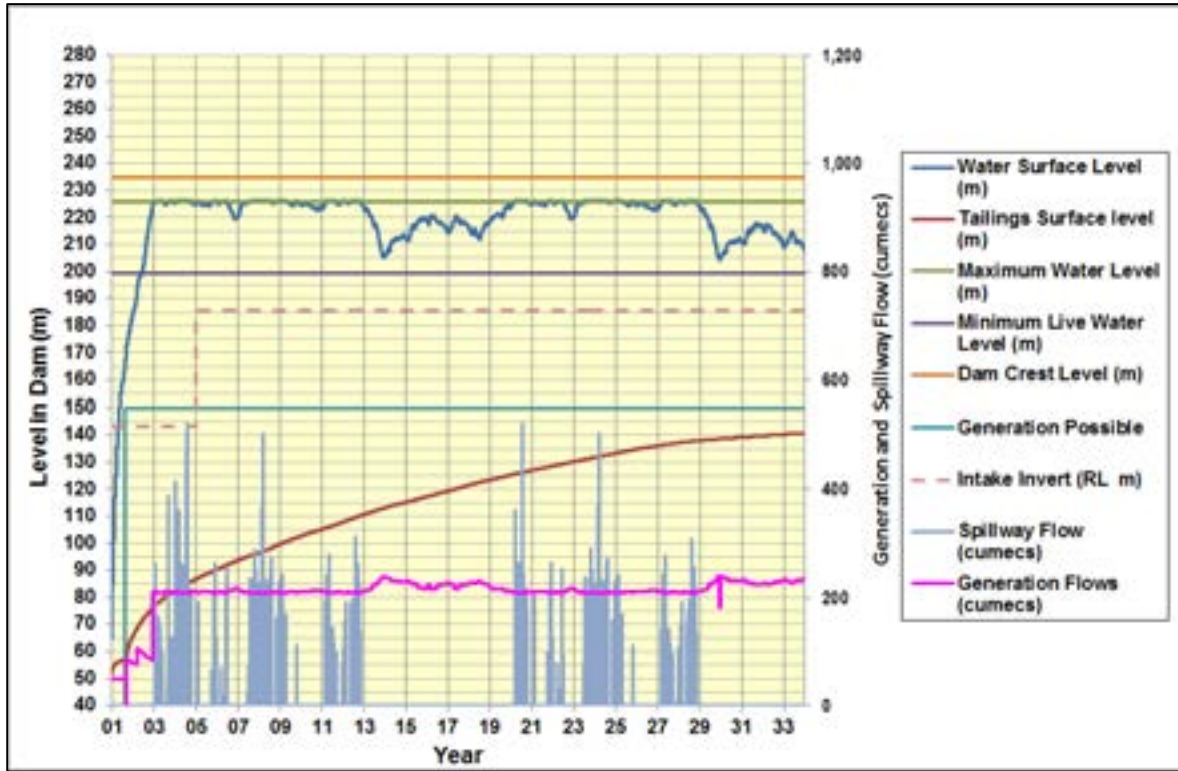


Figure 18-3: Reservoir level variation for least reliable sequence – Years - 1–33

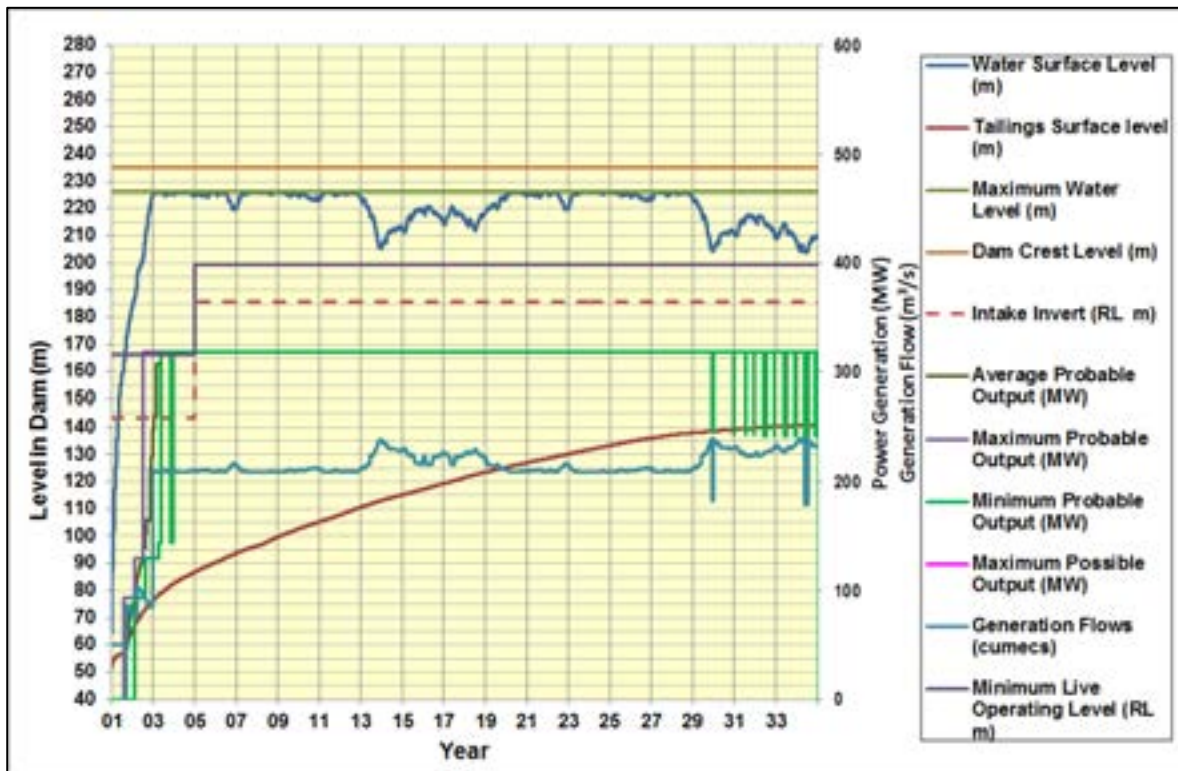


Figure 18-4: Reservoir water levels and power generation for least reliable sequence – Years -1–33

18.2 Energy production (200 × 38 year synthetic flow series)

The synthetic flow series has produced the results of the modelling of 200 flow sequences which have been generated using the hidden Markov model to generate the data. The resulting flow data has been analysed and the results of the comparison with the measured flow series are set out in Section 7.3. As noted, the flow duration curves look very similar. However, not surprisingly, the synthetic flow series has more extreme minimum and maximum inflows. A concern is that the long term events may be too extreme. It should be noted that the analysis of the synthetic flow series has only been carried out for the January electrical loads.

In analysing the synthetic flow series, identical turbine generator configurations and conveyance system parameters have been used as with the measured flow series. The water management rules are also the same.

The energy model used is slightly more accurate than for the measured flow series owing to some simplifications in the measured flow series model that aimed to speed up the running of the model by perhaps 15 times.

The energy production potential of the scheme is presented in Table 18-4. One point to note in particular is the significant variation in the energy production potential with the synthetic flow series in the later years in the worst sequence. The average export potential to the export grid is 996 GWh/a. However, it can fall as low as 425 GWh/a in the worst year of the worst of the 200 sequences. This is equivalent to one year in the 7,600 years modelled.

Table 18-4: Comparison of energy production (varying loads and flow series)

Year	May Loads measured flows	January Loads measured flows	January Loads synthetic flows		
			Best sequence	Average sequence	Worst sequence
-1	413	-	-	-	-
1	1,669	1,007	1,011	1,006	1,006
2	2,768	1,720	2,102	1,692	1,990
3	2,812	2,082	2,083	2,061	2,083
4	2,774	2,102	2,098	2,098	2,098
5	2,789	2,206	2,207	2,207	2,207
6	2,789	2,198	2,199	2,199	2,199
7	2,812	2,098	2,100	2,100	2,100
8	2,774	2,114	2,110	2,109	2,110
9	2,789	2,106	2,108	2,108	2,108
10	2,789	2,104	2,110	2,110	2,110
11	2,812	2,781	2,783	2,781	2,783
12	2,774	2,789	2,784	2,768	2,784
13	2,789	2,763	2,765	2,743	2,765
14	2,789	2,757	2,759	2,749	2,699
15	2,812	2,800	2,802	2,779	2,709
16	2,774	2,829	2,827	2,780	2,342
17	2,789	2,830	2,832	2,775	2,501
18	2,789	2,801	2,805	2,754	2,492
19	2,812	2,812	2,815	2,754	2,504

Year	May Loads measured flows	January Loads measured flows	January Loads synthetic flows		
			Best sequence	Average sequence	Worst sequence
20	2,774	2,798	2,795	2,730	2,795
21	2,789	2,785	2,788	2,747	2,788
22	2,789	2,796	2,798	2,761	2,798
23	2,804	2,810	2,820	2,755	2,648
24	2,774	2,797	2,792	2,716	2,492
25	2,789	2,776	2,778	2,700	2,338
26	2,789	2,783	2,784	2,720	2,695
27	2,812	2,785	2,787	2,712	2,634
28	2,773	2,789	2,783	2,709	2,214
29	2,789	2,779	2,782	2,703	2,458
30	2,788	2,779	2,781	2,713	2,781
31	2,816	2,787	2,782	2,705	2,507
32	2,768	2,785	2,780	2,703	2,279
33	2,779	2,777	2,769	2,687	2,242

The results of the synthetic flow series analysis are presented in a series of tables and charts that follow on the basis of the percentage of time a value is exceeded. The aim is to reduce the volume of data produced by the model and to make clear the trends that are coming out of the model.

Figure 18-5 shows the reliability of generation over the life of the scheme. The analysis is divided into five bands of years:

- Year 1
- Year 5 to 10
- Years 11 to 20
- Years 21–33
- Years 1–33.

It is not possible to produce data simply for Years 2 to 3. The reason is that the first day of the generation sequence is the first time power is supplied to the FRCGP. The export grid supply has to wait for the reservoir to reach a level where generation can commence for the export grid. The amount of the delay varies by more than a year from the shortest to the longest sequence generation to reach the required level. This affects the data for Years 2 and 3 and the start of Year 4 significantly and makes a simple comparison impossible. However, a review of the detail shows that the loads were met over this period with 100% reliability. This has been factored into the values presented for the Years 1–33 summary value. It can be seen that the first year reliability is 99.5% while for Years 2 to 10 it is 100%, owing to the fact that the combined load of the FRCGP and export grid can be met under all inflow sequences in combination with the live storage buffer.

In Years 11–33 it can be seen that the reliability of the generation supply starts to reduce at 40 to 60% exceedance and drops to 94% reliability in the most extreme case with a probability of 1 in 200. This corresponds with the mean inflow over the entire flow sequence approaching the mean inflow over all values in the synthetic flow series of 223.3 m³/s.

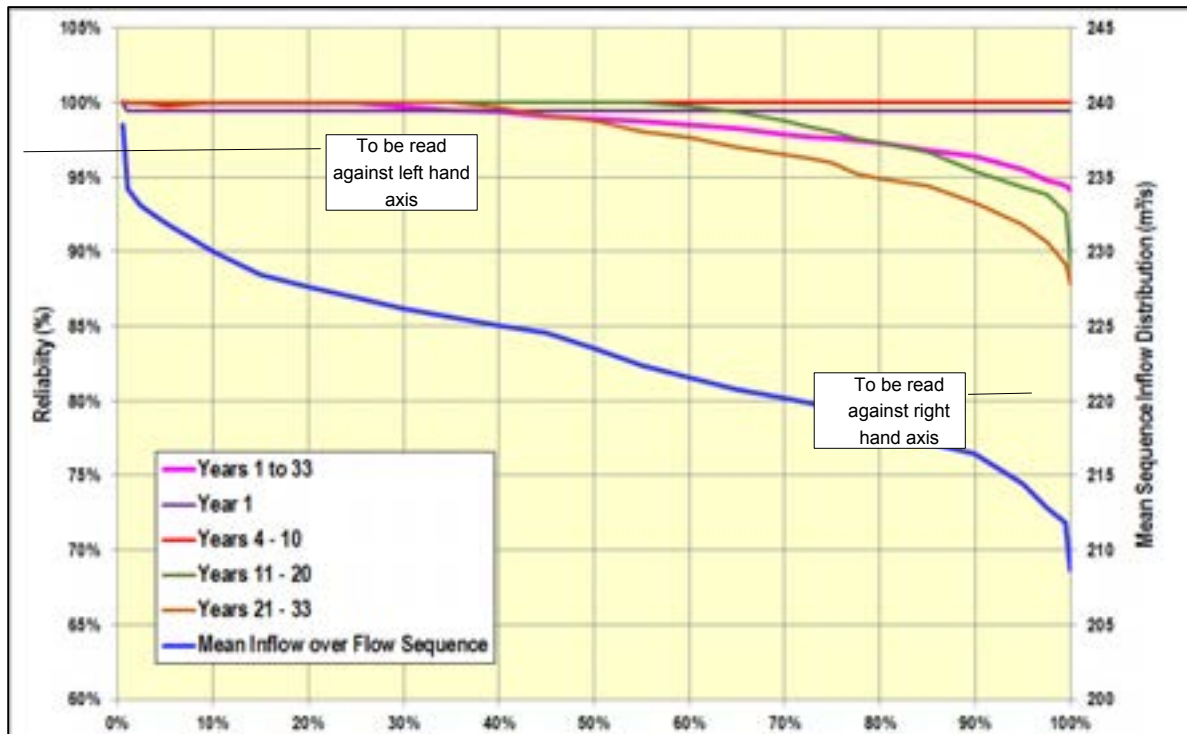


Figure 18-5: Generation reliability in different years

The long term reliability of the sixteen measured flow projections can be seen in Figure 18-5. The long term reliability is 99.58% overall and 98.99% for the worst flow sequence. The reliability of supply to the FRCGP is 100%. With the synthetic flow series, the reliability of supply to the FRCGP is 100%. However, the overall value starts to reduce at flow exceedances of 40 to 60%, depending on the year being looked at. In the worst event it reaches 94.13% with 200-year return periods. The overall average is 98.52%. This is summarised in the Table 18-5 below. The table shows data for both the water reliability and the generation plant reliability, the latter information is derived from the information in Section 15.4.3. It can be seen overall the reliability from the synthetic flow series is 1% less than from the measured flow series. In Years 11–33 when the load is at a maximum, the reliability using the synthetic data is down from 99.97% to 98.06%, almost 2% less. In the worst flow sequence for the two data sources the difference is more extreme – 99.81% and 92.30% for the measured and synthetic flow series respectively. However, this is still an extremely high level of reliability for a hydroelectric power scheme for a 1 in 200-year event.

Table 18-5: Reliability of generation using the measured and synthetic flow series (January electrical load)

Reliability measure	Measured series inflows	Synthetic series inflows	Measured series inflows	Synthetic series inflows
Water supply reliability measure	Years 1–33 (All years)		Years 11–33 (Peak demand years)	
Average over all sequences	99.97%	98.52%	99.96%	98.06%
Worst sequence	99.81%	94.13%	99.74%	92.30%
Reliability of supply to the FRCGP	100.00%	100.00%	100.00%	100.00%
Generation reliability measure	Generation reliability Years 1–33 (All years)		Generation reliability Years 11–33 (Peak demand years)	
Generating plant reliability at peak load + a spinning reserve unit	99.98%		98.71%	
Generating plant reliability at normal load + a spinning reserve unit	100.00%		99.98%	
Overall plant reliability at all loads + a spinning reserve unit	100.00%		99.96%	

Table 18-6 shows the same information but compares the reliability results using modelled data for the January and May Electrical Load profiles. Information for the May Electrical Loads analysed using the synthetic flow series is not be available for this study phase.

Table 18-6: Comparison of reliability in meeting the January and May electrical load profiles

Flow Sequence	January Loads*	May Loads*	January Loads*	May Loads*
Water supply reliability measure	Years 1–33 (All years)		Years 11–33 (Peak demand years)	
Average over all sequences	99.97%	99.97%	99.96%	99.97%
Worst sequence	99.81%	99.86%	99.74%	99.82%
Reliability of supply to the FRCGP	100.00%	100.00%	100.00%	100.00%
Generation reliability measure	Generation reliability Years 1–33 (All years)		Generation reliability Years 11–33 (Peak demand years)	
Generating plant reliability at peak load + a spinning reserve unit	99.98%		98.71%	
Generating plant reliability at normal load + a spinning reserve unit	100.00%		99.98%	
Overall plant reliability at all loads + a spinning reserve unit	100.00%		99.96%	

Note: * = Using measured series inflows over 16 sequences

As can be seen there is very little difference between the reliability of the two load profiles even though the maximum energy generation is maintained throughout the years with the May loads and the firm supply to the FRCGP is 15% higher.

The trend of falling reliability for the synthetic series is expected. However, the point at which the reliability starts to reduce is slightly unexpected. The more accurate synthetic Water Balance and Energy Model produces slightly more power than the measured series Water Balance and Energy

Model. The difference is small but is between 0.1% and 0.5%. This may seem insignificant. However, during sustained periods of low inflows, this difference is important because the water level rises faster and stays high for longer. This improves the head and as a result there are times when the water required for a given output can exceed 5% as a result. The solution to obtaining the required reliability seems to lie in the differences between synthetic and measured flow series.

Both series have a similar mean flow. However, there are more extreme events in the synthetic series with sustained periods of high inflows and sustained periods of very low inflows. This was noted in the comparison of the series in Section 7.3 and shown in Figure 7-5 and Figure 7-6 for periods of up to one year. However, the issue extends to even longer events. Figure 18-6 compares the average inflows, maximum and minimum over periods of up to 16 years for the measured flow series and 24 years for the synthetic flow series. The driest one-year period in the measured flow series occurred over 1996/97 when the inflow averaged 144 m³/s. This is almost certainly the lowest inflow since 1981 when flow measurements commenced on the Frieda River. A comparison between the NOAA El Nino Index confirms this and also suggests that it may have been the lowest inflow since 1871, although a few other years may have been similar. The synthetic series has significantly drier periods – flows equivalent to the 1996/97 event last 3 years in the synthetic series.

The net effect of these very long dry periods is to drain the live storage allowance which is 42.5% of the annual long term inflow to the reservoir. Years of low flows simply drain the live storage and mean the level does not recover as fast as normal, increasing the water use per unit of energy produced. A similar but less sustained effect occurs with very high inflows. The reservoir spill in the synthetic flow series is greater because the peak inflows are higher and there is insufficient live storage to take advantage of this. Trying to run the load dispatch more aggressively to capture these high inflows means using more water on average and risking longer periods when the generation capacity is restricted.

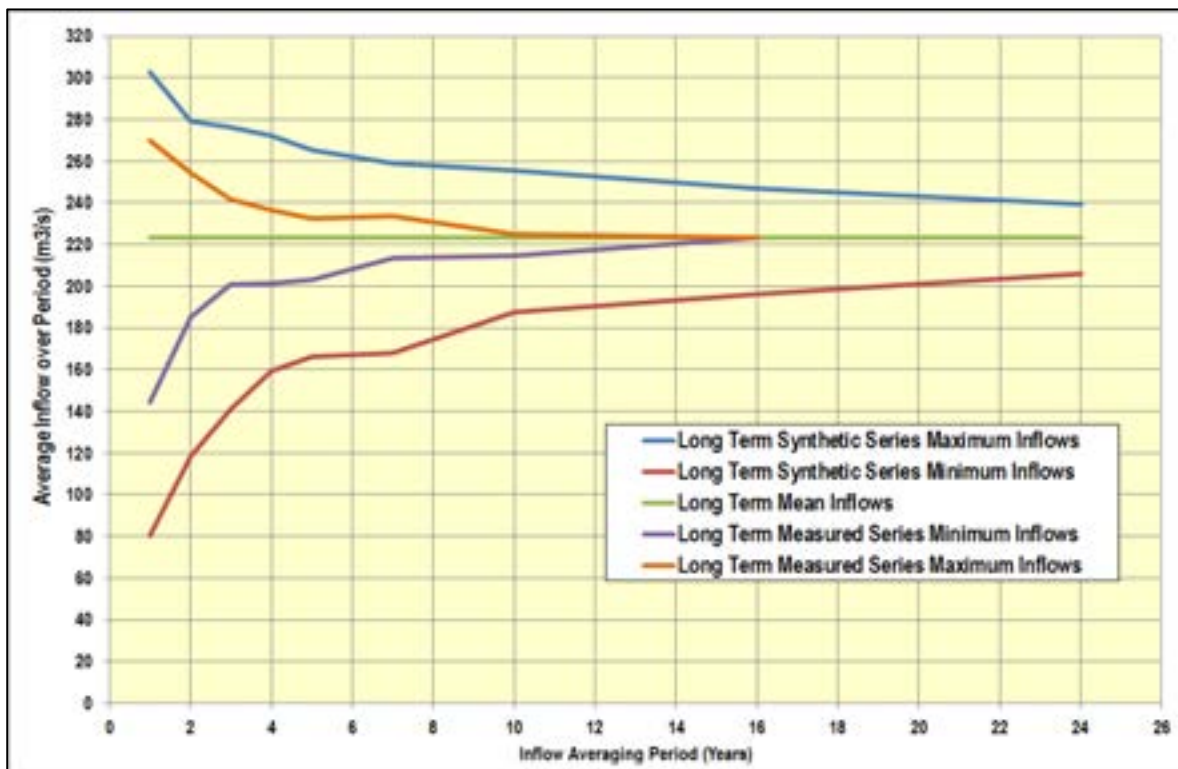


Figure 18-6: Very long term inflows to the reservoir in the measured and synthetic flow series

The extent of the spillway flows in the synthetic series is seen in Figure 18-7. It does suggest that the extra water could be used to generate power at a lower reliability. A review of the analysis details shows that an average spill of 4.9% of the total inflow with the measured flows is likely to maximise generation overall by balancing the risk of spill with high head and greater water to wire efficiency. In the synthetic flow series this point is 6.5% of the total inflow.

Figure 18-8 shows the potential additional annual generation that is possible by reducing the spillway flows. Figure 18-9 shows the total annual generation if the spillway flow is utilised. As can be seen the additional generation potential could be as much as 195 GWh/a with the annual total reaching 2,986 GWh/a in the best year. However, the average boost is 30 GWh/a to 2,767 GWh/a in total from 2,737 GWh/a. The additional power is available for supply to the export grid. Over the 200 years modelled the supply to the export grid could vary from 792 to 1,192 GWh/a with a mean of 973 GWh/a over the years of peak FRCGP demand from Years 11–33. By comparison the measured flow series generation is 2,790 GWh/a over the period of maximum demand from Years 11–33.

As noted previously this does mean a potential shortfall in power supplied to the export grid, given that the full needs if the FRCGP are met without restriction. The measured flow series determined that 996 GWh/a could be made available to the export grid at a reliability in excess of 99.5%. The synthetic series reduces this. The average supply to the export grid is 943 GWh/a and 973 GWh/a if the enhanced generation is considered. The amount of power available at 99.5% reliability is 2,587 GWh/a in total making 793 GWh/a available to the remote grid. This information is presented in Table 18-7.

Table 18-7: Predicted generation from the measured and synthetic flow series (January loads)

Case	Generation potential	
	Measured series inflows (GWh/a)	Synthetic series inflows (GWh/a)
Average generation over peak demand Year 11–33	2,790	2,737
Generation to FRCGP in all cases	1,794	1,794
Average generation to export grid	966	943
Total generation at 99.5% reliability	2,790	2,587
Total generation to export grid at 99.5% reliability	996	793
Total 'firm power' generation at 95% reliability	2,790	2,627
Total 'firm power' generation to export grid at 95% reliability	996	833

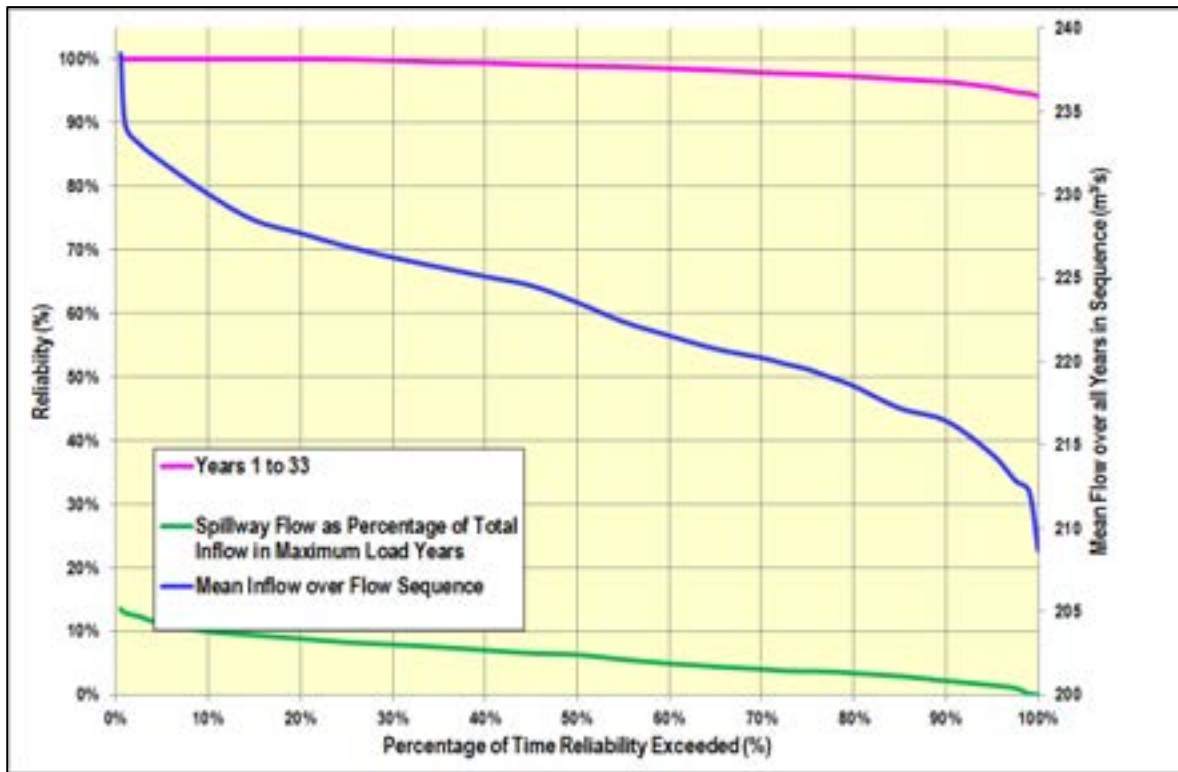


Figure 18-7: Generation reliability, inflow and spill

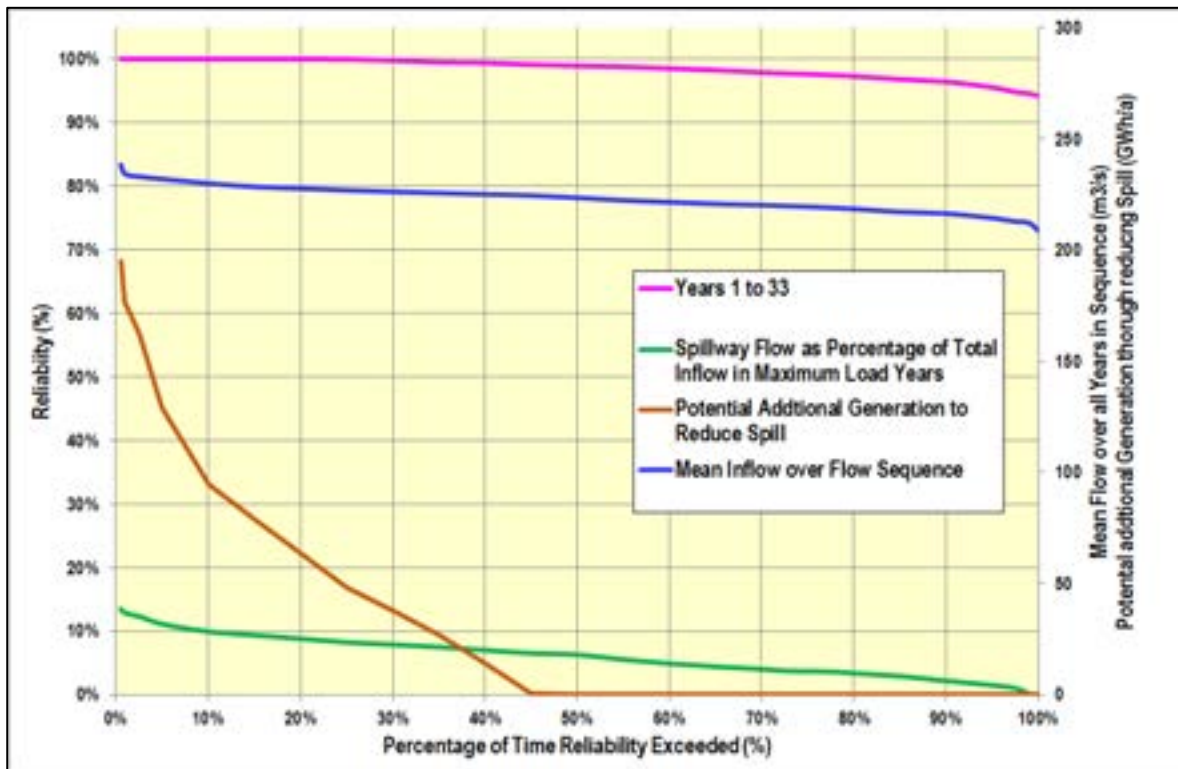


Figure 18-8: Potential additional generation by reducing spill in wet years

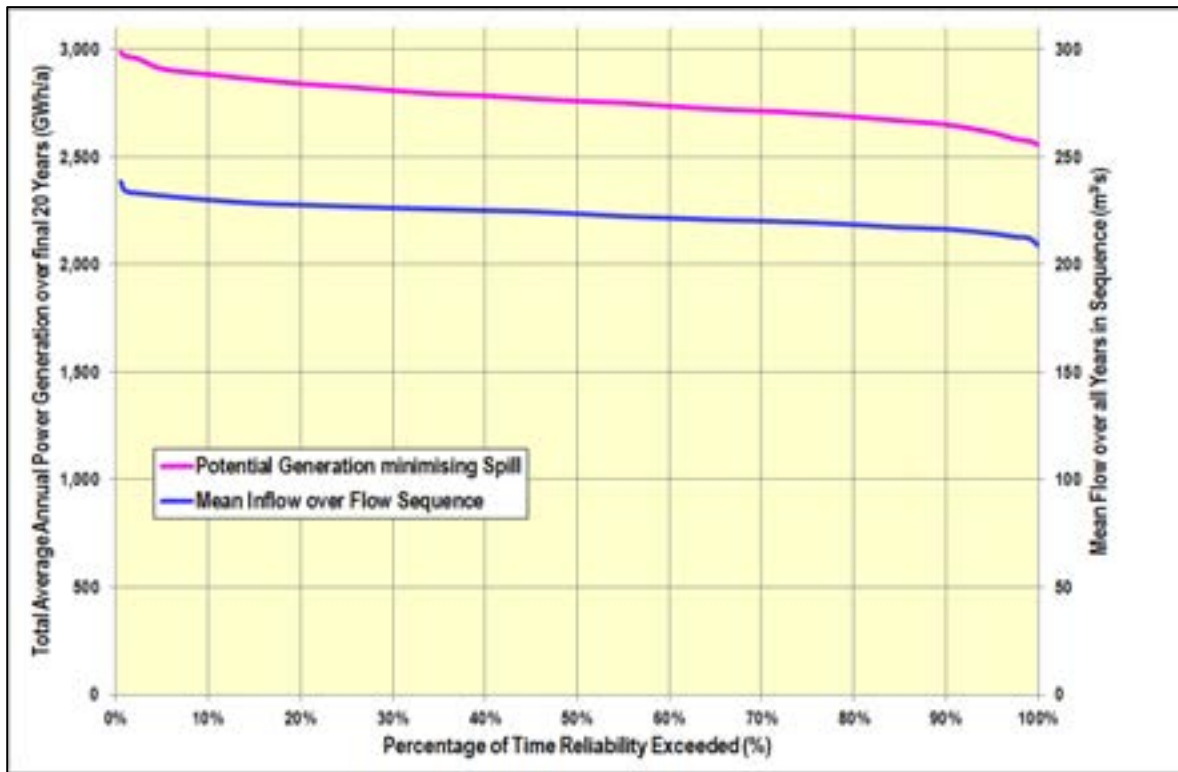


Figure 18-9: Comparison of total generation potential and mean inflow

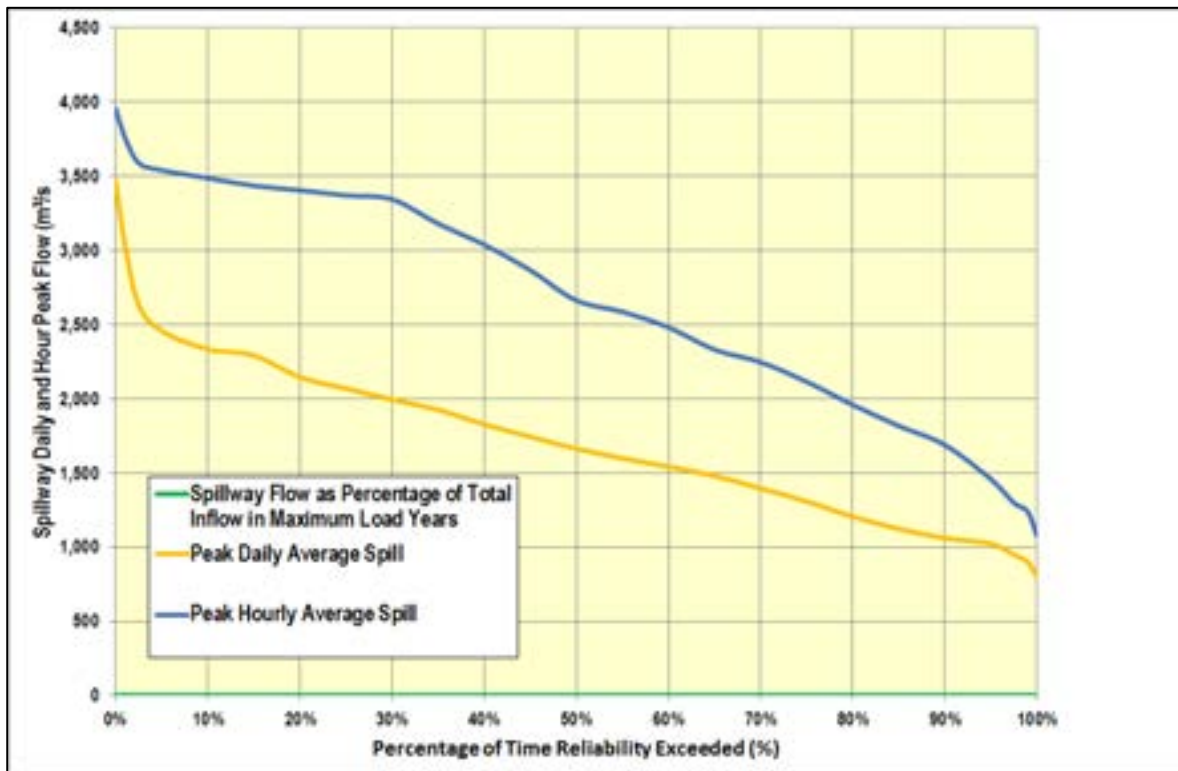


Figure 18-10: Peak hourly and daily spillway flows over the 33 years modelled

19 Operations and Closure

This section discusses the operational and closure requirements of the FRHEP. The FRHEP will require a site-specific and ongoing stewardship program committed during construction and operation that must be continued in perpetuity. Closure and post-closure management and maintenance requirements have been considered for both temporary and permanent closure scenarios.

19.1 Operations

19.1.1 Stewardship

The combination of hydroelectric power supply and storage of tailings and waste in the impounded reservoir makes the FRHEP a unique project. Therefore, the construction, operation and closure of the facility will require a level of stewardship exceeding that which is implemented elsewhere. The stewardship program must address the responsibility of normal hydroelectric dam safety standards while also providing a management/ oversight structure for tailings and waste from the mine operations and downstream water quality and should be developed as part of further studies.

Key components of that stewardship can therefore be separated into two main components, the hydroelectric dam safety program, and tailings and waste disposal oversight, both with associated corporate systems.

A detailed stewardship program can be developed once there is better understanding of the stakeholders involved in the FRHEP. At this stage, it is understood that these entities will include:

- The PNG Government
- The owner of the FRHEP
- The owner of the FRCGP.

The owner of the FRHEP will ultimately remain responsible for the reservoir, including water quality and material stored within the reservoir. The FRCGP operators will need to comply with the standards set by the FRHEP owner.

The SPS study identified several risks that are important for the development of the stewardship program. It is evident from the risk assessment that diligent commercial structuring will play an important role to secure the required roles and responsibilities. Third party, independent oversight is also highly recommended and should continue throughout the life of the FRHEP.

19.1.2 Dam safety program

Dam safety programs are described by the International Commission on Large Dams (ICOLD) and most of its associated national organisations, including the Australian National Committee on Large Dams (ANCOLD) and the Canadian Dam Association (CDA). The Mining Association of Canada has produced similar guidance specific to tailings dams which is still considered to be the industry standard. Table 19-1 provides references to the most relevant international, national and industry guidance documents.

Table 19-1: Dam safety guidance documents

Source	Document
ANCOLD	Guidelines on Dam Safety Management (2003) Guidelines for Tailings Dams – Planning, Construction, Design, Operation, and Closure (2012)
Canadian Dam Association	Dam Safety Guidelines issued 2007, (revised 2013) Technical Bulletin – Application of Dam Safety Guidelines to Mining Dams (2014)
Mining Association of Canada	A Guide to the Management of Tailings Facilities Second Edition (2011) Developing an Operating, Maintenance and Surveillance Manual for Tailings and Water Management Facilities (2011) A Guide to the Audit and Assessment of Tailings Facilities (2011)
ICOLD	Bulletin 158 – Dam Surveillance Guide (2015) Bulletin 154 – Dam Safety Management: Operational Phases of the Dam Life Cycle Bulletin 139 – Improving Tailings Dam Safety – Critical Aspects of management, Design, Operations and Closure (2011) Bulletin 59 – Dam Safety Guidelines (1987)

Design of the hydroelectric dam safety program should incorporate the integrity, operational management and monitoring of the hydro intakes, gates, surge chamber, tunnel drainage systems and the turbine inlet valves. Design of the tailings and waste safety program should include the tailings and waste disposal schedule, barge and pipeline operations, exclusion zones and depositional management zones.

Figure 19-1 shows the typical components of dam safety programs. Policy is the link between the dam safety program, corporate policies, local regulations and industry guidance.

Planning requires identification of roles and execution responsibilities, including objectives, standards, procedures, resources and schedules.

Implementation includes operational and financial controls, construction management, operations, maintenance, and emergency preparedness.

Monitoring and Evaluation includes regular or daily surveillance, inspection and review activities, as well as risk identification and evaluation, and risk management systems.

Audit, Review and Reporting includes formal reviews and reports on an annual or less frequent basis.

Continuous Improvement includes corrective actions as well as reporting to executive officers.

Supporting Processes occur throughout the safety program and include training programs, communication and record keeping.

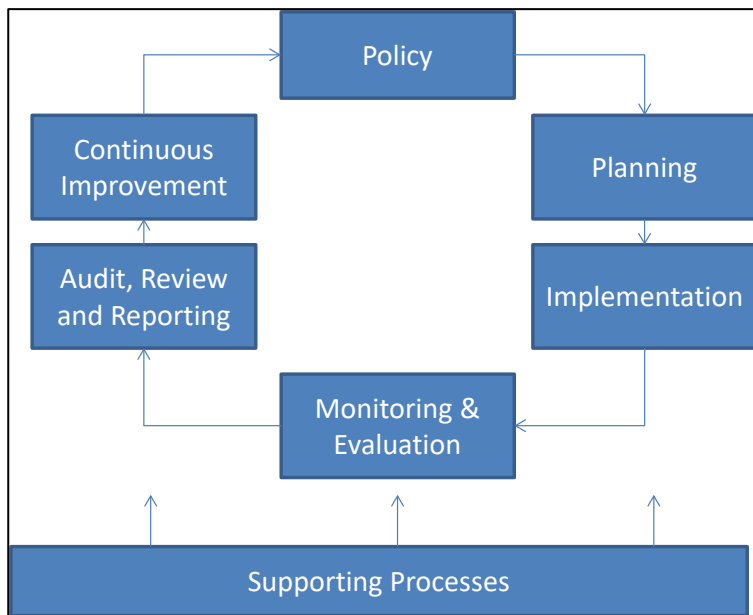


Figure 19-1: Components of a typical dam safety program

Figure 19-1 is a generic summary intended to show common features of the guidance documents. More specific guidance can be found in the sources listed in Table 19-1. Specific requirements common to all guidance documents that should be incorporated include:

- Development of an Operations, Maintenance and Surveillance Manual
- Development of an Emergency Preparedness Manual
- Responsible on-site senior engineers and geotechnical personnel
- Daily inspections by trained operators
- Annual inspections by the Engineer of Record
- Independent Dam Safety Reviews on a predefined interval
- Periodic review by an External Geotechnical Review Boards.

19.1.3 Corporate systems

Stewardship also requires structures of governance and reporting at a higher level than the dam and tailings and waste safety programs. While there is less published guidance on these components of stewardship, there are examples of effective systems in both the hydroelectric power and mining industry. Critical elements include:

- Specific accountability for construction, operation and safety at the Board and senior management and executive levels
- Training at all levels, including senior management, executive and Board, to ensure a full understanding that dam safety is fundamental to the business
- Executive and senior management commitment to ensuring that a dam safety culture is established, monitored and continuously improved
- Clear management accountabilities, reporting relationships and business systems that make dam safety part of the normal work flow and reward systems
- At the Corporate and site level, a clear understanding of post-mining scenarios to ensure long term management of dam safety for the hydroelectric power plant
- A clear understanding of management systems and the risks involved.

At the site level, specific requirements include:

- Clear accountabilities and reporting relationships among site staff
- Well-established procedures for engineering, construction, QA/QC, operations and maintenance
- Well-qualified construction contractors working under clear lines of oversight and communication
- Adequately trained and supported staff
- Coordination of tailings and waste management systems, staff and oversight with water and environmental management systems, staff and oversight.

The above lists highlight key factors and are not intended to be comprehensive. Stewardship requirements specific to the FRHEP dam and tailings and management safety programs and corporate systems will need to be developed during future study phases and once management, corporate and regulatory stakeholders have been defined.

19.1.4 Proposed role definitions

Figure 19-2 shows an illustrative organisational chart for FRHEP stewardship. It is recognised that the actual organisational chart will vary depending on personnel capabilities, but the intention here is to show key roles and how they should relate to company, site management and external organisations.

The most critical roles for the dam safety will be the FRHEP Manager and the Engineer of Record (EOR). They may also be the same individual. The roles of the FRHEP Manager and the EOR should be clearly defined in the Operation, Maintenance and Surveillance (OMS) Manual, to be reviewed annually at a minimum or with any changes to roles or individuals.

The FRHEP Manager will be ultimately responsible for all day-to day hydroelectric power generation and dam safety operations of FRHEP and planning activities associated with tailings and mine waste disposal within the reservoir. All functional leads at the FRHEP will report to the FRHEP Manager. The FRHEP Manager should ideally be independent due to the complexity of the FRHEP, its relationship to multiple activates and the Extreme risk of dam failure¹⁰³. Tailings and mine waste disposal activities would fall under the FRCGP.

The overarching responsibility of the EOR is to determine if the FRHEP meets applicable regulations, guidelines and standards. To execute this responsibility, the EOR should be completely familiar with the design, history and current conditions of the dam. Where the EOR is also the designer of record, involved through construction and operations, this knowledge would be implicit in the design, as-built, monitoring and inspection reports. If the EOR is not the designer, or is not present during construction and operations, this knowledge needs to be built through a comprehensive and detailed design and performance dam safety review (guidelines for such reviews are being established by, among others, the Canadian Dam Safety Association). Given the complexity of the FRHEP, the EOR will need to rely on other qualified professional engineers to provide assurances of ancillary facilities related to the hydroelectric power structures, including the diversion and spillway structures. Other qualified professionals will need to provide assurances related to water management, tailings and waste stability, waste geochemistry and water quality.

The EOR needs to be supported by a team that has the necessary range of technical expertise and the capability to provide for succession. This means that the EOR may be an employee of an engineering consultancy, and any in-house expertise resides in the position of Corporate FRHEP

¹⁰³ SRK 2018, Frieda River HEP SPS Design- Dam Break Assessment, Document number PNA009_Frieda River HEP SPS Design - Dam Break Assessment_Rev0

Manager. The responsibilities of the Corporate FRHEP Manager should include reviews and assurances that FRHEP management systems are in place and functioning properly, as well as providing technical advice and support.

External parties that will also play important roles in the FRHEP stewardship are shown on the right side of Figure 19-2. A Dam Safety Inspector, independent of the EOR and Design Team, must carry out regular inspections according to specifications documented in the guidelines cited above. A Technical Review Board, comprised of highly experienced technical experts familiar with the dam history, will provide independent technical advice to the FRHEP Manager and EOR. To preserve the independence of the Technical Review Board, they should report to one or more corporate Directors.

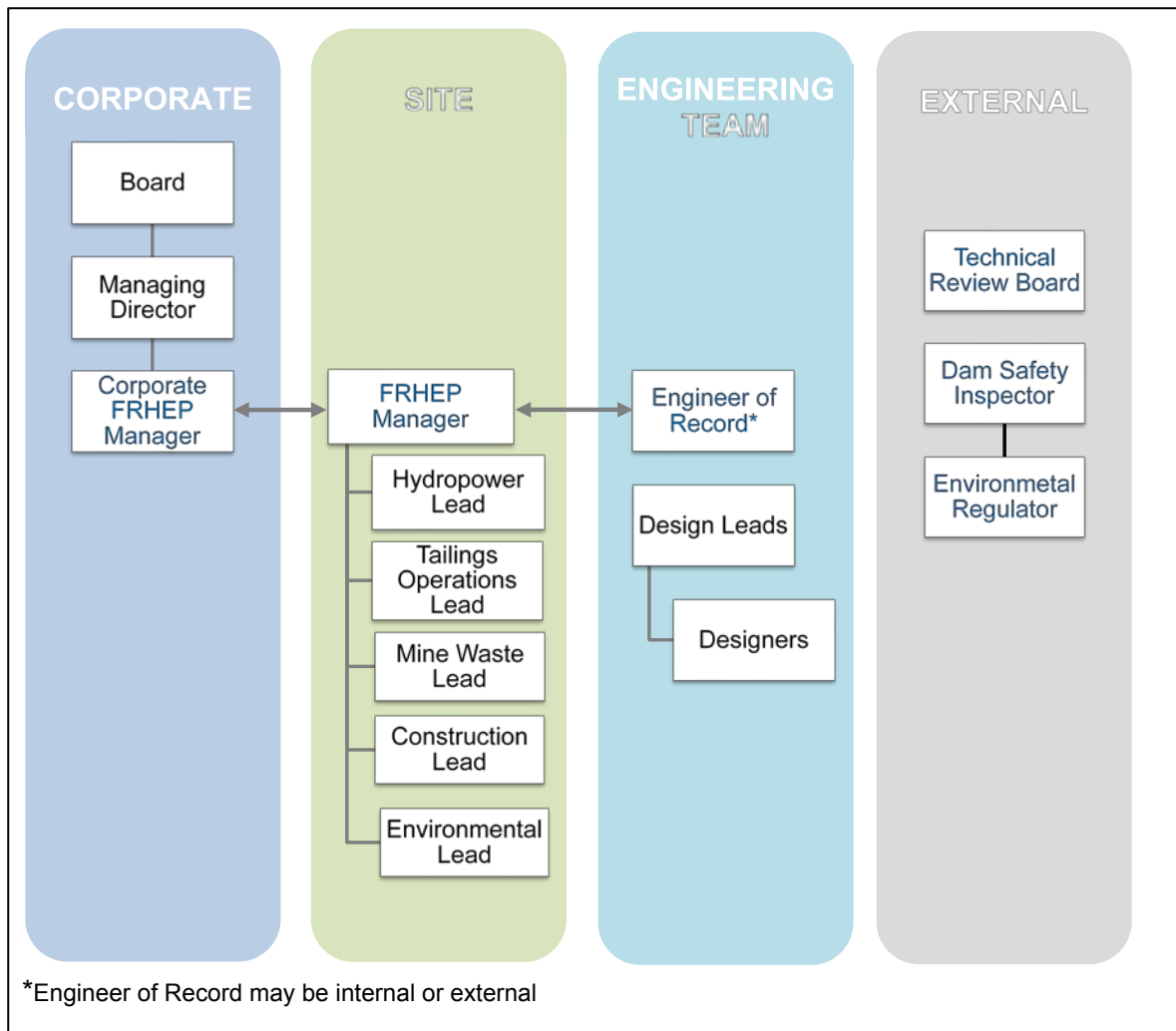


Figure 19-2: Organisation chart for FRHEP stewardship

19.2 Tailings and waste rock disposal

The risks associated with tailings and waste disposal are such that tailings and waste deposition and storage deserves equal attention to power generation. The following section describes the deposition strategy that has been developed, taking into account water quality, the results of the limnology study, sediment transport, potential risks associated with tsunami type wave generation due to failure of underwater spoil mounds, stratification within the reservoir resulting in a deeper anoxic zone, early filling of the reservoir, operational sequencing, critical levels for operational control, proximity of the embankment intake structures and preferred methods of deposition.

Tailings will be pumped as a slurry via floating pipelines on the surface of the reservoir, and primary crushed waste rock will be dumped by barge.

The following section outlines the tailings and waste deposition stages and locations, pipeline routes, proposed deposition methods and supporting operational limitations.

Key critical levels for control of the FRHEP, including control levels related to early filling of the reservoir, were incorporated in the embankment design and forms the basis of this assessment (Figure 8-1).

19.2.1 Objectives

The objectives of the tailings and waste deposition strategy are summarised as follows:

- To reduce and/ or delay capital and operational expenditure where practically possible
- To limit the tailings and waste management risk by simplifying the operational demands
- To mitigate the environmental risks associated with the deposition and storage of tailings and waste within the reservoir; chemical and total suspended solids (TSS) limits are to comply with environmental guidelines for water quality within the reservoir and downstream of the embankment
- To build sufficient contingency in the design to accommodate acceptable levels of change
- To maximise the use of available storage capacity
- To allocate storage capacity for operational and maintenance requirements, including an emergency tailings compartment for unforeseen circumstances such as pump breakdowns and allocated space close to the processing plant for waste storage due to unforeseen circumstances such as diesel shortages or a reduction in operatable barge numbers that limits cycle times and distances
- To limit the exposure of tailings and waste within the oxidizing zone, to minimise the risk of metals leaching
- To maintain sufficient water cover over the tailings and waste, to prevent the formation of acid
- To limit the risk of re-suspension of tailings, waste and sediments to manage environmental and operational risks
- To restrict the tailings and waste deposition to specific levels proximal to the embankment, reducing the risk of particles being sucked into the hydroelectric conveyance system and resulting in excessive wear to the hydroelectric equipment; this level was limited to RL 180 m
- To minimise the potential impact of underwater spoil mound failures and landslides on the facility, stored tailings and waste and the operation, and identify appropriate measures to mitigate the associated risks

The following section highlights key considerations and assumptions:

- The LOM is 33 years.
- Production profiles as detailed in the basis of design – these profiles were used as the basis for determining capacity requirements.
- The waste dry density value is 1.5 t/m³ – SRK has assumed this parameter based on previous experience at Frieda River.
- The tailings dry density remains unchanged from previous studies and varies between 1.1 t/m³ and 1.4 t/m³.
- As specific flow rates throughout the reservoir and how they affect beaching angles are unknown and are likely to be variable due to significantly different catchment characteristics and seasonal

climatic changes, it is likely that the associated tailings particle settlement characteristics will be affected. A beaching angle of 1% has been selected for the tailings spoil face.

- FRL indicated that the waste will undergo single-stage gyratory crushing and be transported by conveyor from the mine to the barge-loading facility.
- FRL has provisionally indicated that 5,000 t (2,300 m³) barges will be used with dimensions of 80 m × 16 m.
- Barges will be stationary during dumping. Dumping will be completed before recommencing the next trip.
- The barge travel speed is approximately 8–10 knots.
- The subaqueous natural angle of repose of the dumped waste could reach 30°–40°.
- Due to the typical flat beaching characteristics of the fines, it can be expected that the fraction of the fines not trapped within the tailings and waste mass will run out to the far reaches of the reservoir. This has not been modelled, as the exact configuration is unknown.
- To inform the volumetric modelling for the FRHEP, it has been assumed that the sediment contribution to the reservoir will be evenly distributed as a blended mass within the tailings and waste.
- The combined tailings and sediment storage requirement at the earlier defined range of dry densities is 1.11 Bm³.
- The combined waste and sediment storage requirement at a waste dry density of 1.5 t/m³ is 1.06 Bm³.
- Waste is classified in three categories relating to density, size and settling characteristics – hard, medium and soft
- Additional space has been allocated to storage compartments adjacent to the processing plant to provide options for deposition should unforeseen circumstances require a reduction of barging and piping distances. These have capacity for two years of deposition – 65.1 Mm³ of blended tailings and sediment, and 62.3 Mm³ of blended waste and sediment.
- Assuming the levels permit, the emergency tailings compartment may be designed (by others) to allow deposition by gravity feed should pumps fail or power outages occur during operations.
- The tailings grading remains unchanged from previous studies – however, the waste crushing methodology and waste particle size distribution have changed. While the grading curve has not yet been supplied, SRK has been informed that the particles will be smaller than 300 mm.

Once early filling commences, the reservoir's water level is predicted to rise at the rates shown in Figure 19-3. The lines represent various rates of water level rise developed from a series of historical rainfall periods.

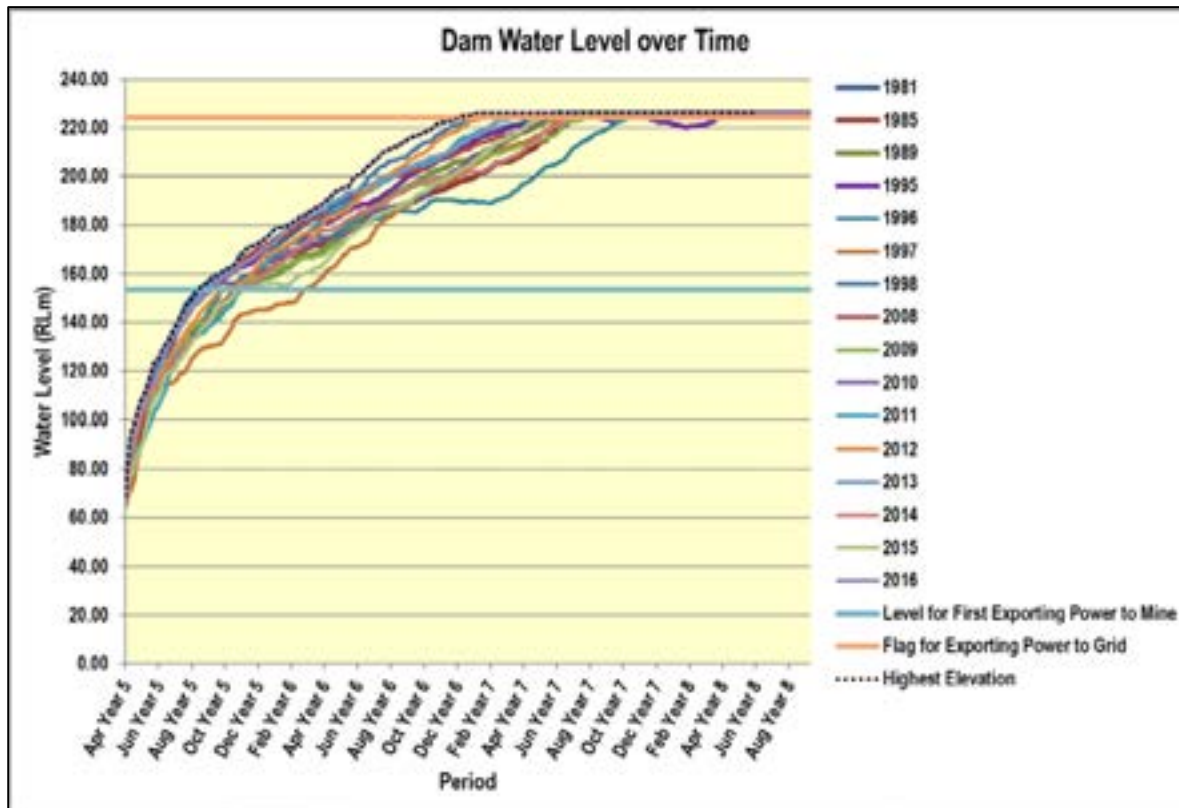


Figure 19-3: Rates of reservoir water level rise during early filling

19.2.2 Limnology and geochemistry

The detailed 3D limnology model developed during the SPS¹⁰⁴ indicates that the reservoir is likely to be stratified, with an anoxic zone in the deeper metalimnion and hypolimnion strata (Figure 19-4 for a simplified representation of the expected stratification). Further refinement of this model will be undertaken in future study phases.

The layers are typically representative of the following:

- Epilimnion: upper, well-mixed and least-dense layer in a stratified lake or reservoir, occurring above the metalimnion and deeper hypolimnion. For the FRHEP operating at RL 226 m, the stratification consists of a warm, mixed epilimnion above ~RL 215 m.
- Metalimnion: layer in which density changes more rapidly with depth than it does in the layers above (epilimnion) or below (hypolimnion). The metalimnion in the FRHEP during operation extends below the epilimnion to ~RL 160 m, with steps in the density gradient created by the hydroelectric operation.
- Hypolimnion: most dense, weakly stratified and often quiescent bottom layer of water beneath the metalimnion of a stratified lake or reservoir. During operations the FRHEP hypolimnion occurs below ~RL 160 m.

The limnology study estimates the interface of the epilimnion and metalimnion is expected to occur at approximately 40 m below the minimum operating level; RL 159.4 m. Reservoir conditions below this level are expected to be more stable with less current activity and movement of water.

¹⁰⁴ HydroNumerics 2018,

Generation of acid occurs from oxidation of potentially acid forming material. The risk of oxidation is significantly limited by deposition of tailings and waste below the cover of water.

The geochemical assessment of the tailings and waste indicates that an oxidising environment will exacerbate release of metals from the tailings and waste. The limnology and water quality review therefore recommends that the duration of exposure of the active tailings and waste must be minimised to avoid excessive levels of metal leaching.

The re-suspension of tailings and waste must also be limited to prevent potential transport of the tailings and mine waste through the FRHEP intake structures and spillway and further downstream. Deposition of finer material by barge dumping near the embankment increases the risk of fines being transported through the FRHEP intake structures. To this end, dumping must not occur within 1 km of the embankment and restrictions regarding the type of material deposited in proximity to the embankment must be applied. Hard waste material is to be dumped a minimum of 1 km from the embankment, and medium and soft materials are to be deposited a minimum of 2 km and 4 km from the embankment respectively.

The limnology study has indicated that inflows may, at times, develop sufficient shear stresses to cause re-suspension of fines deposited in the upper reaches of the Nena and Niar rivers and must therefore be limited or eliminated. The bed shear resistance of the tailings is not well understood and must be studied to better define the risk.

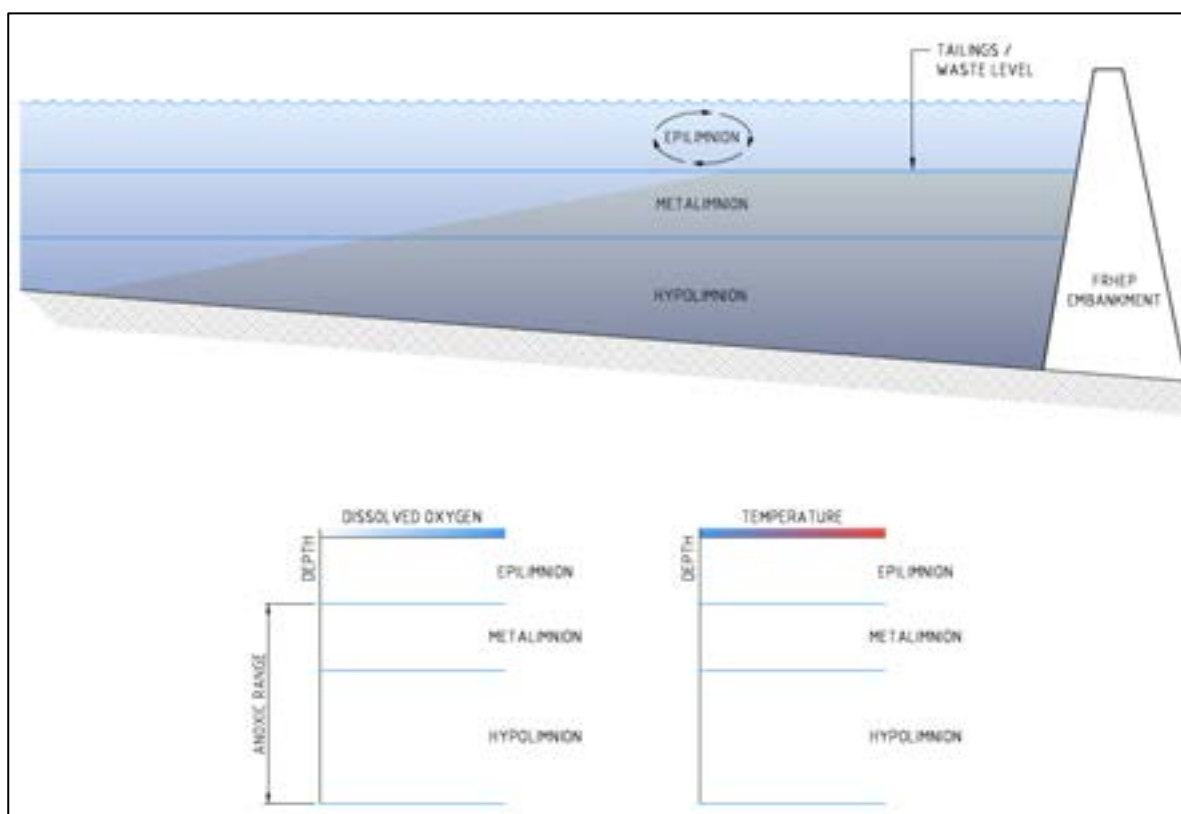


Figure 19-4: Stratification within the reservoir

19.2.3 Capacity

SRK undertook a capacity assessment for the entire basin using Rift TD software, and considering a 0% beach slope. The total available storage capacity of 3.3 Bm³ was determined at the RL 159.4 m control level and represents the maximum available tailings, waste and sediment storage capacity as a function of the reservoir basin profile.

To limit the potential for sediment re-suspension, SRK recommends that deposition within the narrow and shallow valleys and extremities of the reservoir be limited where possible, and notes that deposition at the shallow extremities will not be possible using barges. Based on the assumption that the reservoir's extremities may, as a result, only be partially used and that the tailings will develop a beach steeper than 0% (approximately 1%), the available storage capacity of 3.3 Bm³ will be reduced.

The sediment generation values defined by Golder Associates have been used to estimate the total sediment contribution. The total sediment generation over the LOM was estimated to be 43.6 Mm³ based on a 33-year LOM. For simplicity, the sediment load was equally shared between the tailings and waste to establish individual capacity requirements within the designated compartments of the reservoir. The total combined volume of tailings, waste rock and sediment generation equates to 2.17 Bm³, resulting in approximately 1.1 Bm³ of spare capacity within the reservoir, at RL 159.4 m. Complete utilisation of the available 1.1 Bm³ capacity is unlikely, as reaching extremities of the reservoir and far-reaching valleys will be difficult, and would potentially result in re-suspension of fine particles in the upper Nena and Niar river compartments.

Although SRK does not yet have a comprehensive understanding of the exact behaviour of the finer waste fraction, it is expected that this portion, being a small percentage of the total waste volume, will run out into the reservoir's extremities.

Although the expected tailings beach profiles may vary across the reservoir due to varied flow rates entering the reservoir, it is likely that these beach profiles will be very flat. This will result in some tailings flowing out into the extremities of the reservoir and possibly filling most of the available space at a particular elevation. This may result in the final upper level of the tailings not reaching RL 159.4 m. The potential lowest possible upper level of the tailings mass could be at RL 135 m, assuming a 0% beaching angle and that the entire footprint of the Frieda compartment is reached. The upper reaches of the Niar and Nena rivers will experience large inflows, which will increase the risk of re-suspension of tailings during high inflow conditions.

19.2.4 Mound failure and landslides

Subaqueous mounds and failures

SRK refined a preliminary assessment to determine potential wave sizes that may be generated due to failure of underwater structures. The maximum potential wave amplitude is estimated to be ~5.4 m high, and it is therefore recommended that waste rock and tailings material be deposited at angles to promote stable conditions to mitigate the risk of failure and subsequent wave generation. For the purpose of this assessment, it is assumed that the waste rock material can safely be stockpiled at a slope of 5% and the tailings at a slope of 1%. It is likely that cone formation will continue to occur on a small scale, including slumping during deposition; however, large-scale cone formation and potential failure must be avoided through deposition control.

SRK recommends that a stability assessment be undertaken to define the recommended safe angle, and establish a realistic size for the failure wedge, as a basis for refining the wave size assessment.

Cones will develop at the bottom of the reservoir during tailings and waste rock deposition, resulting in continuous small-scale failures. While such failures cannot be avoided, they are not expected to pose any significant risk to the reservoir. However, large-scale failures must be prevented. Smaller scale failures may induce larger failures, and loads induced during deposition must be considered in the slope stability assessment.

The control of spoil slopes at depth will be difficult, and will require the expertise of trained personnel, suitable control measures and operating protocol.

Subaerial landslide risk

Apart from naturally occurring landslides, reservoir -induced landslides can be expected, especially due to the presence of water and fluctuations in the water level that will promote the occurrence of landslides along the headwaters of the lake.

Landslides into the reservoir will generate waves, resulting in the potential to compromise the integrity of the FRHEP, re-suspend sediment and metals, and introduce additional sediments to the reservoir.

The potential wave size in large-scale landslides could be significantly larger than for the underwater spoil mound failures and is further discussed in Section 11.

The desktop geohazard assessment completed by SRK (Section 3.2) categorised landslides according to geohazard rating and associated risk. Smaller landslides are expected at the headwater of the reservoir, especially in the zone of water fluctuation. Large landslides that would significantly impact the reservoir have also been identified; however, further fieldwork assessment of these landslides would need to be undertaken to either gain a better understanding of the risk, or identify mitigation measures.

19.2.5 Deposition strategy

This section describes the approximate tailings and waste rock deposition locations, staging, and proposed pipeline routes, considering operational activities and other relevant constraints.

Layout and staging

The basis for the following footprint is the maximum permissible waste and tailings elevation, i.e. RL 159.4 m and the expected volumes to be generated during the 33-year mine life. Waste is partially disposed in the lower Ok Binai/ Nena and Frieda compartments, with the Nena River valley almost exclusively used for waste disposal (Figure 19-5). Tailings will predominantly be disposed in the Frieda compartment. A small fraction of tailings is disposed in the upper Ok Binai compartment. This configuration will require a larger fraction of the waste rock to be disposed in the Frieda compartment, resulting in a longer barging distance from the plant.

This strategy limits the risk of potential re-suspension of finer tailings material due to the overhead movement of barges and the associated development of overhead currents.

Waste rock is not designed to fill the extremities of the reservoir due to limited access and area for manoeuvring of barges.

Of the spare capacity that remains below RL 159.4 m, a large fraction is located in the Frieda compartment, with extremities and small valleys unlikely to be filled in this compartment due to their horizontal profiling, distance from the larger reservoir and deposition points that are difficult to reach.

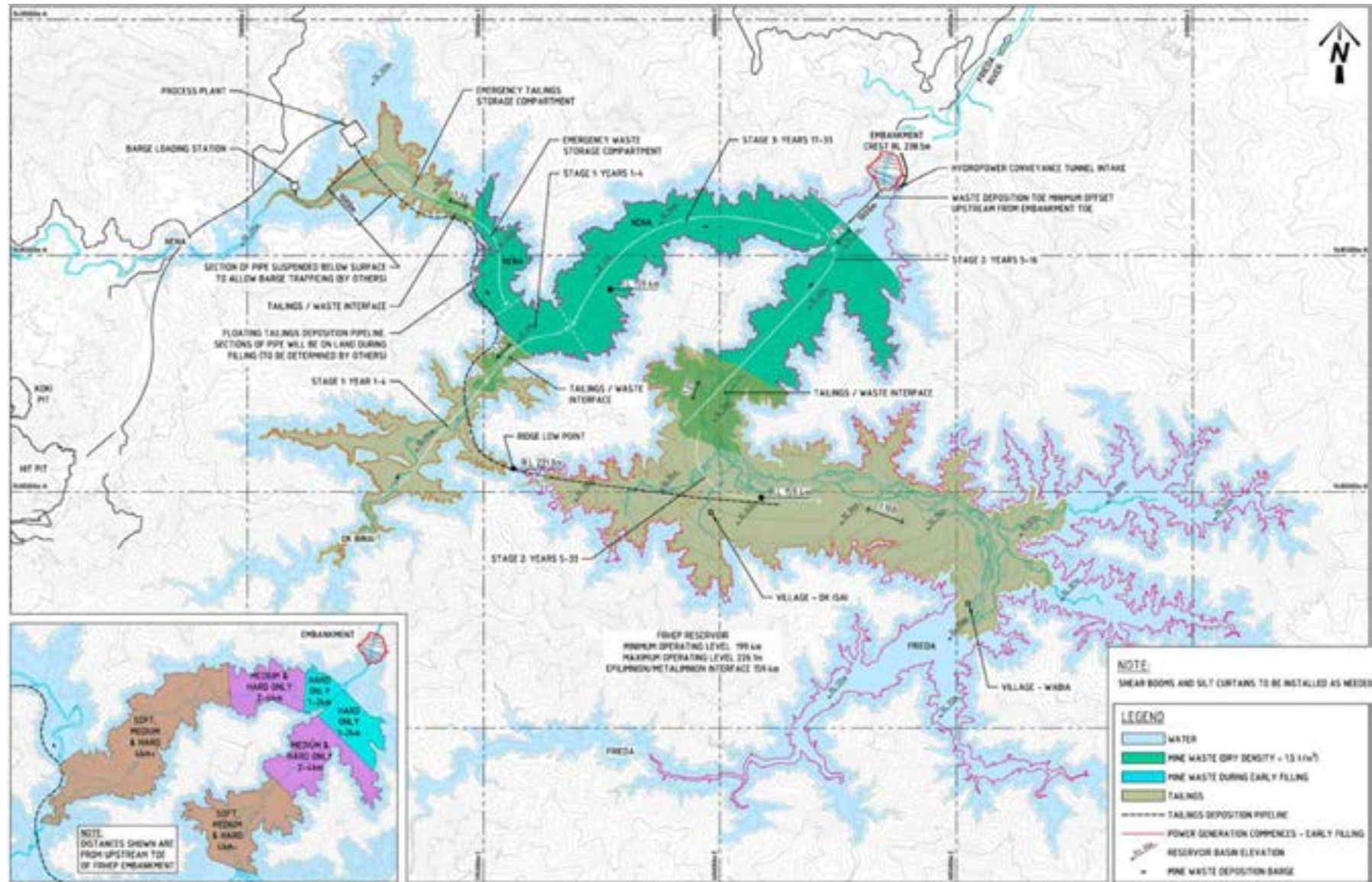


Figure 19-5: Tailings and waste deposition layout assuming a waste density of 1.5 t/m³

The deposition sequence must be controlled whereby tailings deposition is permitted on top of waste, but not vice versa (Figure 19-6). Dumping heavier boulder and gravelly waste material onto pre-deposited tailings will result in significant disturbance and re-suspension of finer tailings particles. The additional load may also induce failure of the tailings spoil mound. The interface between the tailings and waste must be limited where practically possible. The placement of fine-grained tailings over the already-deposited heavier waste mass will require careful management. Bathymetric instrumentation could be used to monitor the subaqueous profiles.

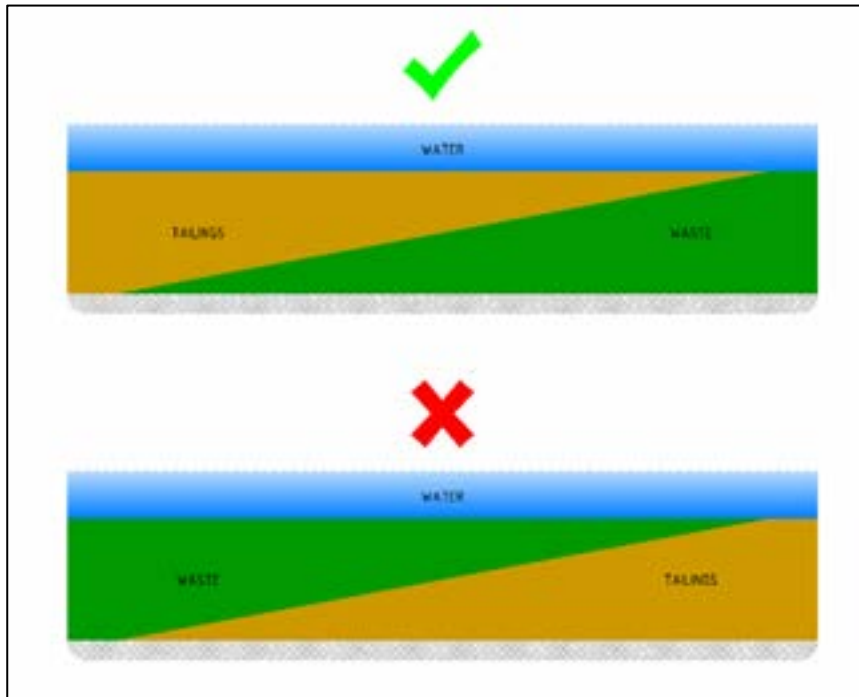


Figure 19-6: Deposition sequence

Unless confined, deposition of tailings will result in material migrating into the waste rock storage compartments. SRK recommends an underwater mound be developed to limit the extent of migrating tailings. Failure to limit the tailings migration into the allocated waste rock storage compartment, will, under the current constraints, require a portion of the waste rock to be deposited into the upper reaches of the Frieda compartment which introduces some logistical risks, including:

- The requirement to barge the waste rock to the far ends of the reservoir
- A potential requirement for additional capital (additional barges)
- A potential increase in operational expenditure (fuel, crews, etc).

Considering the above, SRK recommends developing underwater waste rock toes by early deposition of waste rock where an interface between the tailings and waste rock deposition is anticipated. Tailings can then be deposited adjacent to the exposed outer face of the underwater barrier formed by the waste rock, and allowed to develop upstream away from the embankment. Although the exact subaqueous beach angles have not been validated by laboratory testing, it is likely that the waste rock beaching angle will be higher than the tailings beaching angle. This, in turn, implies that the waste rock spoil will develop vertically at a higher rate of rise compared to the tailings mass, ensuring the barrier is continually progressed ahead of the tailings. An initial spoil barrier will be required at the confluence of the Frieda and Nena/ Lower Ok Binai compartments. An underwater barrier will also be required to separate tailings migration from the emergency compartment and the adjacent waste rock deposition compartment, and to prevent the migration of tailings to the adjacent designated waste rock storage area. This barrier must be developed as and when required, to ensure a division is always

ahead of the top of tailings. When the waste rock material from the pit is fine, especially during early mining activities, the beaching angles may be flat and would not result in any significant barrier development, in which case the waste rock needs to be progressed simultaneously or slightly ahead of the tailings such that the interface between waste rock and tailings prevent the tailings from migrating towards the embankment.

The underwater toe will be developed as part of the planned waste rock deposition, with waste rock being dumped at the anticipated location of the interface between the waste rock and tailings. The waste rock must be dumped at angles not steeper than 5% to promote stable waste rock slope conditions, which serves as a physical spoil barrier to constrain the tailings upstream from the interface. At all times, the underwater spoil barrier along the length of the tailings and waste rock interface must be progressed such that the elevation is always at least a few metres higher than the top of tailings.

As the stability of the underwater waste mass is not yet fully understood, it has been assumed that a 5% slope would provide adequate stability. If the results of further studies reveal that the underwater mound is at an unacceptably high risk of failure, it may be necessary to progressively develop the tailings deposition to buttress the upstream face. This will change the deposition sequence and timing such that waste rock deposition will alternate between different zones. An alternative is to flatten the outer waste rock slopes to suitable angles. A benefit of spreading the tailings and waste rock across a larger footprint during development is the increased time for material to consolidate, resulting in improved material strengths and additional storage capacity.

For FRL's preferred strategy, waste rock will initially be deposited at the confluence of the Nena and Ok Binai rivers, followed by deposition towards the embankment. The underwater barrier between the tailings and waste rock needs to be developed in the Frieda compartment prior to deposition of tailings moving across from the upper Ok Binai compartment. Tailings will then be deposited progressively upstream in the Frieda compartment from the underwater toe. This will result in the tailings and waste rock initially being deposited closer to the plant.

For the purposes of this assessment, the interface between the various stages has been depicted as vertical divisions, and slight variations to the staging are likely to be required following development of a more detailed 3D model.

Risks associated with transport of tailings and waste rock derived sediments through the FRHEP and downstream are increased by deposition into the epilimnion layer, and by deposition of the finer tailings and waste rock material close to the embankment intake structures. The potential risk of finer-grained tailings being deposited on the upstream face of the embankment is the reduction of the embankment's material strength properties. It is therefore recommended that waste material be deposited below the epilimnion layer at a minimum distance of 1 km from the embankment upstream toe, and that material deposited in proximity to the embankment has strict distance limitations based on hardness (SRK Drawing PNA009-0010). To this end, material must be deposited as follows:

- Hard: not closer than 1 km from the upstream toe of the embankment
- Medium: not closer than 2 km from the upstream toe of the embankment
- Soft: not closer than 4 km from the upstream toe of the embankment.

Tailings deposition in the upper reaches of the Nena and Niar rivers must be avoided, as significantly higher shear stresses due to concentrated flows are experienced in these parts of the reservoir. The tailings shear resistance to flow may be exceeded, resulting in particles being resuspended under higher flow conditions.

An alternative to reduce sediment transport through the FRHEP could include implementation of management systems to reduce the intensity of barge deposition near the embankment. Limiting the

frequency of barge dumping close to the embankment would reduce the volume of sediment being transported through the lake.

Although this alternative method will be evaluated as part of future study phases, the initial indicators are that the solution is viable.

Tailings and pipeline pumping

SRK envisages the use of a single pipeline for the tailings stream. A second pipeline could be utilised for redundancy; however, this is not a requirement, as the allocated tailings emergency compartment could be used during periods of downtime on the main pipeline. In this case, the addition of a separate, shorter pipeline would allow tailings deposition in the designated emergency compartment which should be operable by gravity feed, in case of pump failure or power outages during operations. The second pipeline may also be required to allow maintenance activities on the main pipeline to be carried out.

FRL has advised that the pipelines will be floating on the surface of the reservoir. The main pipeline is routed across the surface of the reservoir, via the upper Ok Binai compartment and along an east-west alignment to achieve the shortest practical route to the end of the pipeline in the Frieda compartment.

During filling of the reservoir, the section of pipeline closest to the plant will be supported on land before floating on the surface of the reservoir. Fluctuating water levels will also leave the section of pipeline between the upper Ok Binai and Frieda compartments supported on land. Parts of the pipeline must therefore be designed to be supported on both land and on the reservoir surface; factors such as the time needed for construction and installation can be estimated by the pipeline designer.

The pipeline route was also selected to minimise obstruction of the barge trafficking routes. The main pipeline and barging routes will intersect at a location close to the plant where the pipeline will be submerged below the surface (as advised by FRL) of the reservoir to enable barges to safely pass overhead. Pipeline routes have been located close to the reservoir's shores to maximise space for barge trafficking. However, if pipelines are too close to the shore, the pipeline may be affected by waves in the wave-breaking zone. Pipeline locations therefore need to be reviewed during operations to prevent damage to the pipeline.

To mitigate risks associated with subaqueous spoil mound failure, deposition of tailings must be controlled to limit spoil slopes to less than 1%. The discharge end of the pipeline therefore needs to be regularly manoeuvred both horizontally and vertically to permit control of discharge from the end.

Although diffusers are not an operational requirement, modifications to the discharge section of the pipeline are recommended to prevent cavitation and associated development of air bubbles, which would result in flotation of tailings particles. Bleeding of the air would need to be done before discharging tailings into the reservoir.

Stratification within the reservoir is sensitive to temperature variations and it is necessary to control the slurry temperature before deposition. Energy introduced through the various stages of processing, such as chemical reactions and heat from the sun during pumping across the surface of the reservoir, will increase the slurry temperature that may lead to buoyant plumes that transport fines vertically during deposition. Whilst initially the slurry is likely to be more dense than ambient water due to the TSS load, as the large particles settle a positive buoyancy due to temperature may lead to instability and vertical mixing, dependant on the rate of settling compared to the rate of diffusion of heat. To this end, it is recommended that water from the uppermost layer of the reservoir is introduced to the slurry stream before deposition. Other facilities have implemented a double wall vertical riser system to achieve this. Other alternatives may also be considered, such as methods of reducing the absorption

of energy from the sun, and placement methods at or near the bed of the reservoir, that will be refined during further studies.

The pipeline needs to be anchored or restrained at a reasonable distance from the edge of the reservoir to prevent resting on land due to rising or falling water levels. To facilitate better manoeuvring, it is preferable to have all sections of the pipeline floating at all times. Resting on land will generate unnecessary stresses within the pipeline and result in the requirement for additional pumping capacity across the pipeline which will then have variable grades.

Sacrificial anchors have been recommended to ensure pipelines remain in their intended location and their use should be considered by pipeline designers. Underwater slumping and potential landslides may affect the integrity of the anchors.

Pipe bursts must be considered a risk where uncontrolled discharge of tailings may occur within the epilimnion layer. While the risks are not yet well defined, pipe ratings should be specified, as the use of correctly specified pipes will mitigate the potential risk of failure. The effect of sediment transport due to pipeline failure was not assessed as part of the SPS and must be studied during future study phases.

During filling, the pipeline section closest to the plant will be supported on land before floating on the surface of the reservoir. The affected section of pipe is dependent on various factors, including the time needed for construction and installation, and can be estimated by the pipeline designer.

Additional risks to the integrity of pipelines floating on the reservoir include the potential for wave development (discussed in Section 19.2.3). Hazards from biodegradable matter, including trees, floating on the surface of the reservoir will be managed by installing shear booms and wood/ debris collection points.

19.2.6 Tailings deposition

Tailings disposition must always occur below the epilimnion/ metalimnion interface, at least 40 m below the reservoir's surface. The operational water level of the reservoir could fluctuate between RL 199.4 m and RL 226.1 m. This would result in a maximum depth to the depositional limit of RL 159.4 m of up to 67 m.

Deposition at levels deeper than the epilimnion/ hypolimnion interface will improve discharge conditions by limiting potential transport of tailings and waste rock through the FRHEP and further downstream, and will therefore need to be implemented. A clearance of 20 m must be maintained between the reservoir bottom or previously deposited tailings, and the discharge end of the pipeline where possible. The depth to the deposition location will require constant monitoring and adjustment of the discharge end of the pipeline.

The final surface of the tailings may not reach the same elevation as the waste due to the tailings' beaching characteristics and potential for the tailings to be spread across a larger area.

Equipment on the reservoir's surface to operate the discharge end of the pipeline needs to be designed to address buoyancy requirements due to significant pipeline weights and hydraulic uplift forces during operation.

Pipeline anchors may require occasional tensioning to accommodate fluctuating water levels.

19.2.7 Waste rock deposition

Barge dumping was identified by FRL as the preferred method for waste deposition following a formal trade-off assessment which included consideration of pumping the waste rock.

Single-stage crushing via gyratory crushers will reduce the waste to a sizeable fraction that facilitates conveyor transport from the mine to the barge-loading facility (Figure 19-7). The barges, provisionally specified as 5,000 t vessels, will be loaded at the loading station located south of the process plant. The barge-loading station will be designed to maintain operations within the operating range of the reservoir. The operating range for the barge-loading facility is between RL 199.4 m and RL 226.1 m. The maximum waste rock particle size is expected to be 300 mm and will include a finer fraction.

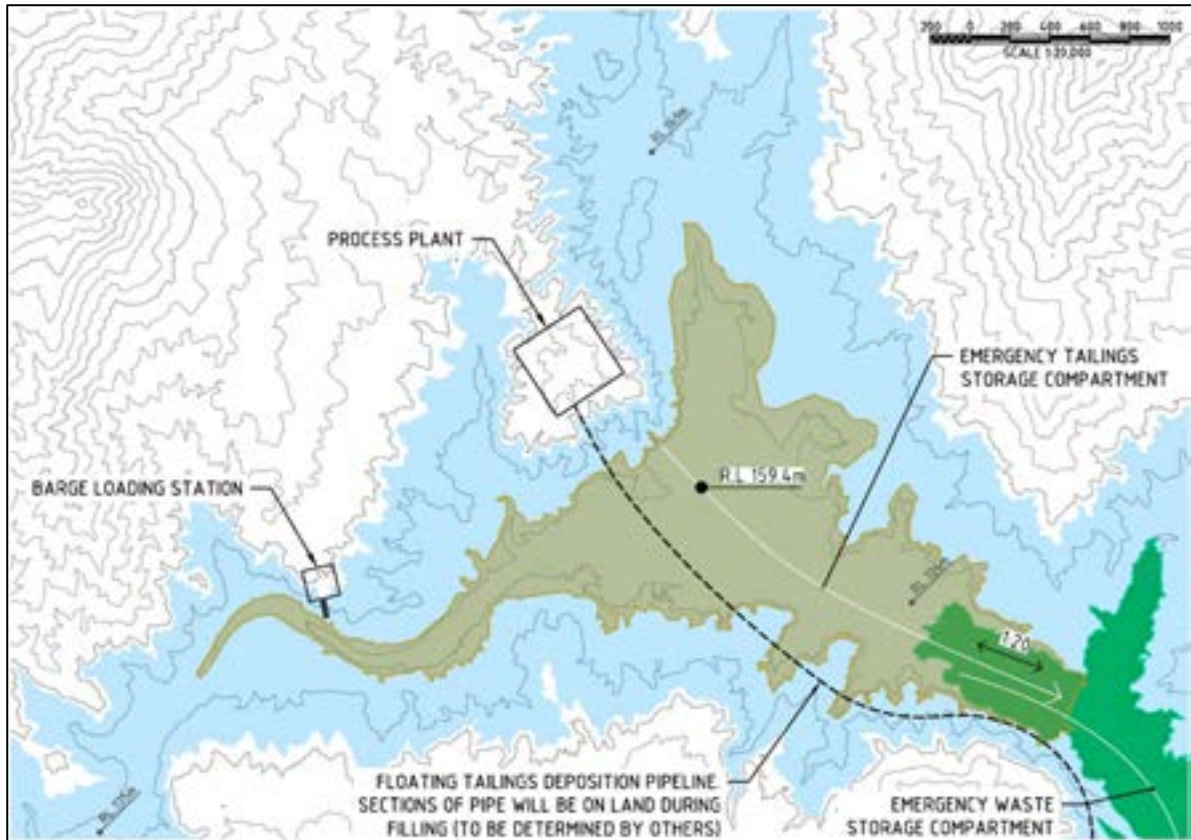


Figure 19-7: Proposed location of barge-loading facility

The barges will travel across the surface of the reservoir to the designated waste rock compartments and come to a complete standstill before off-loading commences. A latching system in the centre of the barge will be opened to release the barge’s waste contents (Figure 19-8).

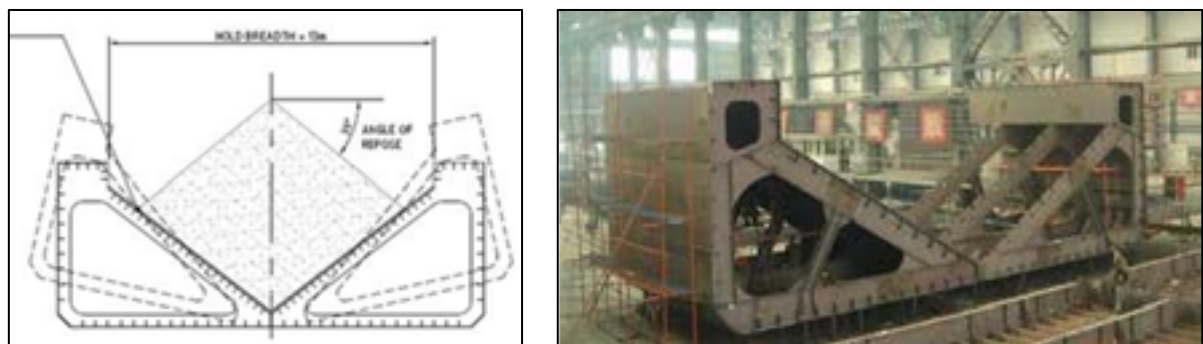


Figure 19-8: Barge latching system

The waste rock will then be dropped through the water column before landing on the bottom of the reservoir or on previously deposited waste rock. Sediment re-suspension from the bottom of the reservoir will occur, including transport of sediments retained in the water column. The latches must

be completely closed before recommencing the next trip to limit flushing and associated drag behind the barge of any fines retained in the storage compartment.

A single off-loading event was simulated in the limnology model, which indicated that sediment transport levels during off-loading are within acceptable limits. Simulation of continuous off-loading needs to be undertaken in future assessments. The limnology modelling highlighted issues with increased sediment transport due to discharge close to the embankment. A depositional strategy as discussed in Section 19.2.4 is therefore recommended. Once the operator has a better understanding of sediment transport characteristics, this limitation may be reconsidered. Other sediment transport mitigating measures can be considered at a later stage; for example, the use of more silt curtains.

The waste rock must be contained below RL 159.4 m to prevent it from being exposed to the epilimnion layer for extended periods.

The slopes of the deposited waste rock should be limited to less than 5% to prevent building up of potential unstable underwater waste masses. Implementation of appropriate monitoring procedures and protocols will be important in mitigating the risks associated with slopes that are too steep.

The barge operator must consider the impact of barge-generated waves to limit any potential negative impacts. The impact to pipelines, other traffic across the reservoir, tailings operations and the development of surface currents should be considered during the design.

Dumping close to the tailings pipelines must be controlled to limit wave generation, and prevent interference with any anchoring system that may be in place. A demarcated exclusion zone close to the pipelines will likely be required.

Biodegradable matter, including trees, floating on the surface of the reservoir may also impede barge operations. Shear booms will be installed at strategic locations to manage floating debris. A-floating shear boom would extend the length of the tailings/ waste boundary to prevent interference between trash and/ or waste rock disposal barges and the tailings deposition system area.

It is noted that silt-fencing costs have been included in the budget to mitigate the risk of sediment discharge, but only during the early days of operation.

Wave generation by wind, underwater embankment failures and landslides may affect the integrity of the barging operations and should be regarded as an operational risk.

19.2.8 Operations and maintenance

A comprehensive operations and maintenance manual will be developed prior to commissioning. The manual will be updated once the properties of the tailings and waste material and depositional characteristics are better understood, and will continue to be updated throughout the operating life of the facility.

Redundancy

Although provision of pipe, pump and barge redundancy is not a requirement, for operational reasons, provision for such redundancy is recommended. Downtime on pipelines, pumps and barges due to blockages, damage, maintenance and failures, should be considered. These events may necessitate the use of additional tailings pipeline and/ or barges to limit operational downtime. It is proposed that a short tailings pipeline should be provided to discharge to the emergency storage compartment.

19.2.9 Summary

The tailings and waste deposition strategy allows for tailings to be pumped and waste rock to be deposited by barge. The selected deposition layout has the primary objective of maintaining waste rock deposition close to the plant, particularly during early operations. The FRHEP facility has a 3.3 Bm³ total capacity, which exceeds the total current FRCGP storage requirements of 2.17 Bm³.

Waste rock and tailings characteristics and underwater spoil slope failure mechanisms are not yet fully understood and the risks need to be refined. Maximum slopes of 5% and 1% for waste rock and tailings respectively have been assumed for underwater embankments and the exact final tailings footprint is unknown. The tailings beach is expected to be very flat and therefore underwater spoil toes are required to prevent tailings migrating from tailings to waste rock compartments.

It is important to minimise the transport of potentially acid-forming material through the FRHEP and downstream for water quality compliance and to minimise turbine wear. Barge-dumping within 1 km of the embankment must therefore be avoided and hard, medium and soft material (classified according to density, size and settling characteristics) must not be dumped closer than 1 km, 2 km and 4 km respectively. Inflows may, at times, develop sufficient shear stresses to cause significant re-suspension of fines located in the upper reaches of the Nena and Niar rivers. Further work on material characterisation is needed in future study phases to clearly understand this risk.

The deposition of tailings and waste rock material requires monitoring to manage the risks associated with metal leaching due to exposure of material in the oxidising zone, and potential re-suspension of fines due to deposition in the epilimnion zone, underwater landslides, and deposition of waste on top of tailings. Interaction between the pipeline and barge operation must be avoided. Operational controls, including procedure manuals for use by barge and tailings pipeline operators, will be developed and regularly updated.

Wave action from underwater embankment failures, landslides, wind or barge operations may interfere with surface operations and affect the integrity of the pipeline and the embankment. Potential wave amplitudes due to a submerged landslide are estimated to be no higher than 6 m. Biodegradable matter, including trees, floating on the surface of the reservoir may also impede surface operations and shear booms will be installed at strategic locations to manage floating debris.

It is recommended that the tailings be de-aerated and mixed with colder water from the reservoir before being deposited subaqueously.

The effect of prolonged periods of drought on sediment resuspension due to a water level being lower than operational requirements has not been evaluated in the SPS and must be considered during further studies, including the option of limiting barge dumping frequency close to the embankment.

19.3 Hydroelectric power operation and control philosophy

This section sets out the operating philosophy for the hydroelectric power generation project including black start capability, independence of unit operations, security of auxiliary supplies and generation dispatch at the commencement and ultimate embankment operating levels. For the purposes of this report, the following is provided:

- Options for control of frequency, and voltage and unit output using the unit governors and excitation; recommendations have been provided.
- Possible control system architectures for both the gates and hydroelectric powerstation are discussed.
- Options for a high level supervisory system are discussed, but a recommendation has not been provided in this report.

19.3.1 Embankment and reservoir operating rules

As a result of the Water Balance and Energy modelling (Section 7), and the power generation requirements (Section 18), the reservoir and embankment crest rules are presented in Table 19-2.

Table 19-2: Water management operating rules

Item	Values	Comment
Embankment crest level	RL 238.50 m	This is the final dam height.
Embankment spillway crest level	RL 212.44 m	This is the crest level required for four gates 7.5 m (W) × 16.2 m (H) to achieve the required spillway discharge in a PMF event.
Embankment crest level less slump following seismic event	RL 231.50 m	This is the design maximum water level in a 72-hour PMF flood event and is based on the dam condition following an MCE seismic event.
Maximum PMF water level with four spillway gates operating	RL 231.80 m	This is the maximum level during the PMF with all four gates operating correctly throughout the flood event.
Maximum PMF water level with three spillway gates operating	RL 232.40 m	This is the maximum level during the PMF with only three of the four gates operating correctly throughout the flood event. The fourth gate remains fully closed.
Maximum PMF water level with three spillway gates operating and the bypass valves operating	RL 231.18 m	This is the maximum level during the PMF with only three of the four gates operating correctly throughout the flood event. The fourth gate remains fully closed. The four powerstation bypass valves work in parallel with the gates.
Normal reservoir maximum operating level	RL 226.14 m	This is the maximum operating level without spill. This level could possibly be raised slightly.
Minimum reservoir level to commence supply to the export grid for the first time	RL 224.14 m	Supply to the export grid for the first time is delayed until the reservoir is almost full.
Minimum reservoir operating level for full power to FRCGP and export grid	RL 204.39 m	Supply to export grid shuts down when the reservoir falls below this level.
Minimum reservoir operating level for full power to FRCGP alone	RL 199.39 m	Supply to FRCGP shuts down when the reservoir falls below this level.
Minimum reservoir operating level for start of power generation using the lower intake	RL 162.65 m January Loads RL 171.20 m May Loads	Power supply to the FRCGP can commence at this level.
Minimum reservoir operating level for start of power generation using the lower intake	RL 157.65 m January Loads RL 166.20 m May Loads	Power supply to the FRCGP would need to be stopped or limited if the water level falls below this value with the lower intake operating.
Minimum embankment level to commence filling	RL 151.48 m	This provides the storm buffer, 2 months bypass valve operation delay and a 3.5 m slump allowance plus other revisions.
Minimum embankment level at start of generation	RL 201.69 m May Loads	This provides the storm buffer, 6 months construction delay and a 3.5 m slump allowance. This change is due to the higher initial loads requiring a higher initial water level being offset by the reduction from 6 to 2 months in the allowance for delay and recognising that the reliable operation of the bypass valves is an inherent part of the dam safety during filling.

Item	Values	Comment
Lower intake invert	RL 143.30 m	This needs to be reviewed following the model study results during the next phase of the project. It is possible that it may need to be lowered by 5–10 m.
Upper intake invert	RL 185.60 m	This needs to be reviewed following the model study results.
Minimum water level above tailings/ waste rock	40 m	This value is based on the results of the limnology study.
Maximum tailings and sediment level	RL 159.4 m	Based on a depth of 40 m below the minimum long term operating level
Maximum tailings and sediment level assuming the mine is shut down	~RL 180 m	Continued use of the gates will keep flushing the reservoir and help maintain a useful live storage volume for power generation. The absolute maximum level for tailings and sediment is the spillway crest. However, the peak output may need to reduce because of submergence issues and the intakes will need protection or modification to allow generation to continue.
Minimum water level above conveyance invert for hydroelectric power operations	14.5 m	This is determined by the submergence required for the intake.
PMF storage volume	621 Mm ³	Preliminary routing studies found that 55% of this volume will be retained in the reservoir when the levels peak during a 72-hour PMF event.
FRHEP minimum live storage volume	3,001 Mm ³	This is the volume between the maximum and minimum operating levels (RL 226.14 m to RL 199.39 m).
FRHEP storm storage buffer	815–532 Mm ³	This is the buffer to allow the powerstation bypass valves to drain the reservoir during early filling. The storm volume required is dependent on the water level.

19.3.2 Spillway gates

This section describes the mechanical and electrical system required for the spillway gate operation (hydraulic). Details of the gate flow capacity and the reservoir level rise are provided in Section 10.5.3. The key features of the gates are set out in Table 19-3.

Table 19-3: Spillway gate key parameters

Parameter	Value
Number of gates	4
Type of gate	Radial
Width	7.5 m
Height	16.4 m
Gate actuation	Hydraulic
Normal maximum water level at which gates commence opening	RL 226.14 m
Maximum water level at which gates open fully	RL 227.64 m
Maximum gate vertical opening above crest while controlling flows	10.50 m
Corresponding maximum gate opening angle	104.9°
Gate discharge coefficient	0.744
Maximum gate opening normal to the flow	10.67 m
Maximum gate discharge prior to opening fully	3,243 m ³ /s

In order to ensure reliable gate operation, the following facilities are required:

- Each gate has a dedicated hydraulic lifting system each housed in separate fire compartment within the spillway gate control building.
- A mobile trailer mounted HPU system can also be provided. This allows the piping between the control building and gates to be bypassed.
- Each gate has a diesel and electrically driven pump.
- Two standby generators would be provided. A third standby generator may be required to handle lighting loads around the dam crest area. Each generator will be in its own fire compartment.
- Dual DC systems would be provided.
- Each gate would have a dedicated PLC. Dual PLCs, including all I/O may need to be provided to meet the reliability criteria. As a minimum, duplicated CPUs and communications modules will be provided.
- Each gate needs to be able to receive the reservoir levels from three sensors directly without being routed through other PLCs. A two out of three logic will be applied to deciding the correct reservoir level when there is a difference.

The spillway gate control building will provide accommodation for operators should they be forced to work 24 hours per day. The gates would be able to operate fully automatically or manually through the PLC based control system.

19.3.3 Governor control modes

Fixed MW set point control

Base loading means that a unit is running at a constant load and its output will not be affected by system changes. Base loading is used (in parallel operation with the grid infinite source) and it can be accomplished by MW control. This mode of operation is highly desirable where different types of generating units have different responses to load changes. It is highly desirable for hydroelectric power units where the efficiency of water use varies with the flow. In addition, there can be rough running regions in the power output caused by pressure fluctuations and vortices in the draft tube; these running points must be avoided.

In this mode the governor will not try to control the speed, rather it will look at the generating set output directly and match it to a given reference. As a result, MW control is not affected by frequency changes in the grid and a steady base loading is achieved. MW control is only possible when running in parallel with the grid system (frequency control must exist). Whenever the generating set is running in an island system, the control will operate in droop mode.

In MW control mode, the load reference is compared with the actual load of the engine. The difference between these signals constitutes the input to a PID-controller. The regulation output of this controller will accordingly vary in order to sustain the reference level. This output will control the diesel fuel rack position with the actuator. The PID-controller's dynamic settings have load-dependent mapping.

There are additional modes, for frequency support. The most suitable for islanded operation is to change to droop or joint droop reactive power sharing control. If the frequency deviates outside a fixed window, the control mode will automatically trip to speed control. The speed reference is updated continuously by the speed control loop also in load control, which means that if a trip occurs, the transfer will basically be bump less (no load swing). The magnitude of the frequency control dead band varies but it could be +/-0.15 to 0.20 Hz for FRHEP.

Speed droop control

Droop control refers to a speed control system whereby the control internal speed setting is lowered as a parameter of the load. Originally the term is derived from the old flyball governors that provided proportional control of frequency. However, this mode of operation is still required even in the days of PID loop controlled governors. Droop control is a universal load sharing mode and it can be used both for parallel operation in an island system and in special cases (small grids) for parallel operation with the utility.

The speed reference is compared with the measured generator speed. The difference between these signals constitutes the input to a PID-controller. The regulation output of this controller will vary, to sustain the reference level. This output will control the diesel fuel rack position with the actuator.

The PID-controller has different sets of dynamic parameters for operation with the generator breaker open speed dependent mapping (for synchronising) and closed load dependent (mapping) to obtain an optimal stability under all conditions. Some adaptive speed deviation dependent features can be provided, to minimise large speed fluctuations in islanded mode.

Speed droop control in island mode operation

In island/ speed droop controlled system, changes in active load will be shared (proportionally) equally between parallel units. The level of active power for each individual generating set depends on the speed reference. If all units have exactly the same speed reference and same droop value, they will have equal active loads. If the references or droop settings vary, the active loads will vary respectively.

A change in active load will result in a change in the system speed (frequency) as the controller speed setting will be affected by the amount of active load (MW). The higher the active load is, the lower the frequency will be. Usually droop is set to 4% which will be also the change in system speed if speed references are not changed. The operator can manually increase or decrease the speed reference on all machines to compensate for steady-state change in frequency. However, changing the speed reference on one engine will affect the kilowatt output on other parallel units; hence, keeping the engine load equally shared and the system speed correct may turn out to be laborious. In these operation modes, it is recommended to utilise isochronous load sharing system controlled by the Station PLC or a dedicated PLC for joint control of the unit governors and Automatic Voltage Regulators (AVRs). This controller will automatically share the load between the units. In special cases when load sharing is not possible, the PLC frequency fine tuning functionality will support maintaining nominal frequency.

Active frequency control

This is a special case of speed droop control. The difficulty with speed droop is that the PID controls the frequency to the permanent droop offset value. The offset ensures units share the load, assuming they all respond equally in any situation. However, no unit is in control of the frequency to correct any offset. Active frequency control is where one unit is given the job of controlling the frequency without the permanent droop offset. It is possible that this can be done with several units working jointly to ensure equal loading of the units.

Speed droop control in parallel with grid operation

When operating parallel with grid, the grid determines the system frequency. A droop controlled generating set can be operated parallel with the grid in base load principle. Decreasing or increasing the speed reference will change the unit output as the crossing point of the droop curve and the frequency is changed. Theoretically, the system works as a base load system as long as the frequency is steady; however, experience has shown that especially in weak grids where the frequency variation is noticeable, base loading cannot be properly achieved; the output of the unit will be fluctuating with the frequency changes. MW control should be applied for optimised operation.

Synchronous generation and tailwater depression

This is an operating mode that can be used for Francis and Kaplan turbines. The unit is started and synchronised in the normal way. While it is running at no load, compressed air is forced rapidly into the draft tube allowing the runner to spin air. The generator is synchronised to the grid and its excitation can be varied to provide reactive power for the site. The generator losses are incurred but this is the only cost of this mode of operation. Its big advantage is that it allows the unit to load immediately if required. The loading rate is limited only by the rate of opening the wicket gates. At FRHEP, each unit would require a compressed air reservoir with a capacity of approximately 2 m³. The station compressed air system used for the generator braking can be used to recharge the vessel.

19.3.4 Generator reactive power and voltage control

Reactive power setpoint control

In this mode the AVR is sent a fixed reactive power setpoint. Depending on the design of the AVR the setpoint may come from the operator or from a control loop. The actual variable being controlled in the excitation is unlikely to be the reactive power and this is frequently controlled by an external control loop. This may be in the AVR or it could be in the unit PLC. The danger with this mode is that with changes in load the voltage of the system may be too high or too low. Some of the units must be controlling the system voltage at all times.

Power factor

Power factor control is a method of controlling the generator excitation and reactive load when the generator is running in parallel with the grid. When in power factor control, the AVR is trying to match the reactive load proportionally to the active load. Power factor control is only possible when in parallel with the grid. Voltage control must be provided elsewhere in the system. Whenever the generating set is running in an islanded system, it must be in Voltage Droop Compensation (VDC), reactive load sharing control or droop control.

Voltage droop

Voltage droop control has similar characteristics to speed droop control, but the parameters are different. Whereas in speed droop control the system frequency is controlled by means of controlling water to the unit and the droop is derived from the active load, in voltage droop control the intention is to control the system voltage by means of controlling the generator field excitation and the droop is derived from the reactive load. Essentially this means that if all units are running in voltage droop control in an island system, the bus voltage will vary as a function of reactive load. The changes in reactive load will be shared proportionally equally providing that the droop settings are the same.

Reactive load sharing (joint voltage control)

Reactive load sharing between the units in islanded mode operation is highly desirable. This is achieved through special control functionality in the AVR. Each unit AVR reads these values and calculates a common average AVR setpoint, and compensates the effect of voltage droop. Therefore, the voltage level on the busbar is always kept at 100%. This is the recommended operation mode in pure island mode and is not an allowed operation when parallel with the grid. Some AVRs have this option the enabled by an inbuilt feature. Alternatively, if the AVR does not have the required functionality, an external controller reads the individual unit reactive power and sends a reactive power setpoint to the AVR. The controller could be the Station PLC or separate PLC dedicated both governor and AVR load sharing functions.

Frequently a dedicated communication bus is used to provide this functionality. The AVRs of each generating set are connected through a communication bus and the principle is that each AVR writes the value of its own amount of reactive power to the load sharing communication bus. Each unit reads

these values and calculates a common average AVR setpoint, and compensates the effect of voltage droop. Therefore, the voltage level on the busbar is always kept at 100%. This is the recommended operation mode in pure island mode and is not an allowed operation when parallel with the grid.

19.3.5 Recommended control settings for FRHEP generating plant

In deciding how the generating plant is to operate at the FRHEP there are several issues to be resolved:

- FRHEP is the only power supply available to the FRCGP. This means the generating plant supplying the FRCGP must be set to control frequency. The output of the units will be controlled by the governors in order to meet the demand from the mine. To achieve this, it would be normal to set one unit in active frequency control and the other units in joint speed droop control
- Exporting power to the export grid is different in that the FRHEP is contributing a contracted output. The units would normally operate in MW set point control for this duty and change to speed droop if the frequency moves outside certain bounds. The aim of this is to ensure the export grid provides other power sources for frequency control and aims to ensure that only the contracted amount of power is taken. If the units supplying power to the export grid are operated in speed droop control, the FRHEP will supply all the power demanded by the remote system without limitation
- The FRCGP requires a unit available on spinning reserve to meet the required reliability targets. If the two grids are operated jointly, frequency control will be the primary issue. While some units could be in MW set point control, the units on speed droop or active frequency control will compensate for the lack of response from the units in MW set point control
- The Power System Study suggests that the export grid and FRCGP grid operate interconnected. The logic is that the larger grid has advantages in that any disturbance such as a unit trip or SAG mill trip is a smaller percentage of the total load than with the separate grids. The result will be reduced amplitude of frequency swings. Also, there is less efficiency disadvantage in operating an extra unit loaded and eliminating the spinning reserve unit – this improves the response when a unit trips. These are all valid points. However, there is the conflicting issue of how to control the power flow to the export grid and how the governors should be configured for operation on the two systems. A further advantage of operating the grids separately is that different philosophies can be adopted for the control of voltage without compromising the two systems. The FRCGP bus units could control the voltage on the FRCGP bus while the export grid bus units could control the voltage on the export grid bus 400 km away.

Currently, there is insufficient information concerning the export grid to make definitive decisions, and it is recommended that the substation be configured with the three buses to allow the FRCGP and the export grid to be supplied from separate buses, but also provide the facilities required to allow the two buses to be connected and operate as a single system. The reserve bus should be used for bringing up the large remote transformers and for the operation of the load bank.

The recommended governor settings are as follows:

- If the two loads are segregated, the units on the FRCGP bus should operate in joint speed droop control with possibly a single unit operating in active frequency control and another on spinning reserve. The units supplying the export grid should be in MW setpoint control
- If the two loads are connected, a single unit will be in active frequency control and the remaining operating units will be in joint speed droop control with possibly one unit on spinning reserve.

19.3.6 Control system architecture and function

Hydroelectric power and gate controls

Hydroelectric power control systems tend to come in two types:

- Dedicated control system provided by the original equipment supplier. These can be very good at the turbine generator level and often have full integration with the governors and excitation systems. However, there can be issues with auxiliaries such as intake gates or special control requirements and also with new mechanical and control equipment additions as time passes. There is also an issue with dedicated systems becoming redundant and having a relatively small installed base on a worldwide basis. Maintaining a trained software support can be an issue that increases over time
- PLC based control systems with standard industrial packages used for the HMI display and Historian facilities for data storage and reporting. These are open access systems and can be easy to support an upgrade. This option can experience difficulties with obtaining the optimum integration with the governor and excitation systems.

The key features of the proposed hydroelectric power control system are:

- A dual optic fibre Ethernet is provided at the powerstation and a second dual Ethernet is provided at the intake and spillway gates. The two systems will be connected by two means;
 - Using fibre and a second path using either fibre following a different route
 - A line of sight radio link.
- Unit PLCs with dual processors to control the units and communicating directly with the unit governor and excitation
- Bypass valve PLCs for each valve connected to the dual Ethernet
- Three penstock pressure sensors in total communicating directly with the dual Ethernet. This allows accurate information concerning the penstock pressures and hence the embankment water level to be provided. This backs up the embankment water level sensors which is important during early filling when the embankment depends on the bypass valves for safety.
- Station PLC to handle station auxiliaries, substation and joint control issues
- Protection relays with their own network to allow communication and interfacing with the relevant PLCs
- A dedicated PLC at the intake covering the high and lower intake gates and the residual flow valve operation
- Dedicated PLCs with dual processors for each individual spillway gate
- Three embankment level sensors communicating directly on to the Ethernet to provide reliable information concerning the embankment water level
- PLCs are used to provide distributed intelligence in the system and to allow the safe operation or shutdown of plant items in the event of faults or a loss of communications
- Dual optic fibre systems are provided for communications
- Dedicated networks can be used for communication between unit governors and excitation systems for high speed operations during joint control operation of the units
- Remote control from a centre remote from the powerstation of all powerstation and embankment functions can be implemented.

The proposed control system architecture is shown over three schematic diagrams in Figure 19-9 to Figure 19-11.

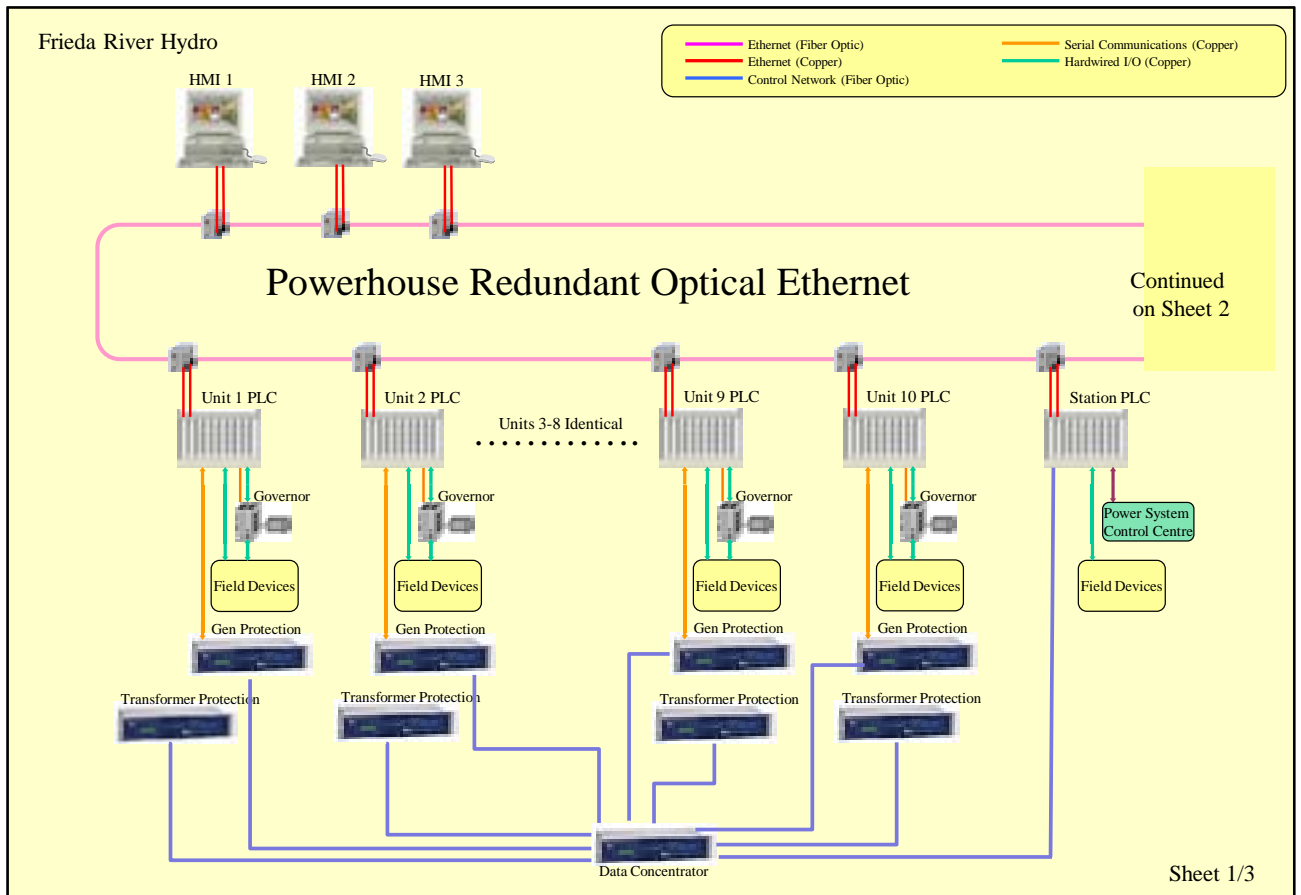


Figure 19-9: Powerhouse generation control system

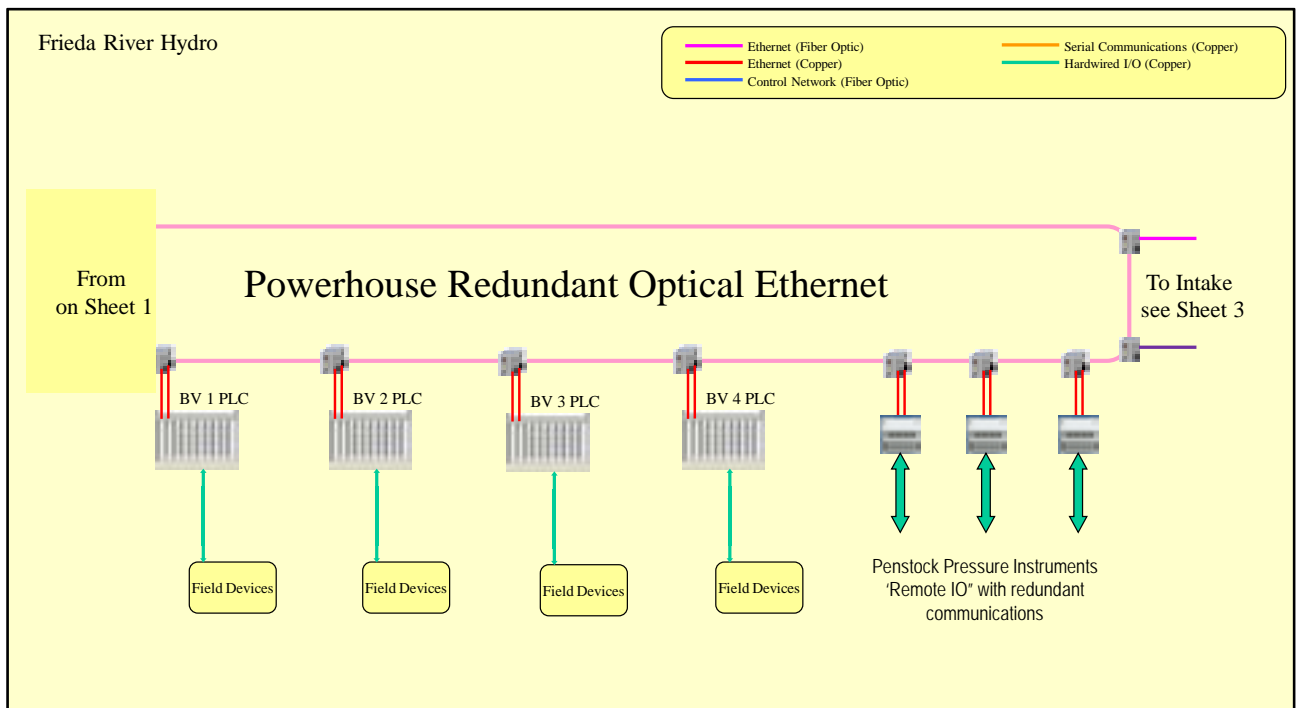


Figure 19-10: Bypass valve control system

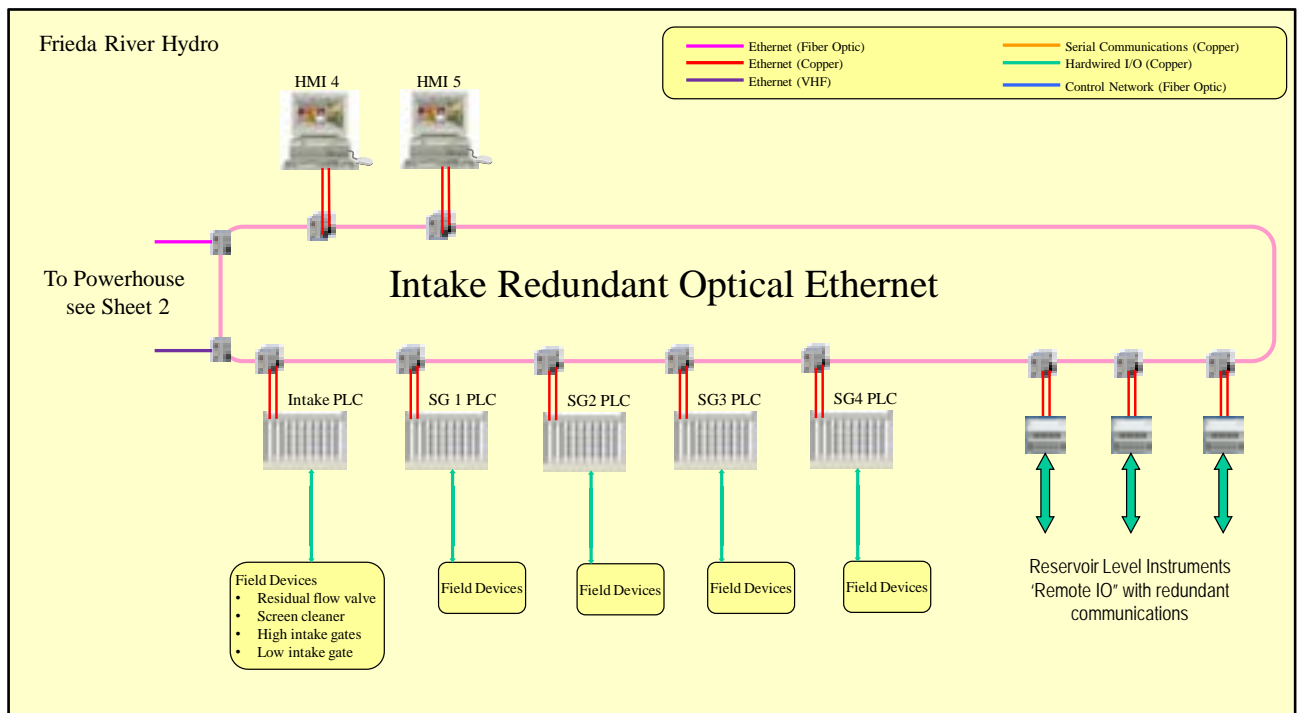


Figure 19-11: Intake gates, spillway gates and residual flow valve control system

High level supervisory system

Overall supervision of the power system can be provided by a high level Joint Generation Control System covering both the transmission system and hydroelectric power. Operationally, this should include the transformers and HV breakers at the FRCGP and the transformers and HV breakers on the transmission system to the export grid. This functionality is required for the switching operations required to liven the large transformers that supply the mine and export grid.

Software functionality of the supervisory system could include:

- Scheduling water and loads over the long term to ensure reliability of supply in accordance with the contractual agreements with the FCGP and the export grid
- Providing advance warning of potential shortfalls in supply
- Determining the optimum hydroelectric power generation and comparing it with the site load; this can be modified to allow the efficiency of the hydroelectric power generation to be maximised
- Determining the number of generators to operate taking into account spinning reserve requirements
- Allocating specific units to the frequency control role, spinning reserve and the reactive power support role for both the FRCGP and export grid power systems
- Supervising the starting and stopping units for planned and routine maintenance or simply for rotation of plant operation
- Determining the governor and AVR control mode for each operating unit
- Allocating spinning reserve based on the hydroelectric power load and the site load; the reserve will be in the form of spare operating hydroelectric power capacity and spinning reserve unit on tailwater depression.

Some of these activities can be carried out manually – especially those relating to the starting and stopping of units. However, other activities that affect the overall efficiency of the power system

generation and its ability to perform rapidly in a trip situation are best handled through a high level software supervisory system.

Switching operations associated with the livening of remote transformers are complex and likely to be carried out manually because of the liaison required with operators at the mine and at the far end of the export grid transmission line.

Situations such as black starting the system or individual generating station are likely to be best carried out by the operators.

19.4 Facility closure

Closure plans have been developed for the most likely closure categories:

- Temporary suspension
- Planned permanent closure
- Early permanent closure
- Closure during construction.

The FRHEP is designed on the basis that for the first 33 years, power will be supplied to the FRCGP and all surplus power will be supplied to the export grid, if required. After mine closure, all power will be supplied to the export grid (if required) for the remainder of the FRHEP operating life. Closure scenarios for each category are summarised in Table 19-4. Relevance of each of the closure categories will be determined by the long-term power supply requirements of the FRHEP and must be considered during future study phases. Once mining operations have ceased, the continued use of the FRHEP (after mine closure) will likely only result in the requirement for planned permanent closure, unless temporary suspension is needed for repairs due to damage to the facility. The other three closure categories will apply if power generation is for mine use only.

Table 19-4: Closure scenarios

Closure scenario	Potential closure scenarios
Temporary suspension	<ul style="list-style-type: none"> • Temporary suspension of mine operations, with FRHEP supplying power for sole use of the FRCGP • Temporary suspension of mine operations, with FRHEP supplying power to the FRCGP and export grid.
Planned permanent closure	<ul style="list-style-type: none"> • Mine operations cease at the planned LOM, with FRHEP supplying power for sole use of the FRCGP • Mine operations cease at the planned LOM, with FRHEP supplying power to the FRCGP and export grid (closure of mine infrastructure components only) • Post-mine closure power supply to export grid is no longer required.
Early permanent closure	<ul style="list-style-type: none"> • Early closure of the mine, with FRHEP supplying power for sole use of the FRCGP • Early closure of the mine, with FRHEP supplying power to the FRCGP and export grid (closure of mine infrastructure components only).
Closure during construction	<ul style="list-style-type: none"> • Mine closes prior to completion of the FRHEP construction; power supply to export grid is not required.

With the inclusion of tailings and mine waste, the general objective of closure is to ensure physical and chemical stability, with minimum requirements for active intervention and maintenance. As the water contained in the FRHEP cannot be drained and the embankment cannot be removed, the facility will require ongoing maintenance in perpetuity.

Specific objectives and requirements for closure of the FRHEP are as follows:

- Prevent uncontrolled release of the tailings and waste rock
- Prevent oxidation and contaminant release from the stored tailings and waste rock
- Minimise the risk of failure of the embankment and/ or spillway.

To limit oxygen ingress and prevent solute generation from the waste rock and tailings, a water cover or water-saturated soil cover must be maintained over the waste and tailings in all closure scenarios. Specific measures for each closure scenario are discussed in the following sections.

19.4.1 Temporary suspension

Supply of power for the FRCGP

Mining operations may go into suspension for extended periods as dictated by market conditions, socio-political constraints and/ or natural disruptive events. Suspension periods arising from global economic changes and low metal prices can last for several years. Those arising from socio-political impacts may last from several months to several years. Suspension periods arising from natural events, such as the El Niño drought that has affected other PNG operations, can last for months. Other natural events have the potential to disrupt operations for variable periods and include landslides, earthquakes and storms.

In the event of a temporary suspension, the critical requirement for the FRHEP is water and water quality management, including freeboard management. An active care-and-maintenance approach would need to be adopted to ensure that any potential risks associated with the FRHEP are managed and mitigated. A skeleton crew would be required on site to operate and maintain the spillway system, maintain freeboards, ensure water coverage of the waste and tailings, monitor and maintain embankments, and undertake water quality monitoring. Spillway gates may need to be completely opened and conveyance tunnel outlet valves may need to be closed depending on the expected duration of suspension. Residual flows would be maintained via the spillway.

Road maintenance must continue to ensure access when the FRHEP start-up commences.

Key mechanical and electrical equipment may require intermittent inspection and may need to be operated to maintain good working order. The FRCGP will need to make a decision with respect to management of the floating tailings pipeline during this period. At a minimum, SRK recommends that the tailings pipes are flushed. Should the suspension period be extended, the pipes would be removed from the reservoir and returned to a central storage yard, or secured against theft and damage. Similarly, the FRCGP will need to make a decision regarding the barge management. For a short suspension period, the barges will be moored and secured at a docking facility. For longer suspension periods, the barges will be removed above the high-water mark and stored on dry land in a secure environment (fenced or in sheds). The barges will need to be prepared for extended storage periods following the manufacturers' instructions (fuel removal, for example). Intermittent inspections of the surface of the reservoir will also be required to investigate changing conditions such as potential landslides, or the presence of unauthorised activities around the reservoir.

Due to the FRHEP's remote location, temporary closure could leave the FRHEP exposed to a risk of theft because of reduced numbers of site personnel. This would require regular security control measures to be implemented.

Periods of temporary suspension are also ideal opportunities for maintenance of key mechanical and electrical equipment, including pipelines and barges, to be carried out.

Supply of power to the FRCGP and the export grid

Temporary suspension periods arising from natural events, such as the El Niño drought that has affected other operations in PNG, can last for months. Other natural events with the potential to disrupt operations for variable periods include landslides, earthquakes and storms. In periods of low rainfall, such as during an El Niño event, the FRHEP would likely still be required to meet some reduced power generation targets, and this may impact mining operations.

The temporary FRHEP closure requirements will be similar to the temporary mine closure procedures described above.

19.4.2 Planned permanent closure

The main activities associated with the planned permanent closure of the FRHEP relate to removal of infrastructure and specific access roads, potential grouting of the embankment cut-off, maintenance of other infrastructure, and considerations in terms of sedimentation and impact on the schedule.

Infrastructure removal

All tailings and waste rock disposal infrastructure, equipment and mining materials will be removed. This includes barges, barge-loading infrastructure and the tailings disposal pipeline. The tailings pipeline is to be flushed prior to disposal.

The FRHEP will be completely decommissioned once power generation is no longer required. This includes demolition of the powerhouse and removal of the associated electrical infrastructure, plugging of the hydroelectric power conveyance tunnels and surge chambers, and removal of the operational spillway radial gates.

Salvageable equipment and materials will be recycled or sold if practical. Hazardous wastes will be removed from the site and disposed of at an appropriate waste facility. Non-hazardous wastes are assumed to be either disposed of underwater on the tailings facility or in a dedicated landfill on site.

Earthworks

Access roads not required for long-term monitoring and maintenance will be removed and rehabilitated. To promote natural revegetation, all disturbed surfaces will be prepared by scarification or ripping of compacted surfaces.

Embankment cut-off

Degradation of the asphalt core and grout curtain is not expected; however, should long-term degradation occur, grouting of the foundation cut-off system in such extreme cases may be required.

Associated infrastructure

Roads and other key components of the facility, such as the spillway, may require intermittent maintenance and repairs after closure to ensure the embankment remains functional in the case of temporary closure.

Sediment

Natural sediments will continue to inundate the FRHEP post-closure. When a RL 180 m level has been reached, suction from the intake could potentially cause sediments in the facility to be extracted through the tunnels; this will start to increase turbine wear. However, at the predicted annual rate of sediment loads deposited in the reservoir, the facility will be closed before this level is reached.

The limnology study during future study phases needs to further investigate the long-term effects of sediments settling in the upper reaches of the reservoir, and the potential for re-suspension and transport through the FRHEP over the long term.

Schedule

Removal of the tailings and waste rock disposal infrastructure, along with associated earthworks, would occur at the end of the 33-year mine life. Closure of the FRHEP and its associated earthworks will occur once power generation is no longer required, which will depend on the requirement of the facility to continue supplying power to the export grid.

19.4.3 Early permanent closure

Should mining operations cease earlier than planned and power to the export grid is no longer required, the early permanent closure measures are expected to be the same as for the planned permanent closure scenario (Section 19.5).

19.4.4 Closure during construction

Should the FRHEP cease during the embankment construction phase and prior to filling of water, the following additional closure measures would be undertaken as required:

- Depending on the embankment construction progress, the embankment will either be breached, or a permanent spillway will be constructed around one of the abutments.
- Where practical, exposed bedrock within the footprint area will be covered with topsoil from the spoil storage area and the area revegetated.
- The spoil storage area will be re-graded to a stable landform and revegetated.
- The quarry will be re-graded or backfilled, as required, to prevent ponding of water.
- The diversion inlet tunnel will be plugged and the inlet area re-graded and/ or filled to prevent any surface water ponding.
- Stormwater diversion and silt collection channels, diversion bunds, and sedimentation ponds will be decommissioned once they are no longer required.

19.5 Post-closure surface water management

After closure, natural inflows from the river system will pass through the facility via the spillway, once the gates are removed. The spillway has been sized to then allow flows in excess of the probable maximum flood (PMF) to be safely conveyed around the embankment.

The surrounding catchment will contribute significant sediment loads to the facility, and it is expected that the facility will eventually become completely silted. The sediments will reduce the storage capacity of the FRHEP, but will also result in the formation of a saturated cover over the tailings and mine waste. Landslides or other mass movement into the FRHEP will further reduce the available storage. Consequently, the spillway has been sized to pass flows in excess of the PMF without relying on attenuation within the reservoir.

19.6 Post-closure maintenance and monitoring

The embankment, spillway and water will continue to require long-term monitoring, inspection and maintenance in perpetuity. Detailed plans that establish post-closure maintenance and monitoring criteria will need to be developed prior to closure, noting that long-term requirements will not be limited to the FRHEP. The current expectation is that the mine's pit water will require treatment over the long term, which will require personnel presence and long-term access.

The post-closure maintenance and monitoring requirements specific to the FRHEP are expected to include the following:

- Embankment surveillance: continued inspections and monitoring as per the dam safety program developed in the later design stages, which is based on ANCOLD, CDA and ICOLD guidance
- Maintenance requirements: routine and event-driven maintenance of the embankment and spillway
- Post-closure monitoring requirements: reservoir elevation, sedimentation rates in the FRHEP, depths of the reservoir over tailings and waste, performance of the embankment, performance of the spillway, and water chemistry in the FRHEP and at the embankment seepage outlet.

Compiled by



Claude Prinsloo

Senior Consultant

Peer Reviewed by



Pepé Moreno

Principal Consultant

SRK Report Client Distribution Record

Project Number: PNA009

Report Title: Frieda River Hydroelectric Project Selection Phase Study

Date Issued: 5 November 2018

Name/Title	Company
Edward Chong	Frieda River Limited

Rev No.	Date	Revised By	Revision Details
0	01/06/2018	Claude Prinsloo	Draft Report
1	20/07/2018	Claude Prinsloo	Final Report
2	23/07/2018	Claude Prinsloo	Revised Final Report
3	27/09/2018	Pepe Moreno	Revised Final Report
4	04/10/2018	Claude Prinsloo	Revised Final Report
5	02/11/2018	Claude Prinsloo	Revised Final Report

This Report is protected by copyright vested in SRK Consulting (Australasia) Pty Ltd. It may not be reproduced or transmitted in any form or by any means whatsoever to any person without the written permission of the copyright holder, SRK.

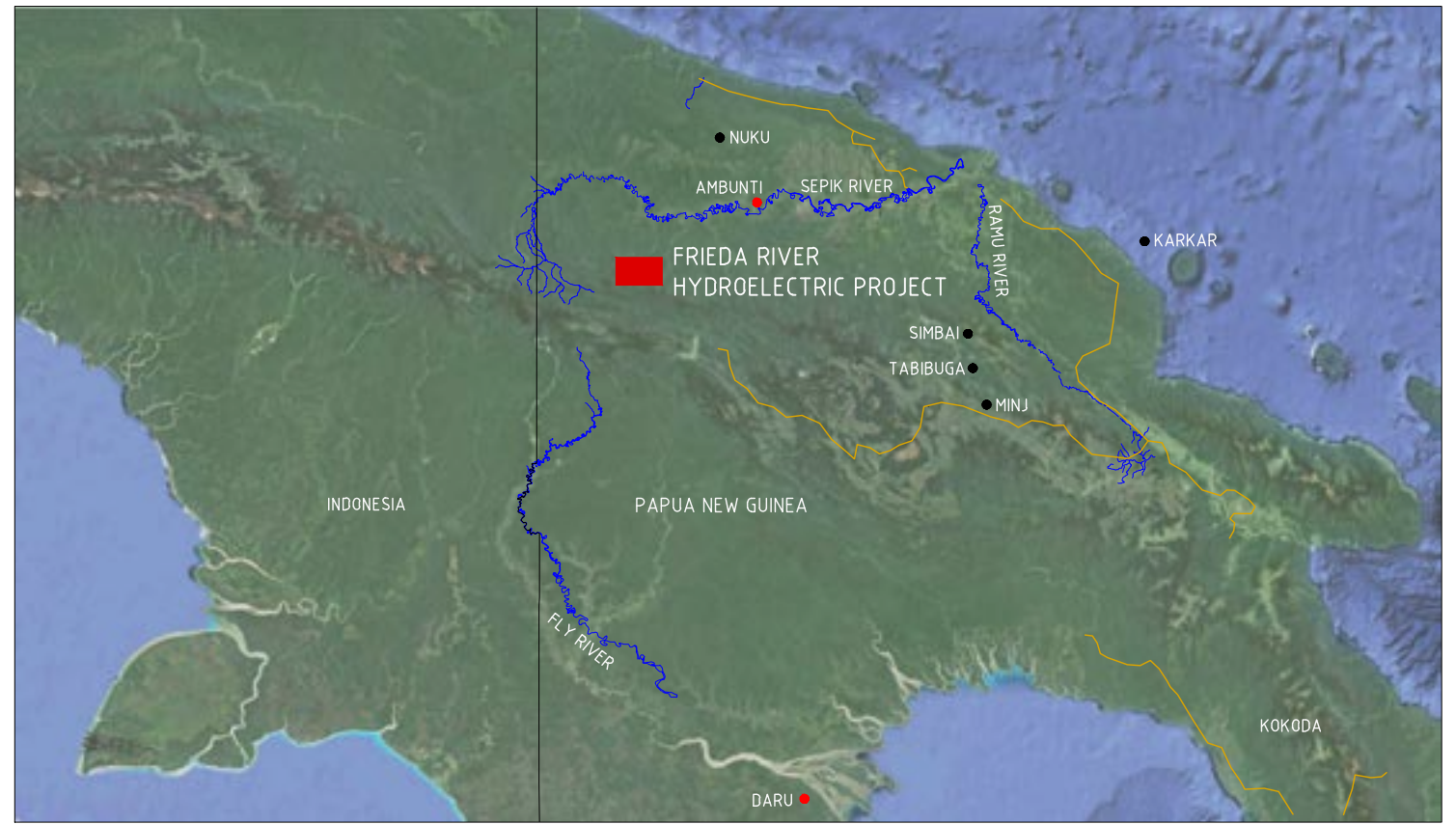
Appendix 1: Drawings (SRK and Stantec)

FRIEDA RIVER HEP DRAWING LIST

Study	Origin	Vendor Drawing Number	PanAust Drawing Number	Drawing Title	Description	REV
SPS	SRK	PNA009-0000	FRP-2-D-00-01-X-030-001	PROJECT LOCATION & DRAWING LIST COVER SHEET	COVER SHEET	D
SPS	SRK	PNA009-0005	FRP-2-D-00-01-D-030-001	FINAL INUNDATION PLAN	PLAN	C
SPS	SRK	PNA009-0010	FRP-2-D-00-01-D-030-002	WASTE ROCK & TAILINGS DEPOSITION LAYOUT (33 YEAR LOM.)	LAYOUT	C
SPS	SRK	PNA009-0020	FRP-2-D-00-01-D-030-003	SITE GENERAL ARRANGEMENT	LAYOUT	D
SPS	SRK	PNA009-0030	FRP-2-D-00-01-D-030-004	SURFICIAL GEOLOGY SECTIONS SHEET 1 OF 2	SECTIONS	C
SPS	SRK	PNA009-0032	FRP-2-D-00-01-D-030-005	SURFICIAL GEOLOGY SECTIONS SHEET 1 OF 2	SECTIONS	C
SPS	SRK	PNA009-0034	FRP-2-D-00-01-D-030-006	STABILISED ZONE EXCAVATION LAYOUT & SECTIONS	LAYOUT AND SECTIONS	C
SPS	SRK	PNA009-0040	FRP-2-D-00-01-D-030-007	INITIAL INUNDATION ZONES FOR DIVERSION & COFFERDAMS	PLAN	C
SPS	SRK	PNA009-0042	FRP-2-D-00-01-D-030-008	CONSTRUCTION SEQUENCE LAYOUT	LAYOUT	D
SPS	SRK	PNA009-0044	FRP-2-D-04-01-D-030-001	FOUNDATION EXCAVATION DEPTH MAP	PLAN	C
SPS	SRK	PNA009-0052	FRP-2-D-00-01-D-030-009	DOWNSTREAM DRAINAGE & SEDIMENT MANAGEMENT LAYOUT	LAYOUT	C
SPS	SRK	PNA009-0056	FRP-2-D-02-01-D-030-001	TYPICAL ROADS LAYOUT	LAYOUT	D
SPS	SRK	PNA009-0058	FRP-2-D-02-01-D-030-002	TYPICAL ROADS SECTIONS	SECTIONS	C
SPS	SRK	PNA009-0060	FRP-2-D-02-01-D-030-003	SPOIL STORAGE 1 LAYOUT & SECTIONS	LAYOUT AND SECTIONS	C
SPS	SRK	PNA009-0062	FRP-2-D-02-01-D-030-004	SPOIL STORAGE 2 LAYOUT & SECTIONS	LAYOUT AND SECTIONS	C
SPS	SRK	PNA009-0070	FRP-2-D-02-01-D-030-005	DIVERSION & COFFERDAMS LAYOUT AND CONSTRUCTION SEQUENCE	LAYOUT	C
SPS	SRK	PNA009-0072	FRP-2-D-02-01-D-030-006	DIVERSION & COFFERDAMS TYPICAL SECTIONS	SECTIONS	C
SPS	SRK	PNA009-0080	FRP-2-D-04-01-D-030-002	EMBANKMENT FINAL LAYOUT	LAYOUT	C
SPS	SRK	PNA009-0082	FRP-2-D-04-01-D-030-003	EMBANKMENT TYPICAL CROSS SECTION & DETAILS	SECTION AND DETAILS	C
SPS	SRK	PNA009-0084	FRP-2-D-04-01-D-030-004	EMBANKMENT TYPICAL LONG SECTION & PLINTH LAYOUT	LAYOUT AND SECTION	C
SPS	SRK	PNA009-0086	FRP-2-D-04-01-D-030-005	EMBANKMENT PLINTH & CUT-OFF WALL CONNECTIONS DETAILS	DETAILS	C
SPS	SRK	PNA009-0088	FRP-2-D-04-01-D-030-006	EMBANKMENT PLINTH & CUT-OFF WALL GROUTING LAYOUT & SECTION	LAYOUT AND SECTION	C
SPS	SRK	PNA009-0090	FRP-2-D-04-01-D-030-007	EMBANKMENT INSTRUMENTATION LAYOUT	LAYOUT	C
SPS	SRK	PNA009-0092	FRP-2-D-04-01-D-030-008	EMBANKMENT INSTRUMENTATION SECTIONS	SECTIONS	C
SPS	SRK	PNA009-0100	FRP-2-D-00-01-D-030-010	CRITICAL LEVELS SECTION	SECTION	C
SPS	SRK	PNA009-0110	FRP-2-D-10-01-D-030-001	SPILLWAY LAYOUT	LAYOUT	D
SPS	SRK	PNA009-0112	FRP-2-D-10-01-D-030-002	SPILLWAY LONG SECTION	LONG SECTION	C
SPS	SRK	PNA009-0114	FRP-2-D-10-01-D-030-003	SPILLWAY SECTION AND DETAILS	SECTION AND DETAILS	C
SPS	SRK	PNA009-0116	FRP-2-D-10-01-D-030-004	SPILLWAY INLET GATE LAYOUT, SECTION & ELEVATION	LAYOUT, SECTION & ELEVATION	C
SPS	SRK	PNA009-0117	FRP-2-D-10-01-D-030-005	SPILLWAY BRIDGE LAYOUT, SECTIONS & DETAILS	LAYOUT, SECTIONS & DETAILS	C
SPS	SRK	PNA009-0118	FRP-2-D-10-01-D-030-006	SPILLWAY INLET RETAINING WALL TYPICAL SECTION	SECTION	C
SPS	Stantec	80510050	FRP-2-D-10-01-D-030-007	SPILLWAY GATE PLAN	PLAN	B
SPS	Stantec	80510050	FRP-2-D-10-01-D-030-008	SPILLWAY GATE SECTION	SECTION	B
SPS	Stantec	80510050	FRP-2-D-10-01-D-030-009	SPILLWAY GATE ELEVATION	ELEVATION	B
SPS	SRK	PNA009-0120	FRP-2-D-06-01-D-030-001	DIVERSION TUNNEL LAYOUT, SECTIONS & DETAIL	LAYOUT, SECTIONS AND DETAIL	C
SPS	SRK	PNA009-0122	FRP-2-D-06-01-D-030-002	DIVERSION TUNNEL INLET LAYOUT & SECTIONS	LAYOUT AND SECTIONS	C
SPS	SRK	PNA009-0124	FRP-2-D-06-01-D-030-003	DIVERSION TUNNEL OUTLET LAYOUT, SECTION & DETAIL	LAYOUT, SECTION & DETAIL	C
SPS	SRK	PNA009-0130	FRP-2-D-00-01-D-030-011	GEOTECHNICAL INVESTIGATION PLAN	PLAN	D
SPS	SRK	PNA009-0201	FRP-2-D-04-01-D-030-009	EMBANKMENT PLINTH CUT-OFF WALL DEVELOPMENT PLAN LAYOUT	LAYOUT	B
SPS	SRK	PNA009-0202	FRP-2-D-04-01-D-030-010	EMBANKMENT PLINTH CUT-OFF WALL PANEL LAYOUT & SECTIONS	LAYOUT & SECTIONS	C
SPS	SRK	PNA009-0203	FRP-2-D-04-01-D-030-011	EMBANKMENT PLINTH CUT-OFF WALL CONNECTION DETAILS 1	DETAILS	C
SPS	SRK	PNA009-0204	FRP-2-D-04-01-D-030-012	EMBANKMENT PLINTH CUT-OFF WALL CONNECTION DETAILS 2	DETAILS	B

FRIEDA RIVER HEP DRAWING LIST

Study	Origin	Vendor Drawing Number	PanAust Drawing Number	Drawing Title	Description	REV
SPS	SRK	PNA009-0205	FRP-2-D-04-01-D-030-013	EMBANKMENT PLINTH CUT-OFF WALL CONNECTION DETAILS 3	DETAILS	C
SPS	SRK	PNA009-0206	FRP-2-D-04-01-D-030-014	EMBANKMENT PLINTH CUT-OFF WALL PANEL TYPES	DETAILS	C
SPS	SRK	PNA009-0211	FRP-2-D-04-01-D-030-015	EMBANKMENT PLINTH CUT-OFF WALL TRANSITION DETAILS	DETAILS	C
SPS	Stantec	80510050	FRP-2-D-14-01-D-030-001	SCHEME LAYOUT PLAN	PLAN	B
SPS	Stantec	80510050	FRP-2-D-14-01-D-030-002	INTAKE SITE PLAN	PLAN	B
SPS	Stantec	80510050	FRP-2-D-14-01-D-030-003	RESIDUAL FLOW LAYOUT PLAN AND LONGSECTION	PLAN AND LONGSECTION	B
SPS	Stantec	80510050	FRP-2-D-14-01-D-030-004	RESIDUAL FLOW INTAKE AND CHAMBER PLANS AND ELEVATIONS	PLANS AND ELEVATIONS	B
SPS	Stantec	80510050	FRP-2-D-14-01-D-030-005	LOWER INTAKE AND GATE SHAFT PLANS AND LONGSECTION	PLANS AND LONGSECTION	B
SPS	Stantec	80510050	FRP-2-D-14-01-D-030-006	UPPER INTAKE TOWER PLANS	PLANS	B
SPS	Stantec	80510050	FRP-2-D-14-01-D-030-007	UPPER INTAKE TOWER SECTION AND ELEVATION	SECTION AND ELEVATION	B
SPS	Stantec	80510050	FRP-2-D-14-01-D-030-008	WATER CONVEYANCE LONGSECTION	LONG SECTION	B
SPS	Stantec	80510050	FRP-2-D-14-01-D-030-009	TUNNEL SECTIONS	SECTIONS	B
SPS	Stantec	80510050	FRP-2-D-14-01-D-030-010	SURGE CHAMBER PLAN AND SECTION	PLAN AND SECTION	B
SPS	Stantec	80510050	FRP-2-D-14-01-D-030-011	PENSTOCK PLAN AND ELEVATIONS	PLAN AND ELEVATIONS	B
SPS	Stantec	80510050	FRP-2-D-14-01-D-030-012	DRAIN VALVE STRUCTURE PLAN AND SECTION	PLAN AND SECTION	B
SPS	Stantec	80510050	FRP-2-D-12-01-D-030-001	POWERHOUSE SITE PLAN	PLAN	B
SPS	Stantec	80510050	FRP-2-D-12-01-D-030-002	POWERHOUSE SWITCHGEAR AND OFFICES LEVEL AND ROOF PLANS	PLANS	B
SPS	Stantec	80510050	FRP-2-D-12-01-D-030-003	POWERHOUSE MACHINE HALL AND CONTROL ROOM LEVEL PLANS	PLANS	B
SPS	Stantec	80510050	FRP-2-D-12-01-D-030-004	POWERHOUSE WICKET GATE AND GENERATOR LEVEL PLANS	PLANS	B
SPS	Stantec	80510050	FRP-2-D-12-01-D-030-005	POWERHOUSE TURBINE LEVEL PLAN	PLAN	B
SPS	Stantec	80510050	FRP-2-D-12-01-D-030-006	POWERHOUSE DRAFT TUBE LEVEL PLAN	PLAN	B
SPS	Stantec	80510050	FRP-2-D-12-01-D-030-007	POWERHOUSE LARGE TURBINE CROSS SECTION	CROSS SECTION	B
SPS	Stantec	80510050	FRP-2-D-12-01-D-030-008	POWERHOUSE SMALL TURBINE CROSS SECTION	CROSS SECTION	B
SPS	Stantec	80510050	FRP-2-D-12-01-D-030-009	POWERHOUSE LONGSECTION	LONG SECTION	B
SPS	Stantec	80510050	FRP-2-D-12-01-D-030-010	POWERHOUSE SINGLE LINE DIAGRAM	DIAGRAM	B

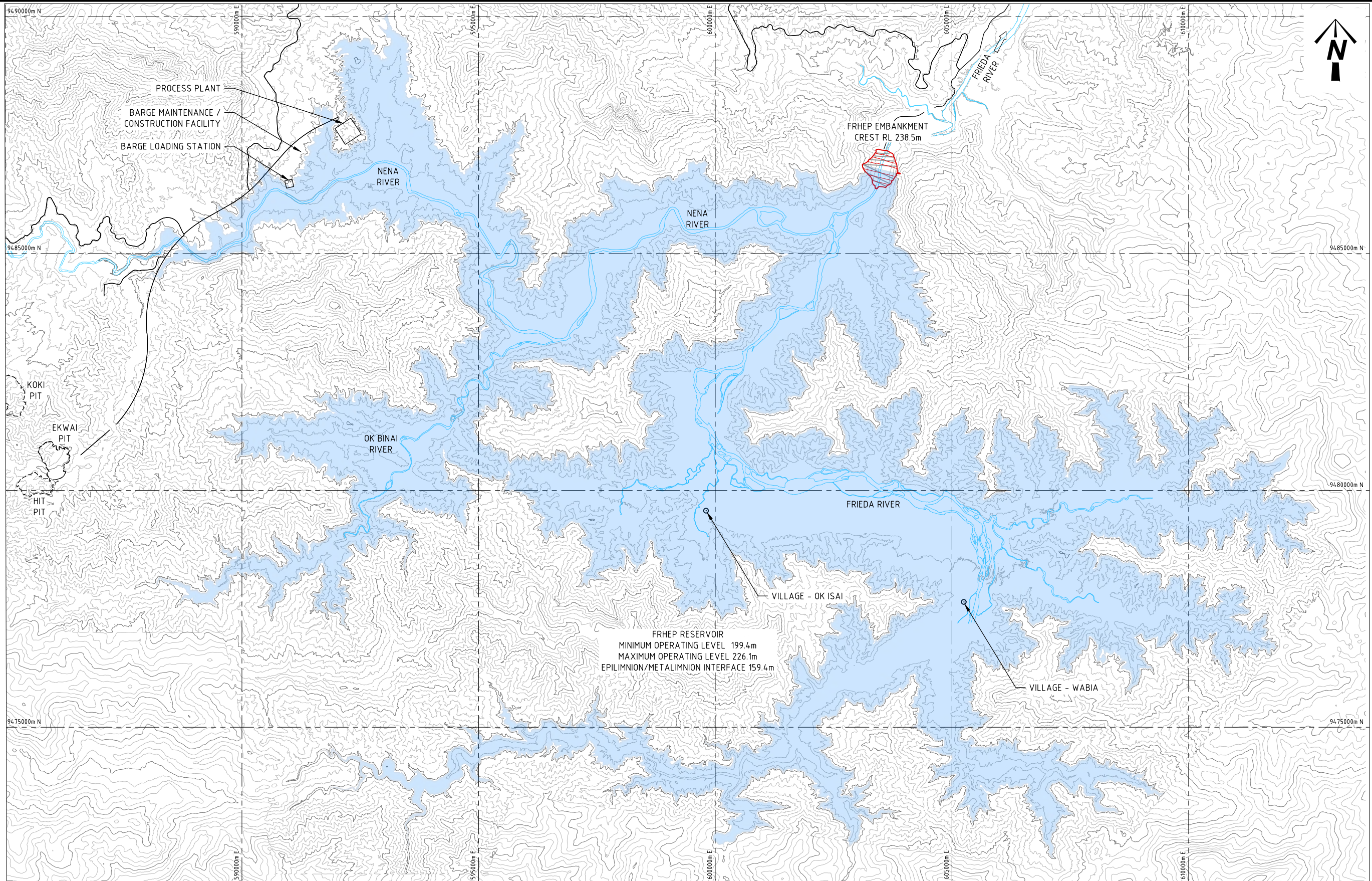


PROJECT LOCALITY MAP

NOTE:
SECTION AND DETAIL DRAWING REFERENCES THROUGHOUT THE DRAWING SET REFER TO THE VENDOR DRAWING NUMBER LOCATED BENEATH THE ENGINEERING COMPANY LOGO

P:\PNA009 - FRIEDA RIVER HEP PFS\04_WORKING_FILES\2_DRAFTING\00 - DRAWINGS\01 - SHEETS\PNA009-0000.DWG - 23/10/2018 1:46:17 PM

				<p>ENGINEERING COMPANY</p> <p>SRK Perth 10 Richardson Street, West Perth, Western Australia 6005 Tel: +61 8 9288 2000 - Fax: +61 8 9288 2001 http://www.srk.com.au</p>			<p>DRAWN: TREV 31.05.18 DESIGN: PRIN 31.05.18 DES.CHKD: MORE 31.05.18 LD ENG. APPR: MORE 31.05.18 PM APPR: MORE 31.05.18</p>			<p>OWNER</p> <p>FRIEDA RIVER LIMITED</p>		<p>STATUS</p> <p>FOR INFORMATION</p>		
							<p>TITLE</p> <p>FRIEDA RIVER HYDROELECTRIC PROJECT PROJECT LOCATION & DRAWING LIST COVER SHEET</p>		<p>SCALE AS SHOWN</p> <p>ALL DIMENSIONS IN METRES</p>					
									<p>REV No. D</p> <p>SIZE A1</p>					
									<p>DRAWING No</p> <p>FRP-2-D-00-01-X-030-001</p>					
REF. DWG No.	DWG. DESCRIPTION	No	DATE	REVISION DETAILS	LD ENG.	PM	VENDOR DRG NO.	PNA009-0000						



FINAL INUNDATION PLAN
SCALE 1:40,000

P:\PNA009 - FRIEDA RIVER HEP PFS\04_WORKING_FILES_V2_DRAFTING\00 - DRAWINGS\01 - SHEETS\PNA009-0005.DWG - 17/10/2018 10:35:15 AM

REF. DWG No.	DWG. DESCRIPTION	No	DATE	REVISION DETAILS	LD ENG.	PM
		C	25.09.18	ISSUED FOR FINAL REPORT	MORE	MORE
		B	18.07.18	REISSUED FOR CLIENT REVIEW	MORE	MORE
		A	31.05.18	ISSUED FOR CLIENT REVIEW	MORE	MORE

ENGINEERING COMPANY



SRK Perth 10 Richardson Street, West Perth, Western Australia 6005
Tel: +61 8 9288 2000 - Fax: +61 8 9288 2001
<http://www.srk.com.au>

DRAWN	TREV	31.05.18
DESIGN	PRIN	31.05.18
DES.CHKD	MORE	31.05.18
LD ENG. APPR	MORE	31.05.18
PM, APPR	MORE	31.05.18

VENDOR DRG NO. PNA009-0005



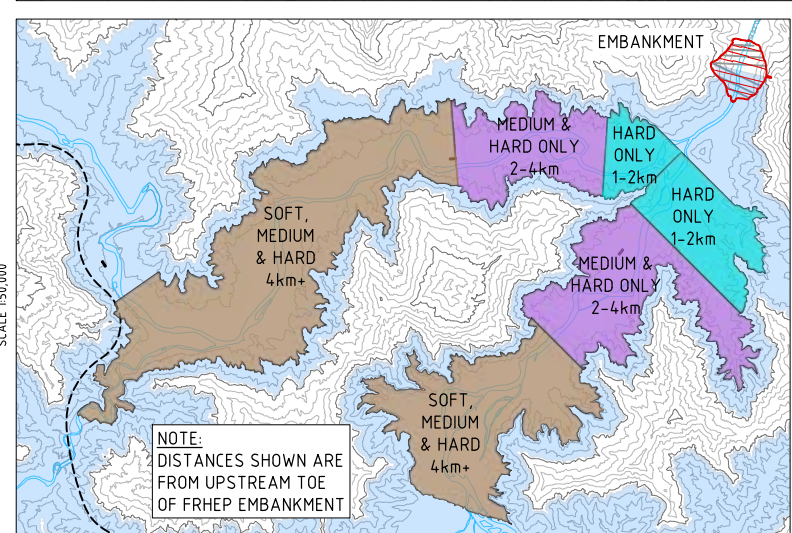
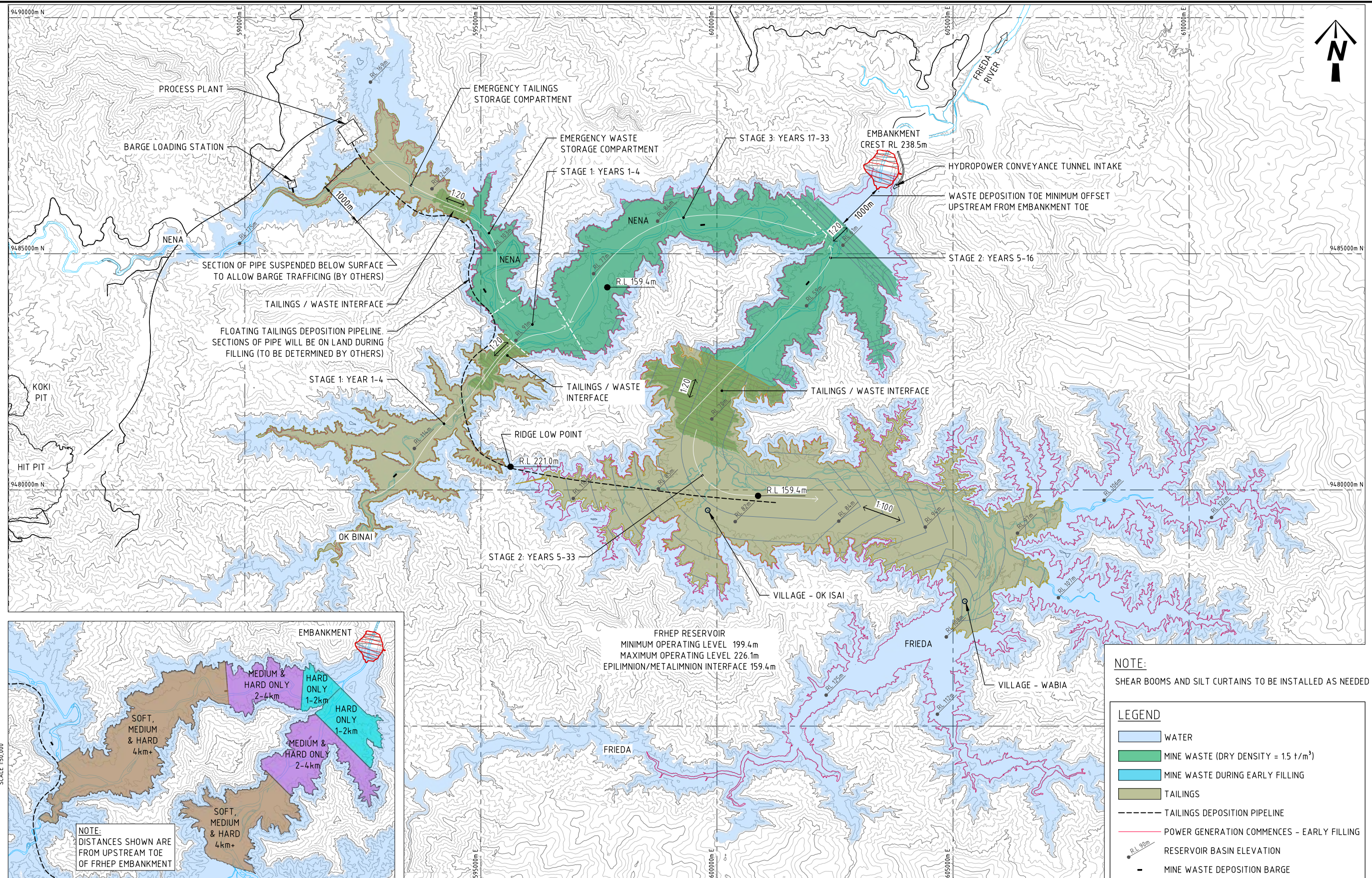
FRIEDA RIVER

OWNER
FRIEDA RIVER LIMITED

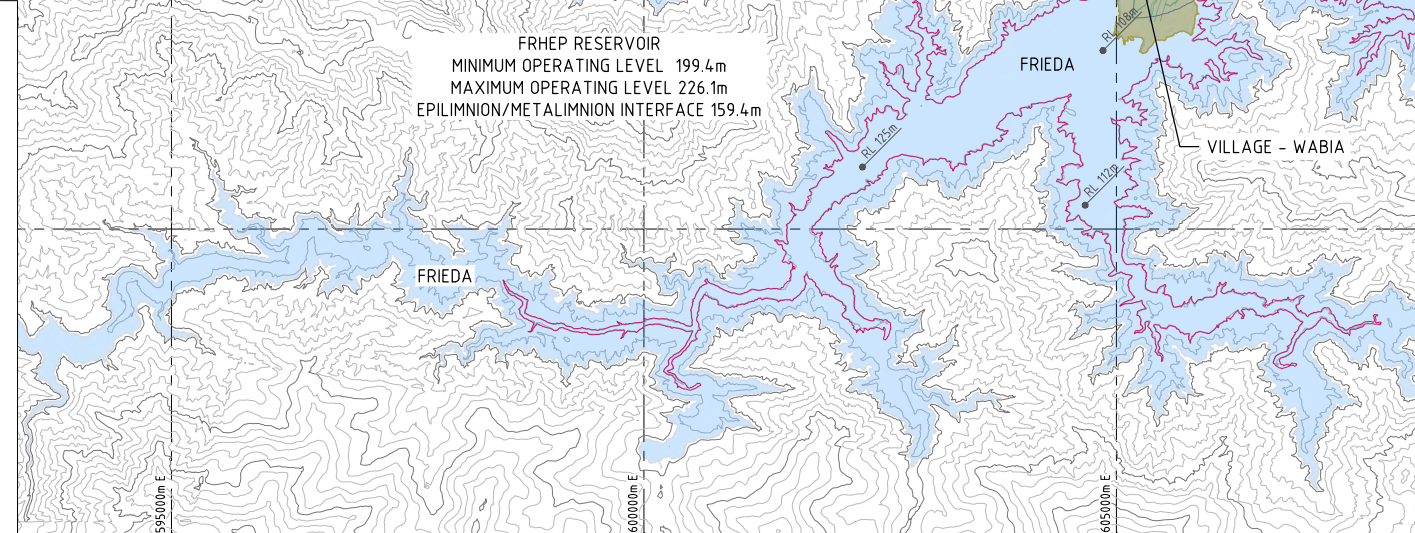
TITLE
FRIEDA RIVER HYDROELECTRIC PROJECT

FINAL INUNDATION PLAN

STATUS FOR INFORMATION		
SCALE	AS SHOWN	REV No.
		SIZE
ALL DIMENSIONS IN METRES		C A1
DRAWING No		
FRP-2-D-00-01-D-030-001		



WASTE ROCK STAGED DEPOSITION LAYOUT
SCALE 1:50,000



WASTE ROCK & TAILINGS DEPOSITION LAYOUT (33 YEAR LOM.)
SCALE 1:40,000

NOTE:
SHEAR BOOMS AND SILT CURTAINS TO BE INSTALLED AS NEEDED

LEGEND

- WATER
- MINE WASTE (DRY DENSITY = 1.5 t/m³)
- MINE WASTE DURING EARLY FILLING
- TAILINGS
- TAILINGS DEPOSITION PIPELINE
- POWER GENERATION COMMENCES - EARLY FILLING
- RESERVOIR BASIN ELEVATION
- MINE WASTE DEPOSITION BARGE

SCALE 1:40,000

P:\PNA009 - FRIEDA RIVER HEP PFS\04_WORKING_FILES_V2_DRAFTING\00 - DRAWINGS\01 - SHEETS\VPNA009-0010.DWG - 17/10/2018 10:36:22 AM

REF. DWG No.	DWG. DESCRIPTION	No	DATE	REVISION DETAILS	LD ENG.	PM
		C	25.09.18	ISSUED FOR FINAL REPORT	MORE	MORE
		B	18.07.18	REISSUED FOR CLIENT REVIEW	MORE	MORE
		A	31.05.18	ISSUED FOR CLIENT REVIEW	MORE	MORE

ENGINEERING COMPANY

srk

SRK Perth 10 Richardson Street, West Perth, Western Australia 6005
Tel: +61 8 9288 2000 - Fax: +61 8 9288 2001
<http://www.srk.com.au>

DRAWN	TREV	31.05.18
DESIGN	PRIN	31.05.18
DES.CHKD	MORE	31.05.18
LD ENG. APPR	MORE	31.05.18
PM APPR	MORE	31.05.18

VENDOR DRG NO. PNA009-0010

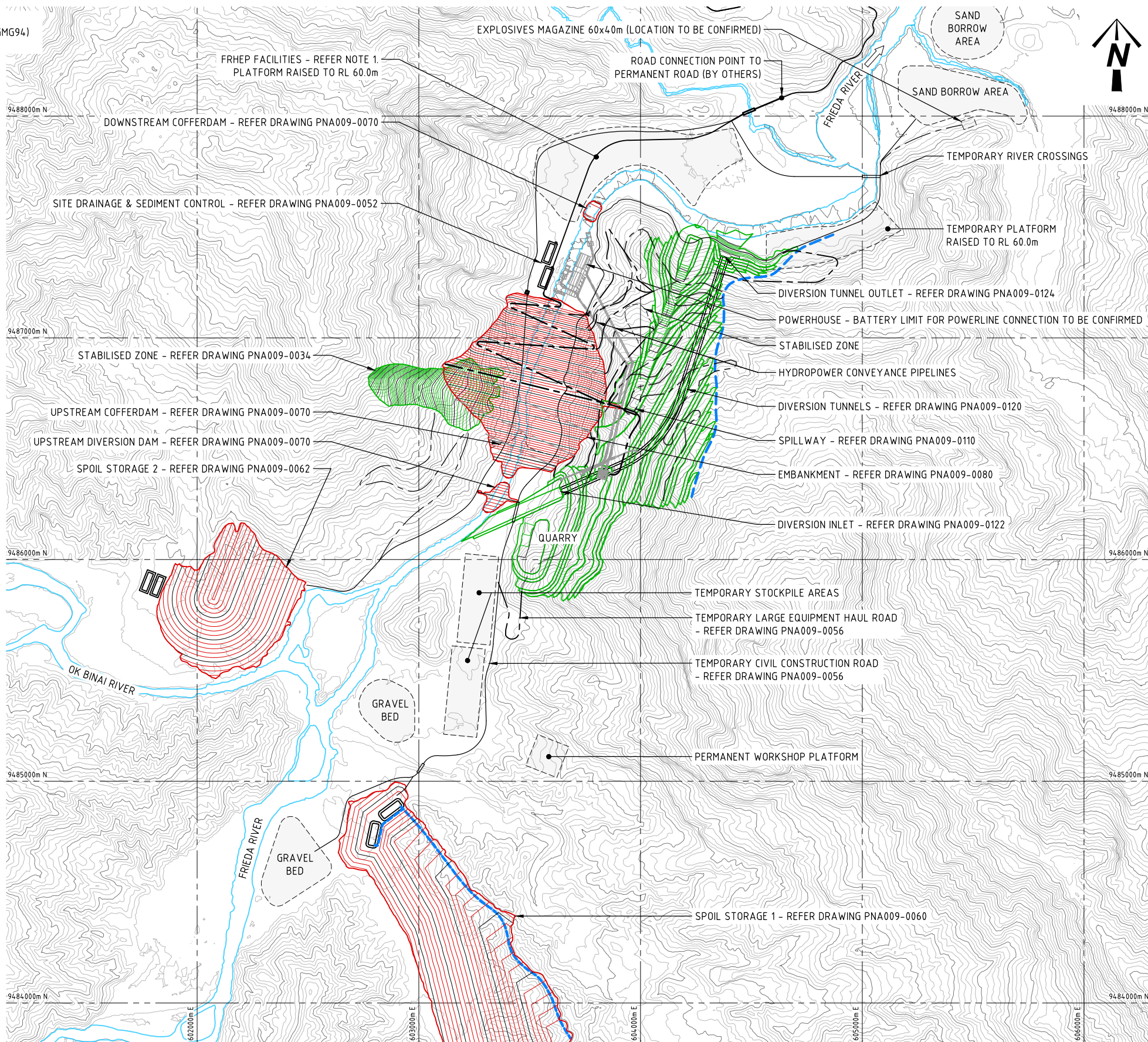


OWNER
FRIEDA RIVER LIMITED

TITLE
**FRIEDA RIVER HYDROELECTRIC PROJECT
WASTE ROCK & TAILINGS
DEPOSITION LAYOUT (33 YEAR LOM.)**

STATUS FOR INFORMATION		
SCALE	AS SHOWN	REV No.
		C
		SIZE
		A1
DRAWING No		
FRP-2-D-00-01-D-030-002		

PROJECTION: UNIVERSAL TRANSVERSE MERCATOR, ZONE 54
 HORIZONTAL DATUM: PAPUA NEW GUINEA MAP GRID 1994 (PNGMG94)
 VERTICAL DATUM: AITAPE MEAN SEA LEVEL (MSL)

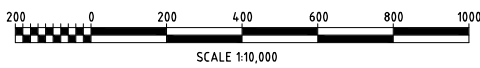


NOTE:

1. - FRHEP FACILITIES:
 - 1.1. OFFICES
 - 1.2. LABORATORY
 - 1.3. EQUIPMENT WORKSHOPS FOR CIVIL EQUIPMENT
 - 1.3. EQUIPMENT WORKSHOPS FOR QUARRY EQUIPMENT
 - 1.4. GENERAL WORKSHOPS
 - 1.5. STORAGE FOR EQUIPMENT AND TOOLS
 - 1.6. CONCRETE BATCHING PLANT
 - 1.7. ASPHALT BATCHING PLANT
 - 1.7. GROUTING PLANT
 - 1.8. CRUSHER FACILITIES
 - 1.9. TEMPORARY STOCKPILE AREA
 - 1.10. OFFICES (CLIENT)
 - 1.11. STORAGE FOR EQUIPMENT (CLIENT)

LEGEND:

- DESIGN SURFACE CONTOURS (CUT)
- DESIGN SURFACE CONTOURS (FILL)
- TUNNEL (DIVERSION & POWER HOUSE)
- ROAD (TEMPORARY)
- ROAD RIVER CROSSING
- ROAD (PERMANENT)
- SEDIMENT PONDS



SITE GENERAL ARRANGEMENT
 SCALE 1:10,000

P:\PNA009 - FRIEDA RIVER HEP PFS\04_WORKING_FILES_V2_DRAFTING\00 - DRAWINGS\01 - SHEETS\PNA009-0020.DWG - 27/09/2018 9:55:37 AM

REF. DWG No.	DWG. DESCRIPTION	No	DATE	REVISION DETAILS	LD ENG.	PM
		D	25.09.18	ISSUED FOR FINAL REPORT	MORE	MORE
		C	03.09.18	REISSUED FOR CLIENT REVIEW	MORE	MORE
		B	18.07.18	REISSUED FOR CLIENT REVIEW	MORE	MORE
		A	31.05.18	ISSUED FOR CLIENT REVIEW	MORE	MORE

ENGINEERING COMPANY



SRK Perth 10 Richardson Street, West Perth, Western Australia 6005
 Tel: +61 8 9288 2000 - Fax: +61 8 9288 2001
<http://www.srk.com.au>

DRAWN	TREV	31.05.18
DESIGN	PRIN	31.05.18
DES.CHKD	MORE	31.05.18
LD ENG. APPR	MORE	31.05.18
PM, APPR	MORE	31.05.18

VENDOR DRG NO. PNA009-0020



FRIEDA RIVER

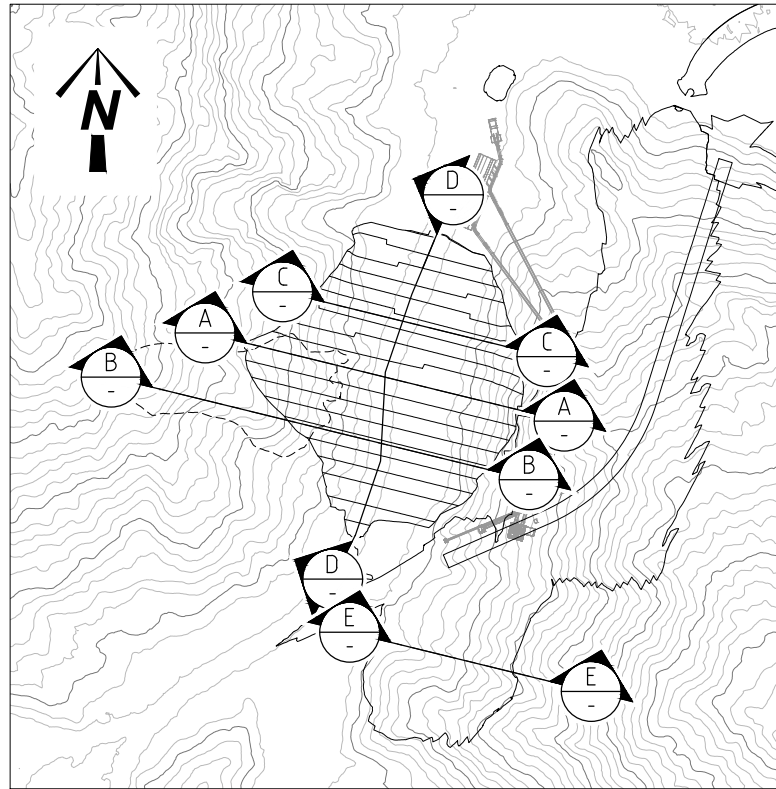
OWNER
 FRIEDA RIVER LIMITED

TITLE
 FRIEDA RIVER HYDROELECTRIC PROJECT

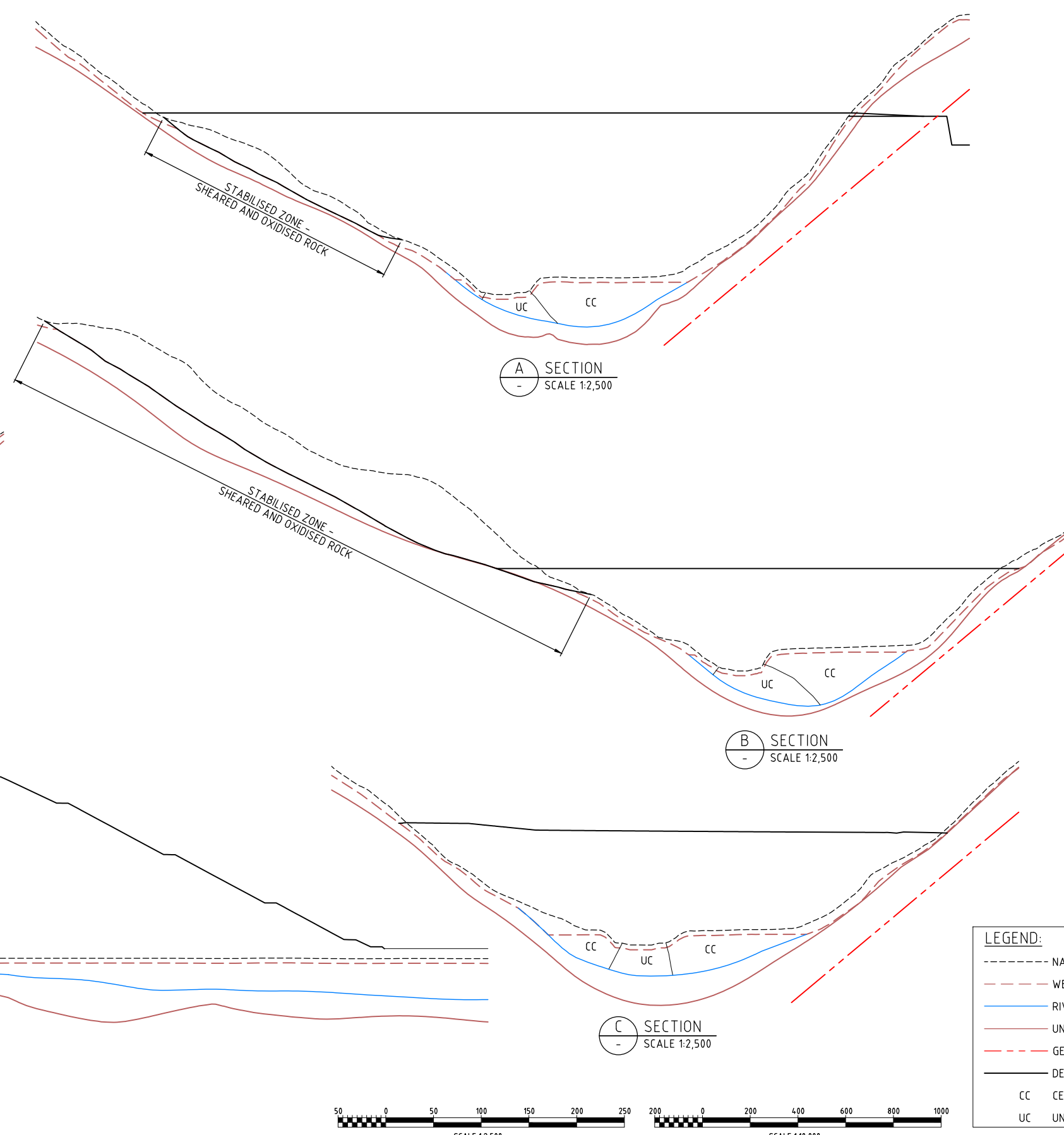
SITE GENERAL ARRANGEMENT

STATUS FOR INFORMATION			
SCALE	AS SHOWN	REV No.	SIZE
ALL DIMENSIONS IN METRES		D	A1
DRAWING No FRP-2-D-00-01-D-030-003			

PROJECTION: UNIVERSAL TRANSVERSE MERCATOR, ZONE 54
 HORIZONTAL DATUM: PAPUA NEW GUINEA MAP GRID 1994 (PNGMG94)
 VERTICAL DATUM: AITAPE MEAN SEA LEVEL (MSL)



HEP SURFICIAL GEOLOGY SECTIONS KEY PLAN
 SCALE 1:10,000



E SECTION
 SCALE 1:2,500

A SECTION
 SCALE 1:2,500

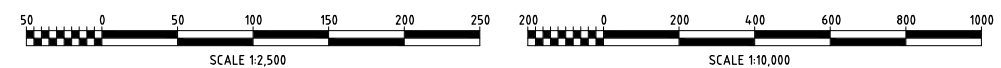
B SECTION
 SCALE 1:2,500

D SECTION
 SCALE 1:2,500

C SECTION
 SCALE 1:2,500

LEGEND:

- NATURAL GROUND
- - - WEATHERED BEDROCK
- RIVER CHANNEL
- UNWEATHERED BEDROCK
- - - GEOLOGICAL FEATURE
- DESIGN SURFACE
- CC CEMENTED CO/ALLUVIUM
- UC UNCEMENTED ALLUVIUM



P:\PNA009 - FRIEDA RIVER HEP PFS\04_WORKING_FILES_V2_DRAFTING\00 - DRAWINGS\01 - SHEETS\PNA009-0030.DWG - 27/09/2018 9:55:52 AM

REF. DWG No.	DWG. DESCRIPTION	No	DATE	REVISION DETAILS	LD ENG.	PM
		C	25.09.18	ISSUED FOR FINAL REPORT	MORE	MORE
		B	18.07.18	REISSUED FOR CLIENT REVIEW	MORE	MORE
		A	31.05.18	ISSUED FOR CLIENT REVIEW	MORE	MORE

ENGINEERING COMPANY

 SRK Perth 10 Richardson Street, West Perth, Western Australia 6005
 Tel: +61 8 9288 2000 - Fax: +61 8 9288 2001
<http://www.srk.com.au>

DRAWN	TREV	31.05.18
DESIGN	PRIN	31.05.18
DES.CHKD	MORE	31.05.18
LD ENG. APPR	MORE	31.05.18
PM, APPR	MORE	31.05.18

VENDOR DRG NO. PNA009-0030

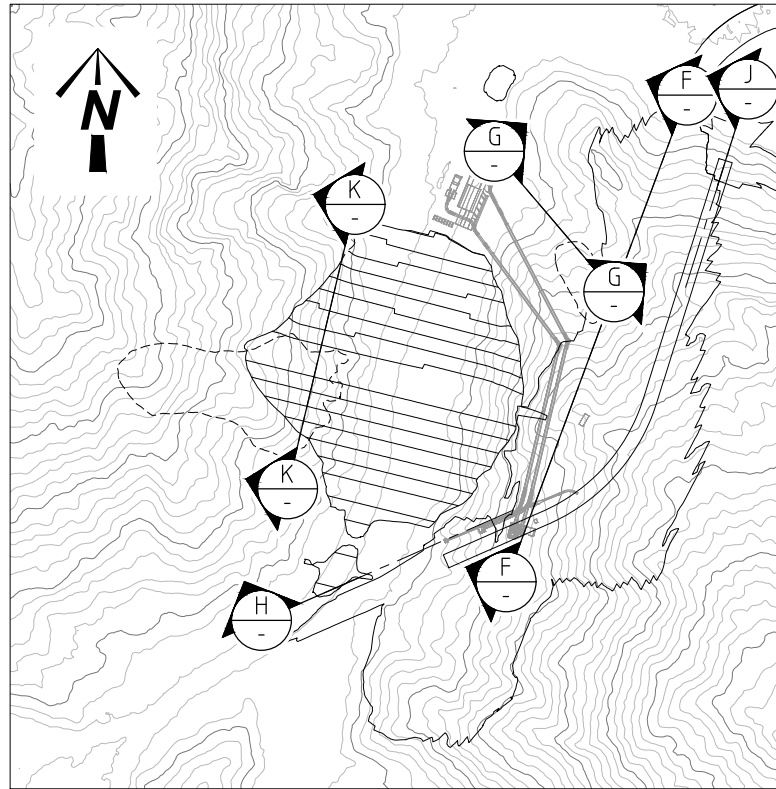
OWNER
 FRIEDA RIVER LIMITED

TITLE
 FRIEDA RIVER HYDROELECTRIC PROJECT
 SURFICIAL GEOLOGY
 SECTIONS SHEET 1 OF 2

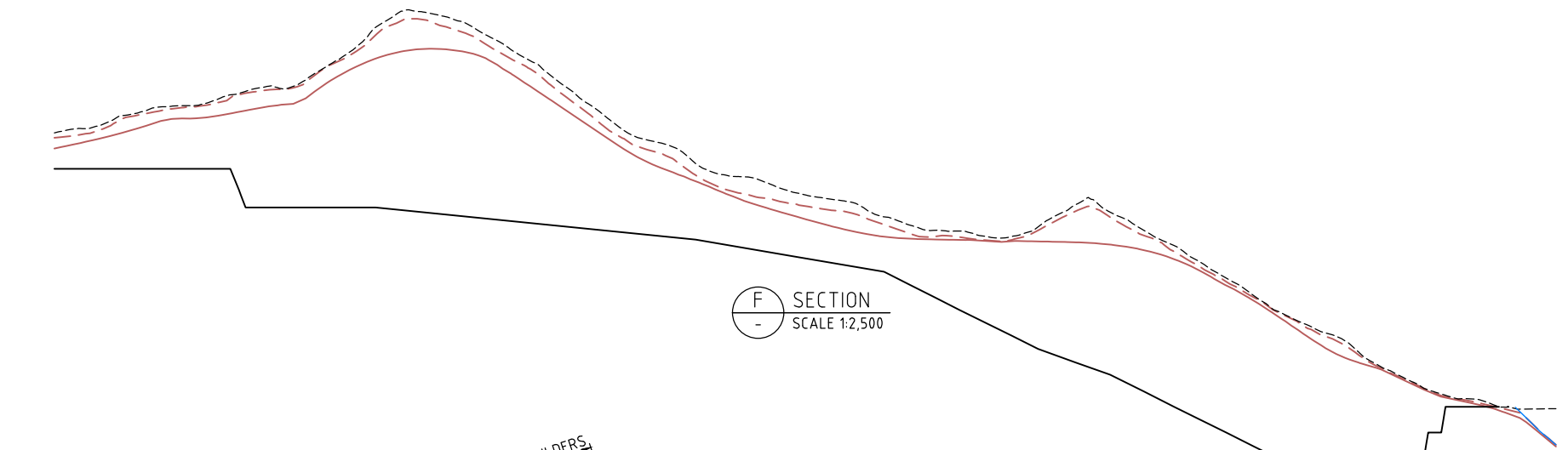
STATUS FOR INFORMATION

SCALE	AS SHOWN	REV No.	C	SIZE	A1
ALL DIMENSIONS IN METRES					
DRAWING No FRP-2-D-00-01-D-030-004					

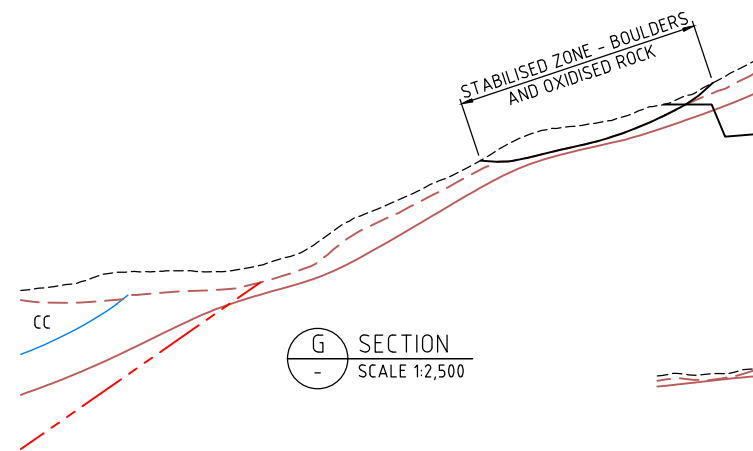
PROJECTION: UNIVERSAL TRANSVERSE MERCATOR, ZONE 54
 HORIZONTAL DATUM: PAPUA NEW GUINEA MAP GRID 1994 (PNGMG94)
 VERTICAL DATUM: AITAPE MEAN SEA LEVEL (MSL)



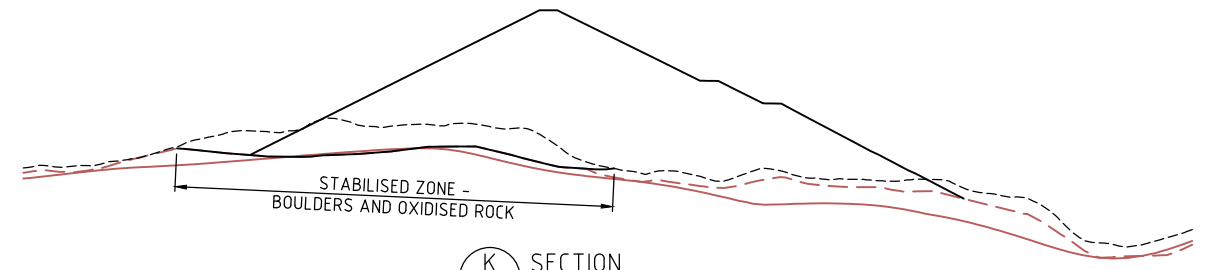
HEP SURFICIAL GEOLOGY SECTIONS KEY PLAN
 SCALE 1:10,000



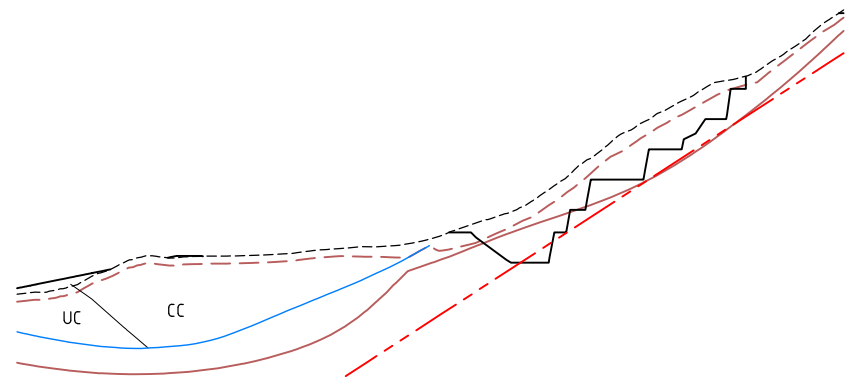
F SECTION
 SCALE 1:2,500



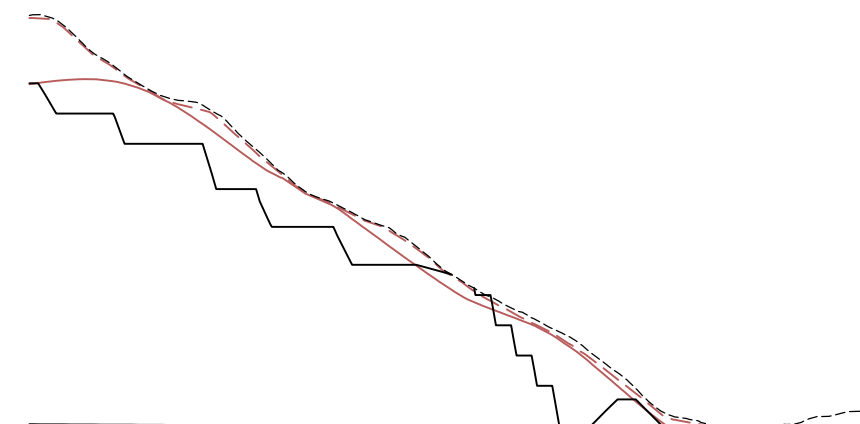
G SECTION
 SCALE 1:2,500



K SECTION
 SCALE 1:2,500



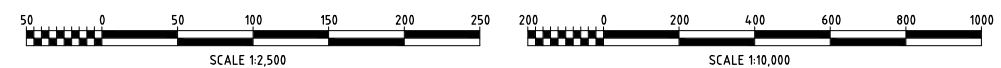
H SECTION
 SCALE 1:2,500



J SECTION
 SCALE 1:2,500

LEGEND:

- NATURAL GROUND
- WEATHERED BEDROCK
- RIVER CHANNEL
- UNWEATHERED BEDROCK
- GEOLOGICAL FEATURE
- DESIGN SURFACE
- CC CEMENTED CO/ALLUVIUM
- UC UNCEMENTED ALLUVIUM



P:\PNA009 - FRIEDA RIVER HEP PFS\04_WORKING_FILES_V2_DRAFTING\00 - DRAWINGS\01 - SHEETS\PNA009-0032.DWG - 27/09/2018 9:56:04 AM

REF. DWG No.	DWG. DESCRIPTION	No	DATE	REVISION DETAILS	LD ENG.	PM
		C	25.09.18	ISSUED FOR FINAL REPORT	MORE	MORE
		B	18.07.18	REISSUED FOR CLIENT REVIEW	MORE	MORE
		A	31.05.18	ISSUED FOR CLIENT REVIEW	MORE	MORE

ENGINEERING COMPANY

SRK Perth 10 Richardson Street, West Perth, Western Australia 6005
 Tel: +61 8 9288 2000 - Fax: +61 8 9288 2001
<http://www.srk.com.au>

DRAWN	TREV	31.05.18
DESIGN	PRIN	31.05.18
DES.CHKD	MORE	31.05.18
LD ENG. APPR	MORE	31.05.18
PM, APPR	MORE	31.05.18

VENDOR DRG NO. PNA009-0032

OWNER
FRIEDA RIVER LIMITED

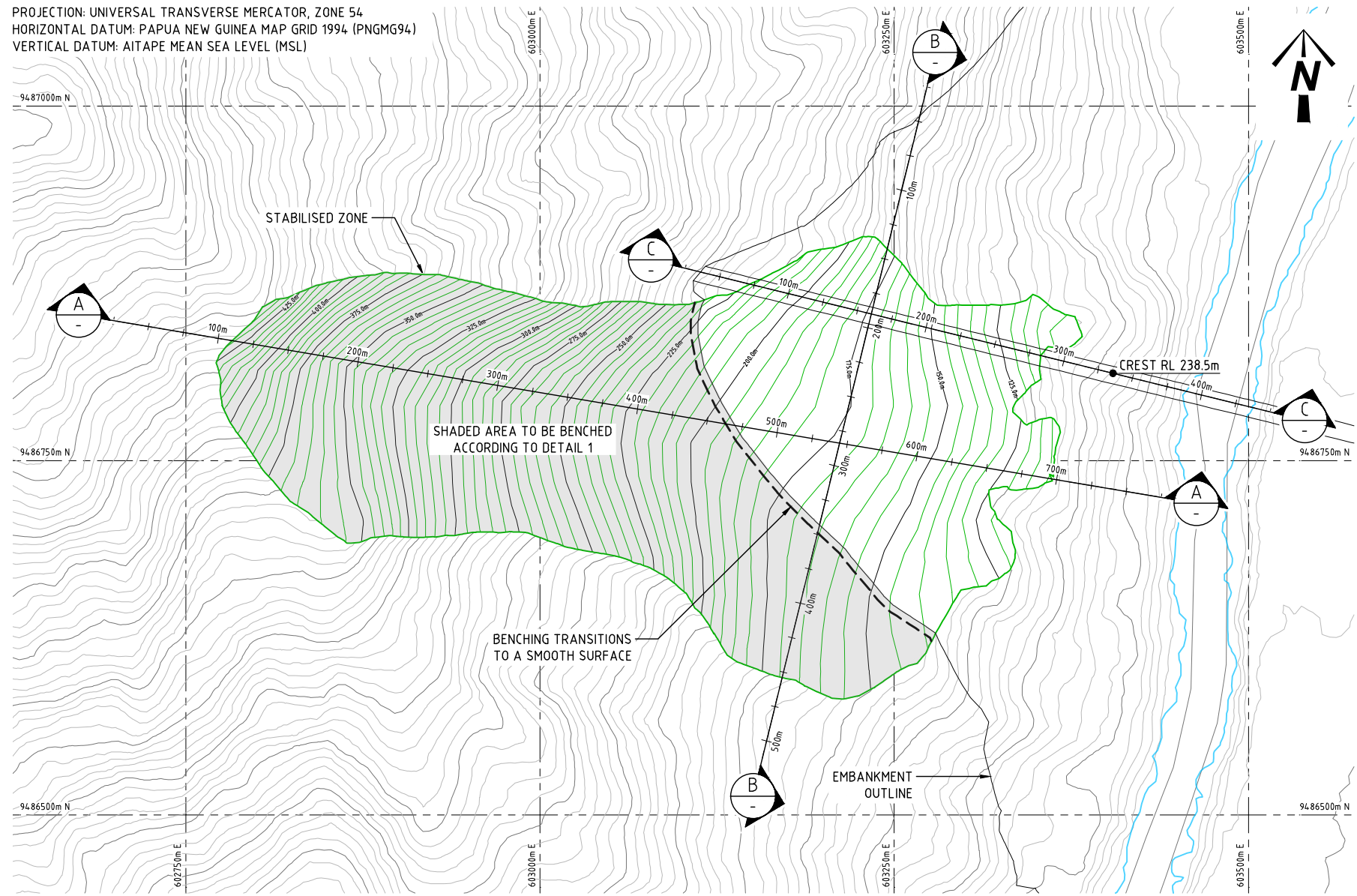
TITLE
**FRIEDA RIVER HYDROELECTRIC PROJECT
 SURFICIAL GEOLOGY
 SECTIONS SHEET 2 OF 2**

STATUS
FOR INFORMATION

SCALE	AS SHOWN	REV No.	SIZE
		C	A1

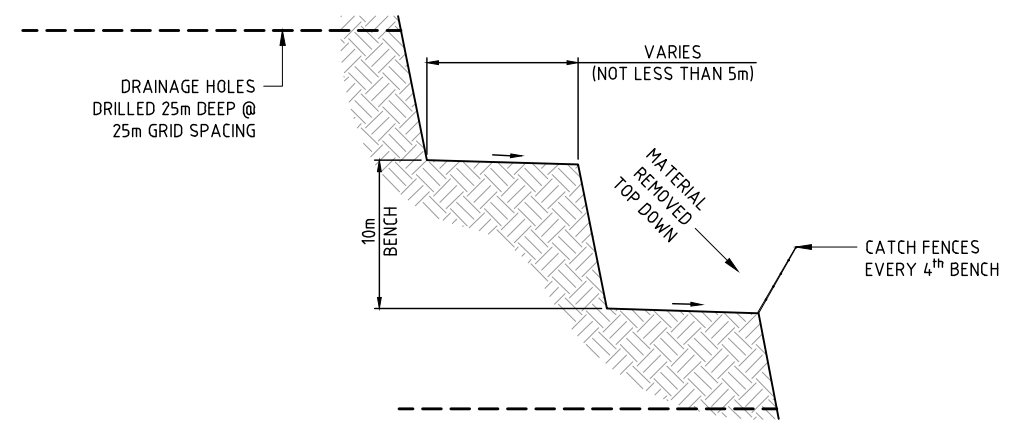
DRAWING No
FRP-2-D-00-01-D-030-005

PROJECTION: UNIVERSAL TRANSVERSE MERCATOR, ZONE 54
 HORIZONTAL DATUM: PAPUA NEW GUINEA MAP GRID 1994 (PNGMG94)
 VERTICAL DATUM: AITAPE MEAN SEA LEVEL (MSL)

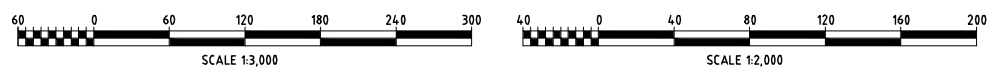


POTENTIAL UNSTABLE ZONE EXCAVATION LAYOUT
 SCALE 1:2,000

NOTE:
 MOUNTAINOUS CUT FACES TO HAVE SPOT BOLTING



1 DETAIL
 SCALE 1:250



P:\PNA09 - FRIEDA RIVER HEP PFS\04_WORKING_FILES_V2_DRAFTING\00 - DRAWINGS\01 - SHEETS\PNA09-0034.DWG - 27/09/2018 1:20:20 PM

REF. DWG No.	DWG. DESCRIPTION	No	DATE	REVISION DETAILS	LD ENG.	PM
		C	25.09.18	ISSUED FOR FINAL REPORT	MORE	MORE
		B	18.07.18	REISSUED FOR CLIENT REVIEW	MORE	MORE
		A	31.05.18	ISSUED FOR CLIENT REVIEW	MORE	MORE

ENGINEERING COMPANY

 SRK Perth 10 Richardson Street, West Perth, Western Australia 6005
 Tel: +61 8 9288 2000 - Fax: +61 8 9288 2001
<http://www.srk.com.au>

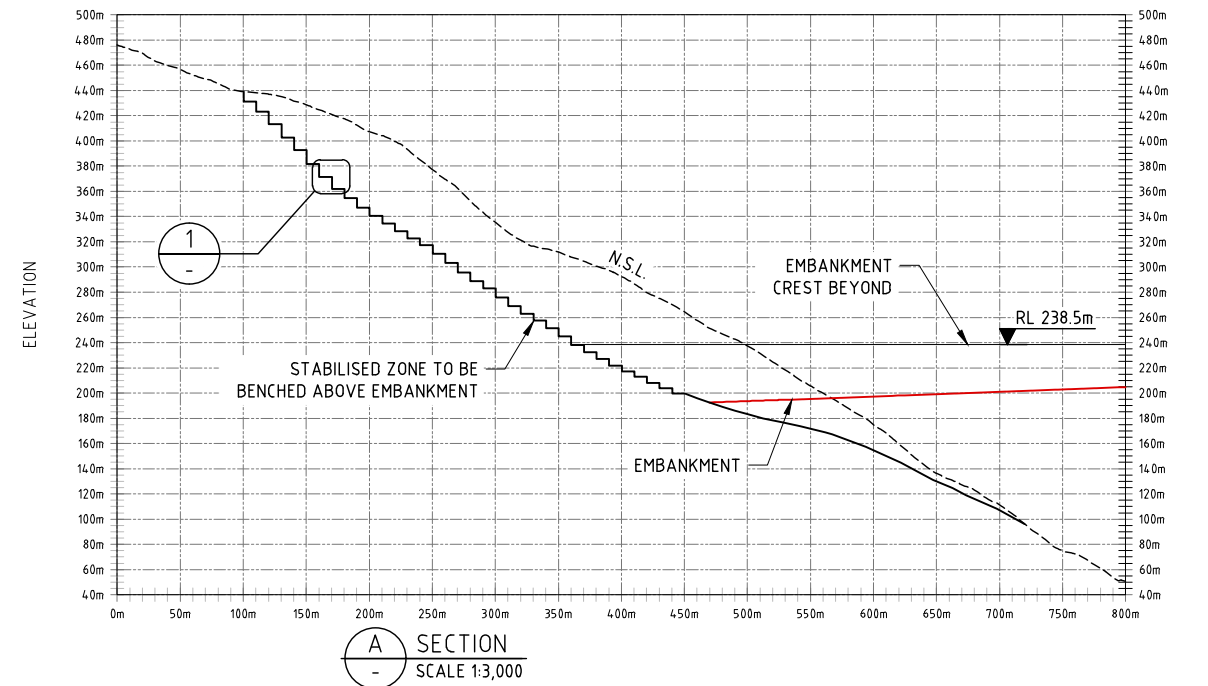
DRAWN	TREV	31.05.18
DESIGN	PRIN	31.05.18
DES.CHKD	MORE	31.05.18
LD ENG. APPR	MORE	31.05.18
PM. APPR	MORE	31.05.18

VENDOR DRG NO. PNA09-0034

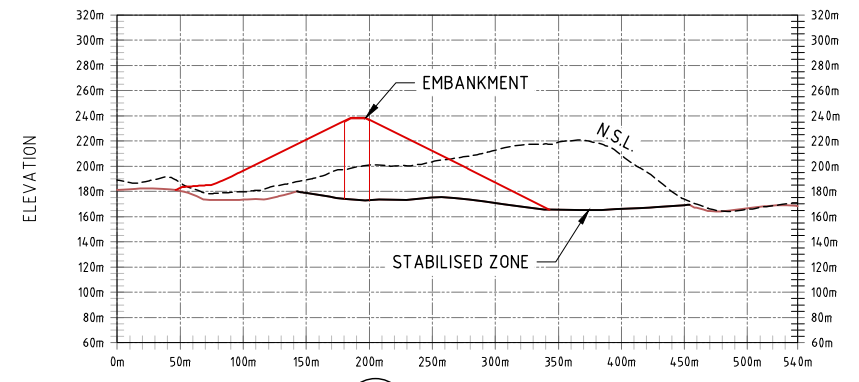
OWNER
FRIEDA RIVER LIMITED

TITLE
**FRIEDA RIVER HYDROELECTRIC PROJECT
 STABILISED ZONE EXCAVATION LAYOUT &
 SECTIONS**

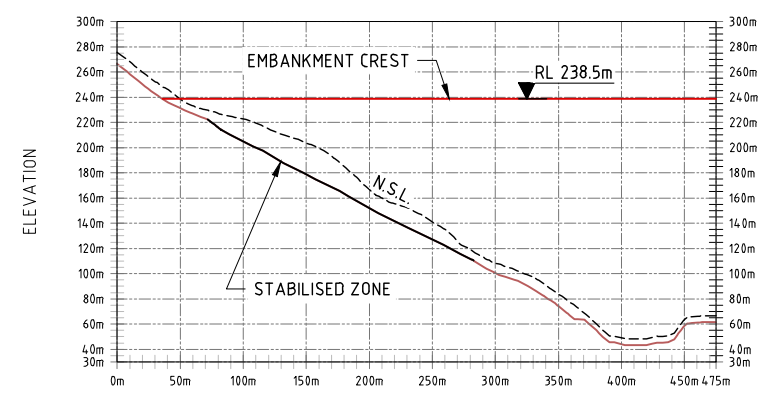
STATUS FOR INFORMATION		
SCALE	AS SHOWN	REV No.
		C
ALL DIMENSIONS IN METRES		SIZE
		A1
DRAWING No		
FRP-2-D-00-01-D-030-006		



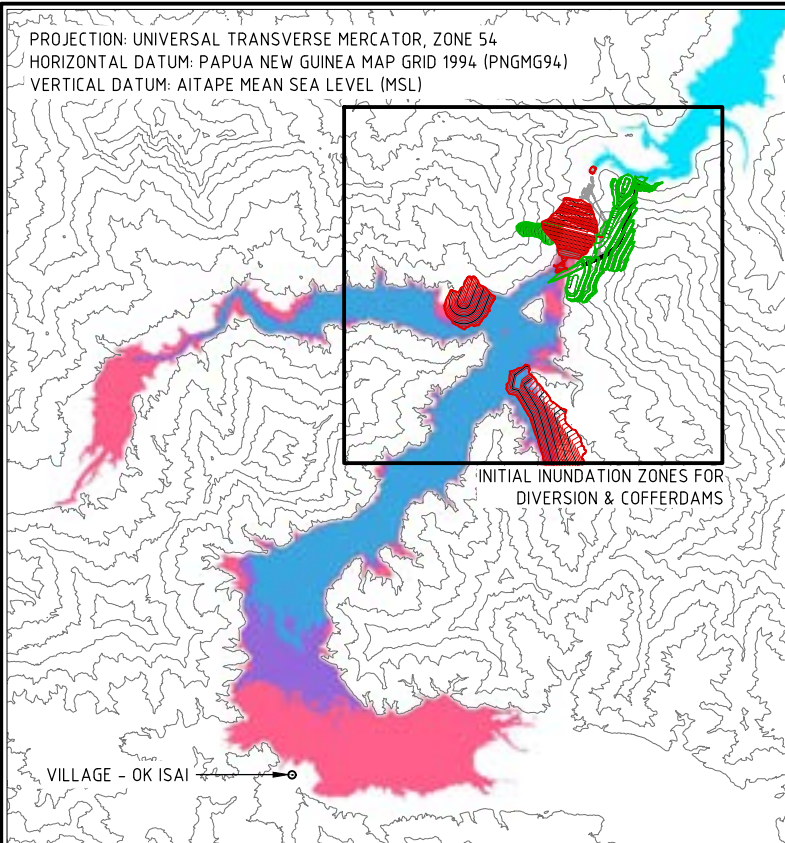
A SECTION
 SCALE 1:3,000



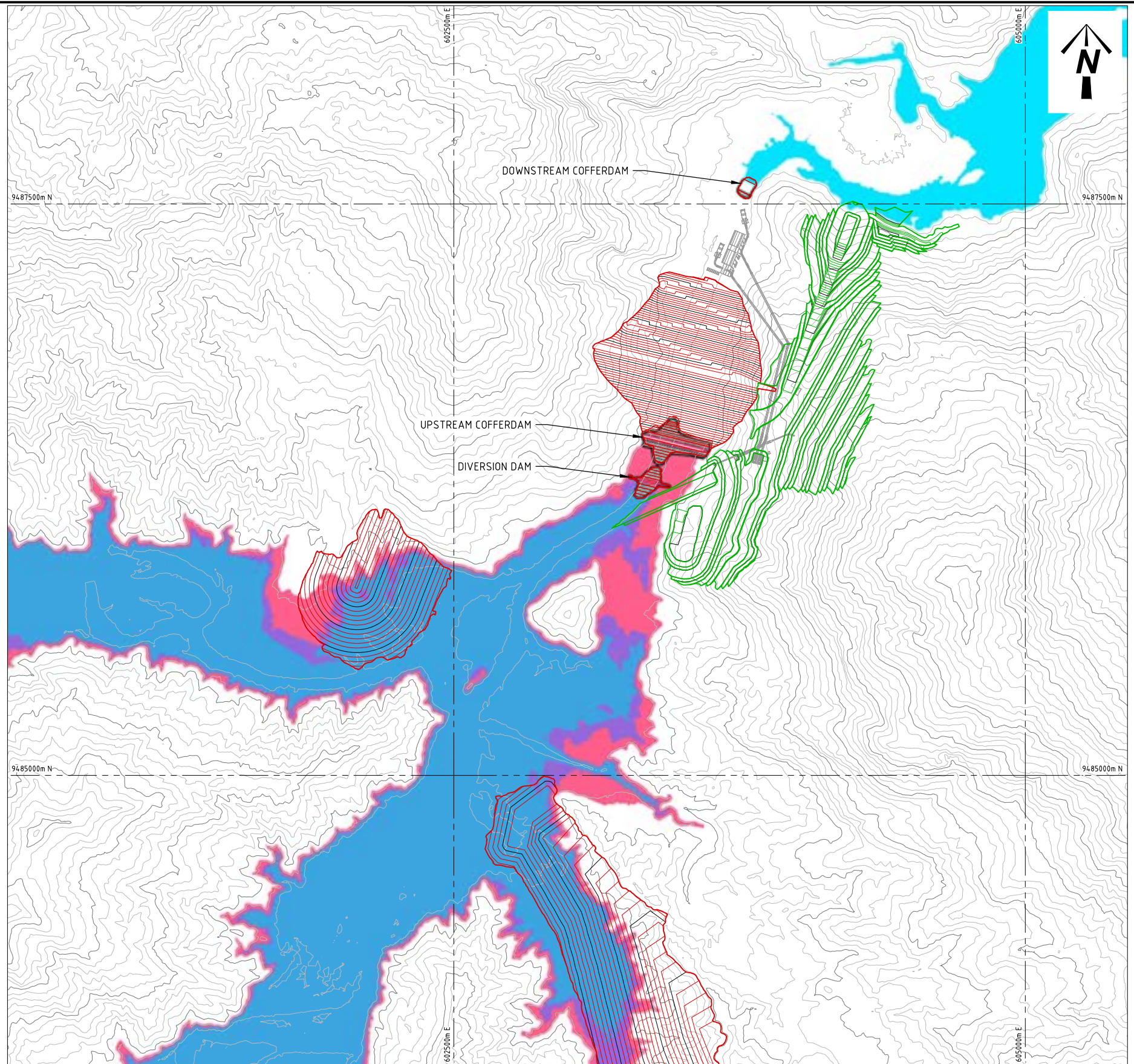
B SECTION
 SCALE 1:3,000



C SECTION
 SCALE 1:3,000



INITIAL INUNDATION LAYOUT
 SCALE 1:50,000



INITIAL INUNDATION ZONES FOR DIVERSION & COFFERDAMS
 SCALE 1:10,000

LEGEND	
	RL 82.3 (0.7m BELOW TOP OF MAIN COFFERDAM)
	RL 74.0 (0.5m BELOW TOP OF DIVERSION DAM)
	RL 70.1 (LARGEST RECORDED STREAM FLOW EVENT DURING 2012-13)
	RL 55.1 (0.4m BELOW TOP OF D/S COFFERDAM)



P:\PNA009 - FRIEDA RIVER HEP PFS\04_WORKING_FILES_V2_DRAFTING\00 - DRAWINGS\01 - SHEETS\PNA009-0040.DWG - 27/09/2018 9:57:20 AM

REF. DWG No.	DWG. DESCRIPTION	No	DATE	REVISION DETAILS	LD ENG.	PM
		C	25.09.18	ISSUED FOR FINAL REPORT	MORE	MORE
		B	18.07.18	REISSUED FOR CLIENT REVIEW	MORE	MORE
		A	31.05.18	ISSUED FOR CLIENT REVIEW	MORE	MORE

ENGINEERING COMPANY

SRK Perth 10 Richardson Street, West Perth, Western Australia 6005
 Tel: +61 8 9288 2000 - Fax: +61 8 9288 2001
<http://www.srk.com.au>

DRAWN	TREV	31.05.18
DESIGN	PRIN	31.05.18
DES.CHKD	MORE	31.05.18
LD ENG. APPR	MORE	31.05.18
PM, APPR	MORE	31.05.18

VENDOR DRG NO. PNA009-0040

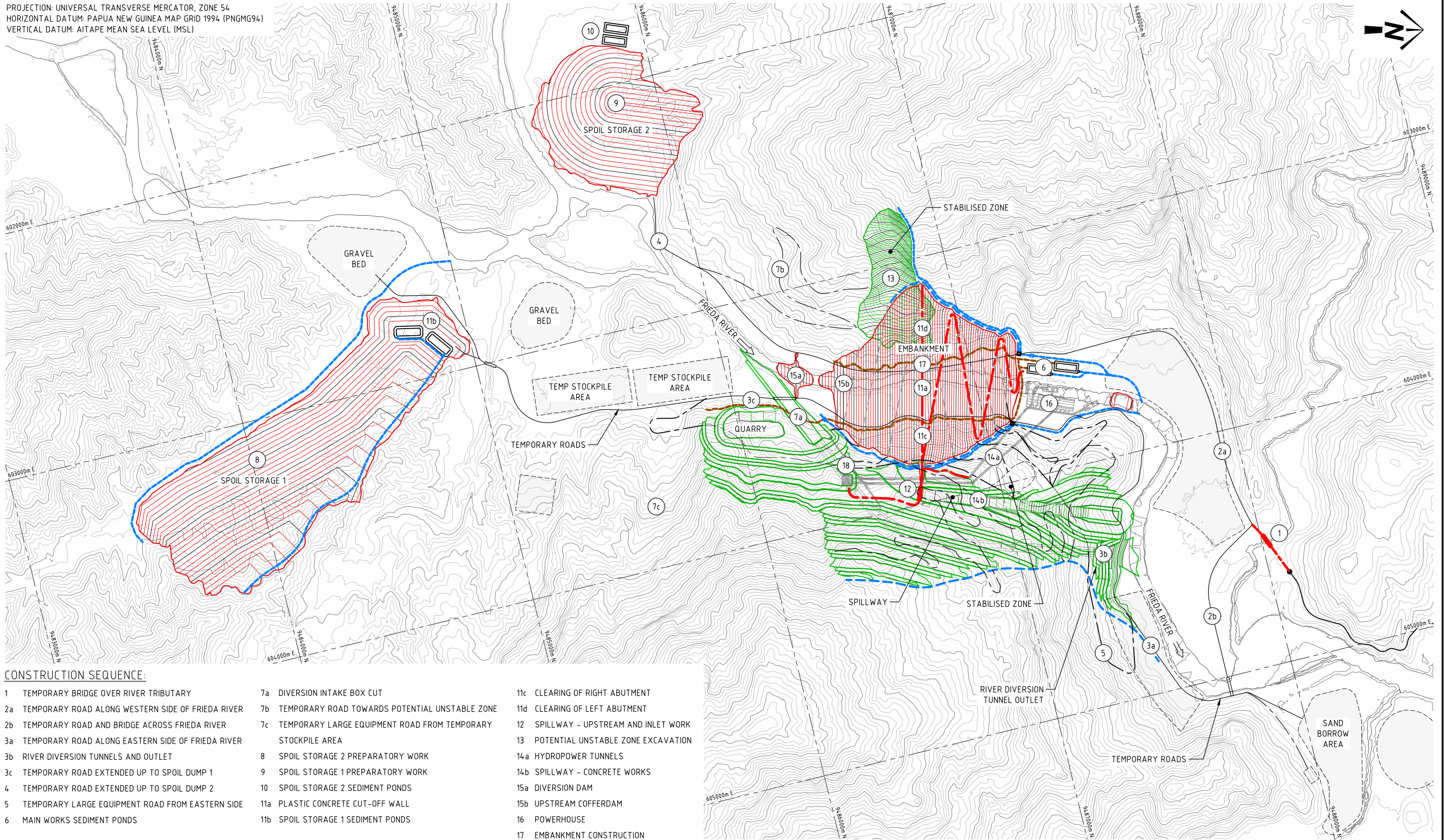
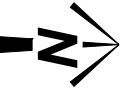
FRIEDA RIVER

OWNER
FRIEDA RIVER LIMITED

TITLE
**FRIEDA RIVER HYDROELECTRIC PROJECT
 INITIAL INUNDATION ZONES FOR
 DIVERSION & COFFERDAMS**

STATUS FOR INFORMATION			
SCALE	AS SHOWN	REV No.	SIZE
ALL DIMENSIONS IN METRES		C	A1
DRAWING No FRP-2-D-00-01-D-030-007			

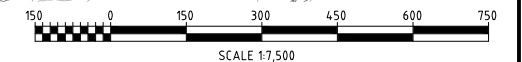
PROJECTION: UNIVERSAL TRANSVERSE MERCATOR, ZONE 54
 HORIZONTAL DATUM: PAPUA NEW GUINEA MAP GRID 1994 (PNGMG94)
 VERTICAL DATUM: AITAPE MEAN SEA LEVEL (MSL)



CONSTRUCTION SEQUENCE:

- | | | |
|------------------------------------------------------|-----------------------------------------------------------------|---------------------------------------|
| 1 TEMPORARY BRIDGE OVER RIVER TRIBUTARY | 7a DIVERSION INTAKE BOX CUT | 11c CLEARING OF RIGHT ABUTMENT |
| 2a TEMPORARY ROAD ALONG WESTERN SIDE OF FRIEDA RIVER | 7b TEMPORARY ROAD TOWARDS POTENTIAL UNSTABLE ZONE | 11d CLEARING OF LEFT ABUTMENT |
| 2b TEMPORARY ROAD AND BRIDGE ACROSS FRIEDA RIVER | 7c TEMPORARY LARGE EQUIPMENT ROAD FROM TEMPORARY STOCKPILE AREA | 12 SPILLWAY - UPSTREAM AND INLET WORK |
| 3a TEMPORARY ROAD ALONG EASTERN SIDE OF FRIEDA RIVER | 8 SPOIL STORAGE 2 PREPARATORY WORK | 13 POTENTIAL UNSTABLE ZONE EXCAVATION |
| 3b RIVER DIVERSION TUNNELS AND OUTLET | 9 SPOIL STORAGE 1 PREPARATORY WORK | 14a HYDROPOWER TUNNELS |
| 3c TEMPORARY ROAD EXTENDED UP TO SPOIL DUMP 1 | 10 SPOIL STORAGE 2 SEDIMENT PONDS | 14b SPILLWAY - CONCRETE WORKS |
| 4 TEMPORARY ROAD EXTENDED UP TO SPOIL DUMP 2 | 11a PLASTIC CONCRETE CUT-OFF WALL | 15a DIVERSION DAM |
| 5 TEMPORARY LARGE EQUIPMENT ROAD FROM EASTERN SIDE | 11b SPOIL STORAGE 1 SEDIMENT PONDS | 15b UPSTREAM COFFERDAM |
| 6 MAIN WORKS SEDIMENT PONDS | | 16 POWERHOUSE |
| | | 17 EMBANKMENT CONSTRUCTION |
| | | 18 HYDROPOWER INTAKES |

CONSTRUCTION SEQUENCE LAYOUT
 SCALE 1:7,500



P:\PNA009 - FRIEDA RIVER HEP PFS\04_WORKING_FILES_V2_DRAFTING\00 - DRAWINGS\01 - SHEETS\PNA009-0042.DWG - 27/09/2018 9:57:45 AM

REF. DWG No.	DWG. DESCRIPTION	No	DATE	REVISION DETAILS	LD ENG.	PM
		D	25.09.18	ISSUED FOR FINAL REPORT	MORE	MORE
		C	03.09.18	REISSUED FOR CLIENT REVIEW	MORE	MORE
		B	18.07.18	REISSUED FOR CLIENT REVIEW	MORE	MORE
		A	31.05.18	ISSUED FOR CLIENT REVIEW	MORE	MORE

ENGINEERING COMPANY

SRK Perth 10 Richardson Street, West Perth, Western Australia 6005
 Tel: +61 8 9288 2000 - Fax: +61 8 9288 2001
<http://www.srk.com.au>

DRAWN	TREV	31.05.18
DESIGN	PRIN	31.05.18
DES.CHKD	MORE	31.05.18
LD ENG. APPR	MORE	31.05.18
PM, APPR	MORE	31.05.18

VENDOR DRG NO. PNA009-0042

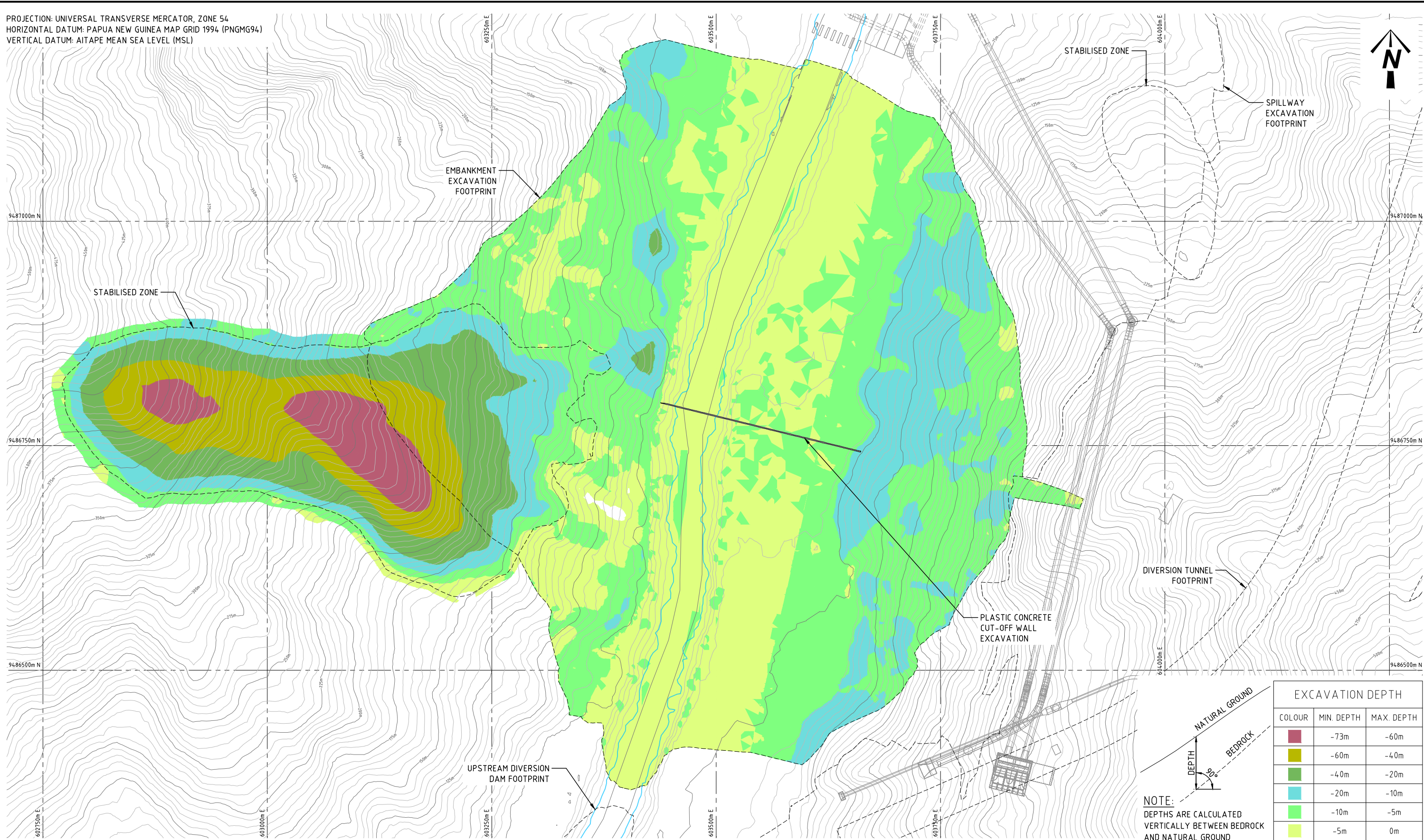
FRIEDA RIVER

OWNER
FRIEDA RIVER LIMITED

TITLE
FRIEDA RIVER HYDROELECTRIC PROJECT
CONSTRUCTION SEQUENCE LAYOUT

STATUS FOR INFORMATION		
SCALE	AS SHOWN	REV No.
		D
SIZE		A1
DRAWING No		
FRP-2-D-00-01-D-030-008		

PROJECTION: UNIVERSAL TRANSVERSE MERCATOR, ZONE 54
 HORIZONTAL DATUM: PAPUA NEW GUINEA MAP GRID 1994 (PNGMG94)
 VERTICAL DATUM: AITAPE MEAN SEA LEVEL (MSL)



FOUNDATION EXCAVATION DEPTH MAP
 SCALE 1:2,000

P:\PNA009 - FRIEDA RIVER HEP PFS\04_WORKING_FILES_V2_DRAFTING\00 - DRAWINGS\01 - SHEETS\PNA009-0044.DWG - 27/09/2018 12:25:58 PM

REF. DWG No.	DWG. DESCRIPTION	No	DATE	REVISION DETAILS	LD ENG.	PM
		C	25.09.18	ISSUED FOR FINAL REPORT	MORE	MORE
		B	18.07.18	REISSUED FOR CLIENT REVIEW	MORE	MORE
		A	31.05.18	ISSUED FOR CLIENT REVIEW	MORE	MORE

ENGINEERING COMPANY



SRK Perth 10 Richardson Street, West Perth, Western Australia 6005
 Tel: +61 8 9288 2000 - Fax: +61 8 9288 2001
<http://www.srk.com.au>

DRAWN	TREV	31.05.18
DESIGN	PRIN	31.05.18
DES.CHKD	MORE	31.05.18
LD ENG. APPR	MORE	31.05.18
PM. APPR	MORE	31.05.18

VENDOR DRG NO. PNA009-0044



FRIEDA RIVER

OWNER
FRIEDA RIVER LIMITED

TITLE
**FRIEDA RIVER HYDROELECTRIC PROJECT
 FOUNDATION EXCAVATION
 DEPTH MAP**

STATUS FOR INFORMATION			
SCALE	AS SHOWN	REV No.	SIZE
ALL DIMENSIONS IN METRES		C	A1
DRAWING No FRP-2-D-04-01-D-030-001			

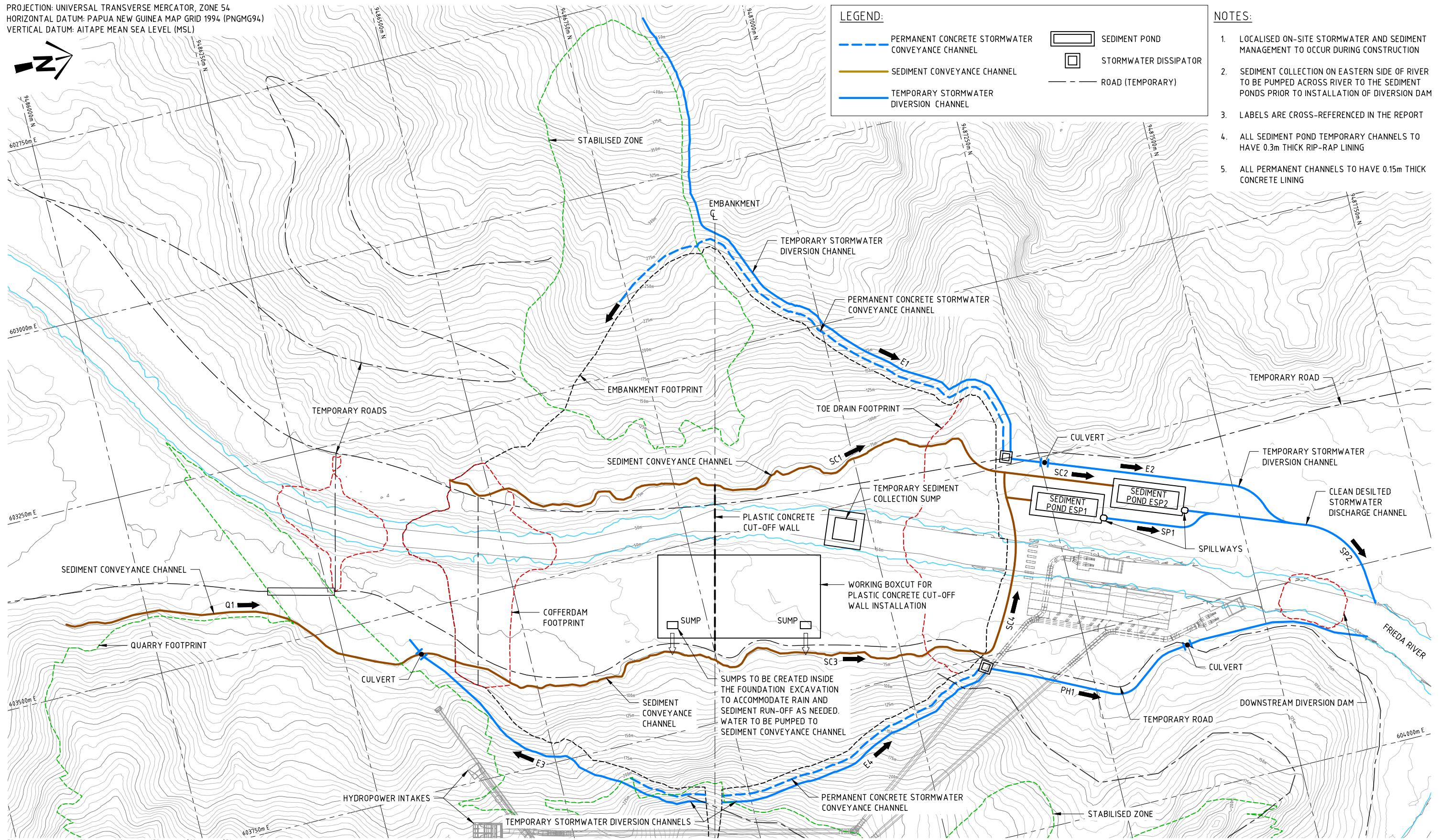
PROJECTION: UNIVERSAL TRANSVERSE MERCATOR, ZONE 54
 HORIZONTAL DATUM: PAPUA NEW GUINEA MAP GRID 1994 (PNGMG94)
 VERTICAL DATUM: AITAPE MEAN SEA LEVEL (MSL)



LEGEND:

- PERMANENT CONCRETE STORMWATER CONVEYANCE CHANNEL
- SEDIMENT CONVEYANCE CHANNEL
- TEMPORARY STORMWATER DIVERSION CHANNEL
- SEDIMENT POND
- STORMWATER DISSIPATOR
- ROAD (TEMPORARY)

- NOTES:**
1. LOCALISED ON-SITE STORMWATER AND SEDIMENT MANAGEMENT TO OCCUR DURING CONSTRUCTION
 2. SEDIMENT COLLECTION ON EASTERN SIDE OF RIVER TO BE PUMPED ACROSS RIVER TO THE SEDIMENT PONDS PRIOR TO INSTALLATION OF DIVERSION DAM
 3. LABELS ARE CROSS-REFERENCED IN THE REPORT
 4. ALL SEDIMENT POND TEMPORARY CHANNELS TO HAVE 0.3m THICK RIP-RAP LINING
 5. ALL PERMANENT CHANNELS TO HAVE 0.15m THICK CONCRETE LINING



DOWNSTREAM DRAINAGE & SEDIMENT MANAGEMENT LAYOUT
 SCALE 1:2,500

P:\PNA009 - FRIEDA RIVER HEP PFS\04_WORKING_FILES_V2_DRAFTING\00 - DRAWINGS\01 - SHEETS\PNA009-0052.DWG - 27/09/2018 1:24:46 PM

REF. DWG No.	DWG. DESCRIPTION	No	DATE	REVISION DETAILS	LD ENG.	PM
		C	25.09.18	ISSUED FOR FINAL REPORT	MORE	MORE
		B	18.07.18	REISSUED FOR CLIENT REVIEW	MORE	MORE
		A	31.05.18	ISSUED FOR CLIENT REVIEW	MORE	MORE

ENGINEERING COMPANY

srk

SRK Perth 10 Richardson Street, West Perth, Western Australia 6005
 Tel: +61 8 9288 2000 - Fax: +61 8 9288 2001
<http://www.srk.com.au>

DRAWN	TREV	31.05.18
DESIGN	PRIN	31.05.18
DES.CHKD	MORE	31.05.18
LD ENG. APPR	MORE	31.05.18
PM APPR	MORE	31.05.18

VENDOR DRG NO. PNA009-0052

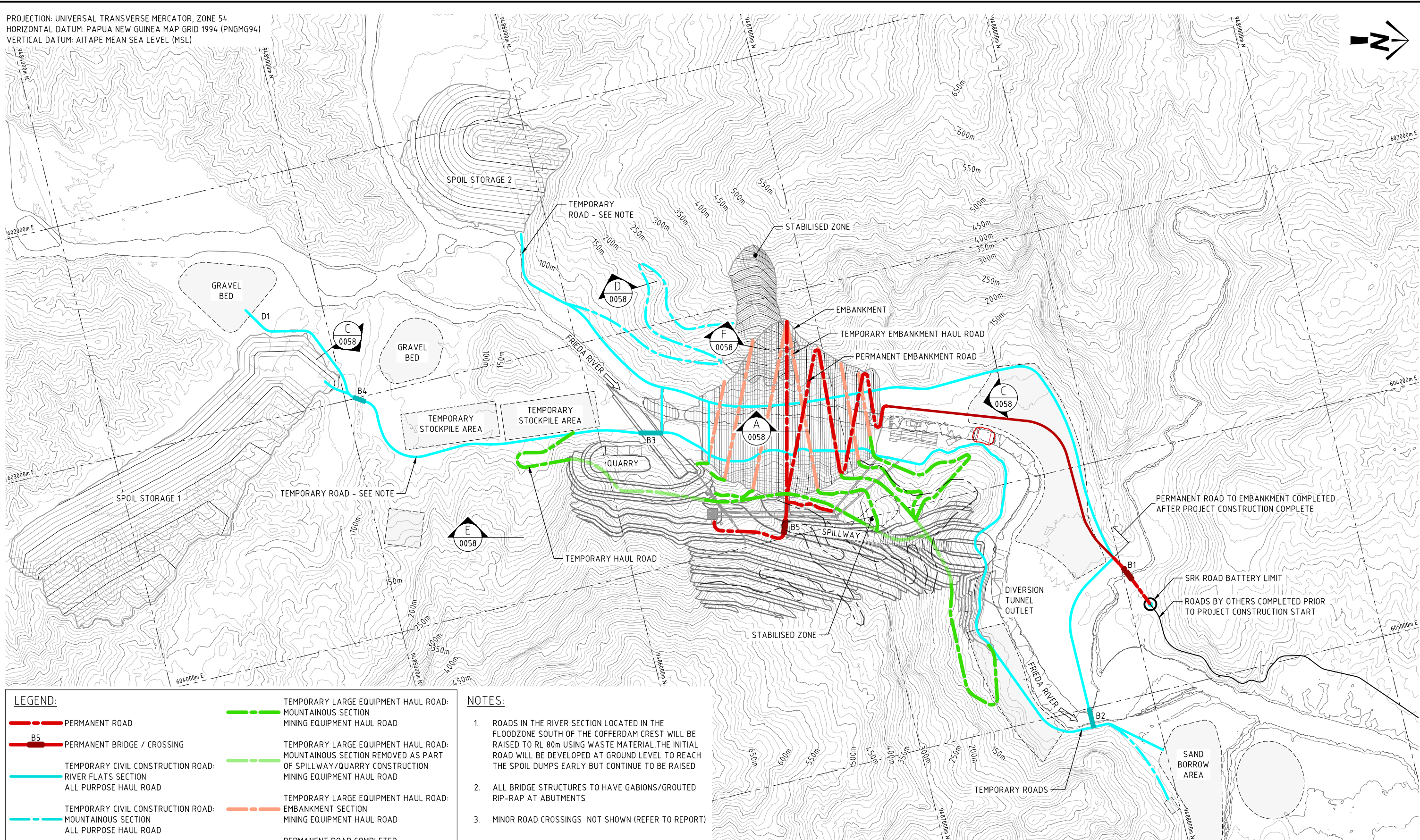
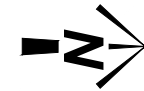


OWNER
 FRIEDA RIVER LIMITED

TITLE
 FRIEDA RIVER HYDROELECTRIC PROJECT
 DOWNSTREAM DRAINAGE & SEDIMENT MANAGEMENT LAYOUT

STATUS FOR INFORMATION			
SCALE	AS SHOWN	REV No.	SIZE
	ALL DIMENSIONS IN METRES	C	A1
DRAWING No		FRP-2-D-00-01-D-030-009	

PROJECTION: UNIVERSAL TRANSVERSE MERCATOR, ZONE 54
 HORIZONTAL DATUM: PAPUA NEW GUINEA MAP GRID 1994 (PNGMG94)
 VERTICAL DATUM: AITAPE MEAN SEA LEVEL (MSL)



LEGEND:	
	PERMANENT ROAD
	PERMANENT BRIDGE / CROSSING
	TEMPORARY CIVIL CONSTRUCTION ROAD: RIVER FLATS SECTION
	TEMPORARY CIVIL CONSTRUCTION ROAD: MOUNTAINOUS SECTION
	TEMPORARY BRIDGE / CROSSING
	TEMPORARY LARGE EQUIPMENT HAUL ROAD: MOUNTAINOUS SECTION
	TEMPORARY LARGE EQUIPMENT HAUL ROAD: MOUNTAINOUS SECTION REMOVED AS PART OF SPILLWAY/QUARRY CONSTRUCTION
	TEMPORARY LARGE EQUIPMENT HAUL ROAD: EMBANKMENT SECTION
	PERMANENT ROAD COMPLETED AFTER PROJECT CONSTRUCTION

- NOTES:**
- ROADS IN THE RIVER SECTION LOCATED IN THE FLOODZONE SOUTH OF THE COFFERDAM CREST WILL BE RAISED TO RL 80m USING WASTE MATERIAL THE INITIAL ROAD WILL BE DEVELOPED AT GROUND LEVEL TO REACH THE SPOIL DUMPS EARLY BUT CONTINUE TO BE RAISED
 - ALL BRIDGE STRUCTURES TO HAVE GABIONS/GROUTED RIP-RAP AT ABUTMENTS
 - MINOR ROAD CROSSINGS NOT SHOWN (REFER TO REPORT)

SITE ROADS LAYOUT
 SCALE 1:7,500

P:\PNA009 - FRIEDA RIVER HEP PFS\04_WORKING_FILES_V2_DRAFTING\00 - DRAWINGS\01 - SHEETS\VPNA009-0056.DWG - 27/09/2018 9:58:41 AM

REF. DWG No.	DWG. DESCRIPTION	No	DATE	REVISION DETAILS	LD ENG.	PM
		D	25.09.18	ISSUED FOR FINAL REPORT	MORE	MORE
		C	03.09.18	REISSUED FOR CLIENT REVIEW	MORE	MORE
		B	18.07.18	REISSUED FOR CLIENT REVIEW	MORE	MORE
		A	31.05.18	ISSUED FOR CLIENT REVIEW	MORE	MORE

ENGINEERING COMPANY

SRK Perth 10 Richardson Street, West Perth, Western Australia 6005
 Tel: +61 8 9288 2000 - Fax: +61 8 9288 2001
<http://www.srk.com.au>

DRAWN	TREV	31.05.18
DESIGN	PRIN	31.05.18
DES.CHKD	MORE	31.05.18
LD ENG. APPR	MORE	31.05.18
PM APPR	MORE	31.05.18

VENDOR DRG NO. PNA009-0056

FRIEDA RIVER

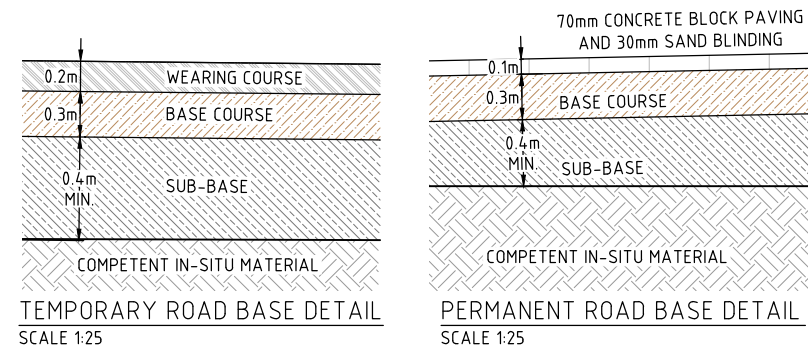
OWNER
FRIEDA RIVER LIMITED

TITLE
FRIEDA RIVER HYDROELECTRIC PROJECT

TYPICAL ROADS LAYOUT

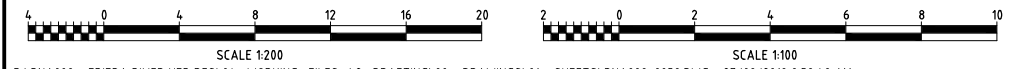
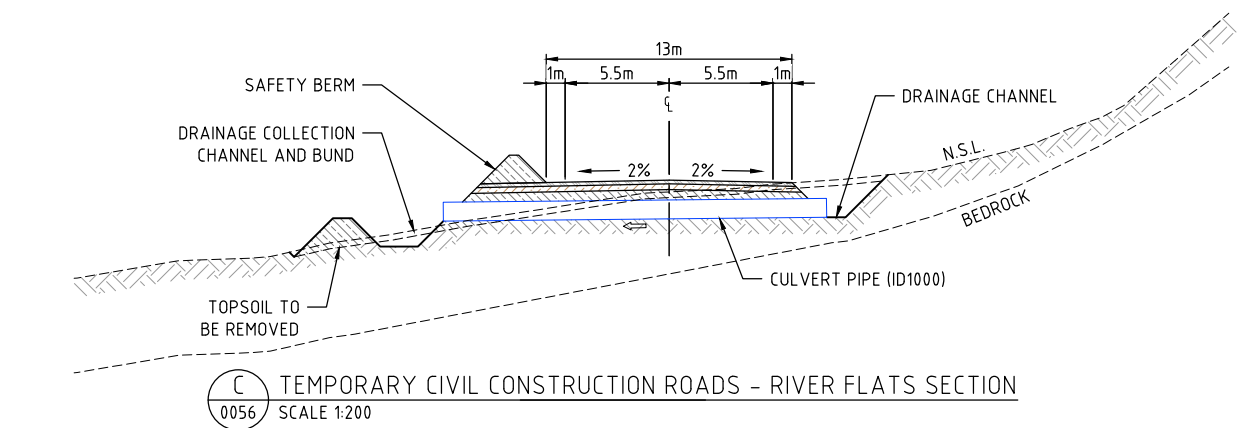
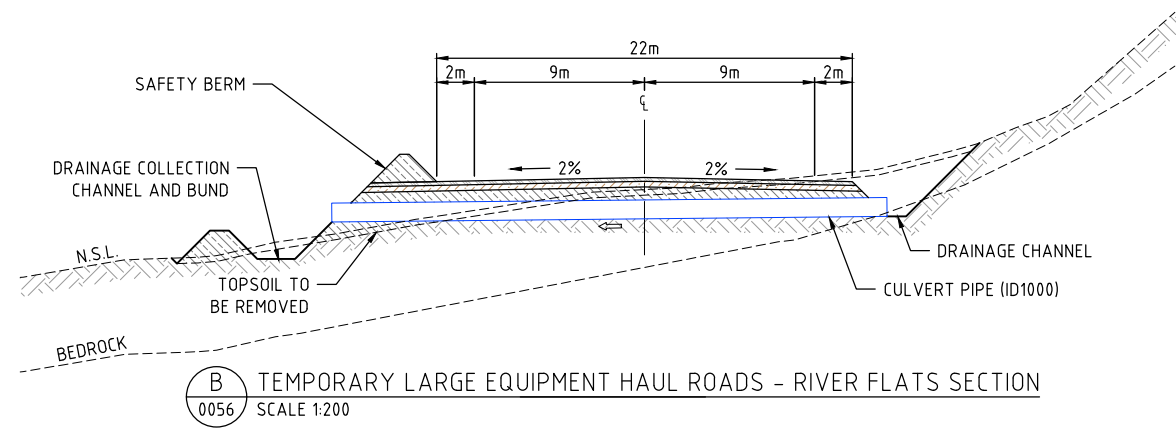
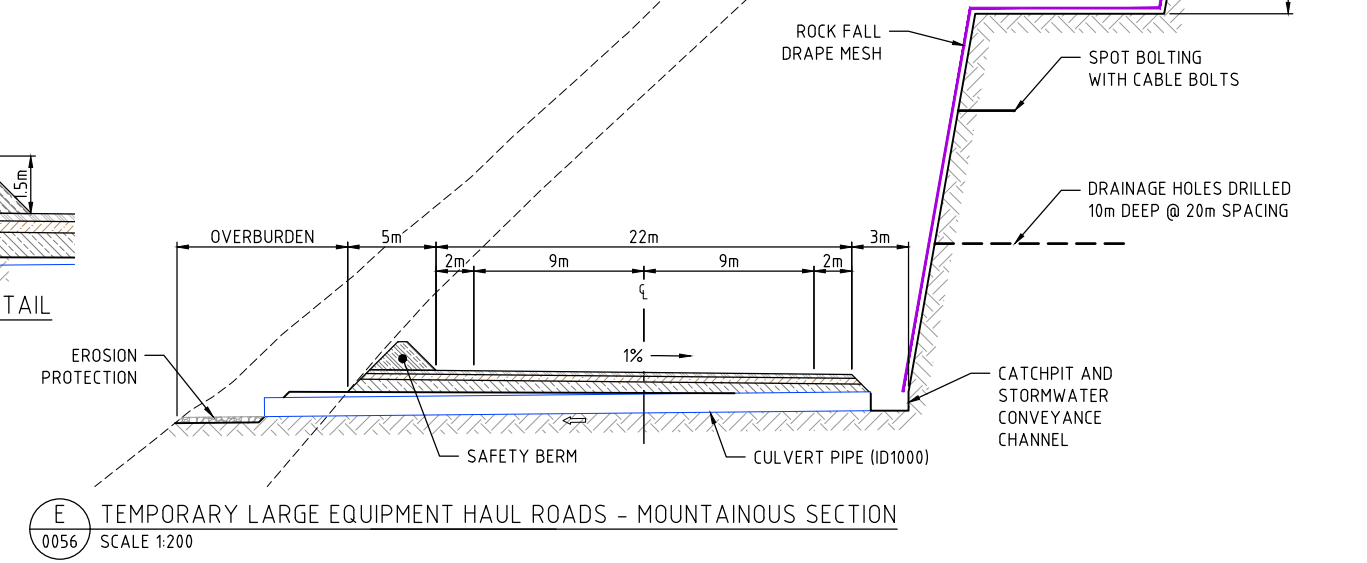
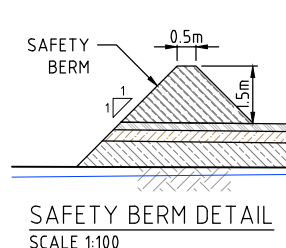
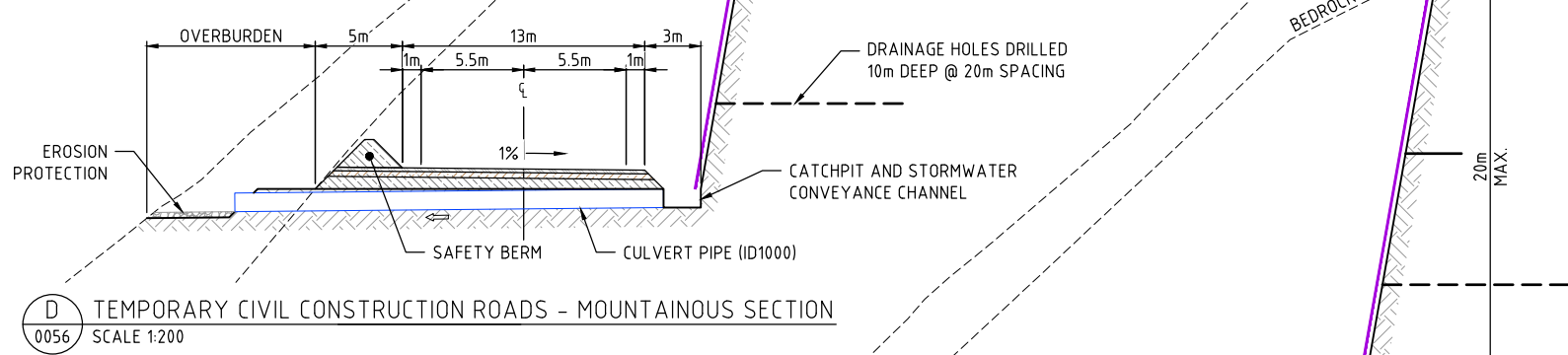
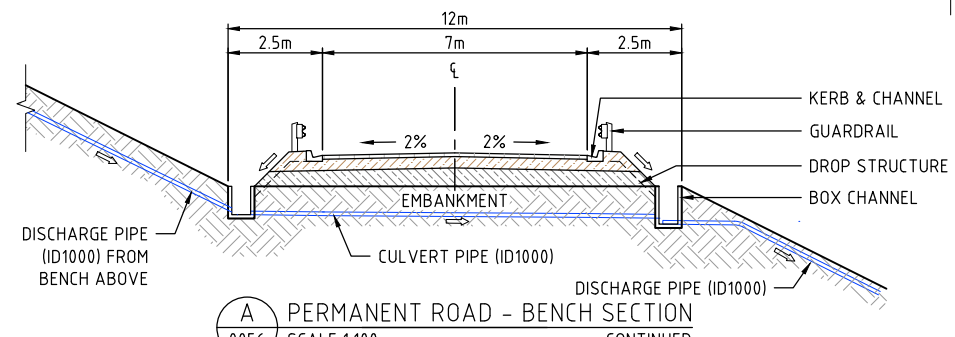
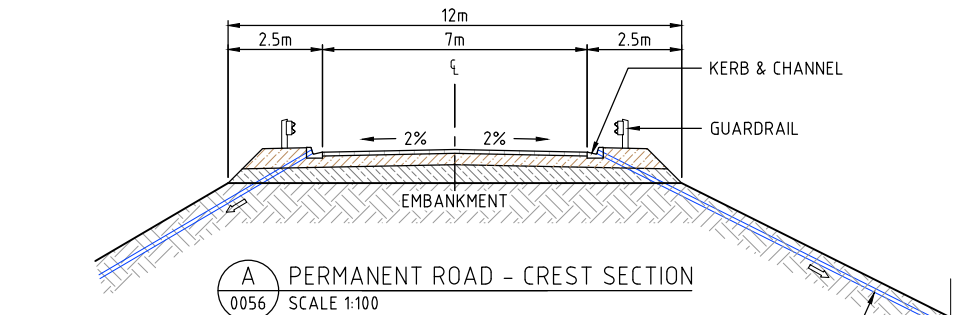
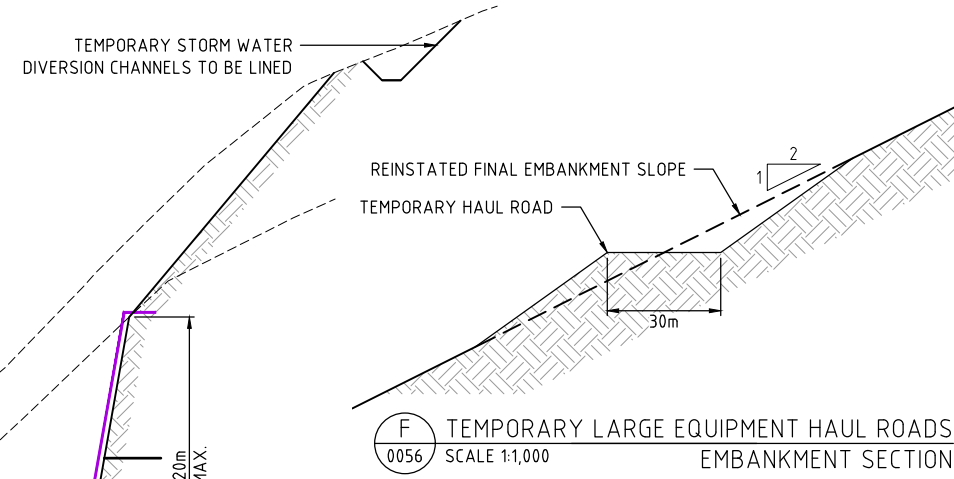
STATUS FOR INFORMATION		
SCALE	AS SHOWN	REV No.
ALL DIMENSIONS IN METRES		D
DRAWING No	FRP-2-D-02-07-D-030-001	

PROJECTION: UNIVERSAL TRANSVERSE MERCATOR, ZONE 54
 HORIZONTAL DATUM: PAPUA NEW GUINEA MAP GRID 1994 (PNGMG94)
 VERTICAL DATUM: AITAPE MEAN SEA LEVEL (MSL)



NOTE:

- ROADS IN THE RIVER SECTION LOCATED IN THE FLOOD ZONE SOUTH OF THE COFFERDAM CREST WILL BE RAISED TO RL 80m USING WASTE MATERIAL. THE INITIAL ROAD WILL BE DEVELOPED AT GROUND LEVEL TO REACH THE SPOIL DUMPS EARLY BUT CONTINUE TO BE RAISED
- THREE CULVERT PIPES (ID1000) TO BE INSTALLED EVERY 200m ALONG ROAD LENGTH
- STORMWATER PIPES HAVE NOT BEEN DESIGNED
- MOUNTAINOUS CUT FACES TO HAVE SPOT BOLTING



P:\PNA009 - FRIEDA RIVER HEP PFS\04_WORKING_FILES_V2_DRAFTING\00 - DRAWINGS\01 - SHEETS\PNA009-0058.DWG - 27/09/2018 9:58:49 AM

REF. DWG No.	DWG. DESCRIPTION	No	DATE	REVISION DETAILS	LD ENG.	PM
		C	25.09.18	ISSUED FOR FINAL REPORT	MORE	MORE
		B	18.07.18	REISSUED FOR CLIENT REVIEW	MORE	MORE
		A	31.05.18	ISSUED FOR CLIENT REVIEW	MORE	MORE

ENGINEERING COMPANY

 SRK Perth 10 Richardson Street, West Perth, Western Australia 6005
 Tel: +61 8 9288 2000 - Fax: +61 8 9288 2001
<http://www.srk.com.au>

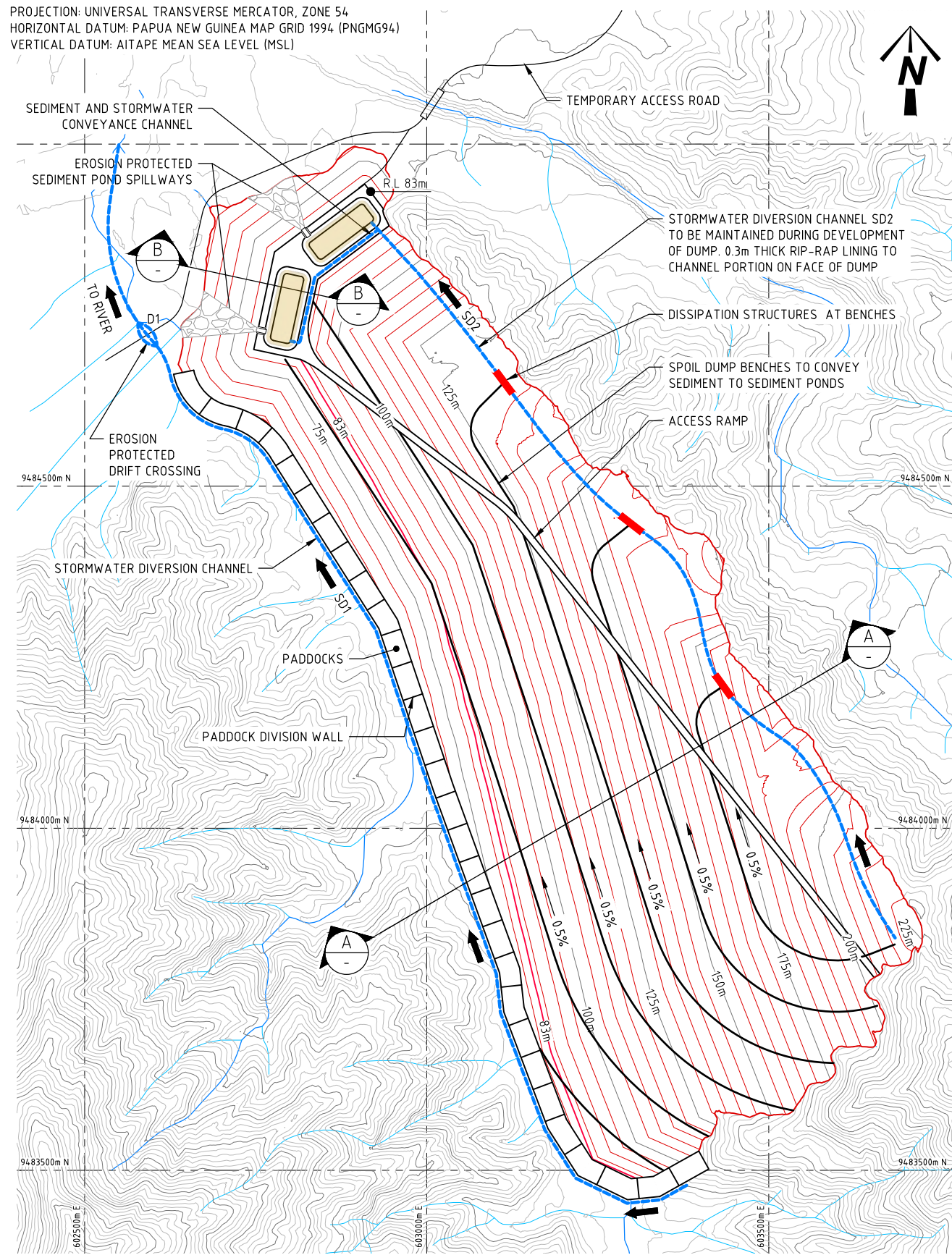
OWNER
FRIEDA RIVER LIMITED

TITLE
FRIEDA RIVER HYDROELECTRIC PROJECT

TYPICAL ROADS SECTIONS

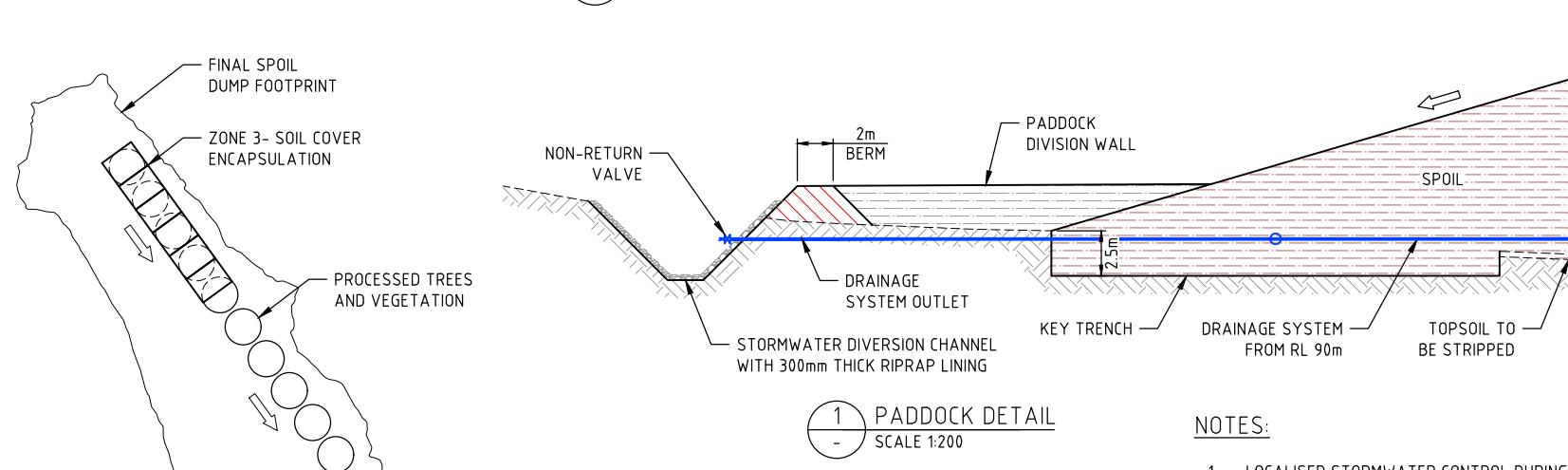
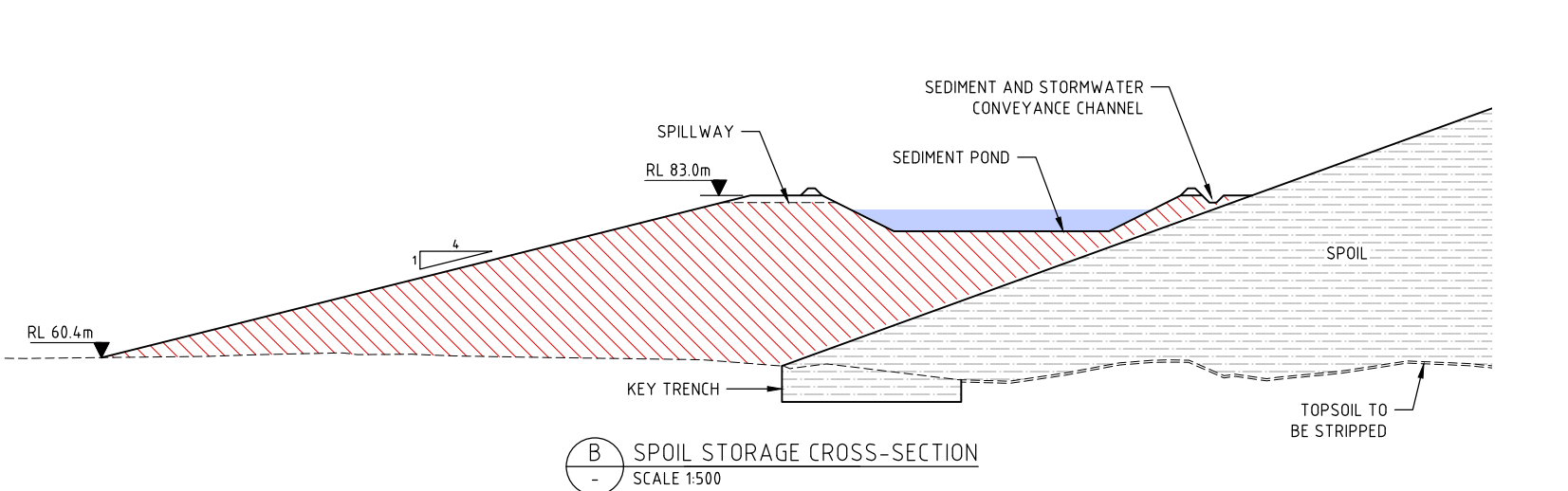
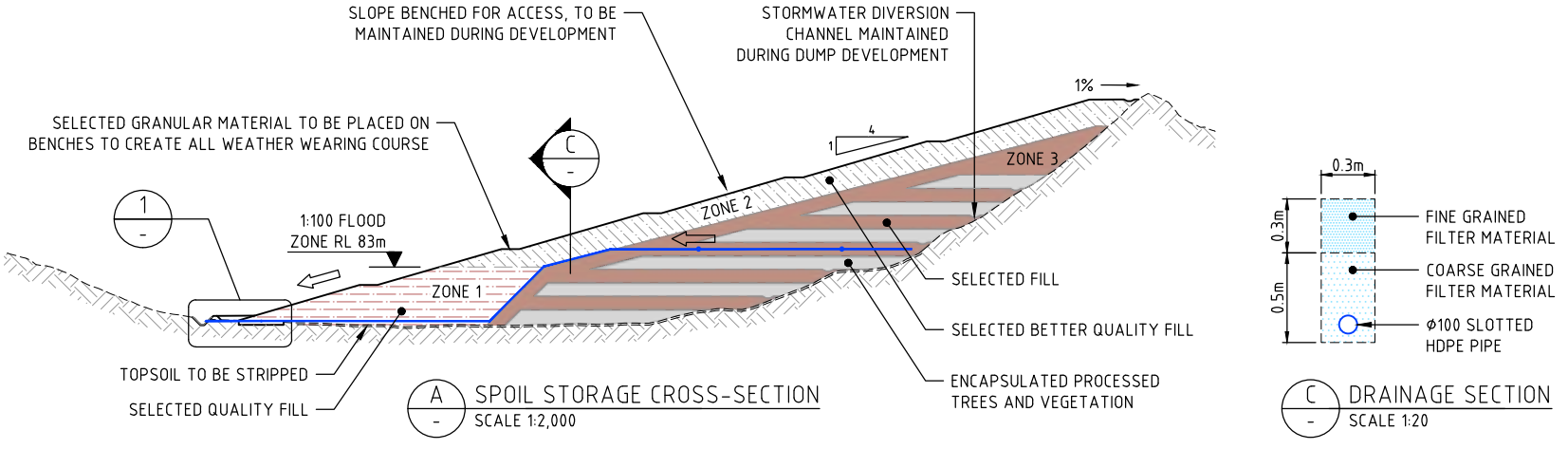
STATUS FOR INFORMATION		
SCALE	AS SHOWN	REV No.
		C
SIZE		A1
DRAWING No		
FRP-2-D-02-07-D-030-002		

PROJECTION: UNIVERSAL TRANSVERSE MERCATOR, ZONE 54
 HORIZONTAL DATUM: PAPUA NEW GUINEA MAP GRID 1994 (PNGMG94)
 VERTICAL DATUM: AITAPE MEAN SEA LEVEL (MSL)



SPOIL STORAGE 1 LAYOUT
 SCALE 1:4,000

P:\PNA009 - FRIEDA RIVER HEP PFS\04_WORKING_FILES_V2_DRAFTING\00 - DRAWINGS\01 - SHEETS\VPNA009-0060.DWG - 27/09/2018 9:59:04 AM



SPOIL STORAGE DEPOSITION SEQUENCE
 SCALE 1:10,000

NOTES:

- LOCALISED STORMWATER CONTROL DURING SPOIL DUMP BASE DEVELOPMENT TO BE DETERMINED ON-SITE DURING CONSTRUCTION
- ZONE 1 TO BE COMPACTED
- SPOIL TO BE COMPACTED IN DESIGNATED AREAS TO IMPROVE MATERIAL STRENGTH

SCALE 1:200

SCALE 1:200

SCALE 1:500

SCALE 1:2,000

REF. DWG No.	DWG. DESCRIPTION	No	DATE	REVISION DETAILS	LD ENG.	PM
		C	25.09.18	ISSUED FOR FINAL REPORT	MORE	MORE
		B	18.07.18	REISSUED FOR CLIENT REVIEW	MORE	MORE
		A	31.05.18	ISSUED FOR CLIENT REVIEW	MORE	MORE

ENGINEERING COMPANY

SRK Perth 10 Richardson Street, West Perth, Western Australia 6005
 Tel: +61 8 9288 2000 - Fax: +61 8 9288 2001
<http://www.srk.com.au/>

VENDOR DRG NO. PNA009-0060

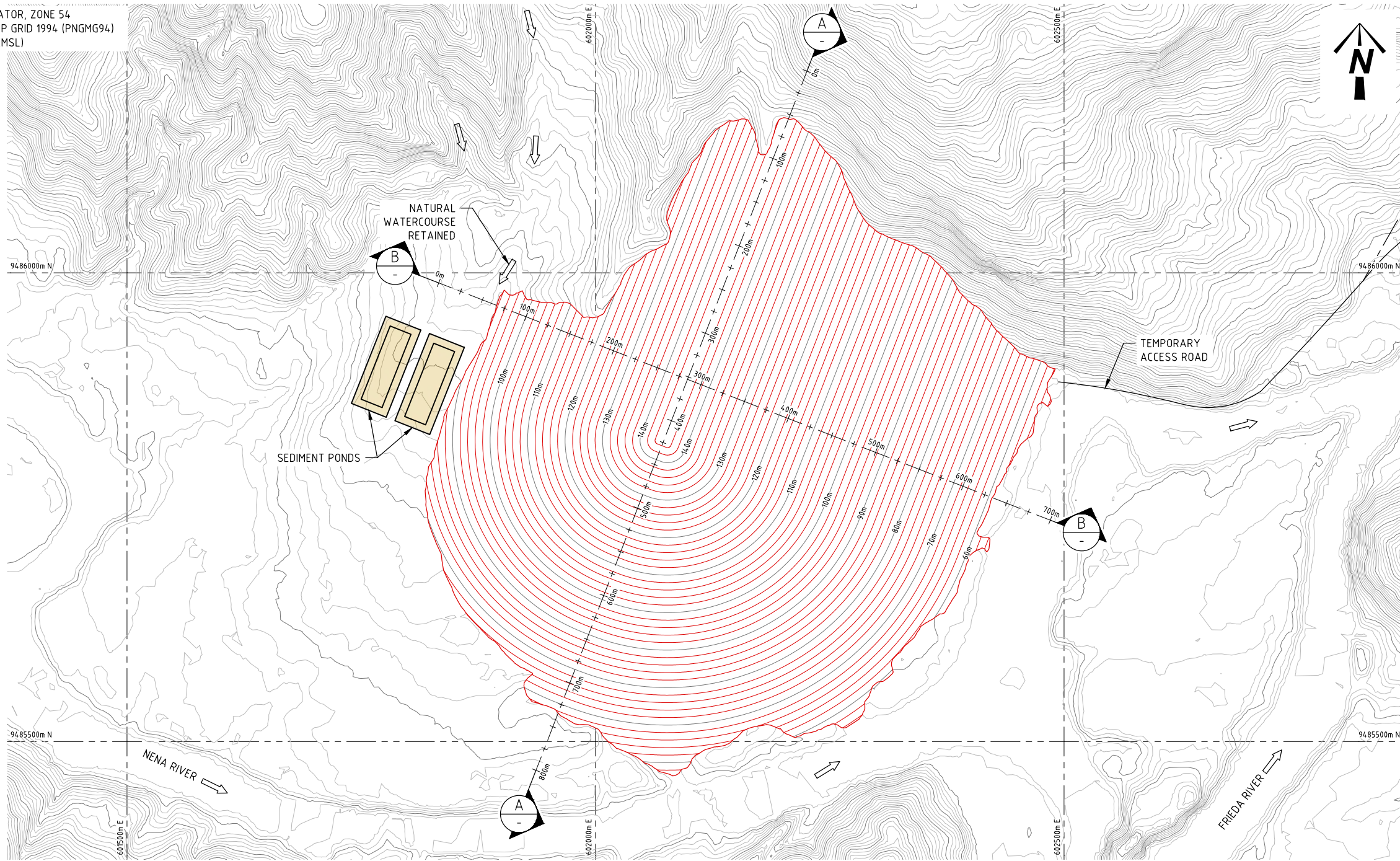
DRAWN	TREV	31.05.18
DESIGN	PRIN	31.05.18
DES.CHKD	MORE	31.05.18
LD ENG. APPR	MORE	31.05.18
PM APPR	MORE	31.05.18

OWNER
FRIEDA RIVER LIMITED

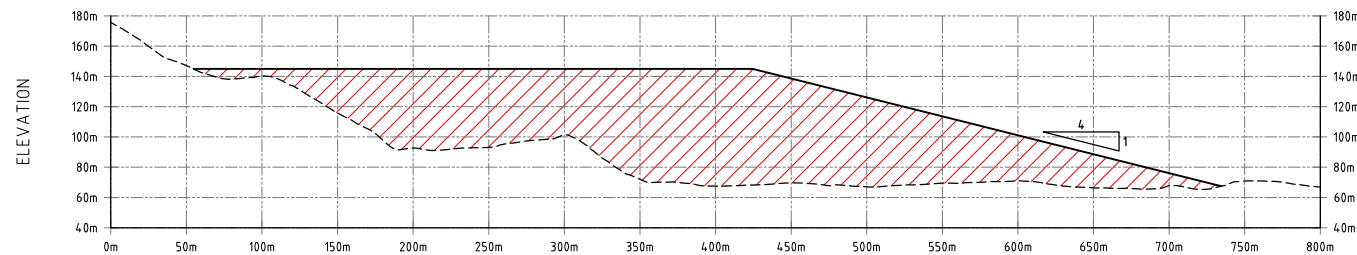
TITLE
**FRIEDA RIVER HYDROELECTRIC PROJECT
 SPOIL STORAGE 1
 LAYOUT & SECTIONS**

STATUS FOR INFORMATION		
SCALE	AS SHOWN	REV No.
		C
		SIZE
		A1
DRAWING No		
FRP-2-D-02-07-D-030-003		

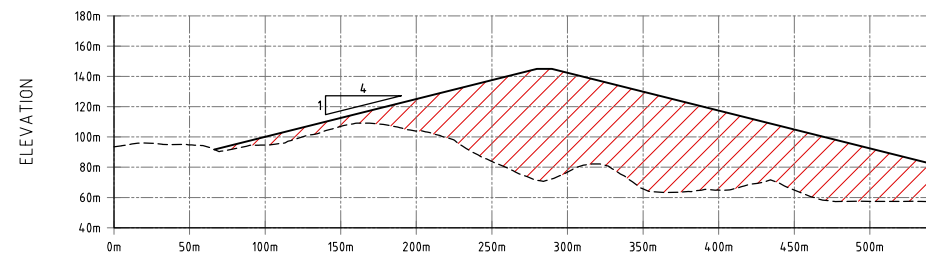
PROJECTION: UNIVERSAL TRANSVERSE MERCATOR, ZONE 54
 HORIZONTAL DATUM: PAPUA NEW GUINEA MAP GRID 1994 (PNGMG94)
 VERTICAL DATUM: AITAPE MEAN SEA LEVEL (MSL)



SPOIL STORAGE 2 LAYOUT
 SCALE 1:2,500

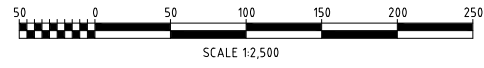


A - SPOIL STORAGE CROSS-SECTION
 SCALE 1:2,500



B - SPOIL STORAGE CROSS-SECTION
 SCALE 1:2,500

NOTE:
 REFER DRAWING PNA009-0060
 FOR TYPICAL SPOIL DUMP DETAILS



P:\PNA009 - FRIEDA RIVER HEP PFS\04_WORKING_FILES_V2_DRAFTING\00 - DRAWINGS\01 - SHEETS\PNA009-0062.DWG - 27/09/2018 9:59:20 AM

REF. DWG No.	DWG. DESCRIPTION	No	DATE	REVISION DETAILS	LD ENG.	PM
		C	25.09.18	ISSUED FOR FINAL REPORT	MORE	MORE
		B	18.07.18	REISSUED FOR CLIENT REVIEW	MORE	MORE
		A	31.05.18	ISSUED FOR CLIENT REVIEW	MORE	MORE

ENGINEERING COMPANY



SRK Perth 10 Richardson Street, West Perth,
 Western Australia 6005
 Tel: +61 8 9288 2000 - Fax: +61 8 9288 2001
[http://www.srk.com.au/](http://www.srk.com.au)

DRAWN	TREV	31.05.18
DESIGN	PRIN	31.05.18
DES.CHKD	MORE	31.05.18
LD ENG. APPR	MORE	31.05.18
PM APPR	MORE	31.05.18

VENDOR DRG NO. PNA009-0062



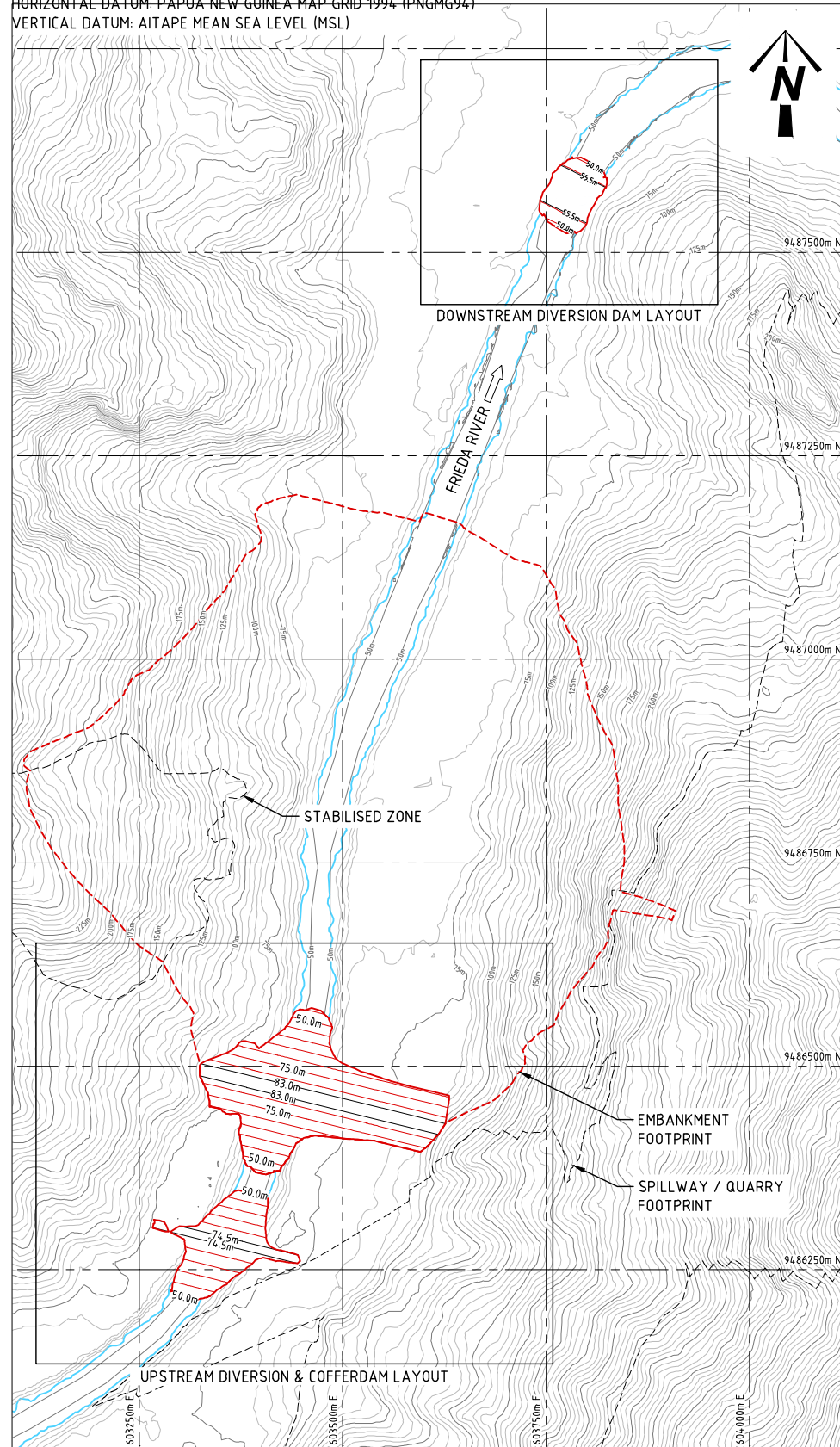
FRIEDA RIVER

OWNER
FRIEDA RIVER LIMITED

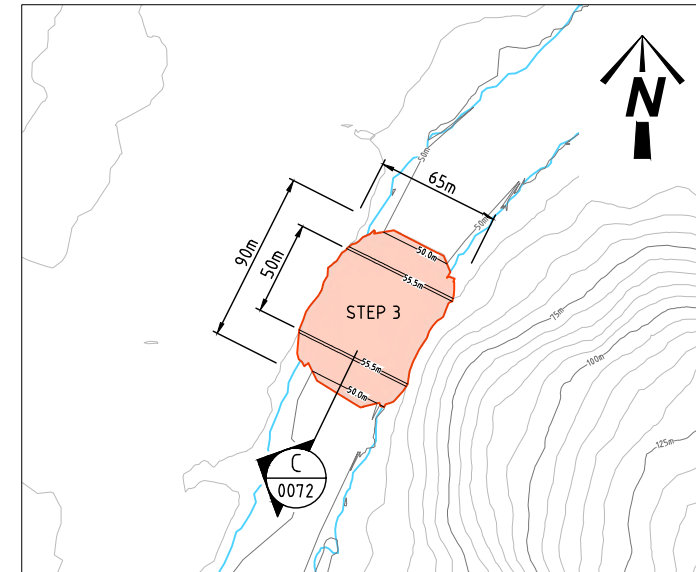
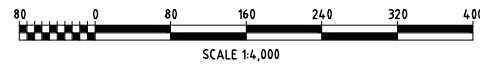
TITLE
**FRIEDA RIVER HYDROELECTRIC PROJECT
 SPOIL STORAGE 2 LAYOUT &
 SECTIONS**

STATUS FOR INFORMATION		
SCALE	AS SHOWN	REV No.
ALL DIMENSIONS IN METRES		C
DRAWING No	FRP-2-D-02-07-D-030-004	
	SIZE	A1

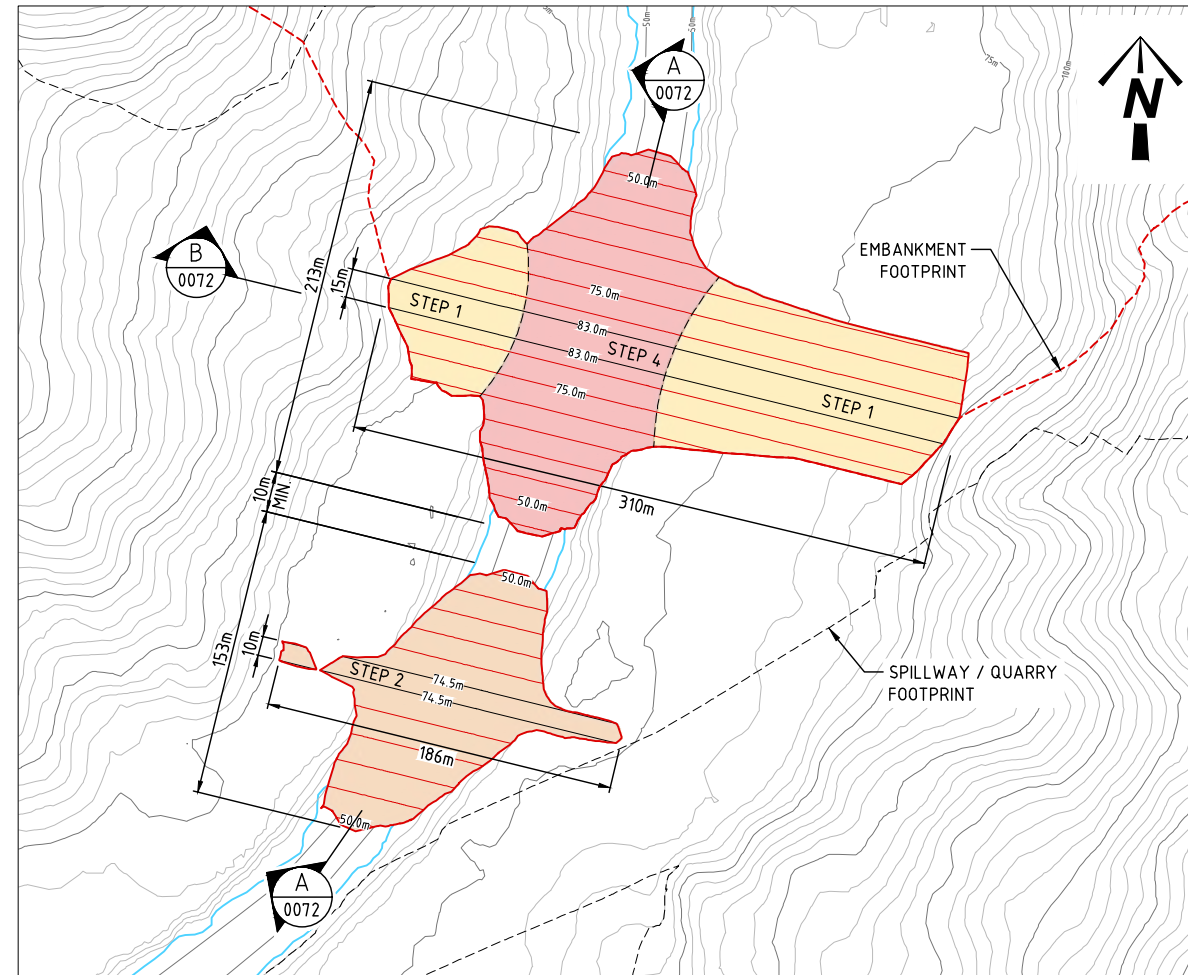
PROJECTION: UNIVERSAL TRANSVERSE MERCATOR, ZONE 54
 HORIZONTAL DATUM: PAPUA NEW GUINEA MAP GRID 1994 (PNGMG94)
 VERTICAL DATUM: AITAPE MEAN SEA LEVEL (MSL)



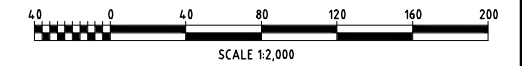
DIVERSION & COFFERDAM KEY PLAN
 SCALE 1:4,000



DOWNSTREAM DIVERSION DAMS LAYOUT
 SCALE 1:2,000



UPSTREAM DIVERSION & COFFERDAM LAYOUT
 SCALE 1:2,000



P:\PNA009 - FRIEDA RIVER HEP PFS\04_WORKING_FILES_V2_DRAFTING\00 - DRAWINGS\01 - SHEETS\PNA009-0070.DWG - 27/09/2018 1:26:18 PM

REF. DWG No.	DWG. DESCRIPTION	No	DATE	REVISION DETAILS	LD ENG.	PM
		C	25.09.18	ISSUED FOR FINAL REPORT	MORE	MORE
		B	18.07.18	REISSUED FOR CLIENT REVIEW	MORE	MORE
		A	31.05.18	ISSUED FOR CLIENT REVIEW	MORE	MORE

ENGINEERING COMPANY



SRK Perth 10 Richardson Street, West Perth, Western Australia 6005
 Tel: +61 8 9288 2000 - Fax: +61 8 9288 2001
<http://www.srk.com.au>

DRAWN	TREV	31.05.18
DESIGN	PRIN	31.05.18
DES.CHKD	MORE	31.05.18
LD ENG. APPR	MORE	31.05.18
PM. APPR	MORE	31.05.18

VENDOR DRG NO. PNA009-0070

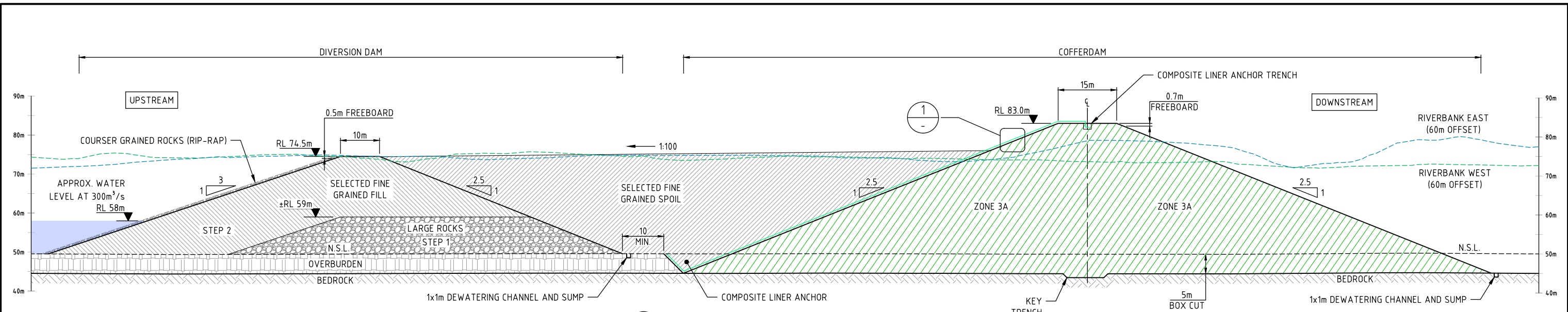


FRIEDA RIVER

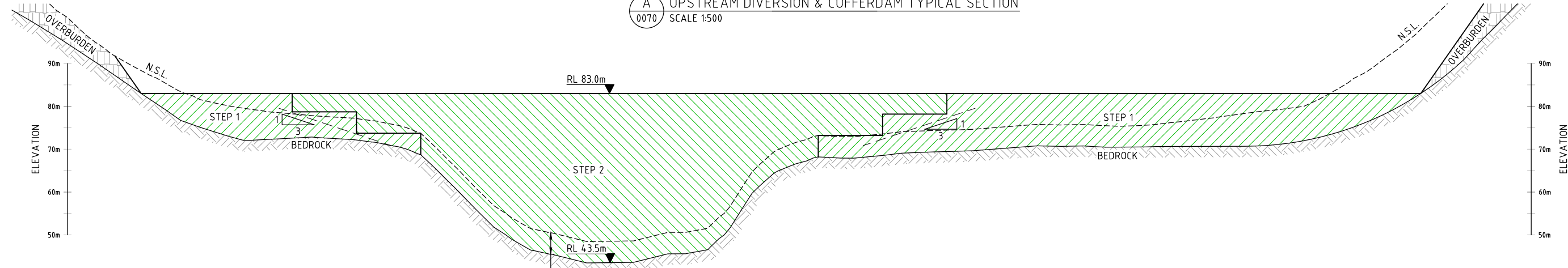
OWNER
FRIEDA RIVER LIMITED

TITLE
**FRIEDA RIVER HYDROELECTRIC PROJECT
 DIVERSION & COFFERDAMS LAYOUT AND
 CONSTRUCTION SEQUENCE**

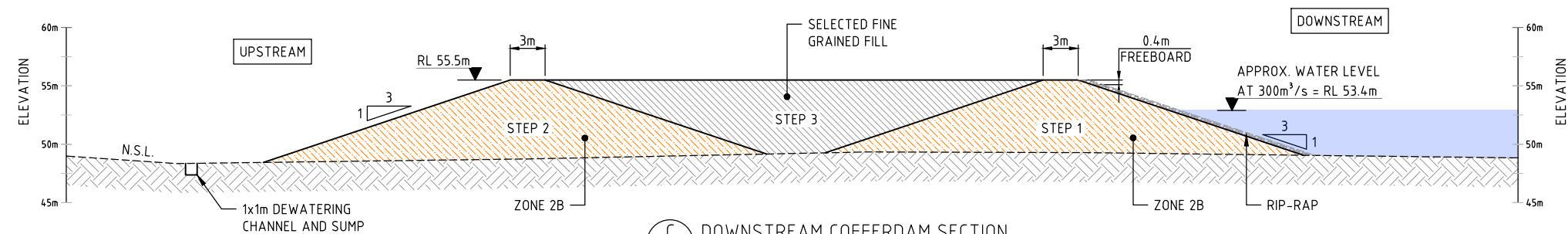
STATUS FOR INFORMATION		
SCALE	AS SHOWN	REV No.
		C
		A1
DRAWING No FRP-2-D-02-07-D-030-005		



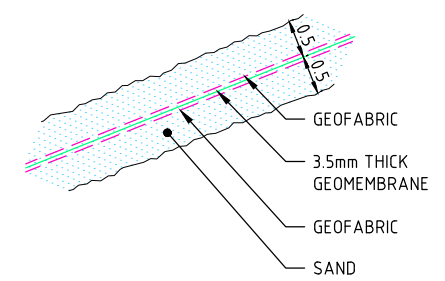
A UPSTREAM DIVERSION & COFFERDAM TYPICAL SECTION
0070 SCALE 1:500



B UPSTREAM COFFERDAM LONG SECTION
0070 SCALE 1:500



C DOWNSTREAM COFFERDAM SECTION
0070 SCALE 1:250



1 COMPOSITE LINER TYPICAL DETAIL
SCALE 1:50

NOTE:
SIPHON TO BE INSTALLED FOR EMPTYING WATER FROM THE ZONE BETWEEN MAIN AND DOWNSTREAM COFFERDAMS

LEGEND:

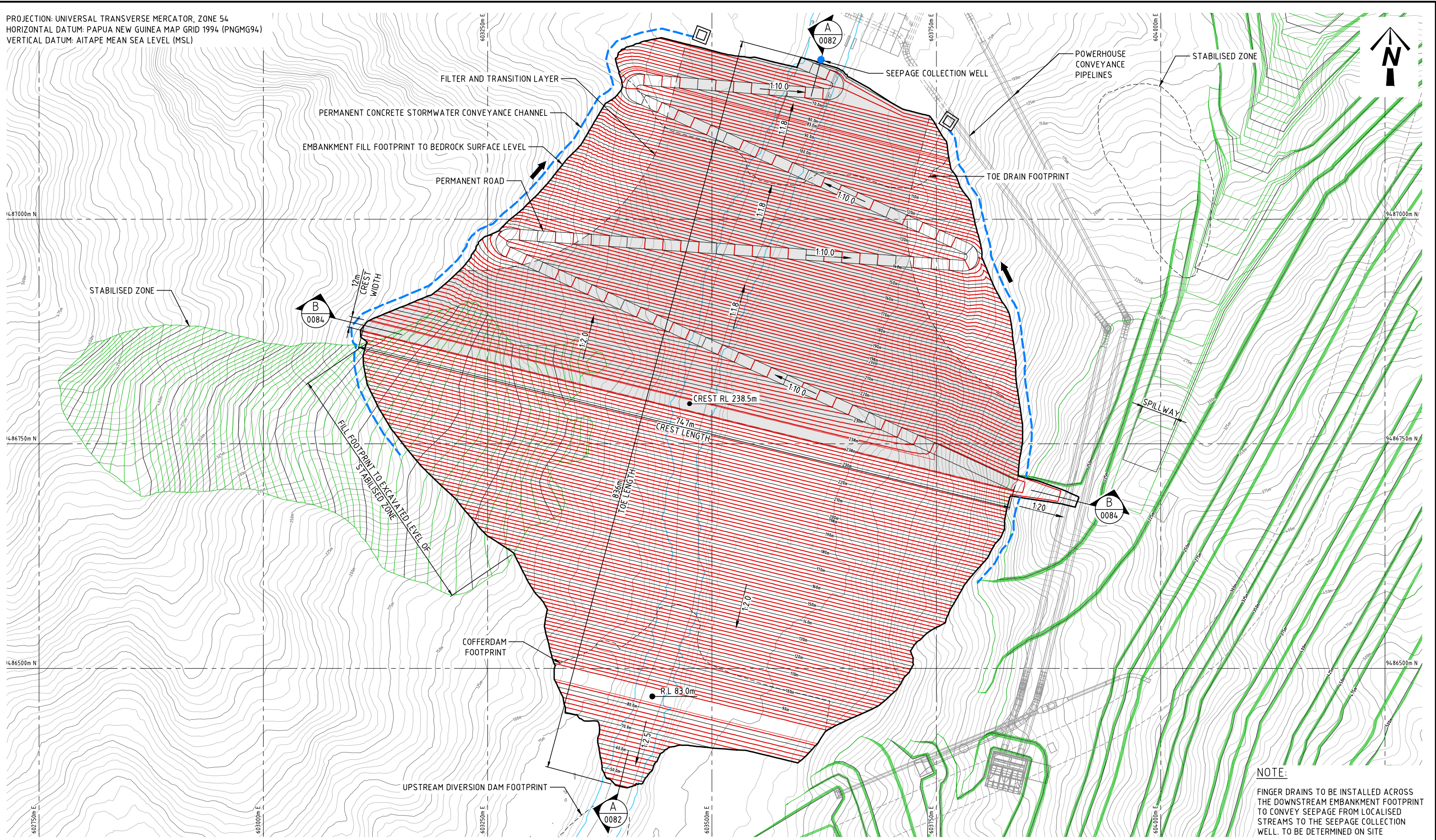
	ZONE 2A - FILTER MATERIAL (0-60mm)		BEDROCK
	ZONE 2B - TRANSITION MATERIAL (0-200mm)		FINE GRAINED FILL
	ZONE 3A - HIGHLY COMPACTED ROCK FILL (0-600mm)		LARGE ROCKS (>0.5m³)



P:\PNA009 - FRIEDA RIVER HEP PFS\04_WORKING_FILES_V2_DRAFTING\00 - DRAWINGS\01 - SHEETS\PNA009-0072.DWG - 27/09/2018 9:59:47 AM

				<p>ENGINEERING COMPANY</p> <p>SRK Perth 10 Richardson Street, West Perth, Western Australia 6005 Tel: +61 8 9288 2000 - Fax: +61 8 9288 2001 http://www.srk.com.au</p>			<p>DRAWN TREV 31.05.18</p> <p>DESIGN PRIN 31.05.18</p> <p>DES.CHKD MORE 31.05.18</p> <p>LD ENG. APPR MORE 31.05.18</p> <p>PM, APPR MORE 31.05.18</p>			<p>OWNER</p> <p>FRIEDA RIVER LIMITED</p>			<p>STATUS</p> <p>FOR INFORMATION</p>		
				<p>FRIEDA RIVER</p>			<p>TITLE</p> <p>FRIEDA RIVER HYDROELECTRIC PROJECT</p> <p>DIVERSION & COFFERDAMS TYPICAL SECTIONS</p>			<p>SCALE AS SHOWN</p> <p>REV No. C</p> <p>SIZE A1</p>					
				<p>REF. DWG No.</p> <p>DWG. DESCRIPTION</p> <p>No</p> <p>DATE</p> <p>REVISION DETAILS</p> <p>LD ENG.</p> <p>PM</p> <p>VENDOR DRG NO. PNA009-0072</p>			<p>DRAWING No</p> <p>FRP-2-D-02-07-D-030-006</p>								

PROJECTION: UNIVERSAL TRANSVERSE MERCATOR, ZONE 54
 HORIZONTAL DATUM: PAPUA NEW GUINEA MAP GRID 1994 (PNGMG94)
 VERTICAL DATUM: AITAPE MEAN SEA LEVEL (MSL)



EMBANKMENT FINAL LAYOUT
 SCALE 1:2,000

NOTE:
 FINGER DRAINS TO BE INSTALLED ACROSS THE DOWNSTREAM EMBANKMENT FOOTPRINT TO CONVEY SEEPAGE FROM LOCALISED STREAMS TO THE SEEPAGE COLLECTION WELL. TO BE DETERMINED ON SITE

P:\PNA009 - FRIEDA RIVER HEP PFS\04_WORKING_FILES_V2_DRAFTING\00 - DRAWINGS\01 - SHEETS\PNA009-0080.DWG - 27/09/2018 1:27:38 PM

REF. DWG No.	DWG. DESCRIPTION	No	DATE	REVISION DETAILS	LD ENG.	PM
		C	25.09.18	ISSUED FOR FINAL REPORT	MORE	MORE
		B	18.07.18	REISSUED FOR CLIENT REVIEW	MORE	MORE
		A	31.05.18	ISSUED FOR CLIENT REVIEW	MORE	MORE

ENGINEERING COMPANY

 SRK Perth 10 Richardson Street, West Perth, Western Australia 6005
 Tel: +61 8 9288 2000 - Fax: +61 8 9288 2001
<http://www.srk.com.au>

	DRAWN	TREV	31.05.18
	DESIGN	PRIN	31.05.18
	DES.CHKD	MORE	31.05.18
	LD ENG. APPR	MORE	31.05.18
	PM. APPR	MORE	31.05.18



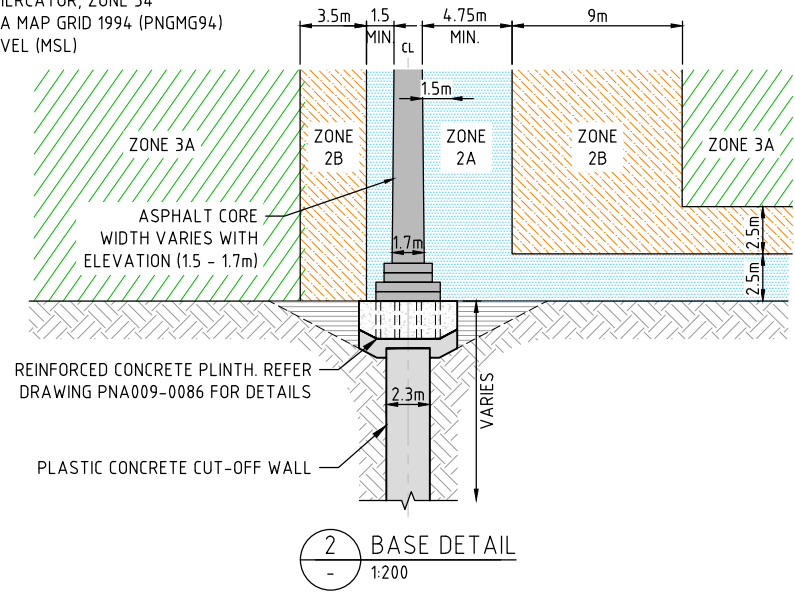
OWNER
FRIEDA RIVER LIMITED

TITLE
FRIEDA RIVER HYDROELECTRIC PROJECT

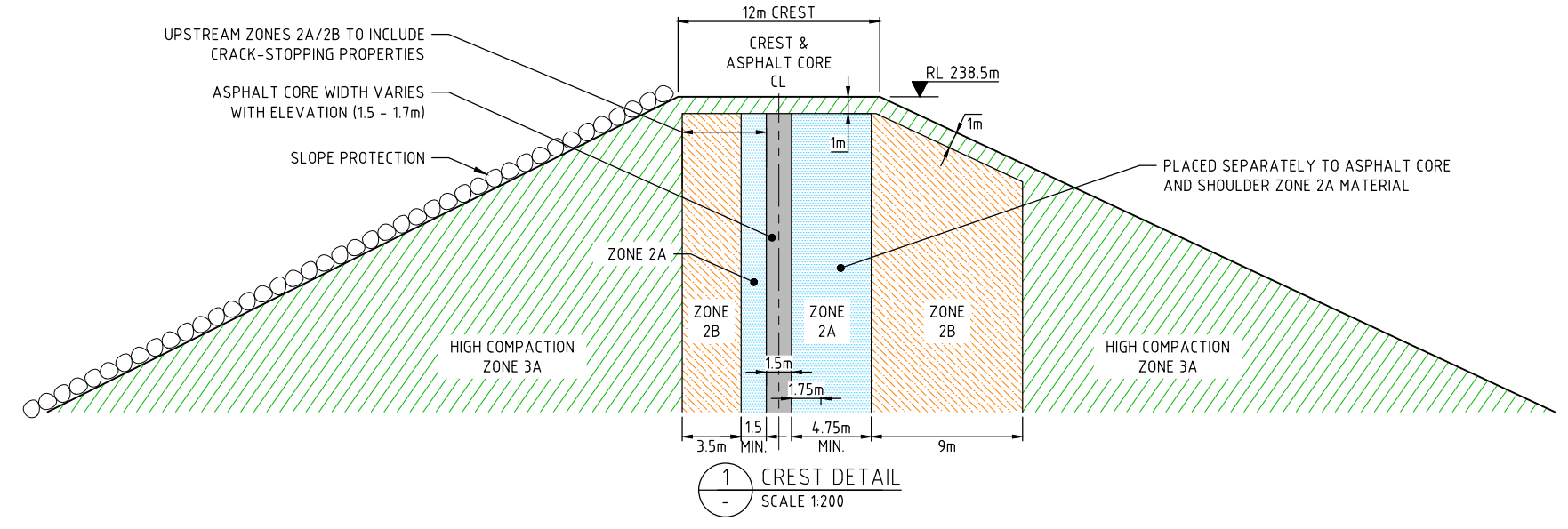
EMBANKMENT FINAL LAYOUT

STATUS FOR INFORMATION			
SCALE	AS SHOWN	REV No.	SIZE
ALL DIMENSIONS IN METRES		C	A1
DRAWING No FRP-2-D-04-01-D-030-002			

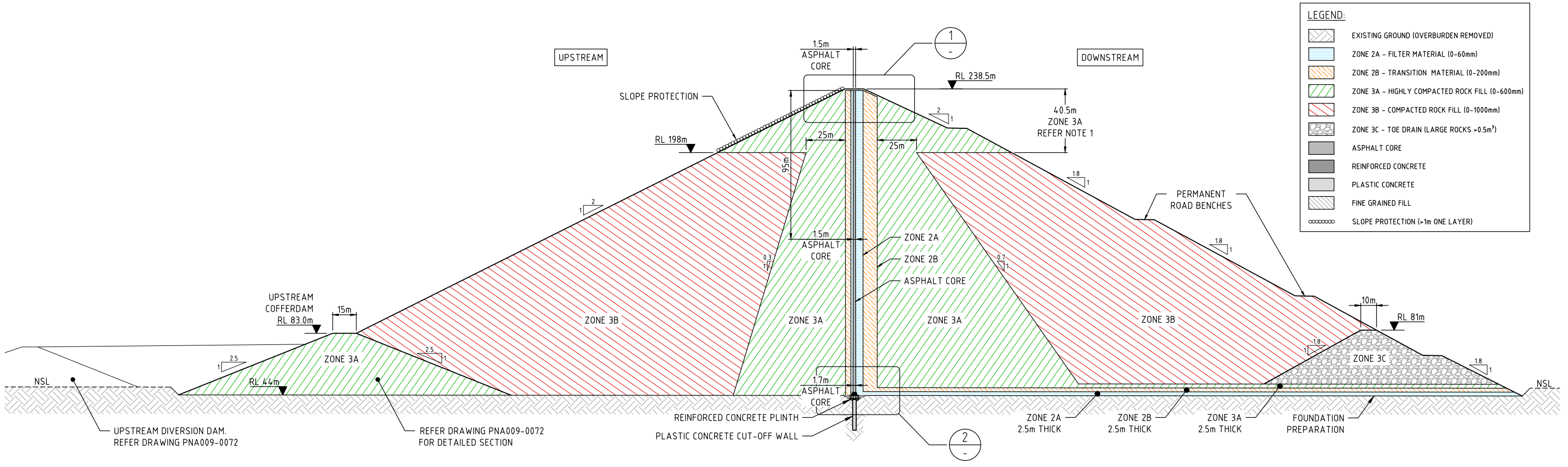
PROJECTION: UNIVERSAL TRANSVERSE MERCATOR, ZONE 54
 HORIZONTAL DATUM: PAPUA NEW GUINEA MAP GRID 1994 (PNGMG94)
 VERTICAL DATUM: AITAPE MEAN SEA LEVEL (MSL)



2 BASE DETAIL
 1:200



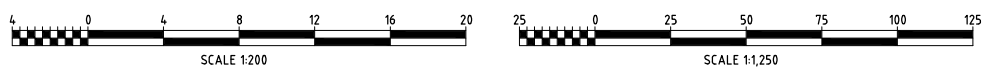
1 CREST DETAIL
 SCALE 1:200



A EMBANKMENT TYPICAL CROSS SECTION
 0080 SCALE 1:1,250

LEGEND:

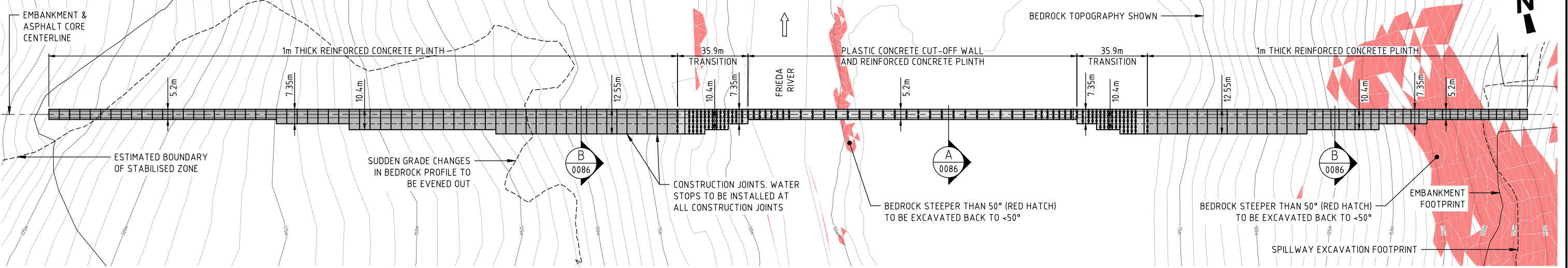
	EXISTING GROUND (OVERBURDEN REMOVED)
	ZONE 2A - FILTER MATERIAL (0-60mm)
	ZONE 2B - TRANSITION MATERIAL (0-200mm)
	ZONE 3A - HIGHLY COMPACTED ROCK FILL (0-600mm)
	ZONE 3B - COMPACTED ROCK FILL (0-1000mm)
	ZONE 3C - TOE DRAIN (LARGE ROCKS >0.5m³)
	ASPHALT CORE
	REINFORCED CONCRETE
	PLASTIC CONCRETE
	FINE GRAINED FILL
	SLOPE PROTECTION (>1m ONE LAYER)



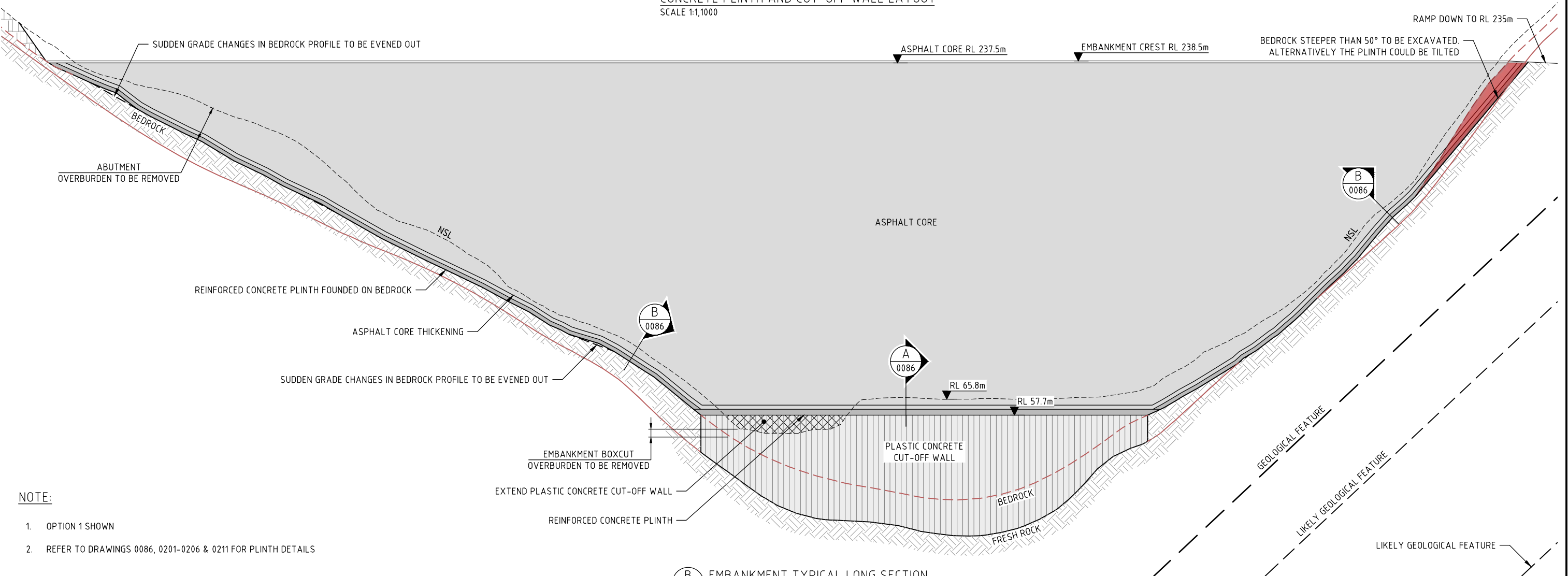
P:\PNA009 - FRIEDA RIVER HEP PFS\04_WORKING_FILES_V2_DRAFTING\00 - DRAWINGS\01 - SHEETS\PNA009-0082.DWG - 27/09/2018 10:00:09 AM

				ENGINEERING COMPANY SRK Perth 10 Richardson Street, West Perth, Western Australia 6005 Tel: +61 8 9288 2000 - Fax: +61 8 9288 2001 http://www.srk.com.au			DRAWN: TREV 31.05.18 DESIGN: PRIN 31.05.18 DES.CHKD: MORE 31.05.18 LD ENG. APPR: MORE 31.05.18 PML APPR: MORE 31.05.18			OWNER FRIEDA RIVER LIMITED		STATUS FOR INFORMATION	
							TITLE FRIEDA RIVER HYDROELECTRIC PROJECT EMBANKMENT TYPICAL CROSS SECTION & DETAILS			SCALE AS SHOWN ALL DIMENSIONS IN METRES			
				REF. DWG No. DWG. DESCRIPTION No DATE REVISION DETAILS LD ENG. PM VENDOR DRG NO. PNA009-0082			REV No. SIZE C A1			DRAWING No FRP-2-D-04-01-D-030-003			

PROJECTION: UNIVERSAL TRANSVERSE MERCATOR, ZONE 54
 HORIZONTAL DATUM: PAPUA NEW GUINEA MAP GRID 1994 (PNGMG94)
 VERTICAL DATUM: AITAPE MEAN SEA LEVEL (MSL)



CONCRETE PLINTH AND CUT-OFF WALL LAYOUT
 SCALE 1:1,000



B EMBANKMENT TYPICAL LONG SECTION
 0080 SCALE 1:1,000

- NOTE:
- OPTION 1 SHOWN
 - REFER TO DRAWINGS 0086, 0201-0206 & 0211 FOR PLINTH DETAILS



P:\PNA009 - FRIEDA RIVER HEP PFS\04_WORKING_FILES_V2_DRAFTING\00 - DRAWINGS\01 - SHEETS\PNA009-0084.DWG - 17/10/2018 10:36:39 AM

REF. DWG No.	DWG. DESCRIPTION	No	DATE	REVISION DETAILS	LD ENG.	PM
		C	25.09.18	ISSUED FOR FINAL REPORT	MORE	MORE
		B	18.07.18	REISSUED FOR CLIENT REVIEW	MORE	MORE
		A	31.05.18	ISSUED FOR CLIENT REVIEW	MORE	MORE

ENGINEERING COMPANY

SRK Perth 10 Richardson Street, West Perth, Western Australia 6005
 Tel: +61 8 9288 2000 - Fax: +61 8 9288 2001
<http://www.srk.com.au>

VENDOR DRG NO. PNA009-0084

DRAWN	TREV	31.05.18
DESIGN	PRIN	31.05.18
DES.CHKD	MORE	31.05.18
LD ENG. APPR	MORE	31.05.18
PM, APPR	MORE	31.05.18

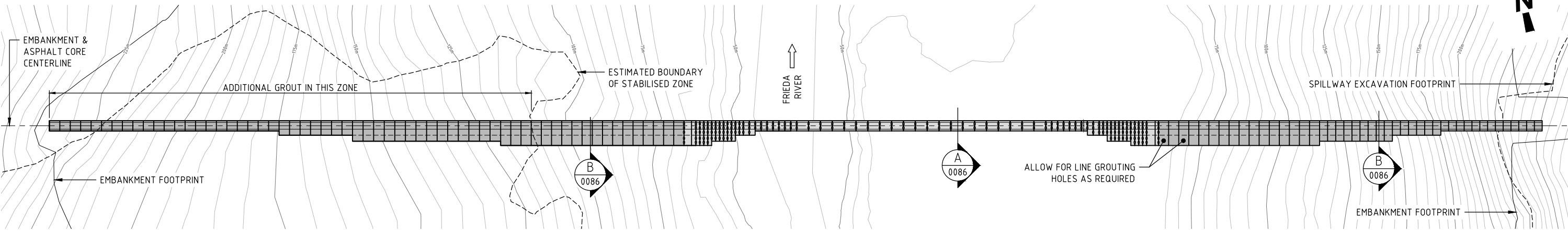
OWNER
FRIEDA RIVER LIMITED

TITLE
**FRIEDA RIVER HYDROELECTRIC PROJECT
 EMBANKMENT TYPICAL LONG SECTION &
 PLINTH LAYOUT**

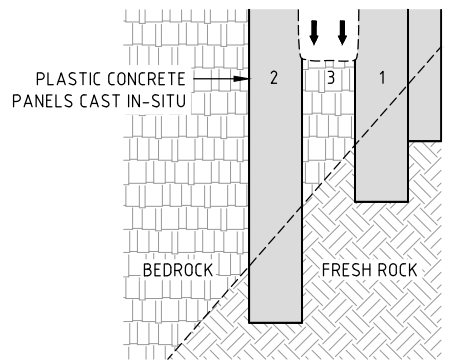
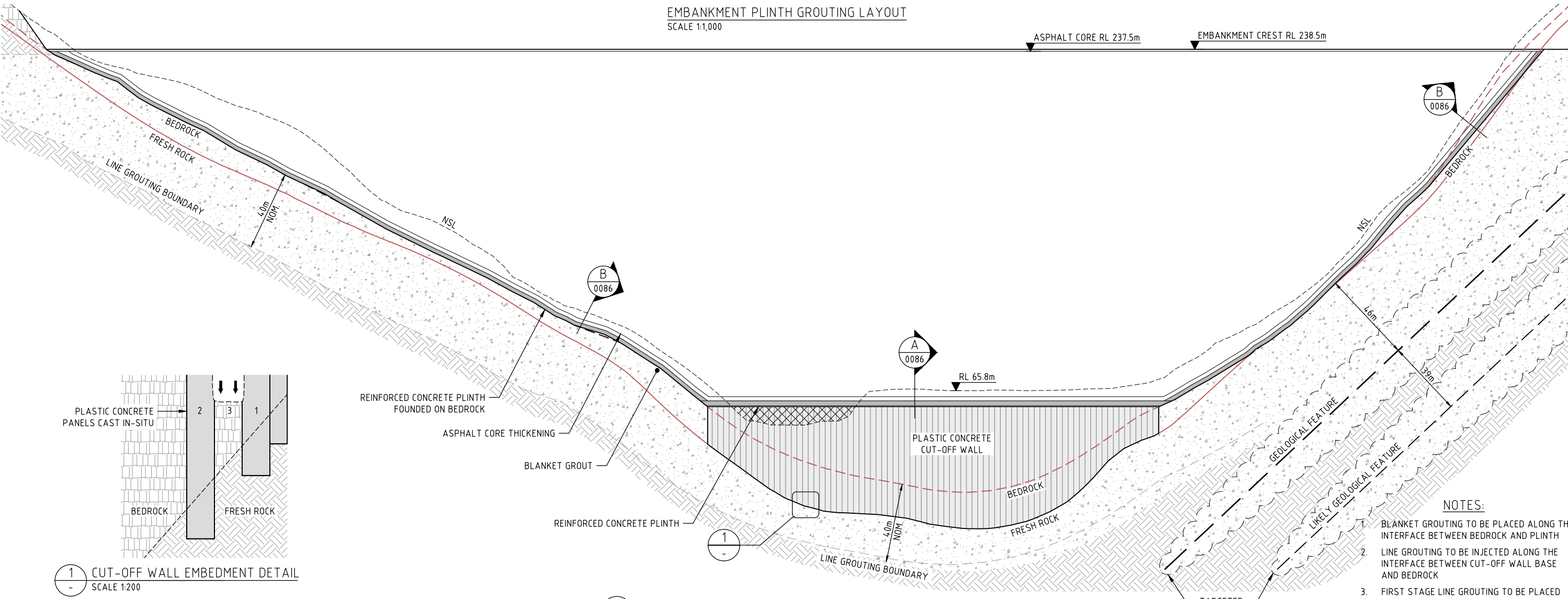
STATUS FOR INFORMATION		
SCALE	AS SHOWN	REV No.
		C
	ALL DIMENSIONS IN METRES	SIZE
		A1
DRAWING No FRP-2-D-04-01-D-030-004		

NOTE:
 GRADE CHANGE BETWEEN PANELS TO BE LIMITED TO 35°

PROJECTION: UNIVERSAL TRANSVERSE MERCATOR, ZONE 54
 HORIZONTAL DATUM: PAPUA NEW GUINEA MAP GRID 1994 (PNGMG94)
 VERTICAL DATUM: AITAPE MEAN SEA LEVEL (MSL)



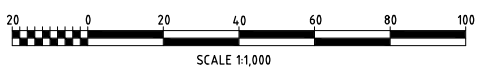
EMBANKMENT PLINTH GROUTING LAYOUT
 SCALE 1:1,000



1 CUT-OFF WALL EMBEDMENT DETAIL
 SCALE 1:200

B EMBANKMENT PLINTH & CUT-OFF WALL GROUTING SECTION
 SCALE 1:1,000

- NOTES:**
1. BLANKET GROUTING TO BE PLACED ALONG THE INTERFACE BETWEEN BEDROCK AND PLINTH
 2. LINE GROUTING TO BE INJECTED ALONG THE INTERFACE BETWEEN CUT-OFF WALL BASE AND BEDROCK
 3. FIRST STAGE LINE GROUTING TO BE PLACED AT 10m SPACING, FOLLOWED BY SECOND STAGE GROUTING AT INTERVALS IN THE CENTRE BETWEEN 10m GRID.
 4. FAULTS REQUIRE TARGETED GROUTING
 5. GROUTING OF THE FRIEDA FAULT MAY BE REQUIRED PENDING FURTHER INVESTIGATION



P:\PNA009 - FRIEDA RIVER HEP PFS\04_WORKING_FILES_V2_DRAFTING\00 - DRAWINGS\01 - SHEETS\PNA009-0088.DWG - 17/10/2018 10:36:50 AM

REF. DWG No.	DWG. DESCRIPTION	No	DATE	REVISION DETAILS	LD ENG.	PM
		C	25.09.18	ISSUED FOR FINAL REPORT	MORE	MORE
		B	18.07.18	REISSUED FOR CLIENT REVIEW	MORE	MORE
		A	31.05.18	ISSUED FOR CLIENT REVIEW	MORE	MORE

ENGINEERING COMPANY

SRK Perth 10 Richardson Street, West Perth, Western Australia 6005
 Tel: +61 8 9288 2000 - Fax: +61 8 9288 2001
<http://www.srk.com.au>

DRAWN	TREV	31.05.18
DESIGN	PRIN	31.05.18
DES.CHKD	MORE	31.05.18
LD ENG. APPR	MORE	31.05.18
PM, APPR	MORE	31.05.18

VENDOR DRG NO. PNA009-0088

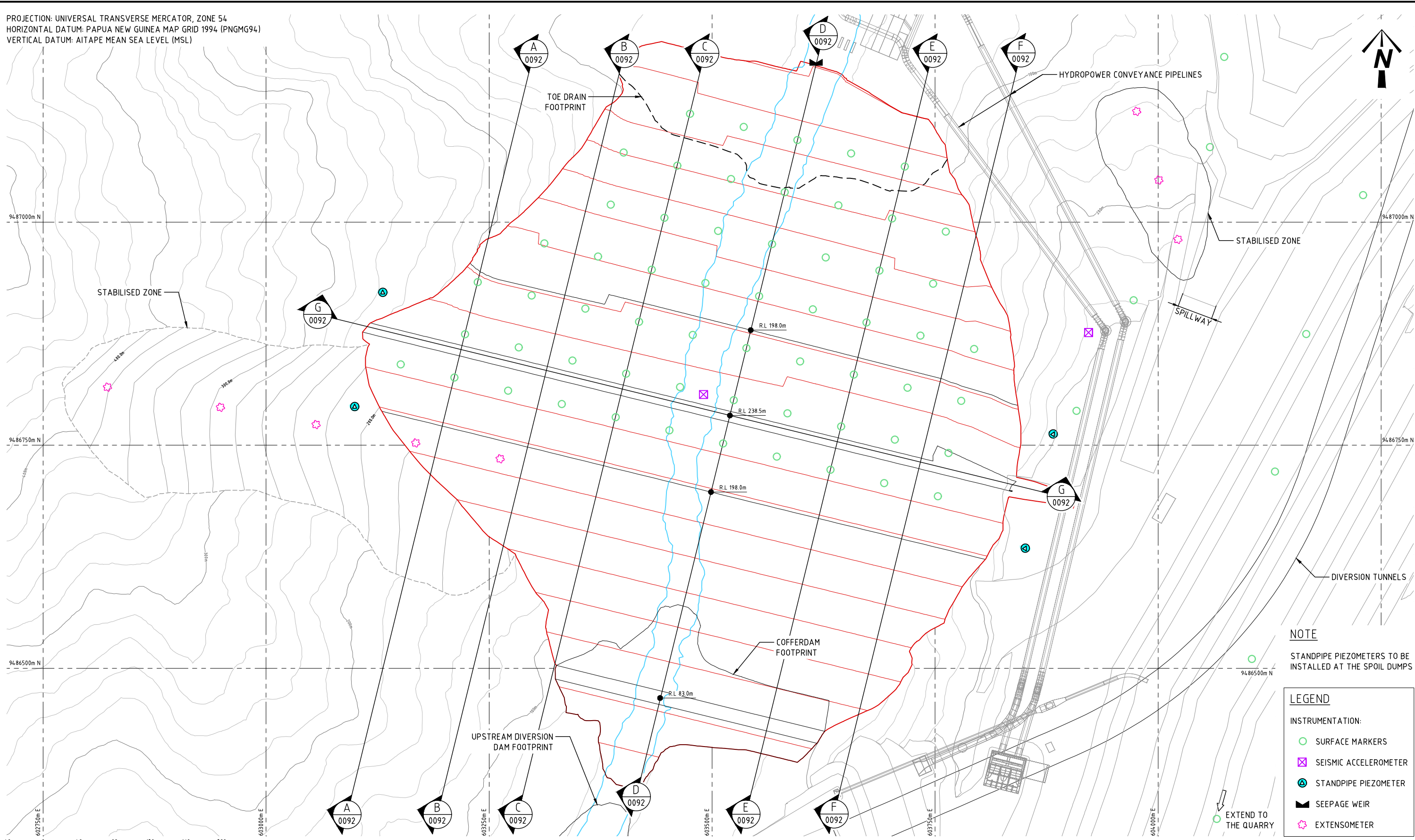
FRIEDA RIVER

OWNER
FRIEDA RIVER LIMITED

TITLE
**FRIEDA RIVER HYDROELECTRIC PROJECT
 EMBANKMENT PLINTH & CUT-OFF WALL
 GROUTING LAYOUT & SECTION**

STATUS FOR INFORMATION		
SCALE	AS SHOWN	REV No.
ALL DIMENSIONS IN METRES		C
DRAWING No	FRP-2-D-04-01-D-030-006	

PROJECTION: UNIVERSAL TRANSVERSE MERCATOR, ZONE 54
 HORIZONTAL DATUM: PAPUA NEW GUINEA MAP GRID 1994 (PNGMG94)
 VERTICAL DATUM: AITAPE MEAN SEA LEVEL (MSL)



NOTE
 STANDPIPE PIEZOMETERS TO BE INSTALLED AT THE SPOIL DUMPS

LEGEND

INSTRUMENTATION:

- SURFACE MARKERS
- ⊗ SEISMIC ACCELEROMETER
- ⊕ STANDPIPE PIEZOMETER
- ▲ SEEPAGE WEIR
- ★ EXTENSOMETER

EMBANKMENT INSTRUMENTATION LAYOUT
 SCALE 1:2,000

P:\PNA009 - FRIEDA RIVER HEP PFS\04_WORKING_FILES_V2_DRAFTING\00 - DRAWINGS\01 - SHEETS\PNA009-0090.DWG - 27/09/2018 1:33:27 PM

REF. DWG No.	DWG. DESCRIPTION	No	DATE	REVISION DETAILS	LD ENG.	PM
		C	25.09.18	ISSUED FOR FINAL REPORT	MORE	MORE
		B	18.07.18	REISSUED FOR CLIENT REVIEW	MORE	MORE
		A	31.05.18	ISSUED FOR CLIENT REVIEW	MORE	MORE

ENGINEERING COMPANY



SRK Perth 10 Richardson Street, West Perth, Western Australia 6005
 Tel: +61 8 9288 2000 - Fax: +61 8 9288 2001
<http://www.srk.com.au>

DRAWN	TREV	31.05.18
DESIGN	PRIN	31.05.18
DES.CHKD	MORE	31.05.18
LD ENG. APPR	MORE	31.05.18
PM APPR	MORE	31.05.18



OWNER
 FRIEDA RIVER LIMITED

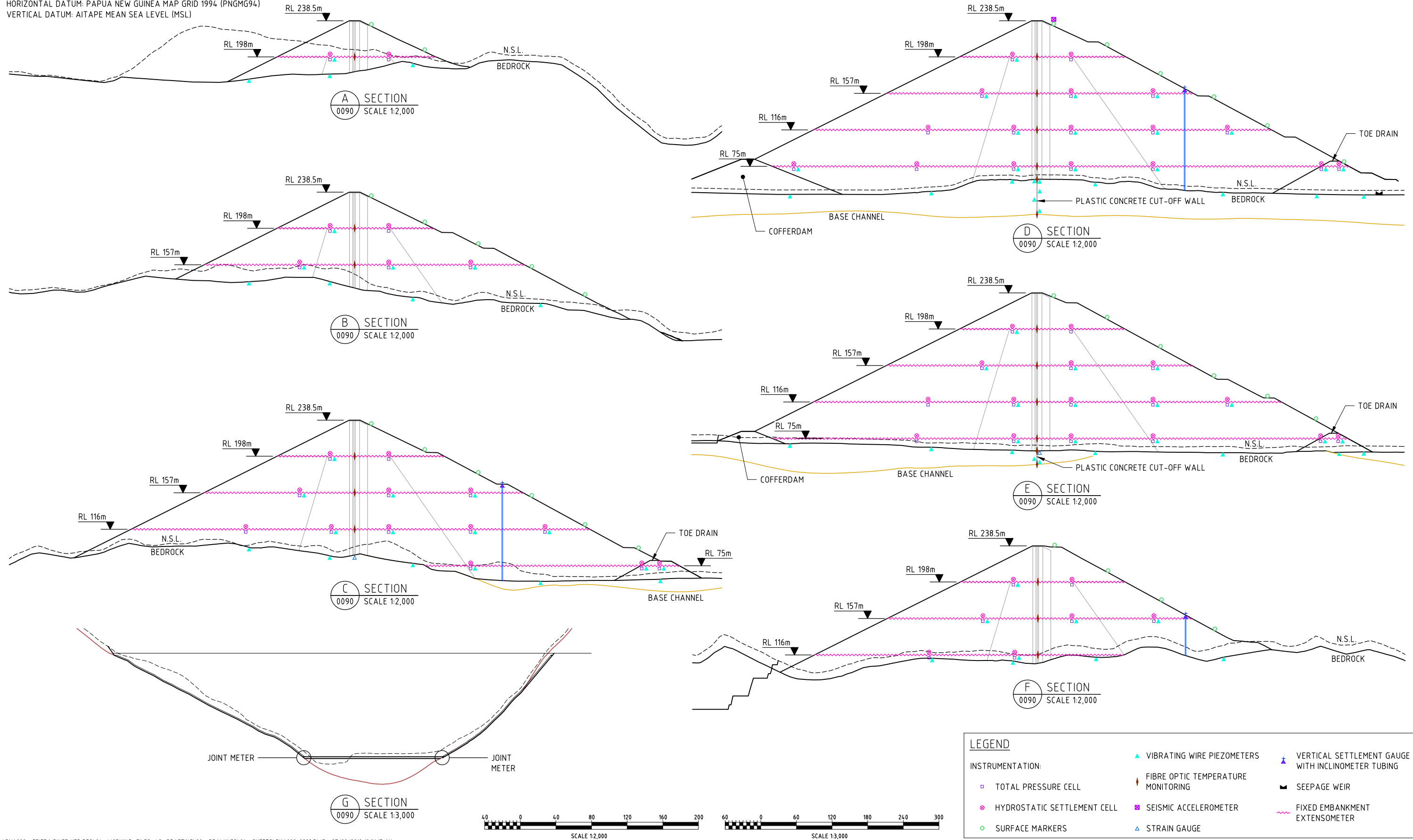
TITLE
 FRIEDA RIVER HYDROELECTRIC PROJECT
 EMBANKMENT INSTRUMENTATION
 LAYOUT

STATUS FOR INFORMATION

SCALE	AS SHOWN	REV No.	SIZE
		C	A1

DRAWING No
 FRP-2-D-04-01-D-030-007

PROJECTION: UNIVERSAL TRANSVERSE MERCATOR, ZONE 54
 HORIZONTAL DATUM: PAPUA NEW GUINEA MAP GRID 1994 (PNGMG94)
 VERTICAL DATUM: AITAPE MEAN SEA LEVEL (MSL)



LEGEND			
INSTRUMENTATION:			
□	TOTAL PRESSURE CELL	▲	VIBRATING WIRE PIEZOMETERS
○	HYDROSTATIC SETTLEMENT CELL	▲	VERTICAL SETTLEMENT GAUGE WITH INCLINOMETER TUBING
●	SURFACE MARKERS	■	SEEPAGE WEIR
○	SEISMIC ACCELEROMETER	■	FIXED EMBANKMENT EXTENSOMETER
○	STRAIN GAUGE		
○	FIBRE OPTIC TEMPERATURE MONITORING		

P:\PNA009 - FRIEDA RIVER HEP PFS\04_WORKING_FILES_V2_DRAFTING\00 - DRAWINGS\01 - SHEETS\PNA009-0092.DWG - 27/09/2018 10:01:17 AM

REF. DWG No.	DWG. DESCRIPTION	No	DATE	REVISION DETAILS	LD ENG.	PM
		C	25.09.18	ISSUED FOR FINAL REPORT	MORE	MORE
		B	18.07.18	REISSUED FOR CLIENT REVIEW	MORE	MORE
		A	31.05.18	ISSUED FOR CLIENT REVIEW	MORE	MORE

ENGINEERING COMPANY

SRK Perth 10 Richardson Street, West Perth, Western Australia 6005
 Tel: +61 8 9288 2000 - Fax: +61 8 9288 2001
<http://www.srk.com.au>

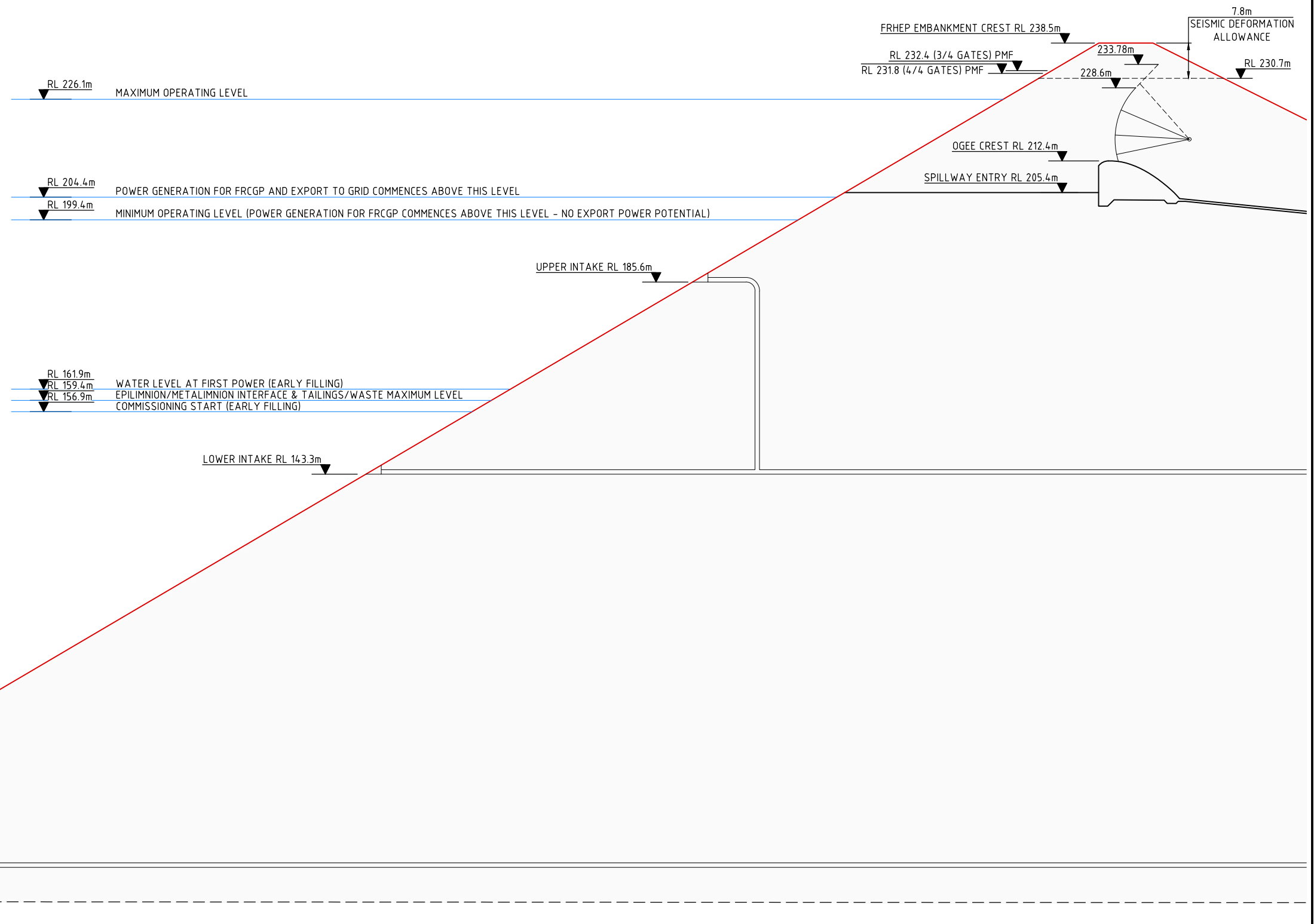
VENDOR DRG NO. PNA009-0092

OWNER
FRIEDA RIVER LIMITED

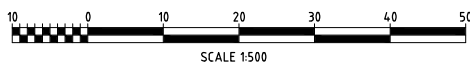
TITLE
**FRIEDA RIVER HYDROELECTRIC PROJECT
 EMBANKMENT INSTRUMENTATION
 SECTIONS**

STATUS FOR INFORMATION			
SCALE	AS SHOWN	REV No.	SIZE
ALL DIMENSIONS IN METRES		C	A1
DRAWING No		FRP-2-D-04-01-D-030-008	



PROJECTION: UNIVERSAL TRANSVERSE MERCATOR, ZONE 54
 HORIZONTAL DATUM: PAPUA NEW GUINEA MAP GRID 1994 (PNGMG94)
 VERTICAL DATUM: AITAPE MEAN SEA LEVEL (MSL)



FRHEP CRITICAL LEVELS SECTION
 SCALE 1:500



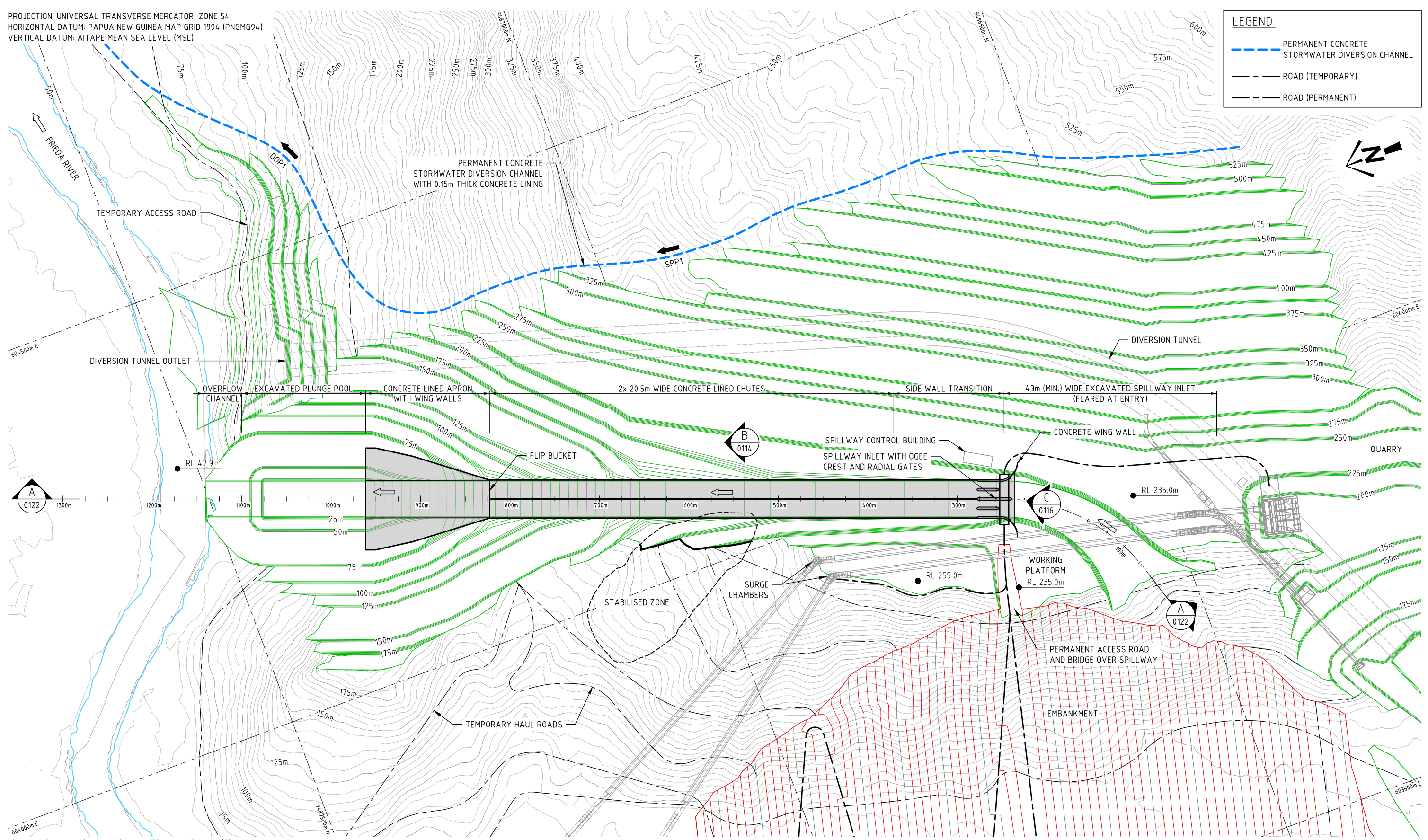
P:\PNA009 - FRIEDA RIVER HEP PFS\04_WORKING_FILES_V2_DRAFTING\00 - DRAWINGS\01 - SHEETS\PNA009-0100.DWG - 27/09/2018 10:01:22 AM

				ENGINEERING COMPANY  SRK Perth 10 Richardson Street, West Perth, Western Australia 6005 Tel: +61 8 9288 2000 - Fax: +61 8 9288 2001 http://www.srk.com.au			DRAWN: TREV 31.05.18 DESIGN: PRIN 31.05.18 DES.CHKD: MORE 31.05.18 LD ENG. APPR: MORE 31.05.18 PM APPR: MORE 31.05.18			OWNER FRIEDA RIVER LIMITED		STATUS FOR INFORMATION SCALE AS SHOWN ALL DIMENSIONS IN METRES DRAWING No FRP-2-D-00-01-D-030-010		
							TITLE FRIEDA RIVER HYDROELECTRIC PROJECT CRITICAL LEVELS SECTION			REV No. C SIZE A1				
REF. DWG No.	DWG. DESCRIPTION	No	DATE	REVISION DETAILS	LD ENG.	PM	VENDOR DRG NO.	PNA009-0100						
		C	25.09.18	ISSUED FOR FINAL REPORT	MORE	MORE								
		B	18.07.18	REISSUED FOR CLIENT REVIEW	MORE	MORE								
		A	31.05.18	ISSUED FOR CLIENT REVIEW	MORE	MORE								

PROJECTION: UNIVERSAL TRANSVERSE MERCATOR, ZONE 54
 HORIZONTAL DATUM: PAPUA NEW GUINEA MAP GRID 1994 (PNGMG94)
 VERTICAL DATUM: AITAPE MEAN SEA LEVEL (MSL)

LEGEND:

- PERMANENT CONCRETE STORMWATER DIVERSION CHANNEL
- ROAD (TEMPORARY)
- ROAD (PERMANENT)



SCALE 1:2,000
 0 40 80 120 160 200

SPILLWAY LAYOUT
 SCALE 1:2,000

P:\PNA009 - FRIEDA RIVER HEP PFS\04_WORKING_FILES_V2_DRAFTING\00 - DRAWINGS\01 - SHEETS\PNA009-0110.DWG - 27/09/2018 10:01:36 AM

REF. DWG No.	DWG. DESCRIPTION	No	DATE	REVISION DETAILS	LD ENG.	PM
		D	25.09.18	ISSUED FOR FINAL REPORT	MORE	MORE
		C	03.09.18	REISSUED FOR CLIENT REVIEW	MORE	MORE
		B	18.07.18	REISSUED FOR CLIENT REVIEW	MORE	MORE
		A	31.05.18	ISSUED FOR CLIENT REVIEW	MORE	MORE

ENGINEERING COMPANY

SRK Perth 10 Richardson Street, West Perth, Western Australia 6005
 Tel: +61 8 9288 2000 - Fax: +61 8 9288 2001
<http://www.srk.com.au>

DRAWN	TREV	31.05.18
DESIGN	PRIN	31.05.18
DES.CHKD	MORE	31.05.18
LD ENG. APPR	MORE	31.05.18
PM, APPR	MORE	31.05.18

VENDOR DRG NO. PNA009-0110

FRIEDA RIVER

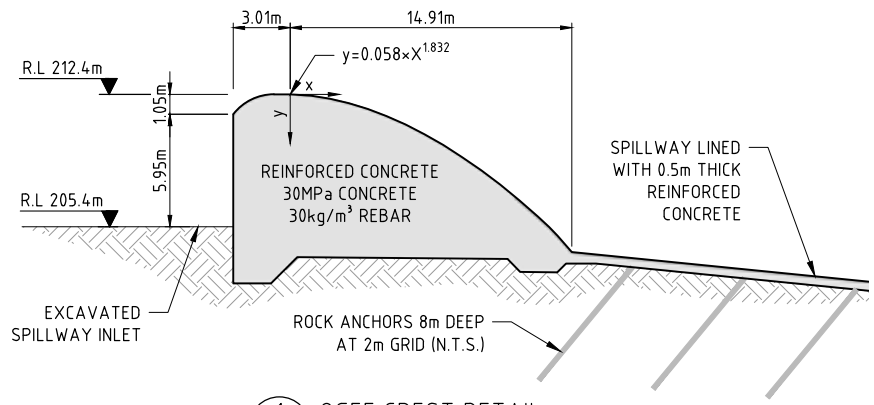
OWNER
FRIEDA RIVER LIMITED

TITLE
FRIEDA RIVER HYDROELECTRIC PROJECT

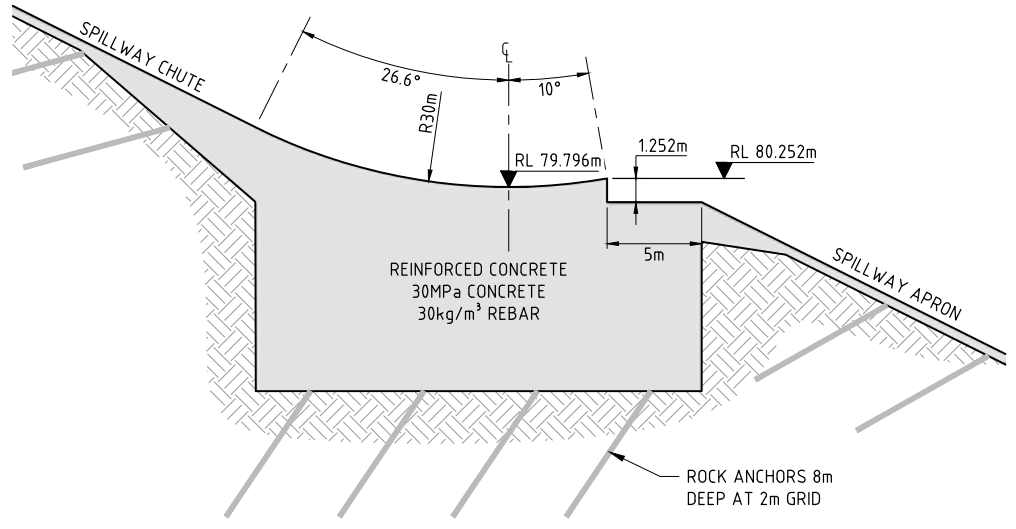
SPILLWAY LAYOUT

STATUS FOR INFORMATION		
SCALE	AS SHOWN	REV No.
ALL DIMENSIONS IN METRES		D
DRAWING No		A1
FRP-2-D-10-01-D-030-001		

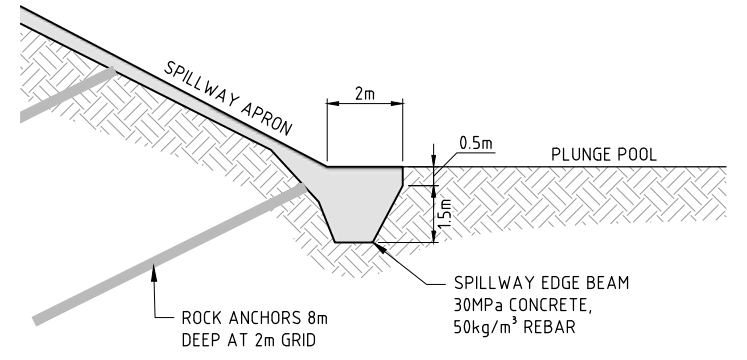
PROJECTION: UNIVERSAL TRANSVERSE MERCATOR, ZONE 54
 HORIZONTAL DATUM: PAPUA NEW GUINEA MAP GRID 1994 (PNGMG94)
 VERTICAL DATUM: AITAPE MEAN SEA LEVEL (MSL)



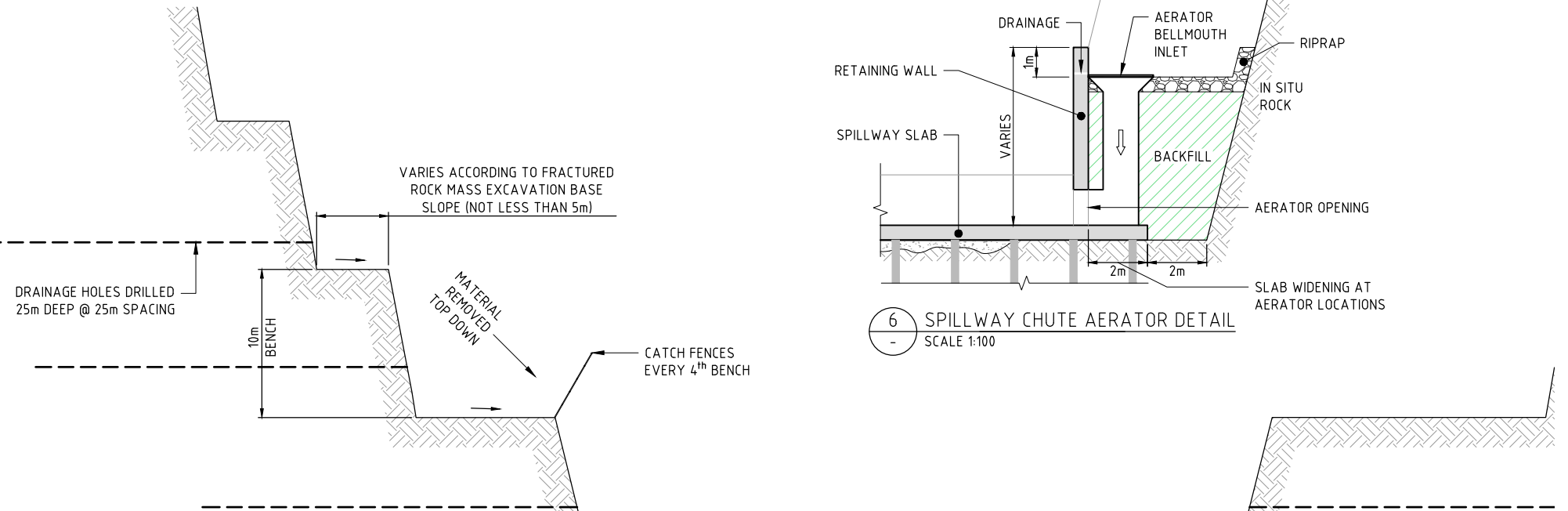
1 Ogee Crest Detail
 0122 SCALE 1:200



2 Flip Bucket Detail
 0122 SCALE 1:200

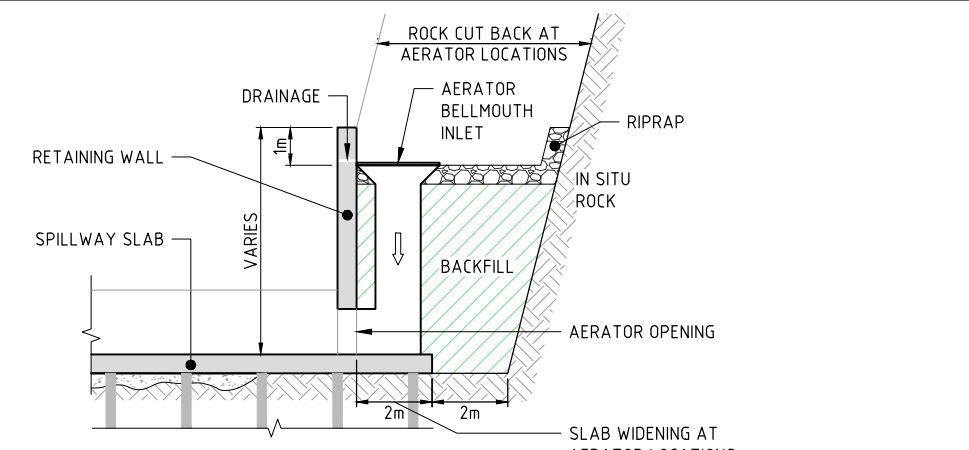


3 Spillway Toe Wall Detail
 0122 SCALE 1:100

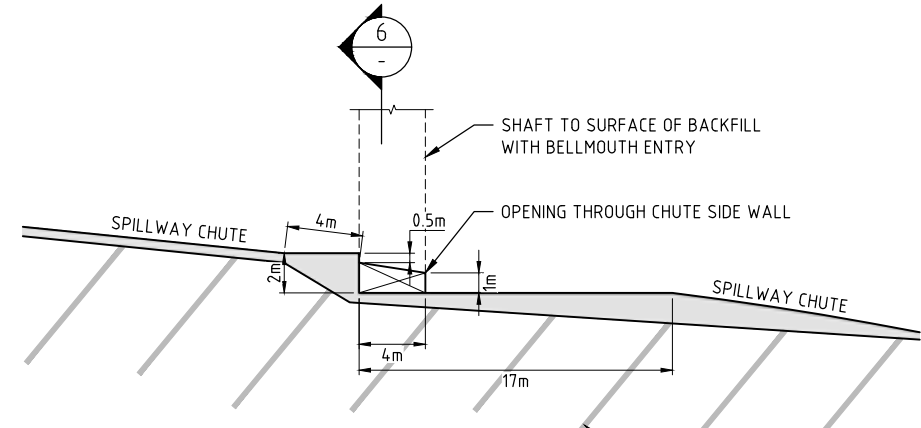


NOTE: SPILLWAY EXCAVATION CUT TO HAVE SPOT-BOLTING (3m LENGTH)

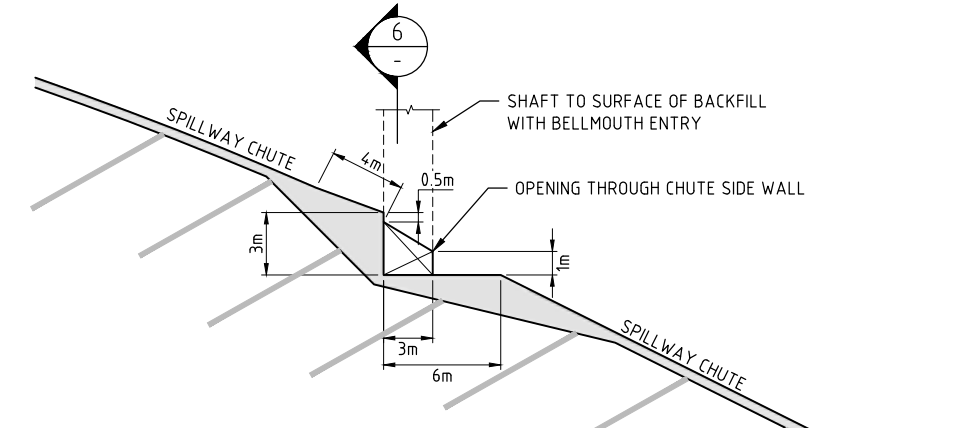
B Spillway Chute Section
 0110 SCALE 1:200



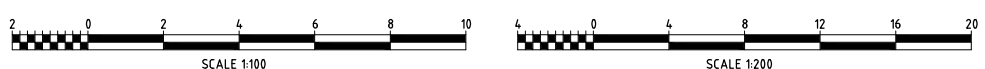
6 Spillway Chute Aerator Detail
 SCALE 1:100



4 Aerator Detail
 0122 SCALE 1:200



5 Aerator Detail
 0122 SCALE 1:200



P:\PNA009 - FRIEDA RIVER HEP PFS\04_WORKING_FILES_V2_DRAFTING\00 - DRAWINGS\01 - SHEETS\PNA009-0114.DWG - 27/09/2018 10:01:54 AM

REF. DWG No.	DWG. DESCRIPTION	No	DATE	REVISION DETAILS	LD ENG.	PM
		C	25.09.18	ISSUED FOR FINAL REPORT	MORE	MORE
		B	18.07.18	REISSUED FOR CLIENT REVIEW	MORE	MORE
		A	31.05.18	ISSUED FOR CLIENT REVIEW	MORE	MORE

ENGINEERING COMPANY

SRK Perth 10 Richardson Street, West Perth, Western Australia 6005
 Tel: +61 8 9288 2000 - Fax: +61 8 9288 2001
<http://www.srk.com.au>

DRAWN	TREV	31.05.18
DESIGN	PRIN	31.05.18
DES.CHKD	MORE	31.05.18
LD ENG. APPR	MORE	31.05.18
PM APPR	MORE	31.05.18

VENDOR DRG NO. PNA009-0114

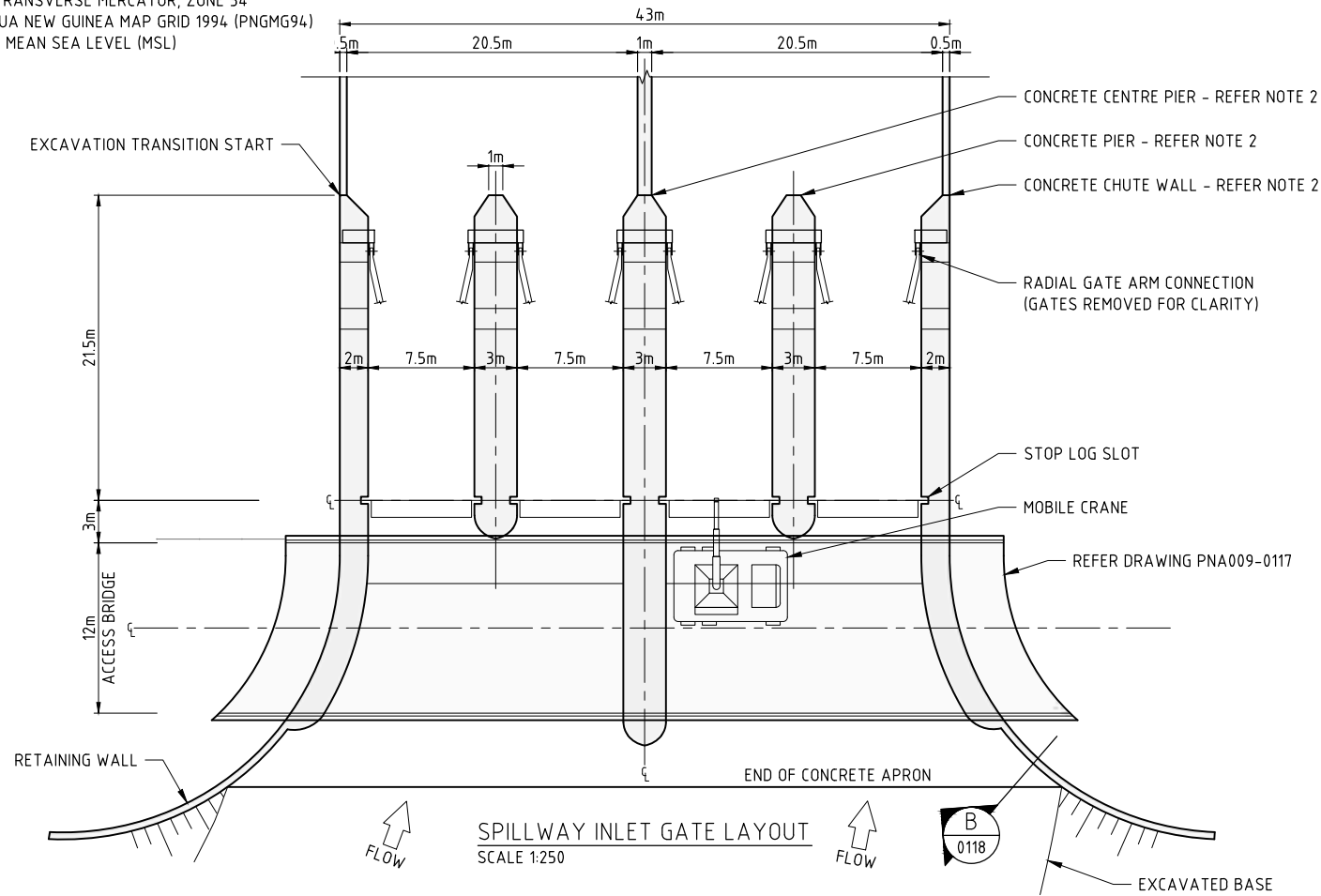
OWNER
FRIEDA RIVER LIMITED

TITLE
FRIEDA RIVER HYDROELECTRIC PROJECT

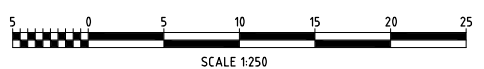
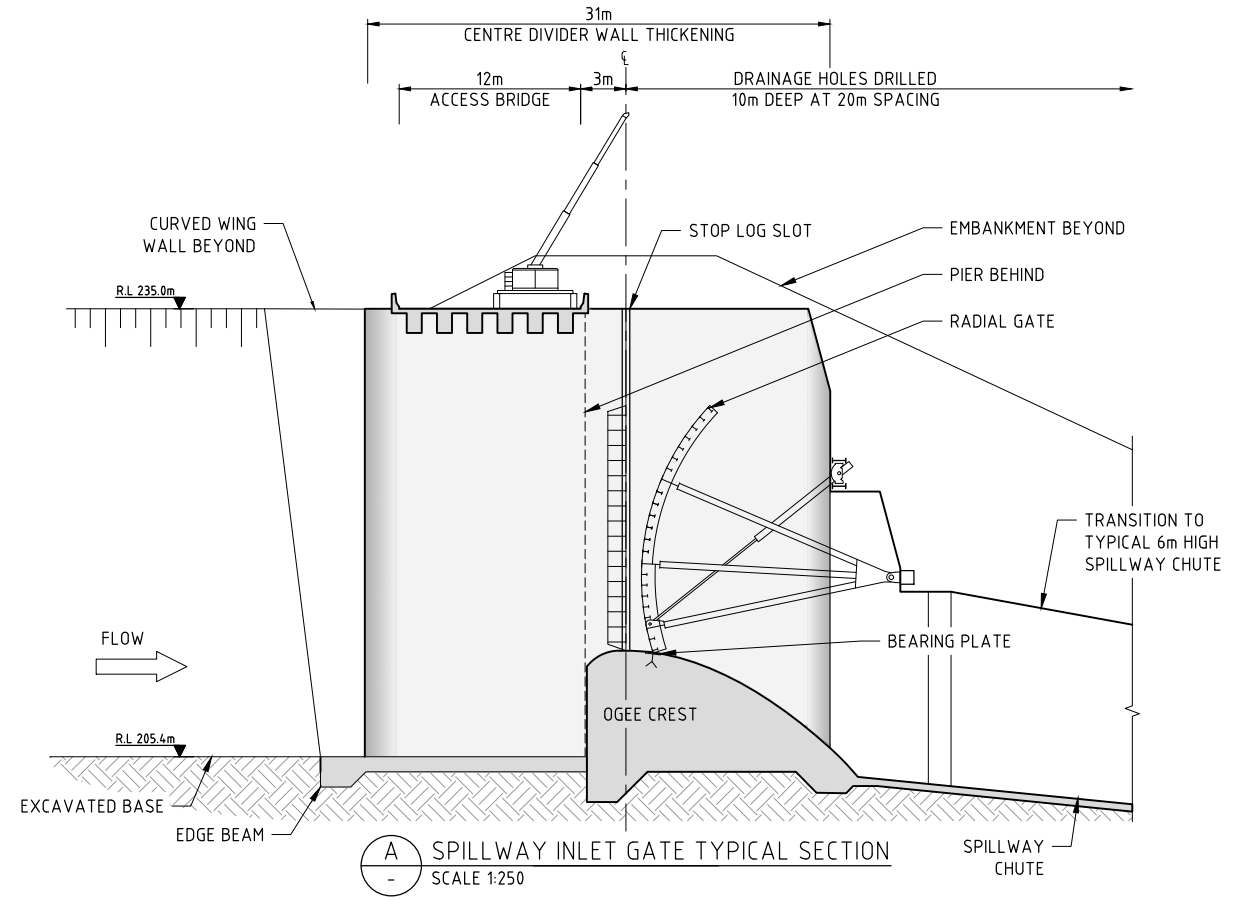
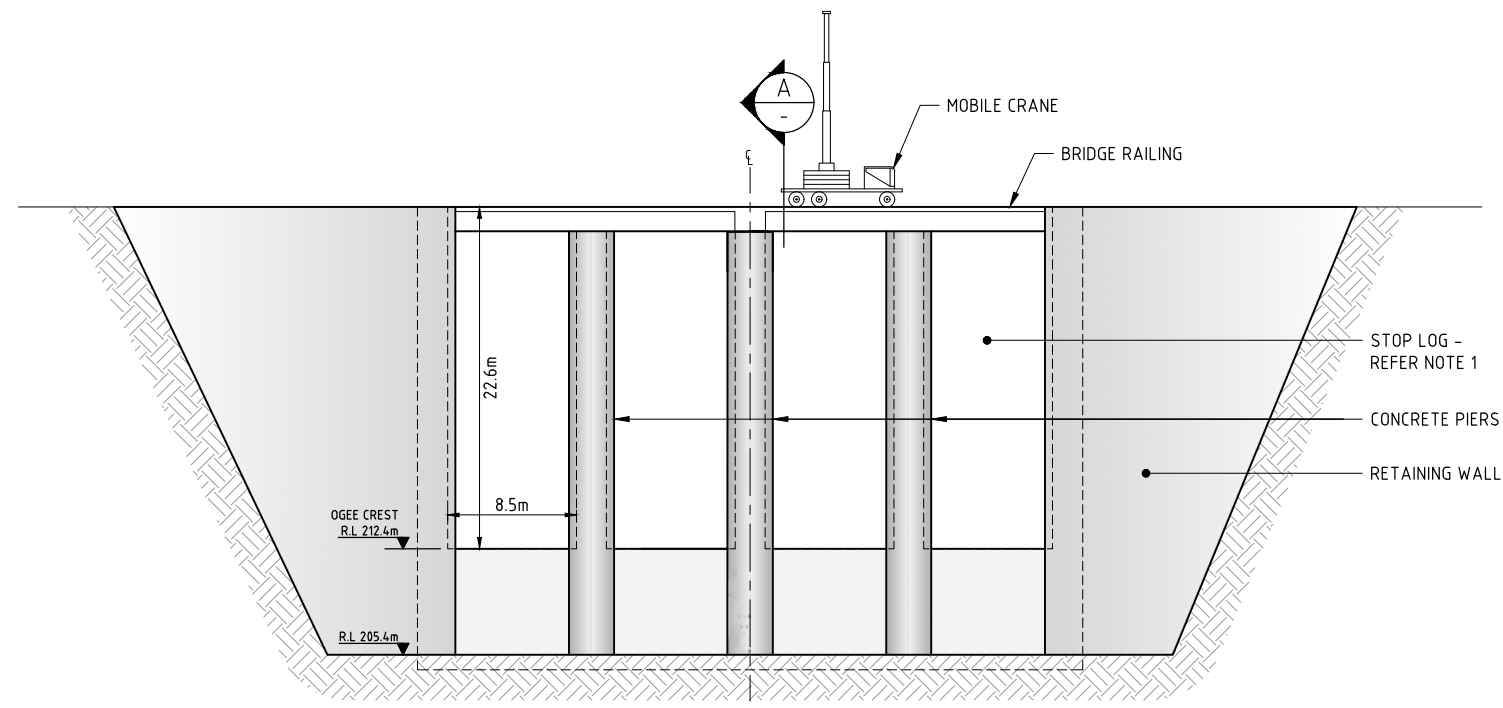
SPILLWAY SECTION & DETAILS

STATUS FOR INFORMATION		
SCALE	AS SHOWN	REV No.
		C
SIZE		A1
DRAWING No FRP-2-D-10-01-D-030-003		

PROJECTION: UNIVERSAL TRANSVERSE MERCATOR, ZONE 54
 HORIZONTAL DATUM: PAPUA NEW GUINEA MAP GRID 1994 (PNGMG94)
 VERTICAL DATUM: AITAPE MEAN SEA LEVEL (MSL)



- NOTES:**
- 1 STOP LOGS TO BE FABRICATED IN SECTIONS
 - 2 REINFORCING TO PIERS WITH 30 MPa CONCRETE AND 100 kg/m³ HIGH TENSILE REBAR
 - 3 JOINTS AND WATER STOPS TO BE SPECIFIED



P:\PNA009 - FRIEDA RIVER HEP PFS\04_WORKING_FILES_V2_DRAFTING\00 - DRAWINGS\01 - SHEETS\PNA009-0116.DWG - 27/09/2018 10:01:58 AM

REF. DWG No.	DWG. DESCRIPTION	No	DATE	REVISION DETAILS	LD ENG.	PM	VENDOR DRG NO.

ENGINEERING COMPANY

 SRK Perth 10 Richardson Street, West Perth, Western Australia 6005
 Tel: +61 8 9288 2000 - Fax: +61 8 9288 2001
<http://www.srk.com.au>

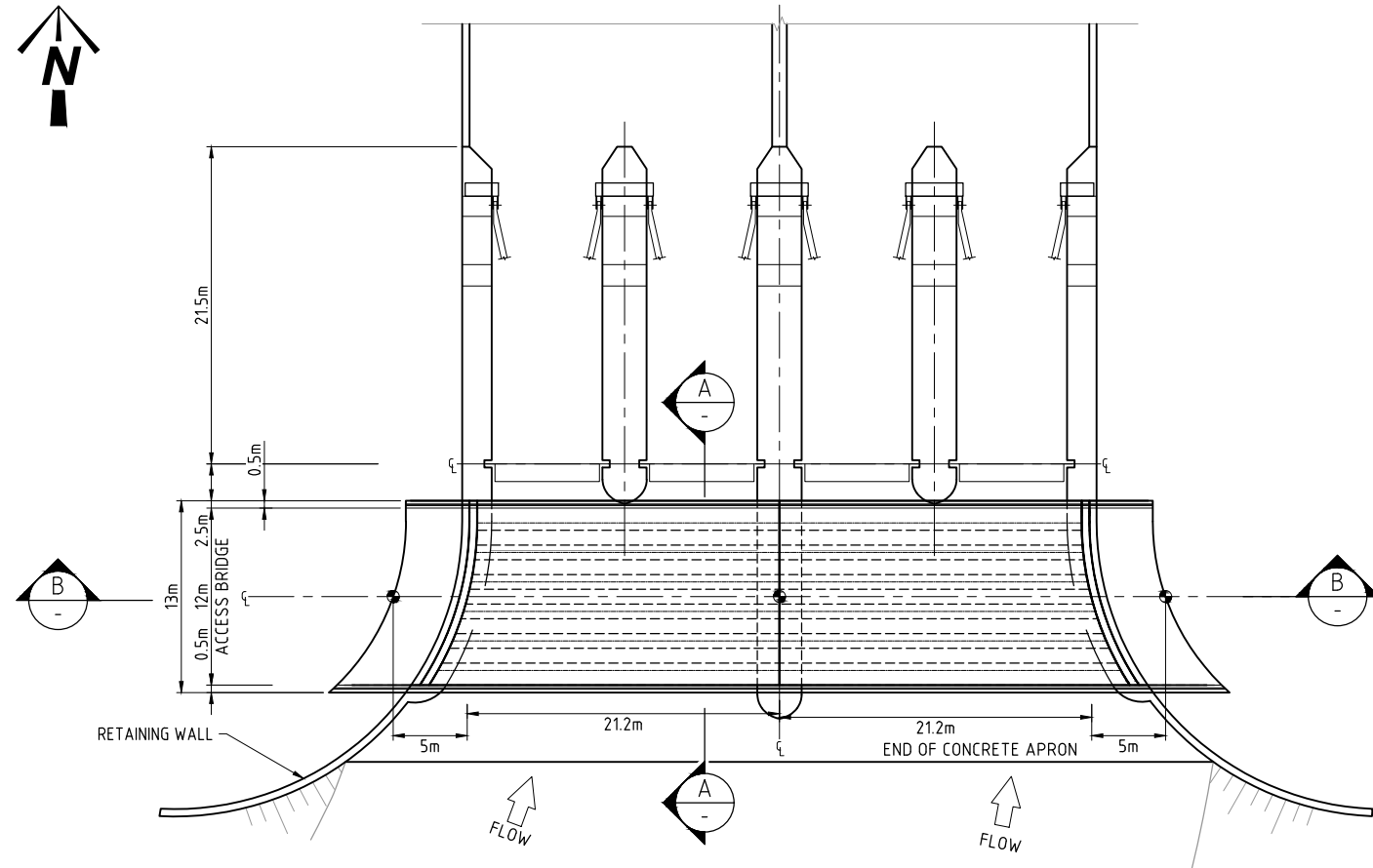
FRIEDA RIVER

OWNER
 FRIEDA RIVER LIMITED

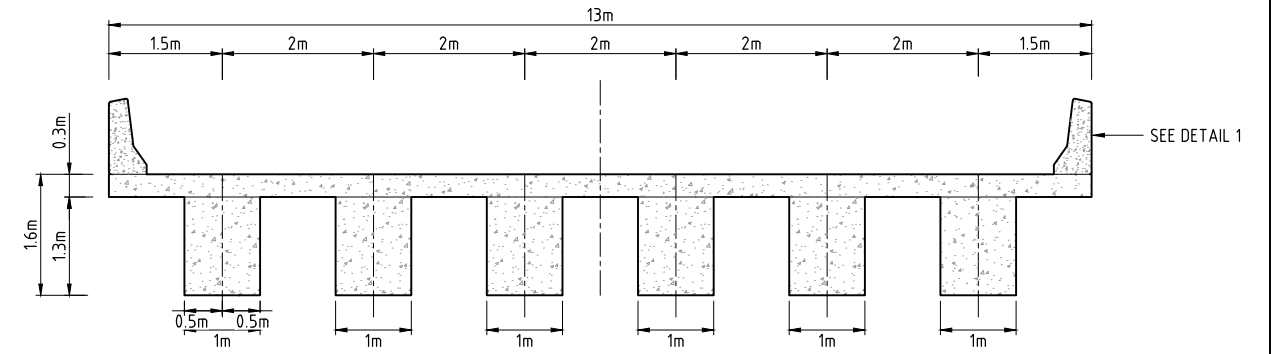
TITLE
 FRIEDA RIVER HYDROELECTRIC PROJECT
 SPILLWAY INLET GATE LAYOUT,
 SECTION & ELEVATION

STATUS FOR INFORMATION			
SCALE	AS SHOWN	REV No.	SIZE
ALL DIMENSIONS IN METRES		C	A1
DRAWING No FRP-2-D-10-01-D-030-004			

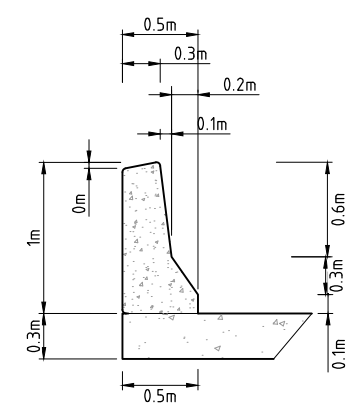
PROJECTION: UNIVERSAL TRANSVERSE MERCATOR, ZONE 54
 HORIZONTAL DATUM: PAPUA NEW GUINEA MAP GRID 1994 (PNGMG94)
 VERTICAL DATUM: AITAPE MEAN SEA LEVEL (MSL)



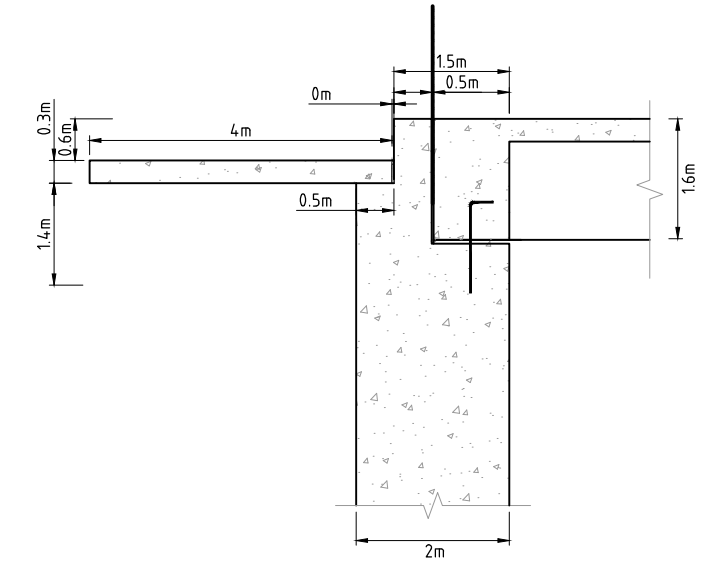
SPILLWAY BRIDGE LAYOUT
 SCALE 1:250



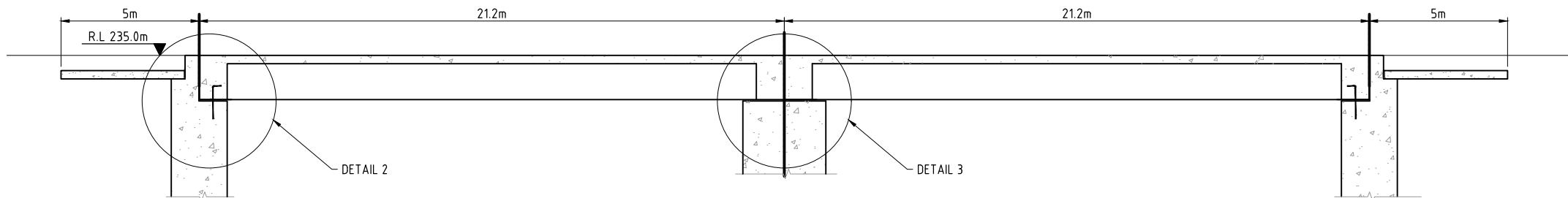
A SECTION
 SCALE 1:50



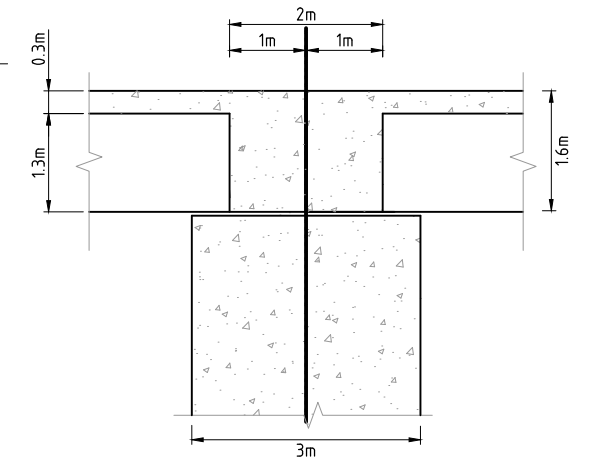
1 DETAIL
 SCALE 1:25



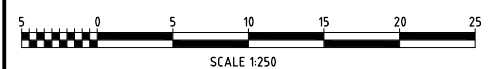
2 DETAIL
 SCALE 1:50



B SECTION
 SCALE 1:100



3 DETAIL
 SCALE 1:50



P:\PNA009 - FRIEDA RIVER HEP PFS\04_WORKING_FILES_V2_DRAFTING\00 - DRAWINGS\01 - SHEETS\PNA009-0117.DWG - 27/09/2018 10:02:02 AM

REF. DWG No.	DWG. DESCRIPTION	No	DATE	REVISION DETAILS	LD ENG.	PM
		C	25.09.18	ISSUED FOR FINAL REPORT	MORE	MORE
		B	18.07.18	REISSUED FOR CLIENT REVIEW	MORE	MORE
		A	31.05.18	ISSUED FOR CLIENT REVIEW	MORE	MORE

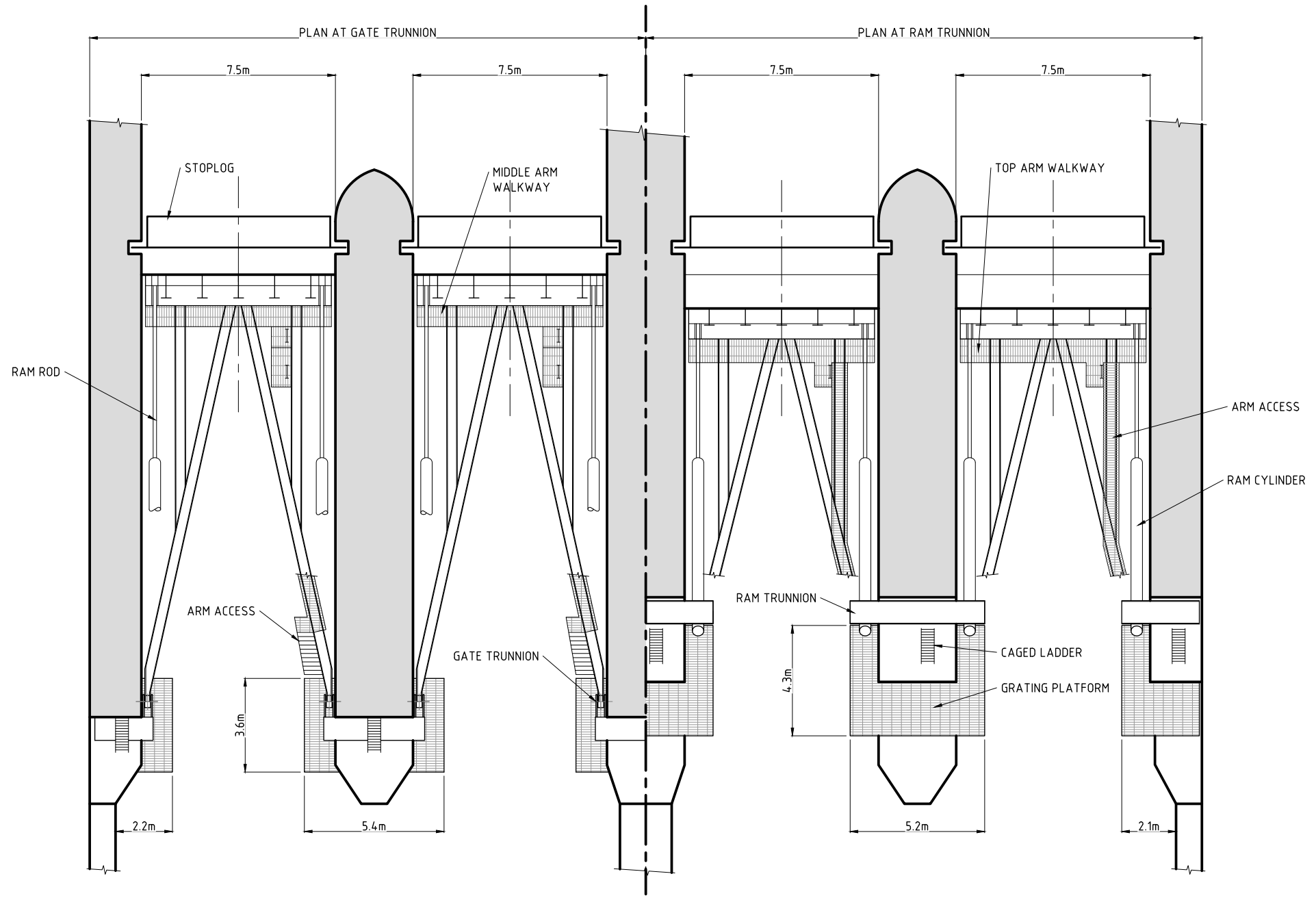
ENGINEERING COMPANY			DRAWN	TREV	31.05.18
 SRK Perth 10 Richardson Street, West Perth, Western Australia 6005 Tel: +61 8 9288 2000 - Fax: +61 8 9288 2001 http://www.srk.com.au			DESIGN	PRIN	31.05.18
			DES.CHKD	MORE	31.05.18
			LD ENG. APPR	MORE	31.05.18
PM, APPR	MORE	31.05.18			



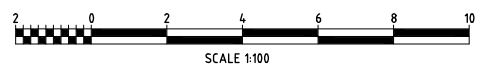
OWNER	FRIEDA RIVER LIMITED
TITLE	FRIEDA RIVER HYDROELECTRIC PROJECT SPILLWAY BRIDGE LAYOUT, SECTIONS & DETAILS

STATUS FOR INFORMATION		
SCALE	AS SHOWN	REV No.
ALL DIMENSIONS IN METRES	C	A1
DRAWING No FRP-2-D-10-01-D-030-005		

PROJECTION: UNIVERSAL TRANSVERSE MERCATOR, ZONE 54
 HORIZONTAL DATUM: PAPUA NEW GUINEA MAP GRID 1994 (PNGMG94)
 VERTICAL DATUM: AITAPE MEAN SEA LEVEL (MSL)



PLAN



C:\DATA\PDF\FRIEDA RIVER\FRP-2-D-10-01-D-030-007.DWG

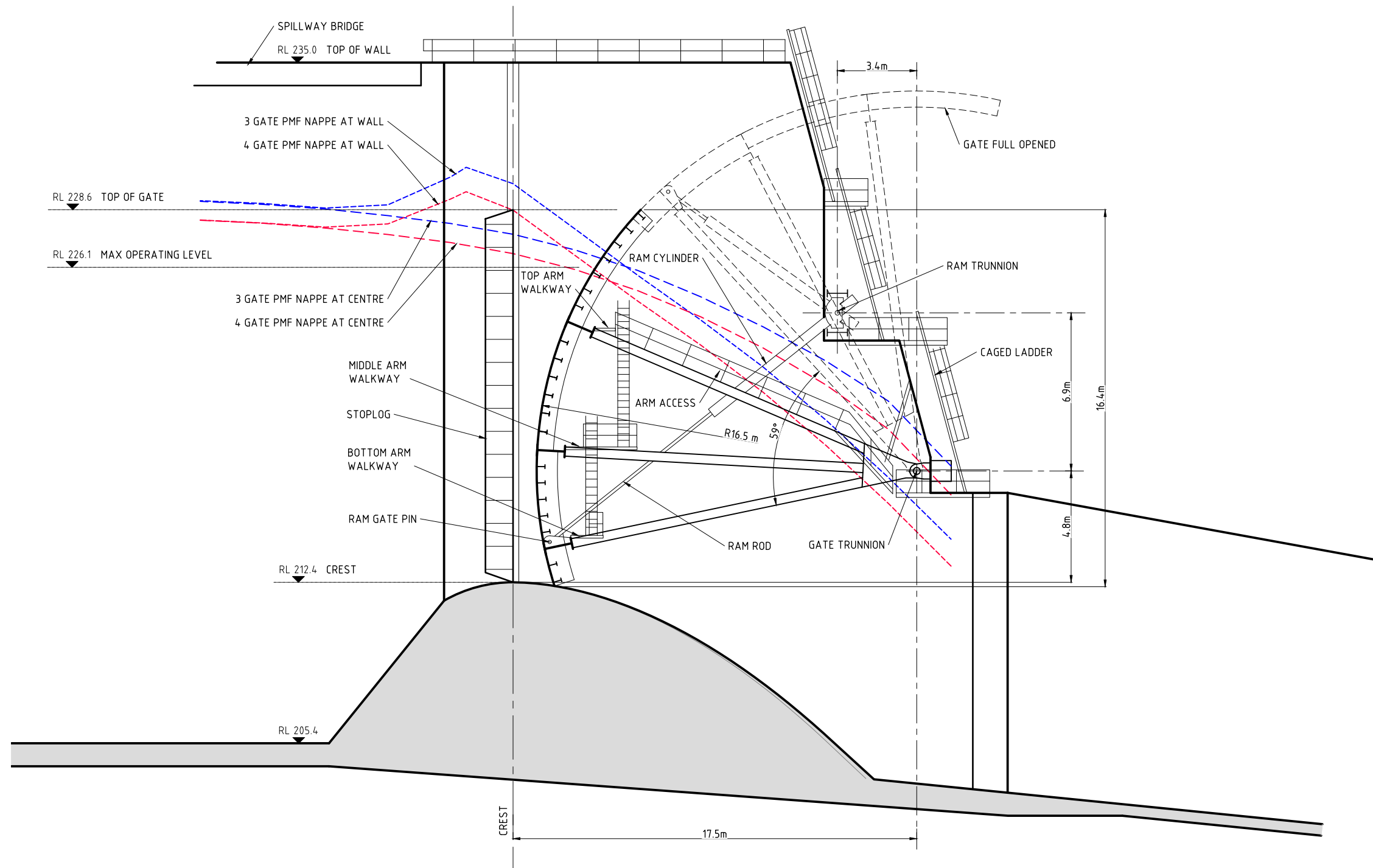
REF. DWG No.	DWG. DESCRIPTION	No	DATE	REVISION DETAILS	LD ENG.	PM
		B	24.09.18	ISSUED FOR FINAL REPORT	BROW	BROW
		A	28.06.18	ISSUED FOR CLIENT REVIEW	BROW	BROW

ENGINEERING COMPANY			DRAWN	MURR	28.06.18
 			DESIGN	ROBI	28.06.18
			DES.CHKD	ROBI	28.06.18
			LD ENG. APPR	BROW	28.06.18
			PM, APPR	BROW	28.06.18
VENDOR DRG NO. 80510050					

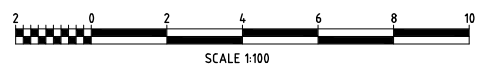
OWNER	FRIEDA RIVER LIMITED	
TITLE	FRIEDA RIVER HYDROELECTRIC PROJECT SPILLWAY GATE PLAN	

STATUS FOR INFORMATION		
SCALE 1:100	REV No.	SIZE
ALL DIMENSIONS IN METRES	B	A1
DRAWING No FRP-2-D-10-01-D-030-007		

PROJECTION: UNIVERSAL TRANSVERSE MERCATOR, ZONE 54
 HORIZONTAL DATUM: PAPUA NEW GUINEA MAP GRID 1994 (PNGMG94)
 VERTICAL DATUM: AITAPE MEAN SEA LEVEL (MSL)



SECTION



C:\DATA\PDF\FRIEDA RIVER\FRP-2-D-10-01-D-030-008.DWG

REF. DWG No.	DWG. DESCRIPTION	No	DATE	REVISION DETAILS	LD ENG.	PM
		B	24.09.18	ISSUED FOR FINAL REPORT	BROW	BROW
		A	28.06.18	ISSUED FOR CLIENT REVIEW	BROW	BROW

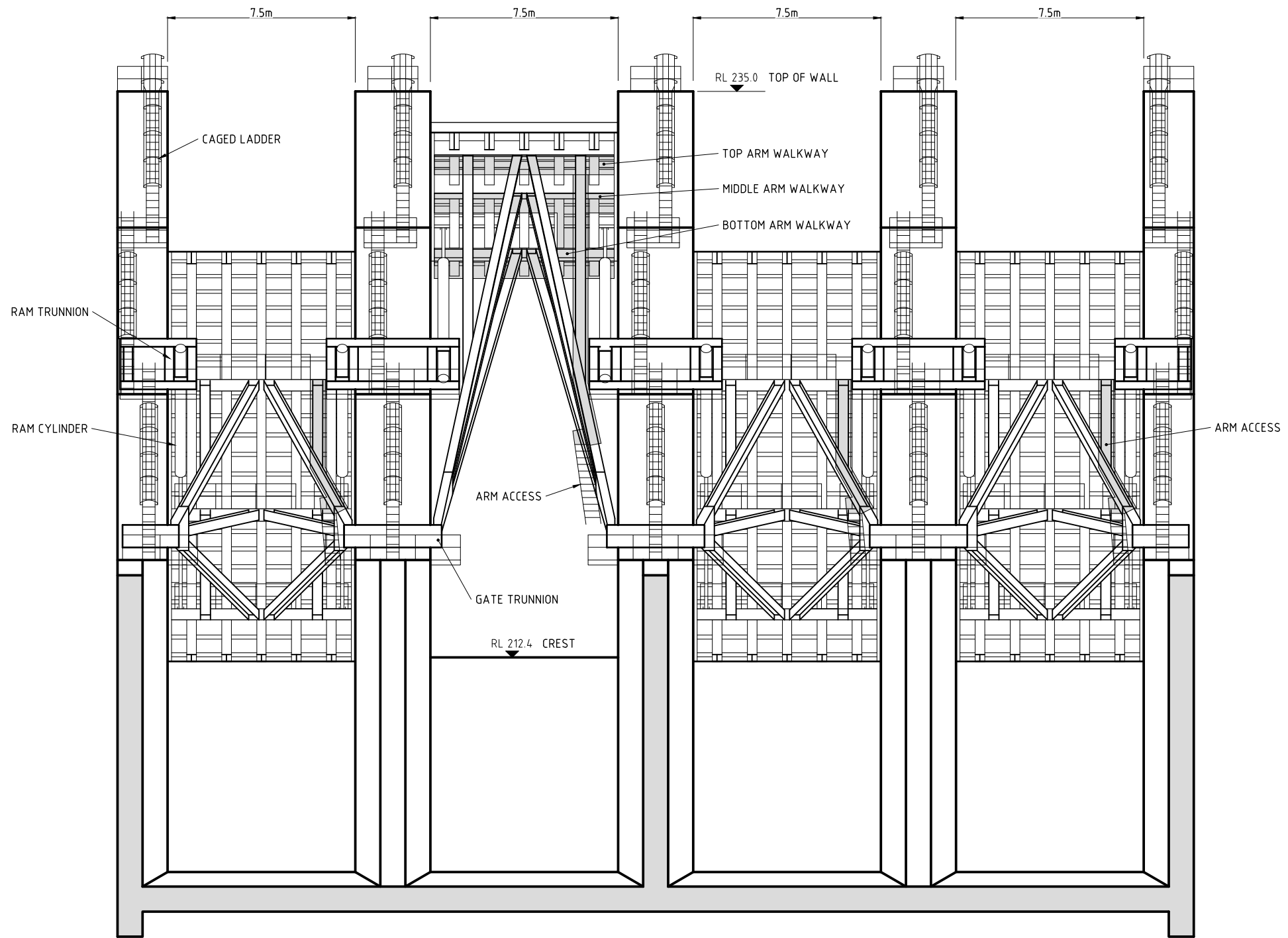
ENGINEERING COMPANY			DRAWN	MURR	28.06.18
 			DESIGN	ROBI	28.06.18
			DES.CHKD	ROBI	28.06.18
			LD ENG. APPR	BROW	28.06.18
			PM APPR	BROW	28.06.18
VENDOR DRG NO.			80510050		

OWNER
FRIEDA RIVER LIMITED

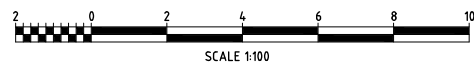
TITLE
 FRIEDA RIVER HYDROELECTRIC PROJECT
 SPILLWAY GATE SECTION

STATUS FOR INFORMATION		
SCALE 1:100	REV No.	SIZE
ALL DIMENSIONS IN METRES	B	A1
DRAWING No FRP-2-D-10-01-D-030-008		




PROJECTION: UNIVERSAL TRANSVERSE MERCATOR, ZONE 54
 HORIZONTAL DATUM: PAPUA NEW GUINEA MAP GRID 1994 (PNGMG94)
 VERTICAL DATUM: AITAPE MEAN SEA LEVEL (MSL)



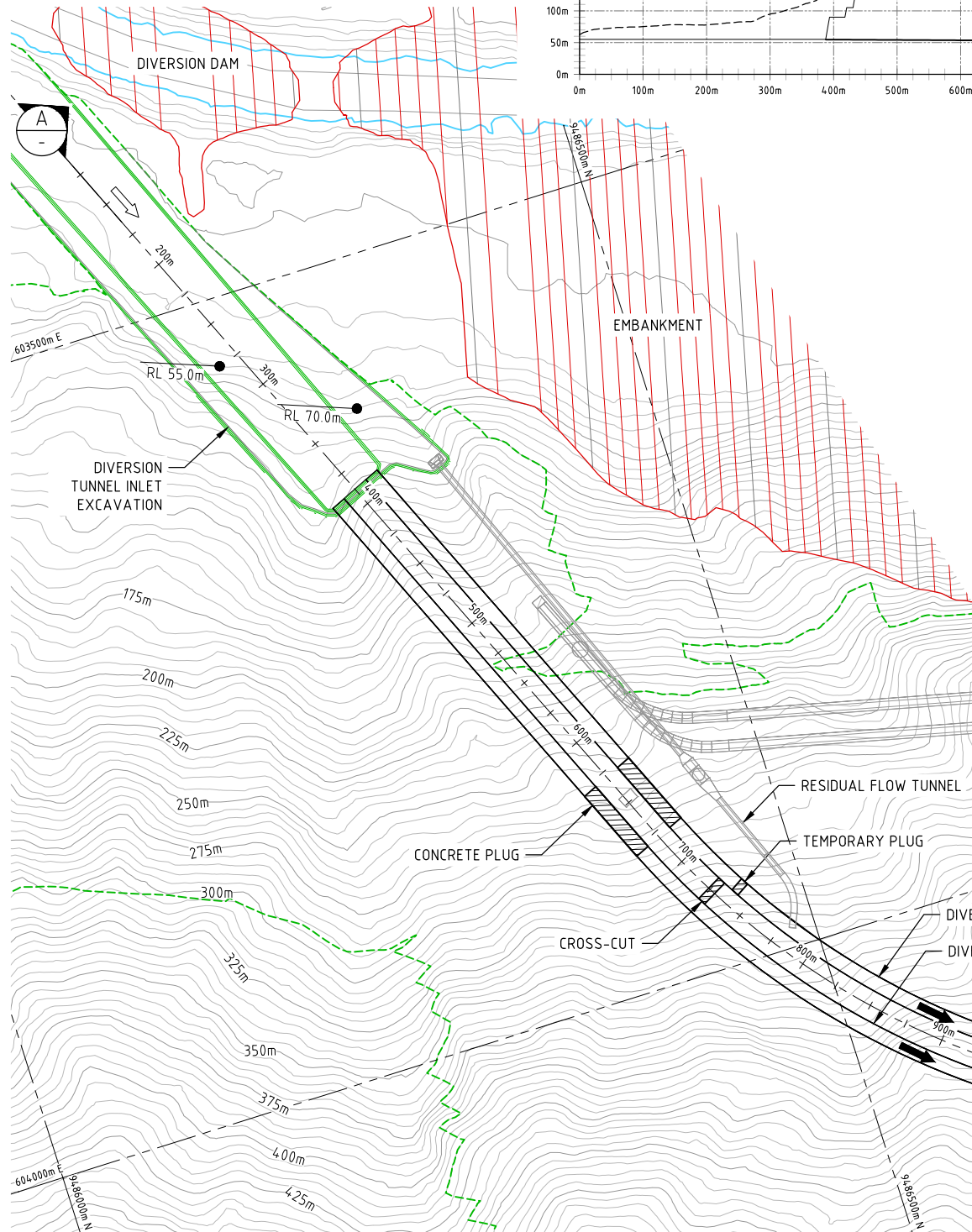
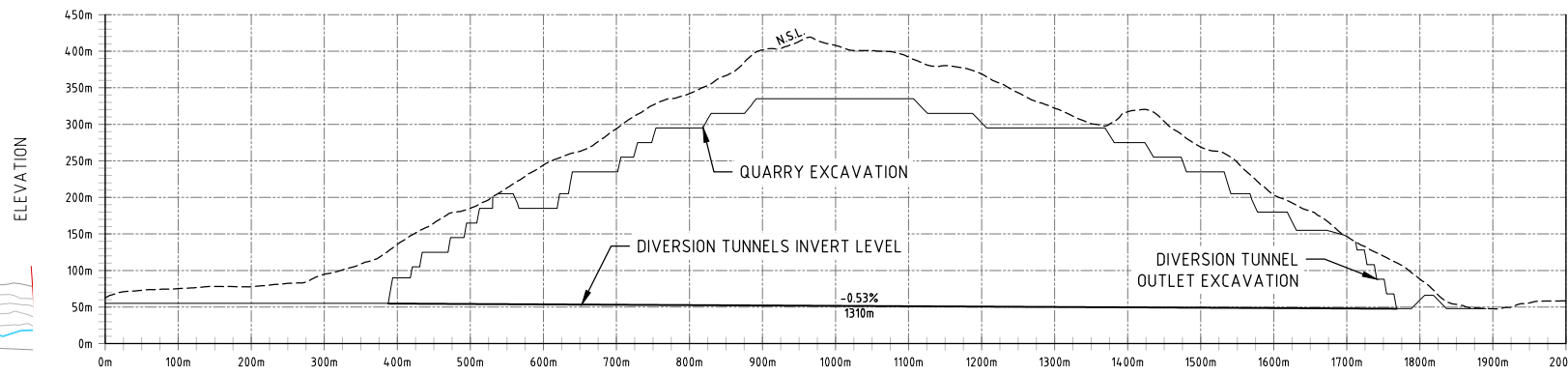
ELEVATION



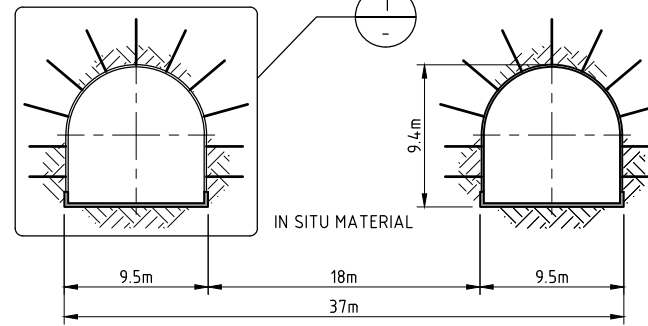
C:\DATA\PDF\FRIEDA RIVER\FRP-2-D-10-01-D-030-009.DWG

				ENGINEERING COMPANY		DRAWN	MURR	28,06,18	  	OWNER		FRIEDA RIVER LIMITED		STATUS		FOR INFORMATION	
						DESIGN	ROBI	28,06,18		TITLE		FRIEDA RIVER HYDROELECTRIC PROJECT SPILLWAY GATE ELEVATION		SCALE	1:100	REV No.	SIZE
						DES.CHKD	ROBI	28,06,18						ALL DIMENSIONS IN METRES		B	A1
						LD ENG. APPR	BROW	28,06,18						DRAWING No		FRP-2-D-10-01-D-030-009	
REF. DWG No.	DWG. DESCRIPTION	No	DATE	REVISION DETAILS		LD ENG.	PM	VENDOR DRG NO.	80510050	PM, APPR	BROW	28,06,18					

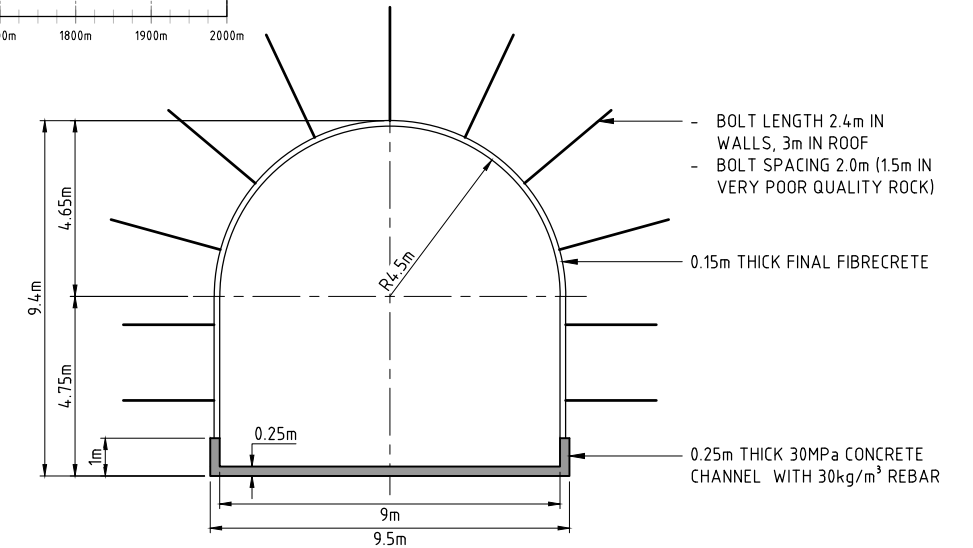
PROJECTION: UNIVERSAL TRANSVERSE MERCATOR, ZONE 54
 HORIZONTAL DATUM: PAPUA NEW GUINEA MAP GRID 1994 (PNGMG94)
 VERTICAL DATUM: AITAPE MEAN SEA LEVEL (MSL)



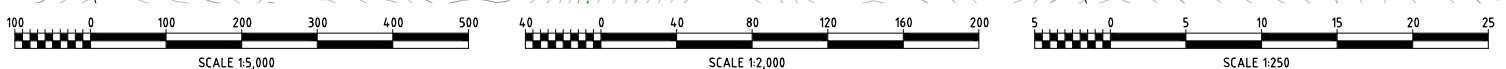
A SECTION
SCALE 1:5,000



B DIVERSION TUNNELS CROSS-SECTION
SCALE 1:250



1 DIVERSION TUNNEL DETAIL
SCALE 1:100



DIVERSION TUNNEL LAYOUT
SCALE 1:2,000

P:\PNA009 - FRIEDA RIVER HEP PFS\04_WORKING_FILES_V2_DRAFTING\00 - DRAWINGS\01 - SHEETS\PNA009-0120.DWG - 27/09/2018 10:02:19 AM

REF. DWG No.	DWG. DESCRIPTION	No	DATE	REVISION DETAILS	LD ENG.	PM
		C	25.09.18	ISSUED FOR FINAL REPORT	MORE	MORE
		B	18.07.18	REISSUED FOR CLIENT REVIEW	MORE	MORE
		A	31.05.18	ISSUED FOR CLIENT REVIEW	MORE	MORE

ENGINEERING COMPANY

 SRK Perth 10 Richardson Street, West Perth, Western Australia 6005
 Tel: +61 8 9288 2000 - Fax: +61 8 9288 2001
<http://www.srk.com.au>

DRAWN	TREV	31.05.18
DESIGN	PRIN	31.05.18
DES.CHKD	MORE	31.05.18
LD ENG. APPR	MORE	31.05.18
PM, APPR	MORE	31.05.18

VENDOR DRG NO. PNA009-0120

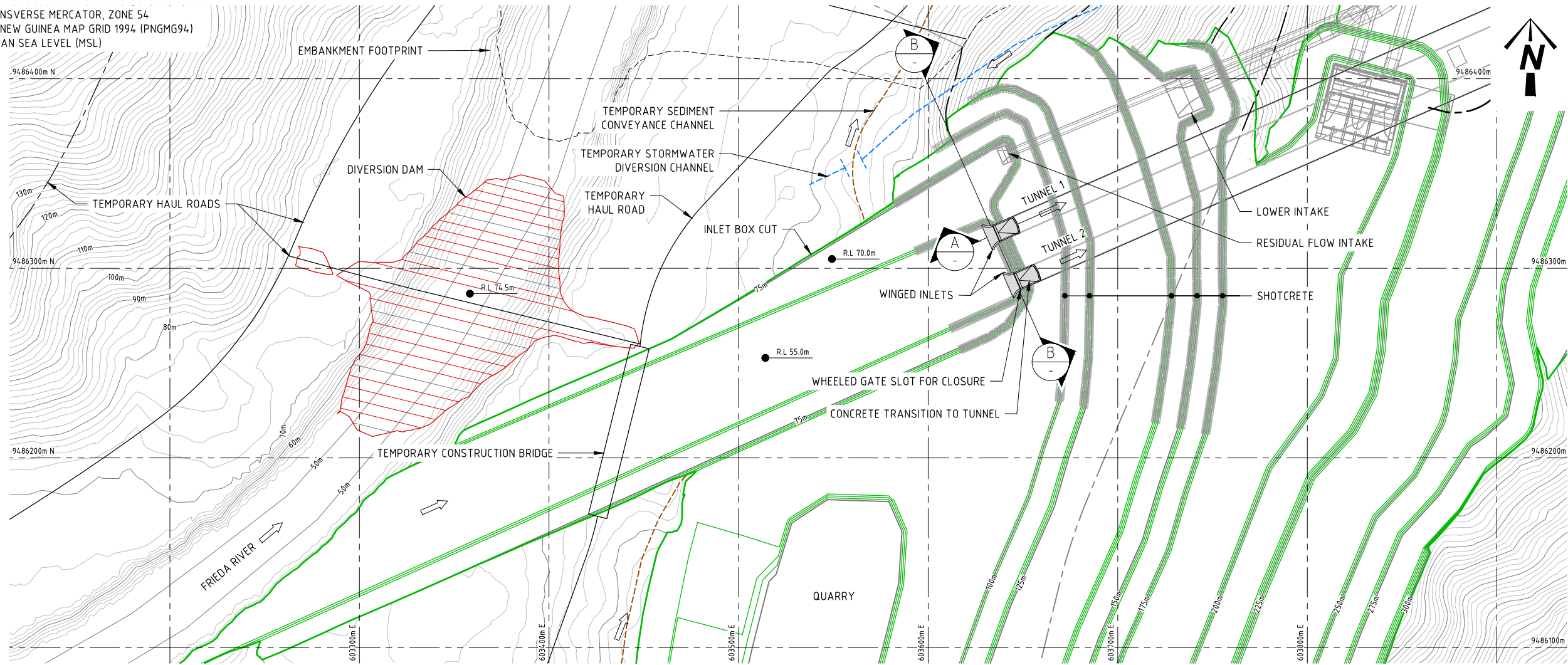
FRIEDA RIVER

OWNER
FRIEDA RIVER LIMITED

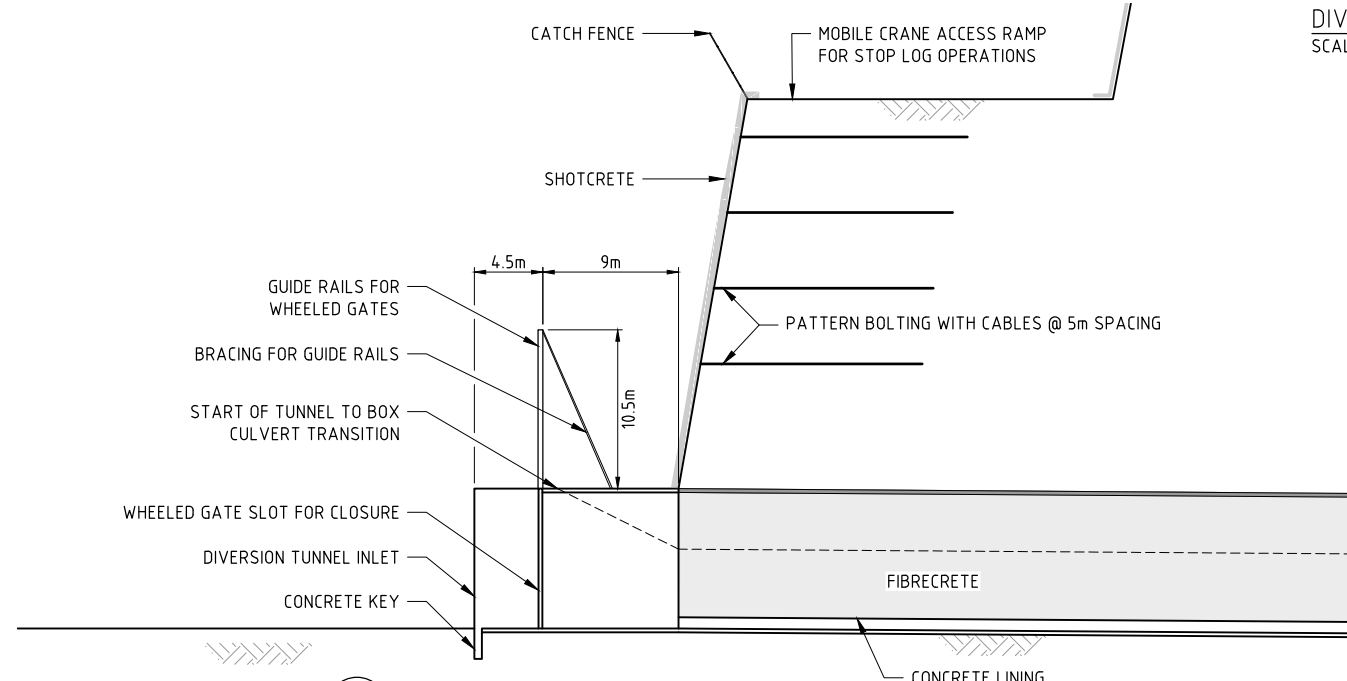
TITLE
**FRIEDA RIVER HYDROELECTRIC PROJECT
 DIVERSION TUNNEL LAYOUT,
 SECTIONS & DETAIL**

STATUS FOR INFORMATION		
SCALE	AS SHOWN	REV No. SIZE
ALL DIMENSIONS IN METRES		C A1
DRAWING No FRP-2-D-06-01-D-030-001		

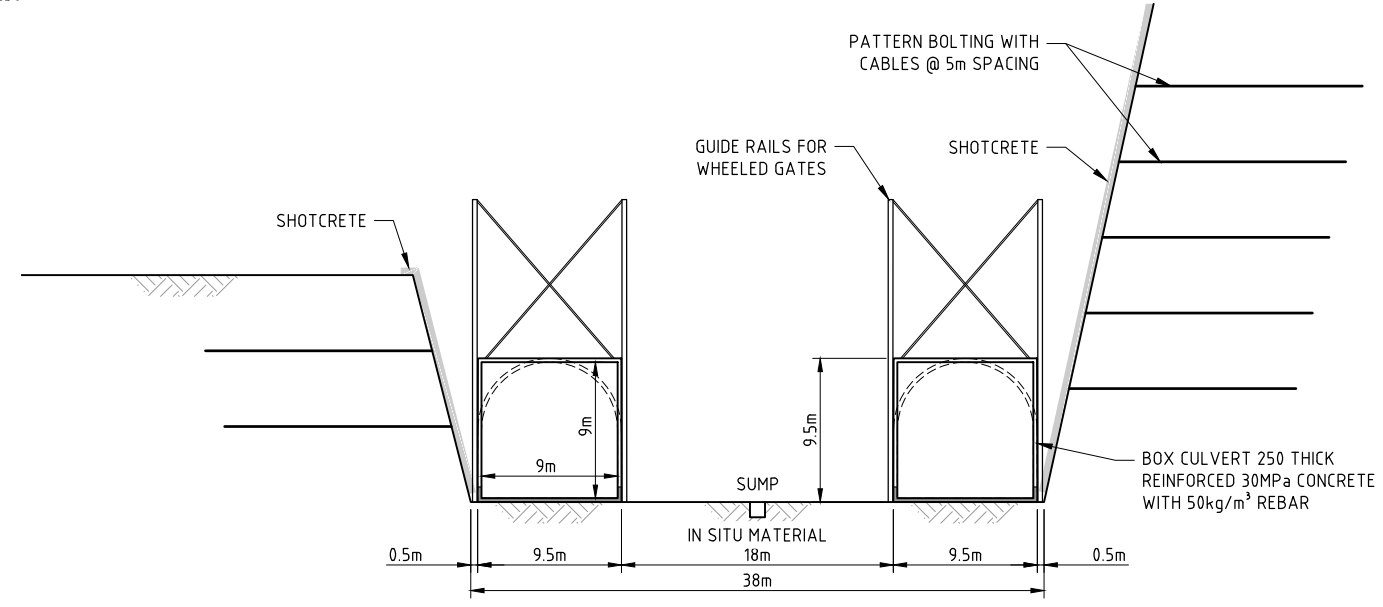
PROJECTION: UNIVERSAL TRANSVERSE MERCATOR, ZONE 54
 HORIZONTAL DATUM: PAPUA NEW GUINEA MAP GRID 1994 (PNGMG94)
 VERTICAL DATUM: AITAPE MEAN SEA LEVEL (MSL)



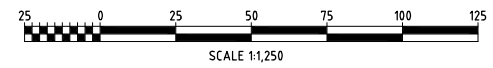
DIVERSION TUNNEL INLET LAYOUT
 SCALE 1:1,250



A - DIVERSION TUNNEL INLET SECTION
 SCALE 1:250



B - DIVERSION TUNNEL CROSS-SECTION
 SCALE 1:250



P:\PNA009 - FRIEDA RIVER HEP PFS\04_WORKING_FILES_V2_DRAFTING\00 - DRAWINGS\01 - SHEETS\PNA009-0122.DWG - 27/09/2018 10:02:33 AM

REF. DWG No.	DWG. DESCRIPTION	No	DATE	REVISION DETAILS	LD ENG.	PM
		C	25.09.18	ISSUED FOR FINAL REPORT	MORE	MORE
		B	18.07.18	REISSUED FOR CLIENT REVIEW	MORE	MORE
		A	31.05.18	ISSUED FOR CLIENT REVIEW	MORE	MORE

ENGINEERING COMPANY



SRK Perth 10 Richardson Street, West Perth, Western Australia 6005
 Tel: +61 8 9288 2000 - Fax: +61 8 9288 2001
<http://www.srk.com.au>

DRAWN	TREV	31.05.18
DESIGN	PRIN	31.05.18
DES.CHKD	MORE	31.05.18
LD ENG. APPR	MORE	31.05.18
PM, APPR	MORE	31.05.18

VENDOR DRG NO. PNA009-0122

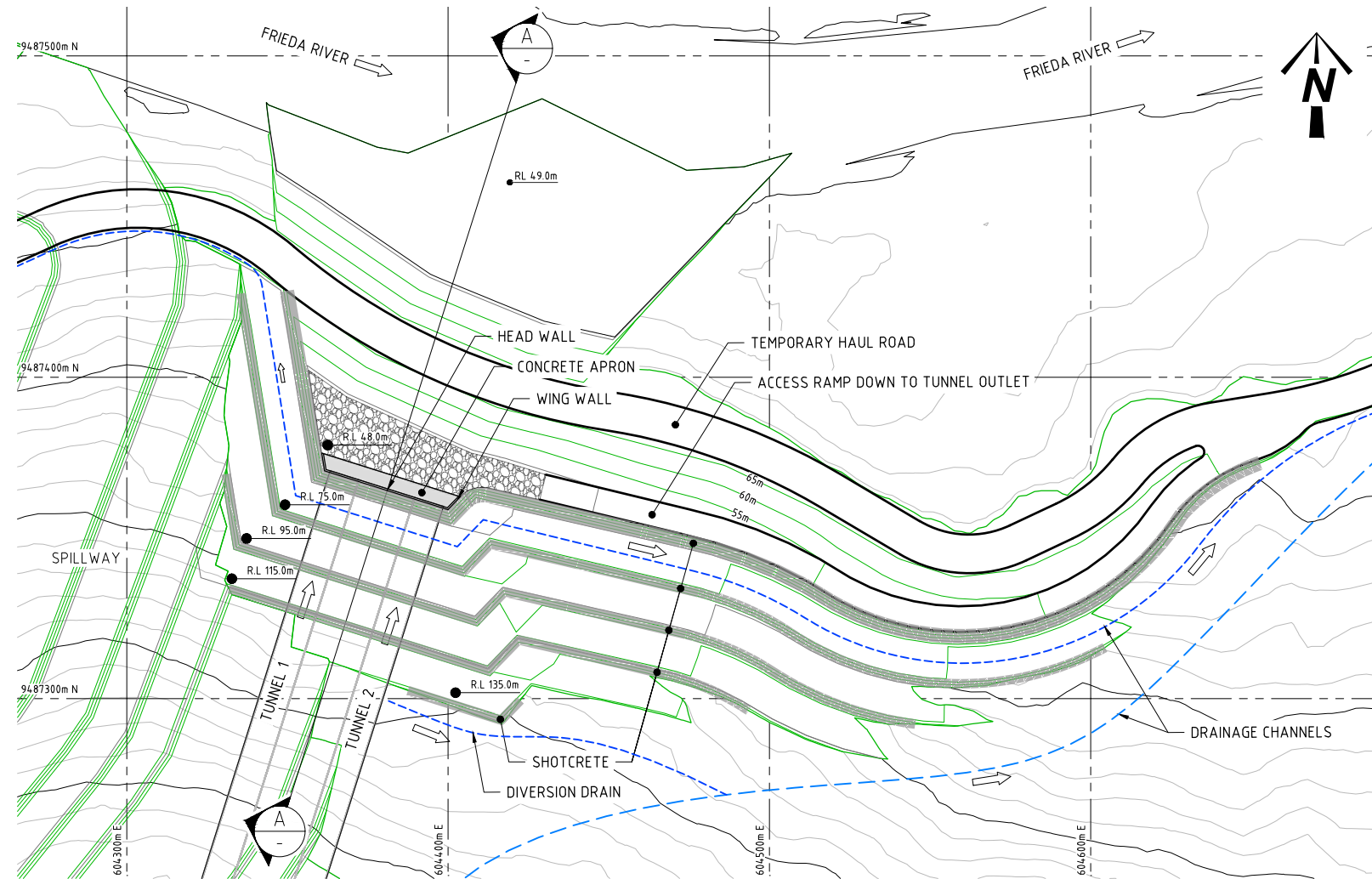


OWNER
FRIEDA RIVER LIMITED

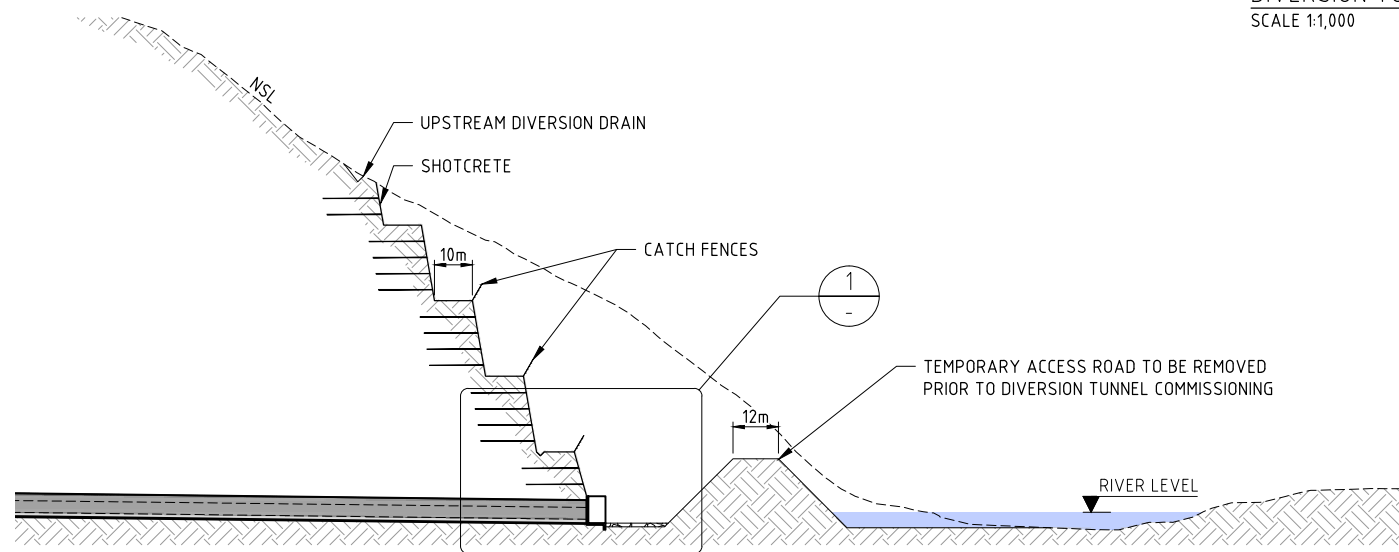
TITLE
**FRIEDA RIVER HYDROELECTRIC PROJECT
 DIVERSION TUNNEL INLET
 LAYOUT & SECTIONS**

STATUS FOR INFORMATION		
SCALE	AS SHOWN	REV No.
		C
		A1
DRAWING No		FRP-2-D-06-01-D-030-002

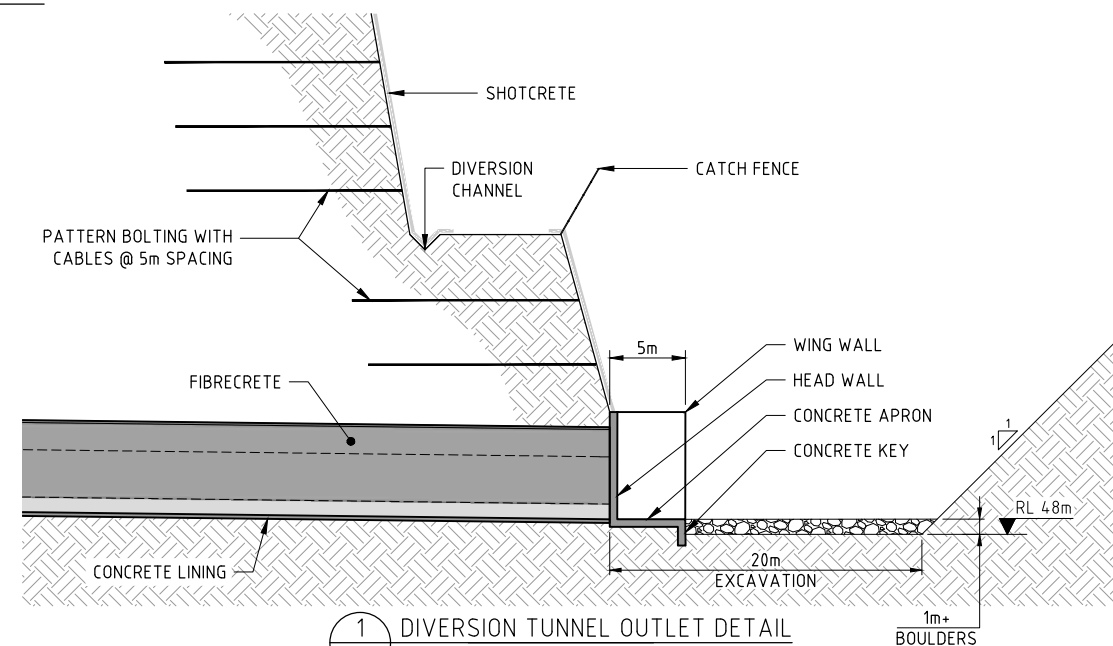
PROJECTION: UNIVERSAL TRANSVERSE MERCATOR, ZONE 54
 HORIZONTAL DATUM: PAPUA NEW GUINEA MAP GRID 1994 (PNGMG94)
 VERTICAL DATUM: AITAPE MEAN SEA LEVEL (MSL)



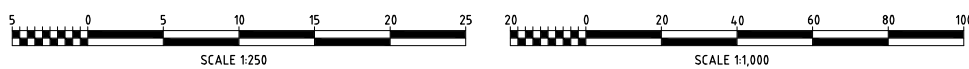
DIVERSION TUNNEL OUTLET LAYOUT
 SCALE 1:1,000



A
 -
 DIVERSION TUNNEL OUTLET SECTION
 SCALE 1:1,000



1
 -
 DIVERSION TUNNEL OUTLET DETAIL
 SCALE 1:250



P:\PNA009 - FRIEDA RIVER HEP PFS\04_WORKING_FILES_V2_DRAFTING\00 - DRAWINGS\01 - SHEETS\PNA009-0124.DWG - 27/09/2018 10:02:40 AM

REF. DWG No.	DWG. DESCRIPTION	No	DATE	REVISION DETAILS	LD ENG.	PM
		C	25.09.18	ISSUED FOR FINAL REPORT	MORE	MORE
		B	18.07.18	REISSUED FOR CLIENT REVIEW	MORE	MORE
		A	31.05.18	ISSUED FOR CLIENT REVIEW	MORE	MORE

ENGINEERING COMPANY
srk
 SRK Perth 10 Richardson Street, West Perth, Western Australia 6005
 Tel: +61 8 9288 2000 - Fax: +61 8 9288 2001
<http://www.srk.com.au>

DRAWN	TREV	31.05.18
DESIGN	PRIN	31.05.18
DES.CHKD	MORE	31.05.18
LD ENG. APPR	MORE	31.05.18
PM, APPR	MORE	31.05.18

VENDOR DRG NO. PNA009-0124

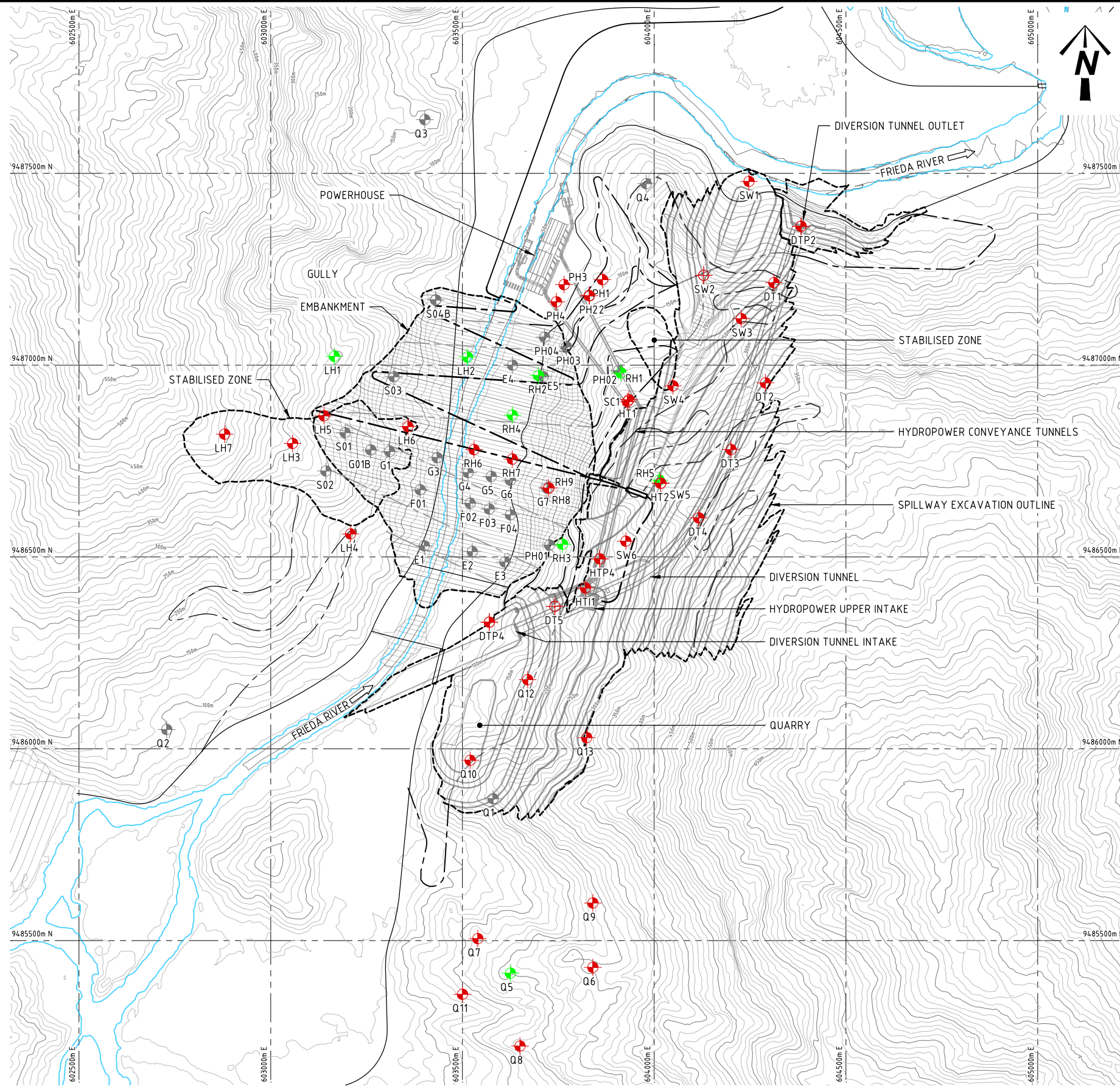


OWNER
FRIEDA RIVER LIMITED

TITLE
**FRIEDA RIVER HYDROELECTRIC PROJECT
 DIVERSION TUNNEL OUTLET
 LAYOUT, SECTION & DETAIL**

STATUS FOR INFORMATION		
SCALE	AS SHOWN	REV No.
		C
		SIZE
		A1
DRAWING No		
FRP-2-D-06-01-D-030-003		

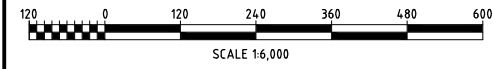
PROJECTION: UNIVERSAL TRANSVERSE MERCATOR, ZONE 54
 HORIZONTAL DATUM: PAPUA NEW GUINEA MAP GRID 1994 (PNGMG94)
 VERTICAL DATUM: AITAPE MEAN SEA LEVEL (MSL)



LEGEND

- SKM BOREHOLE LOCATIONS
- SRK BOREHOLE LOCATIONS - IPS (STAGE 1)
- SRK BOREHOLE LOCATIONS - SPS (STAGE 2)
- SRK BOREHOLE - REMOVED FROM PROGRAM

NOTE:
 FOR HOLE DETAILS REFER TO "Stage 2 HEP Drilling Investigation_Rev8 (20180228).xlsx"



GEOTECHNICAL INVESTIGATION PLAN
 SCALE 1:6,000

P:\PNA009 - FRIEDA RIVER HEP PFS\04_WORKING_FILES_V2_DRAFTING\00 - DRAWINGS\01 - SHEETS\PNA009-0130.DWG - 27/09/2018 10:02:57 AM

REF. DWG No.	DWG. DESCRIPTION	No	DATE	REVISION DETAILS	LD ENG.	PM

ENGINEERING COMPANY

SRK Perth 10 Richardson Street, West Perth, Western Australia 6005
 Tel: +61 8 9288 2000 - Fax: +61 8 9288 2001
<http://www.srk.com.au>

DRAWN	TREV	31.05.18
DESIGN	PRIN	31.05.18
DES.CHKD	MORE	31.05.18
LD ENG. APPR	MORE	31.05.18
PM, APPR	MORE	31.05.18

VENDOR DRG NO. PNA009-0130

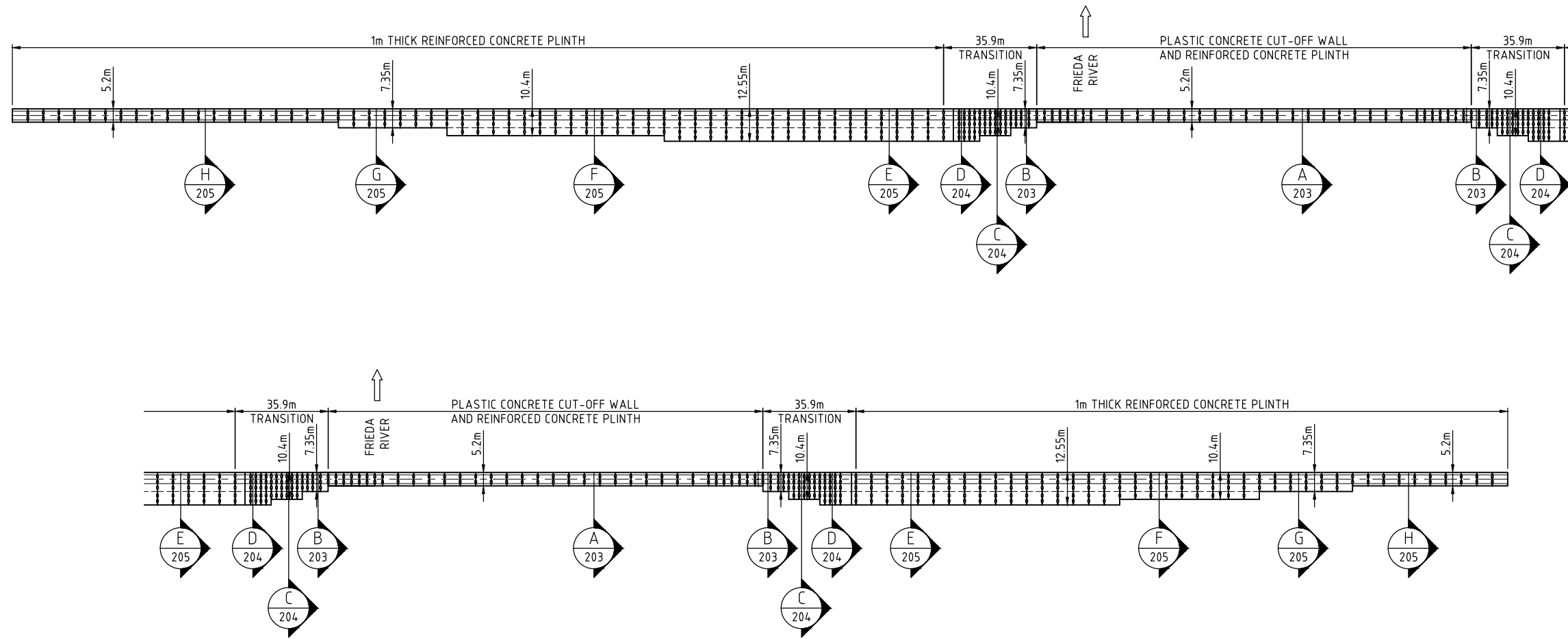
FRIEDA RIVER

OWNER
FRIEDA RIVER LIMITED

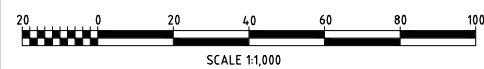
TITLE
**FRIEDA RIVER HYDROELECTRIC PROJECT
 GEOTECHNICAL INVESTIGATION
 PLAN**

STATUS FOR INFORMATION			
SCALE	AS SHOWN	REV No.	SIZE
ALL DIMENSIONS IN METRES		D	A1
DRAWING No FRP-2-D-00-01-D-030-011			



PROJECTION: UNIVERSAL TRANSVERSE MERCATOR, ZONE 54
 HORIZONTAL DATUM: PAPUA NEW GUINEA MAP GRID 1994 (PNGMG94)
 VERTICAL DATUM: AITAPE MEAN SEA LEVEL (MSL)



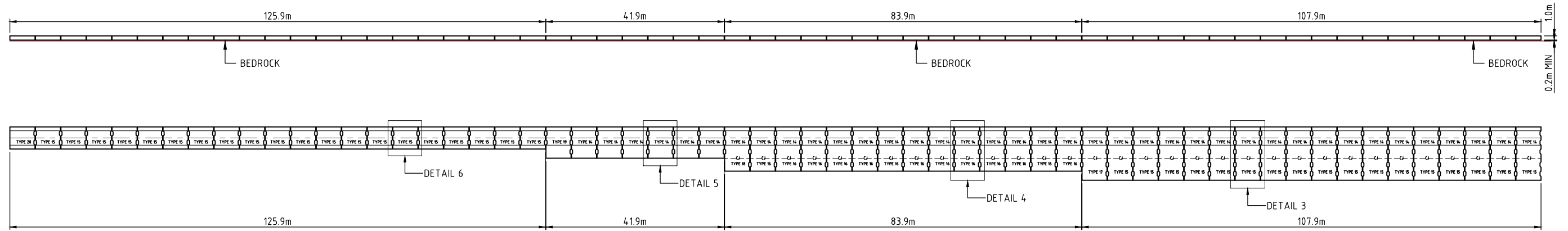
CONCRETE PLINTH DEVELOPMENT PLAN LAYOUT
 SCALE 1:1000



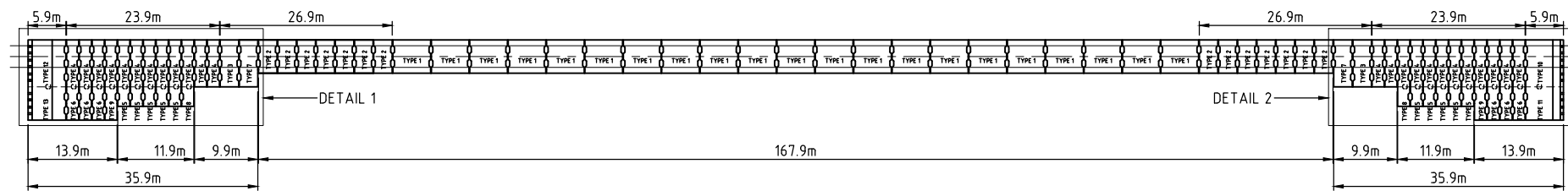
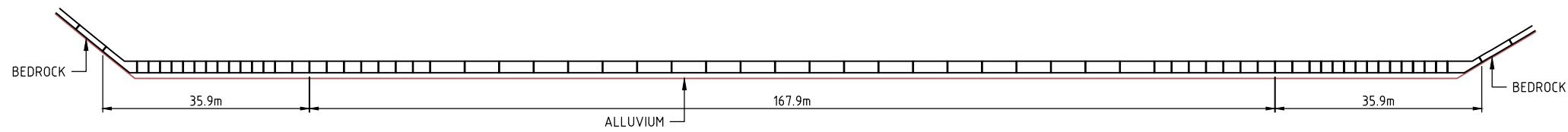
P:\PNA009 - FRIEDA RIVER HEP PFS\04_WORKING_FILES_V2_DRAFTING\00 - DRAWINGS\01 - SHEETS\PNA009-0201_0214.DWG - 27/09/2018 10:03:05 AM

						ENGINEERING COMPANY  SRK Perth 10 Richardson Street, West Perth, Western Australia 6005 Tel: +61 8 9288 2000 - Fax: +61 8 9288 2001 http://www.srk.com.au			DRAWN: TREV 18.07.18 DESIGN: PRIN 18.07.18 DES.CHKD: MORE 18.07.18 LD ENG. APPR: MORE 18.07.18 PM, APPR: MORE 18.07.18						OWNER: FRIEDA RIVER LIMITED TITLE: FRIEDA RIVER HYDROELECTRIC PROJECT EMBANKMENT PLINTH CUT-OFF WALL DEVELOPMENT PLAN LAYOUT			STATUS: FOR INFORMATION SCALE: AS SHOWN ALL DIMENSIONS IN METRES DRAWING No: FRP-2-D-04-01-D-030-009		
						B 25.09.18 ISSUED FOR FINAL REPORT MORE MORE A 18.07.18 ISSUED FOR CLIENT REVIEW MORE MORE														
REF. DWG No.	DWG. DESCRIPTION	No	DATE	REVISION DETAILS	LD ENG.	PM	VENDOR DRG NO.	PNA009-0201	PM, APPR	MORE	18.07.18									

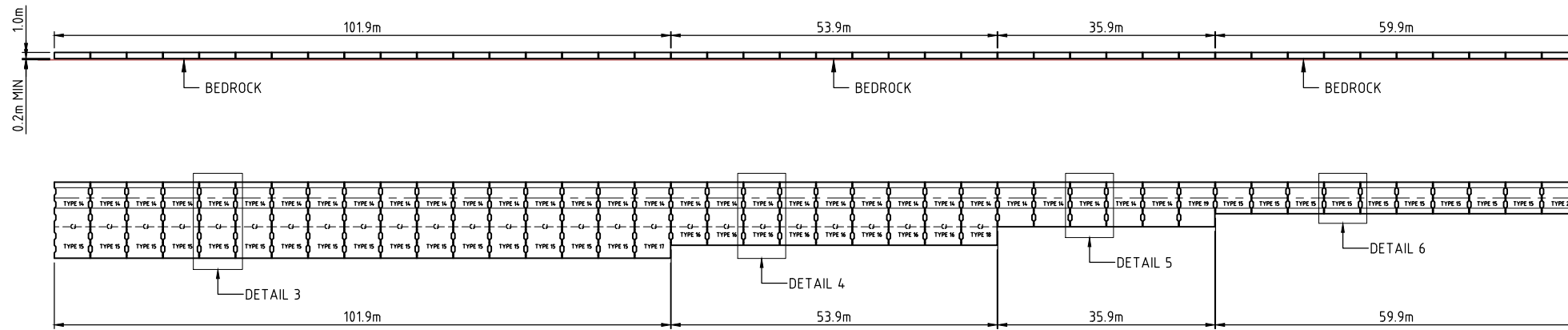
PROJECTION: UNIVERSAL TRANSVERSE MERCATOR, ZONE 54
HORIZONTAL DATUM: PAPUA NEW GUINEA MAP GRID 1994 (PNGMG94)
VERTICAL DATUM: AITAPE MEAN SEA LEVEL (MSL)



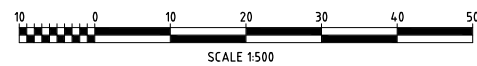
LEFT EMBANKMENT - CONCRETE PLINTH PANEL LAYOUT
SCALE 1:500



CUT OFF WALL - CONCRETE PLINTH PANEL LAYOUT
SCALE 1:500



RIGHT EMBANKMENT - CONCRETE PLINTH PANEL LAYOUT
SCALE 1:500



P:\PNA009 - FRIEDA RIVER HEP PFS\04_WORKING_FILES_V2_DRAFTING\00 - DRAWINGS\01 - SHEETS\PNA009-0201_0214.DWG - 27/09/2018 10:03:12 AM

REF. DWG No.	DWG. DESCRIPTION	No	DATE	REVISION DETAILS	LD ENG.	PM

ENGINEERING COMPANY



SRK Perth 10 Richardson Street, West Perth,
Western Australia 6005
Tel: +61 8 9288 2000 - Fax: +61 8 9288 2001
<http://www.srk.com.au>

DRAWN	TREV	31.05.18
DESIGN	PRIN	31.05.18
DES.CHKD	MORE	31.05.18
LD ENG. APPR	MORE	31.05.18
PM, APPR	MORE	31.05.18

VENDOR DRG NO. PNA009-0202

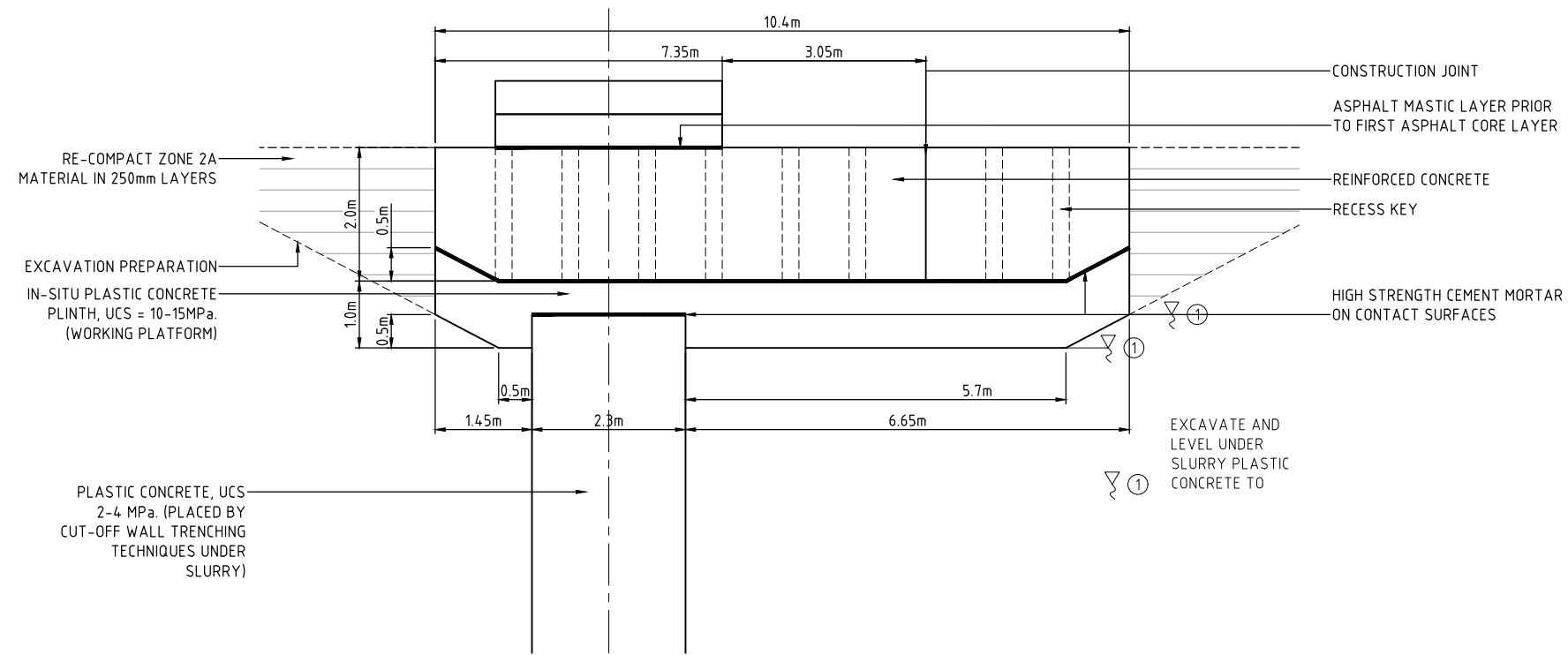


OWNER
FRIEDA RIVER LIMITED

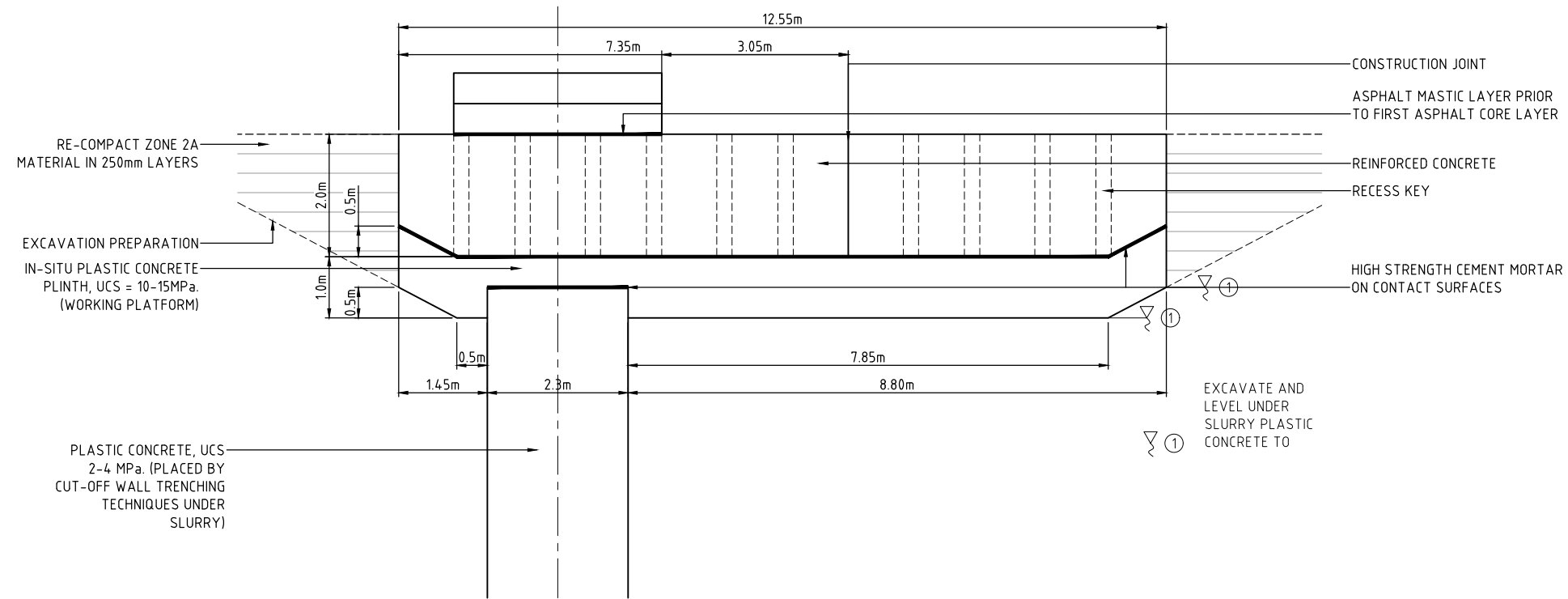
TITLE
**FRIEDA RIVER HYDROELECTRIC PROJECT
EMBANKMENT PLINTH CUT-OFF WALL
PANEL LAYOUT & SECTIONS**

STATUS FOR INFORMATION		
SCALE	AS SHOWN	REV No.
		SIZE
ALL DIMENSIONS IN METRES		C A1
DRAWING No		
FRP-2-D-04-01-D-030-010		

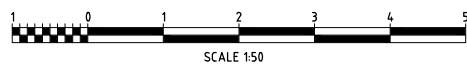
PROJECTION: UNIVERSAL TRANSVERSE MERCATOR, ZONE 54
 HORIZONTAL DATUM: PAPUA NEW GUINEA MAP GRID 1994 (PNGMG94)
 VERTICAL DATUM: AITAPE MEAN SEA LEVEL (MSL)



C PLINTH CONNECTION DETAIL
 201 1:50



D PLINTH CONNECTION DETAIL
 201 1:50



P:\PNA009 - FRIEDA RIVER HEP PFS\04_WORKING_FILES_V2_DRAFTING\00 - DRAWINGS\01 - SHEETS\PNA009-0201_0214.DWG - 27/09/2018 10:03:21 AM

REF. DWG No.	DWG. DESCRIPTION	No	DATE	REVISION DETAILS	LD ENG.	PM
		B	25.09.18	ISSUED FOR FINAL REPORT	MORE	MORE
		A	18.07.18	ISSUED FOR CLIENT REVIEW	MORE	MORE

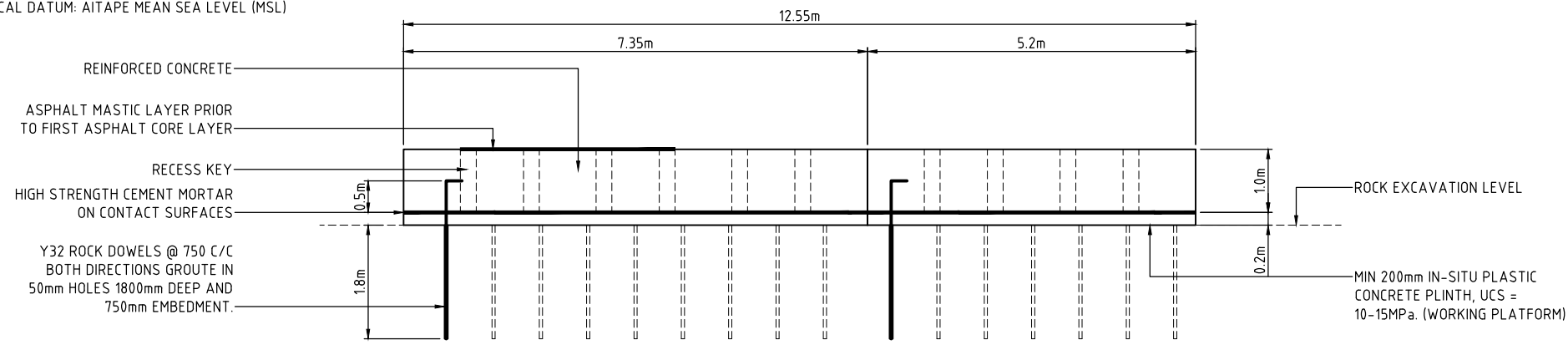
ENGINEERING COMPANY		
	DRAWN	18.07.18
	DESIGN	18.07.18
	DES.CHKD	18.07.18
	LD ENG. APPR	18.07.18
	PM, APPR	18.07.18
SRK Perth 10 Richardson Street, West Perth, Western Australia 6005 Tel: +61 8 9288 2000 - Fax: +61 8 9288 2001 http://www.srk.com.au		
VENDOR DRG NO.	PNA009-0204	



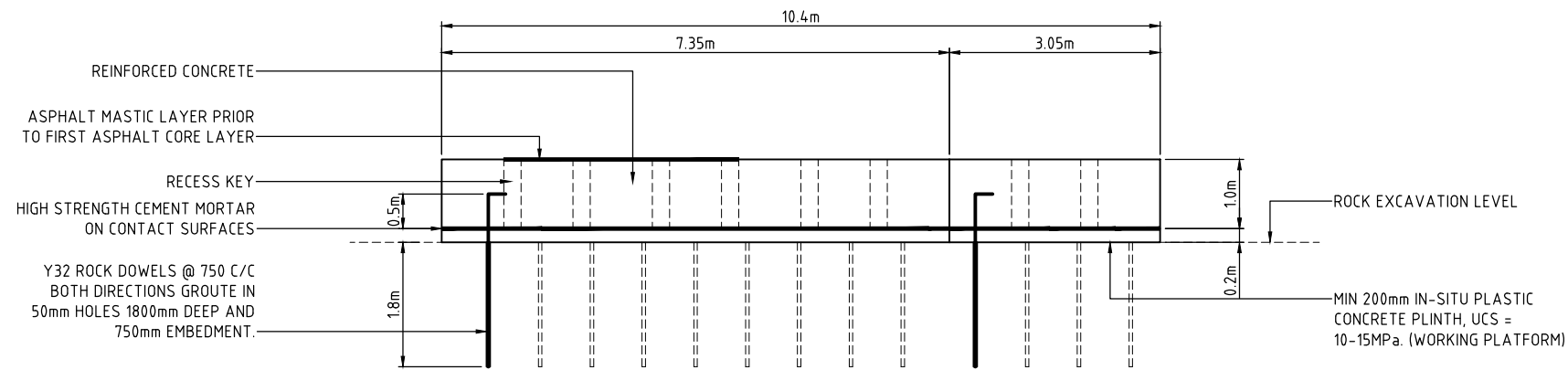
OWNER	FRIEDA RIVER LIMITED		
TITLE	FRIEDA RIVER HYDROELECTRIC PROJECT EMBANKMENT PLINTH CUT-OFF WALL CONNECTION DETAILS 2		

STATUS FOR INFORMATION			
SCALE	AS SHOWN	REV No.	SIZE
ALL DIMENSIONS IN METRES		B	A1
DRAWING No		FRP-2-D-04-01-D-030-012	

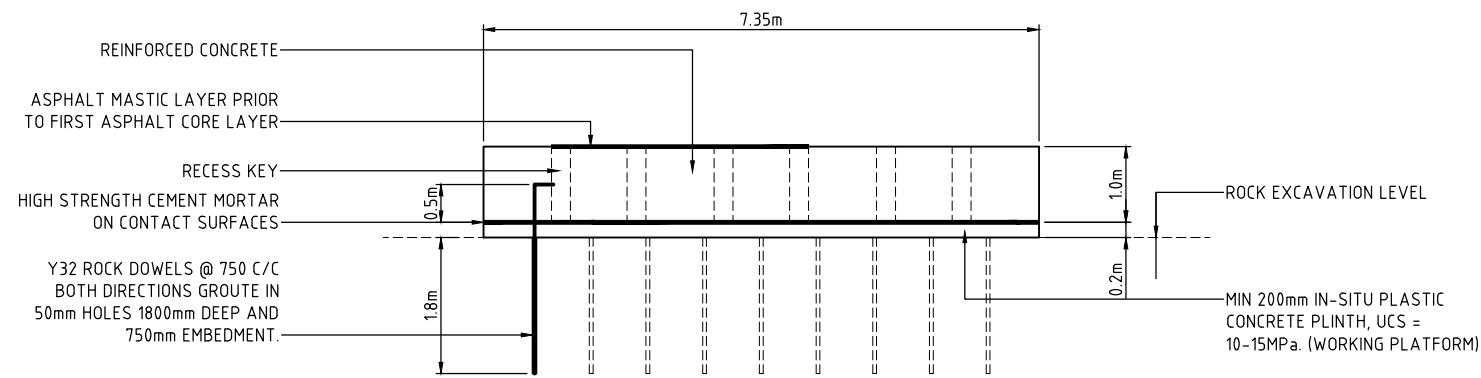
PROJECTION: UNIVERSAL TRANSVERSE MERCATOR, ZONE 54
 HORIZONTAL DATUM: PAPUA NEW GUINEA MAP GRID 1994 (PNGMG94)
 VERTICAL DATUM: AITAPE MEAN SEA LEVEL (MSL)



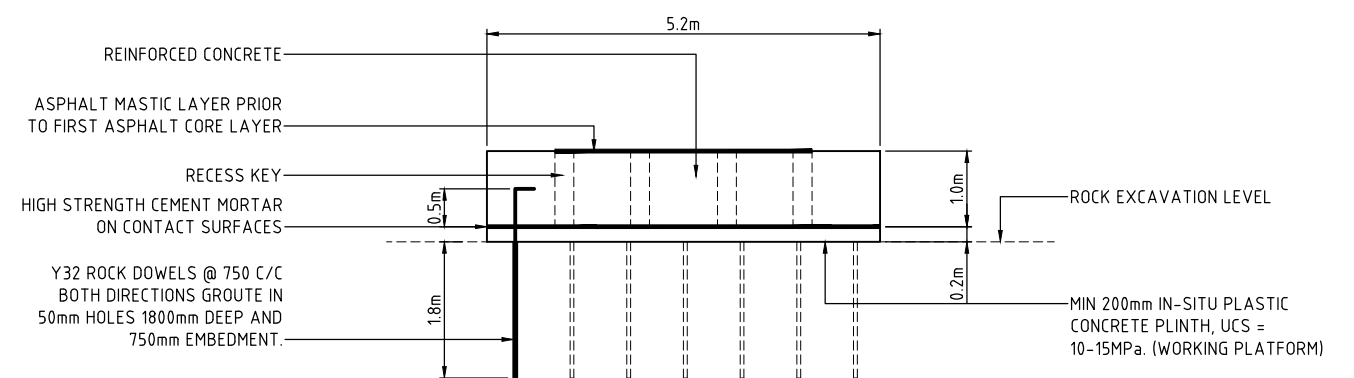
E PLINTH CONNECTION SECTION DETAIL
 205 1:50



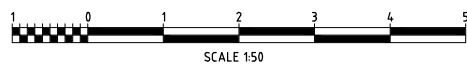
F PLINTH CONNECTION DETAIL 2
 205 1:50



G PLINTH CONNECTION SECTION DETAIL
 205 1:50



H PLINTH CONNECTION SECTION DETAIL
 205 1:50



P:\PNA009 - FRIEDA RIVER HEP PFS\04_WORKING_FILES_V2_DRAFTING\00 - DRAWINGS\01 - SHEETS\PNA009-0201_0214.DWG - 27/09/2018 10:03:27 AM

REF. DWG No.	DWG. DESCRIPTION	No	DATE	REVISION DETAILS	LD ENG.	PM
		C	25.09.18	ISSUED FOR FINAL REPORT	MORE	MORE
		B	18.07.18	REISSUED FOR CLIENT REVIEW	MORE	MORE
		A	31.05.18	ISSUED FOR CLIENT REVIEW	MORE	MORE

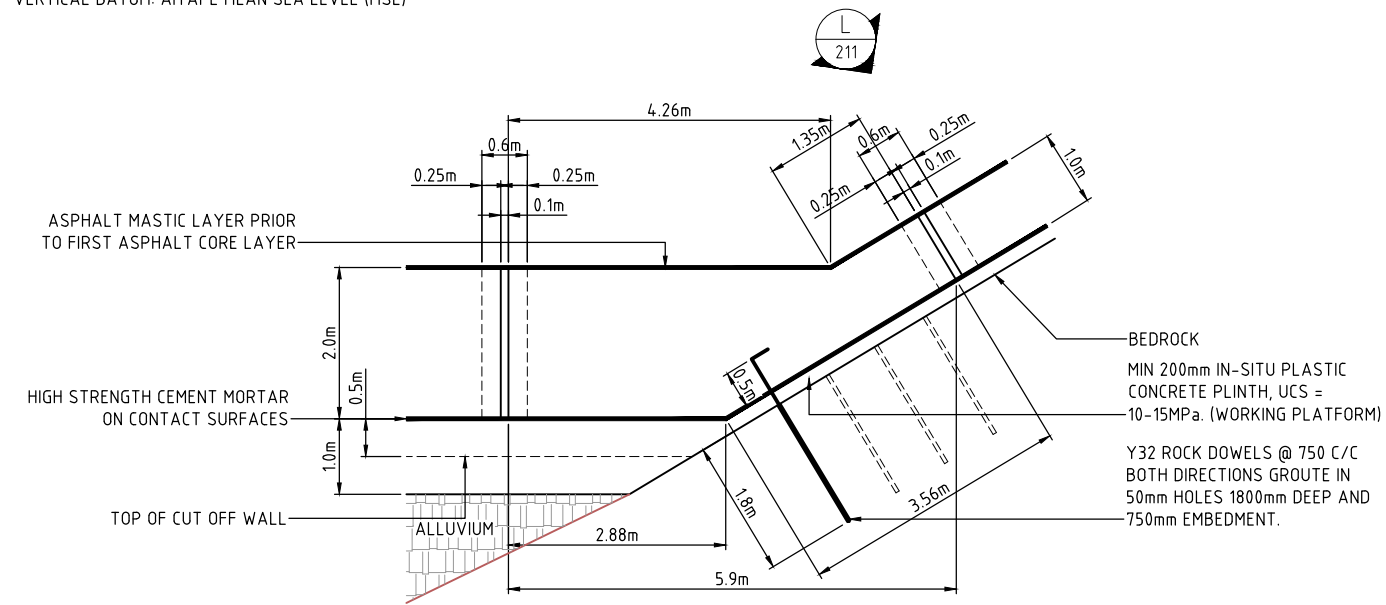
ENGINEERING COMPANY		
	DRAWN	TREV 31.05.18
	DESIGN	PRIN 31.05.18
	DES.CHKD	MORE 31.05.18
	LD ENG. APPR	MORE 31.05.18
	PM, APPR	MORE 31.05.18
SRK Perth 10 Richardson Street, West Perth, Western Australia 6005 Tel: +61 8 9288 2000 - Fax: +61 8 9288 2001 http://www.srk.com.au		
VENDOR DRG NO. PNA009-0205		



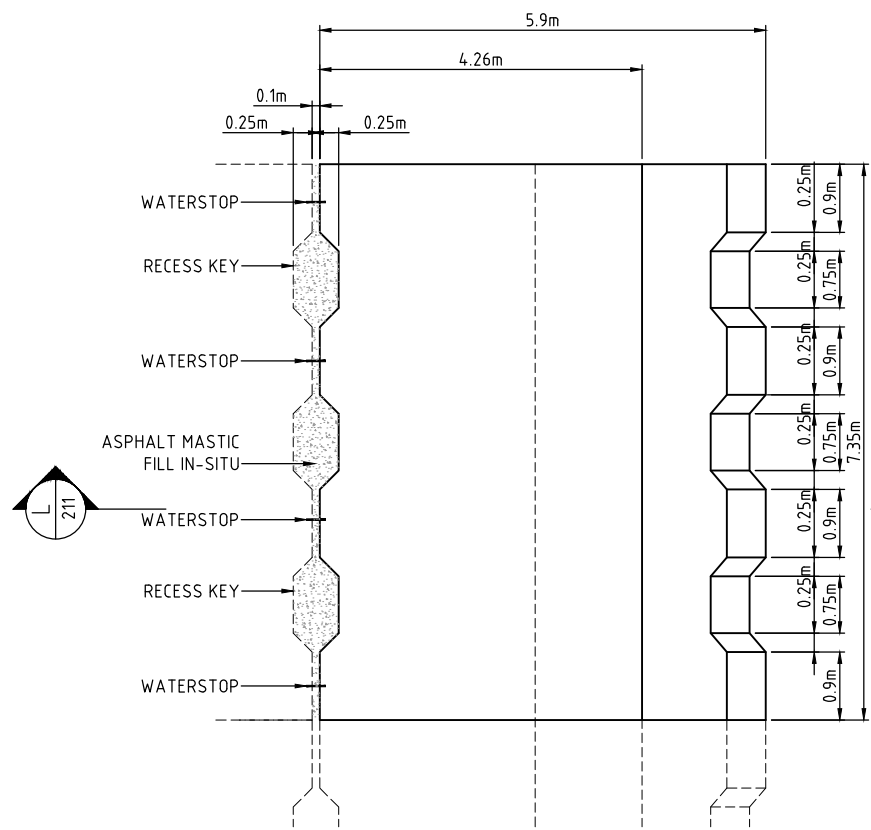
OWNER	FRIEDA RIVER LIMITED
TITLE	FRIEDA RIVER HYDROELECTRIC PROJECT EMBANKMENT PLINTH CUT-OFF WALL CONNECTION DETAILS 3

STATUS FOR INFORMATION		
SCALE	AS SHOWN	REV No.
		C
		SIZE
		A1
DRAWING No		
FRP-2-D-04-01-D-030-013		

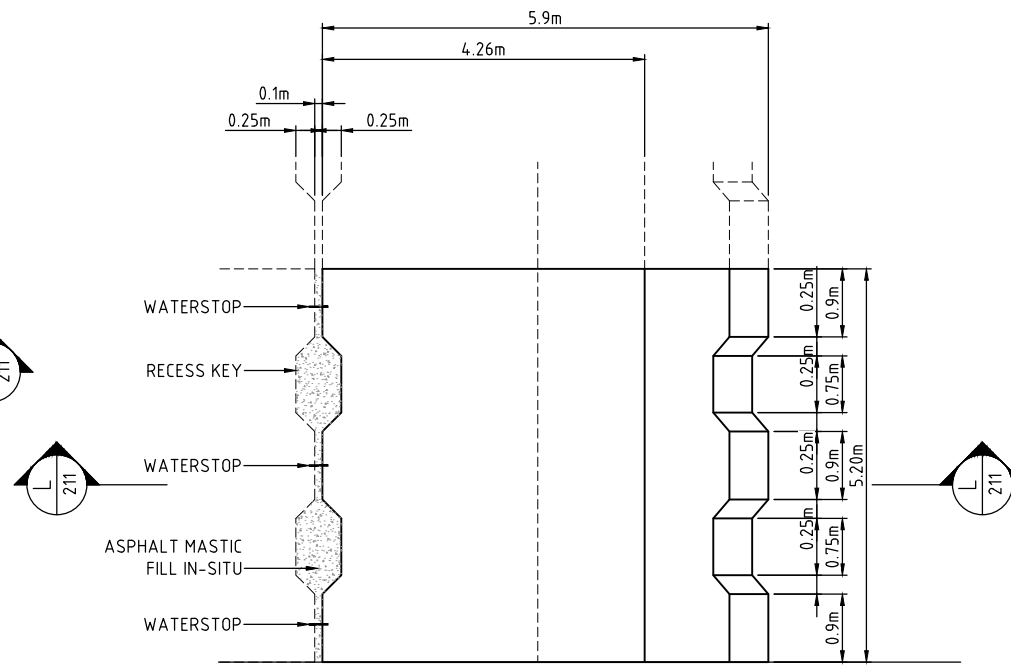
PROJECTION: UNIVERSAL TRANSVERSE MERCATOR, ZONE 54
 HORIZONTAL DATUM: PAPUA NEW GUINEA MAP GRID 1994 (PNGMG94)
 VERTICAL DATUM: AITAPE MEAN SEA LEVEL (MSL)



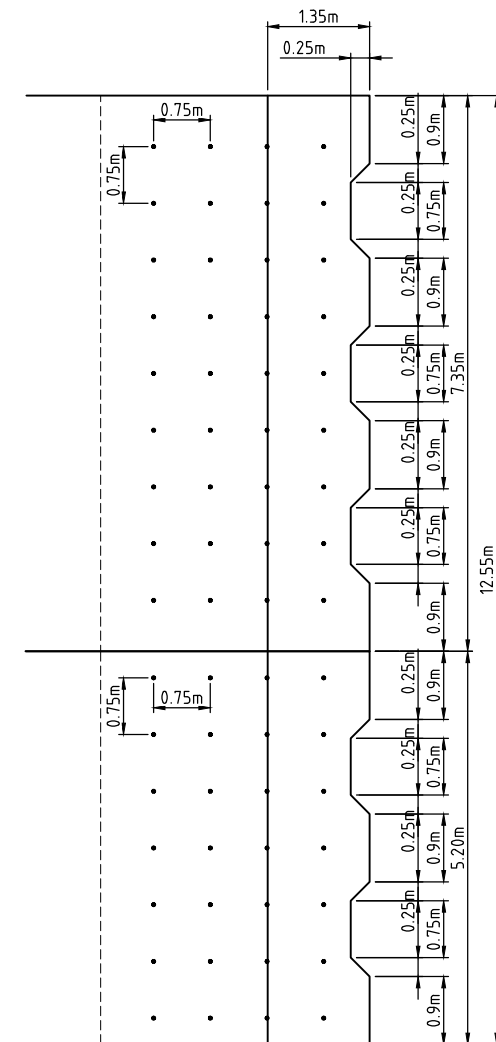
L 211
 PLINTH CONNECTION DETAIL
 1:50



PLAN VIEW - PLINTH CONNECTION DETAIL - TYPE 10
 1:50



PLAN VIEW - PLINTH CONNECTION DETAIL - TYPE 11
 1:50



PLAN VIEW ON L- PLINTH CONNECTION DETAIL
 1:50



SCALE 1:50

P:\PNA009 - FRIEDA RIVER HEP PFS\04_WORKING_FILES_V2_DRAFTING\00 - DRAWINGS\01 - SHEETS\PNA009-0201_0214.DWG - 27/09/2018 10:03:43 AM

REF. DWG No.	DWG. DESCRIPTION	No	DATE	REVISION DETAILS	LD ENG.	PM
		C	25.09.18	ISSUED FOR FINAL REPORT	MORE	MORE
		B	18.07.18	REISSUED FOR CLIENT REVIEW	MORE	MORE
		A	31.05.18	ISSUED FOR CLIENT REVIEW	MORE	MORE

ENGINEERING COMPANY



SRK Perth 10 Richardson Street, West Perth, Western Australia 6005
 Tel: +61 8 9288 2000 - Fax: +61 8 9288 2001
<http://www.srk.com.au>

VENDOR DRG NO. PNA009-0211

DRAWN	TREV	31.05.18
DESIGN	PRIN	31.05.18
DES.CHKD	MORE	31.05.18
LD ENG. APPR	MORE	31.05.18
PM, APPR	MORE	31.05.18



FRIEDA RIVER

OWNER

FRIEDA RIVER LIMITED

TITLE FRIEDA RIVER HYDROELECTRIC PROJECT
 EMBANKMENT PLINTH CUT-OFF WALL
 TRANSITION DETAILS

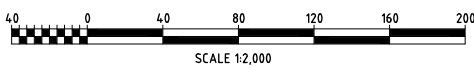
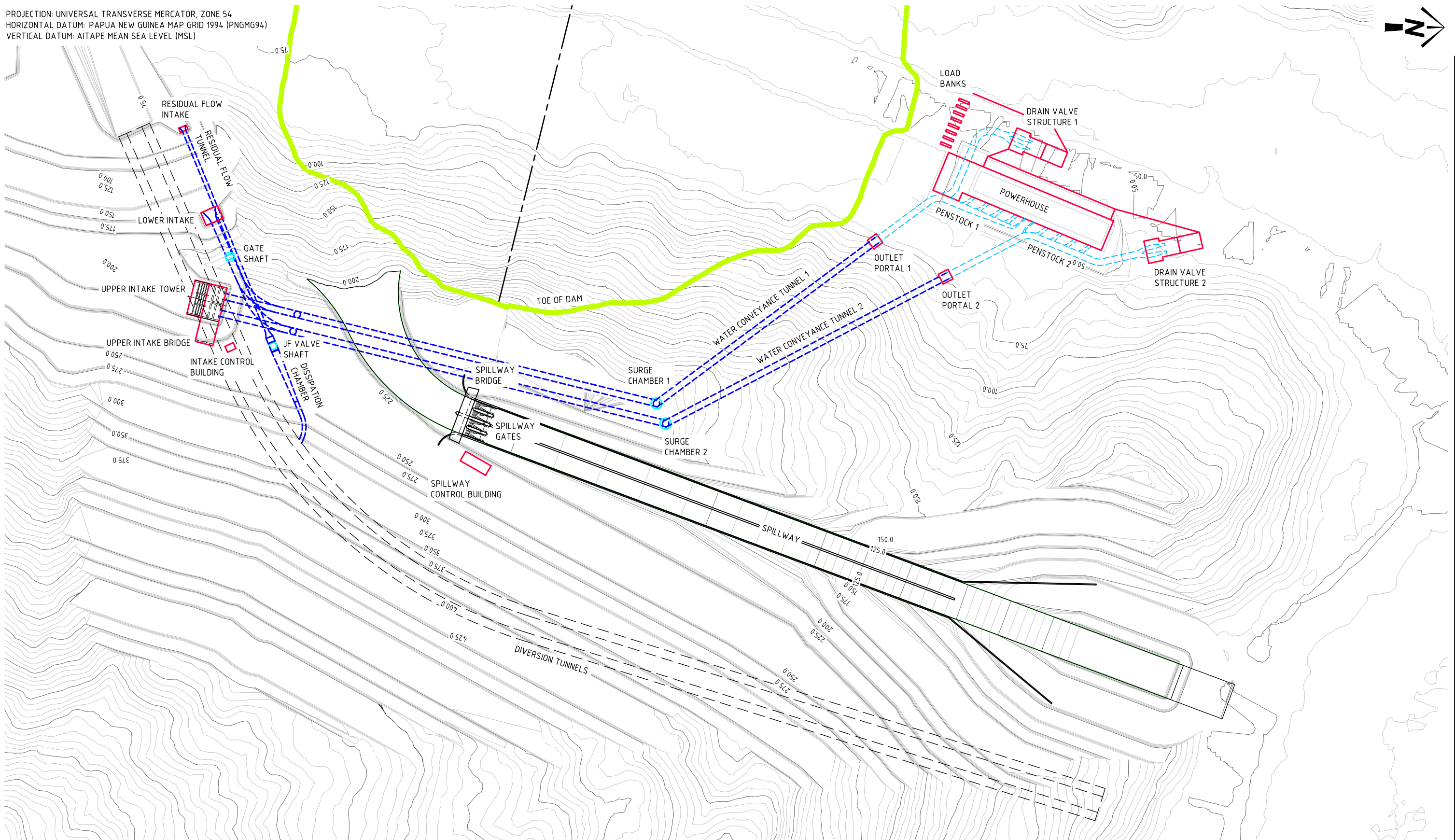
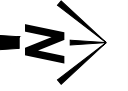
STATUS FOR INFORMATION

SCALE AS SHOWN REV No. SIZE

ALL DIMENSIONS IN METRES C A1

DRAWING No FRP-2-D-04-01-D-030-015

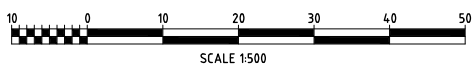
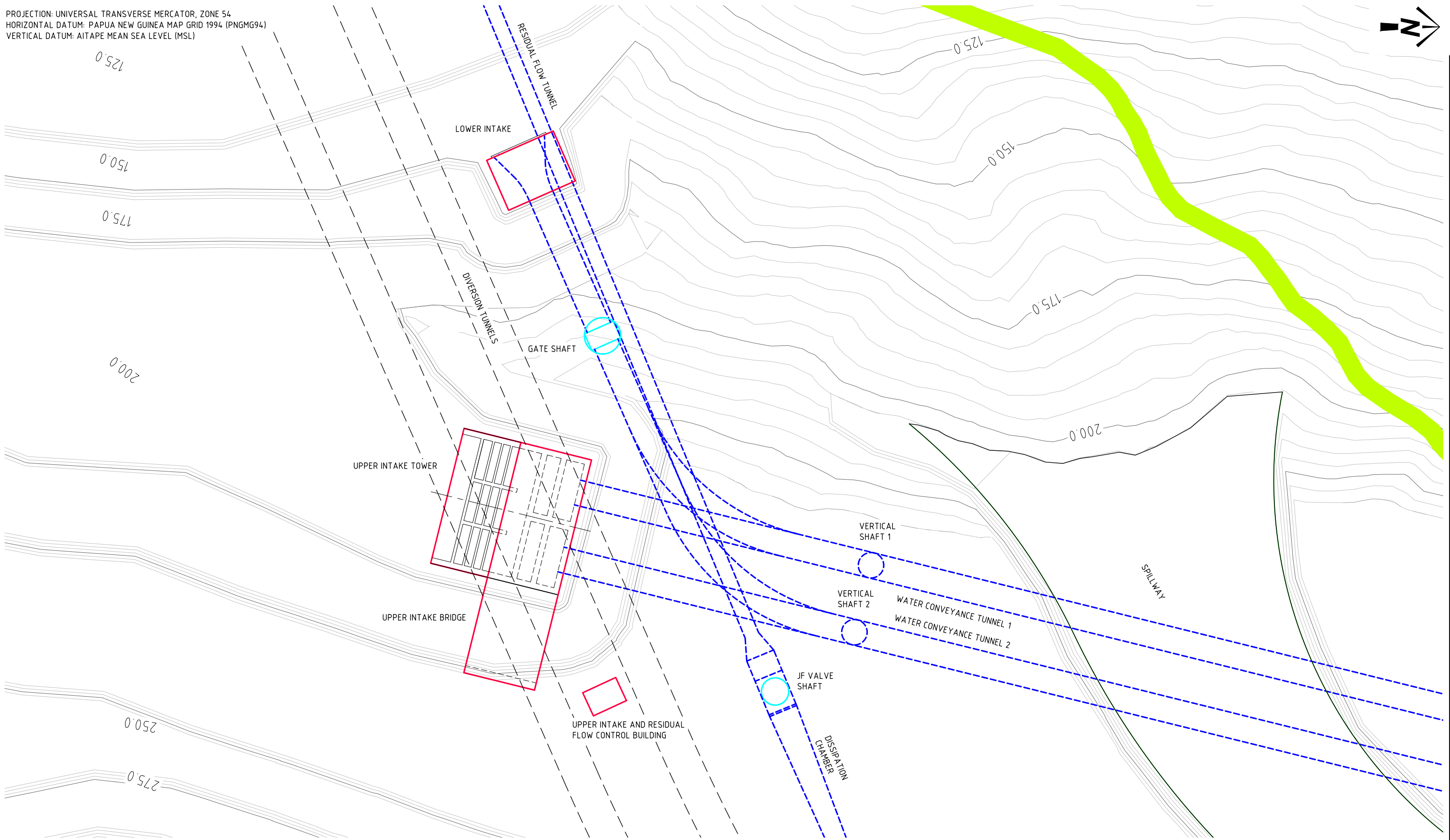
PROJECTION: UNIVERSAL TRANSVERSE MERCATOR, ZONE 54
 HORIZONTAL DATUM: PAPUA NEW GUINEA MAP GRID 1994 (PNGMG94)
 VERTICAL DATUM: AITAPE MEAN SEA LEVEL (MSL)



C:\DATA\PDF\FRIEDA RIVER\FRP-2-D-14-01-D-030-001.DWG

						ENGINEERING COMPANY 			DRAWN MURR 28.06.18 DESIGN DEVL 28.06.18 DES.CHKD ROBI 28.06.18 LD ENG. APPR BROW 28.06.18 PM APPR BROW 28.06.18			OWNER FRIEDA RIVER LIMITED			STATUS FOR INFORMATION		
									TITLE FRIEDA RIVER HYDROELECTRIC PROJECT SCHEME LAYOUT PLAN			SCALE 1:2,000		REV No.	SIZE		
												ALL DIMENSIONS IN METRES		B	A1		
												DRAWING No FRP-2-D-14-01-D-030-001					
REF. DWG No.	DWG. DESCRIPTION	No	DATE	REVISION DETAILS		LD ENG.	PM	VENDOR DRG NO. 80510050									
		B	24.09.18	ISSUED FOR FINAL REPORT		BROW	BROW										
		A	28.06.18	ISSUED FOR CLIENT REVIEW		BROW	BROW										

PROJECTION: UNIVERSAL TRANSVERSE MERCATOR, ZONE 54
 HORIZONTAL DATUM: PAPUA NEW GUINEA MAP GRID 1994 (PNGMG94)
 VERTICAL DATUM: AITAPE MEAN SEA LEVEL (MSL)



C:\DATA\PDF\FRIEDA RIVER\FRP-2-D-14-01-D-030-002.DWG

REF. DWG No.	DWG. DESCRIPTION	No	DATE	REVISION DETAILS	LD ENG.	PM
		B	24.09.18	ISSUED FOR FINAL REPORT	BROW	BROW
		A	28.06.18	ISSUED FOR CLIENT REVIEW	BROW	BROW

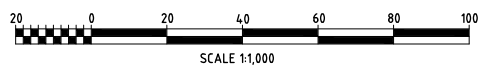
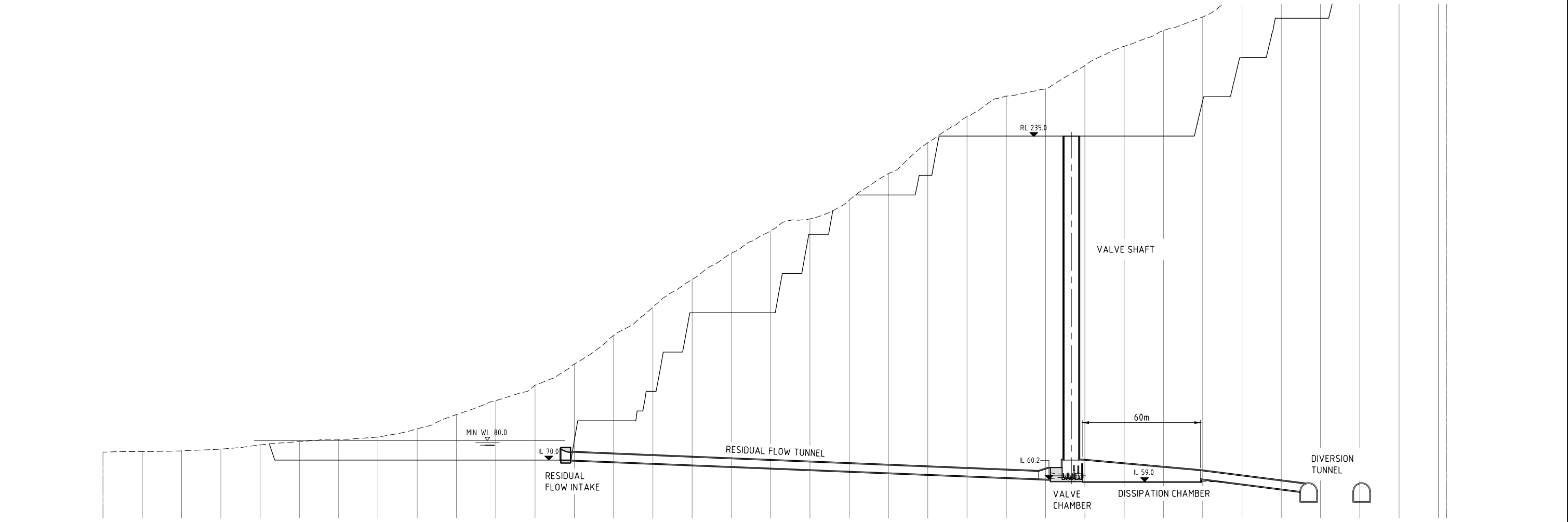
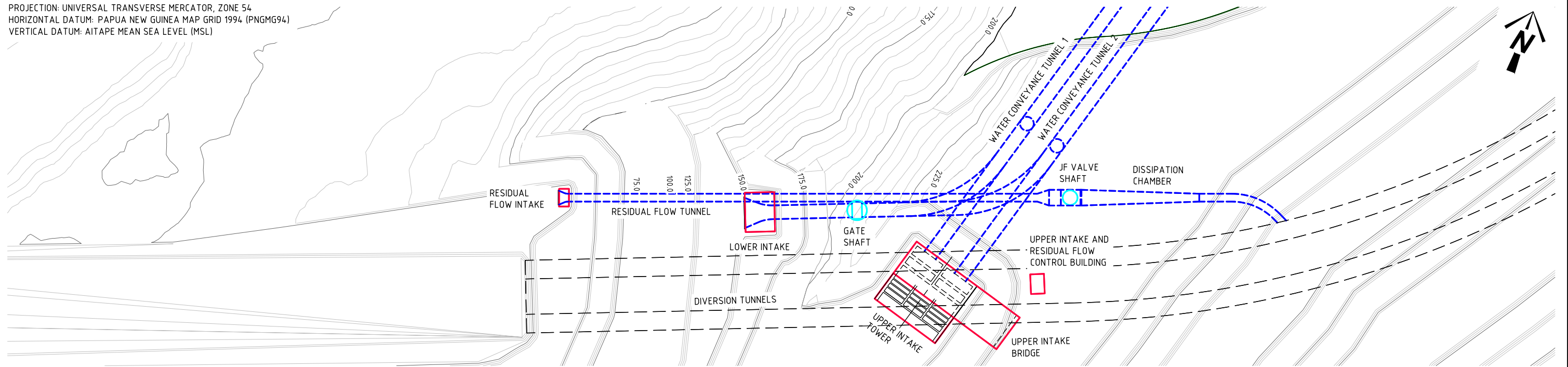
ENGINEERING COMPANY			DRAWN	MURR	28.06.18
 			DESIGN	DEVL	28.06.18
			DES.CHKD	ROBI	28.06.18
Vendor DRG No. 80510050			LD ENG. APPR	BROW	28.06.18
			PM APPR	BROW	28.06.18



OWNER	FRIEDA RIVER LIMITED	
TITLE	FRIEDA RIVER HYDROELECTRIC PROJECT INTAKE SITE PLAN	

STATUS FOR INFORMATION		
SCALE 1:500	REV No.	SIZE
ALL DIMENSIONS IN METRES	B	A1
DRAWING No FRP-2-D-14-01-D-030-002		

PROJECTION: UNIVERSAL TRANSVERSE MERCATOR, ZONE 54
 HORIZONTAL DATUM: PAPUA NEW GUINEA MAP GRID 1994 (PNGMG94)
 VERTICAL DATUM: AITAPE MEAN SEA LEVEL (MSL)



C:\DATA\PDF\FRIEDA RIVER\FRP-2-D-14-01-D-030-003.DWG

REF. DWG No.	DWG. DESCRIPTION	No	DATE	REVISION DETAILS	LD ENG.	PM
		B	24.09.18	ISSUED FOR FINAL REPORT	BROW	BROW
		A	28.06.18	FOR CLIENT REVIEW	BROW	BROW

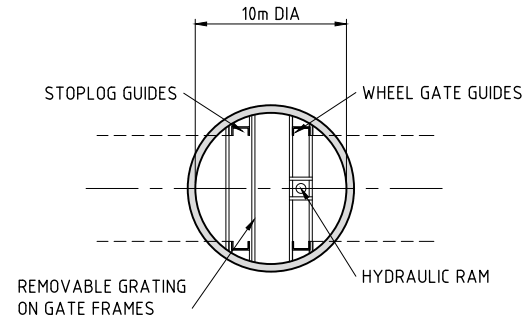
ENGINEERING COMPANY			DRAWN	MURR	28.06.18
 			DESIGN	DEVL	28.06.18
			DES.CHKD	ROBI	28.06.18
			LD ENG. APPR	BROW	28.06.18
			PM, APPR	BROW	28.06.18



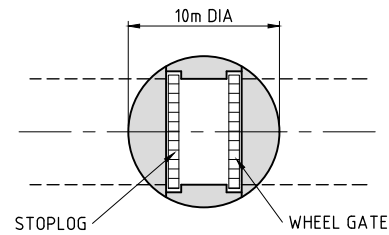
OWNER	FRIEDA RIVER LIMITED
TITLE	FRIEDA RIVER HYDROELECTRIC PROJECT RESIDUAL FLOW LAYOUT PLAN AND LONGSECTION

STATUS FOR INFORMATION		
SCALE	1:1,000	REV No.
ALL DIMENSIONS IN METRES		SIZE
	B	A1
DRAWING No FRP-2-D-14-01-D-030-003		

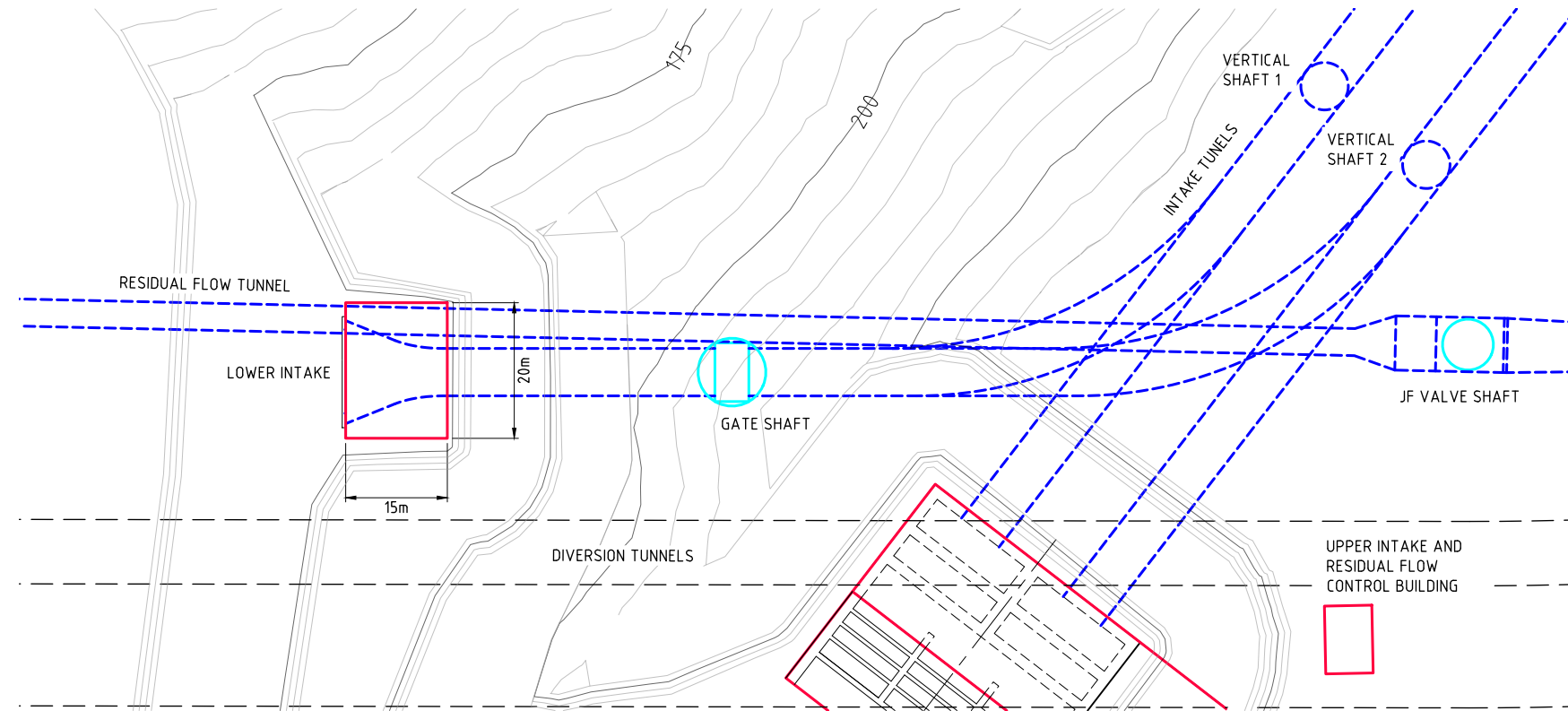
PROJECTION: UNIVERSAL TRANSVERSE MERCATOR, ZONE 54
 HORIZONTAL DATUM: PAPUA NEW GUINEA MAP GRID 1994 (PNGMG94)
 VERTICAL DATUM: AITAPE MEAN SEA LEVEL (MSL)



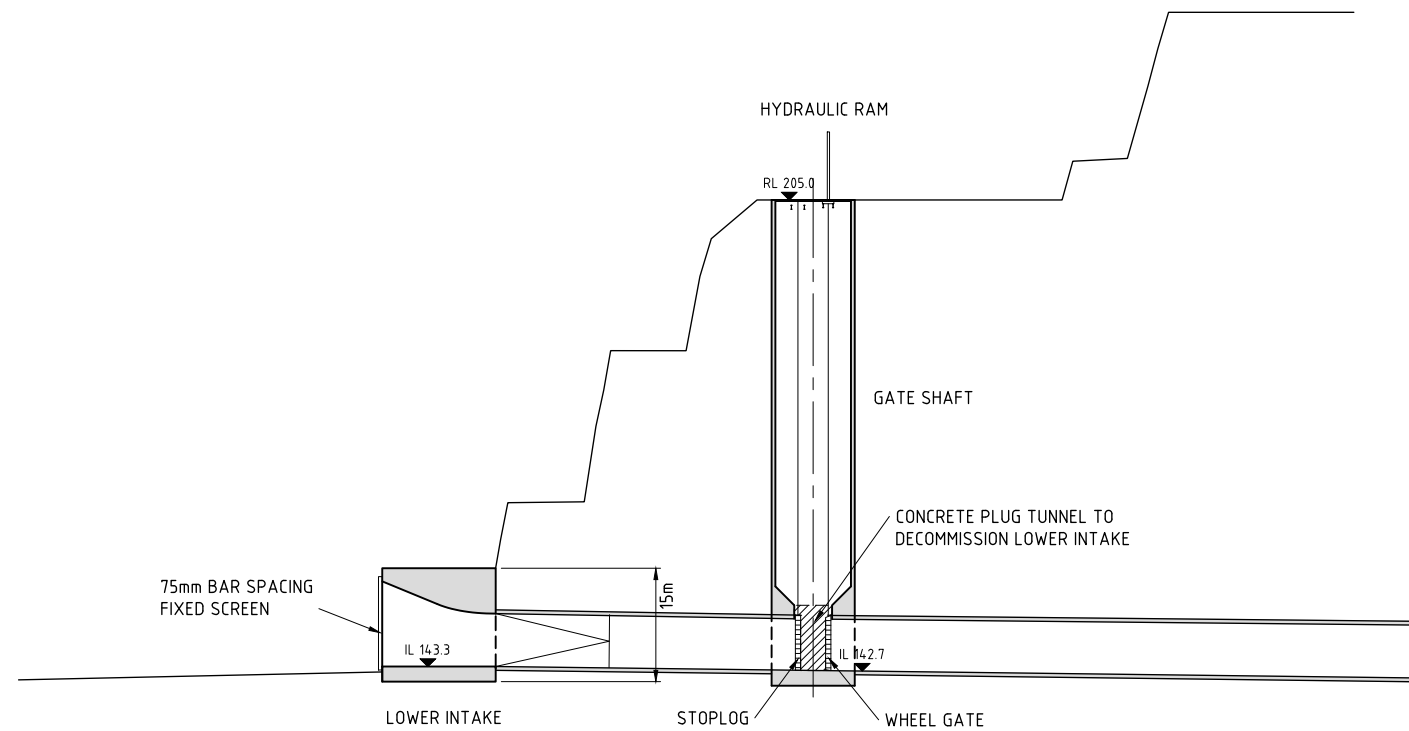
GATE SHAFT TOP PLAN



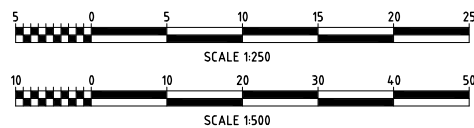
GATE SHAFT BASE PLAN



LOWER INTAKE AND GATE SHAFT LAYOUT PLAN



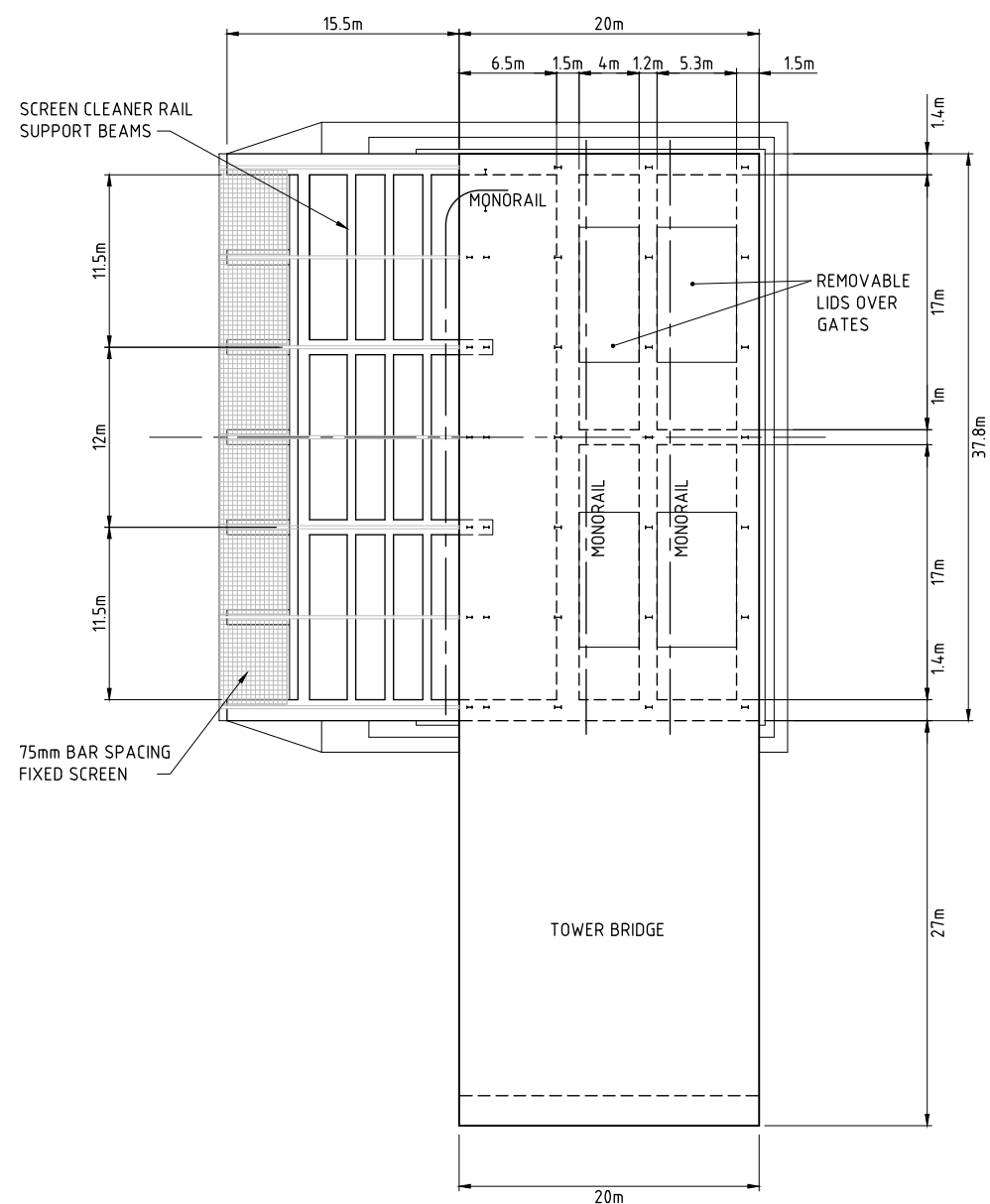
LOWER INTAKE AND GATE SHAFT LONGSECTION



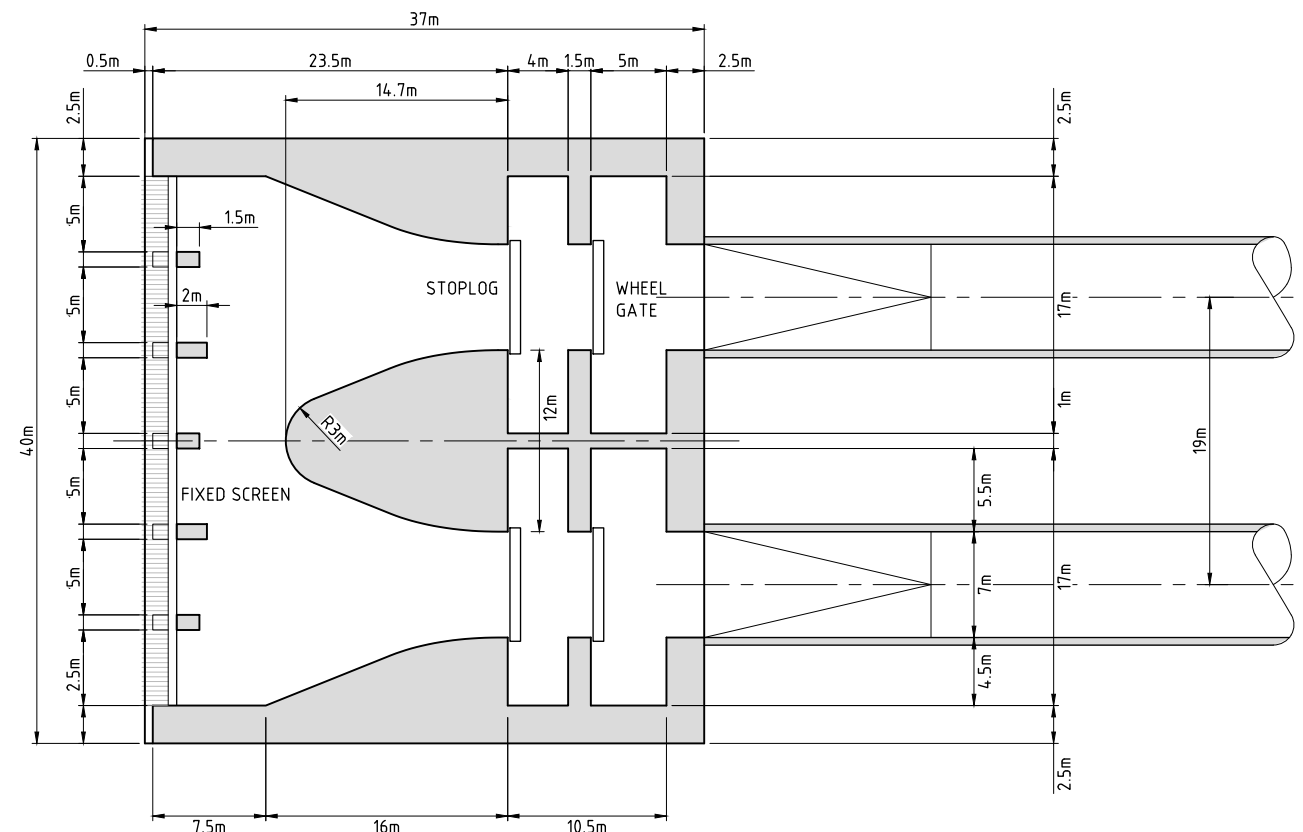
C:\DATA\PDF\FRIEDA RIVER\FRP-2-D-14-01-D-030-005.DWG

				ENGINEERING COMPANY		DRAWN MURR 28.06.18 DESIGN DEVL 28.06.18 DES.CHKD ROBI 28.06.18 LD.ENG. APPR BROW 28.06.18 PM APPR BROW 28.06.18	 	OWNER	FRIEDA RIVER LIMITED	STATUS FOR INFORMATION		
				B 24.09.18 ISSUED FOR FINAL REPORT BROW BROW A 28.06.18 ISSUED FOR CLIENT REVIEW BROW BROW				TITLE	FRIEDA RIVER HYDROELECTRIC PROJECT LOWER INTAKE AND GATE SHAFT PLANS AND LONGSECTION	SCALE 1:500 1:250	REV No.	SIZE
REF. DWG No.	DWG. DESCRIPTION	No	DATE	REVISION DETAILS	LD ENG.	PM	VENDOR DRG NO.	80510050		ALL DIMENSIONS IN METRES	B	A1
										DRAWING No	FRP-2-D-14-01-D-030-005	

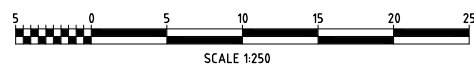
PROJECTION: UNIVERSAL TRANSVERSE MERCATOR, ZONE 54
 HORIZONTAL DATUM: PAPUA NEW GUINEA MAP GRID 1994 (PNGMG94)
 VERTICAL DATUM: AITAPE MEAN SEA LEVEL (MSL)





TOWER TOP PLAN



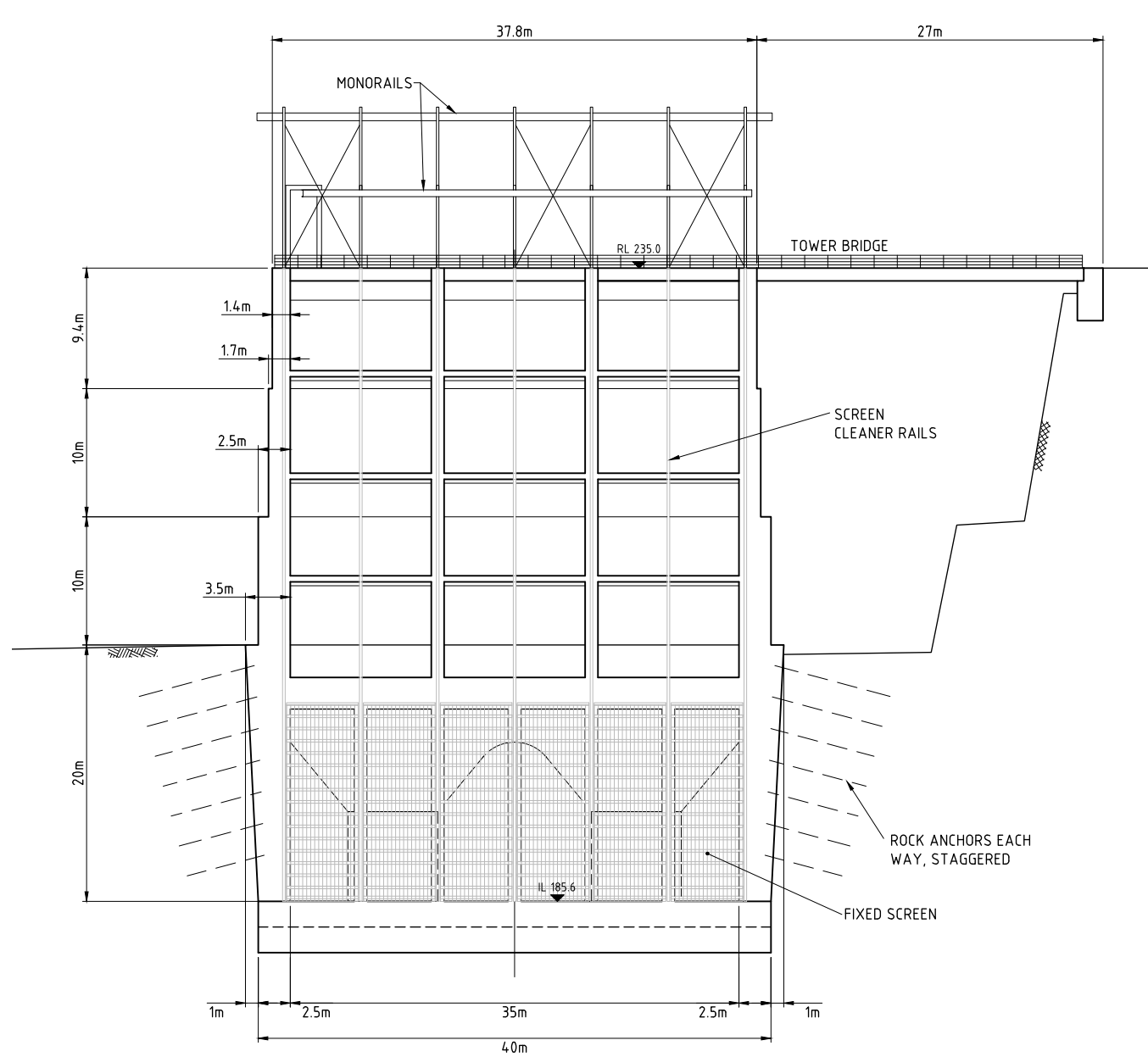
TOWER BASE PLAN



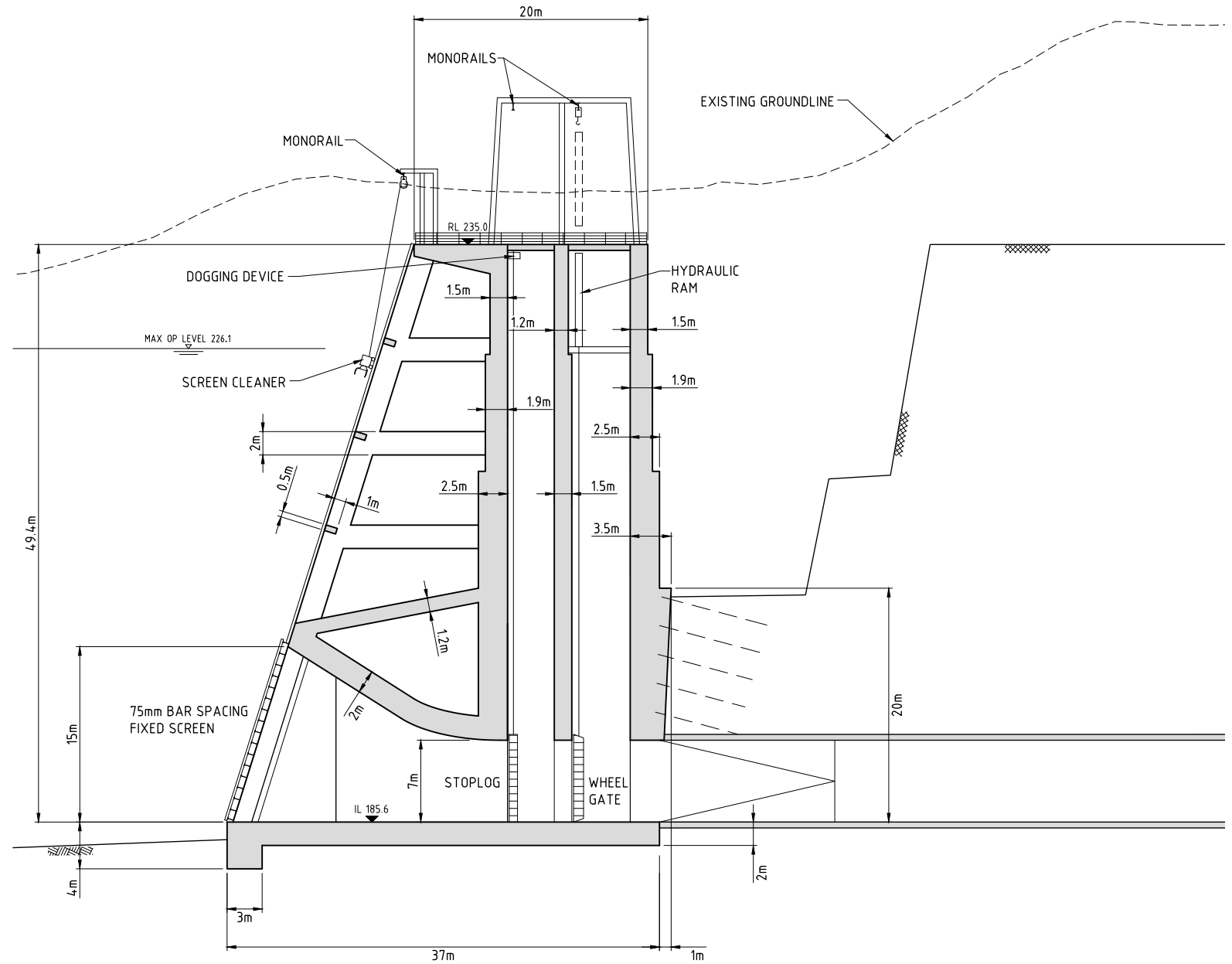
C:\DATA\PDF\FRIEDA RIVER\FRP-2-D-14-01-D-030-006.DWG

				ENGINEERING COMPANY		DRAWN MURR 28.06.18			 	OWNER		STATUS		
						DESIGN DEVL 28.06.18				FRIEDA RIVER LIMITED		FOR INFORMATION		
						DES.CHKD ROBI 28.06.18				FRIEDA RIVER HYDROELECTRIC PROJECT		SCALE 1:250	REV No.	SIZE
						LD ENG. APPR BROW 28.06.18				UPPER INTAKE TOWER PLANS		ALL DIMENSIONS IN METRES	B	A1
REF. DWG No.	DWG. DESCRIPTION	No	DATE	REVISION DETAILS		LD ENG.	PM	VENDOR DRG NO. 80510050	PM, APPR BROW 28.06.18	FRIEDA RIVER		DRAWING No		
											FRP-2-D-14-01-D-030-006			

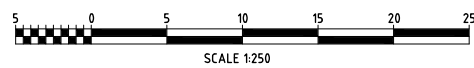
PROJECTION: UNIVERSAL TRANSVERSE MERCATOR, ZONE 54
 HORIZONTAL DATUM: PAPUA NEW GUINEA MAP GRID 1994 (PNGMG94)
 VERTICAL DATUM: AITAPE MEAN SEA LEVEL (MSL)



TOWER ELEVATION



TOWER SECTION



C:\DATA\PDF\FRIEDA RIVER\FRP-2-D-14-01-D-030-007.DWG

REF. DWG No.	DWG. DESCRIPTION	No	DATE	REVISION DETAILS	LD ENG.	PM
		B	24.09.18	ISSUED FOR FINAL REPORT	BROW	BROW
		A	28.06.18	ISSUED FOR CLIENT REVIEW	BROW	BROW

ENGINEERING COMPANY



VENDOR DRG NO. 80510050

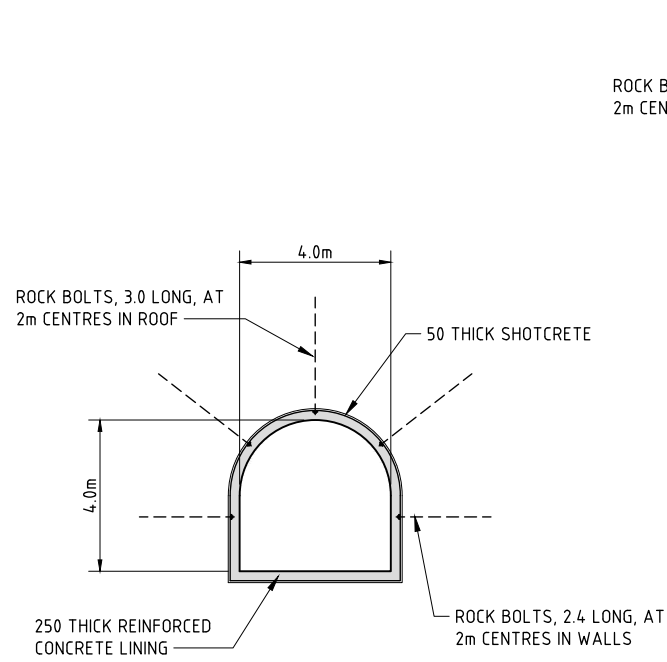
DRAWN	MURR	28.06.18
DESIGN	DEVL	28.06.18
DES.CHKD	ROBI	28.06.18
LD ENG. APPR	BROW	28.06.18
PM APPR	BROW	28.06.18



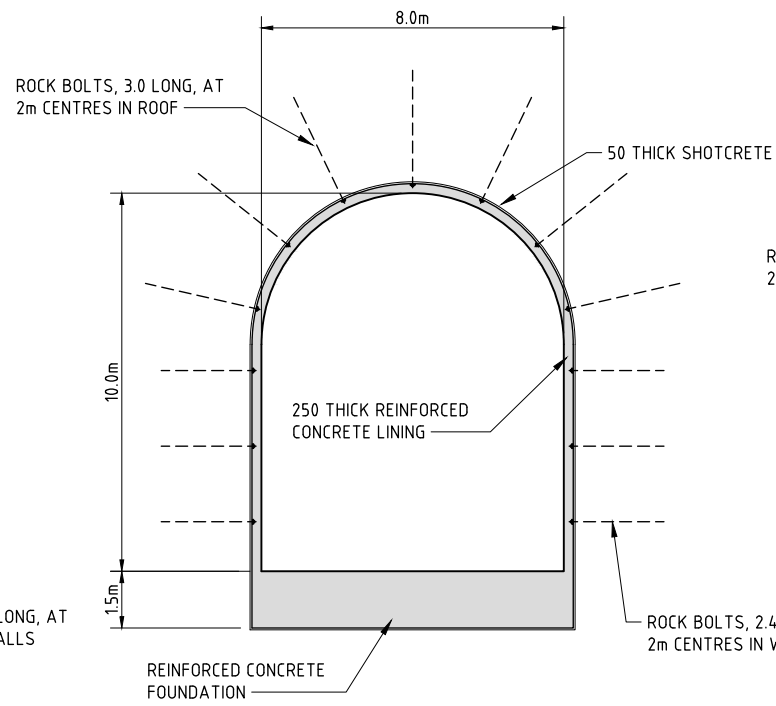
OWNER
FRIEDA RIVER LIMITED

TITLE
 FRIEDA RIVER HYDROELECTRIC PROJECT
 UPPER INTAKE TOWER SECTION AND ELEVATION

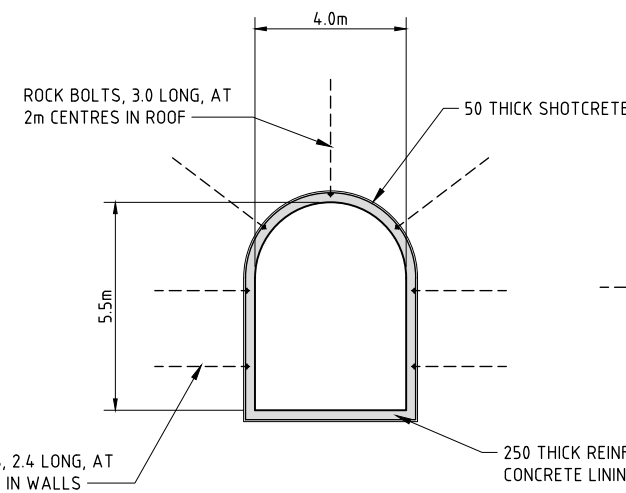
STATUS FOR INFORMATION		
SCALE 1:250	REV No.	SIZE
ALL DIMENSIONS IN METRES	B	A1
DRAWING No FRP-2-D-14-01-D-030-007		



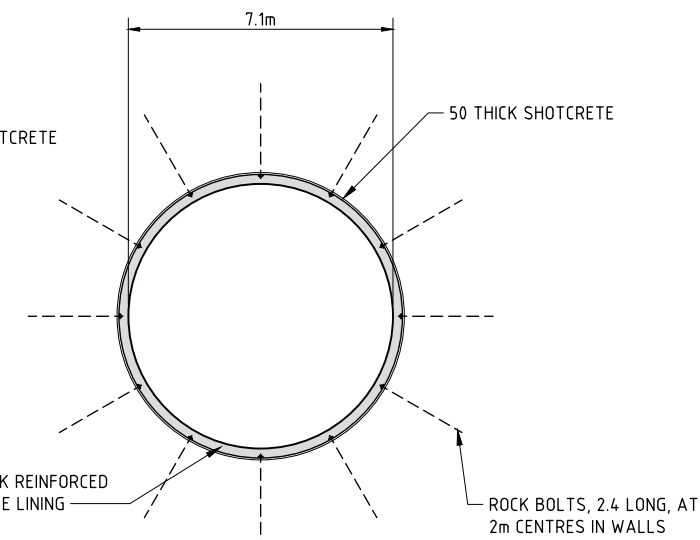
RESIDUAL FLOW TUNNEL



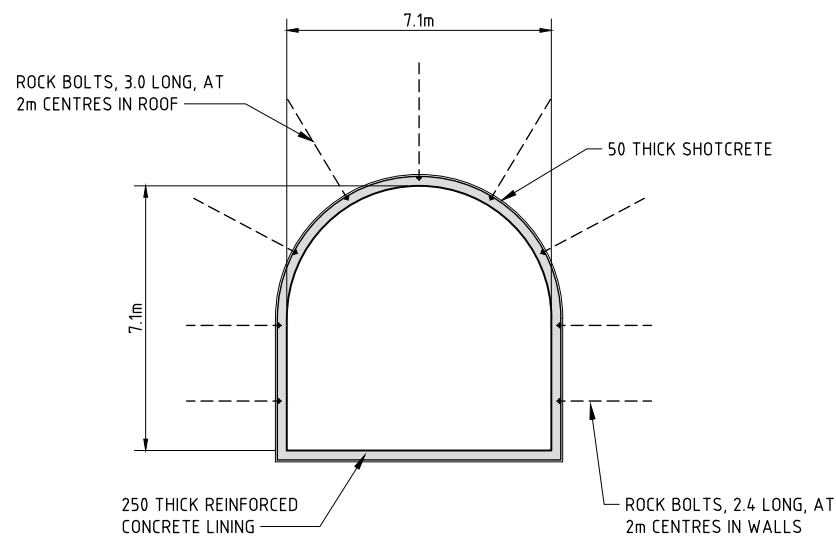
RESIDUAL FLOW VALVE CHAMBER



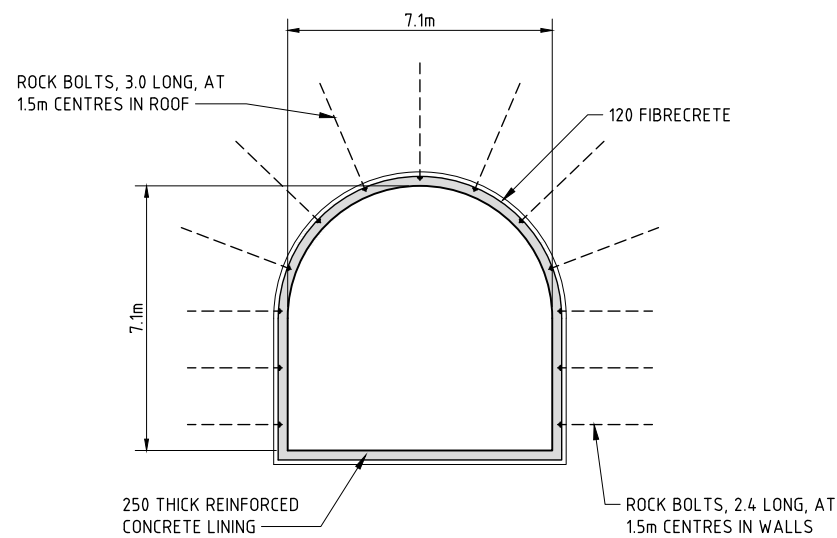
RESIDUAL FLOW DISSIPATION CHAMBER



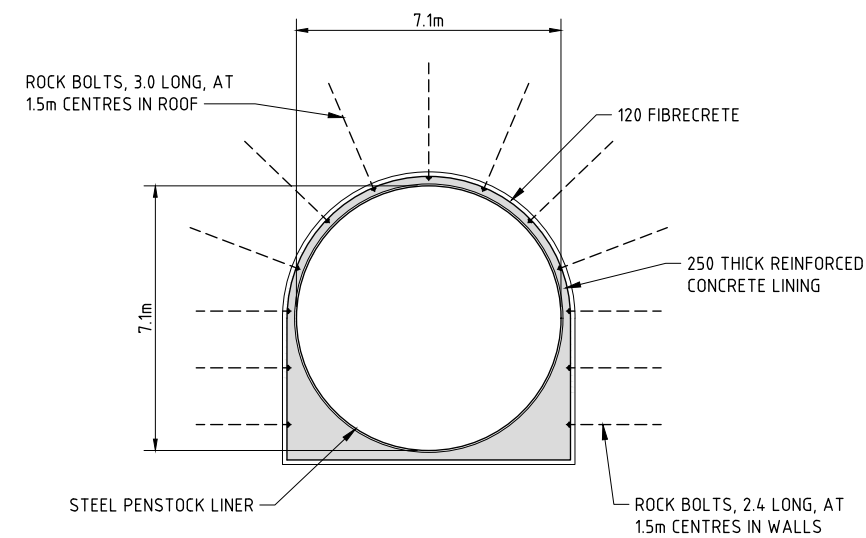
**WATER CONVEYANCE POWER SHAFT
RESIDUAL FLOW VALVE SHAFT SIMILAR**



**TYPE A - FAIR QUALITY ROCK
Q INDEX RANGE 1-10**

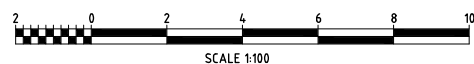


**TYPE B - VERY POOR QUALITY ROCK
Q INDEX RANGE 0.1-1.0**



STEEL LINER AT DOWNSTREAM PORTAL

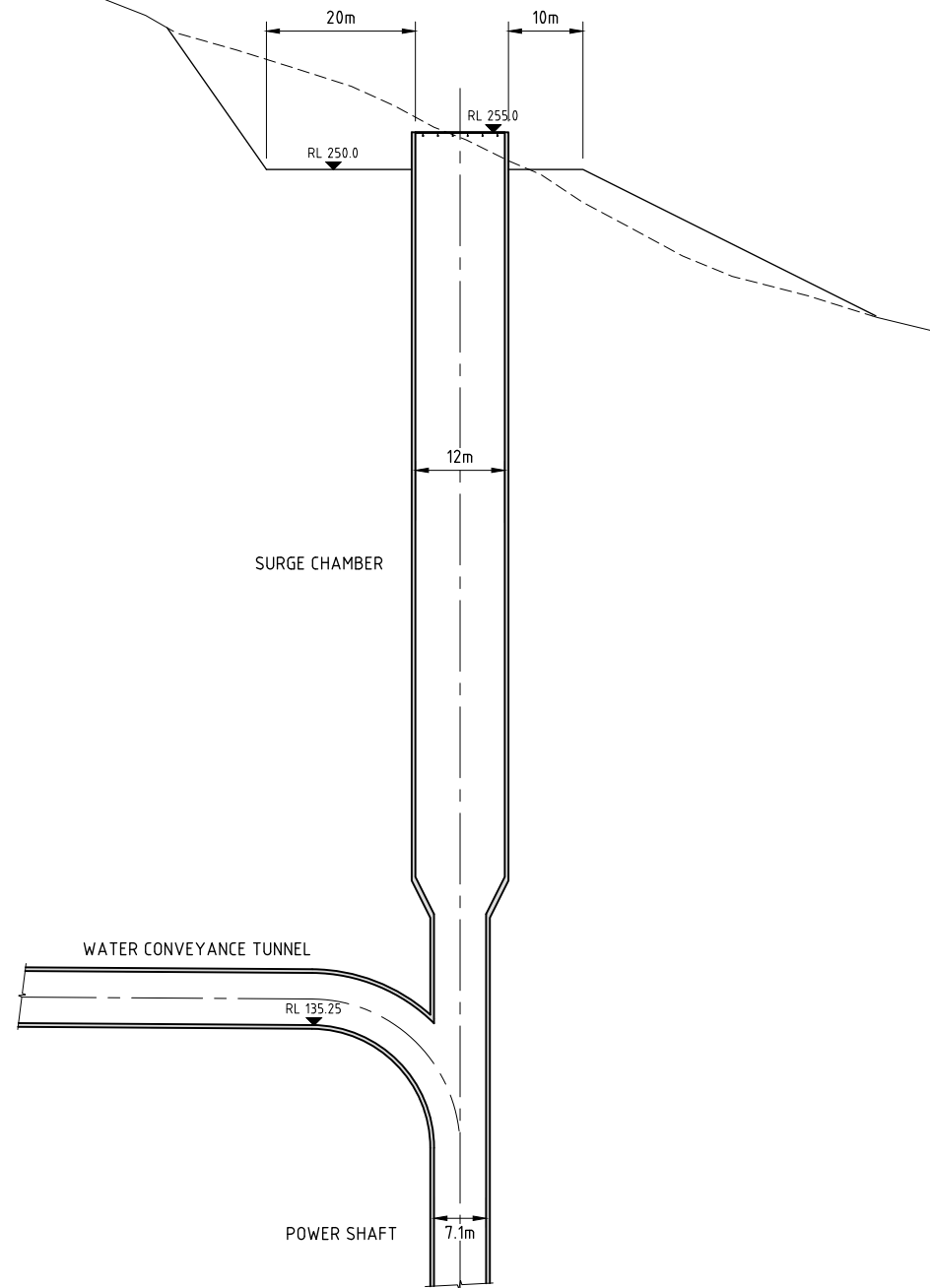
WATER CONVEYANCE TUNNEL



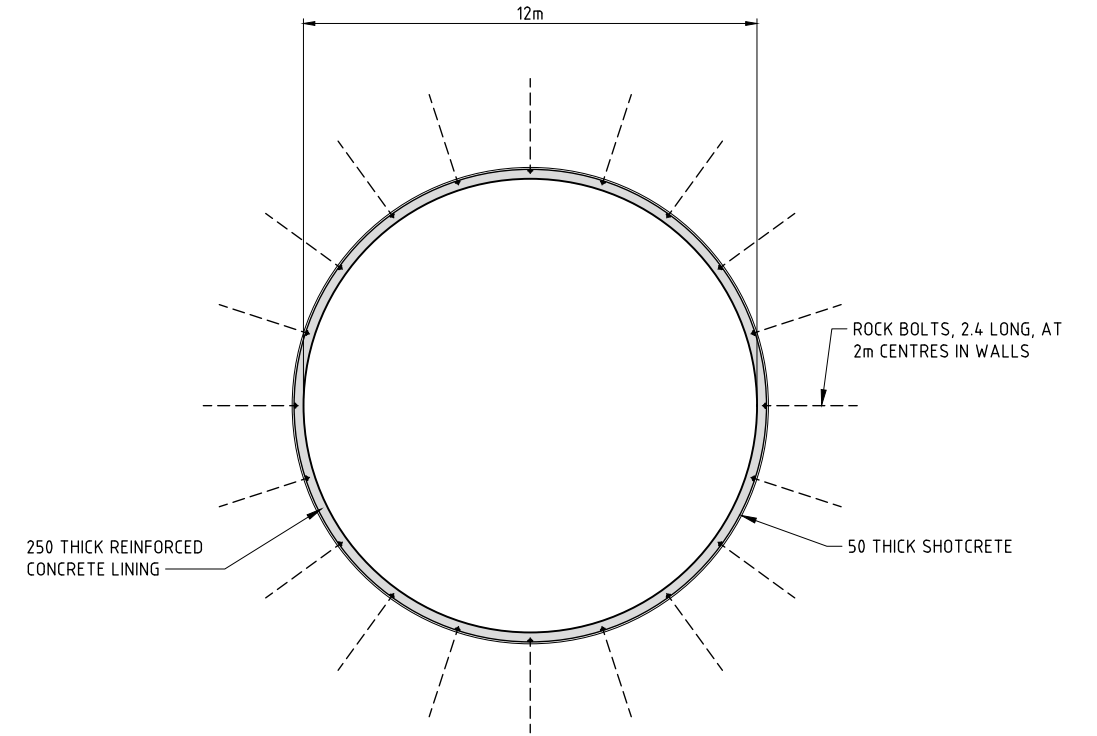
C:\DATA\PDF\FRIEDA RIVER\FRP-2-D-14-01-D-030-009.DWG

				ENGINEERING COMPANY			DRAWN MURR 28.06.18				OWNER		STATUS		
				DESIGN DEVL 28.06.18			DESIGN DEVL 28.06.18				FRIEDA RIVER LIMITED		FOR INFORMATION		
				DES.CHKD ROBI 28.06.18			LD ENG. APPR BROW 28.06.18				TITLE		SCALE 1:100	REV No.	SIZE
				PM APPR BROW 28.06.18			PM APPR BROW 28.06.18				FRIEDA RIVER HYDROELECTRIC PROJECT TUNNEL SECTIONS		ALL DIMENSIONS IN METRES	B	A1
REF. DWG No.	DWG. DESCRIPTION	No	DATE	REVISION DETAILS		LD ENG.	PM	VENDOR DRG NO.	80510050	DRAWING No		FRP-2-D-14-01-D-030-009			

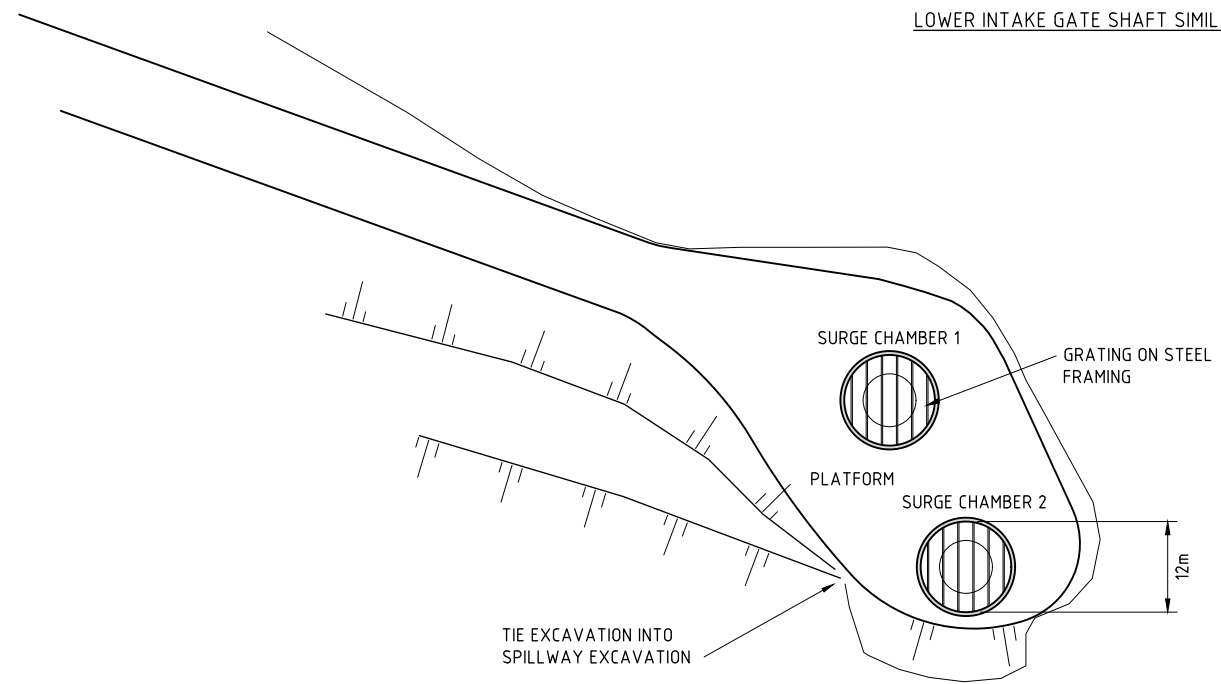
PROJECTION: UNIVERSAL TRANSVERSE MERCATOR, ZONE 54
 HORIZONTAL DATUM: PAPUA NEW GUINEA MAP GRID 1994 (PNGMG94)
 VERTICAL DATUM: AITAPE MEAN SEA LEVEL (MSL)



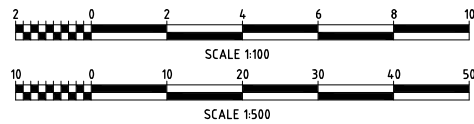
SURGE CHAMBER SECTION






SURGE CHAMBER TYPICAL SECTION
 LOWER INTAKE GATE SHAFT SIMILAR



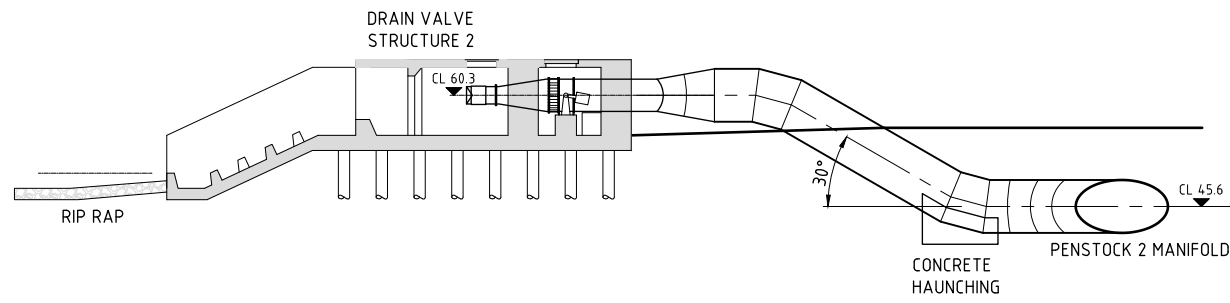
SURGE CHAMBER PLAN



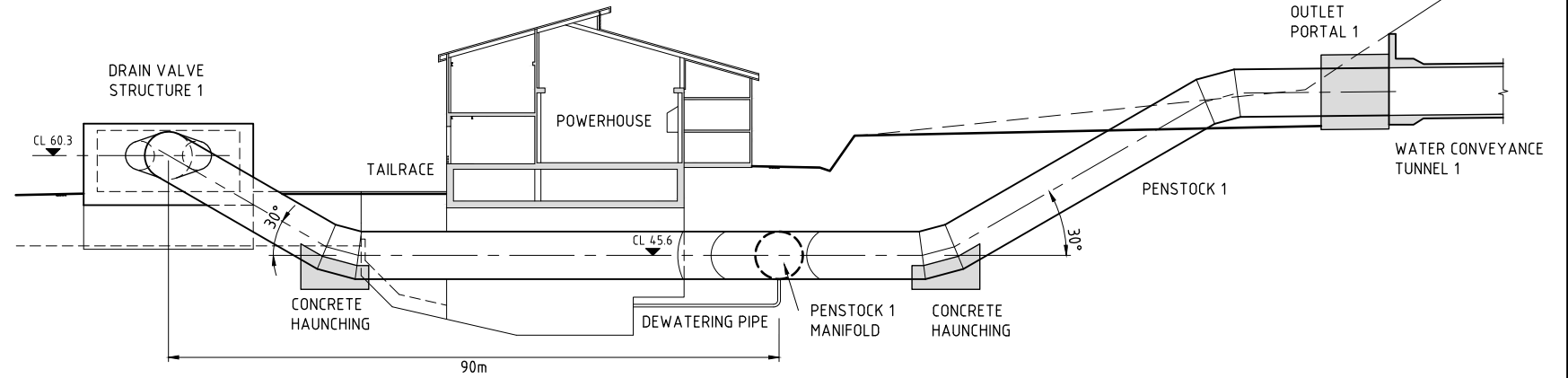
C:\DATA\PDF\FRIEDA RIVER\FRP-2-D-14-01-D-030-010.DWG

				ENGINEERING COMPANY		DRAWN MURR 28.06.18			  	OWNER FRIEDA RIVER LIMITED		STATUS FOR INFORMATION	
				DESIGN LUSK 28.06.18			SCALE 1:500 1:100			REV No.	SIZE		
				DES.CHKD ROBI 28.06.18			ALL DIMENSIONS IN METRES			B	A1		
				LD ENG. APPR BROW 28.06.18			DRAWING No			FRP-2-D-14-01-D-030-010			
REF. DWG No.	DWG. DESCRIPTION	No	DATE	REVISION DETAILS		LD ENG.	PM	VENDOR DRG NO. 80510050	PM APPR BROW 28.06.18				

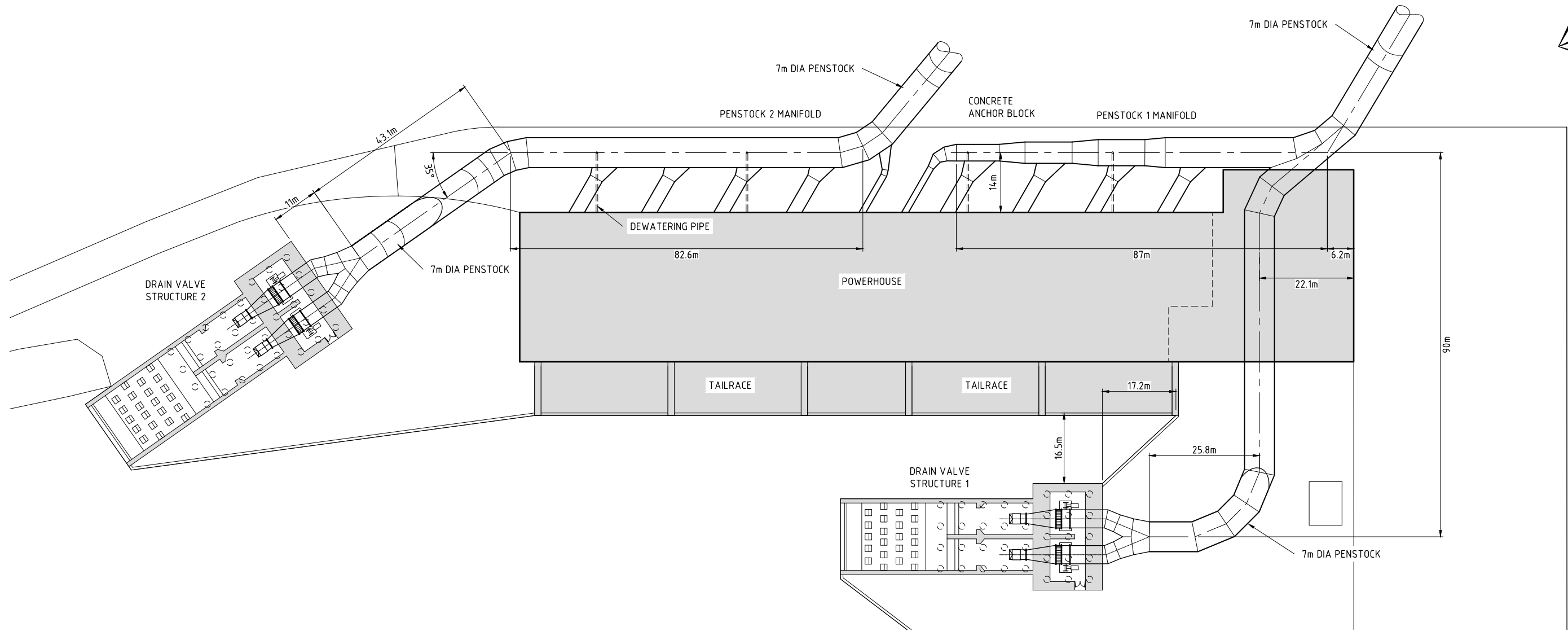
PROJECTION: UNIVERSAL TRANSVERSE MERCATOR, ZONE 54
 HORIZONTAL DATUM: PAPUA NEW GUINEA MAP GRID 1994 (PNGMG94)
 VERTICAL DATUM: AITAPE MEAN SEA LEVEL (MSL)



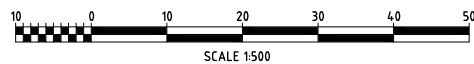
PENSTOCK 2 TO DRAIN VALVE ELEVATION



PENSTOCK 1 TO DRAIN VALVE ELEVATION



PENSTOCK PLAN



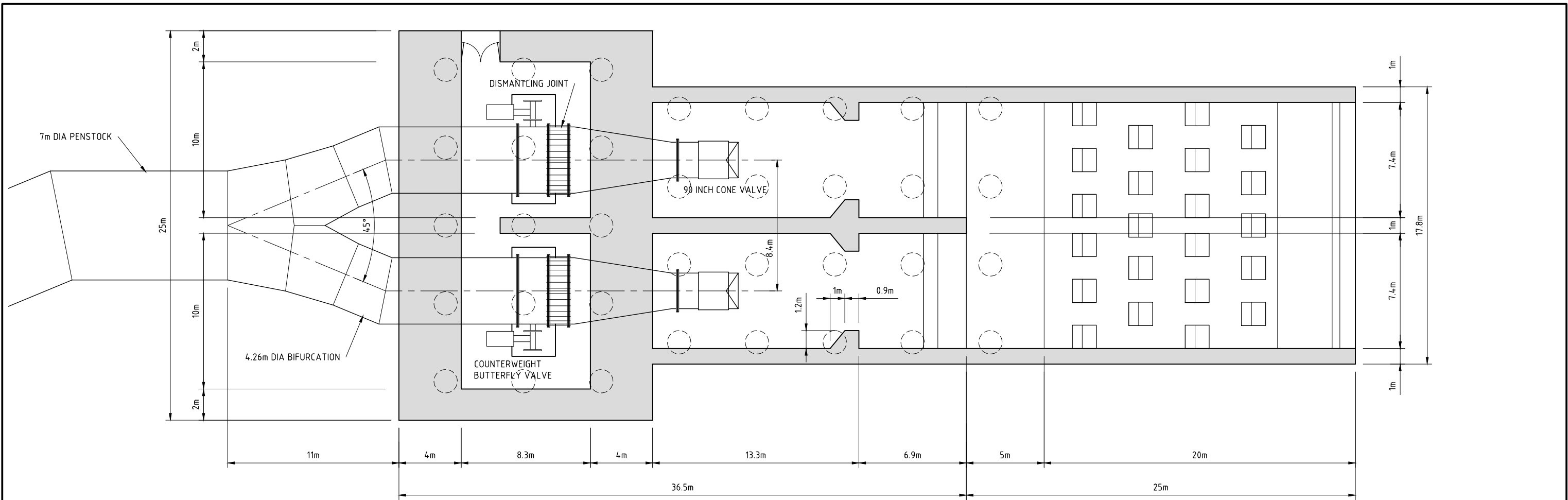
C:\DATA\PDF\FRIEDA RIVER\FRP-2-D-14-01-D-030-011.DWG

REF. DWG No.	DWG. DESCRIPTION	No	DATE	REVISION DETAILS	LD ENG.	PM
		B	24.09.18	ISSUED FOR FINAL REPORT	BROW	BROW
		A	28.06.18	ISSUED FOR CLIENT REVIEW	BROW	BROW

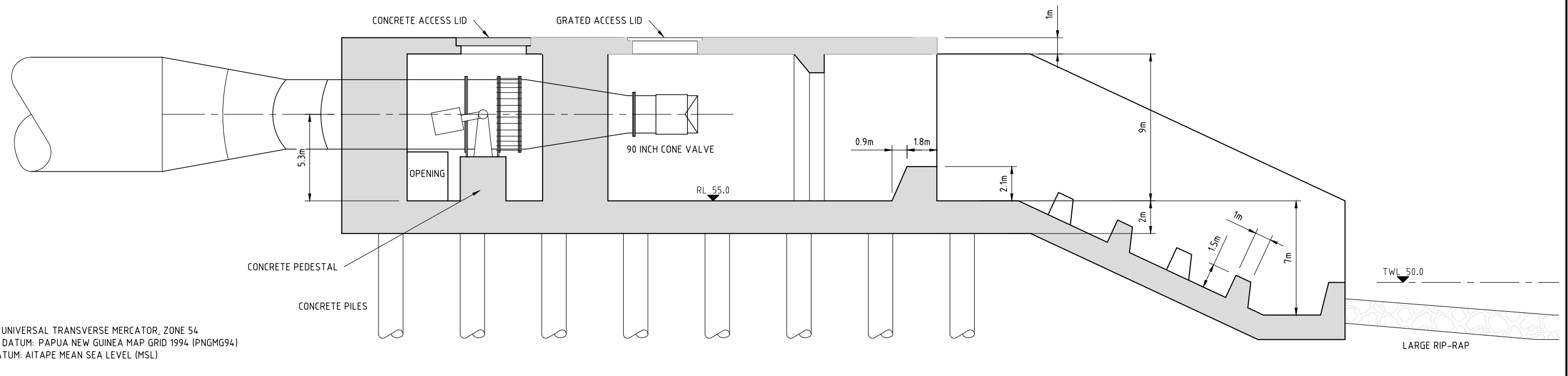
ENGINEERING COMPANY			DRAWN	MURR	28.06.18
			DESIGN	LUSK	28.06.18
			DES.CHKD	ROBI	28.06.18
			LD ENG. APPR	BROW	28.06.18
			PM APPR	BROW	28.06.18

OWNER	FRIEDA RIVER LIMITED	
TITLE	FRIEDA RIVER HYDROELECTRIC PROJECT PENSTOCK PLAN AND ELEVATIONS	

STATUS FOR INFORMATION		
SCALE 1:500	REV No.	SIZE
ALL DIMENSIONS IN METRES	B	A1
DRAWING No FRP-2-D-14-01-D-030-011		

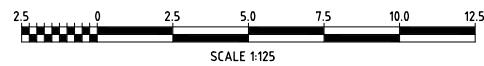


DRAIN VALVE STRUCTURE PLAN



DRAIN VALVE STRUCTURE SECTION

PROJECTION: UNIVERSAL TRANSVERSE MERCATOR, ZONE 54
 HORIZONTAL DATUM: PAPUA NEW GUINEA MAP GRID 1994 (PNGMG94)
 VERTICAL DATUM: AITAPE MEAN SEA LEVEL (MSL)



C:\DATA\PDF\FRIEDA RIVER\FRP-2-D-14-01-D-030-012.DWG

REF. DWG No.	DWG. DESCRIPTION	No	DATE	REVISION DETAILS	LD ENG.	PM
		B	24.09.18	ISSUED FOR FINAL REPORT	BROW	BROW
		A	28.06.18	ISSUED FOR CLIENT REVIEW	BROW	BROW

ENGINEERING COMPANY



VENDOR DRG NO. 80510050

DRAWN	MURR	28.06.18
DESIGN	DEVL	28.06.18
DES.CHKD	ROBI	28.06.18
LD ENG. APPR	BROW	28.06.18
PM APPR	BROW	28.06.18



OWNER
FRIEDA RIVER LIMITED

TITLE
 FRIEDA RIVER HYDROELECTRIC PROJECT
 DRAIN VALVE STRUCTURE PLAN AND SECTION

STATUS FOR INFORMATION		
SCALE 1:125	REV No.	SIZE
ALL DIMENSIONS IN METRES	B	A1
DRAWING No FRP-2-D-14-01-D-030-012		

PROJECTION: UNIVERSAL TRANSVERSE MERCATOR, ZONE 54
 HORIZONTAL DATUM: PAPUA NEW GUINEA MAP GRID 1994 (PNGMG94)
 VERTICAL DATUM: AITAPE MEAN SEA LEVEL (MSL)



100.0

75.0

CONCRETE LINED WATER CHANNEL

OUTLET PORTAL 2

OUTLET PORTAL 1

PENSTOCK 2

PENSTOCK 1

WATER CHANNEL

RL 56.0

HARDSTAND
RL 59.0

FFL 59.2

POWERHOUSE

RL 55.0

DRAIN VALVE
STRUCTURE 2

RETAINING WALL

TAILRACE

RL 56.0

RIP RAP
RL 48.0

RETAINING WALL

LOAD BANKS

TRANSFORMER

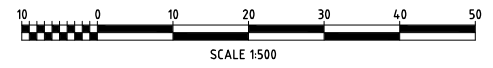
DRAIN VALVE
STRUCTURE 1

RL 55.0

RETAINING WALL

RL 58.0

WATER CHANNEL



C:\DATA\PDF\FRIEDA RIVER\FRP-2-D-12-01-D-030-001.DWG

REF. DWG No.	DWG. DESCRIPTION	No	DATE	REVISION DETAILS	LD ENG.	PM
		B	24.09.18	ISSUED FOR FINAL REPORT	BROW	BROW
		A	28.06.18	ISSUED FOR CLIENT REVIEW	BROW	BROW

ENGINEERING COMPANY



DRAWN	MURR	28.06.18
DESIGN	DEVL	28.06.18
DES.CHKD	ROBI	28.06.18
LD ENG. APPR	BROW	28.06.18
PM APPR	BROW	28.06.18

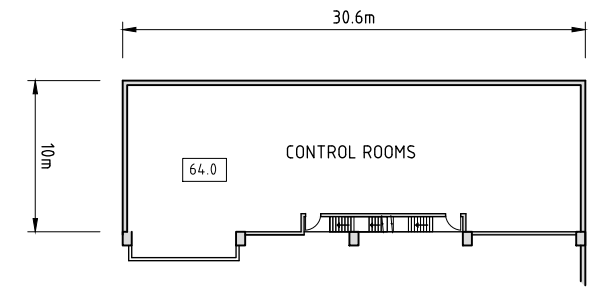


OWNER
FRIEDA RIVER LIMITED

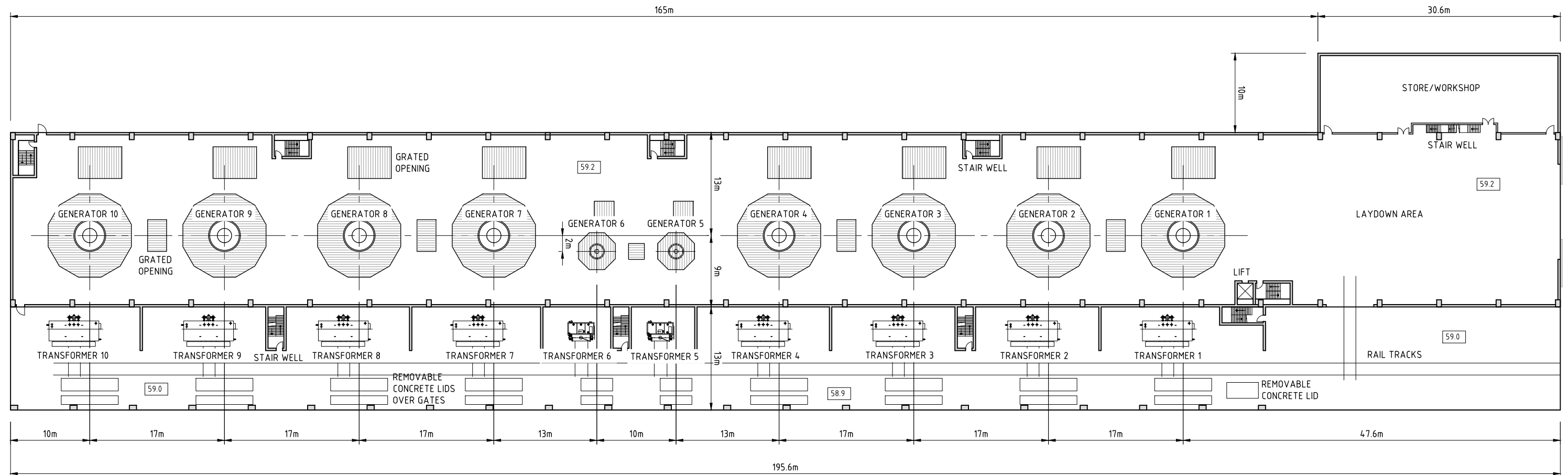
TITLE
**FRIEDA RIVER HYDROELECTRIC PROJECT
POWERHOUSE SITE PLAN**

STATUS FOR INFORMATION		
SCALE 1:500	REV No.	SIZE
ALL DIMENSIONS IN METRES	B	A1
DRAWING No FRP-2-D-12-01-D-030-001		

PROJECTION: UNIVERSAL TRANSVERSE MERCATOR, ZONE 54
 HORIZONTAL DATUM: PAPUA NEW GUINEA MAP GRID 1994 (PNGMG94)
 VERTICAL DATUM: AITAPE MEAN SEA LEVEL (MSL)



CONTROL ROOM LEVEL PLAN



MACHINE HALL LEVEL PLAN



C:\DATA\PDF\FRIEDA RIVER\FRP-2-D-12-01-D-030-003.DWG

REF. DWG No.	DWG. DESCRIPTION	No	DATE	REVISION DETAILS	LD ENG.	PM
		B	24.09.18	ISSUED FOR FINAL REPORT	BROW	BROW
		A	28.06.18	ISSUED FOR CLIENT REVIEW	BROW	BROW

ENGINEERING COMPANY



VENDOR DRG NO. 80510050

DRAWN	MURR	28.06.18
DESIGN	DEVL	28.06.18
DES.CHKD	ROBI	28.06.18
LD ENG. APPR	BROW	28.06.18
PM APPR	BROW	28.06.18

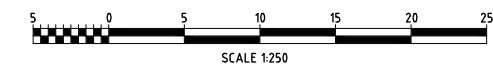
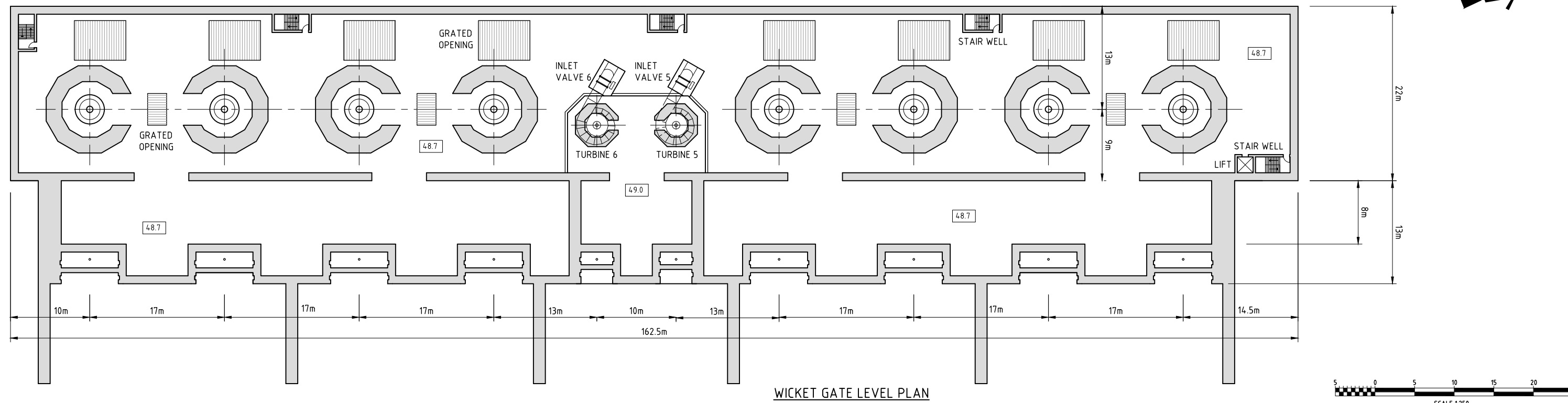
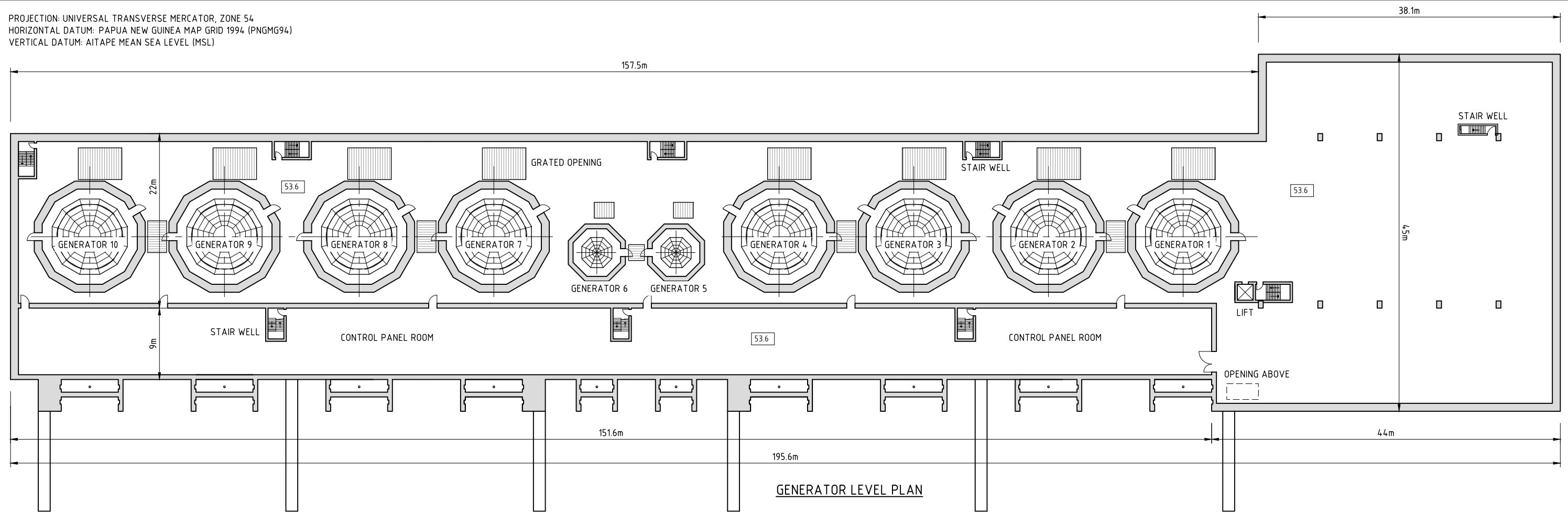


OWNER
FRIEDA RIVER LIMITED

TITLE
**FRIEDA RIVER HYDROELECTRIC PROJECT
 POWERHOUSE MACHINE HALL AND
 CONTROL ROOM LEVEL PLANS**

STATUS FOR INFORMATION		
SCALE 1:250	REV No.	SIZE
ALL DIMENSIONS IN METRES	B	A1
DRAWING No FRP-2-D-12-01-D-030-003		

PROJECTION: UNIVERSAL TRANSVERSE MERCATOR, ZONE 54
 HORIZONTAL DATUM: PAPUA NEW GUINEA MAP GRID 1994 (PNGMG94)
 VERTICAL DATUM: AITAPE MEAN SEA LEVEL (MSL)



C:\DATA\PDF\FRIEDA RIVER\FRP-2-D-12-01-D-030-004.DWG

REF. DWG No.	DWG. DESCRIPTION	No	DATE	REVISION DETAILS	LD ENG.	PM
		B	24.09.18	ISSUED FOR FINAL REPORT	BROW	BROW
		A	28.06.18	ISSUED FOR CLIENT REVIEW	BROW	BROW

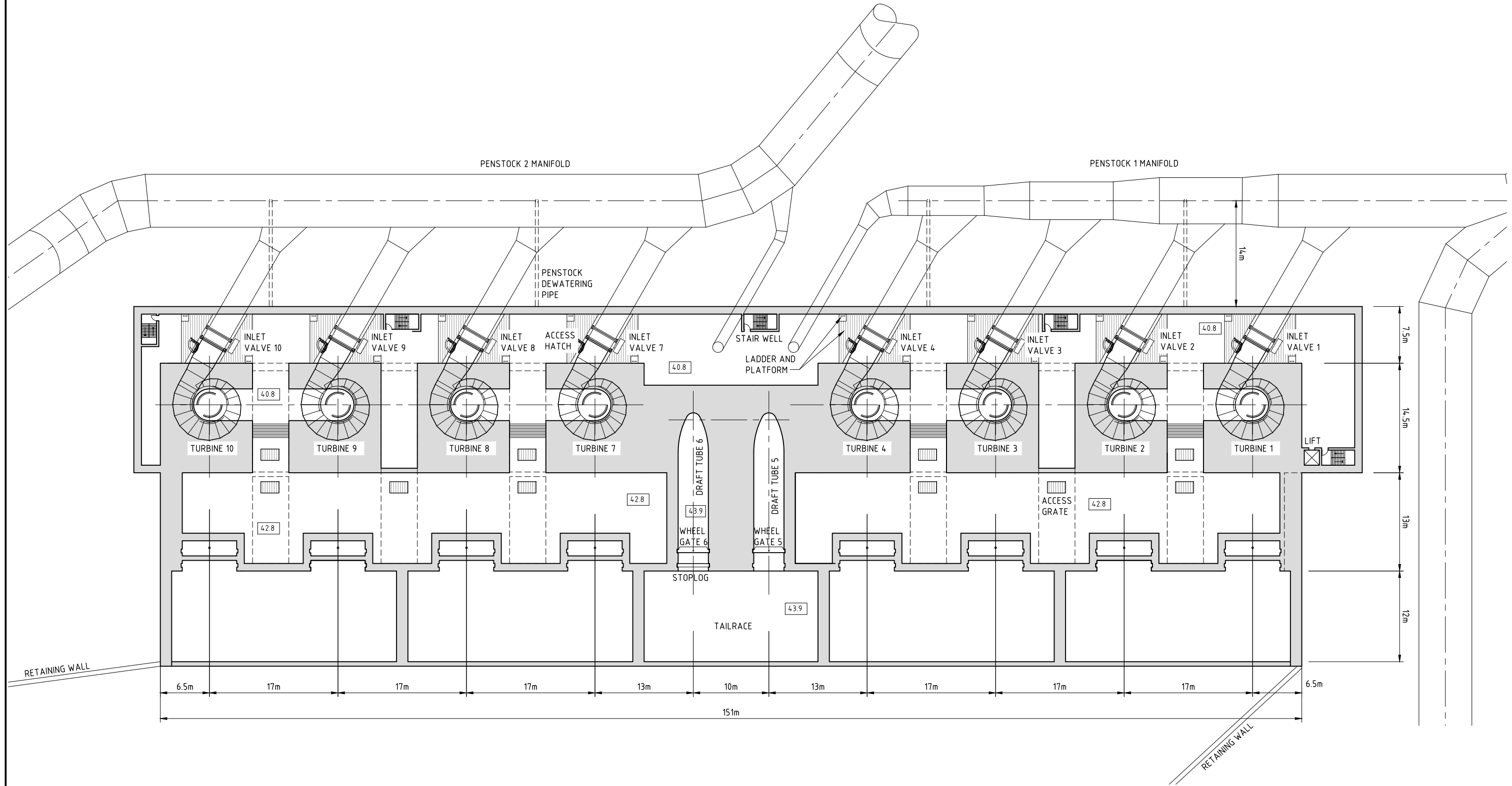
ENGINEERING COMPANY			DRAWN	MURR	28.06.18
 PANAUST Stantec			DESIGN	DEVL	28.06.18
			DES.CHKD	ROBI	28.06.18
FRIEDA RIVER			LD ENG. APPR	BROW	28.06.18
			PM APPR	BROW	28.06.18



OWNER	FRIEDA RIVER LIMITED	
TITLE	FRIEDA RIVER HYDROELECTRIC PROJECT POWERHOUSE WICKET GATE AND GENERATOR LEVEL PLANS	

STATUS FOR INFORMATION		
SCALE	1:250	REV No.
ALL DIMENSIONS IN METRES	B	SIZE A1
DRAWING No FRP-2-D-12-01-D-030-004		

PROJECTION: UNIVERSAL TRANSVERSE MERCATOR, ZONE 54
 HORIZONTAL DATUM: PAPUA NEW GUINEA MAP GRID 1994 (PNGMG94)
 VERTICAL DATUM: AITAPE MEAN SEA LEVEL (MSL)



TURBINE LEVEL PLAN

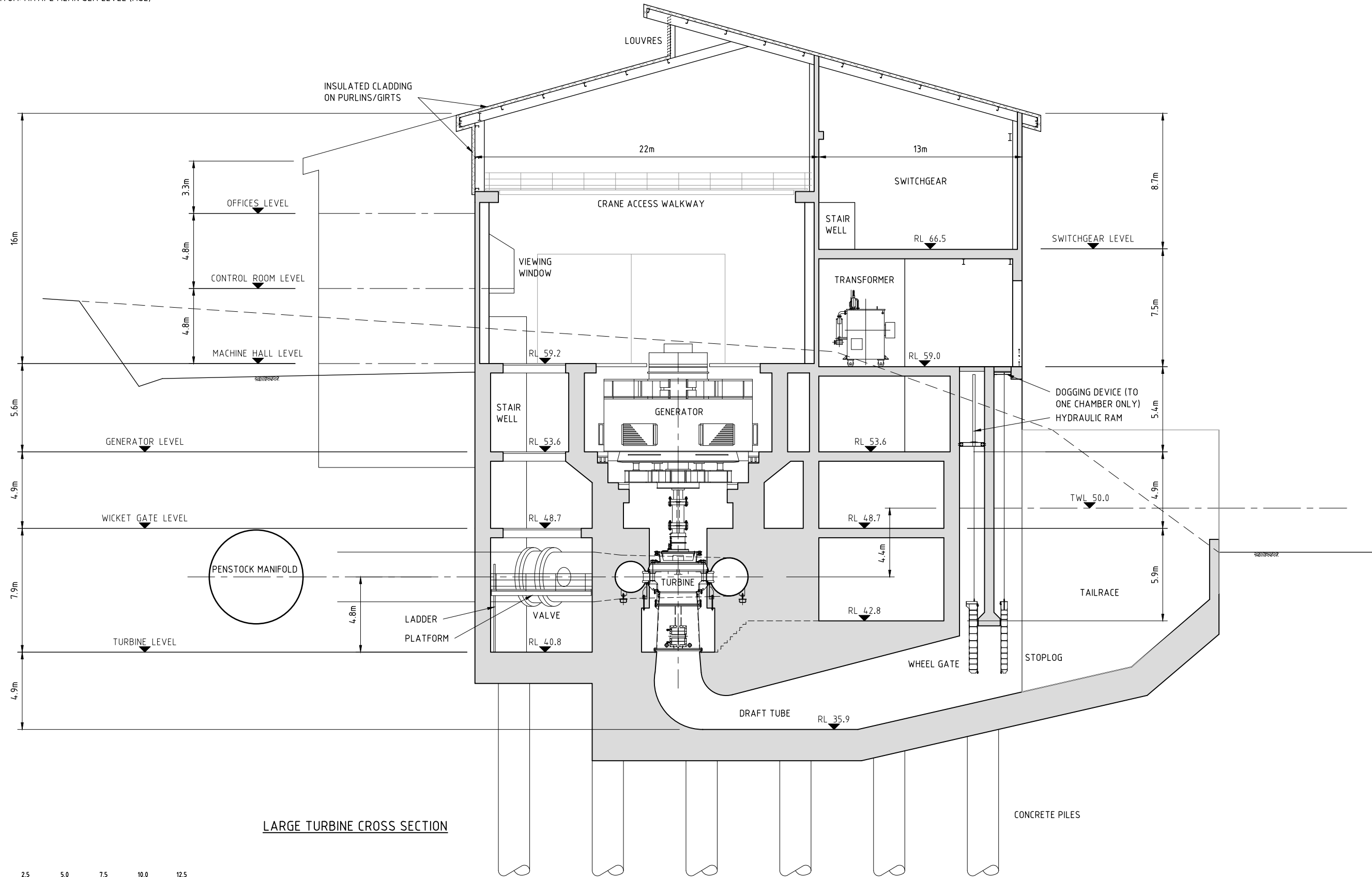


C:\DATA\PDF\FRIEDA RIVER\FRP-2-D-12-01-D-030-005.DWG

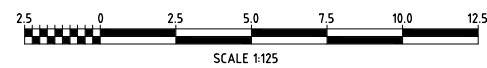
				ENGINEERING COMPANY		DRAWN MURR 28.06.18			OWNER FRIEDA RIVER LIMITED		STATUS FOR INFORMATION	
				 		DESIGN DEVL 28.06.18					SCALE 1:250	REV No.
						DES.CHKD ROBI 28.06.18			TITLE FRIEDA RIVER HYDROELECTRIC PROJECT POWERHOUSE TURBINE LEVEL PLAN		ALL DIMENSIONS IN METRES	
						LD ENG. APPR BROW 28.06.18					B	A1
REF. DWG No.	DWG. DESCRIPTION	No	DATE	REVISION DETAILS		LD ENG.	PM	VENDOR DRG NO. 80510050	PM, APPR BROW 28.06.18	DRAWING No FRP-2-D-12-01-D-030-005		



PROJECTION: UNIVERSAL TRANSVERSE MERCATOR, ZONE 54
 HORIZONTAL DATUM: PAPUA NEW GUINEA MAP GRID 1994 (PNGMG94)
 VERTICAL DATUM: AITAPE MEAN SEA LEVEL (MSL)



LARGE TURBINE CROSS SECTION



C:\DATA\PDF\FRIEDA RIVER\FRP-2-D-12-01-D-030-007.DWG

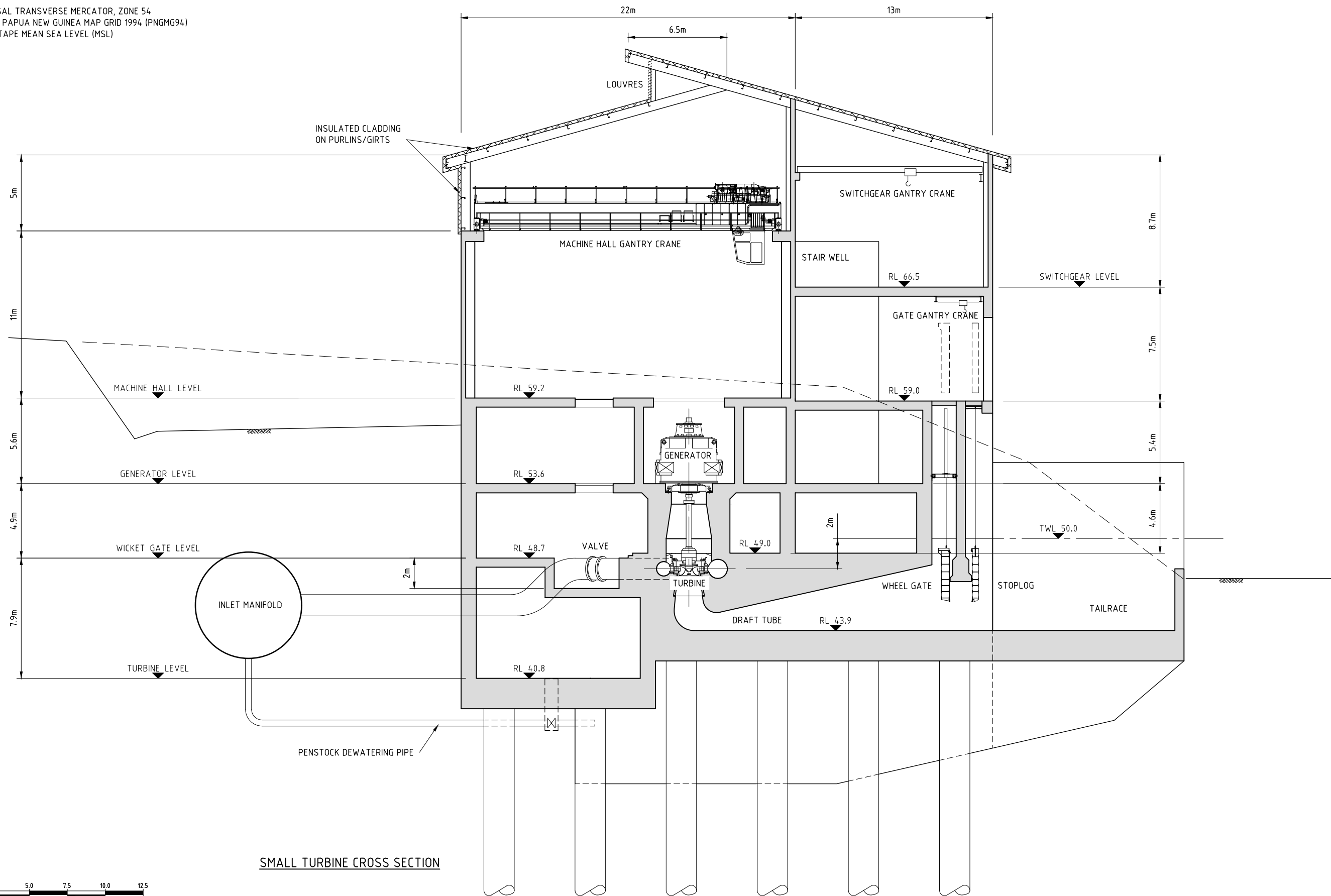
REF. DWG No.	DWG. DESCRIPTION	No	DATE	REVISION DETAILS	LD ENG.	PM
		B	24.09.18	ISSUED FOR FINAL REPORT	BROW	BROW
		A	28.06.18	ISSUED FOR CLIENT REVIEW	BROW	BROW

ENGINEERING COMPANY			DRAWN	MURR	28.06.18
 			DESIGN	DEVL	28.06.18
			DES.CHKD	ROBI	28.06.18
			LD ENG. APPR	BROW	28.06.18
			PM APPR	BROW	28.06.18

OWNER	FRIEDA RIVER LIMITED
TITLE	FRIEDA RIVER HYDROELECTRIC PROJECT POWERHOUSE LARGE TURBINE CROSS SECTION

STATUS FOR INFORMATION		
SCALE	1:125	REV No.
ALL DIMENSIONS IN METRES	B	SIZE A1
DRAWING No FRP-2-D-12-01-D-030-007		

PROJECTION: UNIVERSAL TRANSVERSE MERCATOR, ZONE 54
 HORIZONTAL DATUM: PAPUA NEW GUINEA MAP GRID 1994 (PNGMG94)
 VERTICAL DATUM: AITAPE MEAN SEA LEVEL (MSL)



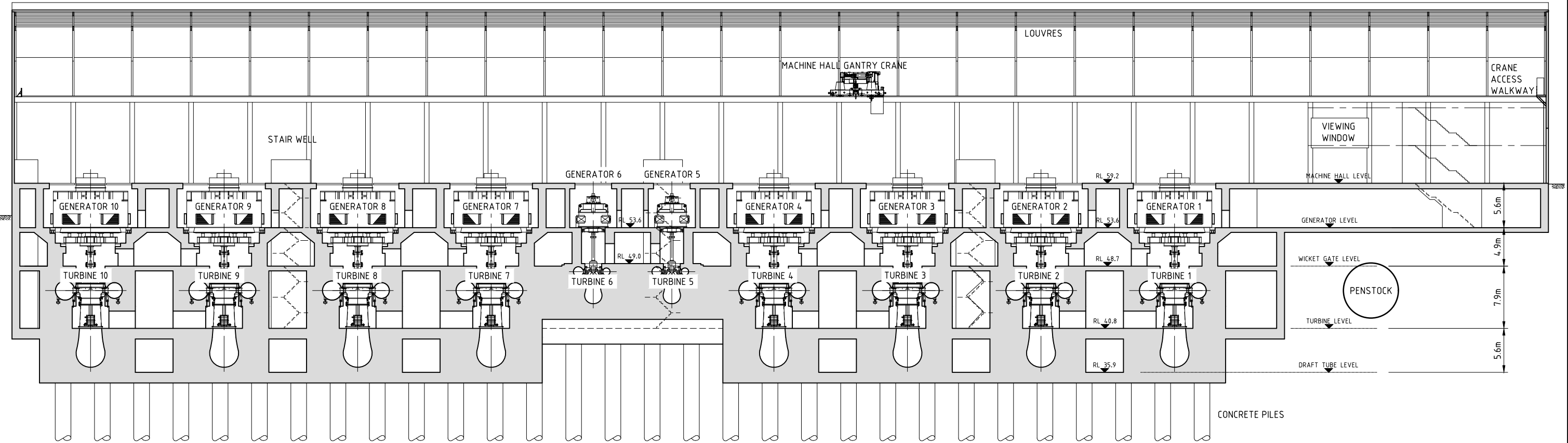
SMALL TURBINE CROSS SECTION



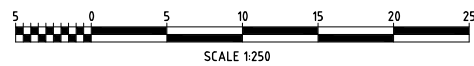
C:\DATA\PDF\FRIEDA RIVER\FRP-2-D-12-01-D-030-008.DWG

				ENGINEERING COMPANY		DRAWN MURR 28.06.18			OWNER		STATUS			
				 		DESIGN DEVL 28.06.18			FRIEDA RIVER LIMITED		FOR INFORMATION			
						DES.CHKD ROBI 28.06.18			TITLE		SCALE 1:125	REV No.	SIZE	
				LD ENG. APPR BROW 28.06.18		PM APPR BROW 28.06.18			FRIEDA RIVER HYDROELECTRIC PROJECT		ALL DIMENSIONS IN METRES		B	A1
				VENDOR DRG NO. 80510050					POWERHOUSE SMALL TURBINE CROSS SECTION		DRAWING No		FRP-2-D-12-01-D-030-008	
REF. DWG No.	DWG. DESCRIPTION	No	DATE	REVISION DETAILS		LD ENG.	PM							
		B	24.09.18	ISSUED FOR FINAL REPORT		BROW	BROW							
		A	28.06.18	ISSUED FOR CLIENT REVIEW		BROW	BROW							

PROJECTION: UNIVERSAL TRANSVERSE MERCATOR, ZONE 54
 HORIZONTAL DATUM: PAPUA NEW GUINEA MAP GRID 1994 (PNGMG94)
 VERTICAL DATUM: AITAPE MEAN SEA LEVEL (MSL)

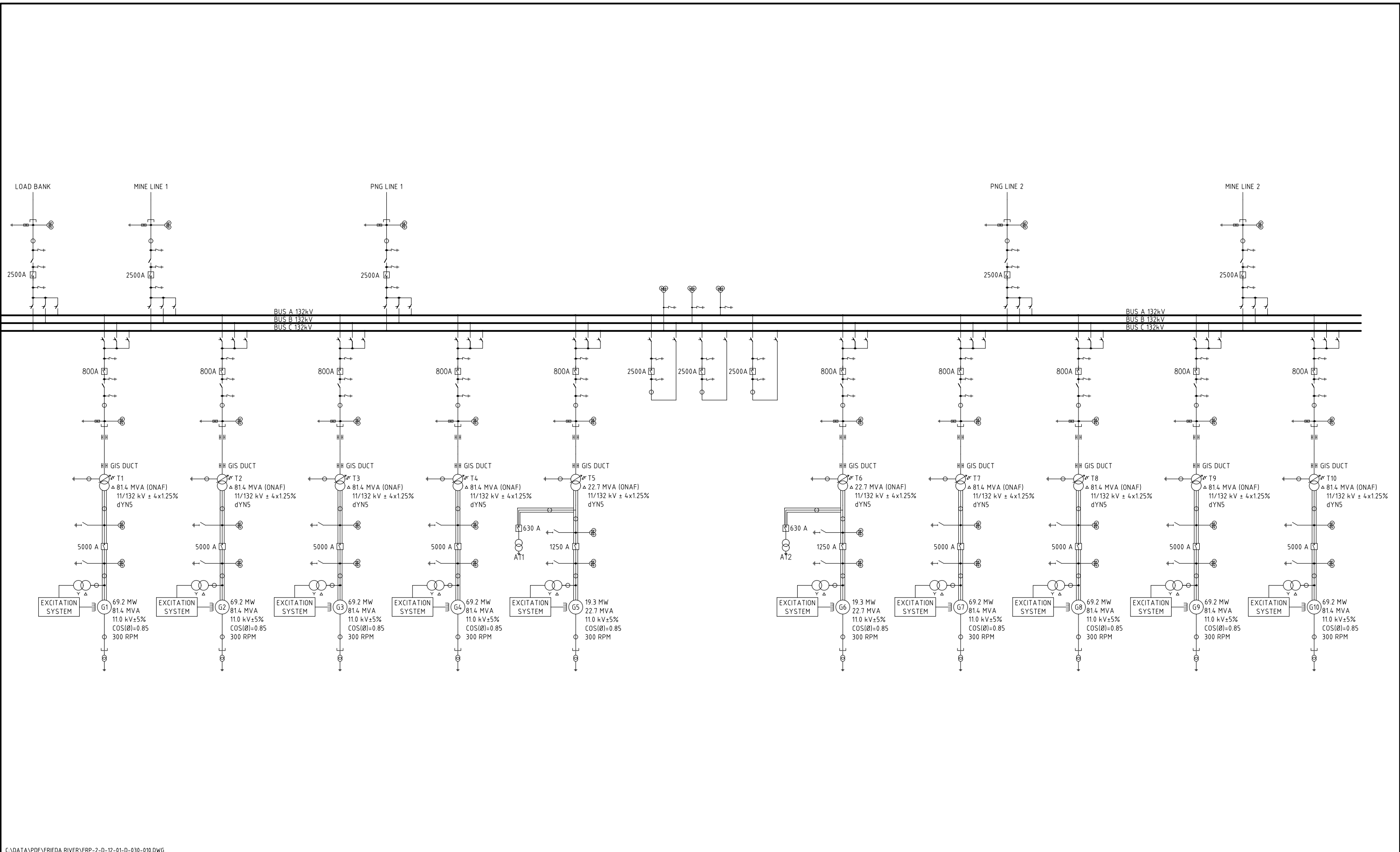


LONGSECTION



C:\DATA\PDF\FRIEDA RIVER\FRP-2-D-12-01-D-030-009.DWG

							ENGINEERING COMPANY 			DRAWN MURR 28.06.18 DESIGN DEVL 28.06.18 DES.CHKD ROBI 28.06.18 LD ENG. APPR BROW 28.06.18 PM APPR BROW 28.06.18			OWNER FRIEDA RIVER LIMITED			STATUS FOR INFORMATION		
										TITLE FRIEDA RIVER HYDROELECTRIC PROJECT POWERHOUSE LONGSECTION			SCALE 1:250 ALL DIMENSIONS IN METRES					
							BROW BROW BROW BROW			REV No. B SIZE A1								
							REF. DWG No. DWG. DESCRIPTION No DATE REVISION DETAILS LD ENG. PM VENDOR DRG NO. 80510050			DRAWING No FRP-2-D-12-01-D-030-009								



C:\DATA\PDF\FRIEDA RIVER\FRP-2-D-12-01-D-030-010.DWG

REF. DWG No.	DWG. DESCRIPTION	No	DATE	REVISION DETAILS	LD ENG.	PM
		B	24.09.18	ISSUED FOR FINAL REPORT	BROW	BROW
		A	28.06.18	ISSUED FOR CLIENT REVIEW	BROW	BROW

ENGINEERING COMPANY			DRAWN	SPIT	DATE
			DESIGN	SPIT	28.06.18
			DES.CHKD	ROBI	28.06.18
			LD ENG. APPR	BROW	28.06.18
			PM APPR	BROW	28.06.18



OWNER	
FRIEDA RIVER LIMITED	
TITLE	
FRIEDA RIVER HYDROELECTRIC PROJECT POWERHOUSE SINGLE LINE DIAGRAM	

STATUS FOR INFORMATION		
SCALE	NTS	REV No.
ALL DIMENSIONS IN METRES		SIZE
		B A1
DRAWING No		
FRP-2-D-12-01-D-030-010		

Appendix 2: Artist's Impression

